Palaeontology

VOLUME 41 · PART 5 · SEPTEMBER 1998

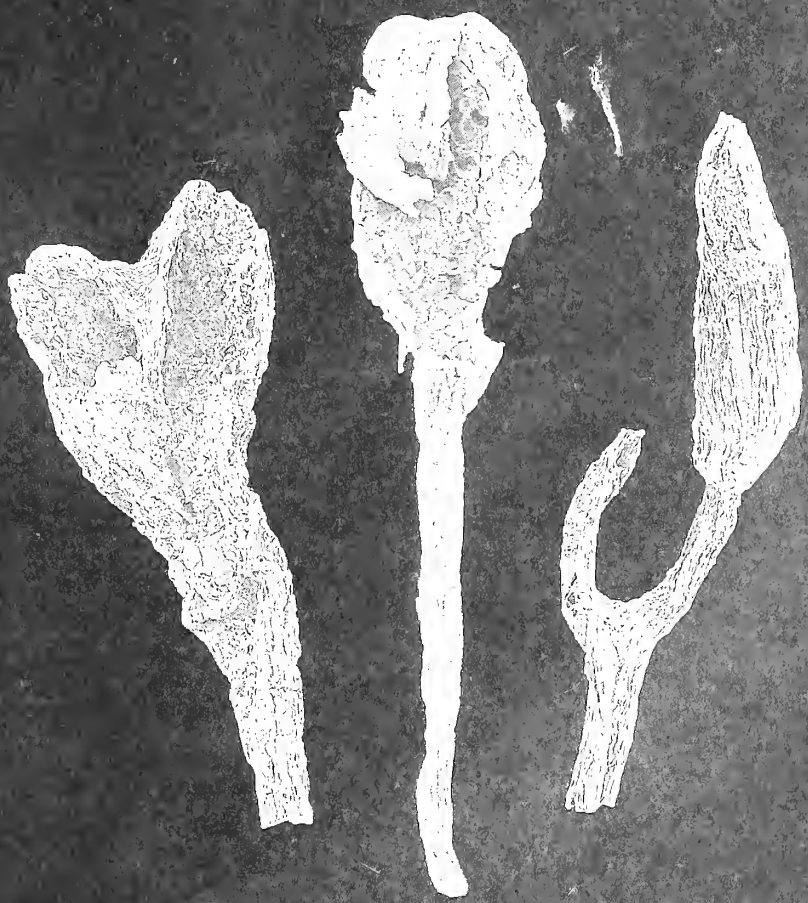

Published by
The Palaeontological Association · London
Price £38·00

THE PALAEONTOLOGICAL ASSOCIATION

(Registered Charity No. 276369)

The Association was founded in 1957 to promote research in palaeontology and its allied sciences.

COUNCIL 1997–1998

President: Professor E. N. K. CLARKSON, Department of Geology and Geophysics, University of Edinburgh, West Mains Road, Edinburgh EH9 3JW

Vice-Presidents: Dr R. M. OWENS, Department of Geology, National Museum and Gallery of Wales, Cardiff CF1 3NP
Dr P. DOYLE, Department of Earth Sciences, University of Greenwich, Grenville Building, Pembroke, Chatham Maritime, Kent ME4 4AW

Treasurer: Dr T. J. PALMER, Institute of Geography and Earth Sciences, University of Wales, Aberystwyth, Dyfed SY23 3DB

Membership Treasurer: Dr M. J. BARKER, Department of Geology, University of Portsmouth, Burnaby Road, Portsmouth PO1 3QL

Institutional Membership Treasurer: Dr J. E. FRANCIS, Department of Earth Sciences, The University, Leeds LS2 9JJ

Secretary: Dr M. P. SMITH, School of Earth Sciences, University of Birmingham, Birmingham B15 2TT

Newsletter Editor: Dr S. RIGBY, Department of Geology and Geophysics, University of Edinburgh, West Mains Road, Edinburgh EH9 3JW (co-opted)

Newsletter Reporter: Dr P. PEARSON, Geology Department, University of Bristol, Wills Memorial Building, Queens Road, Bristol BS8 1RJ

Marketing Manager: Dr A. KING, English Nature, Northminster House, Peterborough PE1 1UA

Publicity Officer: Dr M. A. PURNELL, Department of Geology, University of Leieester, University Road, Leicester LE1 7RH

Editors

Dr D. M. UNWIN, Geology Department, University of Bristol, Wills Memorial Building, Queens Road, Bristol BS8 1RJ
Dr R. WOOD, Department of Earth Sciences, University of Cambridge, Downing Street, Cambridge CB2 3EQ
Dr D. A. T. HARPER, Geologisk Museum, Copenhagen University, Øster Voldgade 5–7, 1350 Copenhagen K, Denmark
Dr A. R. HEMSLEY, Department of Earth Seiences, University of Wales College of Cardiff, Cardiff CF1 3YE
Dr J. CLACK, University Museum of Zoology, University of Cambridge, Downing Street, Cambridge CB2 3EJ
Dr B. M. COX, British Geologieal Survey, Keyworth, Nottingham NG12 5GG
Dr D. K. LOYDELL (Technical Editor), Department of Geology, University of Portsmouth, Burnaby Building, Burnaby Road, Portsmouth PO1 3QL

Other Members: Dr M. J. SIMMS, Department of Geology, Ulster Museum, Botanic Gardens, Belfast BT9 5AB
Mr F. W. J. BRYANT, 27, The Creseent, Maidenhead, Berkshire SL6 6AA

Overseas Representatives

Argentina: Dr M. O. MANCEÑIDO, Division Paleozoologia invertebrados, Faeultad de Cienеias Naturales y Museo, Paseo del Bosque, 1900 La Plata. *Australia*: Dr K. J. MCNAMARA, Western Australian Museum, Francis Street, Perth, Western Australia 6000. *Canada*: Professor S. H. WILLIAMS, Department of Earth Sciences, Memorial University, St John's, Newfoundland A1B 3X5. *China*: Dr CHANG MEE-MANN, Institute of Vertebrate Palaeontology and Palaeoanthropology, Academia Sinica, P.O. Box 643, Beijing. Dr RONG JIA-YU, Nanjing Institute of Geology and Palaeontology, Chi-Ming-Ssu, Nanjing. *France*: Dr J.-L. HENRY, Institut de Géologie, Université de Rennes, Campus de Beaulieu, Avenue du Général Leclerc, 35042 Rennes Cédex. *Iberia*: Professor F. ALVAREZ, Departamento de Geologia, Universidad de Oviedo, C/. Jésus Arias de Velasco, s/n. 33005 Oviedo, Spain. *Japan*: Dr I. HAYAMI, University Museum, University of Tokyo, Hongo 7-3-1, Tokyo. *New Zealand*: Dr R. A. COOPER, New Zealand Geological Survey, P.O. Box 30368, Lower Hutt. *Scandinavia*: Dr R. BROMLEY, Fredskovvej 4, 2840 Holte, Denmark. *USA*: Professor A. J. ROWELL, Department of Geology, University of Kansas, Lawrenee, Kansas 66044. Professor N. M. SAVAGE, Department of Geology, University of Oregon, Eugene, Oregon 97403. Professor M. A. WILSON, Department of Geology, College of Wooster, Wooster, Ohio 44961. *Germany*: Professor F. T. FÜRSICH, Institut für Paläontologie, Universität, D8700 Würzburg, Pleieherwall 1

MEMBERSHIP

Membership is open to individuals and institutions on payment of the appropriate annual subscription. Rates for 1998 are:

Institutional membership . . .	£90·00 (U.S. $175)	Student membership	£10·00 (U.S. $20)
Ordinary membership . . .	£28·00 (U.S. $50)	Retired membership	£14·00 (U.S. $25)

There is no admission fee. Correspondence concerned with Institutional Membership should be addressed to **Dr J. E. Francis, Department of Earth Sciences, The University, Leeds LS2 9JJ.** Student members are persons receiving full-time instruction at educational institutions recognized by the Council. On first applying for membership, an application form should be obtained from the Membership Treasurer: **Dr M. J. Barker, Department of Geology, University of Portsmouth, Burnaby Road, Portsmouth PO1 3QL.** Subscriptions cover one calendar year and are due each January; they should be sent to the Membership Treasurer. All members who join for 1998 will receive *Palaeontology*, Volume 41, Parts 1–6. Enquiries concerning back numbers should be directed to the Marketing Manager.

Non-members may subscribe, and also obtain back issues up to five years old, at cover price through Blackwell Publishers Journals, P.O. Box 805, 108 Cowley Road, Oxford OX4 1FH, UK. For older issues contact the Marketing Manager.

US Mailing: Periodicals postage paid at Rahway, New Jersey. Postmaster: send address corrections to *Palaeontology*, c/o Mercury Airfreight International Ltd, 2323 E–F Randolph Avenue, Avenel, NJ 07001, USA (US mailing agent).

Cover: coalified terminal sporangia from the Lower Devonian of the Welsh Borderland containing permanent tetrads (far left) and dyads. Similar spores found dispersed in Ordovician rocks are considered the earliest evidence for embryophytic life on land (from left to right, NMW94.76G.1; NMW96.11G.6; NMW97.42G.4. All × 45).

THE SIGNIFICANCE OF A NEW NEPHROPID LOBSTER FROM THE MIOCENE OF ANTARCTICA

by RODNEY M. FELDMANN *and* J. ALISTAIR CRAME

ABSTRACT. The nephropid lobster, *Hoploparia gazdzicki* sp. nov., is described from Early Miocene glacio-marine sedimentary rocks of King George Island, South Shetland Islands, Antarctica. Such an occurrence considerably extends the stratigraphical range of a widespread lobster genus that reached its acme in the Late Cretaceous. The previous youngest records were from the Eocene of western Europe, and it would appear that, by the Early Miocene, the genus may have become a relict in relatively cold and deep waters in Antarctica. Although the full phylogenetic implications of this extension to the stratigraphical range are not yet apparent, there are some important palaeoecological ones. This occurrence can be taken as a further indication that certain benthic decapods were able to survive the onset of glacio-marine conditions in Antarctica. Perhaps other factors, such as the availability of food, habitat space, or decline in seasonal temperature fluctuation, ultimately controlled the decline of this major benthic group in the Southern Ocean.

THE fossil record of decapod crustaceans in Antarctica is remarkably robust in rocks ranging in age from Late Jurassic through to Eocene (Feldmann and Tshudy 1989). However, there are currently only two known occurrences of fossil decapods on the continent in post-Eocene rocks and there are only a few living pelagic decapods known from the region today. The decapods are certainly one of the key benthic groups to be grossly under-represented in the living Antarctic marine fuana and their demise has often been linked in a general way to Cenozoic climatic deterioration (Clarke and Crame 1989; Arntz *et al.* 1997). The two post-Eocene records of decapods in Antarctica are those of the homolodromiid crab, *Antarctidromia inflata* Förster, from the Cape Melville Formation (CMF) on King George Island, South Shetland Islands (Förster *et al.* 1985; see below), and an extremely fragmentary specimen of a palinurid lobster from the Pliocene of the Vestfold Hills, Princess Elizabeth Land (Feldmann and Quilty 1997). Although such a sparse record may be due to the restricted onshore occurrences of Cenozoic marine sedimentary rocks in Antarctica, it is also thought to reflect a very real decline in taxonomic diversity (Clarke and Crame 1989).

In this context, it is particularly significant that a new species of fossil lobster has been collected from the Lower Miocene at Cape Melville, King George Island (Text-fig. 1). It is even more noteworthy that this lobster, *Hoploparia gazdzickii* sp. nov., represents a significant upward extension in the stratigraphical range of a lineage whose acme was reached in the Late Cretaceous, and whose youngest known representative, prior to this discovery, was from the Eocene of the northern hemisphere. It is the purpose of this paper to describe this new species and to speculate on the implications of this occurrence for both decapod evolution and biogeography in the high southern latitudes.

GEOGRAPHICAL AND STRATIGRAPHICAL SETTING

The three specimens to be described here were collected from a sequence of glacio-marine sedimentary rocks which is virtually unique to the Cape Melville peninsula (Text-fig. 1). Collectively, the sequence comprises the CMF, which is in turn a component of the Moby Dick Group, King George Island Supergroup (Birkenmajer 1987). Estimated to be between 175 and 200 m thick, the CMF is in sharp contact at its easternmost extremity with underlying columnar-jointed basalts/andesites of the Sherratt Bay Formation. On the western margins of the peninsula,

[Palaeontology, Vol. 41, Part 5, 1998, pp. 807–814]

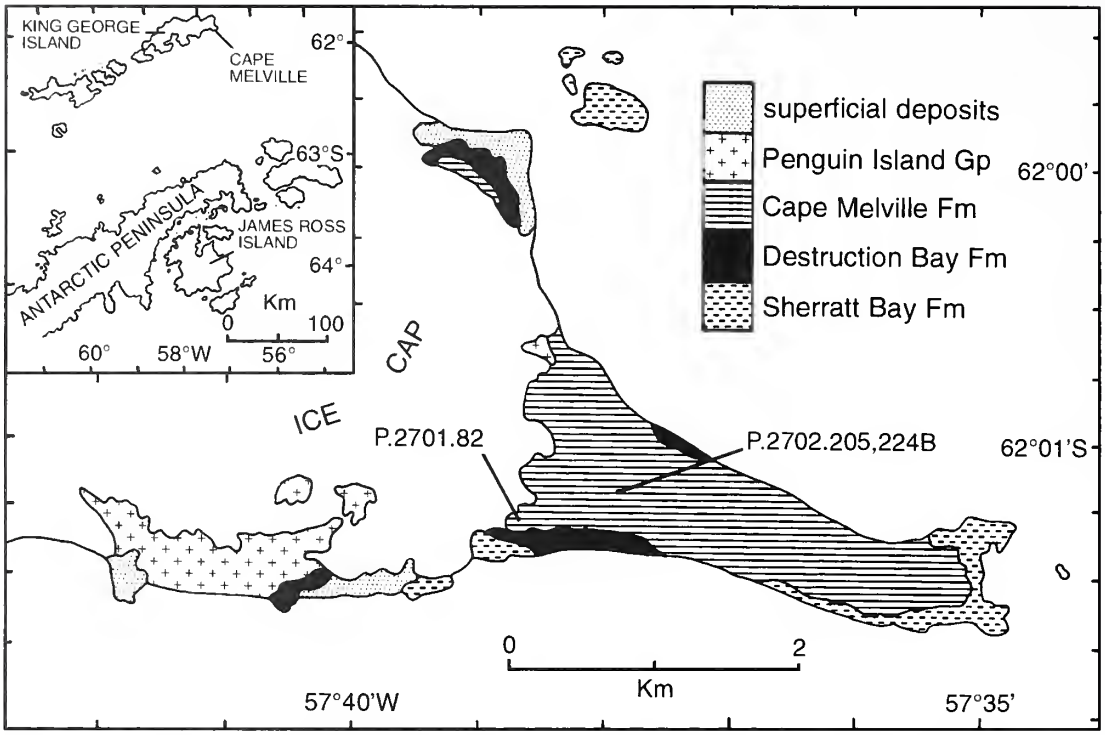

TEXT-FIG. 1. Locality and geological sketch map for Cape Melville, King George Island, South Shetland Islands. Localities of type specimens shown. Geological information based on Birkenmajer (1987, fig. 5).

the CMF is underlain by a further sedimentary unit, the Destruction Bay Formation (Birkenmajer 1987; Text-fig. 1). The CMF is overlain to the west by sub-Recent volcanic rocks assignable to the Penguin Island Volcanic Group.

The predominant lithology within the CMF is a pale grey/green/brown-weathering mudstone to silty mudstone bearing conspicuous, small to very large lonestones. Occasionally, the matrix coarsens to fine- or even medium-grained sandstone, and in places there are irregular seams and lenses of very coarse- to pebbly-sandstones. The lonestones comprise an extremely wide range of igneous, metamorphic and sedimentary lithologies, and are undoubtedly glacial dropstones. Some of them are of only local (i.e. northern Antarctic Peninsula) origin, but others, such as archaeocyath-bearing limestones, ripple cross-laminated red sandstones, and pink-weathering polymict conglomerates, indicate a source region as far distant as the Transantarctic Mountains (i.e. at least some 2000 km to the south).

The CMF varies from a subhorizontal structural disposition to a gentle east or north-east dip of about 5°. It is cut by a prominent north-west–south-east trending dyke swarm, which is in turn cut by a later series of north-north-east–south-south-west trending normal faults. Two of these andesitic–basaltic dykes have been dated radiometrically (K–Ar) at 20 Ma, and this puts a minimum age constraint on the entire Moby Dick Group (Birkenmajer 1990). In addition, a tuff from close to the base of the Destruction Bay Formation has been dated (K–Ar) at 23 Ma, and both brachiopods and foraminifera from the same unit have strong Lower Miocene affinities. A consensus of radiometric and palaeontological age determinations indicates that the CMF is best regarded as Early Miocene (Birkenmajer 1987, 1990).

All three specimens were collected from the plateau surface extending along the top of the peninsula (Text-fig. 1). The holotype, P.2701.82, comes from the south-western corner, close to the

moraine material associated with the edge of the ice cap; the two paratypes (P.2702.205, 224B) were collected from the eastern slopes of 'Crab Creek'. Such locations indicate a stratigraphical position within approximately the uppermost 75 m of the CMF, and a close association with a rich benthic marine invertebrate assemblage dominated by infaunal bivalves, gastropods, solitary corals and crabs.

As might be expected in such a mud-rich environment, the bivalve assemblage is dominated by deposit-feeding nuculids and nuculanids. Other taxa include limopsids, several small heteroconchs, and a comparatively large number of anomalodesmatans. The prolific crab remains range from disarticulated chelae and incomplete carapaces to whole, articulated specimens associated with burrow structures. They have been assigned to just one taxon, *Antarctidromia inflata* Förster (Förster *et al.* 1985, 1987). The solitary corals have been identified as *Flabellum rariseptatum* (Roniewicz and Morycowa 1987), and the common gastropods include a medium-large volutid, at least two types of buccinid, a large turrid (*Austrotoma*), and several forms of naticid. Brachiopods, echinoids, scaphopods, bryozoans and large foraminiferans are also present, and overall the assemblage has a relatively deep-water, outer-shelf aspect.

SYSTEMATIC PALAEONTOLOGY

Order DECAPODA Latreille, 1803
Infraorder ASTACIDEA Latreille, 1803
Family NEPHROPIDAE Dana, 1852

Genus HOPLOPARIA McCoy, 1849

Type species. Astacus longimanus G. B. Sowerby, 1826, by subsequent designation of Rathbun, 1926.

Hoploparia gazdzickii sp. nov.

Text-figures 2–3

Derivation of name. The trivial name recognizes the significant contributions of Andrzej Gaździcki, Polish Academy of Sciences, Warszawa, to the study of the geology and palaeontology of King George Island.

Types. The holotype, P.2701.82, and two paratypes, P.2702.205 and 2702.224B, are deposited in the collections of the British Antarctic Survey, Cambridge, England.

Description. Moderate to small sized (for genus) carapace more than twice as long as high, with diminutive cephalic spines, and with well defined groove pattern.

Dorsal margin biconvex with postcervical groove crossing midline behind midlength. Posterior margin incomplete, convex. Ventral margin smoothly convex with narrow marginal rim and furrow. Frontal margin broken but with shallow, rimmed orbital margin. Rostrum not preserved. Two weak spine rows developed on dorso-anterior portion of cephalic region. Rostral spine row with four spines of which anteriormost is largest. Supraorbital spine row with three spines increasing in size anteriorly. Single, prominent antennal spine. Carapace grooves narrow, deeply incised, distinct. Cervical groove (e of Text-fig. 3) originates at point about one-third total height from midline, becoming narrower and better defined ventrally; curving anteriorly in smooth arc terminating abruptly against nearly straight, anteriorly-inclined antennal groove (b). Gastroorbital groove (d) an indistinct depression. Postcervical groove (c) with straight dorsal segment crossing midline behind midpoint of carapace, weakly convex-forward midsection inclined at about 45° to dorsum, and short anterior section curving toward cervical groove. Branchiocardiac groove (a) smoothly convex forward, coalescing with postcervical groove at midsection and merging with deeply incised, tightly curved hepatic groove (b_1) defining presumed position of adductor testis muscle insertion (χ) which is swollen and bears several fine granules. Region of mandibular external articulation (ω) broadly and subtly swollen. Branchiostegite with very fine, uniformly spaced setal pits overall and few very fine pustules along ventral margin.

Abdomen with well differentiated tergal and pleural surfaces separated by distinct convex-downward ridge (Text-fig. 3). Terga with coarsely punctate irregularly undulating axial regions and transversely ovoid, irregular

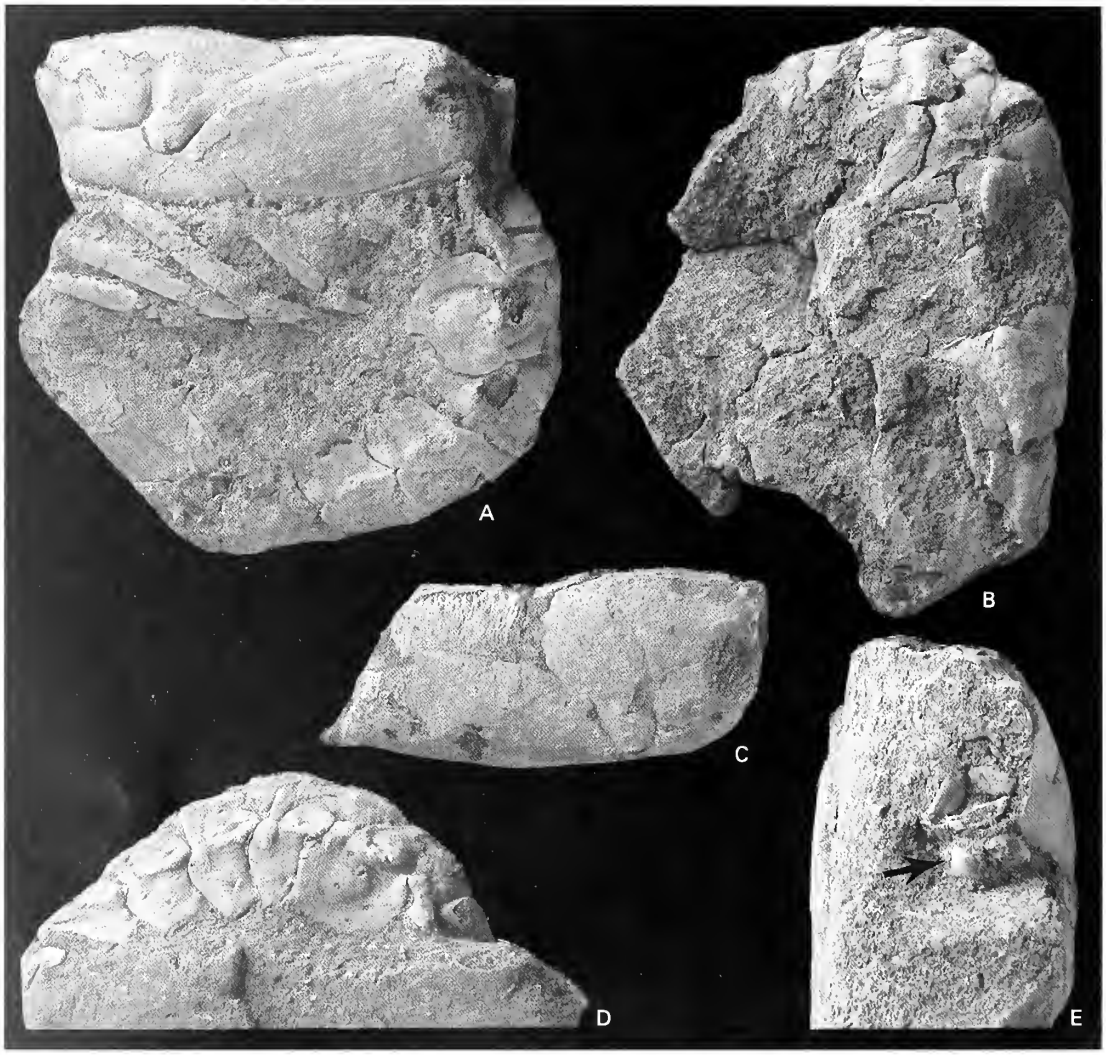

TEXT-FIG. 2. *Hoploparia gazdzickii* sp. nov. A, left lateral view of holotype, P.2701.82, showing nearly complete cephalothorax and abdomen. B, left lateral view of paratype, P.2702.205, showing incompletely preserved abdomen. C, right lateral view of paratype, P.2702.244B, showing crushed, incomplete cephalothorax. D, right lateral view of abdomen of holotype. E, frontal view of holotype showing mandibles (arrow) and fragments of maxillipeds. All × 1·5.

swellings laterally. Posterior rim of each tergum smooth, elevated. Pleura smoother than terga, domed medially, swollen at posterodorsal corner where somites articulate. Pleuron of first somite small, triangular, anteriorly directed; that of second somite larger than any of the others, broadly obovate with posteriorly directed acute spine. Remaining pleura lanceolate with acute tips directed slightly toward posterior. Single pit situated at midpoint of pleura 3–5. Telson margins not preserved; axis depressed, bounded by two broadly elevated longitudinal ridges diverging slightly toward posterior. Uropods large, elongate, oval, with diaresis.

Mandibles strongly inflated, occlusal surface of right mandible overlaps that on left. First pereiopods not known. Proximal elements of pereiopods 2–5 of uniform size, long, narrow, cylindrical.

Measurements. Dimensions of carapace, in mm, are given on Text-figure 3.

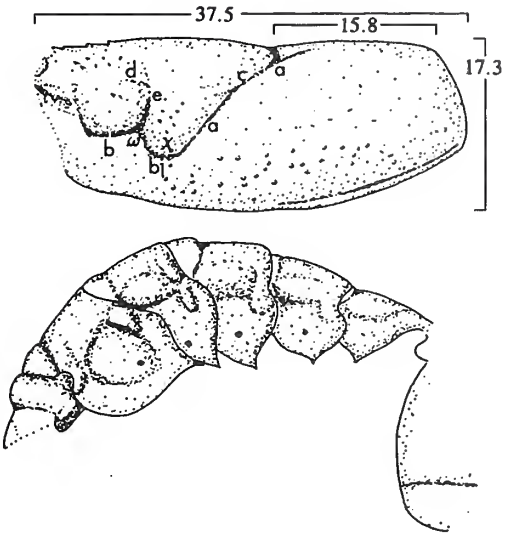

TEXT-FIG. 3. Line drawings of *Hoploparia gazdzickii* sp. nov. showing the positions of the carapace features, orientation of measurements taken, in millimetres, and details of morphology of the abdomen (composite drawing based primarily on the holotype) a, branchiocardiac groove; b, antennar groove; b_1, hepatic; c, postcervical; d, gastroorbital; e, cervical; ω, position of mandibular external articulation; χ, inferred position of 'adductor testis' muscle attachment.

Remarks. Hoploparia, along with other nephropid lobsters, was recently subjected to a cladistic analysis (Tshudy and Babcock 1997) which tested morphological characters used to define genera as well as the affinities of included genera. On the basis of this, and previous works, representatives of the genus *Hoploparia* may be distinguished from those in the closely related genus *Homarus* in several ways. With reference to the specimens described above, the development of a cervical groove that extends dorsal to the level of the gastroorbital groove, possession of a postcervical groove that is strongly developed throughout and that extends toward the cervical groove, projection of the branchiocardiac groove ventral to the presumed attachment site of the adductor testis muscle merging with the hepatic groove to intercept the cervical groove, and development of strong ornament on the abdomen resulting in clear demarcation of the tergal and pleural regions, are all characters that permit confident assignment to *Hoploparia*. Other distinguishing features, including the nature of the rostrum and the conformation of the chelae (Glaessner 1969), cannot be used because they are not preserved on the available material.

Species within the genus are distinguished on the basis of carapace ornament, relative degrees of development of the carapace grooves, morphology of the chelae, and details of the ornament on the abdomen. The combination of the characters exhibited by *Hoploparia gazdzickii* sp. nov. clearly distinguishes it from previously described species. It possesses an antennal groove that is nearly straight, instead of smoothly curved, and that is steeply inclined in an anterodorsal direction; this feature is unique. In addition, the carapace of the new species is nearly devoid of nodes, spines, or other ornament. In this regard, it more closely resembles species of *Homarus*. The only distinctive carapace ornament is that of the two rows of spines on the cephalic region and a large antennal spine, characters exhibited by all, or nearly all, species within the genus. Those spines, however, are diminutive in *H. gazdzickii* sp. nov. Finally, although the carapace is nearly smooth, the abdomen is heavily ornamented.

The type species of the genus, *Hoploparia longimanus* (G. B. Sowerby), from the Upper Cretaceous of England, possesses rows of nodes just posterior to the cervical and postcervical grooves, pustulose ornament on the cephalic region, an antennar groove that is nearly parallel to the ventral carapace margin, and highly ornamented abdominal pleura; none of these characters is evident on *H. gazdzickii*.

Two species of *Hoploparia* have been described previously from Antarctica. *Hoploparia stokesi* (Weller 1903), has been collected from numerous sites on Snow Hill, Seymour, James Ross, and Vega islands in rocks ranging from Campanian through to Paleocene (Feldmann and Tshudy 1989).

Individuals within this species can be distinguished readily from *H. gazdzickii*. *Hoploparia stokesi* tends to be much larger, exhibits a more granular carapace, more strongly developed spines on both the mandibular articulation and the adductor testis region, a prominent spine on the ridge separating the abdominal pleura from the terga, a nodose surface on the telson, and keeled uropods. *Hoploparia antarctica* Wilckens, 1907, is known from the Campanian of James Ross Island as well as the Campanian–Maastrichtian of southern and central Patagonia, Argentina. This latter species bears a prominent row of antennal spines, moderate to weakly developed intermediate and branchial carinae on the branchiostegite, nearly smooth tergal surfaces, and strongly inflated borders on the abdominal pleura.

DISCUSSION

Prior to this study, the youngest occurrences of *Hoploparia* were those in the Eocene of Europe; there are, for example, references to *Hoploparia* sp. from both Germany (Ebert 1887) and Italy (Ristori 1889). The overall pattern of distribution for the genus would appear to be one of origin in the Early Cretaceous, at least by the Hauterivian (Feldmann 1974), and possibly as early as the Berriasian–early Valanginian in the Americas (Aguirre Urreta 1989). By the Late Cretaceous, the genus was distributed world-wide: in the epicontinental seaways of North America, the Atlantic Ocean basin, Europe, Madagascar, South America and Antarctica. The geographical range of the genus declined significantly during the Paleogene, after which it was thought to have vanished, either by true extinction or by giving rise to one or more of the modern nephropid genera (Aguirre Urreta 1989). However, it is now apparent that the genus persisted as a relict in the Antarctic region at least into the Early Miocene.

There remain unanswered questions regarding the origins of the modern nephropid genera. Although that topic is not directly relevant to the present work, this new discovery of a Miocene *Hoploparia* does raise the question of whether it formed the rootstock of at least some of the modern genera or whether it was a contemporary of genera which had arisen earlier. *Metanephrops* Jenkins, 1972 is reported to have arisen at least by the Late Cretaceous in the form of *Metanephrops jenkinsi* Feldmann, 1989, from the James Ross Basin, Antarctica. Tshudy and Babcock (1997) concluded that the genera most closely allied to *Hoploparia* arose in the Early Cretaceous. Difficulty in testing the relationships of the other nephropids using palaeontological evidence arises because most of the modern nephropids are inhabitants of outer shelf and slope habitats (Holthuis 1974), and these are not well represented in the fossil record.

There are also unresolved questions regarding the palaeoecological implications of the occurrence of *Hoploparia* in the CMF fauna. Certainly the preponderance of occurrences of the genus throughout its geological history have been in inner shelf, moderate to high energy settings (Aguirre Urreta 1989). In almost all instances too, biotic associations indicate normal marine settings. As fossil occurrences of *Hoploparia* range from as far north as Greenland to as far south as Antarctica, this could be taken to represent original water temperatures ranging from cool-temperate to subtropical. Nevertheless, the outer limit of the bathymetric range has never been adequately constrained, and these records from the Lower Miocene of Antarctica indicate that the genus also inhabited moderately deep waters. A comparison can be made here with modern *Homarus* Weber, which is known to occur at virtually all depths on the continental shelf and, before active capture by humans, was observed in tide pools in intertidal settings (Herrick 1911).

Finally, it is striking how two quite different benthic decapod genera, *Antarctidromia* and *Hoploparia*, co-occur in the CMF. This is without doubt a glacial deposit, for the dropstones could only have been deposited from very large icebergs originating along the southernmost margins of the Weddell Sea (present day Ronne Ice Shelf). Thus, at least two distinct decapod taxa were able to survive cold-water (glacial) conditions and it may be that there was no simple link between the onset of glaciation and the extinction of many benthic marine taxa (Clarke and Crame 1989). Perhaps the extinctions were phased over a long period of time, or factors other than low temperature *per se* were of paramount importance. There is a growing volume of evidence to suggest that the ability to cope with oligotrophic conditions may be just as important to survival within the

present-day Southern Ocean benthos as the ability to withstand near-freezing conditions (Arntz *et al.* 1997).

Acknowledgements. RMF's work at the British Antarctic Survey was supported by NSF grant OPP 9526252. JAC thanks S. M. Redshaw for helping to collect the specimens during the 1995 field season.

REFERENCES

AGUIRRE URRETA, M. B. 1989. The Cretaceous decapod Crustacea of Argentina and the Antarctic Peninsula. *Palaeontology*, **32**, 499–552.

ARNTZ, W. E., GUTT, J. and KLAGES, M. 1997. Antarctic marine biodiversity 3–14. *In* BATTAGLIA, B., VALENCIA, J. and WALTON, D. W. H. (eds). *Antarctic communities: species, structure and survival.* Cambridge University Press, Cambridge, 464 pp.

BIRKENMAJER, K. 1987. Oligocene–Miocene glacio-marine sequences of King George Island (South Shetland Islands), Antarctica. *Palaeontologia Polonica*, **49**, 9–36.

—— 1990. Geochronology and climatostratigraphy of Tertiary glacial and interglacial successions on King George Island, South Shetland Islands (West Antarctica). *Zentralblatt für Geologie und Paläontologie*, **1**, No. 1–2, 141–151.

CLARKE, A. and CRAME, J. A. 1989. The origin of the Southern Ocean marine fauna. 253–268. *In* CRAME, J. A. (ed.) *Origins and evolution of the Antarctic biota.* Geological Society, London, Special Publication, 47, 322 pp.

DANA, J. D. 1852. *Crustacea. United States Exploring Expedition during the years 1838, 1839, 1840, 1841, 1842 under the command of Charles Wilkes, U.S.N., 13.* C. Sherman, Philadelphia, 1620 pp.

EBERT, T. 1887. Beitrag zur Kenntnis der tertiären Dekapoden Deutschlands. *Jahrbuch der (Königlich) Preussischen Geologischen Landesanstalt und Bergakademie, Berlin*, 262–271.

FELDMANN, R. M. 1974. *Hoploparia riddlensis*, a new species of lobster (Decapoda: Nephropidae) from the Days Creek Formation (Hauterivian, Lower Cretaceous) of Oregon. *Journal of Paleontology*, **48**, 587–593.

—— 1989. *Metanephrops jenkinsi* n. sp. (Decapoda: Nephropidae) from the Cretaceous and Paleocene of Seymour Island, Antarctica. *Journal of Paleontology*, **63**, 64–69.

—— and QUILTY, P. G. 1997. First Pliocene decapod crustacean (Malacostraca: Palinuridae) from the Antarctic. *Antarctic Science*, **9**, 56–60.

—— and TSHUDY, D. M. 1989. Evolutionary patterns in macrurous decapod crustaceans from Cretaceous to early Cenozoic rocks of the James Ross Island region, Antarctica, 183–195. *In* CRAME, J. A. (ed.). *Origins and evolution of the Antarctic Biota.* Geological Society, London, Special Publication 47, 322 pp.

FÖRSTER, R., GAZDZICKI, A. and WRONA, R. 1985. First record of a homolodromiid crab from a Lower Miocene glacio-marine sequence of West Antarctica. *Neues Jarbuch für Geologie und Paläontologie, Monatshefte*, **8**, 399–404.

—— —— —— 1987. Homolodromiid crabs from the Cape Melville Formation (Lower Miocene) of King George Island, West Antarctica. *Palaeontologia Polonica*, **49**, 147–161.

GLAESSNER, M. F. 1969. Decapoda. R399–R651, R626–R628. *In* MOORE, R. C. (ed.). *Treatise on invertebrate paleontology. Part R. Arthropoda 4.* Geological Society of America and University of Kansas Press, Lawrence, 651 pp.

HERRICK, F. H. 1911. Natural history of the American lobster. *Bulletin of the U.S. Bureau of Fisheries*, **29**, 1–408.

HOLTHUS, L. B. 1974. The lobsters of the superfamily Nephropidae of the Atlantic Ocean (Crustacea: Decapoda). *Bulletin of Marine Science*, **24**, 723–884.

JENKINS, R. J. F. 1972. *Metanephrops*, a new genus of late Pliocene to Recent lobsters (Decapoda, Nephropidae). *Crustaceana*, **22**, 161–177.

LATREILLE, P. A. 1802–1803. *Histoire naturelle, générale et particulère, des crustacés, des arachnides, des myriapodes et des insectes: Volume 3.* F. Dufart, Paris, 468 pp.

McCOY, F. 1849. On the classification of some British fossil Crustacea with notices of new forms in the University Collection at Cambridge. *Annals and Magazine of Natural History, Series 2*, **4**, 161–179, 330–335.

RATHBUN, M. J. 1926. The fossil stalk-eyed Crustacea of the Pacific slope of North America. *Bulletin of the U.S. National Museum*, **138**, 1–155.

RISTORI, G. 1889. Crostacei Piemontesi del miocene inferiore. *Bollettino della Società geologica italiana*, **7**, 397–412.

RONIEWICZ, E. and MORYCOWA, E. 1987. Development and variability of Tertiary *Flabellum rariseptatum* (Scleractinia), King George Island, West Antarctica. *Palaeontologia Polonica*, **49**, 83–103.

SOWERBY, G. B. 1826. Description of a new species of *Astacus*, found in a fossil state at Lyme Regis. *Zoological Journal*, **2**, 493–494.

TSHUDY, D. and BABCOCK, L. E. 1977. Morphology-based phylogenetic analysis of the clawed lobsters (family Nephropidae and the new family Chilenophoberidae). *Journal of Crustacean Biology*, **17**, 253–261.

WELLER, S. 1903. The Stokes collection of Antarctic fossils. *Journal of Geology*, **11**, 413–419.

WILCKENS, O. 1907. Die Lamellibranchiaten, Gastropoden U.S.W. der oberen Kreide Südpatagoniens. *Berichte der Naturforschended Gesellschaft zu Freiburg i. Br.*, **15**, 97–166.

RODNEY M. FELDMANN
Department of Geology
Kent State University
Kent, Ohio 44242, USA

J. ALISTAIR CRAME
British Antarctic Survey
High Cross, Madingley Road
Cambridge CB3 0ET, UK

Typescript received 2 October 1997
Revised typescript received 6 February 1998

NEW PYGOCEPHALOMORPH CRUSTACEANS FROM THE PERMIAN OF CHINA AND THEIR PHYLOGENETIC RELATIONSHIPS

By ROD S. TAYLOR, SHEN YAN-BIN *and* FREDERICK R. SCHRAM

ABSTRACT. Members of the malacostracan order Pygocephalomorpha are among the most characteristic elements in nearshore marine and freshwater communities in the Carboniferous and Permian of Europe and North America. A new family of pygocephalomorph Eumalacostraca, Tylocarididae, with two new monospecific genera, is described from China, where it occurs in the Early Permian Tungtzeyen Formation of Fujian, and in the Late Permian Lungtan Formation of Hunan. The descriptions of *Fujianocaris bifurcatus* gen. et sp. nov. and *Tylocaris asiaticus* gen. et sp. nov. are based on dorsally preserved isolated carapaces, some showing incomplete abdominal details, but with no complete tail fans. Opinions on the affinities of Pygocephalomorpha to other malacostracans have varied but they are generally regarded as a separate order of 'mysidacean' peracarids. Hitherto the phylogeny of the group has not been considered, and the current family level taxonomy remains rather artificial. A cladistic analysis of fossil and Recent 'mysidacean' and pygocephalomorph crustaceans is presented here which outlines the affinities within the group and holds promise for an eventual natural taxonomy of the Pygocephalomorpha.

LITTLE work has been done on the palaeobiology and taxonomy of fossil Crustacea in China, especially with respect to global biogeography (Shen 1983), with the exception of extensive taxonomic work on conchostracans, which range from the Devonian to the Cretaceous (Shen 1978, 1981, 1984, 1990; Zhang *et al.* 1990). Palaeobiological research has increased in China recently due to the discovery of such important localities as the Cambrian *Lagerstätte* at Chengjiang (e.g. Chen *et al.* 1995*a*, 1995*b*), and a result has been the discovery of new crustaceans in Early Permian strata in south-east China. This paper describes the new taxa *Fujianocaris bifurcatus* and *Tylocaris asiaticus*, both apparently belonging to the Pygocephalomorpha. Whilst these new species are only the second reported discovery of Pygocephalomorpha in China (see Shen 1983), members of this order have long been recognized elsewhere as one of the most prominent and striking crustacean groups in late Palaeozoic nearshore marine and freshwater communities, in particular from North America and Europe. However, determination of the phylogenetic affinities of this enigmatic group has remained problematical.

Prestwich (1840) was the first to describe a pygocephalomorph, a carapace from the British Coal Measures; he named it *Apus dubius*, and believed that its affinities might be with the notostracan phyllopods. Later, Huxley (1857) described *Pygocephalus cooperi*, also from the British Coal Measures; in this specimen the ventral aspect of the thorax is preserved, but he did not compare it with *A. dubius*. Salter (1861) realized that the carapace described by Prestwich was not a phyllopod, and erected the genus *Anthrapalaemon* to accommodate it and some newly discovered carapace specimens that he ascribed to another species, *A. grossarti*. No-one appreciated at that time that these various taxa had affinities to one another. Indeed, there persisted in the literature an unnatural dichotomous taxonomy: fossils preserving a dorsal view of the carapace were placed in *Anthrapalaemon*, while those preserving the ventral aspects of the thorax bore the name *Pygocephalus*. The confusion increased when Woodward (1879) applied the generic name *Necroscilla* to separate abdomina and Salter (1863) placed a tail fan in a separate genus *Diplostylus*.

The generic name *Anthrapalaemon* became widely employed for any large lobster-like carapace.

[Palaeontology, Vol. 41, Part 5, 1998, pp. 815–834, 2 pls]

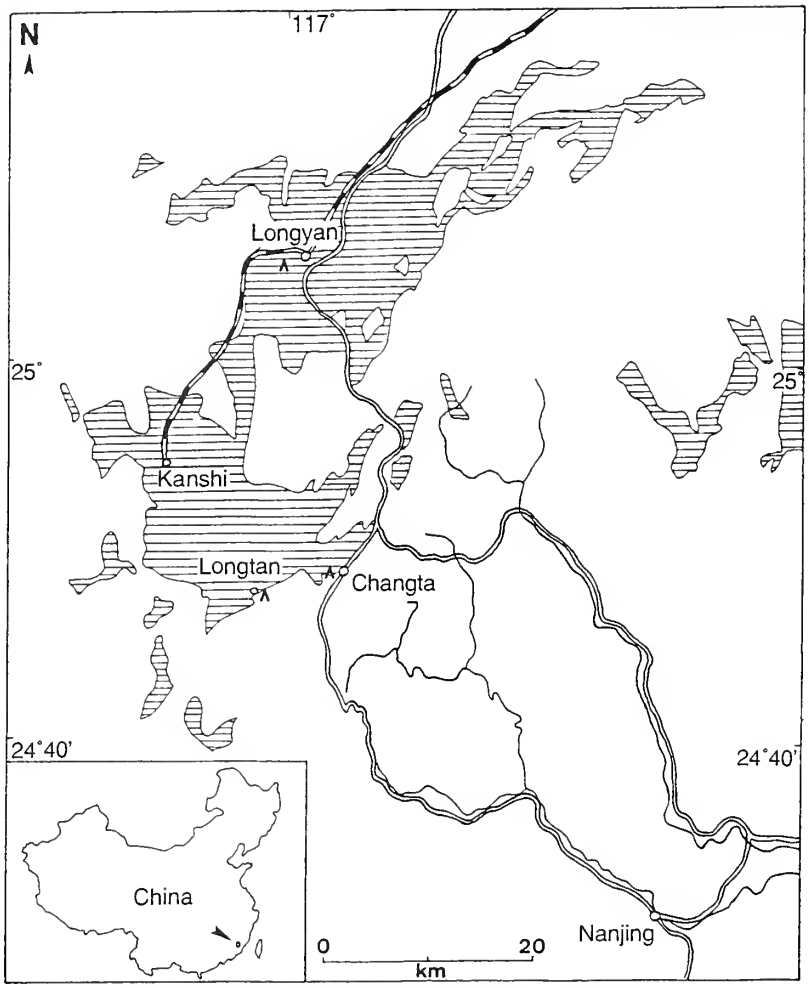

TEXT-FIG. 1. Localities from which *Fujianocaris bifurcatus* and *Tylocaris asiaticus* have been collected, indicated by arrowheads. Shaded areas represent the Lower Permian.

Peach (1883) erected a separate genus, *Pseudogalathea*, for some distinctly ridged forms, and did the same for some other Scottish taxa that he segregated under the genus *Tealliocaris*. Brooks (1962) made a major contribution towards resolving the taxonomy of this group. He proposed *Pseudotealliocaris*, for some distinctly decorated taxa, recognized the synonymy of *Pygocephalus* and *Anthrapalaeomon* (former is senior synonym), confirmed the taxonomic status of the North American species *Anthracaris gracilis*, erected *Mamayocaris* for another North American species, and made some assumptions about the supposed higher taxonomic affinities of the pygocephalomorphs. Brooks suggested that one should not compare pygocephalomorphs with phyllopods, schizopods or decapods, as had been done in the past, but placed them in a distinct order, Eocarida, with various other Palaeozoic forms. Finally, Schram (1974*a*, 1974*b*, 1979) imposed some order on the species level taxonomy in the group, especially among the British faunas, clarified the issues of thoracopod anatomy that had coloured Brooks' interpretation of the higher taxonomy, and performed a cladistic analysis that advanced a clear hypothesis about the possible

higher affinities of the pygocephalomorphs. In addition, Schram (1978) also recognized another genus in the Permian of Russia, *Jerometichenoria*.

All these discoveries focused largely on 'northern hemisphere' taxa from Laurentia. Nevertheless, another important source of pygocephalomorphs occurs in 'southern hemisphere', essentially Gondwanan, localities. Broom (1931) described a South African species, *Notocaris tapscotti*, and Clarke (1920) first recognized a Brazilian form, *Paulocaris pachecoi*. Later, Beurlen (1931, 1934) expanded on the South American fauna with his erection of *Liocaris* and *Pygaspis*, both again from Brazil. Brooks (1962) synonymized both of these genera with *Paulocaris*, but they have since been resurrected by other authors (e.g. Pinto 1971), reflecting the taxonomic confusion that has marked the history of this group. Unfortunately, these Gondwanan taxa are based on rare and poorly preserved material, making definitive taxonomic assignments difficult. Brooks (1969) set these poorly known, southern hemisphere forms aside as a separate family, Notocarididae, but its only diagnostic character, reduced abdomen flexed under the thorax, clearly does not apply to all southern forms and may merely be an artefact of preservation. The Brazilian *Pygaspis* bear a regular, large, posteriorly directed abdomen (Pinto 1971), and the supposed diagnostic flexure under the thorax is also present on many specimens of northern hemisphere pygocephalomorphs.

In the course of this work, we noted similarities between our two new genera and the Scottish Carboniferous genus *Pseudogalathea*. However, there are palaeobiogeographical implications arising from this, with phylogenetically highly derived animals, with many apomorphic carapace features, arriving at disparate parts of the Palaeozoic world. Whilst we could not preclude this possibility, it caused us to re-examinee the total array of anatomical information that could be derived from fossil pygocephalomorphs and possible near relatives, and we performed a cladistic analysis to test more rigorously our initial conclusions on the affinities of the Chinese taxa.

The material used in this study was obtained from the Permian of Fujian Province, south-east China (Text-fig. 1). Most specimens were collected from a coal mine in the village of Changta, Nanjing County, in the third member of the Early Permian Tungtzeyen Formation (one specimen has also been reported from an equivalent horizon at Longtan village, Yongdin County, Fujian (Zhu 1990, pl. 21, fig. 15)). One specimen was found at each of the following: Xihushan, Longyan County, Fujian Province, Early Permian Tungtzeyen Formation; Shitangpu Village, Lukou Town, Zhuzhou City, Hunan Province, Late Permian Lungtan Formation; and an undetermined locality from the Permian of Fujian. This last specimen, due to its uncertain provenance is not considered further. All specimens are deposited in the Nanjing Institute of Geology and Palaeontology (NIGP), Academia Sinica.

SYSTEMATIC PALAEONTOLOGY

Class MALACOSTRACA Latrielle, 1802
Order PYGOCEPHALOMORPHA Beurlen, 1930
Family TYLOCARIDIDAE fam. nov.

Diagnosis. Carapace with large falciform rostrum with central groove and papillated margin; prominent mid-dorsal keel, with posterior bifurcation merging with posterior carapace margin; well-developed cervical and rostro-gastric ridges, surrounding papillated rostral ridge; antero-lateral and posterio-lateral spines present; heavily thickened carapace margin. Abdomen with medial and one set of lateral ridges on tergites; elongate telson with finely bifurcated tip; endopods and exopods with serrate margins and no diaresis associated with exopod.

Genus FUJIANOCARIS gen. nov.

Derivation of name. From Fujian Province, China.

Type species. Fujianocaris bifurcatus.

Diagnosis. Carapace with prominent mid-dorsal keel, bifurcated at both anterior and posterior ends, and pair of prominent lateral keels; carapace margin, rostrum, cervical ridge and keels decorated with papillations, slightly smaller on the carapace margin and rostrum; remainder of carapace smooth; cervical ridges well developed, with shallow cervical grooves; large falciform rostrum with central groove present.

Fujianocaris bifurcatus sp. nov.

Plate 1, figures 1–5; Text-figures 2B, 3A

Derivation of name. From the posterior bifurcations of the telson and the mid-dorsal keel of the carapace.

Holotype. NIGP 126323 A/B; part and counterpart of a carapace and associated abdomen (Pl. 1, fig. 1).

Paratypes. NIGP 126324A-2, 3, NIGP 126327, NIGP 126328, NIGP 126329-1, 2, NIGP 126330-1, 2, NIGP 126331B-2, NIGP 126332A, B, NIGP 126333A/B, NIGP 126334-2, NIGP 126335, NIGP 126336A-1, 2/B-1, 2.

Horizon and locality. No. 25 coal bed, third member of Lower Permian Tungtzeyen Formation, Xiangshuping, Changta coal mine, Nanjing County, Fujian Province (Text-fig. 1).

Diagnosis. As for genus.

Description. The carapace appears to have been heavily sclerotized. A prominent mid-dorsal keel is present, extending two-thirds to three-quarters its length to the posterior margin (NIGP 126328; Pl. 1, fig. 4). This keel is continuous with a greatly thickened ridge along the posterior, lateral and anterior margins of the carapace. At the immediate anterior end of the medial keel is a pair of antero-laterally directed cervical ridges (in some specimens, these appear to be almost continuous with the keel (NIGP 126330-1; Pl. 1, fig. 3)). These ridges are curved slightly outwards and extend approximately one-third of the distance to the lateral margins of the carapace; they appear to run parallel to what seems to be a set of very shallow cervical grooves (NIGP 126329-1, 2). At its posterior end, the medial keel terminates in a pair of mid-lateral, posteriorly directed spines (NIGP 126323B, NIGP 126331B-2). A pair of lateral keels extends from just posterior of the cervical grooves to the posterior carapace margin, approximately midway between the medial keel and the lateral margin of the carapace (NIGP 126328). These lateral keels extend for approximately the same distance as the medial one. Papillations decorate all keels, more heavily on the medial, and the thickened posterior and lateral carapace margins (NIGP 126330-1; Pl. 1, fig. 3). No branchiostegal spines are present.

The rostrum is long, approximately one-quarter the length of the carapace, and curves slightly ventrally. It is semicircular in cross section, with a dorsal, central groove (NIGP 126330-1, NIGP 126334-2, NIGP 126329-1, 2), and originates from a triangular rostral ridge anterior to the cervical ridges (NIGP 126330-1). The rostral margin and rostral ridge are papillated. There emerges from this rostral ridge a pair of papillated antero-lateral gastric ridges, running approximately parallel to the antero-lateral margin of the carapace (NIGP 126336B-1, NIGP 126329-1, 2). These ridges are wider and more robust laterally than mid-dorsally. At their lateral extent they turn posteriorly, adjacent to the termination of the cervical ridges (NIGP 126330-1, 2). Short,

---

EXPLANATON OF PLATE 1

Figs 1–5. *Fujianocaris bifurcatus* gen. et sp. nov. 1–2, NIGP 126323A, holotype. 1, × 4; 2, tail fan (small arrow = telson, large arrows = endopods, tailless arrows = expods); × 11. 3, NIGP 126329-1; × 11. 4, NIGP 126328, × 5·5. 5, NIGP 126322, × 5. 1–3 from the Early Permian Tungtzeyen Formation, Changta, Nanjing County, Fujian Province; 4 from the same formation, Xihushan, Longyan County, Fujian Province; 5 from the Late Permian Lungtan Formation, Shitangpu, Lukou, Zhuzhou, Hunan Province.

1

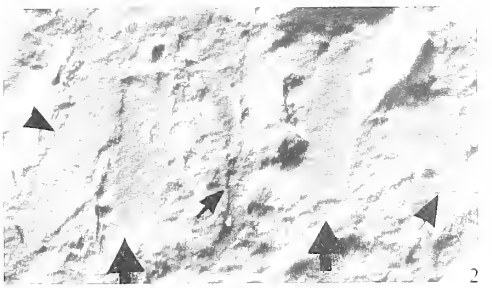

2

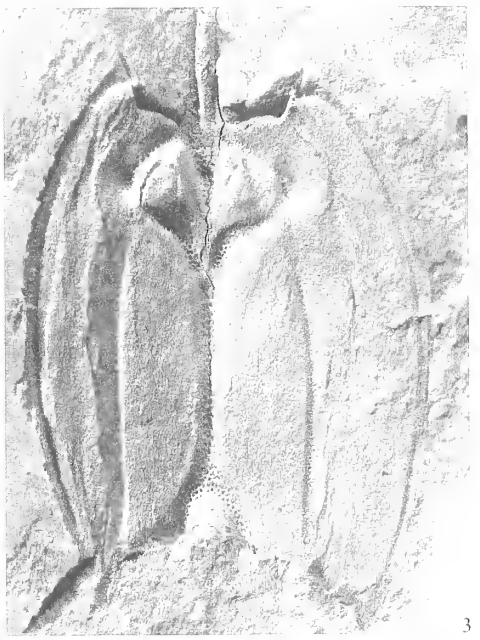

3

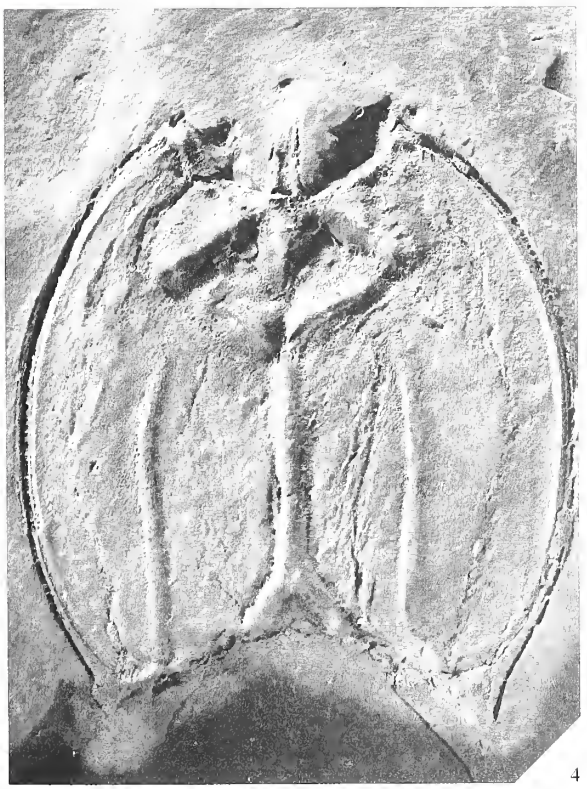

4

5

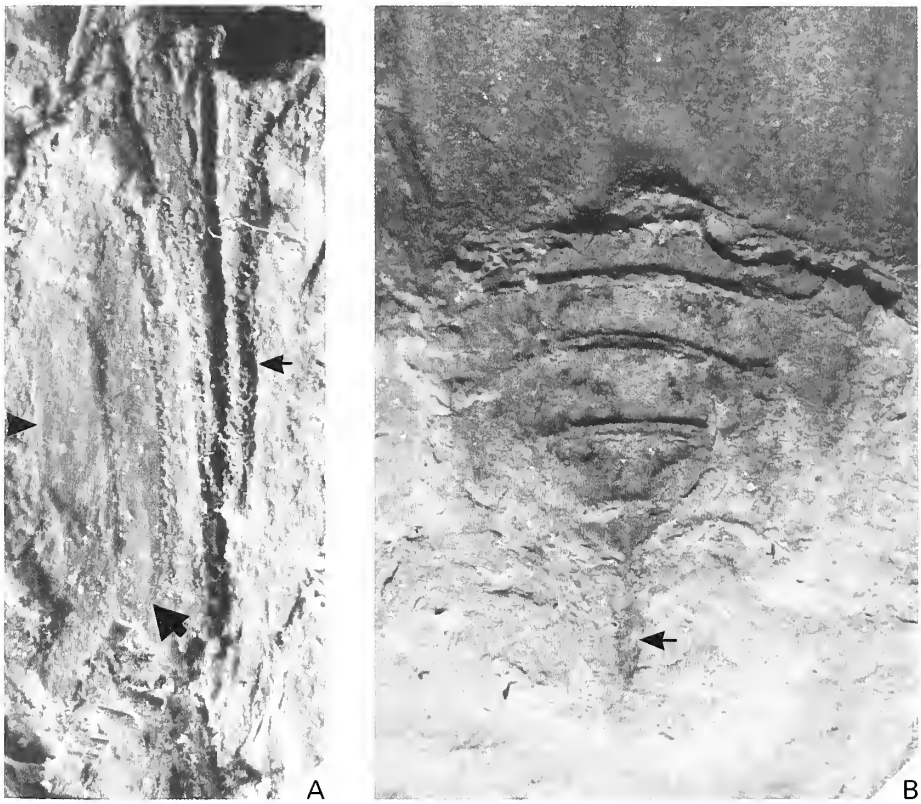

TEXT-FIG. 2. A, *Tylocaris asiaticus* gen. et sp. nov.; NIGP 126324A; partial tail fan; × 14·5. B, *Fujianocaris bifurcatus* gen. et sp. nov.; NIGP 126334; abdomen and tail fan; × 12·5. Both specimens from the Early Permian Tungtzeyen Formation, Changta village, Nanjing County, Fujian Province (small arrow = telson; large arrows = endopods; tailless arrows = exopods).

rounded, antero-lateral and long, postero-lateral spines are present (NIGP 126323B, NIGP 126327, NIGP 126331B-2, NIGP 126334A-2, 3). A set of broad optic notches is located between the rostrum to the antero-lateral spine.

The abdomen is short, slightly less than one-half the length of the carapace (NIGP 126323A, NIGP 126334-2). Four abdominal segments are exposed (the first two shielded under the carapace), each possessing well-developed pleura with posteriorly-directed processes. Each abdominal tergite possesses a mid-dorsal triangular boss (best developed on the last two pleomeres) as well as a pair of small lateral ridges (NIGP 126332B). The length of the segments remains constant whilst the width decreases markedly in the series, such that the sixth abdominal segment is approximately one-half the width of the third (NIGP 126323A, NIGP 126327, NIGP 126334-2). The telson is narrow and very long, with a length *c.* 2·5 times that of the last abdominal segment (NIGP 126323A, NIGP 126334-2) (Text-fig. 2B). The telson possesses a longitudinal, medial ridge (Pl. 1, fig. 2), whilst its distal terminus appears to form a small fork (NIGP 126323A). The uropods consist of lobate exopods and endopods, the latter with medially serrate margins (NIGP 126323A). No diaresis is noted on the exopods, nor are statocysts visible.

Remarks. The sole specimen (Pl. 1, fig. 5) collected from the Late Permian Lungtan Formation of Shitangpu village, Hunan Province is of particular interest. It is included here in *Fujianocaris bifurcatus*, despite some small differences from other members of this species. In most aspects (e.g. the cervical and gastric ridges and the mid-dorsal keel) it is like other specimens of *F. bifurcatus*, but

TABLE 1. Measurements in millimetres of *Fujianocaris bifurcatus*.

Specimen	Rostrum length	Carapace length	Abdomen length	Abdominal segment width				Telson length
				1	2	3	4	
126322	> 1·7	12·2						
126323A	> 1·3	9·3	5·8	8·5	7·4	5·9	4·5	6·7
126327	> 3·8	15·3	11·8	10·5	9·8	8·0	6·3	
126328	2·8	12·2						
126329-1	> 1·8	8·0						
126329-2	1·6	6·6						
126330-1	> 3·0	14·0						
126330-2		7·8						
126331B-2		13·3						
126332A	2·7	10·5		6·7	5·8	4·7		
126334-2			3·75	5·3	4·75	3·2	2·7	> 2·0
126336-1	3·0	9·5						
126336-2	1·7	6·8						

it lacks the lateral keels, that are characteristic of this species. This specimen is preserved such that there is little contrast between it and the surrounding matrix, making it difficult to determine whether all relevant details of the carapace have been preserved, or whether the absence of these keels is an artefact of preservation. Due to the overall similarities between this specimen and the Early Permian *F. bifurcatus*, it is considered for the time being as an unusual member of this taxon rather than a separate species.

Genus TYLOCARIS gen. nov.

Derivation of name. From the Greek *tylos*, knob, referring to the presence of numerous papillations over the carapace.

Type species. Tylocaris asiaticus.

Diagnosis. Carapace with prominent mid-dorsal keel, bifurcated at posterior end, with gastric and cardiac ridges anterior to, and hepatic ridges flanking the anterior end; small papillations highly concentrated on mid-dorsal keel and carapace margin, and more loosely distributed over remainder of carapace; cervical and cardiac ridges well developed; rostrum falciform with central goove; telson long and narrow, with elongate medial ridge and small fork on terminus; a pair of pits on the dorsal surface of each endopod and exopod.

Tylocaris asiaticus sp. nov.

Plate 2, figures 1–3; Text-figures 2A, 3B

Derivation of name. From its discovery in Asia.

Holotype. NIGP 126324 A-1/B; part and counterpart of an incomplete carapace and its associated abdomen (Pl. 2, fig. 1).

Paratypes. NIGP 126325, NIGP 126326A/B, NIGP 126331A/B-1, NIGP 126334-1.

Horizon and locality. No. 25 coal bed, third member of Lower Permian Tungtzeyen Formation, Xiangshuping, Changta coal mine, Nanjing County, Fujian Province (Text-fig. 1).

Diagnosis. As that for genus.

Description. The carapace was probably not heavily sclerotized in life, as suggested by wrinkling of some specimens (NIGP 126326B; see Pl. 2, fig. 2). It posseses a very prominent mid-dorsal ridge, extending two-thirds the length of the carapace from the cervical groove to the posterior margin. This median ridge forks posteriorly and is continuous with a thickened ridge along the posterior margin of the carapace. At the point at which these ridges merge, there is a set of tiny, posteriorly directed processes (NIGP 126326B). The posterior thickened ridge continues along the lateral and anterior margins of the carapace (NIGP 126324A-1). Flanking the anterior end of the median ridge is a pair of highly arched hepatic ridges, with concave surfaces facing inwards (Pl. 2, fig. 2). Immediately anterior to these is a fine cervical groove, which is in turn adjacent to a pair of antero-laterally directed cervical ridges (NIGP 126324A-1/B, NIGP 126331B-1).

A pair of broad optic notches is present between the rostrum and a set of tiny, rounded antero-lateral spines (NIGP 126324-1/B, NIGP 126326B). Papillations are densely concentrated on the medial keel and the posterior and lateral carapace margins (NIGP 126324A-1, NIGP 126325), and this ornament is also distributed over the central portion of the carapace, becoming less densely aggregated near the lateral margins (Pl. 2, figs 1–2). No branchiostegal serrations on the lateral margins are present.

The rostrum is long, one-quarter to one-third the length of the carapace. It is slightly falciform, is an extension of the papillated mid-dorsal rostral ridge (NIGP 126331A/B-1), and possesses papillations along its margin. A pair of narrow, weakly developed, antero-lateral ridges emerges from the anteriormost region of the rostral ridge. These extend posteriorly and laterally from the rostral ridge to the cervical groove (NIGP 126331B-1). The carapace bears a pair of short, rounded, antero-lateral spines lateral to the optic notch and a pair of well-developed postero-lateral spines (NIGP 126324B, NIGP 126326B). One specimen (NIGP 126324A/B; Pl. 2, fig. 1) possesses what appear to be dislocated, regularly segmented antennal fragments near the anterior end of the carapace.

The abdomen is approximately the same length as the carapace. Five abdominal segments are exposed, which possess posteriorly pointed pleura. Segment width decreases whilst length increases distally along the abdominal series, such that the sixth abdominal segment is approximately one-half the width but twice the length of the second segment (NIGP 126324A-1). Each of the tergites bears a broad, triangular medial ridge, as well as a pair of narrow, longitudinal lateral ridges (NIGP 126325; Pl. 2, fig. 1). The elongate and narrow telson appears to terminate in a finely forked tip (NIGP 126331A). It is longer by approximately one-third than the final abdominal tergite, and carries a narrow medial keel running its entire length. Two specimens each show what may be a single caudal furca, occurring at approximately the middle (NIGP 126331A) and near the end (NIGP 126323A-1) of the telson. A pair of lobate uropods, possibly distally pointed, are present, the endopod possessing serrate margins (NIGP 126324A-1; Text-fig. 2A). A diaresis is not visible on the exopods. One specimen (NIGP 126325; Pl. 2, fig. 3) exhibits a pair of small pits along the dorsal midline of the exopods and endopods. Statocysts are not seen.

Remarks. There is one anomalous specimen (NIGP 126326 A/B; Pl. 2, fig. 2), which possesses, immediately anterior to the cardiac groove, two sets of three well-developed spines/nodes instead of cardiac ridges, with spine/node size decreasing antero-laterally. It it slightly deformed, but appears to be considerably wider (length/width *c*. 0·8) than the others (length/width *c*. 1·3 in undeformed specimens). Despite these differences, with the small sample it is considered here to be an unusual member of this taxon, and is perhaps an example of sexual dimorphism; more material might demonstrate that it is a different species.

EXPLANATION OF PLATE 2

Figs 1–3. *Tylocaris asiaticus* gen. et sp. nov. 1, NIGP 126324A; × 5; 2, NIGP 126326A; × 5; 3, NIGP 126325; × 10·75 (arrows = pits). All from the Early Permian Tungtzeyen Formation, Changta village, Nanjing County, Fujian Province.

1

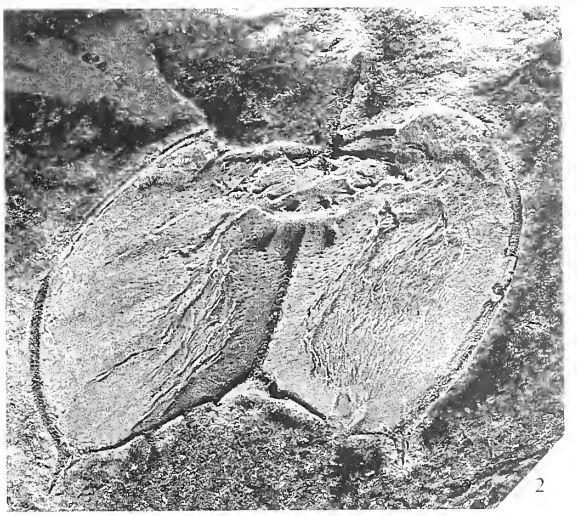

2

3

TABLE 2. Measurements in millimetres of *Tylocaris asiaticus*.

Specimen	Rostrum length	Carapace length	Abdomen length	Abdominal segment width 1	2	3	4	5	Telson length
126324A-1		~ 16	14·0		7·0	5·7	5·0	4·2	~ 6·5
126325			9·2		5·4	4·6	3·8	2·7	~ 5·3
126326	2·7	7·6							
126331A-1	2·9	8·0	6·3			3·3	2·7	1·8	
126334-1	2·7	9·6							

METHODS

A data matrix based on 33 morphological characters from 31 taxa (Table 3) was created using MacClade 3.01. Taxa were chosen based on several criteria. All 18 known pygocephalomorphs were included, with most data derived from the literature. Some information on British pygocephalomorphs was obtained from examination of material at the Hunterian and Kelvingrove museums in Glasgow, the National Museum of Scotland in Edinburgh, and the British Geological Survey in Keyworth.

PAUP 3.1.1 was used to perform a cladistic analysis of this matrix. Heuristic searches were the only practical option, due to the large size of the matrix and the high number of unknowns within it. After an initial unweighted analysis of the matrix, a successive reweighting option was employed, in which the unweighted matrix underwent an heuristic search and was then reweighted using the rescaled consistency index (RCI). This was in turn followed by another heuristic search, and so on until there was no further reduction in the minimum tree lengths obtained. This method provided a set of the most parsimonious trees for a matrix in which the most 'important' characters are granted the highest influence on the outcome of the analysis (see Table 4).

Representative recent mysidacean and lophogastrid taxa were included in this analysis, as well as all known fossil mysid forms, to determine whether the new Chinese species were more closely associated to the similar mysidacean/lophogastrid forms than to the pygocephalids. A hypothetical ancestor was used as an outgroup, scored with zeros for all character states – a so-called Lundberg rooting. Whilst such a procedure is not regarded as an ideal solution to the outgroup problem, it proved useful in this analysis as there was no clear choice in the selection of an outgroup: the most obvious choice would be the mysids and lophogastrids, but since these taxa were actually included in the analysis, their use as outgroups would heavily bias the results.

It is important to note that several alternative options were explored in these cladistic analyses, including the exclusion of certain 'problematical' taxa (i.e. *N. tapscotti*, and both *Pygaspis* species) whose positions appeared to be very unstable, the ordering of selected characters, the treatment of the lophogastrid and mysid taxa as outgroup taxa with the exclusion of the hypothetical ancestor from the analysis, and so forth. In each of these cases, the resolution of the tree as well as the consistency index (CI) were reduced, suggesting that the set of trees described here, whilst far from perfect, is probably the best possible based on the currently available information. It is hoped that current work being done in South America by Professor Pinto and his associates (Pinto, pers. comm.) on some of the less well-known pygocephalomorph species, such as *P. pachecoi*, will provide more information on some of the more problematical taxa. This may, in turn, greatly improve the resolution and informational content of analyses of this difficult group.

CHARACTERS

To arrive at our cladistic analysis we assembled a list of 33 features based largely on carapace and tail fan morphology. The commonly incomplete pygocephalomorph specimens forced us to focus

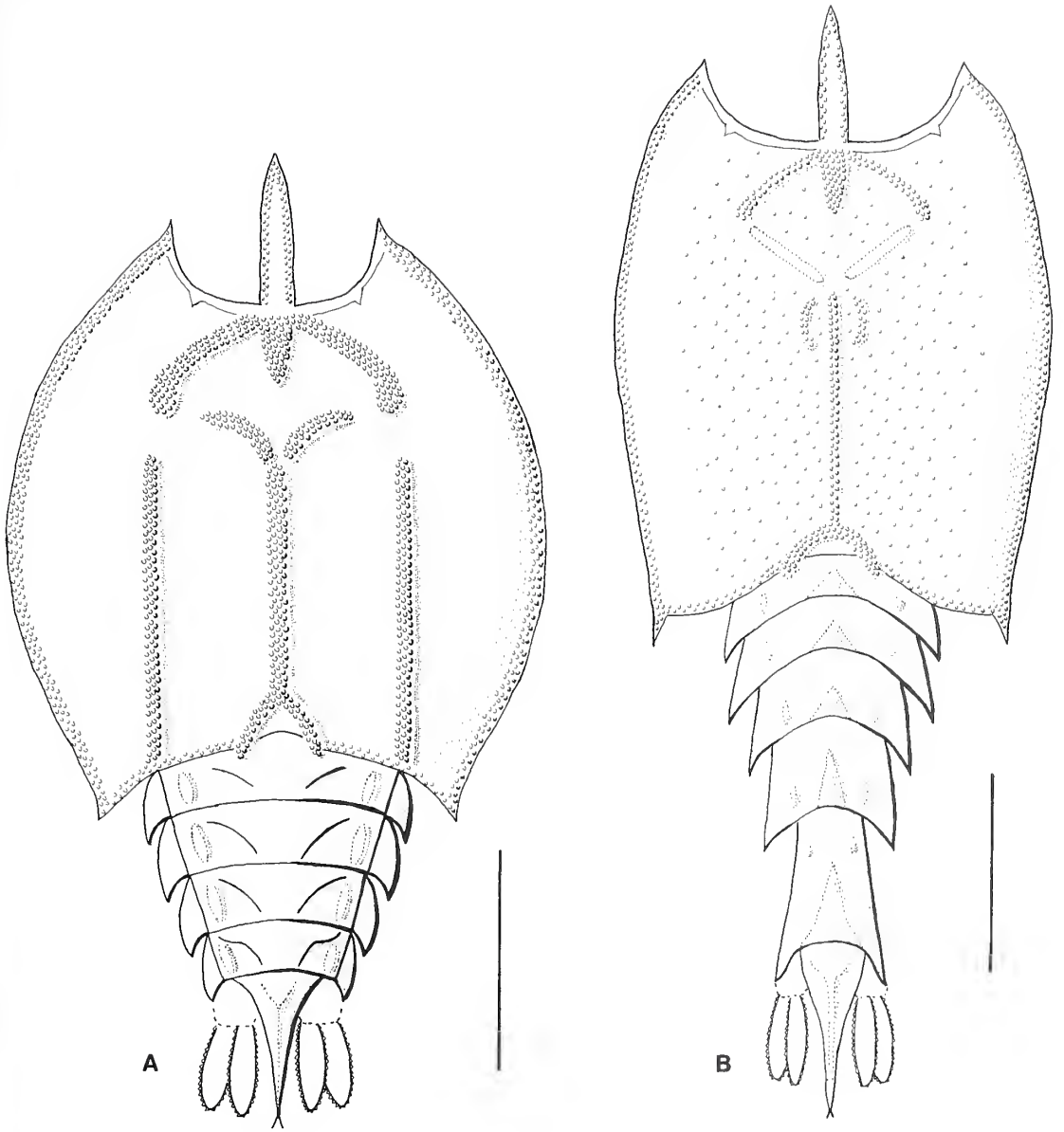

TEXT-FIG. 3. Reconstructions of: A, *Fujianocaris bifurcatus*; B, *Tylocaris asiaticus*. Scale bars represent 5 mm.

on these parts of the exoskeleton, which are those most often preserved and thus provide the majority of the taxonomic characters that are used to define genera and species. The characters and observations on them are listed below, and they include both binary and multi-state features.

1. Hepatic spines absent (0) or present (1). These spines constitute a frequently encountered set anterior to the cervical grooves.
2. Gastric spines absent (0) or present (1). This set of spines characterizes only the monotypic genus *Anthracaris*.

TABLE 3. Data matrix used in the phylogenetic analysis (see Methods and Table 1 for information regarding the identity of the characters).

Taxon	Character 0 0 0 0 0 0 0 0 0 1 1 1 1 1 1 1 1 1 2 2 2 2 2 2 2 2 2 2 3 3 3 3 1 2 3 4 5 6 7 8 9 0 1 2 3 4 5 6 7 8 9 0 1 2 3 4 5 6 7 8 9 0 1 2 3
Hypothetical ancestor	0 0 0 0 0 0 0 0 0 0 0 0 0 0 0 0 0 0 0 0 0 0 0 0 0 0 0 0 0 0 0 0
Lophogaster intermedius	0 0 0 1 0 0 0 1 0 0 0 0 0 0 0 5 0 0 1 0 0 1 0 0 0 1 0 0 0 0 0 0 0
Gnathophausia longispina	0 1 1 0 0 1 0 2 0 0 0 0 0 0 0 6 0 0 1 0 1 2 1 1 1 1 0 2 2 3 0 2 0 0
Paralophogaster glaber	0 1 1 0 0 0 0 2 0 0 0 0 0 0 0 5 0 0 ? 0 1 0 0 0 2 1 0 2 0 0 0 0 0 0
Eucopia unguiculata	0 0 0 0 0 1 0 2 0 0 0 0 0 0 0 6 0 0 1 0 1 0 0 0 2 1 0 0 0 0 0 0 0
Chalaraspidum alatum	0 0 1 0 0 1 0 1 1 0 0 0 0 0 0 5 0 0 0 0 0 2 0 0 0 ? 0 ? 3 0 0 0 0 0
Ceratolepis hamata	0 1 0 0 0 0 0 2 0 0 0 0 0 0 0 6 0 0 1 0 0 2 0 0 1 1 0 ? 0 0 0 1 0 0
Neognathophausia ingens	0 0 1 1 0 1 0 2 0 0 0 ? 0 0 6 0 1 1 0 1 1 0 0 1 1 0 ? 2 3 0 1 0 0
Peachocaris strongi	0 0 0 0 0 0 0 2 0 0 0 0 ? ? ? ? ? ? 0 0 1 0 0 1 ? 0 0 0 0 0 0 0 0
Schimperella beneckei	0 0 0 0 0 0 0 0 1 0 0 0 0 0 0 4 0 0 0 0 1 1 0 0 2 1 0 ? 0 0 0 0 0 0
Mysis flexuosa	0 0 0 0 0 0 0 0 0 0 0 0 0 0 0 3 0 0 1 0 0 0 0 0 1 1 0 0 0 0 0 0 0 0
Pygocephalus cooperi	0 1 1 0 1 0 0 1 0 0 0 0 2 2 1 0 1 0 0 1 2 0 0 0 0 0 1 0 0 0 1 0 0
Pygocephalus dubius	0 1 1 0 1 1 0 1 0 0 2 0 2 2 1 0 1 0 0 1 2 0 0 0 0 0 1 0 0 0 1 0 0
Pygocephalus aisenvergi	0 1 1 0 0 0 0 1 0 0 2 0 2 2 1 0 1 0 0 1 2 0 0 1 0 0 1 0 0 0 1 0 0
Tealliocaris woodwardi	0 1 0 0 0 1 0 0 1 0 2 0 ? 1 2 1 0 0 0 1 1 0 0 1 0 0 1 2 3 0 1 0 0
Pseudogalathea macconochiei	0 0 1 1 0 1 0 0 0 1 0 1 1 1 1 0 0 0 0 1 2 0 0 0 0 ? ? 3 0 0 2 0 0
Fujianocaris bifurcatus	0 0 1 1 0 1 1 1 0 1 1 1 ? ? 4 1 0 1 1 ? 2 1 1 0 2 1 ? 2 0 0 1 1 1
Tylocaris asiaticus	0 0 1 1 0 1 1 ? 0 1 2 1 ? ? 6 1 0 1 1 ? 2 1 1 2 1 1 ? 0 0 0 1 1 1
Chaocaris chinensis	0 ? 1 1 0 0 1 0 0 1 2 ? ? ? ? ? ? ? ? ? ? ? ? ? ? ? ? ? 1 2 1 2 0 0
Anthracaris gracilis	1 1 1 0 2 1 0 0 0 0 0 0 1 2 1 0 1 0 0 1 2 0 0 0 0 0 1 0 0 0 2 0 0
Pseudotealliocaris caudafimbriata	0 1 1 0 ? 1 0 0 0 0 0 0 ? 0 1 1 0 0 ? ? 2 1 0 0 ? 0 1 2 1 0 2 0 0
Pseutotealliocaris etheridgei	0 1 1 0 0 1 0 0 1 0 0 0 1 1 2 1 0 0 0 1 2 0 1 0 0 0 1 2 1 0 2 0 0
Pseudotealliocaris palinscari	0 0 0 0 0 1 0 0 1 0 0 0 2 2 1 1 0 0 0 1 1 1 0 0 1 0 ? 2 3 0 1 0 0
Jerometichenoria grandis	0 1 1 0 0 0 0 0 1 0 3 0 ? ? ? ? ? ? ? ? ? ? ? ? ? ? ? 0 0 0 1 0 0
Mamayocaris jepseni	0 1 1 0 1 0 0 2 0 0 0 0 1 2 1 0 0 0 0 1 2 0 0 0 0 0 1 0 0 0 0 0 0
Mamayocaris jaskoski	0 1 1 0 1 0 0 2 0 0 0 0 1 1 1 0 1 0 0 1 1 0 0 0 0 0 1 0 0 0 0 0 0
Notocaris tapscotti	0 0 0 0 0 0 0 ? 0 ? 0 0 1 ? 1 0 0 0 0 ? ? 0 0 ? 0 ? ? 0 0 0 0 0 0
Paulocaris pachecoi	0 0 1 0 0 1 0 1 0 0 0 1 ? ? ? ? ? ? ? ? 2 0 0 ? 0 ? 2 0 0 0 1 0 0
Liocaris	0 0 0 0 0 0 0 2 0 0 0 0 ? ? ? ? ? ? ? ? 1 0 ? 0 0 0 2 0 0 0 1 0 0
Pygapsis brasiliensis	0 0 0 0 0 0 0 0 0 0 0 1 0 2 2 1 0 0 0 0 ? 1 0 0 0 0 1 1 0 0 0 0 0 0
Pygaspis ginsburghi	0 0 0 0 0 0 0 0 0 0 0 0 0 ? ? ? ? ? ? ? ? 2 0 1 ? 0 ? 1 0 0 0 0 0 0

3. Anterolateral spine absent (0) or present (1). These spines can mark the lateral extent of the optic notch on the anterior margin of the carapace.
4. Postero-lateral 'process' absent (0) or present (1). These variably developed spines can be found at the postero-lateral aspects of the carapace.
5. Branchiostegal spines/serrations absent (0), only on the anterior carapace margin (1) or along the entire carapace margin (2). These distinctive features can ornament either the anterior or the entire lateral margins of the carapace.
6. Mid-dorsal ridge/keel (extending between the cervical groove and posterior carapace margin) absent (0) or present (1). This forms the most prominent component of a complex series of possible grooves and ridges on the carapace of mysidacean-like pericarids.
7. Medio-lateral spines absent (0) or present (1). A set of spines on the posterior margin of the carapace just lateral to the mid-dorsal ridge or keel.
8. Cervical groove whole (0), split (1) or strongly posteriorly directed (2). This is the principal groove

TABLE 4. Final results of the Rescaled Consistency Index (RCI) reweighting of the characters used in this analysis.

	Character	Final weight
1	Hepatic spines	1000
2	Gastric spines	133
3	Anterolateral spine	97
4	Posterolateral 'process'	200
5	Branchiostegal spines/serrations	444
6	Mid-dorsal keel	58
7	Medio-lateral spines	1000
8	Cervical groove	111
9	Cervical constriction	100
10	Marginal thickening	1000
11	Carapace papillations	200
12	Branchiostegal inflation	1000
13	Telson lobe number	389
14	Telson spine	267
15	Telson l/w ratio	300
16	Telson medial ridge	400
17	Telson terminal process	400
18	Telson terminus	429
19	Uropod margin	1000
20	Uropod diaresis	100
21	Abdominal pleurae	81
22	Abdominal medial keel	63
23	Abdominal lateral keel	63
24	Length of sixth abdominal segment	127
25	Abdominal posterior narrowing	389
26	Abdominal segments visible	250
27	Sternal field	571
28	Primary lateral keels	286
29	Secondary lateral keels	563
30	Tertiary lateral keels	1000
31	Rostral keel	156
32	Cervical ridge	1000
33	Rostro-gastral ridge	1000

on the carapace of these crustaceans and stands in contrast to the more complex series of grooves seen on the carapace of decapod eucarids.

9. Constriction of carapace margin at cervical groove absent (0) or present (1).

10. Massive thickening of carapace margin absent (0) or present (1). This forms distinctive structures along the margin.

11. Surface papillations on the carapace absent (0), restricted to specific regions of carapace (1), covering entire carapace (2) or merged to form texture/sculpturing (3). A multi-state feature typically useful in distinguishing between pygocephalomorph species.

12. Branchiostegal inflation absent (0) or present (1). It is difficult to categorize just what this feature represents. It is well developed in several genera. One could assume it bears some relationship to the possible development of gills in the branchiostegal chamber, but this cannot be easily confirmed in the fossils. It might also bear some relationship to streamlining necessary to facilitate surface flow over the thoracic region of the body.

13. Telson lobe/furca number zero (0), one pair (1) or two pairs (2). This and the following five characters often form a most coherent set of features for generic diagnoses in the order.
14. Telson spine absent (0), rounded (1) or pointed (2).
15. Telson length/width ratio < 0·5 (0), 0·51–1·0 (1), 1·01–1·5 (2), 1·51–2·0 (3), 2·01–2·5 (4), 2·51–3·0 (5), > 3·01 (6).
16. Telson medial ridge absent (0) or present (1).
17. Telson terminal process absent (0) or present (1).
18. Telson terminus whole (0) or forked (1).
19. Uropod margins straight (0) or serrate (1).
20. Uropod diaresis absent (0) or present (1).
21. Abdominal pleurae absent (0), gently rounded (1) or angular (2). Insofar as they are preserved, decorative features of the abdomen (here and in the succeeding characters) can help to delineate species.
22. Abdominal medial keel/ridge absent (0) or present (1).
23. Abdominal lateral keels absent (0) or one pair (1).
24. Length of sixth abdominal segment same as fifth (0), slightly longer than fifth (1) or much longer than fifth (2).
25. Abdominal posterior narrowing: none (0) slight (1) or great (2).
26. Abdominal segments visible: six (0) or one or two covered (1). This feature actually reflects the degree of posterior development of the carapace. Typically the carapace covers only the thorax, but in some instances it extends backwards to cover the anterior part of the abdomen.
27. Sternal field narrow (0), wide and triangular (1) or wide and rectangular (2). This feature is not always evident, unless the ventral part of the thorax is preserved. It appeared (e.g. Schram 1986) that essentially only two forms of thoracic sternite field prevailed: narrow, with little development of sternites; or triangular, with narrow sternites anteriorly and wider ones posteriorly. In examination of some of the pygocephalomorphs from Brazil, it became clear that the observations of Pinto (1971) concerning wide anterior sternites on the thorax to form a more rectangular field have great value. Whilst this feature is unknown in many pygocephalomorph genera at present, we suspect that as more information becomes available this may prove to be a very important character for sorting higher relationships in the group.
28. Primary lateral keels absent (0), medio-lateral (1), gastro-lateral (2) or postero-lateral (3).
29. Secondary lateral keels absent (0), free (1), postero-lateral (2), close to lateral margin (3) or 'fused' with lateral margin (4).
30. Tertiary lateral margin absent (0) or present (1).
31. Rostral keel absent (0), not reaching cervical groove (1) or reaching cervical groove (2).
32. Cervical ridge absent (0) or present (1).
33. Rostro-gastral ridge absent (0) or present (1).

RESULTS

For the initial, unweighted analysis, a total of 30 most parsimonious trees with a length of 129 steps was found, with a CI of 0·411. These trees, whilst showing some trends for specific groups in the analysis did not provide sufficient resolution to deduce relationships for all taxa involved, and thus we employed the use of the reweighting methods discussed above. This successive weighting regime provided a total of 15 most parsimonious trees of length 132, with a CI of 0·402. A 50 per cent. majority rule tree for these trees is shown in Text-figure 4.

Several interesting relationships emerged from this analysis. First, the recent and fossil mysids plus the recent lophogastrids form a distinct (if somewhat confused) clade, even when not specifically treated as an outgroup in the analysis. Within the pygocephalomorph 'ingroup', several distinct clades are evident which show considerable overall support for some of the taxonomic divisions outlined by Brooks (1962). As seen in the tree in Text-figure 4, the three species of

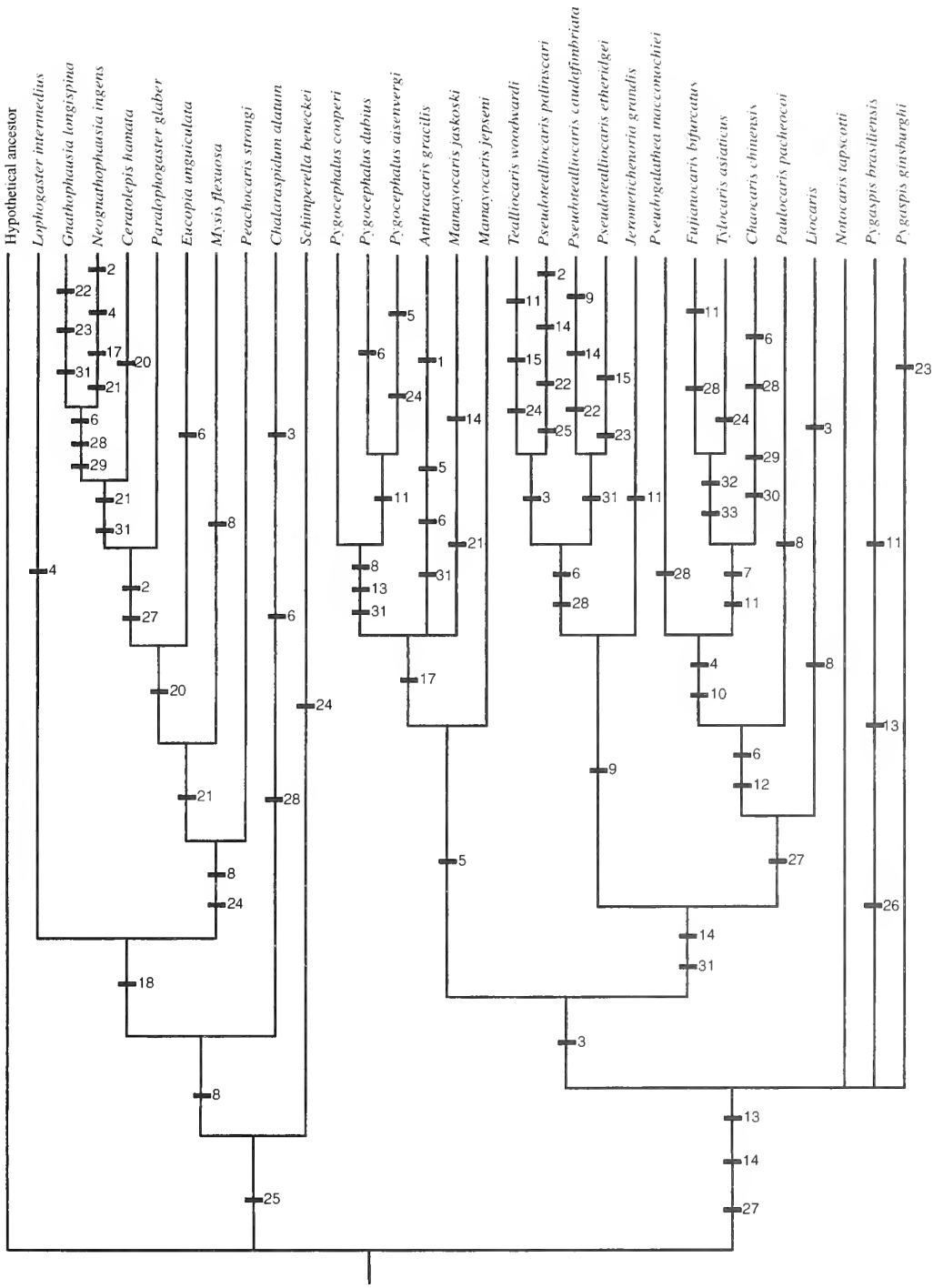

TEXT-FIG 4. Strict consensus tree of the 15 trees obtained from an analysis incorporating successive reweighting of a pygocephalomorph and lophogastrid data set, using a hypothetical ancestor as outgroup. Character state changes are plotted (see Methods section for further details).

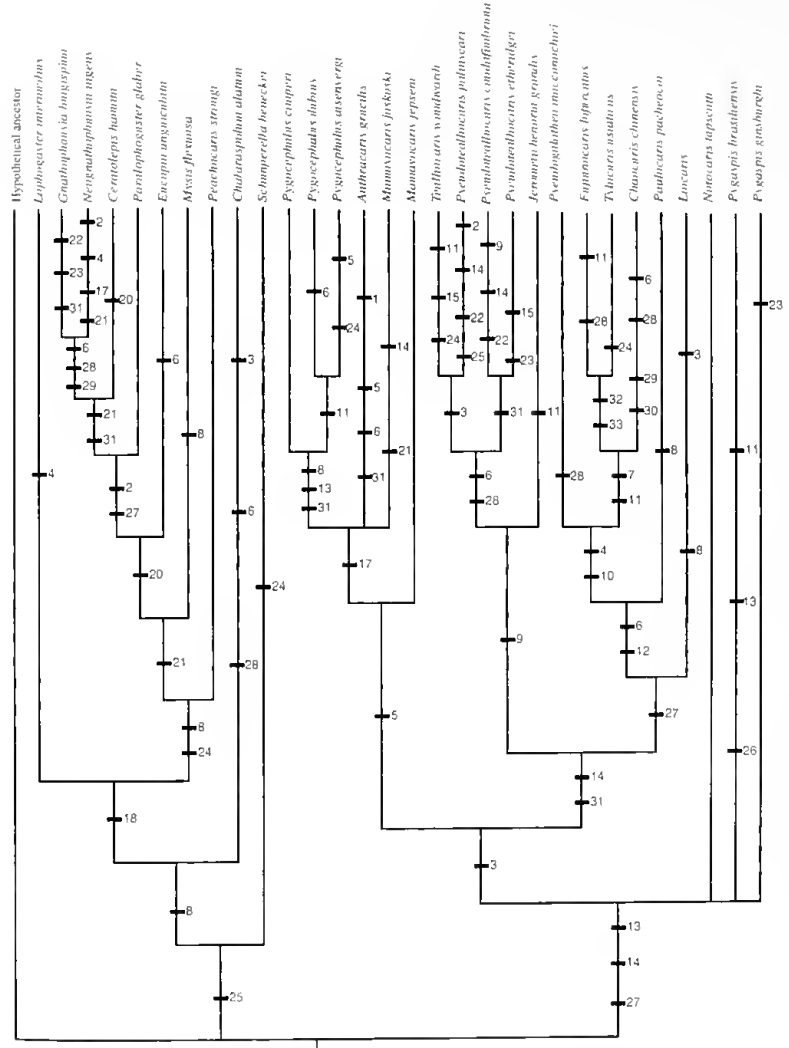

TEXT-FIG 4 Strict consensus tree of the 15 trees obtained from an analysis incorporating successive reweighting of a pygocephalomorph and lophogastrid data set, using a hypothetical ancestor as outgroup. Character state changes are plotted (see Methods section for further details).

Pygocephalus form a monophyletic group with *Anthracaris* and both species of *Mamayocaris*. This closely reflects Brooks' (1962) taxonomic scheme, in which *Anthracaris* and *Mamayocaris* are included with *Pygocephalus* in the family Pygocephalidae. One major disagreement with Brooks (1969) is the unification of *Tealliocaris* with the three species of *Pseudotealliocaris* to form a monophyletic clade; he had placed the latter in Pygocephalidae and the former in Tealliocarididae. Thus, Brooks' generic distinction between *Tealliocaris* and *Pseudotealliocaris* may be an unnatural taxonomic separation. His familial separation of these genera is certainly suspect. *Jerometichenoria* is united by this analysis with this tealliocaridid clade, suggesting that the family Jerometichenoriidae, proposed by Schram (1978), may also be unnecessary.

A close relationship seems to exist between the three Chinese forms, *Fujianocaris* and *Tylocaris* and the Carboniferous *Chaocaris*, and the British *Pseudogalathea*, and this may also extend to the problematical South American genera *Paulocaris* and *Liocaris*. This is perhaps the most interesting relationship to emerge from this analysis, as it could indicate taxonomic and palaeobiogeographical relationships between these geographically widely separated taxa. This result also contrasts with Brooks' (1962) interpretation, in that his placement of *Pseudogalathea* with *Tealliocaris* in Tealliocarididae is not supported by this analysis. In addition, Brooks placed *Paulocaris* in Notocarididae with *Notocaris*, another association that does not appear to be supported by this analysis. Both the *Pygaspis* species and *N. tapscotti* occur basally in the pygocephalomorph 'clade', with no clear associations to any of the three major pygocephalomorph clades expressed in the analysis. We hope that a more adequate understanding of the anatomy of the southern hemisphere species will resolve the polychotomies in this part of the tree, and allow us to address definitively the issues of pygocephalomorph classification.

DISCUSSION

Age

Beds of the Tungtzeyen Formation containing *Fujianocaris bifurcatus* also contain several other taxa, including plants, conchostracans, bivalves, brachiopods, gastropods, ammonoids, fusilinids and crinoids. These taxa collectively are the basis for the assignment of an Early Permian age for the Tungtzeyen Formation (Sheng *et al.* 1982).

Morphology

At the outset of this study, it was assumed that the two new species were members of the extinct Carboniferous/Permian order Pygocephalomorpha, based on overall morphology and similar time ranges. However, we also considered that they might be related to Recent mysids or, more likely, Recent Lophogastrida. There is a great number of morphological similarities between the latter and the Pygocephalomorpha. They have both been considered as sub-orders of the Mysida, and were elevated to the status of separate orders by Schram (1984). The main distinguishing characters for the Pygocephalomorpha are the presence of a triangular field of sternites on the ventral surface of the thorax and the development of a complex tail fan, including at least one pair of caudal furcae associated with the telson (Schram 1986). Since none of the specimens described here shows either ventral preservation or a complete fail fan, these unfortunately could not be used.

Important characters that distinguish these new species from the morphologically similar pygocephalomorph *Pseudogalathea* are: the complex cervical and rostro-gastric ridges; the medial ridge of the telson in the tylocaridids; and the highly elongated postero-lateral spines of *Pseudogalathea*. *Pygocephalus*, another pygocephalomorph to which *F. bifurcatus* and *T. asiaticus* could be compared (Brooks 1962, 1969), is distinguishable from the tylocaridids by the absence of antero-lateral serrations on the carapace margin, the presence of a medial ridge on the telson, and the presence of carapace ridges. A third pygocephalomorph genus, *Chaocaris*, occurs in China (Shen 1983) and has several similarities to the tylocaridids, but is distinguished by its possession of a set of mid-lateral carapace keels, the absence of a medial carapace keel, and an elongate, narrow rostral

ridge extending from the anterior end of the carapace to the cervical ridge. The taxonomic placement of *Chaocaris* with the pygocephalomorphs is uncertain, as this taxon is based on a single carapace.

T. asiaticus and *F. bifurcatus* also show similarities to mysidacean species known from the fossil record, in particular *Schimperella beneckei* and *Peachocaris strongi*. *S. beneckei* can be distinguished by its six exposed abdominal somites and its possession of a truncate telson that is shorter than its associated uropods (Hessler 1969), and *P. strongi* by its rounded abdominal pleurae, the exposure of all six abdominal somites, and the presence of large, rounded postero-lateral lappets on the carapace (Brooks 1962).

One important morphological character that suggested to us a possible relationship between *F. bifurcatus* and *T. asiaticus* and the lophogastrids instead of the pygocephalomorphs is the apparent presence of a bifurcation at the terminal end of the telson, resembling a pair of terminal spines. This is a common occurrence in the order Lophogastrida but is generally absent among pygocephalomorphs. This is, however, an uncertain character at best, due to the usually poor nature of preservation of the tail fan in these animals.

Associated faunas and ecology

Specimens of *Tylocaris asiaticus* and *Fujianocaris bifurcatus* were collected from three different localities in south-east China: most are from the Early Permian Tungtzeyen Formation at Changta, Fujian, which comprises alternating thin beds of grey to dark grey, fine-grained quartz sandstone and siltstone, interbedded with mudstone and coal beds. The accompanying flora and fauna includes plants (*Gigantonoclea fukiensis*, *Sphenophyllum sino-coreanum*, *Pecopteris* (*Rajahia*) *rigida*, *P. helitelioides*, *Sphenopteris tenuis*, *Asterophyllites longifolius*, *Lobatannularia lingulata*, *Gigantopteris dictyophylloides*, *Compsopteris* sp., and *Cordaites* sp.), bivalves (*Bakevellia ceratophaga*, *Wikingia elegans*, *Vosellina* aff. *yunnanensis*, *Astartella* cf. *ambiensis*, *Stuchburia* sp. and *Palaeoneilo* sp.), brachiopods (*Cathaysia* sp., *Neoplicatifera* sp., *Linoproductus* sp., *Lingula* sp. and *Pygnochonetes* sp.), gastropods (*Cyclozyga* sp., *Baylea* sp. and *Bellerophon* sp.), ammonoids (*Altudoceras* sp. and *Schouchangoceras* sp.), crinoids (*Cyclocylicus quinquelobus*) and unidentified insect wing fragments.

The flora at these south-east Chinese localities may represent the Late Palaeozoic Cathaysian flora (see Zhang and He 1985). The gigantopterids probably represent tropical woody climbers, carried to the site of deposition by streams or winds (Yao 1983). The brachiopod *Lingula* and the bivalves *B. ceratophaga*, *Stuchburia* sp. and *V.* aff. *yunnanensis* are all euryhaline forms, which lived in shallow marine settings. These floral and faunal characters, along with the lithological characteristics, suggests deposition in a nearshore marine environment, with possible repeated deepening cycles. This high-salinity environment may be largely responsible for the relative scarcity of specimens and their general incompleteness, as such shallow water fully marine faunas are rarely preserved in the fossil record (Schram 1981; Briggs and Clarkson 1989). It is perhaps due to the highly sclerotized nature of the carapace of *F. bifurcatus* that it is preserved in such high numbers, in comparison with *T. asiaticus*. There is considerable generic (*Sphenophyllum*, *Pecopteris*, *Sphenopteris* and *Asterophyllites*) and some specific overlap (*A. longifolius*) between this south-east Chinese flora and that of the Late Carboniferous Mazon Creek Essex assemblage, which has been interpreted as a nearshore marine fauna (Janssen 1965; Pfefferkorn 1979; Schram 1979*b*). Whilst not closely related geologically during the Permian (Scotese and McKerrow 1990; Ziegler *et al.*, pers. comm.), southern China and continental southern North America were both located near the equator and probably shared tropical environments, which might account for the similar floras.

The single specimen of *F. bifurcatus* from the Lower Permian at Xihushan, Fujian Province was found in dark grey mudstones, with no associated faunal or floral elements. There is a lack of data for this section, due to little collecting having been done. Based on its lithology, this unit is assumed to have been deposited in a coastal marine environment, similar to that inferred for the better known Lower Permian at Changta, Xiangshuping.

A further single specimen of *F. bifurcatus* was collected from an exposure of the Upper Permian at Shitangpu, Hunan Province where the Lungtan Formation is composed of yellowish to dark grey thin-bedded mudstone. It also contains brachiopods (*Spinomarginifera pseudosintanensis*, *Spinomarginifera* sp., *Leptodus tenuis*, *Martinia* sp., *Punctospirifer* sp., *Oldhamina* sp., *Haydenella* sp., and *Gubleria* sp.) and bivalves (*Schizodus* sp., *Palaeoneilo* sp., *Nuculopsis*? sp. and *Stutchburia*? sp.). The absence of terrestrial or freshwater plant material indicates a system isolated from freshwater runoff. The relative abundance of brachipods, seemingly preserved *in situ*, suggests a quiet marine environment, as does the presence of exclusively fine-grained sediments, which were probably deposited in a nearshore marine or paralic setting, possibly lagoonal or a protected bay (Wang 1985; Zhang 1992).

The occasional presence of carapaces of *F. bifurcatus* and *T. asiaticus* on closely associated bedding planes suggests that these two species lived in the same or closely associated communities. It is difficult to establish their rôle within these communities, however, as their preservation is insufficient to discern such features as mouthpart anatomy and thus insight into feeding type. These eumalacostracans may represent low-level carnivores, as suggested for seemingly similar forms by Schram (1981), but only the collection and description of further material, with better or new morphological details, can answer this question.

Palaeobiogeography

The placement of these new Chinese taxa into the order Pygocephalomorpha presents some new and difficult questions about Palaeozoic palaeobiogeography. Based on this order alone, there is evidently some palaeobiogeographical relationship between central North America, South America, South Africa, Great Britain, and, tentatively, southern China during the Carboniferous and Permian. However, it is not known whether this is due to similar ecological conditions, or to a true biogeographical connection. Whilst Permian maps (e.g. Scotese and McKerrow 1990) show similar latitudinal positions for several areas in which pygocephalomorphs occur (i.e. North America, Great Britain), there is no physical connection between these regions and the land masses destined to make up China. However, the same can also be said for the taxa found in such areas as South Africa and Brazil, which were not closely related palaeogeographically to North America and Great Britain. Thus, the question of historical biogeography for the order Pygocephalomorpha is a difficult one, regardless of the taxonomic position of the tylocaridids.

One possibly important trend can be seen in the temporal distribution of the pygocephalomorphs. All of the 11 known Carboniferous species occur in close association with Laurentia. Conversely, of the six known Permian species, five have a Gondwanan distribution (the exception being *Mamayocaris jepseni*, which is Laurentian in origin). Thus, there was a general shift in the distribution of the pygocephalomorphs from the Laurentian to the Gondwanan coastal margins over the Carboniferous to the Permian, with the exception of isolated populations which remained in Laurentian waters throughout the Permian. This concurs with the observations of Schram (1977), who discussed malacostracan crustacean distributions during the Palaeozoic and the Triassic. He suggested a restriction to Laurentian waters during the Late Palaeozoic for the malacostracans, followed by an expansion of their distribution to other parts of the world with the formation of the Pangaean supercontinent during the Permian. The new information provided by the tylocaridid pygocephalomorphs clearly supports this observation. It is difficult to draw further conclusions about Palaeozoic palaeobiogeography, especially with respect to the pygocephalomorph crustaceans, from the data as it currently stands.

The same biogeographical problems exist, however, in the alternative hypothesis, in which the tylocaridids might be members of the Lophogastrida rather than Pygocephalomorpha. Little is known about the fossil record of the lophogastrids with the exception of the Carboniferous species *Peachocaris strongi* from North America and the Triassic species *Schimperella beneckei* from Alsace, France. Thus, the same problematical issue arises: trying to draw connections between the closely related North American and European regions to the distant Chinese land masses.

Acknowledgements. This research was made possible by a grant (no. 750.195.17) from 'de Stichting Geologisch, Oceanografisch en Atmosferisch Onderzoek', Nederlandse Organisatie voor Wetenschappelijk Onderzoek (The Department of Geological, Oceanographic and Atmospheric Research, the Dutch Organization for Scientific Research). Thanks are also extended to Dr Ronald Jenner III, for his valuable assistance and comments on the manuscript.

REFERENCES

BEURELEN, K. 1930. Vergleichende Stammesgeschichte Grundlagen, Methoden, Probleme unter besonderer Berüksichtigung der höheren Krebse. *Fortschriften der Geologie und Palaeontologie*, **8**, 317–464.

—— 1931. Crustacean reste aus den Mesosaurierschichten (Unterperm) von Brasilien (São Paulo). *Palaeontologische Zeitschrift*, **13**, 35–50.

—— 1934. Die Pygaspiden, eine neue Crustaceen (Entomostracen) Gruppe aus den Mesosaurier-führenden Iraty-Schichten Brasiliens. *Palaeontologische Zeitschrift*, **16**, 122–138.

BRIGGS, D. E. G. and CLARKSON, E. N. K. 1989. Environmental controls on the taphonomy and distribution of Carboniferous malacostracan crustaceans. *Transactions of the Royal Society of Edinburgh: Earth Sciences*, **80**, 293–301.

BROOKS, H. K. 1962. The Palaeozoic Eumalacostraca of North America. *Bulletins of American Paleontology*, **44**, 163–338.

—— 1969. Eocarida. R341–R345. *In* MOORE, R. C. (ed.). *Treatise on invertebrate paleontology. Part R. Arthropoda 4*. Geological Society of America and University of Kansas Press, Lawrence.

BROOM, R. 1931. On the *Pygocephalus*-like crustacean of the South African Dwyka. *Proceedings of the Zoological Society of London*, 571–573.

CHEN JUN-YUAN, ZHU MAO-YAN and ZHOU GUI-QING 1995. The Early Cambrian medusiform metazoan *Eldonia* from the Chengjiang Lagerstätte. *Acta Palaeontologica Polonica*, **40**, 213–244.

—— ZHOU GUI-QING and RAMSKÖLD, L. 1995. The Cambrian lobopodian *Microdictyon sinicum*. *Bulletin of the National Museum of Natural Science*, **5**, 1–93.

CLARKE, J. M. 1920. Crustacea from the Permian of São Paulo, Brazil. *Bulletin of the New York State Museum*, **219/220**, 135–137.

HESSLER, R. R. 1969. Pericarida. R360–R393. *In* MOORE, R. C. (ed.). *Treatise on invertebrate paleontology. Part R. Arthropoda 4*. Geological Society of America and University of Kansas Press, Lawrence.

HUXLEY, T. H. 1857. Description of a new crustacean (*Pygocephalus cooperi*) from the Coal Measures. *Quarterly Journal of the Geological Society, London*, **13**, 363–369.

JANSSEN, R. E. 1965. *Leaves and stems from fossil forests*. Popular Science Series 1. Illinois State Museum.

LATRIELLE, P. A. 1802. *Histoire naturelle générale et particulière, des crustacés at des insects*. 3. F. Dufort, Paris, 486 pp.

PEACH, B. N. 1883. Further researches among the Crustacea and Arachnida of the Carboniferous rocks of the Scottish Border. *Proceedings of the Royal Society of Edinburgh*, **30**, 511–529.

PFEFFERKORN, H. W. 1979. High diversity and stratigraphic age of the Mazon Creek flora. *In* NITECKI, M. H. (ed.). *Mazon Creek fossils*. Academic Press, New York, 581 pp.

PINTO, I. D. 1971. Reconstituição de *Pygaspis* Beurlen, 1934 (Crustacea – Pygocephalomorpha). Sua Posição Sistemática, seu significado e de outros fósseis para o Gondwana. *Anais da Academia Brasil Ciências*, **43** (supplemento).

PRESTWICH, J. 1840. On the geology of the Coalbrookdale. *Transactions of the Geological Society, London*, **5**, 413–495.

SALTER, J. W. 1861. On some higher Crustacea of the British Coal Measures. *Quarterly Journal of the Geological Society, London*, **17**, 528–533.

—— 1863. On some fossil Crustacea from the Coal-measures and Devonian rocks of British North America. *Quarterly Journal of the Geological Society, London*, **19**, 76.

SCHRAM, F. R. 1974*a*. Mazon Creek caridoid Crustacea. *Fieldiana: Geology*, **30**, 9–65.

—— 1974*b*. Convergences between Late Paleozoic and modern caridoid Malacostraca. *Systematic Zoology*, **23**, 323–332.

—— 1977. Paleozoogeography of Late Paleozoic and Triassic malacostracans. *Systematic Zoology*, **26**, 367–379.

—— 1978. *Jerometichenoria grandis* n. gen., n. sp. (Crustacea: Mysidacea) from the Lower Permian of the Soviet Union. *Journal of Paleontology*, **52**, 605–607.

—— 1979*a*. British Carboniferous Malacostraca. *Fieldiana: Geology*, **40**, 1–129.

—— 1979*b*. The Mazon Creek biotas in the context of a Carboniferous faunal continuum. 159–190. *In* NITECKI, M. H. (ed.). *Mazon Creek fossils*. Academic Press, New York, 581 pp.
—— 1981. Late Paleozoic crustacean communities. *Journal of Paleontology*, **55**, 126–137.
—— 1984. Relationships within eumalacostracan crustaceans. *Transactions of the San Diego Society of Natural History*, **20**, 301–312.
SCOTESE, C. R. and McKERROW, W. S. 1990. Revised world maps and introduction. 1–21. *In* McKERROW, W. S. and SCOTESE, C. R. (eds). Palaeozoic palaeogeography and biogeography. *Memoir of the Geological Society*, **12**, 1–435.
SHENG JINZHANG, JIN YUGAN, RUI LIN, ZHANG LINXIN, ZHENG ZHOUQUAN, WANG YUJING, LIAO ZHOUTING and ZHAO JIAMIN 1982. [Correlation chart of the Permian in China with explanatory text.] 153–170. *In* [*Stratigraphic correlation chart in China with explanatory text.*] Science Press, Beijing. [In Chinese.]
SHEN YAN-BIN 1978. Leaid conchostracans from the Middle Devonian of south China with notes on their origin, classification and evolution. *Papers for the International Symposium on the Devonian System*, 1–15.
—— 1981. Cretaceous conchostracan fossils from eastern Shandong. *Acta Palaeontologica Sinica*, **20**, 518–526.
—— 1983. A new pygocephalomorph genus (Eumalacostraca) of Lower Carboniferous from Anhui. *Acta Palaeontologica Sinica*, **22**, 663–668.
—— 1984. Occurrence of Permian leaid conchostracans in China and its palaeogeographical significance. *Acta Palaeontologica Sinica*, **23**, 505–513.
—— 1990. A new conchostracan genus from Lower Permian Tungziyan Formation, Fujian. *Acta Palaeontologica Sinica*, **29**, 309–314.
WANG HUNGZHEN 1985. *Atlas of the palaeogeography of China*. Cartographic Publishing House, Beijing, 300 pp. [In Chinese and English.]
WOODWARD, H. 1879. On *Necroscilla wilsoni* a supposed stomatopod crustacean from the Middle Coal Measures, Cossall, near Ilkeston. *Quarterly Journal of the Geological Society, London*, **35**, 551–552, pl. 26.
YAO ZHAOQI 1983. Ecology and taphonomy of gigantopterids. *Bulletin of the Nanjing Institute of Geology and Palaeontology, Academia Sinica*, **6**, 63–84.
ZHANG SHANZHEN and HE YUANLIANG 1985. Late Palaeozoic palaeophytogeographic provinces in China and their relationships with plate tectonics. *Palaeontologia Cathayana*, **2**, 77–86.
ZHANG WENTANG, SHEN YANBIN and NIU SHAOWU 1990. Discovery of Jurassic conchostracans with well-preserved soft parts and notes on its biological significance. *Palaeontologia Cathayana*, **5**, 311–352.
ZHANG YANGYU 1992. Sedimentary environments and its evolution of Tungziyan Formation in Fujian. *Coal Field Geology of China*, **4**, 20–25.
ZHU TONG 1990. *The Permian coal-bearing strata and palaeobiocoenosis of Fujian*. Geological Publishing House, Beijing, 127 pp.

ROD S. TAYLOR
FREDERICK R. SCHRAM
Institute for Systematics and Population Biology
University of Amsterdam
P.O. Box 94766
1090 GT Amsterdam
The Netherlands
e-mail taylor@bio.uva.nl
e-mail schram@bio.uva.nl

SHEN YAN-BIN
Nanjing Institute of Geology and Palaeontology
Academia Sinica
39 East Beijing Road, Nanjing
The People's Republic of China
210008
e-mail LPSNIGP@nanjing.jspta.chinamail.sprint.com

Typescript received 16 April 1997
Revised typescript received 18 September 1997

THREE-DIMENSIONALLY MINERALIZED INSECTS AND MILLIPEDES FROM THE TERTIARY OF RIVERSLEIGH, QUEENSLAND, AUSTRALIA

by IAN J. DUNCAN, DEREK E. G. BRIGGS *and* MICHAEL ARCHER

ABSTRACT. An assemblage of three-dimensionally preserved insects and millipedes from the late Oligocene/early Miocene limestones of Riversleigh (north-west Queensland) augments a sparse Tertiary insect record from Australia. The fauna includes four species of Coleoptera, one of Trichoptera represented only by the larva, and a myriapod. The arthropods are uncompacted and have been replicated in calcium phosphate. Early phosphatization has preserved original structures such as the overlapping layers and helicoidal pore canals of the procuticle, and wrinkles in the arthrodial membrane. The most remarkable preservation is of the ocular apparatus. The hexagonal lenses and their rhabdom emplacements are preserved in the Coleoptera. The trichopteran larva displays an unusual form of compound eye, consisting of large, separate circular lenses. Where the cornea has been lost, an irregular lattice of 'cups' is exposed. This is the first example of this 'schizochroal'-type eye reported in a fossil insect. Bacteria and fungi associated with the decay of the insects are themselves mineralized.

DESPITE the great success of insects through time in terms of both abundance and diversity, surprisingly little is known about the fossil insects of Australia. The majority of remains so far uncovered consist of wings or indeterminate fragments. Only rarely are wings attached to bodies and even when this occurs, most fossils are preserved in a crushed and distorted condition (Riek 1970*a*). Approximately 350 fossil species in 19 orders have been described from Australia, covering a period extending from the Upper Permian to the Pliocene (for reviews see Riek 1970*a*, 1970*b*; Jell and Duncan 1986). However, this record includes only three significant Tertiary insect deposits besides those at Riversleigh (Text-fig. 1): Redbank and Dinmore, southern Queensland (Riek 1967) and Vegetable Creek, NSW (Riek 1954). The information provided by these sites is limited by the quality of the fossil material. The Lower Tertiary Redbank assemblage is dominated by Coleoptera and Homoptera, but Blattodea, Hemiptera-Heteroptera, Neuroptera, Mecoptera and Diptera are also represented (Riek 1970*a*). Insects are much rarer in the Dinmore assemblage, with single wings of an orthopteran, an isopteran, a homopteran and an odonatan comprising the total fauna (Riek 1970*a*). The Vegetable Creek fauna is restricted to immature aquatic insects, predominantly Ephemeroptera and Diptera. Only beetle elytra have been recovered from other Tertiary sites (Riek 1970*a*). The remarkable three-dimensionally preserved insects from Riversleigh represent an important addition to this Tertiary record.

THE RIVERSLEIGH FAUNA

Riversleigh's major importance is the data that it provides on the Tertiary mammals of Australia (Archer and Bartholomai 1978; Archer and Clayton 1984), nearly trebling the species of this age previously recorded for the entire continent (Archer *et al.* 1994*a*, 1994*b*, 1995). The insects were first discovered in the course of processing the vertebrate-packed limestone in search of small bones and teeth. Acetic acid digestion may have introduced a bias, as specimens which are not phosphatized would have been destroyed. Specimens which preserve organics were recovered from other Riversleigh sites (D. A. Arena, pers. comm.). Coleopteran specimens are rare. At least four different species, each belonging to a different family, have been found. Fragmentary larval specimens of a

[Palaeontology, Vol. 41, Part 5, 1998, pp. 835–851]

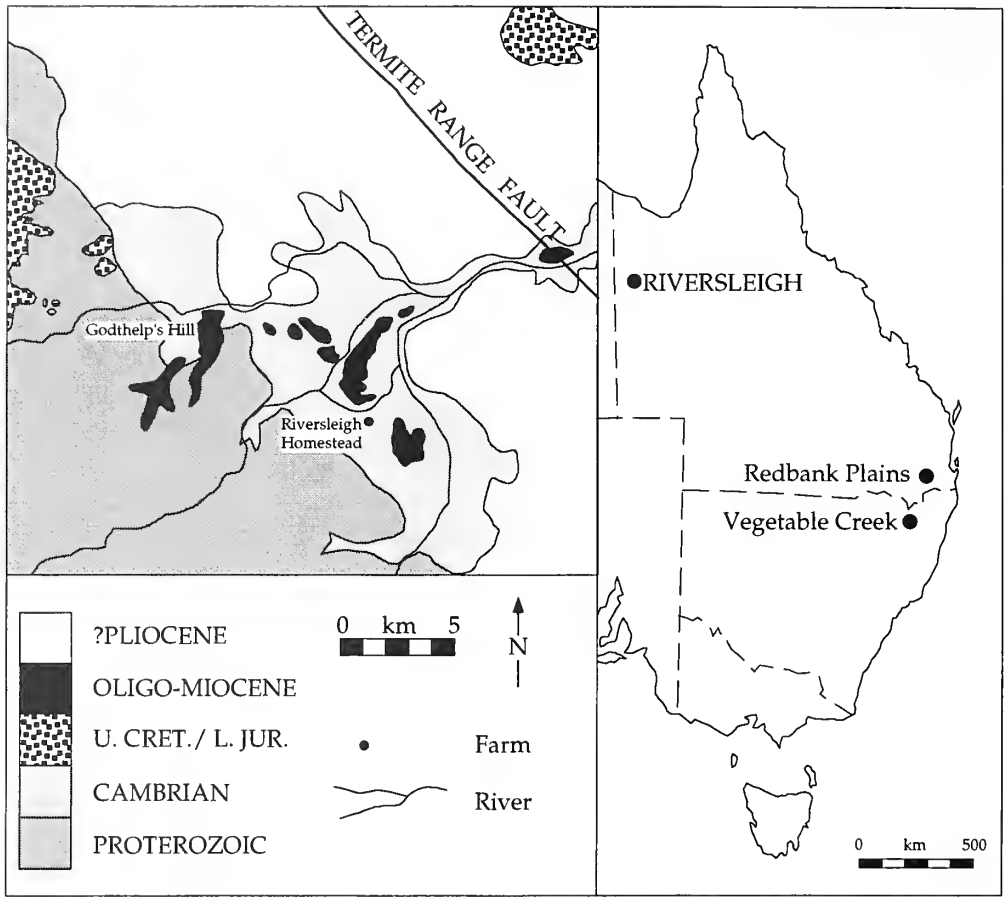

TEXT-FIG. 1. Location map. Left, detail of Upper site, Godthelp's Hill and geology of the surrounding area. Right, locations of Riversleigh and principal Tertiary insect-bearing *Lagerstätten* in eastern Australia (after Megerian 1992).

single species of Trichoptera are much more common. A myriapod, and a previously documented isopod (Archer *et al.* 1994*a*), complete the arthropod fauna as presently known.

Locality and stratigraphy

Although Riversleigh was originally thought to represent a single, distinct mid Miocene assemblage (Tedford 1967), fossils have now been recovered from over 100 different sites, ranging in age from late Oligocene to near present day (Archer *et al.* 1989, 1994*a*, 1994*b*, 1995). For a detailed discussion of the stratigraphy, see Megerian (1992).

The arthropods reported here were recovered from one locality, the Upper Site of Godthelp's Hill (Text-fig. 1). Arthropods are also known from other Riversleigh sites (Camel Sputum and Dunsinane sites). At the Upper Site, the vertebrate fauna is particularly diverse, with almost twice the number of marsupial species as any surviving Australian ecosystem, as well as a diverse range of birds, reptiles and amphibians (Archer *et al.* 1989, 1994*a*). The Upper Site is interpreted as a former shallow (*c.* 1 m deep), lime-rich pool in a rain forest (Archer *et al.* 1994*a*), where levels of calcium carbonate were sufficient to result in the precipitation of a thin peripheral crust.

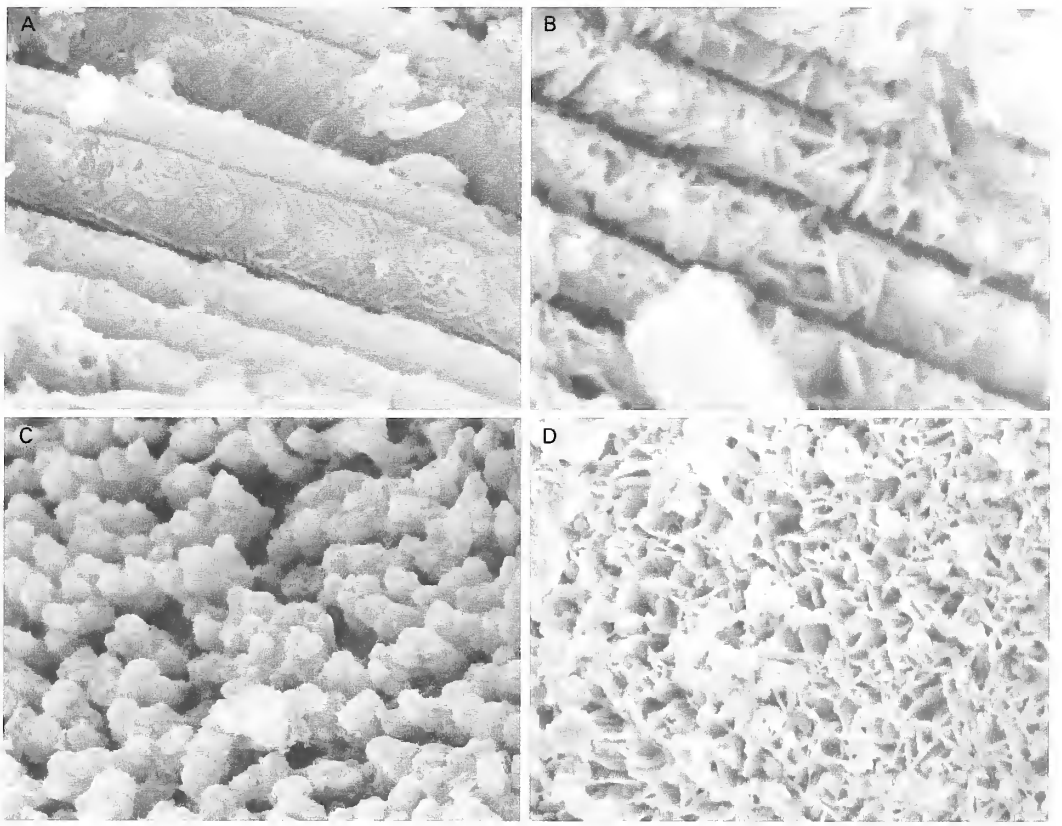

TEXT-FIG. 2. Micro-environments of preservation in a trichopteran larva (QM F34592). A, cuticular fragment from within the tail assemblage displaying distinct chevron structures arranged in parallel rows; structural detail is lost to the lower right; ×65000. B, cuticle a few micrometres distant to 'A'; the structures have been replicated by plates of calcium phosphate such that the gross structure is retained while the detail is lost; ×65000. C, 'nodular' surface of the dorsal cuticle; ×25000. D, replacement of the nodules within a few micrometres of 'C' with plates of calcium phosphate; ×30000. Specimens are gold coated.

Accumulations of piles of crystalline shards, interspersed with animal remains, are common in many of the Riversleigh deposits. The crystal crust may have given the appearance of firmness, only to give way under the weight of an animal that strayed onto it, which then drowned. The Upper Site limestone is characterized by black, iron-rich bands that may reflect periods of anaerobic conditions, where an absence of oxygen inhibited scavengers, contributing to the lack of disarticulation of the vertebrate remains. Wrinkled sheets, interpreted as algal mats, have also been recovered from acid residues (Archer *et al.* 1994*a*). The trichopteran larvae are found in tube-like extensions of this mat-like material. The range of vertebrates found at the Upper Site suggests that all the surrounding micro-environments are represented, from tree tops (many possums) to the forest floor (wynyariids, macropopoids, perameloids, etc.), and the water itself (frogs) (Archer *et al.* 1994*a*).

TAPHONOMY

The most striking feature of the Riversleigh arthropods is their preservation in three dimensions. However, only the more recalcitrant tissues have survived; the internal soft tissues have decayed.

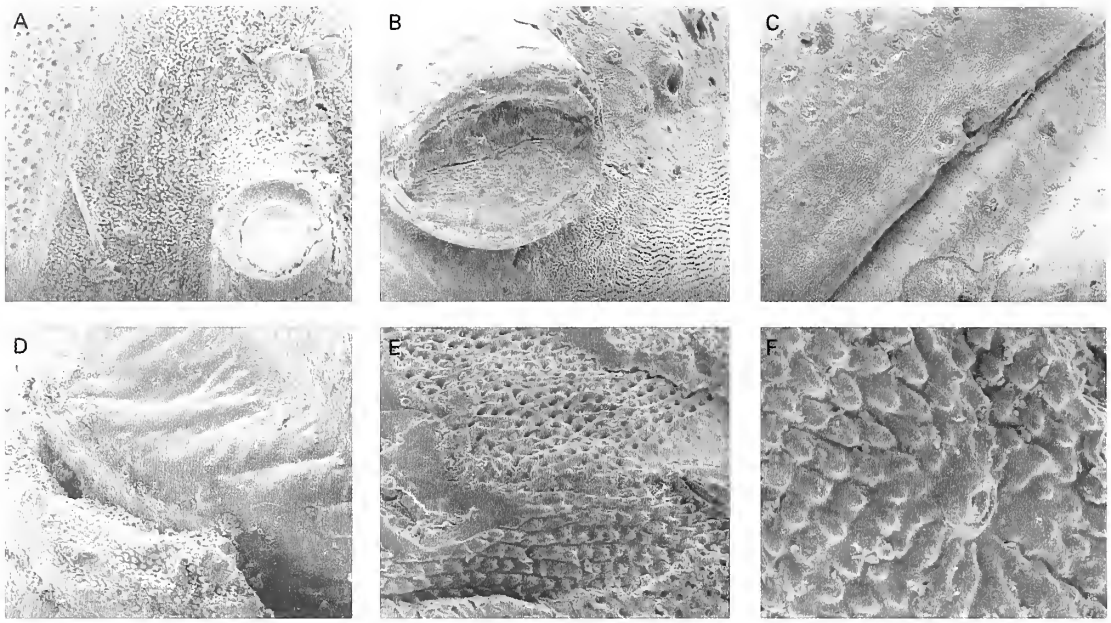

TEXT-FIG. 3. Ornamentation of cuticle of trichopteran larva (QM F34587). A, prescutum with irregular pattern of pits; a spiracle is also present; × 4500. B, interface between the scutum, showing sites of hair emplacement in its upper half, and the scutellum; the scutellum is more regularly patterned than the prescutum; × 5000. C, scutum and scutellum, overlapping the next segment (to the right); × 4000. D, limb of first thoracic segment, surrounded by arthrodial membrane; × 700. E, arthrodial membrane; × 1750. F, close-up of hair emplacement; × 2250.

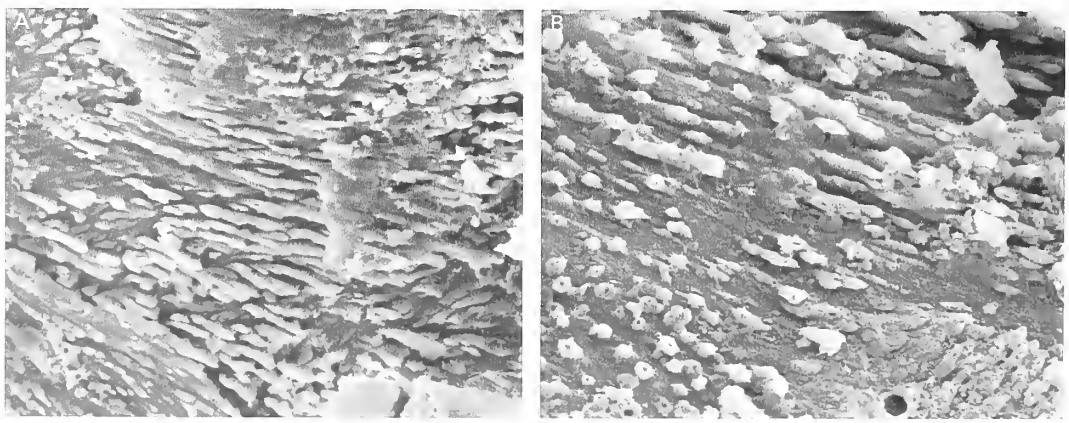

TEXT-FIG. 4. Underlying arrangement of microfibrils within the cuticle of coleopteran species C (QM F34582). A, longitudinal arrangement of microfibrils; × 13000. B, longitudinal and cross sectional arrangement of microfibrils; × 32500.

The overlapping layers that make up the cuticle are preserved, as are the ocular framework, rhabdom and individual lenses of the eye. Microprobe analysis confirms that the specimens are preserved in carbonate-fluorapatite. Some specimens are infilled with detrital matter that appears to have been phosphatized contemporaneously.

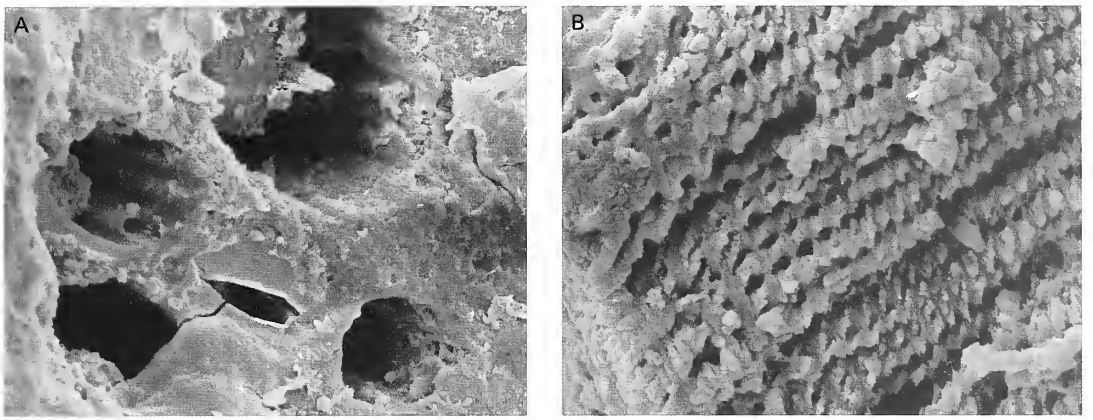

TEXT-FIG. 5. Canals within the cuticle of the trichopteran larva (QM F34591). A, series of parallel canals exposed in tail segment; ×9000. B, helicoidal pore canals (cf. Bouligand 1965) in a cuticle fragment; ×27500.

Cuticle

Structures less than 1 μm in dimensions are preserved on the surface of the cuticle (Text-fig. 3). The distinctive arrangement of the microfibrils (Text-figs 4, 9A) is evident in section, as is the helicoidal structure observed by Bouligand (1965) and Neville *et al.* (1969) in living insects (Text-fig. 5B). The orientation of the crystals follows that of the structural proteins and other biomolecules within the cuticle, emphasizing the high fidelity of replication by calcium phosphate. Parallel canals can be discerned within the tail segment of one of the larvae (Text-fig. 5A).

The cuticle of the trichopteran larva displays distinct chevron structures arranged in parallel rows (Text-fig. 2A) just a few micrometres distant from a point where the cuticle has been replaced by plates of phosphate that replicate the gross structure but obliterate the detail (Text-fig. 2B). A similar phenomenon is evident where the nodular patterning of the larval cuticle (Text-fig. 2C) is replaced within a few micrometres by plates of phosphate (Text-fig. 2D). This indicates that the conditions under which decay and mineralization took place varied on a sub-millimetre scale (see Martill 1988; Briggs and Kear 1994).

Eye

Perhaps the most striking evidence of the fidelity of preservation occurs in the eyes (Text-fig. 6; Duncan and Briggs 1996). The insect compound eye is composed of arrays of ommatidia – the basic visual unit (Snodgrass 1935; Text-fig. 6F). Each ommatidium is composed of a dioptric apparatus and rhabdom, isolated from the next ommatidium by pigment cells; the dioptric apparatus of lens and crystalline cone controls the focusing of light. The cuticle of this apparatus is composed predominantly of chitin, which differs ultrastructurally from that surrounding it (Neville 1970). The rhabdom contains the visual pigments that trigger impulses in the optic nerve (Snodgrass 1935). The entire ocular apparatus of the Riversleigh specimens is replicated in calcium phosphate.

The eyes exhibit varying degrees of alteration through decay and diagenesis. Where the lenses (diameter 30 μm) are preserved, the characteristic hexagonal-packing arrangement of the compound eye is apparent (Text-fig. 6A, I). With the deflation of an individual lens through decay, crystal aggregates are evident in the interior. Where the dioptric apparatus is lost, the rhabdom emplacement is exposed (Text-fig. 6B, D, K). In cross section the rhabdoms can be discerned

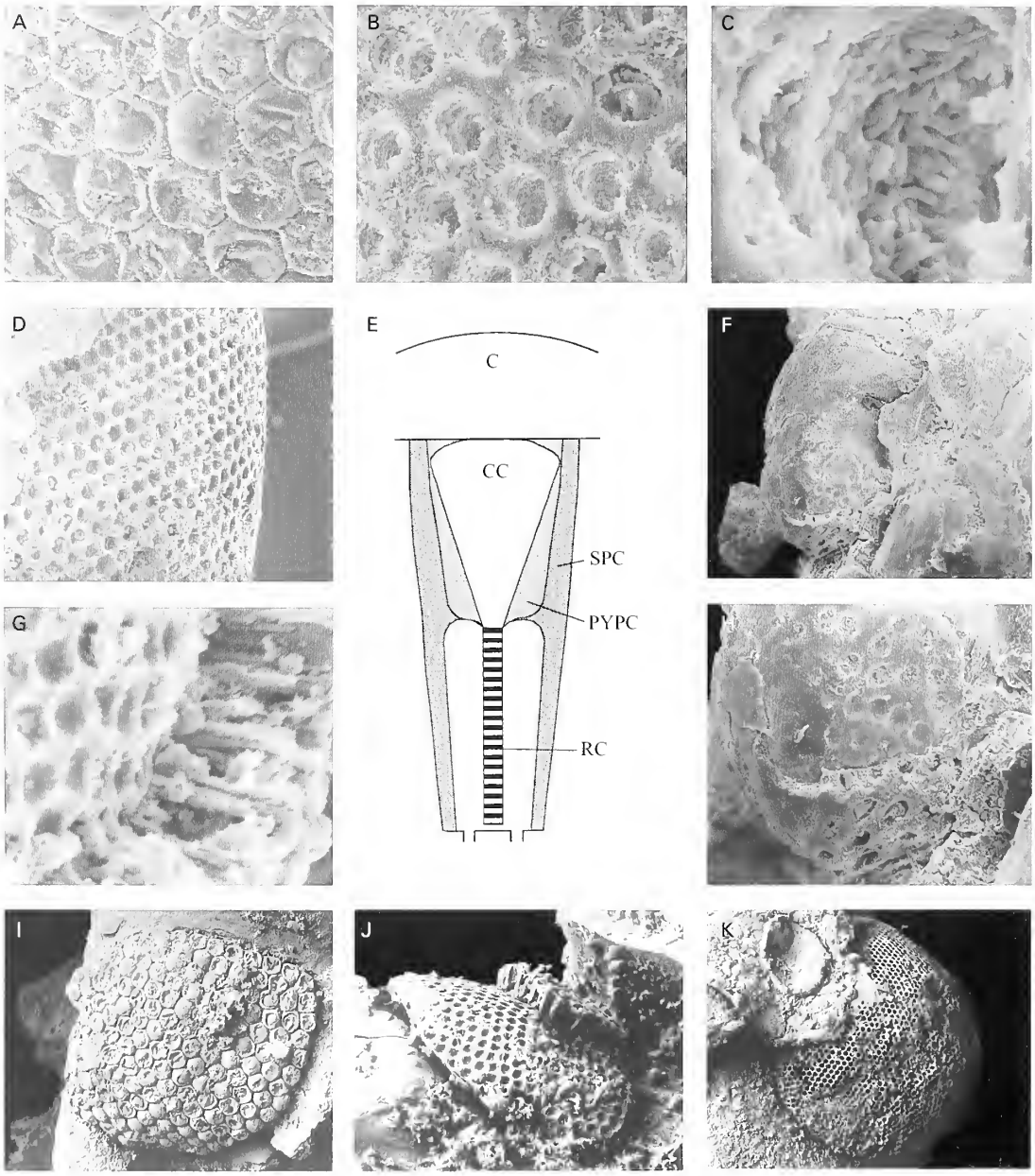

TEXT-FIG. 6. Compound eyes. A, I, coleopteran species A; B–D, K, coleopteran species B; G, J, coleopteran species C; F, H, trichopteran larva. A, lenses displaying characteristic hexagonal packing (QM F16648); ×2500. B, framework of pigment cells revealed by loss of dioptric apparatus (QM F34583); ×7000. C, walls of rhabdomal emplacement lined with bacteria (QM F34583); ×20000. D, framework of the eye (QM F34583); ×1500. E, schematic of ommatidium of apposition eye. Abbreviations: C, corneal lens; CC, crystalline cone; PYPC, primary pigment cells; SPC, secondary pigment cells; RC, retinal cells; R, rhabdom. F, 'schizochroal-type' eye (QM F34584); ×2750. G, cross section through rhabdomal emplacement showing ommatidial cups (QM F34582); ×2000. H, close-up of 'schizochroal-type' eye, showing ommatidial cups (QM F34584); ×2750. I, complete eye (QM F16648); ×720. J, complete eye (QM F34582); ×2500. K, complete eye (QM F34583); ×480.

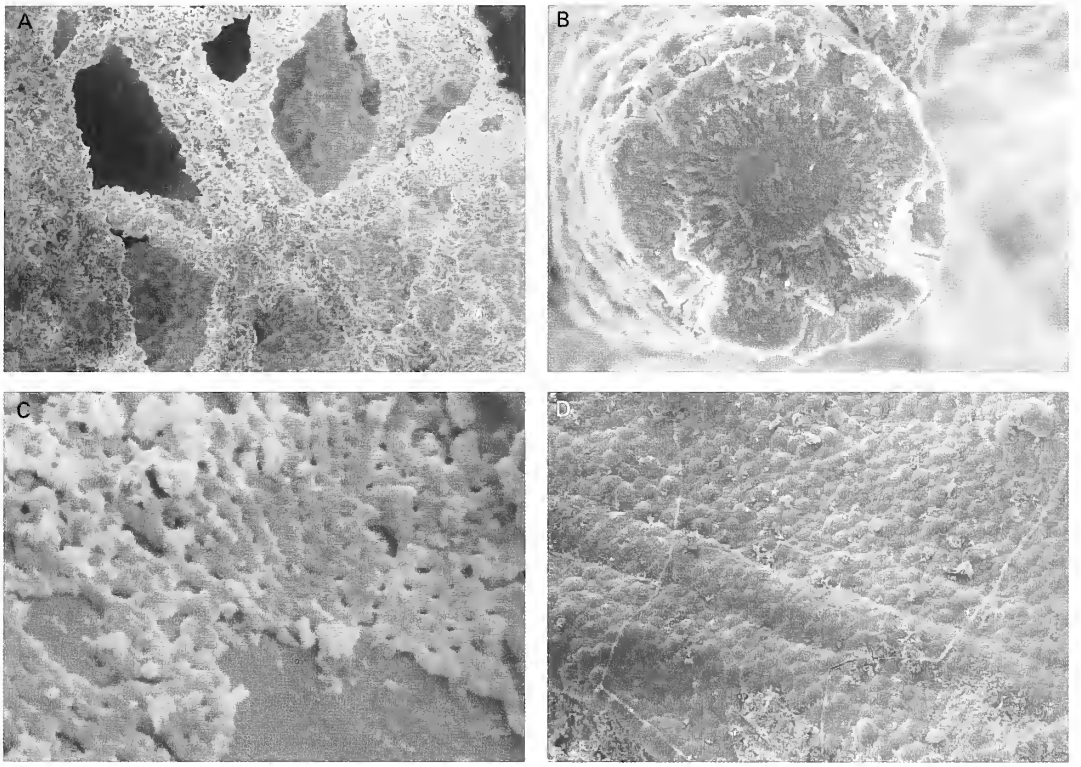

TEXT-FIG. 7. Fossil fungi and bacteria. A, fungal hyphae criss-crossing the interior of head and thorax of larva (QM F34584); × 1750, B, cross section through single fungal strand (QM F34584); × 9000. C, fungal colony covering sternite of larva (QM F34592); × 225000. D, bacterial mat covering surface of coleopteran wing (QM F34595); × 600.

extending radially from the surface of the eye (Text-fig. 6G, J). With the rhabdoms stripped away, the ommatidial cups, the concave receptacles of the ocular apparatus, are evident. The pigment cells that once lined the rhabdom interior of one specimen have been destroyed by bacteria, which are now preserved as rod-like protuberances from the walls (Text-fig. 6C). Bacteria are also preserved enshrouding the hind wings of a beetle (Text-fig. 7D). Mineralized bacteria have been reported from other localities (e.g. Messel; Wuttke 1983).

The trichopteran larva displays an unusual form of compound eye consisting of large, separate circular lenses rather than the more usual closely packed hexagonal type (Text-fig. 6F, H). Where the cornea and dioptric apparatus have been lost, an irregular arrangement of 'cups' is exposed. This 'schizochroal-type' eye occurs in only a small number of living insects (Kinzelbach, 1967; Clarkson 1979; Paulus 1979; see Horváth *et al.* 1997 for a review), where it is thought to maximize light reception. Caterpillars of the Lepidoptera, the sister group of Trichoptera, normally have six isolated biconvex lenses, widely distributed on each side of the head. Coleopteran and megalopteran larvae can have up to six well-separated stemmata on each side of the head, the Neuroptera and Raphidioptera up to seven, and the Strepsiptera five. Larvae of most Mecoptera have dispersed faceted eyes consisting of 30–35 typical ommatidia.

Fungi

A trichopteran larva preserves fungal hyphae in the head capsule and trunk (Text-fig. 7A). Individual strands criss-cross the interior of the insect displaying a simple lateral dichotomous

branching (Text-fig. 7A). In cross section (Text-fig. 7B) an individual strand shows a structureless core (12 μm in diameter) surrounded by a layer displaying a distinct radial pattern (17 μm broad). The outer layer represents a crystalline overgrowth around the original fungal strand, which is presumably represented by the core which has a diameter (12 μm) comparable to that of modern hyphae (10 μm). Extant hyphae consist of an outer wall of hemicellulose or chitin around a cavity, the strands forming a filamentous system (Talbot 1971).

An unusual fungal growth is also noted covering the external surface of a larval segment, where a number of strands appear to radiate from a central point, each joined by short lengths to form a distinctive meshwork (Text-fig. 7C).

Environmental conditions

The exceptional preservation of the Riversleigh insects raises several questions regarding both the rate and mechanism of mineralization. Most models for the preservation of non-mineralized tissues require rapid burial, anoxicity, or both, in order to preclude scavenging (Seilacher *et al.* 1985). The presence of a surface crust and algal mats at the Upper Site at Riversleigh would have inhibited circulation and promoted anoxicity. Only the more recalcitrant tissue (i.e. cuticle, or calcified cuticle in the case of the myriapod) is preserved and this, coupled with the presence of bacteria within the rhabdom emplacements and fungal hyphae in the head capsule of one of the specimens, suggests that decay proceeded for some time prior to mineralization. The fungal strands criss-cross the interior of some specimens indicating that the fungus colonized the carcass *after* the internal tissue was lost through decay.

It is clear that the limited number of arthropod species recovered from this site cannot reflect the total diversity of this rain forest environment. Those taxa (and life stages) that are preserved, and survived the acid digestion, are probably the more readily phosphatized elements of the biota. Their higher preservation potential may reflect the original biochemistry of the cuticle.

Other examples of three-dimensionally preserved insects

Three-dimensional preservation normally relies on sufficiently early mineralization to prevent collapse through decay, and to protect the fossil from overburden-induced compaction. Thus insects preserved as organic remains are rarely three-dimensional, except in conservation traps (*sensu* Seilacher *et al.* 1985) such as amber (Poinar and Hess 1982; Henwood 1992, 1993; Grimaldi *et al.* 1994) and asphalt (Miller 1983; Stock 1992; Stankiewicz *et al.* 1997). The insects of the Oligocene Bembridge Marls, Isle of Wight, England (Jarzembowski 1980) are an exception. Here they are preserved essentially as a void left by the decayed internal tissues, lined with the cuticle, which is represented by a micrometre-thick, highly altered, organic layer.

Most three-dimensionally preserved insects occur in early diagenetic concretions, such as the siderite nodules that are known from a variety of Carboniferous sites (see Bolton 1905; Woodward 1907; Heyler 1980; Baird *et al.* 1985*a*, 1985*b*), notably at Mazon Creek in north-eastern Illinois (Richardson 1956; Johnson and Richardson 1966; Nitecki 1979; Baird *et al.* 1985*a*). These Carboniferous insects rarely preserve ultrastructural details of the cuticle (see Baird *et al.* 1985*a*) in contrast to those preserved in Tertiary concretions. Calcareous nodules from the Miocene of Barstow, California (Palmer 1957) exhibit micrometre-scale replication of the cuticle and internal tissue by a suite of minerals including quartz, apatite, celestite, gypsum and zeolite (Park 1995). The concretions of the Eocene London Clay, England, which are composed of pyrite, apatite or calcite (Britton 1960; Allison 1988), have yielded various beetles (Britton 1960), and a pyritized maggot (Rundle and Cooper 1971) which preserves surface details of the cuticle, but not the internal tissues. Phosphatic concretions from the mid Tertiary Dunsinane Site at Riversleigh, preserve insects (D. A. Arena, pers. comm.).

The Riversleigh insects are exceptional in that phosphatization of the cuticle has led to three-dimensional preservation without the formation of a concretion. Phosphatized insects have also been reported from the Eocene Quercy Phosphorites of France (Handschin 1944), and the Oligocene fissure fillings of Ronheim, Germany (Hellmund and Hellmund 1996), but in both cases crystallization is coarser than at Riversleigh and less detail is preserved. A similar style of preservation in calcite is known from the Miocene volcanic deposits of Rusinga and M'fwangano Islands, Lake Victoria, Kenya (Leakey 1952, 1963) but only the gross morphology of taxa with thickened cuticles, such as millipedes and beetles, is preserved. Calcified millipedes are also known from Holocene cave deposits in the West Indies (Donovan and Veltkamp 1994), but the cuticle is likely to have been biomineralized in life.

SYSTEMATIC PALAEONTOLOGY

The morphological terminology and classification used here is that of *The Insects of Australia* (C.S.I.R.O. 1992). An open nomenclature is employed, as identification to the lowest taxonomic level is impossible due to the incomplete nature of the specimens. The specimens of Coleoptera lack appendages, including wings and elytra. In some cases only the head and thorax have been recovered. Thus identification must be based primarily upon the emplacement of the coxae and features of the head. No complete specimen of the trichopteran larva has been found. Details are often obscured by debris adhering to the ventral surface which cannot be removed without damage to the specimen. The only myriapod specimens are undifferentiated segments.

The specimens are held in the Queensland Museum, Brisbane, to which the abbreviation QM refers.

Phylum ARTHROPODA
Superclass HEXAPODA Latreille, 1825
Class INSECTA Linné, 1758
Subclass PTERYGOTA Brauer, 1885
Division ENDOPTERYGOTA Sharp, 1899
Order COLEOPTERA Linné, 1758
Suborder POLYPHAGA Emery, 1886
Superfamily CURCULIONOIDEA Latreille, 1802
Family CURCULIONIDAE Latreille, 1802?

Coleopteran species A

Text-figures 6A, I, 8A

Material. QM F16648, QM F34585, incomplete adults with only damaged head and prothorax present.

Description

Head. The head is large and produced forward into a rostrum, which is longer than broad. The compound eyes are large, bulging and situated dorsolaterally at the base of the rostrum.

Thorax. The prothorax is broad, half as long as wide, with gently convex lateral margins. The anterolateral corners of the pronotum project to form protective 'shoulders' about the head. The prosternum is bounded laterally by concave sternopleural sutures. The posterior margin of this plate curves round and between the fore coxae. The first pair of coxae are contiguous and meet along the midline. They are globular in shape and incorporate a lateral facing concavity to accommodate the femur.

Dimensions. Maximum length of head and prothorax: 5 mm.

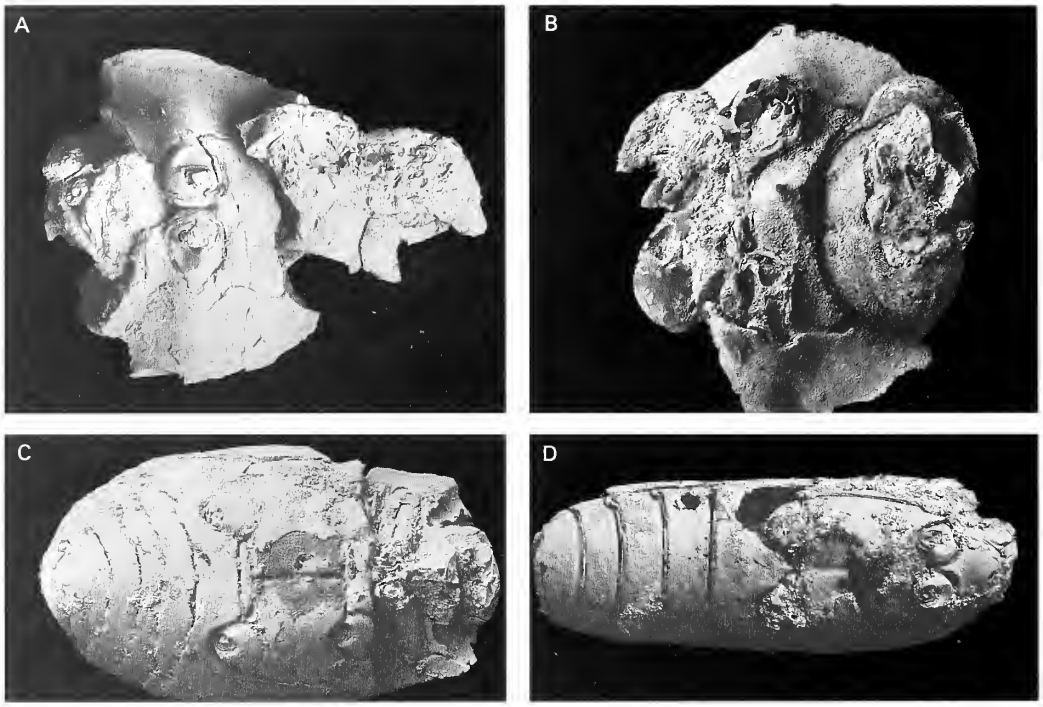

TEXT-FIG. 8. Coleoptera. A, species A, undetermined curculionid (QM F16648); ×100. B, species B, undetermined polyphagan (QM F34583); ×120. C, species C, undetermined histerid (QM F34582); ×120. D, species D, undetermined ommatid (QM F34595); ×60.

Remarks. This species is referred to Curculionidae on the basis of its stout rostrum, large eyes toward the rostral base and contiguous, projecting, fore coxae. The incompleteness of the specimens prevents a more detailed interpretation.

Superfamily and Family indet.

Coleopteran species B

Text-figures 6B–D, K, 8B

Material. QM F34583, an incomplete adult, with only head and prothorax intact; QM F34586, an incomplete adult, consisting only of the pronotum.

Description. The body is highly convex in cross section.

Head. The head is hooded by the pronotum (Text-fig. 8B) and is all but concealed from above. The anterior margin is gently convex. The large, bulbous compound eyes are ventrolateral in position, and approach the anterior margin (Text-fig. 6K). The mouth is hypognathous.

Thorax. In plan view, the prothorax is a longitudinally elongate semicircle. The anterior margin is convex. On the ventral surface the sternopleural suture of the prosternum runs from the lateral margins of the head to the

coxae of the first limbs. These sutures mark the lateral margins of the prosternum, which is bounded anteriorly by the head and posteriorly by the transverse suture of the mesosternal plate. The plate rises to an elevated process between the first pair of limbs. The sternopleural sutures of the mesothorax form a gently curved semicircular outline. The thorax slopes rapidly from the sternopleural sutures to the lateral margin of the prothorax.

Dimensions. Maximum length of head and pronotum: 5 mm.

Remarks. The specimens show a number of characters that support assignment to the Polyphaga: notopleural sutures are absent on the prothorax, the ventral portion of the notum (hypomeron) is joined directly to the sternum on each side along the notosternal suture, and the pleuron is reduced and concealed. Insufficient detail is preserved to allow a more detailed taxonomic assignment.

Superfamily HYDROPHYLOIDEA Latreille, 1802
Family HISTERIDAE Latreille, 1802

Coleopteran species C

Text-figures 4A–B, 6G, J, 8C

Material. QM F34582, an almost complete adult, with only mid and hind legs missing.

Description. The outline of the body is a near perfect oval.

Head. The head is small (less than one-eighth body length) and sub-rectangular in outline, almost half as long as wide. It is sunk deeply into the pronotum and is concealed when viewed from above. The eyes are flattened and occupy the entire lateral margin of the head, approaching the anterior margin (Text-fig. 6J). The mouth is hypognathous.

Thorax. A distinct pronotum, narrower than the meso- and metathorax, hoods the head. When viewed from above it appears rectangular in outline, and extends laterally beyond the head. The outline of the pronotum tapers gently from the posterior to the anterior margin. On the anterior margin of the prosternum is a raised median process which becomes a ridge running the length of the prosternum, decreasing in height as it does so. The first pair of limbs immediately flanks this ridge. The fore coxae, although partially obscured by the encrusted tibia, appear both large and transverse. Fore trochantins appear absent. The pronotum and the mesonotum are united along a transverse suture. The mesosternum is bound laterally by the coxae of the second pair of limbs, which appear to open laterally. Its anterior margin is marked by the boundary between the pronotum and the mesonotum, its posterior by the metasternal transverse anterior suture. The metasternal surface is divided along the midline by the longitudinal suture. Both the fore and hind coxae incorporate a concavity to accommodate the femur.

Abdomen. The abdomen tapers gently posteriorly, forming a rounded pygidium. The elytra are truncate leaving the propygidium and pygidium exposed. There are five ventrites.

Dimensions. Maximum length of beetle: 5 mm.

Remarks. The ovoid body shape, truncate elytra exposing two complete tergites, and head all but concealed by the pronotum, are indicative of superfamilies Hydrophyloidea and Staphylinoidea. A median metasternal suture is unknown in the latter. The separation of the mid-coxae by more than the width of one coxa, and the wider separation of the hind coxae, indicate that the species belongs to the family Histeridae, and not Hydrophilidae.

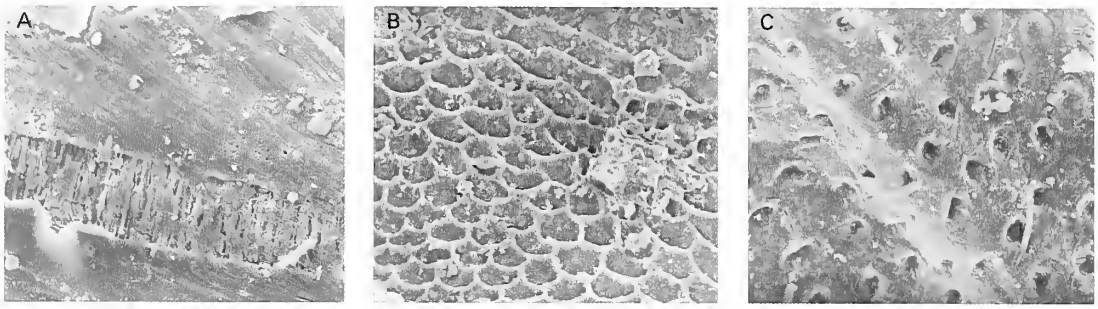

TEXT-FIG. 9. Cuticle and wing of ommatid (coleopteran species D) (QM F34595). A, break in cuticle reveals distinct alignment of microfibrils; ×9000. B, terrace-like pattern of cuticle between wings on ventral surface; ×6000. C, close-up of wing; ×6000.

Suborder ARCHOSTEMATA Kolbe, 1908
Superfamily CUPIDOIDEA Latreille, 1802
Family OMMATIDAE Newman, 1839

Coleopteran species D

Text-figures 7D, 8D, 9A–C

Material. QM F34595, an almost complete adult, missing head and prothorax, with the wings covering much of the dorsal surface of the body (Text-fig. 8D).

Description

Thorax. The lateral margins of the mesothorax are parallel for much of their length, but begin to converge gently towards the anterior. The mesothoracic coxae are contiguous, globular in shape, with a posterior-facing concavity. A median suture divides the metasternum. The meta-coxae are also globular and adjoin the anterior margin of the metasternum, the margin of which curves between and around them. The lateral metasternal sutures diverge gently from the mesothoracic coxae, so that the metasternum increases in width posteriorly. The metathoracic coxae are larger than the mesothoracic but are not contiguous. The cuticle displays distinct lineation (Text-fig. 9A).

The dorsal surface is almost entirely shrouded by the exposed hind wings. They slope from the anterior 'shoulders' toward the midline. The gap separating them decreases in width posteriorly. It extends one-quarter of the length of the thorax, at which point the wings meet. The cuticle within the gap displays a distinct terracing (Text-fig. 9B). At the anterior margin is a small pinnacle, posterior of which is a narrow ridge which runs the length of the gap.

The remains of the wings shrouding the dorsal surface show traces of venation (Text-fig. 9C), but the detail is obscured by a coating of mincralized bacteria (Text-fig. 7D).

Abdomen. The abdomen consists of five segments, and has a distinct blunt appearance, the lateral margins tapering gently to a rounded pygidium. The first ventrite, which is the largest, curves around and between the metathoracic coxae. The other four are smaller, and all are of similar length.

Dimensions. Maximum length of specimen, 7 mm.

Remarks. This species is assigned to the suborder Archostemata on the basis of the metathoracic trochantins. The presence of five ventrites indicates that the species belongs to either Cupedidae or Ommatidae. The lack of grooves on the ventral surface to accommodate the legs precludes assignment to the former, and indicates that this species belongs to the latter.

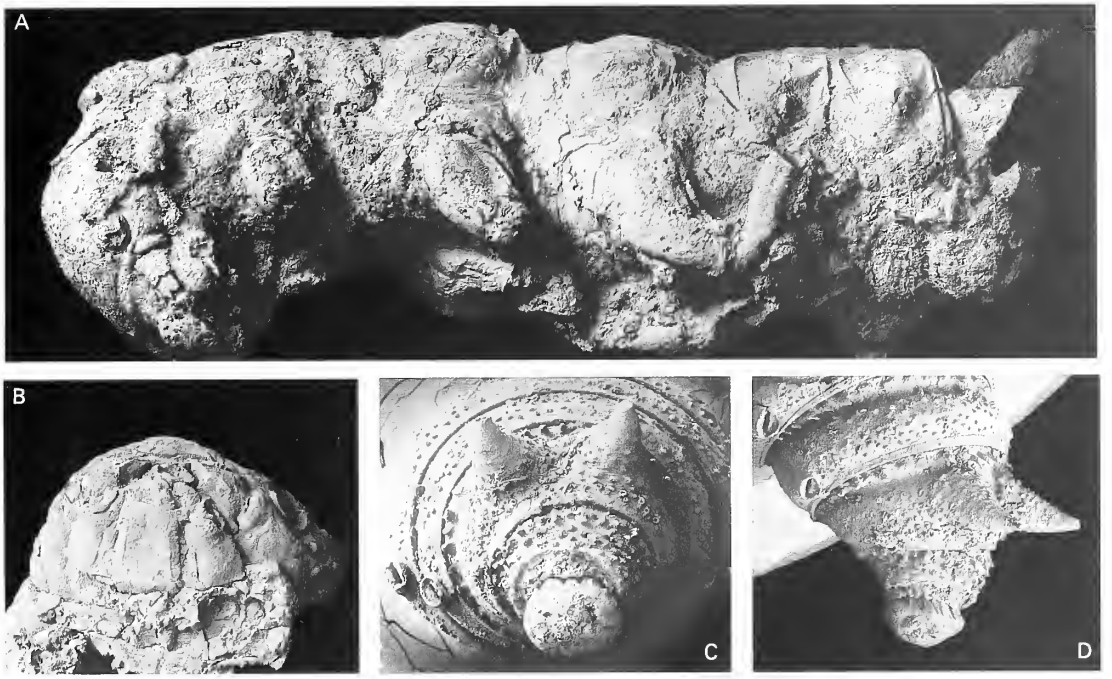

TEXT-FIG. 10. Trichopteran larva. A, composite image of head, thorax and upper abdomen (QM F34587); × 80. B, ventral view of head (QM F34593); × 100. C–D, tail assemblage (QM F34594); × 140.

Order TRICHOPTERA Kirkby, 1815

Superfamily and Family indet.

Text-figures 2A–D, 3A–F, 5A–B, 6F, H, 10A–D

Material. QM F34584, QM F34587–QM F34594, all of which are incomplete larval stages.

Description. In cross section the dorsal surface is strongly curved, whilst the ventral surface is flattened.

Head. The head is globular in shape with a slightly flattened anterior margin, and is broader than long. It is marked by two large ventrolateral antennal sockets, which protrude downwards. The scape of the antenna is large, and circular in cross section. The lateral epicranial sutures arise at the posterior margins of the head, pass around the sockets of the antennae on the lateral side and converge to form the median suture. The general outline of the suture is that of an inverted 'Y'. The epicranium is patterned by a random arrangement of setae emplacements. Five ocelli form a semicircle about a central ocellus towards the anterior margin of the head. The clypeal region, which is divided into two equal segments, is slightly produced and evenly convex over the entire margin. The sutura frontoclypealis is dorsally convex. The labrum is short and gently tapered. The mandibles are curved and opposable with a double saw-toothed edge. The ventral surface of the cranium is covered by a bilaterally symmetrical labium. Flanking this is a pair of gently convex maxillae (Text-fig. 10B). Anterior to this, also flanking the labium, is a small, flattened eye of 'schizochroal'-type (Text-fig. 6F, H).

Thorax. The thorax consists of three segments, with the pronotum being the largest (Text-fig. 10A). All are much wider than long, with the cuticle of the dorsal surface more heavily sclerotized than that of the ventral surface and the abdomen. There is a distinct ridge around the periphery of the pronotum. There are three distinct units to each tergite. The anterior prescutum (Text-fig. 3A) is relatively narrow but increases in thickness dorsally, forming a 'saddle-like' feature and patterned by an irregular arrangement of pits (Text-fig. 3B). The scutum, the largest of the three units, is patterned by a random arrangement of raised setae emplacements. The posterior scutellum is wider than the prescutum, although similarly patterned (Text-fig. 3C). The scutellum of each segment overlies the prescutum of that behind. The individual tergites are

separated by intersegmental membranes. A large spiracle is present on the lateral surface of the pronotum. There is a slight bulging of each segment laterally, just above the first pair of limbs. The limbs themselves are robust and decrease in size posteriorly. The base of each is protected by a coxal collar (Text-fig. 3D). The adjacent arthrodial membrane is distinctly patterned (Text-fig. 3E–F).

Abdomen. The abdomen bears at least nine tergites, although no complete specimen exists. There is a slight swelling of the abdomen about the fifth-last tergite and it tapers gently posterior to this. The scutellum of each tergite overlaps the prescutum of the following one, as with the thorax. The last few tergites have a distinctive appearance, the penultimate segment bearing two posteriorly projecting conical 'horns', or terminal prolegs, which are fused to the dorsal surface (Text-fig. 10C–D). The final tergite terminates in a hemispherical 'bulb' (although this may be an extrusion of internal tissue, since this 'bulb' is absent from a second specimen). A tube-like spiracle projects posteriorly from the ventral surface of each abdominal somite, although poor preservation prevents confirmation that such a spiracle is present on segment 1. The cuticle of the abdomen, including that of the tergite with the 'horns', is ornamented in a similar fashion to the thorax. The only difference is the presence of small 'fang-like', posteriorly projecting barbs on the prozonite, which decrease in size towards the ventral surface, where they are absent. On the ventral surface are small, longitudinally aligned setae. However, their arrangement is obscured by encrusting material.

Dimensions. Almost complete specimens suggest an overall length of 50–70 mm.

Remarks. The orders Trichoptera and Lepidoptera are united in the informal rank Amphiesmenoptera. Accordingly, the larvae possess many similarities. However, the presence of a pair of projecting conical 'horns', or terminal abdominal prolegs, allows the Riversleigh species to be assigned with some confidence to the order Trichoptera. More detailed taxonomic assignment would require information on the position of setae or spicules on the abdomen.

Class MYRIAPODA Latreille, 1796
Order JULIDA Brandt, 1833
Family indet.

Material. QM F34596 (two specimens), mid sections of the trunk composed of four and five segments respectively.

Description. The trunk consists of a number of leg-bearing rings. The sclerites of each ring are fused together and to the pleurotergal arch to form a completely cylindrical sclerite (Monozonian condition). The prozonite of one ring is overlapped by the metazonite of that preceding it. The two zonites are separated by a distinct suture. Each ring carries two pairs of limbs and constitutes a diplosegment. The coxal openings are small and project laterally. The limbs are slender.

Dimensions. Length of single ring 3 mm, diameter 4 mm.

Remarks. The presence of only disarticulated segments precludes assignment beyond the level of suborder.

Acknowledgements. The research at Riversleigh was supported by the Australian Research Grants Scheme (Archer); the National Estate Grants Scheme, Queensland (Archer); the University of New South Wales; the Commonwealth Department of Environment, Sports and Territories; the Queensland National Parks and Wildlife Service; the Commonwealth World Heritage Unit; ICI Australia Pty Ltd; the Australian Geographic Society; the Queensland Museum; the Australian Museum; the Royal Zoological Society of N.S.W.; the Linnean Society of N.S.W.; Century Zinc Pty Ltd; Mount Isa Mines Pty Ltd; Surrey Beatty and Sons Pty Ltd; the Riversleigh Society Inc.; and private supporters including E. Clark, M. Beavis, M. Dickson, S. and J. Laverack and S. and D. Scott-Orr. We thank P. A. Jell for access to the Riversleigh arthropods and D. A. Arena for supplying a preprint of a paper on the Dunsinane Site and for stratigraphical and other information. Skilled preparation of the specimens was carried out by A. Gillespie. Useful discussion was

provided by E. N. K. Clarkson, P. R. Wilby and A. C. Neville. E. A. Jarzembowski and P. Hammond reviewed an earlier draft. Additional SEM assistance was provided by Chris Jones of The Natural History Museum (London). IJD is a NERC research student.

REFERENCES

ALLISON, P. A. 1988. Taphonomy of the Eocene London Clay biota. *Palaeontology*, **31**, 1079–1110.

ARCHER, M. and BARTHOLOMAI, A. 1978. Tertiary mammals of Australia: a synoptic review. *Alcheringa*, **2**, 1–19.

—— and CLAYTON, G. (eds). 1984. *Vertebrate zoogeography and evolution in Australasia*. Hesperian Press, Perth, 136 pp.

—— GODHELP, H., HAND, S. J. and MEGERIAN, D. 1989. Fossil mammals of Riversleigh, northwestern Queensland: preliminary overview of biostratigraphy, correlation and environmental change. *Australian Zoologist*, **25**, 29–65.

—— HAND, S. J. and GODHELP, H. 1994*a*. *Riversleigh, the story of animals in ancient rainforests of inland Australia*. Second edition. Reed Books, Chatswood, NSW, 264 pp.

—— —— —— 1994*b*. Patterns in the history of Australia's mammals and inferences about palaeohabitats. 80–103. *In* HILL, R. (ed.). *History of the Australian vegetation: Cretaceous to Recent*. Cambridge University Press, Cambridge, 340 pp.

—— —— —— 1995. Tertiary environmental and biotic change in Australia. 77–90. *In* VRBA, E. S., DENTON, G. H., PARTRIDGE, T. C. and BURCKLE, L. H. (eds). *Paleoclimate and evolution, with emphasis on human origins*. Yale University Press, New Haven, 265 pp.

BAIRD, G. C., SROKA, S. C., SHABICA, C. W. and BEARD, T. L. 1985*a*. Mazon Creek-type fossil assemblages in the U.S. midcontinent Pennsylvanian: their recurrent character and paleoenvironmental significance. *Philosophical Transactions of the Royal Society, Series B*, **311**, 87–99.

—— SHABICA, C. W., ANDERSON, J. L. and RICHARDSON, E. S. Jr 1985*b*. The biota of a Pennsylvanian muddy coast: habitats within the Mazonian Delta Complex, northeastern Illinois. *Journal of Paleontology*, **59**, 253–281.

BOLTON, H. 1905. Notes on the geological horizon and palaeontology of the 'Soapstone Bed' in the Lower Coal Measures, near Colne, Lancashire. *Geological Magazine*, (5), **2**, 433–444.

BOULIGAND, Y. 1965. Sur une architecture torsadée répandue dans de nombreuses cuticules d'arthropodes. *Compte rendu hebdomadaire des séances de l'Académie des Sciences, Paris*, **261**, 3665–3668.

BRANDT, X. 1833. Ueber die inder Regentschaft Algier beobachteten Myriopoden. *In* WAGNER, M. (ed.). *Alger III*. Leopold Voss, Leipzig, 135 pp.

BRAUER, F. 1885. Systematische-zoologische Studien. *Sitzungsberichte der (K.) Akademie der Wissenschaften in Wien, mathematische-naturwissenschaftlichen Klasse*, **91**, 237–431.

BRIGGS, D. E. G. and KEAR, A. J. 1994. Decay and mineralization of shrimps. *Palaios*, **9**, 431–456.

BRITTON, E. B. 1960. Beetles from the London Clay (Eocene) of Bognor Regis, Sussex. *Bulletin of the British Museum, Natural History (Geology)*, **4**, 27–50.

CLARKSON, E. N. K. 1979. The visual system of trilobites. *Palaeontology*, **22**, 1–22.

COMMONWEALTH SCIENTIFIC AND INDUSTRIAL RESEARCH ORGANIZATION (C.S.I.R.O) 1992. *The insects of Australia*. Melbourne University Press, Melbourne, 1029 pp.

DONOVAN, S. K. and VELTKAMP, C. J. 1994. Unusual preservation of late Quaternary millipedes from Jamaica. *Lethaia*, **27**, 355–362.

DUNCAN, I. J. and BRIGGS, D. E. G. 1996. Three-dimensionally preserved insects from the Tertiary of Riversleigh, Australia. *Nature*, **381**, 30–31.

EMERY, C. 1886. Ueber Phylogenie und Systematik der Insekten. *Biologisches Zentralblatt*, **5**, 648–656.

GRIMALDI, D. A., BONWICH, E., DELANNOY, M. and DOBERSTEIN, S. 1994. Electron microscope studies of mummified tissues in amber fossils. *American Museum Novitates*, **3097**, 1–31.

HANDSCHIN, E. 1944. Insekten aus den Phosphoriten des Quercy. *Schweizer Paläontologische Abhandlungen*, **64**, 1–23.

HELLMUND, M. and HELLMUND, W. 1996. Phosphoritisierte Insekten- und Annelidenreste aus der mitteloligozänen Karstpaltenfüllung 'Ronheim 1' bei Harburg (Bayern, Süddeutschland). *Stuttgarter Beiträge zur Naturkunde, Series B*, **241**, 1–21.

HENWOOD, A. 1992. Exceptional preservation of dipteran flight muscle and the taphonomy of insects in amber. *Palaios*, **7**, 203–212.

—— 1993 Recent plant resins and the taphonomy of organisms in amber: a review. *Modern Geology*, **19**, 35–59.

HEYLER, D. 1980. Fossiles du Stephanian de Montceau-les-Mines (France). *Bulletin du Société Histoire Naturelle, Autun*, **94**, 3–6.

HORVÁTH, G. and CLARKSON, E. N. K. 1993. Computational reconstruction of the probable change of form of the corneal lens and the maturation of optics in the post-ecdysial development of the Devonian Trilobite *Phacops rana milleri* Stewart 1927. *Journal of Theoretical Biology*, **160**, 343–373.

—— —— and PIX, W. 1997. Survey of modern counterparts of schizochroal trilobite eyes: structural and functional similarities and differences. *Historical Biology*, **12**, 229–264.

JARZEMBOWSKI, E. A. 1980. Fossil insects from the Bembridge Marls, Palaeogene of the Isle of Wight, southern England. *Bulletin of the British Museum, Natural History (Geology)*, **33**(4), 237–293.

JELL, P. A. and DUNCAN, P. M. 1986. Invertebrates, mainly insects, from the freshwater, Lower Cretaceous, Koonwarra Fossil Bed (Korumburra Gp), South Gippsland, Victoria. *Memoir of the Association of Australasian Palaeontologists*, **3**, 111–205.

JOHNSON, R. G. and RICHARDSON, E. S., Jr 1966. A remarkable Pennsylvanian fauna from the Mazon Creek area, Illinois. *Journal of Geology*, **74**, 626–631.

KINZELBACH, R. 1967. Zur Kopfmorphologie der Fächerflügler (Strepsiptera, Insecta). *Zoologische Jahrbücher Anatomie*, **84**, 559–684.

KIRKBY, W. 1815. *An introduction to entomology*. Longman, London, 512 pp.

KOLBE, H. J. 1908. Mein System der Coleopteran. *Zeitschrift für wissenschaftliche Insektbiologie*, **4**, 116–123.

LATREILLE, P. A. 1802. *Histoire naturelle, générale et particulière, des crustacés et des insectes*. 3. Dufart, Paris, 467 pp.

—— 1825. *Familles naturelles du régne animal, exposées succinctement et dans un ordre analytique, avec l'indication de leurs genre*. Dufart, Paris, 570 pp.

LEAKEY, L. S. B. 1952. Lower Miocene invertebrates from Kenya. *Nature*, **169**, 1020–1021.

—— 1963. Adventures in the search for man. *National Geographic*, **123**(1), 132–152.

LINNÉ, C. von 1758. *Systema Naturae Regna Tria Naturae: secundum classes, ordines, genera, species, cum characteribus differentiis synonymis, locis*. 10th edition, revised. Laurentius Salvius, Holmiae, 824 pp.

MARTILL, D. M. 1988. Preservation of fish in the Cretaceous of Brazil. *Palaeontology*, **31**, 1–18.

MEGERIAN, D. 1992. Interpretation of the Miocene Carl Creek Limestone, northwestern Queensland. *The Beagle*, **9**, 219–248.

MILLER, S. E. 1983. Late Quaternary insects of Rancho La Brea and McKittrick, California. *Quaternary Research*, **20**, 90–104.

MILLS, J. S., WHITE, R. and GOUGH, L. J. 1984. The chemical composition of Baltic amber. *Chemical Geology*, **47**, 15–39.

NEVILLE, A. C. 1970. Cuticle ultrastructure in relation to the whole insect. 17–39. *In* NEVILLE, A. C. (ed.). *Insect ultrastructure*. Symposium of the Royal Entomological Society of London, 5.

—— THOMAS, M. G. and ZELAZNY, B. 1969. Pore canal shape related to molecular architecture of arthropod cuticle. *Tissue and Cell*, **1**, 183–200.

NITECKI, M. H. (ed.) 1979. *Mazon Creek fossils*. Academic Press Inc., New York, 581 pp.

PALMER, A. R. 1957. Miocene arthropods from the Mojave desert, California. *Professional Papers of the U.S. Geological Survey*, **294**, 237–80.

PARK, L. E. 1995. Geochemical and paleoenvironmental analysis of lacustrine arthropod-bearing concretions of the Barstow Formation, southern California. *Palaios*, **10**, 44–57.

PAULUS, H. F. 1979. Eye structure and the monophyly of the Arthropoda. 299–383. *In* GUPTA, A. P. (ed.). *Arthropod phylogeny*. Van Nostrand Reinhold, New York, 330 pp.

POINAR, G. O. Jr 1992. *Life in amber*. Stanford University Press, Stanford, California, 349 pp.

—— and HESS, R. 1982. Ultrastruture of 40-million-year-old insect tissue. *Science*, **215**, 1241–1242.

RICHARDSON, E. S. Jr 1956. Pennsylvanian invertebrates of the Mazon Creek area, Illinois. *Fieldiana Geology*, **12**, 1–76.

RIEK, E. F. 1954. A re-examination of the Upper Tertiary mayflies described by Etheridge and Olliff from the Vegetable Creek tin-field. *Records of the Australian Museum*, **23**, 159–160.

—— 1967. Further evidence of Panorpidae in the Australian Tertiary (Insecta: Mecoptera). *Journal of the Australian Entomological Society*, **6**, 71–72.

—— 1970*a*. Fossil history. 168–187. *In* C.S.I.R.O. Division of Entomology. *The Insects of Australia*. 3rd edition. Melbourne University Press, Carlton, Victoria.

—— 1970*b*. Origin of the Australian insect fauna. *Second Gondwana Symposium – 1970*, 593–598.

RUNDLE, A. J. and COOPER, J. 1971. Occurrence of a fossil insect larva from the London Clay of Herne Bay, Kent. *Proceedings of the Geologists' Association*, **82**, 293–295.

SEILACHER, A., REIF, W.-E. and WESTPHAL, F. 1985. Sedimentological, ecological and temporal patterns of fossil Lagerstätten. *Philosophical Transactions of the Royal Society of London, Series B*, **311**, 5–23.

SHARP, D. 1899. Some points in the classification of the Insecta Hexapoda. *In Proceedings of the fourth International Congress of Zoology, Cambridge, England*, 246–249.

SNODGRASS, R. E. 1935. *Principles of insect morphology*. McGraw Hill, New York, 667 pp.

STANKIEWICZ, B. A., BRIGGS, D. E. G., EVERSHED, P. R. and DUNCAN, I. J. 1997. Chemical preservation of the insect cuticles from the asphalt deposits of California. *Geochimica et Cosmochimica Acta*, **61**, 2247–2252.

STOCK, C. H. 1992. *Rancho La Brea. A record of Pleistocene life in California*. Natural History Museum of Los Angeles County, Science Series, 37. 79 pp.

TALBOT, P. H. B. 1971. *Principles of fungal taxonomy*. Macmillan, London, 274 pp.

TEDFORD, R. H. 1967. Fossil mammal remains from the Tertiary Carl Creek Limestone, northwestern Queensland. *Bulletin of the Bureau of Mineral Resources, Australia*, **92**, 217–36.

WOODLAND, B. A. and STENSTROM, R. C. 1979. The occurrence and origin of siderite concretions in the Francis Creek Shale (Pennsylvanian) of northeastern Illinois. 69–104. *In* NITECKI, M. H. (ed.). *Mazon Creek fossils*. Academic Press Inc., New York, 581 pp.

WOODWARD, H. 1907. Further notes on the Arthropoda of the British Coal Measures. *Geological Magazine*, (5), **4**, 539–549.

WUTTKE, M. 1983. 'Weichteil-Erhaltung' durch lithizierte Mikroorganismen bei mitteleozänen Vertebraten aus den Ölschiefern der 'Grube-Messel' bei Darmstadt. *Senckenbergiana Lethaea*, **64**, 509–527.

IAN J. DUNCAN

DEREK E. G. BRIGGS

Department of Earth Sciences
University of Bristol
Wills Memorial Building
Queen's Road
Bristol BS8 1HQ, UK
e-mail ian.j.duncan@bristol.ac.uk
D.E.G.Briggs@bristol.ac.uk

MICHAEL ARCHER

Vertebrate Palaeontological Research
Laboratory
School of Biological Sciences
University of New South Wales
Sydney 2052, Australia

Typescript received 24 February 1997
Revised typescript received 23 June 1997

EFFACED STYGINID TRILOBITES FROM THE SILURIAN OF NEW SOUTH WALES

by D. J. HOLLOWAY *and* P. D. LANE

ABSTRACT. Eight species of illaenimorph trilobites belonging to five genera of the Styginidae are described from limestones of the mid–late Wenlock to Ludlow Mirrabooka Formation and its stratigraphical equivalents in the Orange district, New South Wales. The morphology of illaenimorph (= effaced) styginids is discussed; the term 'omphalus' is introduced for the socketed, tubercle-like projection present in some genera on the interior of the cranidium at or in front of the anterior end of the axial furrow. Amongst other characters, the gross convexity of the exoskeleton, the form of the rostral plate, the presence of the omphalus, the form of the thorax, and possibly the form of the hypostome are deemed most useful for generic diagnosis; characters used for discrimination at a lower taxonomic level include the proportions of the exoskeleton, the degree of effacement, the pattern of cranidial muscle scars, the size and position of the eye, and the character and disposition of sculpture. New taxa are *Excetra iotops* gen. et sp. nov., *Lalax olibros* gen. et sp. nov., *L. lens* gen. et sp. nov., *Rhaxeros synaimon* sp. nov. and *R. trogodes* sp. nov. *Bumastus* (*Bumastella*) Kobayashi and Hamada is raised to generic status and its diagnosis emended; specimens from New South Wales are assigned to the type species *B. spicula*, which is considered to be synonymous with five other Japanese species assigned to three different genera by Kobayashi and Hamada. *Bumastus* is tentatively recorded on the basis of a single rostral plate; the genus is otherwise known with certainty only from Laurentia and eastern Avalonia. Meraspid transitory pygidia of *Bumastella* and *Lalax* from New South Wales are up to eight times larger than those of other styginids with well documented ontogenies; transitory pygidia of large size are known also in some other Silurian effaced styginids, and it is suggested that the phenomenon may result from neoteny. The assumption that sexual maturity in trilobites coincided with the meraspid–holaspid transition is refuted. The effaced styginids from New South Wales show strong faunal affinity with those from the Upper Wenlock or Lower Ludlow of Japan.

TRILOBITES are abundant in Silurian limestones west of the city of Orange in central western New South Wales. Few of the species have been described, although they constitute the most diverse and best preserved Silurian trilobite faunas known from Australia. Although at least nine major groups of invertebrates are present in the limestones, the largely disarticulated elements of trilobite exoskeletons are predominant, and most of them are effaced (illaenimorph) forms belonging to the Styginidae. Faunas of this type also occur in lithologically similar relatively pure limestones of Silurian age elsewhere in the world, and were named the 'Styginid-Cheirurid-Harpetid Assemblage' by Thomas and Lane (1998, p. 447, figure 36.1–36.2), who described the lithology in which it occurs, and its stratigraphical and geographical distribution. The reasons for the dominance of effaced trilobite elements in such assemblages are not known; large and small elements of trilobites occur together, and with large and small specimens of other invertebrate groups (ostracodes and brachiopods, respectively with dimensions as little as 2 mm and up to 50 mm), so that hydrodynamic sorting seems not always to be a factor. In some cases it might have been; some 'nested' occurrences of effaced cranidia and/or pygidia were noted, for example of *Rhaxeros trogodes* from locality PL1996. The effect upon the aspect of the association as preserved of discarded exuviae cannot be assessed; however, the commonness of this type of association in rocks ranging from Ordovician to Permian indicates that effaced trilobites might have been the dominant forms in life.

In the present paper, the effaced styginids from only the mid to late Wenlock and Ludlow limestones of the Orange district sequences are described.

[Palaeontology, Vol. 41, Part 5, 1998, pp. 853–896, 8 pls]

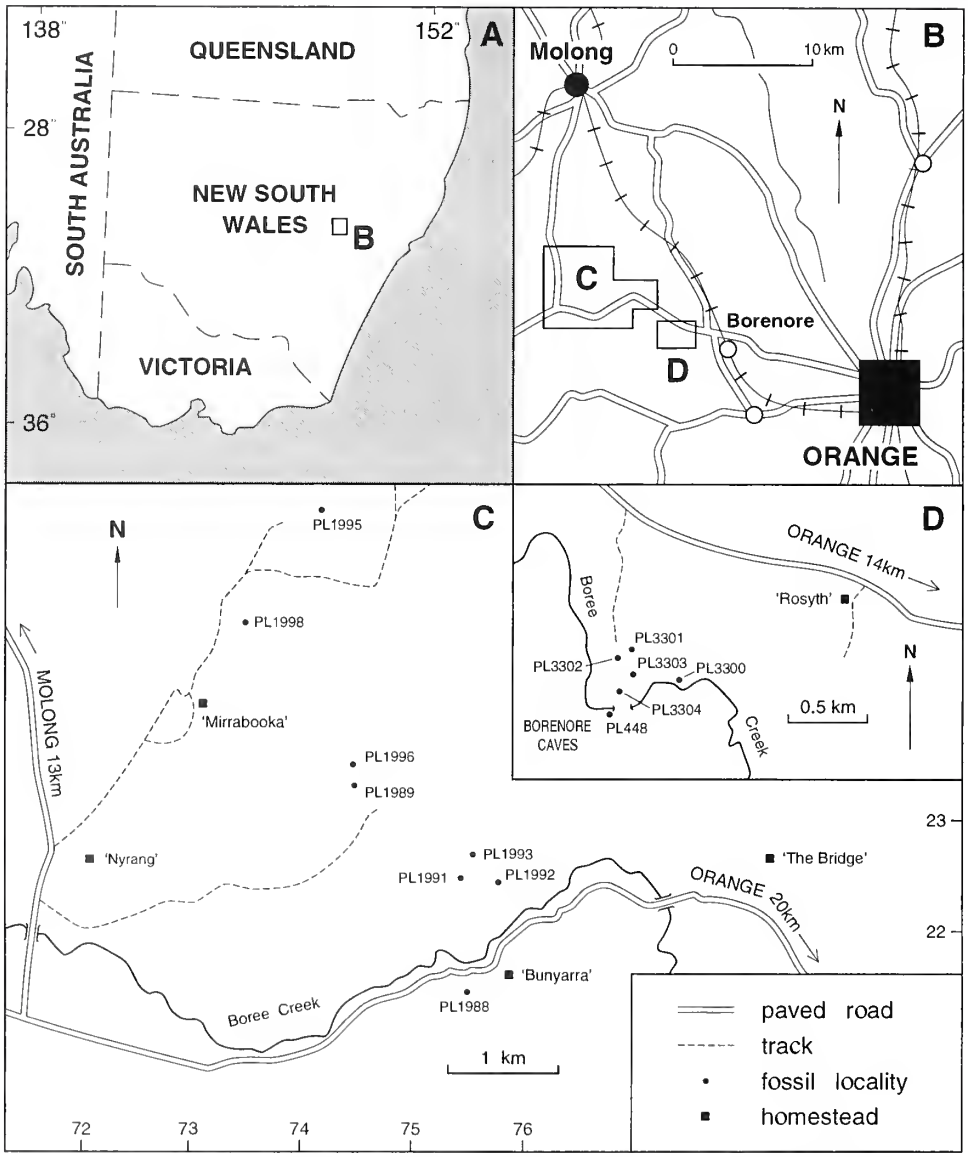

TEXT-FIG. 1. A, South-eastern Australia; approximate area of Text-figure 1B indicated by square. B, general area from which the trilobites were collected. C–D, location of fossiliferous localities.

STRATIGRAPHY

The Silurian sequence in the area between Borenore and Molong, 20–30 km west-north-west of Orange (Text-fig. 1), is characterized by marked and complex changes in lithofacies which, together with the geographically restricted nature of previous geological mapping, has led to the recognition of a variety of stratigraphical units in different parts of the area (Text-fig. 2).

In the western part of the area, near 'Mirrabooka' homestead, the lowermost Silurian unit is the Boree Creek Formation (Sherwin 1971*a*, p. 210), an impure limestone up to 60 m thick (Sherwin and Pickett, *in* Pickett 1982, p. 141) which unconformably overlies late Ordovician andesitic

volcanics. The Boree Creek Formation was divided by Sherwin (1971*a*) into lower and upper limestone units, informally named Limestones A and B respectively, separated by a calcareous tuffaceous sandstone referred to as the 'tuffaceous trilobite bed'. A possible disconformity between Limestone A and the 'tuffaceous trilobite bed' was considered by Sherwin and Pickett (*in* Pickett 1982, p. 140) to be probably of only very local significance, and not to represent a significant break. These authors also expressed doubts about the lateral extent of the lithological subdivisions of the Boree Creek Formation; observations by DJH suggest that the subdivisions can be recognized only locally, that the lithology of the 'tuffaceous trilobite bed' is only the result of decalcification of the limestone, and that trilobites are not restricted to the middle part of the formation. Conodonts from the Boree Creek Formation were correlated by Bischoff (1986, p. 36; text-fig. 8) with the latest Llandovery to early Wenlock *amorphognathoides* and *ranuliformis* biozones.

Disconformably overlying the Boree Creek Formation is the Mirrabooka Formation. This consists of 500 m of predominantly fine sandstones and siltstones but also includes several lenticular limestone bodies that were referred to by Sherwin (1971*a*) as Limestones C, H and I. The following graptolite species from near the base of the Mirrabooka Formation were recorded by Pickett (1982, p. 147): *Pristiograptus meneghini*, *Monoclimacis* cf. *flemingi*, *M.* cf. *flumendosae*, *Dendrograptus* sp. and *Dictyonema* sp. – which are considered to represent a mid to late (but not latest) Wenlock age. The age indicated by an assemblage (*Bohemograptus bohemicus*, *Lobograptus* '*scanicus*', *Linograptus posthumus* and *Dictyonema* sp.) from about the horizon of Limestone I (Text-fig. 2), in the upper part of the formation is equivocal; correlation with the Ludlow *scanicus* and *leintwardinensis* biozones was suggested (Pickett 1982, p. 147), but Dr D. Loydell (pers. comm.) suggests that although the Ludlow is indicated, the named species are not all known to occur stratigraphically together elsewhere, and re-examination of the fauna should be undertaken.

Overlying the Mirrabooka Formation with apparent conformity are up to 400 m of shales and siltstones that are commonly olive green or red; they were assigned by Sherwin (1971*a*, p. 219) to the Wallace Shale, the type locality of which lies some 25 km to the south. In the 'Mirrabooka' area the formation also contains pods of limestone up to 250 m long, and a boulder bed and exotic blocks of Ordovician sediments and volcanics. The graptolites *Monograptus* cf. *ultimus* and *M. bouceki*, indicative of the Upper Ludlow, occur in the lower part of the formation (Byrnes, *in* Pickett 1982, p. 154), and the upper part is considered to extend into the Devonian.

In the eastern part of the area, just west of Borenore, the Rosyth Limestone (Walker 1959, p. 42) is equivalent to at least part of the Boree Creek Formation. Problems with the definition of the Rosyth Limestone were discussed by Pickett (1982, p. 161), who restricted the name to the lowermost part of the sequence, which consists of richly fossiliferous limestones and calcareous shales with a thickness of 50 m to more than 100 m. Overlying these strata, apparently disconformably, are 100 m of unnamed lithic arenites, shales and bedded limestones. These are in turn overlain disconformably by the 600 m thick massive white, grey and red limestones of the Borenore Limestone, which is equivalent to the Mirrabooka Formation and probably the lowermost Wallace Shale. Bischoff (1986, p. 38; text-fig. 8) reported conodonts of the early Wenlock *ranuliformis* Biozone in the lower part of the Borenore Limestone; it is possible, however, that the specimens did not come from this formation but from the underlying unnamed limestone unit mentioned above.

To the north of 'Mirrabooka', towards Molong, the Mirrabooka Formation grades into the Molong Limestone (Adrian 1971, p. 193), which directly overlies late Ordovician andesitic volcanics with unconformity, and is unconformably overlain by Late Devonian sandstones. Several discrete limestone bodies occurring to the south of the main outcrop area of the Molong Limestone in the vicinity of 'Mirrabooka' homestead were referred to by Sherwin (1971*a*) as Limestones D–G and J; these were considered by Sherwin (1971*a*, p. 212) to be southern extremities of the Molong Limestone, but Pickett (1982, p. 147) assigned them to the Mirrabooka Formation. The stratigraphical range of the Molong Limestone is uncertain, but the upper part is believed to be equivalent to part of the Wallace Shale and the lower part may contain equivalents of the Rosyth Limestone (Pickett 1982, p. 148).

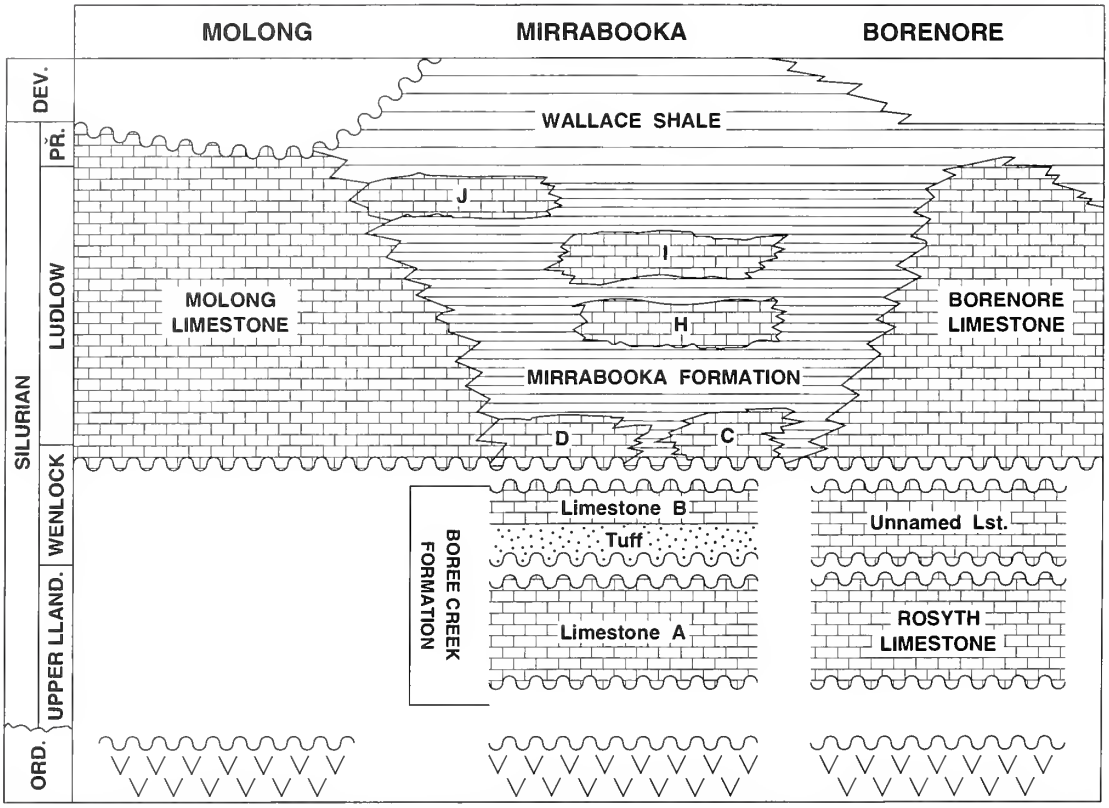

TEXT-FIG. 2. General stratigraphy of the collection area; modified from Pickett (1982, fig. 18). Abbreviations: Lst. = limestone; Tuff. = tuffaceous trilobite bed of Sherwin (1971*a*); LLAND. = Llandovery; PŘ = Přídolí.

TRILOBITE FAUNAS

The earliest record of trilobites from the area was by de Koninck (1876) who identified *Illaenus wahlenbergi* Barrande?, *Bronteus partschi* Barrande and *Harpes ungula* Sternberg from Borenore Caves, in strata now assigned to the Borenore Limestone. Etheridge (1909) assigned specimens from a similar horizon in the same area to his earlier established species *Illaenus johnstoni*. Etheridge and Mitchell (1917) described the new species *Bronteus angusticaudatus* from the Borenore Limestone south of Borenore Caves, and also *B. mesembrinus* and *B. molongensis* from 'limestone-beds adjacent to Molong', a locality that could refer either to the Molong Limestone or to the Early Devonian Garra Formation. Other trilobites to have been recorded from the Borenore Limestone are *Calymene*, *Encrinurus* and *Sphaerexochus* (Süssmilch 1907; Campbell *et al.* 1974); Dun (1907, p. 265, pl. 40, fig. 7) also identified *Phacops*, but the specimen illustrated is an encrinurid pygidium.

From the Silurian sequence below the Borenore Limestone just to the east of Borenore Caves, Fletcher (1950) described the new species *Dicranogmus bartonensis* (= *Trochurus bartonensis*; see Thomas and Holloway 1988, p. 221), *Encrinurus borenorensis* (= *Batocara borenorense*; see Edgecombe and Ramsköld 1992, p. 259, and Holloway 1994, p. 255) and *Phacops macdonaldi* (= *Ananaspis macdonaldi*; see Holloway 1980, p. 63), as well as *Phacops crossleii* Etheridge and Mitchell. Also present in Fletcher's collections, although not recorded by him, is a species of *Youngia* (Holloway 1994, p. 244). The precise locality from which the material was collected is unknown, but the occurrence of some of the same species in the Boree Creek Formation suggests that the material came from a similar stratigraphical level.

From the Boree Creek Formation, Sherwin (1971*a*, fig. 8) listed the trilobites *Bumastus*,

Decoroproetus?, *Ananaspis macdonaldi*, *Batocara borenorense*, *Trochurus bartonensis* and *Dicranurus*, and Sherwin (1971*b*) described *Acernaspis*? *oblatus* (a junior synonym of *Ananaspis macdonaldi*; see Holloway 1980, p. 64). Work in progress indicates that the trilobite fauna of this formation includes at least 24 other genera belonging to the families Styginidae, Proetidae, Scharyiidae, Brachymetopidae, Cheiruridae, Staurocephalidae, Calymenidae, Lichidae and Odontopleuridae.

The most abundant trilobite faunas in the overlying Mirrabooka Formation occur in limestones H and I, from which Sherwin (1971*a*, fig. 8) listed *Scutellum*, *Bunastus* sp. B, *Bunastus* sp. C, *Kosovopeltis*, *Decoroscutellum* cf. *molongensis* (Etheridge and Mitchell), *Decoroproetus*? and *Cheirurus*. Apart from the effaced styginids that are the subject of the present work, preliminary investigations on the remaining trilobites indicate that the fauna is at least as diverse as that of the underlying Boree Creek Formation, with representatives of the same families. In addition to the trilobites, other invertebrates present in the Mirrabooka Formation include brachiopods, gastropods, bivalves, rostroconchs, ostracodes, ?stromatoporoids, corals, and pelmatozoan debris.

From siltstones just above the base of the Wallace Shale near 'Mirrabooka' homestead, Sherwin (1968) described the trilobite *Denckmannites rutherfordi*, and also recorded *Encrinurus mitchelli* (Foerste) and an indeterminate odontopleurid.

MATERIALS, METHODS AND LOCALITIES

The material is preserved as largely dissociated exoskeletal elements in indurated limestones, which vary from predominantly white to pale grey, pink or, in the case of the Borenore Limestone, red. The cuticle of the trilobites is invariably present and usually adheres preferentially to the internal mould. The matrix is commonly sparry calcite, although sugary-textured and micritic patches occur; mechanical exposure of the exoskeletal elements by Vibrotool is normally relatively easy since the matrix readily parts from the outer surface of the cuticle. Removal of the cuticle from the internal mould, which is necessary to expose features of its internal surface, is correspondingly difficult.

Localities. The trilobites were collected from the following horizons and localities; the localities are marked on Text-figure 1. The PL prefix to locality numbers refers to the Museum of Victoria invertebrate fossil locality register. Grid references apply to the Molong 8631-I & IV and Cudal 8631-II & III 1:50,000 topographic sheets (1st edition) published by the Central Mapping Authority of New South Wales.

1. Limestone H, about middle of Mirrabooka Formation:
   PL1989, GR FD74502330;
   PL1996, GR FD74502350.
2. Limestone I, upper half of Mirrabooka Formation:
   PL1991, GR FD75452250;
   PL1992, GR FD75802245;
   PL1993, GR FD75552265;
   PL1988, GR FD75452155 (correlation with Limestone I tentative).
3. Limestone J, equivalent to the uppermost part of the Mirrabooka Formation:
   PL1998, GR FD73502480.
4. Borenore Limestone, ?lower half:
   PL448, GR FD80351865;
   PL3301, GR FD80501905;
   PL3302, GR FD804190;
   PL3303, GR FD805189;
   PL3304, GR FD804188.
5. Molong Limestone, horizon indeterminate:
   PL1995, GR FD74202580.

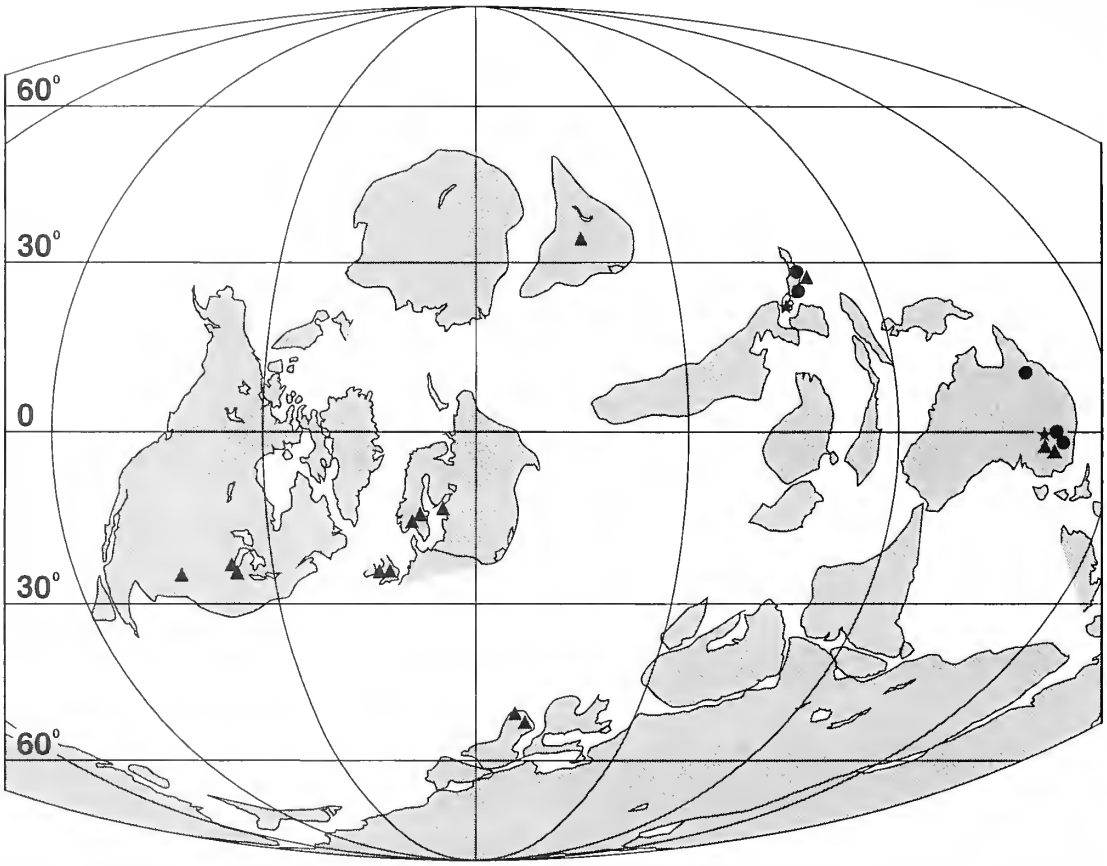

TEXT-FIG. 3. Palaeogeographical map for the Ludlow, showing distribution of *Bumastella* (stars), *Rhaxeros* (solid circles) and *Lalax* (triangles); base map modified from Scotese and McKerrow (1990).

Repository. All illustrated material is housed in the invertebrate palaeontological collections of the Museum of Victoria, Melbourne (NMV).

PALAEOBIOGEOGRAPHICAL IMPLICATIONS

The most significant palaeobiogeographical pattern to emerge from our study is the close affinity of the effaced styginids from New South Wales with those from the Late Wenlock or Early Ludlow limestones of Mt Yokokura, Japan (Kobayashi and Hamada 1974, 1984, 1986, 1987). Two of the genera, *Bumastella* and *Rhaxeros*, are known only from eastern Australia and Japan (Text-fig. 3); however, *Leioscutellum* Wu, 1977, from the Llandovery of China, may be a senior synonym of *Rhaxeros*. *Bumastella* is represented in Australia and Japan by the same species, *B. spicula* (Kobayashi and Hamada, 1974), although it has been recorded from Japan under a number of different names (see below). *Rhaxeros synaimon* and *R. trogodes*, described herein from New South Wales, also possibly occur in Japan (see below). *Lalax* occurs in both New South Wales (*L. olibros* sp. nov., *L. lens* sp. nov.) and Japan (e.g. *L. kattoi* (Kobayashi and Hamada, 1984)) but is more widely distributed, being known also from Bohemia (e.g. *L. bouchardi* (Barrande, 1846)), Norway (e.g. *L. inflatus* (Kiaer, 1908)), Estonia ('*Illaenus* (*Bumastus*) *barriensis*' of Holm 1886; see below), Kazakhstan (*L. bandaletovi* (Maksimova, 1975)), the United Kingdom (e.g. *L. xestos* (Lane and Thomas, 1978*a*)), and the eastern United States (e.g. *L. chicagoensis* (Weller, 1907)).

Work in progress on other elements of the trilobite faunas of the Orange district supports the

close affinity with Japan, suggesting the existence of a distinctive eastern Gondwanan fauna during the Silurian.

SEGMENTAL VARIATION IN POSTERIOR TAGMATA OF *BUMASTELLA* AND *LALAX*

Many of the dissociated posterior tagmata of *Bumastella spicula*, *Lalax olibros* and *L. lens* from New South Wales include in their anterior part various numbers of fused segments that appear to be unreleased thoracic segments. These specimens thus have the morphology of meraspid transitory pygidia, but there are two aspects of the specimens that are unusual: (1) they are much larger than meraspid transitory pygidia of other trilobites; and (2) unlike meraspid transitory pygidia of other trilobites, some specimens of *Bumastella spicula* from New South Wales show no correlation between the number of fused segments and size.

Tables 1–2 and Text-figures 4–5 show the size of specimens from New South Wales and number of fused segments present. In *Lalax olibros* the number of fused segments decreases progressively from five to zero as the specimen size increases up to a maximum width of *c.* 9 mm; all specimens larger than this lack fused segments. In *L. lens* the smallest known specimen has just one fused segment, and all other specimens, with maximum widths greater that 7 mm, lack fused segments. In relatively small specimens of *Bumastella spicula* the number of fused segments generally decreases with increasing specimen size up to a maximum width of about 15 mm, at which size no fused segments are present; there are, however, several exceptions to this pattern (see Table 2). The smallest specimen of *B. spicula* has five fused segments whereas a slightly larger one has six, the posteriormost segment having a pleural furrow like the segments in front but lacking an interpleural furrow posteriorly. Most specimens of *B. spicula* with maximum widths of 15 mm or more (11 out of 17 specimens) lack fused segments; the remainder have from one to three fused segments (mostly two), there being no correlation between the number of fused segments and specimen size.

In all three species from New South Wales, the pygidium behind the fused segments is identical in form to that of pygidia lacking them. This indicates that the general reduction in the number of fused segments with increasing specimen size in *Lalax olibros* and at least the smaller specimens of *Bumastella spicula* (maximum widths up to 15 mm) is due to the progressive release of segments into the thorax rather than to effacement. Release of segments into the thorax is also demonstrated by some specimens in which the anteriormost segment is only partially fused (e.g. Pl. 6, fig. 7). Hence the fused segments are protothoracic segments, and the specimens are meraspides according to the definition of Whittington (1957, 1959).

TABLE 1. Numbers of fused thoracic segments in posterior tagmata of *Lalax olibros* sp. nov. and *L. lens* sp. nov., arranged in order of increasing maximum width. For both species, all specimens larger than those listed lack fused thoracic segments.

Species	Registration no.	Maximum width (mm)	Fused segments	Figured herein
Lalax olibros	P144944	4·3	5	Pl. 5, fig. 20
	P144810	4·8	4	Pl. 5, fig. 14
	P144808	6·2	2	Pl. 5, fig. 13
	P144809	6·4	2	–
	P144816	6·8	2	–
	P144807	7·6	2	–
	P144806	*c.* 9	1	Pl. 5, fig. 14
	P144844	*c.* 9	0	–
	P144805	9·2	0	–
Lalax lens	P144836	6·9	1	Pl. 6, fig. 7
	P144837	7·1	0	–

TABLE 2. Numbers of fused thoracic segments in posterior tagmata of *Bumastella spicula* from New South Wales, arranged in order of increasing maximum width. All known measurable specimens are listed.

Registration no.	Maximum width (mm)	Fused segments	Formation	Figured herein
P145038	4·7	5	Borenore Lst	Pl. 2, fig. 8
P144943	5·2	6	Mirrabooka Fm	Pl. 2, fig. 12
P144942	9·3	3	Mirrabooka Fm	–
P144940	*c.* 9·5	3	Mirrabooka Fm	–
P145045	*c.* 9·5	1	Borenore Lst	–
P144939	10·0	4	Mirrabooka Fm	Pl. 2, fig. 15
P144941	*c.* 10	3	Mirrabooka Fm	–
P144938	10·5	1	Mirrabooka Fm	Pl. 2, fig. 17
P144969	*c.* 13	1	Molong Lst	–
P145039	*c.* 13	1	Borenore Lst	–
P144968	14·6	1	Molong Lst	–
P145036	15·0	0	Borenore Lst	–
P144937	15·3	0	Mirrabooka Fm	–
P145042	*c.* 15·5	0	Borenore Lst	–
P145037	15·7	0	Borenore Lst	–
P145043	17·5	0	Borenore Lst	–
P145027	17·8	2	Mirrabooka Fm	–
P145035	19·5	0	Borenore Lst	Pl. 2, fig. 5
P144936	20·4	2	Mirrabooka Fm	Pl. 2, figs 3, 6
P144930	21·0	3	Mirrabooka Fm	Pl. 2, figs 9–10
P144965	*c.* 22	0	Molong Lst	–
P144935	*c.* 23	2	Mirrabooka Fm	Pl. 2, fig. 18
P144970	24·3	0	Molong Lst	–
P144934	26·6	0	Mirrabooka Fm	Pl. 2, figs 1–2
P144964	*c.* 27	0	Molong Lst	–
P144933	*c.* 30	2	Mirrabooka Fm	–
P144932	*c.* 32	1	Mirrabooka Fm	Pl. 2, fig. 13
P144931	*c.* 60	0	Mirrabooka Fm	–

Further circumstantial evidence supports the conclusion that pygidia of *Bumastella spicula* with fused segments belong to meraspides. It is provided by two specimens having articulated thoracic segments attached: NMV P144943 (Pl. 2, fig. 12) has four segments in the thorax and six fused segments in the pygidium; and NMV P144930 (Pl. 2, figs 9–10) has seven segments in the thorax and three fused segments in the pygidium. With the possible exception of *Dysplanus*, which was diagnosed as having only nine thoracic segments, all known styginids, effaced or not, for which there is information available have ten thoracic segments in the holaspis. It seems likely, therefore, that NMV P144943 and NMV P144930 exhibit the total number of segments, some thoracic and some still fused, that are going to satisfy the completion of the holaspid thorax (i.e. they are degree 4 and degree 7 meraspides respectively). Of course, because these specimens lack cephala, it is possible that their thoraces are incomplete anteriorly; however, the progressive and marked increase in width (tr.) of the articulating facets on the anteriormost segments present suggests to us that these are from the front of the thorax, and that no segments are missing.

The apparently random occurrence of fused segments in pygidia of *Bumastella spicula* more than 15 mm wide requires further discussion. It might be suggested that, although the fused segments in pygidia less than 15 mm wide are protothoracic segments, those in larger pygidia were added after the release of segments into the thorax had ceased (i.e. after the holaspid stage had been attained). Segments are known to be added to the holaspid pygidium in some trilobites (e.g. *Shumardia*, *Dionide*; see Whittington 1957, p. 442), although the process is unknown in Styginidae. If this process

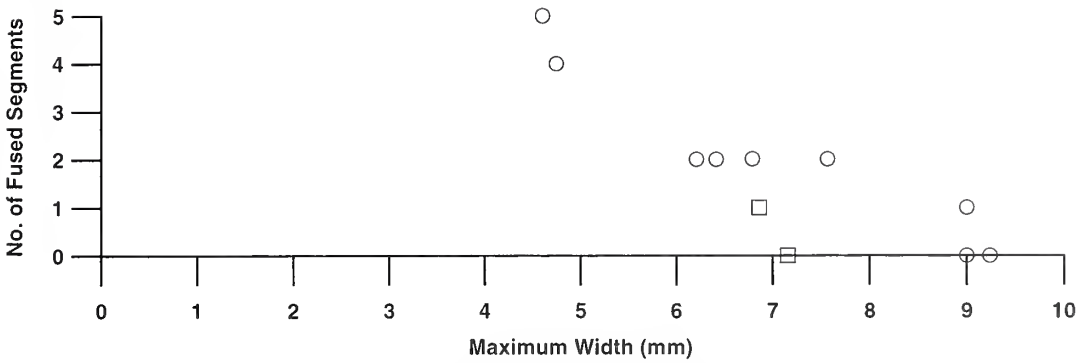

TEXT-FIG. 4. Plot of number of fused thoracic segments in posterior tagmata of *Lalax olibros* (circles) and *L. lens* (squares) versus maximum width of specimen; all specimens larger than those plotted lack fused segments.

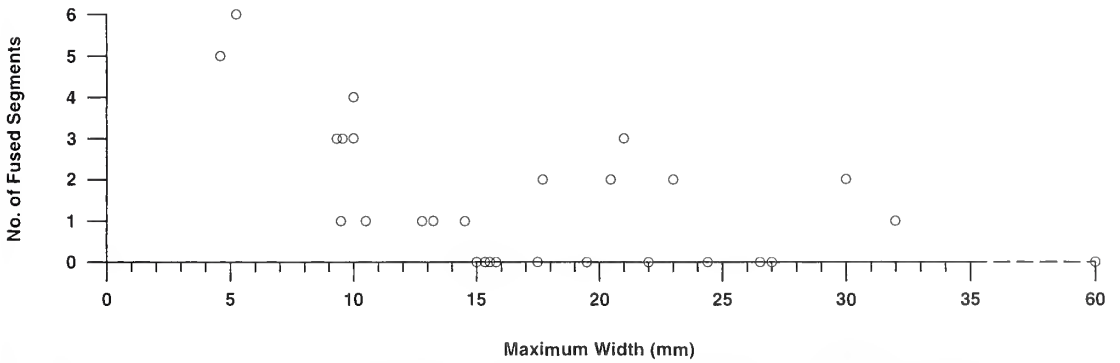

TEXT-FIG. 5. Plot of number of fused thoracic segments in posterior tagmata of *Bumastella spicula* from New South Wales versus maximum width of specimen.

had occurred in *B. spicula*, it would mean that specimen NMV P144930 (discussed above), with seven segments in the thorax and three fused segments in a pygidium 21 mm wide, is not a meraspis displaying the complete number of postcephalic segments, as we have suggested, but a holaspis with the first three thoracic segments broken off. We consider this to be unlikely, in view of the similarity (except for size) between such specimens and smaller transitory pygidia of the species. Other evidence suggesting that the fused segments in the larger pygidia were not added in the holaspid stage is: (1) the fused segments occur at the front of the pygidia, not at the back where new segments are formed; and (2) the number of fused segments in specimens wider than 15 mm does not show a general increase with increasing specimen size.

It is notable that specimens of *Bumastella spicula* more than 15 mm wide with fused segments are known only from the Mirrabooka Formation (locality PL1989; see Table 2) and not from localities in the Borenore and Molong limestones. This suggests that the apparently random occurrence of fused segments in large specimens may reflect either the presence of more than one species within the sample, or the influence of environmental factors that affected the rate of segment release into the thorax in individuals at that locality. However, we can detect no other morphological evidence to support the first possibility, nor is there any evidence (lithological, faunal or taphonomic) that environmental conditions at PL1989 differed from those at other localities where *B. spicula* is found.

In other styginids for which relatively complete ontogenies are known, meraspid transitory pygidia are up to a little more than 3 mm wide (Table 3). Somewhat larger transitory pygidia, up to a little more than 4 mm wide (excluding marginal spines) in a specimen with one protothoracic segment, were recorded in *Kosovopeltis borealis* (Poulsen) by Ludvigsen and Tripp (1990, text-fig.

4F, pl. 4, fig. 5). The largest transitory pygidia of *Lalax olibros* and *L. lens* are almost two to three times the size of the largest transitory pygidium of *Kosovopeltis* (Table 1), whereas the largest transitory pygidium of *Bumastella spicula* is eight times larger (Table 2; however, the smallest pygidium of *B. spicula* without fused segments is three to four times larger than the largest transitory pygidia of *K. borealis*). The smallest transitory pygidia of *L. olibros* and *B. spicula* known, with five fused segments (i.e. meraspid degree 5 if there are ten segments in the holaspid thorax), are between two and four times larger than degree five transitory pygidia of *Scutellum calvum* and *Dentaloscutellum hudsoni* (Chatterton 1971, figs 5A, 7).

TABLE 3. Range in width of transitory pygidia, excluding marginal spines, in some styginids (meraspid degrees 0–9).

Species	Age	Width of transitory pygidia (mm)	Reference
Failleana calva	Ordovician	0·7–2·7	Chatterton (1980, pl. 5, figs 10, 20–21, 30–31)
Kosovopeltis svobodai	Silurian	0·6–3·2	Káchka and Šarič (1991, fig. 6)
Scutellum calvum	Devonian	1·0–1·9	Chatterton (1971, fig. 7)
Dentaloscutellum hudsoni	Devonian	1·0–2·3	Chatterton (1971, fig. 5A)

Meraspid transitory pygidia of large size are also known in other Silurian effaced styginids. A transitory pygidium of *Lalax bouchardi* from Bohemia was figured by Šnajdr (1957, pl. 10, fig. 7); the specimen, which has two protothoracic segments, is *c.* 5·8 mm wide. Transitory pygidia of effaced styginids from Arkansas have also been observed by one of us (DJH); widths of these specimens are 6·3 mm for a specimen of *Lalax* with one protothoracic segment, 4–4·2 mm for specimens of *Illaenoides* with five protothoracic segments, and 5·8 mm for a specimen of *Illaenoides* with three protothoracic segments. This evidence indicates that large meraspides are not unique to the species under discussion here, and in fact the phenomenon may be widespread amongst effaced Silurian styginids. The evolution of such forms with large meraspides from an ancestor or ancestors with normal-sized meraspides may be the result of neoteny (reduced rate of morphological development). Assuming the same rates of growth and moulting in ancestor and descendent, the latter must have undergone a greater number of moults in order to reach a larger size at the same stage of ontogeny. Hence the rate of morphological change (in this case, release of protothoracic segments into the thorax) must have been delayed at each moult in the descendent. If the delay was cumulative at each moult, then throughout ontogeny the descendent form would have fallen further and further behind its ancestor in release of segments into the thorax, accounting for the very large size of some of the meraspides.

Meraspid transitory pygidia comparable in size to those of *Bumastella spicula* are known in the nileid *Illaenopsis harrisoni* from the Arenig of South Wales. Fortey and Owens (1987, p. 197) reported that in this species, which they considered to have the largest merapides of any trilobite, transitory pygidia with one protothoracic segment reach a width of 20 mm, which is two-thirds the size of the largest known transitory pygidia of *B. spicula*. Neoteny was also cited by Fortey and Owens (1987, p. 197) as a possible mechanism for the development of the giant meraspid transitory pygidia of *I. harrisoni*.

A question raised by such giant meraspides is whether they have any bearing on the attainment of sexual maturity (i.e. whether they were biologically adult, although not morphologically complete). From study of the many well-documented and relatively complete trilobite ontogenies known there is no direct evidence for the onset of sexual maturity, and to no organs or structures of the exoskeleton of any trilobite can be ascribed a sexual function. However, sexual maturity is commonly assumed, unjustifiably, to have coincided with attainment of the holaspid stage (e.g.

McNamara 1986, p. 124), although this was defined by Whittington (1957, 1959) in purely morphological terms by the acquisition of the full complement of thoracic segments. It is recognized that protaspid, meraspid and holaspid stages are not developmentally homologous amongst all trilobites (Hughes and Chapman 1995, p. 349), suggesting that sexual maturity may have occurred at different growth stages in different taxa. Whittington (1957, p. 445) noted that some trilobites may increase in length 30- to 40-fold during the holaspid stage (e.g. holaspides of *Isotelus gigas* range from 8–9 mm to 400 mm long, whilst those of *Paradoxides* range from 13·5 mm to over 400 mm). This very large increase in size leads us to suspect that sexual maturity was attained later than the meraspid-holaspid transition in such forms.

Some of the meraspid transitory pygidia of *Bumastella spicula* from New South Wales are amongst the largest specimens of the species known. Assuming that specimens in our collections are representative of the full size attained by individuals of the species, some of these meraspides must have been mature. If so, the release of protothoracic segments into the thorax must have continued in those individuals after maturity, although perhaps at a much slower rate in respect to the moult rate than prior to maturity. If none of the meraspides of *B. spicula* was mature, and assuming that sexual maturity is related to size, it is reasonable to conclude that holaspides smaller than the largest meraspis were also immature. This would mean that the breeding population of the species is virtually unrepresented amongst our collections, a possibility that we believe to be unlikely. We consider, therefore, that sexual maturity and attainment of the holaspid stage are unrelated in *B. spicula*, and that they may be unrelated in many other trilobite species.

SYSTEMATIC PALAEONTOLOGY

Remarks. Because of the great to extreme effacement of the forms described below, it has not been possible to produce brief generic diagnoses. As diagnosed, genera are distinguished on combinations of characters, all of which are therefore listed. However, it is our belief that the gross convexity of the exoskeleton, the form of the rostral plate, the presence or lack of the 'omphalus' and 'anterolateral internal pit' (see terminology below), and the form of the thorax (width of axis, distance between axial furrow and fulcrum) are of paramount importance in diagnosing genera of effaced styginids. Of possible importance also is the form of the hypostome, which is all too often unknown in the present material and in previously described species of effaced styginids. We consider that the proportions of the exoskeleton, the degree of effacement, the pattern of cranidial muscle scars, and the size and position of the eye (which can, however, vary greatly during ontogeny; see *Bumastella spicula* below) have less taxonomic value, and may be of more use in diagnosing species.

Descriptions commence with the gross morphology of the exoskeleton, followed by descriptions of sculpture, muscle scars and ontogeny where these headings are appropriate. In view of the significant differences in appearance between testiferous and exfoliated specimens of the same species, all descriptions are of the external surface of the exoskeleton, unless otherwise stated.

Terminology. Muscle scars on the glabella are numbered G0, G1, etc. from the posterior forward. The feature associated with the cephalic axial furrow often referred to as the 'lateral muscle impression' is here termed the 'lunette'. The 'holcos' (Helbert and Lane, *in* Helbert *et al.* 1982, p. 132) is the concave zone parallel to and near the lateral and posterior margins of some styginid pygidia. Anteriorly, the holcos is deflected adaxially to unite with an oblique depression running subparallel to the posterior edge of the articulating facet; examination of the ontogenetic development of *Failleana* (Chatterton 1980, pl. 5; Ludvigsen and Chatterton 1980, pl. 1) indicates that this oblique depression is the pleural furrow on the anterior segment of the pygidium.

On the interior of the cranidium of some effaced styginids is a raised boss, commonly with a median depression (often figured as a pit with a central swelling on the internal mould), at which the axial furrow may terminate anteriorly, as in *Cybantyx* (see Lane and Thomas 1978*a*, text-fig. 4f), *Paracybantyx* (see Ludvigsen and Tripp 1990, pl. 1, figs 5–9) and *Lalax* (see Pl. 5, fig. 10); the

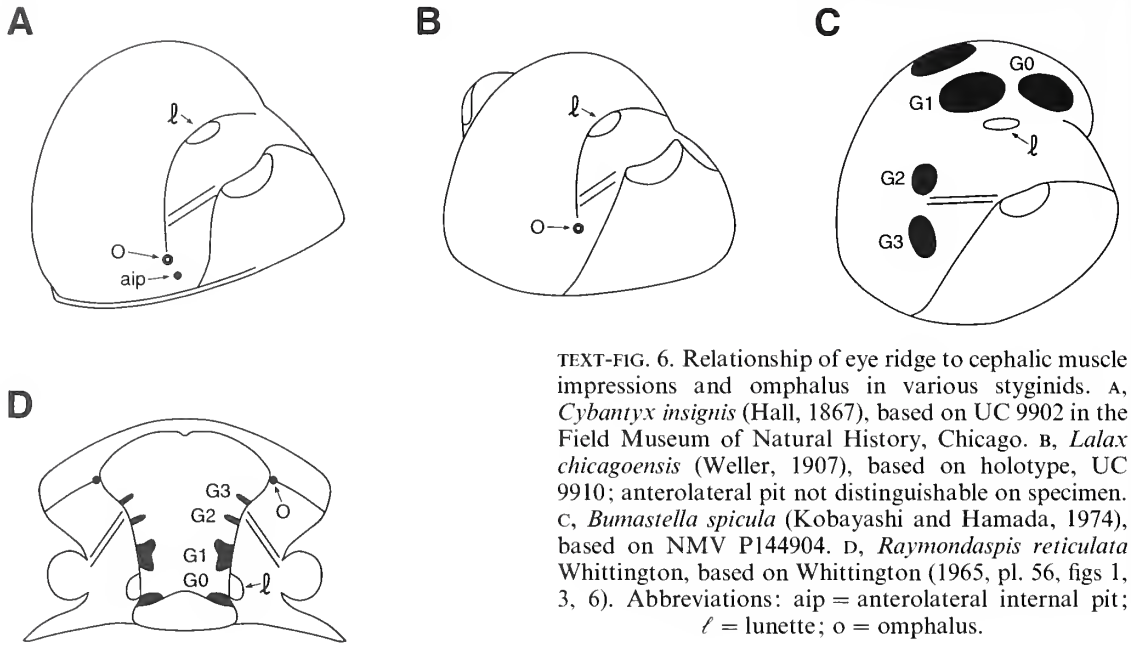

TEXT-FIG. 6. Relationship of eye ridge to cephalic muscle impressions and omphalus in various styginids. A, *Cybantyx insignis* (Hall, 1867), based on UC 9902 in the Field Museum of Natural History, Chicago. B, *Lalax chicagoensis* (Weller, 1907), based on holotype, UC 9910; anterolateral pit not distinguishable on specimen. C, *Bumastella spicula* (Kobayashi and Hamada, 1974), based on NMV P144904. D, *Raymondaspis reticulata* Whittington, based on Whittington (1965, pl. 56, figs 1, 3, 6). Abbreviations: aip = anterolateral internal pit; ℓ = lunette; o = omphalus.

term 'omphalus' (latinized from the Greek for navel) is introduced for this structure. The omphalus may be reflected on the exterior of the exoskeleton as a pit or as a small patch devoid of sculpture. Even when the axial furrow cannot be recognized anteriorly, because of a high degree of effacement, the omphalus may be clearly defined and is useful in indicating the transverse extent of the glabella, as in *Lalax* gen. nov. Other effaced styginids in which the omphalus occurs are *Dysplanus* Burmeister, 1843, *Failleana* Chatterton and Ludvigsen, 1976, *Litotix* Lane and Thomas, 1978*a*, *Opsypharus* Howells, 1982 and *Platillaenus* Jaanusson, 1954. Situated just in front of the omphalus, and usually slightly adaxial or abaxial to it, there may be a small pit on the interior of the cranidium (appearing as a node on internal moulds), as in *Lalax* (see Pl. 5, figs 3, 7, 9–10; Lane and Thomas 1978*a*, pl. 3, fig. 14a) and also *Cybantyx*; this pit is here termed the anterolateral internal pit.

The omphalus was described by Ludvigsen and Chatterton (1980, p. 476) as a 'socketed pit' (illustrated as a pitted tubercle in their pl. 1, fig. h) and considered by them to be one of the diagnostic features of Bumastinae (Raymond, 1916; as conceived by Jaanusson 1959). Of the genera normally assigned to the subfamily, however, the omphalus is absent in the type species of *Bumastus*, *B. barriensis* Murchison, 1839, and in *Goldillaenus* Schindewolf, 1924, *Illaenoides* Weller, 1907 and *Thomastus* Öpik, 1953. More recently described effaced styginid genera in which the omphalus is absent are *Bumastella* Kobayashi and Hamada, 1974, *Excetra* gen. nov., *Ligiscus* Lane and Owens, 1982, *Meitanillaenus* Chang, 1974, *Ptilillaenus* Lu, 1962 and *Rhaxeros* Lane and Thomas, 1980.

From its position, the omphalus is not the homologue of the 'fossula', which is defined as lying at the anterior edge of the eye ridge. In *Cybantyx insignis* and *Lalax chicagoensis*, the omphalus is situated well in front of the anterior end of the eye ridge (Text-fig. 6A–B). In *Bumastella spicula* (described below) the eye ridge is directed towards a point between G2 and G3 (Text-fig. 6C); *Bumastella* lacks an omphalus, but in other effaced styginids in which the omphalus is present it is situated level with or in front of G3. Hence, although no fossula is present in these forms or the others under discussion here, the omphalus lies morphologically anterior to where such a structure would be expressed. Chatterton and Ludvigsen (1976, p. 39) stated, however, that in *Failleana calva* the omphalus is situated where '... a very shallow furrow that is posteriorly continuous with palpebral furrow joins axial furrow' (i.e. at the posterior edge of the eye ridge); this statement is not

supported by their illustrations (Chatterton and Ludvigsen 1976, pl. 6, figs 6, 39) which show the omphalus lying well in front of the weak furrow defining the anterior edge of the eye ridge.

The omphalus seems to be homologous with the pit (as expressed on the exterior of the exoskeleton) that lies in the axial furrow at or just behind the junction with the lateral border furrow in some non-effaced Ordovician styginids, including species of *Stygina* Salter, 1853, *Raymondaspis* Přibyl, *in* Prantl and Přibyl, 1949 (see Text-fig. 6D) and *Turgicephalus* Fortey, 1980, and also in *Theamataspis* Öpik, 1937 (see Skjeseth 1955, pl. 3, fig. 1; Whittington 1965, pl. 56, figs 3, 7, pl. 59, figs 1, 5–8; Fortey 1980, pl. 6, figs 1–2, 5, pl. 7, figs 1–3, pl. 9, figs 1–3, 5). In *Platillaenus*, the omphalus ('Vordergrube' of Jaanusson 1954, pl. 3, fig. 6) also lies at the junction of the axial and lateral border furrows.

Functionally, the omphalus was apparently involved with the attachment of the hypostome to the cranidium. Jaanusson (1954, p. 548, text-fig. 1, pl. 3, figs 2, 4) showed that in *Dysplanus centrotus* the anterior wing process of the hypostome projects well forward above the cephalic doublure and is in close proximity with the omphalus. Chatterton and Ludvigsen (1976, p. 39, pl. 6, figs 2, 11, 16) described a protuberance similar in form to the omphalus on the inner (dorsal) margin of the librigenal doublure of *Failleana calva*; this librigenal protuberance faces the omphalus and the two are adjacent in a complete cephalon. Although they were unsure of its function, Chatterton and Ludvigsen (1976, p. 39) suggested that the librigenal structure may have been associated with ligament or muscle attachment to the anterior wing of the hypostome, or with the omphalus.

Orientation. In convex to highly convex trilobites, it is difficult to indicate the exact orientation of specimens for description and photography. As applied herein to cephala and cranidia, 'dorsal view' indicates that the posterior margin adaxial to the fulcrum is vertical, 'palpebral view' that the upper edge of the visual surface (or palpebral suture) is horizontal, and 'plan view' that the maximum sagittal length is being shown. For pygidia, 'dorsal view' indicates that the anterior margin adaxial to the articulating facet is vertical, and 'plan view' that the lateral and posterior margins are horizontal (in plan view a little less than the maximum sagittal length of the pygidium is shown). As convexity varies during ontogeny of individual species, and between species, 'plan' and 'palpebral' views are not necessarily identical at all stages of ontogeny and in different species, and in other cases the two views may coincide.

Suborder ILLAENINA Jaanusson, 1959
Family STYGINIDAE Vogdes, 1890

Remarks. The family name is used here in the emended sense of Lane and Thomas (1983, p. 156), who recognized no subfamilial divisions because of the inability at present to recognize phyletic lines of development. Ludvigsen and Tripp (1990, p. 8) retained the division of Styginidae into Stygininae, Scutelluinae and Bumastinae 'as an aid to grouping the large number of genera in the family' but did not indicate which characters could be used as a basis for this subdivision. We consider, however, that the only justification for the recognition of supraspecific taxa is evolutionary relationship. Although also rejecting Ludvigsen and Tripp's concept of styginid subfamilies as taxa of convenience, Adrain *et al.* (1995, p. 726) recognized Scutelluinae and Bumastinae as phylogenetic entities that 'may very likely prove to be monophyletic', but no evidence to support this statement was offered. Nielsen (1995, pp. 295, 320) recently used Stygininae and Bumastinae as subdivisions of Styginidae without any discussion on the characters he regarded as diagnostic.

Genus BUMASTELLA Kobayashi and Hamada, 1974

Type species. By original designation; *Bumastus* (*Bumastella*) *spiculus* Kobayashi and Hamada, 1974 from the Upper Wenlock (or Lower Ludlow), Gomi, Yokokura-yama, Kôchi Prefecture, Shikoku, Japan.

Emended diagnosis. Cephalon extremely convex (sag., exsag., tr.), almost hemispherical; in dorsal profile, posterior margin transverse medially, deflected posteroventrally abaxial to fulcrum towards

broadly rounded genal angle. Axial furrow shallow and poorly defined close to posterior margin, not impressed farther forwards. Eye small, in palpebral view placed with posterior edge in transverse line with posterior edge of lunette, in lateral view placed at half height of cephalon; visual surface borne on steep, concave band of librigena. Anterior branch of facial suture gently convergent forwards, posterior branch gently divergent backwards. Rostral plate sub-triangular, lacking posterior flange, convexity in sagittal line greatest anteriorly. Thorax with gently convex axis narrowing markedly backwards; articulating furrows not impressed; pleurae with horizontal portion adaxial to fulcrum widening (tr.) in more posterior segments, as wide (tr.) as or wider than gently downturned portion abaxial to fulcrum. Pygidium wider than long (sag.), much less convex than cephalon, with strongly developed holcos.

Remarks. The above diagnosis is an attempt to characterize the genus allowing for the considerable morphological changes which are seen during ontogeny. These changes, which are outlined below in the section on ontogeny, are partly the reason that we consider the type species to be synonymous with two other species of *Bumastella* and one of *Bumastus* erected by Kobayashi and Hamada (1974) at the same time, and with at least one (and possibly another) form described as possible species of *Illaenoides* by the same authors in a later work (see synonymy of *Bumastella spicula* herein).

Kobayashi and Hamada (1974, p. 50) erected *Bumastella* as a subgenus of *Bumastus*, and diagnosed it as having a 'narrower axial lobe which is clearly separated in thorax from pleurae by pronounced axial furrows. Eyes are very large in comparison with those of *Stenopareia* Holm, 1886 (see Owen and Bruton 1980, pl. 2, fig. 11). Short genal spines are present in the type species.' We consider that, apart from the effacement, *Bumastella* has little similarity with *Bumastus* and is not closely related to it. In our opinion, *Bumastella* has more similarities to *Illaenoides* and *Thomastus* (for comparison with the latter see Sandford and Holloway 1998).

The similarities with *Illaenoides* (type species *I. triloba* Weller, 1907, p. 226, pl. 17, figs 6–9, pl. 19, figs 12–14) from the Niagaran (upper Llandovery or Wenlock) of Illinois include the extreme convexity of the cephalon, the glabella that narrows weakly forwards from the posterior cephalic margin to the lunette, the small eyes, the subparallel anterior branch and weakly divergent posterior branch of the facial suture, and the strong holcos. *Illaenoides* differs from *Bumastella* in that the eyes are even smaller and are situated farther forwards, with the posterior margin in front of the lunette in palpebral view; the posterior cephalic margin is deflected less strongly backwards abaxial to the fulcrum; the rostral plate is lenticular in outline rather than triangular, with connective sutures that are distinctly sigmoidal rather than almost straight; the pleurae on the posteriormost thoracic segments are wider abaxial to the fulcra than adaxially; and the pygidium is longer.

In view of the differences, even from closely related forms, we consider it necessary to raise Kobayashi and Hamada's taxon to generic status.

Stratigraphical range and distribution. Late Wenlock to ?early Ludlow; Japan and New South Wales.

EXPLANATION OF PLATE 1

Figs 1–21. *Bumastella spicula* (Kobayashi and Hamada, 1974); locality PL1989, Mirrabooka Formation, unless otherwise indicated. 1–3, 5, NMV P144906; cephalon, anterior and palpebral views; ×2; ventral view; ×2·5; lateral view; ×2. 4, NMV P144928; rostral plate, ventral view; ×4. 6, NMV P144953; locality PL1995, Molong Limestone; small cephalon, oblique view; ×5. 7–8, NMV P145028; locality PL448, Borenore Limestone; cephalon, lateral and palpebral views; ×1·75. 9, NMV P144907; cephalon, palpebral view; ×3. 10, 13, NMV P144905; cephalon, palpebral and dorsal views; ×1·75. 11, 14, 21, NMV P144904; largest cephalon, dorsal, anterior and oblique views; ×1·75. 12, NMV P144908; small cephalon, anterior view; ×5. 15–16, 18, NMV P144910; smallest cephalon, palpebral, oblique and lateral views; ×6. 17, 19, NMV P144951; locality PL1995, Molong Limestone; small cephalon, palpebral and oblique views; ×4·5. 20, NMV P144950; locality PL1995, Molong Limestone; small cephalon, oblique view; ×4·5.

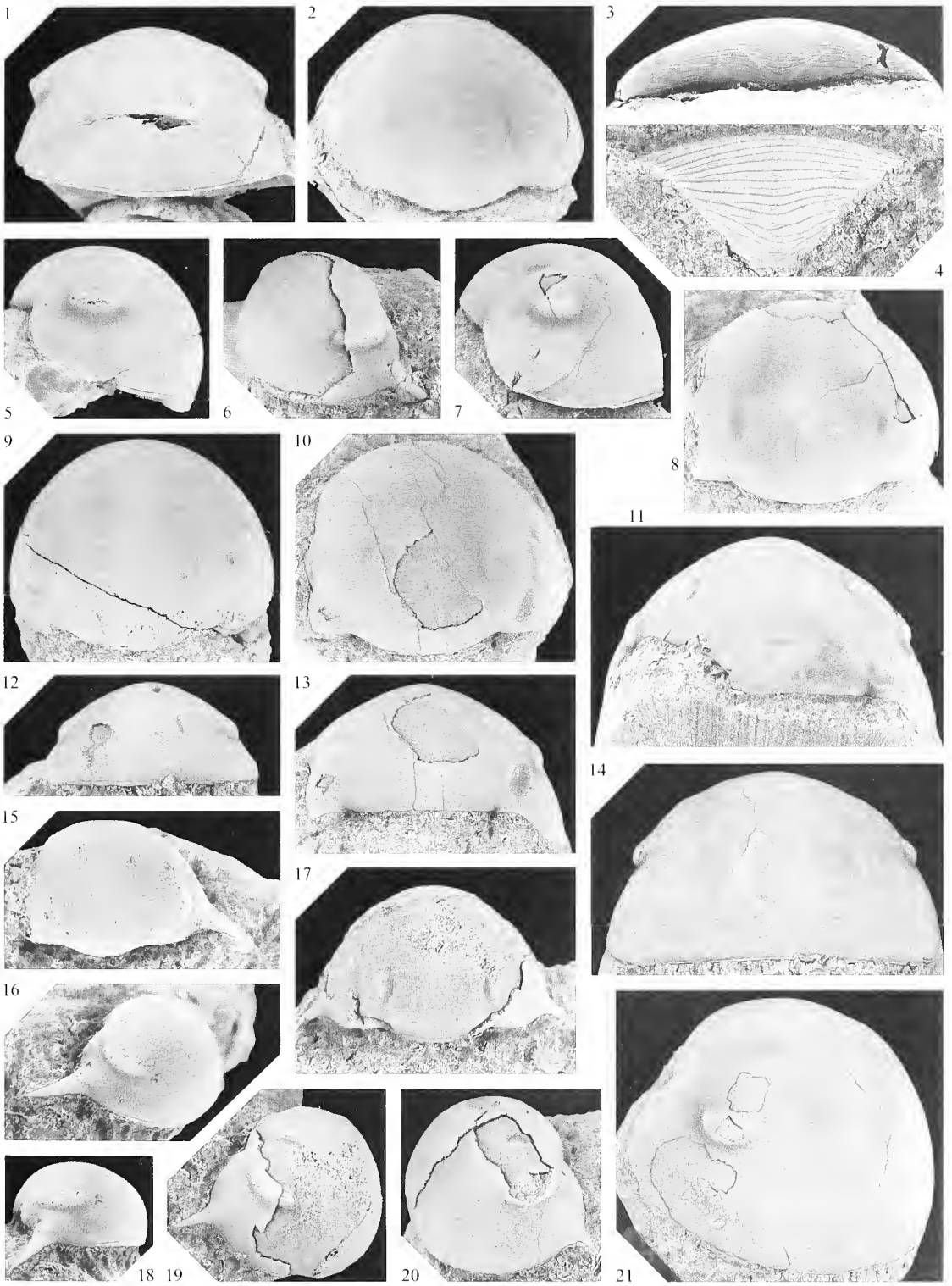

HOLLOWAY and LANE, *Bumastella*

Bumastella spicula (Kobayashi and Hamada, 1974)

Plate 1, figures 1–21; Plate 2, figures 1–15, 17–18;
Text-figure 6C

1909	*Illaenus Johnstoni* Etheridge; Etheridge, p. 1, figs 1–2 [*non* Etheridge 1896, p. 33, pl. fig. 3].
1974	*Bumastus glomerosus* Kobayashi and Hamada [*partim*], p. 47, pl. 1, figs 3–6, 8 [*non* fig. 7 = *Rhaxeros subquadratus*]; text-fig. 2A.
1974	*Bumastus* (*Bumastella*) *spiculus* Kobayashi and Hamada, p. 51, pl. 2, fig 3; text-fig. 2D.
1974	*Bumastus* (*Bumastella*) *bipunctatus* Kobayashi and Hamada, p. 51, pl. 2, figs 4–9; ?pl. 3, fig. 1; text-fig. 2E.
1974	*Bumastus* (*Bumastella*) *aspera* Kobayashi and Hamada [*partim*], p. 52, pl. 3, figs 3–5 [*non* fig. 6 = *Rhaxeros* cf. *synaimon*]; text-fig. 2F, cephalon only [pygidium = *Rhaxeros* cf. *synaimon*].
1985*a*	*Bumastus glomerosus*; Kobayashi and Hamada [*partim*], p. 345.
1985*a*	*Bumastus* (*Bumastella*) *spiculus*; Kobayashi and Hamada, p. 345.
1985*a*	*Bumastus* (*Bumastella*) *bipunctatus*; Kobayashi and Hamada, p. 345.
1985*a*	*Bumastus* (*Bumastella*) *aspera*; Kobayashi and Hamada [*partim*], p. 345.
1985*a*	*Illaenoides* (?) *magnisulcatus* Kobayashi and Hamada [*nom. nud.*], p. 345.
?1985*a*	*Illaenoides* (?) *abnormis* Kobayashi and Hamada [*nom. nud.*], p. 345.
1986	*Illaenoides* (?) *magnisulcatus* Kobayashi and Hamada, p. 452, pl. 90, fig. 5.
?1986	*Illaenoides* (?) *abnormis* Kobayashi and Hamada, p. 453, pl. 90, fig. 6.
*non*1987	*Bumastus glomerosus*; Kobayashi and Hamada, p. 110, figs 1A, 2.1a–d [= *Lalax*? sp.].

Holotype. University of Tokyo Museum No. 7345; from the Upper Wenlock (or Lower Ludlow); Gomi, Yokokura-yama, Kôchi Prefecture, Shikoku, Japan.

Other material. Approximately 17 cephala, 19 cranidia, 18 librigenae, one rostral plate, six thoracopyga and 26 pygidia (including meraspid transitory pygidia), from PL448, PL1988, PL1989, PL1995, and PL3301–PL3304.

Description. Cephalon almost semicircular in lateral and dorsal views, more than semicircular in anterior and palpebral views; in palpebral view, sagittal length 85 per cent. of maximum transverse width which is level with posterior edge of eye. Axial furrow forming shallow notch in posterior cephalic margin, rapidly dying out just in front of posterior margin but in some specimens very faintly discernible as far forward as lunette, towards which it converges weakly; width of glabella at posterior margin slightly more than half maximum cephalic width. From posterior end of axial furrow, a short (tr.), indistinct furrow is directed laterally and slightly forwards, just in front of narrow (tr.), horizontal portion of posterior fixigenal margin adaxial to fulcrum. Lunette weakly expressed, rather more than 50 per cent. of length of visual surface, situated with anterior edge level with cephalic midlength (sag.) in palpebral view. Fixigena adaxial to palpebral lobe slightly inflated above general transverse convexity (in anterior view); palpebral lobe narrow (tr.), sloping less steeply abaxially than adjacent part of fixigena, length *c.* 20 per cent. of sagittal length of cephalon in palpebral view, placed at 100–150 per cent. its own length from posterior margin; palpebral furrow shallow and poorly defined, weakly curved in palpebral view. Eye ridge (faintly visible in one specimen under the microscope but not in photographs; see Text-fig. 6C) very narrow, running anteromedially from close to front of palpebral lobe towards midway between G2 and G3, but dying out before reaching line of these impressions. Anterior section of facial suture subparallel to sagittal line posteriorly, curving adaxially anteriorly to cut cephalic margin in line (exsag.) with abaxial edge of lunette; palpebral section of suture very gently curved; posterior section diverging gently backwards, almost straight for most of its course but deflected slightly more strongly abaxially near posterior margin. Librigena gently convex exsagittally and weakly convex transversely; visual surface gently convex dorso-ventrally, subparallel sided with rounded anterior and posterior margins; lenses very small and very numerous.

Cephalic doublure steeply inclined, more convex medially than laterally. Rostral plate with maximum width a little more than twice sagittal length, and 50 per cent. of width of cranidium at palpebral lobes. Anterior margin broadly rounded; lateral margins converging backwards at *c.* 110–120°, slightly more strongly near anterior margin than farther back; posterior margin transverse or weakly convex forwards.

Hypostome unknown.

Number of thoracic segments unknown. In a specimen with seven thoracic segments articulated with a meraspid transitory pygidium having three protothoracic segments (Pl. 2, figs 9–10), thoracic axis is 80 per cent.

as wide (tr.) posteriorly as anteriorly, and horizontal portion of pleurae adaxial to fulcrum is twice as wide posteriorly as anteriorly; overall, thorax becomes slightly wider backwards. Axial furrow broad and shallow. Anterior segments with pleurae flexed strongly backwards at fulcrum, and with large articulating facets occupying most of segmental length; more posterior segments successively less strongly flexed backwards at fulcrum but curving forwards slightly distally, with successively smaller articulating facets.

Pygidium more convex sagittally than transversely, semi-elliptical in outline, in plan view sagittal length 70 per cent. of maximum width, which is at posterior outer angle of articulating facet. Anterior margin gently arched forwards across axis, between anterior ends of holcos; anterior width of axis 50 per cent. of maximum pygidial width; short (sag., exsag.) articulating half ring defined by absence of sculpture and by faint articulating furrow abaxially. Articulating facet short (exsag.), occupying *c.* 60 per cent. of width (tr.) of anterior pleural margin; anterior edge of facet with small process situated closer to abaxial than adaxial extremity. Anteriormost pleural furrow strongly developed, joining in a broad curve with holcos which dies out quite suddenly at *c.* 66 per cent. of maximum pygidial length. Doublure occupying *c.* 20 per cent. of sagittal length of pygidium, slightly less convex medially than anteriorly but more steeply inclined.

Sculpture. Cephalon everywhere covered by dense, small and indistinct pits; especially at posterior margin, and for a little way forward on glabella, this pattern of pits has very narrow, irregular, anastomosing furrows superimposed. Near to anterior margin of cranidium, a few weakly developed terrace ridges are present. Lateral and anterior margins of cephalon bear a very narrow but distinct marginal thread. Rostral plate with ten non-anastomosing terrace ridges present on ventral surface; most anterior of these ridges run parallel to anterior margin, medial ones become transverse, and posterior few ridges curve convex backwards to become subparallel to posterior margin.

Thorax and pygidium bear packed indistinct pits like those of cephalon. In addition, distinct terrace ridges are present on and behind articulating facets of thoracic pleurae and pygidium, forming a chevron pattern on lateral parts of pygidium abaxial to the holcos (Pl. 2, fig. 13).

Muscle scars. Glabella bears four pairs, distinguished by weak wrinkling of exterior of exoskeleton in some specimens. G0 and G1 elongated, of similar size and in line exsagittally; G0 situated less than its own length from posterior cephalic margin, extending forwards almost level with posterior edge of lunette in palpebral view; G1 with posterior margin just in front of transverse line through back of lunette and anterior margin opposite front of eye in palpebral view. G2 smallest, sub-circular, slightly more abaxially placed than G1, equidistant from G1 and G3. G3 also sub-circular, slightly larger than G2 (but much smaller than G0 and G1) and placed slightly farther abaxially, about twice as far from anterior cephalic margin as from G2.

Pygidia have two or more pairs of relatively small, sub-circular and poorly defined muscle scars situated anteriorly close to the sagittal line; another pair of larger, sub-circular scars, situated farther from the sagittal line just in front of the pygidial midlength (sag.), is defined by a reticulate appearance of the exterior of the exoskeleton. Surrounding the region of the paired muscle scars laterally and posteriorly, and extending backwards as far as 75 per cent. of the sagittal pygidial length, is a broad, arcuate band of scattered, small (*c.* 0·1–0·2 mm diameter), circular pits, possibly representing muscle attachment sites on the interior of the exoskeleton (Pl. 2, fig. 13)

The smallest meraspid transitory pygidium (Pl. 2, fig. 8), with five protothoracic segments, has a pair of elliptical scars impressed on the interior of the exoskeleton, either side of a small, raised (on internal mould) sub-triangular area apparently representing the axis. These scars are probably the posterior pair described above.

Ontogeny. The above description is based on some of the largest exoskeletal elements from New South Wales, which differ from the smallest growth stages in a number of respects. Morphological changes that occur during ontogeny (apart from the change in number of protothoracic segments in meraspid transitory pygidia; see above) are as follows.

1. The genal spine gradually deceases in length and finally disappears. In the smallest cephalon, with a width of 5 mm (Pl. 1, figs 15–16, 18; librigena 2·5 mm maximum length) the genal spine is 1·6 mm long; on a cephalon 8·2 mm wide (Pl. 1, figs 17, 19; librigena 4·5 mm long) it is 1·4 mm long; on a librigena about 9·5 mm long (Pl. 2, fig. 14) it is developed only as a very short, thorn-like point (the tip of which is broken off); and on a librigena 10·2 mm long (Pl. 2, fig. 11) it is represented by a very small swelling.
2. The cranidium changes from slightly wider than long to slightly longer than wide in plan view.
3. The length of the visual surface changes from about one-third to about one-tenth of the length of the cephalon in plan view.

4. The eye changes in position from less than one-half its own length, to more than its own length from the posterior edge of the cephalon.
5. Overall convexity of the cephalon increases (compare Pl. 1, figs 7, 18), and the cephalic outline in plan view changes from semicircular to circular.
6. Sagittal length of the pygidium increases slightly relative to width.
7. Overall convexity of the pygidium increases.
8. The holcos and anteriormost pleural furrow are very weak in the smallest meraspid transitory pygidia (Pl. 2, figs 8, 12) and become more distinct in larger specimens.

In some other effaced styginids, for example *Bumastus barriensis* (see Lane and Thomas 1978*a*, pl. 4, fig. 6) and *Failleana calva* (see Ludvigsen and Chatterton 1980, pl. 1, figs s–v), a genal spine is present in small specimens but is absent later in ontogeny.

Remarks. Study of the ontogenetic changes in *Bumastella* collected from a single locality (PL1989), discussed above, led us to the conclusion that those Kobayashi and Hamada species we have synonymized, each of which is based on only one or a few specimens (mostly cranidia), all from the Yokokura limestone of Mt Yokokura (possibly the same locality; see Kobayashi and Hamada 1985*a*, p. 345), represent different stages in the ontogeny of a single species. The smallest form available in our collections has the morphology of *B. spicula* (the type species), which is followed by specimens in order of increasing size having the form of *B. bipunctata*, *B. aspera*, '*Illaenoides*?' *magnisulcatus*, possibly '*I.*?' *abnormis*, and finally the largest morph '*Bumastus*' *glomerosus* which Kobayashi and Hamada (1974, p. 47) noted 'is the largest illaenid species in the Yokokura fauna'. The Japanese material, of which we have examined plaster casts, is not as well preserved as that from New South Wales, so that it has not been possible to compare all details, such as sculpture. However, based on a comparison of general proportions and convexity of cranidia during growth, we believe that the latter material is conspecific.

We consider that the pygidium Kobayashi and Hamada (1974) assigned to *Bumastella aspera*, and one of the pygidia they assigned to '*Bumastus*' *glomerosus*, do not belong to *Bumastella* but to two different species of *Rhaxeros* (see discussions of *R. synaimon* and *R. trogodes*).

Three cephala from the Borenore Limestone at Borenore Caves were referred by Etheridge (1909) to his species *Illaenus johnstoni*, originally based (Etheridge 1896) on material from the Ordovician

---

EXPLANATION OF PLATE 2

Figs 1–15, 17–18. *Bumastella spicula* (Kobayashi and Hamada, 1974); locality PL1989, Mirrabooka Formation, unless otherwise indicated. 1–2, NMV P144934; pygidium, dorsal and lateral views; ×2. 3, 6, NMV P144936; transitory pygidium with two protothoracic segments, lateral and dorsal views; ×2·25. 4, NMV P145041; locality PL3301, Borenore Limestone; librigenal doublure, ventral oblique view; ×3. 5, NMV P145035; locality PL448, Borenore Limestone; pygidium and posteriormost thoracic segment, dorsal view; ×2·25. 7, NMV P144924; librigena, oblique view; ×4. 8, NMV P145038; locality PL448, Borenore Limestone; transitory pygidium with five protothoracic segments, dorsal view; ×8. 9–10, NMV P144930; transitory pygidium with three protothoracic segments and seven articulated thoracic segments, dorsal and lateral views; ×2·25. 11, NMV P144920; librigena, oblique view; ×4. 12, NMV P144943; transitory pygidium with six protothoracic segments and four articulated thoracic segments, dorsal view; ×7. 13, NMV P144932; transitory pygidium with one protothoracic segment and with last thoracic segment articulated; detail showing sculpture, oblique view; ×4. 14, NMV P144962; locality PL1995, Molong Limestone; librigena, oblique view; ×4. 15, NMV P144939; transitory pygidium with four protothoracic segments, dorsal view; ×4. 17, NMV P144938; transitory pygidium with one protothoracic segment, dorsal view; ×4. 18, NMV P144935; transitory pygidium with two protothoracic segments, latex cast in ventral view; ×2.

Figs 16, 19. *Bumastella* sp.; NMV P144972; locality PL1989, Mirrabooka Formation; pygidium, lateral and dorsal views; ×2·25.

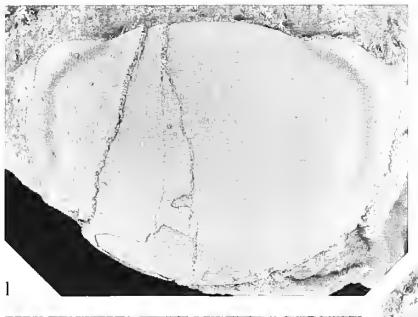
1


2


3

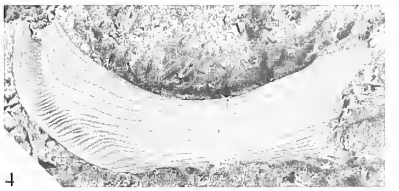
4

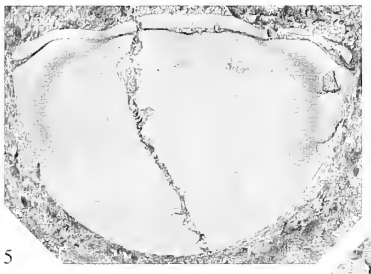
5

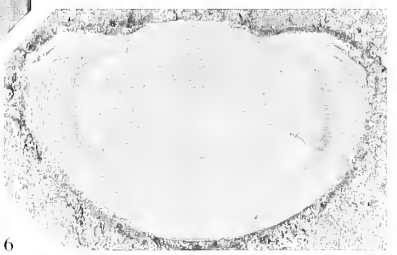
6

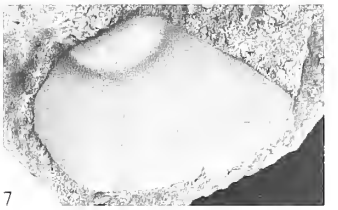
7

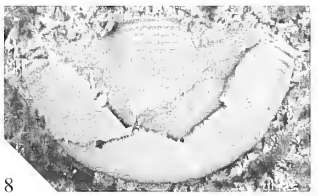
8

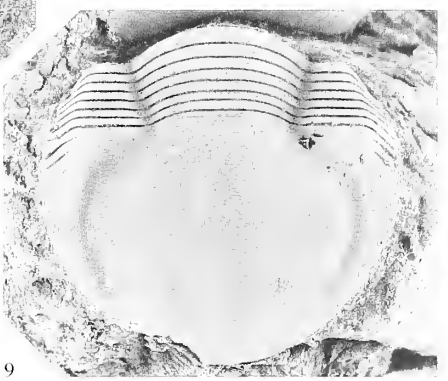
9

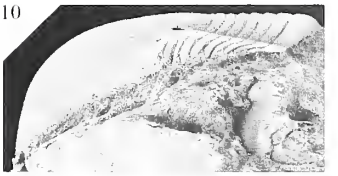
10

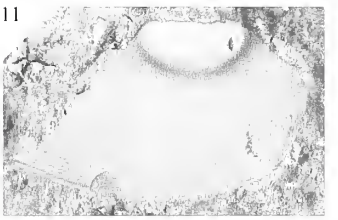
11

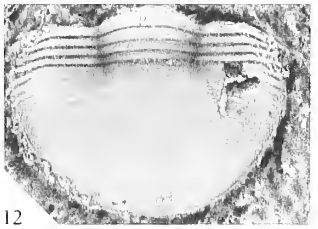
12


13

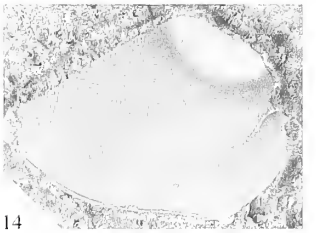
14


16

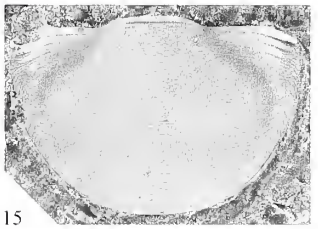
15

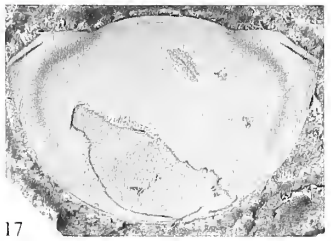
17


18

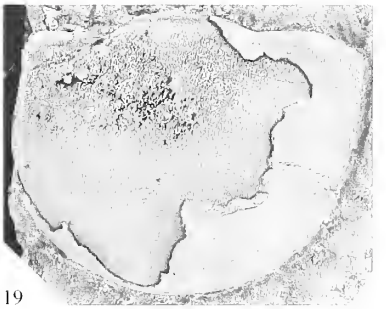
19

HOLLOWAY and LANE, *Bumastella*

of Tasmania. The specimens were deposited in the former Mining and Geological Museum in Sydney, but Dr I. Percival of the Geological Survey of New South Wales has advised us that they were transferred in the 1930s to the Australian Museum, where there is now no record of their existence (Mr R. Jones, pers. comm.). Nevertheless, Etheridge's illustrations of one of the cephala clearly show that it belonged to *Bumastella*. Other specimens of *Bumastella* collected by us in the vicinity of Borenore Caves are indistinguishable from *B. spicula* from the Mirrabooka Formation and the Molong Limestone farther to the west, and we consider them to be conspecific.

A tiny pygidium from the Borenore Limestone at Borenore Caves was tentatively assigned to *Illaenus wahlenbergi* Barrande by de Koninck (1876). The small size of the specimen (3 mm long by 2 mm wide), and de Koninck's description of it as having 'four segments of the thorax ... connected to it', suggest that it may have been a meraspid. It was not illustrated and has since been destroyed by fire, so its identity is indeterminate, but the fact that it was longer than wide suggests that it did not belong to *Bumastella spicula*.

Bumastella sp.

Plate 2, figures 16, 19

Material. A single pygidium from PL1989.

Remarks. This pygidium differs from similarly sized pygidia of *Bumastella spicula*, including those from the same locality, and apparently belongs to a separate species. The differences from *B. spicula* include a more elongate outline, much lower convexity, a narrower axis anteriorly, a narrower (tr.) articulating facet and a correspondingly wider anterior pleural margin adaxial to the facet, a shallower holcos that does not extend as far backwards, finer pitting on the exterior of the exoskeleton, and several prominent ridges around the lateral and posterior margins instead of a single one. This is the only other species-group form of *Bumastella* known.

Genus BUMASTUS Murchison, 1839

Type species. By monotypy; *Bumastus Barriensis* Murchison, 1839; Barr Limestone Member of the Coalbrookdale Formation; Hay Head lime works, Great Barr, West Midlands Metropolitan County, UK.

Other species. *B. danielsi* (Miller and Gurley, 1893), *B. graftonensis* (Meek and Worthen, 1870), *B. ioxus* (Hall, 1867).

Diagnosis. See Lane and Thomas 1978*a*, p. 11.

Remarks. The taxonomic problems that effacement in trilobites has caused historically are well illustrated by this genus. Since 1839, many species of Ordovician and Silurian effaced trilobites have been referred to *Bumastus* which, until the early part of the twentieth century, was almost universally considered to be a subgenus of *Illaenus* (e.g. Barrande 1852; Burmeister 1843; Salter 1867; Holm 1886; Vogdes 1890; Weller 1907). Most of these species have since been assigned to other genera. We consider that only the three species listed above, in addition to the type species, can be assigned with confidence to *Bumastus*.

Stratigraphical range and distribution. ?Late Llandovery to earliest Ludlow; USA (Arkansas, Illinois and Oklahoma) and UK (Welsh Borderland and West Midlands).

Bumastus? sp.

Plate 4, figures 17–18

Material. A single rostral plate from PL1995.

Remarks. This rostral plate cannot be assigned to any of the other effaced styginid species known from PL1995. The specimen is tentatively assigned to *Bunastus* because it has an upwardly flexed flange posteriorly, in this respect resembling the rostral plates of *B. barriensis* (see Lane and Thomas 1978*a*, pl. 2, fig. 1b–c) and *B.* cf. *ioxus* (Hall, 1867). The rostral plates of those species differ from the present specimen, however, in that the line along which the flange is flexed upwards is strongly convex backwards rather than transverse, and the flange itself is more concave (sag.) and is smooth instead of bearing well developed terrace ridges.

Genus EXCETRA gen. nov.

Derivation of name. Latin, referring to the fanciful resemblance of the cephalon, when viewed anterolaterally, to the head of a snake; gender feminine.

Type species. Excetra iotops gen. et sp. nov.

Diagnosis. Cephalon strongly convex in transverse profile, in sagittal profile gently convex in posterior half and strongly convex in anterior half. Axial furrow subparallel to sagittal line immediately behind lunette but diverging backwards closer to posterior cephalic margin, diverging gently forwards in front of lunette and dying out just in front of glabellar midlength (sag.); omphalus and anterolateral internal pit absent. G0 large, elliptical, not reaching axial furrow, situated less than its own length from posterior margin; G1 longer (exsag.) than G0, kidney-shaped, extending close to axial furrow anteriorly; G2 comma-shaped; G3 small, transverse. Posterior fixigenal margin with well-developed articulating flange bounded anteriorly by furrow that is flexed backwards distally. Eye small, of low convexity, with posterior edge transversely opposite midlength of lunette; socle absent. Posterior branch of facial suture weakly diverging backwards; anterior branch strongly diverging. Genal angle broadly rounded. Librigenal doublure with flattened facet on posterior edge. Connective suture converging backwards across anterior part of doublure and diverging backwards across posterior part, meeting inner edge of doublure close to outer end of hypostomal suture. Rostral plate gently inflated medially; posterolaterally with acute, upwardly curved projections abaxial to strongly transversely arched hypostomal suture. Thoracic axis parallel-sided, comprising about half segmental width (tr.); articulating furrows present on axial rings; axial furrow distinct; pleurae steeply downturned abaxial to narrow (tr.), horizontal proximal portion. Pygidium moderately to strongly convex, with articulating half ring defined by well impressed articulating furrow; anteriormost pleural furrow very weakly defined adaxially, holcos absent; articulating facet rather weakly defined posteriorly.

Remarks. The cephalon of *Excetra* resembles that of *Ligiscus*, known from the type species, *L. arcanus* Lane and Owens, 1982 (p. 47, pl. 3, figs 4–8; fig. 3) from the uppermost Llandovery or lowest Wenlock of western North Greenland, and *L. smithi* Adrain, Chatterton and Blodgett, 1995 (p. 726, figs 2.1–2.2, 2.4–2.15, 3.13, 3.15–3.16) from the upper Llandovery of Alaska. The similarities include the moderate convexity of the cephalon, the axial furrow that is subparallel immediately behind the lunette and posteriorly divergent farther backwards, the absence of the omphalus, the articulating flange on the posterior cephalic margin bounded in front by a distinct furrow, the medially inflated rostral plate, and the thorax with relatively narrow (tr.), subparallel-sided axis, deep axial furrow, and articulating furrows on each of the axial rings (see Adrain *et al.* 1995). The cephalon of *Ligiscus* differs from that of *Excetra* in that the eye is much larger and is situated farther back, with its anterior edge opposite the front of the lunette; the axial furrow is more distinct in front of the lunette; G0 and G1 both extend laterally to the axial furrow, G0 is situated farther from the posterior cephalic margin and G1 is sub-quadrate rather than kidney-shaped; G2 is ovate rather than comma-shaped; the anterior branch of the facial suture is more divergent; the genal angle has a short, broad spine; the connective suture apparently converges backwards across the entire doublure instead of diverging across the posterior part; and the rostral

plate apparently lacks upturned projections posterolaterally. The pygidium of *Ligiscus*, very poorly known in the type species but well documented in *L. smithi*, is not similar to that of *Excetra*, being much less convex and having a distinct axis and well-defined pleural ribs and furrows.

Excetra iotops sp. nov.

Plate 3, figures 1–19; Plate 4, figures 1–10, 13

Derivation of name. Combination of Greek 'iota' – small, and 'ops' – eye.

Holotype. Cephalon NMV P144713 (Pl. 3, figs 1–3); from PL1989.

Paratypes. Cephala NMV P144712, NMV P144717; cranidia NMV P144714–P144716, P144718, P144721, P144723–P144725, P144727, P144730, P144733; librigenae NMV P144736–P144737; rostral plates NMV P144739, P144903; incomplete thorax NMV P144751; pygidium with attached thoracic segment NMV P144731; pygidia NMV P144734, P144741–P144747, P144749–P144750, P144752, P144754; all from PL1989.

Other material. Two fragmentary cephala, five cranidia and five pygidia from PL1989.

Diagnosis. As for the genus.

Description. Cephalon *c.* 80 per cent. as long as wide (sag.) in dorsal view, widest just in front of genal angle; anterior and lateral margins uniformly curved; posterior margin of glabella gently convex backwards. Glabella gently convex (tr.) in posterior half, slightly more than half maximum width of cephalon at posterior margin, width at lunette *c.* 75 per cent. of posterior width. Median pit present on glabellar interior opposite posterior edge of G0. Lunette sub-circular, situated more than its own length from posterior edge of cephalon. Eye situated more than twice its own length from posterior cephalic margin; palpebral lobe bounded adaxially by weak furrow. Anterior and posterior branches of facial suture meeting cephalic margin approximately on same exsagittal line as palpebral suture; posterior branch with gentle sigmoidal curve; anterior branch almost straight just in front of eye, where it diverges at about 40° to sagittal axis, and broadly curved anteriorly. Posterior articulating flange strongly downturned at mid-width (tr.); articulating furrow deeper than axial furrow.

Cephalic doublure expanding and greatly increasing in convexity anteromedially towards abaxial end of hypostomal suture; facet on posterior edge of doublure not extending abaxially as far as genal angle. Median part of hypostomal suture gently arched in transverse profile, convex backwards in ventral profile; lateral part of suture deflected posterolaterally and dorsally. Narrowest (tr.) part of rostral plate situated on transverse line through median part of hypostomal suture.

Thoracic axial rings strongly arched (tr.), decreasing very slightly in length sagittally; articulating furrows short (sag., exsag.) and shallow. Inner part of pleurae (about 40 per cent. of transverse width) with very short (exsag.) articulating flange on anterior edge; outer part of pleurae gently convex (tr.), with pointed tips.

Pygidium 110–120 per cent. as wide as long (sag.) in plan view. Articulating half ring slightly less than half maximum pygidial width, gently convex (sag., exsag.). Adaxial part of anterior pleural margin with narrow (tr.)

EXPLANATION OF PLATE 3

Figs 1–19. *Excetra iotops* gen. et sp. nov.; locality PL1989, Mirrabooka Formation. 1–3, NMV P144713, holotype; cephalon, dorsal, anterior and lateral views; ×4·5. 4, NMV P144717; cephalic doublure, ventral view; ×4. 5–6, NMV P144903; rostral plate, ventral and posterior views; ×3·5. 7, NMV P144730; cranidium, palpebral view; and NMV P144731; pygidium with posteriormost thoracic segment (see Pl. 4, fig. 6), oblique view; ×4. 8–10, NMV P144727; smallest cranidium, palpebral, anterior and lateral views; ×8. 11–12, NMV P144723; cranidium, palpebral and lateral views; ×6. 13, NMV P144718; cranidium, palpebral view; ×5. 14–15, 18–19, NMV P144712; largest cephalon, palpebral, lateral and oblique views; ×3; and detail showing muscle scars on interior of glabella and fixigena; ×5. 16–17, NMV P144737; librigena, oblique dorsal and oblique ventral views; ×5.

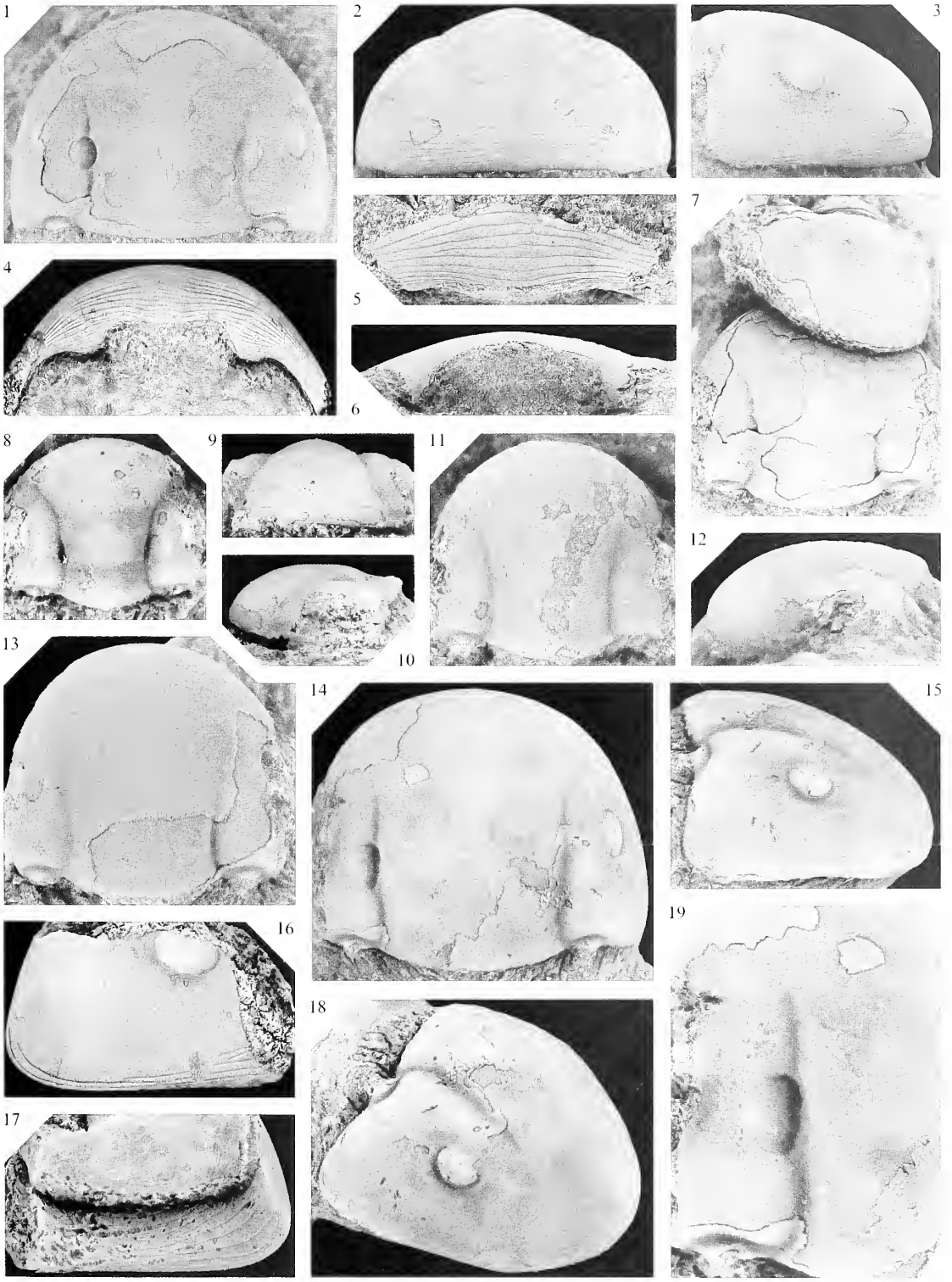

HOLLOWAY and LANE, *Excetra*

articulating flange similar to, but weaker than, that on cephalon; abaxial to flange, anterior edge of articulating facet is weakly deflected forwards in plan view. Doublure steeply inclined, increasing slightly in width toward sagittal line where it is *c.* 40 per cent. of pygidial length in plan view; outer part of doublure gently convex, inner part gently concave and bearing about six pairs of weak radial furrows.

Sculpture. Fine, dense pits extend over external surface of cephalon and pygidium. Marginal band of subparallel terrace ridges present on anterior and lateral parts of cephalon, and curving inwards for a short distance adaxial to genal angle; this band very narrow (one to two ridges wide) posterolaterally, widest anteromedially (ten to thirteen ridges wide). Upturned part of cephalic doublure abaxial to hypostomal suture with terrace ridges more widely spaced than on narrow outer portion of doublure; terrace ridges on outer portion of doublure diverge adaxially onto rostral plate. Pygidium with terrace ridges present anterolaterally on dorsal surface, where they are largely restricted to articulating facet, running subparallel to pygidial margin on front of facet and curving posterolaterally farther back; one or two ridges extend along pygidial margin behind facet to about 75 per cent. pygidial length from anterior in plan view. Terrace ridges on outer part of pygidial doublure more closely spaced than on inner part of doublure.

Muscle scars. Glabellar muscle scars faint on external surface; on interior slightly raised (i.e. impressed on internal mould), sharply delimited and with a weak dendritic pattern on G0 and G1. G0 longer (exsag.) than wide, length equal to that of eye; G1 with posterior edge opposite front of lunette and anterior edge opposite front of axial furrow, extending closer to axial furrow anterolaterally than does G0; G2 broader abaxially than adaxially, not extending as far abaxially as G1, anterior edge at about 25 per cent. glabellar length from anterior in palpebral view; G3 close to G2 and extending farther abaxially. Interior of fixigena with numerous, small, raised scars, except on lunette (Pl. 3, fig. 9).

Pygidia with a pair of weakly impressed, sub-circular or exsagittally elongated scars (slightly raised on interior), situated either side of sagittal line a short distance behind articulating furrow (Pl. 4, fig. 5); in some specimens, these scars joined to articulating furrow by faint, anteriorly diverging furrows (Pl. 4, fig. 8). Lateral and posterolateral to these paired scars, interior of pygidium has numerous, mostly small, raised scars, some of which are arranged in six or more radial rows (Pl. 4, fig. 5) that are reflected on external surface of some specimens as extremely faint furrows; larger, radially elongated scars present towards adaxial ends of some rows (Pl. 4, fig. 9).

Ontogeny. The two smallest cranidia (sagittal length 3·3 mm in palpebral view; Pl. 3, figs 8–10) show distinct differences from the largest ones on which the preceding description is based. The differences are as follows.

1. The axial furrow is deeper, especially anteriorly where it extends almost to the cranidial margin, diverging quite strongly forwards from a point transversely opposite the front of the palpebral lobe.
2. The glabella is narrower in its posterior half (in relation to the sagittal length of the cranidium and the width across the palpebral lobes).
3. The occipital furrow is present as a shallow depression that is longer (sag., exsag.) than the occipital ring and contains muscle scar G0 laterally.
4. The occipital ring is slightly inflated medially and bears two median tubercles: a larger one on the posterior edge of the ring and a smaller one just in front.
5. G1 is more distinct on the exterior of the exoskeleton.
6. The fixigena behind the front of the palpebral lobe is not as steeply declined abaxially (compare Pl. 3, figs 2, 9).
7. There is a shallow depression on the front of the fixigena, running subparallel to and close to the anterior cephalic margin.
8. The palpebral lobe is relatively longer, the palpebral furrow is more distinct, and there is a weak eye ridge directed anteromedially from the front of the palpebral lobe.
9. The anterior and posterior branches of the facial suture diverge more strongly from either end of the palpebral lobe.
10. The lunette is larger and extends farther back, to about its own length from the posterior edge of the cephalon.

Remarks. The position of the paired muscle impressions on the anteromedian part of the pygidium of *Excetra iotops*, and the fact that in some specimens they are joined to the articulating furrow by a faint, anteriorly diverging furrow, suggest that they are homologous with the pits at the posterior end of the furrow that divides the pygidial axis longitudinally in some non-effaced styginids (see

Planiscutellum kitharos Lane and Thomas, 1978*a*, pl. 6, fig. 4b). Also probably homologous are the smooth, ovate areas on the posterolateral part of the pygidial axis of *Meroperix ataphrus*, described and illustrated by Lane (1972, p. 345, pl. 60, fig. 4b). This evidence suggests that the pygidial axis of *Excetra iotops* is very short, as in other styginids.

Genus LALAX gen. nov.

Derivation of name. Greek 'frog', alluding to the protuberant eye and palpebral area; gender masculine.

Type species. Lalax olibros gen. et sp. nov.

Other species. L. bandaletovi (Maksimova, 1975); *L. bouchardi* (Barrande, 1846) (= *Bumastus praeruptus* Kiær, 1908; see Helbert *et al.* 1982, p. 133); *L. chicagoensis* (Weller, 1907); *L. clairensis* (Thomas, 1929); *L. hornyi* (Šnajdr, 1957); *L. inflatus* (Kiær, 1908) (= *Bumastus phrix* Lane and Thomas, 1978*a*; see Helbert 1984, p. 134); *L. kattoi* (Kobayashi and Hamada, 1984); *L. lens* sp. nov.; *L. xestos* (Lane and Thomas, 1978*a*); *L.*? *sakoi* (Kobayashi and Hamada, 1984); *L.*? *transversalis* (Weller, 1907).

Diagnosis. Cephalon strongly convex (sag.), curvature in sagittal plane subtending more than 90°, height in lateral profile greater than or equal to sagittal length. Omphalus and anterolateral internal pit present. Axial furrow diverging moderately behind and immediately in front of lunette, dying out anteriorly behind omphalus. Eye large, situated less than its own length from posterior cephalic margin; socle not strongly convex (tr.). Posterior branch of facial suture strongly diverging backwards; anterior branch diverging moderately forwards. Genal angle broadly rounded. Rostral plate sub-triangular, gently convex (sag., exsag.) over anterior 70 per cent. and gently concave in posterior part, without upturned posterior flange; connective suture meeting hypostomal suture close to sagittal line; vincular furrow present across posterior edge of doublure. Thorax with very wide, gently arched axis comprising 60–70 per cent. segmental width (tr.); axial furrow weak; fulcrum situated very close to axial furrow; pleurae abaxial to fulcrum almost continuous in slope with lateral part of axial rings. Pygidium moderately convex (sag., exsag.), lenticular in dorsal view, maximum width just in front of midlength; anteriormost pleural furrow and holcos very weak or not defined. Terrace ridges present over most of dorsal surface of cephalon and pygidium.

Remarks. Bumastus is most easily distinguished from *Lalax* by its rostral plate that is lenticular rather than triangular in outline in ventral view and has a vertical, concave (sag.) posterior flange, and by the connective suture meeting the hypostomal suture a little farther from the sagittal line. Distinguishing the genera may be difficult in the absence of information on the rostral plate, but in *Bumastus* G0 and G1 are confluent rather than separate (compare Lane and Thomas 1983, text-fig. 2a, d); the omphalus is absent, although the anterolateral internal pit may be present; the visual surface is longer (exsag.) and narrower (tr.), with upper and lower margins parallel over almost their entire length; and the socle is more convex (tr.) and is separated from the visual surface by a deeper furrow.

In the presence of the omphalus and the anterolateral internal pit, and the outline of the rostral plate, *Lalax* is similar to *Cybantyx* (see Lane and Thomas 1978*a*, pl. 5, figs 1–8). *Cybantyx* differs from *Lalax* in having a narrow, upturned anterior and lateral cephalic border; the lunette is situated slightly farther forwards, with its anterior edge slightly in front of the anterior edge of the eye in palpebral view; the axial furrow is more distinct in front of the lunette, extending as far as the omphalus; the anterior branch of the facial suture converges weakly in front of the palpebral lobe instead of diverging; the posterior part of the rostral plate is not concave (sag.); and the pygidium is longer.

Litotix Lane and Thomas, 1978*a*, with type and only known species *L. armata* (Hall, 1865; see annotation of this reference below; Lane and Thomas 1978*a*, pl. 4, figs 8–18; text-fig. 4a–e) resembles *Lalax* in the convexity and proportions of the cephalon and pygidium, and in the presence of the omphalus. The rostral plate of *Litotix* is unknown, but the weak sagittal carina on the

cephalon, the axial furrow that extends anteriorly to the omphalus, the absence of the anterolateral internal pit, and the spinose genal angle are differences from *Lalax*.

Two species are assigned to the genus with question. *L. sakoi* (see Kobayashi and Hamada 1985*b*, pl. 30, fig. 1) is known only from a cranidium, but may be synonymous with *L. kattoi* (see Kobayashi and Hamada 1985*b*, pl. 30, fig. 5), which is from the same locality and appears to differ only in its larger size; also possibly belonging to the same species is the pygidium assigned to *Bumastus glomerosus* by Kobayashi and Hamada (1987, p. 110, fig. 1A, 2.1a–d; see synonymy of *Bumastella spicula* herein). *L.? transversalis* is based on incomplete cephala differing from those of other species in the transverse outline and the convexity of the librigenal field; the form of the rostral plate is unknown. The only specimen of *L. clairensis* that has been figured is an internal mould of a cranidium (Thomas 1929, pl. 1, fig. 6), but one of us (DJH) has studied additional material, including librigenae and an incomplete cephalon with part of a rostral plate, allowing confident assignment of the species to *Lalax*. Also assigned here to *Lalax* are the specimens from the Estonian islands of Saaremaa and Muhu figured by Holm (1886, p. 164, pl. 11, figs 12–16) as '*Illaenus*' *barriensis*.

Stratigraphical range and distribution. ?Late Llandovery (or early Wenlock) to Ludlow; eastern USA, UK (Welsh Borders), southern Norway, Estonia, Bohemia, Kazakhstan, Japan and New South Wales.

Lalax olibros sp. nov.

Plate 4, figures 11–12, 14–16, 19–20; Plate 5, figures 1–23;
Plate 6, figures 9, 13, 16, 18

Derivation of name. Greek 'slippery', referring to the smooth, effaced appearance of the exoskeleton.

Holotype. Pygidium NMV P144800, Pl. 6, figs 9, 13, 16, 18; from PL1993.

Paratypes. From PL1993: cephala NMV P144758–P144760, P144762–P144763; cranidia NMV P144765–P144767, P144770, P144772; cranidium with incomplete thorax NMV P144771; librigenae NMV P144780–P144785, P144788–P144790; rostral plates NMV P144792–P144794; hypostome NMV P144796; incomplete thorax NMV P145048; pygidia (including meraspid transitory pygidia) NMV P144773, P144797, P144801–P144804, P144806–P144808, P144810. From PL1991: cephalon NMV P144819; cranidium P144817; pygidium with incomplete thorax NMV P144822. From PL1998: cranidium NMV P144811; librigena NMV

EXPLANATION OF PLATE 4

Figs 1–10, 13. *Excetra iotops* gen. et sp. nov.; locality PL1989, Mirrabooka Formation. 1–2, 4, NMV P144746; pygidium, dorsal, lateral and anterodorsal views; ×4·5. 3, NMV P144751; incomplete thorax, dorsal view; ×7. 5, NMV P144747; pygidium, dorsal view; ×4. 6, NMV P144731; pygidium with posteriormost thoracic segment articulated, dorsal view; ×5. 7, 10, 13, NMV P144743; pygidium with dorsal surface excavated to expose external mould of doublure, dorsal, posterior and lateral views; ×3·25. 8, NMV P144744; pygidium, detail to show weak longitudinal furrows connecting paired muscle scars to articulating furrow, dorsal view; ×5·5. 9, NMV P144741; pygidium, detail showing muscle scars arranged in longitudinal rows on interior of exoskeleton, dorsal view; ×5.

Figs 11–12, 14–16, 19–20. *Lalax olibros* gen. et sp. nov.; Mirrabooka Formation; locality PL1993 unless otherwise indicated. 11, NMV P144812; locality PL1998; librigena, oblique view; ×5. 12, NMV P144780; librigena, latex cast, ventral oblique view; ×4. 14, NMV P144789; librigena, oblique view; ×7. 15, NMV P144782; librigena, oblique view; ×4. 16, NMV P144796; hypostome, latex cast in ventral view; ×5. 19, NMV P144771; cranidium with three articulated thoracic segments, dorsal view; ×3. 20, NMV P145048; incomplete thorax, dorsal view; ×4.

Figs 17–18. *Bumastus*? sp.; locality PL1995, Molong Limestone; NMV P145047; rostral plate, ventral and posteroventral views; ×4.

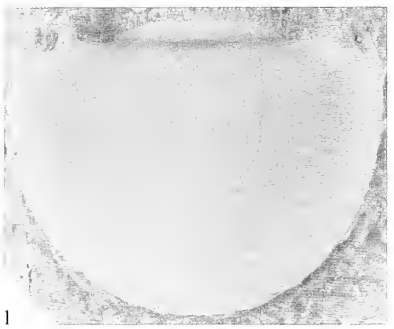
1


2


3

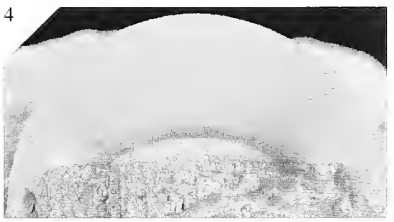
4

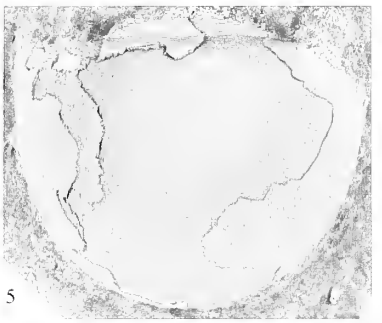
5


6


7

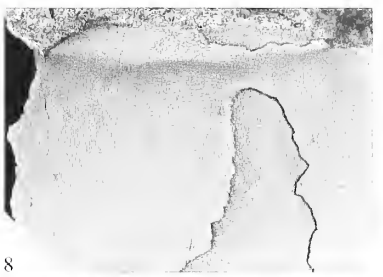
8

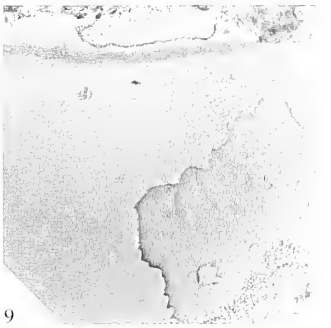
9

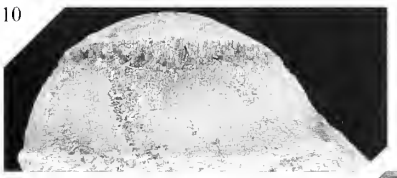
10

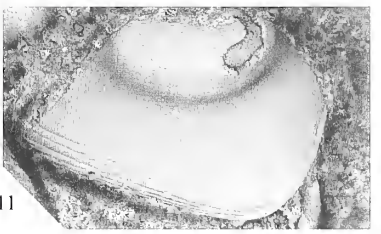
11

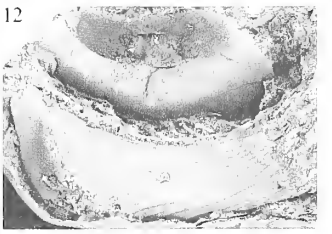
12

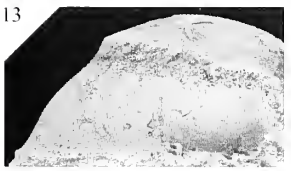
13

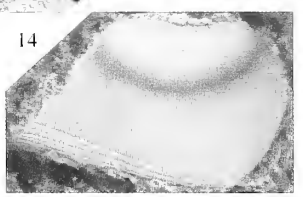
14

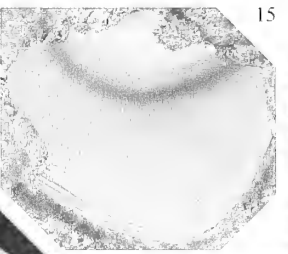
15

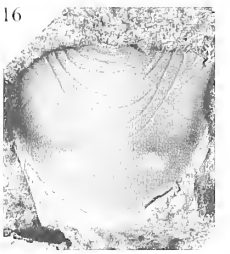
16

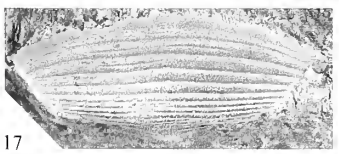
17


18


19

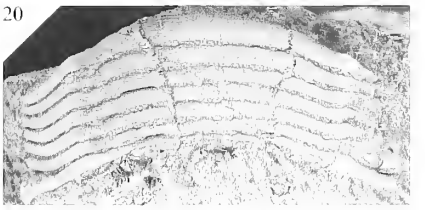
20

HOLLOWAY and LANE, *Excetra*, *Lalax*, *Bumastus*?

P144812; pygidia (including meraspid transitory pygidia) NMV P144813–P144814, P144816, P144944. From PL3301: cranidium NMV P145052; pygidium NMV P145049. From PL3303: cranidium NMV P145051.

Other material. Five cephala, 14 cranidia, five librigenae, a rostral plate, a pygidium with incomplete thorax and seven pygidia from PL1993, PL1991, PL1995 and PL3303.

Diagnosis. Cranidium *c.* 130 per cent. as wide across palpebral lobes as long (sag.) in palpebral view. Axial furrow almost indistinguishable behind lunette; latter situated with posterior edge just in front of posterior edge of palpebral lobe. Anterolateral internal pit lying slightly adaxial to exsagittal line through omphalus. Connective suture subtending angle of *c.* 105° at back of rostral plate. Pygidium strongly convex, more so in posterior than in anterior half; anteriormost pleural furrow and holcos not defined. Terrace ridges confined to anterior, lateral and posterior margins of cephalon, posterior part of librigenal field, and anterior margin of pygidium. Cranidial muscle impressions indistinguishable.

Description. Cephalon convex, in lateral view sagittal profile describing an arc of *c.* 120°, in anterior view transverse profile rather less that semicircular; in palpebral view sagittal length 70 per cent. of maximum transverse width, which is level with posterior half of palpebral lobe. Axial furrow barely discernible posterior to very weakly impressed lunette, not defined in front of lunette. Interior of cephalon with median pit (forming median node on internal moulds) about half way between posterior margin and transverse line through back of lunette. Palpebral lobe indicated in anterior view by slight upward break in slope from uniform transverse convexity of glabella and adjacent fixigena; in palpebral view, palpebral lobe about 40 per cent. of sagittal length of cephalon, situated about 60 per cent. of its own length from posterior cephalic margin. Anterior section of facial suture gently sigmoidal, diverging slightly forwards from front of palpebral lobe, converging fairly strongly anteriorly in a broad arc to meet rostral suture more-or-less on an exsagittal line through anterolateral internal pit; posterior section of suture short, weakly sigmoidal, directed posterolaterally at an angle of *c.* 30° to transverse direction. Librigena convex (exsag., tr.), steeply inclined, slightly overhanging lateral margin; genal angle broadly rounded. Visual surface gently convex dorsoventrally, in dorsal view almost paralleling curvature of lateral margin of librigena; lenses (visible only as impression on internal moulds) tiny, increasing slightly in size towards top of eye. Socle highest at midlength, weakly convex (tr.) except anteriorly where it dies out into broad, shallow furrow at front of eye.

Rostral plate 40 per cent. as long (sag.) as maximum width (tr.); width across hypostomal suture *c.* 10 per cent. maximum width; rostral suture gently convex forwards; connective sutures weakly convex outwards in anterior half and weakly concave outwards in posterior half. Abaxial to rostral plate, doublure decreases in convexity posteriorly; vincular furrow well rounded in cross section.

Hypostome about twice as wide across anterior wings as long (sag.); lateral margin almost straight and converging strongly backwards between anterior and posterior wings; posterior margin rounded. Maculae

---

EXPLANATION OF PLATE 5

Figs 1–23. *Lalax olibros* gen. et sp. nov.; Mirrabooka Formation unless otherwise indicated. 1–2, NMV P144817; locality PL1991; cranidium, palpebral and lateral views; ×2·5. 3–4, 7, NMV P144762; locality PL1993; small cephalon, anterior, lateral and palpebral views; ×4·5. 5, NMV P144819; locality PL1991; cephalic doublure, ventral view; ×3. 6, NMV P144793; locality PL1993; rostral plate, ventral view; ×4. 8–10, NMV P144766; locality PL1993; largest cranidium, posterodorsal, palpebral and oblique views; ×2. 11–12, 17, NMV P144813; locality PL1998; pygidium, latex cast in ventral view; ×2·5; detail of internal mould showing muscle scars; ×4; internal mould, lateral view; ×2·5. 13, NMV P144808; locality PL1993; transitory pygidium with two protothoracic segments, dorsal view; ×6. 14, NMV P144806; locality PL1993; transitory pygidium with one protothoracic segment, dorsal view; ×4·5. 15, NMV P144810; locality PL1993; transitory pygidium with four protothoracic segments, dorsal view; ×8. 16, NMV P144760; locality PL1993; cephalon, lateral view; ×3. 18–19, NMV P144802; locality PL1993; pygidium, lateral and dorsal views; ×3. 20, NMV P144944; locality PL1998; smallest transitory pygidium, with five protothoracic segments, dorsal view; ×8. 21–22, NMV P145049; locality PL3301, Borenore Limestone; pygidium, lateral and dorsal views; ×2. 23, NMV P144797; locality PL1993; pygidium, dorsal view; ×1·75.

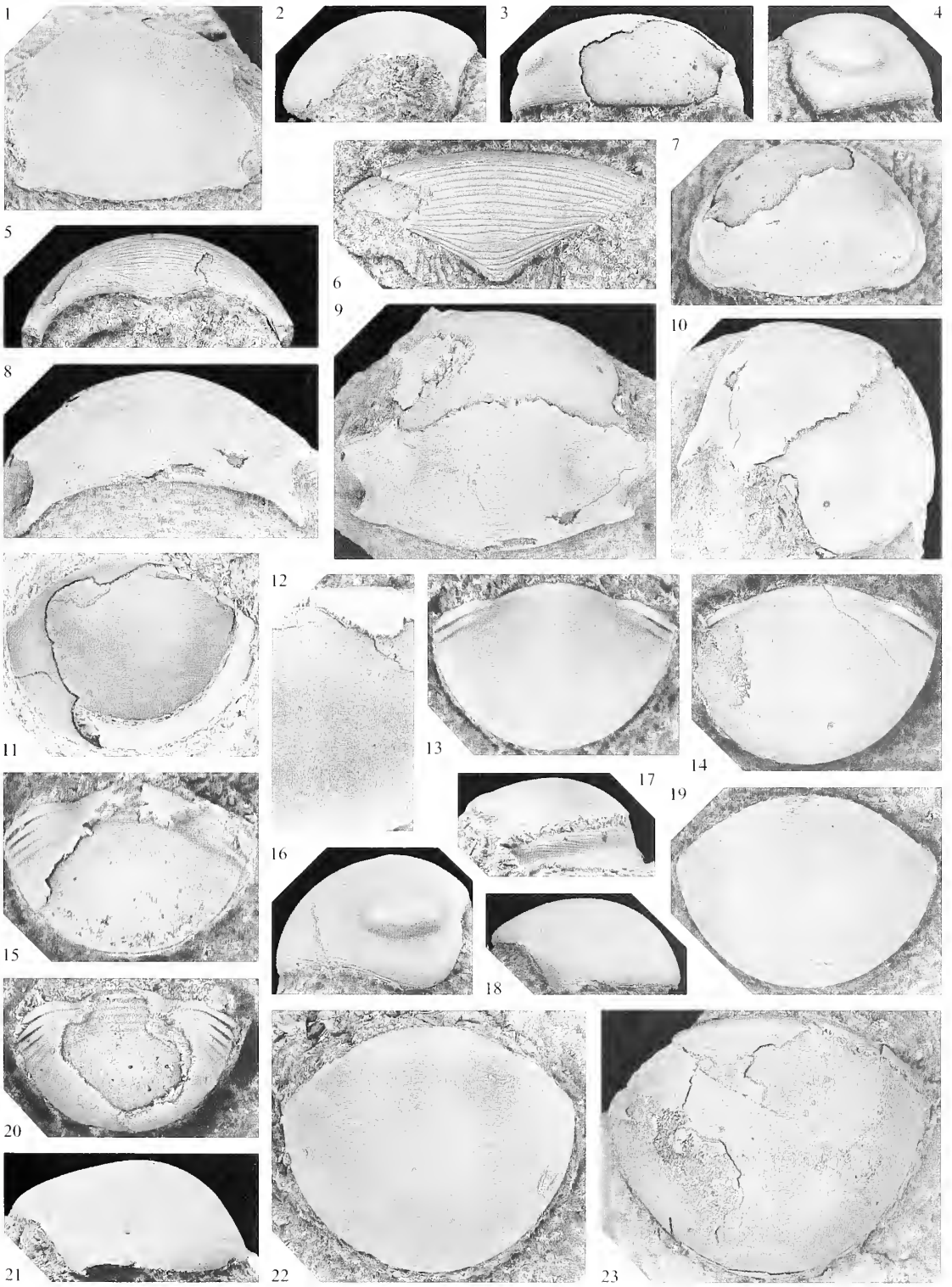

HOLLOWAY and LANE, *Lalax*

inflated, situated at about 60 per cent. of hypostomal length (sag.) from anterior; middle furrow shallow abaxially, not impressed medially. Anterior lobe of middle body sub-trapezoidal, strongly convex transversely and weakly convex sagittally, sloping fairly steeply backwards; posterior lobe of middle body crescentic, moderately convex transversely and gently concave sagittally. Lateral and posterior borders narrow, rounded in section; border furrows shallow.

Thoracic axis narrowing gently backwards, comprising 60–65 per cent. of total segmental width (tr.); pleurae successively more weakly flexed backwards at fulcrum from front to back of thorax; anterior edge of segments with wide (tr.) articulating flange at inner end of facet.

Pygidium ovate; in plan view length (sag.) 75 per cent. of maximum width, which is situated in front of midlength. Anterior margin gently arched forwards between fulcra, distance between fulcra *c.* 65 per cent. maximum pygidial width; articulating facet short (exsag.), with panderian protuberance on anterior edge at *c.* 40 per cent. distance from abaxial to adaxial extremities of facet. Posterior pygidial margin broadly rounded. Doublure convex, steeply inclined, occupying *c.* 15 per cent. of sagittal length of pygidium in plan view, narrowing forwards a little and increasing in convexity near anterolateral extremity of pygidium.

Sculpture. Dorsal surface of cephalon and pygidium covered with fine pits, except on lunette and visual surface of eye; these pits are external openings of perforations that are surrounded on interior of exoskeleton by raised rims (visible on internal moulds as tiny pits *c.* 0·1 mm in diameter). Anterior and posterior parts of cranidium with terrace ridges running subparallel to cephalic margins; terrace ridges on posterior part of librigenal field weakly sinuous, anastomosing and running subparallel to base of eye, dying out on anterior part of librigenal field. Terrace ridges on cephalic margins, rostral plate and strongly convex outer part of librigenal doublure are higher, more closely spaced and more continuous than on dorsal surface and on steeply inclined inner part of librigenal doublure; narrow (sag., exsag.) band devoid of terrace ridges present across front of rostral plate (Pl. 5, fig. 6); on posterior part of librigenal doublure, terrace ridges do not extend behind anterior slope of vincular furrow. Terrace ridges on front of pygidium running subparallel to anterior margin, most closely spaced laterally on and just behind articulating facet, deflected backwards at lateral pygidial margin. On pygidial doublure terrace ridges run concentrically, except anterolaterally where they gently curve abaxially across doublure. Interior of pygidium with a narrow, slightly impressed (slightly raised on internal mould) sagittal band extending over posterior half of pygidium; this sagittal band is devoid of openings of exoskeletal perforations.

Muscle scars. A pygidium of moderate size (maximum width 16·3 mm) has a pair of small, circular muscle scars, situated close to sagittal line opposite maximum pygidial width in plan view (Pl. 5, figs 11–12); these scars are slightly raised on interior of exoskeleton (weakly impressed on internal mould). Adjacent to these scars posterolaterally there may be a pair of larger, extremely weak sub-circular scars.

The two smallest meraspid transitory pygidia have a pair of elliptical or ovate muscle scars gently impressed on the interior of the exoskeleton (slightly raised on internal mould) opposite the lateral extremity of the future pygidium (Pl. 5, figs 15, 20). Between the scars, and extending forwards to the front of the future pygidium, is a conical, slightly raised (on internal mould) area, probably representing at least in part the axis. Similar scars are present in pygidia of *L. bouchardi* (see Šnajdr 1957, pl. 11, fig. 11) and *L. inflatus* (= *Bumastus phrix*) of Lane and Thomas (1978*a*, pl. 3, figs 3, 10).

Ontogeny. The progressive decrease in the number of protothoracic segments with increasing size of meraspid transitory pygidia has been outlined above in the section on segmental variation. Other morphological changes occurring during ontogeny include the following.

1. A slight node is present on the genal angle in the smallest cephala and librigenae (Pl. 4, fig. 14; Pl. 5, fig. 4) but is lost in larger specimens.
2. The eye decreases in size relative to the sagittal length of the cephalon, and the librigenal field correspondingly increases in width (compare Pl. 4, figs 14–15).

Remarks. Of previously described species of this genus, the best known are *L. bouchardi* from the Wenlock of Bohemia (Šnajdr 1957, p. 109, pl. 10, figs 1–9, pl. 11, figs 1–13) and the Oslo Region, Norway (Whittard 1939, p. 287, pl. 3, figs 1–4), and *L. inflatus* from the Wenlock of Norway (Whittard 1939, p. 289, pl. 3, figs 5–8) and the Welsh Borderlands (Lane and Thomas 1978*a*, p. 14, pl. 3, figs 1–22). Both of these species differ from *L. olibros* in having terrace ridges more widely distributed on the cephalon and pygidium, and forming a concentric elliptical pattern on the

librigenal field; and in having a less convex pygidium with weak but distinct anteriormost pleural furrow and holcos. Examination of type and other specimens of *L. bouchardi* shows that this species also differs from *L. olibros* in having a more distinct cephalic axial furrow; the palpebral lobe is situated closer to the posterior cephalic margin and the cranidium in front of the palpebral lobe is relatively longer; there is a short (sag., exsag.), slightly convex border on the anterior and lateral cephalic margins; and the anterior section of the facial suture is straighter. *Lalax inflatus* also differs from *L. olibros* in having the anterolateral internal pit situated closer to the omphalus and slightly abaxial rather than adaxial to it; the eye socle is more convex posteriorly where it is separated from the visual surface by a deeper furrow; and the terrace ridges on the librigenal doublure extend farther posteriorly, across the vincular furrow.

Šnajdr (1957, pl. 10, figs 10–11) illustrated only a pygidium and an incomplete cranidium of *Lalax hornyi*, from the Ludlow of Bohemia, but an articulated dorsal exoskeleton (see Barrande 1872, pl. 16, figs 15–18; Šnajdr 1990, p. 147) from a similar horizon at a different locality was assigned to this species by Marek (*in* Horný and Bastl 1970, p. 83). This specimen differs from *L. olibros* in having terrace ridges arranged in a concentric ellipse on the librigenal field, a deeper furrow below the eye socle, the anterolateral internal pit (visible on exterior of exoskeleton) situated anterolateral to the omphalus instead of anteromedial to it, a less convex pygidium with a distinct holcos, terrace ridges covering almost the entire dorsal surface of the pygidium, and a weak sagittal ridge on the posterior half of the pygidium.

The smallest meraspid transitory pygidia of *Lalax olibros* and *Bumastella spicula* are exceedingly alike (compare Pl. 2, fig. 8 and Pl. 5, fig. 20). The specimen of *B. spicula* is distinguished by its much weaker convexity and very weakly developed anteriormost pleural furrow on the future pygidium.

Lalax lens sp. nov.

Plate 6, figures 1–8, 10–12, 14–15, 17, 19–20

Derivation of name. Greek 'lens', referring to the similarity of the outline of the pygidium to a biconvex lens.

Holotype. Cranidium NMV P144824 (Pl. 6, figs 1–3); from PL1989.

Paratypes. Cranidia NMV P144823, P144825–P144826; librigenae NMV P144827–P144829; rostral plates NMV P144831–P144832; pygidia with incomplete thoraces NMV P144836–P144837; pygidia NMV P144833–P144835, P144929, P145046; all from PL1989.

Diagnosis. Cranidium *c.* 110 per cent. as wide across palpebral lobes as long (sag.) in palpebral view. Axial furrow shallow but distinct behind lunette; latter situated with posterior edge well in front of posterior edge of palpebral lobe. Connective suture subtending angle of *c.* 145° at back of rostral plate. Pygidium evenly convex in sagittal profile. Terrace ridges present over entire dorsal surface of pygidium, and all of cephalon except for median part of cranidium between front of palpebral lobe and posterior edge of lunette.

Description. The description of *L. olibros* applies also to *L. lens*, except for details of muscle scars and the differences listed below in the remarks.

Muscle scars. These are most easily seen in largest cranidium (Pl. 6, fig. 4), in which they are weakly impressed and also defined by fine wrinkling or reticulate ridging of external surface, although edges of scars are poorly defined. G0 largest, sub-circular, situated midway between sagittal line and axial furrow, and less than its own length from posterior cephalic margin; anterior edge of scar opposite back of palpebral lobe in palpebral view. G1 situated slightly closer to sagittal line than G0, elongated exsagittally, in palpebral view with posterior edge level with narrowest part of glabella and anterior edge opposite or just behind front of palpebral lobe. G2 and G3 sub-circular; G2 situated same distance from sagittal line as G0 and at *c.* 38 per cent. of cephalic length from anterior in palpebral view; G3 slightly larger than G2, situated farthest from sagittal line, and in front of transverse line through omphalus in palpebral view.

Remarks. L. lens differs from *L. olibros* in the following.

1. The cranidium is relatively longer, especially in front of the palpebral lobe. In plan view, the anterior edge of the palpebral lobe is situated almost opposite the cephalic midlength (sag.) in *L. lens* but in front of the midlength in *L. olibros*.
2. The lunette is situated slightly farther forwards, with its posterior edge well in front of the back of the palpebral lobe, whereas in *L. olibros* the posterior edge of the lunette is almost level with the back of the palpebral lobe (compare Pl. 6, fig. 1 and Pl. 5, fig. 9).
3. The rostral plate is less acute in outline posteromedially (compare Pl. 6, fig. 17 and Pl. 5, fig. 6).
4. The pygidium is distinctly less convex (sag., exsag., tr.; compare Pl. 6, figs 9–11, 13).
5. Terrace ridges are more widely distributed on the exoskeleton. On the cranidium they extend from the anterior margin backwards almost to the front of the palpebral lobe, from the posterior margin as far forwards as the posterior edge of the lunette, and over most of the palpebral area. On the librigena terrace ridges cover most of the field and are separated from longer, straighter, more prominent and more closely spaced ridges on the lateral margin by a narrow groove that gradually converges with the librigenal margin towards the genal angle and becomes deeper; adaxial to the genal angle, this groove is crossed by several prominent, forwardly deflected terrace ridges and dies out. Terrace ridges are present over the entire dorsal surface of the pygidium.

Genus RHAXEROS Lane and Thomas, 1980

Type species. Rhax pollinctrix Lane and Thomas, 1978*b* from the Quinton Formation (Upper Llandovery) of northern Queensland.

Other species. R. latus (Chatterton and Campbell, 1980); *R. subquadratus* (Kobayashi and Hamada, 1974); *R. synaimon* sp. nov.; *R. trogodes* sp. nov; *R.? shinoharai* (Kobayashi and Hamada, 1974).

Diagnosis. Cephalon gently convex (sag., tr.); axial furrow converging anteriorly and posteriorly towards lunette, joining posterior border furrow in a curve; preglabellar and lateral border furrows may be weakly defined. Omphalus and anterolateral internal pit absent. Librigena with posterior margin slightly concave in outline and genal angle rounded or subangular; eye small to large, with bean-shaped visual surface; socle absent. Rostral plate lenticular in outline, without upturned posterior flange, gently transversely arched just in front of hypostomal suture; connective suture meeting hypostomal suture rather far from sagittal line. Librigenal doublure with fan-shaped vincular depression posterolaterally, just in front of flattened, triangular facet on posterior margin. Hypostome about twice as wide across anterior wings as long (sag.), with subangular shoulder and posterior margin strongly rounded in outline; middle furrow deep abaxially; macula inflated. Thorax with evenly arched axis comprising 60–70 per cent. segmental width (tr.), and with pleurae

---

EXPLANATION OF PLATE 6

Figs 1–8, 10–12, 14–15, 17, 19–20. *Lalax lens* sp. nov.; locality PL1989, Mirrabooka Formation. 1–3, NMV P144824, holotype; cranidium, palpebral, anterior and lateral views; ×1·75. 4, NMV P144823; largest cranidium, palpebral view; ×1·5. 5–6, NMV P144825; cranidium, palpebral and lateral views; ×3. 7, NMV P144836; transitory pygidium with one protothoracic segment incompletely separated and two thoracic segments articulated, dorsal view; ×5. 8, 12, NMV P145046; pygidium, latex cast in ventral view and internal mould in lateral view; ×1·75. 10–11, 14, NMV P144833; pygidium, lateral, posterior and dorsal views; ×3. 15, NMV P144828; librigena, oblique view; ×2·5. 17, NMV P144832; rostral plate, ventral view; ×4. 19–20, NMV P144929; largest pygidium, lateral and dorsal views; ×1·5.

Figs 9, 13, 16, 18. *Lalax olibros* gen. et sp. nov.; NMV P144800, holotype; locality PL1993, Mirrabooka Formation; pygidium, lateral, posterior, dorsal and ventral views; ×2·25.

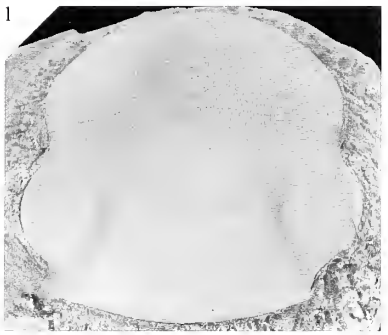
1

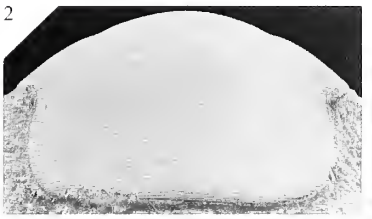
2

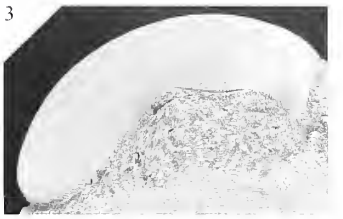
3

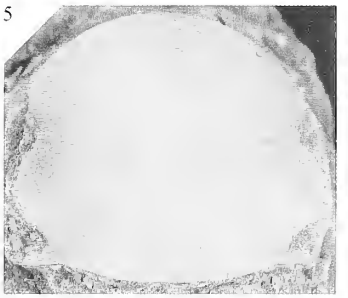
5


6

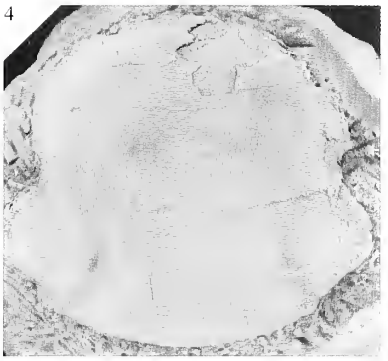
4

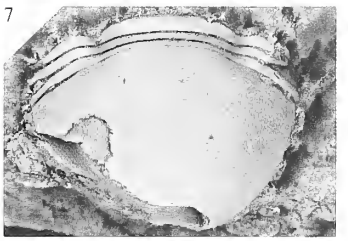
7


8

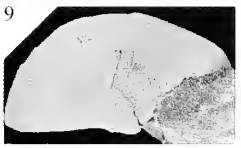
9

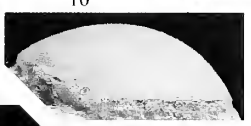
10

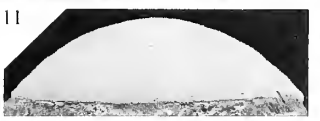
11


12

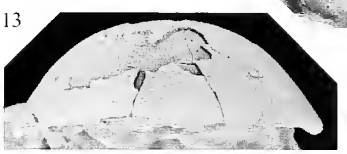
13

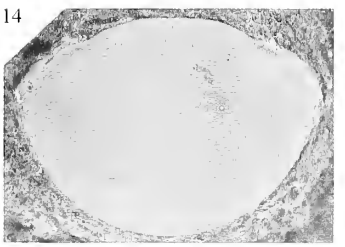
14

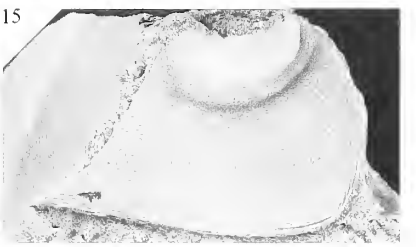
15

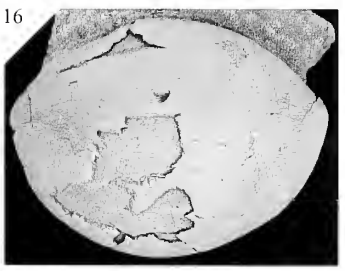
16

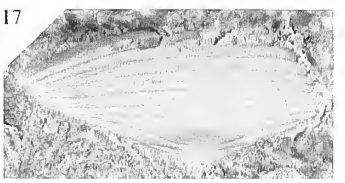
17


18

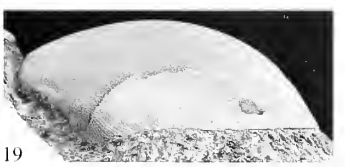
19

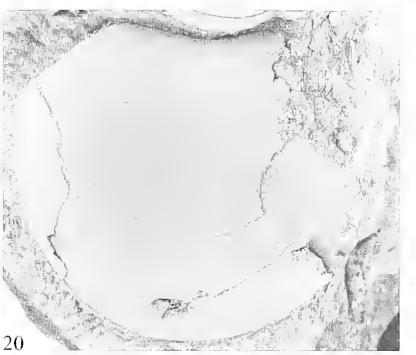
20

HOLLOWAY and LANE, *Lalax*

strongly downturned abaxial to very narrow (tr.) articulated portion; first segment longer (sag., exsag.) than remainder, with axial ring expanding strongly backwards and with articulating furrow impressed; articulating furrow very weak or absent on more posterior segments. Pygidium more convex than cephalon, a little wider than long, commonly with weak, radially disposed ribs and furrows laterally; holcos weak to absent.

Remarks. Lane and Thomas (1980, p. 191) proposed *Rhaxeros* as the replacement name for *Rhax* Lane and Thomas, 1978*b* (*non* Hermann, 1804).

Failleana Chatterton and Ludvigsen, 1976, resembles *Rhaxeros* in many features, including the convexity of the cephalon, the course of the axial furrow, the size and position of the eye, the shape of the rostral plate, the thorax with a very broad axis and very narrow (tr.) articulated portion of the pleurae, and the pygidium with holcos weak or absent. *Failleana* is distinguished from *Rhaxeros* mainly by the presence of the omphalus, a character to which we attribute considerable taxonomic importance.

Leioscutellum Wu, 1977 closely resembles *Rhaxeros* in the glabella that expands strongly backwards close to the posterior margin, the very large eye, the rounded genal angle, the weak lateral border furrow on the librigena, the shape and convexity of the pygidium, the weak radial ribs and furrows on the lateral part of the pygidium, and the very shallow holcos. The type and only known species, *L. tenuicaudatus* Wu, 1977, (p. 98, pl. 1, figs 1–2; text-fig. 4.1a–b) from the upper Llandovery (Telychian) of south-west China, apparently differs from *Rhaxeros* species in having a distinct occipital furrow, but comparison of cephalic characters is hindered by the fact that the material of *L. tenuicaudatus* lacks the anterior part of the cephalon. *Leioscutellum* may yet be shown to be a senior synonym of *Rhaxeros*, but until *L. tenuicaudatus* becomes better known we believe that *Leioscutellum* should be restricted to the type material.

Goldillaenus shinoharai Kobayashi and Hamada, 1974 (p. 53, pl. 3, fig. 6, text-fig. 2G) is based on a single cranidium that resembles *Rhaxeros* in the moderate convexity and the course of the axial furrow, but the illustration of the specimen does not allow further assessment. Pending revision of the species, we assign it to *Rhaxeros* with question.

Stratigraphical range and distribution. Late Llandovery to ?early Ludlow; Queensland, New South Wales, Australian Capital Territory and Japan.

Rhaxeros synaimon sp. nov.

Plate 7, figures 1–21; Plate 8, figures 18–19

Derivation of name. Greek 'kinsman' referring to its relationship with the type species.

Holotype. Cranidium NMV P144847 (Pl. 7, figs 8, 11–12); from PL1989.

Paratypes. Cephala NMV P144845–P144846, P144863; cranidium with rostral plate NMV P144860; cranidium with anteriormost thoracic segment NMV P144890; cranidia NMV P144848–P144851, NMV P144853–P144859, P144861–P144862; librigenae NMV P144865–P144870, P144917; rostral plate NMV P144892; thoracic segments NMV P144735, P144872–P144875, P144893; pygidia NMV P144876–P144881, P144883–P144884, P144887–P144889; all from PL1989.

Other material. Eight cranidia, two librigenae, a rostral plate, two thoracic segments and three pygidia from PL1989, PL1991, PL1992, PL1993, PL1995 and PL1998.

Diagnosis. Axial furrow dying out anteriorly in front of lunette; preglabellar and anterior border furrows not defined; lateral border furrow very weak on librigena. Eye less than half maximum length of librigena, gently curved in dorsal view, its anterior edge level with front of lunette. Posterior section of facial suture meeting posterior cephalic margin in line (exsag.) with its origin

at posterior of visual surface; connective suture evenly curved, meeting rostral suture at an acute angle. Pygidium with shallow holcos and up to four, weakly defined pleural ribs and furrows. Sculpture of distinct, small pits present over most of dorsal surface; terrace ridges on cranidium restricted to narrow band anteriorly; pygidium with terrace ridges on and just behind articulating facet, and close to lateral and posterior margins.

Description. Cephalon gently convex in sagittal line, with maximum curvature anteriorly, describing less than a semicircle transversely; in palpebral view sagittal length almost 65 per cent. of maximum transverse width, which is situated just in front of genal angle and level with posterior edge of eye. Axial furrow clearly impressed posterior to lunette, diverging gently backwards, very weak behind junction with distinct posterior border furrow that runs slightly obliquely forward abaxially on fixigena. Axial furrow less distinct in front of lunette than behind, diverging at *c.* 40° to sagittal axis, dying out as an obvious feature at about 60 per cent. of cephalic length from posterior margin and close to anterior section of facial suture. Small, weak median glabellar (occipital) node present on both exterior of exoskeleton and internal mould opposite posterior edge of eye. Lunette ovate, width (tr.) *c.* 60 per cent. maximum length (which is slightly oblique to an exsagittal line), adaxial margin more distinct than abaxial, especially on internal mould. Palpebral lobe *c.* 25 per cent. sagittal length of cephalon, placed less than 50 per cent. of its length from posterior cephalic margin. Palpebral furrow broad, very weak, running subparallel to palpebral rim. Palpebral area very gently inflated. Anterior section of facial suture gently convex adaxially immediately in front of palpebral lobe, thereafter almost straight and diverging at *c.* 20° to sagittal line, near anterior margin strongly curved adaxially. Posterior section of suture very short, curved abaxially and then adaxially.

Lateral margin of librigena gently curved, meeting gently concave-forwards posterior margin at sharply rounded genal angle. Lateral border furrow broad and weak, running about mid-way between base of eye and lateral margin, dying out anteriorly against facial suture, extending close to cephalic margin posteriorly where it joins in strong curve with equally weak librigenal portion of posterior border furrow (Pl. 7, fig. 15). Visual surface bounded below by a distinct furrow which is narrowest at midlength of eye, widest anteriorly, and confluent with posterior border furrow behind eye. Lenses visible on external surface of eye, increasing in size towards top of visual surface. Librigenal doublure gently convex (tr.) anteriorly, increasing greatly in width at outer end of hypostomal suture due to dorsal deflection of inner margin; posterolateral to this expansion, outer part of doublure gradually decreases in convexity and inner part becomes gently concave. Rostral plate more convex exsagittally than sagittally due to transverse arching of hypostomal suture; connective suture converging at *c.* 65° to sagittal line.

Thorax incompletely known but similar to that of *R. trogodes*.

Pygidium *c.* 75 per cent. as long as wide in plan view, more convex transversely than sagittally, lateral and posterior margins with greatest curvature medially. Articulating half ring marked by very indistinct articulating furrow (Pl. 7, fig. 21), indicating anterior width of axis which is 60 per cent. maximum pygidial width. Abaxial extremity of articulating half ring separated from adaxial extremity of articulating facet by only a very narrow section of anterior pleural margin that is almost horizontal in anterior profile and has the appearance of a shallow notch in dorsal profile (Pl. 7, figs 6, 21). Posterior edge of articulating facet marked adaxially by most anterior and most distinct of up to four pleural ribs; facet not as clearly differentiated abaxially from shallow holcos situated adjacent to lateral and posterior margins. Doublure in plan view about 20 per cent. of maximum pygidial width anterolaterally, posteriorly somewhat less than 50 per cent. sagittal length. Outer portion (about 30 per cent.) of doublure gently convex, inner portion weakly concave; inner portion bears a sagittal ridge which is widest and most distinct anteriorly.

Sculpture. Dense pits covering most of dorsal exoskeleton are absent on lunette, rim of palpebral lobe adjacent to palpebral suture, posterior to eye on cranidium and librigena, in a narrow band across front of thoracic segments and pygidium, and on articulating facets of thorax and pygidium. Terrace ridges on front of cephalon run parallel to anterior margin, becoming discontinuous and more sinuous posteriorly; abaxially, they increase in height and become restricted to cephalic margin, only a single, prominent ridge extending backwards along lateral librigenal margin as far as genal angle (Pl. 7, fig. 15). Pygidium with terrace ridges on articulating facet and anteriormost pleural rib, short oblique ones close to lateral margin, and a few close to and subparallel to posterior margin. Terrace ridges on cephalic and pygidial doublure higher and more continuous than on dorsal surface, closely spaced on rostral plate, widely spaced on inner part of librigenal doublure.

Muscle scars. G0 sub-circular, slightly inflated on exterior of exoskeleton, placed at its own diameter from posterior margin and nearer to axial furrow than to sagittal line, its anterior margin just behind transverse line

through posterior edge of lunette. G1 sub-circular or sub-triangular, slightly larger than G0, placed well forward with its posterior margin about opposite anterior edge of lunette. G2 sub-circular, a little smaller than G1 and placed close to it at about 30 per cent. cephalic length (sag.) from anterior. G3 small, transversely elliptical, situated immediately in front of G2 and lateral to it. Small, accessory muscle scar possibly present between G0 and G1. Internal surface of palpebral area with numerous small, sub-circular, raised scars (impressed on internal moulds).

Remarks. The largest cranidium (the holotype; Pl. 7, figs 8, 11–12) and an incomplete cephalon of similar size have a weak sagittal carina running forward from a point opposite the lunette. In the holotype, the carina swells anteriorly into an elongated oval feature which terminates near the posterior edge of the zone of terrace ridges. The most complete known thorax of *Rhaxeros synaimon* consists of five segments (Pl. 7, fig. 19); comparison with *R. trogodes* (see below) indicates that these are the first five thoracic segments (anteriormost segment longer (sag., exsag.) than remainder, with strongly backwardly expanding axial ring, with large anterior articulating flange at fulcrum, and with strongly backwardly deflected articulating facet).

Many detailed characters serve to distinguish *Rhaxeros synaimon* from the type species. In general, *R. pollinctrix* is not as effaced, having very shallow preglabellar and anterior border furrows on the abaxial part of the cranidium, a cephalic axial furrow that does not die out anteriorly, and better developed pygidial pleural ribs and furrows, especially in smaller specimens; in *R. synaimon* pleural ribs and furrows are not discernible in small pygidia although they are very weakly indicated in large ones. *R. pollinctrix* also differs in that the glabella narrows more strongly forwards towards the lunette; the lunette is situated slightly farther backwards opposite the midlength (exsag.) of the palpebral lobe; the eye is proportionately larger and much more convex in both anterior and palpebral views; the posterior border furrow is weaker on the fixigena; the posterior branch of the facial suture is more divergent; and the cephalon and pygidium have more extensive terrace ridges dorsally but lack dense pitting.

Goldillaenus? *latus* Chatterton and Campbell, 1980 (p. 83, pl. 7, figs 7–9, 11–21) from the Walker Volcanics (Wenlock) near Canberra is here assigned to *Rhaxeros*. It differs from *R. synaimon* in that the cephalic axial furrow diverges more strongly backwards behind the lunette, the palpebral lobe is more strongly curved in outline, the posterior branch of the facial suture diverges strongly backwards, and the pygidium lacks a distinct holcos. In addition, the pygidium of *R. latus* appears to lack weak radial ribs and furrows laterally, although this may be due to the relatively poor preservation of the material.

Examination of a cast of the pygidium figured by Kobayashi and Hamada (1974, pl. 3, fig. 6a–c) as *Bumastus* (*Bumastella*) *aspera* shows that it does not belong to *Bumastella* but to *Rhaxeros*, and closely resembles or is possibly conspecific with *R. synaimon*. The similarities with *R. synaimon* include the convexity, the shallow holcos, the very weak radial ribs anterolaterally, the dense sculpture of fine pits, and the distribution of terrace ridges on the first rib and close to the lateral margin.

EXPLANATION OF PLATE 7

Figs 1–21. *Rhaxeros synaimon* sp. nov.; locality PL1989, Mirrabooka Formation. 1–2, 5, NMV P144863; small cephalon, lateral, anterior and palpebral views; ×4·5. 3, 6, NMV P144888; pygidium, lateral and dorsal views; ×4. 4, 7, 9, NMV P144860; small cranidium with rostral plate, lateral and palpebral views; ×5; rostral plate, ventral view; ×6·25. 8, 11–12, NMV P144847, holotype; cranidium, anterior, palpebral and lateral views; ×2·75. 10, NMV P144890; small cranidium with anteriormost thoracic segment, palpebral view; ×6. 13, NMV P144892; rostral plate, ventral view; ×4·5. 14, NMV P144865; librigenal doublure, ventral oblique view; ×4·5. 15, NMV P144845; incomplete cephalon, oblique view; ×2·75. 16, NMV P144846; incomplete cephalon, palpebral view; ×3·5. 17, NMV P144861; cranidium, palpebral view; ×5·5. 18, 21, NMV P144879; pygidium, posterior and dorsal views; ×3. 19, NMV P144735; first five thoracic segments, dorsal view; ×4·5. 20, NMV P144866; librigena, oblique view; ×5.

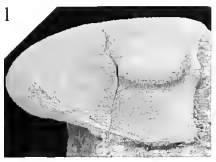
1

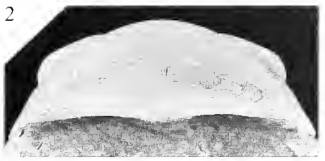
2


3

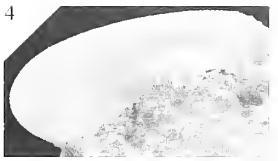
4

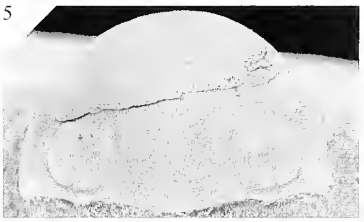
5

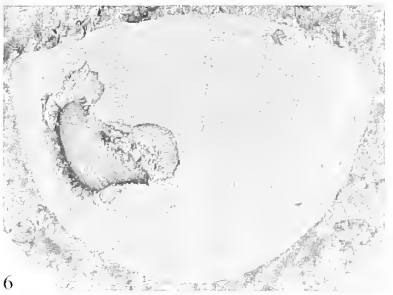
6


7

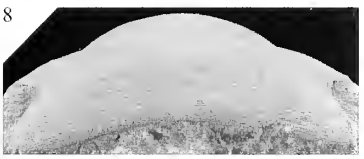
8


9


10

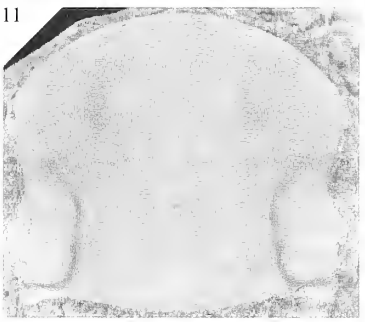
11

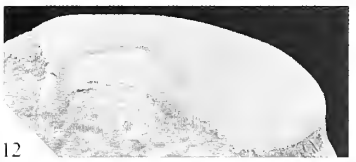
12

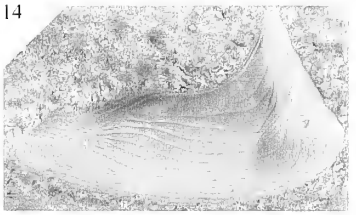
14

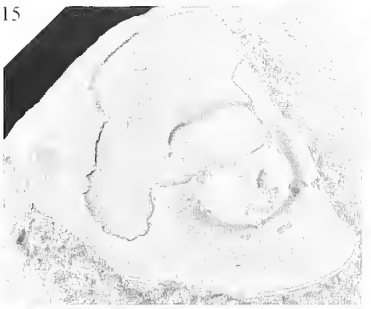
15


13

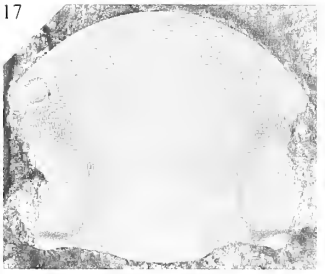
17

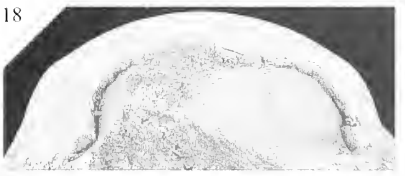
18

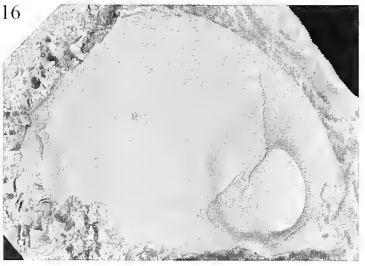
16

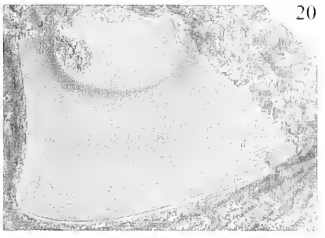
20

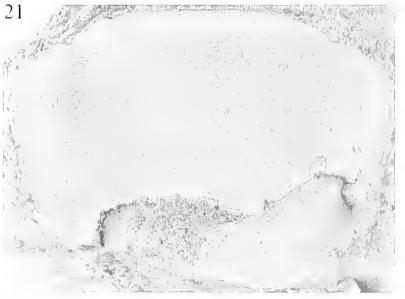
21

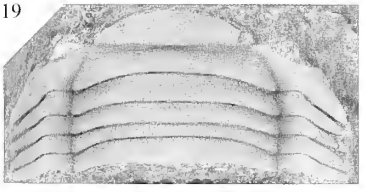
19

HOLLOWAY and LANE, *Rhaxeros*

Rhaxeros trogodes sp. nov.

Plate 8, figures 1–17, 20

Derivation of name. Greek 'trox' – caterpillar, together with the suffix '-odes' – denoting likeness, referring to the appearance of the exoskeleton.

Holotype. Pygidium NMV P145017, Pl. 8, figs 5, 9, 12; from PL1996.

Paratypes. Incomplete cephala NMV P144981, P144985; cranidia NMV P144975, P144977–P144979, P144983, P144986; incomplete cranidium with partial thorax NMV P144980; librigenae NMV P144987, P144989–P144991, P144993–P144994, P144996, P145002–P145003; rostral plates NMV P145000–P145001, P145004, P145024; hypostomes NMV P144998–P144999, P145006, P145025; incomplete thoraces NMV P144984, P144995, P145007–P145008; pygidia with incomplete thoraces NMV P145010–P145011; pygidia NMV P144974, P144988, P145009, P145014–P145016, P145018, P145023; all from PL1996.

Other material. A large number of disarticulated and mostly disarticulated exoskeletal remains from PL1996; three pygidia from PL3303 and other localities within the Borenore Limestone.

Diagnosis. Cephalon moderately convex; axial furrow dying out anteriorly, preglabellar and lateral border furrows not defined. Librigena with posterior margin very weakly concave forwards and genal angle broadly rounded; eye small, situated almost its own length from posterior cephalic margin. Posterior branch of facial suture barely curved. Connective suture more strongly curved abaxially than adaxially, meeting rostral suture at almost 90°. Pygidium strongly convex, with weak sagittal carina extending for posterior 60 per cent. in plan view; radial ridges and furrows very faint or indistinguishable laterally; holcos absent. Terrace ridges present on anterior 25 per cent. of cranidium, on pygidium restricted to articulating facets.

Description. Hypostome with middle body *c.* 150 per cent. as wide anteriorly as long (sag.); anterior lobe comprising 65 per cent. sagittal length of middle body, strongly convex transversely and gently convex sagittally; posterior lobe crescentic, much less convex transversely than anterior lobe, flattened and sloping backwards sagittally, dominated anterolaterally by large, inflated macula; middle furrow dying out abruptly at adaxial extremity of macula. Lateral border furrow deepest at outer end of middle furrow; posterior border furrow very shallow. Lateral border decreasing in convexity (tr.) between anterior wing and shoulder; posterior border very weakly convex, barely increasing in length medially.

Thorax strongly arched transversely; very narrow (tr.), subhorizontal proximal portion of pleurae only slightly interrupting curve of axis and steeply downturned portion of pleurae abaxial to fulcrum; anteriormost

EXPLANATION OF PLATE 8

Figs 1–17, 20. *Rhaxeros trogodes* sp. nov.; locality PL1996, Mirrabooka Formation, unless otherwise indicated. 1–2, NMV P144979; cranidium, palpebral and lateral views; ×4. 3, NMV P144983; cranidium, palpebral view; and NMV P144984; thoracic segment, oblique view; ×4. 4, NMV P145025; hypostome, ventral view; ×8. 5, 9, 12, NMV P145017, holotype; pygidium, lateral, posterior and dorsal views; ×4·75. 6, NMV P144998; hypostome, ventral view; ×8. 7, NMV P145001; rostral plate, ventral view; ×5. 8, NMV P144993; librigena, oblique view; ×5·5. 10, 13, NMV P145018; pygidium, dorsal and lateral views; ×4·75. 11, NMV P144994; librigena, oblique view; ×5·5. 14, NMV P144980; incomplete cranidium with first four thoracic segments, dorsal view; ×4. 15–16, NMV P145050; locality PL3303, Borenore Limestone; largest pygidium, dorsal and lateral views; ×2·25. 17, NMV P145011; incomplete thorax and pygidium, lateral view; ×3. 20, NMV P145010; incomplete thorax and pygidium, dorsal view; ×3.

Figs 18–19. *Rhaxeros synaimon* sp. nov.; locality PL1989, Mirrabooka Formation. 18, NMV P144881; pygidium, latex cast in ventral view showing doublure; ×3. 19, NMV P144887; pygidium, plan view; ×3.

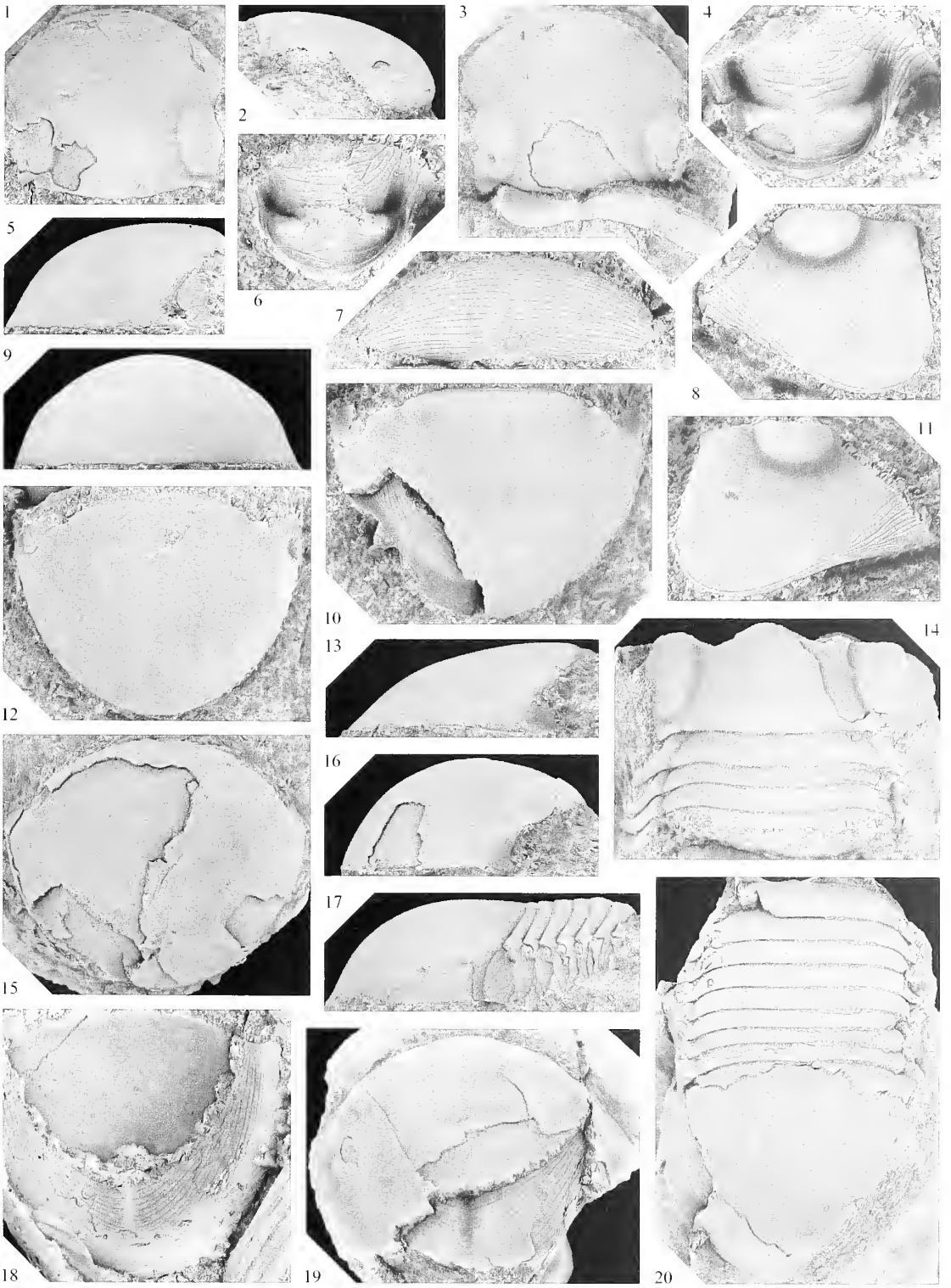

HOLLOWAY and LANE, *Rhaxeros*

segment longer (sag., exsag.) than remainder (Pl. 8, fig. 14). Axis comprising *c.* 70 per cent. of segmental width (tr.); axial furrow firmly impressed, diverging strongly backwards on anterior segments, less strongly on subsequent segments, converging backwards on posterior segment (Pl. 8, fig. 20). Articulating half ring on first segment longer sagittally than ring, from which it is separated by weak, convex-backwards articulating furrow; articulating half rings not differentiated on subsequent segments. Pleurae with articulating flange on anterior margin at fulcrum; this flange most strongly developed on first segment, bounded posteriorly by oblique furrow (Pl. 8, fig. 14). Pleurae beyond fulcrum with broad articulating facet and rounded tip (Pl. 8, fig. 3).

Muscle scars. G0 not clearly seen, but apparently similar in shape and position to that in *R. synaimon*. G1 large, kidney- or bean-shaped, posterior edge opposite middle (exsag.) of lunette, anterior edge level with cephalic midlength (sag.) and extending close to axial furrow. G2 and G3 similar to those of *R. synaimon*. Internal surface of pygidium with traces of axial segmentation anteriorly, defined by three pairs of weak, transverse scars that are comma-shaped abaxially and straight medially. More posteriorly, between about 30 per cent. and 50 per cent. pygidial length in plan view, are two pairs of small, elongated, elliptical or lachrymate scars, with rippled surface in some specimens; adaxial pair of scars slightly larger than abaxial pair and extending farther back.

Remarks. A full description of *R. trogodes* is not warranted as in overall morphology this species is similar to *R. synaimon*; the hypostome and thorax are described as the former is unknown and the latter less completely known in *R. synaimon*. The most obvious differences between *R. trogodes* and *R. synaimon* are the greater convexity of the former, especially in the pygidium, the much smaller and more anteriorly placed eye, and the broadly rounded genal angle. *R. trogodes* also differs from *R. synaimon* in that the cephalic axial furrow is slightly deeper, the posterior section of the facial suture is almost straight, the posterior margin of the librigena is not as concave in outline, the lateral and posterior border furrows are not weakly developed on the librigena, the posterior edge of the rostral plate is not as evenly curved but is transverse medially, radial ribs and furrows are very weak or indistinguishable on the pygidium, there is no holcos, and the sagittal ridge on the pygidial doublure is weaker. In *R. trogodes* the terrace ridges on the front of the cranidium are more closely spaced and extend farther back than in *R. synaimon*, and terrace ridges on the pygidium are restricted to the articulating facets, being absent around the lateral and posterior margins. Most of the differences between *R. trogodes* and *R. synaimon* also serve to distinguish the former from the type species.

Kobayashi and Hamada (1974, p. 50) stated that the two cranidia on which they based their species '*Bumastus*' *subquadratus* were found together with the incomplete thorax and pygidium they described as '*Bumastus* aff. *barriensis*'. We assign all of these specimens to *Rhaxeros* and consider them to be probably conspecific; the short axial furrow shown by Kobayashi and Hamada (1974, text-fig. 2c) in their reconstruction of the pygidium is not evident in the specimen. Also possibly belonging to *Rhaxeros subquadratus* is one of the pygidia assigned by Kobayashi and Hamada (1974, pl. 1, fig. 7) to '*Bumastus*' *glomerosus* (= *Bumastella spiculus*); this pygidium differs from that of *Bumastella* in its greater convexity, the absence of the holcos, and the wider doublure that is convex over much of its width. *Rhaxeros subquadratus* shows similarities to *R. trogodes* in the convexity of the cranidium and pygidium, and possibly in the distribution of terrace ridges on the pygidium, but the specimens are too poorly preserved to judge whether they are conspecific with the material from New South Wales.

Acknowledgements. PDL gratefully acknowledges the Council of the Museum of Victoria for financial support and provision of research facilities while in Australia; the cost of his travel to Australia was generously provided by the British Council (Australia), and that to Tokyo by the NERC. We thank Penelope Clark, Lars Ramsköld, and Andrew Sandford for assistance in collecting material; Lawrence Sherwin for providing information on localities; Barry Webby for arranging the loan of material from the Sydney University collections; Akira Kawazoe for sending moulds of specimens described by Kobayashi and Hamada (1974) from the collections of the Kôchi Prefectural Fossil Museum; and Ken McNamara and Bob Owens for

discussion on the giant meraspid transitory pygidia of *Bumastella* and *Lalax*. Terry Doyle (Department of Earth Sciences, Keele University) patiently drafted several versions of the text-figures.

REFERENCES

ADRAIN, J. M., CHATTERTON, B. D. E. and BLODGETT, R. B. 1995. Silurian trilobites from southwestern Alaska. *Journal of Paleontology*, **69**, 723–736.

ADRIAN, J. 1971. Stratigraphic units in the Molong district, New South Wales. *Records of the Geological Survey of New South Wales*, **13**, 179–198.

BARRANDE, J. 1846. *Notice préliminaire sur le système Silurien et les Trilobites de Bohême*. Leipzig, vi+97 pp.

—— 1852. *Système Silurien du centre de la Bohême. 1ère partie. Recherches paléontologiques, vol. 1. Crustacés, Trilobites*. Published by the author, Prague and Paris, xxx+935 pp., 51 pls.

—— 1872. *Systême Silurien du centre de la Bohême. 1ère partie. Recherches paléontologiques, vol. 1. Trilobites, Crustaces divers et Poissons, supplément*. Published by the author, Prague and Paris, xxx+647 pp., 35 pls.

BISCHOFF, G. C. O. 1986. Early and middle Silurian conodonts from midwestern New South Wales. *Courier Forschungsinstitut Senckenberg*, **89**, 1–337.

BURMEISTER, H. 1843. *Die Organisation der Trilobiten, aus ihren lebenden Verwandten entwickelt; nebst einer systematischen Uebersicht aller zeither beschriebenen Arten*. G. Reimer, Berlin, 147 pp., 6 pls.

CAMPBELL, K. S. W., HOLLOWAY, D. J. and SMITH, W. D. 1974. A new receptaculitid genus, *Hexabactron*, and the relationships of the Receptaculitaceae. *Palaeontographica, Abteilung A*, **146**, 52–77, pls 12–17.

CHANG [ZHANG] WEN-TANG 1974. [Silurian] Trilobites. 173–187, pls 80–85. *In* NANJING INSTITUTE OF GEOLOGY AND PALAEONTOLOGY, ACADEMIA SINICA (ed.). [*A handbook of the palaeontology and stratigraphy in southwest China.*] Science Press, Beijing, iii+454 pp., 202 pls. [In Chinese].

CHATTERTON, B. D. E. 1971. Taxonomy and ontogeny of Siluro-Devonian trilobites from near Yass, New South Wales. *Palaeontographica, Abteilung A*, **137**, 1–108, pls 1–24.

—— 1980. Ontogenetic studies of Middle Ordovician trilobites from the Esbataottine Formation, Mackenzie Mountains, Canada. *Palaeontographica, Abteilung A*, **171**, 1–74, pls 1–19.

—— and CAMPBELL, K. S. W. 1980. Silurian trilobites from near Canberra and some related forms from Yass. *Palaeontographica, Abteilung A*, **167**, 77–119, pls 1–16.

—— and LUDVIGSEN, R. 1976. Silicified Middle Ordovician trilobites from the South Nahanni River area, District of Mackenzie, Canada. *Palaeontographica, Abteilung A*, **154**, 1–106, pls 1–22.

DUN, W. S. 1907. Notes on Palaeozoic Brachiopoda and Pelecypoda from New South Wales. *Records of the Geological Survey of New South Wales*, **8**, 265–269, pl. 40.

EDGECOMBE, G. D. and RAMSKÖLD, L. 1992. The Silurian encrinurine trilobite *Pacificurus*; new species from North America. *Journal of Paleontology*, **66**, 255–262.

ETHERIDGE, R. 1896. Description of a small collection of Tasmanian Silurian fossils presented to the Australian Museum by Mr A. Montgomery, MA, Government Geologist, Tasmania. *Report of the Secretary of Mines for Tasmania*, **1895–96**, 41–48, pls 1–2. [Reprinted 1897 in *Papers and Proceedings of the Royal Society of Tasmania*, **1896**, 29–46, pl. 1].

—— 1909. The trilobite *Illaenus* in the Silurian rocks of New South Wales. *Records of the Geological Survey of New South Wales*, **8**, 319–321. [Reprint pages numbered 1–3].

—— and MITCHELL, J. 1917. The Silurian trilobites of New South Wales, with references to those of other parts of Australia. *Proceedings of the Linnean Society of New South Wales*, **42**, 480–510, pls 24–27.

FLETCHER, H. O. 1950. Trilobites from the Silurian of New South Wales. *Records of the Australian Museum*, **22**, 220–233.

FORTEY, R. A. 1980. The Ordovician trilobites of Spitsbergen. 3. Remaining trilobites of the Valhallfonna Formation. *Norsk Polarinstitutt Skrifter*, **171**, 1–163.

—— and OWENS, R. M. 1987. The Arenig Series in South Wales. *Bulletin of the British Museum (Natural History), Geology Series*, **41**, 69–307.

HALL, J. 1865. Account of some new or little-known species of fossils from rocks of the age of the Niagara group. *Report of the New York State Museum of Natural History*, **18**. [Issued as advance copies].

—— 1867. Account of some new or little known species of fossils from rocks of the age of the Niagara Group. *Report of the New York State Cabinet of Natural History*, **20**, 305–401, pls 10–23. [Reprint of Hall 1865 with additions]

HELBERT, G. J. 1984. The Silurian trilobites of the Oslo district, Norway. Unpublished Ph.D. thesis, University of Keele.

—— LANE, P. D., OWENS, R. M., SIVETER, DEREK J. and THOMAS, A. T. 1982. Lower Silurian trilobites from the Oslo region. 129–148. *In* WORSLEY, D. (ed.). *International Union of Geological Sciences Subcommission on*

Silurian Stratigraphy. Field meeting, Oslo region, 1982. Palaeontological contributions from the University of Oslo, 278, Paleontologisk Museum, Oslo, vii + 175 pp.

HERMANN, J. F. 1804. *Mémoire aptérologique*. Strasbourg, vi + 144 pp.

HOLLOWAY, D. J. 1980. Middle Silurian trilobites from Arkansas and Oklahoma, USA. *Palaeontographica, Abteilung A*, **170**, 1–85, pls 1–20.

—— 1994. Early Silurian trilobites from the Broken River area, north Queensland. *Memoirs of the Museum of Victoria*, **54**, 243–269.

HOLM, G. 1886. Revision der Ostbaltischen Silurischen Trilobiten von Fr. Schmidt. Abtheilung 3. Illaeniden. *Mémoires de l'Académie Impériale des Sciences de St.-Pétersbourg, 7e Série*, **33**, i–ii + 1–173, pls 1–12. [*Zapiski Imperatorskoi Academii Nauk*].

HORNÝ, R. and BASTL, F. 1970. *Type specimens of fossils in the National Museum Prague. Volume 1. Trilobita*. Museum of Natural History, Prague, 354 pp.

HOWELLS, Y. 1982. Scottish Silurian trilobites. *Monograph of the Palaeontographical Society*, **135** (561), 1–76, pls 1–15.

HUGHES, N. C. and CHAPMAN, R. E. 1995. Growth and variation in the Silurian proetide trilobite *Aulacopleura koninckі* and its implications for trilobite palaeobiology. *Lethaia*, **28**, 333–353.

JAANUSSON, V. 1954. Zur Morphologie und Taxonomie der Illaeniden. *Arkiv för Mineralogie och Geologi*, **1**, 545–583, pls 1–3.

—— 1959. Family Illaenidae Hawle & Corda, 1847. 372–376. *In* MOORE, R. C. (ed.). *Treatise on invertebrate paleontology. Part O. Arthropoda 1*. Geological Society of America and University of Kansas Press, Boulder, Colorado and Lawrence, Kansas, xix + 560 pp.

KÁCHA, P. and ŠARIČ, R. 1991. Ontogeny of the trilobite *Kosovopeltis svobodai* Šnajdr from the Bohemian Silurian. *Věstník Ústředního ústavu geologického*, **66**, 257–273, pls 1–6.

KIÆR, J. 1908. Das Obersilur im Kristianagebiete. Eine stratigraphisch-faunistische Untersuchung. *Skrifter utgitt af VidenskabsSelskabet i Christiania, Matematisk–Naturvidenskapelig Klasse*, **2**, i–xvi + 1–596 [for 1906].

KOBAYASHI, T. and HAMADA, T. 1974. Silurian trilobites of Japan in comparison with Asian, Pacific and other faunas. *Special Papers of the Palaeontological Society of Japan*, **18**, i–viii + 1–155, pls 1–12.

—— —— 1984. Advance report on a new trilobite collection of the Silurian Yokokura-yama fauna, Shikoku island, Japan. *Research Report of the Kôchi University, Natural Sciences*, **32**, 253–258.

—— —— 1985*a*. On the Silurian trilobites and cephalopods of Mt. Yokokura, Shikoku, Japan. *Proceedings of the Japan Academy, Series B*, **61**, 345–347.

—— —— 1985*b*. Additional Silurian trilobites to the Yokokura-yama fauna from Shikoku, Japan. *Transactions and Proceedings of the Palaeontological Society of Japan*, **139**, 206–217.

—— —— 1986. The second addition to the Silurian trilobite fauna of Yokokura-yama, Shikoku, Japan. *Transactions and Proceedings of the Palaeontological Society of Japan, New Series*, **143**, 447–462, pl. 90.

—— —— 1987. The third addition to the Silurian trilobite fauna of Yokokura-yama, Shikoku, Japan. *Transactions and Proceedings of the Palaeontological Society of Japan, New Series*, **147**, 109–116.

KONINCK, L.-G. de 1876. *Recherches sur les fossiles paléozoïques de la Nouvelle-Galles du Sud (Australie). Première partie. Espèces siluriennes*. 1–65. F. Hayez, Bruxelles, 140 pp. [English translation published in 1898 as *Memoirs of the Geological Survey of New South Wales, Palaeontology*, **6**, i–xiii + 1–298, pls 1–24].

LANE, P. D. 1972. New trilobites from the Silurian of north-east Greenland, with a note on trilobite faunas in pure limestones. *Palaeontology*, **15**, 336–364.

—— and OWENS, R. M. 1982. Silurian trilobites from Kap Schuchert, Washington Land, North Greenland. *Rapports Gronlands Geologisk Undersøgelse*, **108**, 41–69.

—— and THOMAS, A. T. 1978*a*. Family Scutelluidae. 8–29, pls 1–7. *In* THOMAS, A. T. British Wenlock trilobites. Part 1. *Monograph of the Palaeontographical Society*, **131** (552), 1–56, pls 1–14.

—— —— 1978*b*. Silurian trilobites from NE Queensland and the classification of effaced trilobites. *Geological Magazine*, **115**, 351–358.

—— —— 1980. A replacement name for *Rhax* Lane & Thomas (Trilobita) *non* Hermann, 1804. *Geological Magazine*, **117**, 191.

—— —— 1983. A review of the trilobite suborder Scutelluina. *Special Papers in Palaeontology*, **30**, 141–160.

LU YEN-HAO 1962. Restudy on Grabau's types of three Silurian trilobites from Hupei. *Acta Palaeontologica Sinica*, **10**, 158–166, pl. 1. [In Chinese; English summary 167–173].

LUDVIGSEN, R. and CHATTERTON, B. D. E. 1980. The ontogeny of *Failleana* and the origin of the Bumastinae (Trilobita). *Geological Magazine*, **117**, 471–478, 1 pl.

—— and TRIPP, R. P. 1990. Silurian trilobites from the Northern Yukon Territory. *Life Sciences Contributions from the Royal Ontario Museum*, **153**, i–iv + 1–59.

MAKSIMOVA, Z. A. 1975. [*Trilobites*.] 119–133, pls 30–32. *In* MENNER, V. V. (ed.). *Kharakteristika fauny pogranichnikh sloev Silura i Devona tsentral'nogo Kazakhstana*. [*Characteristic fauna of the boundary beds between the Silurian and Devonian of central Kazakhstan*.] Materialy po geologii tsentral'nogo Kazakhstana, 12. Nedra, Moscow, 248 pp.

McNAMARA, K. J. 1986. The role of heterochrony in the evolution of Cambrian trilobites. *Biological Reviews*, **61**, 121–156.

MEEK, F. B. and WORTHEN, A. H. 1870. Descriptions of new species and genera of fossils from the Palaeozoic rocks of the western states. *Proceedings of the Academy of Natural Science of Philadelphia*, **1870**, 22–56.

MILLER, S. A. and GURLEY, W. F. E. 1893. Description of some new species of invertebrates from the Palaeozoic rocks of Illinois and adjacent states. *Bulletin of the Illinois State Museum of Natural History*, **3**, 1–81, pls 1–8.

MURCHISON, R. I. 1839. *The Silurian System*. John Murray, London, xxxii + 768 pp.

NIELSEN, A. T. 1995. Trilobite systematics, biostratigraphy and palaeoecology of the Lower Ordovician Komstad Limestone and Huk Formations, southern Scandinavia. *Fossils and Strata*, **38**, 1–374.

ÖPIK, A. A. 1937. Trilobiten aus Estland. *Acta et Commentationes Universitatis Tartuensis*, *A*, **32**, 1–163.

—— 1953. Lower Silurian fossils from the "*Illaenus* Band" Heathcote, Victoria. *Memoirs of the Geological Survey of Victoria*, **19**, 1–42, pls 1–13.

OWEN, A. W. and BRUTON, D. L. 1980. *Late Caradoc–early Ashgill trilobites of the central Oslo Region, Norway*. Palaeontological Contributions from the University of Oslo, No. 245. Paleontologisk Museum, Oslo, 63 pp.

PICKETT, J. W. 1982 (ed.). The Silurian System in New South Wales. *Bulletin of the Geological Survey of New South Wales*, **29**, i–v, 1–264.

PRANTL, F. and PŘIBYL, A. 1949. O nových nebo málo známých trilobitech českého ordoviku. *Rozpravy České akademie věd a umění*, **58** (8), 1–22, pls 1–3. [English translation published in *Bulletin international de l'Académie tchéque des sciences*, **49** (8), 1–23, pls 1–3.]

RAYMOND, P. E. 1916. New and old Silurian trilobites from south-eastern Wisconsin, with notes on the genera of the Illaenidae. *Bulletin of the Museum of Comparative Zoology, Harvard University*, **60**, 1–41, pls 1–4.

SALTER, J. W. 1853. On a few genera of Irish Silurian fossils. *Report of the British Association for the Advancement of Science*, **22**, 59–61.

—— 1867. A monograph of the British trilobites from the Cambrian, Silurian and Devonian Formations. Part 4. *Monograph of the Palaeontographical Society*, **20** (86), 177–214, pls 25*–30.

SANDFORD, A. C. and HOLLOWAY, D. J. 1998. The effaced styginid trilobite *Thomastus* from the Silurian of Victoria, Australia. *Palaeontology*, **41**, 913–928.

SCHINDEWOLF, O. H. 1924. Vorläufige Übersicht über die Obersilur-Fauna des "Elbersreuther Orthoceratitenkalkes". 1. Allgemeine Vorbemerkungen und Trilobitenfauna. *Senckenbergiana*, **6**, 187–221.

SCOTESE, C. R. and McKERROW, W. S. 1990. Revised world maps and introduction. 1–21. *In* McKERROW, W. S. and SCOTESE, C. R. (eds). Palaeozoic palaeogeography and biogeography. *Memoir of the Geological Society, London*, **12**, 1–435.

SHERWIN, L. 1968. *Denckmannites* (Trilobita) from the Silurian of New South Wales. *Palaeontology*, **11**, 691–696.

—— 1971*a*. Stratigraphy of the Cheesemans Creek district, New South Wales. *Records of the Geological Survey of New South Wales*, **13**, 199–237.

—— 1971*b*. Trilobites of the subfamily Phacopinae from New South Wales. *Records of the Geological Survey of New South Wales*, **13**, 83–99, pls 1–8.

SKJESETH, S. 1955. The Middle Ordovician of the Oslo region, Norway. 5. The trilobite family Styginidae. *Norsk Geologisk Tidsskrift*, **35**, 9–28, pls 1–5.

ŠNAJDR, M. 1957. Klasifikace čeledě Illaenidae (Hawle a Corda) v českém starším paleozoiku. [Classification of the family Illaenidae (Hawle and Corda) in the Lower Palaeozoic of Bohemia.] *Sborník Ústředního Ústavu Geologického*, **23**, 125–254, pls 1–12 [English summary 270–284].

—— 1990. *Bohemian trilobites*. Geological Survey, Prague, 265 pp.

SÜSSMILCH, C. A. 1907. Note on the Silurian and Devonian rocks occurring to the west of the Canoblas Mountains near Orange, N.S.W. *Journal and Proceedings of the Royal Society of New South Wales*, **40**, 130–141.

THOMAS, A. T. and HOLLOWAY, D. J. 1988. Classification and phylogeny of the trilobite order Lichida. *Philosophical Transactions of the Royal Society of London, Series B*, **321** (1205), 179–262.

—— and LANE, P. D. 1998. *Trilobite associations of the North Atlantic region*. 444–457. *In* BOUCOT, A. J. and

LAWSON, J. D. (eds). *Project ecostratigraphy; an encyclopaedia of palaeoecology*. Cambridge University Press, Cambridge.

THOMAS, N. L. 1929. Hypoparia and opisthoparia from the St Clair Limestone, Arkansas. *Bulletin of the Scientific Laboratories of Denison University*, **24**, 1–25.

VOGDES, A. W. 1890. A bibliography of Paleozoic Crustacea from 1698 to 1889, including a list of North American species and a systematic arrangement of genera. *Bulletin of the United States Geological Survey*, **63**, 1–177.

WALKER, D. B. 1959. Palaeozoic stratigraphy of the area to the west of Borenore, N.S.W. *Journal and Proceedings of the Royal Society of New South Wales*, **93**, 39–46.

WELLER, S. 1907. The paleontology of the Niagaran Limestone in the Chicago area. The Trilobita. *Bulletin of the Chicago Academy of Science*, **4**, 163–281, pls 16–25.

WHITTARD, W. F. 1939. The Silurian illaenids of the Oslo region. *Norsk Geologisk Tidsskrift*, **19**, 275–295, pls 1–4.

WHITTINGTON, H. B. 1957. The ontogeny of trilobites. *Biological Reviews*, **32**, 421–469.

—— 1959. Ontogeny of Trilobita. 127–145. *In* MOORE, R. C. (ed.). *Treatise on invertebrate paleontology. Part. O. Arthropoda 1*. Geological Society of America and University of Kansas Press, Boulder, Colorado and Lawrence, Kansas. xix + 560 pp.

—— 1965. Trilobites of the Ordovician Table Head Formation, western Newfoundland. *Bulletin of the Museum of Comparative Zoology, Harvard University*, **132**, 275–442.

WU HONG-JI 1977. Comments on new genera and species of Silurian–Devonian trilobites in south-west China and their significance. *Acta Palaeontologica Sinica*, **16**, 95–119, pls 1–3 [In Chinese; English summary p. 117].

D. J. HOLLOWAY
Invertebrate Palaeontology
Museum of Victoria
PO Box 666E
Melbourne
Victoria 3001, Australia
e-mail dhollow@mov.vic.gov.au

P. D. LANE
Department of Earth Sciences
University of Keele
Staffordshire ST5 5BG, UK
e-mail gga15@esci.keele.ac.uk

Typescript received 14 July 1997
Revised typescript received 26 November 1997

VARIATION IN THE EYES OF THE SILURIAN TRILOBITES *EOPHACOPS* AND *ACASTE* AND ITS SIGNIFICANCE

by A. T. THOMAS

ABSTRACT. Among the compound eyes of trilobites, the most remarkable are the schizochroal type of the suborder Phacopina. As well as representing an ancient visual system of probably unique kind, schizochroal eyes show patterns of variation in lens distribution which have figured in discussions of possible dimorphism and polymorphism in trilobites species, and have been used by some authors as taxonomic characters. *Eophacops musheni* is a common species in the British Wenlock, and variation in the lens pattern on the visual surface is described from about 40 well preserved specimens. Adults typically have 19 or 20 files of lenses, and two cases are described of individuals with 20 files in the left eye and 19 in the right. Comparable cases occur in *Acaste*. Dimorphism in the visual surface of *A. downingiae* is doubtful. The new data on the variation of the visual surfaces of *E. musheni* and *A. inflata* indicate that visual surface morphology provides a reliable guide to species identity only in some cases. They also allow Clarkson's developmental model for the visual surface to be extended to imply that the initial length of the section of the generative zone actively producing lenses was variable, and that lens emplacement was initiated at different times relative to the descent of the generative zone in different individuals. If development of a lens was controlled by the distance from adjacent lens centres, and given that lenses are round and that emplacement began in a single horizontal row, hexagonal close packing and the development of dorso-ventral files result automatically. Cubic close packing could be produced by modifying the spacing factor in successive horizontal rows. The number of dorso-ventral files of lenses and their relative height are controlled by the length of the active section of the generative zone and its pattern of growth. The existence of individuals with eyes differing in the number of files demonstrates that file number is a consequence of a developmental programme, rather than being under immediate genetic control. Variation in the timing of termination of lens emplacement accounts for the observed variation posteriorly and near the base of the visual surface.

THE calcite compound eyes of trilobites, notable for being the oldest preserved visual system, have been the subject of scientific investigation for more than a hundred years. The structures which originally underlay the lentiferous visual surface are unknown, thus limiting our understanding of the animals' vision. Nevertheless, the morphology and function of trilobite eyes have been the study of intensive investigation in recent decades (see Clarkson 1975, 1979 for reviews). Two principal types of eye morphology have been distinguished: the more primitive holochroal eyes, characteristic of most trilobite groups, and the schizochroal type of the suborder Phacopina. A possible third kind of eye, which has at least some features in common with the schizochroal type, occurs in eodiscid trilobites, but its distinctiveness remains to be confirmed (see Zhang and Clarkson 1990, p. 912).

Schizochroal eyes differ from holochroal ones in possessing separated, thick, biconvex lenses, which are relatively large (sometimes < 1 mm across; Clarkson 1979, p. 12), compared with the average lens diameter of 100 μm in holochroal eyes (Horváth *et al.* 1997, p. 233) and circular in plan view (square lenses occur in some trilobites with holochroal eyes: see Clarkson 1975, fig. 5K, p. 17; Fortey 1997, p. 403). All schizochroal lenses are doublet structures: an upper lens unit composed of calcite with the c-axis orientated perpendicular to the visual surface, underlain by an intralensar bowl. The aplanatic character of the doublets corrected for spherical aberration (Clarkson and Levi-Setti 1975). It is possible, however, for spherical aberration to be corrected by singlet lenses of the appropriate shape. Horváth (1996) argued that a possible function of the intralensar bowl might

[Palaeontology, Vol. 41, Part 5, 1998, pp. 897–911, 1 pl.]

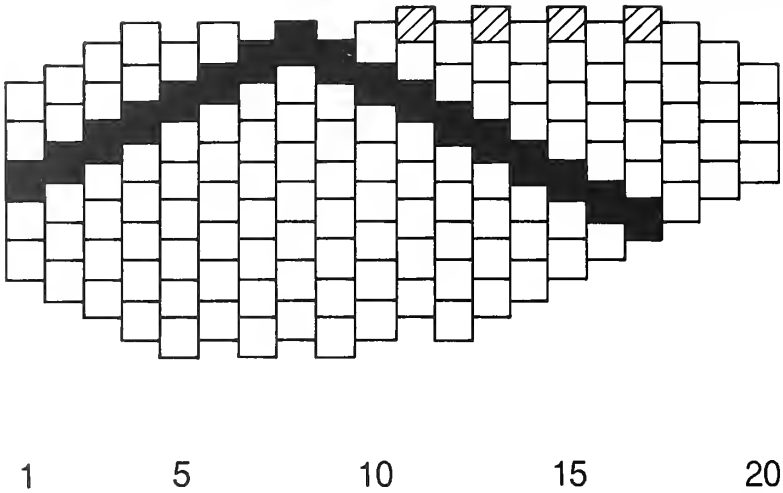

TEXT-FIG. 1. Schematic representation of visual surface in a paralectotype of *Eophacops musheni* (Salter, 1864) (BU 59a), showing the terminology used in the text. Front of eye is to left; numbers below drawing denominate individual dorso-ventral *files*, counting from the front. Black boxes indicate single examples of *ascending* and *descending diagonal rows*; oblique shading indicates *accessory upper horizontal row*.

be reflectivity reduction and enhanced light transmission. The overall features of the schizochroal eye suggest that a unique kind of visual system might be represented, which acted as an aggregate of simple eyes rather than being directly comparable to the compound eyes of most other arthropods (Fordyce and Cronin 1993; Horváth *et al.* 1997). The geometrical arrangement of lenses on the visual surface is such that schizochroal-eyed trilobites may have possessed stereoscopic vision throughout the visual field (Stockton and Cowen 1976).

Partly because they are such striking features, eye morphology and the pattern of lens distribution have figured in discussions concerning possible dimorphism and polymorphism in various phacopine species, and have sometimes been used in separating genera and species. Often, however, the available material has been poorly localized, and sample sizes have been small. Continuing studies of trilobites from the British Wenlock have included examination of eight named species of the phacopid genera *Eophacops* and *Ananaspis*, and the acastomorphs *Acaste*, *Acastoides* and *Acastocephala*. Full descriptions of the species will be published in the next part of my monograph (1978, 1981, continuing) of the fauna. This paper describes the pattern of eye lens variation in *Eophacops musheni*, where the number of suitably preserved specimens is relatively large and the material is tolerably well localized. Additionally, examples of *E. musheni* and *Acaste inflata* are described in which the right and left eyes of individual specimens show different patterns of lens distribution. The developmental significance of these abnormalities, and the use of eye lens patterns in taxonomy and the discrimination of dimorphs and polymorphs, are reviewed below.

Terminology and eye lens diagrams. Terminology follows Clarkson (1966*a*, p. 2, text-fig. 1). Lens plots for the species (Text-fig. 1) generally follow the method of Clarkson and Tripp (1982, fig. 6, p. 293), a development of Campbell's (1977, p. 40) system, which allows the characteristic hexagonal close packing to be represented (also see Howells 1982, p. 42). For the reasons explained in the text, however, positionally equivalent lenses are first identified at the front of the visual surface rather than at the back. The characteristic arrangement of lenses in dorso-ventral files and horizontal rows is preserved. The additional arrangement of lenses in ascending and descending diagonal rows, which is a geometrical consequence of the packing arrangement, is also represented.

Stereographic plots are needed if it is desired to represent the sizes of lenses and their separation with minimal distortion (Clarkson 1996*a*, p. 7).

SYSTEMATIC PALAEONTOLOGY

Remarks. The species considered here will be revised fully elsewhere. Because none of them has been described in recent years, however, sufficient taxonomic data are given to make my concept of the species clear. Descriptive details refer to aspects of eye morphology only.

Order PHACOPIDA Hawle and Corda, 1847
Suborder PHACOPINA Hawle and Corda, 1847
Family PHACOPIDAE Hawle and Corda, 1847
Subfamily PHACOPIDELLINAE Delo, 1935

Genus EOPHACOPS Delo, 1935

Remarks. This name has been conserved by the International Commission on Zoological Nomenclature in Opinion 1846 (*Bulletin of Zoological Nomenclature*, **53** (for 1996), p. 205; see Owens and Thomas 1995).

Eophacops musheni (Salter, 1864)

Plate 1, figures 1–5, 7–8; Text-figures 1–4, 6

v*.1864 *P.* (*Phacops*) *Musheni*, n. sp., Salter, p. 23, pl. 2, figs 7–12.
.1966*b* *Phacops musheni* Salter 1864; Clarkson, p. 77, pl. 1.
.1967 *E. musheni* (Salter); Campbell, p. 38, pl. 12, fig. 20.
.1985 *Eophacops musheni* (Salter, 1864); Ramsköld, p. 28, pl. 5, figs 2–3, 5–7, text-fig. 4B.

Material, localities and horizons. The syntypes include BU59a–c and two untraced specimens (Morris 1988, p. 2), from the Coalbrookdale Formation (?), Malvern, Hereford and Worcester; NHM 58898, It9660, from the Much Wenlock Limestone Formation (Homerian), Dudley, West Midlands. Salter's figures are partly restored: the closest match with an actual specimen is between his plate 2, figure 9 and BU59c (Pl. 1, fig. 5). That specimen shows the cephalic doublure as well as the dorsal morphology, and is here selected as lectotype. There is some doubt about the horizon from which the BU59 specimens came. Salter gave the horizon as 'Wenlock Shale' (= Coalbrookdale Formation), but the BU catalogue records it as 'Woolhope Shale' (= Wych Beds, Telychian). The specimens were originally part of the Ketley Collection, but no primary documentation relating to them survives. If the BU catalogue is correct, the range quoted for this species by Thomas *et al.* (1984, fig. 23, p. 52) is extended downwards. Several other typically Wenlock species are recorded from this horizon also (Thomas *et al.* 1984, p. 54). The Dudley syntypes probably came from the storm-generated obrution deposits which occur towards the top of the Nodular Beds Member of the Much Wenlock Limestone Formation (see Dorning (1983) for formalization of Butler's (1939) lithostratigraphy).

There are many good, articulated (commonly enrolled) specimens of this species in the major British palaeontological collections. Most are from the Coalbrookdale Formation of the Malvern area or the Much Wenlock Limestone Formation of the West Midlands inliers or Malvern. Similarities in preservation suggest that most of the specimens came from a small number of horizons.

The species also occurs in the Wenlock of Gotland. In describing that material, Ramsköld (1985, p. 30) noted contrasts between the smaller Malvern specimens and the larger ones from Dudley figured by Salter, suggesting that he might have confounded two *Eophacops* species. Study of all the available British material suggests that Salter was correct in assigning his specimens to a single species.

Description. Because Ramsköld (1985) suggested that separate species might be represented in the Dudley and Malvern areas, data relating to specimens from the two localities are plotted separately (Text-fig. 2A–B). A two-tailed version of the non-parametric Mann–Whitney test indicates that the samples do not significantly differ from each other in size ($U = 55{\cdot}5$; a significant difference at the 5 per cent. level requires $U < 42$). The overall morphology of the visual surface is very similar in the samples from the two localities. Some Dudley specimens

have an additional lens at the base of each of files 1–4 and at the top of files 5 and 8. At both localities specimens have either 19 or 20 files (Text-fig. 3): the Malvern sample has a higher proportion with 19. A one-tailed Mann–Whitney test shows that the number of files present is not directly correlated with specimen size ($U = 79{\cdot}5$; a significant correlation at the 5 per cent. level requires $U < 48$).

The minimum number of lenses is 103; the maximum number preserved is 140 (allowing for preservation, < 144 may have been present originally). The lenses shaded in files one and two in Text-figure 2 occur in all specimens, and the distribution of the other lenses is plotted accordingly. At the maximum height of the eye, files of six (rarely), seven or eight lenses alternate with seven, eight or nine respectively. The material from the Wenlock of Gotland (Ramsköld 1985, p. 25, fig. 4B) shows a pattern of variation which falls within that described here. All those specimens had 20 files.

A single Malvern specimen (Pl. 1, fig. 4; Text-fig. 4B) has 21 files in its left eye. Comparison with other specimens suggests that the additional file, which contains just one lens, lies in a position which might be termed file '0'. The right visual surface is not uniformly well preserved, and a full lens count is impossible. It is well preserved anteriorly, and no single lens in this position is seen. A small depression at the anterior margin of the right visual surface may mark its position, however. Alternatively, the two eyes may have been asymmetrical in this regard. There are two specimens which certainly show different numbers of files in each eye (Text-fig. 4C–D). The right eye of OUM C16680/1 has 19 files whilst 20 occur in the left. Slight damage to the left eye makes an exact lens count impossible, but the additional file seems to occupy the position indicated by the crosses in Text-figure 4D. OUM C16680/3 (Text-fig. 4D) shows a similar posterior extension, also at the back of the left eye. There is no measurable difference in the exsagittal lengths of the eyes on the right and left sides of these specimens, but the minor distortion suffered by both makes minor differences in length impossible to establish reliably (Pl. 1, figs 7–8).

Remarks. Most variation in the pattern of lens distribution in *E. musheni* occurs dorsally, ventrally and posteriorly (Text-fig. 2): only occasionally is the front of the visual surface affected. A similar pattern of variation was noted in Devonian phacopids by Campbell (1977, p. 40), and is documented also for *Acernaspis superciliexcelsis* from the Scottish Llandovery (Howells 1982, text-fig. 8, p. 42), and for Silurian *Eophacops* species from Gotland (Ramsköld 1985, fig. 4, p. 25). In describing material of the Ordovician *Calyptaulax brongniartii*, Clarkson and Tripp (1982, fig. 6, p. 293) noted that populations from different localities differed in the pattern of lens distribution. Comparable variation is seen in samples of *Eophacops sprogensis* from Gotland (Ramsköld 1985, fig. 4C–E). As described above, however, consistent differences between the Dudley and Malvern samples of *E. musheni* are small. This could be due to the averaging effect of combining populations from several separate original collections.

With one exception, the eyes of *E. musheni* have 19 or 20 files of lenses. The two specimens which possess 20 files in their left eyes and 19 in their right are notable in this context. There is no obvious sign of injury, yet the variation in file number between the two sides of the same specimen is comparable with that occurring between individuals in the population as a whole. Specimens of *Acaste* showing comparable asymmetries are described below.

EXPLANATION OF PLATE 1

Figs 1–5, 7–8. *Eophacops musheni* (Salter, 1864); Coalbrookdale Formation (?), Malvern district, Hereford and Worcester. 1–3, paralectotype, BU 59a; anterior, palpebral and left lateral views; ×4. 4, OUM C16880/2; slightly oblique anterior view of part of cephalon; arrowhead indicates lens comprising file '0' (see text for details); ×10. 5, lectotype, BU 59c; oblique anterolateral view; ×4. 7, OUM C16680/1; palpebral view; ×4. 8, OUM C16680/3; palpebral view; ×4.

Figs 6, 9–11. *Acaste inflata* Salter, 1864; lectotype, OUM C9; Much Wenlock Limestone Formation, Ledbury Railway Tunnel, Hereford and Worcester. 6, 9, palpebral and anterior views of whole specimen; ×3. 10–11, lateral views of left and right eyes; ×9.

Figs 12–14. *Acaste* cf. *inflata* Salter; NMW 27.110.G998.3; Much Wenlock Limestone Formation, Dudley, West Midlands. 12, 14, lateral views of left and right eyes; ×9. 13, palpebral view of cephalon; ×4.

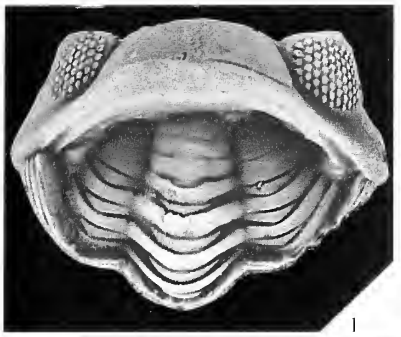
1

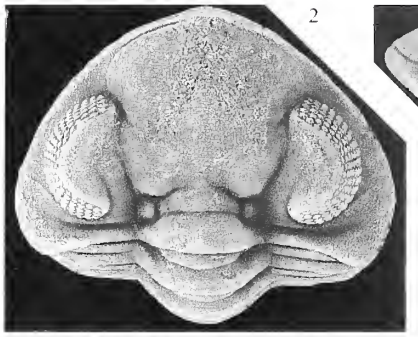
2

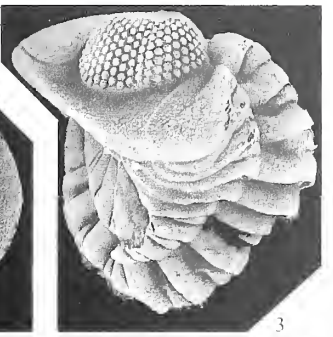
3

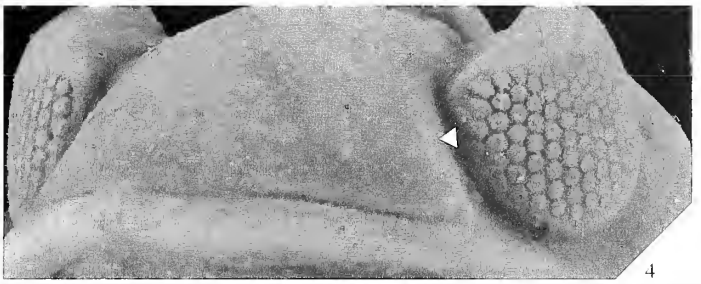
4

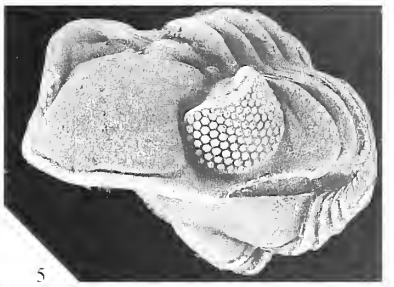
5

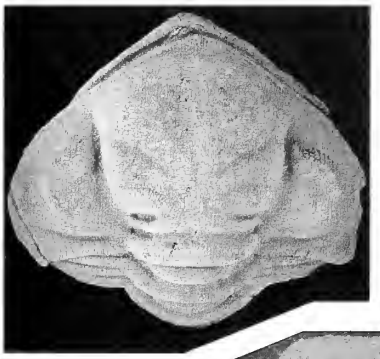
6


7

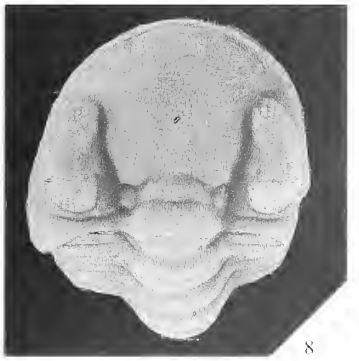
8

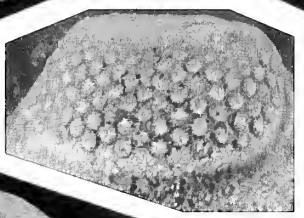
10

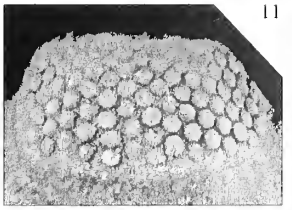
11

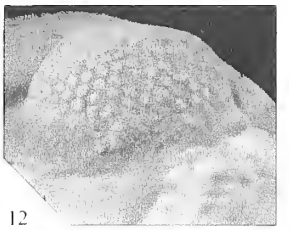
12

9

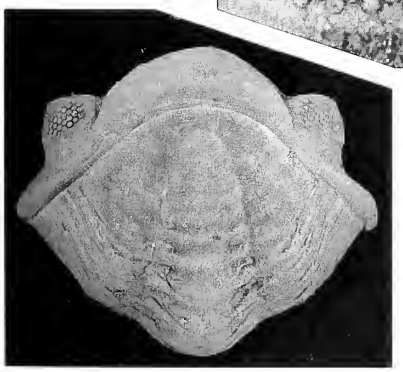

13

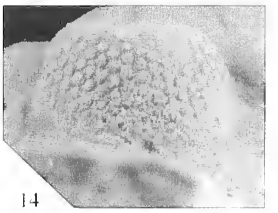
14

THOMAS, *Eophacops*, *Acaste*

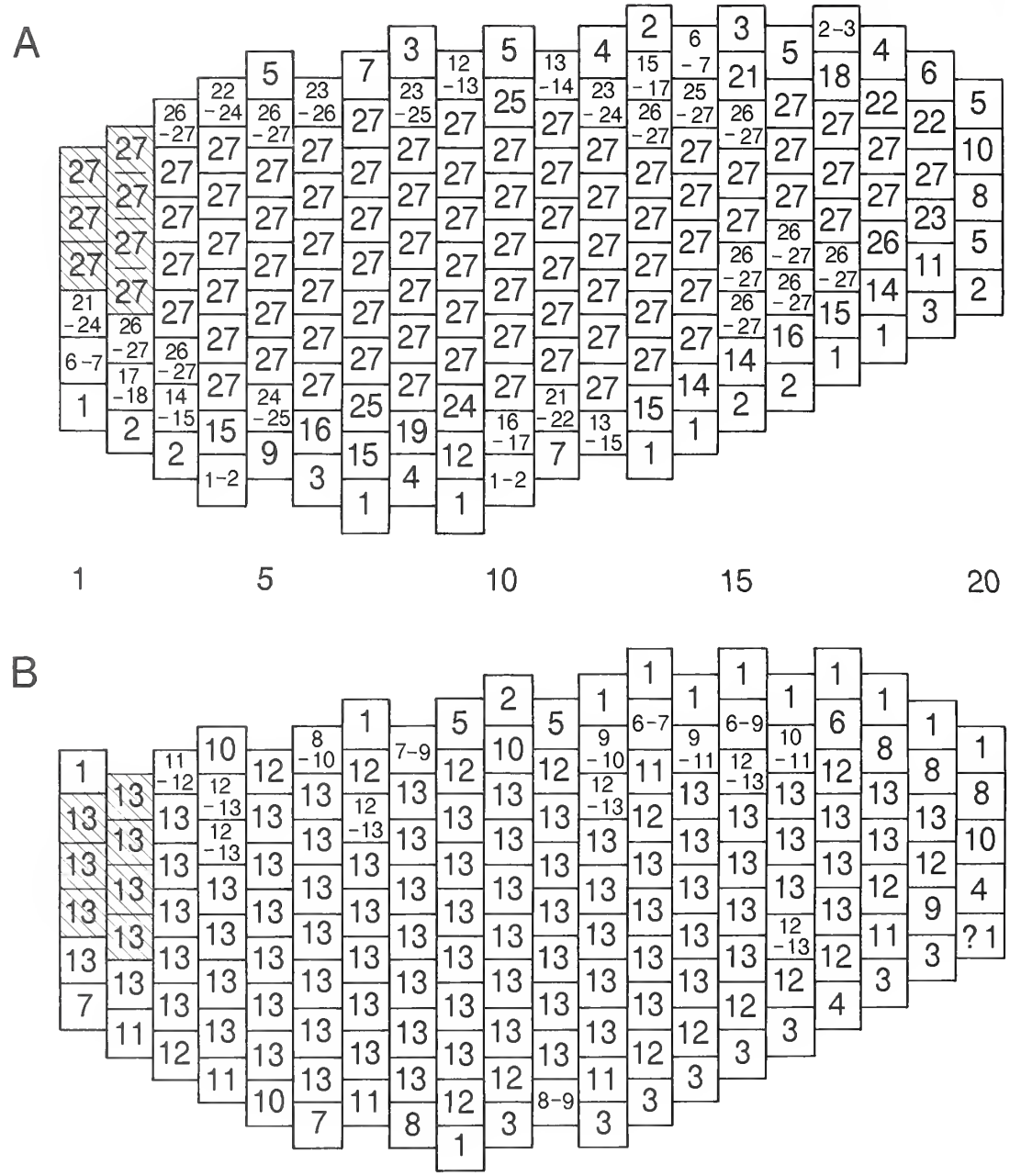

TEXT-FIG. 2. Schematic representation of visual surfaces in *Eophacops musheni* (Salter, 1864). Front of eye is to left; numbers below drawing denominate individual dorso-ventral files, counting from the front. A, sample from Much Wenlock Limestone Formation, Dudley, and Walsall (two specimens); 27 eyes of 26 specimens. B, sample from Coalbrookdale Formation (?), Malvern district; 13 eyes of 13 specimens. Numbers in boxes indicate the number of surfaces having that lens; ranges indicate uncertainty due to preservation. Positionally equivalent lenses in files 1 and 2 shaded; see text for further explanation.

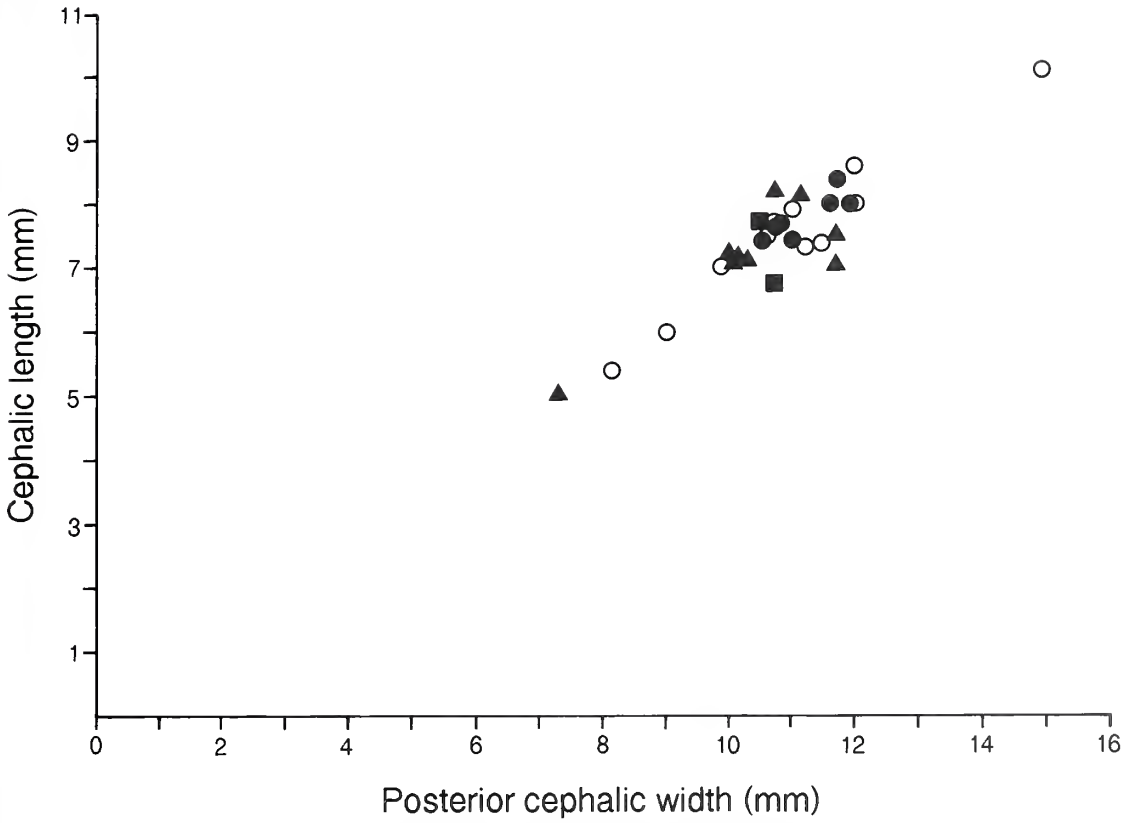

TEXT-FIG. 3. Scatter diagram of cephalic length (in palpebral view) versus posterior cephalic width in 29 specimens of *Eophacops musheni* (Salter, 1864). Circles indicate Dudley specimens, triangles those from Malvern; squares are used for Walsall material. Solid symbols denote specimens with 20 files of lenses, open symbols those with 19.

In most cases where phacopine specimens with both eyes well preserved have been described, the visual surfaces are identical. Rare asymmetries have been recorded, however. Clarkson (1966*a*, p. 12, text-fig. 4a–b) described one specimen of *A. downingiae* with two extra lenses in the right eye and a hiatus in the centre of the left. Similar minor irregularities have been described in *Reedops* species from the Devonian of Bohemia (Clarkson 1969, pp. 195, 197). Such asymmetries could arise either from minor injuries or developmental irregularities. Ludvigsen (1979, p. 77, fig. 51c, p. 82) described a specimen of *Phacops rana*, from the Devonian of Ontario, with markedly asymmetrical eyes: the left eye is much smaller than the right, and has only about 20 lenses (compared with 67 in the right eye). Ludvigsen attributed the condition to an early injury. However, Owen (1985, p. 259) noted that the whole left cheek is reduced in size but has an otherwise normal morphology. I agree with him that this makes a genetic or developmental abnormality more likely.

There are no recent descriptions of several named species of *Eophacops* (for species list see Ramsköld and Werdelin 1991, p. 66), but good descriptions and illustrations are available for the species from Gotland (Ramsköld 1985) and Bohemia (Chlupáč 1977). Within these species, there are 18–21 files of lenses, with the maximum number per file varying from five to nine. The visual surfaces of *E. musheni* are at the larger end of the spectrum in terms of the number of lenses present. Some of the smaller-eyed species, such as *E. lauensis* Ramsköld (1985, pl. 6, fig. 5B, fig. 6F, p. 25), could be distinguished from larger-eyed forms on the morphology of the visual surface alone. In

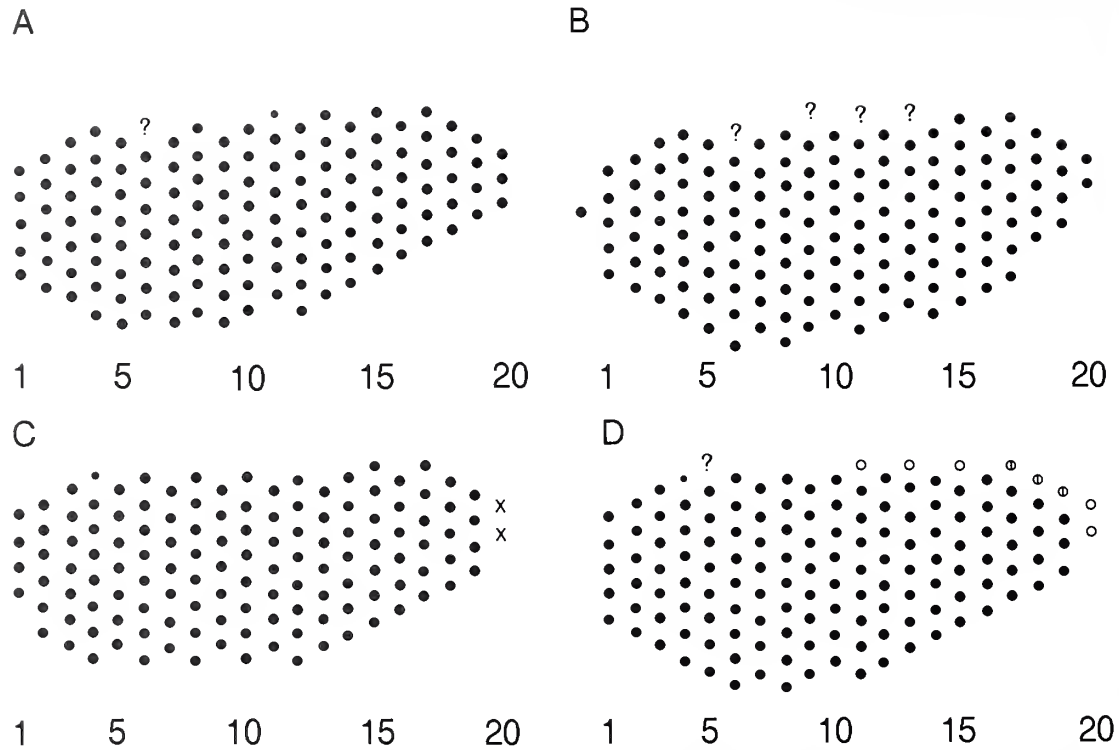

TEXT-FIG. 4. Schematic representation of visual surfaces in *Eophacops musheni* (Salter); Coalbrookdale Formation (?), Malvern district. Front of eye is to left; numbers below drawing denominate individual dorso-ventral files, counting from the front. A, paralectotype BU 591 (both eyes). B, OUM C16680/2 (left eye). C, OUM C16680/1 (right eye). Twenty files occur in the less well preserved left eye, the additional file apparently in the position marked by the crosses. D, OUM C16680/3: solid shading indicates presence of lens in both eyes; blank circles, presence in left eye only; circles with vertical bar, lens present in left eye but occurrence in less well preserved right eye uncertain.

other cases, however, lens patterns would provide only a more general guide to species identity, particularly given the degree of variation which occurs.

Family ACASTIDAE Delo, 1935
Subfamily ACASTINAE Delo, 1935

Remarks. The family level classification of acastomorph trilobites has been fluid ever since the group was first recognized. Edgecombe's (1993) arrangement is followed here.

Genus ACASTE Goldfuss, 1843

Type species. By subsequent designation of Burmeister (1843, p. 139); *Calymene? Downingiae* Murchison, 1839; from the Much Wenlock Limestone Formation (Homerian), Wren's Nest Hill, Dudley, West Midlands.

Acaste inflata Salter, 1864

Plate 1, figures 6, 9–11; Text-figure 5

v*.1864 *Phacops* (*Acaste*) *Downingiae* Murchison, var. *γ*, *inflatus*, Salter, p. 27, pl. 2, fig. 30 only.

1966a *A. downingiae inflatus* (Salter); Clarkson, p. 11.
v.1966 *Acaste inflata* (Salter 1864); Shergold, p. 192, pl. 29, figs 9–16.

Lectotype. Selected by Shergold 1966, p. 192; OUM C9, complete enrolled specimen figured Salter 1864, pl. 2, fig. 30, refigured Shergold 1966, pl. 29, figs 9–14; from the Much Wenlock Limestone Formation, Ledbury Railway Tunnel, Hereford and Worcester.

Material localities and horizons. A. inflata is a rare species, with about 20 specimens being known from the Much Wenlock Limestone Formation of the Dudley and Walsall inliers (West Midlands) and the Ledbury area, near Malvern. Morphologically similar specimens occur in rocks of late Wenlock age in the Tortworth and Usk inliers and in the Elton Beds (lower Ludlow) of Shropshire. The BGS, NHM and OUM house most of the material.

Description. Clarkson (1966*a*, p. 11) had no material with the visual surface preserved, but Shergold (1966, p. 192) diagnosed the species as having vertical files of seven lenses alternating with six at the maximum height of the eye. In his description (p. 193), he recorded a maximum of 130 lenses in an individual visual surface.

Text-figure 5A shows the pattern of lens distribution in the visual surfaces of four specimens of this species. There are 21 or 22 dorso-ventral files. The minimum number of lenses is 108 (allowing for preservation, 113 lenses may have been present originally); the maximum number is 122. Files 1–4 are identical in all specimens: the distribution of other lenses is plotted accordingly. The lectotype of *A. inflata* has eyes which differ in the number of files (Text-fig. 5B–C). The left eye (Pl. 1, fig. 10) has 21 files and, allowing for minor damage to the top of the visual field, compares very closely with other specimens of the species. Only 19 files occur in the right eye (Pl. 1, fig. 11), however, and the total number of lenses is 99. Files 5–9 and 11–16 contain either five or six lenses, and only file ten has seven. The right eye is *c.* 13 per cent. shorter (exsag.) than the left (Pl. 1, fig. 6; this is less evident in Shergold's 1966, pl. 29, fig. 9 because the specimen is there illustrated in occipital view, and the palpebral lobes are consequently foreshortened). In the other specimens, six is the minimum number of lenses in these files and files 4–7 have seven. Packing irregularities occur in files 7–12, but these are minor. A specimen possibly belonging to this species also has asymmetrical eyes (Pl. 1, figs 12–14; Text-fig. 5D–E). In both, files of six and seven lenses alternate at the maximum height of the visual surface. However, the left eye has 21 files and 118 preserved lenses (possibly 121 originally) whilst the right has 22 files and 126 lenses (?128 originally). In this case, the right eye is slightly shorter (exsag.) than the left (compare anterior limit of palpebral lobes relative to abaxial ends of 3S furrows on Pl. 1, fig. 13), despite the higher number of files. Packing irregularities are evident between files 15 and 19 of the right eye.

Remarks. The lectotype of *A. inflata* is notable for possessing two more files of lenses in the left eye than in the right. Increased length of the left visual field has been achieved by the development of additional files posteriorly, as appeared to be the case in comparable specimens of *Eophacops musheni*. The specimen is undistorted, and the right eye is noticeably shorter than the left, indicating that lens size and spacing have remained constant. The presence of minor packing irregularities in the right eye might indicate that the smaller number of files there reflects incomplete development of that visual surface, rather than reflecting extended development of the left surface. In the specimen of *A.* cf. *inflata* the slightly smaller right eye is the one with the larger number of files, again suggesting that it is that eye which is abnormal. Files 1–15 are normally developed, but file 16, while straight, does not extend to the top of the visual surface: it has the appearance of having been intercalated (Text-fig. 5E). Slight packing irregularities develop posterodorsally, because the upper parts of files 17 and 18 curve slightly forwards. I argue later in this paper that these eye asymmetries result from developmental abnormalities, although of course these could have been precipitated by injuries. Babcock (1993) recognized that sublethal injuries are more common on the right hand side of trilobites than on the left.

A. inflata resembles *A. downingiae*, a species which is more common and more widely distributed in the British Homerian. The number of specimens with well preserved visual surfaces, however, is small. The eyes of *A. downingiae* are generally larger than those of *A. inflata*, and were described in detail by Clarkson (1966*a*, p. 11). He distinguished two eye variants, basing his description on seven well preserved specimens (figures quoted below include some additional data collected by ATT and from Shergold 1966, p. 189). The more common form, Clarkson's eye variant A, has larger

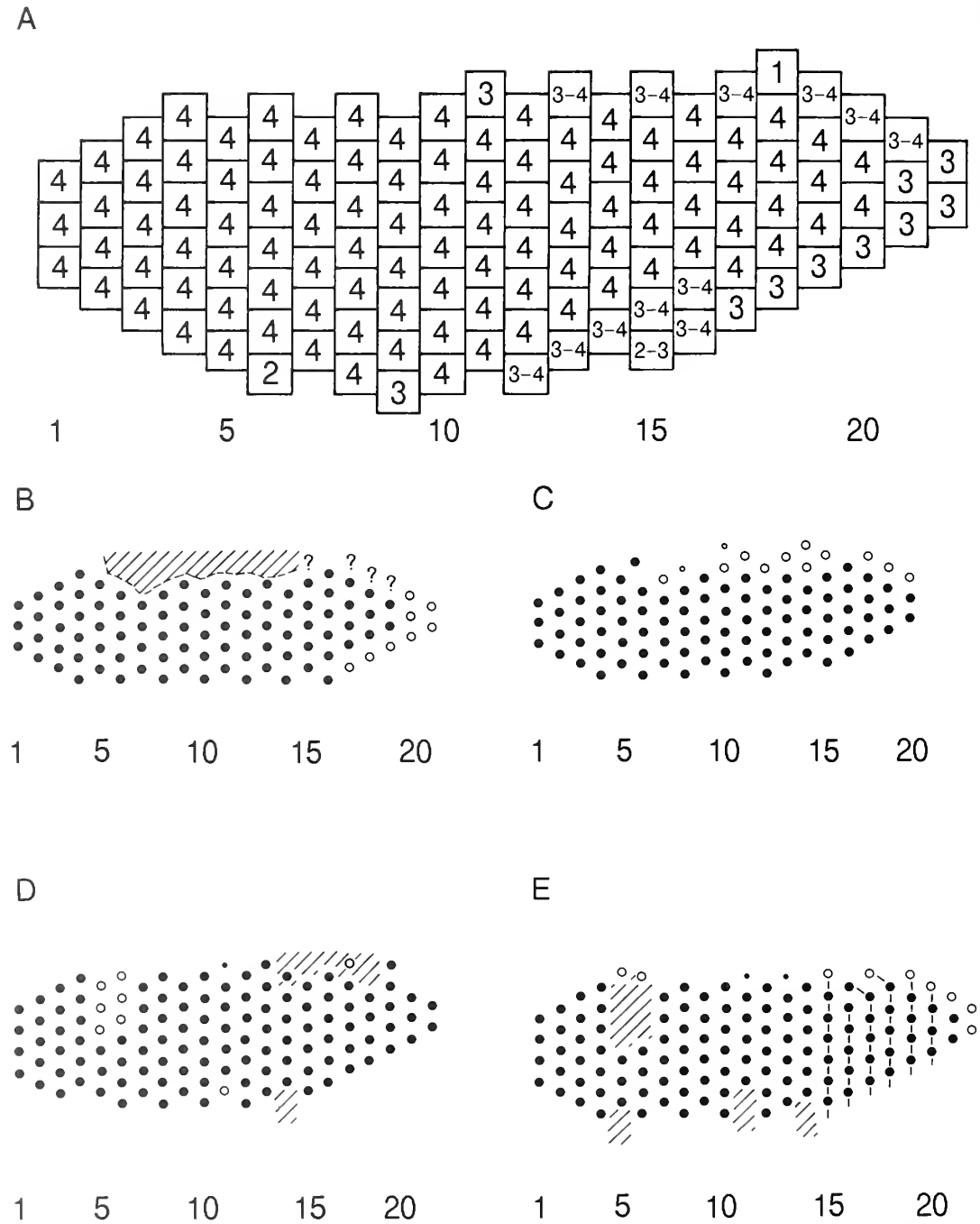

TEXT-FIG. 5. Schematic representation of visual surfaces in *Acaste inflata* Salter, 1864 and *A.* cf. *inflata*. Front of eye is to left; numbers below drawing denominate individual dorso-ventral files, counting from the front. A, *A. inflata*; plan of lens distribution in four surfaces of four specimens (OUM C559, C614, C617, NHM I1520). Numbers in boxes indicate the number of surfaces having that lens; ranges indicate uncertainty due to preservation. B–C, *A. inflata*; plan of lens distribution in left and right eyes of lectotype, OUM C9; Much

TABLE 1. Distribution of lenses in the visual surfaces of *Acaste* species, anterior of eyes to left. Top row shows number of lenses per file in *A. inflata* (left eye of OUM C614). Data below are counts from *A. downingiae* eye variant B (from Clarkson 1966*a*, table 1, p. 13; based on SM A28737 and A28741).

A. inflata	345	666	677	777	767	665	543	2
A. downingiae	345	566	567	666	656	655	543	
	345	677	778	787	777	676	654	32

eyes, with 22–25 files. The total number of lenses recorded ranges from 111 to 168, with files of 7 (8) alternating with 8 (9) at the maximum height of the visual field. Specimens of eye variant B have smaller eyes, containing 109–136 lenses arranged in 21–23 dorso-ventral files. At the maximum height of the visual field, files of 6 (7) lenses alternate with 7 (8). The two eye variants occur in collections made from a single locality and are otherwise similar morphologically.

The range of variation in eye variant B overlaps with that found in the generally smaller-eyed *A. inflata* (Table 1). These data indicate that lens patterns provide a less reliable guide to species identification in acastomorphs than Shergold (1966) believed.

Given this overlap in morphology with a related species and the degree of variation known to occur in some other phacopines, I doubt that *A. downingiae* really displays dimorphism in its visual surface. It seems more likely that the apparent dimorphism reflects the small number of specimens on which the analysis was based: certainly, a significantly larger sample would be needed to demonstrate dimorphism convincingly. Dimorphism and polymorphism in eye morphology have been claimed quite widely in the Phacopina, and some cases were critically reviewed by Ramsköld and Werdelin (1991, p. 59). They concluded that some of the morphs may represent distinct taxa, whilst in other cases it is not known whether different morphs originally occurred at the same horizons. Among Silurian trilobites, the most convincing case of polymorphism was described by Siveter (1989) in his *Ananaspis* aff. *stokesii* (= *A.* (*s.l.*) *nuda* Salter, 1864; see Ramsköld and Werdelin 1991, p. 73), from western Ireland. In that species, a morph with 21? or 22 files with up to nine lenses in each co-occurs with a smaller-eyed form possessing 17–20 files, with a maximum of six lenses per file (Siveter 1989, p. 136, pl. 19). The differences in the visual surface are associated with other minor morphological contrasts.

DEVELOPMENT OF THE VISUAL SURFACE IN PHACOPINA

The existing state of knowledge was reviewed by Clarkson (1975, p. 13). Eyes first appear in the protaspis stage. They are anteriorly placed, and migrate posteriorly during ontogeny. The first lenses are emplaced in a generative zone lying directly below the palpebral margin, and these form a single horizontal row (the accessory upper horizontal row on Text-fig. 1). This generative zone has the form of an anteriorly expanding logarithmic spiral in plan view (Clarkson 1975, fig. 3a–c, p. 14). As the eye grows, the generative zone migrates downwards so that subsequent lenses are always emplaced below existing ones, at the bottom of the visual surface. Clarkson distinguished two components to the developmental programme: (1) growth of the generative zone; (2) lens

Wenlock Limestone Formation, Ledbury Railway Tunnel, Hereford and Worcester. Shaded circles indicate presence of lens in both eyes. D–E, *A.* cf. *inflata*; plan of lens distribution in left and right eyes of NMW 27.110.G998.3; Much Wenlock Limestone Formation, Dudley, West Midlands. Shaded circles indicate presence of lens in both eyes. Dashed lines in E indicate the traces of files 15–20: packing irregularities occur in this part of the eye.

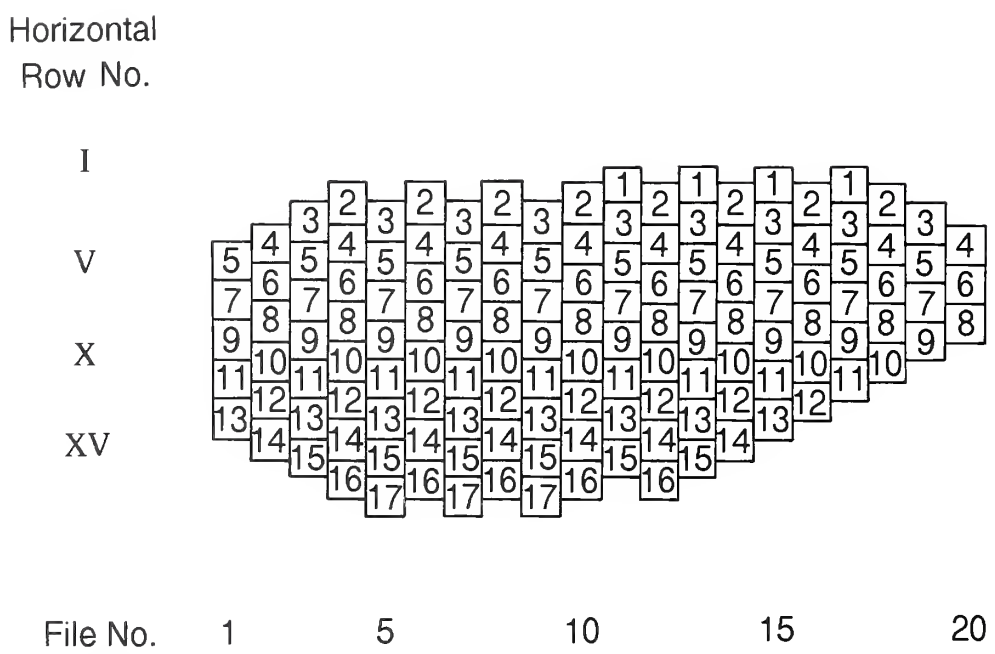

TEXT-FIG. 6. Schematic representation of visual surface in a paralectotype of *Eophacops musheni* (Salter). Front of eye is to left; numbers below drawing denominate individual dorso-ventral files, counting from the front. Roman numerals denote successive horizontal rows; boxes representing lenses are numbered accordingly. See text for discussion.

emplacement. He noted that lens addition may begin while the generative zone is still growing anteriorly, and used this to account for the accessory upper horizontal row of lenses in the rear part of the eye in dalmanitids. The patterns of variation described here further clarify the process of visual surface development in phacopine trilobites.

In the simplest case, several centres in the generative zone would become active simultaneously, thus creating a simple accessory upper horizontal row. The variation at the top of the visual field in *E. musheni* and *A. inflata* implies that initiation of lens emplacement was not synchronous in all individuals. Although a pattern of vertical files and horizontal rows could be constructed by an inclined generative zone, the pattern of lengthening of successive horizontal rows at the top of the visual surface described below indicates that the generative zone was orientated horizontally (i.e. at right angles to the file axes) during its descent. Additional active centres arose anteriorly and posteriorly as each new horizontal row was added: this would allow for the emplacement of new lenses as the visual surface expanded, and lenses in equivalent positions should be identifiable posteriorly and dorsally (Clarkson and Tripp 1982, p. 293). Text-figure 6 illustrates the inferred sequence of lens emplacement in a single specimen of *E. musheni*. Lens emplacement began posterodorsally, with the development of an accessory upper horizontal row of four lenses. In forming horizontal row II (eight lenses), the active section of the generative zone had extended anteriorly to a considerable extent, but to a much smaller degree posteriorly. By row IV, the maximum number of lenses (ten) was achieved. By this stage, the active section of the generative zone had expanded forward to its full extent, so that positionally equivalent lenses can be recognized in the upper anterior portion of the visual field (Text-fig. 2). An individual with eyes asymmetrical in terms of file number could be produced either by arrested development of the active section of the generative zone on one side, or by its continued extension on the other. This seems to have

occurred in the specimens of *E. musheni* and *A. inflata*, and could account for the possession of additional files either anteriorly or posteriorly. The apparent intercalation of an additional, incomplete, file into one visual surface of the specimen of *A.* cf. *inflata*, implies the development of an additional centre of lens development within the active section of the generative zone during its downwards migration.

Horizontal rows IV to IX all contain ten lenses, so that the eye contains 20 files. Termination of lens emplacement began at the rear of the eye (row IX), and somewhat later at the front (row XIII), the anterior and posterior descending diagonal rows at the base of the eye indicating that emplacement persisted longest anteromedially (files 5–9). Again, variation in the timing of the termination of lens emplacement in different individuals would lead to the observed variation in lens patterns in the lower part of the eye.

The additional developmental instructions needed to produce the patterns documented are: initiation of lens emplacement along an active section of the generative zone; growth of this section to a maximum size and its differential development anteriorly; and termination of lens emplacement.

Initiation of lens emplacement. A trigger must have caused lens emplacement to begin in an active section of the generative zone. If initiation of an individual lens was controlled by the distance between adjacent lens centres, then lenses in each horizontal row would be equally spaced, and those in vertically adjacent horizontal rows would alternate: this automatically leads to hexagonal close packing and to the production of dorso-ventral files. A characteristic of certain Phacopina is that the lenses increase in size from top to bottom of the dorso-ventral files, reflecting increased spacing of lens centres through a constant arithmetic factor in successive horizontal rows (Clarkson 1975, p. 20; Pl. 1, fig. 3). This device allows areally efficient hexagonal close packing to be combined with arrangement of lenses in files and rows while the visual surface simultaneously expands outwards as well as downwards.

Fortey and Morris (1977) described variation in lens packing in *Phacops turco* aff. *praecedens* from the Eifelian of Morocco. Their sample is dominated by individuals whose eye lenses are emplaced on the cubic close packing system, although one specimen displays hexagonal close packing, and two show an intermediate arrangement. All specimens have clear dorso-ventral files. Evidently the regular arrangement of lenses was of greater importance to the animals than the efficiency of the packing system. In the case of the specimens showing cubic close packing, the retention of dorso-ventral files must reflect modification of the spacing factor between adjacent lens centres in successive horizontal rows.

Growth to a maximum size of the active section of the generative zone and its differential growth anteriorly. Differences in the number of lenses in the horizontal row results in eyes with different numbers of dorso-ventral files. The existence of individual specimens possessing eyes which differ in the number of files indicates that file number is not an expression of direct genetic control. Rather, it is a consequence of a developmental programme.

Termination of lens emplacement. Once initiated at the back of the eye, termination of lens emplacement progressed continuously. The maximum number of lenses in each dorso-ventral file is thus a consequence of the timing of onset of termination of lens emplacement and the number of files which occur (the latter, in turn, reflects the maximum number of lenses in a horizontal row).

Acknowledgements. I thank the curators of the British Geological Survey (BGS), Lapworth Museum, University of Birmingham (BU), the National Museum of Wales (NMW), The Natural History Museum (NHM), and Oxford University Museum (OUM) for the loan of specimens in their care (abbreviated prefixes of specimen numbers shown in brackets). Dr J. R. Ashworth kindly advised on statistical methodology. Drs E. N. K. Clarkson, P. D. Lane and M. P. Smith commented on an earlier version of the manuscript and made useful suggestions for its improvement.

REFERENCES

BABCOCK, L. E. 1993. Trilobite malformations and the fossil record of behavioural asymmetry. *Journal of Paleontology*, **67**, 217–229.

BURMEISTER, H. 1843. *Die Organisation der Trilobiten, aus ihren lebenden Verwandten entwickelt; nebst einer systematischen Uebersicht aller zeither beschriebenen Arten*. G. Reimer, Berlin, 146 pp., 6 pls.

BUTLER, A. J. 1939. The stratigraphy of the Wenlock Limestone of Dudley. *Quarterly Journal of the Geological Society, London*, **95**, 37–74.

CAMPBELL, K. S. W. 1967. Henryhouse trilobites. *Bulletin of the Oklahoma Geological Survey*, **115**, 1–68, pls 1–19.

—— 1977. Trilobites of the Haragan, Bois d'Arc and Frisco Formations (Early Devonian), Arbuckle Mountains region, Oklahoma. *Bulletin of the Oklahoma Geological Survey*, **123**, i–vi + 1–227, pls 1–40.

CHLUPÁČ, I. 1977. The phacopid trilobites of the Silurian and Devonian of Czechoslovakia. *Rozpravy Ústředního Ústavu Geologického*, **43**, 1–172, pls 1–32.

CLARKSON, E. N. K. 1966*a*. Schizochroal eyes and vision of some Silurian acastid trilobites. *Palaeontology*, **9**, 1–29, pls 1–3.

—— 1966*b*. The life attitude of the Silurian trilobite *Eophacops musheni* Salter 1864. *Scottish Journal of Geology*, **2**, 76–83, 1 pl.

—— 1969. On the schizochroal eyes of three species of *Reedops* (Trilobita: Phacopidae) from the Lower Devonian of Bohemia. *Transactions of the Royal Society of Edinburgh*, **68**, 183–205, 3 pls.

—— 1975. The evolution of the eye in trilobites. *Fossils and Strata*, **4**, 7–31.

—— 1979. The visual system of trilobites. *Palaeontology*, **22**, 1–22.

—— and LEVI-SETTI, R. 1975. Trilobite eyes and the optics of Des Cartes and Huygens. *Nature*, **254**, 663–667.

—— and TRIPP, R. P. 1982. The Ordovician trilobites *Calyptaulax brongniartii* (Portlock). *Transactions of the Royal Society of Edinburgh: Earth Sciences*, **72** (for 1981), 287–294.

DELO, D. M. 1935. A revision of the phacopid trilobites. *Journal of Paleontology*, **9**, 402–420.

DORNING, K. J. 1983. Palynology and stratigraphy of the Much Wenlock Limestone Formation, Dudley, central England. *Mercian Geologist*, **20**, 31–40.

EDGECOMBE, G. D. 1993. Silurian acastacean trilobites of the Americas. *Journal of Paleontology*, **67**, 535–548.

FORDYCE, D. and CRONIN, T. W. 1993. Trilobite vision: a comparison of schizochroal and holochroal eyes with the compound eyes of modern arthropods. *Paleobiology*, **19**, 288–303.

FORTEY, R. A. 1997. Late Ordovician trilobites from southern Thailand. *Palaeontology*, **40**, 397–449.

—— and MORRIS, S. F. 1977. Variation in lens packing of *Phacops* (Trilobita). *Geological Magazine*, **114**, 25–32.

GOLDFUSS, A. 1843. Systematische Übersicht der Trilobiten un Beschreibung einiger neuen Arten derselben. *Neues Jahrbuch für Mineralogie, Geologie und Paläontologie*, **1843**, 537–567, pls 4–6.

HAWLE, I. and CORDA, J. C. 1847. *Prodrom einer Monographie der böhmischen Trilobiten*. J. G. Calve, Prague, 176 pp., 7 pls.

HORVÁTH, G. 1996. The lower lens unit in schizochroal trilobite eyes reduces reflectivity: on the possible optical function of the intralensar bowl. *Historical Biology*, **12**, 83–92.

—— CLARKSON, E. N. K. and PIX, W. 1997. Survey of modern counterparts of schizochroal trilobite eyes: structural and functional similarities and differences. *Historical Biology*, **12**, 229–263.

HOWELLS, Y. 1982. Scottish Silurian trilobites. *Monograph of the Palaeontographical Society*, **135** (561), 1–76, pls 1–15.

LUDVIGSEN, R. 1979. Fossils of Ontario. Part 1: the trilobites. *Royal Ontario Museum, Life Sciences Miscellaneous Publications*, 96 pp.

MORRIS, S. F. 1988. A review of British trilobites, including a synoptic revision of Salter's monograph. *Monograph of the Palaeontographical Society*, **140** (574), 1–316.

MURCHISON, R. I. 1839. *The Silurian System, founded on geological researches in the counties of Salop, Hereford, Radnor, Montgomery, Caermarthen, Brecon, Pembroke, Monmouth, Gloucester, Worcester and Stafford; with descriptions of the coalfields and overlying formations*. John Murray, London, xvi + 523 pp., 37 pls.

OWEN, A. W. 1985. Trilobite abnormalities. *Transactions of the Royal Society of Edinburgh: Earth Sciences*, **76**, 252–272.

OWENS, R. M. and THOMAS, A. T. 1995. *Eophacops* Delo, 1935 and *Acernaspis* Campbell, 1967 (Trilobita): proposed conservation. *Bulletin of Zoological Nomenclature*, **52**, 34–36.

RAMSKÖLD, L. 1985. Silurian phacopid and dalmanitid trilobites from Gotland. *Stockholm Contributions in Geology*, **40**, 1–62, pls 1–12.

—— and WERDELIN, L. 1991. The phylogeny and evolution of some phacopid trilobites. *Cladistics*, **7**, 29–74.

SALTER, J. W. 1864. A monograph of the British trilobites from the Cambrian, Silurian and Devonian formations. Part 1. *Monograph of the Palaeontographical Society*, **16** (67), 1–80, pls 1–6.

SHERGOLD, J. H. 1966. A revision of *Acaste downingiae* (Murchison) and related trilobites. *Palaeontology*, **9**, 183–207, pls 28–32.

SIVETER, D. J. 1989. Silurian trilobites from the Annascaul Inlier, Dingle Peninsula, Ireland. *Palaeontology*, **32**, 109–161.

STOCKTON, W. L. and COWEN, R. 1976. Stereoscopic vision in one eye: paleophysiology of the schizochroal eye of trilobites. *Paleobiology*, **2**, 304–315.

THOMAS, A. T. 1978. British Wenlock trilobites. Part 1. *Monograph of the Palaeontographical Society*, **132** (552), 1–56, pls 1–14.

—— 1981. British Wenlock trilobites. Part 2. *Monograph of the Palaeontographical Society*, **134** (559), 57–99, pls 15–25.

—— OWENS, R. M. and RUSHTON, A. W. A. 1984. Trilobites in British stratigraphy. *Geological Society of London, Special Report* no. 16, 78 pp.

ZHANG XI-GUANG and CLARKSON, E. N. K. 1990. The eyes of Lower Cambrian eodiscid trilobites. *Palaeontology*, **33**, 911–932.

A. T. THOMAS

School of Earth Sciences
The University of Birmingham
Edgbaston
Birmingham, B15 2TT, UK

Typescript received 3 September 1997
Revised typescript received 1 December 1997

THE EFFACED STYGINID TRILOBITE *THOMASTUS* FROM THE SILURIAN OF VICTORIA, AUSTRALIA

by ANDREW SANDFORD *and* DAVID J. HOLLOWAY

ABSTRACT. *Thomastus* is a blind effaced styginid trilobite that occurs in strata of Wenlock age in Victoria, Australia. The genus is most closely related to *Bumastella* and *Illaenoides*, with which it shares characters such as a highly convex cephalon, the absence of the omphalus and the anterolateral internal pit, a weakly forwardly converging facial suture, a transverse furrow in front of the articulating flange on the posterior fixigenal margin, and a pygidium with a deep holcos. Of the four species previously assigned to *Thomastus*, *T. collusor* and *T. vicarius* are considered to be synonyms of the type species *T. thomastus*. One new species, *T. aops*, is described.

THE trilobite *Thomastus* Öpik, 1953 is known only from strata of Wenlock age cropping out in the region between Melbourne and Heathcote in central Victoria, Australia (Text-fig. 1). Four species have been assigned to the genus: *T. thomastus* Öpik, 1953, *T. collusor* Öpik, 1953, and *T. vicarius* Öpik, 1953, all from the Wapentake Formation in the Heathcote district; and *T. jutsoni* (Chapman, 1912) from the Anderson Creek Formation at Bulleen and Balwyn in the eastern suburbs of Melbourne. Another species, *T. aops* sp. nov., from the Bylands Siltstone in the Bylands area, is newly described herein.

Since *Thomastus* was established it has remained poorly understood because of the indifferent preservation of many of the specimens, and because of the limited material on which three of the four previously named species are based. The opportunity to revise the genus has been provided by an enlarged collection of material acquired through recent field collecting and the transfer to the Museum of Victoria of specimens formerly housed in the Geological Survey of Victoria and the University of Melbourne.

FAUNAS AND AGE

Heathcote. The Wapentake Formation in the Heathcote district consists of approximately 1900 m of siltstones and sandstones conformably overlying the Costerfield Siltstone (Text-fig. 2). Low in the Wapentake Formation is a relatively thin band of siltstone characterized by the presence of siliceous concretions, many of them containing fossils, of which *Thomastus thomastus* is the most abundant. This horizon was named the '*Illaenus*' band by Chapman and Thomas (1935) and Thomas (1937), who considered it to mark the base of the Wapentake Formation. However, Rickards and Sandford (in press) note that the fauna of the '*Illaenus*' band ranges well above and below this level, and they redefined the base of the Wapentake Formation 400 m lower in the sequence at the appearance of prominent sandstones. Conformably overlying the Wapentake Formation are 2200 m of sandstones, siltstones and mudstones, named the Dargile Formation by Thomas (1937); Rickards and Sandford (in press) assign these beds to the Yan Yean Formation (lower) and the Melbourne Formation (upper), and raised the Dargile Formation to group status to incorporate the entire Wenlock–lowermost Ludlow sequence.

The fauna of the '*Illaenus*' band, described by Öpik (1953) and revised by Talent (1964), includes brachiopods, bryozoans, bivalves, gastropods, trilobites, ostracodes and conulariids. Some of the

[Palaeontology, Vol. 41, Part 5, 1998, pp. 913–928, 2 pls]

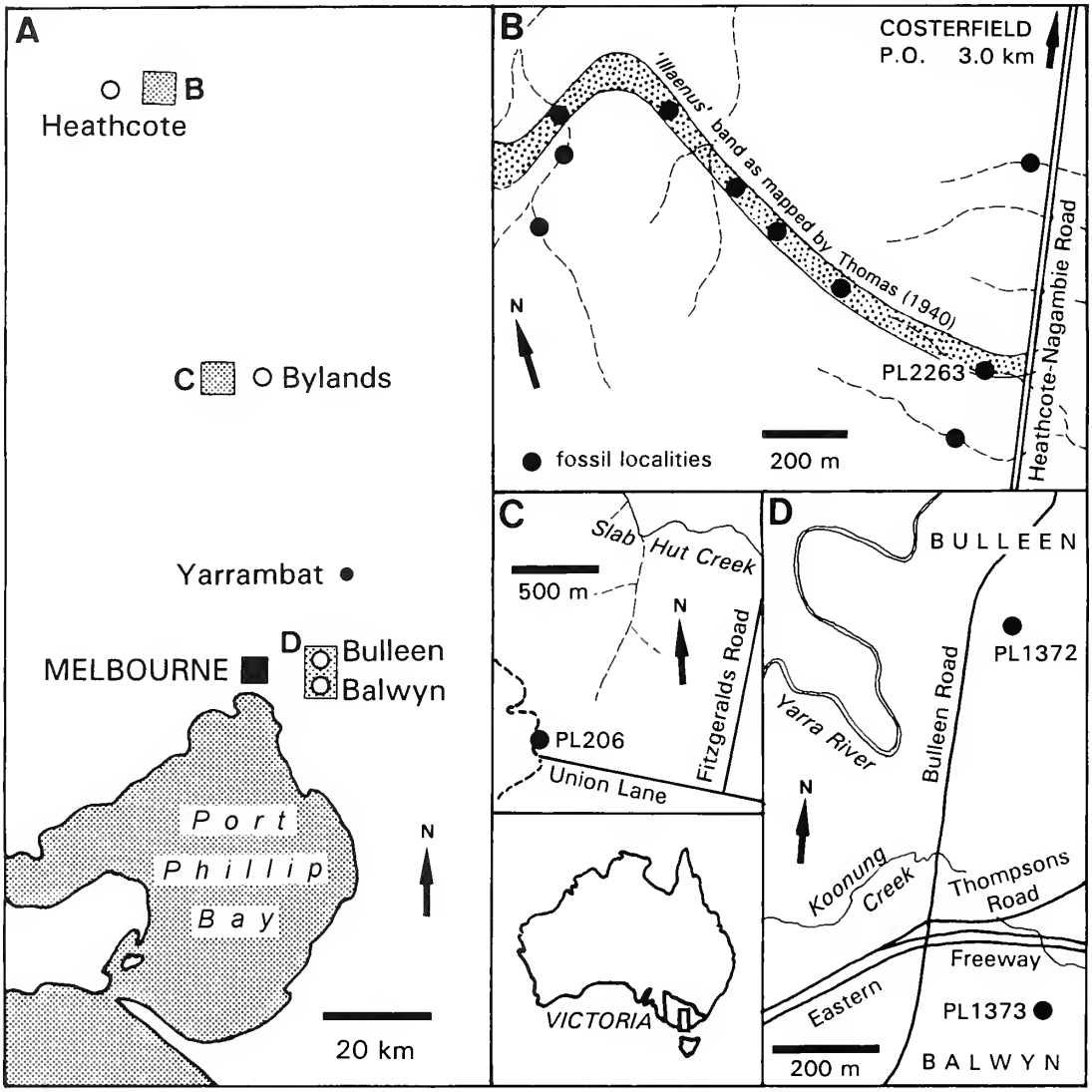

TEXT-FIG. 1. A, map of central Victoria showing localities from which *Thomastus* has been recorded; approximate areas of figures B–D indicated by shaded squares. B–D, location of *Thomastus* localities in the Heathcote, Bylands and Bulleen-Balwyn areas. Inset shows location of Victoria and area of figure A in Australia.

siliceous nodules from the band were interpreted by Öpik as coprolites, but they are probably concretions. At least 80 per cent. of the trilobites recovered from the band belong to *Thomastus*, but Öpik (1953) also described '*Phacops*' *typhlagogus* (= *Ananaspis*; see Campbell 1967, p. 32), *Dalmanites athamas* and '*Dalmanitina* (*Eudolatites*)' *aborigenum* (a junior synonym of *Dalmanites athamas*; see below). Other trilobites that we have identified from limited material are *Maurotarion* sp., *Trimerus*? sp., and indeterminate specimens of a calymenid, a proetid and an odontopleurid; the last includes a cephalon and the isolated thoracic segment identified by Öpik (1953) as *Ceratocephala* sp.

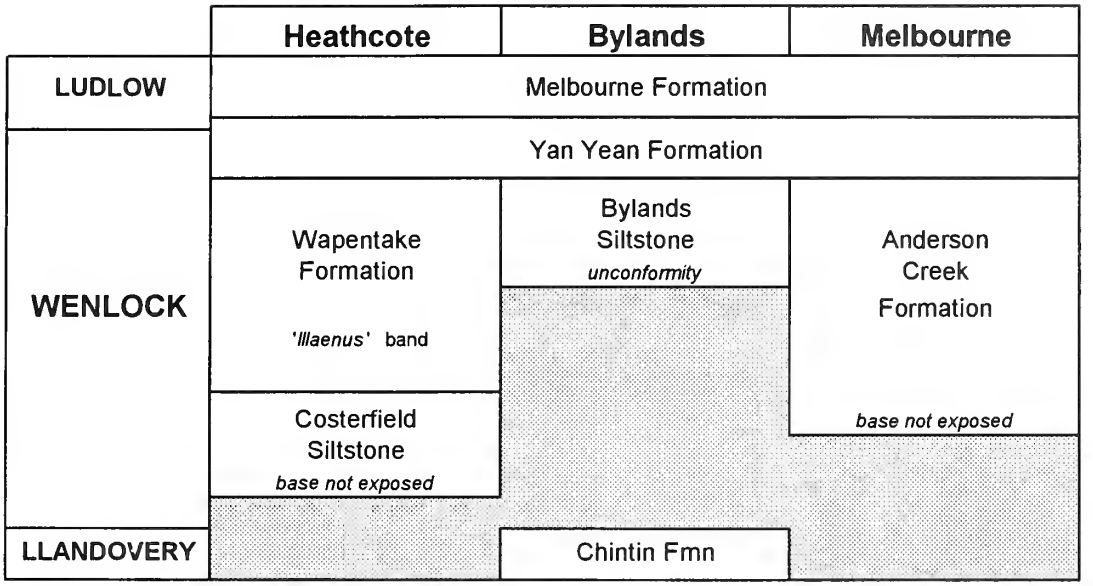

TEXT-FIG. 2. Upper Llandovery–Lower Ludlow stratigraphy at localities where *Thomastus* has been collected; stratigraphical terminology follows Rickards and Sandford (in press).

The '*Illaenus*' band was considered by Öpik (1953, p. 10) to be of mid to late Llandovery age, based mainly on the presence of graptolites identified as *Climacograptus hughesi* and *Monograptus* cf. *jaculum*. The present whereabouts of these graptolite specimens are unknown, so their identifications cannot be verified. However, the occurrence of *Ananaspis typhlagogus*, belonging to a genus not known to range below the Wenlock, and the presence of earliest Ludlow (*nilssoni* Biozone) graptolites at a stratigraphical level 2800 m higher in the sequence (high in the overlying Yan Yean Formation; see Rickards and Sandford in press, fig. 4), indicate that the Wapentake Formation, including the '*Illaenus*' band, is of Wenlock age.

Bylands. Siltstones at a locality in the Bylands area contain a sparse but diverse fossil fauna, including trilobites, articulate and inarticulate brachiopods, bivalves, gastropods, nautiloids, hyolithids, conulariids and carpoids. Apart from the new species of *Thomastus*, *T. aops*, trilobites present include *Decoroproetus*?, a species of *Ananaspis* distinct from *A. typhlagogus*, a pygidium of *Struveria*?, a new genus of blind acastid, a thoracic segment of an indeterminate homalonotid, *Dicranurus*, and other indeterminate odontopleurids. Mapping by VandenBerg (1992) placed this locality at the top of the Chintin Formation; Rickards and Sandford (in press), however, included the locality in their newly named Bylands Siltstone, which they considered to overlie the Chintin Formation disconformably (Text-fig. 2). The presence of *Ananaspis* indicates that the strata at this locality are no older than Wenlock, and this age is consistent with the occurrence of graptolites of the latest Wenlock *ludensis* Biozone low in the overlying Yan Yean Formation at a locality about 7 km to the east (PL1675 = locality Q2 of Williams 1964, fig. 2; see Rickards and Sandford in press, fig. 4).

Blind trilobites are rare in the Silurian, so it is noteworthy that two blind forms, *Thomastus* and a new acastid genus, are the most common trilobites in the Bylands fauna. *Thomastus* also dominates the fauna in the '*Illaenus*' band at Heathcote. With the possible exception of the homalonotids, which generally have relatively small eyes, none of the other trilobites present at either locality appears to have reduced eyes. The two species of *Ananaspis* have eyes of normal size for the genus, and the size of the palpebral lobes in *Decoroproetus*? and *Dicranurus* from Bylands,

and *Maurotarion* from Heathcote, indicate that the eyes in these forms were also of normal size. In the other trilobites occurring at Bylands and Heathcote neither the eyes nor the palpebral lobes are preserved, so their size is unknown.

A fauna of blind or almost blind trilobites from the Arenig of South Wales was described by Fortey and Owens (1987), who named it the atheloptic association. It was found together with large-eyed trilobites of the cyclopygid families, but these were considered to have been mesopelagic forms inhabiting the water column above the benthic fauna of blind or almost blind forms. The trilobites at Bylands and Heathcote lacking reduced eyes do not have the morphology of pelagic forms (e.g. a wide axis) and would have been benthic like *Thomastus* and the blind acastid. Hence, the blind trilobites at Bylands and Heathcote, unlike those in the atheloptic assemblage of Fortey and Owens, occurred together with normal-eyed forms in a natural benthic community.

Melbourne. The Anderson Creek Formation in the Melbourne district was considered by VandenBerg (1988, p. 107) to consist of 2300 m of sandstones, siltstones and minor conglomerates of late Llandovery to early Ludlow age. Rickards and Sandford (in press), however, restricted the unit to strata of early and mid Wenlock age, with a thickness of about 1300 m; overlying strata of latest Wenlock to early Ludlow age were assigned by Rickards and Sandford to the Yan Yean and Melbourne formations.

The Anderson Creek Formation is mostly unfossiliferous, but sparse shelly faunas and graptolites, mostly undescribed, are known from a few scattered localities. *Thomastus jutsoni*, known only from two specimens from separate localities near the top of the formation (as redefined by Rickards and Sandford), is the only trilobite described. Graptolites from the formation listed by Rickards and Sandford (in press, fig. 4) are indicative of the *riccartonensis* and *testis* biozones.

SYSTEMATIC PALAEONTOLOGY

Repositories and terminology. Specimens are housed in the invertebrate palaeontological collections of the Museum of Victoria (NMV), and the Commonwealth Palaeontological Collection, Australian Geological Survey Organisation, Canberra (CPC). For specimens previously housed in the Geological Survey of Victoria (GSV) and the Geology Department of the University of Melbourne (MUGD), the old registration numbers of those institutions are given as well as the new Museum of Victoria numbers. Locality numbers with a PL prefix are listed in the invertebrate fossil locality register of the Museum of Victoria.

Morphological terminology follows Holloway and Lane (1998, p. 863).

Note on 'Dalmanitina (Eudolatites)' aborigenum. This species was based by Öpik (1953, p. 26, pl. 10, figs 85–87) only on an incomplete fixigena and a fragmentary pygidium from the '*Illaenus*' band of the Wapentake Formation in the Heathcote district. The fixigena, the holotype of the species, actually belongs to the Dalmanitinae rather than to the Dalmanitininae or to the Mucronaspidinae (see Holloway 1981), as shown by the lanceolate posterior border furrow that does not meet the lateral border furrow distally, and by the broad, flattened genal spine. Öpik believed that the course of the posterior branch of the facial suture suggested that the eye, which is not preserved, was very small and set far forward, unlike the large eyes of most Dalmanitinae. However, only the abaxial part of the suture is preserved, and its course is similar to that in other large-eyed Dalmanitinae, in which the suture is deflected anterolaterally from the back of the eye in a convex forwards curve (e.g. Campbell 1967, pl. 18, fig. 2). We therefore assign this specimen to *Dalmanites athamas* and consider *aborigenum* to be a junior synonym of that species. The paratype pygidium of *aborigenum* does not belong to *D. athamas*, as the pleural furrows are short (exsag.) and sharply incised instead of being expanded (exsag.) and asymmetrical in profile. We consider the specimen to be too incomplete for reliable generic assignment.

Suborder ILLAENINA Jaanusson, 1959
Family STYGINIDAE Vogdes, 1890

Genus THOMASTUS Öpik, 1953

Type species. *Thomastus thomastus* Öpik, 1953 from the Wapentake Formation (Wenlock) of central Victoria, Australia; original designation.

Diagnosis. Cephalon highly convex (sag., tr.), curving through more than 90° in sagittal line, very steep anteriorly. Glabella narrowest at or behind lunette; axial furrow very weak or absent in front of lunette. Omphalus and anterolateral internal pit absent. Posterior part of fixigena with distinct transverse furrow in front of articulating flange. Eyes absent; facial suture gently convex abaxially, exsagittally aligned or weakly diverging forwards in posterior part, converging forwards in anterior part, situated far from axial furrow. Librigena narrow (tr.), posterior margin concave in outline, genal angle with spine or more or less orthogonal. Cephalic doublure with vincular furrow running oblique to posterior margin; rostral plate lenticular in outline, lacking posterior flange; connective suture meeting hypostomal suture rather far from sagittal line. Hypostome with middle furrow and maculae very weak or absent; lateral and posterior borders narrow, lacking shoulder. Thorax with ten segments; axis 50–60 per cent. segmental width; axial furrow distinct; pleurae adaxial to fulcrum as wide (tr.) as or wider than abaxial to fulcrum. Pygidium much less convex than cephalon; anterior margin with distinct transverse portion just adaxial to articulating facet; holcos well developed.

Remarks. In erecting *Thomastus*, Öpik (1953, pp. 22–23) proposed an ancestry for it in *Bumastus*, and suggested that it might perhaps be included in *Bumastus* as a subgenus, although he preferred to regard it as an independent genus in order to preserve the concept of *Bumastus* as having characteristically large eyes. A relationship with *Bumastus* was accepted by Jaanusson (1957, p. 93; 1959, p. 374) who assigned *Thomastus* to the Bumastinae (*sensu* Raymond 1916). Lane and Thomas (1983, pp. 156–157), however, included *Thomastus* in a list of genera they assigned to the Illaenidae, whereas they placed *Bumastus* in the Styginidae. We do not consider that *Thomastus* belongs to the Illaenidae, because of the absence of an upwardly and forwardly curved posterior flange on the rostral plate. We agree with Öpik and Jaanusson that the affinities of *Thomastus* lie with *Bumastus*, although we interpret the latter in a more restricted sense (see Holloway and Lane 1998, p. 872) and do not consider it to be most closely related to *Thomastus*. In our opinion, *Thomastus* is most closely related to *Bumastella* Kobayashi and Hamada, 1974 (see Holloway and Lane 1998) and *Illaenoides* Weller, 1907. Characters shared with those genera include the extreme convexity of the cephalon, the absence of the omphalus and anterolateral internal pit, the facial suture that converges weakly forwards, the transverse furrow on the posterior part of the fixigena in front of the articulating flange, and the deep pygidial holcos. Apart from the presence of eyes, *Illaenoides* differs from *Thomastus* in that the cephalic axial furrow converges forwards more weakly behind the lunette, the facial suture is situated closer to the axial furrow, the genal angle is more rounded, and the hypostome is more elongated with a distinct posterior lobe of the middle body. *Bumastella* differs from *Thomastus* in having eyes, the posterior cephalic margin is deflected strongly backwards abaxial to the fulcrum, the lunette is situated farther forwards in dorsal view, the facial suture is situated closer to the axial furrow, the genal angle is broadly rounded, the rostral plate is subtriangular in outline rather than lenticular, the thoracic axis narrows more strongly backwards, so that the pleurae on the posterior thoracic segments are wider adaxial to the fulcrum, and the pygidium is more transverse.

In thoracic and pygidial morphology, including the well developed holcos, *Thomastus* shows similarities with *Opsypharus* Howells (1982, p. 10, pl. 2, figs 8–20), but striking differences in the cephalon indicate that the two genera are not closely related. The differences in *Opsypharus* include the low convexity of the cephalon, the presence of the omphalus, the axial furrow extending in front

of the lunette, the much narrower fixigena, the strongly divergent anterior and posterior branches of the facial suture, the wide librigenae with shallow lateral border furrow, and the well rounded genal angle.

Thomastus thomastus Öpik, 1953

Plate 1, figures 1–16

1937 *Illaenus* sp.; Thomas, p. 66.
1953 *Thomastus thomastus* Öpik, p. 23, pl. 8, figs 61–71; text-fig. 8.
1953 *Thomastus collusor* Öpik, p. 24, pl. 9, figs 72–74.
1953 *Thomastus vicarius* Öpik, p. 24, pl. 9, figs 75–79.
1957 *Thomastus vicarius* Öpik; Jaanusson, p. 94.
1964 *Thomastus thomastus* Öpik; Talent, p. 47.
1964 *Thomastus collusor* Öpik; Talent, p. 47.
1964 *Thomastus vicarius* Öpik; Talent, p. 48.
non 1975 *Thomastus thomastus* Öpik; Fletcher, p. 69, fig. 2B–D.

Holotype. Dorsal exoskeleton NMV P52474 (*ex* GSV 36570), figured Öpik (1953, pl. 8, figs 61–62, text-fig. 8), Plate 1, figures 1, 4, 15; from locality PL2263 (= F44 of Thomas 1940; and locality 44, Parish of Heathcote in Talent 1964, fig. 1), Heathcote district, Victoria (grid reference CV03021272 on the Costerfield 1:25000 topographic sheet 7824-2-3).

Paratypes. From the same locality as the holotype: dorsal exoskeleton NMV P52475 (*ex* GSV 36573, figured Öpik 1953, pl. 8, figs 63–64). From locality PL2269 (= F51 of Thomas 1940; and locality 51, Parish of Heathcote in Talent 1964, fig. 1), Heathcote district, Victoria (grid reference CV06401145): dorsal exoskeleton NMV P52476 (*ex* GSV 46602; Öpik 1953, pl. 8, figs 65–66); incomplete dorsal exoskeleton NMV P52478 (*ex* GSV 46604, 46619, counterparts; Öpik 1953, pl. 8, figs 69–70); incomplete cranidium NMV P52479 (*ex* GSV 46620; Öpik 1953, pl. 8, fig. 71); hypostome NMV P52477 (*ex* GSV 46599; Öpik 1953, pl. 8, fig. 67). From locality PL1460, Heathcote district, Victoria (grid reference CV02531335): incomplete cranidium and thorax NMV P139848 (*ex* GSV 46570; not illustrated). From 'South Heathcote': dorsal exoskeleton NMV P140676 (*ex* MUGD 1959; Öpik 1953, pl. 8, fig. 68).

Type material of T. collusor. Öpik (1953, p. 24) stated that he had identified three specimens of this species, but the only specimen that can be located now is the holotype, an incomplete cephalon and partial thorax NMV P52480 (*ex* GSV 46631; Öpik 1953, pl. 9, figs 72–74), from locality PL2269.

Type material of T. vicarius. Holotype: dorsal exoskeleton CPC 691, figured Öpik (1953, pl. 9, figs 75–76); the counterpart external mould, consisting of the thorax and pygidium but lacking the cephalon, is NMV P139889;

EXPLANATION OF PLATE 1

Figs 1–16. *Thomastus thomastus* Öpik, 1953; lower part of Wapentake Formation (Wenlock), Heathcote district, Victoria. 1, 4, 15, NMV P52474, holotype; locality PL2263; dorsal exoskeleton. 1, dorsal view of cephalon. 4, anterior view. 15, lateral view of cephalon and part of thorax. All ×2·25. 2, NMV P147066; locality PL2263; cranidium, oblique view; ×1·5. 3, NMV P139827; '*Illaenus*' band, exact locality uncertain; hypostome, ventral view; ×3. 5–6, NMV P139977; locality PL2263; dorsal exoskeleton. 5, lateral view of cephalon. 6, dorsal view of cephalon. Both ×2. 7, NMV P139887; locality PL386; dorsal exoskeleton, dorsal view; ×1·5. 8–9, NMV P139979; locality PL2263; latex cast of pygidium. 8, lateral view; ×2·75. 9, dorsal view; ×2. 10, NMV P139914; from '2 km west of Costerfield'; dorsal exoskeleton, dorsal view; ×1·25. 11, NMV P139906; locality PL2263; pygidium, dorsal view; ×1·5. 12, NMV P139864; locality PL2269; incomplete cranidium, detail of anterior part in anterior view showing terrace ridges; ×2·5. 13, NMV P139932; '*Illaenus*' band, exact locality uncertain; cephalon, ventral view showing rostral plate; ×2·5. 14, NMV P139839 (ex GSV 36575); locality PL2263; incomplete dorsal exoskeleton, detail of back of cranidium and front of thorax showing sculpture; ×3·75. 16, NMV P139922; '*Illaenus*' band, exact locality uncertain; dorsal exoskeleton, lateral view; ×1·75.

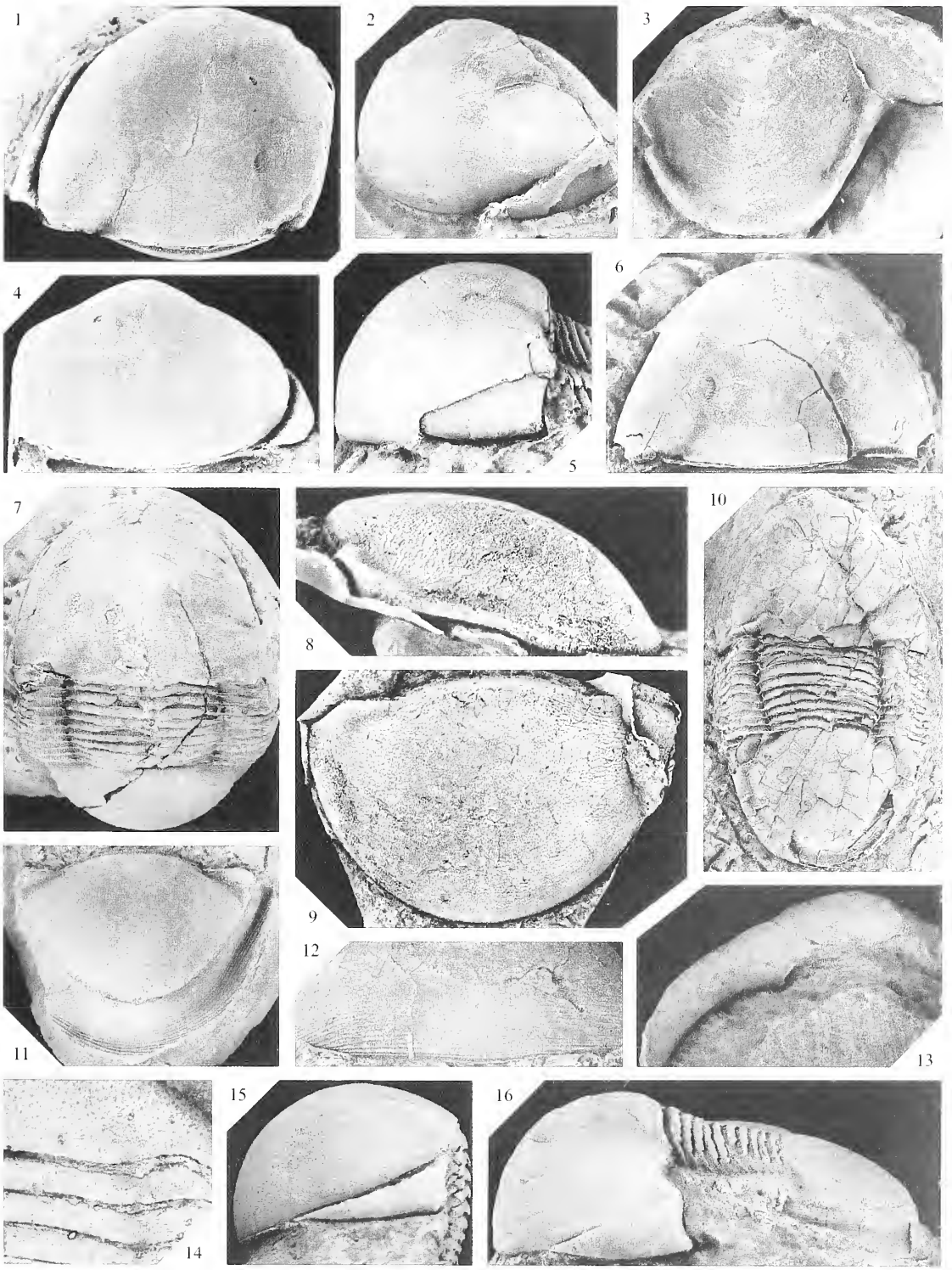

SANDFORD and HOLLOWAY, *Thomastus*

collection locality not recorded by Öpik (1953) but is probably PL2263. Paratypes: dorsal exoskeleton NMV P140675 (*ex* MUGD 1960; Öpik 1953, pl. 9, figs 78–79), from 'South Heathcote'; incomplete pygidium NMV P52481 (*ex* GSV 46624; Öpik 1953, pl. 9, fig. 77), from locality PL2269.

Other material. NMV P33135, P55955–P55956, P55959–P55965, P139806–P139847, P139849–P139864, P139975–P139888, P139890–P139984, P146118, P147047–P147048, P147058–P147061, P147066–P147069, from various localities in the Heathcote district.

Horizon. Wenlock Series; Wapentake Formation.

Diagnosis. Glabella narrowest at lunette. Facial suture gently and evenly curved in dorsal view, almost exsagittally aligned at posterior end, converging anteriorly. Librigena slightly wider than fixigena posteriorly; posterior margin of librigena weakly concave in outline; genal angle orthogonal or with very short spine. Pygidium moderately convex; lateral margin weakly arched upwards; holcos non-existent posteriorly; doublure angular in cross section anteriorly.

Description. Cephalon in dorsal view *c.* 160 per cent. as wide as long (sag.), widest posteriorly; anterior outline parabolic, posterior margin more-or-less transverse; in lateral view, cephalon almost as high as long, vertical or slightly overhanging anteriorly, highest point situated well in front of posterior margin and opposite lunette. Axial furrow describing abaxially concave arc, shallow behind lunette, faint to effaced in front of lunette. Small, conical apodeme present just in front of posterior cephalic margin, at junction of axial furrow and transverse furrow in front of articulating flange. Glabella forming low arch (tr.) at posterior margin, retaining slight independent convexity (tr.) as far forward as lunette; width of glabella almost 50 per cent. maximum cephalic width posteriorly, width at lunette *c.* 60 per cent. posterior width. Lunette weakly impressed, situated at *c.* 40 per cent. of cephalic length (sag.) in dorsal view. Fixigena wide, decreasing in convexity (tr.) anteriorly, width opposite lunette equal to width of glabella measured across same transverse line. Posterior fixigenal margin gently flexed downwards and backwards about half way between axial furrow and posterior end of facial suture. Librigena as wide posteriorly as fixigena, narrowing forwards, sloping very steeply abaxially; genal angle with short spine (Pl. 1, fig. 16) or almost orthogonal; posterior librigenal margin always gently concave adaxial to genal angle. Facial suture in lateral view horizontal or sloping backwards slightly at posterior end, thereafter sloping forwards at *c.* 20° to horizontal.

Cephalic doublure steeply inclined and gently convex posteriorly, increasing greatly in convexity anteriorly, its inner edge deeply embayed medially by strongly transversely arched hypostomal suture. Vincular furrow shallow, bounded in front by a ridge that is subangular in cross section at inner edge of doublure and dies out abaxially. Rostral plate *c.* 20 per cent. as wide posteriorly as anteriorly, gently convex (sag., exsag.) over most of its length, weakly concave (sag., exsag.) just in front of posterior margin; posterior margin gently concave in outline. Connective suture concave abaxially in anterior half and gently convex abaxially in posterior half, converging backwards at *c.* 60° to sagittal line overall.

Hypostome twice as wide across anterior wings as long (sag.), outline excluding anterior wings semielliptical. Middle body inflated, in transverse profile strongly rounded in sagittal line and flattened on flanks, in lateral profile weakly concave just in front of posterior border furrow; middle furrow and maculae indistinguishable. Lateral border rounded (tr.), narrowing backwards; lateral border furrow increasing in depth slightly towards anterior end. Posterior border very short (sag., exsag.), with sharply rounded crest; posterior border furrow long (sag., exsag.), shallow, poorly differentiated from middle body. Posterior wing triangular, situated opposite posteromedial edge of middle body.

Thorax with axis gently arched (tr.), weakly expanding backwards in anterior half, narrowing more distinctly backwards in posterior half. Axial rings gently convex (sag., exsag.), expanding only very weakly medially; articulating furrow not defined. Portion of pleurae adaxial to fulcrum horizontal, successively increasing in width (tr.) from front to back of thorax. Abaxial to fulcrum, anterior segments strongly flexed backwards, posterior segments successively more weakly flexed backwards and curving forwards slightly distally. Close to posterior edge of segment on internal surface is a small, conical apodeme situated directly beneath axial furrow.

Pygidium 62 per cent. to more than 90 per cent. as long as wide, widest across posterior edge of articulating facet; posterior and lateral margins with strongest curvature medially. In lateral profile, pygidium highest at about half sagittal length. Articulating facet short (exsag.), extending adaxially about half anterior width (tr.) of pleura. Anterior width of axis (marked by forward arching of anterior margin between anterior ends of holcos) about half maximum width of pygidium. Holcos broad, well-rounded, deepest anteriorly where it runs subparallel to posterior edge of articulating facet, dying out opposite about 60 per cent. of pygidial length (sag.)

from anterior. Doublure widest medially where it is almost 30 per cent. sagittal length of pygidium. Anterolaterally, doublure divided into a flattened, gently abaxially sloping outer portion and a flattened, steeply inclined inner portion by a subangular flexure; posteromedially, this flexure fades, outer portion of doublure becomes gently convex and slopes weakly outwards, and inner portion becomes weakly concave and slightly less steeply inclined.

Sculpture. Cephalon with terrace ridges close to and running subparallel with anterior and posterior margins; away from margins, terrace ridges grade into coarse pits covering reminder of dorsal surface of cephalon. Thorax with terrace ridges running subparallel to anterior and posterior margins of segments. Terrace ridges on pygidium more extensive than on cephalon, running parallel with pygidial margins peripherally, becoming more transverse adaxially opposite pygidial midlength, grading into pits medially. Cephalic and pygidial doublures with terrace ridges running subparallel to margins; terrace ridges more closely spaced on outer part of cephalic doublure than on inner part, and very closely spaced on subangular flexure subdividing anterolateral part of pygidial doublure. Terrace ridges on hypostome run concentrically on lateral and posterior borders, and in convex-backwards arcs on middle body.

Remarks. Specimens of *T. thomastus* not preserved in concretions are flattened and crushed, as noted by Öpik (1953, p. 23), and the exoskeleton is commonly fractured into angular fragments (e.g. Pl. 1, fig. 10). Specimens in concretions are less deformed, but the steeply inclined librigenae are commonly displaced slightly inwards and upwards beneath the cranidium, resulting in the abaxial part of the fixigena lying above the librigena being broken off (e.g. Pl. 1, fig. 5). In all specimens, the surface of the exoskeleton is coated with a very thin layer of a grey or brown crystalline mineral that X-ray diffraction analysis has shown to be siliceous. Whether this mineral has partly replaced the outermost layers of the exoskeleton or has been deposited in a thin layer on internal and external moulds is unclear. However, in specimens in concretions, which are preserved in positive relief and have some of the characteristics of internal moulds (e.g. expression of apodemes), the siliceous coating commonly also shows details of external sculpture (e.g. Pl. 1, fig. 12). No muscle scars have been observed either on specimens preserved in positive relief or on the corresponding external moulds.

Two specimens, NMV P139900 and NMV P147066 (Pl. 1, fig. 2), each have a large swelling on the cheek situated fairly close to the axial furrow. In the first specimen the swelling is level with the back of the lunette in dorsal view, and in the second it is level with the front of the lunette. In neither is it possible, because of preservational factors, to determine whether there was a corresponding swelling on the opposite cheek. The swellings contain no evidence of lenses and therefore do not appear to be eyes. It is possible that they are non-functional remnants of eyes; if so, their position well adaxial to the facial suture indicates that the suture must have migrated from its former course. However, the slightly different position of the swellings in relation to the lunette in the two specimens leads us to believe that the swellings are not associated with eyes, and that they are probably pathological.

Many specimens of *T. thomastus*, especially those in concretions, are preserved in a posture in which, if the lateral margins of the cephalon are oriented in a horizontal plane, the thorax and pygidium slope steeply downwards and backwards. This posture, known as the bumastoid stance, is similar to the inferred life orientation of other highly convex illaenimorph trilobites (Bergström 1973, figs 13–14; Stitt 1976, text-fig. 6; Westrop 1983, fig. 3; Fortey 1986, fig. 7) and, as in those forms, suggests that *Thomastus* may have led a sedentary, infaunal, suspension feeding existence. Specimens of *T. thomastus* not in concretions are less commonly preserved in the life orientation; the greater compaction suffered by these specimens has in most cases caused the front of the cephalon to be rotated upwards so that the posterior edge of the occipital region has ridden over the first few axial rings of the thorax (Pl. 1, fig. 10).

It is normally considered that in trilobites adopting the bumastoid stance the pygidium and most of the thorax were buried in the sediment, and the cephalon protruded above the surface. Being blind, *Thomastus* may have lived with the top of its cephalon below the sediment surface, and used its anterior appendages to draw water into its burrow for feeding and respiration.

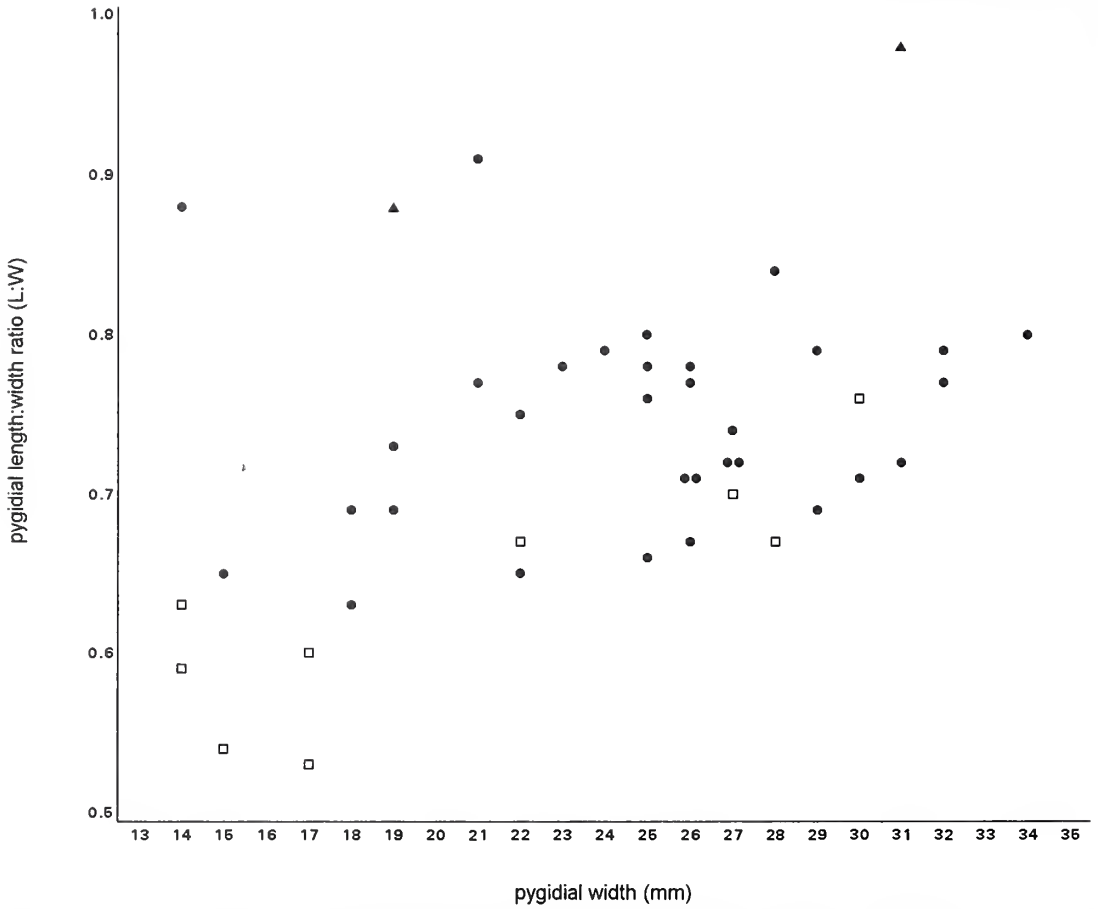

TEXT-FIG. 3. Plot of pygidial length:width ratio versus pygidial width for *Thomastus thomastus* (dots), *T. aops* (open squares) and *T. jutsoni* (triangles).

Variation in *Thomastus thomastus* in the shape of the genal angle is related to specimen size. The smallest cephalon (maximum width *c.* 13 mm) in which the shape of the genal angle is clear has a short genal spine subtending an angle of about 50°; with increasing specimen size, the genal spine decreases in length, and in the largest cephalon (maximum width *c.* 27 mm) with the genal angle preserved it is obtuse (*c.* 110°) and lacks a spine. Proportions of the pygidium vary considerably between specimens of similar size, but a general increase in elongation (L:W ratio) with increasing size can be recognized in the sample population (Text-fig. 3). Two specimens have pygidia as elongated as that of *T. jutsoni*, with L:W ratios close to 0·9, but these specimens resemble others of *T. thomastus* in having the narrowest part of the glabella situated at the lunette, instead of well behind the lunette as in *T. jutsoni* (see Table 1). Pygidia of *T. thomastus* have the lateral margin and the outer part of the doublure just behind the articulating facet weakly deflected upwards in a long (exsag.) arch (see Pl. 1, figs 8, 16), resulting in the doublure becoming angular in cross section (Pl. 1, fig. 11). This arch appears to match the ventral curvature of the librigenal margin, and presumably ensured a close fit between the cephalon and pygidium on enrolment.

Doubts about the distinctness of *T. collusor* and *T. vicarius* were raised by Talent (1964, p. 48), who suspected that one of them may be a sexual dimorph of *T. thomastus*. We consider both *collusor* and *vicarius* to be synonyms of *T. thomastus*. Öpik (1953, p. 25) considered *T. vicarius* to be distinguished from *T. thomastus* mainly by the more widely spaced terrace ridges on the doublure,

especially the pygidial doublure. Our observations indicate that the spacing of the terrace ridges is greater in larger specimens than in smaller ones, and we attribute the relatively wide spacing in the types of *vicarius* to the large size of these specimens. Other features in which Öpik considered *vicarius* to differ from *T. thomastus* were a less inflated cephalon with a sub-triangular rather than 'broad elliptical' outline, rounded rather than spinose genal angles, and a wider thoracic axis at the fourth segment. We can detect no significant differences in the convexity and outline of the cephalon nor in the relative width of the axis, and the genal angle is incomplete in both the holotype and one of the paratypes of *vicarius* but does not appear to have been rounded. Öpik (1953, p. 24) distinguished *T. collusor* from *T. thomastus* by the rounded genal angle, the more inflated fixigenae, the deeper transverse furrow ('pleuro-occipital furrow') on the posterior part of the fixigena, the transverse curvature of the glabella just in front of the posterior margin, the coarser pitting of the exoskeleton, and the subparallel course of the thoracic axial furrow. In the holotype of *collusor* (Öpik 1953, pl. 9, figs 72–74), the only member of the type series that can now be recognized, the genal angle is broken so its shape is indeterminate, and we can detect no significant differences from *T. thomastus* in the other characters mentioned.

The horizon from which Fletcher (1975) recorded 'numerous cephala and pygidia' of *Thomastus thomastus* in the Cobar district of western New South Wales is uncertain. Fletcher gave the horizon as the Mallee Tank Beds, but that stratigraphical name is obsolete. The specimens may have come from either the Baledmund Formation or the Burthong Formation, both considered to be of Lochkovian age (MacRae 1987); however, we do not know of any other records of effaced styginids in rocks younger than Silurian. Fletcher stated that *T. thomastus* is also very common in the Rosyth Limestone (Upper Llandovery; Pickett 1982, fig. 18) near Orange, *c.* 400 km south-west of Cobar. The specimens illustrated by Fletcher (1975, fig. 2B–D) are internal moulds of three pygidia, two from the Cobar district and one from the Rosyth Limestone. They differ from pygidia of *T. thomastus* in lacking the distinct transverse portion of the anterior margin adaxial to the articulating facet, the entire anterior margin instead forming an almost continuous curve with the facet. In addition, there is no holcos in the specimen from the Rosyth Limestone, and probably in the specimens from Cobar; in the latter specimens the lateral part of the dorsal surface is broken away, revealing the external mould of the doublure, but there is no trace of a holcos anteromedially. These differences preclude assignment of the specimens to *Thomastus*.

Thomastus aops sp. nov.

Plate 2, figures 1–10

1988 *Thomastus* cf. *thomastus* Öpik; VandenBerg, p. 105.
1992 *Thomastus* cf. *thomastus* Öpik; VandenBerg, p. 44.

Derivation of name. Greek 'blind', referring to the absence of eyes.

Holotype. Dorsal exoskeleton NMV P139969, figured Plate 2, figure 8; from locality PL206, near the western end of Union Lane, Bylands, Victoria (grid reference CU154644 on the Kilmore 1:25,000 topographic sheet 7823-2-1).

Paratypes. Dorsal exoskeletons NMV P139339, P139345–P139346, P139968, P139970–P139973; pygidia with incomplete thoraces NMV P139340, P139343; pygidium NMV P139966; all from the same locality as the holotype.

Other material. NMV P139341–P139342, P139344, P139347–P139349, P139967, P139974, P147051–P147054, from the same locality as the holotype.

Horizon. Wenlock Series, Bylands Siltstone.

Diagnosis. Glabella narrowest at lunette. Facial suture with distinct flexure opposite (tr.) lunette, diverging gently forwards behind flexure, converging forwards in front of flexure. Librigena much

wider (tr.) than fixigena posteriorly; posterior margin of librigena markedly concave in outline; genal spine long. Pygidium gently convex; holcos continuous but very shallow posteriorly.

Remarks. The rostral plate and hypostome of *Thomastus aops* sp. nov. are unknown. The pygidium on one of the specimens appears to have a weakly defined axis (Pl. 2, fig. 10), which occupies about half the sagittal length of the pygidium, is about as wide anteriorly as long, and narrows strongly backwards to a well-rounded terminus. Another specimen has four pairs of muscle scars arranged in backwardly converging rows on the anteromedial part of the pygidium (Pl. 2, fig. 7); the scars are more distinct on the internal mould than on the exterior of the exoskeleton, are circular, and successively decrease in size posteriorly. The cephalon of the same specimen appears also to have three or four pairs of very poorly defined muscle scars on the internal mould of the glabella.

Thomastus aops is most easily distinguished from *T. thomastus* by its longer genal spine and more deeply embayed posterior librigenal margin (Table 1). Additional points of difference in *T. aops* are that the facial suture is not evenly curved but has a distinct flexure opposite the lunette, just behind the midlength of the cephalon in dorsal and lateral profiles (Pl. 2, figs 1–2); the facial suture is not exsagittally aligned at its posterior end but diverges forwards as far as the flexure; the lateral pygidial margin is not arched upwards; and the pygidial doublure is evenly curved rather than angular in cross section anteriorly. Small pygidia (14–20 mm wide) of *T. aops* are relatively wider than those of *T. thomastus* of similar size, whereas larger pygidia of *T. aops* have L:W ratios falling in the lower part of the range of *T. thomastus* (Text-fig. 3). Some other apparent differences, such as the slightly deeper cephalic axial furrows, the lower convexity of the cephalon and pygidium, and the continuation of the holcos posteromedially, are difficult to assess given the greater tectonic flattening suffered by specimens of *T. aops* in comparison with specimens of *T. thomastus* preserved in concretions.

Thomastus jutsoni (Chapman, 1912)

Plate 2, figures 11–12

1912 *Illaenus jutsoni* Chapman, p. 295, pl. 61, figs 4–5.
1952 *Illaenus jutsoni*; Gill, p. 42.
1952 *Illaenus* aff. *jutsoni* Chapman; Gill, p. 43, pl. 1, fig. 1.
1953 *Thomastus jutsoni*; Öpik, p. 22.
1953 *Illaenus jutsoni* Chapman 1912; Öpik, p. 25, pl. 9, fig. 80.
?1955 *Thomastus* sp. indet.; Whiting, p. 32.
1965 *Thomastus jutsoni* (Chapman); Gill, p. 24, pl. 6, fig. 1.
1971 *Illaenus jutsoni* Chapman; Kobayashi and Hamada, p. 127.

EXPLANATION OF PLATE 2

Figs 1–10. *Thomastus aops* sp. nov.; locality PL206, Bylands Siltstone (Wenlock), Bylands, Victoria. 1–2, 9, NMV P139345; dorsal exoskeleton. 1, internal mould, dorsal view of cephalon. 2, internal mould, lateral view of cephalon. 9, latex cast, dorsal view. All × 2·5. 3–4, NMV P139968; latex cast of dorsal exoskeleton. 3, dorsolateral view of cheek; × 3·75. 4, dorsal view of cephalon; × 2·5. 5, 7, NMV P139339; dorsal exoskeleton. 5, latex cast of pygidium, dorsal view; × 1·5. 7, internal mould of dorsal exoskeleton, dorsal view; × 1·6. 6, NMV P139340; pygidium and incomplete thorax; latex cast of pygidium, dorsal view; × 3. 8, NMV P139969, holotype; dorsal exoskeleton; latex cast, dorsal view; × 2. 10, NMV P139346; dorsal exoskeleton; latex cast, dorsal view; × 3.

Figs 11–12. *Thomastus jutsoni* (Chapman, 1912); Anderson Creek Formation (Wenlock), Melbourne district, Victoria. 11, NMV P12299, holotype; locality PL1372; internal mould of dorsal exoskeleton, dorsal view; × 2. 12, NMV P14719; locality PL1373; internal mould of dorsal exoskeleton, dorsal view; × 1·5.

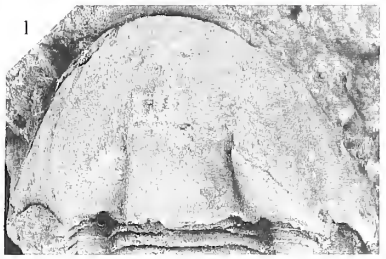
1

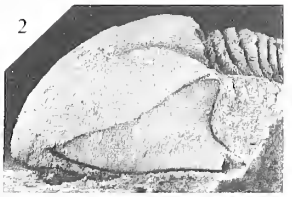
2

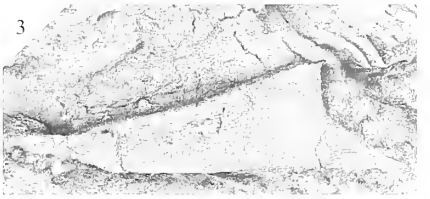
3


4

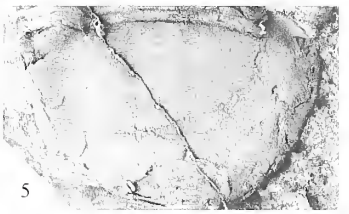
5

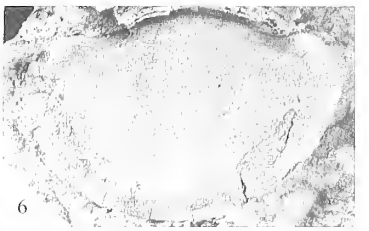
6

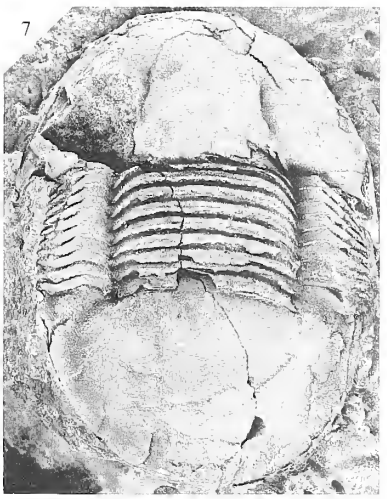
7

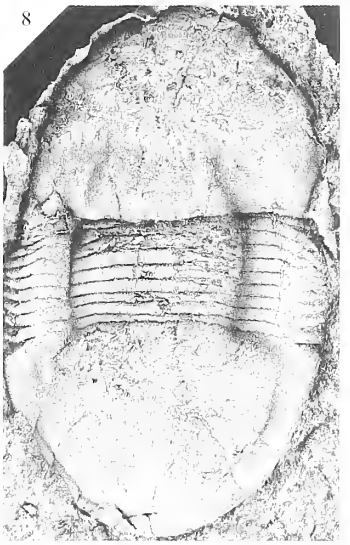
8

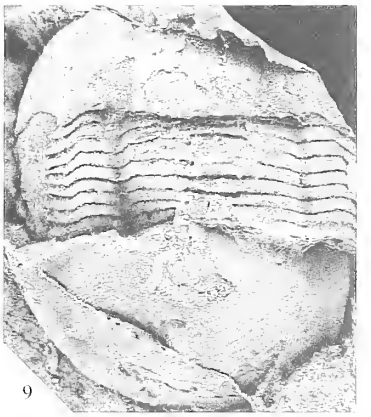
9


10


11

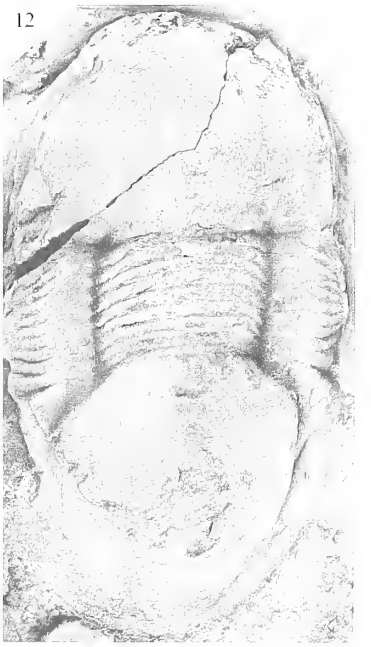
12

SANDFORD and HOLLOWAY, *Thomastus*

1971 *Thomastus jutsoni*; VandenBerg, p. 3.
1974 *Thomastus* (?) *jutsoni*; Kobayashi and Hamada, p. 30.
1974 *Bumastus* (?) *jutsoni*; Kobayashi and Hamada, p. 33.

Holotype. Internal mould of dorsal exoskeleton NMV P12299, figured Chapman (1912, pl. 61, figs 4–5), Öpik (1953, pl. 9, fig. 80), Gill (1965, pl. 6, fig. 1), Plate 2, figure 11; from locality PL1372, a former quarry site in Bulleen Road, Bulleen, 12 km east-north-east of Melbourne city centre, Victoria.

Other material. Internal mould of dorsal exoskeleton NMV P14719, from locality PL1373, a sewerage excavation in Hill Road, North Balwyn, Melbourne district, Victoria.

Horizon. Wenlock Series; Anderson Creek Formation.

Diagnosis. Occipital furrow very weakly defined. Glabella narrowing forwards as far as occipital furrow, subparallel just in front of occipital furrow, subsequently expanding gently forwards to lunette; width at lunette slightly less than width at posterior cephalic margin. Pygidium rather elongate, 80–90 per cent. as long as wide; doublure very wide, *c.* 30 per cent. sagittal length of pygidium.

Remarks. Both specimens are poorly preserved. As noted by Öpik (1953, p. 25), the description of the holotype by Chapman (1912) is very inaccurate, particularly in the account of eyes, which apparently do not exist, and the form of the facial suture and genal spine, which are not preserved. Crushing of the specimen appears to have caused the sagittal ridge on the cephalon described by Chapman, and has probably also exaggerated the depth of the holcos. The specimen from North Balwyn retains the right librigena, which has been flexed downwards so that it stands vertically, the resulting fracturing of the cephalon obscuring the facial suture; the librigena is very poorly

TABLE 1. Comparison of diagnostic characters of *Thomastus thomastus*, *T. aops* and *T. jutsoni*.

	T. thomastus	*T. aops*	*T. jutsoni*
Narrowest part of glabella	At lunette	At lunette	Posterior to lunette
Occipital furrow	Absent	Absent	Weak
Facial suture	Evenly curved, converging forwards	Distinct flexure opposite lunette, diverging forwards behind flexure, converging forwards in front of flexure	Unknown
Posterior width of librigena	Slightly greater than width of fixigena	Much greater than width of fixigena	Much greater than width of fixigena?
Posterior margin of librigena	Gently concave	Strongly concave	Unknown
Genal angle	Orthogonal or with very short spine	Long genal spine	Short spine?
Holcos	Non-existent posteriorly	Continuous but shallow posteriorly	Unknown
Lateral margin of pygidium	Gently arched	Not arched	Not arched
Pygidial doublure	Narrow, angular in cross section anteriorly	Narrow, evenly curved in cross section anteriorly	Very wide

913-28

897-911

853-96

CHAPMAN ADD 2NOV98

CALL NO.	Journal title with vol. & yr. OR author of book
QE701 P155 no.41	PALAEONTOLOGY 41(5) 1998

Journal article author & pages OR title, edition, date of book

CHARGED	RECEIVED BY (Name and date)	See notes on back of card
	SMITHSONIAN INSTITUTION LIBRARIES Natural History Branch, Room 51-A, 2nd Floor Washington, D.C. 20560 SI-862B (Rev. 2-9-82)	

preserved but appears to have a short genal spine. Despite the lack of so much morphological information in both specimens, we consider them to belong to the same species because of the similarities in the poorly defined occipital furrow and the course of the cephalic axial furrow. Gill (1952, p. 43) did not assign the specimen from North Balwyn to *jutsoni* with confidence, stating that it differed from the holotype in size and in 'the lines (i.e. terrace ridges) on the pygidial border'. However, we do not consider size to be a useful taxonomic character in the styginids. We also dismiss the second supposed difference, as the dorsal surface of the pygidium above the doublure is broken off in the North Balwyn specimen, so it appears that Gill was comparing the terrace ridges on the external mould of the doublure with those on the dorsal surface of the holotype.

Thomastus jutsoni is easily distinguished from both *T. thomastus* and *T. aops* (Table 1) by the weak occipital furrow, the glabella that is subparallel-sided at its narrowest part, which is situated well behind the lunette, the longer pygidium (Text-fig. 3), and the wider pygidial doublure.

Whiting (1955, footnote on p. 32) reported a specimen of *Thomastus* sp. indet. from the Golden Crown Mine, Yarrambat, 25 km north-north-east of Melbourne. This specimen is possibly NMV P139965, an internal mould of a dorsal exoskeleton. The elongate pygidium and the depth of the holcos medially suggest assignment to *T. jutsoni*, but the specimen is too damaged and sheared to be assigned to the species with certainty.

Acknowledgements. We thank A. H. M. VandenBerg (Geological Survey of Victoria) for bringing to our attention the material of *Thomastus aops* which he collected; R. B. Rickards (University of Cambridge) for identifying graptolite specimens; D. L. Strusz (Australian Geological Survey Organisation) for the loan of specimens; and W. D. Birch (Museum of Victoria) for X-ray diffraction analysis of the mineral coating on specimens of *Thomastus thomastus*. Improvements to the manuscript were suggested by R. M. Owens and two anonymous referees.

REFERENCES

BERGSTRÖM, J. 1973. Organization, life, and systematics of trilobites. *Fossils and Strata*, **2**, 1–69, pls 1–5.

CAMPBELL, K. S. W. 1967. Trilobites of the Henryhouse Formation (Silurian) in Oklahoma. *Bulletin of the Oklahoma Geological Survey*, **115**, 1–68.

CHAPMAN, F. 1912. New or little known Victorian fossils in the National Museum. Part 14. On some Silurian trilobites. *Proceedings of the Royal Society of Victoria*, **24**, 293–300, pls 61–63.

—— and THOMAS, D. E. 1935. Silurian. 106–110. *In Handbook for Victoria. Prepared for the members of the Australian and New Zealand Association for the Advancement of Science on the occasion of its meeting held in Melbourne, January, 1935*. Government Printer, Melbourne, 151 pp.

FLETCHER, H. O. 1975. Silurian and Lower Devonian fossils from the Cobar area of New South Wales. *Records of the Australian Museum*, **30**, 63–85.

FORTEY, R. A. 1986. The type species of the Ordovician trilobite *Symphysurus*: systematics, functional morphology and terrace ridges. *Paläontologische Zeitschrift*, **60**, 255–275.

—— and OWENS, R. M. 1987. The Arenig Series in South Wales. *Bulletin of the British Museum (Natural History), Geology Series*, **41**, 69–307.

GILL, E. D. 1952. On the age of the bedrock between Melbourne and Lilydale, Victoria. *Victorian Naturalist*, **69**, 41–47.

—— 1965. Palaeontology of Victoria. 1–24. *In* ARNOLD, V. H. (ed.). *Victorian Year Book 1965* (No. 79). Commonwealth Bureau of Census and Statistics, Victorian Office, Melbourne, 821 pp.

HOLLOWAY, D. J. 1981. Silurian dalmanitacean trilobites from North America and the origins of the Dalmanitidae and Synphoriidae. *Palaeontology*, **24**, 695–731.

—— and LANE, P. D. 1998. Effaced styginid trilobites from the Silurian of New South Wales. *Palaeontology*, **41**, 853–896.

HOWELLS, Y. 1982. Scottish Silurian trilobites. *Monograph of the Palaeontographical Society*, **135** (561), 1–76, pls 1–15.

JAANUSSON, V. 1957. Unterordovizische Illaeniden aus Skandinavien. *Bulletin of the Geological Institutions of the University of Uppsala*, **37**, 79–165, pls 1–10.

—— 1959. Family Illaenidae Hawle & Corda, 1847. 372–376. *In* MOORE, R. C. (ed.). *Treatise on invertebrate paleontology. Part O. Arthropoda 1.* Geological Society of America and University of Kansas Press, Boulder, Colorado and Lawrence, Kansas, xix + 560 pp.

KOBAYASHI, T. and HAMADA, T. 1971. Silurian trilobites from the Langkawi Islands, West Malaysia, with notes on the Dalmanitidae and Raphiophoridae. *Geology and Palaeontology of Southeast Asia*, **9**, 87–134, pls 18–23.

—— —— 1974. Silurian trilobites of Japan in comparison with Asian, Pacific and other faunas. *Special Papers of the Palaeontological Society of Japan*, **18**, i–viii + 1–155, pls 1–12.

LANE, P. D. and THOMAS, A. T. 1983. A review of the trilobite suborder Scutelluina. *Special Papers in Palaeontology*, **30**, 141–160.

MACRAE, G. P. 1987. *Geology of the Nymagee 1:100,000 sheet 8133.* New South Wales Geological Survey, Sydney, viii + 137 pp.

ÖPIK, A. A. 1953. Lower Silurian fossils from the '*Illaenus* Band', Heathcote, Victoria. *Memoirs of the Geological Survey of Victoria*, **19**, 1–42, pls 1–13.

PICKETT, J. W. (ed.) 1982. The Silurian System in New South Wales. *Bulletin of the Geological Survey of New South Wales*, **29**, i–v, 1–264.

RAYMOND, P. E. 1916. New and old Silurian trilobites from southeastern Wisconsin, with notes on the genera of the Illaenidae. *Bulletin of the Museum of Comparative Zoology, Harvard University*, **60**, 1–41.

RICKARDS, R. B. and SANDFORD, A. C. in press. Llandovery–Ludlow graptolites from central Victoria: new correlation perspectives of the major formations. *Australian Journal of Earth Sciences.*

STITT, J. H. 1976. Functional morphology and life habits of the Late Cambrian trilobite *Stenopilus pronus* Raymond. *Journal of Paleontology*, **50**, 561–576.

TALENT, J. A. 1964. The Silurian and Early Devonian faunas of the Heathcote district, Victoria. *Memoirs of the Geological Survey of Victoria*, **26**, 1–55, pls 1–27. [Publication date incorrectly altered to 1965 on many copies.]

THOMAS, D. E. 1937. Some notes on the Silurian rocks of the Heathcote area. *Mining and Geological Journal, Victoria*, **1** (1), 64–67.

—— 1940. *Heathcote, County of Dalhousie, 40 chains to 1 inch geological parish map.* Department of Mines, *Victoria, Melbourne.*

VANDENBERG, A. H. M. 1971. Explanatory notes on the Ringwood 1:63,360 Geological Map. *Report of the Geological Survey of Victoria*, **1971/1**, 1–35.

—— 1988. Silurian–Middle Devonian. 103–146. *In* DOUGLAS, J. G. and FERGUSON, J. A. (eds). *Geology of Victoria.* 2nd edition. Victorian Division, Geological Society of Australia Incorporated, Melbourne, xv + 663 pp.

—— 1992. Kilmore 1:50,000 map geological report. *Report of the Geological Survey of Victoria*, **91**, 1–86.

VOGDES, A. W. 1890. A bibliography of Paleozoic Crustacea from 1698 to 1889, including a list of North American species and a systematic arrangement of genera. *Bulletin of the United States Geological Survey*, **63**, 1–177.

WELLER, S. 1907. The paleontology of the Niagaran Limestone in the Chicago area. The Trilobita. *Bulletin of the Chicago Academy of Science*, **4**, 163–281, pls 16–25.

WESTROP, S. R. 1983. The life habits of the Ordovician illaenine trilobite *Bumastoides. Lethaia*, **16**, 15–24.

WHITING, R. G. 1955. Report on the Golden Crown Mine, Yarrambat. *Mining and Geological Journal, Victoria*, **5** (6), 32–34.

WILLIAMS, G. E. 1964. The geology of the Kinglake district, central Victoria. *Proceedings of the Royal Society of Victoria*, 77, 273–327, pls 47–51.

ANDREW SANDFORD
DAVID J. HOLLOWAY
Museum of Victoria
P.O. Box 666E
Melbourne
Victoria 3001, Australia
e-mail dhollow@mov.vic.gov.au

Typescript received 1 July 1997
Revised typescript received 12 December 1997

FIRST RECORDS OF FOSSIL TREMECINE HYMENOPTERANS

by SONJA WEDMANN

ABSTRACT. Two Hymenoptera, from the Upper Oligocene of Enspel (Germany) and the Upper Pliocene of Willershausen (Germany), are described and their systematic position is discussed. The fossil from Enspel shows parts of the body and almost the complete wing venation. After analysis of the phylogeny of Tremecinae (Siricidae) it could be placed near *Eriotremex* and *Afrotremex*. The specimen from Willershausen has only the apical part of one forewing preserved and belongs to *Tremex*.

THE earliest representatives of hymenopterous insects are from the Triassic of Australia (Riek 1955) and Russia (Rasnitsyn 1980, 1988). They are exclusively members of the Xyelidae. Only in the Jurassic do more hymenopterous taxa (Rasnitsyn 1988) appear. Many of these belong to the Siricidae or their stem-group. One of the oldest records of a stem-group member of the Siricidae is that of *Sinosirex* Hong, 1975 from the Upper Jurassic or Lower Cretaceous of China (Königsmann 1977). Myrmiciidae (= Pseudosiricidae) from the Upper Jurassic and Cretaceous was synonymized with Siricidae by Rasnitsyn (1988) because the thorax shows features typical of siricids. Perhaps these fossils belong to the stem-group of the Siricidae, too. The Auliscinae from the Upper Jurassic of Karatau are placed in Siricidae by Rasnitsyn (1969, 1980), but Königsmann (1977) considered this placement to be problematical. The Praesiricidae from Lower Cretaceous of Transbaikalia and from the Upper Jurassic of Kazakhstan have been removed from the Siricidae (Rasnitsyn 1983).

The extant Siricidae consist of the Siricinae (not necessarily a monophyletic group) and the Tremecinae. The oldest fossil siricine is from the Lower Cretaceous of eastern Russia; it is possibly related to *Xeris* Costa, 1894 and *Eoxeris* Maa, 1949 (Gromov *et al.* 1993). The oldest Tertiary find is *Urocerus patagonicus* Fidalgo and Smith, 1987, described from Paleocene shales in Patagonia (Fidalgo and Smith 1987); *Urocerus ligniticus* (Piton, 1940) and two other *Urocerus* fossils are recorded from the Paleocene of Menat, Puy-de-Dôme, France (Nel 1988). *Eoxeris klebsi* (Brues, 1926) is known from Baltic amber (Brues 1926). Other fossil Siricinae were mentioned by Nel (1991) from Oligocene and Miocene shales in France. *Urocerites spectabilis* Heer, 1867 has been described from the Miocene shales of Radoboj, Croatia.

The two fossils described here are the first reports of Tremecinae in the geological record. One fossil was found in the lake deposits of Enspel (*c.* 25 Ma; Storch *et al.* 1996; Wuttke 1997), near Bad Marienberg, Westerwald Mountains, Rheinland-Pfalz, Germany. The second fossil is from the lake deposits (Upper Pliocene) of Willershausen near Osterode in the Harz Mountains, Lower Saxony, Germany.

Before determining the exact systematic position of a fossil species or higher taxon, the phylogenetic relationships among the related extant taxa should be clarified. So far only Gauld and Mound (1982) have attempted to reconstruct the phylogeny of Siricidae. A new evaluation of characters has led to the reconstruction of phylogenetic relationships presented here.

EXTANT MATERIAL

I examined the venation of the forewings of the following extant material from the general collection of the Muséum National d'Histoire Naturelle in Paris: *Eriotremex insignis* Smith, 1859: 2 ♀; *Tremex*

[Palaeontology, Vol. 41, Part 5, 1998, pp. 929–938]

alchymista Mocsáry, 1886: 3 ♂, 2 ♀; *Tremex columba* (Linnaeus, 1763): 1 ♂, 9 ♀; *Tremex fuscicornis* (Fabricius, 1787): 4 ♂, 4 ♀; *Tremex longicollis* Konow, 1896: 1 ♀; *Tremex magus* (Fabricius, 1787): 1 ♂, 2 ♀; *Tremex pandora* Westwood, 1874: 1 ♂. The following material was borrowed for further study: *Eriotremex insignis*: 1 ♀; *Tremex alchymista*: 2 ♀; *Tremex columba*: 3 ♀; *Tremex fuscicornis*: 1 ♂, 3 ♀; *Tremex magus*: 1 ♀.

PHYLOGENY OF TREMECINAE

Siricidae

Siricidae is very probably a monophyletic group (Königsmann 1977). There are several autapomorpic features for this taxon (Text-fig. 1, characters 1–6): Both the labium and maxilla are very hairy, the maxillary palp is 1-segmented (Ross 1937). The mesonotum has two diagonal grooves separating off side lobes (Ross 1937; Benson 1938). This feature seems not to be present in *Sinosirex* (Hong 1975), which can be interpreted either as a plesiomorphic feature or as an apomorphic loss in *Sinosirex*. Apomorphic characters of the wing venation are the basad inclined first part of Rs (Königsmann 1977; Rasnitsyn 1988) and the short fused part of Rs+M (Königsmann 1977). The last abdominal segments of both sexes are modified: in the female tergite 9 is short with a distinct precornal basin, tergite 10 is long, horn-like and strongly protruding caudad (Maa 1949). In the male the ninth tergite is divided into two triangular plates and the last sternite is drawn out pointedly (Königsmann 1977).

Extant Siricidae are divided into two groups, Siricinae and Tremecinae (Ashmead 1898). In this investigation the classification of Rohwer (1911) is followed.

Siricinae

The Siricinae are not necessarily monophyletic because no autapomorpic characters are known. The 3-segmented labial palp is a plesiomorphic character which is shared with Orussidae, Anaxyelidae, most Xiphydriidae and other taxa (Ross 1937). Another plesiomorphic feature is the long, slender, multi-segmented antenna. Further characters used to separate Siricinae from Tremecinae are the attachment of the larvae of Siricinae to conifers, short distance between the antennae, ratio of width to length of eyes being not more than 1·5 and contraction of the anal cell from about the middle (Benson 1943). These characters are not present in all genera of Siricinae or not only in genera of Siricinae. Gauld and Mound (1982) regarded the contraction of the anal cell from about the middle as an autapomorphic feature of Siricinae without *Siricosoma* Forsius, 1933. But, this is a rather vague character which is present also in *Teredon* (Bradley 1913, text-fig. 10), and therefore I consider this feature to be unsuitable to confirm the monophyly of Siricinae without *Siricosoma*. Further investigations are necessary to resolve the phylogenetic relationships of these taxa.

Gauld and Mound (1982) established a sister-group relationship between *Siricosoma* and Tremecinae (*sensu* Rohwer 1911) because these taxa have only one hind tibial spur (termed the mid tibial spur by Gauld and Mound (1982)). However, in *Xeris* Costa, 1894 and in the closely related *Neoxeris* Saini and Singh, 1987, there is only one spur present, too, which is rated as a convergent development by Gauld and Mound (1982). Even in *Urocerus flavicornis* Fabricius, 1781, about 10 per cent. of the males possess only a single spur on the hind tibia (Bradley 1913), which is why I consider this character to be very weak. As a second autapomorphic feature for *Siricosoma*+Tremecinae the shape of the distal flagellar segments is listed (Gauld and Mound 1982), a feature which is not defined more closely. The third apomorphy of Gauld and Mound (1982) is that the antennal bases of *Siricosoma* and of the taxa belonging to the Tremecinae are set far apart. This character is also found in *Sirotremex* Smith, 1988, which is placed currently in the Siricinae (Smith 1988). As stated before, it is necessary to investigate many more characters before a well-founded analysis of phylogenetic relationships is possible.

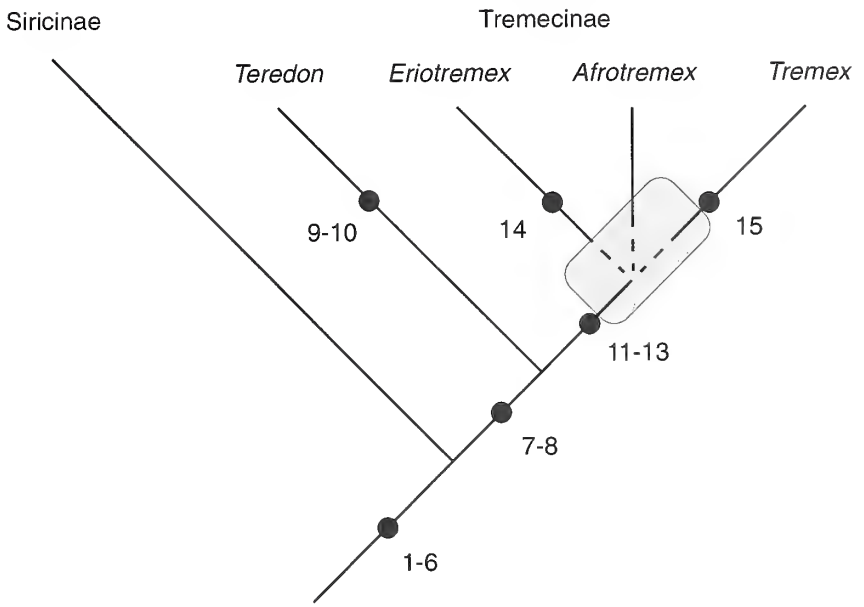

TEXT-FIG. 1. Phylogenetic relationships of extant Siricidae. The shaded area shows the possible phylogenetic position of *Eriotremex* or *Afrotremex* sp. from Enspel. The numbers refer to the following list of apomorphic characters. 1, labium and maxilla very hairy. 2, maxillary palp 1-segmented. 3, mesonotum with two diagonal grooves setting off side lobes. 4, first part of Rs directed diagonally towards wing base. 5, fused part of Rs and M very short. 6, abdominal segments 9 and 10 modified. 7, labial palp two-segmented. 8, vein 1r-m in hindwing shifted apically and located near middle of cell 1M. 9, antenna with five or six segments. 10, hindleg of male widely dilated. 11, vein 2r-m absent in forewing. 12, hindwing without closed anal cell. 13, veins M and cu-a of forewing (almost) in line. 14, disc on ninth abdominal tergite convex in the middle and hairy. 15, apical position of vein 2r-rs in forewing.

Tremecinae

Tremecinae *sensu* Rohwer (1911) comprises *Teredon*, *Eriotremex*, *Afrotremex* and *Tremex*. This taxon is most probably monophyletic. A synapomorphic feature of the Tremecinae is probably the 2-segmented labial palp (Text-fig. 1, character 7) which is present in *Teredon* (Konow 1905), *Tremex* (Bradley 1913; Benson 1943), *Eriotremex* (Benson 1943) and *Afrotremex* (David R. Smith, pers. comm.).

In the hindwing, vein 1r-m (nomenclature after Ross 1936) is shifted towards the apex so that it is located at about the middle of cell 1M at least in the following species: *Teredon latitarsis* (Bradley 1913, fig. 10), *Eriotremex formosanus* (Matsumura 1930, pl. 6, fig. 4; Smith 1975, fig. 1), *E. smithi* (Kirby 1882, pl. 15, fig. 1), *E. yamasakii* (Togashi 1990, fig. 1) and *E. insignis*, *Afrotremex hyalinatus* (Guiglia 1937, pl. 15), *Tremex apicalis* (Matsumura 1930, pl. 6, fig. 7), *T. chujoi* (Sonan 1938, fig. 5), *T. longicollis* (Matsumura 1930, pl. 6, fig. 3), *T. niger* (Sonan 1938, fig. 4), *T. pandora* (Westwood 1874, pl. 21, fig. 9), *T. rugicollis* (Westwood 1874, pl. 20, fig. 9), *T. columba*, *T. fuscicornis* and *T. magus*. In Siricinae and in many taxa whose wing venation is considered to be rather primitive, e.g. Xyelidae (Königsmann 1977), vein 1r-m is located at the basal part of cell 1M. Thus, the apical position of vein 1r-m is probably another synapomorphic feature of the Tremecinae (Text-fig. 1, character 8).

Bradley (1913) mentioned the loss of cerci in Tremecinae. This could be another apomorphic character of Tremecinae, since in *Teredon* (David R. Smith, pers. comm.), *Afrotremex* (David R. Smith, pers. comm.) and *Tremex* (Benson 1943) cerci are entirely absent. However, species of

TEXT-FIG. 2. *Eriotremex* or *Afrotremex* sp.; Landesamt für Denkmalpflege Rheinland-Pfalz No. 9604; Enspel, Germany, Upper Oligocene; whole fossil; × 3·3.

Eriotremex possess cerci (Benson 1943). On condition that loss of cerci is apomorphic for Tremecinae the presence of cerci in *Eriotremex* would have to be rated as a reversal. This would be an autapomorphic feature of *Eriotremex*. The alternative is to assume independent loss of cerci in *Teredon*, *Afrotremex* and *Tremex*. This could support a sister group relationship of *Afrotremex* and *Tremex*.

The attachment of Tremecinae to angiosperm trees (Benson 1943) is not necessarily apomorphic for the Tremecinae since the larval host plants of *Teredon* and of *Afrotremex* are not known. One species of *Eriotremex* is associated with angiosperm plants and the larvae of *Tremex* species seem to live exclusively in angiosperm trees (Smith 1978).

Teredon

The two species of *Teredon* have the following apomorphic characters (Text-fig. 1, characters 9–10): The antennae are 5- or 6-segmented. The hindleg of the male has a widely expanded tibia and basitarsus (Cresson 1865).

Eriotremex + Afrotremex + Tremex

The taxa *Eriotremex*, *Afrotremex* and *Tremex* probably form a monophylum. In these taxa vein 2r-m is absent, M and cu-a almost are in line in the forewing, and the hindwing lacks a closed anal cell (Text-fig. 1, characters 11–13).

There are several diagnostic characters for *Eriotremex* (Benson 1943). The basal position of vein 2r-rs in the forewing is a plesiomorphic feature and the rating of the presence of cerci is not clear (see above). The only possible apomorphic feature of *Eriotremex* is that the disc on the ninth abdominal tergite is convex in the middle and hairy (Text-fig. 1, character 14). In *Teredon*, *Afrotremex* and *Tremex* this disc is flat and bald (Pasteels 1951; David R. Smith, pers. comm.) as in the Siricinae.

The diagnostic features of *Afrotremex* are the basal position of vein 2r-rs in the forewing, a flat ninth abdominal tergite, and the presence of a genal carina (Pasteels 1951). Probably all of these character states are plesiomorphic since they can be found in several taxa of Siricinae, too. A genal carina is absent in *Eriotremex*, *Tremex* and some taxa of the Siricinae. The state of this character is not known for *Teredon*. Independent loss could have occurred easily.

Tremex has an apomorphic character in the apical position of vein 2r-rs in the forewing (Text-fig. 1, character 15).

The phylogenetic relationships between *Eriotremex*, *Afrotremex* and *Tremex* cannot be resolved with the characters presently available.

Characters of the wing venation should be used with caution. Because of potential variability of the wing venation of lower Hymenoptera (Kloiber 1936; Zirngiebl 1939; Jansen 1987) and especially of woodwasps (Cockerell 1921), 28 individuals of six species of *Tremex* and two specimens of *Eriotremex insignis* were examined. Although there were several aberrations, no significant variability in the above mentioned characters of the wing venation could be detected. Thus, the use of the venational characters is justified.

Altogether, this phylogenetic analysis is based on characters for which homoplasy is possible. It is desirable to find many more additional characters to test the proposed relationships.

SYSTEMATIC PALAEONTOLOGY

Genus ERIOTREMEX Benson, 1943 or AFROTREMEX Pasteels, 1951

Eriotremex or *Afrotremex* sp.

Text-figures 2–4

Material. Collection-no. 9604, deposited in the Landesamt für Denkmalpflege Rheinland-Pfalz, Referat Erdgeschichtliche Denkmalpflege, Mainz, Germany.

Locality. Enspel, near Bad Marienberg, Westerwald Mountains, Germany. Fossil site 6, horizon 16.

Age. Upper Oligocene, *c.* 25 Ma (Storch *et al.* 1996; Wuttke 1997).

Preservation. The fossil is seen from the ventral side. The body is fragmentarily preserved (Text-fig. 2). In the head the lower parts of the two eyes are visible. Fragments of the antennae are preserved in front of the head. The thorax shows no detailed structures. The left forewing is only partly present (Text-fig. 2). On the right side both wings can be seen clearly (Text-fig. 3). The abdomen is fragmentarily preserved. From the presence of an ovipositor the fossil can be determined as female.

Morphology. Length 33 mm from head to tip of ovipositor. Forewing 19 mm long. Lower part of forewing and upper part of hindwing overlap, veins in this area cannot be seen (Text-fig. 3). In forewing, 2r-rs is located basally, 2r-m absent with 1Rs and 2Rs united, and M and cu-a in line (Text-fig. 3). Vein 1r-m seems shifted backwards in hindwing, no trace of it above proximal part of cell M, possibly located at middle of upper margin of cell M. Hindwing lacks closed anal cell. Dark shadow below vein A1 in hindwing, probably caused

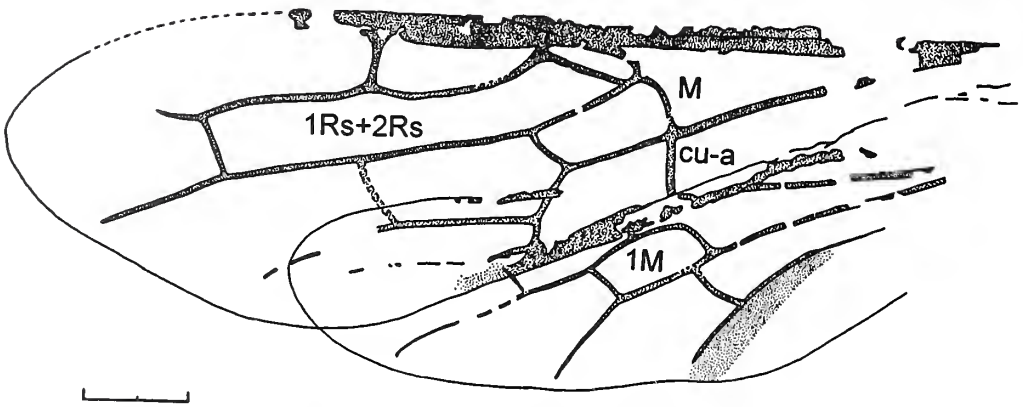

TEXT-FIG. 3. *Eriotremex* or *Afrotremex* sp.; Landesamt für Denkmalpflege Rheinland-Pfalz No. 9604; Enspel, Germany, Upper Oligocene; *Camera lucida* drawing of right wings. Scale bar represents 2 mm. For abbreviations see text.

TEXT-FIG. 4. *Eriotremex* or *Afrotremex* sp.; Landesamt für Denkmalpflege Rheinland-Pfalz No. 9604; Enspel, Germany, Upper Oligocene; *Camera lucida* drawing of hind part of abdomen. Scale bar represents 2 mm. rv = rami valvularum, v3 = third valvulae.

by folded wing membrane (Text-fig. 3). Semicircular structures at base of ovipositor (Text-fig. 4) are rami valvularum (Snodgrass 1935). Ovipositor length 15 mm from base to tip, but it is unclear if ovipositor is completely preserved. Ratio length of forewing/length of ovipositor 1·27.

Systematic position. The fossil belongs to the monophyletic group *Eriotremex* + *Afrotremex* + *Tremex* because in the forewing 2r-m is absent, M and cu-a are almost in line and the hindwing lacks a closed anal cell (complex of apomorphic features 11–13 in Text-fig. 1). The fossil can be distinguished from *Tremex* by having 2r-rs in a basal position (Text-fig. 3). This is the plesiomorphic condition which is present in *Eriotremex* and *Afrotremex*. The appearance of the disc on the ninth abdominal tergite is not visible in the fossil. Consequently, the phylogenetic position must be within the monophylum consisting of *Eriotremex* + *Afrotremex* + *Tremex*, whilst *Tremex* can be excluded. In Text-figure 1 the area of possible phylogenetic positions is shaded.

Genus TREMEX Jurine, 1807

Tremex sp.

Text-figure 5

Material. Collection-no. 27670, Staatliches Museum für Naturkunde in Stuttgart, Germany.

Locality. Willershausen near Osterode, Harz Mountains, Lower Saxony, Germany. No further data available.

Age. Upper Pliocene.

Preservation. Only one forewing (Text-fig. 5) is present. The basal part of the wing is missing. The venation is almost completely preserved. Parts of the veins are not dark but can be recognized because they are raised.

Morphology. Wing length 14 mm. Membrane apically undulated. Vein 2r-rs in apical position, M and cu-a in line. Vein 2rm absent, resulting in fusion of cells 1Rs and 2Rs. In cell 2M, veins M and Cu1a are parallel to each other (Text-fig. 5).

Systematic position. The fossil belongs to *Tremex* because of the apical position of vein 2r-rs in the forewing. This position of 2r-rs is an autapomorphic feature of *Tremex* (Text-fig. 1, character 14). A determination of the species is not possible since there are no known significant differences in the wing venation of *Tremex* at species level.

ZOOGEOGRAPHICAL AND EVOLUTIONARY CONSIDERATIONS

The two extant species of *Teredon* occur only in Cuba (Smith 1978). There are 11 recent species of *Eriotremex* which are native to the Oriental Region (Maa 1956; Smith 1978; Togashi 1991). One species also occurs in Papua-New Guinea (Smith 1978). *E. formosanus* was recently introduced in North America (Smith 1975, 1996). The two species of *Afrotremex* are native to Central Africa (Guiglia 1937; Pasteels 1951). Currently, there are 23 species of *Tremex* (Smith 1978; Togashi 1979). One species occurs in North America, but most species occur in the Palaearctic Region and a few species are confined to the Oriental Region (Smith 1978). The present geographical pattern of Tremecinae can be interpreted as a relict distribution. Probably the Tremecinae formerly were much more widely distributed than today.

For Siricinae, a formerly much wider distribution is proven by the discovery of a fossil *Urocerus*-species in Paleocene shales in Argentina (Fidalgo and Smith 1987). Today there are no Siricidae native in South America.

The specimen from the Upper Oligocene of Enspel belongs to the monophyletic group consisting of *Tremex* + *Afrotremex* + *Eriotremex*. If the reconstruction of the phylogenetic relationships

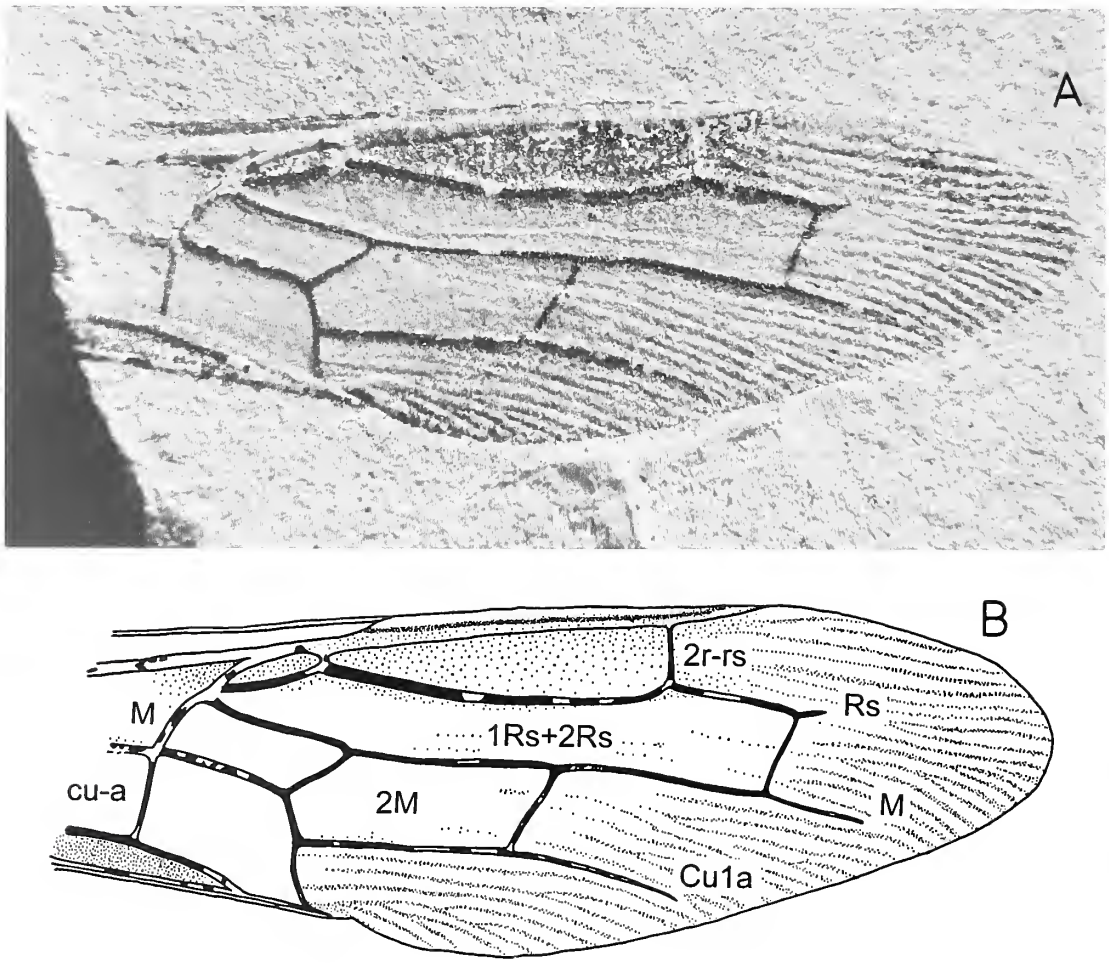

TEXT-FIG. 5. *Tremex* sp.; Staatliches Museum für Naturkunde Stuttgart, No. 27670; Willershausen, Germany, Upper Pliocene. A, photograph of whole fossil; B, *Camera lucida* drawing. Scale bar represents 2 mm. For abbreviations see text.

presented above is correct, not only must *Tremex*+*Afrotremex*+*Eriotremex* have been present in Upper Oligocene times, but also *Teredon* as its supposed sister taxon.

The zoogeographical implications of the fossil from Enspel are unclear. It is possible that the fossil does not belong to *Eriotremex* or *Afrotremex* but to the stem-lineage of *Tremex*+*Afrotremex*+*Eriotremex* or to the stem-lineage of one of these three taxa (Text-fig. 1).

The Pliocene *Tremex* from Willershausen indicates the minimum age for *Tremex*, but the taxon probably is much older.

Acknowledgements. I am very grateful to Dr D. R. Smith (Washington) for examining several characters in the taxa *Afrotremex* and *Teredon*, for commenting on the manuscript critically and for providing literature. I thank Dr G. Tröster, Prof. Dr R. Willmann, Dipl-Biol., Th. Hörnschemeyer (all Göttingen), Dr A. P. Rasnitsyn (Moscow) and the editor Dr R. Wood (Cambridge, UK) for critical comments on the manuscript. I thank Dr M. Wuttke (Mainz) for the loan of the fossil from Enspel, and Dr M. Urlichs (Stuttgart) who lent me the

Willershausen fossil. Drs A. Nel and J. Casevitz-Weulersse (both Paris) were so kind as to make a loan of the extant material possible. This study was supported financially by the Deutsche Forschungsgemeinschaft (TR 262/3-1).

REFERENCES

ASHMEAD, W. H. 1898. Classification of the horntails and sawflies. *Canadian Entomologist*, **30**, 177–182.

BENSON, R. B. 1938. On the classification of sawflies (Hymenoptera, Symphyta). *Transactions of the Royal Entomological Society of London*, **87**, 353–384.

—— 1943. Studies in Siricidae, especially of Europe and Southern Asia (Hymenoptera, Symphyta). *Bulletin of Entomological Research*, **34**, 27–51.

BRADLEY, J. C. 1913. The Siricidae of North America. *Journal of Entomology and Zoology*, **36**, 1–30.

BRUES, C. T. 1926. A species of *Urocerus* from Baltic amber. *Psyche*, **33**, 168–169.

COSTA, A. 1894. *Prospetto degli Imenotteri Italiani da servire di Prodomo di Imenotterologia Italiana. Parte Terza. Tenthredinidei e Siricidei*. Naples, 290 pp.

COCKERELL, T. D. A. 1921. Some British fossil insects. *Canadian Entomologist*, **53**, 22–23.

CRESSON, E. T. 1865. On the Hymenoptera of Cuba. *Proceedings of the Entomological Society of Philadelphia*, **4**, 1–200.

FABRICIUS, J. C. 1781. *Species Insectorum*. Vol. 1. Hamburg and Kiel, 552 pp.

—— 1787. *Mantissa Insectorum*. Vol. 1. Hafniae, 348 pp.

FIDALGO, P. and SMITH, D. R. 1987. A fossil Siricidae (Hymenoptera) from Argentina. *Entomological News*, **98**, 63–66.

FORSIUS, R. 1933. Notes on a collection of Malaysian Tenthredinoidea (Hym.). *Bulletin of the Raffles Museum*, **8**, 169–193.

GAULD, I. D. and MOUND, L. A. 1982. Homoplasy and the delineation of holophyletic genera in some insect groups. *Systematic Entomology*, **7**, 73–86.

GROMOV, V. V., DMITRIEV, V. Yu., ZHERICHIN, V. V., LEBEDEV, E. L., PONOMARENKO, A. G., RASNITSYN, A. P. and SUKATSHEVA, I. D. 1993. [Cretaceous insects from Uljya-River Basin (West Okhot region).] 5–57. *In* PONOMARENKO, A. G. (ed.). [Mesozoic insects and ostracods from Asia.] *Transactions of the Paleontological Institute, Academy of Sciences of the USSR*, **252**, 1–159. [In Russian].

GUIGLIA, D. 1937. Alcune osservazioni intorno al *Tremex hyalinatus* Mocsáry (Hymen. Phytophaga). *Annali del Museo Civico di Storia Naturale Giacomo Doria*, **59**, 433–437.

HEER, O. 1867. Fossile Hymenopteren von Oeningen und Radoboj. *Neue Denkschriften der allgemeinen Schweizerischen Gesellschaft für die gesammten Naturwissenschaften*, **22**, 1–42.

HONG YOU-CHONG 1975. Eine neue fossile – Sinosiricidae (Hymenoptera: Siricoidea) in West-Weichang der Provinz Hebei. *Acta Entomologica Sinica*, **18**, 240–241.

JANSEN, E. 1987. Die europäischen Arten der Gattung *Konowia* Brauns (Hymenoptera: Xiphydriidae). *Stuttgarter Beiträge zur Naturkunde A*, **400**, 1–12.

JURINE, L. 1807. *Nouvelle méthode de classer les Hyménoptères et les Diptères*. Pasehoud, Geneva, 319 pp.

KIRBY, W. F. 1882. *List of Hymenoptera, with descriptions and figures of the typical specimens in the British Museum. Vol. 1, Tenthredinidae and Siricidae*. London, 450 pp.

KLOIBER, J. 1936. Abnormales Flügelgeäder von Tenthrediniden (Hym.). *Konowia*, **15**, 152–154.

KONOW, F. W. 1896. Verschiedenes aus der Hymenopteren-Gruppe der Tenthrediniden. *Wiener Entomologische Zeitschrift*, **15**, 41–59.

—— 1905. Hymenoptera Fam. Siricidae. *Genera Insectorum*, **28**, 1–14.

KÖNIGSMANN, E. 1977. Das phylogenetische System der Hymenoptera. Teil 3: 'Symphyta'. *Deutsche Entomologische Zeitschrift*, **24**, 1–111.

LINNAEUS, C. 1763. Centuria Insectorum. *Amoenitates Academicae*, **6**, 384–415.

MAA, T. 1949. A synopsis of Asiatic Siricoidea with notes on certain exotic and fossil forms (Hymenoptera Symphyta). *Musée Heude, Notes d'Entomologie Chinoise*, **13**, 11–189.

—— 1956. Notes on the genus *Eriotremex* Benson (Hymenoptera: Siricidae). *Proceedings of the Hawaiian Entomological Society*, **16**, 91–94.

MATSUMURA, S. 1930. *The illustrated thousand insects of Japan*. Vol. 2. (*Hymenoptera*). The Toko-Shoin, Tokio, 198 pp.

MOCSÁRY, S. 1886. A magyrországi fa-ronto darázsok. *Rovart Lapok*, **3**, 1–9.

NEL, A. 1988. Redescription de *Eosirex ligniticus* Piton, 1940 (Hymenoptera Symphyta Siricidae). *L'Entomologiste*, **44**, 287–292.

—— 1991. Description et révision de trois 'Siricidae' fossiles du Cénozoique (Hymenoptera). *Bulletin de la Société entomologique de France*, **96**, 247–253.

PASTEELS, J. 1951. Sur quelques Tenthredinoidea africains. *Bulletin et Annales de la Société entomologique de Belgique*, **87**, 195–205.

PITON, L. 1940. Paléontologie du Gisement Éocène de Menat (Puy-de-Dôme). Thèses presentées a la Faculté des Sciences de l'Université de Clermont, Clermont-Ferrand, Vallier.

RASNITSYN, A. P. 1969. [The origin and evolution of lower Hymenoptera.] *Transactions of the Paleontological Institute, Academy of Sciences of the USSR*, **3**, 1–196. [In Russian].

—— 1980. [The origin and evolution of the hymenopteran insects.] *Transactions of the Paleontological Institute, Academy of Sciences of the USSR*, **174**, 1–192. [In Russian].

—— 1983. Fossil Hymenoptera of the superfamily Pamphiloidea. *Paleontological Journal*, **2**, 56–70.

—— 1988. An outline of evolution of the hymenopterous insects (order Vespida). *Oriental Insects*, **22**, 115–145.

RIEK, E. F. 1955. Fossil insects from the Triassic beds at Mt. Crosby, Queensland. *Australian Journal of Zoology*, **3**, 654–691.

ROHWER, S. A. 1911. A classification of the suborder Chalcogastra of the Hymenoptera. *Proceedings of the Entomological Society of Washington*, **13**, 215–226.

ROSS, H. H. 1936. The ancestry and wing venation of the Hymenoptera. *Annals of the Entomological Society of America*, **29**, 99–111.

—— 1937. A generic classification of the Nearctic sawflies (Hymenoptera, Symphyta). *Illinois Biological Monographs*, **15**, 1–173.

SAINI, M. S. and SINGH, D. 1987. A new genus and a new species of Siricinae (Insecta, Hymenoptera, Siricidae) from India with a revised key to its world genera. *Zoologica Scripta*, **16**, 177–180.

SMITH, D. R. 1975. *Eriotremex formosanus* (Matsumura), an Asian horntail in North America (Hymenoptera: Siricidae). *United States Department of Agriculture Cooperative Economic Insect Report*, **25**, 851–854.

—— 1978. Suborder Symphyta (Xyelidae, Pararchexyelidae, Parapamphiliidae, Xyelydidae, Karatavitidae, Gigasiricidae, Sepulcidae, Pseudosiricidae, Anaxyelidae, Siricidae, Xiphydriidae, Paroryssidae, Xyelotomidae, Blasticotomidae, Pergidae). *In* VAN DER VECHT, J. and SHENEFELT, R. D. (eds). *Hymenopterorum Catalogus* (nova editio), Pars 14. The Hague, Holland, 193 pp.

—— 1988. A synopsis of the sawflies (Hymenoptera: Symphyta) of America south of the United States: introduction, Xyelidae, Pamphiliidae, Cimbicidae, Diprionidae, Xiphydriidae, Siricidae, Orussidae, Cephidae. *Systematic Entomology*, **13**, 205–261.

—— 1996. Discovery and spread of the Asian horntail, *Eriotremex formosanus* (Matsumura) (Hymenoptera: Siricidae), in the United States. *Journal of Entomological Science*, **31**, 166–171.

SMITH, F. 1859. Catalogue of hymenopterous insects collected by Mr. A. R. Wallace at the islands of Aru and Key. *Journal of the Proceedings of the Linnean Society, Zoology*, **3**, 132–178.

SNODGRASS, R. E. 1935. *Principles of insect morphology*. McGraw-Hill, New York, 667 pp.

SONAN, J. 1938. Siricidae of Formosa. *Transactions of the Natural History Society of Formosa*, **28**, 88–94.

STORCH, G., ENGESSER, B. and WUTTKE, M. 1996. Oldest fossil record of gliding in rodents. *Nature*, **378**, 439–441.

TOGASHI, I. 1979. A new species of *Tremex* Jurine from Taiwan (Hymenoptera: Symphyta–Siricidae). *Transactions of the Shikoku Entomological Society*, **14**, 187–189.

—— 1990. A new *Eriotremex* from Japan (Hymenoptera: Siricidae). *Transactions of the Shikoku Entomological Society*, **19**, 105–108.

WESTWOOD, J. O. 1874. *Thesaurus Entomologicus Oxoniensis*. Clarendon Press, Oxford, 205 pp.

WUTTKE, M. 1997. Die Fossillagerstätten Enspel und Messel. *Spektrum der Wissenschaft*, **3**, 110–112.

ZIRNGIEBL, L. 1939. Veränderungen am Flügelgeäder von *Xiphydria prolongata* Geoff. *Abhandlungen des naturwissenschaftlichen Vereins Bremen*, **31**, 106–108.

SONJA WEDMANN

Georg-August-Universität Göttingen,
II. Zoologisches Institut und Museum,
Abt. Morphologie und Systematik,
Berliner Str. 28, D-37073 Göttingen, Germany

Typescript received 24 June 1997
Revised typescript received

SILURIAN POLYPLACOPHORAN MOLLUSCS FROM GOTLAND, SWEDEN

by LESLEY CHERNS

ABSTRACT. A new, unusually diverse and abundant polyplacophoran (chiton) assemblage occurs in the Silurian of Gotland, Sweden, largely as silicified material. The paleoloricate fauna described here includes: *Thairoplax pelta* gen. et sp. nov., *Plectrochiton tegulus* gen. et sp. nov., *Alastega lira* gen. et sp. nov., *Heloplax papilla* gen. et sp. nov., *Enetoplax decora* gen. et sp. nov. and *Arctoplax ornata* gen. et sp. nov.; *Gotlandochiton* Bergenhayn is revised. One genus represented by an intermediate sclerite, and two unassociated end sclerites, are left under open nomenclature. Most material is from the late Wenlock Halla Formation. Three of the new genera have a holoperipheral growth style and dorsal mucronate apex, normally found only in tail sclerites; plates of these genera display prominent subapical muscle cavities. Patterns of growth banding that associate several such plates as coming from the same individual are important in suggesting that most represent intermediate, and not tail, sclerites. The morphological evidence from sclerites for musculature, and muscle function are assessed for all of the chitons. Recent chiton plates, which have sutural laminae for physical articulation, do not show comparable indications of insertion sites. Several of the Gotland chitons had elongate sclerites, and were elongate animals by comparison with Recent chitons; others had shorter, broader plates and hence a more ovoid body form.

THE only widely known early Palaeozoic polyplacophoran (chiton) genus, *Chelodes*, was first described from the Silurian of Gotland, Sweden (*C. bergmani* Davidson and King, 1874). On the basis of existing and new collections, Gotland species were revised by Cherns (1998). The new collections, from extensive sampling of silicified horizons (Laufeld and Jeppsson 1976) by Dr L. Jeppsson (Lund University, Sweden) and Dr L. Liljedahl (Liljedahl 1984), are dominated quantitatively by sclerites of the large chiton *Chelodes actinis* Cherns, 1998. However, in addition, the relatively abundant and well-preserved acid-isolate assemblages include a diverse range of other chiton taxa, which are described here. *Gotlandochiton* Bergenhayn, 1955 from museum collections is revised. All the material is deposited at the Naturhistoriska Riksmuseet, Stockholm (RM).

The general depositional setting of the stable platform carbonates that dominate the Silurian (Llandovery–Ludlow) succession of Gotland (Text-fig. 1) is discussed by Cherns (1998). Among silicified samples taken from several hundred localities throughout the succession, chitons are restricted to only four localities (Text-fig. 1); three are Wenlock (lower Silurian), of which one (Krakfot) yielded exclusively *Spicuchelodes* (Cherns 1998), and one Ludlow (upper Silurian). Productive localities for the chitons described here are Möllbos (Möllbos-1, Grid Reference Rikets nät RN 637645 165970; Liljedahl 1984), from where most material is derived, and Klintebys (Klintebys-1, RN 636515 164685; Laufeld 1974), both in the Halla Formation, and Ängvards (Ängvards-4, RN 631953 164607) in the Hamra Formation. In addition, the type locality for *Gotlandochiton interplicatus* Bergenhayn, 1955 is Klints Othem (Laufeld 1974; = Spillings 1–2, Jaanusson 1986, p. 10) in the Wenlock Slite Group, and *Thairoplax birhombivalvis* (Bergenhayn, 1955) comes from localities Visby (Lindström 1884, locality Wisby) and Kålens kvarn (Lindström 1884, Kålens qvarn) in the Upper Llandovery to Lower Wenlock, Visby to Högklint formations. All other chiton localities have yielded only *Chelodes* spp.

[Palaeontology, Vol. 41, Part 5, 1998, pp. 939–974, 9 pls]

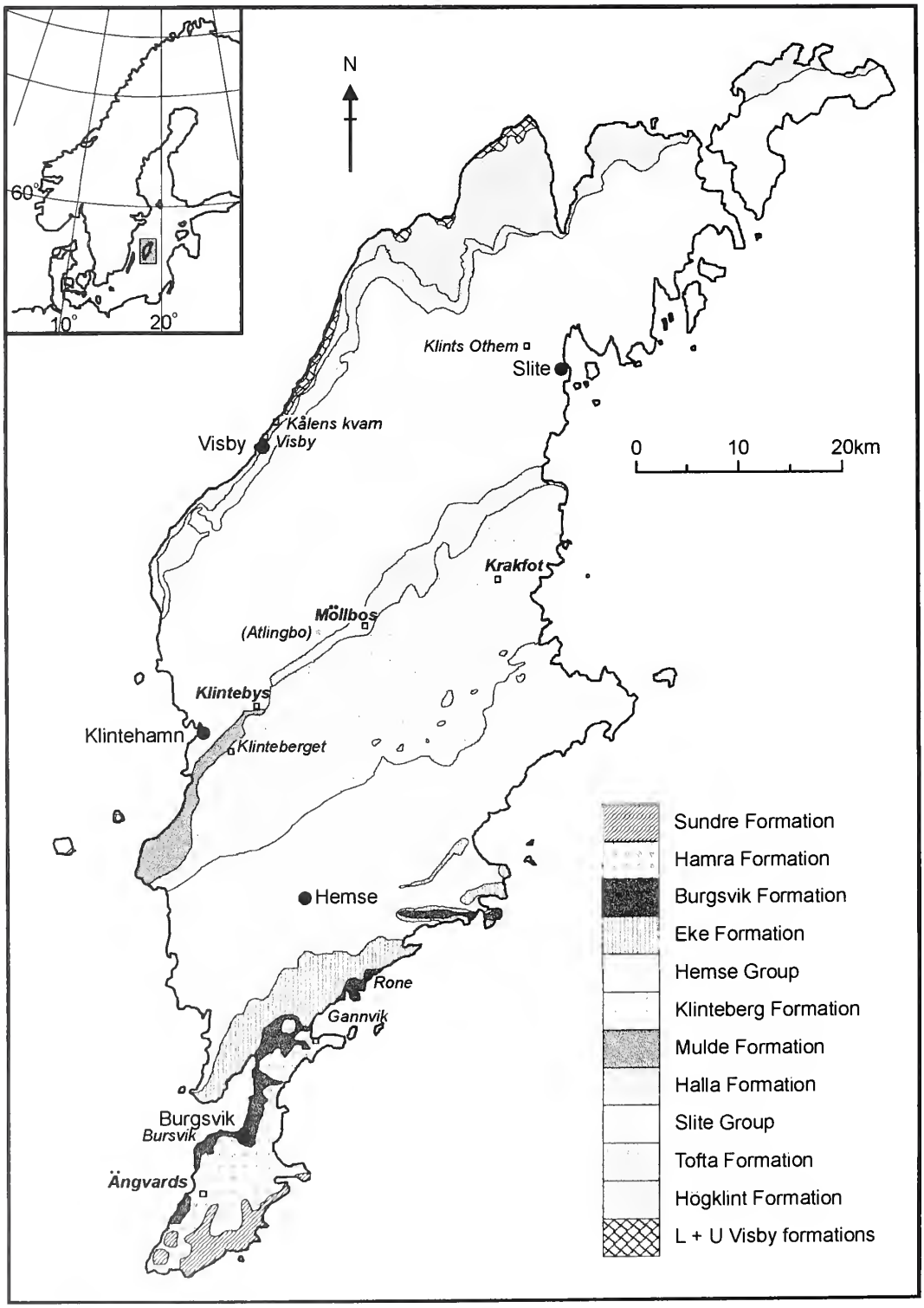

TEXT-FIG. 1. For caption see opposite.

PRESERVATION

The existing Riksmuseum collections used here are limestone specimens with sclerites partly embedded, preserved as recrystallized, coarse calcite mosaics, and with consequent loss of surface detail. These collections are from the Llandovery locality Visby (*T. birhombivalvis*), and Wenlock localities at Kålens kvarn (*T. birhombivalvis*) and Klints Othem (*G. interplicatus*). Limited taxonomic data were derived from these specimens.

In contrast, the silicified material comprises isolated sclerites, including small and delicate specimens. The vast majority of chitons are from the Möllbos-1 locality in the Late Wenlock (Homerian) Halla Formation, from < 1 m thickness of very thin bedded (< 0·1 m), hard, pale grey micritic limestones with some thinner (< 0·05 m) marl intercalations (e.g. Liljedahl 1984, fig. 35). Macrofossil material appears sparse in hand specimen, and is difficult to extract from the compact lithology. However, acid extraction from several hundred kg of limestones has yielded a rich and diverse fauna; the total, diverse chiton material is < 300 sclerites, limited in comparison with some other groups (e.g. > 3400 determinable bivalves; Liljedahl 1984), but still unusually numerous compared with most Palaeozoic chiton occurrences. A fairly low energy depositional environment is evident from the generally small degree of wear and breakage. The chiton assemblage includes *Thairoplax pelta*, *T.*? aff. *pelta*?, *Plectrochiton tegulus*, *Alastega lira*, *Heloplax papilla*, *Enetoplax decora*, *Arctoplax ornata*, head B and head/tail C, as well as a large number of *C. actinis* (Cherns 1998). The preservation of silicified sclerites shows little distinction in crystal size between surface and inner layers, superficially a mosaic of fairly small, inward growing quartz crystals (Schmitt and Boyd 1981, cf. Pattern 1, evident in *C. actinis* from this locality; Cherns 1998). Evidence for rapid precipitation of chalcedony and fine quartz suggests relatively high silica concentrations. Details of surface features are well preserved, indicating early cementation of the micritic carbonate matrix, before delayed precipitation into dissolution cavities. Preserved shell thickness and convexity indicate replacement before significant compaction.

Some of the silicified material is from Klintebys-1, also in the Halla Formation. These specimens are more coarsely crystalline and beekitized, fairly worn, with loss of surface detail. Fragmented specimens typically have sealed edges. The preservation suggests coarser surrounding sediment, a higher energy environment producing more fragmentation, and again delayed precipitation into cavities. Coarser replacement might also indicate slower precipitation and lower silica concentrations than at Möllbos-1 (Schmitt and Boyd 1981). As with Möllbos-1, the preservation of the convexity of shells means that replacement preceded compaction. The Klintebys collections yielded only *A. lira*, including head and tail sclerites, together with *Chelodes* spp. (Cherns 1998). Gen. A from Ängvards-4 in the Hamra Formation shows similar coarse beekitization.

TERMINOLOGY AND MEASUREMENTS

The Silurian chitons are paleoloricates, lacking the sutural laminae for insertion beneath the adjacent plate which characterize neoloricate, and hence living chitons (e.g. Smith 1960). The measurements and terminology for paleoloricate sclerites with a posterior apex, ventral apical area and mixoperipheral growth follow those outlined by Cherns (1998, text-fig. 2). Most chitons, paleoloricates and neoloricates, have a ventral extension of the outer dorsal shell layer, the tegmentum, to form the apical area (Smith and Toomey 1964). In contrast, several of the paleoloricate chitons described here have a dorsal apex and holoperipheral growth style, typically found only in tail sclerites of Recent neoloricate chitons. These sclerites have a prominent raised dorsal apex, or mucro, which corresponds on the ventral surface to a deep subapical cavity, and

TEXT-FIG. 1. Map of Gotland showing the geological succession of Silurian (upper Llandovery to Ludlow) strata, all localities for chitons in existing Riksmuseum collections (italics) and new silicified collections (bold italics). (For discussion of the locality Atlingbo, see Cherns 1998.)

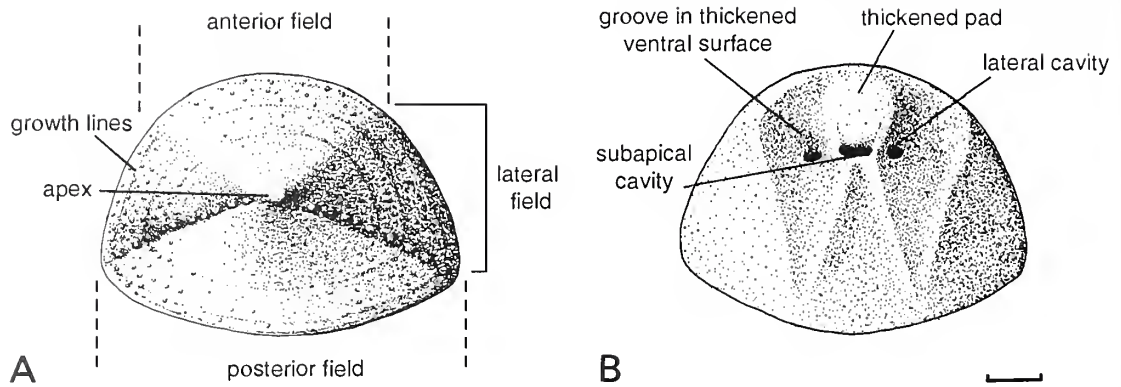

TEXT-FIG. 2. Diagram of holoperipheral sclerites of *Heloplax papilla* gen. et sp. nov., to illustrate terminology used in description of A, dorsal and B, ventral surfaces. Intermediate sclerites have a prominent mucronate subcentral apex, elevated anterior and posterior shell fields, and transverse flexure through the depressed lateral fields. A line of coarser granular ornament delimits the lateral from posterior shell fields. The sculpted ventral surface of a thickened sclerite has additional, smaller lateral cavities as well as the deep, anteriorly slanting subapical cavity, and a pattern of longitudinal and oblique furrows and pads around the cavities. Scale bar represents 1 mm.

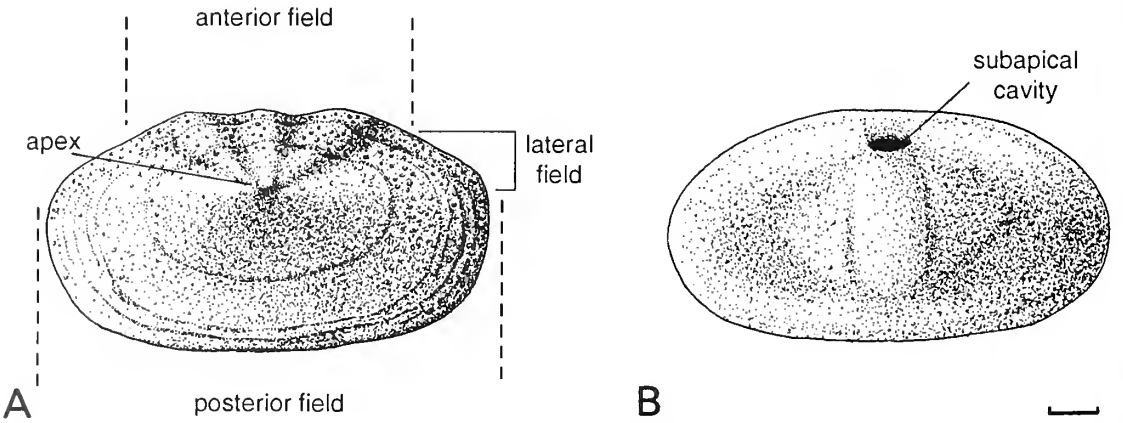

TEXT-FIG. 3. Diagram of holoperipheral sclerites of *Enetoplax decora* gen. et sp. nov. to illustrate terminology used in description of A, dorsal and B, ventral surfaces. Intermediate sclerites have an anteriorly displaced mucronate apex, elevated short anterior shell field, long, gently curved and elevated posterior field, gentle transverse flexure through short, depressed lateral fields; lateral and posterior fields without distinct separation. The ventral surface of thickened sclerites has a deep, anteriorly slanting subapical cavity, nearer to the anterior margin and associated with shallower development of pads and longitudinal furrows than in *Heloplax papilla* (Text-fig. 2). Scale bar represents 1 mm.

dorsal shell with anterior, lateral and posterior fields. Terminology for such plates in two genera is shown in Text-figures 2–3.

In the systematic descriptions below, figured specimens are indicated by an asterisk against specimen numbers.

SYSTEMATIC PALAEONTOLOGY

Class POLYPLACOPHORA de Blainville, 1816
Subclass PALEOLORICATA Bergenhayn, 1955

Remarks. Suprageneric classification requires revision encompassing other Palaeozoic chitons, and will be considered in a wider review.

Genus GOTLANDOCHITON Bergenhayn, 1955

Type species. G. interplicatus Bergenhayn, 1955 (p. 15, pl. 1, fig. 6; pl. 2, fig. 4 (reconstruction)), by original designation, from the Upper Wenlock, Silurian, of Gotland, Sweden.

Diagnosis (emended from Bergenhayn 1955). Intermediate sclerites broad, arched, with straight, deep, trapezoidal side slopes; jugum rounded, jugal angle close to perpendicular; shell fields not evident. Wide anterior margin gently convex to transverse; anterolateral corners rounded, anterolateral margins short, parallel to slightly divergent; posterolateral margins longer, straight, tapering rapidly across triangulate posterior shell to posterior apex; apical angle close to perpendicular. Ornament of low rounded ridges and narrow grooves parallel to growth lines. Apical area apparently broad and short.

Remarks. Gotlandochiton was erected by Bergenhayn (1955) to include four new species described from Gotland. The original generic diagnosis stated that the form of the intermediate sclerites resembled that of most living chitons, with distinct shell fields and with jugal or complete coverage (across the following sclerite). The new family Gotlandochitonidae Bergenhayn, 1955 had a more discrete diagnosis of intermediate sclerites wider than long, variable in shape within the genus, and with weak but distinct shell fields. In the *Treatise on invertebrate paleontology* (Smith 1960, p. I50), relatively small size was noted as a family character.

Bergenhayn (1955) distinguished this genus from *Chelodes* on the basis of sclerites that were wider than long, and with distinct shell areas/fields. In the type species, the broad sclerite has straight side slopes flexed across the jugum, but shell fields are not evident. However, Bergenhayn (1955) also erected and included three other species within *Gotlandochiton*: *G. laterodepressus*, *G. troedssoni* and *G. birhombivalvis*. Of these, the first two, in which central and lateral shell fields are developed, have been synonymized with *C. gotlandicus* (Cherns 1998), and *Chelodes* is now recognized as including species that have distinct shell fields (Cherns 1998). For *Chelodes*, Cherns (1998) noted that sclerites only consistently become longer than wide with increasing size, so that as a criterion particularly for smaller sclerites this is of limited value. *G. birhombivalvis* is transferred here to the new genus *Thairoplax*, described below.

Smith and Toomey (1964) noted that *Gotlandochiton* should display clearly defined shell areas, and suggested an 'apical area less than 1·5 mm wide, extending across the entire posterior margin or present mainly in the vicinity of the valve apex' (p. 18). *G. hani* Smith, *in* Smith and Toomey, 1964, from the lower Ordovician of southern Oklahoma, USA, has broad, rectangular flexed sclerites which have a very narrow band-like ventral apical area and some ventral transverse thickening (Smith and Toomey 1964). The emended generic diagnosis above does not include shell fields, the approximately straight posterior margin in *G. hani* compares with a triangulate posterior shell in both *Gotlandochiton interplicatus* and *Thairoplax* gen. nov., and the very short apical area is also apparently different in form from those of both genera.

Gotlandochiton interplicatus Bergenhayn, 1955

Plate 1, figure 1a–d

v* 1955 *Gotlandochiton interplicatus* Bergenhayn, p. 15, pl. 1 fig. 6; pl. 2 fig. 4 [reconstruction].

1960 *Gotlandochiton interplicatus* Bergenhayn; Smith, p. 150, fig. 34, 4 [reconstruction, Bergenhayn 1955].
1975 *Gotlandochiton interplicatus* Bergenhayn; Van Belle, p. 125.
1977 *Gotlandochiton interplicatus* Bergenhayn; Sirenko and Starobogatov, p. 31.
1987 *Gotlandochiton interplicatus* Bergenhayn; Smith and Hoare, p. 34.

Material and locality. Holotype RM Mo6012*, intermediate sclerite, with fragment of adjacent plate; Klints Othem (= Spillings 1–2, Laufeld 1974; Jaanusson 1986), Gotland; Slite Formation, Slite g, Upper Wenlock (Homerian).

Diagnosis. As for the genus.

Description (emended from Bergenhayn 1955). Holotype an intermediate sclerite in limestone matrix obscuring ventral surface, right posterolateral edge broken; fragment of anterior left portion of second, more posterior sclerite partially covered only by apex. Broad (width 12·3 mm), arched sclerite, wider than long (length 11·3 mm), with straight and deep, trapezoidal side slopes (Pl. 1, fig. 1b–c), jugal ridge rounded, jugal angle 98°. Shell fields not evident. Anterior margin wide and gently convex, rounding into short anterolateral margins that are parallel to slightly divergent. Posterolateral margins longer, straight, tapering rapidly to posterior apex, apical angle 94°. Maximum width of sclerite near posterolateral corners, behind mid-length. Dorsal surface fairly worn, but ornament of low rounded ridges and incised narrow grooves (= ribs of Bergenhayn 1955, p. 16) parallel to growth lines, i.e. to anterior and anterolateral margins, crossing posterolateral margins (Pl. 1, fig. 1a–c). Granular sculpture identified by Bergenhayn (1955, p. 16; Pl. 1, fig. 1c) is a patchy, replacement fabric. In lateral profile, jugal ridge slightly convex (Pl. 1, fig. 1b–c). In transverse profile, shell flexed across rounded jugal ridge (Pl. 1, fig. 1d), height/length 0·38.

Remarks. On the basis of the limited overlap of the holotype onto a second sclerite, with coverage apparently confined to the jugal area, Bergenhayn (1955) deduced that the apical area was narrow and restricted to the apex. He commented that this would leave triangular areas of the body wall exposed laterally between plates (Bergenhayn 1955, p. 15). However, growth lines transect the posterolateral margins onto the ventral apical area (Cherns 1988), which would have spanned the breadth between posterolateral corners and was thus apparently wide, close to the maximum width. The broken right posterolateral margin, curved from apex to posterolateral corner (Pl. 1, fig. 1c, cf. the straight left margin in fig. 1a–b may represent breaking away of the apical area here. Its length (= median length; Cherns 1998, text-fig. 2) and shape of the anterior margin are unknown, the former at most the length from the posterolateral corners, and thus less than half the length of the sclerite. The apparently wide apical area suggests a greater degree of overlap of sclerites than is apparent in the specimen, where the plates may have separated during preservation.

EXPLANATION OF PLATE 1

Fig. 1. *Gotlandochiton interplicatus* Bergenhayn, 1955; RM Mo6012, holotype; intermediate sclerite; Klints Othem, Gotland; Slite Group, Upper Wenlock (Homerian). 1a, dorsal view, showing also fragment of following sclerite; 1b, left lateral view, showing also fragment of following sclerite; 1c, right lateral view, broken posterolateral margin; 1d, anterior view. All × 3.

Figs 2–5. *Thairoplax birhombivalvis* (Bergenhayn, 1955); intermediate sclerites. 2, holotype, RM Mo6031; Visby, Gotland; ?Lower Visby Formation, Upper Llandovery (Telychian); ventral external mould. 3, RM Mo6023; Kålens kvarn, Gotland; lower Högklint Formation, Lower Wenlock (Sheinwoodian). 3a, dorsal view; 3b, left lateral view; note coarse replacement fabric; 3c, anterior view. 4, RM Mo6024a; Kålens kvarn, Gotland; lower Högklint Formation, Lower Wenlock (Sheinwoodian); dorsal view, posterior shell broken. 5, RM Mo6024b; Kålens kvarn, Gotland; lower Högklint Formation, Lower Wenlock (Sheinwoodian); left lateral view, partly embedded sclerite. All × 3.

Fig. 6. gen. A indet.; RM Mo160.061; Ängvards-4, Gotland; Hamra Formation, Upper Ludlow (upper Ludfordian); broken intermediate sclerite. 6a, dorsal view; 6b, ventral view; 6c, left lateral view; 6d, posterior view. All × 3.

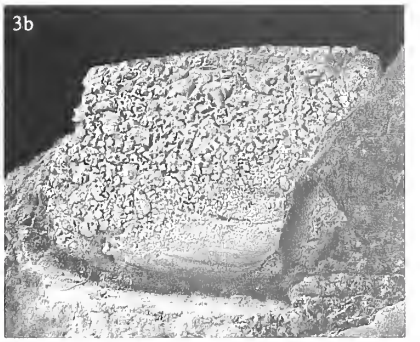

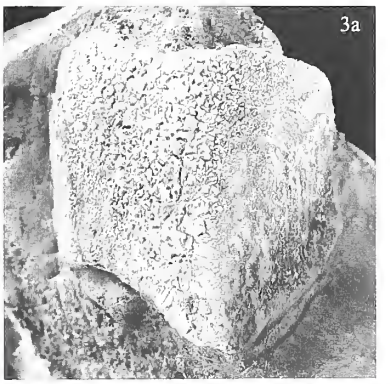

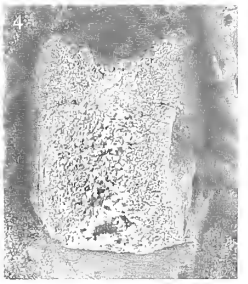

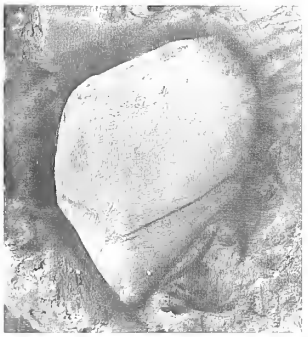

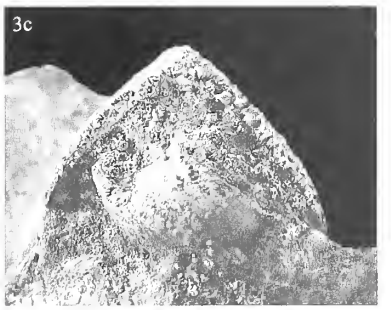

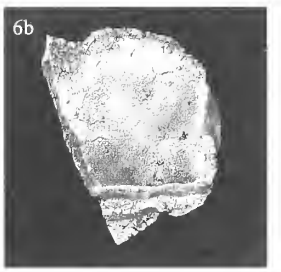

CHERNS, Silurian chitons

A silicified sample from Ängvards-4, from the younger, late Ludlow Hamra Formation, yielded one partial sclerite (gen. A, below) that has a broad form and distinctive shallow ridge-and-groove ornament somewhat similar to that of *G. interplicatus*, and an unusual, transverse anterior margin to the apical area. *Gotlandochiton birhombivalvis* Bergenhayn, 1955, in which sclerites are not notably wide, has a V-shaped ventral apical area (Bergenhayn 1955, pl. 1, fig. 7). Until more material becomes available to verify this ventral feature in *G. interplicatus*, the genus should be restricted to the type species. *G. birhombivalvis* is therefore transferred to the new genus *Thairoplax*.

gen. A indet.

Plate 1, figure 6a–d

Material, locality and horizon. One partial silicified (beekitized) intermediate sclerite, RM Mo160.061*, Gotland (RN 631953 164607), Hamra Formation, Upper Ludlow (Ludfordian).

Description. One broken and beekitized intermediate sclerite, the left side without the apex. Sclerite apparently wider than long, slightly cordate, with jugal flexure and straight side slope, without shell fields. Side slope fairly deep, trapezoidal (Pl. 1, fig. 6c). Broad, transverse, slightly rounded anterior margin having only shallow and narrow median embayment, rounding into only slightly convex to straight anterolateral margin parallel to jugal ridge, rounding sharply into straight posterolateral margin tapering steeply towards posterior apex. Anterolateral and posterolateral margins apparently roughly equal in length. Strong ornament of rounded ridges and incised grooves parallel to growth lines. Maximum width at posterolateral corners, well behind mid-length. Ventral apical area broad, triangulate, with raised transverse anterior margin across breadth of shell to posterolateral corners. Apical length/length in specimen 0·28, estimated for complete sclerite possibly *c.* 0·3. Ventral surface smooth.

Remarks. The broad shell has strong ornament of rounded ridges and narrow incised grooves parallel to growth lines that is fairly similar to that of the holotype of *G. interplicatus*, and unlike that of all other Gotland chitons. The transverse anterior margin is slightly embayed medially, by comparison with the smoothly rounded anterior in *G. interplicatus*, and the jugal angle on the broken sclerite appears to be slightly greater at *c.* 105°. The side slope is less deep, the antero- and posterolateral margins appear roughly equal in length, i.e. longer, and shorter and steeper, respectively. No shell fields are apparent. The broad apical area would imply complete coverage across the adjacent sclerite; its transverse anterior margin is unique among the Gotland chiton fauna.

The specimen is notably younger than *G. interplicatus*, from the Upper Ludlow as opposed to Upper Wenlock. Because it is only a single specimen, from a stratigraphical horizon that has previously yielded only *Chelodes gotlandicus* Lindström, 1884, it has been left under open nomenclature.

Genus THAIROPLAX gen. nov.

Derivation of name. From the Greek *thairos*, hinge, and *plax*, plate, to indicate the flexed form of sclerites.

Type species. Thairoplax pelta gen. et sp. nov.; Upper Wenlock, Silurian, Gotland, Sweden.

Diagnosis. Arched intermediate sclerites flexed longitudinally across jugum, jugal angle perpendicular to slightly obtuse, side slopes straight, trapezoidal; anterior margin transverse; posterolateral shell triangulate, posterior apex pointed, acute. Ventral apical area broad, V-shaped, less than one-third of length. Shell becoming medium to large size, typically longer than wide, thicker medially, tapering outwards; ventral surface smooth, without localized thickening. Ornament of fine growth lines. Shell fields weak. Broad central and narrower lateral fields.

Remarks. Thairoplax gen. nov. is similar to *Chelodes* in having fairly large, wedge-shaped sclerites with a posterior apex, but differs in its marked jugal flexure between straight trapezoidal side slopes, and in limited ventral thickening, greater medially, in contrast to the thick to massive, sculptured ventral surface in larger sclerites of *Chelodes*. *Thairoplax* differs from *Gotlandochiton*, which is similar in having flexed intermediate sclerites with straight side slopes, in having sclerites at least as long as wide, a transverse anterior margin, a more acute apex, and a distinctly V-shaped apical area.

Paleochiton Smith, 1964 (*P. kindbladensis* Smith, *in* Smith and Toomey, 1964) and *Kindbladochiton* Van Belle, 1975 (*K. arbucklensis* (Smith, *in* Smith and Toomey, 1964); Van Belle 1975) are monospecific early Ordovician genera from southern Oklahoma, USA, which have broadly rectangular intermediate sclerites, but both have transverse posterior margins, in contrast to the extended, triangulate posterior portion of the sclerite in *Thairoplax*. In *Paleochiton* the ventral apical area is short and bandlike. *Kindbladochiton* has a ventral transverse thickened ridge lacking in the smooth ventral surface of *Thairoplax*. Kluessendorf (1987) described chiton morphotype A from the middle–upper Silurian of Wisconsin, USA, for a flexed shell with flat side slopes and parallel lateral margins, which on general form and V-shaped anterior margin of the apical area could belong within *Thairoplax* (see discussion of *T. birhombivalvis* below).

Thairoplax pelta gen. et sp. nov.

Plate 2, figures 1–3

Derivation of name. From the Greek *pelte*, shield, to describe the shape of sclerites.

Material, locality and horizon. Seven intermediate sclerites, Möllbos-1, Gotland, Halla Formation, Upper Wenlock (Homerian); holotype RM Mo159.901*, isolated plate with dorsal small bryozoan encrustation; syntypes RM Mo159.937, 159.952*, 159.972, 159.973*, 160.019, 160.026.

Diagnosis. Shield-shaped intermediate sclerites flexed slightly obtusely across jugum, rounded jugal ridge, side slopes long; sclerites elongate. Ventral apical area short, apical length/length $< 0{\cdot}2$.

Description. Shield-shaped intermediate sclerites of medium size (mean length 15·3 mm, s.d. = 2·86, $n = 6$; holotype length 12·1 mm), elongate, mean length/width 1·4 (s.d. = 0·09, $n = 6$; holotype 1·38). Flexed and thickened slightly medially across rounded jugal ridge, tapering across flat, trapezoidal side slopes towards lateral margins; mean jugal angle 103° (s.d. = 3·8, $n = 7$; holotype 108°). Anterior part of shell roughly rectangular, long, with anterior margin close to transverse, very slightly embayed to convex, median length/length 0·99 (s.d. = 0·02, $n = 6$; holotype 1·0), anterolateral corners rounded. Straight anterolateral margins more than half the length of the sclerite, almost parallel, maximum width towards anterior, in front of midlength; posterolateral corners distinct; shorter, straight posterolateral margins tapering rapidly to acute posterior pointed apex, mean apical angle 69° (s.d. = 5·6, $n = 7$; holotype 70°). Dorsal sculpture of fine growth lines parallel to anterior and anterolateral margins, crossing onto ventral apical area (e.g. Pl. 2, fig. 3a, c); parallel, prominent larger growth steps (e.g. Pl. 2, figs a, c). The latest growth lines may be entirely ventral, forming a narrow ventral rim, e.g. holotype (Pl. 2, fig. 1b). Weak dorsal radial folds give poor definition of broad central and narrow posterolateral areas (Pl. 2, figs 1a, 3a).

Ventral apical area short, narrow band tapering across to posterolateral corners, to markedly V-shaped (Pl. 2, figs b), mean apical length/length 0·18 (s.d. = 0·02, $n = 5$; holotype 0·10). Apical area ornamented with growth lines, anterior margin slightly raised above smooth ventral surface.

Lateral profile (Pl. 2, figs c) shows straight jugal ridge, roughly parallel anterolateral margin, transverse anterior margin and rapidly tapering, shorter posterolateral margin. Transverse section (Pl. 2, figs d) V-shaped posteriorly, becoming more rounded anteriorly, side slopes straight and tapering. Mean height/length 0·34 (s.d. = 0·05, $n = 7$; holotype 0·37).

Remarks. T. pelta differs from the similar-aged (late Wenlock) *Gotlandochiton interplicatus* in having elongate sclerites, weakly defined shell areas with a broad triangular central field, a bandlike to strongly V-shaped ventral apical area, and ornament of only fine growth lines.

T. pelta is found among collections from Möllbos-1 dominated quantitatively by *C. actinis*, from which it is easily distinguished by its flexed, shield-shaped, non-massive form.

Thairoplax? aff. *pelta*?

Plate 3, figure 4

Material, locality and horizon. Möllbos-1, Gotland, Halla Formation, Upper Wenlock (Homerian); one isolated intermediate sclerite, RM Mo160.020*.

Description. Arched, medium sized intermediate sclerite, similar length to width, flexed across jugum, side slopes straight; length 12·1 mm, length/width 1·04, height/length 0·42, jugal angle 96°. Anterior margin transverse, slightly embayed, rounding through fairly long, gently convex and divergent anterolateral margins; maximum width at posterolateral corners, behind midlength. Posterolateral margins straight, similar length to anterolateral margins, tapering rapidly across triangulate posterior shell to pointed apex, apical angle 85°. Ventral apical area broad, V-shaped, tapering outwards, apical length/length 0·31. Ventral surface smooth, not greatly thickened, but with rounded, low triangular transverse ridge between posterolateral corners, tapering anteriorly, posteriorly extending as narrow median pad flanked by low furrows towards anterior rim of apical area (Pl. 3, fig. 4b). Dorsal weak low radial jugal fold across fairly narrow anterior embayment; fine growth lines.

Remarks. This specimen occurred in a sample with *T. pelta* and *C. actinis*, and is broadly similar in its flexed form with straight side slopes and V-shaped apical area to *T. pelta*. However, it differs in having rounded anterolateral margins, slightly tapering anteriorly and of similar length to the posterolateral margins, in having a relatively long apical area (apical length/length 0·31, cf. mean 0·18 for *T. pelta*), and particularly in the localized ventral thickening into a low transverse ridge. It may represent an anterior intermediate sclerite of *T. pelta*, tapering towards a typically small head sclerite, but the pattern of ventral thickening, unseen otherwise in *T. pelta*, may indicate that it does not belong within this species (or genus?).

Thairoplax birhombivalvis (Bergenhayn, 1955)

Plate 1, figures 2–5

v* 1955 *Gotlandochiton birhombivalvis* Bergenhayn, p. 18, pl. 1, fig. 7; pl. 2, fig. 6 [reconstruction].
1977 *Gotlandochiton birhombivalvis* Bergenhayn; Sirenko and Starobogatov, p. 31.
1987 *Gotlandochiton birhombivalvis* Bergenhayn; Smith and Hoare, p. 15.

Material, locality and horizon. Four intermediate sclerites; holotype RM Mo6031*, external mould of ventral surface, Visby, Gotland, Lower Visby Formation (Visby a), Upper Llandovery (Telychian); syntypes RM Mo6023* and 6024* (two specimens), Kålens kvarn (= Kolens kvarn), Visby, Gotland, Högklint Formation, Lower Wenlock (Sheinwoodian).

EXPLANATION OF PLATE 2

Figs 1–3. *Thairoplax pelta* gen. et sp. nov.; Möllbos-1, Gotland; Halla Formation, upper Wenlock (Homerian); intermediate sclerites. 1, holotype (with small bryozoan encrustation on left anterior), RM Mo159.901; 1a, dorsal view; 1b, ventral view; 1c, right lateral view; 1d, posterior view. 2, RM Mo159.973; 2a, dorsal view, showing prominent growth increment; 2b, ventral view; 2c, right lateral view; 2d, posterior view. 3, RM Mo159.952; 3a, dorsal view, showing prominent growth increment, broad central shell field; 3b, ventral view; 3c, right lateral view; note weak fold defining broad central shell field, fine growth ornament; 3d, posterior view. All ×3.

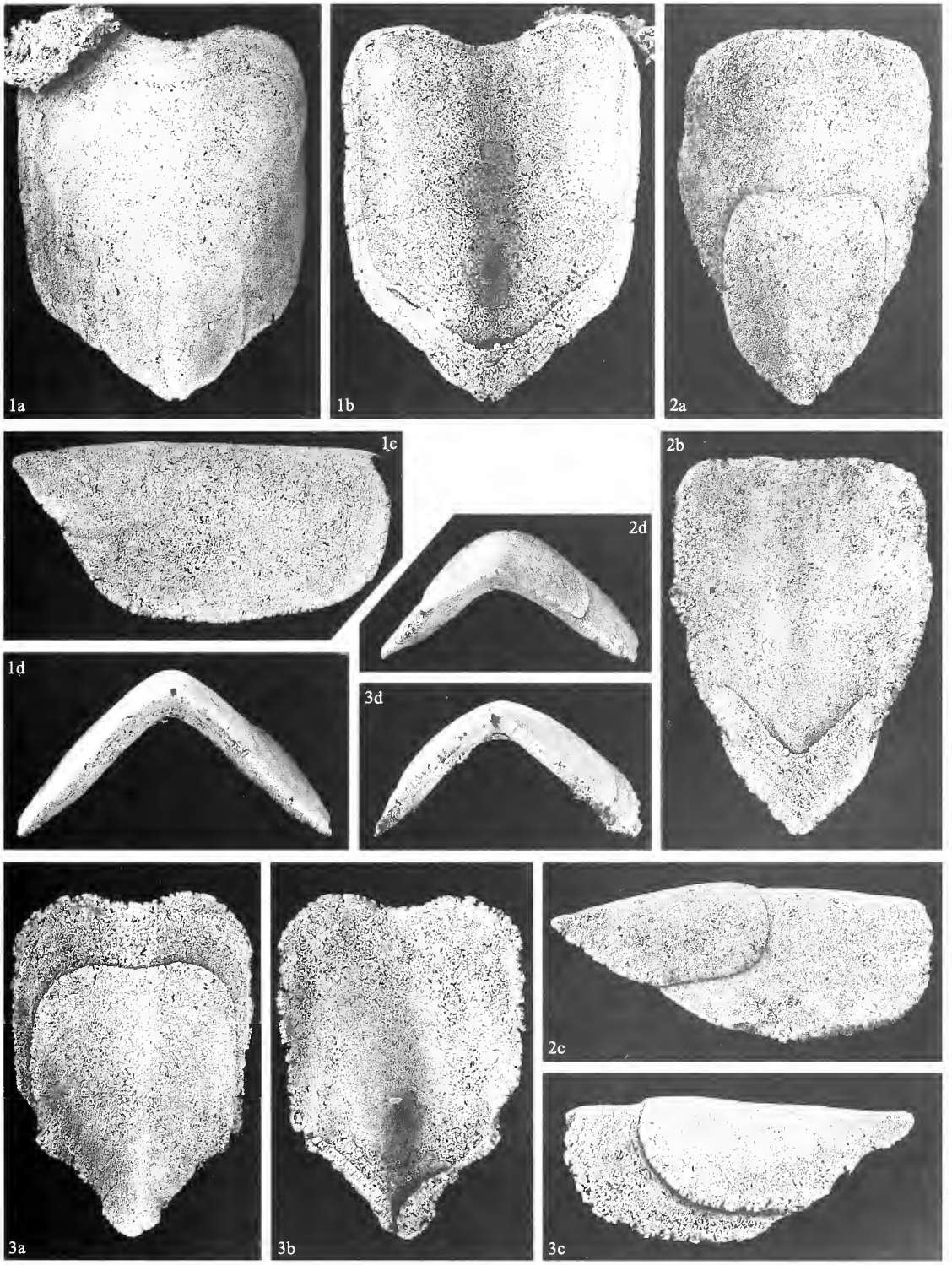

CHERNS, *Thairoplax*

Diagnosis (emended from Bergenhayn 1955, p. 18). Intermediate sclerites with deep side slopes, jugal ridge sharp to more rounded, jugal angle almost perpendicular; anterolateral margins slightly divergent, posterolateral margins longer, maximum width at posterolateral corners, apical angle acute. Ventral apical area tapering rapidly outwards, apical length/length *c.* 0·3.

Description. The holotype is a distorted, arched, ventral external mould, showing flat, deep trapezoidal side slopes diverging almost perpendicularly (87°) across a sharp jugal ridge, and with a broad, V-shaped apical area that tapers rapidly outwards from its central flexure, apical length/length 0·31. Triangulate posterior shell to pointed apex, apical angle 71°, straight posterolateral margins, longer than anterolateral margins, bordered by apical area (Pl. 1, fig. 2). RM Mo6023 (Pl. 1, fig. 3) shows only the dorsal surface, strongly arched (height/length 0·58) across a jugal flexure (86°) sharper posteriorly but becoming more rounded anteriorly, and with weakly defined, broad triangular central shell field expanding from apex to outside anterolateral corners on deep trapezoidal side slopes. Sclerite fairly large (length 13·9 mm), slightly longer than wide (length/width 1·07), not greatly thickened. Anterior margin straight across flexed central area, anterolateral corners sharply rounded into straight to only slightly convex lateral margins, and longer, straight posterolateral margins tapering rapidly to apex; apical angle 73°. Growth lines, or possibly slightly stronger ornament of very shallow ridges and grooves, follow anterior and anterolateral margins, crossing onto the ventral apical area at posterolateral corners behind mid-length; larger growth increments indicated by spaced narrow ridges/grooves (Pl. 1, fig. 3b). Two worn and coarsely replaced chiton specimens on RM 6024, both partially embedded in limestone, come from the same locality as RM Mo6023, from a slightly younger horizon than the holotype. One has the apex broken off, but shows part of the dorsal surface arched strongly across the jugal ridge, as in RM Mo6023, and appears from growth lines to have a transverse anterior margin and straight anterolateral margins (Pl. 1, fig. 4). The other specimen shows the left dorsal surface including the apex, with a long straight posterolateral margin tapering to a pointed apex (Pl. 1, fig. 5). Bergenhayn (1955) noted a granular sculpture preserved on one sclerite, presumably RM Mo6023, where coarse sparite replacement of the shell has produced an apparent surface pattern.

Remarks. Bergenhayn (1955, p. 18) based this species, which he considered very distinct, on the four intermediate sclerites described above from Visby and Kålens kvarn, Visby, from the Upper Llandovery to Lower Wenlock. Specific characters, of two rhomboid shaped sides hinged along the midline at a jugal angle of *c.* 90°, an ornament of very low, evenly spaced growth lines (= larger growth increments), and total coverage across the adjacent plate (indicated by a broad apical area), he noted as combined with an absence of shell fields. Despite the lack of shell fields, he still assigned the species to *Gotlandochiton* on the basis that the shell form and, more questionably, complete coverage did not belong within *Chelodes*.

In comparison with *T. pelta*, the older species *T. birhombivalvis*, based on more limited, non-isolate material, has deeper, shorter side slopes, a more perpendicular flexure, longer posterolateral margins across the triangulate posterior shell, and a longer V-shaped apical area. Intermediate sclerites are broader and less elongate.

EXPLANATION OF PLATE 3

Figs 1–3. *Plectrochiton tegulus* gen. et sp. nov.; Möllbos-1, Gotland; Halla Formation, Upper Wenlock (Homerian). 1, RM Mo160.032, holotype; intermediate sclerite. 1a, dorsal view; 1b, ventral view, note ?weak transverse ridge between anterolateral corners; 1c, left lateral view; 1d, posterior view. All × 5. 2, RM Mo159.942; intermediate sclerite. 2a, dorsal view; 2b, ventral view; 2c, left lateral view; 2d, posterior view. All × 5. 3, RM Mo159.900; intermediate sclerite. 3a, dorsal view; 3b, ventral view; 3c, left lateral view; 3d, posterior view. All × 4.

Fig. 4. *Thairoplax*? aff. *pelta*?, Möllbos-1, Gotland; Halla Formation, Upper Wenlock (Homerian); RM Mo160.020, intermediate sclerite. 4a, dorsal view showing weak narrow jugal fold; 4b, ventral view; note low transverse ridge anterior to apical area, with tapering extension beneath apical area rim; 4c, left lateral view; 4d, posterior view. All × 3.

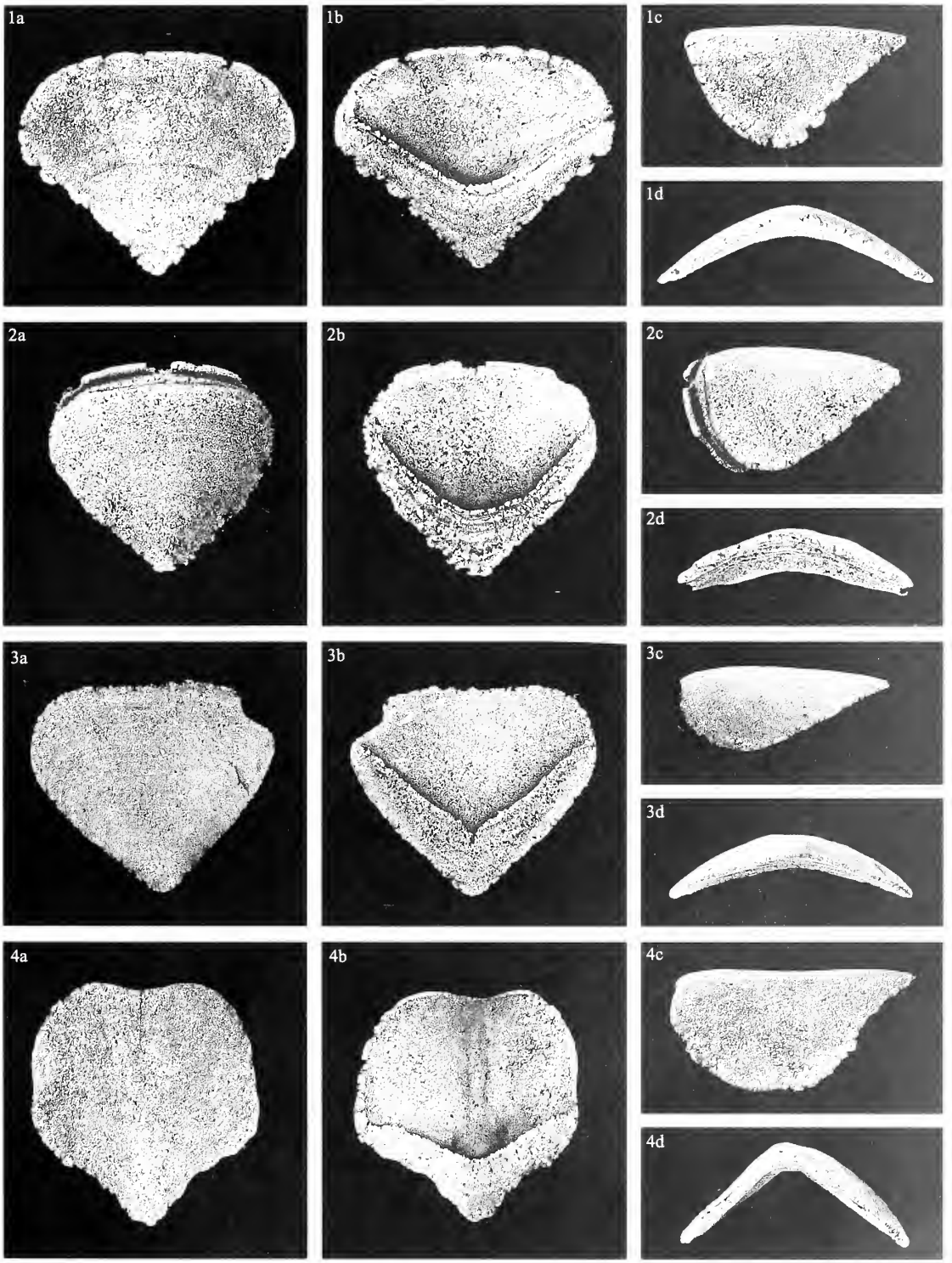

CHERNS, *Plectrochiton*, *Thairoplax*?

Kluessendorf (1987) compared Morphotype A, an incomplete specimen showing the ventral surface, from the Racine Dolomite (Wenlock/Ludlow) of Wisconsin, USA, with *T. birhombivalvis*, on the basis of a flexed form with flat side slopes and parallel lateral margins. The elongate form and apparently short apical area are more similar to *T. pelta*, although there are insufficient diagnostic characters to allow close comparison.

PLECTROCHITON gen. nov.

Derivation of name. From the Greek *plektron*, a tool for plucking a stringed instrument, to describe the triangulate shape of sclerites.

Type species. *P. tegulus* gen. et sp. nov., from the Upper Wenlock, Silurian of Gotland, Sweden.

Diagnosis. Broad and short, small low-arched triangulate sclerites, wider than long; transverse to gently convex anterior margin, rounded anterolateral corners, tapering straight posterolateral margins to broad, pointed posterior apex, apical angle almost perpendicular. Ornament of fine growth lines; no shell fields, jugal angle obtuse, *c*. 125°. Apical area approximately one-third of length, wide, tapering outwards to anterolateral corners, V-shaped to concave anterior margin. Ventral surface smooth, concave, triangulate to lozenge-shaped.

Remarks. The small, broad and only gently arched, triangulate form of intermediate sclerites in *Plectrochiton* gen. nov., without shell fields and with only fine growth line ornament, is distinct from other genera of Palaeozoic chitons (e.g. Smith and Toomey 1964, p. 17). By comparison with other Gotland chitons, *Chelodes* Davidson and King, 1874 has commonly large, elongate, wedge- to heart-shaped intermediate sclerites, in some species with shell fields. *Gotlandochiton* Bergenhayn, 1955 and *Thairoplax* gen. nov. have medium to large, flexed sclerites with straight trapezoidal side slopes. The triangulate form distinguishes *Plectrochiton* gen. nov. from the roughly rectangular sclerites of Ordovician *Paleochiton* Smith, *in* Smith and Toomey, 1964, and *Kindbladochiton* Van Belle, 1975, and from the Ordovician–Cretaceous *Ivoechiton* Bergenhayn, 1955.

Plectrochiton tegulus gen. et sp. nov.

Plate 3, figures 1–3

Derivation of name. From the Latin *tegulus*, a tile, to describe the very low-arched form.

Material, locality and horizon. Eight intermediate sclerites from Möllbos-1, Gotland; Halla Formation, Upper Wenlock (Homerian); holotype RM Mo160.062*, isolated plate, syntypes 159.865–159.866, 159.874, 159.900*, 159.936, 159.942*, 160.009.

Diagnosis. As for the genus.

Description. Small and low-arched, short broad triangulate intermediate sclerites that are wider than long, without shell fields. Mean length 5·9 mm (s.d. = 2·2, $n = 8$; holotype 7·1 mm), mean length/width 0·87 (s.d. = 0·04, $n = 6$; holotype 0·86), mean jugal angle 125° (s.d. 3·8, $n = 8$; holotype 123°). Wide anterior margin straight to gently convex, with rounded anterolateral corners, no anterolateral margins, tapering straight posterolateral margins to broad, pointed posterior apex, mean apical angle 88° (s.d. = 9·1, $n = 8$; holotype 91°). Maximum width across anterolateral corners, well anterior of midlength. Ornament of fine growth lines parallel to anterior margin, transecting posterolateral margins onto ventral apical area. Apical area with mean apical length/length 0·29 (s.d. = 0·08, $n = 6$; holotype 0·35), wide, with a slightly raised anterior margin V-shaped to rounded and concave anteriorly (Pl. 3, figs 1b, 2b, 3b), tapering outwards along posterolateral margins to anterolateral corners. Ventral surface smooth, concave, triangulate to lozenge-shaped, may have slight transverse thickening across between anterolateral corners (Pl. 3, fig. 1b).

Lateral profile triangular, fairly shallow, with flat to slightly convex dorsal surface, gently convex anterior margin (Pl. 3, figs 1c, 2c, 3c). Transverse section shallow, shell thicker medially, tapering laterally (Pl. 3, figs 1d, 2d, 3d).

Remarks. P. tegulus gen. et sp. nov. is distinguished from small sclerites of *C. actinis* Cherns, 1998, which co-occur in samples from Möllbos, by the absence of anterior invagination, lower length to width ratio, and shallower transverse profile with a more obtuse jugal angle. The slightly elevated anterior rim to the apical area may indicate muscle attachment along this margin (Cherns 1998). The fairly small sized, triangulate sclerites could represent head or tail sclerites, although they lack features commonly found in such sclerites of chitons, such as distinct, commonly radiate, ornament of head sclerites, and a prominent mucro in tail sclerites (e.g. Smith 1960; Hyman 1967). For *C. actinis*, ovoid, ornamented plates that co-occur with the intermediate sclerites have been described as head sclerites (Cherns 1998).

ALASTEGA gen. nov.

Derivation of name. From the Latin *ala*, wing, and Greek *stege*, roof, to described the winged form of the sclerites.

Type species. A. lira gen. et sp. nov. from the Upper Wenlock, Silurian of Gotland, Sweden.

Diagnosis. Small arched sclerites, flexed across jugum, with triangulate, pointed posterior apex; slightly elevated and rounded, broad triangulate jugal shell field flattening anteriorly; apical angle nearly perpendicular, jugal angle slightly obtuse; ornament of shallow rounded ridges and furrows, growth lines, stronger on lateral fields. Intermediate sclerites small, wide and short, strongly arched and winged; jugal ridge rounded anteriorly, broad anterior embayment, side slopes deep and straight, triangulate posterior shell to apex. Ventral apical area short V-shaped band tapering across long posterolateral margins. Transverse ventral thickening forming V-shaped ridge, tapering outwards. Tail sclerites as long as wide, lower arched, more triangulate and weakly trilobed, shallower anterior embayment; jugal field elevated and rounded, side slopes shallower; apical area short, V- to U-shaped anterior margin, tapering across long posterolateral margins, ventral surface with transverse V-shaped thickening. Head sclerites small, elongate, ovoid, low arched; distinct rounded triangulate jugal field, posterior pointed apex; ventral surface smooth, concave, apical area not known.

Remarks. Small, short and wide, winged and strongly arched intermediate sclerites with distinct transverse ventral thickening at around mid-length parallel to the short V-shaped apical area are characteristic of *Alastega* gen. nov. *Ivoechiton* (*I. oklahomensis* Smith, *in* Smith and Toomey, 1964; *I. calathicolus* Smith, *in* Smith and Toomey, 1964) and *Kindbladochiton* (*K. arbucklensis* Smith, *in* Smith and Toomey, 1964) from the lower Ordovician of Oklahoma, USA, have intermediate sclerites wider than long, with a transverse thickening across the ventral surface of sclerites, and with a posterior margin swept back from the apex or transverse (Smith and Toomey 1964). *Alastega* gen. nov. differs from *Ivoechiton* in having defined shell fields, and from both in its long straight posterolateral margins tapering across the triangulate posterior shell to a pointed apex, with a corresponding V-shaped ventral apical band.

Alastega lira gen. et sp. nov.

Plate 4; Text-figure 4

Derivation of name. From the Latin *lira*, plough ridge, to describe the dorsal ornament.

Material, locality and horizon. Möllbos-1, Gotland, Halla Formation, Upper Wenlock (Homerian); 21 isolated sclerites (including four tail sclerites); holotype RM Mo159.845*, intermediate sclerite; RM Mo159.827,

159.846–159.847, 159.848*, 159.852, 159.876–159.882, 159.893–159.894, 159.917, 159.949, 159.987; tail sclerites 159.826*, 159.849*, 159.883, 160.010. Klintebys-1, Gotland, Halla Formation, Upper Wenlock (Homerian); 21 isolated sclerites (including two head, three tail sclerites); 160.036–160.037, 160.039, 160.041, 160.043–160.046, 160.048, 160.050–160.053, 160.057, 160.058*, 160.059, head sclerites 160.047, 160.060*, tail sclerites 160.038, 160.040, 160.049.

Diagnosis. As for the genus.

Description. Intermediate sclerites (Pl. 4, figs 1–2; Text-fig. 4D–G) small, strongly arched and winged, flexed across rounded jugum, side slopes straight and deep. Mean length 3·6 mm (s.d. = 2·0, $n = 28$; holotype 2·7 mm), smaller sclerites much wider than long, becoming less so with growth, mean length/width 0·78 (s.d. = 0·18, $n = 20$; holotype 0·66). Jugal ridge flattening anteriorly over slightly elevated and rounded, broad triangulate jugal field, mean jugal angle 96° (s.d. = 8, $n = 32$; holotype 97°). Anterior margin broad, rounding through shallow median embayment across jugal field, mean median length/length 0·88 (s.d. = 0·06, $n = 27$; holotype 0·85). Strongly rounded anterolateral corners into short, slightly convex, divergent anterolateral margins, maximum width at posterolateral corners. Posterolateral margins longer, straight, tapering rapidly across triangulate posterior to pointed broad apex; mean apical angle 88° (s.d. = 12, $n = 26$; holotype 89°). Ornament of shallow rounded ridges and furrows, and growth lines, sinuate parallel to anterior and anterolateral margins, stronger on lateral fields (Pl. 4, fig. 1a, c; Text-fig. 4D, F). Ventral surface with short, V-shaped apical area as slightly raised band across posterolateral margins, tapering outwards to posterolateral corners, mean apical length/length 0·17 (s.d. = 0·06, $n = 15$; holotype 0·19). Ventral surface smooth, with transverse thickened triangular ridge around midlength, V-shaped, thickest medially, tapering towards and flattening anteriorly and posteriorly (Pl. 4, fig. 1b, e, 2a–b; Text-fig. 4E), becoming relatively more posterior with increased size of sclerite. Lateral profile (Pl. 4, fig. 1c, Text-fig. 4F) gently convex dorsally, weak radial fold elevating low jugal area, deep side slopes to posterolateral corners, steep straight posterolateral margins, sinuate shallowing anterolateral to anterior margins. Transverse profile strongly arched across jugal flexure rounding anteriorly, side slopes straight, tapering outwards (Pl. 4, figs 1d–e, 2b; Text-fig. 4G), mean height/length 0·67 (s.d. = 0·18, $n = 28$; holotype 0·78). Thickened ventral ridge producing longitudinal flexure of ventral surface into two inclined planes, particularly evident in smaller specimens; inclined posterior profile with V-shaped ventral surface, angular ventral flexure (Pl. 4, fig. 2b), inclined anterior profile with lunate ventral surface (Pl. 4, fig. 1e).

Tail sclerites (Pl. 4, fig. 3; Text-fig. 4A–C) roughly as long as wide, mean length 3·6 mm (s.d 1·2, $n = 5$), mean length/width 1·04 (s.d. = 0·27, $n = 3$), lower arched, more triangulate and weakly trilobed. Elevated, rounded and broad triangulate jugal field, narrower, less convex lateral fields, mean jugal angle 101° (s.d. = 9, $n = 5$). Anterior margin more shallowly embayed across jugal field, mean length/length 0·93 (s.d. = 0·06, $n = 4$), strongly rounded anterolateral corners into very short anterolateral margins, long straight posterolateral margins tapering across triangulate posterior to pointed posterior apex, mean apical angle 88° (s.d. = 27, $n = 5$). Ornament of growth lines, low ridges/furrows poorly preserved. Ventral short apical area with V- to U-shaped elevated margin, tapering outwards across posterolateral margins (Pl. 4, fig. 3b; Text-fig. 4B), mean apical length/length 0·21 (s.d. = 0·04, $n = 3$). Ventral surface smooth, flexed across broad transverse triangulate thickened ridge, greatest medially, V-shaped, around midlength. Longitudinal profile showing shallower side slopes, radial fold elevating jugal field, less steep posterolateral margins (Pl. 4, fig. 3c; Text-fig. 4C). Anterior transverse profile lower arched, side slopes straight, mean height/length 0·42 (s.d. = 0·05, $n = 5$); inclined anterior ventral surface lunate, inclined posterior ventral surface with more angular flexure.

EXPLANATION OF PLATE 4

Figs 1–3. *Alastega lira* gen. et sp. nov.; Möllbos-1, Gotland; Halla Formation, Upper Wenlock (Homerian). 1, RM Mo159.845, holotype; intermediate sclerite. 1a, dorsal view; note rounded ridge-and-furrow ornament; 1b, ventral view, showing V-shaped transverse ridge; 1c, right lateral view; 1d, posterior view; 1e, anterior, slightly tilted view to show lunate anterior surface of transverse ridge. 2, RM Mo159.848; intermediate sclerite. 2a, ventral view, showing V-shaped transverse ridge further anterior than in 1b; 2b, posterior, slightly tilted view to show V-shaped posterior surface of transverse ridge. 3, RM Mo159.849; tail sclerite. 3a, dorsal view, note elevated fold of central shell field; 3b, ventral view, V-shaped transverse ridge well in front of apical area; 3c, right lateral view; 3d, anterior view. All ×15.

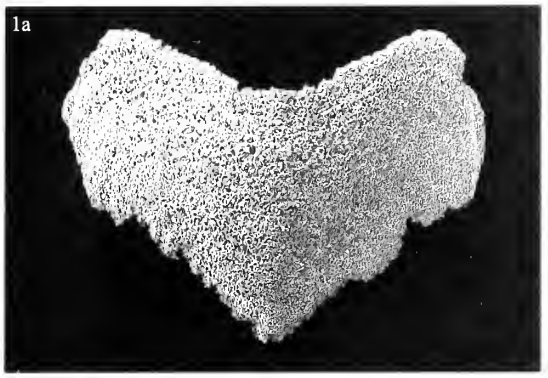

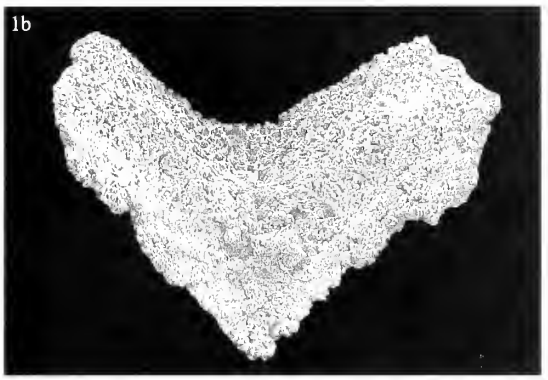

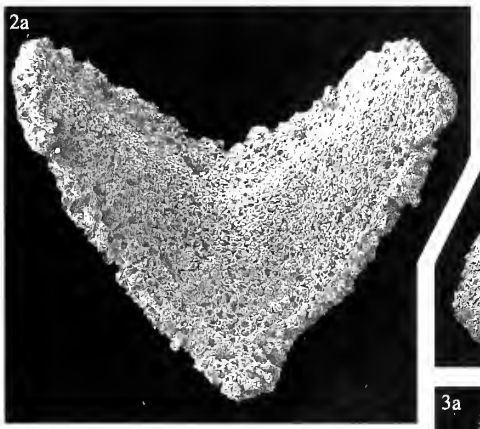

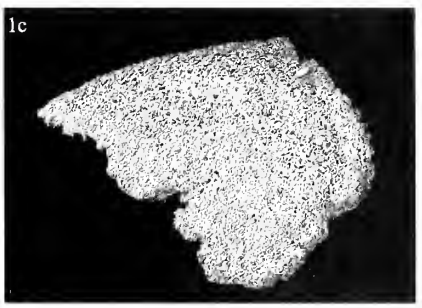

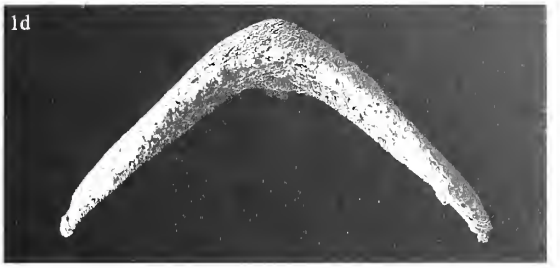

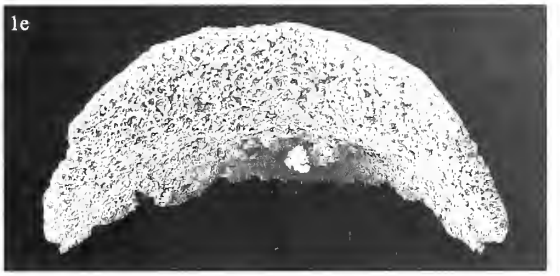

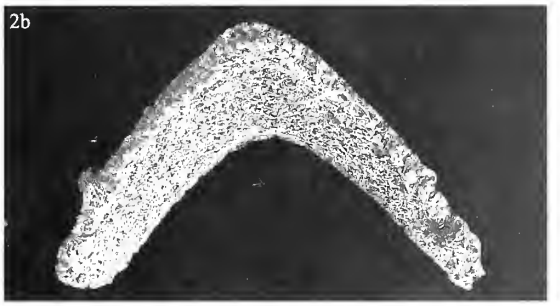

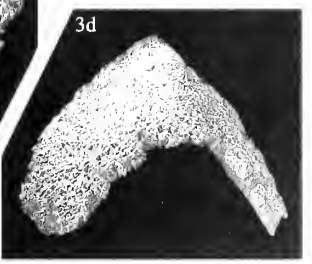

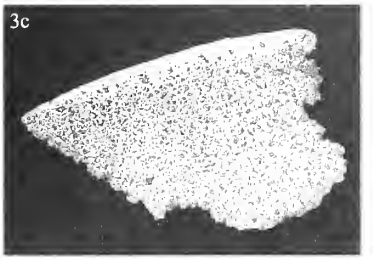

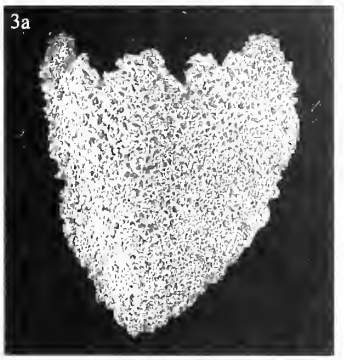

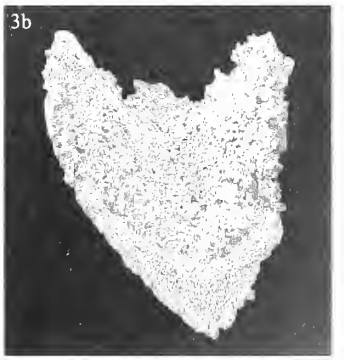

CHERNS, *Alastega*

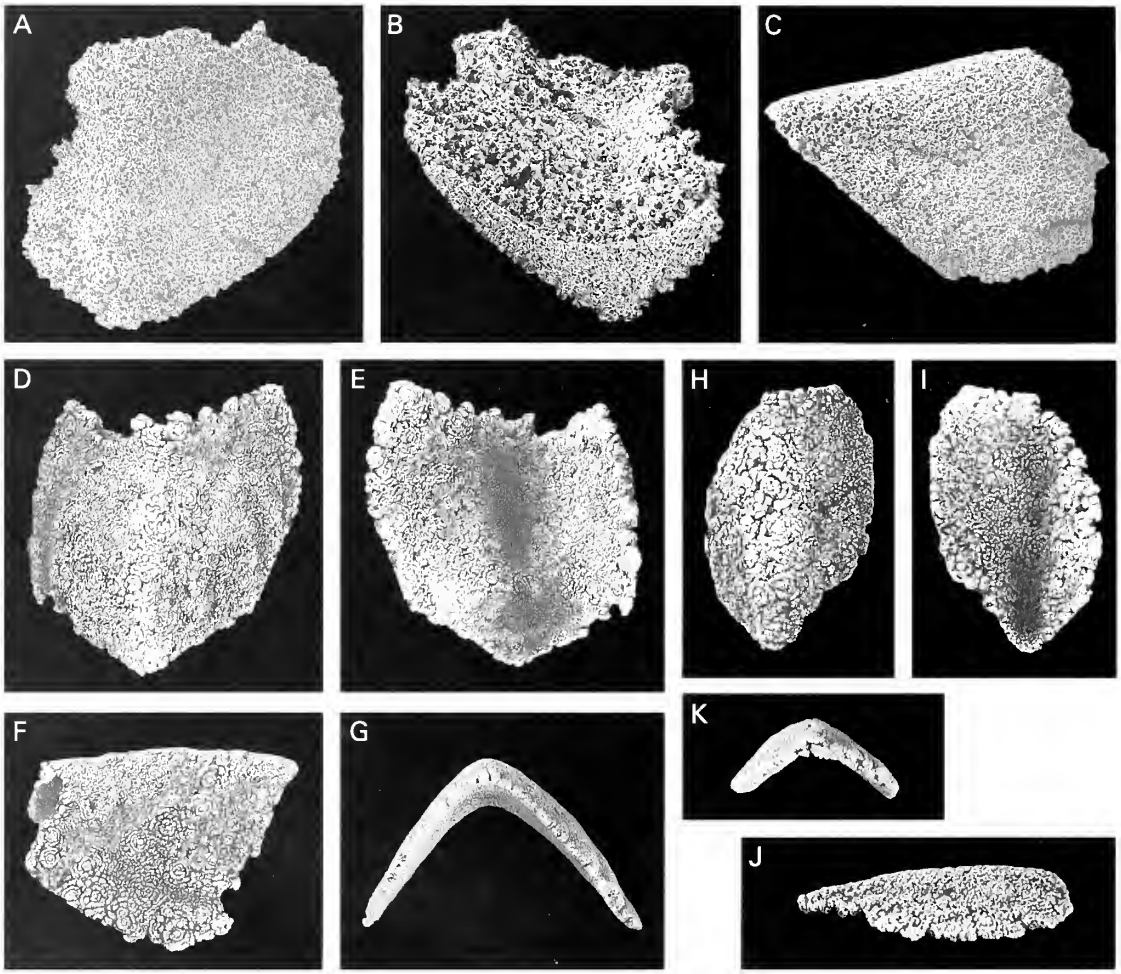

TEXT-FIG. 4. *Alastega lira* gen. et sp. nov. A–C, RM Mo159.826; Möllbos-1, Gotland; Halla Formation, Upper Wenlock (Homerian); tail sclerite, fragmented on left side. A, dorsal view, showing elevated fold of central shell field. B, ventral view, transverse ridge well in front of apical area. C, right lateral view, showing elevated central shell field. All ×20. D–G, RM Mo160.058; Klintebys-1, Gotland; Halla Formation, Upper Wenlock (Homerian); beekitized intermediate sclerite. D, dorsal view; note elevated shell central field, rounded ridge-and-furrow ornament. E, ventral view; note V-shaped transverse ridge. F, left lateral view, showing well developed ornament. G, posterior view. All ×5. H–K, RM Mo160.060; Klintebys-1, Gotland; Halla Formation, Upper Wenlock (Homerian); head sclerite. H, dorsal view, showing elevated central field, rounded ridged ornament on lateral fields. I, ventral view. J, lateral view, showing elevated fold of central field. K, posterior view. All ×7.

Head sclerites (Text-fig. 4H–K) known only from two specimens, both beekitized, one poorly preserved. Small, ovoid, low arched, elongate, with distinct rounded, triangulate jugal field; mean length 4·6 mm (s.d. = 0·57, $n = 2$), mean length/width 1·33 (s.d. = 0·40, $n = 2$), mean jugal angle 95° (s.d. = 1, $n = 2$). Anterior margin transverse to gently convex across jugal field, rounding into long, convex anterolateral margins, short straight posterolateral margins tapering rapidly across triangulate posterior to pointed apex; apical angle *c.* 88°. Ornament of low rounded ridges and furrows, growth lines, particularly developed on lateral fields. Ventral surface smooth, concave, deepest towards posterior, apical area unknown but probably very short. Lateral profile shallow, low fold elevating jugal field. Posterior profile low arched, mean height/length 0·29 (s.d. = 0·07, $n = 2$), short straight side slopes.

Remarks. The thickened transverse ventral ridge characteristic of this genus associates the short, wide, high arched intermediate sclerites with relatively longer, more triangulate, lower arched tail sclerites. In particular, the lunate shape of the anterior ventral surface of the thickening is distinctive. In addition, in both these types of sclerite and in the elongate, ovoid and shallow arched head sclerites the dorsal surface has a triangulate, slightly elevated and rounded jugal field, and distinctive ornament of shallow rounded ridges and furrows, preserved better on the flatter lateral fields. All have almost perpendicular apical angles and slightly obtuse jugal angles. The ovoid elongate shape and shallow form of the head sclerites show similarities to those described recently for the large chiton *C. actinis* (Cherns 1998, text-fig. 4), although the *A. lira* sclerites are much smaller, with coarser ridged ornament, and a more distinct and rounded jugal field.

The material of *A. lira* comes from Möllbos-1 and Klintebys-1, both from the Late Wenlock Halla Formation. All specimens from Möllbos-1 are small but include some that are well preserved. Many of those from Klintebys-1 are poorly preserved and beekitized, but they include also larger examples, of both intermediate and tail sclerites. The size difference is notable, with several 7–9 mm long, compared with the means (including these) of 3·6 mm, and unfortunately the sclerites preserve poor detail. However, they do share the general form and characteristic ventral ridge in both intermediate and tail plates, and co-occur in samples with the more typical, small specimens; hence they are treated here as the same species.

In intermediate sclerites, the ventral thickening becomes relatively more posterior as the shell lengthens, and its anterior lunate surface develops shallow sculpting to enhance lateral pads (Text-fig. 4E, cf. Pl. 4, fig. 1b). The ventral thickening in longer (i.e. larger) intermediate sclerites produces a natural balance, and presumed life position, with gentle anterior tilt of the jugal field, leaving the ventral anterior surface horizontal and the posterior surface behind the ridge elevated slightly.

The intermediate sclerites show variation in the breadth of anterior embayment and degree of divergence of anterolateral margins. These features may relate to different positions of plates along the animal, in particular to narrowing of the broad intermediate sclerites anteriorly towards the elongate head sclerite.

HELOPLAX gen. nov.

Derivation of name. From the Greek *helos*, nail, stud, and *plax*, plate, to describe the rounded form of sclerites.

Type species. H. papilla gen. et sp. nov. from the Upper Wenlock (Silurian) of Gotland, Sweden.

Diagnosis. Small, transversely elongate, ovoid intermediate sclerites with subcentral elevated mucronate apex, rounded margins. Fairly broad, vaulted triangulate anterior field; broader triangulate posterior field, concave becoming flattened to convex posteriorly, elevated; depressed lateral fields across transverse flexure. Maximum shell width slightly posterior of mid-length, at posterolateral corners. Dorsal concentric growth lines; distinct granular ornament, coarser anteriorly and laterally, also coarsening outwards; quincunx pattern but with line of larger granules demarcating posterior field. Ventral surface with small deep median subapical cavity, oblique towards anterior. Ventral thickening leading to strongly sculpted surface around subapical area. ?Tail sclerites smaller, relatively broad, vaulted convex anterior and posterior fields, coarser line of ornament within lateral fields.

Remarks. Heloplax gen. nov. differs from all other paleoloricate chitons, except *Enetoplax* gen. nov. and *Arctoplax* gen. nov. described below, in having small ovoid intermediate plates with a dorsal mucronate apex, and concentric holoperipheral growth (Text-fig. 2). They thereby lack the ventral apical area of sclerites with a posterior apex, representing extension of the dorsal outer tegmentum onto the ventral surface, found in at least most paleoloricate chitons, and in neoloricate chitons except for tail sclerites (e.g. *Pterochiton spatulatus*, *Pedanochiton discomptus*; Smith and Toomey 1964; Debrock *et al.* 1984; Hoare 1989). In *Heloplax*, the sclerites are vaulted and convex anteriorly, and in most the concave post-apical posterior field becomes elevated. This shell morphology

suggests that these are intermediate sclerites, which can become imbricated, and not tail plates. Variations in morphology suggest that both intermediate and tail plates are represented, the latter being vaulted and convex both anteriorly and posteriorly.

From the Lower Carboniferous (Mississippian) of Utah, Hoare (1989) described as a tail plate a single small sclerite of generally similar configuration to *Heloplax*, but with sutural laminae and hence a neoloricate chiton.

Heloplax papilla gen. et sp. nov.

Plates 5–6

Derivation of name. From the Greek *papilla*, bud, nipple, to describe the granular ornament.

Material, locality and horizon. Möllbos-1, Gotland, Halla Formation, Upper Wenlock (Homerian); 25 isolated sclerites; holotype RM Mo159.832*, intermediate sclerite; intermediate sclerites RM Mo159.828*, 159.829*, 159.830–159.831, 159.833, 159.867*, 159.884, 159.891–159.892, 159.896, 159.898, 159.912, 159.920, 159.954, 159.968, 159.997, 160.011, 160.017; ?tail sclerites RM Mo159.834, 159.851*, 159.886–159.887, 159.889, 159.984.

Diagnosis. As for the genus.

Description. (Text-fig. 2). Small broad intermediate sclerites, transversely ovoid, with rounded margins; mean length 3·6 mm (s.d. = 0·3, $n = 16$; holotype 3·7 mm), mean length/width 0·70 (s.d. = 0·05, $n = 16$; holotype 0·67). Prominent sub-central pointed dorsal apex is elevated and mucronate; mean 0·48 (s.d. = 0·06, $n = 17$; holotype 0·46) of length from anterior. Maximum width only slightly posterior of apex at posterolateral corners, mean 0·54 (s.d. = 0·04, $n = 16$; holotype 0·57) of length from anterior. Concentric growth lines about apex, some more distinct growth increments forming low ridges towards outer part of dorsal surface (e.g. Pl. 6, fig. 1a, d). Dorsal surface with vaulted, triangulate, transversely convex anterior and posterior fields, depressed, concave to flattened lateral fields. Anterior field fairly broad, arched, smoothly rounded and convex, elevating to apex, posterior field broader, concave behind apex, flattening and becoming convex to margins. Lateral fields rounding and becoming concave between anterior and posterior fields, most depressed close to apex, flattening outwards. Longitudinal profile strongly convex anteriorly to prominent apex, concave to flattened or becoming convex posteriorly, elevated (Pl. 5, figs 1c, 2c; Pl. 6, figs 1c, 2c). In transverse profile, gently convex, arched, deeper laterally. Granular dorsal ornament, coarser in anterior and lateral fields, and coarsening outwards, generally slightly finer granulation across posterior field. Quincunx arrangement of granules, but with band of coarser granules from apex to posterolateral corners demarcating posterior field (e.g. Pl. 5, figs 1a, b, e, 2a–b). Anterior and lateral fields not differentiated by ornament. Ornament becoming less well defined in thickened sclerites (e.g. Pl. 6, fig. 1a, c).

Ventral surface smooth, with gentle convex transverse flexure corresponding to lateral depressed fields of the dorsal surface. Small deep median cavity beneath apex, slanted obliquely towards anterior, circular to ovoid,

---

EXPLANATION OF PLATE 5

Figs 1–2. *Heloplax papilla* gen. et sp. nov.; Möllbos-1, Gotland; Halla Formation, Upper Wenlock (Homerian); intermediate sclerites. 1, RM Mo159.832, holotype. 1a, dorsal view; note sub-central mucronate apex, line of coarser granules across depressed lateral shell fields; × 15. 1b, ventral view, showing subapical cavity, flanking lateral depressions; × 15. 1c, oblique ventral view, showing transverse flexure of sclerite across lateral fields, behind subapical cavity, obliquely directed lateral depressions, deep subapical cavity slanting anteriorly; × 15. 1d, left lateral view; note line of coarser granules, elevation of posterior shell field behind mucronate apex; × 15. 1e, detail of lateral ornament, showing line of coarser granules; × 25. 2, RM Mo159.867. 2a, dorsal view; note holoperipheral quincunx granular ornament coarsening outwards; × 15. 2b, ventral view; note deep subapical cavity, flanking oblique lateral furrows, transverse flexure of sclerite; × 15. 2c, right lateral view; note line of coarser granules across lateral field, strongly elevated posterior field; × 14. 2d, detail of granular ornament from anterior edge, with new growth increment inserted from below; × 50.

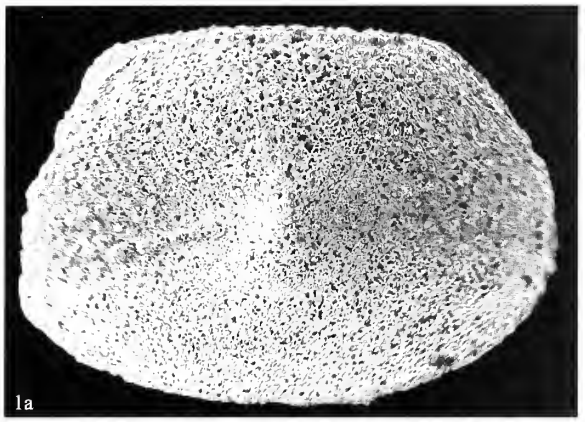

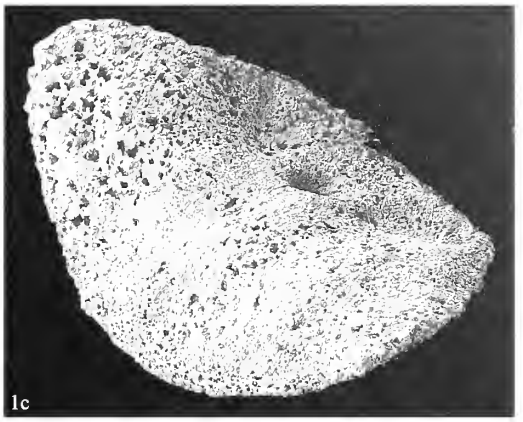

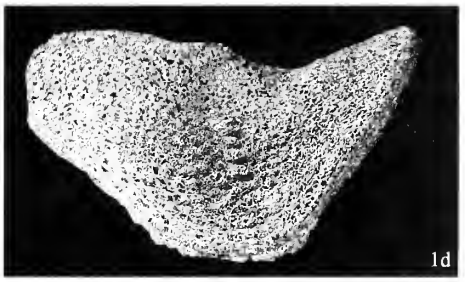

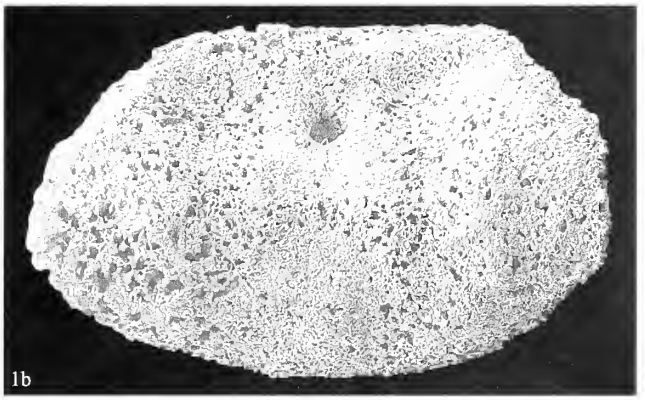

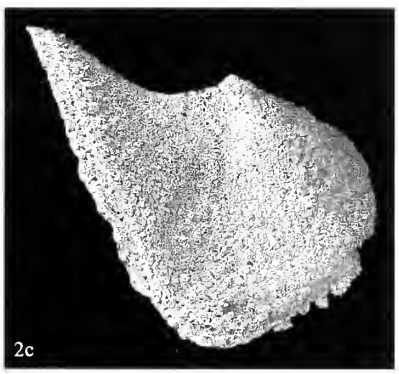

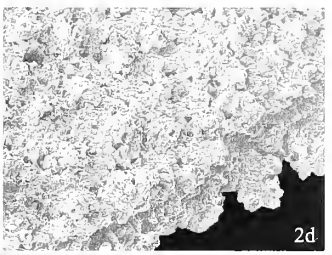

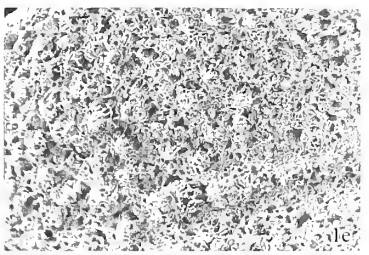

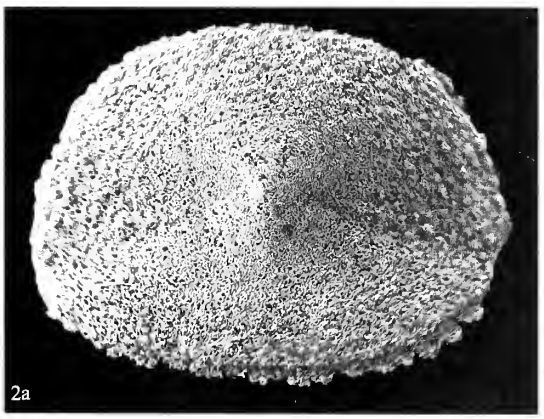

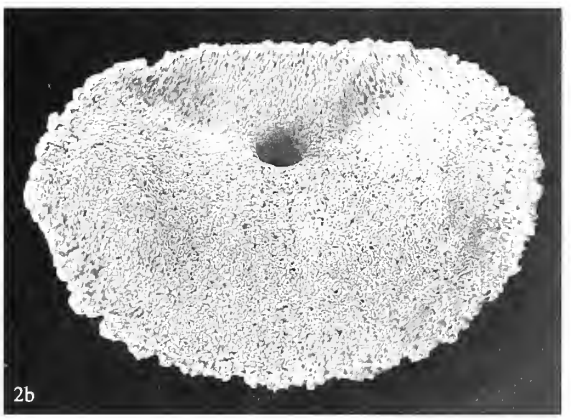

CHERNS, *Heloplax*

with smooth margins; mean 0·32 (s.d. = 0·05, $n = 17$; holotype 0·30) of length from anterior. Ventral thickening leading to surface sculpting around sub-apical cavity, and development of an additional, flanking lateral pair of more anterolaterally directed, smaller shallower cavities beneath apical region; subapical cavity bordered anteriorly by thickened pad, posteriorly by shallow longitudinal furrow flattening outwards, lateral cavities in shallow anterolateral furrows (Pl. 6, fig. 1b, d; also less thickened sclerites in Pl. 5, figs 1b–c, 2b). Anterior surface and flexed region becoming strongly sculpted and thickened, posterior surface with shallow tapering median furrow, shallower outer rim to sclerite.

?Tail sclerites (Pl. 6, fig. 3) smaller and relatively broader than intermediate, mean length 2·3 mm (s.d. = 0·14, $n = 6$), mean length/width 0·55 (s.d. = 0·03, $n = 5$). Ovoid, smoothly rounded with elevated sub-central mucronate apex more anterior of maximum width; apex mean 0·40 (s.d. = 0·08, $n = 6$) of length from anterior, maximum width mean 0·54 (s.d. = 0·04, $n = 6$) of length from anterior. Vaulted convex anterior and posterior fields, without posterior elevation, lateral fields narrow, depressed (Pl. 6, fig. 3c). Transverse profile low arched, broad, deeper laterally. Granular ornament, coarsening outwards, with line of coarser granules from apex across lateral fields (Pl. 6, fig. 3a). Ventral surface with deep, slanting median cavity anterior of transverse flexure beneath apex, mean 0·33 (s.d. = 0·04, $n = 6$) of length from anterior. Ventral surface otherwise smooth, becoming thickened and sculpted particularly in subapical ad flexed region to give shallow median longitudinal furrow and anterolateral furrows flanking subapical cavity.

Remarks. By comparison with intermediate sclerites, the ovoid, rounded ?tail sclerites are smaller, relatively broad, and have a gently convex longitudinal profile, both anterior and posterior fields being vaulted. The mucronate apex is a little more anterior, ventrally the subapical pit is similarly situated. Both have outward coarsening granular ornament, but in the ?tail sclerites the characteristic line of larger granules lies within the lateral fields rather than at their posterior limit. The ?tail sclerites are distinct mainly on size, shape, and the longitudinal profile lacking post-apical concavity to posterior elevation. On the material available, and because of the line of larger granules among the lateral ornamentation of both types of sclerite, and fairly similar form overall, the smaller sclerites are proposed as possible tail plates for this species. They might otherwise represent anterior intermediate plates, but are less likely to represent head plates because those typically differ more in morphology from the other plates in chitons.

No head sclerites are identified for *H. papilla*. Two small end sclerites from Möllbos, described below (pp. 966, 968), may include the appropriate head sclerite for this species.

ENETOPLAX gen. nov.

Derivation of name. From the Greek *enete*, brooch, and Latin *plax*, plate, to describe the form.

Type species. E. decora gen. et sp. nov. from the Upper Wenlock (Silurian) of Gotland, Sweden.

Diagnosis. Small, transversely elongate, ovoid to sub-triangular intermediate sclerites with elevated mucronate apex displaced anteriorly from centre; rounded margins. Strongly vaulted short and fairly narrow triangulate anterior field to pointed apex, elevated by low folds; depressed shallow lateral fields flattening outwards across weak transverse flexure, rounding into broad long triangulate posterior field, concave becoming flattened to convex outwards. Broadening behind apex to maximum width just posterior of mid-length. Dorsal concentric growth lines; granular ornament, coarsening outwards, coarser on anterior area, finer to coarse on lateral to posterior areas. Ventral surface with small deep median subapical cavity near anterior margin, slanted anteriorly. Ventral thickening leading to only weak sculpting of surface. ?Head sclerite round, with elevated mucronate apex close to anterior, vaulted short anterior field, gently convex and long posterolateral field, granular ornament; ventral surface concave, shallow subapical cavity.

Remarks. Enetoplax gen. nov. is similar to *Heloplax* gen. nov. (above) in having small ovoid intermediate sclerites with a dorsal mucronate apex and holoperipheral growth. It differs in that sclerites are less vaulted and flexed, have the apex more anterior, and a correspondingly shorter and narrower anterior field, a longer, shallower and broader posterior field, and maximum width further

displaced posteriorly behind the apex (Text-fig. 3). Ventrally the subapical cavity is more anterior, and transverse flexure is weak. Ventral thickening leads to limited surface sculpting around the subapical area, by contrast to the strong development of this surface in *Heloplax*. Granular ornament in both genera coarsens outwards, and is more developed on the anterior field which in *Enetoplax* is delimited by low radial folds. *Heloplax* has a distinct line of coarser granules radiating from the apex across the lateral fields.

Both *Enetoplax* and *Heloplax* sclerites occur in samples from Möllbos-1, both together and separately. Although the intermediate sclerites are broadly similar, and different from all other chitons described, they are easily distinguished morphologically, and are separated here at generic level.

Enetoplax decora gen. et sp. nov.

Plates 7–8

Derivation of name. From the Latin *decoris*, adorned, to describe the ornamented plates.

Material, locality and horizon. Möllbos-1, Gotland, Halla Formation, Upper Wenlock (Homerian); 40 isolated sclerites; holotype RM Mo159.999*, intermediate sclerite; intermediate sclerites RM Mo159.835* (?tail), 159.836*, 159.837–159.839, 159.840 (?tail), 159.841–159.84, 159.850, 159.868, 159.885, 159.888, 159.890, 159.897, 159.913–159.916, 159.921, 159.923, 159.924 (?tail), 159.955–159.956, 159.960, 159.969, 159.974, 159.983, 160.000*, 160.001, 160.016, 160.025, 160.028–160.029, 160.033–160.035; ?head sclerite RM Mo159.998*.

Diagnosis. As for the genus.

Description. (Text-fig. 3). Small, transversely elongate, intermediate sclerites with rounded, convex margins; mean length 3·3 mm (s.d. = 0·5, $n = 38$; holotype 3·3 mm), length/width 0·68 (s.d. = 0·07, $n = 33$; holotype 0·49). Elevated mucronate apex anterior of centre, mean 0·33 (s.d. = 0·06, $n = 38$; holotype 0·36) of length from anterior; ovoid to sub-triangular, broadening behind apex to maximum width slightly posterior of midlength within lateral areas, mean 0·54 (s.d. = 0·06, $n = 38$; holotype 0·60) of length from anterior. Strongly vaulted, short triangulate anterior field to elevated pointed apex; transversely convex, fairly narrow, elevated by low radial folds above lateral fields, low median radial fold or smoothly rounded, convex (e.g. Pl. 7, fig. 1a, c–d; Pl. 8, fig. 1a, c). Weakly defined triangulate posterior field, long and expanding from apex, shallow becoming slightly elevated; gently convex to flattened transversely, broadening outwards, broader than anterior field. Lateral fields gently concave, depressed, flattening outwards, rounding into posterior field, more clearly bounded against low folds of elevated anterior field. In longitudinal profile, convex short anterior field to apex, concave becoming flattened to slightly convex along long posterior field (Pl. 7, figs 1c, 2c; Pl. 8, figs 1c, 2d, 3c). Transverse profile shallow, broad, deeper laterally (Pl. 7, fig. 1d). Growth lines, concentric about apex, more distinct on outer part of dorsal surface, increments forming low ridges (e.g. Pl. 7, fig. 1a, c–d). Granular ornament coarsening outwards, quincunx pattern, coarser and more prominent across vaulted anterior area (e.g. Pl. 8, fig. 1), finer to coarse laterally and posteriorly (e.g. Pl. 7, figs 1a, 2c).

Ventral surface smooth, with small, deep, round to ovoid median cavity with smooth margins near anterior margin, slanting towards anterior from beneath apex (e.g. Pl. 7, fig. 2e); mean 0·22 (s.d. = 0·05, $n = 38$) of length from anterior. Ventral thickening leading to distinct shallow rim outside thickened surface (e.g. Pl. 7, fig. 2b, e), a pair of very shallow longitudinal furrows flanking median pad behind cavity, lateral pads (e.g. Pl. 7, fig. 1b), but relatively little sculpting of surface. Gently convex transverse flexure behind cavity, but low curvature across ventral surface.

?Tail sclerites not clearly distinct, and hence not separated from the remainder of sclerites for biometrics, but possibly represented by three relatively flatter specimens with apex and, particularly, ventral cavity somewhat more anterior (e.g. Pl. 8, fig. 2). Ovoid to sub-triangular, rounded, with elevated mucronate apex towards anterior, mean 0·27 (s.d. = 0·03, $n = 3$) of length from anterior; maximum width near mid-length, mean 0·51 (s.d. = 0·13, $n = 3$) of length from anterior. Very short, narrow, convex anterior field, elevated by low folds from lateral fields, low median radial fold; much longer, broader, concave to flattened posterior field, with slightly lobed or convex posterior margin (Pl. 8, fig. 2a, c). Lateral fields shallowly depressed, concave to flattened. Ventral surface with anteriorly slanting, round to ovoid deep subapical pit close to anterior margin,

mean 0·18 (s.d. = 0·03, $n = 3$) of length from anterior (Pl. 8, fig. 2b, d). Becoming thickened, distinct shallower outer rim, otherwise smooth. Dorsal coarse granular anterior ornament, concentric growth lines.

?Head sclerite (Pl. 8, fig. 3) fairly poorly preserved, limiting biometric measurements. Small, round, with elevated mucronate apex close to anterior. Very short, convex anterior field to apex; long, gently convex posterolateral fields. Dorsal concentric growth lines, granular ornament (poorly preserved). Ventral surface smooth, concave, shallow subapical cavity.

Remarks. Tail sclerites are only tentatively proposed for *Enetoplax*, differing from intermediate sclerites in being lower arched, with the apex, and particularly the subapical cavity, closer to the anterior margin, and the longer posterior field shallower and flatter. By comparison, possible *Heloplax* tail sclerites are notably smaller than intermediate sclerites, relatively broad and have convex, vaulted anterior and posterior fields and thus a convex longitudinal profile. The round head sclerite is associated with *Enetoplax*, rather than *Heloplax*, because of the apex near to the anterior, and long posterolateral field.

ARCTOPLAX gen. nov.

Derivation of name. From the Latin *arcto*, compress, and Greek *plax*, plate, to describe the pinched form of the sclerites.

Type species. *A. ornata* gen. et sp. nov. from the Upper Wenlock (Silurian) of Gotland, Sweden.

Diagnosis. Small, high arched, elongate spatulate intermediate sclerites with strong constriction to sub-central mucronate apex, triangulate shell fields defined by low radial folds and furrows. Anterior and posterior shell fields vaulted, convex, lateral fields depressed; lateral and posterior fields with triangulate, angled faces; anterior field with weaker triangulate facies, rounded medially. Jugal area flat posteriorly, rounded and downward sloping anteriorly; side slopes deep, steep, tapering anteriorly, height greatest posteriorly; maximum width at anterolateral corners, but tapering little along lateral margins; anterior margin transverse to convex, rounding anterolaterally, posterior margin transverse. Ventral surface smooth; deeply concave transversely, narrowing through apical constriction, small deep narrow subapical cavity. Anterior profile rounded, low arched, posterior profile deeper, high arched, with angular corners between faces. Fine granular dorsal ornament, concentric growth lines.

Remarks. The vaulted spatulate form with sub-central mucronate apex is comparable in its holoperipheral growth, and hence lack of a ventral apical area, to *Heloplax* gen. nov. and *Enetoplax*

EXPLANATION OF PLATE 6

Figs 1–3. *Heloplax papilla* gen. et sp. nov.; Möllbos-1, Gotland; Halla Formation, Upper Wenlock (Homerian). 1, RM Mo159.828; well thickened intermediate sclerite. 1a, dorsal view, note line of coarser granules, concentric growth lines; 1b, ventral view, showing sculpted thickened ventral surface: deep, anteriorly slanting subapical cavity with anterior and posterior thickened pads, flanking smaller lateral cavities at base of anteriorly directed, expanding oblique depressions, transverse flexure of sclerite, median longitudinal furrow across posterior field. 1c, oblique ventral view showing posterior, tapering extension of furrows across lateral cavities, tapering bifurcation of pad behind anteriorly slanting subapical cavity. 1d, right lateral view, showing posterior elevation behind mucronate apex, line of coarser granules across lateral field, holoperipheral granular ornament. 2, RM Mo159.829; intermediate sclerite. 2a, dorsal view; note outward coarsening granular ornament, growth lines; 2b, ventral view, showing deep subapical cavity; 2c, left lateral view. 3, RM Mo159.851; ?tail sclerite. 3a, dorsal view; note line of coarser granules across depressed lateral fields, mucronate sub-central apex; 3b, ventral view, showing transverse flexure behind slanting subapical cavity, median longitudinal furrows across posterior field, flanked by thickened pads; 3c, left lateral view; note lack of elevation of posterior field, holoperipheral growth lines. All × 15.

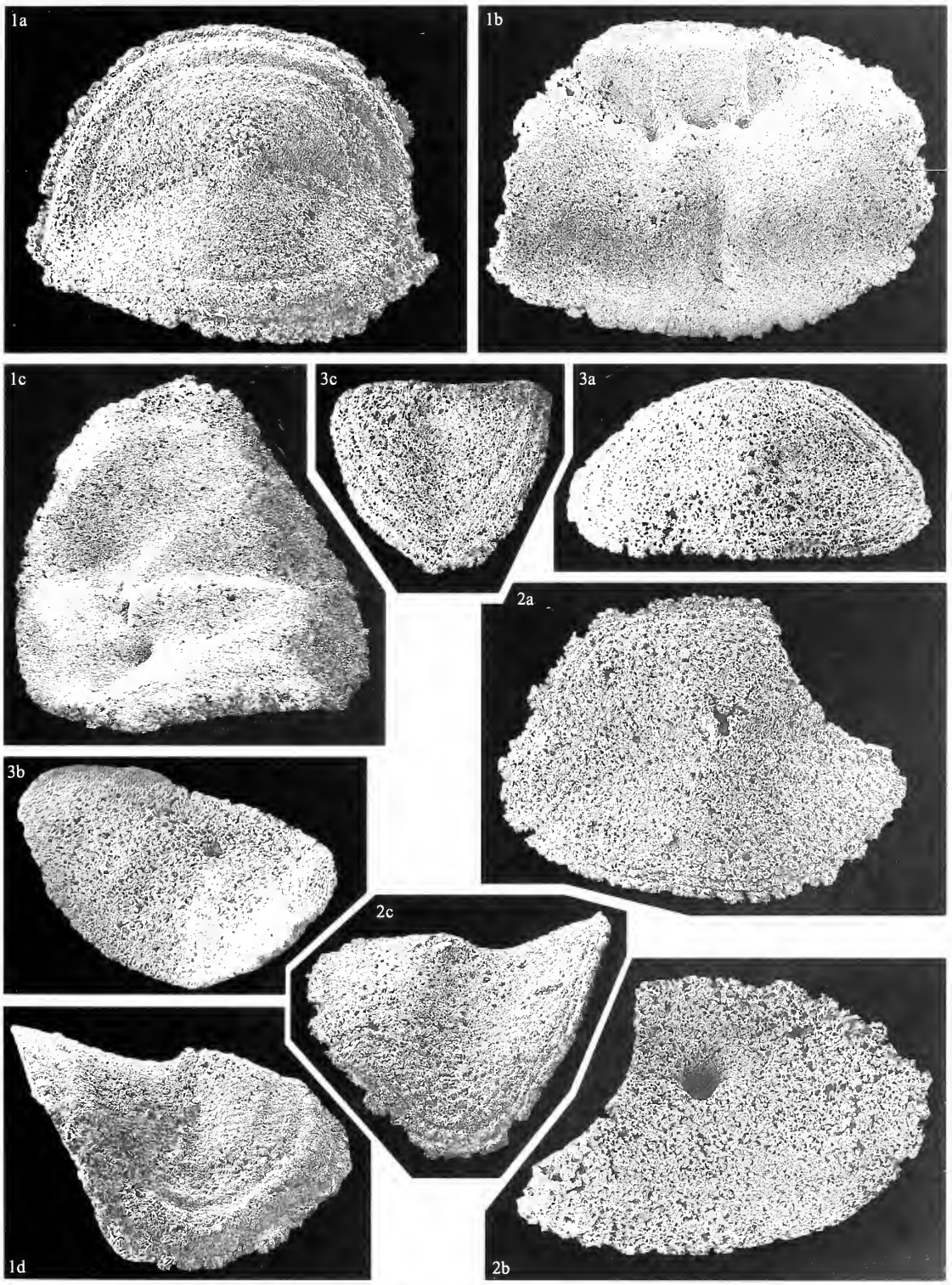

CHERNS, *Heloplax*

gen. nov., and different from other chitons except for some tail sclerites. At Möllbos-1, the sclerites occur not only singly but as several within samples, including some plates of variable size with similar patterns of larger growth increments which probably belonged to the same individual. This would support an interpretation as intermediate plates, and not tail plates of another chiton. Although the ventral subapical cavity in *Arctoplax* compares with similar features in the small ovoid intermediate sclerites of *Heloplax* and *Enetoplax*, the form of *Arctoplax* sclerites is clearly distinct.

The sub-central apex and highly unusual form mean that the anterior–posterior orientation is somewhat equivocal. The normal imbrication of chiton plates produces some overlap of the posterior apical area across the anterior edge of the following plate. In *Arctoplax*, the plates lack an apical area and their form precludes overlap; the deeper, high arched end is interpreted here provisionally as posterior (e.g. Text-fig. 7).

One problematical Ordovician genus *Llandeilochiton* Bergenhayn, 1955, based on a single small specimen from the Llandeilo of southern Scotland (*L. ashbyi* Bergenhayn, 1955), has a rectangular, flexed form with a sub-central apex, and apparently folds delimiting shell areas, but with a marked jugal furrow (Bergenhayn 1955, pl. 2, fig. 12). The specimen has not been examined, and its chiton affinities have been questioned (Smith and Hoare 1987).

Arctoplax ornata gen. et sp. nov.

Plate 9

Derivation of name. From the Latin *orno*, decorate, referring to the fine granular ornament.

Material, locality and horizon. Möllbos-1, Gotland, Halla Formation, Upper Wenlock (Homerian); 15 isolated intermediate sclerites (including one anterior and three posterior fragments); holotype RM Mo159.856*, intermediate sclerite; RM Mo159.853–159.855, 159.857, 159.899*, 159.904, 159.911, 159.925, 159.944, 159.948, 159.986, 159.996*, 160.002, 160.030.

Diagnosis. As for the genus.

Description. Small and high vaulted, elongate spatulate sclerites, mean length 7·0 mm (s.d. = 0·72, $n = 11$; holotype 7·7 mm), mean length/width 1·54 (s.d. = 0·19, $n = 9$; holotype 1·35). Strong constriction to a sub-central mucronate apex, mean 0·51 (s.d. = 0·04, $n = 11$; holotype 0·58) of length from anterior, low angular to rounded radial folds and furrows from apex defining shell fields. Anterior and posterior fields broad, vaulted, convex, with anterior field shallowing from apex, posterior field deepening; steep lateral fields depressed. Lateral and posterior fields folded into triangulate, angled faces, anterior field with weaker, triangulate faces anterolaterally, becoming rounded. Low radial folds elevating anterior and posterior fields, posterior jugal field, central part of lateral fields. Maximum width at anterolateral corners but tapering little along lateral margins; maximum height at posterolateral corners; mean height/length 0·51 (s.d. = 0·08, $n = 11$; holotype 0·48). Anterior field moderately arched, sloping outward, anterior margin rounded, more transverse medially, convex anterolateral corners through steeper radial fold and flexure (Pl. 9, figs 1e, 2e). Long, slightly concave to convex, lateral margins, deepening posteriorly; lateral fields sloping steeply outwards below constricted apex, two triangulate faces flanking central low fold (Pl. 9, figs c). Squarish posterolateral

---

EXPLANATION OF PLATE 7

Figs 1–2. *Enetoplax decora* gen. et sp. nov.; Möllbos-1, Gotland; Halla Formation, Upper Wenlock (Homerian); intermediate sclerites. 1, RM Mo159.999, holotype. 1a, dorsal view; note anteriorly displaced mucronate apex, prominent growth increments, holoperipheral growth; 1b, oblique ventral view; note anteriorly slanting subapical cavity near anterior margin, thickened medial pad flanked by longitudinal furrows; 1c, right lateral view; lateroposterior shell field flat; 1d, anterior view showing mucronate apex, prominent growth increments. 2, RM Mo160.000. 2a, dorsal view; 2b, ventral view; note thickened surface inside marginal rim; 2c, left lateral view; 2d, detail of granular ornament from right hand side, × 50; 2e, details of subapical cavity; note smooth, anteriorly slanting walls, cavity within thickened surface, inside marginal rim, × 50. All except 2d–e × 15.

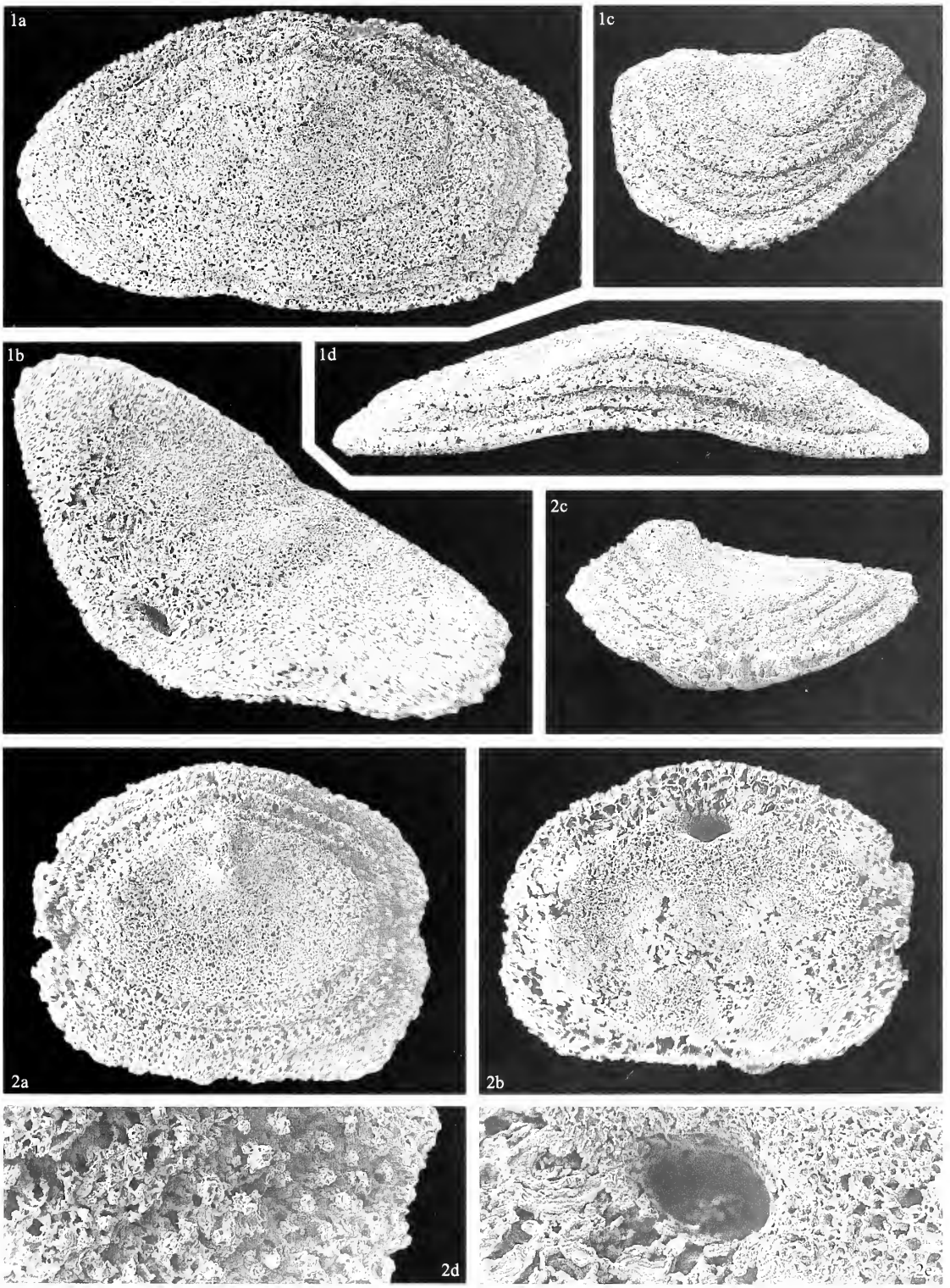

CHERNS, *Enetoplax*

corners through fold and acute flexure, posterior margin straight, transverse; posterior field strongly vaulted across elevated flat triangulate jugal field, flanked either side by two steep, flat triangulate faces angled outwards and downwards respectively (Pl. 9, figs, 1d, 2d). Fine and even, granular dorsal ornament, evident only on some sclerites, coarsening and best preserved towards outer parts of shell across anterior and lateral areas (Pl. 9, figs 1a, c, f, 3a, c–d). Growth lines concentric about apex, larger growth increments more evident towards outer part of dorsal surface.

Ventral surface smooth, concave and strongly folded around a longitudinal axis, deepest posteriorly in triangulate jugal area, apical constriction flanked by depressed side slopes, shallowing anteriorly. Small, deep narrow subapical cavity. All shell areas expanding away from apical constriction, slight corrugation of surface reflecting radial folds.

Remarks. Granular ornament is well preserved on a few sclerites (holotype, Pl. 9, fig. 1, and Pl. 9, fig. 3), but not evident on several other, possibly more thickened, specimens (Pl. 9, fig. 2). Those ornamented sclerites are relatively broad and shallow, with concave lateral margins, while the more thickened sclerites are narrower and deeper, slightly convex laterally. However, differences in ornament may be preservational, and on the basis of the fairly limited material available, variation is regarded here as intraspecific. Tail sclerites have not yet been recognized for *A. ornata*, although the head sclerite may be among the two described below.

head B indet.

Text-figure 5A–E

Material, locality and horizon. Möllbos-1, Gotland, Halla Formation, Upper Wenlock (Homerian); one isolated sclerite, RM Mo159.825*.

Description. Small, vaulted, convex semicircular sclerite (with some damage along the posterior edge) with elevated sub-central mucronate apex. Short, fairly broad and high; length 1·4 mm, length/width 0·58, height/length 1·0. Flat, elevated triangulate face within posterior area, steep, outward sloping, broad convex anterolateral area to rounded semicircular anterolateral margin, shallowing slightly near margin. Slight depressed radial flexure to posterolateral corners, rounding strongly into transverse, arched posterior margin (Text-fig. 5B), posterior shell arched and elevated (Text-fig. 5D), posterior margin transverse. Fine granular dorsal ornament; concentric growth lines more distinct near margins, where a new growth increment secreted from beneath is particularly evident posteriorly (Text-fig. 5E). Ventral surface deeply concave, smooth, deepest subapically and across median posterior face.

Remarks. The small, semicircular and convex form is typical of chiton end plates, and the transverse arched margin and steepness of the outward sloping face suggest that this is a head sclerite. The elevated sub-central mucronate apex, flat triangulate medial posterior face, arched and elevated posterior, and fine granular ornament across the whole shell, are features which associate it most closely with *A. ornata* (Text-fig. 7). However, the size, apical morphology and ornament are also comparable to *Heloplax*, but somewhat less so to *Enetoplax* for which a head sclerite is already tentatively recognized. All three genera are found in other samples from the same horizon.

EXPLANATION OF PLATE 8

Figs 1–3. *Enetoplax decora* gen. et sp. nov.; Möllbos-1, Gotland; Halla Formation, Upper Wenlock (Homerian). 1, RM Mo159.936; intermediate sclerite. 1a, dorsal view; note coarser granular ornament on anterior shell field; 1b, ventral view; 1c, right lateral view, posterolateral shell field gently concave, becoming elevated. 2, RM Mo159.835; ?tail sclerite. 2a, dorsal view; note trilobed, scalloped posterior margin; 2b, ventral view; subapical cavity close to anterior, thickened surface inside marginal rim; 2c, oblique ventral view, showing thickened surface inside marginal rim, medial pad inside weak longitudinal furrows. 3, RM Mo159.998; ?head sclerite. 3a, dorsal view; note mucronate apex close to anterior margin; 3b, ventral view; weak subapical cavity, surface with attached grains; 3c, left lateral view; posterolateral shell field gently convex; 3d, anterior view, showing mucronate apex, convex transverse profile. All ×15.

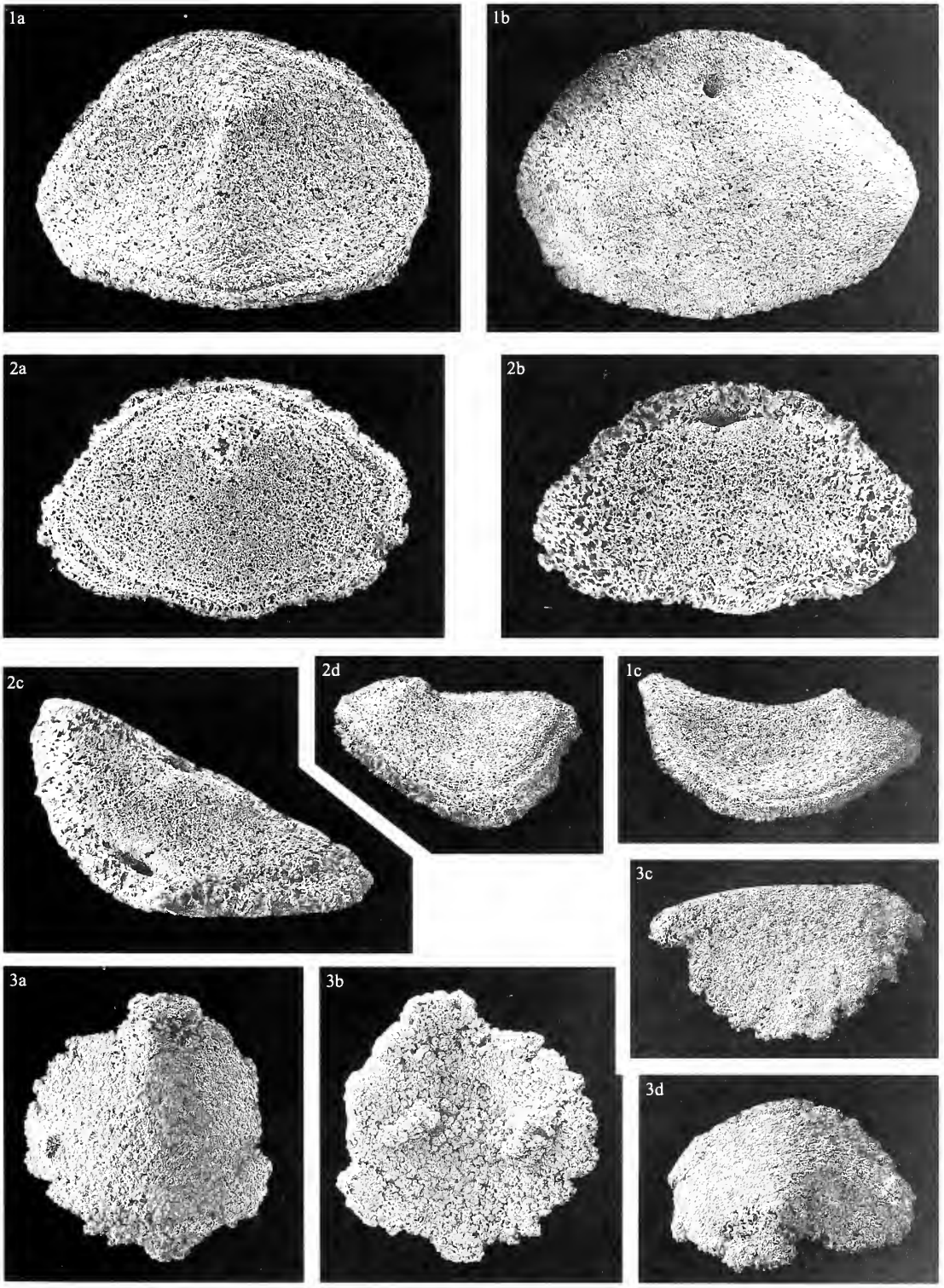

CHERNS, *Enetoplax*

?head or tail C indet.

Text-figure 5F–I

Material, locality and horizon. Möllbos-1, Gotland, Halla Formation, Upper Wenlock (Homerian); one isolated sclerite, RM Mo159.824.

Description. Small, transversely ovoid sclerite, convex becoming arched posteriorly, with dorsal shallow, rounded longitudinal furrows and ribs radiating posteriorly from a weakly elevated ?dorsal apex close to anterior; length 2·5 mm, length/width 0·86, height/length 0·88. Anterior area very short, arched, semicircular margin with distinct rim; strongly rounded posterolateral corners, posterior margin also semicircular, more arched (Text-figs 5F, 5H). Ventral surface smooth, concave, deepest centrally, shallowing outwards (Text-fig. 5G). Concentric growth, ?some weak granular ornament; thickened rim of anterolateral margin showing several growth increments.

Remarks. The fairly poorly preserved sclerite is broken along one edge and across the ventral surface, removing part of a later shell increment and hence the part of the dorsal margin. An apparently continuous marginal rim on an earlier shell layer suggests concentric growth around a dorsal apex, with additional shell increments added as complete layers from the ventral side, leading to significant thickening. The small size, arched convex form and semicircular margins suggest that this is an end plate, but anterior and posterior orientation are somewhat equivocal, only partly dependent upon which end plate it represents. A weak elevation near the unbroken margin apparently represents the apex, from which shallow rounded ribs and furrows, not well preserved, radiate slightly. Positioned with the apex uppermost, both margins remain moderately arched (Text-fig. 5H–I), yet if either margin is positioned flat the other margin becomes steep and raised. Radial ornament from the mucro is fairly common in both head and tail plates of neoloricate chitons (e.g. Smith 1960).

The holoperipheral growth and ovoid shape of this small sclerite are comparable to *Heloplax* and *Enetoplax*, although the ribbed ornament is different. The mode of growth is also similar to the larger, spatulate *Arctoplax*, but different from all other Gotland chitons.

MUSCULATURE IN GOTLAND CHITONS

The musculature of *Chelodes actinis* was discussed from sculpting of the ventral surface in thickened sclerites (Cherns 1998). In living chitons, the complex musculature (e.g. Hyman 1967) between valves and from valves into the body wall leaves no evident insertion sites in the inner shell layer, the ventral hypostracum. The function of the various sets of muscles acting on the valves lies in drawing the plates together and holding them against the body. Sutural laminae and insertion plates, formed of the middle shell layer, the articulamentum, which is absent from paleoloricate chitons, provide physical articulation of plates and attachment to the mantle. Plates are commonly embedded in and partially covered by the mantle.

EXPLANATION OF PLATE 9

Figs 1–3. *Arctoplax ornata* gen. et sp. nov.; Möllbos-1, Gotland; Halla Formation, Upper Wenlock (Homerian); intermediate sclerites. 1, RM Mo159.856, holotype. 1a, dorsal view; note sub-central mucronate apex, radial folds within lateral and posterior shell fields, prominent growth increments; ×7. 1b, ventral view, showing narrow subapical cavity; ×7. 1c, left lateral view; ×7. 1d, posterior view; ×7. 1e, anterior view; ×7. 1f, detail of dorsal granular ornament; ×15. 2, RM Mo159.899. 2a, dorsal view; 2b, ventral view; 2c right lateral view, note prominent growth increments; 2d, posterior view; 2e, anterior view. All ×7. 3, RM Mo159.996; broken left and right posterolateral margins. 3a, dorsal view; ×7. 3b, ventral view; note narrow subapical cavity; ×7. 3c, right lateral view; ×7. 3d, detail of granular ornament; ×15.

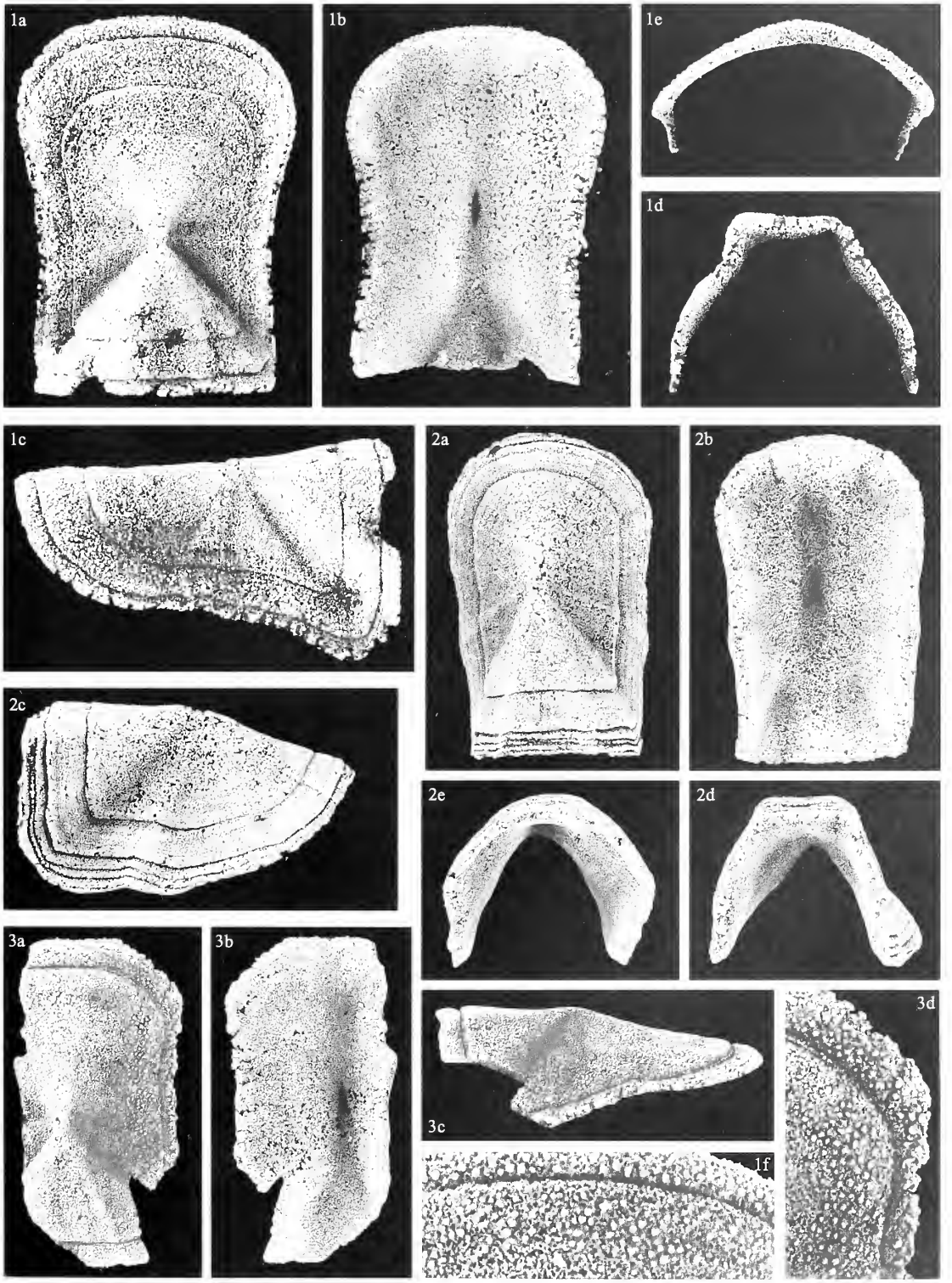

CHERNS, *Arctoplax*

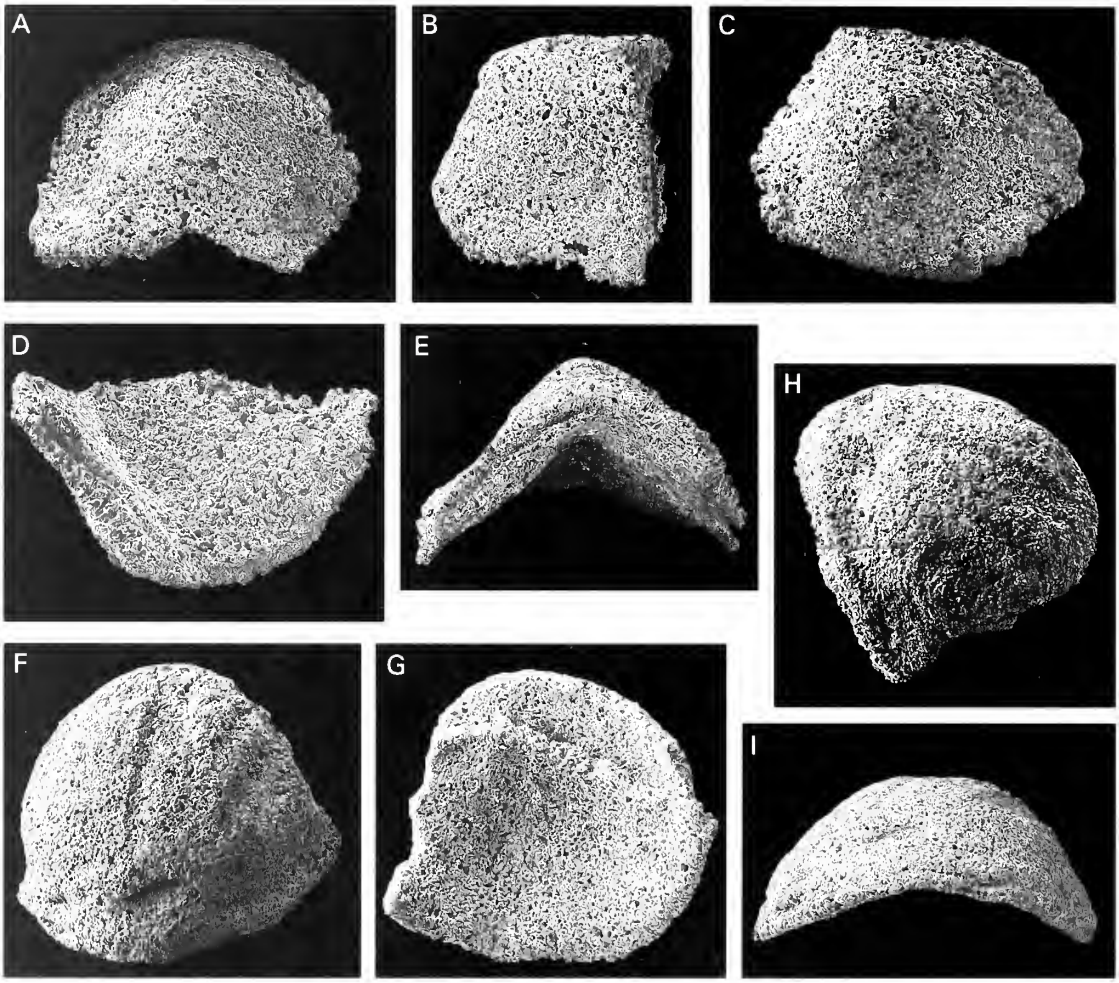

TEXT-FIG. 5. A–E, head B indet.; RM Mo159.825; Möllbos-1, Gotland; Halla Formation, Upper Wenlock (Homerian). A, dorsal view; note sub-central mucronate apex, holoperipheral growth. B, left lateral view. C, oblique anterior view, showing elevated triangular posterior field. D, posterior ventral view. E, posterior view. All × 20. F–I, ?head or tail C indet.; RM Mo159.826; Möllbos-1, Gotland; Halla Formation, Upper Wenlock (Homerian). F, dorsal view, showing radial ridged ornament, thickened posterior margin with growth increment. G, ventral view; note broken growth increment beneath outer shell. H, right lateral view, showing prominent growth increment at posterior, broken anteriorly. I, posterior view. All × 15.

The elongate shield-shaped, flexed intermediate sclerites of *Thairoplax pelta* sp. nov. lack localized ventral thickening, but *T.*? aff. *pelta*? has a low triangulate transverse thickened ridge in front of, and extending medially towards, the apical area (Pl. 3, fig. 4b). Intermediate sclerites of *Plectrochiton tegulus* sp. nov. also show a slight thickening across the equivalent area, although closer to the anterior of these short triangulate sclerites (Pl. 3, fig. 1b). The small, winged intermediate and tail sclerites of *Alastega lira* sp. nov. have well-developed ventral triangulate transverse ridges. In all the genera, the apical area typically has a slightly raised rim above the smooth ventral surface. Other paleoloricate chitons which have thickened transverse ventral ridges include *Kindbladochiton* and the Ordovician *Ivoechiton* spp. (Smith and Toomey 1964). The physical effect of these ridges, which taper outwards, is to elevate slightly the posterior shell, the apical area

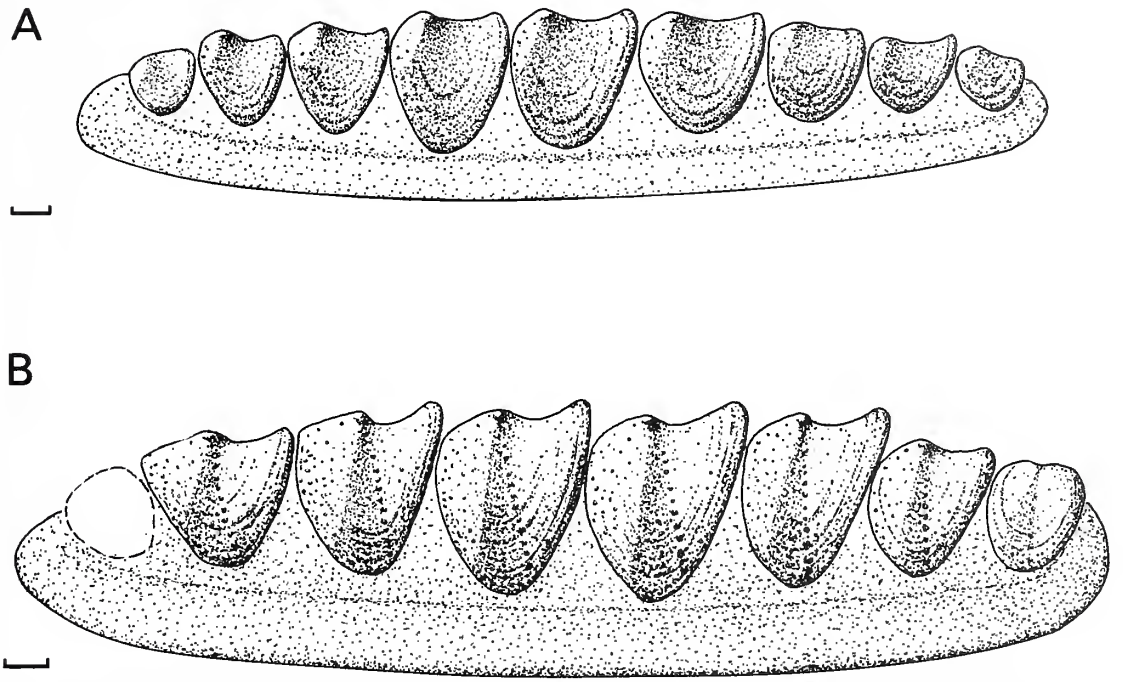

TEXT-FIG. 6. Reconstructions of A, *Enetoplax* and B, *Heloplax* as chitons, shown in left lateral view with normal plate orientations. Sclerites did not overlap but may have become imbricated through muscular rotation to elevate further the posterior shell fields. Scale bars represent 1 mm.

extending above the following sclerite. The ridge would also provide muscle attachment sites. *C. actinis* sclerites lack a similar marked thickening in front of the apical area, although developing shallow furrows flanking a medial pad towards the apical area similar to that of *T.*? aff. *pelta*? (Cherns 1998, pl. 4, fig. 3b). These furrows apparently represent muscle insertion sites, additional to the apical area rim that might serve for muscle attachment. None of the Gotland chitons has marked cavities extending beneath the apical area, as described for the Ordovician *Chelodes whitehousei* and Cambrian *Matthevia* spp. (Runnegar *et al.* 1979).

The three holoperipheral genera have mucronate sclerites with a prominent subapical cavity presumed to function for muscle insertion. In both *Heloplax* and *Enetoplax* (Text-figs 2–3), these small, deep cavities are anteriorly slanting, in front of a transverse flexure of the shell; in the former, the subapical cavity becomes flanked in some sclerites by additional, shallower, anterolaterally directed cavities (Pl. 5, fig. 1b; Pl. 6, fig. 1b). The subapical cavities are circular to transversely ovoid, with smooth margins, tapering into the valve and fairly deep, less even at the basal insertion point (Pl. 7, fig. 2d). Although the main insertion directions for the ventral cavities appear to be anterior and anterolateral, shallow furrows across the posterior field suggest that each also housed posteriorly directed muscles (Pl. 6, fig. 1b–c; Pl. 7, fig. 1b). In *Heloplax*, the posterior field of intermediate sclerites becomes elevated; in *Enetoplax*, a longer field curves more shallowly (Text-fig. 6). Thus the shell flexure serves a similar function to the thickened transverse ridges described above, for other genera; although the sclerites did not overlap, they could probably be drawn down on to the body, drawn closer, rotated and imbricated (cf. *Matthevia* reconstruction in Runnegar *et al.* 1979, text-fig. 1). The tail plates for both *Heloplax* and *Enetoplax* lack posterior elevation, the posterior fields being convex to flat (Text-fig. 6).

Arctoplax sclerites have a deep, tapering, rather slit-like sub-central subapical cavity (Pl. 9, fig. 1b), but in addition their radial angled folds and furrows across the high-arched, elongate shell might

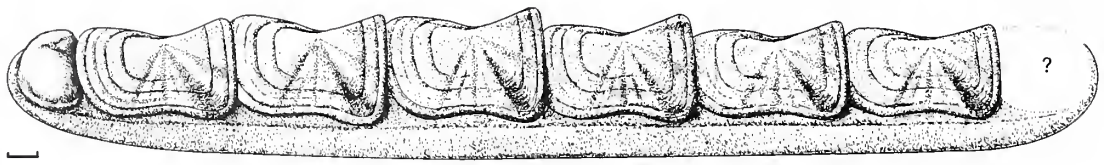

TEXT-FIG. 7. Reconstruction of *Arctoplax* as a chiton in slightly oblique, left lateral view, with the rounded shallower end of sclerites anterior, the squarer and deeper shell field posterior. The head sclerite has been suggested as head B indet. There is no overlap of plates, but muscular rotation of plates may have produced imbrication, elevating the posterior field. Scale bar represents 1 mm.

have provided additional attachment surfaces or muscle tracks into the body wall. The subapical cavity may thus have anchored longitudinal and radial muscles, whereas those in *Heloplax* and *Enetoplax* apparently housed primarily anteriorly and anterolaterally directed muscle blocks. If the function of angled radial faces was connected primarily with the musculature, then by comparison their stronger development at the deeper end, interpreted here tentatively as posterior, might indicate the reverse orientation as more appropriate. However, the deep, long side slopes and marked apical constriction produced lateral cover for a narrow elongate body, where the incongruent, arched anterior and posterior profiles precluded overlap of sclerites. With the more rounded, shallower end as anterior (Text-fig. 7), some rotation of the shell behind the subapical muscle insertion site, to imbricate sclerites as proposed for the other genera, might elevate slightly the deeper, more arched and angular end.

Runnegar *et al.* (1979) interpreted two deep ventral pits in tall conical valves of the late Cambrian *Matthevia variabilis* Walcott, 1885 as muscle insertion sites for dorso-ventral muscles from shell to foot. A comparable single pit was present in the younger late Cambrian *M. walcotti* Runnegar, Pojeta, Taylor and Collins, 1979, and a shallow pit in the early Ordovician *Hemithecella expansa* Ulrich and Bridge, 1941. A concavity beneath the apical area in some early Ordovician *C. whitehousei* Runnegar, Pojeta, Taylor and Collins, 1979 was interpreted as equivalent, and *Matthevia* as a primitive chiton. By contrast, Stinchcomb and Darrough (1995), in discussing Cambrian–Ordovician *Hemithecella*, argued that ventral pits were not chiton features and that *Matthevia*, *Hemithecella* and some *C. whitehousei* should be considered as multi-plated problematical molluscs distinct from chitons.

THE NATURE OF THE SCLERITOME

The majority of the Gotland chitons described above represent isolated sclerites from silicified samples of late Wenlock age. Recent, neoloricate chitons typically have eight plates, of which seven are secreted in the late trochophore stage of ontogeny, the eighth, tail valve somewhat later (Okuda 1947; Hyman 1967). Limited records of articulated fossil chitons indicate a similar valve complement also in older neoloricate and in paleoloricate chitons (e.g. Rolfe 1981; Hoare and Mapes 1989). The only articulated plates among the Gotland material are the type specimen of *G. interplicatus*, which shows a fragment of a second, following sclerite (Pl. 1, fig. 1). The six similar intermediate sclerites in chitons vary in size along the body, but the head particularly, and also tail plates, can be very different (e.g. Smith 1960). The plates have posterior apices and mixoperipheral growth, with the outer tegmentum extending ventrally to form the apical area, except for some tail plates which have a dorsal mucronate apex and holoperipheral growth. In Recent chitons, the apical area is usually a narrow band, but in some early chitons may be much longer (e.g. *Chelodes raaschi*; Kluessendorf 1987).

Fine growth lines are preserved on most of the Gotland chiton sclerites, but also larger, stepped growth increments where similar patterns of growth can be used to associate plates from the same individual as well as indicating intra-individual variation (e.g. *C. actinis*; Cherns 1998, pl. 6; Pl. 7, figs 1–2). Such occurrences for all three of the new genera described here which show holoperipheral

growth are important in the interpretation of these plates as intermediate and not tail sclerites. These and the more typical plates with mixoperipheral growth have highly comparable growth patterns.

Recent chitons mostly range in size up to *c.* 0·05 m, but can be much larger (*Cryptochiton stelleri*, 0·33 m; Hyman 1967), and usually have a flattened, ovoid foot. Overlap of the physically interlocking plates, relating to the length of the apical area, is generally quite small, and plates are normally broad and short. The Gotland chiton assemblage includes several with elongate rather than broad plates. Bergenhayn (1955) used formulae to estimate the length and elongation of Gotland *Chelodes* and *Gotlandochiton*, based on sclerite length, width, and length of apical area, reconstructing large sclerites with relatively long apical areas in *Chelodes* spp. as belonging to very elongate animals, *G. interplicatus* with its broad sclerite rather less so at about three times as long as wide (Bergenhayn 1955, pl. 2). Of the chitons described here, *T. pelta* has long sclerites with a short apical area, little overlap between plates, and hence must have been an elongate animal, and *Arctoplax* without overlap of plates was long but also narrow (Text-fig. 7). The remaining Gotland genera – *Plectrochiton*, *Alastega*, *Enetoplax* and *Heloplax* – had smaller, short and broad sclerites, more similar in shape to Recent chitons, the last two of these genera with no overlap of plates (Text-fig. 6). The stratigraphical evidence suggests that the late Wenlock sequences for the Gotland chiton localities represent very nearshore facies, associated with rocky shorelines (Cherns 1996). Those facies relationships indicate an ecology similar to that of most Recent chitons.

Acknowledgements. I thank Dr L. Jeppsson (Lund University) for providing the silicified collections of Gotland chitons, and for his kind hospitality, also Dr L. Liljedahl for providing some of those silicified samples; Professor M. G. Bassett (National Museum of Wales, Cardiff) for discussion and critical review of the manuscript, and for providing darkroom facilities at NMW; and Mrs G. Evans and Mrs L. Norton (NMW) for drafting Text-figures 2–3 and 6–7. Professor R. D. Hoare (Bowling Green State University, Ohio, USA) kindly read and criticized the manuscript. I am grateful to the Palaeozoology Section, Naturhistoriska Riksmuseum, Stockholm for loan of museum specimens.

REFERENCES

BERGENHAYN, J. R. M. 1943. Preliminary notes on fossil Polyplacophoras from Sweden. *Geologiska Föreningens i Stockholms Förhandlingar*, **65**, 297–303.

—— 1955. Die fossilen Schwedischen Loricaten nebst einer vorläufigen Revision des Systems der ganzen Klasse Loricata. *Lunds Universitets Årsskrift, Nya Förhandlingar, Avdelningen 2*, **51** (8), 1–46, pls 1–2.

—— 1960. Cambrian and Ordovician loricates from North America. *Journal of Paleontology*, **34**, 168–178.

BLAINVILLE, H. M. D. de 1816. Prodrome d'une nouvelle distribution systématique du règne animal. *Bulletin des Sciences, Société Philomathique de Paris*, 105–124.

CHERNS, L. 1996. Silurian chitons as indicators of rocky shores? – new data from Gotland. 41. In JOHNSON, M. E. and BRETT, C. E. (eds). *The James Hall Symposium: Second International Symposium on the Silurian System, Program and Abstracts*. University of Rochester, N.Y., 114 pp.

—— 1998. *Chelodes* and closely related Polyplacophora (Mollusca) from the Silurian of Gotland, Sweden. *Palaeontology*, **41**, 545–573.

DAVIDSON, T. and KING, W. 1874. On the Trimerellidae, a Palaeozoic family of the palliobranchs or Brachiopoda. *Quarterly Journal of the Geological Society, London*, **30**, 124–172, pls 12–19.

DEBROCK, M. D., HOARE, R. D. and MAPES, R. H. 1984. Pennsylvanian (Desmoinesian) Polyplacophora (Mollusca) from Texas. *Journal of Paleontology*, **58**, 1117–1135.

HOARE, R. D. 1989. Mississippian polyplacophoran (Mollusca) from Utah. *Journal of Paleontology*, **63**, 252.

—— and MAPES, R. H. 1989. Articulated specimen of *Acutichiton allynsmithi* (Mollusca, Polyplacophora) from Oklahoma. *Journal of Paleontology*, **63**, 251.

HYMAN, L. H. 1967. *The Invertebrata: Mollusca 1*. Volume 6. McGraw-Hill, New York, vii + 792 pp.

JAANUSSON, V. 1986. *Locality designations in old collections from the Silurian of Gotland*. Swedish Museum of Natural History, Stockholm 19 pp.

KLUESSENDORF, J. 1987. First report of Polyplacophora (Mollusca) from the Silurian of North America. *Canadian Journal of Earth Sciences*, **24**, 435–441.

LAUFELD, S. 1974. Reference localities for palaeontology and geology in the Silurian of Gotland. *Sveriges Geologiska Undersökning, Series C*, **705**, 1–172.

—— and JEPPSSON, L. 1976. Silicification and bentonites in the Silurian of Gotland. *Geologiska Föreningens i Stockholms Förhandlingar*, **97**, 207–222.

LILJEDAHL, L. 1984. Silurian silicified bivalves from Gotland. *Sveriges Geologiska Undersökning, Series C*, **804**, 1–82.

LINDSTRÖM, G. 1884. On the Silurian Gastropoda and Pteropoda of Gotland. *Kongliga Svenska Vetenskaps-Adakamiens Handlingar*, **19**(6), 1–250, pls 1–21.

OKUDA, S. 1947. Notes on the post-larval development of the giant chiton, *Cryptochiton stelleri* (Middendorff). *Journal of Faculty of Science Hokkaido University, Series 6, Zoology*, **9**, 267–275.

ROLFE, W. D. I. 1981. *Septemchiton* – a misnomer. *Journal of Paleontology*, **55**, 675–678.

RUNNEGAR, B., POJETA, J. Jr, TAYLOR, M. E. and COLLINS, D. 1979. New species of the Cambrian and Ordovician chitons *Matthevia* and *Chelodes* from Wisconsin and Queensland: evidence for the early history of polyplacophoran mollusks. *Journal of Paleontology*, **53**, 1374–1394.

SCHMITT, J. G. and BOYD, D. W. 1981. Patterns of silicification in Permian pelecypods and brachiopods from Wyoming. *Journal of Sedimentary Petrology*, **51**, 1297–1308.

SIRENKO, V. I. and STAROBOGATOV, YA. I. 1977. On the systematics of Paleozoic and Mesozoic chitons. *Paleontological Journal*, **1977**(3), 285–294. [K sistematike paleozoyskikh i mesozoyskikh khitonov, *Paleontologischeskii Zhurnal*, **1977**(3), 30–41].

SMITH, A. G. 1960. Amphineura. I41–I76. *In* MOORE, R. G. (ed.). *Treatise on invertebrate paleontology. Volume I. Mollusca 1*. Geological Society of America and University of Kansas Press, Lawrence, Kansas, xxiii + 351 pp.

—— and HOARE, R. D. 1987. Paleozoic Polyplacophora: a checklist and bibliography. *Occasional Papers of the California Academy of Sciences*, **146**, 1–71.

—— and TOOMEY, D. F. 1964. Chitons from the Kindblade Formation (Lower Ordovician), Arbuckle Mountains, Southern Oklahoma. *Circular of the Oklahoma Geological Survey*, **66**, 1–41, pls 1–8.

STINCHCOMB, B. L. and DARROUGH, G. 1995. Some molluscan Problematica from the Upper Cambrian–Lower Ordovician of the Ozark Uplift. *Journal of Paleontology*, **69**, 52–65.

ULRICH, E. O. and BRIDGE, J. 1941. *Hemithecella expansa*. 19–20; pl. 68, fig. 6. *In* BUTTS, C. Geology of the Appalachian Valley in Virginia, Part 2. *Bulletin of the Virginia Geological Survey*, **52**, 1–271.

VAN BELLE, R. A. 1975. Sur la classification des Polyplacophora: 1. Introduction et classification des Paleoloricata, avec la description de *Kindbladochiton* nom. nov. (pour *Eochiton* Smith, 1964). *Informations de la Société Belge de Malacologie, Série 4*, **5**, 121–131, pl. 1.

WALCOTT, C. D. 1885. Notes on some Paleozoic pteropods. *American Journal of Science*, **30**, 17–21.

LESLEY CHERNS

Department of Earth Sciences
Cardiff University
Box 914, Cardiff CF1 3YE, UK

Typescript received 6 June 1997
Revised typescript received 10 November 1997

NEW SILURIAN NEOTAXODONT BIVALVES FROM SOUTH WALES AND THEIR PHYLOGENETIC SIGNIFICANCE

by V. ALEXANDER RATTER *and* JOHN C. W. COPE

ABSTRACT. The arcoidean bivalves, *Trecanolia acincta* gen. et sp. nov. and *Uskardita mikraulax* gen. et sp. nov., are described from the Wenlock of South Wales. These bivalves are accommodated within the new family Frejidae, alongside the closely related Silurian genera *Freja* Liljedahl and *Alytodonta* Cope. The frejids are characterized by an amphidetic, chevron-shaped duplivincular ligament, and a ventrally diverging dental arrangement of pseudocardinals and pseudolaterals. The group provides further evidence that the superfamily Arcoidea evolved from an early Ordovician ancestor, such as *Catamarcaia* Sánchez and Babin. The frejids represent an early diversification of the arcoideans, previously unknown in the Palaeozoic.

THE subclass Neotaxodonta was proposed by Korobkov (1954) to distinguish the arcoid and limopsoid bivalves from the nuculoids. The two groups share a superficially similar taxodont dentition that had long caused them to be taxonomically linked, following an initial proposal by Douvillé (1912). The subclass Palaeotaxodonta, proposed by Korobkov (1954) for the nuculoids, was accepted in the bivalve volumes of the *Treatise* (Cox *et al.* 1969–71). However, the Neotaxodonta – which removed the superfamilies Arcoidea and Limopsoidea from the pteriomorphian bivalves – was not.

Taylor *et al.* (1969, 1973) argued that the shell microstructure of the superfamilies Arcoidea and Limopsoidea provided good grounds for separating them from other pteriomorphians, and Cope (1995) proposed that the Neotaxodonta be recognized as distinct from the Pteriomorphia. As removal of these two superfamilies from the Pteriomorphia, as a restricted order Arcoida, left many former arcoids within the Pteriomorphia without ordinal status, Cope (1996) assigned these to the order Cyrtodontida.

The neotaxodonts have a well established Mesozoic to Recent history, but their Palaeozoic origin and subsequent diversification is contentious. Many previous phylogenetic schemes considered the cyrtodontid pteriomorphians as the probable ancestors of the arcoid neotaxodonts (e.g. Newell 1954, 1965; Cox 1960; Vogel 1962; Cox *et al.* 1969–71; Pojeta 1971, 1978; Waller 1978, 1990). This view was reinforced by the known fossil record, as rich Ordovician faunas of cyrtodonts were known, but the earliest undisputed arcoids were of Devonian age. Possible earlier forms included two poorly known Ordovician species referred to *Parallelodon*. Babin (1966) showed that *P. antiquus* Barrois, 1891 was based on a poorly preserved specimen and that Barrois' figures were highly interpretative. Furthermore, *Glyptarca primaeva* Hicks, 1873 (included in the *Treatise* within *Parallelodon*) was described by Carter (1971) and Cope (1996) as a palaeoheterodont. The earliest undoubted neotaxodont form included in the *Treatise* was therefore the Devonian *Parallelodon*. Recently this view has been challenged (Cope 1997*a*, 1997*b*).

Sánchez and Babin (1993) described the genus *Catamarcaia* from the Middle Arenig of Argentina (see Text-fig. 6). This genus combines continuous dentition (i.e. lacking an edentulous area on the hinge-plate) with a duplivincular ligament; they considered it as a pteriomorphian with palaeoheterodont affinities. However, Cope (1997*a*) concluded that the continuous dentition of *Catamarcaia* was not characteristic of Ordovician pteriomorphs, but was more typical of neotaxodonts. Furthermore, the dental arrangement of *Catamarcaia* is similar to that of the palaeo-

[Palaeontology, Vol. 41, Part 5, 1998, pp. 975–991, 1 pl.]

heterodont *Glyptarca*. This suggests that the neotaxodonts could have evolved directly from the palaeoheterodonts. Cope (1997*b*) carried these arguments further and figured a Silurian neotaxodont, *Alytodonta gibbosa*, showing characters intermediate between *Catamarcaia* and the Wenlock genus *Freja* Liljedahl, 1984.

Herein we describe two new genera of neotaxodonts from the Wenlock Series of South Wales and assess their phylogenetic implications.

SYSTEMATIC PALAEONTOLOGY

All linear measurements are given in millimetres (mm), measured with Vernier callipers under a binocular microscope. Abbreviations used for dimensions, angles and statistics are: $\alpha°$ = angle of obliquity, AL = anterior length, CH = cardinal area height, CL = cardinal area length, L = length, H = height, OL = oblique length, S.D. = standard deviation, U° = umbonal angle, UH = umbonal height, and W = width. The following abbreviations are used to describe preservation: I = internal, E = external, R = right, L = left, A = articulated, C = complete valve, P = slightly fragmented valve, F = fragment, X = recrystallized calcite shell; the letters are combined to describe the preservation of each specimen (e.g. an ILC is a complete internal mould of a left valve). The specimens are housed in the collections of the British Geological Survey, Keyworth (BGS).

Subclass NEOTAXODONTA Korobkov, 1954
Order ARCOIDA Stoliczka, 1871
Superfamily ARCOIDEA Lamarck, 1809
Family FREJIDAE fam. nov.

Type genus. *Freja* Liljedahl, 1984 (p. 36), here designated.

Diagnosis. Equivalved, subequilateral to inequilateral, moderately inflated arcoids, with a sub-orbicular to ovoid outline; ligament external, duplivincular, chevron-shaped and positioned on a cardinal area; hinge line straight; dentition of simple pseudocardinal teeth on the central hinge area, bounded anteriorly and posteriorly by pseudolaterals, elongated obliquely to hinge line; adductor muscle scars anisomyarian; external prosopon of concentric growth lines only.

Remarks. This new family is established to accommodate Silurian representatives of the superfamily Arcoidea. These include the genera *Freja* Liljedahl, 1984, *Alytodonta* Cope, 1997*b*, *Trecanolia* gen. nov. and *Uskardita* gen. nov. (Text-fig. 1). The frejids are characterized by a sub-circular to ovate outline and a straight hinge line. The dentition consists of a series of small, simple pseudocardinal teeth along the central area of the hinge plate, which are terminated by anterior and posterior pseudolateral teeth that are elongated at an oblique angle to the hinge line. The earlier genera, namely *Alytodonta* and *Uskardita*, have much shorter anterior pseudolaterals that are more oblique to the hinge line than later representatives. *Trecanolia* has more modified pseudolateral dentition; the undersides of the ventral teeth have cardinal denticles developing at irregular intervals. All four genera have a chevron-shaped duplivincular ligament between the hinge plate and the beak.

Liljedahl (1984, pp. 36–37) was unsure of the systematic position of *Freja* at the superfamily and family level. At that time, the newly described genus had a unique hinge construction and gross shell morphology. The prosocline outline, straight hinge line and anisomyarian adductors were typical in the cyrtodontoideans, yet the hinge plate and ligament closely resembled the Mesozoic and Cenozoic arcids. With the recent discovery of closely related genera from the Llandovery and Wenlock of Britain, it is possible to view the morphology of *Freja* as typical of this family of Silurian arcoids and it is herein considered as the type genus.

Cope (1997*b*, pp. 740–741) erected the new genus *Alytodonta*, which was based on a single specimen from the Lower Llandovery at Girvan, Ayrshire. *Alytodonta* displays the duplivincular

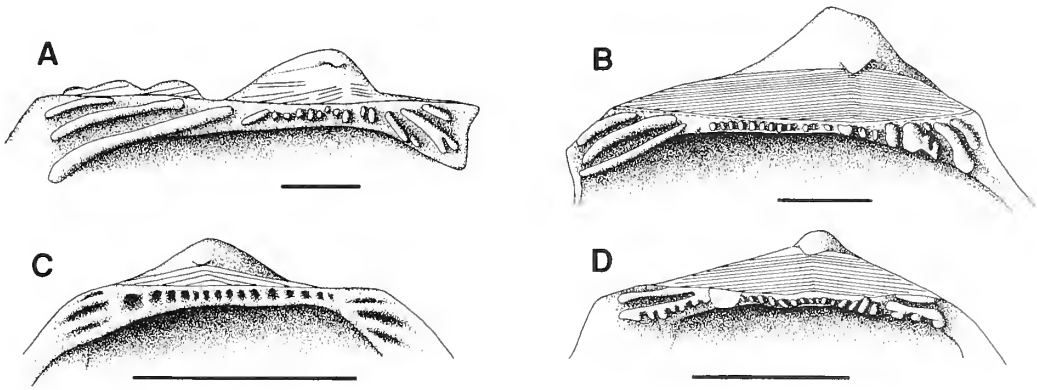

TEXT-FIG. 1. Hinge details of the four frejid genera. A, *Alytodonta gibbosa* Cope, 1997*b*; Natural History Museum L 49858; modified from Cope 1997*b*, text-fig. 4. B, *Uskardita mikraulax* gen. et sp. nov.; BGS GSM 22187. C, *Freja fecunda* Liljedahl, 1984; Geological Survey of Sweden Type 3367; modified from Liljedahl 1984, fig. 21. D, *Trecanolia acincta* gen. et sp. nov.; BGS DEX 2869. Scale bars represent 4 mm.

ligament, subovate outline and continuous dentition that characterize the Frejidae. In his description, Cope (1997*b*) placed *Alytodonta* within the family Parallelodontidae. However, this group contains predominantly Mesozoic and Cenozoic genera that have hinge plates, shell outlines and external prosopon that are easily distinguished from the Frejidae. The parallelodontids have a more inequilateral dental arrangement, chiefly consisting of short, oblique anterior teeth and very long posterior pseudolaterals that are almost parallel with the hinge line. Furthermore, their shells are usually antero-posteriorly elongated and ornamented with both concentric growth lines and radial ridges and gutters.

The family Frejidae cannot accommodate *Catamarcaia*, which displays a duplivincular ligament and a composite dentition of actinodontoid laterals and some small taxodont teeth (Sánchez 1995). The combination of these characters is unique to this bivalve and has resulted in previous uncertainty regarding its sytematic position. It is clearly a neotaxodont but, as yet, cannot be readily accommodated in any existing family.

Stratigraphical range. Lower Llandovery to Upper Wenlock of Britain, Upper Wenlock of Gotland (Sweden), and possibly the Wenlock of Wisconsin, USA.

Genus TRECANOLIA gen. nov.

Derivation of name. From the Welsh *tre* (= settlement), and *canol* (= middle) – the Welsh equivalent of 'Middleton', an allusion to the type locality.

Type species. *Trecanolia acincta* sp. nov., by monotypy.

Diagnosis. Equivalved, inequilateral, moderately inflated, opisthocline, sub-orbicular to oblique shells with a narrow, straight hinge plate, gently rounded posterior and ventral margins and a narrow, strongly convex anterior extremity; umbones elevated above hinge line; beaks orthogyre. Dentition of 11–18 simple, cardinal teeth proximal to umbonal area, terminated by two short anterior pseudolaterals and two longer posterior pseudolaterals; both sets elongated normal to hinge plate; underside of ventral anterior pseudolateral has three to six cardinal denticles; ventral side of posterior pseudolaterals has up to seven taxodont denticles, juvenile specimens may lack the posterior denticles; subumbonal edentulous space present only in juveniles. Adductor scars anisomyarian; anterior adductor scar ovate and supported by shallow myophoric buttress;

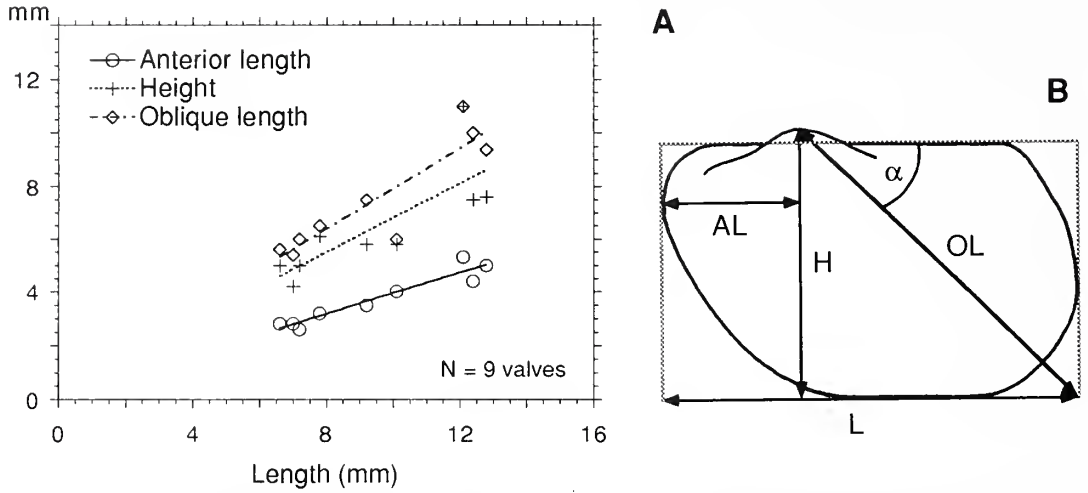

TEXT-FIG. 2. A, bivariate scatter diagram of dimensions measured on *Trecanolia acincta* gen. sp. nov. B, angles and measurements taken on *T. acincta*.

posterior scar larger, but less deeply impressed. Ligament duplivincular and chevron-shaped, located between hinge and beak. External prosopon unknown.

Remarks. Trecanolia is distinguished from other frejids by the oblique and posteriorly elongate shell shape and by the presence of large denticles on the underside of the ventral anterior and posterior pseudolaterals (Text-fig. 3). *Trecanolia* is most closely related to *Freja*; both genera have numerous cardinal teeth and pseudolaterals oriented normal to the hinge plate, similar anisomyarian adductors, and orthogyre beaks. However, *Freja* has an orbicular, subequilateral shell outline, a gently convex anterior margin, less elongate posterior pseudolaterals and lacks the unusual denticles. *Uskardita* is easily distinguished from *Trecanolia* by the large cardinal area, more conspicuous duplivincular ligament, oblique and shorter anterior cardinal teeth and the more upright umbo. *Alytodonta* is more distantly related, as the three posterior pseudolaterals are elongate and rather pterioid in appearance and the beaks are prosogyrate.

Trecanolia acincta gen. et sp. nov.

Plate 1, figures 1–10; Text-figures 2–3

v. 1978 Bivalve gen. et sp. nov.; Squirrel and White, pl. 3, figs 12–14
(?) 1996 *Leiopteria* cf. *undata* (Hall, 1852); Watkins, fig. 2E.

Derivation of name. From the Latin *acinctus* (= well equipped); referring to the numerous teeth and denticles.

EXPLANATION OF PLATE 1

Figs 1–10. *Trecanolia acincta* gen. et sp. nov.; overflow cut from the old lake in Middleton Hall Estate, near Middleton Hall Lodge, 2995 metres S68° W of Dryswlyn Station, Carmarthenshire; grid reference SN 5265 1880; probably Upper Wenlock. 1, BGS DEX 2869A, holotype; internal mould of left valve; ×5. 2, latex cast of holotype; ×5. 3–4, BGS DEX 2834B; internal mould of left valve and latex cast; ×7. 5, 9, BGS DEX 2869B; hinge detail of latex cast and internal mould of right valve; ×6. 6–7, BGS DEX 2843A; internal mould of right valve and latex cast; ×6. 8, BGS DEX 2848; dorsal view of conjoined valves, internal mould; ×4. 10, BGS DEX 2880; internal mould of left valve; ×5.


1

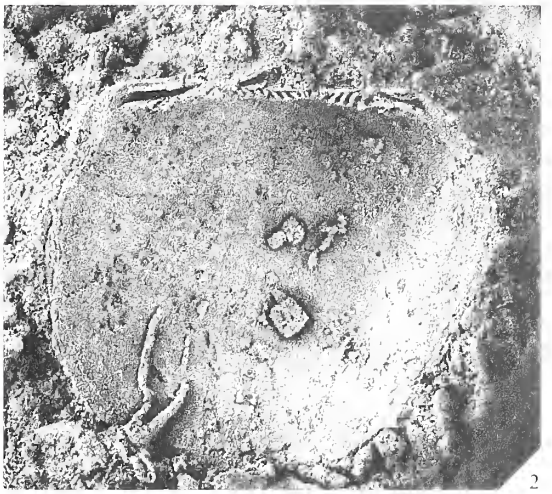
2

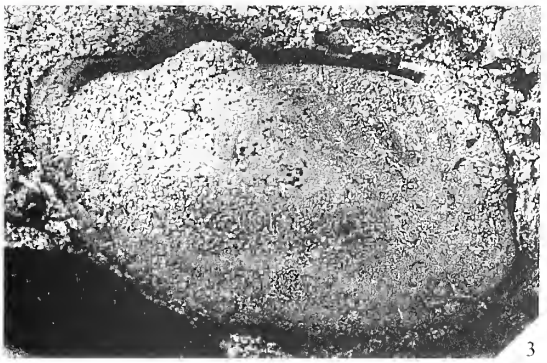
3


4

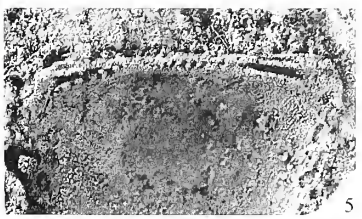
5

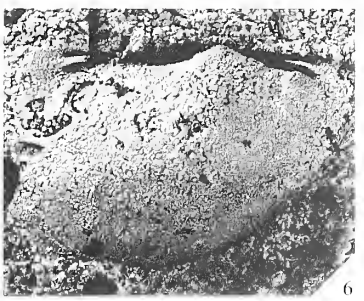
6

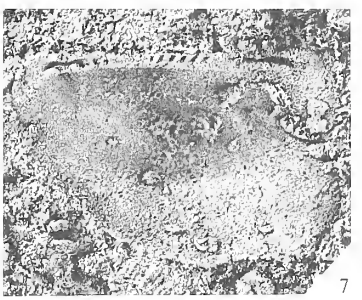
7

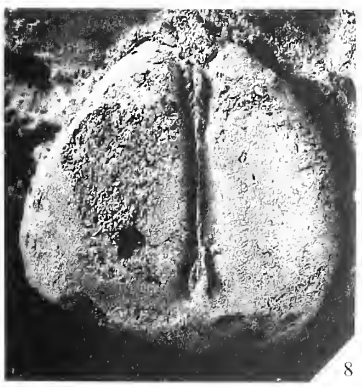
8

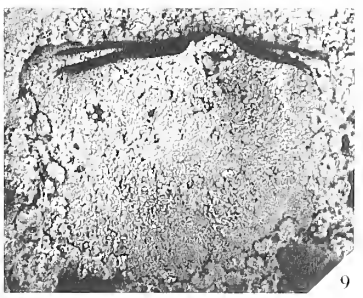
9


10

RATTER and COPE, *Trecanolia*

Holotype. BGS DEX 2869A, a complete internal mould of a left valve. The specimen has been tectonically distorted resulting in a shortened antero-posterior axis. No undeformed specimens have been collected.

Paratypes. BGS DEX 2869B (ILC), BGS DEX 2823A (IRF), BGS DEX 2834A, B, C, D, E (IRC, ILC, IRF, ILC and IRP respectively), BGS DEX 2839A (ILC), BGS DEX 2841 and 2847A (ILF and ELF – part and counterpart), BGS DEX 2847B, C, D (IRF, ILF and IRP respectively), BGS DEX 2843A (IRP), BGS 2848 (IAF), DEX 2880A (ILP). All specimens are from the type locality and horizon.

Type locality and horizon. Overflow cut from old lake in Middleton Hall Estate, near Middleton Hall Lodge, 2995 metres S68° W of Dryswlyn Station, Carmarthenshire, west Wales; grid reference SN 5265 1880. Probably of late Wenlock age (Squirrel and White 1978).

Measurements

BGS DEX	AL	L	H	W	OL	AL/L	H/L	OL/L	U°	α°
2834A	5·0	12·8	7·6	2·0	9·4	0·39	0·59	0·73	117	45
2834B	3·5	9·2	5·8		7·5	0·38	0·63	0·82	117	47
2834D	4·4	12·4	7·5		10·0	0·35	0·60	0·81	115	44
2834E	2·6	7·2	5·0		6·0	0·36	0·69	0·83		
2839A	4·0	10·1	5·8	1·2	6·0	0·40	0·57	0·59	117	51
2843A	2·8	7·0	4·2		5·4	0·40	0·60	0·77	126	46
2869A	5·3	12·1	11·0	3·0	11·0	0·44	0·91	0·91	111	60
2869B	2·8	6·6	5·0		5·6	0·42	0·76	0·85	109	51
2880A	3·2	7·8	6·1		6·5	0·41	0·78	0·83	96	55
Min.	2·6	6·6	4·2	1·2	5·4	0·35	0·57	0·59	96	44
Max.	5·3	12·8	11·0	3·0	11·0	0·44	0·91	0·91	126	60
Mean	3·7	9·5	6·4	2·1	7·5	0·39	0·68	0·82	113·5	49·9
Median	3·5	9·2	5·8	2·0	6·5	0·40	0·63	0·82	116	49·0
S.D.	1·00	2·48	2·04	0·90	2·11	0·03	0·11	0·09	8·68	5·51

Diagnosis. As for genus.

Description. Small, inequilateral, equivalved, opisthocline, moderately inflated, oblique to sub-orbicular shells, with a straight dorsal margin, strongly convex anterodorsal margin, gently rounded anteroventral and ventral margin, slightly angulated posteroventral margin and a somewhat truncate and gently arcuate posterior. The maximum convexity is mid-height and just anterior of the mid-length of the shell. The umbones are situated in the anterior half of the shell, and are conspicuous and elevated above the hinge plate and interumbonal area. The beaks are small and orthogyrate.

BGS DEX	L × H	Cardinal teeth	Anterior denticles	Posterior denticles	Anterior pseudolaterals	Posterior pseudolaterals	Edentulous space?
2834A	97·28	~ 18	2	?	2	2	?
2834B	53·36	13	2–3	3	1	2	No*
2834E	36·00	7	2	~ 3	2	2	Yes (large)
2848 left	~ 96·00	17	3	?	?	?	Yes (small)
2848 right	~ 96·00	18	?	?	?	?	Yes (small)
2869A	133·10	15	3	7	2	2	No
2869B	33·00	12	4	0	2	2	Yes (small)

* Teeth in subumbonal area fused and poorly defined.

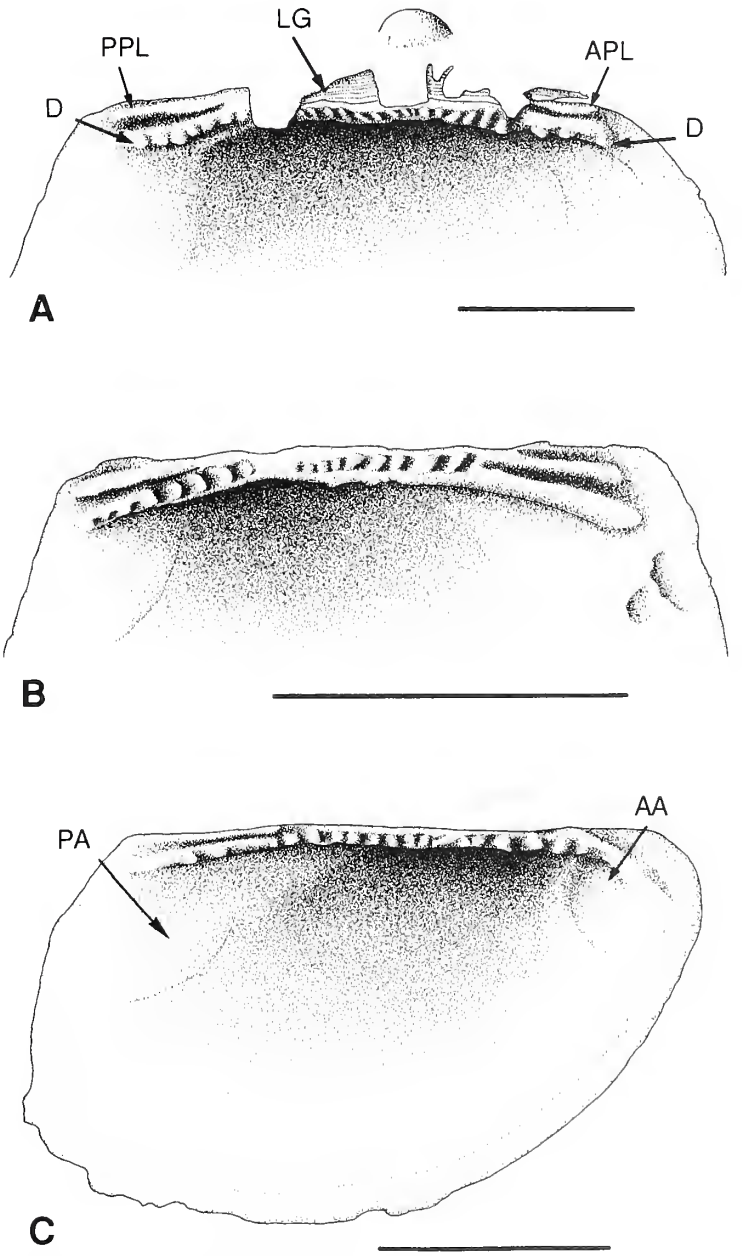

TEXT-FIG. 3. Hinge details of *Trecanolia acincta* gen. et sp. nov. The diagrams are *Camera lucida* drawings of latex casts. A, BGS DEX 2869A, holotype; left valve. B, BGS DEX 2869B; right valve. C. BGS DEX 2834B; left valve. AA = anterior adductor muscle scar; APL = anterior pseudolateral teeth; D = denticles; LG = duplivincular ligament and cardinal area; PA = posterior adductor muscle scar; PPL = posterior pseudolateral teeth. Scale bars represent 3 mm.

The dental arrangement consists of numerous cardinal teeth beneath the cardinal area, terminated by anterior and posterior pseudolaterals. The cardinal teeth are simple, peg-like, are elongated either perpendicular to the hinge line or radiate dorsally, and extend underneath the ligament area and between the anterior and

posterior adductor muscle scars; the number of teeth varies from seven to 12 in juveniles, and from 13 to 18 in more adult specimens; juveniles have a subumbonal edentulous area, but adults have a continuous series of teeth; intermediates display either a very small edentulous area or have small, poorly defined and fused teeth beneath the umbo. The anterior pseudolaterals usually number two and have two to four denticles on the underside of the ventral pseudolateral. The posterior pseudolaterals also number two, but are more elongate; denticles on the underside of the ventral pseudolateral are generally absent in smaller specimens, but number up to seven in the largest individual.

The adductor muscle scars are anisomyarian. The anterior adductor is small, ovate and well impressed; it is positioned ventral to the anteriormost part of the hinge. The posterior adductor is larger, but less well impressed and only visible in a few specimens; the scar is located ventral to the posterior pseudolateral teeth. No pedal muscle scars have been observed. A simple pallial line connects the adductor scars.

Only the holotype displays a chevron-shaped, external, duplivincular ligament on a small, triangular interumbonal or cardinal area, between the beak and the hinge plate.

The external prosopon consists of regularly spaced, commarginal growth lines.

Remarks. The holotype and paratypes were collected by Squirrel and White (1978, pl. 3, figs 12–14, illustrating specimens BGS DEX 2869A, 2869B and 2848) and named as 'Bivalve gen. et sp. nov.'. We have been unable to supplement this collection made in the 1960s, as the section was probably infilled soon after excavation. Within the studied collections, *T. acincta* accounts for approximately one-quarter of the abundant and diverse bivalve fauna. All of the specimens have been slightly deformed tectonically, so that biometric data and details of the shell outline are highly variable.

T. acincta may also occur in the Wenlock of Wisconsin. Watkins (1996) studied the palaeoecology of Silurian reef bivalves from the Racine Formation (mid Sheinwoodian to latest Wenlock in age). Four specimens from this sequence were named as *Leiopteria* cf. *undata* (Hall, 1852), but display some characters that are diagnostic of *T. acincta* (see Watkins 1996, fig. 2E). Denticles are visible beneath the dorsal anterior pseudolateral tooth, whilst the posterior pseudolateral is rather elongate. *L.* cf. *undata* also has a similar shell outline and umbonal area to *T. acincta*. Watkins commented that *L.* cf. *undata* was nearly equivalved (the equivalved condition is diagnostic for the Frejidae but not the Pterineidae), which suggests that this bivalve is not a *Leiopteria* nor indeed any other pterioidean. However, it is uncertain whether these specimens are Laurentian examples of *T. acincta*. This can only be established after examination of the material.

The dental arrangement displays a transition from juvenile to adult stages in this small population. The juvenile shells lack the subumbonal cardinal teeth (e.g. BGS DEX 2869B; Text-fig. 3B) and have either few or no denticles on the underside of the ventral posterior pseudolateral. However, a specimen (BGS DEX 2834B; Text-fig. 3C) transitional between the juvenile and adult stages has fused, poorly defined subumbonal teeth in a position corresponding with the edentulous space in smaller specimens. The largest valve known (BGS DEX 2869A; Text-fig. 3A), which probably represents the final ontogenetic stage, has a complete series of cardinal teeth and seven posterior denticles.

Genus USKARDITA gen. nov.

Derivation of name. The combination of Usk (a south-east Wales town located near the type locality) and *cardita* (Spanish for a small vessel, referring to a mollusc).

Type species. *Uskardita mikraulax* sp. nov., by monotypy.

Diagnosis. Inequilateral, equivalved, sub-orbicular, opisthocline, moderately inflated valves, with elevated, narrow, conspicuous umbo and weakly prosogyrate beaks; cardinal area large, uniconvex lens-shaped, with chevron patterned, external duplivincular ligament; hinge line straight; dentition of approximately 18 cardinal teeth, terminated by three ventrally divergent posterior pseudolaterals and two arcuate, ventrally divergent cardinal teeth; external prosopon of numerous, regular concentric growth lines.

TABLE 1. Comparison of the diagnostic characters of the genera *Alytodonta*, *Uskardita* and *Freja*.

	Alytodonta	*Uskardita*	*Freja*
Shell outline	Sub-orbicular	Sub-orbicular to ovate	Sub-orbicular to ovate
Umbones	Low	Elevated and erect	Low
Beaks	Prosogyrate	Weakly prosogyrate	Orthogyrate
Cardinal area	Small, but elongate	Large and uniconvex	Small and triangular
Ligament	Duplivincular, amphidetic with several furrows	Duplivincular, chevron shaped, several furrows	Duplivincular, chevron shaped, furrows very numerous
Pseudocardinals	11, subumbonal, diverge ventrally	Approximately 18, occupy most of hinge, normal to hinge line	13 in holotype, occupy centre of hinge plate, normal to hinge line
Anterior pseudolaterals	Five, of which two are small and one ventrally bifurcates, diverge ventrally	Two, small, arcuate, diverge ventrally	Three, straight, radiate ventrally but at a very low angle
Posterior pseudolaterals	Three, elongate, decrease in length dorsally, diverge ventrally	Three, short, decrease in length dorsally, diverge ventrally	Three, short, central tooth most elongate, almost parallel with hinge line
Musculature	Anisomyarian adductors plus ?posterior pedal retractor	Unknown	Anisomyarian adductors plus posterior byssal/pedal retractor, gill attachment site and visceral muscle scars
External prosopon	Uncertain	Conspicuous commarginal growth lines	Faint commarginal growth lines
Age	Early Llandovery	? Sheinwoodian, early Wenlock	Late Wenlock

Remarks. Uskardita is known from only seven specimens, but displays characters that warrant the erection of a new genus. *Uskardita* is closely related to both *Alytodonta* and *Freja*, and is most probably an evolutionary intermediate between the two genera. The shell characters are compared in Table 1.

Stratigraphical range. 'Wenlock Shale', Sheinwoodian, of south-east Wales.

Uskardita mikraulax gen. et sp. nov.

Text-figures 4–5

Derivation of name. From the Greek adjective *mikraulax* (= small furrows), referring to the numerous ligament furrows on the cardinal area.

Holotype. BGS GSM 22187, a left valve with a fragmented ventral margin, preserved as recrystallized calcite.

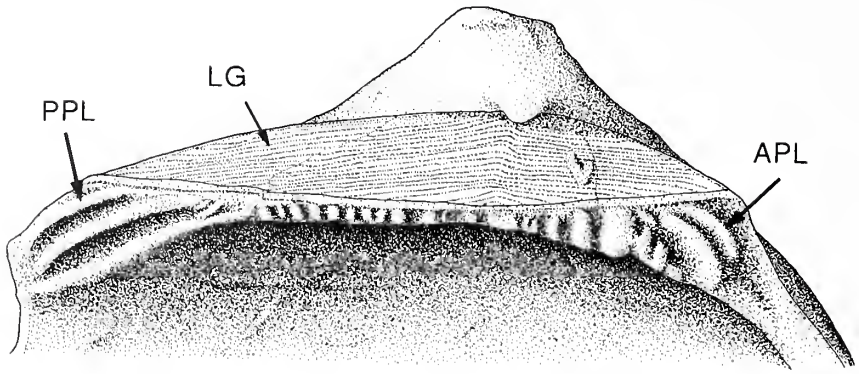

TEXT-FIG. 4. *Uskardita mikraulax* gen. et sp. nov.; holotype, BGS GSM 22187; hinge detail of a left valve. APL = anterior pseudolateral teeth; LG = duplivincular ligament positioned on cardinal area; PPL = posterior pseudolateral teeth.

Paratypes. BGS GSM 21956 (XRP), 22029 (XRF), 22183 (XAP), 22184 (IRC), 22185 (XRC) and 22186 (XRP); all assumed to be from the same locality as the holotype.

Type horizon and locality. 'Wenlock Shale' exposed at Craig y Garcyd, on the southern banks of the River Usk, 2 km north-west of Usk, Monmouthshire (grid reference SO 360 024).

Measurements

BGS GSM	AL	L	H	W	OL	CL	CH	UH	AL/L	H/L	OL/L	H/2 × W	U°	α°
21956	9·5	25·1	~ 24·4	7·5	~ 24·4	~ 16·0	~ 2·5		0·38	0·97	0·97	1·63	132	57
22185	10·3	29·1	25·6	8·2	27·1	~ 18·0	3·0	2·8	0·35	0·88	0·93	1·56	130	54
22186	~ 7·0	~ 23·7	~ 20·9	6·9	~ 23·9	~ 15·0	~ 2·3	~ 2·0	0·29	0·87	1·00	1·51	125	54
22187	8·1	~ 23·7	24·5	~ 7·9	~ 23·0	15·0	2·4	2·5	0·34	1·03	0·97	1·55	97	60

Diagnosis. As for genus.

Description. Inequilateral, equivalved, opisthocline, moderately inflated, medium sized, sub-orbicular to ovate shells with a straight hinge line and gently convex anterior, posterior and ventral margins; the total length is slightly less than the height and oblique length (mean H/L = 0·94; mean OL/L = 0·97); the shell outline is only moderately oblique (mean α° = 56·3); maximum convexity is positioned approximately mid-height and mid-length. The umbones are one-third of the total length from the anterior margin (AL/L averages 0·34) and are conspicuous and elevated above both the cardinal area and the hinge plate; the beaks are weakly prosogyrate and poorly defined.

The dentition consists of pseudocardinal and pseudolateral teeth; the teeth and sockets extend over the entire hinge plate without edentulous spaces. The holotype has 18 small pseudocardinals on the narrow, central portion of the hinge plate which increase in size from the subumbonal area to the anterior; the large anteriormost pseudocardinal consists of three fused small teeth, adjacent to the anterior pseudolaterals. Two small, gently arcuate anterior pseudolaterals are located at the anterior extremity of the hinge plate; the posterior of the two is larger and thicker. Three elongate posterior pseudolaterals also radiate ventrally; the central and posterodorsal teeth are convex when viewed from the posterodorsal direction, whilst the anteroventral tooth is straight to slightly concave.

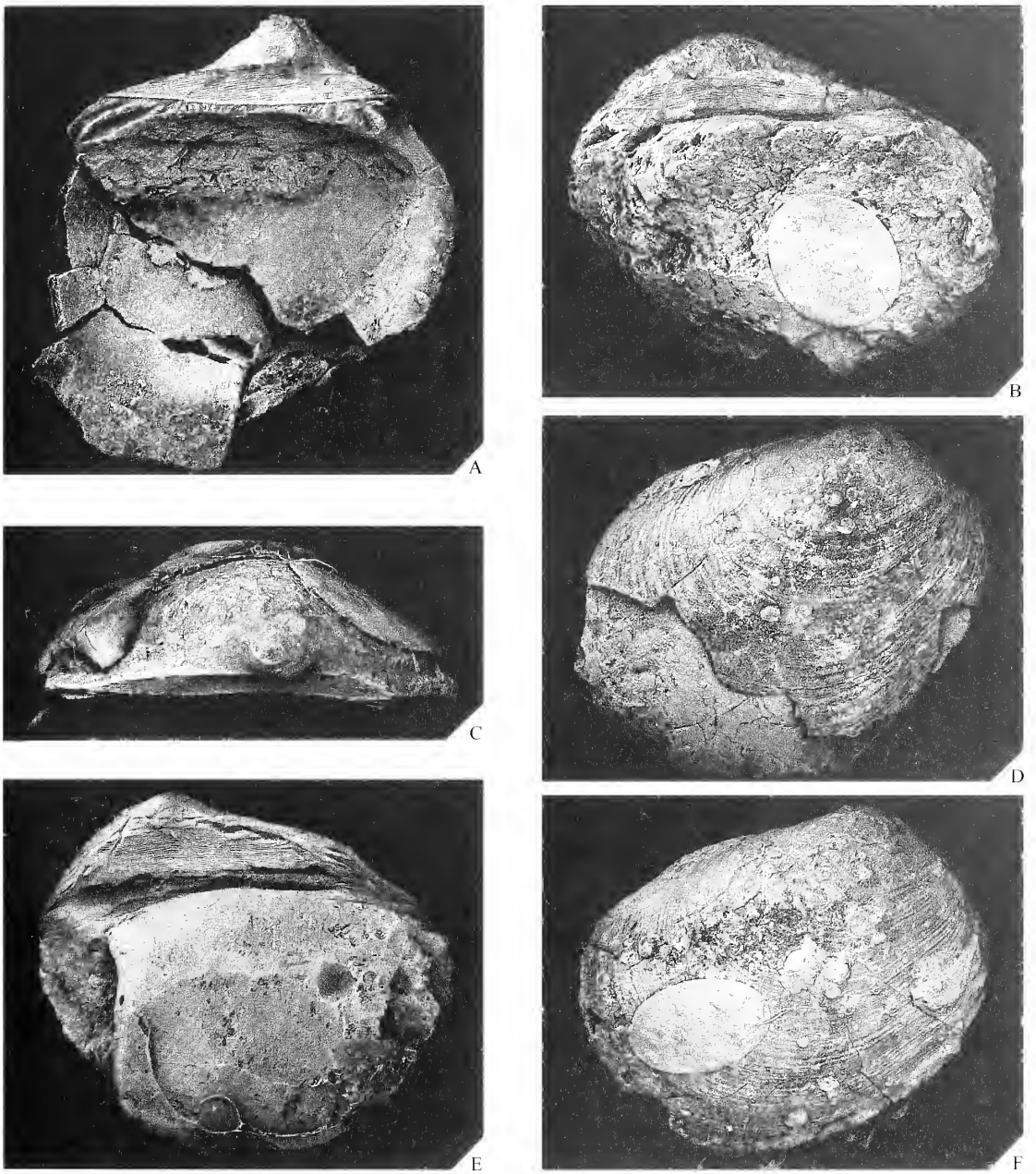

TEXT-FIG. 5. *Uskardita mikraulax* gen. et sp. nov.; Wenlock Shale, Craig y Garcyd, on the south bank of River Usk, 2 km north-west of Usk, Monmouthshire; grid reference SO 360024. A, BGS GSM 22187, holotype; interior of left valve preserved as calcite; × 2·5. B, BGS GSM 22186; right valve displaying cardinal area; × 2·5. C, dorsal view of holotype; × 2·5. D, BGS GSM 22186; exterior view; × 2·5. E–F, BGS GSM 22185; interior and exterior view of a right valve; × 2.

A large, uniconvex lens-shaped cardinal or interumbonal area is situated between the hinge plate and the beak, which supports an external, amphidetic duplivincular ligament; the ligament covers the entire cardinal area and consists of numerous chevron-shaped furrows for the insertion of the ligament lamellar layers; the apices of the chevrons are located slightly posterior to the beaks. Approximately 20 furrows have been measured on the holotype (22 on BGS GSM 22185 and 13 on BGS GSM 22186).

The shell exterior is ornamented with regularly spaced, commarginal growth lines. Muscle scars are not preserved.

Remarks. It is assumed that all the specimens described were collected from a single locality within the 'Wenlock Shale', exposed at Craig y Garcyd on the River Usk, Monmouthshire. The labels that accompany the material either describe the locality simply as 'Usk' or 'Craig y Garcyd, Usk'. The recrystallized calcite preservation of brachiopods, trilobites and a single palaeotaxodont bivalve collected from the 'Wenlock Shale' at Craig y Garcyd (stored within the National Museum of Wales) help to confirm this site as the type locality.

PHYLOGENY

The description of the bivalve genus *Catamarcaia* by Sánchez and Babin (1993, 1994: type species *C. chaschuilensis* Aceñolaza and Toselli, 1977) from the Middle Arenig of Argentina, has resulted in a revision of the early evolutionary history of the Arcoidea (characters summarized in Text-fig. 6). It is apparent that *Catamarcaia* is an innovative genus. Cope (1997*a*) proposed that a hypothetical ancestral arcoidean evolved from a *Glyptarca*-like palaeoheterodont during the Tremadoc with the appearance of a primitive duplivincular ligament and arcoidean dental arrangement. With minor modification of the dentition and ligament this gave rise both to *Catamarcaia* and, after the loss of the subumbonal dentition and shortening of the hinge-plate, to an early cyrtodontoidean lineage. This conclusion suggests that the Arcoidea (Neotaxodonta) appeared before the cyrtodontoidean pteriomorphs and conflicts with earlier phylogenetic schemes. Neotaxodonts are unknown from the middle or upper Ordovician; this is unsurprising if one considers that the arcoids were extremely rare and occupied a near-shore shelf environment. Both of the new South Wales genera are from localities very close to the shoreline of Pretannia, whilst *Alytodonta* also occurred in another close inshore situation at Girvan. The preservation potential of inshore facies is extremely low, resulting in a depleted fossil record.

In addition to *Trecanolia* and *Uskardita*, two other arcoid genera are known from the Silurian. *Freja fecunda* Liljedahl, 1984 was the first to be described. *Alytodonta gibbosa* Cope (1997*b*, pp. 739–741, pl. 4, figs 1, 5, 8) was originally described as a *Cyrtodonta* by Hind (1910), but Liljedahl (1984) showed that its continuous dentition precluded such an assignment. He concluded (1984, fig. 16) that both '*C.*' *gibbosa* and *Freja fecunda* were closely related and shared a radical arcoid ancestor. Furthermore, Liljedahl stated that the radical arcoid descended from an 'actinodont' and was the ancestor of the Cyrtodontoidea. This view was followed by Amler (1989).

With the discovery of *Catamarcaia*, Liljedahl's hypothesis is probably in accordance with the fossil evidence. The rapid development of the duplivincular ligament from the hypothetical ancestor of *Catamarcaia*, postulated by Sánchez (1995, p. 344), may have continued during the Ordovician. If the cardinal area and opisthodetic duplivincular ligament of *Catamarcaia* began to extend towards the anterior, an amphidetic, chevron-shaped duplivincular ligament could have evolved – as seen in Silurian arcoideans. Thomas (1978) and Morris (1979) commented that the chevron-shaped arcoid ligament evolved from the cyrtodontids and early Ambonychioidea. Such a scheme must be questioned if one compares the ligaments of *Catamarcaia* and a typical lower Ordovician cyrtodontid, such as *Cyrtodonta saffordi* (Hall, 1859). Both ligament types are apparently composed of alternating lamellar and fibrous layers to the posterior of the umbones. However, the layers in *Cyrtodonta saffordi* are parallel to the hinge axis and at no point intersect the dorsal hinge margin, whereas in *Catamarcaia* the layers radiate and diverge ventrally so that they terminate on the hinge margin. It is suggested that the chevron-shaped ligament seen in the Silurian frejids is more closely related to the *Catamarcaia* ligament than to the cyrtodontid ligament. If it is assumed that the latter

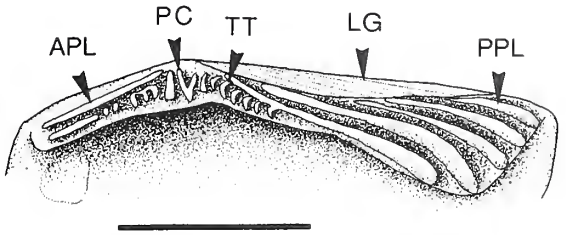

TEXT-FIG. 6. Simplified sketch of the hinge of *Catamarcaia*, modified from Sánchez 1995, figure 1. APL = anterior pseudolateral tooth; LG = duplivincular ligament; PC = pseudocardinal teeth; PPL = posterior pseudolateral teeth; TT = taxodont teeth. Scale bar represents 6 mm.

is more primitive, the fact that the earliest cyrtodontids are from the upper Tremadoc (Pojeta and Gilbert-Tomlinson 1977; Shergold *et al.* 1991) and thus pre-date *Catamarcaia*, indicates that they evolved earlier and feasibly from the hypothetical radical arcoid proposed by Liljedahl (1984) and Cope (1997*a*). The chevron-shaped ligament may have arisen through anterior extension of the opisthodetic half-chevron resulting in another ventrally divergent half-chevron in front of the umbones. An amphidetic full chevron, as seen in the Frejidae, may have arisen subsequently.

The phylogeny of the arcoidean dentition has been discussed by many authors (e.g. Stanley 1972; Pojeta 1978; Thomas 1978; Sánchez 1995). Prior to the recent work of Cope (1997*a*, 1997*b*) it was believed that the arcoidean dental arrangement evolved from the cyrtodontids by the loss of the subumbonal edentulous space. However, the early arcoidean *Catamarcaia* displays a dental arrangement sharing more affinities with *Glyptarca* and the early cycloconchids than the cyrtodontids (Cope 1997*a*, 1997*b*). This again conflicts with the contention that the cyrtodontids are more primitive than the arcoideans. If the cyrtodontids were ancestral to the arcoideans and evolved directly from a *Glyptarca*-like or an 'actinodont' ancestor (as proposed by Pojeta 1978; Thomas 1978; Morris 1979), this would require the loss of the subumbonal dentition, followed by the infilling of the resulting lacuna to produce an arcoidean hinge (Cope 1997*a*, p. 128). Cope (1997*a*) remarked that such a scheme was not parsimonious and that a phylogeny whereby the arcoideans evolved from an ancestor with a continuous dentition was more likely. He also concluded that a hypothetical ancestral arcoid with cardinals and posterior laterals and a newly evolved duplivincular ligament gave rise to both the Cyrtodontidae and a *Catamarcaia*-like bivalve during the Tremadoc.

Knowledge of Lower Palaeozoic bivalve shell microstructure is very limited and extrapolating Ordovician and Silurian bivalve phylogeny using shell microstructural details of younger material must be treated with caution. Cope (1997*b*, pp. 727–733, text-fig. 1) has fully reviewed the early evolution of the shell microstructure. It was concluded that a parent aragonite (prismatic/crossed-lamellar/complex crossed-lamellar) arcoidean shell microstructure probably descended directly from the aragonitic prismato-nacreous palaeoheterodont shell, rather than a calcitic outer layered shell (that probably characterized the early cyrtodontids, pterioids and ambonychioids). Furthermore, as each of these groups is tentatively considered to have had crossed-lamellar middle and complex crossed-lamellar inner shell layers, the most parsimonious phylogeny would dictate that the cyrtodontids evolved from the neotaxodonts with the development of an outer calcitic layer (Cope 1997*a*, 1997*b*).

Previous interpretations regarding the subsequent evolution of the Arcoidea during the remainder of the Palaeozoic have been somewhat confused because the Arcoidea were considered to have evolved directly from the cyrtodontids. As a consequence, malacologists tried to compare possible 'arcoidean descendants' with the cyrtodontid dentition. Further confusion resulted from lack of knowledge of some early Ordovician putative *Parallelodon* (as discussed above).

The fossil record cannot yet confirm that the earliest parallelodontids were more closely related to a *Catamarcaia*-like bivalve than the frejids. Indeed, both groups can be conveniently linked with a *Catamarcaia*-like ancestor (Text-fig. 7). The earliest known frejid, *Alytodonta gibbosa* Cope, 1997*b* (from the Lower Llandovery of Ayrshire), has a continuous series of ventrally diverging pseudocardinal and pseudolateral teeth and an amphidetic, slightly chevron-shaped duplivincular ligament. The subumbonal dentition is reminiscent of the bifurcating subumbonal pseudocardinals and the taxodont teeth seen in *Catamarcaia*. In addition, *Alytodonta* has three posterior

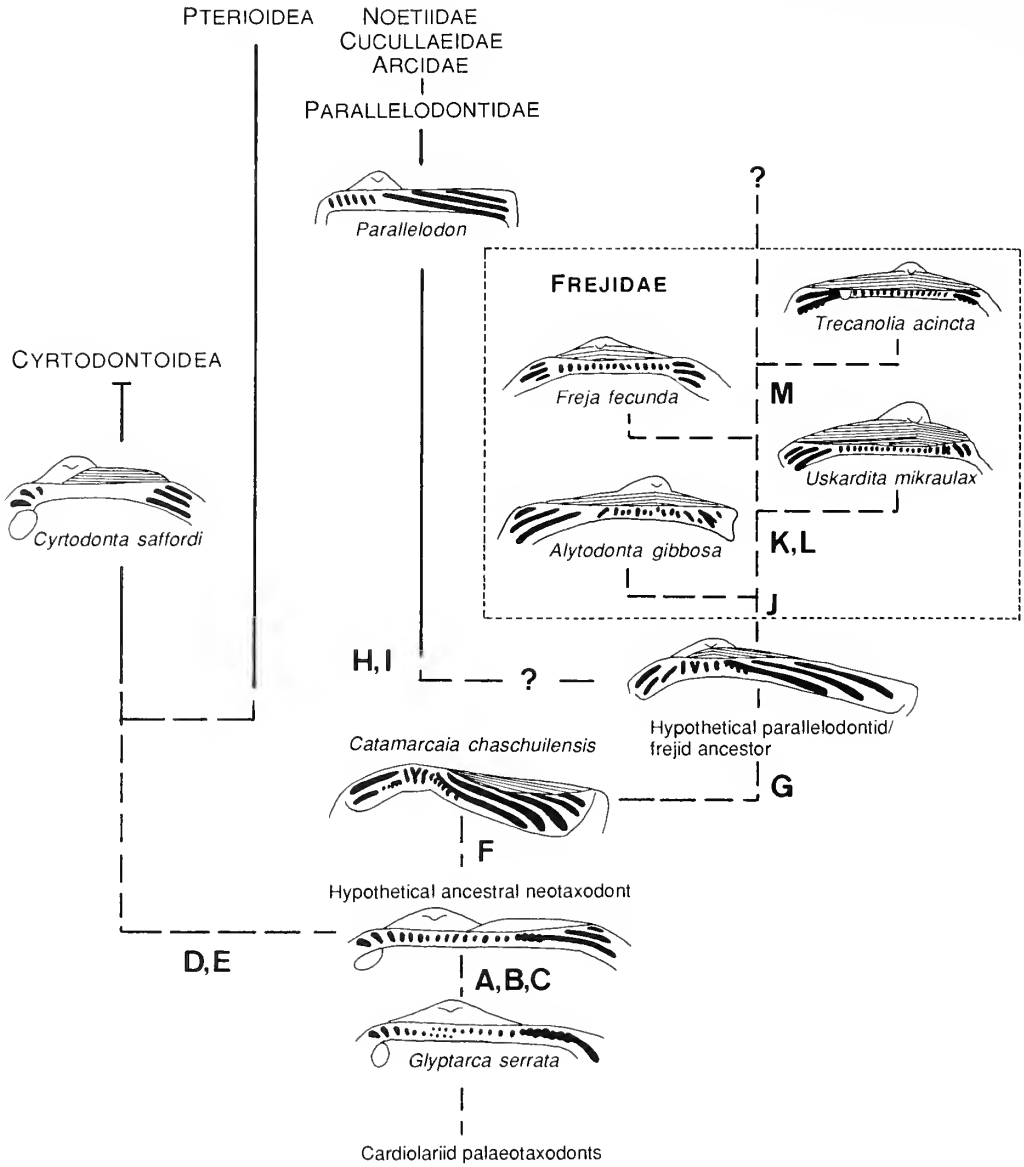

TEXT-FIG. 7. The origin and early evolutionary history of the order Arcoida: a possible phylogenetic scheme. Unbroken lines are based on fossil evidence, broken lines are hypothetical. The four representatives of the Frejidae are highlighted. The scheme is based on the following characters: A = loss of subumbonal dental overlap; B = appearance of an opisthodetic preduplivincular ligament; C = origin of a crossed-lamellar middle layer and complex-crossed-lamellar inner shell layer; D = loss of subumbonal dentition; E = origin of a prismatic calcite outer shell layer; F = appearance of an opisthodetic duplivincular ligament; G = development of an amphidetic duplivincular ligament; H = anteriorwards movement of umbones; I = rotation of anterior teeth to a ventrally convergent position; J = increase in number of pseudocardinals; K = further increase in pseudocardinals and reduction in pseudolateral teeth length; L = enlargement of cardinal area and duplivincular ligament; M = development of denticles.

pseudolaterals that resemble the five seen in *Catamarcaia*. A hypothetical intermediate between the first frejid and the Arenig arcoid would probably display a half chevron-shaped ligament approaching the amphidetic state. The taxodont series seen in *Catamarcaia* may have then separated from the posteriorly migrating posterior pseudolaterals and the anterior pseudocardinals probably rotated anticlockwise.

Between the Lower Llandovery and the Lower Wenlock, evidence for further evolution within the Frejidae is provided by *Uskardita mikraulax*. This genus has a much enlarged cardinal area with numerous lamellar and fibrous ligament layer alternations (preserved as furrows) displaying conspicuous chevrons. *Uskardita* is the first arcoidean known with a chevron-shaped duplivincular ligament that is comparable to that of some of the Mesozoic to Recent Arcidae, Parallelodontidae and Cucullaeidae. The evolutionary significance of the large number of alternating lamellae and fibrous layers is unclear. Experimental work by Thomas (1976) on recent arcoids suggested that the rapid transverse growth of the ligament (as seen in *Uskardita*) results in numerous alternations of fibrous and lamellar layers, widely separated umbones and highly divergent cardinal areas. He found that the rapid growth causes frequent splitting of the ligament layers dorsal to the hinge line resulting in a weak, transversely thin ligament. A weak ligament is disadvantageous for burrowing because it only weakly resists shear stresses and resistance (Thomas 1976, p. 81). It may be concluded that Llandovery and Wenlock arcoideans were evolving from their infaunal ancestors towards a semi-infaunal, byssate life habit.

The dentition of *Uskardita* has clear affinities with that of *Alytodonta*. However, *Uskardita* has shorter pseudolaterals, and more numerous pseudocardinals that are perpendicular to the hinge line. This dental arrangement appears to be intermediate between *Alytodonta* and *Freja* and suggests that during the Wenlock, pseudocardinals began to cover most of the hinge plate (Text-fig. 7). This is of interest because the later arcids, cucullaeids and noetiids have dentitions that are dominated by small pseudocardinal teeth (Cox *et al.* 1969–71).

Two frejid genera are known from the Upper Wenlock, and both can be readily derived from *Uskardita*. *Freja* has similarly arranged pseudocardinals, but displays a further modification to the pseudolaterals and the interumbonal duplivincular ligament. The ventrally diverging anterior and posterior pseudolaterals appear to have rotated so that they are almost parallel with the hinge line. The cardinal area and ligament have reduced in area, so that the umbones are less divergent and closer to the hinge. A reduced ligament may correspond with the small size of *Freja* (the majority of the specimens are less than 10 mm) and this may prevent comparison with *Uskardita*.

The phylogenetic position of *Trecanolia* is more difficult to determine. The genus is probably of similar late Wenlock age to *Freja*. The dental arrangements would suggest that *Trecanolia* is more derived from the ancestral arcoid (Text-fig. 7). In some specimens the pseudocardinal teeth have rotated to a ventrally convergent position which is typical of the arcids and noetiids. Furthermore, the more mature valves have denticles on the underside of the ventral pseudolateral teeth that resemble the pseudocardinals. This may mark a preliminary stage before the evolution of an entirely pseudocardinal dentition, as seen in the Jurassic arcoideans, but such a progression has hitherto not been recorded in the Upper Palaeozoic.

The origins of the later arcoidean families can only be tentatively suggested because of the limited material from the Palaeozoic. The Parallelodontidae may have evolved from a similar ancestor to the Frejidae (considered as a hypothetical parallelodontid/frejid ancestor in Text-fig. 7). The elongate posterior pseudolaterals and ventrally convergent pseudocardinals could have originated from *Catamarcaia*, yet they have a ligament that is more closely related to the frejids. It is therefore proposed that a hypothetical ancestor gave rise to the Frejidae and Parallelodontidae during the mid to late Ordovician; this expains their rather similar cardinal areas and disparate dental arrangements.

The evolution of the Arcidae, Cucullaeidae and Noetiidae during the Mesozoic has been discussed by Stanley (1972, pp. 181–182, text-fig. 15). It was proposed that the parallelodontid subfamily Grammatodontinae arose from a late *Parallelodon* species in the Triassic, and that this subfamily was the ancestor of the family Arcidae. In turn, the families Cucullaeidae and Noetiidae

probably descended from the arcids during the Jurassic period (Stanley 1972). Papers that discuss post-Palaeozoic arcoid evolution include those by Stanley (1972) and Thomas (1976), and these should be referred to for further details.

Acknowledgements. Access to the British Geological Survey collections was kindly provided by Mr S. P. Tunnicliff (British Geological Survey). Miss S. A. Bonnett (Department of Earth Sciences, Cardiff University and Department of Geology, National Museum of Wales) is also acknowledged for photographic assistance. VAR thanks the Department of Earth Sciences, Cardiff University, for funding this research and Professor M. G. Bassett and Dr R. M. Owens for access to facilities in the National Museum of Wales. Comments from an anonymous referee improved part of the manuscript.

REFERENCES

ACEÑOLOZA, G. F. and TOSELLI, A. J. 1977. Observaciones geologicas sobre el Ordovícico de la zona de Chaschuil, Provincia de Catamarca. *Acta Geologica Lilloana*, **14**, 55–81.

AMLER, M. R. W. 1989. Die Gattung *Parallelodon* Meek and Worthen 1866 (Bivalvia, Arcoida) im mitteleuropäischen Unterkarbon. *Geologica et Palaeontologica*, **23**, 53–69, pls 1–2.

BABIN, C. 1966. *Mollusques Bivalves et Céphalopodes du Paléozoïque armoricain*. Imprimerie Commerciale et Administrative, Brest, 471 pp., 114 text-figs, 18 pls.

BARROIS, C. 1891. Mémoire sur la faune du grès armoricain. *Annales de la Société géologique du Nord*, **19**, 134–351, 5 pls.

CARTER, R. M. 1971. Revision of Arenig Bivalvia from Ramsey Island, Pembrokeshire. *Palaeontology*, **14**, 250–261, pls 38–39.

COPE, J. C. W. 1995. The early evolution of the Bivalvia. 361–370. *In* TAYLOR, J. D. (ed.). *Origin and evolutionary radiation of the Mollusca*. Oxford University Press, Oxford, xiv + 392 pp. [Dated 1996].

—— 1996. Early Ordovician (Arenig) bivalves from the Llangynog Inlier, South Wales. *Palaeontology*, **39**, 979–1025.

—— 1997*a*. Affinities of the early Ordovician bivalve *Catamarcaia* Sánchez & Babin, 1993 and its role in bivalve evolution. *Geobios, Mémoire Spécial*, **20**, 127–131.

—— 1997*b*. The early phylogeny of the class Bivalvia. *Palaeontology*, **40**, 713–746.

COX, L. R. 1960. Thoughts on the classification of the Bivalvia. *Proceedings of the Malacological Society of London*, **34**, 60–88.

—— and 24 others. 1969–71. *In* MOORE, R. C. (ed.). *Treatise on invertebrate paleontology. Part N. Mollusca 6, Bivalvia*. Volume 1, 1969: xxxviii + *N*1–*N*489; Volume 2, 1969: ii + *N*491–*N*952; Volume 3, 1971: iv + *N*953–*N*1124. Geological Society of America and University of Kansas Press, Boulder, Colorado and Lawrence, Kansas.

DOUVILLÉ, H. 1912. Classification des lamellibranches. *Bulletin de la Société Géologique de France, 4ème Série*, **12**, 419–467.

HALL, J. 1852. Palaeontology, volume 2, containing descriptions of the organic remains of the lower middle division of the New York System (equivalent in part to the middle Silurian rocks of Europe). *Natural History of New York*. Albany, 362 pp., 85 pls.

—— 1859. Palaeontology: containing descriptions and figures of the organic remains of the lower Helderberg group and the Oriskany sandstone. *Geological Survey of New York*, **3**, 1855–1859, (2), i–xii + 1–532.

HICKS, H. 1873. On the Tremadoc rocks in the neighbourhood of St David's, South Wales and their fossil contents. *Quarterly Journal of the Geological Society of London*, **29**, 39–52.

HIND, W. 1910. The lamellibranchs of the Silurian rocks of Girvan. *Transactions of the Royal Society of Edinburgh*, **47**, 479–548, pls 1–5.

KOROBKOV, I. A. 1954. *Spravochnik i metodicheskoe rukovodstvo po treticlmum mollyuskam Plastinchatozhabernye*. Nauchno-tecnoï Isledov, Leningradskoi Otdelenie, 444 pp., 96 pls. [In Russian].

LAMARCK, J. P. B. A. de M. de 1809. *Philosophie zoologique, ou exposition des considérations relatives à l'histoire naturelle des animaux, la diversité de leur organisation et des facultés qu'ils en obtiennent, aux causes physiques qui maintiennent en leur la vie, et donnent lieu au mouvement qu'ils exécutent; enfin, à celles qui produisent les unes des sentiments et les autres l'intelligence de ceux qui en sont doués*. Dentu, Paris, Vol. 1, 422 pp; Vol. 2, 473 pp.

LILJEDAHL, L. 1984. Silurian silicified bivalves from Gotland. *Sveriges Geologiska Undersökning, Series C*, **804**, 1–82.

MORRIS, N. J. 1979. On the origin of the Bivalvia. 381–413. *In* HOUSE, M. R. (ed.). *The origin of major invertebrate groups*. Systematics Association Special Volume 12, 515 pp.

NEWELL, N. D. 1954. Status of invertebrate paleontology, 1953, V. Mollusca. *Bulletin of the Museum of Comparative Zoology, Harvard University*, **112**, 161–172.

—— 1965. Classification of the Bivalvia. *American Museum Novitates*, **2206**, 1–25.

POJETA, J. 1971. Review of Ordovician pelecypods. *Professional Paper of the United States Geological Survey*, **695**, i–iv + 1–46, pls 1–20.

—— 1978. The origin and early taxonomic diversification of pelecypods. *Philosophical Transactions of the Royal Society of London, Series B*, **284**, 225–246, pls 1–15.

—— and GILBERT-TOMLINSON, J. 1977. Australian Ordovician pelecypod molluscs. *Bulletin of the Bureau of Mineral Resources, Geology and Geophysics*, **174**, 1–64, pls 1–29.

SÁNCHEZ, T. M. 1995. Comments on the genus *Catamarcaia* Sánchez & Babin and the origin of the Arcoida. *Geobios*, **28**, 343–346.

—— and BABIN, C. 1993. Un insolite mollusque bivalve, *Catamarcaia* n. g., de l'Arenig (Ordovicien inférieur) d'Argentine. *Comptes rendus de l'Académie des Sciences, Paris, Série 2*, **316**, 265–271.

—— —— 1994. Los géneros *Redonia* y *Catamarcaia* (Mollusca, Bivalvia) de la Formación Suri (Ordovício Temprano, oeste de Argentina) y su interés palaeobiogeográfico. *Revista Española de Paleontologia*, **9**, 81–90.

SHERGOLD, J. H., GORTER, J. D., NICOLL, R. S. and HAINES, P. W. 1991. Stratigraphy of the Pacoota Sandstone (Cambrian–Ordovician), Amadeus Basin, N. T. *Bulletin of the Bureau of Mineral Resources, Geology and Geophysics*, **237**, 1–14.

SQUIRREL, H. C. and WHITE, D. E. 1978. Stratigraphy of the Silurian and Old Red Sandstone of the Cennen Valley and adjacent areas, south-east Dyfed, Wales. *Report of the Institute of Geological Sciences*, **78/6**, 1–45.

STANLEY, S. M. 1972. Functional morphology and evolution of byssally attached bivalve mollusks. *Journal of Paleontology*, **46**, 165–212.

STOLICZKA, F. 1870–71. Cretaceous fauna of southern India. 3. The Pelecypoda, with a review of all known genera of this class, fossil and Recent. *Geological Survey of India, Palaeontologica Indica, Series 6*, **3**, 1–537.

TAYLOR, J. D., KENNEDY, W. J. and HALL, A. 1969. The shell structure and mineralogy of the Bivalvia. Introduction. Nuculacea–Trigonacea. *Bulletin of the British Museum (Natural History), Zoology Series, Supplement*, **3**, 125–29 pls.

—— —— —— 1973. The shell structure and mineralogy of the Bivalvia. II. Lucinacea–Clavagellacea, conclusions. *Bulletin of the British Museum (Natural History), Zoology Series*, **22**, 256–294, pls 1–15.

THOMAS, R. D. K. 1976. Constraints of ligament growth, form and function on evolution in the Arcoida (Mollusca: Bivalvia). *Paleobiology*, **2**, 64–83.

—— 1978. Shell form and the ecological range of living and extinct Arcoida. *Paleobiology*, **4**, 181–194.

VOGEL, K. 1962. Muscheln mit Schlosszähnen aus dem spanischen Kambrium und ihre Bedeutung für die Evolution der Lamellibranchiaten. *Akademie der Wissenschaft und der Literatur in Mainz, Mathematisch-Naturwissenschaftlichen Klasse, Abhandlungen, Jahrgang* **1962** (4), 193–244, pls 1–5.

WALLER, T. R. 1978. Morphology, morphoclines and a new classification of the Pteriomorphia (Mollusca: Bivalvia). *Philosophical Transactions of the Royal Society of London, Series B*, **284**, 345–365.

—— 1990. The evolution of ligament systems in the Bivalvia. 49–71. *In* MORTON, B. (ed.). *The Bivalvia – Proceedings of a Memorial Symposium in Honour of Sir Charles Maurice Yonge, Edinburgh, 1986*. Hong Kong University Press, Hong Kong.

WATKINS, R. 1996. Palaeoecology of Silurian reef bivalves, Racine Formation, North America. *Lethaia*, **29**, 171–180.

V. ALEXANDER RATTER
JOHN C. W. COPE
Department of Earth Sciences
Cardiff University
P.O. Box 914
Cardiff CF1 3YE, UK

Typescript received 27 January 1998
Revised typescript received 11 March 1998

A NEW AMMONITE GENUS FROM THE LOWER JURASSIC (UPPER SINEMURIAN) OF DORSET, ENGLAND

by DESMOND T. DONOVAN

ABSTRACT. *Bagnolites stuarti* gen. et sp. nov. is described from the lower part of the Lias Group (Lower Jurassic, Upper Sinemurian, Obtusum Zone, Stellare Subzone) of the Dorset coast. It is characterized by an involute shell with smooth, trigonal whorls and a distinctive suture line. Its systematic assignment is uncertain but it may be a derivative of the family Arietitidae.

AMMONITES from the Lias Group of the Dorset coast have been studied for more than two hundred years, and the finding of a new form is now a rare event. This paper reports an ammonite found by the late Stuart Bagnoli which does not belong to a previously described genus.

SYSTEMATIC PALAEONTOLOGY

Suborder AMMONITINA Hyatt, 1889
Superfamily PSILOCERATACEAE Hyatt, 1867
Family ARIETITIDAE Hyatt, 1874?
Subfamily ASTEROCERATINAE Spath, 1946?

Genus BAGNOLITES gen. nov.

Derivation of generic and specific names. For the finder, the late Stuart Bagnoli.

Type species. Bagnolites stuarti sp. nov.

Diagnosis. Involute shell with small umbilicus; umbilical suture opening out from about half a whorl before body-chamber. Whorls triangular in section, whorl sides flat, convergent, umbilical slope undercut. Whorl sides smooth. Blunt keel delimited by concave areas. Suture line with lateral saddles very short and nearly flat-topped. Inner whorls and body-chamber unknown.

Remarks. This new ammonite genus is unlike any other known from the Sinemurian Stage, in which most genera of Ammonitina are evolute and strongly ribbed. For comparisons, one must look to the genera showing a tendency to oxycone shell form which are found in the upper half of the Upper Sinemurian. The closest resemblance is to *Eparietites* of which some species have smooth outer whorls. *Eparietites* is the only genus which has a similar venter to the new form, with the keel flanked by concave areas. Some specimens of *Eparietites* from the Frodingham Ironstone, Lincolnshire have a triangular whorl section with undercut umbilical margin like the present genus, but they have ribbed inner whorls and are more compressed and more evolute than *Bagnolites*. The differences between the two genera, shown in Table 1, are held to be sufficient to justify their separation.

[Palaeontology, Vol. 41, Part 5, 1998, pp. 993–999, 1 pl.]

TABLE 1. Comparison of morphological features of *Eparietites* and *Bagnolites*.

Morphological feature	*Eparietites*	*Bagnolites*
Whorl section	Compressed, almost parallel sided	Triangular
Umbilical slope	Normal	Undercut
Shell coiling	Normal	Excentric for outer whorls
Ornament	Ribs persist to end of phragmocone	Smooth at least on outer part of phragmocone
Suture line	Normal 'arietitid'	Short lateral saddles

TEXT-FIG. 1. Top left, *Xipheroceras dudressieri* (d'Orbigny, 1845); top right, *X.* aff. *ziphus* (Zieten, 1830), bottom, *Bagnolites stuarti* gen. et sp. nov.; Bristol City Museums and Art Gallery no. Ce17364, holotype; oblique view; × 1.

EXPLANATION OF PLATE 1

Figs 1–3. *Bagnolites stuarti* gen. et. sp. nov.; Bristol City Museums and Art Gallery no. Ce17364, holotype; Black Ven Marls, probably Bed 85, Charmouth, Dorset. 1, ventral view showing penultimate preserved whorl exposed by preparation. 2, side view. 3, oblique view, and ventral view of *Xipheroceras* aff. *ziphus* (Zieten, 1830).

Fig. 4. *Promicroceras planicosta* (J. Sowerby, 1814) at left; above it, inner whorls of *Cymbites* sp.; (right), *Asteroceras margaritoides* Spath, 1925*b* in same nodule as figures 1–3.

1

2

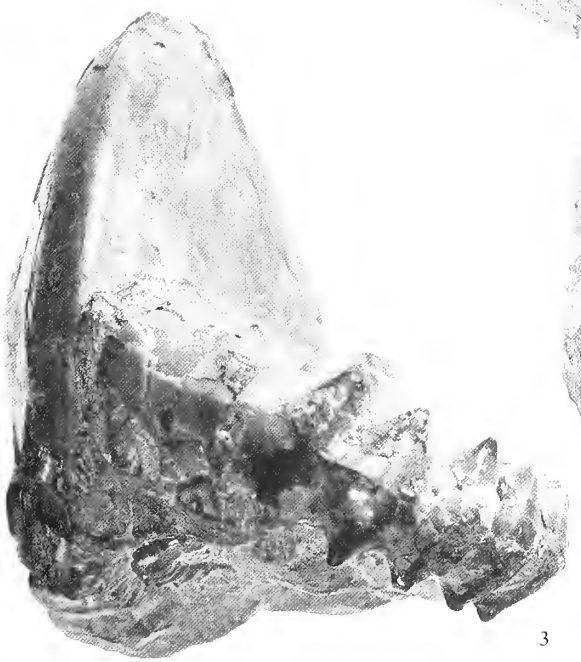

3

4

DONOVAN, Lias Group ammonites

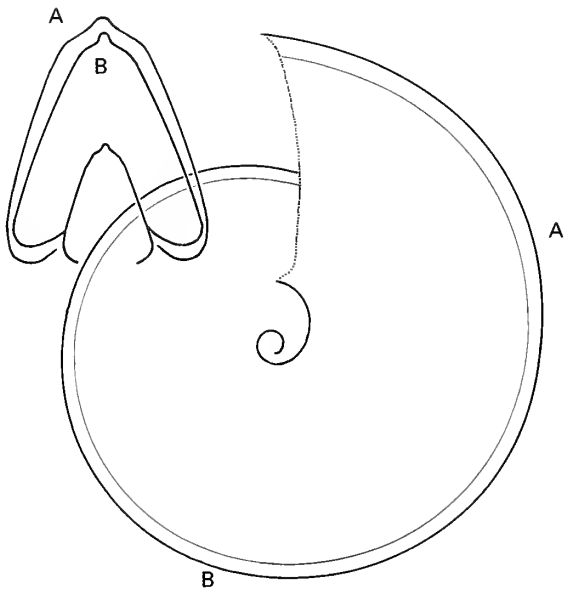

TEXT-FIG. 2. Reconstructed side view of *Bagnolites stuarti* gen. et sp. nov. at a maximum diameter of 128 mm, probably a little less than its final diameter, and whorl sections at diameters of 93 mm (B) and 114 mm (A).

Other oxycone genera, *Gleviceras* (Raricostatum Zone) and *Oxynoticeras* (Oxynotum Zone), do not have the characteristic venter with concave areas flanking a keel, or undercut umbilical margins, besides being younger in age than the new form.

The present writer has suggested (Donovan 1994) that in the Sinemurian there were two evolutionary lineages leading from evolute, ribbed ammonites towards oxycone, smoother ones: one from *Caenisites* via *Eparietites* to *Oxynoticeras*, the second from *Asteroceras* to *Gleviceras*. Both lineages are represented only intermittently in the well-known north-west European sections. *Bagnolites* does not fit easily either of these hypothetical lineages, although if it is related to either it would be to the former because of its limited resemblance to *Eparietites*. On account of specialized features, not present in *Eparietites*, it is difficult to regard *Bagnolites* as an ancestor of that genus. It most probably represents a separate branch from this lineage, but in the absence of more material further speculation is pointless.

Bagnolites stuarti gen. et sp. nov.

Plate 1; Text-figures 1–3

Holotype. No. Ce17364 in the geological collections of the Bristol Museums and Art Gallery.

Material. The holotype was collected by Stuart Bagnoli from the Black Ven Marls in the lower part of the Lias Group on the coast near Charmouth, Dorset. It is in a nodule which is believed to have come from Lang and Spath's (1926, p. 159) Bed 85 in the Obtusum Zone, Stellare Subzone (see below). After Stuart Bagnoli's death, the specimen was presented to Bristol Museums and Art Gallery in his memory by P. A. and C. A. Langham. No other specimens are known.

Stratigraphical horizon. The specimen was probably not found *in situ* and its horizon was not recorded by the finder, but evidence is provided by other ammonites in the same matrix. These are: *Asteroceras margaritoides* Spath, 1925*b* (two specimens); *Cymbites* sp. (inner whorls); *Promicroceras planicosta* (J. Sowerby, 1814); *Xipheroceras* aff. *ziphus* (Zieten, 1830); *X. dudressieri* (d'Orbigny, 1845). This assemblage shows that the age

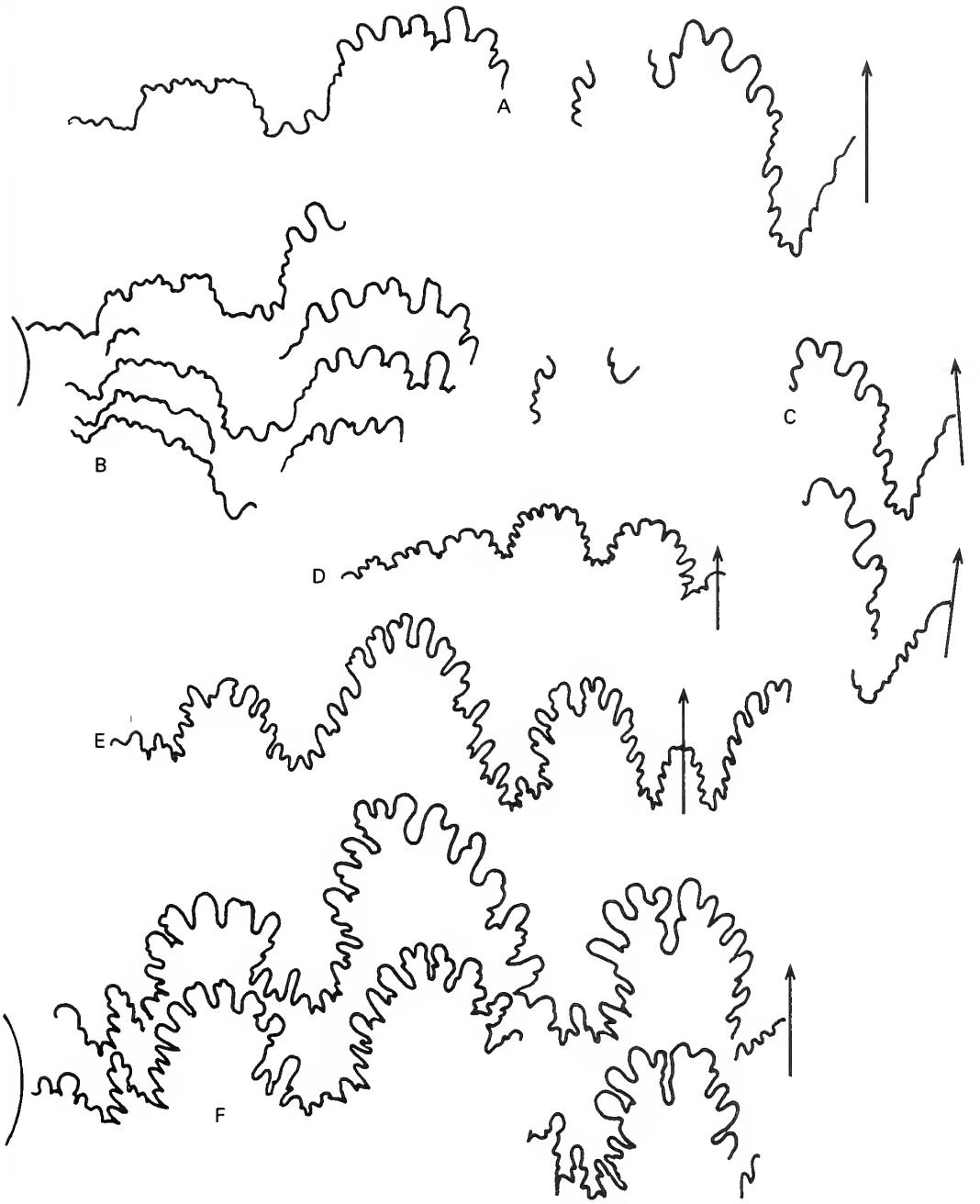

TEXT-FIG. 3. A–C, *Bagnolites stuarti* gen. et sp. nov. A, partial reconstruction of suture line. B, dorsal parts of external suture lines at a diameter of 114 mm. C, external lobes at a diameter of 93 mm, reversed; all × 1·87. D, *Oxynoticeras* aff. *simpsoni* (Simpson, 1843); Natural History Museum no. C17108; from Spath (1925*a*, p. 110, fig. c); × 1·79. E, *Eparietites* aff. *denotatus* (Simpson, 1855); Sedgwick Museum Cambridge, no. J18221; from Wright (1881, pl. 22A, fig. 9); × 1·82. F, *Eparietites denotatus* (Simpson, 1855); holotype, Sedgwick Museum Cambridge, no. J3273; from Wright (1881, pl. 22B, fig. 1); × 1·68.

cannot be older than the Stellare Subzone. On grounds of lithology and fauna, the nodule is likely to have come from Bed 85 of Lang and Spath (1926). Similar accompanying fossils are also found in Bed 87, but this also includes belemnites and brachiopods which are not apparent in the present nodule. Both beds 85 and 87 fall in the Stellare Subzone (Palmer 1972; Page 1992, p. 145). The horizon of the fossil cannot be younger than the Stellare Subzone, because the higher part of that subzone and the succeeding Denotatus Subzone are missing from the Dorset coast section (Page 1992, p. 152, fig. 4) and the accompanying ammonites do not range into the Densinodulum Subzone which forms the next part of the local sequence.

Preparation and method of study. Two areas of the ventral part of the last whorl are missing, having been lost before fossilization. This allowed preparation to expose the ventral part of the penultimate whorl (Text-fig 1). The side view was reconstructed as follows. A cardboard template was made to fit the surviving parts of the venter, and the outline transferred to paper. Assuming that the curve of the venter approximates to a logarithmic spiral, the spiral angle (α) and the centre of the spiral were found by trial and error. For the last half of the penultimate whorl, $\alpha = 84{\cdot}5°$ was found to fit; for the first half of the last whorl, $\alpha = 83°$ and for the second half of the last whorl, $\alpha = 85{\cdot}5°$. These figures are not highly accurate but are considered adequate for the purpose. The missing parts of the ventral curve, back to the part of the penultimate whorl exposed by preparation, were reconstructed using the polar formula:

$$r = ae^{\theta \cot \alpha},$$

where r = radius at an angle of rotation (θ) from initial radius a, and e is the base of natural logarithms (Obata 1960). The ventral curve was extrapolated to a diameter of 128 mm, corresponding to the end of the umbilical suture as preserved. The resulting reconstruction is shown in Text-figure 2. The whorl section at B was drawn by fitting a template, and the inner part completed from the venter of the penultimate whorl exposed by preparation.

Diagnosis. As for genus.

Description. The last preserved part of the venter is at a diameter of 114 mm. The diameter corresponding to the last preserved part of the phragmocone is about 128 mm (see above). Suture lines are visible almost to the end of the last whorl, but it is likely that the beginning of the body-chamber is present. The excentric umbilical suture is likely to be an adult feature. Such 'uncoiling' is typical of the body-chamber of many involute ammonites but is here unusual in starting at least half a whorl before the end of the phragmocone.

The earliest part of the shell seen, revealed by preparation at an estimated diameter of 50 mm, shows the same characters as the last septate whorl. The whorl section is trigonal, the height slightly greater than the thickness, becoming slightly more compressed at the end of the last preserved whorl. The holotype is too incomplete for the standard measurements to be made.

Parts of the external suture line are visible in three places: on the right hand side at a diameter of 114 mm; about half a whorl behind this, where lateral lobes are visible; and on the left hand side, at a diameter of 93 mm, where parts of several external saddles are visible. The suture line is illustrated in Text-figure 3A–C.

The external suture apparently comprises three saddles but the parts seen are inadequate to reconstruct the whole suture beyond doubt (Text-fig. 3A). The first and second lateral saddles are distinctive in being very short with a truncated appearance (Text-fig. 3B). The external saddle appears to be long and narrow (Text-fig. 3C).

Suture lines of *Eparietites* (Text-fig. 3E–F) are similar to that of the new ammonite chiefly as regards the external saddle. Closer comparison may be made with a specimen said to be from beds with *Slatterites* at Drake's Broughton, Worcestershire, identified by Spath as *Oxynoticeras* aff. *simpsoni* (Simpson), the suture of which was figured by him (Spath 1925*a*, p. 110, fig. c) and is reproduced here (Text-fig. 3D). This has short lateral saddles rather like those of *Bagnolites*. It remains possible that the unusual suture line is abnormal but its consistent appearance wherever seen on the specimen argues against this.

Remarks. The inadequate evidence for ammonite phylogenies in the Upper Sinemurian has been referred to above, and not much more can be added. *Bagnolites* has a venter similar to that of *Eparietites* but otherwise has little resemblance to that genus. It seems improbable that it was ancestral to *Eparietites*, and more likely that it was a parallel development from an unknown form which had already evolved the *Eparietites* form of venter in early Obtusum Zone times. The resemblance of the suture line of *Bagnolites* to that of *Oxynoticeras simpsoni*, the earliest species of *Oxynoticeras*, could be held to show that *Bagnolites* was near the (otherwise unknown) immediate ancestors of *Oxynoticeras*.

Acknowledgements. I thank David Hill for preparing the specimen, Simon Powell for photography, and Dr Peter Crowther (formerly of Bristol City Museums and Art Gallery) for drawing my attention to this ammonite and encouraging me to describe it.

REFERENCES

DONOVAN, D. T. 1994. Evolution in some early Jurassic ammonites: Asteroceratinae, Oxynoticeratidae and related forms. *Atti III Convegno Internazionale, Pergola, Italy: Palaeopelagos, Special Publication*, **1**, 383–396.

HYATT, A. 1867. The fossil cephalopods of the Museum of Comparative Zoology. *Bulletin of the Museum of Comparative Zoology*, **1**, 71–102.

—— 1874. Remarks on two new genera of ammonites, *Agassiceras* and *Oxynoticeras*. *Proceedings of the Boston Society of Natural History*, **17**, 225–235.

—— 1889. Genesis of the Arietidae. *Smithsonian Contributions to Knowledge*, **26** (673), i–xii + 1–238.

LANG, W. D. and SPATH, L. F. 1926. The Black Marl of Black Ven and Stonebarrow, in the Lias of the Dorset coast. *Quarterly Journal of the Geological Society, London*, **82**, 144–187.

OBATA, I. 1960. Spirale de quelques ammonites. *Memoirs of the Faculty of Science, Kyushu University, Series D, Geology*, **9** (3), 151–164.

ORBIGNY, A. D. d' 1845. *Paléontologie française. Terrains oolitiques ou jurassiques. Tome premier. Céphalopodes*. Livraison 29, 321–328. Chez l'Auteur, Paris.

PAGE, K. N. 1992. The sequence of ammonite correlated horizons in the British Sinemurian (Lower Jurassic). *Newsletters on Stratigraphy*, **27**, 129–156.

PALMER, C. P. 1972. Revision of the zonal classification of the Lower Lias of the Dorset coast. *Proceedings of the Dorset Natural History and Archaeological Society*, **93**, 102–116.

SIMPSON, M. 1843. *A monograph of the ammonites of the Yorkshire Lias*. Simpkin, Marshall, and Co., London, 60 pp.

—— 1855. *The fossils of the Yorkshire Lias*. Whittaker and Co., London, 149 pp.

SOWERBY, J. 1814. *The mineral conchology of Great Britain*, **1**, part 13, Sowerby, London.

SPATH, L. F. 1925*a*. Notes on Yorkshire ammonites. I.-On the Genus *Oxynoticeras* Hyatt. *The Naturalist*, No. 819 (April, 1925), 107–112.

—— 1925*b*. Notes on Yorkshire ammonites. VI.-On *Ammonites planicosta* J. Sowerby. *The Naturalist*, No. 825 (October, 1925), 299–306.

—— 1946. The type of the genus *Ammonites*. *Annals and Magazine of Natural History*, (11), **12**, 490–497.

WRIGHT, T. 1881. Monograph on the Lias ammonites of the British Islands. Part 4. *Monograph of the Palaeontographical Society*, **35** (165), 265–328, pls 22A, 22B, 41–48.

ZIETEN, C. H. von 1830. *Die Versteinerungen Württembergs*. Lieferungen 1–2. Schweizerbart, Stuttgart, i–viii, 1–16, pls 1–12.

DESMOND T. DONOVAN
Department of Geological Sciences
University College London
Gower Street
London WC1E 6BT, UK

Typescript received 15 May 1997
Revised typescript received 13 October 1997

EVOLUTION AND TAXONOMY OF THE SILURIAN CONODONT *PTEROSPATHODUS*

by PEEP MÄNNIK

ABSTRACT. New data indicate that *Carniodus* is not a separate taxon but the elements considered to belong to it in reality formed a part of the *Pterospathodus* apparatus. The latter contains 14 elements: Pa, Pb_1, Pb_2, Pc, M_1 (+M_2 in *P. pennatus procerus*), Sc_1, Sc_2, Sc_3, Sb_1, Sb_2, Sa, carnuliform with five morphs, carniciform, and curved element with three morphs. Two ecologically distinct lineages existed and evolved separately. One lineage (*P. amorphognathoides angulatus* – *P. amorphognathoides lennarti* ssp. nov. – *P. a. lithuanicus* – *P. a. amorphognathoides*) dominated open shelf carbonate-terrigeneous environments and the other (*P. pennatus pennatus* – *P. p. procerus*) the deeper basinal, graptolite-bearing facies. Both lineages evidently originated from a common ancestral taxon at the top of the *P. eopennatus* Biozone. Three main evolutionary intervals, separated by levels at which the most distinct morphological changes to the elements took place, have been recognized in the *Pterospathodus* sequence. Evolution was more rapid, and the morphological variation within each population considerably higher, in the *P. amorphognathoides* lineage.

P. a. angulatus and *P. p. pennatus* are recognized as separate taxa. *P. celloni* has a short range and originated from the *P. pennatus* lineage. Five morphologically distinct chronological populations are recognized in the *P. a. amorphognathoides* range.

PTEROSPATHODUS is one of the dominant taxa in Telychian conodont faunas, and Walliser (1964) based the first conodont zonation of this interval on *Pterospathodus* species. The genus has been subsequently widely recognized (for summary see Jeppsson 1987). However, although more than 30 years have passed since the first descriptions of *Pterospathodus*, and although its species have been widely used in stratigraphy, knowledge of this genus is still poor. The limitations of existing knowledge of apparatus structure, taxonomic composition, ecology and evolution of *Pterospathodus* have resulted in many different taxonomic and stratigraphical interpretations (Walliser 1964; Barrick and Klapper 1976; Jeppsson 1979; Mabillard and Aldridge 1983; Bischoff 1986; Männik and Aldridge 1989; etc.). Männik and Aldridge (1989) discussed the evolution and relationships within *Pterospathodus* and documented sequential changes shown by populations. They recognized morphological differences between sinistral and dextral Pa elements, and concluded that pennate forms (with a single unbranched or branched lateral process) and non-pennate forms (without a lateral process), previously treated as separate taxa (*P. angulatus*, *P. pennatus* and *P. celloni*), are conspecific. They assigned all these morphotypes to *P. celloni*.

Now, study of rich and well preserved collections (CAI = 1) from Estonia and Gotland, Sweden (Text-fig. 1; Appendix) has provided detailed information about *Pterospathodus* necessitating a re-evaluation of existing ideas about the taxonomy, evolution and ecology of the genus.

APPARATUS

The structure of the *Pterospathodus* apparatus is evidently much more complicated than previous studies suggested. The co-occurrence, similarities in evolutionary patterns and in ecology of *Pterospathodus* and *Carniodus* indicate that both sets of elements belonged to the same apparatus.

Pterospathodus was originally reconstructed as a bimembrate apparatus (Walliser 1964), and later as a quadrimembrate apparatus including Pa, Pb, M and Sc elements (Barrick and Klapper 1976). Mabillard and Aldridge (1983) recognized a fifth – Sa/Sb – element, although it appeared to be

[Palaeontology, Vol. 41, Part 5, 1998, pp. 1001–1050, 6 pls]

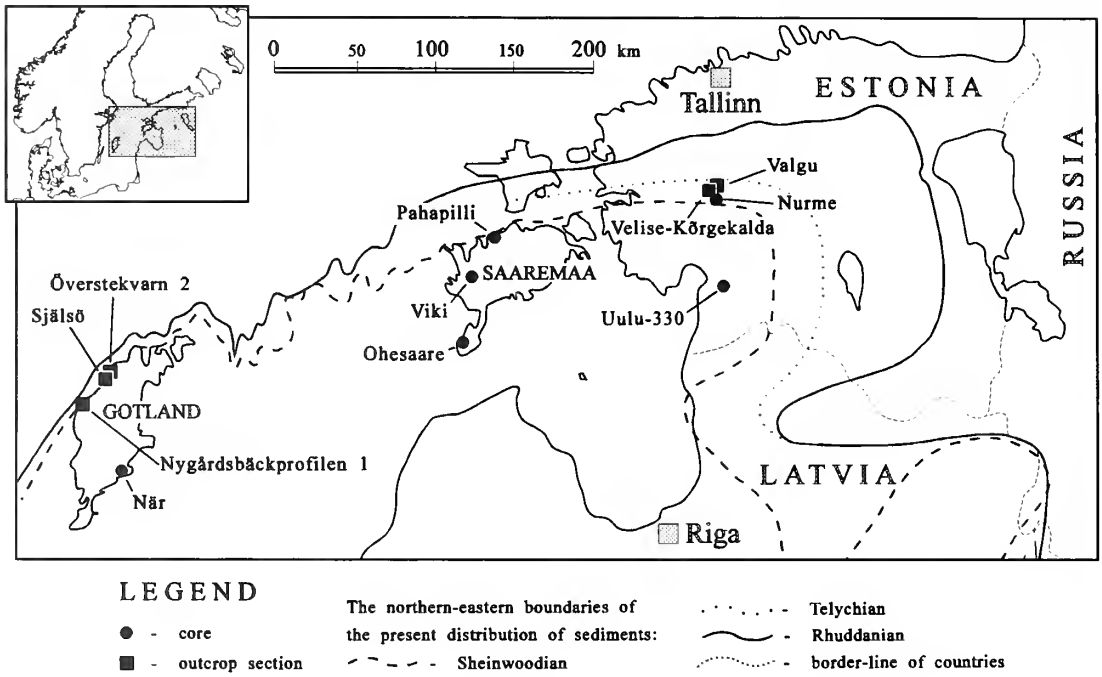

TEXT-FIG. 1. Location of studied sections (for details see Appendix).

morphologically almost identical to its analogue in the *Carniodus* apparatus as reconstructed by Barrick and Klapper (1976). Later, the Sc element of Barrick and Klapper (1976) was re-interpreted to be a Pc element by Aldridge (*in* Männik and Aldridge 1989).

Jeppsson (1979) was the first to propose that elements considered to belong to *Carniodus* in reality formed a part of the *Pterospathodus* apparatus. The main argument against Jeppsson's idea – the difference in stratigraphical ranges (see Männik and Aldridge 1989, pp. 894–895) – has lost its validity in the light of my new information: *Carniodus* has exactly the same stratigraphical range as *Pterospathodus* (Männik 1992). The absence or extreme rarity of *Carniodus* elements in collections from the lowermost part of the *Pterospathodus* range in many sections is most probably caused by their very small size. Small specimens are the most likely to be dissolved or washed away during the laboratory processing of samples.

Each taxon of *Pterospathodus* is associated with a distinct set of elements of *Carniodus* type, and the two sets display parallel evolutionary patterns (see below). It is concluded that *Carniodus* did not exist as a separate apparatus but represents elements of the *Pterospathodus* apparatus, mostly from its primary symmetry transition series. All of the elements (except the Sa) in the *Pterospathodus* apparatus are represented by sinistral and dextral forms, but some of them – Pb_2, Sc_3, carnuliform (morphs a, b, and short morph) – evidently also include symmetrical forms. Elements are morphologically variable and several morphs can be recognized in all of them. All morphs of the same element are closely related to each other and intermediate morphologies between them exist. Only the most distinctive and stratigraphically valuable morphs are described. Below, the elements are characterized briefly and the possible position of them in the apparatus indicated (Text-fig. 2; the main shape categories of elements according to Sweet 1981, 1988).

1. Pa element – carminate, pastinate and stellate (rare) elements in older strata, stelliscaphate and pastiniscaphate elements in younger strata. Originally described as *Pterospathodus amorphognathoides* s.f., *Spathognathodus celloni* s.f. and *S. pennatus* s.f. (Walliser 1964).

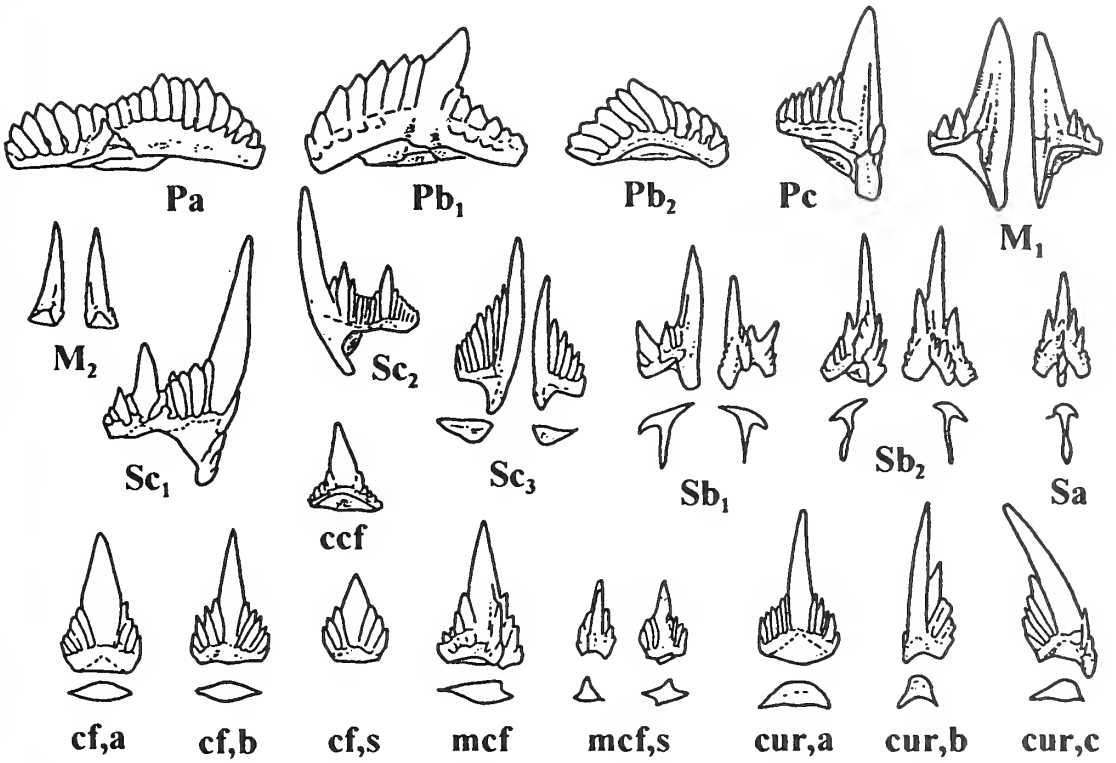

TEXT-FIG. 2. Elements in the *Pterospathodus* apparatus: ccf – carniciform element; cf, a – carnuliform element, morph a; cf, b – carnuliform element, morph b; cf, s – carnuliform element, short morph; mcf – modified carnuliform element; mcf, s – modified carnuliform element, short morph; cur, a – curved element, morph a; cur, b – curved element, morph b; cur, c – curved element, morph c.

2. Pb_1 element – angulate (in older strata) to anguliscaphate (in younger strata), with distinct cusp. Originally described as *Ozarkodina adiutricis* s.f. and *O. gaertneri* s.f. (Walliser 1964).
3. Pb_2 element – dolobrate (in *P. eopennatus*), angulate (in *P. pennatus* and older part of the *P. a. amorphognathoides* lineage) to anguliscaphate (in *P. a. amorphognathoides*), with poorly developed cusp. Originally described as *Carniodus carinthiacus* s.f. (Walliser 1964).
4. Pc element – pastinate, with short anterior and outer lateral, and longer posterior processes. Originally described as *Neoprioniodus costatus* s.f. (Walliser 1964).
5. M_1 element – dolabrate, with short undenticulated anterior (anticusp) and inner lateral processes, and short denticulated posterior process. Originally described as *N. triangularis* s.f. (Walliser 1964).
6. M_2 element – dolabrate, similar to M_1 but is slender, less curved inside, with shorter processes and without anticusp. Recognized only in the *P. pennatus procerus* apparatus.
7. Sc_1 element – bipennate, relatively short anterior process directed steeply downwards and turned only slightly to inner side; longer posterior process almost straight. Originally described as *C. carnus* s.f. (Walliser 1964).
8. Sc_2 element – dolabrate, anterior process directed downwards as a well-developed anticusp; denticulated posterior process relatively long. Originally described as *N. subcarnus* s.f. (Walliser 1964).
9. Sc_3 element – dolabrate, similar to Sc_2 but anticusp is poorly developed; posterior process is short and with denticles which rapidly decrease in size distally. Appears in the *P. eopennatus* ssp. nov. 2 apparatus.

10. Sb_1 element – tertiopedate, outer lateral process denticulated, inner one undenticulated (or with few small denticles) and directed steeply downwards as an anticusp; posterior process denticulated and straight. In *P. eopennatus* ssp. nov. 1, *P. eopennatus* ssp. nov. 2 and *P. p. procerus* the distal part of the outer lateral process is bifurcated. Originally described as *Roudya latialata* s.f. (Walliser 1964, pl. 31, fig. 13).
11. Sb_2 element – tertiopedate, similar to Sa, but lateral processes are asymmetrical and the posterior process is curved sigmoidally to the outer side. In *P. eopennatus* ssp. nov. 1, *P. eopennatus* ssp. nov. 2 and *P. p. procerus* the distal part of the outer lateral process is bifurcated. Originally described as *R. latialata* s.f. (Walliser 1964, pl. 6, fig. 15; pl. 31, figs 11–12).
12. Sa element – alate, all processes denticulated, lateral processes situated symmetrically. Originally described as *R. latialata* s.f. (Walliser 1964)?
13. Carnuliform element, morph a – angulate to carminate, elements with high base and short processes with few relatively wide short denticles. Elements highly variable, forming a transition series of morphologies from elements with almost symmetrically situated anterior and posterior processes and a vertical cusp at one end of the series to strongly posteriorly inclined elements at the other. The latter type possesses a denticulated posterior process but only a single denticle (or none) anterior to the cusp. Based on the form of the cusp and the curvature of processes sinistral, dextral and symmetrical forms can be recognized. Position in apparatus unknown. Originally described as *C. carnulus* s.f. (Walliser 1964).
14. Carnuliform element, morph b – angulate to carminate, carnuliform element with densely denticulated processes. Denticles higher, thinner and more numerous than those on morph a. Forms a morphology transition series similar to that of morph a. Specimens morphologically intermediate between morphs a and b have been found. Sinistral, dextral and symmetrical elements are recognized. Position in apparatus unknown.
15. Carnuliform element, short morph – angulate to carminate, similar to morph a but with short cusp. Less common than morphs a and b. Sinistral, dextral and probably also symmetrical elements exist. Position in apparatus unknown. Appears in the *P. amorphognathoides lennarti* ssp. nov. apparatus.
16. Modified carnuliform element – pastinate, carnuliform element with short straight denticulated outer lateral process. Position in apparatus unknown.
17. Modified carnuliform element, short morph – pastinate and stellate, short morph of carnuliform element with short denticulated lateral process on one or both sides of the element. Position in apparatus unknown. Appears in the *P. amorphognathoides lennarti* ssp. nov. apparatus.
18. Carniciform element – angulate to carminate, elements relatively short, triangular in lateral view, with cusp strongly curved to the inner side. Forms a transition series of morphology from elements with almost symmetrically situated processes and vertical (in lateral view) cusp to those with the cusp moderately inclined posteriorly. Position in apparatus unknown.
19. Curved element, morph a – angulate to carminate, element with high base, high vertical cusp and densely denticulated lateral processes considerably turned to inner side. The length of the processes varies. Position in apparatus unknown.
20. Curved element, morph b – angulate, similar to morph a of curved element but processes shorter and strongly turned to the inner side. Position in apparatus unknown.
21. Curved element, morph c – angulate, resembles morph a of curved element but differs by having fewer and larger denticles on the processes. As a rule the cusp is inclined posteriorly. Position in apparatus unknown. Appears in the *P. amorphognathoides lithuanicus* apparatus.

Hence, the *Pterospathodus* apparatus is probably made of 14 different elements: Pa, Pb_1, Pb_2, Pc, M_1 (joined by the M_2 element in the *P. pennatus procerus* apparatus), Sc_1, Sc_2, Sc_3, Sb_1, Sb_2, Sa and three main groups (carnuliform, carniciform and curved) of highly variable elements with unknown positions in the apparatus. This is many more than is usually recognized in Ordovician and Silurian conodonts. No apparatus known so far from a natural, bedding plane assemblage has so many elements. However, it is quite possible that the carnuliform element at least instead of occupying a

separate position in the apparatus in reality belonged to some of the S elements and its morphology transition series formed continuations of the (posterior) processes of the S elements. The positions of elements, identified here as Pb_2, M_2 and Sc_3, and not known in any other apparatus, are still problematical. The notation used for them in this paper only indicates that, morphologically, these elements are closest to those traditionally considered to occupy the Pb, M and Sc positions respectively in the conodont apparatuses.

SYSTEMATIC PALAEONTOLOGY

Considerable revisions of the taxonomy of *Pterospathodus* are required by the new data. Contrary to the conclusions of Männik and Aldridge (1989), *P. angulatus* and *P. pennatus* are here recognized as separate taxa belonging to different lineages. *P. pennatus* is represented by two chronological subspecies: *P. p. pennatus* and *P. p. procerus*. *P. angulatus* is recognized as the oldest representative of the *P. amorphognathoides* lineage: *P. a. angulatus*.

It appears that the fauna from the Jôhve core discussed in Männik and Aldridge (1989, text-fig. 2) represents only a part (from the *A. kuehni* Subzone to Population 3 of the *P. a. amorphognathoides* Zone above; see Text-fig. 3 and Männik 1995) of the range of *Pterospathodus* in Estonia. No elements of *P. celloni s.s.* were found during a restudy of the Jôhve core collection. The form, identified previously as *P. celloni* in Estonia (and probably also in many collections from other regions of the world – restudy of collections is needed) appears to be multitaxonomic. It is here reidentified as *P. eopennatus* ssp. nov. 1, *P. eopennatus* ssp. nov. 2, *P. a. angulatus* and *P. a. lennarti* ssp. nov.

In the descriptions below only brief characterizations of the morphological features essential to identify each taxon are given.

Figured specimens from Estonia are deposited in the Institute of Geology, Tallinn Technical University, Tallinn, Estonia, and those from Gotland in the Department of Historical Geology and Palaeontology, Lund University, Lund, Sweden.

Genus PTEROSPATHODUS Walliser, 1964

Type species. Pterospathodus amorphognathoides Walliser, 1964, from the Telychian, Cellon, Austria.

Remarks. Pterospathodus is a morphologically complicated genus which evolved rapidly. Eight taxa, representing three distinct lineages (treated here as species) – *P. eopennatus*, *P. pennatus* and *P. amorphognathoides* – are recognized in the Estonian sequence.

In many regions (Alaska – Savage 1985; Australia – Bischoff 1986; north-western Canada – Over and Chatterton 1987; McCracken 1991; Greenland – Armstrong 1990) *P. rhodesi*, all elements of which are characterized by extremely wide platforms/platform ledges, replaced or co-existed with *P. a. amorphognathoides*. The origin of *P. rhodesi* and its relationship to other taxa of *Pterospathodus* are not yet known.

It is possible that also some other species of *Pterospathodus* existed. *Pterospathodus* aff. *P. amorphognathoides* (Nowlan 1981, pl. 7, figs 2–3, 5; later reidentified as *Pterospathodus* n. sp. A by Nowlan 1983), *Pterospathodus* n. sp. B (Nowlan 1983, fig. 4 J, L, Q–R, U) and a conodont identified by Nowlan as *P. pennatus* (Nowlan 1981, pl. 7, figs 1, 4) have been described from eastern Canada (Gaspé Peninsula). *Pterospathodus* n. sp. A has been recognized also on Severnaya Zemlya (Männik, 1983, fig. 5 P) and in the Timan-Pechora region (Melnikov, pers. comm.). It is noteworthy that in all these regions 'real' *Pterospathodus* is extremely rare (Gaspé Peninsula and Timan-Pechora region) or absent (Severnaya Zemlya). So far, only the Pa element of *Pterospathodus* n. sp. A, *Pterospathodus* n. sp. B, and *P. pennatus sensu* Nowlan (1981) are known. It is evident that all these taxa are closely related to each other. However, their relations to the *Pterospathodus* described below are not clear and need further studies.

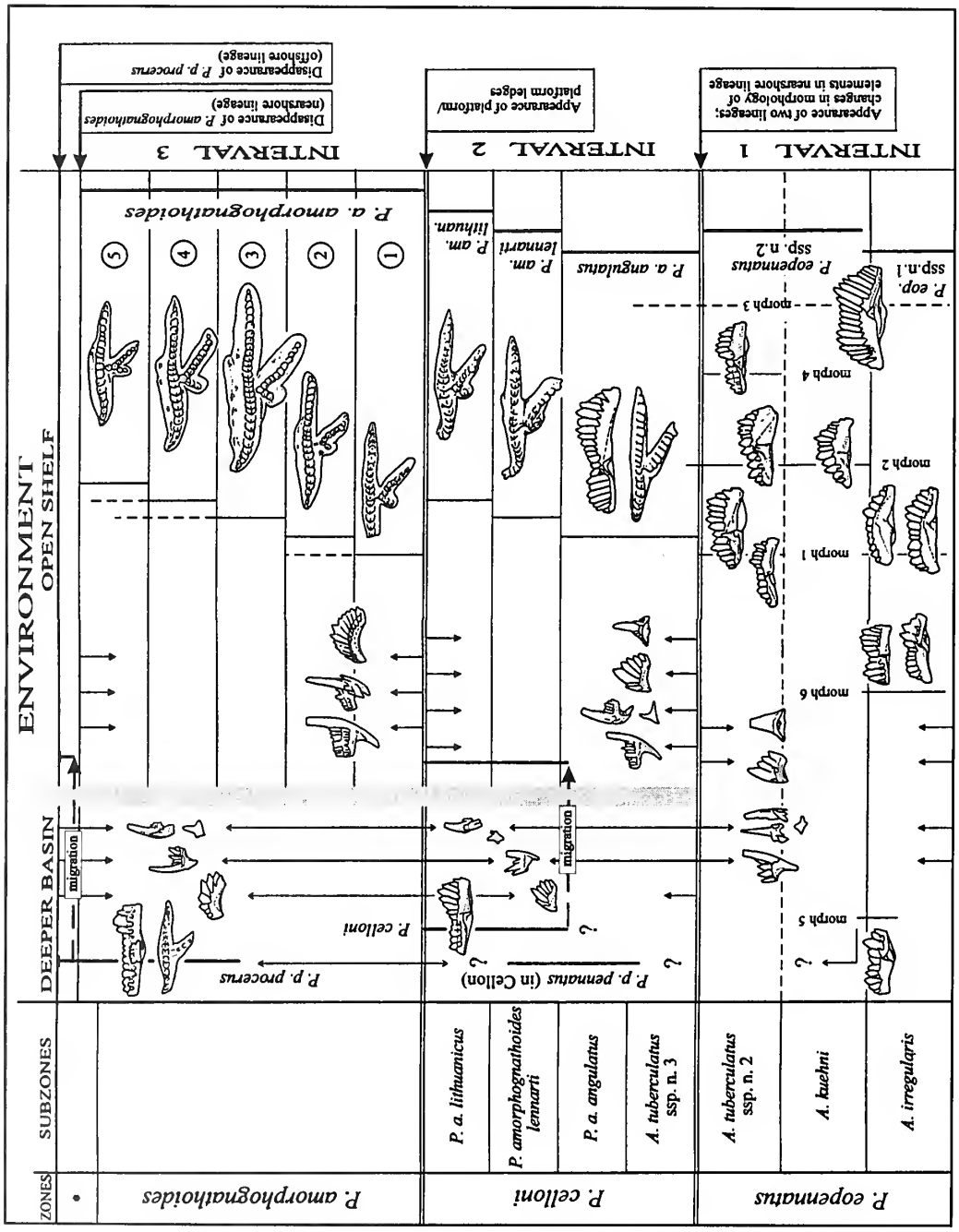

TEXT-FIG. 3. Evolution of *Pterospathodus*. Thick vertical lines – distribution of taxa; '?' at the ends of lines – distribution not known. Thin vertical lines – distribution of selected elements (dotted line = rare occurrence). Thin lines with arrows at the ends – indicate relationships between taxa or similarities between particular elements. Arrows with '?' – relations possible but not proved. Short arrows starting from the boundaries between the zones and pointing to the figures of elements – figured types of elements disappear (arrow points down) or appear (arrow points up) at the indicated boundary. Numbers in circles – populations in *P. a. amorphognathoides*. * – zonation for this interval in Jeppsson (1994, 1997).

Several other taxa, originally also described as species of *Pterospathodus*, appear to belong to some other genera. *P. posteritenuis* (Uyeno and Barnes 1983, pl. 2, figs 1–11, 14–18) is, most probably, identical to *Pranognathus tenuis* (Männik and Aldridge 1989, text-fig. 5). The apparatus of *P. cadiaensis* of Bischoff (1986) was studied in detail by Wang and Aldridge (1996), and reidentified as *Gamachignathus macroexcavatus*. *P. retroramus* of McCracken (1991, pl. 4, figs 24–25; pl. 5, figs 1–5, 8) is most probably related to *Astropentagnathus*, not to *Pterospathodus*.

P. eopennatus *lineage*

P. eopennatus sp. nov.

1971 *Spathognathodus celloni* Walliser, 1964; Schönlaub, p. 44, pl. 2, figs 1–5.
p 1971 *Carniodus carinthiacus* Walliser, 1964; Schönlaub, p. 46, pl. 3, fig. 6 (*non* figs 7–8 [= *P. a. amorphognathoides*]).
vp .1972 *Neoprioniodus costatus paucidentatus* Walliser, 1964; Aldridge, p. 193, pl. 5, fig. 21 (*non* fig. 20 [indet.]).
v. 1972 *Ozarkodina adiutricis* Walliser, 1964; Aldridge, p. 198, pl. 5, figs 2–3.
.1975 *Llandoverygnathus celloni* (Walliser, 1964); Aldridge, pl. 1, figs 20–21.
non 1975 *Llandoverygnathus celloni* (Walliser, 1964); Schönlaub, p. 53, pl. 1, figs 18–19 ([= *Aulacognathus*? sp.]).
1978 *Neoprioniodus costatus paucidentatus* Walliser, 1964; Miller, pl. 2, fig. 12.
1978 *Exochognathus brevialatus* (Walliser, 1964); Miller, pl. 3, figs 7–8.
1978 *Ozarkodina adiutricis* Walliser, 1964; Pickett, pl. 1. fig. 27.
1978 *Neospathognathodus pennatus* (Walliser, 1964); Pickett, pl. 1, figs 24–25.
.1979 *Carniodus* sp. Aldridge, p. 12, pl. 1, fig. 8.
.1979 *Llandoverygnathus celloni* (Walliser, 1964); Aldridge, pl. 1, figs 9–10.
.1979 *Llandoverygnathus pennatus* (Walliser, 1964); Aldridge, pl. 1, fig. 11.
.1979 *Llandoverygnathus* sp. 12 Aldridge, pl. 1, figs 12–15.
1980 *Pterospathodus celloni* (Walliser, 1964); Aldridge, fig. 1.
p? 1983 simple cone element, group 'c' Uyeno and Barnes, p. 26, pl. 8, figs 6–7, 9–12, 18? (*non* fig. 19 [indet.]).
.1985 *Pterospathodus celloni* (Walliser, 1964); Aldridge, p. 80, pl. 3.1, figs 25–26.
1985 *Pterospathodus celloni* (Walliser, 1964); Qiu, pl. 1, figs 1–2.
v. 1986 *Pterospathodus celloni* (Walliser, 1964); Bischoff, p. 194, pl. 28, figs 34–39; pl. 29, figs 1–8.
v. 1986 *Pterospathodus pennatus* (Walliser, 1964); Bischoff, p. 200, pl. 30, figs 12–14, 23–30.
? 1986 *Pterospathodus pennatus* (Walliser, 1964); Jiang *et al.*, pl. 4, fig. 3.
p? 1986 *Spathognathodus celloni* Walliser, 1964; Jiang *et al.*, pl. 4, figs 5, 17 (*non* fig. 6 [indet.]).
? 1987 *Pterospathodus celloni* (Walliser, 1964); Over and Chatterton, p. 2, fig. 1.
1988 *Pterospathodus celloni* (Walliser, 1964); Qiu, pl. 1, fig. 3 [cop. Qiu 1985, pl. 1, fig. 1].
v. 1989 *Pterospathodus*, celloni-morph Männik and Aldridge, text-fig. 3*A*.
1990 *Carniodus* sp. Armstrong, pl. 8, fig. 5.
1990 *Pterospathodus celloni* (Walliser, 1964); Armstrong, p. 118, pl. 19, figs 6–14.
1990 *Pterospathodus pennatus pennatus* (Walliser, 1964); Armstrong, p. 119, pl. 19, figs 15–17.
1990 *Pterospathodus celloni* (Walliser, 1964); Uyeno, p. 65, pl. 3, figs 1–7, 13–14; pl. 11, figs 25–30.
p 1990 *Pterospathodus* cf. *P. celloni* (Walliser, 1964); Uyeno, pl. 11, figs 18–20 (*non* pl. 3, figs 8–10 [= *Astropentagnathus*? sp.]).
v. 1990 *Pterospathodus celloni* (Walliser, 1964); Männik and Viira, pl. 17, figs 18, 21.
? 1991 *Pterospathodus celloni* (Walliser, 1964); McCracken, p. 109, pl. 4, figs 4–11.
? 1996 *Carniodus carnulus* Walliser, 1964; Wang and Aldridge, pl. 4, fig. 12.
? 1996 *Pterospathodus celloni* (Walliser, 1964); Wang and Aldridge, pl. 5, figs 2–3.

Derivation of name. In reference to the morphological similarity and postulated direct evolutionary relationship to *P. pennatus*.

Holotype. Pa element Cn 7879, Nurme core, sample M-889, int. 30·20–30·30 m; Plate 1, figure 19.

Type horizon and locality. Lower part of the Velise Formation, Adavere Regional Stage, Telychian; Nurme core, interval 14·00–30·30 m.

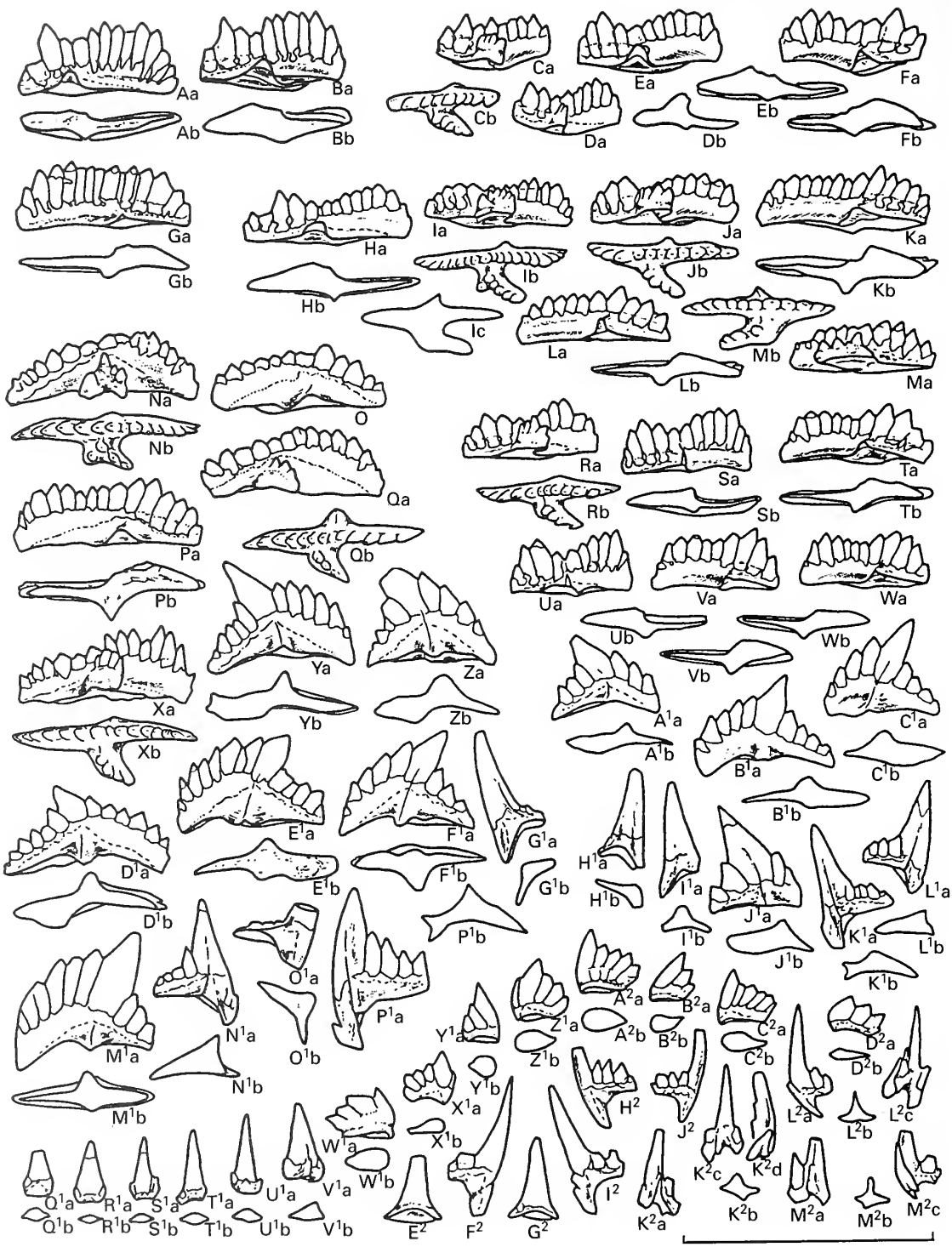

TEXT-FIG. 4. For caption see opposite.

Diagnosis. Pa element morphologically highly variable, with a pennate inner lateral process. Pb_2 element without anterior process. Posterior processes of S elements evenly denticulated. Processes of carniciform element undenticulated.

Description. Pa element is represented by eight main morphs.

Morph 1a – elements relatively long (up to 16–18 denticles). Sinistral elements (Pl. 1, figs 18–19; Pl. 2, fig. 35; Text-figs 4P, 5M, R–S), as a rule, without lateral process. The denticles are lower in the middle of the blade and relatively higher at each end. Dextral elements (Pl. 1, figs 10, 20, 22; Pl. 2, figs 34, 40; Text-figs 4X, 6A) differ by having a pennate lateral process and have higher denticles only at the anterior end of the blade. Both sinistral and dextral elements possess a short, triangular, generally undenticulated outer lateral lobe or process (a few specimens have a single denticle on it). Basal cavity deep and wide under posterior part of element. The lower line of the denticle roots turns steeply down in the posterior part of the blade.

Occurrence. Appears in the *A. irregularis* Subzone, is quite rare in the *A. kuehni* Subzone, but becomes common in the *A. tuberculatus* ssp. nov. 2 Subzone.

Morph 1b (Pl. 1, fig. 21; Text-figs 4N–O, Q, 6E–F, J–K) – similar to morph 1a but differs from it by having considerably shorter denticles and a higher base. Rare dextral specimens may possess a bifurcated lateral process (Text-fig. 4N).

Occurrence. The same as for morph 1a.

Morph 2a – short elements with distinctly higher denticles on the posterior part (sinistral element – Pl. 2, figs 32, 37, 39; Text-figs 5L, 6I, N, T) or anterior part (dextral element – Pl. 2, figs 23, 36; Text-figs 5J–K, 6G–H, M) of the blade. Lateral process better developed on the dextral element. Short triangular undenticulated lateral process is common on the outer side on both elements. Denticles are relatively tall.

Occurrence. Appears in the uppermost part of the *A. irregularis* Subzone and reaches the *A. tuberculatus* ssp. nov. 3 Subzone. Dominates in the *A. kuehni* Subzone but is less common below and above that interval.

Morph 2b (Text-fig. 5O–P) – similar to morph 2a; differs from it by having shorter denticles and higher base.

Occurrence. The same as for morph 2a, but morph 2b is less common.

Morph 3 (Pl. 1, figs 16–17; Text-figs 4A–B, G, 5D, G–I, 7H–I, Q) – dextral and sinistral forms almost identical. Elements relatively long with narrow, tall denticles. Denticle roots (white matter) almost reaches the base line on the distal parts of the blade. The denticles are somewhat lower near the cusp but higher on the distal parts of the blade. A denticulated lateral process is common on dextral, but rare on sinistral elements. Basal cavity shallow and narrow.

Occurrence. Relatively rare but occasionally present from the *A. irregularis* Subzone to *A. tuberculatus* ssp. nov. 3 Subzone.

Morph 4 (Pl. 2, figs 33, 38, 41; Text-fig. 6L, O–P, U) – relatively short, anterior denticles highest proximally, decreasing gradually in height in the distal direction. Posterior denticles are considerably shorter. The sharp decrease in the height of denticles just behind the cusp is the most characteristic feature of this morph. Intermediates between morphs 4 and 2 have been found.

Occurrence. A. tuberculatus ssp. nov. 2 Subzone.

TEXT-FIG. 4. *Pterospathodus eopennatus* ssp. nov. 1; *Astropentagnathus irregularis* Subzone. A–B, G, Pa element, morph 3. C–F, H–M, Pa element, morph 5. N–O, Q, Pa element, morph 1b. P, X, Pa element, morph 1a. R–W, Pa element, morph 6. Y–Z, A^1–F^1, J^1, M^1, Pb_1 element. W^1–D^2, Pb_2 element. G^1–I^1, O^1, M_1 element; K^1–L^1, N^1, P^1, Pc element. Q^1–U^1, carniliform element, morph a. V^1, modified carniliform element. E^2, G^2, carniciform element. F^2, I^2, Sc_1 element. H^2, J^2, Sc_2 element. K^2, Sb_2 element. L^2, Sa element. M^2, Sb_1 element. Scale bar represents 1 mm.

Morph 5 – both sinistral (Pl. 1, figs 25–27, 33; Text-figs 4F, K–M, 5B–C, F) and dextral (Pl. 1, figs 28(?), 30, 35–36; Text-figs 4C–E, H–J, 5A, E) forms relatively short with higher denticles close to the ends of the blade. Those on the anterior blade are slightly higher than on the posterior. Basal margin almost straight in lateral view (Pl. 1, figs 26, 30; Text-fig. 4H–M) or slightly convex (Pl. 1, fig. 28(?); Text-fig. 4C–F). Inner denticulated lateral process well developed on both forms. Shorter outer lateral process better developed (often bearing one or two denticles) on the sinistral forms.

Occurrence. Upper part of the *A. irregularis* Subzone and the lowermost part of the *A. kuehni* Subzone.

Morph 6 (Pl. 1, figs 23(?), 24, 29, 34; Text-fig. 4R–W) – similar to morph 5 but differs by being relatively shorter, possessing higher denticles (particularly on dextral elements – Pl. 1, figs 29, 34; Text-fig. 4R–S, U) and having poorly developed lateral process(es).

Occurrence. *A. irregularis* Subzone.

EXPLANATION OF PLATE 1

Figs 1–9, 11–15. *Pterospathodus eopennatus* ssp. nov. 2. 1, Cn 7861; outer lateral view of sinistral Pb_1 element. 2, Cn 7862; outer lateral view of dextral Pb_2 element. 3, Cn 7863; posterior view of dextral Sb_2 element. 4, Cn 7864; outer lateral view of sinistral modified carnuliform element. 5, Cn 7865; outer lateral view of dextral curved element, morph a. 6, Cn 7866; inner lateral view of dextral Sc_2 element. 7, Cn 7867; outer lateral view of sinistral carnuliform element, morph a. 8, Cn 7868; posterior view of sinistral Sb_1 element. 9, Cn 7869; inner lateral view of dextral carniciform element. 11, Cn 7870; outer lateral view of dextral Pb_1 element. 12, Cn 7871; inner lateral view of dextral Sc_3 element. 13, Cn 7872; inner lateral view of dextral Sc_1 element. 14, Cn 7873; outer lateral view of dextral Pc element. 15, Cn 7874; outer lateral view of dextral Pb_1 element. Figs 1 and 11 from Nurme core, sample M-900, int. 22·65–22·80 m; figs 2–3, 5, 8 and 14 from Nurme core, sample M-907, int. 17·50–17·60 m; figs 4, 6–7, 9, 12–13 and 15 from Viki core, sample M-8, int. 168·60–168·80 m.

Figs 10, 16–46. *Pterospathodus eopennatus* ssp. nov. 1. 10, Cn 7875; inner lateral view of dextral Pa element, morph 1a. 16, Cn 7876; inner lateral view of sinistral Pa element, morph 3. 17, Cn 7877; inner lateral view of dextral Pa element, morph 3. 18, Cn 7878; inner lateral view of sinistral Pa element, morph 1a. 19, Cn 7879; inner lateral view of sinistral Pa element, morph 1a. 20, Cn 7880; upper view of dextral Pa element, morph 1a. 21, Cn 7881; inner lateral view of sinistral Pa element, morph 1b. 22, Cn 7882; inner lateral view of dextral Pa element, morph 1a. 23, Cn 7883; inner lateral view of sinistral Pa element, morph 6(?). 24, Cn 7884; inner lateral view of sinistral Pa element, morph 6. 25, Cn 7885; inner lateral view of sinistral Pa element, morph 5. 26, Cn 7886; inner lateral view of sinistral Pa element, morph 5. 27, Cn 7887; upper view of sinistral Pa element, morph 5. 28, Cn 7888; inner lateral view of dextral Pa element, morph 5(?). 29, Cn 7889; inner lateral view of dextral Pa element, morph 6. 30, Cn 7890; inner lateral view of dextral Pa element, morph 5. 31, Cn 7891; outer lateral view of dextral Pc element. 32, Cn 7892; outer lateral view of dextral Pc element. 33, Cn 7893; upper view of sinistral Pa element, morph 5. 34, Cn 7894; inner lateral view of dextral Pa element, morph 6. 35, Cn 7895; upper view of dextral Pa element, morph 5. 36, Cn 7896; upper view of dextral Pa element, morph 5. 37, Cn 7897; outer lateral view of sinistral Pc element. 38, Cn 7900; lateral view of symmetrical Pb_2 element. 39, Cn 7899; outer lateral view of dextral Pb_2 element. 40, Cn 7898; outer lateral view of sinistral Pb_2 element. 41, Cn 7901; outer lateral view of sinistral Pb_1 element. 42, Cn 7902; outer lateral view of sinistral Pb_1 element. 43, Cn 7903; outer lateral view of dextral Pb_1 element. 44, Cn 7904; inner lateral view of sinistral Sc_2 element. 45, Cn 7905; inner lateral view of dextral Sc_2 element. 46, Cn 7906; inner lateral view of sinistral carniciform element. Figs 10, 18, 20 and 21 from Valgu section, sample M-882; figs 16–17 from Nurme core, sample M-891, int. 29·10–29·20 m; figs 19, 22 and 32 from Nurme core, sample M-889, int. 30·20–30·30 m; figs 23–24, 34 and 41–43 from Viki core, sample M-954, int. 183·17–183·32 m; figs 25, 28 and 35 from Viki core, sample M-960, int. 181·81–181·91 m; fig. 26 from Viki core, sample M-956, int. 182·90–183·04 m; figs 27, 31 and 37 from Viki core, sample M-962, int. 181·29–181·40 m; fig. 29 from Viki core, sample M-958, int. 182·22–182·30 m; figs 30, 33 and 36 from Nurme core, sample M-890, int. 29·50–29·60 m; figs 38–40, 44–46 from Nurme core, sample M-903, int. 20·40–20·50 m.

All × 50.

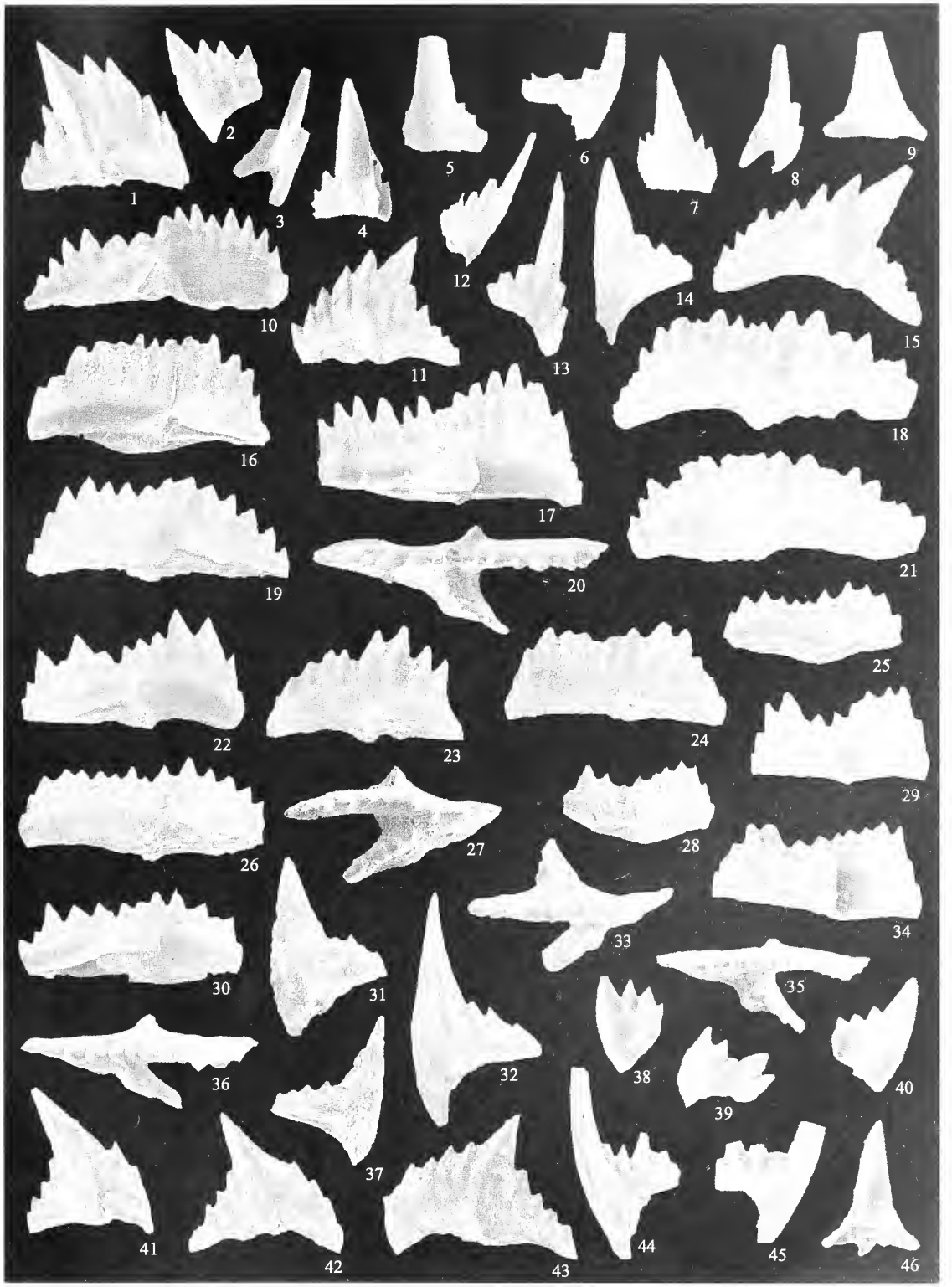

MÄNNIK, *Pterospathodus*

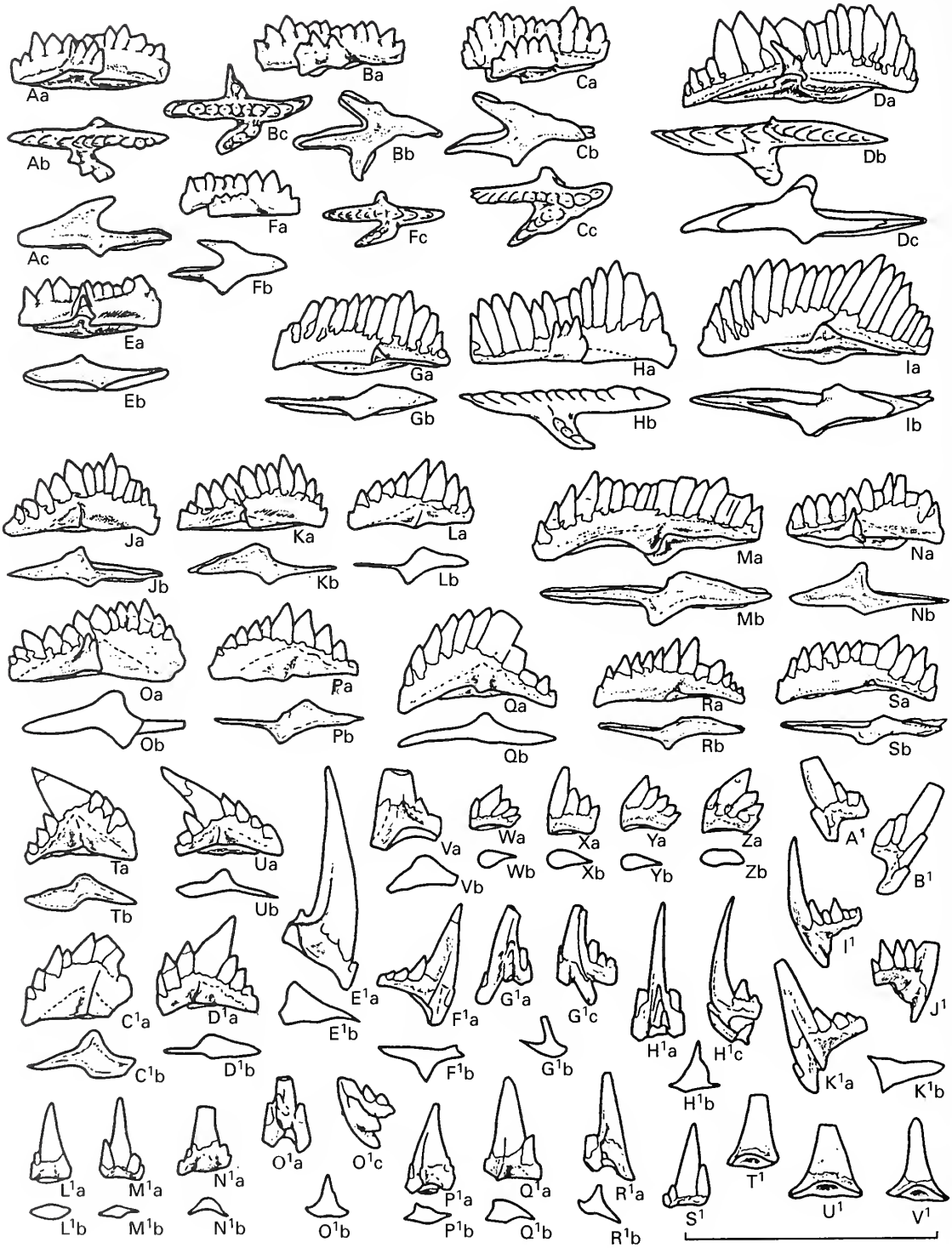

TEXT-FIG. 5. For caption see opposite.

Remarks. In all morphs the sinistral and dextral forms of the Pa element are morphologically different from each other. The pennate inner lateral process tends to be more common on the dextral element. In this paper two populations, evolutionarily connected and stratigraphically following each other, are described as subspecies of *P. eopennatus*: *P. eopennatus* ssp. nov. 1 and *P. eopennatus* ssp. nov. 2.

P. eopennatus can be recognized world-wide (see synonymy). However, a revision of collections is needed to identify subspecies.

Pterospathodus eopennatus ssp. nov. 1

Plate 1, figures 10, 16–46; Text-figures 4, 5A–C, E–F

Material. Several hundred to over a thousand of each of Pa, Pb_1 and Pc elements; tens to hundreds of Pb_2, M, Sc_1, Sc_2, Sb, Sa and carnuliform elements; few tens of carniciform elements.

Diagnosis. P. eopennatus with Pa element represented by morphs 1a, 1b, 3, 5 and 6; the last two are found only in this taxon. Pb_1 element relatively long, arched in lateral view.

Remarks. The relative abundance of morphs varies in different parts of the studied area. Morphs 1a and 1b dominate faunas in the continental part of Estonia whereas morph 6 is the most abundant in the Viki core from the western part of the island of Saaremaa (Text-fig. 1). However, all morphs described above have been found in all studied sections from this interval.

Occurrence. A. irregularis Subzone and the lowermost part of the *A. kuehni* Subzone.

Pterospathodus eopennatus ssp. nov. 2

Plate 1, figures 1–9, 11–15; Plate 2, figures 23, 32–41; Text-figures 5D, G–V¹, 6

v. 1998 *Pterospathodus* sp. nov. e Männik and Małkowski, pl. 1, figs 19, 23–25, 27.

Material. Several hundred Pa and Pb_1 elements; tens to hundreds of Pb_2, Pc, M, Sc_1 and Sc_2 elements; a few tens of Sc_3, Sb, Sa, carnuliform and carniciform elements.

Diagnosis. P. eopennatus with the Pa element represented by morphs 1a, 1b, 2a, 2b, 3 and 4. Pb_1 element short and triangular in lateral view.

Remarks. Pb_1 element dominated by forms which are relatively short and almost triangular in lateral view (Pl. 1, figs 1, 11; Text-figs 5T–U, C¹–D¹, 6Q–R). Rare specimens with a longer anterior process (Pl. 1, fig. 15; Text-fig. 5Q) may be found in the lower part of the *P. eopennatus* ssp. nov. 2 range but become dominant in the upper part (in the *A. tuberculatus* ssp. nov. 2 Subzone). Other elements are morphologically identical in both subspecies.

Two chronological populations are recognized in the range of *P. eopennatus* ssp. nov. 2.

1. The population in the *A. kuehni* Subzone (Text-fig. 5D, G–V¹) is dominated by morph 2a; morphs 1a and 1b are rare and morph 3 can be found occasionally.
2. The population in the *A. tuberculatus* ssp. nov. 2 Subzone (Text-fig. 6) is dominated by morphs 1a and 1b; morphs 2a and 2b occur but are rare. Morph 4 is restricted to this subzone. Also, the oldest Sc_3 elements (Pl. 1, fig. 12; Text-fig. 6I¹–K¹) found so far come from this population.

Occurrence. A. kuehni and *A. tuberculatus* ssp. nov. 2 subzones.

TEXT-FIG. 5. *Pterospathodus eopennatus* ssp. nov.; *Aulacognathus kuehni* Subzone. A–C, E–F. *Pterospathodus eopennatus* ssp. nov. 1, Pa element, morph 5. D, G–V¹, *Pterospathodus eopennatus* ssp. nov. 2. D, G–I, Pa element, morph 3. J–L, Pa element, morph 2a. M–N, R–S, Pa element, morph 1a. O–P, Pa element, morph 2b. Q, T–U, C¹–D¹, Pb_1 element. V, E¹, M_1 element. W–Z, Pb_2 element. A¹–B¹, Sc_1 element. F¹, K¹, Pc element. H¹, Sb_2 element. G¹, R¹, Sb_1 element. I¹–J¹, Sc_2 element. L¹–M¹, S¹, carnuliform element, morph a. N¹, curved element, morph a. O¹, Sa element. P¹–Q¹, modified carnuliform element. T¹–V¹, carniciform element. Scale bar represents 1 mm.

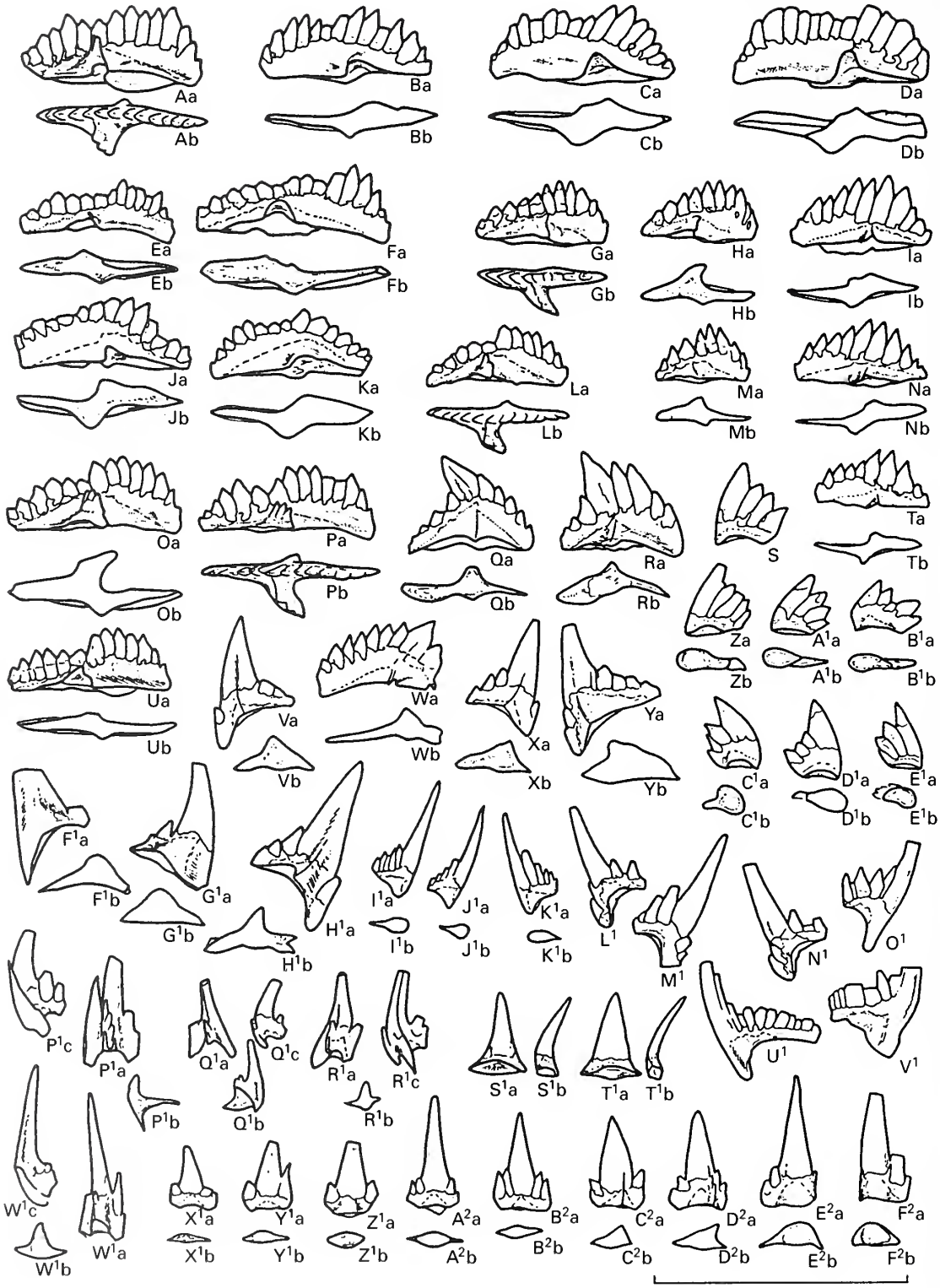

TEXT-FIG. 6. For caption see opposite.

P. amorphognathoides *lineage*

Pterospathodus amorphognathoides Walliser, 1964 *sensu nov.*

Diagnosis. The Pa element of *P. amorphognathoides* is characterized by an inner lateral process, pennate in the older and bifurcated in the younger forms; with (in younger populations) or without (in older ones) a basal platform; may or may not possess a triangular to semiquadrate lateral lobe or short, usually undenticulated process on the outer side of element. Pb_2 element with anterior and posterior processes. Posterior processes of the S elements unevenly denticulated; within the row of short narrow denticles a few larger ones are randomly situated. Processes of the carniciform element bear up to four or five tiny denticles.

Remarks. P. amorphognathoides is represented by a morphologically variable sequence of closely related populations including several evolutionarily connected successive subspecies: *P. a. angulatus*, *P. a. lennarti* ssp. nov., *P. a. lithuanicus* and *P. a. amorphognathoides* (see below). The changes in the morphology of the elements in the apparatus at the boundary between the *P. eopennatus* and *P. amorphognathoides* lineages are relatively sharp and took place at the level corresponding to one of the main events in the evolution of Telychian conodont faunas (Männik 1995).

Pterospathodus amorphognathoides angulatus (Walliser, 1964)

Plate 2, figures 1–22, 24–31; Text-figures 7–8

v.* 1964 *Spathognathodus pennatus angulatus* Walliser, p. 79, pl. 14, figs 19–22.
1975 *Llandoverygnathus pennatus* (Walliser, 1964); Aldridge, pl. 1, figs 24–25.
1981 *Pterospathodus pennatus procerus* (Walliser, 1964); Uyeno and Barnes, pl. 1, fig. 23.
? 1981 *Pterospathodus celloni* (Walliser, 1964); Uyeno and Barnes, pl. 1, figs 20–21.
? 1981 *Carniodus carnulus* Walliser, 1964; Uyeno and Barnes, pl. 1, figs 18–19.
.1982 *Pterospathodus pennatus angulatus* (Walliser, 1964); Aldridge and Mohamed, pl. 2, figs 8–11.
.1982 *Pterospathodus pennatus pennatus* (Walliser, 1964); Aldridge and Mohamed, pl. 2, fig. 12.
1982 *Pterospathodus celloni* (Walliser, 1964); Aldridge and Mohamed, pl. 2, fig. 7.
? 1983 *Carniodus carnulus* Walliser, 1964; Uyeno and Barnes, p. 16, pl. 5, figs 1–10 (figs 2–3 [= cop. Uyeno and Barnes 1981, pl. 1, figs 18–19]).
p? 1983 *Pterospathodus celloni* (Walliser, 1964); Uyeno and Barnes, p. 24, pl. 5, figs 17–18, 20–24 (*non* fig. 18 [indet.]; figs 20–22 [= cop. Uyeno and Barnes 1981, pl. 1, figs 20–21]).
p 1983 *Ozarkodina polinclinata* (Nicoll and Rexroad, 1968); Uyeno and Barnes, p. 22, pl. 5, fig. 19 (*non* figs 11–16 [= *O. polinclinata*]).
1983 *Pterospathodus pennatus procerus* (Walliser, 1964); Uyeno and Barnes, p. 24, pl. 8, figs 1–3 [fig. 1 [= cop. Uyeno and Barnes 1981, pl. 1, fig. 23]).
? 1985 *Pterospathodus pennatus pennatus* (Walliser, 1964); Aldridge, p. 80, pl. 3.1, fig. 27.
1987 *Pterospathodus celloni* (Walliser, 1964); An, p. 202, pl. 33, figs 8–10.
1987 *Neoprioniodus triangularis paucidentatus* Walliser, 1964; An, pl. 35, figs 21–22.
1987 *Pterospathodus pennatus* (Walliser, 1964); Dumoulin and Harris, fig. 4*N*.
? 1988 *Pterospathodus pennatus procerus* (Walliser, 1964); Qiu, pl. 1, figs 5–7 [cop. Qiu 1985, pl. 1, figs 5, 8–9]).
v. 1989 *Pterospathodus*, angulatus-morph Männik and Aldridge, text-fig. 3*B*.
v. 1989 *Pterospathodus*, pennatus-morph Männik and Aldridge, text-fig. 3*C*.

TEXT-FIG. 6. *Pterospathodus eopennatus* ssp. nov. 2; *Apsidognathus tuberculatus* ssp. nov. 2 Subzone. A–D, Pa element, morph 1a. E–F, J–K, Pa element, morph 1b. G–I, M–N, T, Pa element, morph 2a. L, O–P, U, Pa element, morph 4. Q–R, W, Pb_1 element. S, Z–E^1, Pb_2 element. V, X–Y, H^1, Pc element. F^1–G^1, M_1 element. L^1–N^1, Sc_1 element. I^1–K^1, Sc_3 element. O^1, U^1–V^1, Sc_2 element. P^1, Sb_2 element. Q^1–R^1, Sb_1 element. S^1–T^1, carniciform element. W^1, Sa element. X^1–Z^1, carnuliform element, morph a. A^2–B^2, carnuliform element, morph b(?). C^2–D^2, modified carnuliform element. E^2–F^2, curved element, morph a. Scale bar represents 1 mm.

v. 1998 *Pterospathodus* cf. *amorphognathoides angulatus* (Walliser, 1964); Männik and Małkowski, pl. 1, figs 20–22.

Material. Several hundred of each of the P, M, Sc and carnuliform elements; tens to hundreds of Sb, Sa and carniciform elements.

Diagnosis. P. amorphognathoides with elements without platform. Pa element long, with pennate inner lateral process and lower denticles in the middle part of the blade.

Remarks. Pa element of *P. a. angulatus* is similar to the morphs 1a and 1b of the Pa element of *P. eopennatus* ssp. nov. 2 (Pl. 2, figs 34–35; Text-fig. 6A–F, J–K) but differs by having a very long blade with at least 20, usually even more denticles on mature specimens. The Pa element of *P. a. angulatus* is represented by two morphs, one of them with tall denticles (Pl. 2, figs 1, 3–4, 9; Text-figs 7A–B, D, 8B–C, F–H) and the other with short denticles (Pl. 2, fig. 12; Text-figs 7C, G, K, 8A). The ends of lateral processes on Sb elements lack bifurcation.

In the lower part of the range of *P. a. angulatus* morphs 2 and 3 of the Pa, but also extremely rare specimens of the Pb_2 and the carniciform elements typical of *P. eopennatus* ssp. nov. 2 occur occasionally.

P. a. angulatus is the oldest representative of the *P. amorphognathoides* lineage and was evolutionarily followed by *P. amorphognathoides lennarti* ssp. nov.

EXPLANATION OF PLATE 2

Figs 1–22, 24–31. *Pterospathodus amorphognathoides angulatus* (Walliser, 1964). 1, Cn 7907; inner lateral view of dextral Pa element, morph a. 2, Cn 7908; outer lateral view of dextral Pb_2 element. 3, Cn 7909; inner lateral view of sinistral Pa element, morph a. 4, Cn 7910; upper view of dextral Pa element, morph a. 5, Cn 7911; outer lateral view of sinistral Pb_2 element. 6, Cn 7912; outer lateral view of sinistral Pb_1 element. 7, Cn 7913; outer lateral view of sinistral Pc element. 8, Cn 7914; outer lateral view of sinistral Pb_2 element. 9, Cn 7915; inner lateral view of sinistral Pa element, morph a. 10, Cn 7916; outer lateral view of dextral Pb_1 element. 11, Cn 7917; outer lateral view of dextral Pb_1 element. 12, Cn 7918; inner lateral view of sinistral Pa element, morph b. 13, Cn 7919; outer lateral view of sinistral carnuliform element, morph a. 14, Cn 7920; outer lateral view of sinistral carnuliform element, morph a(?). 15, Cn 7921; outer lateral view of sinistral modified carnuliform element. 16, Cn 7922; inner lateral view of sinistral Sc_3 element. 17, Cn 7923; inner lateral view of sinistral Sc_1 element. 18, Cn 7924; inner lateral view of dextral M_1 element. 19, Cn 7925; inner lateral view of sinistral M_1 element. 20, Cn 7926; inner lateral view of sinistral Sc_2 element. 21, Cn 7927; inner lateral view of dextral Sb_1 element. 22, Cn 7928; inner lateral view of dextral Sc_2 element. 24, Cn 7929; inner lateral view of dextral carniciform element. 25, Cn 7930; outer lateral view of sinistral curved element, morph a. 26, Cn 7931; outer lateral view of sinistral curved element, morph b. 27, Cn 7932; posterior view of dextral Sb_1 element. 28, Cn 7933; posterior view of dextral Sb_2 element. 29, Cn 7934; lateral view of Sa element. 30, Cn 7935; outer lateral view of dextral Sb_2 element. 31, Cn 7936; posterior view of Sa element. Figs 1, 3–4, 6–7, 9, 11, 15 and 24 from Nurme core, sample M-1051, int. 12·70–12·85 m; figs 2, 5 and 10 from Uulu-330 core, sample M-1298, int. 139·84–139·92 m; figs 8 and 12 from Nurme core, sample M-1050, int. 13·30–13·40 m; figs 13–14, 16–22 and 25–31 from Velise-Kõrgekalda section, sample VE-2.

Figs 23, 32–41. *Pterospathodus eopennatus* ssp. nov. 2. 23, Cn 7937; inner lateral view of dextral Pa element, morph 2a. 32, Cn 7938; inner lateral view of sinistral Pa element, morph 2a. 33, Cn 7939; upper view of dextral Pa element, morph 4. 34, Cn 7940; inner lateral view of dextral Pa element, morph 1a. 35, Cn 7941; inner lateral view of sinistral Pa element, morph 1a. 36, Cn 7942; inner lateral view of dextral Pa element, morph 2a. 37, Cn 7943; inner lateral view of sinistral Pa element, morph 2a. 38, Cn 7944; upper view of dextral Pa element, morph 4(?). 39, Cn 7945; inner lateral view of sinistral Pa element, morph 2a. 40, Cn 7946; inner lateral view of dextral Pa element, morph 1a. 41, Cn 7947; inner lateral view of dextral Pa element, morph 4. Figs 23, 34–35 and 37–38 from Nurme core, sample M-907, int. 17·50–17·60 m; figs 32 and 36 from Viki core, sample M-11, int. 175·60–175·80 m; figs 33, 39 and 41 from Nurme core, sample M-900, int. 22·65–22·80 m; fig. 40 from Viki core, sample M-8, int. 168·60–168·80 m.

All × 50.

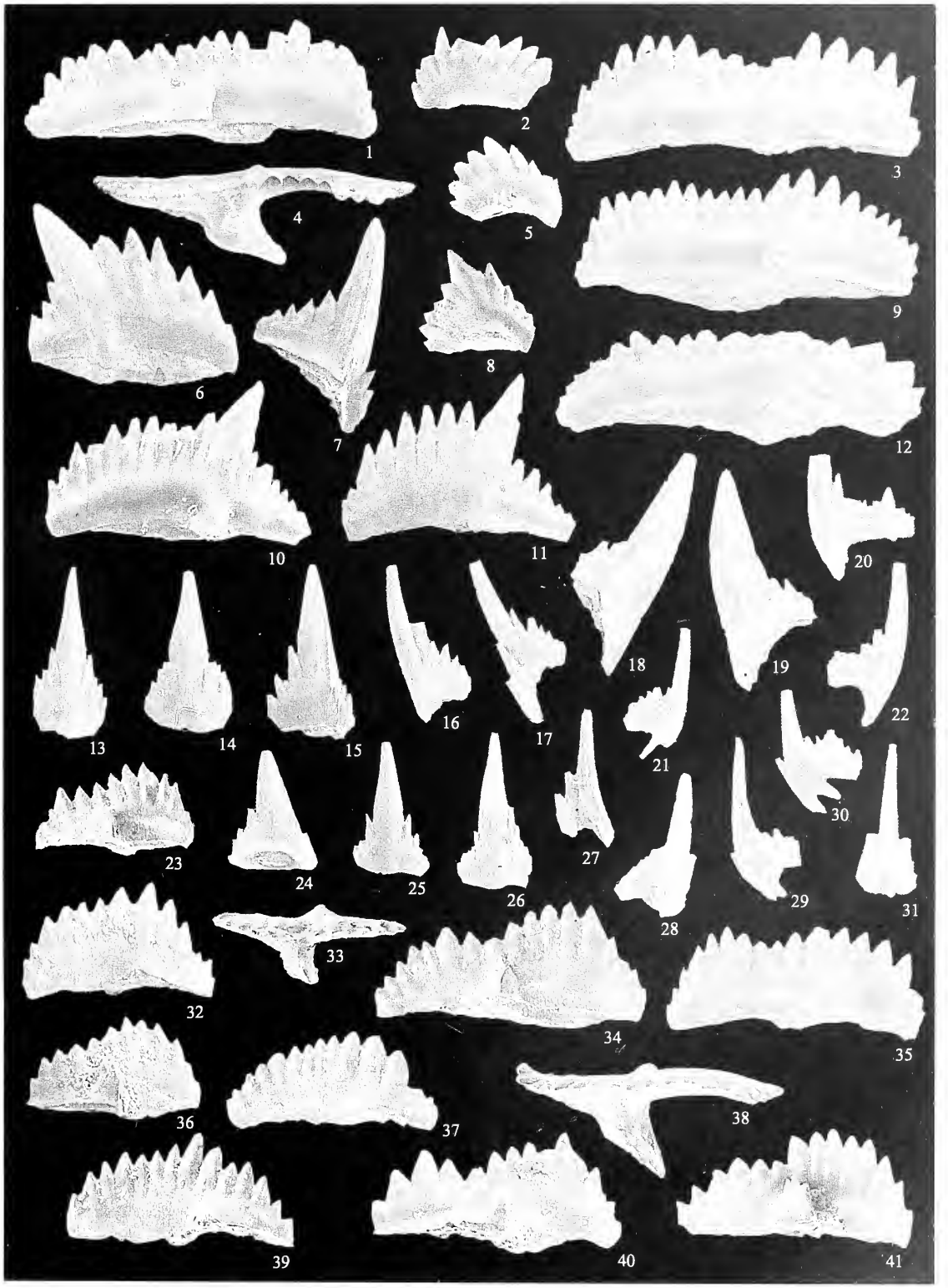

MÄNNIK, *Pterospathodus*

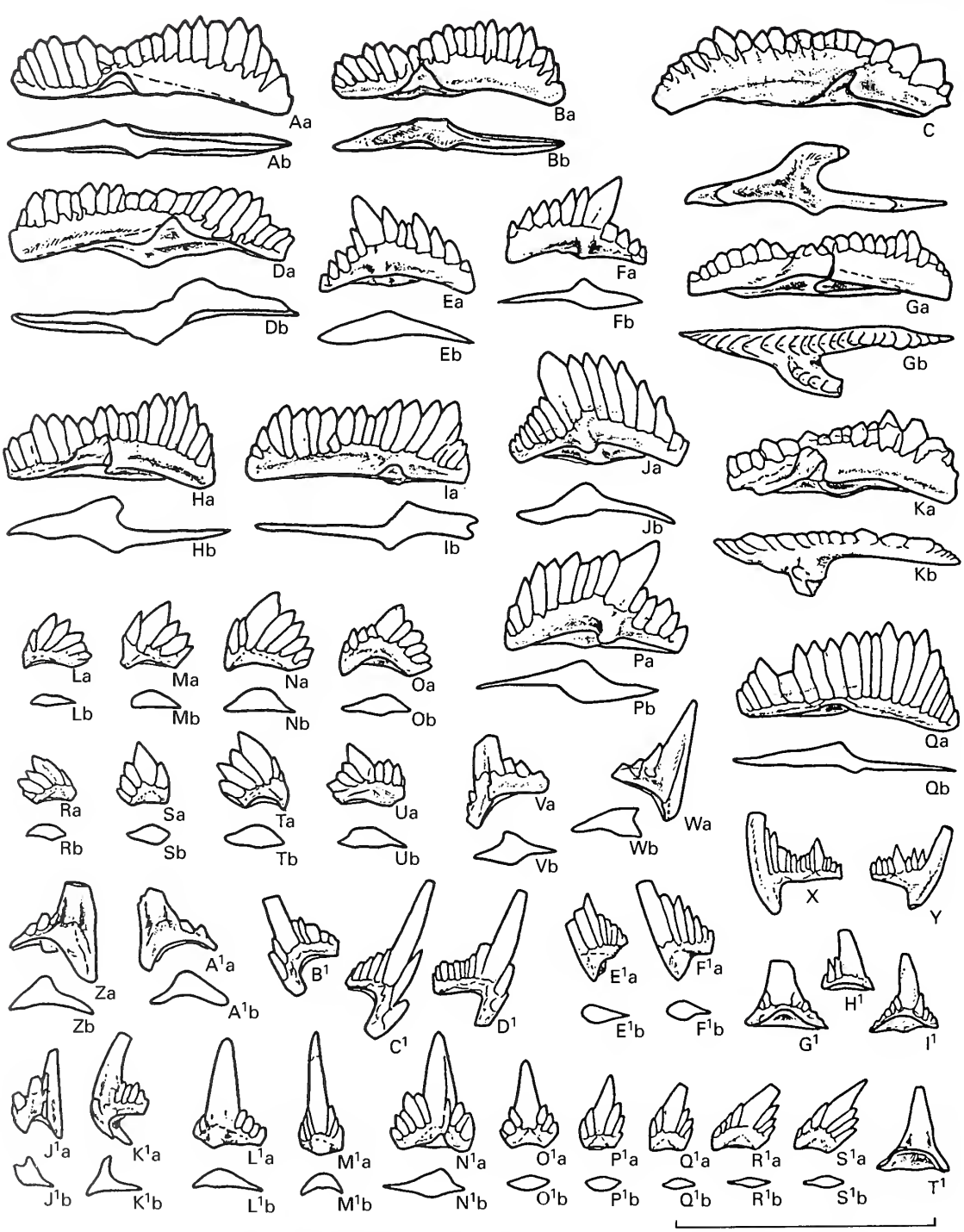

TEXT-FIG. 7. *Pterospathodus amorphognathoides angulatus* (Walliser, 1964); *Apsidognathus tuberculatus* ssp. nov. 3 Subzone. A–B, D, Pa element, morph a. C, G, K, Pa element, morph b. H–I, Q, Pa element, morph 3. E–F, J, P, Pb_1 element. L–O, R–U, Pb_2 element. V–W, Pc element. X–Y, Sc_2 element. Z, A^1, M_1 element. B^1–D^1, Sc_1

Occurrence. A. tuberculatus ssp. nov. 3 and *P. a. angulatus* subzones. *P. a. angulatus* can be recognized worldwide (see synonymy).

Pterospathodus amorphognathoides lennarti ssp. nov.

Plate 3, figures 21–46; Text-figure 9

p. 1972 *Pterospathodus amorphognathoides* Walliser, 1964; Aldridge, p. 208, pl. 3, fig. 18 (*non* figs 17, 19 [= *P. a. amorphognathoides*]).
? 1972 *Neoprioniodus costatus costatus* Walliser, 1964; Aldridge, p. 193, pl. 5, fig. 22.
? 1972 *Ozarkodina gaertneri* Walliser, 1964; Aldridge, p. 200, pl. 5, fig. 7.
.1985 *Pterospathodus pennatus* subsp. nov. Aldridge, p. 81, pl. 3.1, fig. 28.
v. 1986 *P. celloni* (Walliser); Nakrem, fig. 6*a*.
vp. 1986 *Carniodus carnulus* Walliser, 1964; Nakrem, fig. 6*l* (*non* fig. 7*c*, *f* [= *P. a. lithuanicus*]).

Derivation of name. In honour of Dr Lennart Jeppsson, an expert on Silurian conodonts.

Material. Several hundred to a thousand carnuliform elements; several hundred P, M, Sc, carniciform and curved elements; many tens to hundreds of Sb and Sa elements.

Holotype. Dextral Pa element Cn 7968, Pahapilli core, sample M-1520, int. 47·30–47·20 m (Velise Formation, northern Saaremaa, Estonia); Plate 3, figure 21.

Type horizon and locality. Middle part of the Velise Formation, Adavere Regional Stage; Pahapilli core, interval 46·60–50·30 m.

Diagnosis. P. amorphognathoides with elements without platform. The first denticle on the bifurcated lateral process of the Pa element is situated away from the main row of denticles and is connected with the last one by a narrow high ridge.

Remarks. The most characteristic feature separating the Pa element of *P. amorphognathoides lennarti* ssp. nov. from that of younger subspecies (e.g. *P. a. lithuanicus*; Pl. 4, figs 29–32, 34–35; Text-fig. 10A–B, D–E) is the deep groove between the main row of denticles and the first one on the inner lateral process (Text-fig. 9A, D–E). As a rule, that denticle is connected with the main row by a narrow high ridge (Pl. 3, figs 21–22, 25, 27; Text-fig. 9A, D–E). The configuration (the direction of the branches) of the lateral process is highly variable. The distal part of the posterior branch is usually turned parallel to the anterior one (Pl. 3, fig. 27).

The Pa element of *P. amorphognathoides lennarti* ssp. nov. is represented by two morphs. Morph 1 has tall denticles and a relatively low base (Text-fig. 9A, C, G) whereas morph 2 is characterized by short denticles and a higher base (Text-fig. 9E). The denticulation of morph 1 tends to be more irregular and includes overgrown denticles (Text-fig. 9G). A sub-triangular outer lateral lobe/short process is also characteristic, better developed on the sinistral element.

P. amorphognathoides lennarti ssp. nov. is a direct descendant of *P. a. angulatus*. These two taxa differ mainly in the lack (or extremely rare occurrence) of bifurcation on the inner lateral process in *P. a. angulatus* and in the development of an outer lateral lobe on the Pa elements of *P. a. lennarti* ssp. nov. The apparatus of *P. a. lennarti* ssp. nov. differs from earlier taxa in the presence of short

---

element. E^1–F^1, Sc$_3$ element. G^1–I^1, T^1, carniciform element. J^1, Sb$_1$ element. K^1, Sb$_2$ element. L^1, curved element, morph a. M^1, curved element, morph b. N^1, modified carnuliform element. O^1–S^1, carnuliform element, morph a. Scale bar represents 1 mm.

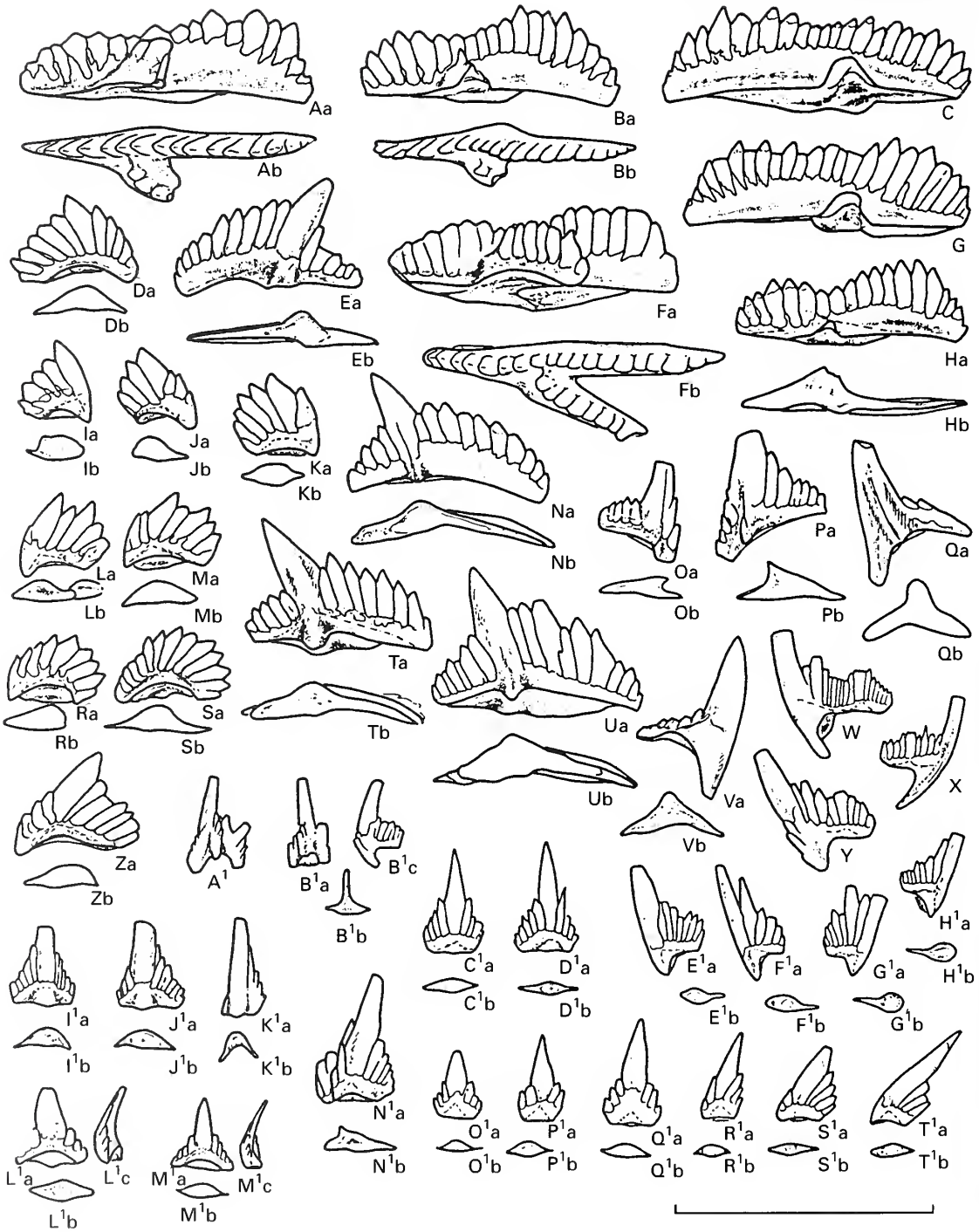

TEXT-FIG. 8. *Pterospathodus amorphognathoides angulatus* (Walliser, 1964); *P. a. angulatus* Subzone. A, Pa element, morph b. B–C, F–H, Pa element, morph a. E, N, T–U, Pb_1 element. D, I–M, R–S, Z, Pb_2 element. O–P, Pc element. Q, V, M_1 element. W–X, Sc_2 element. Y, Sc_1 element. A^1, Sb_1 element. B^1, Sb_2 element. C^1–D^1, carniuliform

and modified short morphs of the carnuliform element (Pl. 3, figs 24, 33; Text-fig. 9V–W, L¹–M¹, V¹–W¹).

Occurrence. The *P. amorphognathoides lennarti* Subzone. On Gotland *P. a. lennarti* ssp. nov. has been found in loose pebbles from Själsö (collection of L. Jeppsson – sample G88-637LJ). *P. a. lennarti* ssp. nov. has also been found in Carnic Alps (Seewarte section – collection of H. P. Schönlaub, sample 195/1–2, and probably in the Cellon section – collection of O. H. Walliser, one fragment in sample 10 H/J), in Great Britain (Aldridge 1972, pl. 3, fig. 18, Ticklerton 2 section; 1985, pl. 3.1, fig. 28, loc. 23 – uppermost Purple Shales of small stream 850 m south-west of Ticklerton, Shropshire) and Norway (Nakrem 1986, fig. 6*a*, Malmoyakalven section, Vik Fm., 42·5 m).

Pterospathodus amorphognathoides lithuanicus Brazauskas, 1983 *sensu novo*

Plate 3, figures 1–20, Plate 4, figures 21, 28–35; Text-figure 10

v.* 1983 *Pterospathodus amorphognathoides lithuanicus* Brazauskas, p. 60, figs 1–7.
v. 1986 *Pterospathodus amorphognathoides* Walliser, 1964; Nakrem, fig. 6*b–d, e*(?), *f–g, i*.
v.? 1986 *Pterospathodus pennatus pennatus* (Walliser, 1964); Nakrem, fig. 6*h*.

Material. Several hundreds to a thousand of each of the Pa, Pb and carnuliform elements; many hundreds of the Pc, M, S, carniciform and curved elements.

Emended diagnosis. *P. amorphognathoides* without basal platform. The first denticle on the bifurcated inner lateral process is situated close to the main row of denticles.

Remarks. Brazauskas (1983) described only the Pa element of the apparatus. Here *P. a. lithuanicus* is considered to include the complete set of elements of the *Pterospathodus* apparatus. Morphologically the most distinct element in this apparatus is the Pa element (Pl. 4, figs 21, 29–32, 34, 45; Text-fig. 10A–B, D–E). The Pb_1 (Pl. 3, figs 15, 17; Text-fig. 10C, F, O, U) and Pb_2 (Pl. 3, fig. 1; Pl. 4, fig. 28; Text-fig. 10G–L, P) elements can also be quite easily separated from those of the older subspecies, as they possess a weak lateral basal thickening lacking on the corresponding elements of *P. a. lennarti* ssp. nov.

As a rule, the sinistral Pa element (Pl. 4, figs 31–32; Text-fig. 10B, E) possesses a distinct rounded or triangular lateral lobe on the outer side of the element. This structure is almost absent on the dextral element (Pl. 4, figs 29–30; Text-fig. 10A, D). In the apparatus of *P. a. lithuanicus* a new modification of curved element, morph c, appears (Pl. 3, fig. 16; Text-fig. 10Y¹–Z¹).

Occurrence. In the *P. a. lithuanicus* Subzone. Outside the Baltic (Estonia, Lithuania) *P. a. lithuanicus* has so far been illustrated only from Norway (Nakrem 1986, fig. 6*d, e*(?), *g–i*, Malmoyakalven section, Vik Fm.). However, it is most probable, that after revision of collections from other regions of the world this taxon will be recognized to have a much wider distribution.

Pterospathodus amorphognathoides amorphognathoides Walliser, 1964

Plate 4, figures 1–20, 22–27; Plate 5; Text-figures 11–15

v.* 1964 *Pterospathodus amorphognathoides* Walliser, p. 67, pl. 15, figs 9–15.
v. 1964 *Ozarkodina gaertneri* Walliser, p. 57, pl. 27, figs 12–19.
v. 1964 ?*Carniodus carinthiacus* Walliser, p. 31, pl. 27, figs 20–26.
v. 1964 *Carniodus carnulus* Walliser, p. 32, pl. 27, figs 27–38; pl. 28, fig. 1.

---

element, morph b. E¹–H¹, Sc_3 element. I¹–J¹, curved element, morph a. K¹, curved element, morph b. L¹–M¹, carniciform element. N¹, modified carnuliform element. O¹–T¹, carnuliform element, morph a. Scale bar represents 1 mm.

v. 1964 *Carniodus carnus* Walliser, p. 34, pl. 28, figs 2–7.
v. 1964 *Carniodus carnicus* Walliser, p. 32, pl. 28, figs. 8–11.
vp. 1964 *Neoprioniodus subcarnus* Walliser, p. 51, pl. 28, figs 13–18 (*non* fig. 12 [= *P. celloni*]).
v. 1964 *Neoprioniodus triangularis triangularis* Walliser, p. 52, pl. 28, figs 25–30.
v. 1964 *Neoprioniodus costatus costatus* Walliser, p. 48, pl. 28, figs 36–41.
v. 1964 *Roundya latialata* Walliser, p. 71, pl. 31, figs 11–14.
.1966 *Ozarkodina gaertneri* Walliser, 1964; Spasov and Filipović, p. 44, pl. 1, figs 1–2.
.1966 *Carniodus carinthiacus* Walliser, 1964; Spasov and Filipović, p. 38, pl. 1, fig. 3.
.1966 *Pterospathodus amorphognathoides* Walliser, 1964; Spasov and Filipović, p. 48, pl. 1, figs 4–5.
.1966 *Neoprioniodus subcarnus* Walliser, 1964; Spasov and Filipović, p. 42, pl. 1, figs 8–9.
.1966 *Neoprioniodus costatus costatus* Walliser, 1964; Spasov and Filipović, p. 42, pl. 1, figs 10–11.
.1966 *Carniodus carnus* Walliser, 1964; Sapsov and Filipović, p. 40, pl. 1, figs 12–13.
1966 *Roundya brevialata* Walliser, 1964; Spasov and Filipović, p. 49, pl. 1, fig. 14.
.1966 *Carniodus carnulus* Walliser, 1964; Spasov and Filipović, p. 39, pl. 1, fig. 15.
.1966 *Carniodus carnicus* Walliser, 1964; Spasov and Filipović, p. 38, pl. 1, fig. 16.

EXPLANATION OF PLATE 3

Figs 1–20. *Pterospathodus amorphognathoides lithuanicus* Brazauskas, 1983. 1, Cn 7948; outer lateral view of dextral Pb_2 element. 2, Cn 7949; outer lateral view of sinistral Sb_1 element. 3, Cn 7950; inner lateral view of dextral Sc_2 element. 4, Cn 7951; inner lateral view of sinistral Sc_2 element. 5, Cn 7952; outer lateral view of sinistral curved element, morph a. 6, Cn 7953; inner(?) lateral view of dextral(?) modified carnuliform element, short morph. 7, Cn 7954; outer lateral view of sinistral curved element, morph b. 8, Cn 7955; posterior view of dextral Sb_1 element. 9, Cn 7956; inner lateral view of sinistral M_1 element. 10, Cn 7957; inner lateral view of dextral Sc_2 element. 11, Cn 7958; posterior view of sinistral Sb_1 element. 12, Cn 7959; inner lateral view of dextral Sc_3 element. 13, Cn 7960; posterior view of sinistral Sb_2 element. 14, Cn 7961; outer lateral view of sinistral Pc element. 15, Cn 7962; outer lateral view of dextral Pb_1 element. 16, Cn 7963; outer lateral view of dextral curved element, morph c. 17, Cn 7964; outer lateral view of dextral Pb_1 element. 18, Cn 7965; inner lateral view of sinistral Sc_3 element. 19, Cn 7966; outer lateral view of dextral carnuliform element, short morph. 20, Cn 7967; inner lateral view of dextral carniciform element. Figs 1, 5–8, 10, 13 and 18–20 from Viki core, sample M-976, int. 149·95–150·08 m; figs 2 and 11 from Viki core, sample M-362, int. 151·87–152·00 m; figs 3–4, 9 and 14–15 from Viki core, sample M-979, int. 148·75–148·85 m; fig. 12 from Viki core, sample M-972, int. 151·25–151·40 m; fig. 16 from Viki core, sample M-971, int. 151·54–151·64 m; fig. 17 from Viki core, sample M-367, int. 146·70–146·80 m.

Figs 21–46. *Pterospathodus amorphognathoides lennarti* ssp. nov. 21, Cn 7968; upper view of dextral Pa element. 22, Cn 7969; upper view of sinistral Pa element. 23, Cn 7970; outer lateral view of dextral curved element, morph b. 24, Cn 7971; inner lateral view of sinistral modified carnuliform element, short morph. 25, Cn 7972; upper view of dextral Pa element. 26, Cn 7973; outer lateral view of sinistral Pb_2 element. 27, Cn 7974; upper view of dextral Pa element. 28, Cn 7975; inner lateral view of dextral Sc_3 element. 29, Cn 7976; outer lateral view of sinistral Pc element. 30, Cn 7977; inner lateral view of sinistral Sc_2 element. 31, Cn 7978; inner lateral view of dextral M_1 element. 32, Cn 7979; inner lateral view of dextral Sc_3 element. 33, Cn 7980; outer(?) lateral view of dextral(?) modified carnuliform element, short morph. 34, Cn 7981; outer lateral view of dextral Sb_2 element. 35, Cn 7982; outer lateral view of dextral Pb_1 element. 36, Cn 7983; outer lateral view of sinistral Pb_1 element. 37, Cn 7984; inner lateral view of sinistral Sc_3 element. 38, Cn 7985; inner lateral view of sinistral Sc_3 element. 39, Cn 7986; inner lateral view of sinistral M_1 element. 40, Cn 8080; outer lateral view of sinistral curved element, morph a. 41, Cn 7987; posterior view of Sa element. 42, Cn 7988; outer lateral view of dextral Pb_1 element. 43, Cn 7989; inner lateral view of dextral Sc_2 element. 44, Cn 7990; posterior view of dextral Sb_1 element. 45, Cn 7991; lateral view of symmetrical(?) carnuliform element, morph b. 46, Cn 7992; outer lateral view of dextral modified carnuliform element. Fig. 21 from Pahapilli core, sample M-1520, int. 47·20–47·30 m; figs 22–25, 33, 35, 42–43 and 45–46 from Viki core, sample M-966, int. 153·88–154·05 m; figs 26–27 from Uulu-330 core, sample M-1070, int. 137·70–137·85 m; figs 28, 34, 40–41 and 44 from Uulu-330 core, sample M-1301, int. 138·05–138·15 m; figs 29–31 and 39 from Viki core, sample M-967, int. 153·60–153·72 m, figs 32 and 37–38 from Viki core, sample M-360, int. 153·35–153·50 m; fig. 36 from Viki core, sample M-968, int. 153·05–153·20 m.

All × 50.

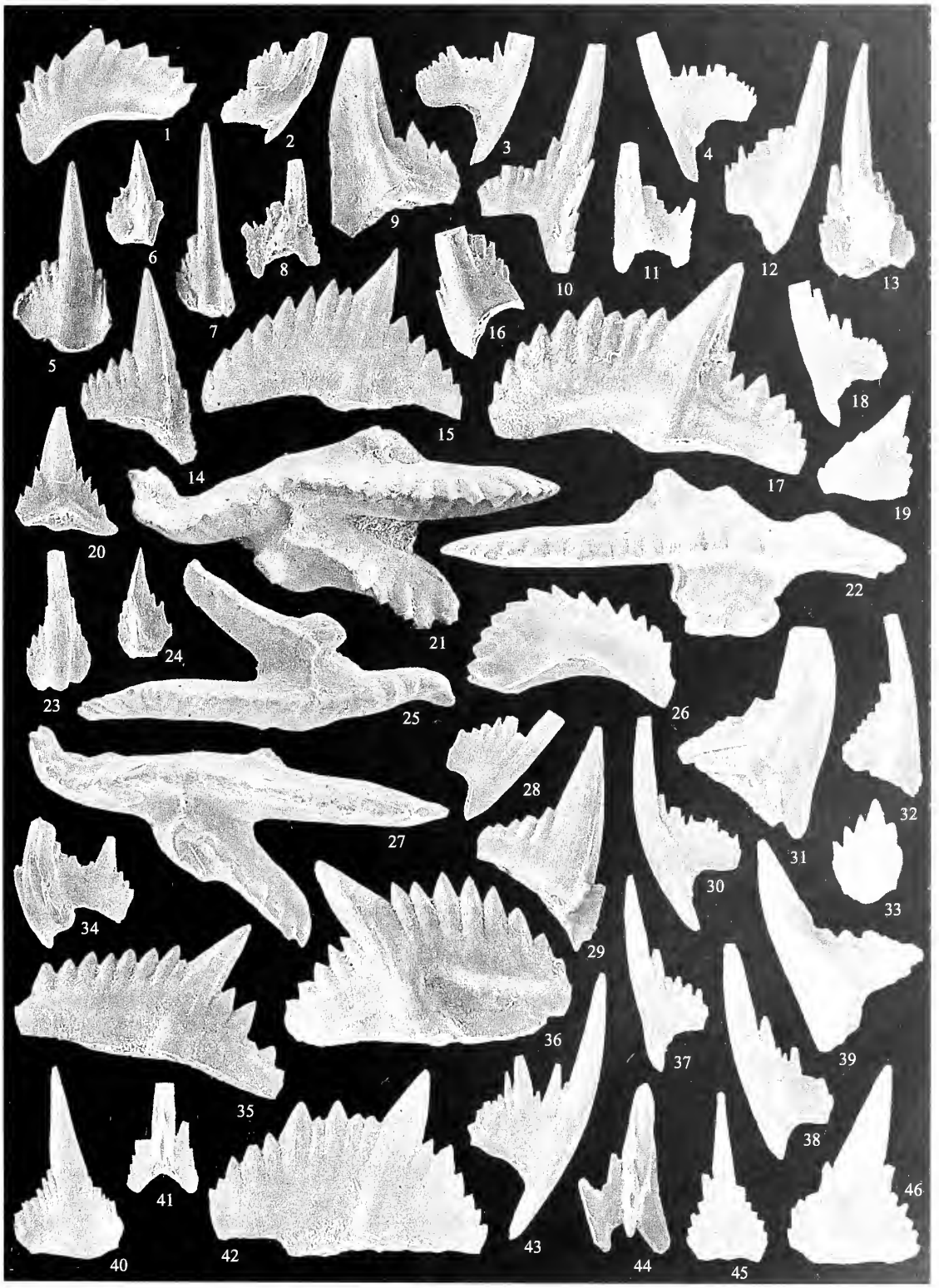

MÄNNIK, *Pterospathodus*

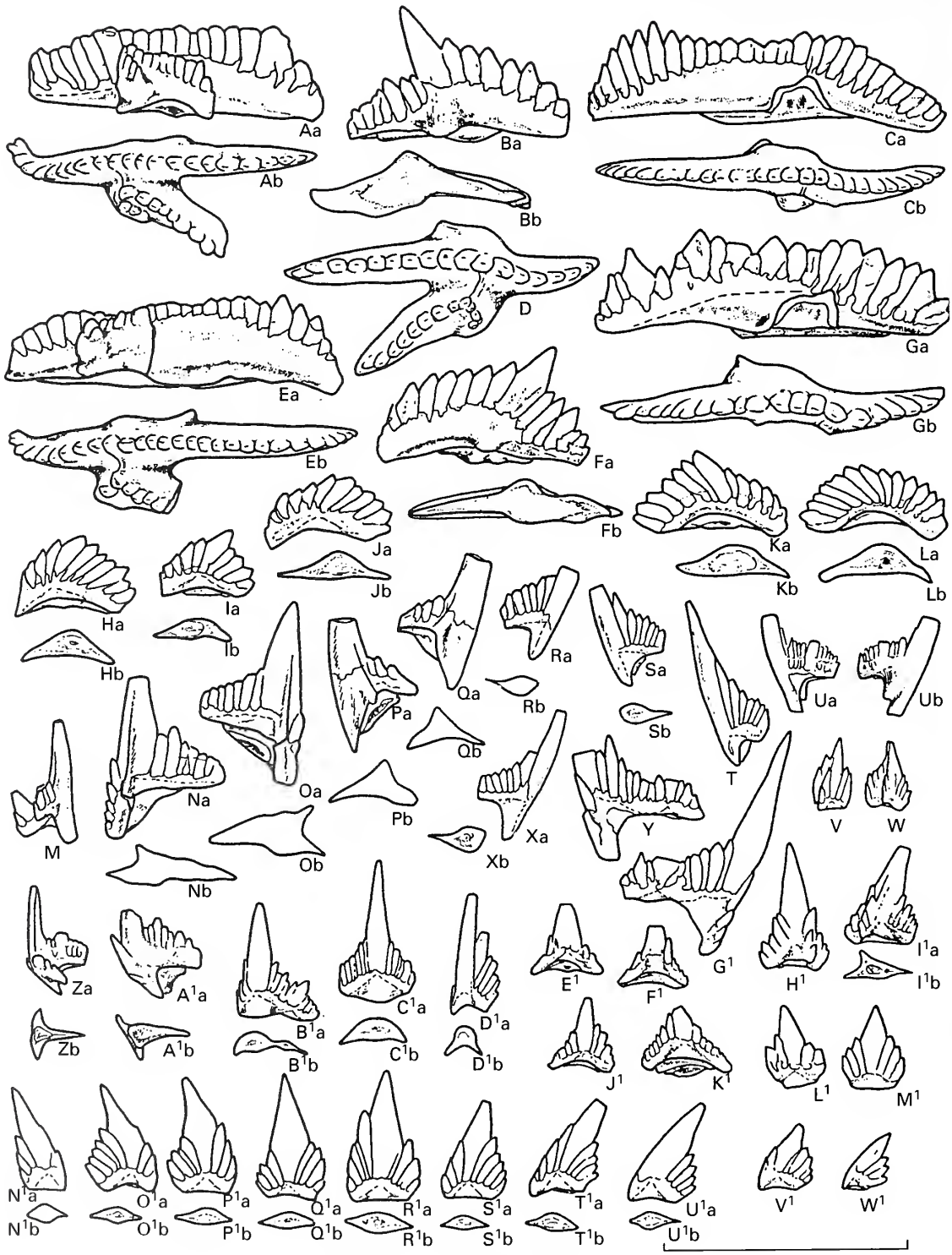

TEXT-FIG. 9. For caption see opposite.

p. 1968 *Ozarkodina gaertneri* Walliser, 1964; Igo and Koike, p. 14, pl. 1, figs 5–6 (*non* figs 7–9 [= *P. pennatus procerus*]).
1968 *Pterospathodus amorphognathoides* Walliser, 1964; Igo and Koike, p. 16, pl. 2, figs 12–13.
p. 1968 *Carniodus* sp. A Igo and Koike, p. 8, pl. 3, fig. 3 (*non* fig. 2 [= *P. p. procerus*?]).
p. 1968 *Neoprioniodus* spp. Igo and Koike, p. 14, pl. 3, fig. 4 (*non* fig. 24 [= *P. p. procerus*?]).
.1968 *Ozarkodina gaertneri* Walliser, 1964; Nicoll and Rexroad, p. 49, pl. 2, figs 12–14.
.1968 *Ozarkodina neogaertneri* Nicoll and Rexroad, p. 50, pl. 2, figs 15–16.
1968 *Pterospathodus amorphognathoides* Walliser, 1964; Nicoll and Rexroad, p. 56, pl. 3, figs 1–5, 6?, 7.
.1968 *Carniodus carinthiacus* Walliser, 1964; Nicoll and Rexroad, p. 24, pl. 5, figs 1–2.
1968 *Carniodus carnicus* Walliser, 1964; Nicoll and Rexroad, p. 25, pl. 5, fig. 3.
.1968 *Carniodus carnulus* Walliser, 1964; Nicoll and Rexroad, p. 25, pl. 5, figs 4–5.
p. 1968 *Carniodus carnus* Walliser, 1964; Nicoll and Rexroad, p. 26, pl. 5, figs 6, 8 (*non* fig. 7 [indet.]).
.1968 *Neoprioniodus subcarnus* Walliser, 1964; Nicoll and Rexroad, p. 41, pl. 5, fig. 10.
.1968 *Neoprioniodus costatus* Walliser, 1964; Nicoll and Rexroad, p. 40, pl. 5, figs 15–16.
.1968 *Neoprioniodus triangularis* Walliser, 1964; Nicoll and Rexroad, p. 42, pl. 5, fig. 17.
1969 *Carniodus carnulus* Walliser, 1964; Schönlaub, pl. 1, fig. 5.
.1969 *Pterospathodus amorphognathoides* Walliser, 1964; Schönlaub, pl. 1, fig. 8.
.1969 ?*Carniodus carinthiacus* Walliser, 1964; Schönlaub, pl. 1, fig. 12.
.1969 *Ozarkodina gaertneri* Walliser, 1964; Schönlaub, pl. 1, fig. 15.
1969 *Pterospathodus amorphognathoides* Walliser, 1964; Drygant, p. 49, pl., fig. 6.
.1969 *Carniodus*? *carinthiacus* Walliser, 1964; Drygant, p. 54, pl., fig. 5.
? 1969 *Neoprioniodus subcarnus* Walliser, 1964; Drygant, p. 53, pl., figs 12–14.
.1970 *Pterospathodus amorphognathoides* Walliser, 1964; Manara and Vai, p. 494, pl. 62, fig. 15.
.1970 *Ozarkodina gaertneri* Walliser, 1964; Manara and Vai, p. 487, pl. 62, fig. 17.
.1971 *Pterospathodus amorphognathoides* Walliser, 1964; Schönlaub, p. 45, pl. 2, figs 6–12.
p. 1971 *Carniodus carinthiacus* Walliser, 1964; Schönlaub, p. 46, pl. 3, figs 7–8 (*non* fig. 6 [= *P. eopennatus*]).
.1971 *Neoprioniodus subcarnus* Walliser, 1964; Rexroad and Nicoll, pl. 1, fig. 11.
.1971 *Pterospathodus amorphognathoides* Walliser, 1964; Rexroad and Nicoll, pl. 2, figs 20–21.
.1971 *Ozarkodina gaertneri* Walliser, 1964; Rexroad and Nicoll, pl. 2, fig. 22.
.1971 *Ozarkodina neogaertneri* Nicoll and Rexroad, 1968; Rexroad and Nicoll, pl. 2, fig. 23.
.1972 *Ozarkodina gaertneri* Walliser, 1964; Rexroad and Nicoll, pl. 1, figs 1–3.
.1972 *Pterospathodus amorphognathoides* Walliser, 1964; Rexroad and Nicoll, pl. 1, figs 4–7.
.1972 *Carniodus carnulus* Walliser, 1964; Rexroad and Nicoll, pl. 1, figs 8–11.
.1972 *Carniodus carnus* Walliser, 1964; Rexroad and Nicoll, pl. 1, figs 12–13.
.1972 *Carniodus carinthiacus* Walliser, 1964; Rexroad and Nicoll, pl. 2, figs 1–3.
1972 *Carniodus carnicus* Walliser, 1964; Rexroad and Nicoll, pl. 2, figs 4, 5?.
.1972 *Neoprioniodus subcarnus* Walliser, 1964; Rexroad and Nicoll, pl. 2, figs 6–7.
.1972 *Neoprioniodus costatus* Walliser, 1964; Rexroad and Nicoll, pl. 2, figs 8–11.
.1972 *Neoprioniodus triangularis* Walliser, 1964; Rexroad and Nicoll, pl. 2, figs 12–13.
1972 *Exochognathus brevialatus* (Walliser, 1964); Rexroad and Nicoll, pl. 2, figs 21?, 22.
.1972 *Ozarkodina neogaertneri* Nicoll and Rexroad, 1968; Rexroad and Nicoll, pl. 2, fig. 34.
p. 1972 *Ozarkodina gaertneri* Walliser, 1964; Aldridge, p. 200, pl. 5, fig. 5 (*non* fig. 7 [= *P. amorphognathoides lennarti* ssp. nov or *P. a. lithuanicus*]).
.1972 *Carniodus carinthiacus* Walliser, 1964; Aldridge, p. 168, pl. 5, figs 8–10.
.1972 *Carniodus carnicus* Walliser, 1964; Aldridge, p. 168, pl. 5, fig. 11.
.1972 *Carniodus carnulus* Walliser, 1964; Aldridge, p. 169, pl. 5, figs 12–14.
.1972 *Carniodus carnus* Walliser, 1964; Aldridge, p. 169, pl. 5, figs 15–16.

TEXT-FIG. 9. *Pterospathodus amorphognathoides lennarti* ssp. nov. A, C–D, G?, Pa element, morph a. E, Pa element, morph b. B, F, Pb_1 element. H–L, Pb_2 element. N–O, Pc element. P–Q, M_1 element. R–T, X, Sc_3 element. U, Sc_2 element. V–W, modified carnuliform element, short morph. Y, G^1, Sc_1 element. Z, Sa element. A^1, Sb_2 element. B^1–C^1, curved element, morph a. D^1, curved element, morph b. E^1–F^1, J^1–K^1, carniciform element. H^1–I^1, modified carnuliform element. L^1–M^1, V^1–W^1, carnuliform element, short morph. N^1–U^1, carnuliform element, morph a. Scale bar represents 1 mm.

.1972 *Neoprioniodus subcarnus* Walliser, 1964; Aldridge, p. 195, pl. 5, fig. 17.
p. 1972 *Pterospathodus amorphognathoides* Walliser, 1964; Aldridge, pl. 3, figs 17, 19 (*non* fig. 18 [= *P. a. lennarti* ssp. nov.]).
.1974 *Pterospathodus amorphognathoides* Walliser, 1964; Aldridge, fig. 1*E–F*.
.1975 *Pterospathodus amorphognathoides* Walliser, 1964; Aldridge, pl. 1, figs 22–23.
.1975 *Carniodus carnulus* Walliser, 1964; Aldridge, pl. 1, figs 3–4, 8–9.
.1975 *Exochognathus latialatus* (Walliser, 1964); Aldridge, pl. 3, fig. 15.
1975 *Neoprioniodus costatus costatus* Walliser, 1964; Aldridge, pl. 3, fig. 17.
1975 *Distomodus triangularis* (Walliser, 1964); Aldridge, pl. 3, fig. 19.
1975 *Pterospathodus amorphognathoides* Walliser, 1964; Saladžius, pl. 2, figs 7, 8(?).
1975 *Carniodus carinthiacus* Walliser, 1964; Saladžius, pl. 1, fig. 5.
1975 *Neoprioniodus costatus* Walliser, 1964; Saladžius, pl. 1, fig. 9.
1975 *Neoprioniodus subcarnus* Walliser, 1964; Saladžius, pl. 1, fig. 11.
1975 *Neoprioniodus triangularis* Walliser, 1964; Saladžius, pl. 1, fig. 12.
1975 *Neoprioniodus triangularis triangularis* Walliser, 1964; Saladžius, pl. 1, fig. 13.
.1976 *Carniodus carnulus* Walliser, 1964; Barrick and Klapper, p. 68, pl. 1, figs 1–2, 6–8, 12–14.
.1976 *Pterospathodus amorphognathoides* Walliser, 1964; Barrick and Klapper, p. 82, pl. 1, figs 4, 9–11, 16.
.1976 *Pterospathodus amorphognathoides* Walliser, 1964; Kuwano, pl. 2, fig. 2.
.1976 *Pterospathodus amorphognathoides* Walliser, 1964; Miller, fig. 822.
1976 *Ozarkodina gaertneri* Walliser, 1964; Miller, fig. 820.
.1977 *Pterospathodus amorphognathoides* Walliser, 1964; Cooper, p. 1065, pl. 2, figs 3, 6.
1977 *Neoprioniodus subcarnus* Walliser, 1964; Liebe and Rexroad, pl. 1, fig. 1.

EXPLANATION OF PLATE 4

Figs 1–4. *Pterospathodus amorphognathoides amorphognathoides* Walliser, 1964; Population 2. 1, Cn 7993; upper view of dextral Pa element. 2, Cn 7994; upper view of sinistral Pa element. 3, Cn 7995; outer lateral view of sinistral Pb_1 element. 4, Cn 7996; outer lateral view of dextral Pb_1 element. Figs 1 and 3–4 from Viki core, sample M-375, int. 137·95–138·10 m; fig. 2 from Viki core, sample M-374, int. 138·95–139·10 m.

Figs 5–20, 22–27. *Pterospathodus amorphognathoides amorphognathoides* Walliser, 1964; Population 1. 5, Cn 7997; outer lateral view of dextral Pb_1 element. 6, Cn 7998; upper view of dextral Pa element. 7, Cn 7999; outer lateral view of dextral Pb_2 element. 8, Cn 8000; upper view of sinistral Pa element. 9, Cn 8001; outer lateral view of dextral Pb_1 element. 10, Cn 8002; outer lateral view of sinistral Pb_1 element. 11, Cn 8003; outer lateral view of dextral Pb_2 element. 12, Cn 8004; outer lateral view of dextral Pa element. 13, Cn 8005; outer lateral view of dextral carnuliform element, short morph. 14, Cn 8006; outer lateral view of sinistral curved element, morph a. 15, Cn 8007; inner lateral view of sinistral Sc_3 element. 16, Cn 8008; inner lateral view of sinistral Sc_2 element. 17, Cn 8009; inner lateral view of dextral Sc_3 element. 18, Cn 8010; inner lateral view of sinistral Sc_1 element. 19, Cn 8011; lateral view of Sa element. 20, Cn 8012; inner lateral view of dextral carniciform element. 22, Cn 8013; outer lateral view of sinistral curved element, morph b. 23, Cn 8014; outer lateral view of dextral carnuliform element, morph a. 24, Cn 8015; inner lateral view of dextral M_1 element. 25, Cn 8016; posterior view of dextral Sb_2 element. 26, Cn 8017; outer lateral view of dextral Pc element. 27, Cn 8018; posterior view of dextral Sb_1 element. Figs 5–6 and 8–10 from Viki core, sample M-367, int. 146·70–146·80 m; figs 7, 11–17, 19–20 and 22–27 from Viki core, sample M-368, int. 145·40–145·55 m; fig. 18 from Viki core, sample M-369, int. 144·45–144·50 m.

Figs 21, 28–35. *Pterospathodus amorphognathoides lithuanicus* Brazauskas, 1983. 21, Cn 8019; inner lateral view of dextral Pa element. 28, Cn 8020; outer lateral view of sinistral Pb_2 element. 29, Cn 8021; upper view of dextral Pa element. 30, LO 7736t; upper view of dextral Pa element. 31, LO 7737t; upper view of sinistral Pa element, juvenile specimen. 32, Cn 8022; upper view of sinistral Pa element. 33, Cn 8023; outer lateral view of sinistral carnuliform element, morph a(?). 34, Cn 8024; outer lateral view of dextral Pa element. 35, Cn 8025; outer lateral view of sinistral Pa element. Figs 21 and 34–35 from Viki core, sample M-979, int. 148·75–148·85 m; figs 28 and 33 from Viki core, sample M-976, int. 149·95–150·08 m; figs 29 and 32 from Uulu-330 core, sample M-1302, int. 137·44–137·50 m; figs 30–31 from Själsö section (Gotland), sample G88-637LJ.

All × 50.

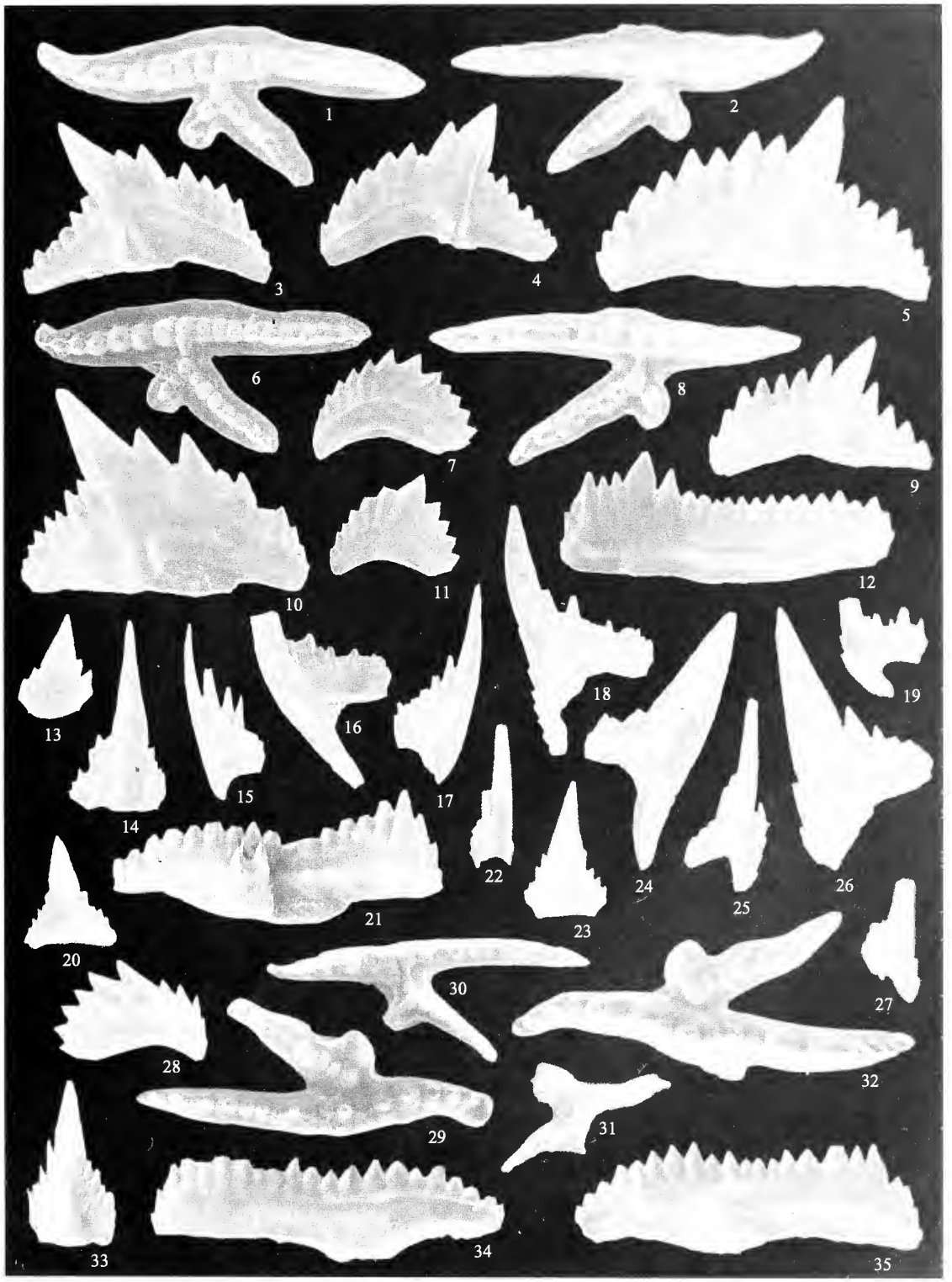

MÄNNIK, *Pterospathodus*

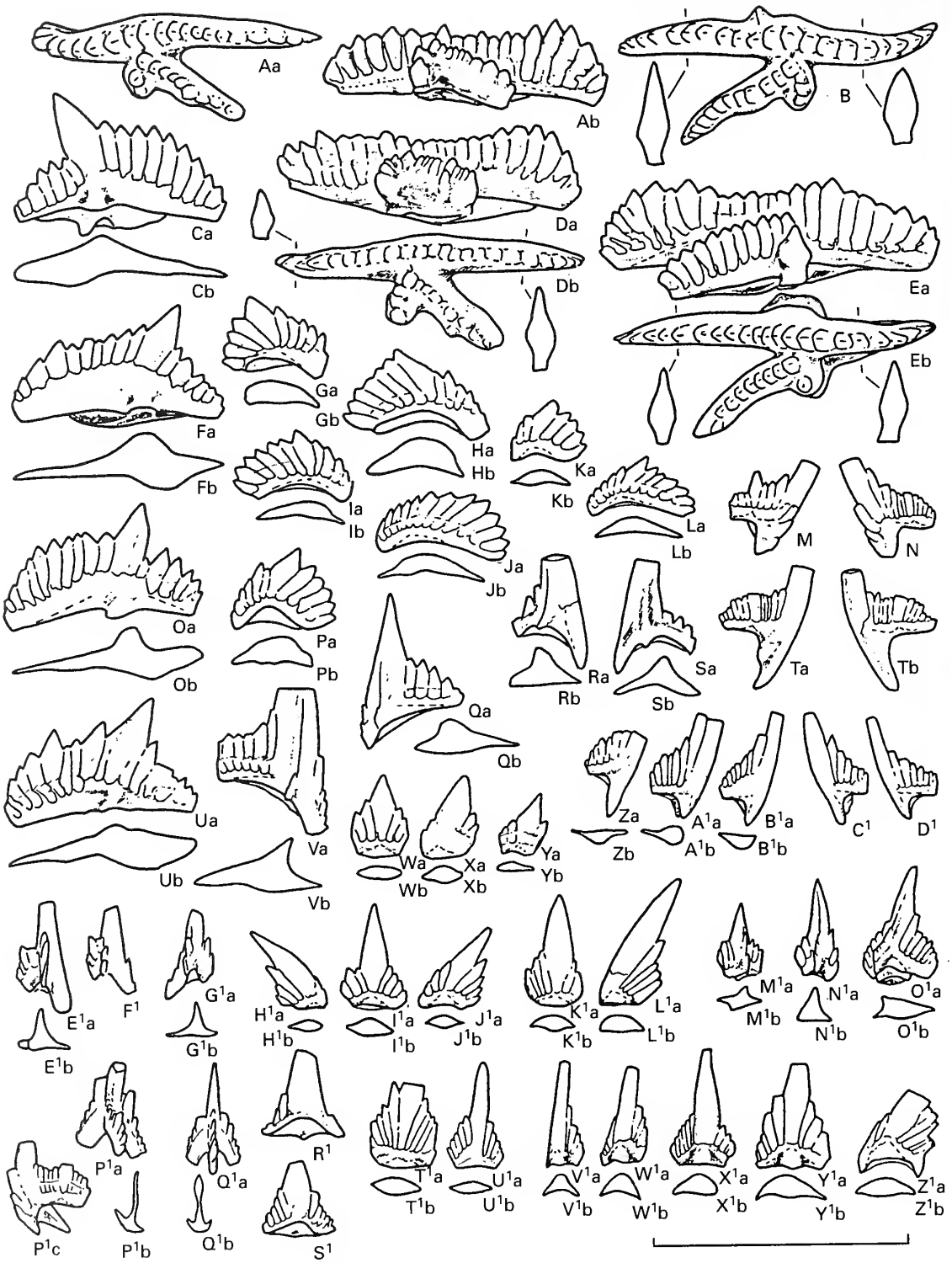

TEXT-FIG. 10. For caption see opposite.

.1977 *Carniodus carinthiacus* Walliser, 1964; Liebe and Rexroad, pl. 1, fig. 2.
.1977 *Carniodus carnulus* Walliser, 1964; Liebe and Rexroad, pl. 1, fig. 3.
.1977 *Carniodus carnicus* Walliser, 1964; Liebe and Rexroad, pl. 1, fig. 4.
.1977 *Pterospathodus amorphognathoides* Walliser, 1964; Liebe and Rexroad, pl. 1, fig. 9.
.1977 *Ozarkodina gaertneri* Walliser, 1964; Liebe and Rexroad, pl. 1, fig. 10.
.1977 *Exochognathus latialatus* (Walliser, 1964); Liebe and Rexroad, pl. 1, fig. 16.
.1977 *Distomodus triangularis* (Walliser, 1964); Liebe and Rexroad, pl. 2, fig. 29.
.1977 *Neoprioniodus costatus* Walliser, 1964; Liebe and Rexroad, pl. 2, figs 30–31.
1977 *Exochognathus brevialatus* (Walliser, 1964); Liebe and Rexroad, pl. 2, fig. 38.
1978 *Neoprioniodus costatus costatus* Walliser, 1964; Miller, pl. 2, figs 10–11.
.1978 *Apparatus 'C' Walliser*, 1964; Miller, pl. 4, figs 8–11.
.1980 *Carniodus carnulus* Walliser, 1964; Helfrich, pl. 1, figs 1–6.
1980 *Pterospathodus amorphognathoides* Walliser, 1964; Helfrich, pl. 2, figs 17–19.
1980 *Pterospathodus celloni* (Walliser, 1964); Helfrich, pl. 2, fig. 30.
.1981 *Pterospathodus amorphognathoides* Walliser, 1964; Nowlan, pl. 7, fig. 6.
.1981 *Pterospathodus amorphognathoides* Walliser, 1964; Uyeno and Barnes, pl. 1, fig. 24.
.1982 *Pterospathodus amorphognathoides* Walliser, 1964; Aldridge and Mohamed, pl. 2, figs 13–16.
.1982 *Carniodus carnulus* Walliser, 1964; Aldridge and Mohamed, pl. 2, figs 17–24.
.1983 *Carniodus carnulus* Walliser, 1964; Mabillard and Aldridge, pl. 2, figs 13–14.
.1983 *Pterospathodus amorphognathoides* Walliser, 1964; Mabillard and Aldridge, pl. 2, figs 25–27.
.1983 *Pterospathodus amorphognathoides* Walliser, 1964; Nowlan, fig. 4*K* [cop. Nowlan 1981, pl. 7, fig. 6].
.1983 *Pterospathodus amorphognathoides* Walliser, 1964; Uyeno and Barnes, p. 24, pl. 8, fig. 24 [cop. Uyeno and Barnes 1981, pl. 1, fig. 24].
.1983 *Pterospathodus amorphognathoides* Walliser, 1964; Barrick, fig. 18*M*.
.1984 *Carniodus? carinthiacus* Walliser, 1964; Drygant, p. 83, pl. 3, figs 8–11.
1984 *Neoprioniodus subcarnus* Walliser, 1964; Drygant, p. 84, pl. 3, figs 14–17.
.1984 *Pterospathodus amorphognathoides* Walliser, 1964; Drygant, p. 109, pl. 7, figs 13–16.
1984 *Ozarkodina gaertneri* Walliser, 1964; Drygant, p. 110, pl. 7, figs 22–27.
(?) 1984 *Carniodus carnicus* Walliser, 1964; Drygant, p. 82, pl. 3, figs 12–13.
v. 1985 *Pterospathodus amorphognathoides* Walliser, 1964; Nehring-Lefeld, p. 635, pl. 1, figs 3–8.
1985 *Carniodus carnulus* Walliser, 1964; Kleffner, pl. 2, figs 26–28.
1985 *Pterospathodus amorphognathoides* Walliser, 1964; Kleffner, pl. 1, fig. 3; pl. 2, figs 29–31.
v. 1985 *Carniodus carnulus* Walliser, 1964; Nehring-Lefeld, p. 632, pl. 2, figs 1–10.
(?) 1985 *Pterospathodus amorphognathoides* Walliser, 1964; Yu, p. 24, pl. 2, fig. 9.
1986 *Pterospathodus amorphognathoides* Walliser, 1964; Jiang *et al.*, pl. 4, figs 1–2.
p. 1987 *Pterospathodus amorphognathoides* Walliser, 1964; Over and Chatterton, pl. 4, figs 1–2 (*non* fig. 3 [= *P. rhodesi*?]).
.1987 *Carniodus carnulus* Walliser, 1964; Kleffner, fig. 5*1–7*.
.1987 *Pterospathodus amorphognathoides* Walliser, 1964; Kleffner, fig. 5*8–9, 11*.
.1987 *Pterospathodus pennatus procerus* (Walliser, 1964); Kleffner, fig. 5*10*.
.1987 *Pterospathodus amorphognathoides* Walliser, 1964; An, p. 201, pl. 33, figs 1–3.
p. 1987 *Pterospathodus pennatus procerus* (Walliser, 1964); An, p. 202, pl. 33, figs 4, 7 (*non* figs 5–6 [= *P. p. procerus*]).
p. 1987 *Exochognathus brassfieldensis* (Branson and Branson, 1947); An, pl. 35, fig. 18 (*non* fig. 17 [indet.]).
1988 *Pterospathodus amorphognathoides* Walliser, 1964; Qiu, pl. 1, fig. 8 [cop. Qiu 1985, pl. 1, fig. 3].
.1989 *Pterospathodus amorphognathoides* Walliser, 1964; Männik and Aldridge, text-fig. 1*G–L*.
v. 1989 *Pterospathodus amorphognathoides* Walliser, 1964; Männik and Aldridge, text-fig. 3*D–E*.

TEXT-FIG. 10. *Pterospathodus amorphognathoides lithuanicus* Brazauskas, 1983. A–B, D–E, Pa element. C, F, O, U, Pb_1 element. G–L, P, Pb_2 element. M–N, Sc_1 element. Q, V, Pc element. R–S, M_1 element. T, Sc_2 element. W–Y, carnuliform element, short morph. Z–D^1, Sc_3 element. E^1–G^1, Sb_1 element. H^1–L^1, carnuliform element, morph a. M^1, modified carnuliform element, short morph. N^1, modified carnuliform element(?). O^1, modified carnuliform element. P^1, Sb_2 element. Q^1, Sa element. R^1–S^1, carniciform element. T^1–U^1, carnuliform element, morph b. V^1–W^1, curved element, morph b. X^1, curved element, morph a. Y^1–Z^1, curved element, morph c. Scale bar represents 1 mm.

p. 1990 *Pterospathodus pennatus procerus* (Walliser, 1964); Uyeno, p. 66, pl. 3, fig. 18 (*non* figs 19–20 [= *P. p. procerus*]).
v. 1990 *Pterospathodus amorphognathoides* Walliser, 1964; Männik and Viira, pl. 17, figs 28, 32.
.1991 *Carniodus carnulus* Walliser, 1964; Kleffner, fig. 5*27–28*.
.1991 *Pterospathodus amorphognathoides* Walliser, 1964; Kleffner, fig. 6*21, 26–27*.
.1992 *Pterospathodus amorphognathoides* Walliser, 1964; Barca *et al.*, pl. 10, figs 7–10.
.1992 *Carniodus carnulus* Walliser, 1964; Barca *et al.*, pl. 10, figs 11–12.
.1996 *Pterospathodus amorphognathoides* Walliser, 1964; Wang and Aldridge, pl. 5, fig. 9.
v. 1998 *Pterospathodus amorphognathoides amorphognathoides* Walliser, 1964; Männik and Małkowski, pl. 1, figs 10, 14–17.

Material. Several hundreds to thousands of all elements.

Emended diagnosis. P. amorphognathoides with distinct basal platform/platform ledges of various configurations and dimensions on all elements.

Remarks. The size and shape of the basal platform of the Pa element is highly variable, evidently due to evolutionary changes (see below). The Pa element may or may not possess a triangular lateral lobe/short usually undenticulated process on the outer side of the element. Occasionally, additional

---

EXPLANATION OF PLATE 5

Figs 1–4, 10, 16. *Pterospathodus amorphognathoides amorphognathoides* Walliser, 1964; Population 5. 1, Cn 8026; upper view of dextral Pa element. 2, Cn 8027; upper view of dextral Pa element. 3, LO 7738t; upper view of sinistral Pa element. 4, Cn 8028; outer lateral view of dextral carnuliform element, short morph. 10, Cn 8029; outer lateral view of dextral modified carnuliform element. 16, Cn 8040; inner lateral view of sinistral Sc_3 element. Figs 1–2 from Viki core, sample M-391, int. 115·45–115·60 m; fig. 3 from Överstekvarn 2 section (Gotland), sample G88-635LJ; figs 4 and 10 from Viki core, sample M-995, int. 113·80–113·95 m; fig. 16 from Viki core, sample M-390, int. 118·40–118·50 m.

Figs 5–9, 11–15, 17–23, 35. *Pterospathodus amorphognathoides amorphognathoides* Walliser, 1964; Population 4. 5, Cn 8030; outer lateral view of sinistral Pb_2 element. 6, Cn 8031; inner lateral view of sinistral Sc_2 element. 7, Cn 8032; outer lateral view of dextral Pb_1 element. 8, Cn 8033; inner lateral view of dextral carniciform element. 9, Cn 8034; outer lateral view of dextral modified carnuliform element, short morph. 11, Cn 8035; inner lateral view of sinistral Sc_1 element. 12, Cn 8036; upper view of dextral Pa element. 13, Cn 8037; upper view of sinistral Pa element. 14, Cn 8038; inner lateral view of dextral Sc_3 element. 15, Cn 8039; outer lateral view of sinistral carnuliform element, morph a. 17, Cn 8041; outer lateral view of sinistral modified carnuliform element. 18, Cn 8042; lateral view of symmetrical carnuliform element, morph a. 19, Cn 8043; posterior view of sinistral Sb_2 element. 20, Cn 8044; posterior view of dextral Sb_2 element. 21, Cn 8045; outer lateral view of dextral curved element, morph b. 22, Cn 8046; posterior view of dextral Sb_1 element. 23, Cn 8047; outer lateral view of sinistral Pc element. 35, Cn 8048; outer lateral view of sinistral modified carnuliform element, short morph. Figs 5, 8–9, 11, 14–15, 17–20 and 22 from Viki core, sample M-386, int. 123·25–123·45 m; fig. 6 from Viki core, sample M-385, int. 124·60–124·75 m; figs 7, 12–13, 21, 23 and 35 from Viki core, sample M-384, int. 125·60–125·75 m.

Figs 24–34, 36–40. *Pterospathodus amorphognathoides amorphognathoides* Walliser, 1964; Population 3. 24, Cn 8049; upper view of sinistral Pa element. 25, Cn 8050; inner lateral view of sinistral Sc_1 element. 26, Cn 8051; outer lateral view of sinistral Pb_1 element. 27, Cn 8052; upper view of sinistral Pa element. 28, Cn 8053; outer lateral view of dextral curved element, morph a. 29, Cn 8054; inner lateral view of dextral Sc_1 element. 30, Cn 8055; inner lateral view of sinistral M_1 element. 31, Cn 8056; outer lateral view of sinistral Pb_2 element. 32, Cn 8057; upper view of dextral Pa element. 33, Cn 8058; inner lateral view of dextral Sc_2 element. 34, Cn 8059; outer lateral view of dextral carnuliform element, morph a. 36, Cn 8060; outer lateral view of sinistral modified carnuliform element. 37, Cn 8061; outer lateral view of dextral Pb_2 element. 38, Cn 8062; inner lateral view of sinistral Sc_3 element. 39, Cn 8063; outer lateral view of sinistral carnuliform element, short morph. 40, Cn 8064; outer lateral view of dextral Sb_2 element. Figs 24, 26, 28, 31–33, 36 and 38–39 from Viki core, sample M-378, int. 134·80–134·90 m; figs 25 and 29 from Viki core, sample M-380, int. 131·85–132·00 m; figs 27, 30, 34, 37 and 40 from Viki core, sample M-381, int. 130·45–130·55 m.

All × 50.

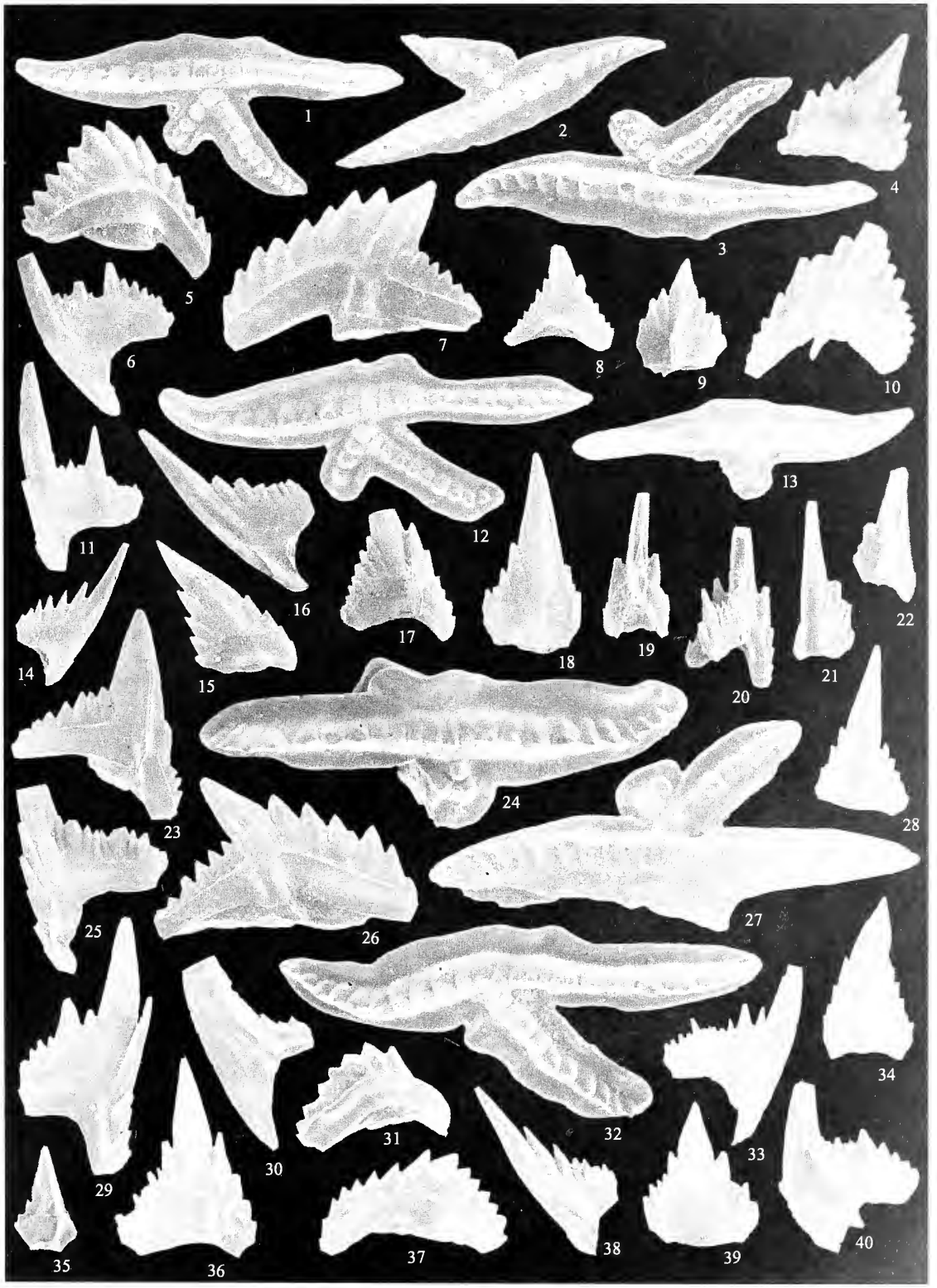

MÄNNIK, *Pterospathodus*

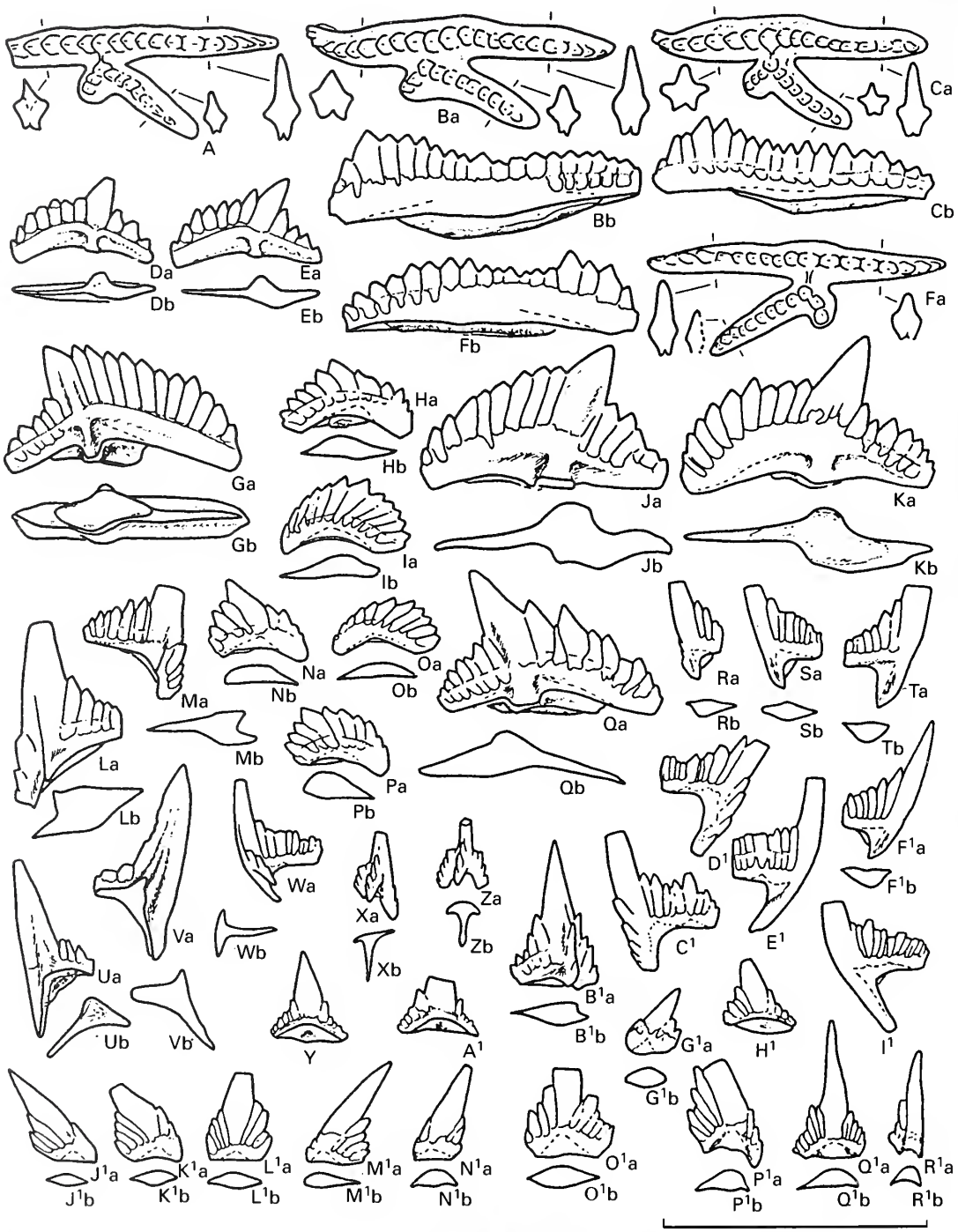

TEXT-FIG. 11. *Pterospathodus amorphognathoides amorphognathoides* Walliser, 1964; Population 1. A–C, F, Pa element. D–E, G, J–K, Q, Pb_1 element. H–I, N–P, Pb_2 element. L–M, Pc element. R–T, F^1, Se_3 element. U–V, M_1 element. W, Sb_2 element. X, Sb_1 element. Y, A^1, H^1, carnieiform element. Z, Sa element. B^1, modified carnuliform

lateral denticle(s) may occur at the distal part of the process. Although the fauna is dominated by elements with a bifurcated lateral process, pennate elements may be found quite often. These are easily separated from pennate elements of *P. p. procerus* on the basis of the configuration of the basal platform and cavity.

Based on changes in the morphology of the Pa element, five main temporal populations can be recognized in *P. a. amorphognathoides* (Pls 4–5; Text-figs 3, 11–15).

Population 1 (Pl. 4, figs 5–20, 22–27; Text-fig. 11). The Pa element possesses a narrow but distinct platform (Pl. 4, figs 6, 8; Text-fig. 11A–C, F). This population also includes rare specimens almost indistinguishable from the elements of *P. a. lithuanicus*. However, in this interval the Pa elements similar to those of *P. a. lithuanicus* possess a short narrow ledge on the outer side of the distal part of the posterior process (Pl. 4, fig. 12). This structure is missing (Pl. 4, figs 29–32, 35), or is very rare (Pl. 4, fig. 34), on the Pa elements of *P. a. lithuanicus*. It is possible that the presence of such Pa elements in Population 1 is evidence that this population forms an evolutionary link between *P. a. lithuanicus* and *P. a. amorphognathoides*. Population 1 is included in *P. a. amorphognathoides* because the subspecies boundary is drawn at the appearance of the new character (platform), not at the point where it was found in all individuals. It is also evident that the initial appearance of platform ledges on the Pa element started on the outer side of the distal part of the posterior process.

Characteristic for Population 1 are at least three morphs of Pb_1 elements.

1. Relatively large and long elements without platform ledges (Pl. 4, figs 5, 10; Text-fig. 11J–K), resembling those of *P. a. lithuanicus* (compare Pl. 3, figs 15, 17; Text-fig. 10C, F, O, U).
2. Small straight elements with a distinct high cusp and narrow platform-ledges (Pl. 4, fig. 9; Text-fig. 11D–E).
3. Relatively large straight elements with a short cusp, high denticles on the long anterior process and low denticles on the shorter posterior process (Text-fig. 11G). This morph is almost identical to the holotype of Walliser's '*Ozarkodina gaertneri*' (Walliser 1964, pl. 27, fig. 14). In the collections studied, this type of element is extremely rare, occurring only in few samples and represented, as a rule, by one or two specimens. Rare elements of this type can be found also in younger populations (Text-fig. 13V).

Morphs 1 and 2 dominate in Population 1, the former being more abundant in older strata and morph 2 in younger strata.

Population 2 (Pl. 4, figs 1–4; Text-fig. 12). The morphologically highly variable platform is widest on the outer proximal side of the Pa element and narrows gradually distally.

Population 3 (Pl. 5, figs 24–40; Text-fig. 13). The platform on the Pa elements reaches its maximum size in this population. The edges of it, particularly on the posterior process, are strongly undulating and partly turned up. Many specimens possess a triangular or semiquadrate outer lateral lobe/short process which may or may not bear denticle(s) (Pl. 5, fig. 27; Text-fig. 12A, C). In Population 3 platform ledges become well developed on most of the elements of the apparatus.

Population 4 (Pl. 5, figs 5–9, 11–15, 17–23; Text-fig. 14). On typical Pa elements of this population the platform is wide on the posterior process and becomes rapidly narrow on the anterior process forming a distinct 'bulge' on the outer side of the element, anterior of the point where the inner bifurcated process joins the main blade. Just behind this 'bulge' the platform is widest and possesses an upturned, undulating edge. The structure described above is distinct on the dextral element (Pl. 5, fig. 12; Text-fig. 14A, C) but less well developed on the sinistral one (Pl. 5, fig. 13; Text-fig. 14B).

Population 5 (Pl. 5, figs 1–4, 10, 16; Text-fig. 15). Most characteristic for this population is a Pa element with the platform widest proximally on the outer side of the element and narrowing equally towards the posterior and anterior ends. Many elements also possess an additional denticle between the main row of denticles and that on the bifurcating lateral process (Text-fig. 15E, G).

Very characteristic of this, the youngest population of *P. a. amorphognathoides*, is the strongly arched (in lateral view) modified carnuliform element (Pl. 5, fig. 10; Text-fig. $15O^1$–P^1). Also, in some sections, a few Pa elements with an extremely wide platform (Text-fig. 15C) were found in the uppermost part of the range of Population 5.

---

element. C^1–D^1, Sc_1 element. E^1, I^1, Sc_2 element. G^1, carnuliform element, short morph. J^1–N^1, carnuliform element, morph a. O^1, carnuliform element, morph b(?). P^1, curved element, morph c. Q^1, curved element, morph a. R^1, curved element, morph b. Scale bar represents 1 mm.

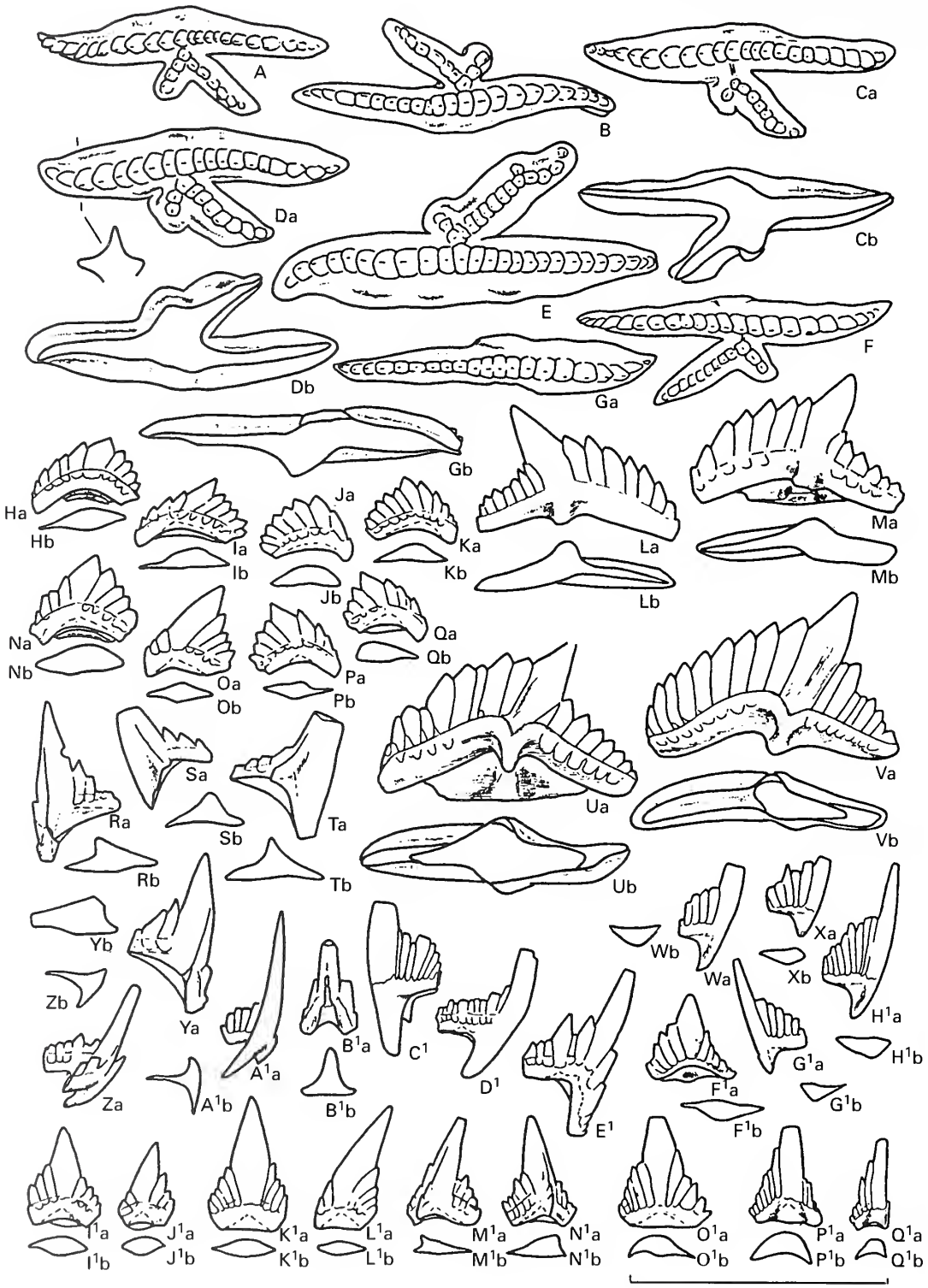

TEXT-FIG. 12. For caption see opposite.

The elements of *P. a. amorphognathoides* in Population 3 are quite similar to those of *P. rhodesi* (see below), differing from them mainly by the less well developed platform/platform ledges. *P. a. amorphognathoides* is abundant and dominates conodont faunas in the open shelf carbonate-terrigeneous facies. Towards the basin it becomes rare and is ecologically replaced by *P. pennatus procerus*.

The populations listed above will in the future probably allow the recognition of several stratigraphically useful subdivisions in the *P. a. amorphognathoides* Zone. However, further studies are needed.

Occurrence. P. a. amorphognathoides, Lower *Pseudooneotodus bicornis* and Upper *Ps. bicornis* zones. *P. a. amorphognathoides* has been recognized world-wide (see synonymy) except for a few regions: Severnaya Zemlya (Männik 1983) and the Sub-Polar Urals (Melnikov, pers. comm.). It is extremely rare in eastern Canada (Gaspé Peninsula; Nowlan 1983). *P. a. amorphognathoides* is evidently also missing in several other regions (e.g. Greenland – Armstrong 1990; Alaska – Savage 1985; some regions in north-western Canada – McCracken 1991; and Australia – Bischoff 1986) where it is replaced by *P. rhodesi*.

P. pennatus *lineage*

As was noted above the *P. pennatus* lineage probably appeared, together with the *P. amorphognathoides* lineage, at the end of the *P. eopennatus* Zone. Both lineages evidently originated from the same ancestral taxon: *P. eopennatus* ssp. nov. 2 (Text-fig. 3; Männik 1995). However, some data suggest also another possibility. Morph 5 of *P. eopennatus* ssp. nov. 1 from the *A. irregularis–A. kuehni* subzones is morphologically very similar to *P. p. pennatus* of Walliser (1964, pl. 14, figs 23–26). In the Cellon section *P. p. pennatus* is found together with *P. celloni* in strata considerably younger than the known range of morph 5 in Estonia. Also, the morphologies of elements and co-occurrences of taxa in Cellon indicate that the oldest *P. celloni* fauna described from that section is no older than the latest *P. eopennatus*, but most probably comes from the earliest *P. celloni* chron (Männik 1996).

In Estonia, in open shelf environments morph 5 disappeared during the end-*irregularis* event. That event caused considerable changes in conodont faunas. Several taxa became extinct or disappeared temporarily and *P. eopennatus* ssp. nov. 1 was replaced by *P. eopennatus* ssp. nov. 2. However, it cannot be excluded that *P. eopennatus* ssp. nov. 1 survived the end-*irregularis* event somewhere in offshore regions and gave rise to the *P. p. pennatus – P. p. procerus* lineage. The morphological similarities between the Pa element of *P. p. pennatus* and morph 5 of *P. eopennatus* ssp. nov. 1 suggest a possibility that these two taxa are directly connected. It is possible that the two ecologically restricted lineages might have appeared already at the end of the *A. irregularis* chron. However, no data about the deeper basin lineage is yet available from the interval between the ranges of *P. eopennatus* ssp. nov. 1 and *P. p. pennatus*. Also, *P. p. pennatus* itself has not been found in Estonia. Therefore, in this paper *P. pennatus* is described as a descendant of *P. eopennatus* appearing in the sequence at the same time as *P. amorphognathoides*.

Pterospathodus pennatus pennatus (Walliser, 1964)

*1964 *Spathognathodus pennatus pennatus* Walliser, p. 79, pl. 14, figs 23–26; pl. 15, fig. 1.
(?)1968 *Neospathognathodus pennatus* (Walliser, 1964); Nicoll and Rexroad, p. 47, pl. 2, fig. 5.

Remarks. P. p. pennatus has not been identified in Estonia. In Cellon *P. p. pennatus* has the same

---

TEXT-FIG. 12. *Pterospathodus amorphognathoides amorphognathoides* Walliser, 1964; Population 2. A–G, Pa element. H–K, N–Q, Pb_2 element. L–M, U–V, Pb_1 element. R, Y, Pc element. S–T, M_1 element. W–X, G^1–H^1, Sc_3 element. Z, Sb_2 element. A^1, Sb_1 element. B^1, Sa element. C^1–D^1, Sc_2 element. E^1, Sc_1 element. F^1, carniciform element. I^1–J^1, carnuliform element, short morph. K^1–L^1, carnuliform element morph a. M^1–N^1, modified carnuliform element. O^1, ?curved element, morph c. P^1, curved element, morph a. Q^1, curved element, morph b. Scale bar represents 1 mm.

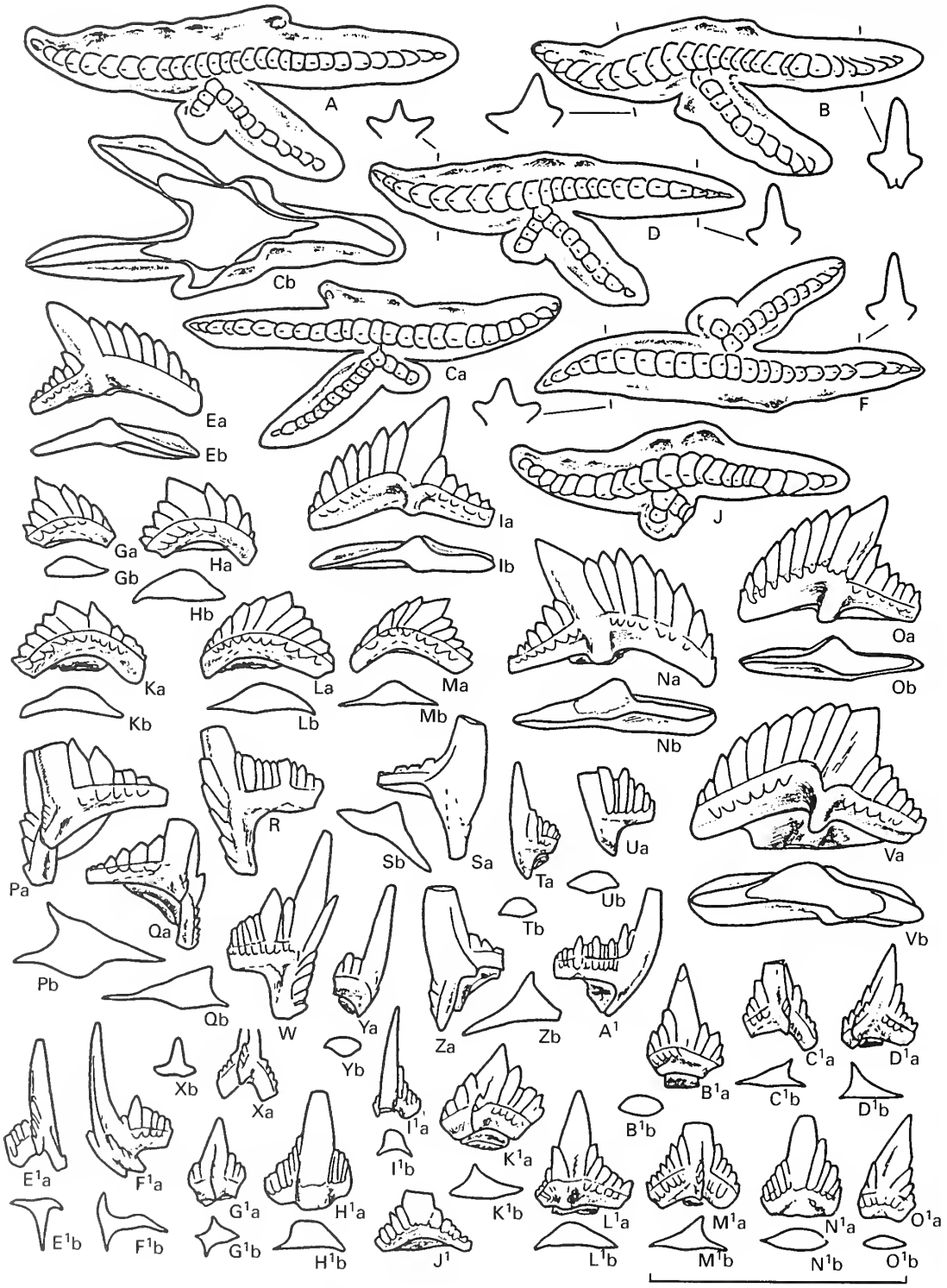

TEXT-FIG. 13. For caption see opposite.

range as *P. celloni* (Walliser 1964). In this section *P. p. pennatus* is very rare in the lowermost sample studied (10 B) which is dominated by elements of *P. a. angulatus*. In sample 10 H/J, I have identified a fragment probably belonging to *P. amorphognathoides lennarti* ssp. nov. together with *P. p. pennatus* and *P. celloni*. In the uppermost sample with *P. p. pennatus* (sample 10 J), a few Pa and Pb elements (Walliser 1964, pl. 15, fig. 1; pl. 27, fig. 5) occur which are morphologically almost identical to those of *P. p. procerus*, indicating a close relationship between these two subspecies.

The morphologically distinct Pb_1, Pb_2, Pc, Sc_1, Sc_2 and Sb_2 elements, which occur in Estonia with the Pa elements of *P. celloni*, are considered to belong to the apparatus of the latter species (see below). However, '*Neoprioniodus triangularis tenuirameus*' (Walliser 1964, pl. 28, figs 22–24; = M_1 element; fig. 21 cannot be identified without direct study of the specimen) and '*Carniodus eocarnicus*' (Walliser 1964, pl. 28, figs 19–20; = Sc_1 element) may belong either to *P. celloni* or *P. p. pennatus* – they all are found together in the same strata. Here these elements are tentatively assigned to *P. celloni* (see synonymy). The specimen illustrated by Walliser (1964, pl. 28, fig. 12) as '*N. subcarnus*' is considered to be the Sc_2 element of *P. celloni*. The majority of the other *Carniodus*-elements illustrated by Walliser (1964) possess distinct platform ledges and evidently belong to *P. a. amorphognathoides* (see above).

Occurrence. *P. celloni* Zone.

Pterospathodus pennatus procerus (Walliser, 1964)

Plate 6, figures 1–25, 27–35; Text-figure 16

v. 1964	*Spathognathodus pennatus procerus* Walliser, p. 80, pl. 15, figs 2–8.
1966	*Spathognathodus pennatus procerus* Walliser, 1964; Spasov and Filipović, p. 50, pl. 1, fig. 6.
p. 1968	*Spathognathodus pennatus procerus* Walliser, 1964; Igo and Koike, pp. 18–19, pl. 2, figs 8–10 (*non* fig. 11 [indet.]).
p. 1968	*Ozarkodina gaertneri* Walliser, 1964; Igo and Koike, p. 14, pl. 1, figs 7–9 (*non* figs 5–6 [= *P. a. amorphognathoides*]).
1968	*Neoprioniodus costatus paucidentatus* Walliser, 1964; Igo and Koike, p. 12, pl. 3, figs 16–17.
.1968	*Neoprioniodus triangularis tenuirameus* Walliser, 1964; Igo and Koike, p. 13, pl. 3, figs 18–19.
p. 1968	*Carniodus* sp. A Igo and Koike, p. 8, pl. 3, fig. 2 (*non* fig. 3 [= *P. a. amorphognathoides*]).
.1968	*Carniodus* sp. B Igo and Koike, p. 8, pl. 3, fig. 20.
.1968	*Roundya*? sp. C Igo and Koike, p. 17, pl. 3, figs 25–28.
p. 1968	*Neoprioniodus* spp. Igo and Koike, p. 14, pl. 3, fig. 24 (*non* fig. 4 [= *P. a. amorphognathoides*]).
1969	*Spathognathodus pennatus procerus* Walliser, 1964; Drygant, p. 50, pl., figs 2–3.
.1976	*Pterospathodus pennatus pennatus* (Walliser, 1964); Barrick and Klapper, p. 86, pl. 1, fig. 19.
v. 1979	*Pterospathodus pennatus procerus* (Walliser, 1964); Jeppsson, p. 235, fig. 7*1–8*.
.1983	*Pterospathodus pennatus procerus* (Walliser, 1964); Savage *et al.*, fig. 2*A–F*.
1984	*Pterospathodus pennatus procerus* (Walliser, 1964); Stouge and Bagnoli Stouge, p. 109, pl. 2, figs 14–17.
1984	*Pterospathodus pennatus procerus* (Walliser, 1964); Drygant, p. 108, pl. 7, figs 17–20.
1985	*Pterospathodus pennatus procerus* (Walliser, 1984); Yu, pl. 1, figs 1–2.
v. 1985	*Pterospathodus pennatus pennatus* (Walliser, 1964); Nehring-Lefeld, p. 637, pl. 1, figs 1–2.
1985	*Pterospathodus pennatus procerus* (Walliser, 1974); Savage, p. 714, fig. 4*A–K*.
vp. 1986	*Pterospathodus procerus* (Walliser, 1964); Bischoff, p. 204, pl. 29, figs 9–10, 15–30 (*non* figs 13–14 [indet.]); pl. 30, figs 1–2 (*non* figs 3–11 [= *P. rhodesi*]).
.1987	*Pterospathodus pennatus procerus* (Walliser, 1964); Over and Chatterton, pl. 4, fig. 4.

TEXT-FIG. 13. *Pterospathodus amorphognathoides amorphognathoides* Walliser, 1964; Population 3. A–D, F, J, Pa element. E, I, N–O, V, Pb_1 element. G–H, K–M, Pb_2 element. P–Q, Pc element. R, W, Sc_1 element. S, Z, M_1 element. T–U, Y, Sc_3 element. X, Sa element. A^1, Sc_2 element. B^1, L^1, carniuliform element, short morph. C^1–D^1, M^1, modified carniuliform element. E^1, Sb^1 element. F^1, Sb_2 element. G^1, modified carniuliform element, short morph. H^1, curved element, morph a. I^1, curved element, morph b. J^1, carniciform element. K^1, modified carniuliform element, short morph. N^1, carniuliform element, morph b. O^1, carniuliform element, morph a. Scale bar represents 1 mm.

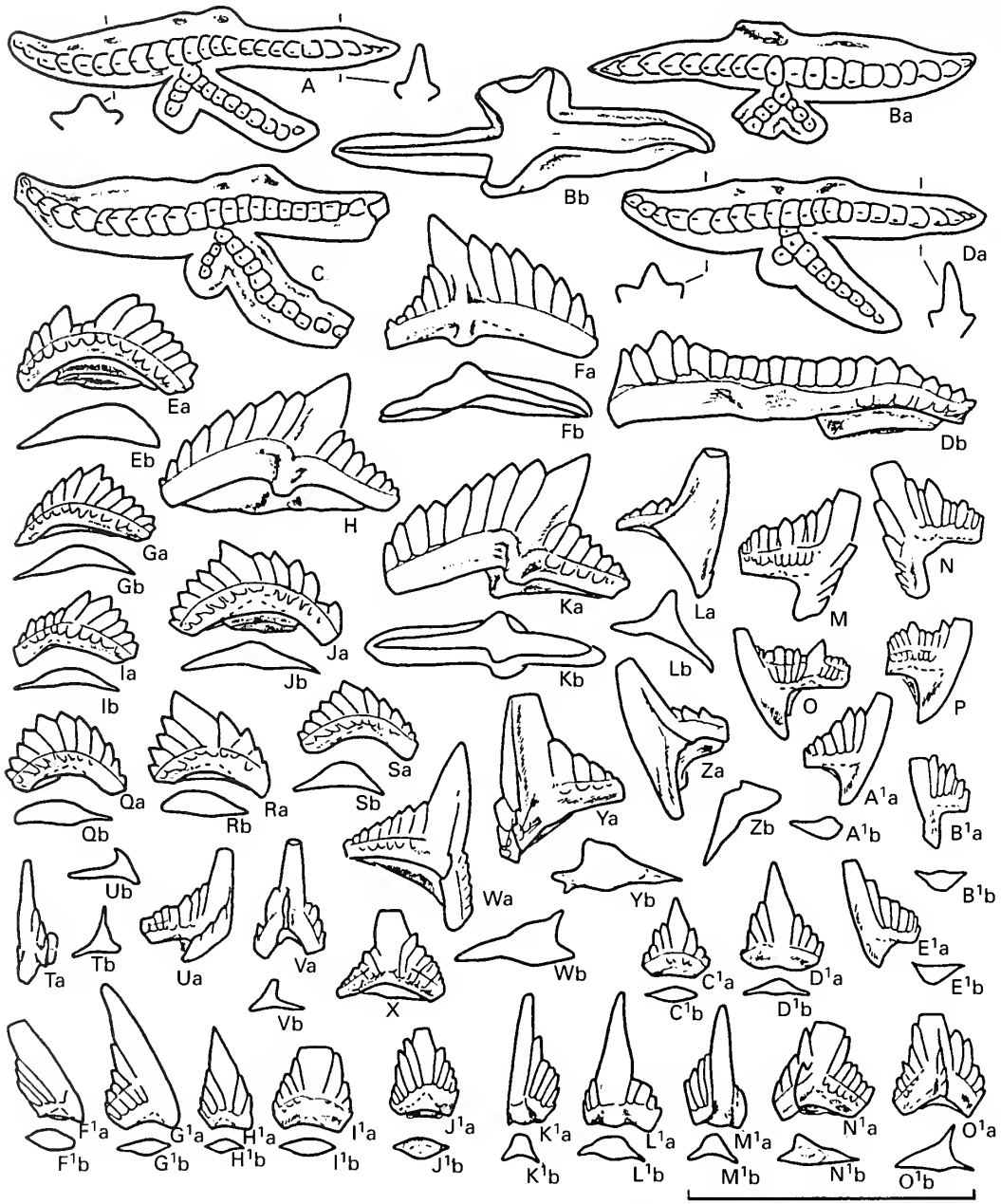

TEXT-FIG. 14. *Pterospathodus amorphognathoides amorphognathoides* Walliser, 1964; Population 4. A–D, Pa element. E, G, I–J, Q–S, Pb_2 element. F, H, K, Pb_1 element. L, Z, M_1 element. M–N, Sc_1 element. O–P, Sc_2 element. T, Sb_1 element. U–V, Sb_2 element. W, Y, Pc element. X, carniciform element. A^1–B^1, E^1, Sc_3 element. C^1–D^1, carnuliform element, short morph. F^1–I^1, carnuliform element, morph a. J^1, carnuliform element, morph b(?). K^1, M^1, curved element, morph b. L^1, curved element, morph a. N^1–O^1, modified carnuliform element. Scale bar represents 1 mm.

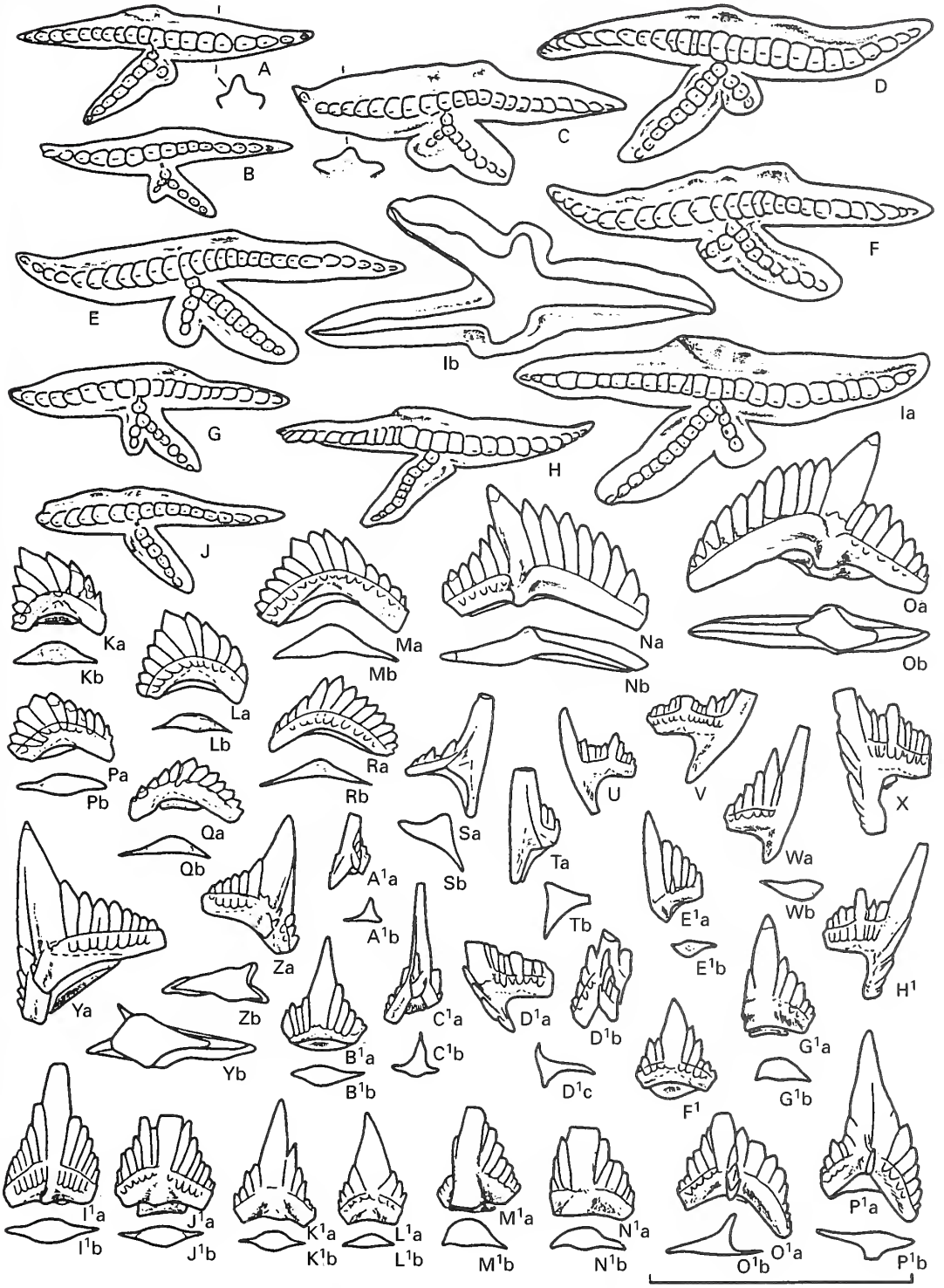

TEXT-FIG. 15. For caption see opposite.

p. 1987 *Pterospathodus pennatus procerus* (Walliser, 1964); An, p. 202, pl. 33, figs 5–6 (*non* figs 4, 7 [= *P. a. amorphognathoides*]).
v. 1990 *Pterospathodus procerus* (Walliser, 1964); Männik and Viira, pl. 17, figs. 29.
p. 1990 *Pterospathodus pennatus procerus* (Walliser, 1964); Uyeno, p. 66, pl. 3, figs 19–20 (*non* fig. 18 [= *P. a. amorphognathoides*]).
.1991 *Pterospathodus procerus* (Walliser, 1964); McCracken, p. 109, pl. 4, figs 12–23.
p? 1991 *Carniodus carnulus* Walliser, 1964; McCracken, p. 108, pl. 3, figs 13–14 (*non* figs 6–12, 15 [= *P. rhodesi*]).
.1992 *Pterospathodus pennatus procerus* (Walliser, 1964); Nehring-Lefeld, pl. 3, figs 1–2.
v. in press *Pterospathodus pennatus procerus* (Walliser, 1964); Männik and Malkowski, pl. 1, figs 6–7, 11–13, 18.

Material. Many tens to about a hundred of the Pa and Pb_1 elements; few to a few tens of all other elements.

Remarks. The apparatus of *P. p. procerus* is well represented in several samples in the studied collections. Pa, Pb_1, Pb_2, Pc, M_1, M_2, Sc_1, Sc_2, Sc_3, Sb_1, Sb_2, Sa, carnuliform morphs a and b, and a possible carniciform element are recognized. The M_2 element (Pl. 6, figs 1, 3; Text-fig. 16W–Z) has so far been found only in the *P. p. procerus* apparatus. The Sc_2 element seems to be represented by two morphs, one without and the other with denticles on the basal part of the anterior edge of the cusp (Pl. 6, figs 9, 22 and 7, 25 respectively; Text-fig. 16P^1–Q^1 and R^1–S^1, V^1–W^1 respectively). Probable carniciform element (Text-fig. 16X^1–A^2, N^2–O^2) of this apparatus possesses a considerably taller cusp than its possible homologues in other apparatuses of *Pterospathodus* (Text-figs 4–15).

The data available allow the recognition of ecological replacement of *P. a. amorphognathoides* by *P. p. procerus* towards offshore environments (Männik 1992). In open shelf environments *P. p. procerus* is extremely rare or completely absent in the *P. a. amorphognathoides* Zone, although in many regions (Estonia – Männik 1992; Gotland – Jeppsson 1979, Jeppsson and Männik 1993; Britain – Männik and Aldridge 1989, Aldridge *et al.* 1993) *P. p. procerus* has been identified from a short interval above the last *P. a. amorphognathoides*. This appearance of *P. p. procerus* in open shelf environments was probably connected with the Ireviken Event, with the extinction of *P. a. amorphognathoides* creating a vacant niche.

Occurrence. P. a. amorphognathoides to Upper *P. p. procerus* zones (Jeppsson 1994, 1997) in deeper basin environments; Lower and Upper *P. p. procerus* zones in open shelf facies. *P. p. procerus* has been found in most known sequences world-wide (see synonymy).

Pterospathodus celloni (Walliser, 1964)

Plate 6, figures 26, 36–54; Text-figure 17

v.* 1964 *Spathognathodus celloni* Walliser, p. 73, pl. 14, figs 3–16.
v. 1964 *Ozarkodina adiutricis* Walliser, p. 54, pl. 27, figs 1–10.
vp. 1964 *Carniodus eocarnicus* Walliser, p. 34, pl. 28, fig. 20 (*non* fig. 19 [= *P. amorphognathoides*]).
vp. 1964 *Neoprioniodus subcarnus* Walliser, p. 51, pl. 28, fig. 12 (*non* figs 13–14 [= *P. a. amorphognathoides*]).
v. 1964 *Neoprioniodus triangularis tenuirameus* Walliser, p. 53, pl. 28, figs 21–24.
v. 1964 *Neoprioniodus costatus paucidentatus* Walliser, p. 48, pl. 28, figs 31–35.
v.? 1964 *Roundya brevialata* Walliser, p. 69, pl. 31, figs 8–10.
? 1968 *Ozarkodina adiutricis* Walliser, 1964; Nicoll and Rexroad, p. 48, pl. 2, fig. 8.
? 1968 *Neospathognathodus celloni* (Walliser, 1964); Nicoll and Rexroad, p. 45, pl. 2, figs 1–4.
1971 *Neospathognathodus celloni* (Walliser, 1964); Rexroad and Nicoll, pl. 1, figs 2–4.
1971 *Ozarkodina adiutricis* Walliser, 1964; Rexroad and Nicoll, pl. 1, fig. 5.

TEXT-FIG. 15. *Pterospathodus amorphognathoides amorphognathoides* Walliser, 1964; Population 5. A–J, Pa element. K–M, P–R, Pb_2 element. N–O, Pb_1 element. S–T, M_1 element. U–V, Sc_2 element. W, E^1, Sc_3 element. X, H^1, Sc_1 element. B^1, carniciform element. C^1, Sa element. D^1, Sb_2 element. F^1, carnuliform element, short morph. G^1, N^1, curved element, morph a. I^1–J^1, carnuliform element, morph b. K^1–L^1, carnuliform element, morph a. M^1, curved element, morph b(?). O^1–P^1, modified carnuliform element. Scale bar represents 1 mm.

1972 *Ozarkodina adiutricis* Walliser, 1964; Rexroad and Nicoll, pl. 1, figs 15–16.
1972 *Spathognathoides celloni* Walliser, 1964; Rexroad and Nicoll, pl. 1, figs 17–19.
1976 *Pterospathodus celloni* (Walliser, 1964); Barrick and Klapper, p. 82, pl. 1, figs 3, 5.
1977 *Ozarkodina adiutricis* Walliser, 1964; Liebe and Rexroad, pl. 1, fig. 11.
1977 *Spathognathodus celloni* Walliser, 1964; Liebe and Rexroad, pl. 1, fig. 12.
1989 *Pterospathodus celloni* (Walliser, 1964); Männik and Aldridge, text-fig. 1*A–F*.
? 1994 *Pterospathodus celloni* (Walliser, 1964); Watkins *et al.*, pl. 10, figs 1–4.

Material. Many tens of Pa and Pb elements; a few Pc, Sc_1 and Sc_2 elements.

Remarks. P. celloni is very rare in the Estonian collections, which mainly represent a proximal carbonate-terrigeneous facies. It is mostly represented by Pa and Pb_1 elements, with the Pb_2 element quite common. However, the identification of the Pb_2 element among co-occurring juvenile Pb_2 elements of *P. amorphognathoides lennarti* ssp. nov. and *P. a. lithuanicus* is quite problematical. Of the other elements of *P. celloni*, only the Sc_1, Sc_2 and extremely rare specimens of the Sb_2 have been identified. Sc_1, Sc_2 and Sb_2 elements of *P. celloni* are morphologically almost identical to their homologues in *P. eopennatus* apparatuses (Pl. 1, figs 3, 6, 13, 44–45; Text-figs 4F^2, H^2–K^2, 5A^1–B^1, H^1–J^1; 6L^1–P^1, U^1–V^1). The Sb_2 is also almost identical to its homologue in *P. p. procerus* (Pl. 6, figs 10–11, 17–19, 27; Text-fig. 16N^1).

Some peculiar carniodiform elements occur together with *P. celloni*. They are here identified as carniciform(?) (Pl. 6, fig. 50; Text-fig. 17L^1–N^1) and carnuliform (Pl. 6, figs 42, 51–52, 54; Text-fig. 17O^1–I^2) elements of *P. celloni* apparatus. It is also probable that at least some of the elements described by Walliser (1964) as '*N. triangularis tenuirameus*' and '*N. costatus paucidentatus*' represent, accordingly, the M_1 and Pc elements of *P. celloni* (see synonymy).

P. celloni seems to have been more abundant in deeper basin environments (graptolite-bearing facies) and was very rare in open shelf regions. Although its origin needs further investigation it is evident that *P. celloni* was closely related to the *P. pennatus* lineage.

Occurrence. From the uppermost part of the *P. a. angulatus* Subzone to the *P. a. lithuanicus* Subzone in open shelf facies. The range in deeper facies needs further studies but may be longer. The distribution of *P. celloni* in other regions needs further studies, with revision of collections. However, based on the published data (see synonymy) it seems quite probable that *P. celloni* can be recognized in most known Telychian sequences.

Pterospathodus rhodesi (Savage, 1985)

.1984 *Pterospathodus* n. sp. A Stouge and Bagnoli Stouge, p. 109, pl. 1, figs 1–6.
.1984 *Carniodus carnulus* Walliser, 1964; Stouge and Bagnoli Stouge, p. 108, pl. 1, figs 11–19.
.* 1985 *Pterospathodus amorphognathoides rhodesi* Savage, p. 714, fig. 3*A–T*.
.1985 *Carniodus carnulus* Walliser, 1964; Savage, p. 714, fig. 2*D–N*.
1985 *Xainzadontus dewukaxiaensis* Yu, p. 25, pl. 1, fig. 14.
1985 *Ozarkodina gaertneri* Walliser, 1964; Yu, pl. 1, fig. 8.
1985 *Roundya triangularis* Yu, p. 25, pl. 1, fig. 13.
v. 1986 *Carniodus carnulus* Walliser, 1964; Bischoff, p. 177, pl. 5, figs 18–34; pl. 6, figs 1–37.
v. 1986 *Pterospathodus procerus* (Walliser, 1964); Bischoff, p. 204, pl. 30, figs 3–11.
v. 1986 *Pterospathodus latus* Bischoff, p. 197, pl. 30, figs 15–18, 31; pl. 31, figs 1–14.
v. 1986 *Pterospathodus amorphognathoides* Walliser, 1964; Bischoff, p. 186, pl. 30, figs 19–22; pl. 31, figs 15–39.
.1987 *Pterospathodus pennatus rhodesi* (Savage, 1985); Over and Chatterton, p. 21, pl. 4, figs 5–6.
p. 1987 *Pterospathodus amorphognathoides* Walliser, 1964; Over and Chatterton, pl. 4, fig. 3 (*non* figs 1–2 [= *P. a. amorphognathoides*]).
.1989 *Pterospathodus rhodesi* (Savage, 1985); Männik and Aldridge, text-fig. 4*A–B*.
.1990 *Carniodus carnulus* Walliser, 1964; Armstrong, p. 68, pl. 4, figs 14–29.
.1990 *Pterospathodus amorphognathoides* Walliser, 1964; Armstrong, p. 115, pl. 19, figs 1–5.

.1990 *Pterospathodus pennatus rhodesi* (Savage, 1985); Armstrong, p. 120, pl. 20, figs 6–16.
p. 1991 *Carniodus carnulus* Walliser, 1964; McCracken, p. 108, pl. 3, figs 6–12, 15 (*non* figs 13–14 [= *P. p. procerus*]).
.1991 *Pterospathodus rhodesi* (Savage, 1985); McCracken, p. 109, pl. 5, figs 6–15.

Remarks. In some regions (Australia, Alaska, Greenland, Tibet). *P. a. amorphognathoides* is replaced by, or co-occurs with, *P. rhodesi*, all elements of which are characterized by extremely wide platform/platform ledges (see illustrations listed in synonymy). The origin of *P. rhodesi* is not known. In general, the morphology of the elements and the architecture of the apparatus suggest that *P. rhodesi* is closely related to the *P. amorphognathoides* lineage. However, the co-occurrence of *P. a. amorphognathoides* and *P. rhodesi* in some sections (e.g. in the southern Mackenzie

---

EXPLANATION OF PLATE 6

Figs 1–25, 27–35. *Pterospathodus pennatus procerus* (Walliser, 1964). 1, LO 7739t; inner lateral view of dextral M_2 element. 2, LO 7740t; inner lateral view of dextral M_1 element. 3, LO 7741t; inner lateral view of sinistral M_2 element. 4, LO 7742t; inner lateral view of sinistral M_1 element. 5, Cn 8065; outer lateral view of dextral Pb_2 element. 6, LO 7743t; outer lateral view of sinistral Pb_2 element. 7, LO 7744t; inner lateral view of sinistral Sc_2 element. 8, Cn 8066; upper view of sinistral Pa element. 9, LO 7745t; inner lateral view of dextral Sc_2 element. 10, LO 7746t; posterior view of dextral Sb_2 element. 11, LO 7747t; outer lateral view of dextral Sb_2 element. 12, LO 7748t; posterior view of dextral Sb_1 element. 13, LO 7749t; posterior view of sinistral Sb_1 element. 14, Cn 8067; outer lateral view of sinistral Sc_1 element. 15, LO 7750t; inner lateral view of sinistral Sc_1 element. 16, Cn 8068; outer lateral view of sinistral Pb_1 element. 17, LO 7751t; posterior view of sinistral Sb_2 element. 18, LO 7752t; outer postero-lateral view of sinistral Sb_2 element. 19, LO 7753t; inner antero-lateral view of sinistral Sb_2 element. 20, LO 7755t; outer lateral view of dextral Pc element. 21, LO 7755t; inner lateral view of dextral curved(?) element. 22, LO 7756t; inner lateral view of dextral Sc_2 element. 23, LO 7757t; inner lateral view of dextral Sc_3 element. 24, LO 7758t; inner lateral view of sinistral Sc_3 element. 25, LO 7759t; inner lateral view of dextral Sc_2 element. 27, LO 7760t; outer lateral view of sinistral Sb_2 element. 28, LO 7761t; outer lateral view of dextral carnuliform element, morph a. 29, LO 7762t; outer lateral view of dextral carnuliform element, morph a. 30, LO 7763t; inner lateral view of sinistral carnuliform element, morph b. 31, LO 7764t; outer lateral view of sinistral curved element. 32, LO 7765t; inner lateral view of sinistral carnuliform element, morph a. 33, LO 7766t; outer lateral view of sinistral carnuliform element, morph a. 34, LO 7767t; posterior view of Sa element. 35, LO 7768t; posterior view of Sa element. Figs 1–4, 7, 10–12, 15, 17–21, 25, 27–29, 31–33 and 35 from Nygårdsbäckprofilen-1 section (Gotland), sample G93-977LJ; figs 5, 8, 14 and 16 from Ohesaare core, sample M-935, int. 348·40–348·60 m; figs 6, 9, 13, 22–24, 30 and 34 from Nygårdsbäckprofilen-1 section (Gotland), sample G93-978LJ.

Figs 26, 36–54. *Pterospathodus celloni* (Walliser, 1964). 26, Cn 8069; outer lateral view of dextral Pb_2 element. 36, LO 7769t; upper view of sinistral Pa element. 37, Cn 8070; outer lateral view of dextral Pc element. 38, Cn 8071; inner lateral view of dextral Sc_2 element. 39, LO 7770t; inner lateral view of sinistral Sc_2 element. 40, Cn 8072; outer lateral view of dextral Pb_1 element. 41, Cn 8073; inner lateral view of dextral Pa element. 42, Cn 8074; inner lateral view of dextral carnuliform(?) element. 43, LO 7771t; inner lateral view of dextral M_1 element. 44, Cn 8075; inner lateral view of sinistral Sc_1 element. 45, LO 7772t; inner lateral view of sinistral Pa element. 46, LO 7773t; outer lateral view of sinistral Pb_1 element. 47, LO 7774t; inner lateral view of dextral Sb_2 element. 48, LO 7775t; outer lateral view of sinistral Sb_2 element. 49, LO 7776t; inner lateral view of dextral Pa element. 50, Cn 8076; inner lateral view of dextral carniciform(?) element. 51, Cn 8077; inner lateral view of dextral carnuliform(?) element. 52, Cn 8078; inner lateral view of sinistral carnuliform element. 53, LO 7777t; outer lateral view of dextral Sb_2 element. 54, Cn 8079; inner lateral view of sinistral carnuliform(?) element. Figs 26 and 44 from Viki core, sample M-967, int. 153·60–153·72 m; fig. 36 from När core (Gotland), int. 351·60–351·65 m; fig. 37 from Viki core, sample M-360, int. 153·35–153·50 m; figs 38 and 41 from Uulu-330 core, sample M-1070, int. 137·70–137·85 m; figs 39, 43, 45–46 and 48–49 from Själsö section (Gotland), sample G88-637LJ; fig. 40 from Uulu-330 core, sample M-1301, int. 138·05–138·15 m; figs 42, 50–52 and 54 from Viki core, sample M-976, int. 149·95–150·08 m; figs 47 and 53 from När core (Gotland), int. 361·30–361·40 m.

All × 50.

MÄNNIK, *Pterospathodus*

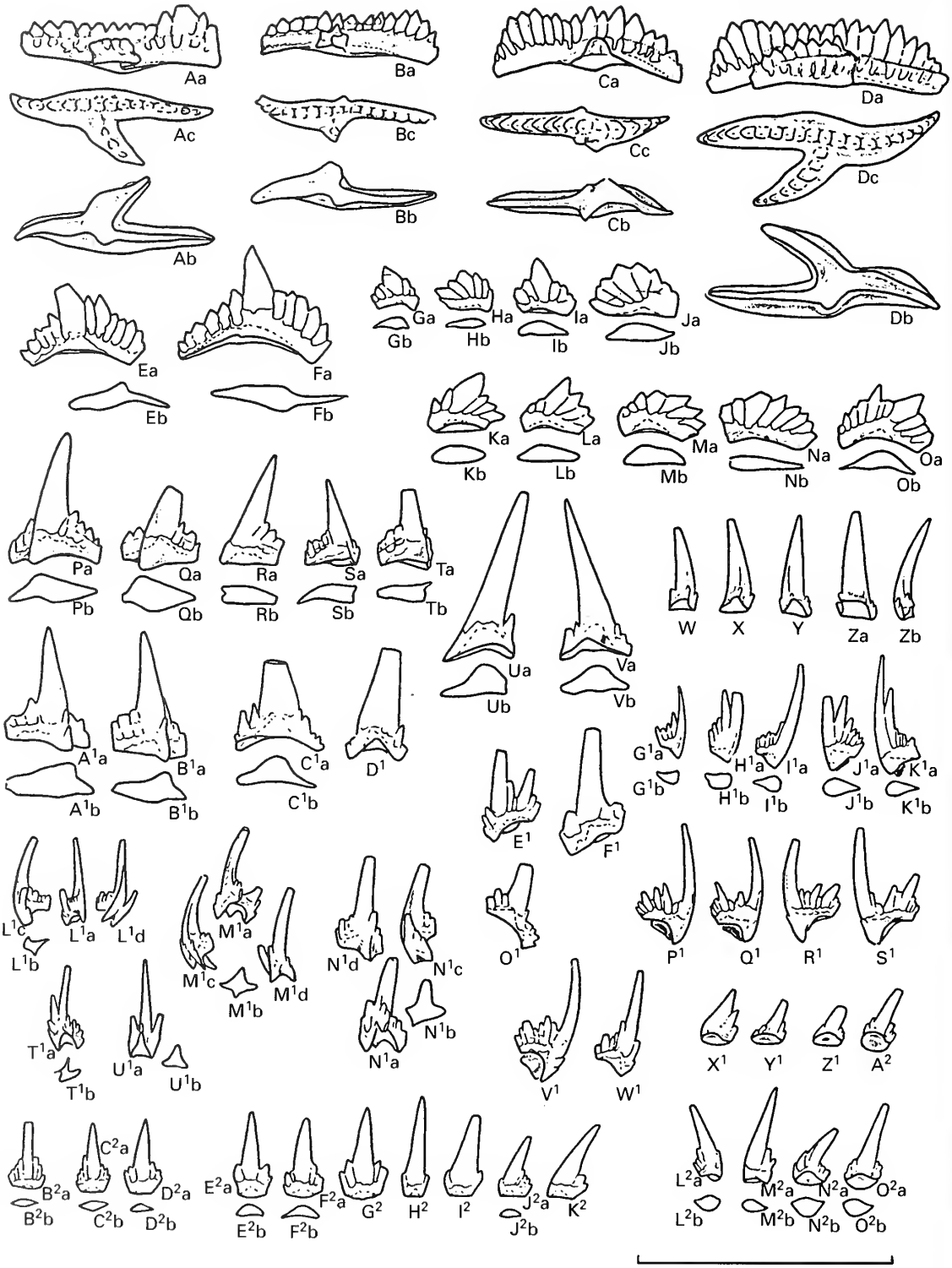

TEXT-FIG. 16. For caption see opposite.

Mountains, Northwest Territories of Canada; Over and Chatterton 1987) indicates that, most probably, they belong to separate species.

The Pa element of *P. rhodesi* is represented at least by two morphs: morph 1 with a bifurcated inner lateral process (Männik and Aldridge 1989, text-fig. 4*A*); and morph 2 with a pennate inner lateral process (Männik and Aldridge 1989, text-fig. 4*B*).

P. rhodesi has not been identified in the Baltic or in other parts of Europe.

Occurrence. *P. a. amorphognathoides* Zone (only?).

ORIGIN

The ancestry of *Pterospathodus* is uncertain. *P. eopennatus* appears widely without a direct antecedent. Bischoff (1986) described a presumed direct ancestor of *P. celloni* (= *P. eopennatus* in this paper) from New South Wales, Australia, which he called *P. cadiaensis*. Elements assigned to this taxon by Bischoff are also known from several other regions (Norway – Aldridge and Mohamed 1982, pl. 1, fig. 33; Severnaya Zemlya – Männik 1983, fig. 4*Y*; Northern Urals – Melnikov, pers. comm.; South China – Aldridge, pers. comm.). Well preserved material from the last region revealed that, in reality, these elements belong to a *Gamachignathus* apparatus, and *P. cadiaensis* was reidentified as *G. macroexcavatus* (Wang and Aldridge, 1996).

The new data presented herein indicate an increased level of similarity between the *Pterospathodus* and *Pranognathus* apparatuses (Männik and Aldridge 1989, text-fig. 5; Uyeno and Barnes 1983, pl. 2, figs 1–11, 14–18, identified as belonging to *Pterospathodus*). However, although the elements of *Pranognathus* can be readily homologized with those of *Pterospathodus* (Pa, Pb_1, Pc, M_1, Sc_1, Sc_2, Sb_1, Sb_2 and Sa can be recognized in *Pranognathus*) there are still too many significant morphological differences between these two apparatuses to allow us to consider *Pranognathus* as a direct ancestor of *Pterospathodus*. In *Pranognathus*, the Pa and Pb_1 elements (Männik and Aldridge 1989, text-fig. 5*A–I*, *U–X*) possess deep wide cavities, the Pc element (Männik and Aldridge 1989, text-fig. 5*J–K*, *Y–Z*) has three long processes, the M_1 element (Männik and Aldridge 1989, text-fig. 5*L–M*) has a denticulated inner lateral process and a large number of denticles on the anterior and posterior processes, and the anterior process of the Sc_2 element (Männik and Aldridge 1989, text-fig. 5*S*) is densely denticulated. Also, several elements known from *Pterospathodus* (Pb_2, Sc_3, canuliform, carniciform and curved), have not been identified in *Pranognathus*. However, as the ranges of *Pterospathodus* and *Pranognathus* are separated by a considerable time interval, it cannot be excluded that these two taxa are related to each other.

Hence, the origin of *Pterospathodus* remains unknown and needs further studies.

CONCLUSIONS

1. Elements previously referred to *Carniodus* do not belong to a separate genus, but formed part of the apparatus of *Pterospathodus*.
2. The structure of the *Pterospathodus* apparatus was evidently much more complicated than previously considered. It consists of at least 14 (15) elements: Pa, Pb_1, Pb_2, Pc, M_1, M_2 (so far recognized only in the *P. p. procerus* apparatus), Sc_1, Sc_2, Sc_3, Sb_1, Sb_2, Sa, carnuliform element with five morphs, curved element with three morphs and carniciform element.
3. In the Telychian, at least two distinct *Pterospathodus* lineages: *P. a. angulatus* – *P. a. amorphognathoides*, and *P. p. pennatus* – *P. p. procerus* existed and evolved separately, the former in the open shelf carbonate-terrigeneous facies and the latter in deeper basin graptolite-bearing facies.

TEXT-FIG. 16. *Pterospathodus pennatus procerus* (Walliser, 1964). A–D, Pa element. E–F, Pb_1 element. G–O, Pb_2 element. P–T, A^1–B^1, Pc element. U–V, C^1–D^1, M_1 element. W–Z, M_2 element. E^1–F^1, O^1, Sc_1 element. G^1–K^1, Sc_3 element. L^1–M^1, Sb_1 element. N^1, T^1, Sb_2 element. P^1–S^1, V^1–W^1, Sc_2 element. U^1, Sa element. X^1–A^2, carniciform element. B^2–C^2, carnuliform element, morph b. D^2–M^2, carnuliform element morph a. N^2–O^2, ?carniciform element. Scale bar represents 1 mm.

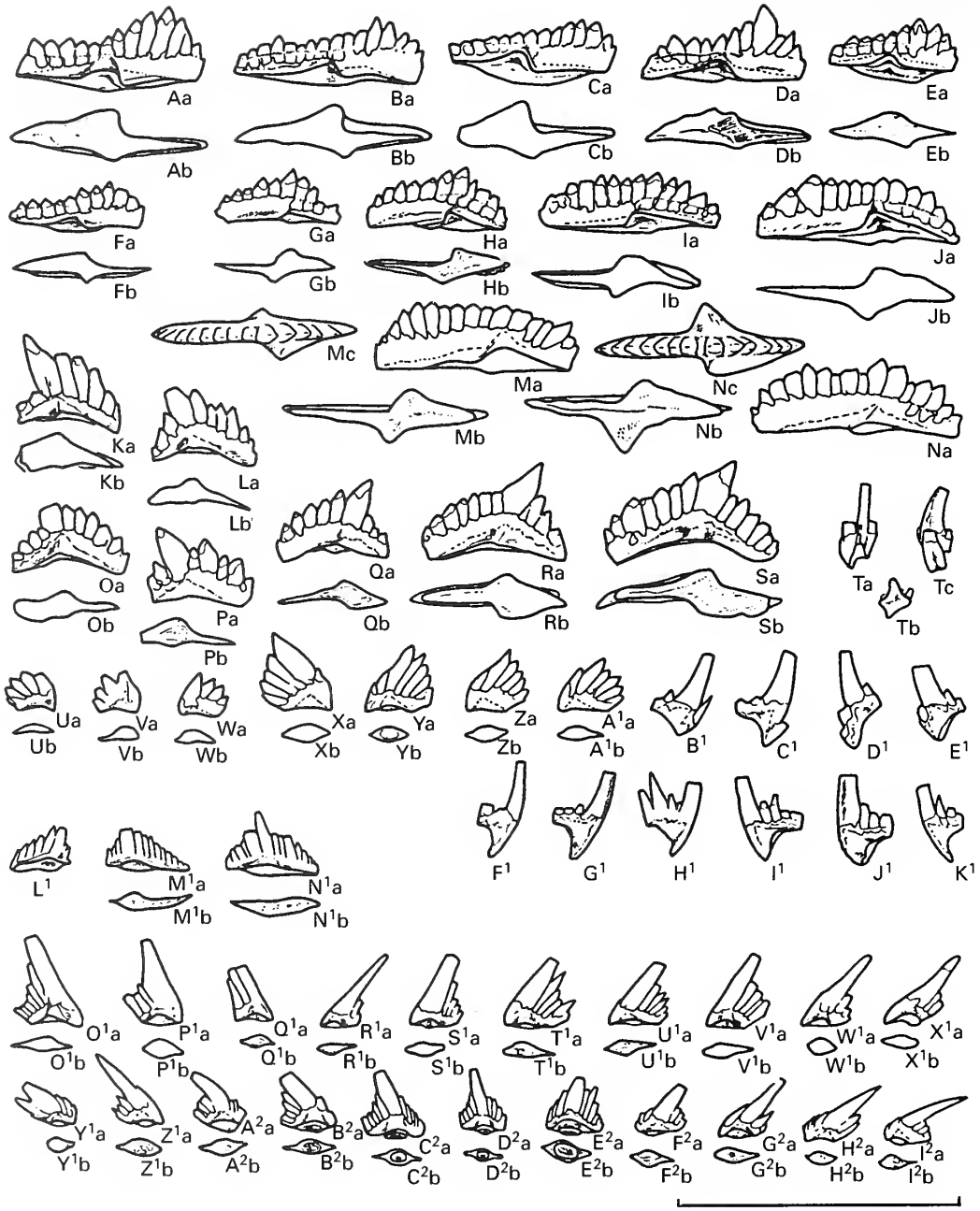

TEXT-FIG. 17. *Pterospathodus celloni* (Walliser, 1964). A–J, M–N, Pa element. K–L, O–S, Pb_1 element. T, Sb_2 element. U–A^1, Pb_2 element. B^1–E^1, Sc_1 element. F^1–K^1, Sc_2 element. L^1–N^1, carniciform(?) element. O^1–I^2, carnuliform(?) element. Scale bar represents 1 mm.

Both probably originated from a common ancestral taxon at the end of the *P. eopennatus* Zone, although they may have appeared in the upper part of the *A. irregularis* Subzone.

4. Evolution was more rapid, and the morphological variation within each population greater, in open shelf environments.

5. Three main intervals of evolution are recognized in the *Pterospathodus* sequence. The boundaries between them are marked by distinct morphological changes in the elements.
6. *P. celloni* was restricted to deeper basin environments, and was closely related to the *P. pennatus* lineage.
7. The appearance of *P. celloni* and *P. p. procerus* in open shelf environments occurred during times when the usual conditions there were partially (or completely – Ireviken Event) altered causing temporary disappearances or the final extinction of several lineages.
8. The evolutionary steps in the *Pterospathodus* lineage, together with changes shown by the rest of the Telychian conodont fauna, provide excellent potential for high resolution stratigraphy (Männik 1995, 1996).

Acknowledgements. Richard J. Aldridge, Howard A. Armstrong, Günther C. O. Bischoff, Antanas Brazuaskas, Lennart Jeppsson, Hans A. Nakrem, Hans P. Schönlaub and Otto H. Walliser kindly gave me free access to their collections of conodonts. Lennart Jeppsson and Richard J. Aldridge read the manuscript critically and suggested many improvements. Claes Bergman and Fredrik Jerre assisted with the SEM, Gennadi Baranov made the prints and Kaie Ronk the drawings of conodonts.

The research was carried out in the Institute of Geology, Tallinn (financed by the Institute of Geology and The Estonian Science Foundation), and in the Department of Historical Geology and Palaeontology, Lund University, Lund (financed by The Swedish Natural Science Research Council). My sincere thanks to everybody.

REFERENCES

ALDRIDGE, R. J. 1972. Llandovery conodonts from the Welsh Borderland. *Bulletin of the British Museum (Natural History), Geology Series*, **22**, 127–231, pls 1–9.

—— 1974. An *amorphognathoides* Zone conodont fauna from the Silurian of the Ringerike area, south Norway. *Norsk Geologisk Tidsskrift*, **54**, 295–303.

—— 1975. The stratigraphic distribution of conodonts in the British Silurian. *Journal of the Geological Society, London*, **131**, 607–618, 3 pls.

—— 1979. An upper Llandovery conodont fauna from Peary Land, eastern North Greenland. *Rapport Grønlands Geologiske Undersøgelse*, **91**, 7–23, pls 1–2.

—— 1980. Notes on some Silurian conodonts from Ireland. *Journal of Earth Sciences of the Royal Dublin Society*, **3**, 127–132.

—— 1985. Conodonts of the Silurian System from the British Isles. 68–92. *In* HIGGINS, A. C. and AUSTIN, R. L. (eds). *A stratigraphical index of conodonts*. Ellis Horwood, Chichester, 263 pp.

—— JEPPSSON, L. and DORNING, K. J. 1993. Early Silurian episodes and events. *Journal of the Geological Society, London*, **150**, 501–513.

—— and MOHAMED, I. 1982. Conodont biostratigraphy of the early Silurian of the Oslo Region, 109–120, 2 pls. *In* WORSLEY, D. (ed.). Subcommission on Silurian Stratigraphy. Field Meeting, Oslo Region, 1982. *Paleontological Contributions from the University of Oslo*, **278**, 175.

AN TAI-XIANG 1987. [*The Lower Palaeozoic conodonts of South China.*] Beijing University Press, Beijing, 238 pp., 35 pls. [In Chinese.]

ARMSTRONG, H. A. 1990. Conodonts from the Upper Ordovician–Lower Silurian carbonate platform of North Greenland. *Grønlands Geologiske Undersøgelse*, **159**, 1–151, pls 1–23.

BARCA, S., FERRETTI, A., MASSA, P. and SERPAGLI, E. 1992. The Hercynian Arburese Tectonic Unit of SW Sardinia. New stratigraphic and structural data. *Rivista Italiana di Paleontologia e Stratigrafia*, **98**, 119–136, pls 1–4.

BRAZAUSKAS, A. Z. 1983. Conodont zones of Lithuanian Llandovery facies. *Nauchnye Trudy Vysshih Uchebnyh Zavedenij Litovskoj SSR, Geologija*, **4**, 41–66. [In Russian, with English and Lithuanian summaries].

BARRICK, J. E. 1983. Wenlockian (Silurian) conodont biostratigraphy, biofacies, and carbonate lithofacies, Wayne Formation, Central Tennessee. *Journal of Paleontology*, **57**, 208–239.

—— and KLAPPER, G. 1976. Multielement Silurian (late Llandoverian–Wenlockian) conodonts of the Clarita Formation, Arbuckle Mountains, Oklahoma, and phylogeny of *Kockelella*. *Geologica et Palaeontologica*, **10**, 59–100, pls 1–4.

BISCHOFF, G. C. O. 1986. Early and middle Silurian conodonts from midwestern New South Wales. *Courier Forschungsinstitut Senckenberg*, **89**, 337, pls 1–34.

COOPER, B. J. 1977. Toward a familial classification of Silurian conodonts. *Journal of Paleontology*, **51**, 1057–1071.

DRYGANT, D. M. 1969. [Konodonty Restevskogo, Kitajgorodskogo i Mukshinskogo gorizontov Silura Podolii.] *Paleontologicheskij Sbornik*, **6** (1), 49–54, 1 pl. [In Russian].

—— 1984. [*Korrelyaciya i konodonty silurijskih-nizhnedevonskih otlozhenij Volyno-Podolij.*] Naukova Dumka, Kiev, 192 pp., 16 pls. [In Russian].

DUMOULIN, A. and HARRIS, A. G. 1987. Off-platform Silurian sequence in the Ambler River Quadrangle. *Geologic Studies in Alaska by the U.S. Geological Survey during 1987*, 35–38.

HELFRICH, C. T. 1980. Late Llandovery–early Wenlock conodonts from the upper part of the Rose Hill and the basal part of the Mifflintown formations, Virginia, West Virginia, and Maryland. *Journal of Paleontology*, **54**, 557–569, 2 pls.

IGO, H. and KOIKE, T. 1968. Ordovician and Silurian conodonts from the Langkawi Island, Malaya, Part 2. *Geology and Palaeontology of Southeast Asia*, **4**, 1–21, pls 1–3.

JIANG WU, ZHANG FANG, ZHOU XIYUN, XIONG JIANFEI, DAI JINYIE and ZHONG DUAN 1986. [*Conodonts – palaeontology.*] Southwestern Petroleum Institute, Sichuan, 264 pp, pls 265–287. [In Chinese].

JEPPSSON, L. 1979. Conodonts. 225–248. *In* JAANUSSON, V., LAUFELD, S. and SKOGLUND, R. (eds). Lower Wenlock faunal and floral dynamics – Vattenfallet section, Gotland. *Sveriges Geologiska Undersökning Avdhandlingar och Uppsatser*, **C762**, 1–294.

—— 1987. Lithological and conodont distributional evidence for episodes of anomalous oceanic conditions during the Silurian. 129–145. *In* ALDRIDGE, R. J. (ed.). *Palaeobiology of conodonts*, Ellis Horwood, Chichester, 180 pp.

—— 1994. A new standard Wenlock conodont zonation. 133. *In* SCHÖNLAUB, H. P. and KREUZER, L. H. (eds). IUGS Subcommission on Silurian Stratigraphy – Field Meeting Eastern + Southern Alps, Austria 1994 in mem. H. Jaeger. *Berichte der Geologischen Bundesanstalt*, **30**, 1–156.

—— 1997. A new latest Telychian, Sheinwoodian and early Homerian (early Silurian) Standard Conodont Zonation. *Transactions of the Royal Society of Edinburgh: Earth Sciences*, **88**, 91–114.

—— and MÄNNIK, P. 1993. High-resolution correlations between Gotland and Estonia near the base of the Wenlock. *Terra Nova*, **5**, 348–358.

KLAAMANN, E. 1990. Locality 8:3. Valgu outcrop. 181–182. *In* KALJO, D. and NESTOR, H. (eds). *Field Meeting, Estonia* 1990. *An excursion guidebook*. Tallinn, 209 pp.

KLEFFNER, M. A. 1985. Conodont biostratigraphy of the stray 'Clinton' and 'Packer Shell' (Silurian, Ohio subsurface) and its bearing on correlation. 219–229, 2 pls. *In* GRAY, J., MASLOWSKI, A., McCULLOUGH, W. and SHAFER, W. E. (eds). *The new Clinton collection – 1985*. Ohio Geological Society, Columbus, Ohio, 243 pp.

—— 1987. Conodonts of the Estill Shale and Bisher Formation (Silurian, southern Ohio): biostratigraphy and distribution. *Ohio Journal of Sciences*, **87** (3), 78–89.

—— 1991. Conodont biostratigraphy of the upper part of the Clinton Group and the Lockport Group (Silurian) in the Niagara Gorge Region, New York and Ontario. *Journal of Paleontology*, **65**, 500–511.

KUWANO, Y. 1976. Finding of Silurian conodont assemblages from the Kurosegawa tectonic zone in Shikoku, Japan. *Memoirs of the National Science Museum*, **9**, 17–22, 2 pls. [In Japanese with English summary].

LIEBE, R. M. and REXROAD, C. B. 1977. Conodonts from Alexandrian and early Niagaran rocks in the Joliet, Illinois, area. *Journal of Paleontology*, **51**, 844–857, pls 1–2.

MABILLARD, J. E. and ALDRIDGE, R. J. 1983. Conodonts from the Coralliferous Group (Silurian) of Marloes Bay, south-west Dyfed, Wales. *Geologica et Palaeontologica*, **17**, 29–43, pls 1–4.

MANARA, C. and VAI, G. B. 1970. La sezione e i conodonti del costone sud del M. Rauchkofel (Paleozoico, Alpi Carniche). *Giornale di Geologia*, **36**, 441–503, pls 59–63.

McCRACKEN, A. D. 1991. Silurian conodont biostratigraphy of the Canadian Cordillera with a description of new Llandovery species. 97–127, 5 pls. *In* ORCHARD, M. J. and McCRACKEN, A. D. (eds). Ordovician to Triassic conodont paleontology of the Canadian Cordillera. *Bulletin of the Geological Survey of Canada*, **417**, 1–335.

MILLER, R. H. 1976. Revision of upper Ordovician, Silurian, and lower Devonian stratigraphy, southwestern Great Basin. *Bulletin of the Geological Society of America*, **87**, 961–968.

—— 1978. Early Silurian to early Devonian conodont biostratigraphy and depositional environments of the Hidden Valley Dolomite, southeastern California. *Journal of Paleontology*, **52**, 323–344, pls 1–4.

MÄNNIK, P. 1983. Silurian conodonts from Severnaya Zemlya. *Fossils and Strata*, **15**, 111–119, 1 pl.

—— 1992. [Upper Ordovician and lower Silurian conodonts in Estonia.] Unpublished Ph.D. thesis, University of Tartu, Estonia. [In Russian].

—— 1995. The evolution of selected conodont lineages and an improved zonation for the Telychian (late Llandovery). 52–54. *In* BROCK, G. A. (ed.). First Australian Conodont Symposium (AUSCOS-I) and the

Boucot Symposium, 18–21 July, 1995, Abstracts and Programme. *Special Publications of the Macquarie University Centre for Ecostratigraphy and Palaeobiology (MUCEP)*, **1**, 1–108.

—— 1996. Telychian (Early Silurian) conodont *Pterospathodus*: evolution and taxonomy. 35. *In* DZIK, J. (ed.). *Sixth European Conodont Symposium (ECOS VI), Abstracts*. Institut Paleobiologii PAN, Warszawa, 70 pp.

—— and ALDRIDGE, R. J. 1989. Evolution, taxonomy and relationships of the Silurian conodont *Pterospathodus*. *Palaeontology*, **32**, 893–906.

—— and MALKOWSKI, K. 1998. Silurian conodonts from the Gołdap core, Poland. *Palaeontologia Polonica*, **58**, 139–149.

—— and VIIRA, V. 1990. Conodonts. 84–89, pls 16–18. *In* KALJO, D. and NESTOR, H. (eds). *Field Meeting, Estonia 1990. An excursion guidebook*. Tallinn, 209 pp.

NAKREM, H. A. 1986. Llandovery conodonts from the Oslo Region, Norway. *Norsk Geologisk Tiddskrift*, **66**, 121–133.

NEHRING-LEFELD, M. 1985. Conodonts of the *amorphognathoides* Zone (Silurian) from eastern part of the Podlasie Depression. *Kwartalnik Geologiczny*, **29** (3/4), 625–652, pls 1–6. [In Polish with English and Russian summaries].

—— 1992. Biostratigraphy of the Old Paleozoic carbonates in the Zawiercie area (NE margin of the Upper Silesian Coal Basin). *Geological Quarterly*, **36**, 171–198, pls 1–5.

NICOLL, R. S. and REXROAD, C. B. 1968. Stratigraphy and conodont paleontology of the Salamonie Dolomite and Lee Creek Member of the Brassfield Limestone (Silurian) in southeastern Indiana and adjacent Kentucky. *Bulletin of the Department of Natural Resources of the Geological Survey of Indiana*, **40**, 1–73, pls 1–7.

NOWLAN, G. S. 1981. Late Ordovician – early Silurian conodont biostratigraphy of the Gaspé Peninsula – a preliminary report. 257–291, 7 pls. *In* LESPÉRANCE, P. J. (ed.). *Subcommission on Silurian Stratigraphy, Ordovician-Silurian Boundary Working Group. Field Meeting, Anticosti–Gaspé, Québec 1981, Vol. 2: stratigraphy and paleontology*. University of Montreal, 321 pp.

—— 1983. Early Silurian conodonts of eastern Canada. *Fossils and Strata*, **15**, 95–110.

OVER, D. J. and CHATTERTON, D. E. 1987. Silurian conodonts from the southern Mackenzie Mountains, Northwest Territories, Canada. *Geologica et Palaeontologica*, **21**, 1–49, pls 1–8.

PICKETT, J. 1978. Silurian conodonts from Blowclear and Liscombe Pools, New South Wales. *Journal and Proceedings of the Royal Society of New South Wales*, **111**, 35–39.

QIU HONGRONG 1985. Silurian conodonts in Xizang (Tibet). *Bulletin of the Institute of Geology of the Chinese Academy of the Geological Science*, **11**, 23–38, pls 1–2. [In Chinese with English summary].

—— 1988. Early Palaeozoic conodont biostratigraphy of Xizang (Tibet). *Symposium on Stratigraphy and Paleontology*, 185–202, 6 pls.

REXROAD, C. R. and NICOLL, R. S. 1971. Summary on conodont biostratigraphy of the Silurian System of North America. *Memoir of the Geological Society of America*, **127**, 207–225, pls 1–2.

—— —— 1972. Conodonts from the Estill Shale (Silurian, Kentucky and Ohio) and their bearing on multielement taxonomy. *Geologica et Palaeontologica*, **SB1**, 57–74, pls 1–2.

SALADŽIUS, V. 1975. Conodonts of the Llandoverian (lower Silurian) deposits of Lithuania. 219–225, pls 1–2. *In* GRIGELIS, A. A. (ed.). *The fauna and stratigraphy of Palaeozoic and Mesozoic of Baltic and Byelorussia*. 'Mintis', Vilnius, 249 pp. [In Russian, with English summary].

SAVAGE, N. M. 1985. Silurian (Llandovery–Wenlock) conodonts from the base of the Heceta Limestone, southeastern Alaska. *Canadian Journal of Earth Sciences*, **22**, 711–727.

—— POTTER, A. W. and WYATT, G. G. 1983. Silurian and Silurian to early Devonian conodonts from West Central Alaska. *Journal of Paleontology*, **57**, 873–875.

SCHÖNLAUB, H. P. 1969. Das Paläozoikum zwischen Bischofalm und Hohem Trieb (Zentrale Karnische Alpen). *Jahrbuch der Geologischen Bundesanstalt*, **112**, 265–320, pls 1–2.

—— 1971. Zur Problematic der Conodonten-Chronologie an der Wende Ordoviz/Silur mit besonderer Berücksichtigung der Verhältnisse im Llandovery. *Geologica et Palaeontologica*, **5**, 35–57, pls 1–3.

—— 1975. Conodonten aus dem Llandovery der Westkarawanken (Österreich). *Verhandlungen der Geologischen Bundesanstalt*, **2–3**, 45–65, pls 1–2.

SPASOV, H. and FILIPOVIĆ, I. 1966. The conodont fauna of the older and younger Palaeozoic in southeastern and northwestern Bosnia. *Geološki Glasnik*, **11**, 33–53, pls 1–3.

STOUGE, S. and BAGNOLI STOUGE, G. 1984. An upper Llandovery conodont fauna from Eastern Hall Land, North Greenland. *Bolletino della Società Paleontologica Italiana*, **23**, 103–112, pls 1–2.

SWEET, W. C. 1981. Morphology and composition of elements. W5–W20. *In* ROBINSON, R. A. (ed.). *Treatise on invertebrate paleontology. Part W. Miscellanea. Supplement 2. Conodonta*. Geological Society of America and University of Kansas Press, Boulder, Colorado and Lawrence, Kansas, 202 pp.

—— 1988. The Conodonta. Morphology, taxonomy, paleoecology, and evolutionary history of a long-extinct animal phylum. *Oxford Monographs on Geology and Geophysics*, **10**, 1–212.

UYENO, T. T. 1990. Biostratigraphy and conodont faunas of Upper Ordovician through Middle Devonian rocks, eastern Arctic Archipelago. *Bulletin of the Geological Survey of Canada*, **401**, 1–210, pls 1–20.

—— and BARNES, C. R. 1981. A summary of Lower Silurian conodont biostratigraphy of the Jupiter and Chicotte formations, Anticosti Island, Québec. 173–184, 1 pl. *In* LESPÉRANCE, P. J. (ed.). *Subcommission on Silurian Stratigraphy, Ordovician-Silurian Boundary Working Group. Field Meeting, Anticosti–Gaspé, Québec 1981, Vol. 2: stratigraphy and paleontology*. University of Montreal, 321 pp.

—— —— 1983. Conodonts of the Jupiter and Chicotte formations (lower Silurian), Anticosti Island, Québec. *Bulletin of the Geological Survey of Canada*, **355**, 1–48, pls 1–9.

WALLISER, O. H. 1964. Conodonten des Silurs. *Abhandlungen des Hessischen Landesamtes für Bodenforschung*, **41**, 1–106, pls 1–32.

WANG CHEN-YUAN and ALDRIDGE, R. J. 1996. Conodonts. 46–55, pls 1–3. *In* CHEN XU and RONG JIA-YU (eds). [*Telychian* (*Llandovery*) *of the Yangtze Region and its correlation with British Isles.*] Science Press, Beijing, 157 pp. [In Chinese].

WATKINS, R., KUGLITSCH, J. J. and McGEE, P. E. 1994. Silurian of the Great Lakes Region, Part 2: paleontology of the Upper Llandovery Brandon Bridge Formation, Walworth County, Wisconsin. *Milwaukee Public Museum Contributions in Biology and Geology*, **87**, 1–71, pls 1–4.

YU HONGJIN 1985. Conodont biostratigraphy of Middle–Upper Silurian from Xainza, Northern Xizang (Tibet). *Contribution to the geology of the Qinghai-Xizang* (*Tibet*) *Plateau*, **16**, 15–31, pls 1–3. [In Chinese with English summary].

PEEP MÄNNIK
Institute of Geology
Tallinn Technical University
Estonia pst. 7
EE0001 Tallinn, Estonia
e-mail mannik@gi.ee

Typescript received 3 July 1997
Revised typescript received 25 March 1998

APPENDIX

List of localities cited in text (see also Text-fig. 1).

A. Exposures

1. Valgu – a drainage canal; studied section corresponds to Point 1 in Klaamann (1990, p. 181).
2. Velise-Kõrgekalda – low cliff on the left bank of the Päärdu (on some maps indicated as Velise) River; *c.* 2·5 km west-south-west of a bridge across the river in Velise village, central Estonia.
3. Själsö – shore exposure; *c.* 4·3 km west of Väskinde church, Gotland, Sweden.
4. Överstekvarn 2 – several small exposures in the southern brook about 200 m north-west of Överstekvarn; *c.* 4·45 km (south-)south-west of Lummelunda church, Gotland, Sweden.
5. Nygårdsbäckprofilen 1 – a brook section at the mouth of Nygårdsbäcken (bäcken = brook) and shore section south-west of it; *c.* 2·97 km north-west of Västerhedje church, Gotland, Sweden.

B. Cores

1. The Nurme, Uulu-330, Viki and Ohesaare cores are housed in the Särghaua field station (central Estonia), Institute of Geology, Tallinn Technical University.
2. The Pahapilli core is housed in the Turja field station (southern Saaremaa, Estonia), Geological Survey of Estonia.
3. The När core is housed in the Geological Survey of Sweden, Uppsala, Sweden.

ON PREDATOR DETERRENCE BY PRONOUNCED SHELL ORNAMENT IN EPIFAUNAL BIVALVES

by HYWEL M. I. STONE

ABSTRACT. Laboratory experiments, undertaken to determine the effectiveness of pronounced shell ornament in epifaunal bivalves against predatory shell boring by subtropical muricid gastropods and extraoral feeding by asteroids, suggest that natural and artificial spines deter muricid predators from attacking ornamented areas of the bivalve shell but do not have a similar effect upon predatory asteroids. These findings are discussed in relation to the extant and often highly spinose cementing bivalve families Spondylidae and Chamidae. The adaptive radiation of the Muricidae in the Albian may have resulted in selection for highly ornamented epifaunal bivalve taxa in shallow, warm water environments where the epifaunal habit renders sessile prey particularly vulnerable to attack by roving durivorous predators. The ability to produce spines, however, was already apparent in ancestral Pectinoida in the late Palaeozoic. It is concluded that the pronounced shell ornament of the free valves of warm water cemented epifaunal bivalve taxa is functional against shell boring muricids. Other hypothesized functions are discussed briefly.

FOR many years it has been argued that shell ornament in bivalved molluscs is directly related to the mode of life of the animal. Thus, shallow infaunal taxa display sculptures that are interpreted as acting as aids to burrowing or as stabilizers for life within soft substrata (Stanley 1970), and cementing epifaunal taxa produce commarginal lamellae or spines on the 'lower' valve as aids to attachment to hard substrata (Stenzel 1971). There have been various hypotheses for the function of spines and commarginal lamellae on the 'upper' free valve of cementing pleurothetic epifauna. It has been suggested, for example, that ornament serves to increase the effective strength of the shell and thus defend it against predators (Vermeij 1987). It has also been proposed that ornament acts to attract the growth of epibionts to the shell. The latter may discourage predation by visually camouflaging the shell or chemically masking secreted metabolites that may act as cues to potential predators (Vance 1978; Feifarek 1987). Ornament may also provide protection for sensory outposts of mantle tissue (by analogy with brachiopod soft part morphology) (Rudwick 1965; Stenzel 1971), or act to deter rasping by certain grazers which may over time erode and weaken the shell. Finally, both spines and commarginal lamellae may act as direct defences against predation (Kauffmann 1969; Vermeij 1987). It is this last hypothesis on which the present study is focused. Historically, however, both the nature of such defences, and the identity of the predators which they may deter, have been far from clear. As Harper and Skelton (1993*a*) have pointed out, much of the literature concerning shell ornament in bivalves has been based upon anecdotal evidence.

The great majority of shell ornament studies have concentrated on infaunal taxa and their adaptations to life within soft substrata (e.g. Stanley 1970, 1981, 1988; Wilson 1979; Watters 1993). However, some work has shown that predation by naticid gastropods may be an important selective force operating on the functional design of certain shallow infaunal bivalve groups, especially in the Indo-Pacific (Ansell and Morton 1983). The effects of shell ornament on other predatory methods, such as smothering by naticids (Ansell and Morton 1987), foraging by crabs, asteroids and birds (Carter 1968; Ansell 1969), and fish predation, have received little attention. Very little evidence has been presented concerning the possible anti-predatory effects of epifaunal bivalve shell sculpture in relation to a variety of predatory methods, including shell boring by muricid gastropod predators and extraoral feeding by asteroids, both subjects of the present study.

Muricids are known to exert heavy predation pressure on organisms in many shallow warm

[Palaeontology, Vol. 41, Part 5, 1998, pp. 1051–1068]

temperate, subtropical and tropical rocky shores and coral reefs (Taylor 1976, 1978). In these environments, spinose epifaunal prey taxa may be an important component of the intertidal and subtidal megafauna. Jackson (1977), for example, in his studies of Jamaican reefs, stated that more than 50 per cent. of spondylid, dimyid and chamid mortalities may be caused by shell boring muricid gastropods. Recently, a possible defensive rôle for the pronounced shell ornament of the intertidal oyster *Saccostrea cucullata* (Born) has been suggested by Taylor (1990), who noted that in Hong Kong the marginal spines of this species may hinder edge-boring by muricids. Preliminary experimental observations of Harper and Skelton (1993*a*) on the same species also suggested that spines are directly effective at deterring muricid predatory activity; they stressed the potential importance of the rise of the shell boring muricids in the early Cretaceous as a factor influencing bivalve defensive traits. Apart from studies such as that of Harper (1994), little work has been published on bivalve predation by subtropical and tropical extraoral feeding asteroids.

Two epifaunal cementing bivalve families, Spondylidae and Chamidae, are of particular interest in the present analysis of the direct inhibitory effect of shell ornament on predators. Although unrelated, both have a wide distribution in warm temperate, subtropical and tropical shallow waters, particularly on rocky shores and reefs (Zavarei 1973; Bernard 1976). Stanley (1970) noted that the spinose ornamentation of these groups, particularly the spondylids, may serve as a defensive adaptation. He considered reef fishes potentially important but did not demonstrate experimentally a link between epifaunal bivalve ornamentation and predation. Likewise, Logan (1974) has suggested that the spines of *Spondylus americanus* Hermann, a species living on the Bermuda Platform, perform a protective function, but did not state which predators would be deterred. This study presents evidence, through manipulative experiments, that spines on bivalve shells may directly hinder a variety of subtropical muricid gastropod predators, but do not have a similar effect against a subtropical extraoral feeding asteroid. The significance of these findings is discussed.

The terminology used to describe shell surface structures and ornamentation has seldom been rigorously applied in the literature. A 'spine' is here defined as a calcareous projection, perpendicular, oblique or subparallel to the general surface of the shell, that arises as a result of the combination of radial and concentric elements of shell growth (Cox 1969), and whose height is greater than that of the shortest dimension of its base. For structures where the basal diameter is equal to or greater than the height, the term 'node' is better applied. A 'lamella' is defined as a calcareous projection, perpendicular, oblique or subparallel to the general surface of the shell, that arises with varying degrees of radial expression but always commarginal with the commissure, and whose height is greater than that of the basal thickness. For structures where the basal thickness is equal to or greater than the height, the term 'commarginal ridge' is better applied.

MATERIALS AND METHODS

To determine the effectiveness of pronounced shell ornamentation in bivalves against predation by shell boring muricids and an extraoral feeding asteroid, a series of experiments was conducted on living animals in flow-through Perspex aquaria at the Swire Institute of Marine Science, Cape d'Aguilar, Hong Kong, from May to July 1995. Over this period, aquarium seawater temperatures reflected those in the field, with an average of 25 °C ± 2 °C. Bivalve prey were offered as a simple choice between ornamented and unornamented individuals (Experiments 1 to 3) or with varying degrees of shell ornamentation (Experiment 4). Different forms of artificial sculptural attachments were produced to form spinose shells in Experiments 1, 3 and 4, and the effects of natural ornament were observed in Experiment 2.

For prey bivalves, the mytilid *Perna viridis* (Linnaeus) was collected intertidally from a pier in the Tolo Channel (New Territories), the mytilid *Septifer virgatus* (Wiegmann) intertidally from the exposed eastern shore of Cape d'Aguilar (Hong Kong Island), and the chamid *Chama reflexa* Reeve subtidally from Hoi Ha Wan (eastern New Territories). In shallow subtidal and low intertidal

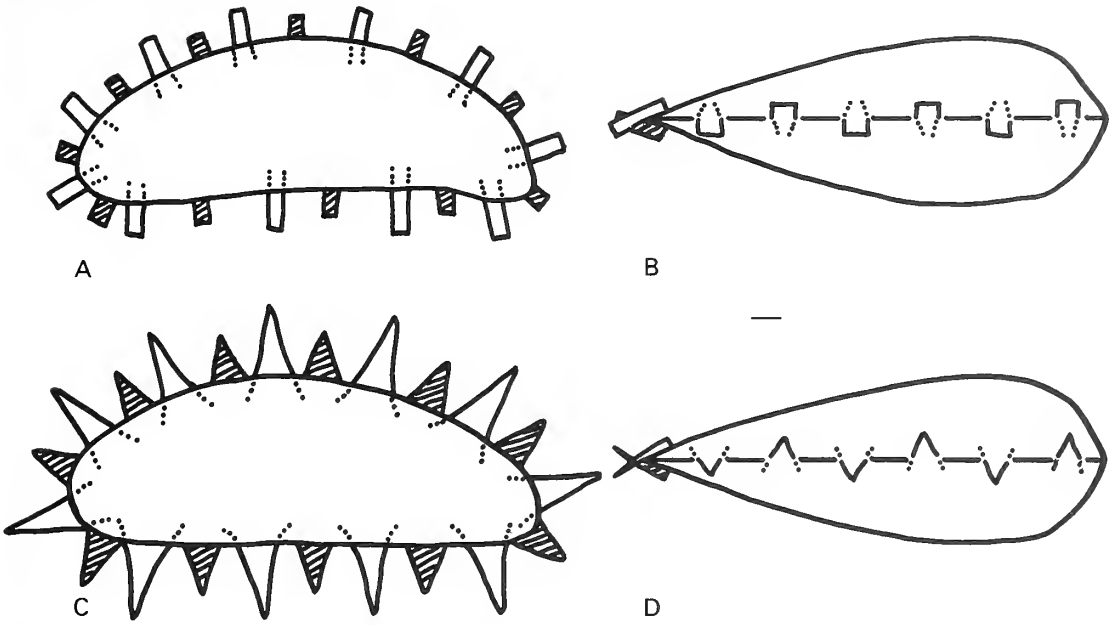

TEXT-FIG. 1. Diagrammatic representation of artificial 'spines' attached to mussel shells in Experiments 1 and 3. A–B, lateral and marginal views of polyethylene 'spines' attached to *Septifer virgatus* offered to *Thais luteostoma* as prey in Experiment 1. C–D, lateral and marginal views of 'spines' attached to *Perna viridis* cut from mussel shell, offered to *Coscinasterias acutispina* as prey in Experiment 3. Scale bar represents 1 mm (A–B) or 2 mm (C–D).

areas around many rocky shores in Hong Kong, *C. reflexa* cements to large boulders, often on their undersides or in crevices (pers. obs.). At the collection site, they were often found aggregated into dense clumps in crevices in the vertical walls of a small jetty.

The shell boring muricid predators *Thais luteostoma* Holten, *T. clavigera* Kuster and *Morula musiva* Kiener, and the extraoral feeding asteroid predator *Coscinasterias acutispina* Stimpson were all collected from sheltered sites in Lobster Bay (Cape d'Aguilar). The asteroids form an important component of the epifauna at the collection site and may feed opportunistically (Harper 1994). The muricid *Chicoreus microphyllus* Lamarck was collected from Hoi Ha Wan. *C. microphyllus*, *T. luteostoma*, *C. acutispina* and *C. reflexa* were all gathered subtidally, whilst *T. clavigera*, *M. musiva*, *P. viridis* and *S. virgatus* were found in the intertidal zone.

Apart from in Experiment 4, all bivalve prey were distributed in a random manner on the base of each tank. For the duration of the experiments the byssate *S. virgatus* and *P. viridis* were not allowed to attach themselves to the floor or walls of each tank in order to reduce the possibility of variation in strength of attachment and to ensure relative homogeneity amongst predator-prey interactions. All predator sizes were recorded. In order to reduce any bias in the observations resulting from death from other possible causes, only those bivalves whose flesh had been completely removed from the shell by the predator were recorded as 'consumed' in the following experiments. Any prey that showed any signs of physical or behavioural deterioration were immediately discarded. For each experiment, predators were initially starved for one week prior to use. All experiments were run for six weeks and aquaria were checked daily. Three replicates were undertaken for each study apart from Experiment 4, with six replicates. Statistical analyses were calculated using the chi square test.

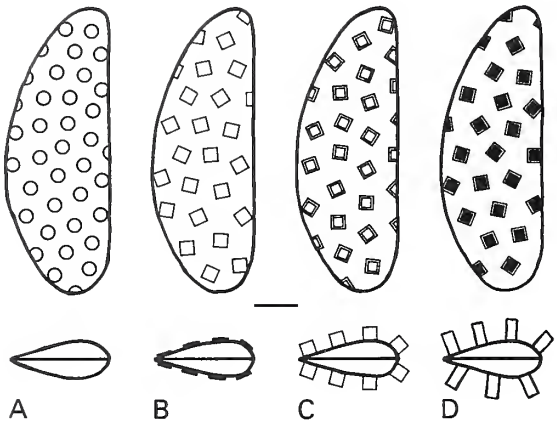

TEXT-FIG. 2. Diagrammatic representation of artificial polyethylene 'spines' attached to the lateral surface of *Perna viridis* shells offered to *Morula musiva* as prey in Experiment 4. A, lateral and posterior views of unornamented mussels dotted with cyanoacrylate as a control. B, lateral and posterior views of 1 mm high 'spines'. C, lateral and posterior views of 2 mm high 'spines'. D, lateral and posterior views of 4 mm high 'spines'. Scale bar represents 5 mm.

Artificial spines

Artificial spines were manufactured and attached to prey bivalve shells in Experiments 1, 3 and 4. Both the form and arrangement of such spines varied according to the experiment, as described below. Apart from in Experiment 4, the process of adhering spines or dotting unornamented prey with epoxy in the laboratory lasted about one hour per specimen at room temperature. All prey, ornamented and unornamented, underwent the same period of emersion.

In the aquarium, the muricid *Thais luteostoma* appeared to be an obligate edge-borer of the prey *Septifer virgatus*, probably the result of alternative prey not being available. The artificial spines required for Experiment 1, therefore, were fixed only along the commissure of both valves, including the area of emergence of the byssus. Since the bivalve prey in this experiment were of relatively small size, and for ease of manipulation, the artificial spines were cut from polyethylene strips to a length of 5 mm, with basal dimensions of 2×2 mm. These were fixed to the bivalves with epoxy resin (Araldite Rapid – Ciba Geigy) at 2 mm distances along the commissure so that they both radiated outwards from the margin and interdigitated by passing through the plane of the commissure at a low angle (Text-fig. 1A–B). The artificial spines were maintained at a length of 5 mm in all cases. As a control for the use of the epoxy, unornamented prey were dotted with Araldite at the same sites as artificial spine attachment in ornamented individuals. Most spines remained secure for the duration of each relevant experiment. If any became dislodged, prey were replaced by newly prepared individuals.

Sculptural augmentation in Experiment 3 consisted of adhering artificial spines all around the commissure of the prey shell, in a similar arrangement to that of Experiment 1, except that, because the prey used in this instance were generally larger than *S. virgatus*, it was possible to cut the spines from dead *Perna viridis* shells with a craft saw, instead of from polyethylene strips. Spines produced in this way were cut to a length of approximately one-third of the length of the shell along the axis of greatest growth, and were attached with epoxy resin. Their natural curvature resulted in interdigitation across the plane of the commissure (Text-fig. 1C–D). This arrangement was chosen for two reasons: (1) the resulting spines were particularly sturdy when fixed and (2), as the mussels are orthothetic in life, a roving predator is likely to come into contact with the margins of the valves, rather that the sides, particularly on sense mussel beds. As a control, epoxy resin was also applied to the shells of unornamented prey so that any differences in asteroid feeding behaviour by, for example, the presence of adhesive chemically masking metabolic cues secreted by the mussels, would apply to both ornamented and unornamented prey alike.

In Experiment 4, artificial spines were cut at varying lengths and arranged over the whole surface of the free unattached valve of artificially cemented *P. viridis* prey. For ease of manipulation, spines were cut from polyethylene strips and attached with cyanoacrylate (Superglue–Loctite) rather than epoxy resin. This provided effective underwater strength of adhesion. The spines were spaced at

2 mm from each other on the free valve surface, mirroring the basal dimensions of the projections themselves (2 × 2 mm) (Text-fig. 2). As a control, the five unornamented bivalves were dotted with cyanoacrylate at 2 mm intervals, thus mimicking the spine distributions on ornamented individuals. All treatments covered the entire free valve from the umbo to the posterior margin. The process of attaching the spines to the shells in the laboratory lasted about ten minutes for each specimen.

The use of epoxy resin and cyanoacrylate in manipulative experiments is far from new. Harper (1991), for example, in her work on the effects of cementation on predation, has shown that daubing the shells of *Mytilus edulis* with epoxy reveals no apparent inhibitory effect on crushing predation by the crabs *Cancer pagarus* and *Carcinus maenas* or extraoral predation by the asteroid *Asterias rubens*. For the work presented here, a pilot study of drilling by *Thais clavigera* revealed no statistically significant difference in consumption between numbers of *Perna viridis* whose shell had been dotted with either epoxy or cyanoacrylate and those that had been left untouched.

Experiment 1

This experiment was designed to show whether artificial spines had an inhibitory effect on shell boring by *Thais luteostoma*. Five *T. luteostoma* were offered 20 *Septifer virgatus* as prey. Ten of the latter were unornamented, and ten had artificial 'spines' attached to both valves all around the commissure. Any differences in the positions of bore holes in ornamented and unornamented prey were noted, and observations were made on the possible inhibitory effects of the spines themselves. All bivalves eaten were replaced with ones of similar size and state of ornamentation.

Experiment 2

This experiment was designed to show if the natural ornamentation of the 'upper' right valve or commissural edge of the prey bivalve *Chama reflexa* inhibits boring by the muricids *Chicoreus microphyllus* and *Thais clavigera*. Two *C. microphyllus* and ten *T. clavigera* were offered 20 *C. reflexa* as prey in each tank. The numbers of each muricid species used merely reflected availability and no attempt at making any inferences about differences in the number of bore holes made by the two muricids was made. Ten bivalves were presented with their natural shell ornament intact, and ten had been filed to a smooth, unornamented finish. The natural sculpture consisted of either very small spines (up to 1·5 mm long) covering the 'upper', right valve, or a crenulate marginal lamella projecting some 2 mm from the commissure, or both. For prey which had been filed smooth, ornament was removed only from the right valve of each specimen. The left valves of all ornamented and unornamented specimens, which were covered by commarginal series of attachment lamellae except at the site of the attachment scar, were left untouched. No attempt was made to cement artificially the prey in the tanks and the bivalves were offered in random distributions and orientations. A range of prey sizes was presented and consumed individuals were replaced by ones of similar size and state of ornamentation. As in Experiment 1, the areas of boring were noted. Exact positions of bore holes are not displayed graphically, however, because of the variable shell morphology of *C. reflexa* and hence the difficulty of projecting such positions onto a standard graphic template.

Experiment 3

This experiment was designed to show if artificial spines deter predation by the extraoral feeding asteroid *Coscinasterias acutispina*. Ten individuals of *C. acutispina* were offered 40 *Perna viridis* as prey, of which 20 were 'ornamented' and 20 'unornamented'. A random size range of prey was presented, and all bivalves consumed were replaced by individuals of similar size and ornament. Numbers of consumed individuals were recorded as well as the feeding behaviour of *C. acutispina* in order to determine any inhibitory effect that the spines may confer. Only animals with three or

more primary arms were selected for use in the study and were chosen at random for each replicate from a holding tank. As noted by Harper (1994), there is a tendency for *C. acutispina* to undergo fissiparity, and this may be a result of stress caused by aquarium confinement or by other factors, such as high levels of prey consumption. Any daughter asteroids produced in this way were immediately removed so that only ten starfishes were present in each replicate at any one time.

Experiment 4

This was essentially a prey choice study and was designed to show if increasingly spinose prey bivalves had a concomitant increasingly inhibitory effect on shell boring by the muricid *Morula musiva*. Twenty *Perna viridis* were cemented artificially to a Perspex sheet in an aquarium and presented to five *M. musiva* predators. Attachment to Perspex was effected by attaching each shell with epoxy resin by either the right or left valve. Both the choice of the valve of attachment and the orientation of each fixed mussel on each sheet were determined at random. Each replicate sheet was slotted vertically into a Perspex frame at the bottom of an aquarium tank, providing individual predator compartments with partitioning sheets of cemented prey separating each compartment. This design was considered satisfactory as it allowed the valves of the mussels to gape normally with apparently little detrimental effect upon feeding and respiration. Of the 20 *P. viridis* on each sheet partition, five were unornamented, five were ornamented with 1 mm long artificial spines, five with 2 mm long spines and five with 4 mm long spines. All artificial spines were applied to the free valve in each case and, as in Experiment 1, the spines were cut from polyethylene strips, with a basal area of 2×2 mm. Artificial attachment of prey to the Perspex sheets did not result in any apparent detrimental effect to normal valve gaping. Moreover, despite this treatment, all the prey in this experiment continued to produce copious byssus threads, suggesting that they were behaving normally. These threads were scraped away from their attachment to the sheet to reduce the possibility of predators being caught and immobilized by them, as has been reported for other mytilids (e.g. Petraitis 1987; Wayne 1987; Day *et al.* 1991), which may have biased the results.

In each replicate, consumed prey were replaced in the same manner as the experiments above until five or more of each particular ornament type were eaten. Subsequently, all remaining mussels of the same type were removed, leaving a reduced amount of sculptural possibilities to be tackled by *M. musiva*. This process was repeated until termination of the experiment when prey preferences could be determined. Consumed prey were also analysed for position of bore holes.

RESULTS

Experiment 1

Thais luteostoma *versus* Septifer virgatus *with artificial marginal spines*. The null hypothesis that equal numbers of ornamented and unornamented prey should be consumed is rejected using the chi square test at a 95 per cent. confidence level (Table 1). Very few spinose bivalves were tackled and, of those that were, there was no evidence of any predator behavioural modification resulting in changes in bore hole positioning. All bore holes, for both spiny and non-spiny prey, were made at the commissural edge and the vast majority located antero-ventrally in the area of the emergence of the byssus (Text-fig. 4A). A byssal gape is present to a greater or lesser degree in all mytilids and, when not permitted to attach to a substrate, is potentially a particularly vulnerable area because it may allow direct entry to the body cavity and metabolites leached from the gape may act as chemical cues to potential predators. The method of experimentation described above is justified because it is even more likely that spines would provide effective defence if the mussels were allowed to attach normally by the byssus and become orthothetically orientated, as in life. This is especially true when shells aggregate side to side in beds and a potential predator would be presented with ornamented dorsal margins rather than the unornamented sides of the valves.

The results show that, in the aquarium, *Thais luteostoma* is an obligate edge-borer on *Septifer virgatus* and that artificial marginal spines attached to prey shells effectively inhibit predation by this

TABLE 1. Numbers of unornamented and artificially ornamented *Septifer virgatus* consumed by the muricid gastropod *Thais luteostoma* in three replicate experiments. Statistical analysis using chi square. Assuming a confidence level of 95 per cent., the null hypothesis that equal numbers of ornamented and unornamented prey are eaten is rejected for all replicates.

Replicate	A	B	C
Spiny prey consumed	2	3	3
Non-spiny prey consumed	36	34	38
Overall total	38	37	41
Predator size (mm)	36·2	36·5	32·7
P	$\ll 0{\cdot}01$	$\ll 0{\cdot}01$	$\ll 0{\cdot}01$

TABLE 2. Numbers of unornamented and naturally ornamented *Chama reflexa* consumed by the muricid gastropods *Chicoreus microphyllus* and *Thais clavigera* in three replicate experiments. Statistical analysis using chi square. Assuming a confidence level of 95 per cent., the null hypothesis that equal numbers of ornamented and unornamented prey are consumed cannot be rejected, and, at the same confidence level the null hypothesis that equal numbers of left and right valves are bored cannot be rejected in two of the three replicates.

Replicate	A	B	C
Ornamented prey consumed	11	16	10
Unornamented prey consumed	14	11	15
Total consumed	25	27	25
P	$\gg 0{\cdot}05$	$\gg 0{\cdot}05$	$\gg 0{\cdot}05$
Right valves bored	10	5	11
Left valves bored	10	17	9
P	$\gg 0{\cdot}05$	$< 0{\cdot}01$	$\gg 0{\cdot}05$

muricid. No attempt was made to bore the sides of any valves and no incomplete bore holes were recorded. It is interesting to note that most boring resulted in damage to both valves either side of the thin byssal gape in any one individual, but the periostracum often remained intact along the commissure (Text-fig. 4A). This provides additional evidence to that already published that the thick periostracum of many mytilids, including that of *S. virgatus* at a thickness of 60 μm (Harper 1997), is difficult to penetrate by gastropod borers and may constitute a defensive adaptation (Harper and Skelton 1993*b*). An inspection of those spinose mussels whose defences had been overcome by *T. luteostoma* showed that one or more spines had been dislodged, suggesting that if all spines had remained completely intact, there would have been even less predation of ornamented individuals. In only one prey individual were all the spines intact after a successful predatory attack (Text-fig. 4B). Aquarium observations revealed that, after making contact with the prey, the muricids would hold the mussels with the foot and orientate them so that the byssal gape was innermost, presumably so that the radula and Accessory Boring Organ could be applied in this area. Physical manipulation of prey by muricid gastropods has not been previously described. Many ornamented and unornamented prey were held in this way, suggesting that chemical stimuli, which have been shown to be a causal factor in attracting muricid gastropods to potential victims (Kohn 1961; Pratt 1974; Carriker 1981; Cross 1983; Williams *et al.* 1983), had not been impaired by the experimental technique, and the rejection of spinose prey was a result of behavioural responses provoked by unfavourable subsequent tactile stimulus. Large numbers of unornamented prey were consumed, despite being dotted with epoxy, and therefore it is concluded that the presence of spines alone is responsible for inhibiting predatory activity.

TABLE 3. Number of bore holes made in different areas of the shell of *Chama reflexa* by the muricid gastropods *Chicoreus microphyllus* and *Thais clavigera* in three replicate experiments.

Replicate	A		B		C	
Valve	Left	Right	Left	Right	Left	Right
Umbonal	—	0	—	0	—	1
Median (ornamented)	—	0	—	0	—	0
Median (unornamented)	1	10	1	5	0	10
Inter-lamellar	2	—	4	—	4	—
Area of attachment	7	—	12	—	5	—
Total	10	10	17	5	9	11

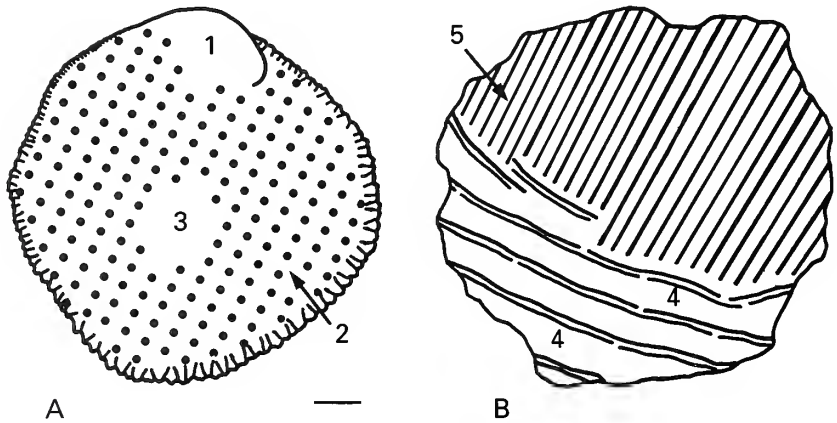

TEXT-FIG. 3. Generalized representation of the bivalve *Chama reflexa* offered to *Chicoreus microphyllus* and *Thais clavigera* in Experiment 2. A, right valve with crenulate marginal lamella, divided into three areas: (1), umbonal; (2), median (ornamented); (3), median (unornamented). Dotted area indicates spinose valve surface. B, left valve, divided into two areas: (4), inter-lamellar; (5), area of attachment. Hatched area indicates flat attachment scar. Scale bar represents 2 mm.

Experiment 2

Chicoreus microphyllus *and* Thais clavigera *versus* Chama reflexa. The results are summarized in Tables 2 and 3. There was no significant difference between the numbers of ornamented and unornamented prey bored, and the null hypothesis that equal numbers of each should be consumed cannot be rejected with chi square analysis at a 95 per cent. confidence level. Upon closer examination, however, some important observations may be made. Table 3 shows the number of times specified areas of the shell were bored successfully for both left and right valves. Five areas are described (Text-fig. 3). For the right, or 'upper' valve, these are: umbonal, median (ornamented) and median (unornamented) (Text-fig. 4C). For the left, or 'lower' valve these are: inter-lamellar and area of attachment. Of the ornamented *C. reflexa* prey, the sculpture on certain areas of the surface of the right valve may be less expressed in some individuals than in others. Bore holes made at these sites are described as median (unornamented). The natural ornament may also have been eroded from the umbonal region during ontogeny, resulting in possible reduced defence in this area (Text-fig. 3A). For the left valve, boring was not observed to have occurred through the

attachment lamellae of the left valve, but only in the commarginal inter-lamellar spaces between adjacent elements (Text-fig. 3B). Table 3 reveals that on no occasion was a bore hole successfully made in a truly ornamented area of a prey shell. The majority of bore holes were either made in the area of attachment of the left valve or unornamented areas of the right valve. In the chamids' natural habitat, boring of the left valve is extremely unlikely to occur unless the bivalve has become forcibly detached, and it is not surprising that the muricids should attack unornamented areas of left valves in the aquarium, in particular the potentially weak area of attachment. However, although the majority of left valves were thinnest in this area, the fact that other areas of both left and right valves were bored, including inter-lamellar areas and the relatively thick right valves, suggests that the degree of ornament expression is the primary determinant of the choice of bore hole site rather than valve thickness. It seems reasonable to suggest that pronounced marginal ornament exhibited by potential prey will additionally afford a degree of protection from boring near the valve edges, in much the same way as the artificial marginal spines of *S. virgatus* in Experiment 1. It may be concluded that the shell spines of lamellae of *C. reflexa* offer a degree of defence against boring by muricids.

TABLE 4. Numbers of unornamented and artificially spinose *Perna viridis* consumed by the extraoral feeding asteroid *Coscinasterias acutispina* in three replicate experiments. Statistical analysis using chi square. Assuming a confidence level of 95 per cent., the null hypothesis that equal numbers of ornamented and unornamented prey are consumed cannot be rejected.

Replicate	A	B	C
Ornamented prey consumed	25	17	46
Unornamented prey consumed	28	24	41
Overall total	53	41	87
P	$\geqslant 0{\cdot}05$	$\geqslant 0{\cdot}05$	$\geqslant 0{\cdot}05$

Experiment 3

Coscinasterias acutispina *versus* Perna viridis. The results are summarized in Table 4. They reveal that there was no significant difference in the numbers of spinose and non-spinose mussel prey consumed. The null hypothesis that equal numbers of each should be eaten could not be rejected using chi square analysis at a 95 per cent. confidence level. The larger number of bivalves eaten in replicate C can probably be attributed to the larger mean size of the starfishes available for this replicate.

In the aquarium, the feeding behaviour of *C. acutispina* is typical of other extraoral feeding asteroids. It assumes a hunched posture over the prey bivalve so that the stomach lobes can be extruded into the shell after prising the valves apart. For mussel prey, the stomach lobes may be extruded into the body cavity through the narrow byssal gape. This has been reported for other genera (Feder 1955; Lavoie 1956; Carter 1968). In contrast to the experiments with muricid borers presented above, *C. acutispina* showed no statistically significant preference for the non-spinose mussels offered. In general, the predatory behaviour of the starfish did not differ when it was confronted by ornamented or unornamented prey. Such behaviour was characterized by an initial encounter with the prey and subsequent manipulation so that the ventral margins, and in particular the byssal gape, were orientated towards the oral region of the predator. In this experiment, the spines of some of the artificially ornamented mussels had been removed by the predators. It is, therefore, probable that the ornament was removed during the process of manipulation or possibly prising of the valves, although the latter was not directly observed. Attached marginal spines were up to one-third the length of the axis of greatest growth in any one individual and, because they

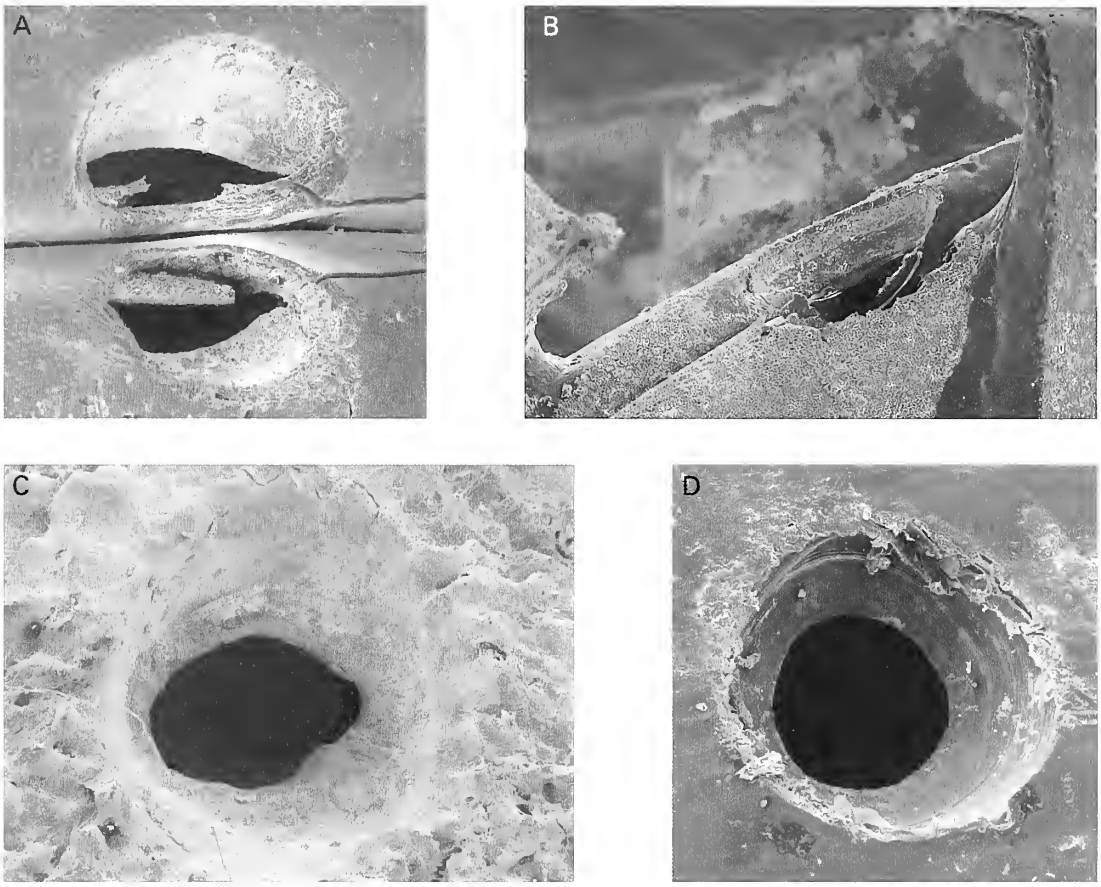

TEXT-FIG. 4. Scanning electron micrographs of muricid bore holes in prey bivalve shells. A, hole bored by *Thais luteostoma* through posterior extremity of the byssal gape of *Septifer virgatus*; ×43. B, single occurrence of a bore hole made by *Thais luteostoma* between intact artificial 'spines' (seen left and right in picture) attached to *Septifer virgatus*; ×33. C, bore hole made by *Chicoreus microphyllus* in median area of a left valve of *Chama reflexa* lacking macro-ornament; ×20. D, bore hole made by *Morula musiva* in an unornamented area between artificial 'spines' attached to the lateral surface of a *Perna viridis* shell; ×45. Material in author's possession.

interdigitated across the plane of the commissure in those mussels whose spines remained intact throughout the feeding process, and would therefore still provide an effective barrier, it is likely that prising the valves apart a short distance would be ineffective in itself. Thus, the stomach lobes may have been extruded to at least the same length as the spines themselves in order to reach the body cavity. The above evidence reveals that *C. acutispina* is adept at dealing with different types of prey and has no difficulty in overcoming the artificially defended bivalves in this experiment.

Experiment 4

Morula musiva *versus* Perna viridis. The results of this choice experiment are summarized in Table 5. The muricid predators chose unornamented mussels as a first choice in three out of the six replicates and as a second choice in two replicates. Highly ornamented prey with 4 mm long spines were chosen only in third place in two replicates. Complete consumption of the other sculptural types, 1 mm and 2 mm spines, was more variable. The results, therefore, suggest that prey with less expressed ornament are preferred to those that are highly spinose (Text-fig. 4D).

TABLE 5. Results of Experiment 4, in which the muricid *Morula musiva* was offered a choice of *Perna viridis* prey: unornamented (NS), with 1 mm long artificial spines, with 2 mm artificial spines or with 4 mm long artificial spines in six replicate experiments. Unornamented prey were chosen as a first choice in three out of six replicates, and as a second choice in two replicates.

Replicate	A	B	C	D	E	F
First choice	1 mm	2 mm	NS	2 mm	NS	NS
Second choice	NS	—	—	NS	1 mm	—
Third choice	4 mm	—	—	4 mm	2 mm	—
Fourth choice	—	—	—	1 mm	—	—
Total prey consumed	21	11	12	20	22	10

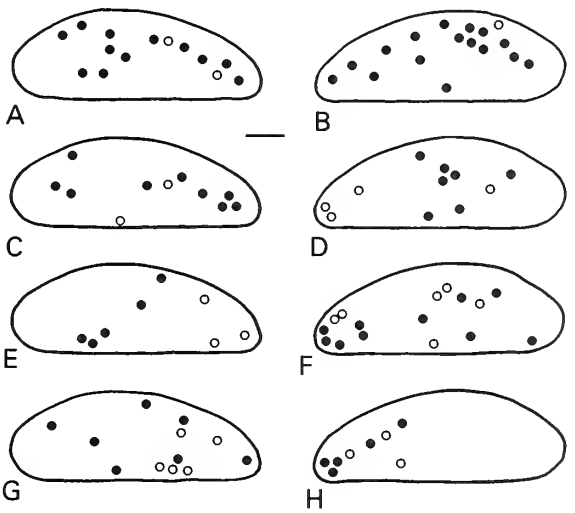

TEXT FIG. 5. Positions of all bore holes made by *Morula musiva* in right (A, C, E, G) and left (B, D, F, H) valves of the mussel *Perna viridis*. Filled circles: holes made in non-attached 'free' valves. Hollow circles: holes made in artificially attached valves. Umbones are towards the centre of the page. A–B, holes made in valves without artificial ornament but dotted with cyanoacrylate as a control. C–D, holes made in valves with 1 mm long artificial 'spines' attached. E–F, holes made in valves with 2 mm long artificial 'spines' attached. G–H, holes made in valves with 4 mm long artificial 'spines' attached. Scale bar represents 5 mm.

Since it was necessary to allow the mussels to function as near normally as possible in this experiment, all prey were cemented for only a portion of the relevant valve so that the valve margins were raised clear of the artificial substrate. This permitted some boring in the attached valve, especially in the area of the umbo. Table 6 reveals that the percentage of bore holes made in attached valves increases from 9·7 per cent in non-spinose mussels to 40·0 per cent. in prey with 4 mm spines. This is additional evidence of the deterrent value of increasing shell ornament. The positions of all bore holes, for both attached and free valves, are shown in Text-figure 5. It is inferred from this experiment, therefore, that the primary effect of pronounced spines on the shells of epifaunal bivalves is that of hindering direct access to the general shell surface.

TABLE 6. Bore hole analysis of the four types of artificially ornamented *Perna viridis* drilled by the muricid *Morula musiva*.

Ornament type	Non-spiny	1 mm spines	2 mm spines	4 mm spines
Percentage bore holes in attached valve	9·7	27·3	37·5	40·0

DISCUSSION

The biotic changes associated with the so-called Mesozoic Marine Revolution (M.M.R.) have been identified by Vermeij (1977, 1978, 1987) as a probable causal factor in the subsequent evolution of strengthening armour in gastropods and bivalves. The M.M.R. was characterized by an increase in the importance of a host of predatory methods and resulted not only in an increase in the development of prey armour in potentially vulnerable molluscan epifaunal taxa but also an expansion of groups escaping predators in other ways, such as those colonizing the infaunal realm (Stanley 1968; Vermeij 1978, 1987). Predatory methods, and the potential consequences of the M.M.R. for molluscan prey, have been assessed by Vermeij (1977, 1987) and Harper and Skelton (1993*a*). Epifaunal bivalves are particularly vulnerable to three predatory strategies: (1) 'insertion and extraction', by extraoral feeding asteroids, prising gastropods, some birds and fish, octopods, arthropods and crustaceans; (2) 'crushing', by many crustaceans, fish, arthropods and some molluscs; and (3) 'boring', by muricid and naticid gastropods and some cephalopods. It has been proposed that these three strategies became dramatically more important as a result of the M.M.R. (Vermeij 1977, 1987).

The experiments presented here were undertaken to examine the effects of two such predatory strategies: shell boring by muricid gastropods and extraoral feeding by asteroids. Both predatory groups have often been held responsible for severe predation impact on epifaunal molluscs, particularly bivalves, in subtropical–tropical and temperate shallow water environments respectively (Galtsoff and Loosanoff 1939; Hancock 1955, 1958; Taylor 1976, 1978), and thus they are particularly suitable for a study of the anti-predatory effects of epifaunal bivalve shell ornament. Cemented bivalves in particular may present themselves as potential sitting targets to muricid gastropods (Harper and Skelton 1993*a*).

Of the principal epifaunal cemented taxa, warm-water oysters, spondylids and chamids display a high degree of morphological plasticity, associated with the habit of cementation, and an ability to construct shells with pronounced spines and/or commarginal lamellae. The results presented here suggest that such ornament in prey taxa is itself directly effective in deterring boring by muricid gastropods. For both chamid and mytilid prey, unornamented areas of the shell are preferentially bored over ornamented areas in each of the three experiments conducted with muricid predators. Where behavioural adaptation seems to have resulted in a high degree of bore hole site specialization, for example in relation to edge-boring by *Thais luteostoma* in Experiment 1, any subsequent site modification that might have been expected when confronted by artificially ornamented prey is lacking. Thus, *T. luteostoma* does not attack the unornamented valve surfaces of *Septifer virgatus* prey and, rather than choosing new bore hole sites in mussels with marginal ornament, this predator takes advantage of the preferential site in unornamented prey (in this case the byssal gape). As new shell ornament of potential prey is formed at the commissure, it is less likely to have been eroded than sculpture formed earlier in ontogeny which cannot be repaired, and predators which attack the valve margins are likely to be at a competitive disadvantage in comparison with those that choose the bore hole site more liberally. This may help to explain why edge-boring of bivalves by muricid gastropods in the field has only rarely been reported (e.g. Morton 1994).

In contrast to the muricid predators, the subtropical extraoral feeding asteroid *Coscinasterias acutispina* is not measurably deterred by artificial spines fixed to mussel prey, even when such spines are positioned around the entire commissure, including the byssal gape. It is through a commissural gape that the stomach lobes of the asteroid are extruded. The gape may be formed mechanically by prising the valves of the prey apart a small distance or it may be a natural element of shell growth. Prising was not directly observed in the current experiment and, as prey were orientated with the byssal gape nearest the oral region of the predator, it was concluded that the stomach lobes were being extruded through this region. In a pilot study, a group of predators were removed from prey during feeding with their everted stomach lobes clearly visible. Despite the presence of large artificial marginal spines on *Perna viridis*, *C. acutispina* is clearly adept at dealing with such 'difficult' prey. It is conceivable that, if spines had been arranged over the general surface of the valves, including the commissure, manipulation of prey by the asteroid might have been more problematical. However, artificial ornament strong enough to withstand such handling could not be attached successfully on the valve surface. Moreover, as stated previously, it is the commissure of the prey bivalve that is most often heavily defended, as this is where new shell material is laid down, and thus it is the ability to extrude stomach lobes through a heavily defended commissure that is of greatest interest. Although naturally cemented bivalves do not present extra-oral feeding asteroids with natural gapes through which stomach lobes can be extruded, it is likely that prising the valves apart a small distance will create a temporary gape, and thus a potentially vulnerable area. In Experiment 3, valve prising was not directly observed but may not have been required for extra-oral feeding because of the presence of the byssal gape in the *Perna viridis* prey offered. The methodology of the present study is therefore considered satisfactory.

It has been stated by some authors, such as Vermeij (1987), that extraoral feeding asteroids are not in general a common component of the benthic megafauna on tropical and subtropical rocky shores. In contrast, muricid gastropods are often abundant and likely to exert strong predatory pressure (Taylor 1976, 1977, 1978). In these areas, therefore, the threat from muricids is potentially far more important than that of extraoral feeding asteroids. The impact of the extraoral method of attack, however, may be particularly severe in cooler waters, where asteroids often aggregate in large numbers and may devastate local epifaunal bivalve populations (Galtsoff and Loosanoff 1939; Hancock 1955, 1958). However, in cooler waters highly ornamented bivalve taxa are rare or non-existent (Nicol 1964, 1965; Harper and Skelton 1993*a*). It seems highly doubtful, therefore, that the presence of marginal ornament in epifaunal bivalves is functional against the extraoral method of attack, and this proposal is strengthened by the results of the experiment presented here.

To determine whether pronounced shell ornament in cementing epifaunal bivalve families, such as the unrelated Spondylidae and Chamidae, arose as an adaptation to the threat posed by muricid gastropod borers, it is necessary to demonstrate agreement between the timing of the onset of the adaptive radiation of muricids in the Albian (Taylor *et al.* 1980, 1983) on the one hand and the appearance of highly ornamented potential prey taxa on the other.

Harper and Skelton have documented the numbers of spinose and non-spinose species of the family Spondylidae from the Jurassic to the present day, and show a general increase in the percentage of spinose species over time (Harper and Skelton 1993*a*, fig. 3). My own unpublished data concur with their results. Despite this increase, however, it is apparent that the rise of spinose ornamentation in Bivalvia predates the adaptive radiation of the muricid gastropods. The ability to construct ornament was already evident in some late Palaeozoic Pectinoida, such as members of the family Pseudomonotidae. It has been proposed that the Spondylidae most probably arose from this family (Newell and Boyd 1970). In their work on Permian ostreiform Bivalvia, Newell and Boyd suggested that the morphological series: *Pseudomonotis* (*Pseudomonotis*)–*Pseudomonotis* (*Trematiconcha*)–*Prospondylus*–*Paleowaagia*–*Newaagia*–*Spondylus*– may represent a phyletic series. Within this series, a number of Permian species display spines and/or scales, most notably *Pseudomonotis* (*Trematiconcha*) *wandageensis* Newell and Boyd, *P. likharevi* Newell and Boyd, *Prospondylus acinetus* Newell and Boyd and *Paleowaagia cooperi* Newell and Boyd (Newell and Boyd 1970, figs 14A, 16A, 23A–G, 24A–E, 28A, 29B, G). Waller (1978) has suggested that spondylids may have evolved

from the superfamily Pectinoidea, rather than from the Pseudomonotidae. Despite the inherent difficulties associated with the assessment of phylogenetic affinities of many pteriomorph groups, ornament construction was nevertheless underway in the pectinoidan families Pseudomonotidae and Aviculopectiniae (for example, *Girtypecten* and *Clavicosta*; see Newell 1969), by the Late Palaeozoic. It is, therefore, unlikely that spinose ornamentation in pteriomorph bivalves arose initially as an adaptation to the muricid borers. It is also difficult to relate ornament to direct deterrence of other predatory methods, such as shell breakage by crustaceans. It is intuitively obvious that, to be effective against the latter group, shell spines and scales would need to be particularly well-developed, stout and strong, especially around the most vulnerable area, the commissure. Evidently, sculptural development in Permian Pectinoida, although present in some genera, was only weakly expressed. Shell ornament in late Mesozoic and particularly Tertiary spondylids is very different (Zavarei 1973; pers. obs.). It seems reasonable to suggest that the faunal changes resulting in a rise in predation pressure concomitant with the M.M.R. was responsible for the adaptive development of large, strong spines that characterize many Mesozoic and Tertiary taxa. Such ornament may be effective against a variety of predators, but it proposed here that muricid borers are potentially one of the most damaging, and potentially the most deterred by pronounced shell ornament, of all predatory groups.

The family Chamidae, unrelated to the Spondylidae but again adopting the cemented habit, probably evolved as a branch of the byssate family Carditidae in the Late Cretaceous (Kennedy *et al.* 1970) and the pronounced shell ornament displayed by the former group may, conceivably, have arisen as a primary adaptation against shell boring predators, especially in view of the evolution of the cemented habit from a byssate precursor. Ornament in extant ribbed carditids, where present, tends to consist of nodes or pronounced scales, but further studies need to be undertaken on the ornament of Palaeozoic and Mesozoic carditids before the geological history of ornament in the Carditidae and Chamidae can be adequately assessed. The evidence, however, seems to suggest that ornamentation of the 'upper' free valve of epifaunal groups evolved initially as a response to some factor other than direct predatory pressure, and may have become coincidentally advantageous under the harsh predatory regimes characterizing the M.M.R. (Vermeij 1977, 1987), particularly with respect to shell boring by muricid gastropods. The original primary function may or may not have been lost and, if the latter is the case, then shell spines and lamellae in extant epifaunal bivalve taxa could be considered multifunctional.

There are several possible hypotheses that may be put forward regarding the primary function of pronounced 'upper' valve shell ornament other than direct predatory inhibition which is the subject of the current study. Firstly, ornament may act to prevent the bivalve from becoming dislodged from cryptic microhabitats such as crevices. This does not apply to cementing taxa such as oysters, spondylids and chamids, although cementation to the sides of crevices may occur. However, some byssate taxa of the families Tridacnidae and Carditidae carry spine-like processes on both valves that may help to prevent dislodgement. The second hypothesis is that ornament may help to alleviate erosion. This applies potentially to both attached and unattached taxa. It has, however, never been satisfactorily demonstrated that the presence of ornament serves to increase shell strength in any way. Moreover, the spines of many widely distributed ornamented genera such as the semi-infaunal *Pinna* and *Atrina*, and certain members of the Spondylidae, such as *Spondylus linguafelis* Sowerby, are often elaborate and delicate and it is difficult to accept such an hypothesis. Erosion and endolithic boring of the shell by organisms such as clionid sponges can remove ornament from all or part of the shell surface and thus render the bivalve vulnerable to predation by muricids or crustaceans if the strength of the valve has been severely weakened, but if the ornament remains intact, it is likely the bivalve will be far more resistant to gastropod borers. Where chamids and spondylids are cemented to rocks in exposed areas, erosion of the shell may be extensive. Bernard (1976) stated that chamids living in such environments are large, thick-shelled with little ornamentation and very shallow in vertical distribution. In these areas, however, the intensity of predation is likely to be considerably less than at sheltered sites, especially for roving predators, such as muricids, that may be dislodged by wave action. In sheltered habitats, the

predation pressure is likely to be more intense and in these areas the ornament of chamids is often highly pronounced (Bernard 1976). The third hypothesis is that ornament may offer protection against the rasping activities of certain roving grazers, for example regular echinoids, feeding on algae growing on shells that may, over time, erode the shell and weaken it. The potential importance of grazing with respect to shell ornament is at present unclear. The fourth hypothesis considers spines and commarginal lamellae acting as stabilizing structures that prevent epifauna lying on soft substrates from being smothered. The spines of the extant chamid genus *Arcinella* may act in this way. This bivalve gains secondary freedom from an initial cemented phase early in ontogeny and rests on sandy or shelly substrates (Nicol 1952). The fifth hypothesis suggests that ornament may act to attract growth of epibionts on the shell, presumably by increasing the surface area of available substrate (Vance 1978; Feifarek 1987). Personal observations of the spondylid *Spondylus americanus* Hermann transferred to aquaria show that the colonizers are often algae, sponges, solitary corals, tube worms and hydroids. Epibiont growth may have a number of potentially beneficial effects. For example, biomineralizing colonizers may increase the effective strength of the shell and help to reduce erosion. Alternatively, epibionts may directly disguise the shell from visually hunting predators or may mask chemical cues released into the ambient environment by the bivalve which may serve as attractants for chemosensitive predators. There is good evidence that predatory gastropods are attracted by such cues (Carriker 1981). Some extant representatives of the families Spondylidae and Chamidae, for example *Spondylus linguafelis* and *Chama lazarus* Linnaeus, possess spines whose distal ends are highly intricate or enlarged into spatulate lamellae. It is conceivable that the consequent large surface area of such processes is particularly attractive to epibiont settlement. Such growth may provide serendipitous defence for sessile organisms such as cementing bivalves. The sixth hypothesis concerns shell ornament as structural supports for areas of sensory mantle tissue (Rudwick 1965; Kauffman 1969; Stenzel 1971). A mechanosensory or chemosensory capability may have several advantages. For example, it may provide the bivalve with an early warning system when under potential threat from an approaching predator, or it may warn against inclement environmental conditions, such as changes in turbidity or salinity. The intricate nature of the ornament of some members of the Spondylidae and Chamidae, referred to above, may indicate a corresponding intricacy of underlying mantle epithelium performing sensory functions. However, a sensory capability has only been suggested by analogy with the soft parts of brachiopods (Rudwick 1965), and comparative morphological evidence to substantiate this hypothesis in the Bivalvia has been lacking. Research is currently being undertaken by the author with regard to the hypothesized functions of pronounced shell ornament detailed above.

The formation of shell ornament in epifaunal bivalves can only proceed within the intrinsic constraints of the bivalve *Bauplan* and extrinsic constraints such as water temperature, food availability, etc. Many epifaunal taxa have demonstrated a remarkable ability to radiate morphologically, particularly in warm waters. Nicol (1965, 1967) has stated that there are very few ornamented bivalves inhabiting cool waters of high latitudes and the deep sea. What ornament is evident, is always subdued. In addition, bivalves that adopt the cemented habit are absent from the Arctic and Antarctic (Nicol 1964). In warm temperate, subtropical and tropical waters many cemented taxa, such as members of the Spondylidae, Chamidae and Ostreidae, are particularly adept at ornament construction. It is suggested here that the sculptural radiation of highly ornamented epifaunal taxa may be a result of pressures imposed by the shell boring muricids from the Albian onwards, resulting in adaptive radiations in potentially vulnerable prey lineages. Whilst the nature and intensity of predation is evidently very different in cool water, the pre-adaptations that may have otherwise permitted the formation of sculpture, such as an ability to produce extensive growth in periodic rapid phases, may also be absent. Feifarek (1987) found that the rate of growth of spines in the spondylid *Spondylus americanus* is extremely rapid, about 1 mm per day. In addition, Paul (1981) has suggested the shell of the highly spinose warm water neogastropod *Murex* (*Murex*) *pecten* Lightfoot grows by rapid episodic incrementation. It is likely that such modes of growth can only be achieved in warm water because of high growth rates which may be associated with a combination of warm water temperatures as well as an adequate food supply,

although the possibility that the effects of cold water enhance the dissolution of biogenic calcareous structures, retarding or preventing growth of pronounced ornament, must also be considered.

SUMMARY

Pronounced shell ornament in epifaunal bivalves has been shown to be effective at deterring shell boring muricid gastropods in aquarium experiments. No apparent inhibitory effect was observed for extraoral predation by asteroids. Gastropod deterrence may have become increasingly important with the adaptive radiation of the muricids in the Albian. Anti-boring defence may not be the sole function of pronounced shell ornament and it is likely that it arose initially for other reasons, in the family Spondylidae at least. Other hypothesized functions include, for example, attracting epibiont growth or outposts for sensory mantle tissue. These may have continued to play an important rôle for the epifaunal bivalve to the present day, despite the value that ornament has been shown to confer in deterring muricids.

Acknowledgements. I am indebted to Dr Elizabeth Harper at the Department of Earth Sciences, University of Cambridge, for discussions concerning the manuscript and to Professor Brian Morton at the Swire Institute of Marine Science, Hong Kong, for use of aquarium facilities. This work forms part of a research studentship funded by the N.E.R.C., ref. GT4/94/136/G. Additional funding was provided by Gonville and Caius College, Cambridge. This is Cambridge Earth Science Publication no. 5263.

REFERENCES

ANSELL, A. D. 1969. Defensive adaptations to predation in the Mollusca. 487–512. *In Proceedings of the Symposium on Mollusca, Cochin*, **2**. Marine Biological Association of India, Mandapam, India.

—— and MORTON, B. 1983. Aspects of naticid predation in Hong Kong with special reference to the defensive adaptations of *Bassina* (*Callanaitis*) *calophylla* (Bivalvia). 635–660. *In* MORTON, B. and DUDGEON, D. (eds). *Proceedings of the 2nd international workshop on the malacofauna of Hong Kong and Southern China, Hong Kong 1983*. Hong Kong University Press, Hong Kong, 681 pp.

—— —— 1987. Alternative predation tactics of a tropical naticid gastropod. *Journal of Experimental Marine Biology and Ecology*, **111**, 109–119.

BERNARD, F. R. 1976. Living Chamidae of the Eastern Pacific (Bivalvia: Heterodonta). *Contributions in Science, Natural History Museum of Los Angeles County*, **278**, 1–43.

CARRIKER, M. R. 1981. Shell penetration and feeding by naticacean and muricacean gastropods: a synthesis. *Malacologia*, **20**, 403–422.

CARTER, R. M. 1968. On the biology and palaeontology of some predators of bivalved Mollusca. *Palaeogeography, Palaeoclimatology, Palaeoecology*, **4**, 29–65.

COX, L. R. 1969. General features of Bivalvia. N2–N129. In MOORE, R. C. (ed.). *Treatise on invertebrate paleontology. Part N. Mollusca 6 (1)*. Geological Society of America and University of Kansas Press, Boulder, Colorado and Lawrence, Kansas, 1224 pp.

CROLL, R. P. 1983. Gastropod chemoreception. *Biological Reviews*, **58**, 293–319.

DAY, R. W., BARKAI, A. and WICKENS, P. A. 1991. Trapping of three drilling whelks by two species of mussel. *Journal of Experimental Marine Biology and Ecology*, **149**, 109–122.

FEDER, H. M. 1955. On the methods used by the starfish *Pisaster ochraceus* in opening three types of bivalve molluscs. *Ecology*, **36**, 764–767.

FEIFAREK, B. P. 1987. Spines and epibionts as antipredator defenses in the thorny oyster *Spondylus americanus* Hermann. *Journal of Experimental Marine Biology and Ecology*, **105**, 39–56.

GALTSOFF, P. S. and LOOSANOFF, V. 1939. Natural history of *Asterias forbesi*. *Bulletin of the U.S. Bureau of Fisheries*, **49**, 79–132.

HANCOCK, D. A. 1955. The feeding behaviour of starfish on Essex oyster beds. *Journal of the Marine Biological Association of the U.K.*, **34**, 313–331.

—— 1958. Notes on starfish on an Essex oyster bed. *Journal of the Marine Biological Association of the U.K.*, **37**, 565–589.

HARPER, E. M. 1991. The role of predation in the evolution of cementation in bivalves. *Palaeontology*, **34**, 455–460.

—— 1994. Molluscivory by the asteroid *Coscinasterias acutispina* (Stimpson). 339–355. *In* MORTON, B. (ed.). *The malacofauna of Hong Kong and Southern China III. Proceedings of the 3rd international workshop on the malacofauna of Hong Kong and Southern China, Hong Kong 13 April–1 May 1992*. Hong Kong University Press, Hong Kong, 504 pp.

—— 1997. The molluscan periostracum: an important constraint in bivalve evolution. *Palaeontology*, **40**, 71–97.

—— and SKELTON, P. W. 1993*a*. The Mesozoic Marine Revolution and epifaunal bivalves. *Scripta Geologica, Special Issue*, **2**, 127–153.

—— —— 1993*b*. A defensive value of the thickened periostracum in the Mytiloidea. *The Veliger*, **36**, 36–42.

JACKSON, J. B. C. 1977. Competition on marine hard substrata: the adaptive significance of solitary and colonial strategies. *American Naturalist*, **111**, 743–767.

KAUFFMANN, E. G. 1969. Form, function and evolution. N129–N205. *In* MOORE, R. C. (ed.). *Treatise on invertebrate paleontology. Part N. Mollusca 6 (1)*. Geological Society of America and University of Kansas Press, Boulder, Colorado and Lawrence, Kansas, 1224 pp.

KENNEDY, W. J., MORRIS, N. J. and TAYLOR, J. D. 1970. The shell structure, mineralogy and relationships of the Chamacea (Bivalvia). *Palaeontology*, **13**, 379–413.

KOHN, A. J. 1961. Chemoreception in gastropod molluscs. *American Zoologist*, **1**, 291–308.

LAVOIE, M. E. 1956. How seastars open bivalves. *Biological Bulletin*, **111**, 114–122.

LOGAN, A. 1974. Morphology and life habits of the Recent cementing bivalve *Spondylus americanus* Hermann from the Bermuda Platform. *Bulletin of Marine Science*, **24**, 568–594.

MORTON, B. 1994. Prey preference and method of attack by *Rapana bezoar* (Gastropoda: Muricidae) from Hong Kong. 339–355. *In* MORTON, B. (ed.). *The malacofauna of Hong Kong and Southern China III. Proceedings of the 3rd international workshop on the malacofauna of Hong Kong and Southern China, Hong Kong 13 April–1 May 1992*. Hong Kong University Press, Hong Kong, 504 pp.

NEWELL, N. D. 1969. N335–N338. *In* MOORE, R. C. (ed.). *Treatise on invertebrate paleontology. Part N. Mollusca (1)*. Geological Society of America and University of Kansas Press, Boulder, Colorado and Lawrence, Kansas, 1224 pp.

—— and BOYD, D. W. 1970. Oyster-like Permian bivalvia. *Bulletin of the American Museum of Natural History*, **143**, 219–281.

NICOL, D. 1952. A revision of the pelecypod genus *Echinochama*. *Journal of Paleontology*, **26**, 803–817.

—— 1964. Lack of shell attached pelecypods in Arctic and Antarctic waters. *The Nautilus*, **77**, 92–93.

—— 1965. Ecologic implications of living pelecypods with calcareous spines. *The Nautilus*, **78**, 109–116.

—— 1967. Some characteristics of cold-water marine pelecypods. *Journal of Paleontology*, **41**, 1330–1340.

PAUL, C. R. C. 1981. The function of the spines in *Murex* (*Murex*) *pecten* Lightfoot and related species (Prosobranchia: Muricidae). *Journal of Conchology*, **30**, 285–294.

PETRAITIS, P. S. 1987. Immobilization of the predatory gastropod, *Nucella lapillus*, by its prey, *Mytilus edulis*. *Biological Bulletin*, **172**, 307–314.

PRATT, D. M. 1974. Attraction to prey and stimulus to attack in the predatory gastropod *Urosalpinx cinerea*. *Marine Biology*, **27**, 37–45.

RUDWICK, M. J. S. 1965. Sensory spines in the Jurassic brachiopod *Acanthothiris*. *Palaeontology*, **8**, 604–617.

STANLEY, S. M. 1968. Post-Paleozoic adaptive radiation of infaunal bivalve molluscs a consequence of mantle fusion and siphon formation. *Journal of Paleontology*, **42**, 214–229.

—— 1970. Relation of shell form to life habits of the Bivalvia (Mollusca). *Memoir of the Geological Society of America*, **125**, 1–296.

—— 1981. Infaunal survival: alternative functions of shell ornamentation in the Bivalvia (Mollusca). *Paleobiology*, **7**, 384–393.

—— 1988. Adaptive morphology of the shell in bivalves and gastropods. 105–141. *In* TRUEMAN, E. R. and CLARKE, M. R. (eds). *The Mollusca, Volume 2. Form and function*. Academic Press.

STENZEL, H. B. 1971. *Oysters*. N953–N1224. *In* MOORE, R. C. (ed.). *Treatise on invertebrate paleontology. Part N. Mollusca (3)*. Geological Society of America and University of Kansas Press, Boulder, Colorado and Lawrence, Kansas, 1224 pp.

TAYLOR, J. D. 1976. Habitats, abundance and diets of muricacean gastropods at Aldabra Atoll. *Zoological Journal of the Linnean Society*, **59**, 155–193.

—— 1977. Diets and habitats of shallow water predatory gastropods around Tolo Channel, Hong Kong. 163–180. *In* MORTON, B. (ed.). *Proceedings of the 1st international workshop on the malacofauna of Hong Kong and Southern China, 23 March–8th April, 1977*. Hong Kong University Press, Hong Kong, 345 pp.

—— 1978. Habitats and diet of predatory gastropods at Addu Atoll, Maldives. *Journal of Experimental Marine Biology and Ecology*, **31**, 83–103.

—— 1990. Field observations of prey selection by the muricid gastropods *Thais clavigera* and *Morula musiva* feeding upon the intertidal oyster *Saccostrea cucullata*. 837–855. *In* MORTON, B. (ed.). *The marine flora and fauna of Hong Kong and Southern China. Proceedings of the 2nd international marine biological workshop, Hong Kong, 1986*. Hong Kong University Press, Hong Kong, 1268 pp.

—— MORRIS, N. J. and TAYLOR, C. N. 1980. Food specialization and the evolution of predatory prosobranch gastropods. *Palaeontology*, **23**, 375–409.

—— CLEEVELY, R. J. and MORRIS, N. J. 1983. Predatory gastropods and their activities in the Blackdown Greensand (Albian) of England. *Palaeontology*, **26**, 521–533.

VANCE, R. R. 1978. A mutualistic interaction between a sessile marine clam and its epibionts. *Ecology*, **59**, 679–685.

VERMEIJ, G. J. 1977. The Mesozoic Marine Revolution: evidence from snails, predators and grazers. *Paleobiology*, **2**, 245–258.

—— 1978. *Biogeography and adaptation. Patterns of marine life*. Harvard University Press, Cambridge, Mass., 332 pp.

—— 1987. *Evolution and escalation. An ecological history of life*. Princeton University Press, Princeton, New Jersey, 527 pp.

WALLER, T. R. 1978. Morphology, morphoclines and a new classification of the Pteriomorphia (Mollusca: Bivalvia). *Philosophical Transactions of the Royal Society of London, Series B*, **284**, 345–365.

WATTERS, G. T. 1993. Some aspects of the functional morphology of the shell of infaunal bivalves (Mollusca). *Malacologia*, **35**, 315–342.

WAYNE, T. A. 1987. Responses of a mussel to shell-boring snails: defensive behaviour in *Mytilus edulis*? *The Veliger*, **30**, 138–147.

WILLIAMS, L. G., RITTSCHOF, D., BROWN, B. and CARRIKER, M. R. 1983. Chemotaxis of oyster drills *Urosalpinx cinerea* to competing prey odors. *Biological Bulletin*, **164**, 536–548.

WILSON, J. G. 1979. What is the function of the shell ornamentation of *Tellina fabula* Gmelin? *Malacologia*, **18**, 291–296.

ZAVAREI, A. 1973. Monographie des Spondylidae (lamellibranches) actuels et fossiles. *Centre d'Études et de Recherches de Paleontologie Biostratigraphique* (*CERPAB*), **4**, 1–230.

HYWEL M. I. STONE
Department of Earth Sciences
University of Cambridge
Downing Street
Cambridge CB2 3EQ, UK
e-mail hywel.stone@btinternet.com

Typescript received 8 October 1996
Revised typescript received 22 July 1997

A CORALLINE-LIKE RED ALGA FROM THE LOWER ORDOVICIAN OF WALES

by ROBERT RIDING, JOHN C. W. COPE *and* PAUL D. TAYLOR

ABSTRACT. A new alga, *Arenigiphyllum crustosum* gen. et sp. nov., from the lower Ordovician (lower Arenig Series, Moridunian Stage) of the Llangynog Inlier, Carmarthenshire, Wales, has a thin crustose dorsiventral thallus. The single specimen is preserved as limonite. Construction is dimerous, consisting of juxtaposed vertical filaments arising from prostrate bases. Cells are closely spaced. There is no evidence of cell fusions, pit connections or reproductive structures. In size and thallus structure, *Arenigiphyllum* closely resembles vegetative parts of extant coralline algae. It is the oldest well-preserved example of a coralline-type alga described to date.

CORALLINALEANS are an important order of red algae that includes the extant Corallinaceae and Sporolithaceae (Verheij 1993). Heavy calcification of the cell wall gives both families an excellent fossil record from the Lower Cretaceous to Recent (Edwards *et al.* 1993, p. 36). However, despite attempts to elucidate their earlier history, the Palaeozoic antecedents of coralline algae have long been uncertain. At first, it was believed that members of the Solenoporaceae held the key to their origins (Nicholson and Etheridge 1885; Brown 1894), but these comparisons encountered difficulties. The central problem was the perception that solenoporaceans had simpler thallus organization and lacked the reproductive structures commonly preserved in corallines (Johnson 1960). As a result, attention switched to Late Palaeozoic fossils that became known as 'ancestral corallines' (Wray 1977, pp. 71–77), in particular to genera such as *Archaeolithophyllum* Johnson (Johnson 1956). However, *Archaeolithophyllum* has not been recorded from rocks older than Carboniferous, leaving the question of possible earlier coralline-like algae unresolved. Blackwell *et al.* (1982) refocused attention on the Lower Palaeozoic by describing reproductive structures in *Solenopora richmondensis* (Miller) Blackwell, Marek and Powell from the upper Ordovician. *Petrophyton kiaeri* Høeg, from the middle–upper Ordovician, has until now been the oldest known Palaeozoic calcified red alga (Riding 1994, p. 428).

Here we describe an older fossil from the lower Ordovician (Arenig) of Wales which, although it lacks reproductive structures, shows closer similarities to coralline vegetative anatomy than either *S. richmondensis* or *P. kiaeri*. It represents the earliest record to date of a well-preserved, originally calcified, coralline-like alga.

LOCALITY AND MATERIAL

The single specimen is from the base of the Bolahaul Member of the Ogof Hên Formation (Fortey and Owens 1978), now referred to the Moridunian Stage of the Arenig Series (Fortey and Owens 1987). The locality is a small quarry in the northern part of the Llangynog Inlier (Cope 1982), 6 km south-west of Carmarthen in south-west Wales (Cope 1996, text-fig. 1). This locality was first mentioned by Strahan *et al.* (1909, p. 16), but their list of fossils is meagre and unremarkable. More recently, extraction of the fossils by one of us (JCWC), using bulk collection of the rock and splitting it in the laboratory, has yielded an extraordinarily diverse fauna, dominated by molluscs, 40 per cent. of which are bivalves constituting the most diverse early Ordovician bivalve assemblage yet

[Palaeontology, Vol. 41, Part 5, 1998, pp. 1069–1076, 1 pl.]

known (Cope 1996). This locality has also yielded the earliest parablastoid (Paul and Cope 1982) and the earliest fully documented bryozoan (Taylor and Cope 1987). In a collection of about 3100 fossils, obtained by splitting some 20 tonnes of rock, ten taxa are represented by single specimens, including the alga described here. The specimen is housed in the National Museum of Wales, Cardiff, with accession number NMW 88. 67G. 2. The specimen is now composed of limonite. Primary calcification is assumed because the preservation is similar to that of parablastoids (Paul and Cope 1982), bryozoans (Taylor and Cope 1987), molluscs, and articulate brachiopods from this locality. The alga is smoothly convex and encrusts what appears to be a trilobite free-cheek. However, substantiating this would require damage to the alga.

In this paper, thin section photography and locality and material description are by JCWC. SEM photographs of *Arenigiphyllum* are by PDT. The systematic section and remainder of the paper are by RR.

SYSTEMATIC PALAEONTOLOGY

Division RHODOPHYTA Wettstein, 1901
Class RHODOPHYCEAE Rabenhorst, 1863
Order CORALLINALES Silva and Johansen, 1986? or GIGARTINALES Schmitz, *in* Engler 1892?
Family uncertain

Genus ARENIGIPHYLLUM Riding gen. nov.

Type species. Arenigiphyllum crustosum gen. et sp. nov.

Derivation of name. After the Arenig Series, in which the fossil was found.

Diagnosis. Thin foliose thallus, with dorsiventral dimerous construction of erect prismatic filaments with rounded interiors, arising from a prostrate base; cell walls closely spaced.

Affinities and comparisons. In general size and filament arrangement, *Arenigiphyllum* closely resembles coralline algae (Pl. 1; Text-fig. 1). At this scale, size becomes a significant criterion and the small size of the filaments and cells makes superficial similarities with sponges, tabulates and bryozoans untenable. In addition to its size, *Arenigiphyllum* distinctly resembles coralline algae in structure. The thallus is thin (less than 1 mm thick) with dorsiventral dimerous construction, i.e. with a basal cell layer (of unistratose basal filaments) and erect upper portion. For example, *Arenigiphyllum* resembles the extant coralline *Exilicrusta* Chamberlain in its thin prostrate thallus and upward curving elongate filaments (compare fig. 5 in Chamberlain 1992 with Pl. 1, fig. 5), and the cell walls (cross partitions) visible in thin section (Text-fig. 2) are comparable to those illustrated by Woelkerling (1988, fig. 219) for *Melobesia*. However, all coralline groups may exhibit the thallus thinness and organization shown by *Arenigiphyllum*, and, in the absence of reproductive structures, it is not possible to decide whether *Arenigiphyllum* could be placed in either of the extant families Sporolithaceae and Corallinaceae.

It is also possible that *Arenigiphyllum* represents a member of the Peyssoneliaceae Denizot (also known as Squamariaceae (Agardh) Hauck). Although not included in the Corallinales, these red algae have broadly similar thallus construction and typically form thin foliose thalli similar to that seen in *Arenigiphyllum*. Peyssoneliaceans have a confirmed record from Lower Cretaceous to Recent (Edwards *et al.* 1993, p. 36), and have been compared to some Late Palaeozoic phylloid algae (Wray 1977, p. 53). A difference from members of the Corallinales is that the peyssoneliacean skeleton is aragonitic. We have no information concerning the original mineralogy of *Arenigiphyllum*. Furthermore, extant peyssonelaceans show dichotomous division of cell filaments which results in a reduction in cell size as the filament grows (e.g. Buchbinder and Halley 1985, figs 6, 7a–b; Wray 1977, figs 37–38). This is not seen in *Arenigiphyllum*. Thus, although an affinity with the Peyssoneliaceae cannot be excluded, comparisons with corallines are closer.

TEXT-FIG. 1. *Lithophyllum incrustans* Philippi, 1837; specimen TJ-24, deposited in the Museum of the Departamento de Estratigrafía y Paleontología, Universidad de Granada; fractured surface showing longitudinal section parallel to prismatic sinuous filaments; compare with *Arenigiphyllum* in Pl. 1, fig. 5; Miocene (Upper Tortonian), Almanzora Corridor, south-east Spain; scanning electron micrograph of coated specimen using secondary electrons; ×221.

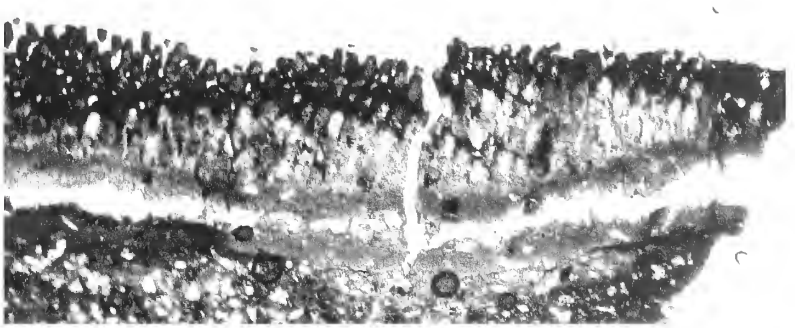

TEXT-FIG. 2. *Arenigiphyllum crustosum* gen. et sp. nov; holotype, NMW 88. 67G. 2; 6 km south-west of Carmarthen; Bolahaul Member, Ogof Hên Formation; thin section showing sub-vertical filaments and closely spaced cell walls near the upper surface; ×27.

The type species of *Solenopora*, *S. spongioides* Dybowski, was described from the upper Ordovician (Dybowski 1877), and the Solenoporaceae has generally been regarded as an extinct family of calcified red algae. However, the Solenoporaceae is a heterogeneous group based on an aggregation of disparate taxa some of which may not be algal (Riding 1977, p. 206, 1993; Brooke and Riding 1987). Corallinalean algae have been recognized among Early Palaeozoic solenoporaceans. Blackwell *et al.* (1982) described sporangial compartments arranged in a sorus in *S. richmondensis* and compared it to the extant coralline *Sporolithon*. The cells of *S. richmondensis* are rounded to polygonal in cross section, are 30–110 μm wide and 60–140 μm long (Blackwell *et al.* 1982, p. 478, fig. 6), appear to be well-aligned between adjacent filaments, and closely resemble those of *Petrophyton kiaeri* from the middle–upper Ordovician. *Petrophyton* has also been recorded by Sinclair (1956) as *P.? floreale* from the Ordovician of Québec, and as *P. kiaeri* from the Silurian of Québec (Mamet and Roux, *in* Héroux *et al.* 1977, p. 2898), but lacks reproductive structures. *Solenopora gotlandica* from the lower Silurian, possesses small cells, radial monomerous or diffuse

thallus organization, and tetrasporangia arranged in sori and also appears to be a sporolithacean (Brooke and Riding in press). Neither *S. gotlandica* nor *S. richmondensis* appears to be congeneric with *S. spongioides*.

Arenigiphyllum is distinguished from *Petrophyton* and species attributed to *Solenopora* by being thin and foliose in form, whereas these other taxa characteristically have inflated nodose thalli. *Arenigiphyllum* is distinguished from *Petrophyton* and *S. richmondensis* by having smaller cells that are wider than high. No pit connections are visible in *Arenigiphyllum*, but this does not preclude their absence since it can be difficult to observe pits even in present-day corallines where they are known to be present (J. C. Braga, pers. comm.). However, larger cell fusions between adjacent filaments do appear to be absent. Among corallines, absence of cell fusions is characteristic of the subfamily Lithophylloideae and some sporolithaceans. More rarely, some corallines lack any kind of cell connection between adjacent filaments. This is characteristic, for example, of the subfamily Austrolithoideae Harvey and Woelkerling, 1995, although these are very small uncalcified plants that are unknown as fossils.

Despite the difficulties of elucidating *Arenigiphyllum*'s precise relationships with extant corallines, due to the absence of reproductive structures and information concerning original mineralogy, available evidence indicates that *Arenigiphyllum* is a calcified red alga closely allied with extant corallines and peyssoneliaceans. Accordingly, it is here tentatively referred to either the Corallinales or Gigartinales.

Remarks. The specimen is preserved as limonite. It is assumed that the original specimen was calcified and that preservation involved infilling by cements and/or matrix, followed by dissolution and replacement. The walls are relatively thick and the final size and shape of the preserved central tube (Pl. 1, fig. 4) may be due to formation of epitaxial cements (see Bosence 1991, figs 1b, 2f; Braga *et al.* 1993, pl. 1, fig. 2) that left the centres of the filaments to be infilled subsequently by matrix. If limonite replaced the calcareous skeleton and cement, but not the matrix-filled tubular filament centres, this would produce the square outer filament surfaces, thick walls and rounded centre. However, it should be noted that present-day corallines such as *Exilicrusta parva* (see Chamberlain 1992, fig. 5) show strikingly similar calcified filaments with planar outer surfaces and rounded interiors prior to any cementation or infilling.

In longitudinal section, the outer planar bounding surface (Pl. 1, figs 1–2) is interpreted as the inner cell wall (see Bosence 1991, fig. 1a, for terminology), which may have been dissolved and infilled to provide the cast preserved. Differential dissolution of parts of the cell wall occurs in dilute acid etching of Recent coralline specimens (see Braga *et al.* 1993, pl. 1, figs 1–2). Cell walls are partially preserved (Text-fig. 2; Pl. 1, figs 1–2). They are unusually closely spaced; most extant corallines have cells whose height is equal to or greater than the filament width. However, some near-surface cells of melobesioids are closely spaced and have a flat appearance similar to those in *A. crustosum* (J. C. Braga, pers. comm.).

EXPLANATION OF PLATE 1

Figs 1–5. *Arenigiphyllum crustosum* gen. et sp. nov.; holotype, NMW 88. 67G. 2; scanning electron micrographs of the uncoated specimen imaged using back-scattered electrons; Llangynog, 6 km south-west of Carmarthen, Wales; Bolahaul Member, Ogof Hên Formation. 1, vertical prismatic filaments, detail of 5; locally ladder-like remains of cell walls are preserved between adjacent filaments; ×110. 2, detail of 1, showing smooth prismatic inner wall of the middle filament, which is removed from adjacent filaments to reveal the surface of the lining or infilling to the filament; ×225. 3, transverse section of regular spaced circular openings interpreted as filaments on the upper surface of the thallus; ×90. 4, detail of 3, showing local infilling of tubes by ?cement/matrix; intervening material is interpreted as filament wall possibly with cement rims; rectilinear cracks may represent inner walls of filaments; ×210. 5, fractured surface of foliose thallus showing dorsiventral dimerous construction with sub-vertical prismatic filaments arising from a prostrate base; ×80.

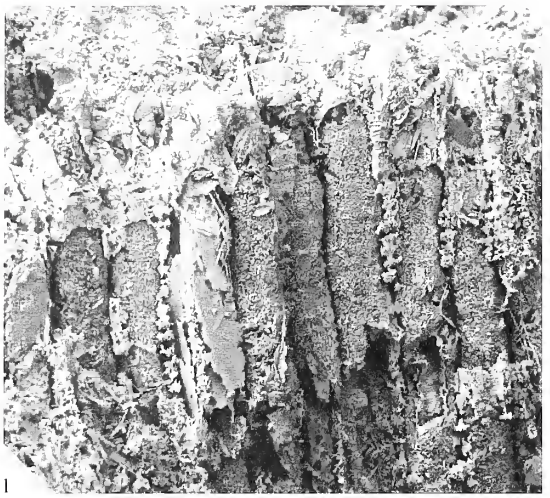

1

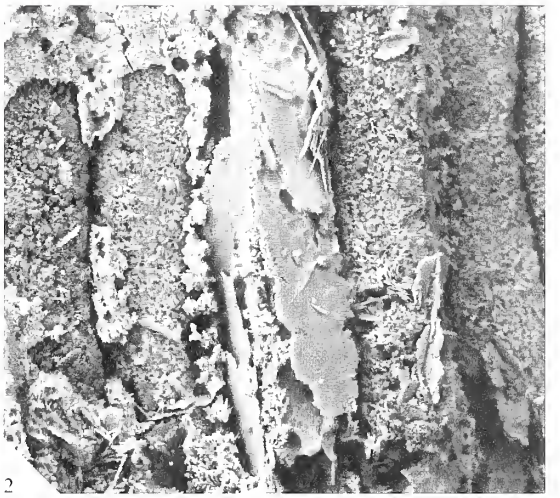

2

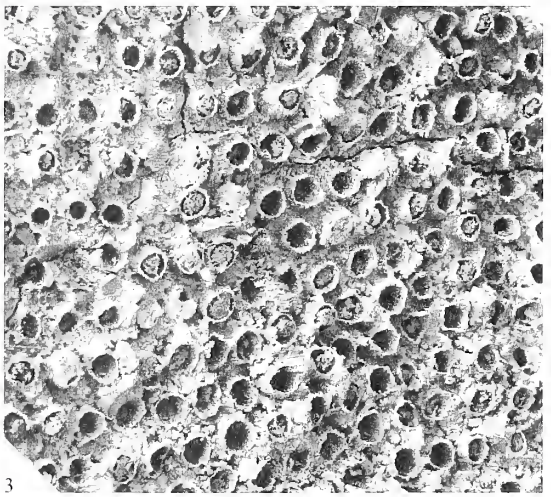

3

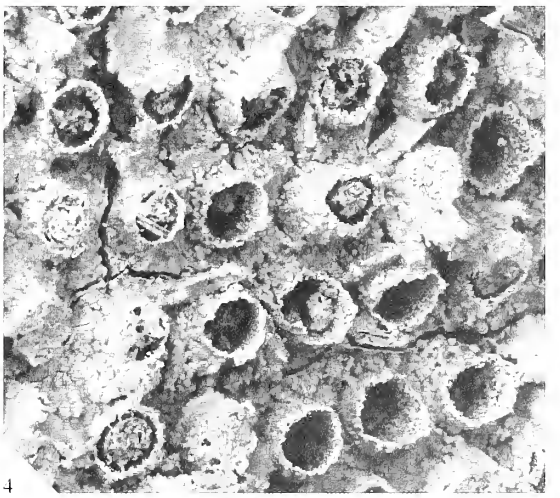

4

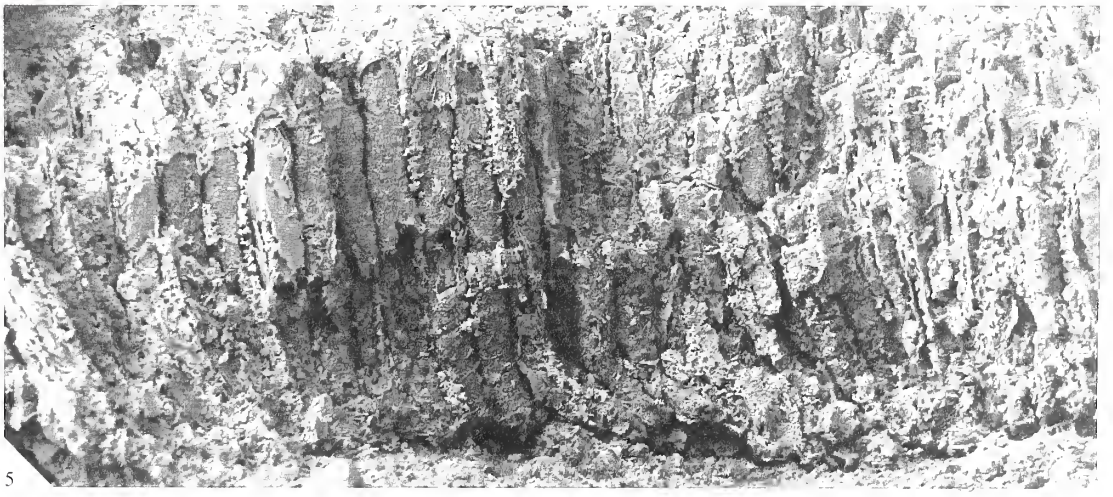

5

RIDING *et al.*, *Arenigiphyllum*

In transverse section, the spaced circular openings (Pl. 1, figs 3–4) are interpreted as cross sections of filaments (see Chamberlain 1992, fig. 5), and the material occupying space between the openings as cement/matrix and/or originally calcified cell wall (compare cement fills of coralline filaments shown by Bosence 1991, fig. 1b, and Braga *et al.* 1993, pl. 1, fig. 2). The circular openings also somewhat resemble epithallial surface concavities of extant corallines (see Woelkerling *et al.* 1985, figs 30–31; Chamberlain 1992, figs 2, 15). The complicated filament infillings observed locally (Pl. 1, fig. 4) appear to be due to replacement of various stages of cement and matrix. An apparent double wall has been produced during preservation of Silurian *Solenopora compacta* (see Rothpletz 1913, pl. 1, fig. 6, lower right centre).

Arenigiphyllum crustosum Riding sp. nov.

Plate 1; Text-figure 2

Derivation of name. From the thin crustose appearance of the fossil.

Holotype. Thin foliose fragment, NMW 88. 67G. 2; Plate 1; Text-figure 2.

Locality and horizon. National Grid Reference SN 3640 1639, Llangynog, Carmarthenshire, Wales. Approximately 5 m above the base of the Bolahaul Member, Ogof Hên Formation (Moridunian Stage, Arenig Series).

Diagnosis. As for genus.

Description. Thin domed layer 800 μm thick and 28 mm across, composed of erect filaments arising vertically from prostrate basal filaments. Filaments tubiform, diameter expanding from 20 μm in basal part up to 60 μm in erect part, where they maintain constant diameter; cell height 15–20 μm; filaments juxtaposed; walls thick, outer surface polygonal with planar faces, inner surface circular.

DISCUSSION

The earliest red alga known is an uncalcified Proterozoic bangiophyte approximately 1000 My old from Somerset Island, Canada (Butterfield *et al.* 1990). Phosphatized red algae (*Thallophyca* Zhang) that probably were not calcified have been reported from the 680 Ma Doushantou Formation of China (Zhang 1989; Zhang and Yuan 1992). The oldest records of possible calcified red algae are based on two reports: Horodyski and Mankiewicz (1990) recorded *Tenuocharta* Horodyski and Mankiewicz from the Neoproterozoic (600–700 Ma) and suggested that it might be a red alga or cyanobacterium; and Grant *et al.* (1991) compared a younger (530–650 Ma) possible alga with phylloid algae, peyssoneliaceans, and corallines. Both of these fossils are calcified and foliose. *Tenuocharta* is distinguished from *Arenigiphyllum* by being extremely thin, apparently consisting of a single layer of 5–10 μm size cell-like structures. The specimens described by Grant *et al.* (1991) appear to have originally been aragonitic and are sheets up to 500 μm thick with elevated structures reminiscent of reproductive structures, which have not been observed in *Arenigiphyllum*. The overall size and appearance are broadly consistent with those of *Arenigiphyllum*, and the possibility that they are related cannot be ruled out. But, poor preservation of internal detail within the sheets precludes any precise comparison with *Arenigiphyllum*. Various early Cambrian calcified fossils have been referred to the red algae (Korde 1959), but are now regarded as probable cyanobacteria (Luchinina 1975; Riding 1991). None has the foliose and cellular structure seen in *Arenigiphyllum*.

Although *Arenigiphyllum* lacks reproductive structures, its possession of dimerous tissue differentiation is much more coralline-like in vegetative anatomy than either S. *richmondensis* (late Ordovician; Blackwell *et al.* 1982) or *P. kiaeri* (mid–late Ordovician; Hoeg 1932, p. 32). *Arenigiphyllum* therefore predates these previous oldest records of confirmed calcified red algae and is the oldest example of a well-preserved coralline-type alga so far known.

Acknowledgements. RR is indebted to Julio Aguirre and Juan Carlos Braga for advice and discussion about coralline anatomy, for critically reading the manuscript and making many helpful suggestions. Juan Carlos Braga suggested the name *Arenigiphyllum*, and kindly provided Text-figure 1.

REFERENCES

BLACKWELL, W. H., MARAK, J. H. and POWELL, M. J. 1982. The identity and reproductive structures of a misplaced *Solenopora* (Rhodophycophyta) from the Ordovician of southwestern Ohio and eastern Indiana. *Journal of Phycology*, **18**, 477–482.

BOSENCE, D. W. J. 1991. Coralline algae: mineralization, taxonomy, and palaeoecology. 98–113. *In* RIDING, R. (ed.). *Calcareous algae and stromatolites*. Springer-Verlag, Berlin 571 pp.

BRAGA, J. C., BOSENCE, D. W. J. and STENECK, R. S. 1993. New anatomical characters in fossil coralline algae and their taxonomic implications. *Palaeontology*, **36**, 535–547.

BROOKE, C. and RIDING, R. 1987. A new look at the Solenoporaceae. *4th International Symposium on Fossil Algae, Cardiff, July 1987, Abstracts*, 7.

—— in press. Ordovician and Silurian coralline red algae. *Lethaia*.

BROWN, A. 1894. On the structure and affinities of the genus *Solenopora*, together with descriptions of new species. *Geological Magazine*, **31**, 145–151, 195–203, pl. 5.

BUCHBINDER, B. and HALLEY, R. B. 1985. Occurrence and preservation of Eocene squamariacean and coralline rhodoliths: Eua, Tonga. 248–256. *In* TOOMEY, D. F. and NITECKI, M. H. (eds). *Paleoalgology: contemporary research and applications*. Springer-Verlag, Berlin, 376 pp.

BUTTERFIELD, N. J., KNOLL, A. H. and SWETT, K. 1990. A bangiophyte red alga from the Proterozoic of Arctic Canada. *Science*, **250**, 104–107.

CHAMBERLAIN, Y. M. 1992. Observations on two melobesioid crustose coralline red algal species from the British Isles: *Exilicrusta parva*, a new genus and species, and *Lithothamnion sonderi* Hauck. *British Phycological Journal*, **27**, 185–201.

COPE, J. C. W. 1982. The geology of the Llanstephan peninsula. 259–269. *In* BASSETT, M. G. (ed.). *Geological excursions in Dyfed, south-west Wales*. National Museum of Wales, Cardiff, 327 pp.

—— 1996. Early Ordovician (Arenig) bivalves from the Llangynog Inlier, South Wales. *Palaeontology*, **39**, 979–1025.

DYBOWSKI, W. 1877. Die Chaetetiden der ostbaltischen Silur-Formation. *Russisch-Kaiserliche Mineralogische Gesellschaft zu St. Petersburg Verhandlungen, Series 2*, **14** (1878), 1–134, pls 1–4.

EDWARDS, D., BALDAUF, J. G., BOWN, P. R., DORNING, K. J., FEIST, M., GALLAGHER, L. T., GRAMBAST-FESSARD, N., HART, M. B., POWELL, A. J. and RIDING, R. 1993. Algae. 15–40. *In* BENTON, M. J. (ed.). *The fossil record 2*. Chapman and Hall, London, 845 pp.

FORTEY, R. A. and OWENS, R. M. 1978. Early Ordovician (Arenig) stratigraphy and faunas of the Carmarthen district, south-west Wales. *Bulletin of the British Museum (Natural History), Geology Series*, **30**, 225–294, pls 1–11.

—— —— 1987. The Arenig Series in South Wales: stratigraphy and palaeontology. *Bulletin of the British Museum (Natural History), Geology Series*, **41**, 69–307.

GRANT, S. W. F., KNOLL, A. H. and GERMS, G. J. B. 1991. Probable calcified metaphytes in the latest Proterozoic Nama Group, Namibia. *Journal of Paleontology*, **65**, 1–18.

HARVEY, A. S. and WOELKERLING, W. J. 1995. An account of *Austrolithon intumescens* gen. et sp. nov. and *Boreolithon van-heurckii* (Heydrich) gen. et comb. nov. (Austrolithoideae subfam. nov., Corallinaceae, Rhodophyta). *Phycologia*, **34**, 362–382.

HÉROUX, Y., HUBERT, C., MAMET, B. and ROUX, A. 1977. Algues siluriennes de la Formation de Sayabec (Lac Matapédia, Québec). *Canadian Journal of Earth Sciences*, **14**, 2865–2908.

HØEG, O. 1932. Ordovician algae from the Trondheim area. *Skrifter utgitt av Det Norske Videnskaps-Akademi i Oslo, I Matematisk-Naturvidenskapelig Klasse*, **4**, 63–96, pls 1–11.

HORODYSKI, R. J. and MANKIEWICZ, C. 1990. Possible late Proterozoic skeletal algae from the Pahrump Group, Kingston Range, southeastern California. *American Journal of Science*, **290-A**, 149–169.

JOHNSON, J. H. 1956. Ancestry of the coralline algae. *Journal of Paleontology*, **30**, 563–567.

—— 1960. Paleozoic Solenoporaceae and related red algae. *Quarterly of the Colorado School of Mines*, **55** (3), 1–77.

KORDE, K. B. 1959. [Morphology and systematic position of representatives of the genus *Epiphyton*.] *USSR Academy of Science Reports, New Series*, **126** (5), 1087–1089. [In Russian].

LUCHININA, V. A. 1975. [Palaeoalgological characteristics of the Early Cambrian of the Siberian Platform.] *USSR Academy of Science, Siberian Section, Institute of Geology and Geophysics*, **216**, 1–98. [In Russian].

NICHOLSON, H. A. and ETHERIDGE, R., JR 1885. On the synonymy, structure, and geological distribution of *Solenopora compacta*, Billings, sp. *Geological Magazine, Decade 3*, **2**, 529–535.

PAUL, C. R. C. and COPE, J. C. W. 1982. A parablastoid from the Arenig of South Wales. *Palaeontology*, **25**, 499–507.

PHILIPPI, R. 1837. Beweis dass die Nulliporen Pflanzen sind. *Archiven Naturgeschichte*, **3**, 387–393.

RABENHORST, L. 1863. *Kryptogamen-Flora von Sachsen, der Ober-Lausitz, Thüringen und Nordböhmen Abteilung 1*. E. Krummer, Leipzig, 653 pp.

RIDING, R. 1977. Problems of affinity in Palaeozoic calcareous algae. 202–211. *In* FLÜGEL, E. (ed.). *Fossil algae, recent results and developments*. Springer-Verlag, Berlin, 375 pp.

—— 1991. Cambrian calcareous cyanobacteria and algae. 305–334. *In* RIDING, R. (ed.). *Calcareous algae and stromatolites*. Springer-Verlag, Berlin, 571 pp.

—— 1993. Calcareous algae. 78–81. *In* KEAREY, P. (ed.). *The encyclopedia of the solid earth sciences*. Blackwell, Oxford, 713 pp.

—— 1994. Evolution of algal and cyanobacterial calcification. 426–438. *In* BENGTSON, S. (ed.). *Early life on Earth*. Nobel Symposium No. 84. Columbia University Press, New York, 630 pp.

ROTHPLETZ, A. 1913. Über die Kalkalgen, Spongiostromen und einige andere Fossilien aus dem Obersilur Gottlands. *Sveriges Geologiska Undersökning, Series Ca*, **10**, 1–57, pls 1–9, map.

SCHMITZ, F. 1892. Florideae. 16–23. *In* ENGLER, A. (ed.). *Syllabus der Pflanzenfamilien*. G. Borntraeger, Berlin, xxiv + 184 pp.

SILVA, P. C. and JOHANSEN, H. W. 1986. A reappraisal of the order Corallinales (Rhodophyceae). *British Phycological Journal*, **21**, 245–254.

SINCLAIR, G. W. 1956. *Solenopora canadensis* (Foord) and other algae from the Ordovician of Canada. *Transactions of the Royal Society of Canada*, **50**, *Series 3*, **4**, 65–81.

STRAHAN, A., CANTRILL, T. C., DIXON, E. E. L. and THOMAS, H. H. 1909. The geology of the South Wales Coalfield. X, The country around Carmarthen. *Memoir of the Geological Survey of Great Britain*, vii + 262 pp.

TAYLOR, P. D. and COPE, J. C. W. 1987. A trepostome bryozoan from the Lower Arenig of South Wales: implications of the oldest described bryozoan. *Geological Magazine*, **124**, 367–371.

VERHEIJ, E. 1993. The genus *Sporolithon* (Sporolithaceae fam. nov., Corallinales, Rhodophyta) from the Spermonde Archipelago, Indonesia. *Phycologia*, **32**, 184–196.

WETTSTEIN, R. R. 1901. *Handbuch der Systematischen Botanik*. Vol. 1. Deuticke, Leipzig, 201 pp.

WOELKERLING, W. J. 1988. *The coralline red algae*. Oxford University Press, Oxford, 268 pp.

—— CHAMBERLAIN, Y.L M. and SILVA, P. C. 1985. A taxonomic and nomenclatural reassessment of *Tenarea*, *Titanoderma* and *Dermatolithon* (Corallinaceae, Rhodophyta) based on studies of type and other critical specimens. *Phycologia*, **24**, 317–337.

WRAY, J. L. 1977. *Calcareous algae*. Developments in palaeontology and stratigraphy, 4. Elsevier, Amsterdam, 185 pp.

ZHANG, YUN 1989. Multicellular thallophytes with differentiated tissues from the late Proterozoic phosphate rocks of south China. *Lethaia*, **22**, 113–132.

—— and YUAN XUN-LAI 1992. New data on multicellular thallophytes and fragments of cellular tissue from Late Proterozoic phosphate rocks, South China. *Lethaia*, **25**, 1–18.

ROBERT RIDING

JOHN C. W. COPE

Department of Earth Sciences
Cardiff University
Cardiff CF1 3YE, UK

PAUL D. TAYLOR

Department of Palaeontology
The Natural History Museum
Cromwell Road, London SW7 5BD, UK

Typescript received 18 June 1997
Revised typescript received 29 October 1997

SPERMATOPHYTE PREOVULES FROM THE BASAL CARBONIFEROUS OF THE AVON GORGE, BRISTOL

by JASON HILTON

ABSTRACT. *Aglosperma avonensis* is a new acupulate species of Early Carboniferous preovule from the VI miospore biozone of the Avon Gorge near Bristol. It is closest in morphology to the slightly older *Aglosperma quadrapartita* from the Taff Gorge near Cardiff, although distinction can be made on the characteristics of the integument, the nucellus and on general size. The possibility that the new preovule represents an ontogenetic stage of *A. quadrapartita* is discounted. The new species displays characteristics of the nucellar apex not observed in the type species, possessing a distinct pollen chamber and tubular salpinx, most probably evidence of a hydrasperman pollen chamber. The distribution of *Aglosperma* and other similar preovulate structures indicates that acupulate preovules were perhaps as cosmopolitan as the previously more widely known cupulate forms during this early period of spermatophyte radiation.

THE origin and subsequent radiation of the seed-plants has been the focus of much palaeobotanical attention, with evidence frequently based on the structure and organization of the ovulate structures, the only features unique to this group in their early evolution. The evolutionary development of the ovule encapsulated the female gametophyte in an entirely new kind of reproductive structure in which monomegaspory (i.e. a single functional megaspore per tetrad and a single tetrad per sporangium) was accompanied by distal modification of the megasporangium for microspore (pollen or pre-pollen) reception and by integumentation (the enclosure of the megasporangium in an additional sterile layer).

Prior to the first geological occurrence of true 'micropylar' ovules, Palaeozoic ovulate structures exhibited a preovular integument, or pre-integument of some authors. In preovules, the integument is proximally complete and distally divides into lobes. These are thus morphologically distinct from true ovules which have a completely enveloping integument except at a micropyle. To date, all pre-Carboniferous ovulate structures are preovulate (Rothwell and Scheckler 1988; Hilton and Edwards 1996).

Recent research has identified that not all of the earliest preovule morphologies occurred within vegetative cupules as had previously been thought (e.g. Rothwell and Scheckler 1988; Serbet and Rothwell 1992), but that certain preovules terminate long slender axes (Hilton and Edwards 1996). These acupulate preovules are morphologically distinct from the cupulate forms and have so far failed to provide unequivocal evidence concerning their reproductive biologies with respect to post-pollination sealing of the megagametophyte. However, in cupulate morphologies evidence of pollination biology has been used as evidence to support theories relating to the phyletic status of the seed plants. Rothwell (1986) interpreted his 'hydrasperman' pollination biology as diagnostic of all ancestral ovulate structures, inferring monophylesis for the seed plants based on the improbability of this kind of elaborate structure having evolved more than once. As yet, the presence of this kind of reproductive biology in the earliest phases of seed plant radiation is only known unequivocally in the cupulate taxa (Rothwell *et al.* 1989; Hilton and Edwards 1996, in press).

During palynological investigations of the Devonian–Carboniferous boundary sequence in the Avon Gorge, Utting and Neves (1969) located plant material within the Shirehampton Beds of the Upper Old Red Sandstone–Lower Limestone Shale transition. The plant megafossils were identified by R. H. Wagner (*in* Utting and Neves 1969) as cf. *Rhacophyton*, and the plant bed was subsequently named the '*Rhacophyton* bed', reflecting the monotypic characteristics of the deposit reported by Utting and Neves (Fairon-Demaret 1986). Subsequent work has identified the presence

[Palaeontology, Vol. 41, Part 5, 1998, pp. 1077–1091, 2 pls]

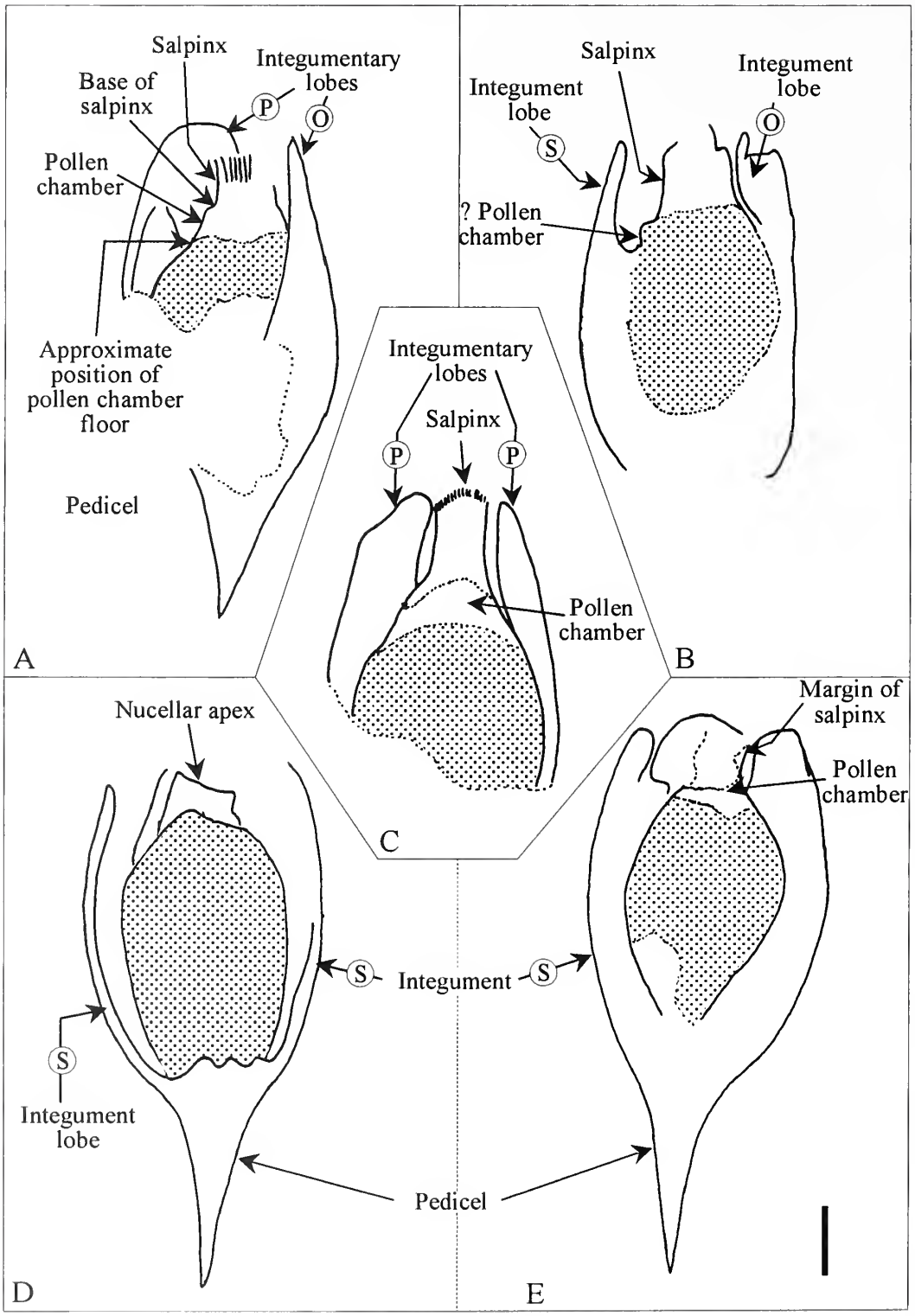

TEXT-FIG. 1. For caption see opposite.

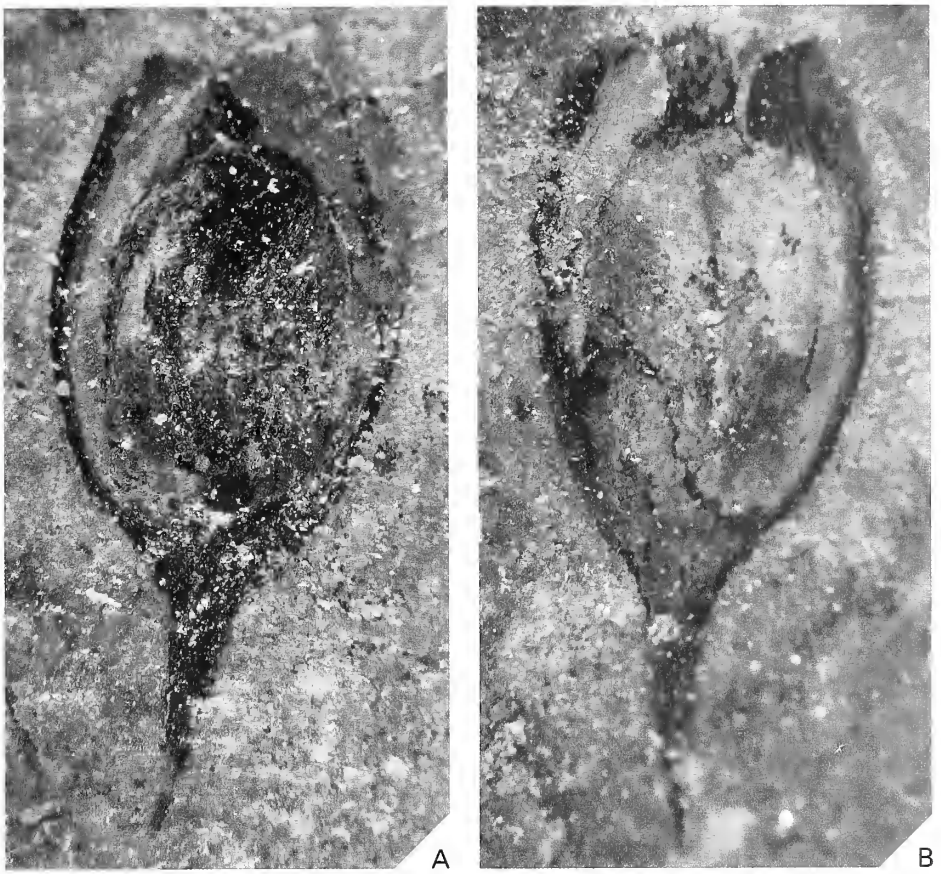

TEXT-FIG. 2. *Aglosperma avonensis* sp. nov.; part (A) and counterpart (B) of holotype. NMW.97.10G.1a–b; two preintegumentary lobes are present in section, either side of the central nucellus. The nucellus is as long as the integument and possesses a nucellar apex with pollen chamber and salpinx (attached to the counterpart). The counterpart possesses a mineral film between the nucellus (on the part). The integument is visible, as most of the nucellus (the proximal 85 per cent.) is attached to the part. The long pedicel is clearly visible. Both × 13.

of numerous dispersed acupulate preovules within the original material and re-collection from the site has provided additional preovules, although none in attachment to a parent plant.

MATERIAL AND METHODS

Plant adpressions from the Avon Gorge locality were prepared by dégagement (Leclercq 1960), using sharpened tungsten needles to remove matrix (and mud) from specimens while viewed under a Wild M3 binocular microscope. Specimens were reinforced during and after dégagement with

TEXT-FIG. 1. Annotated diagrams of four specimens of *Aglosperma avonensis* sp. nov. showing details of gross morphology and characteristics of the nucellar apex. The nucellus of each specimen is shown stippled. Preintegument lobe orientation: P, plan view; S, section view; O, oblique view. A, NMW.97.10G.9 (Pl. 2, figs 4–5); B, NMW.97.10G.2d (Pl. 1, fig. 1; Pl. 2, fig. 7); C, NMW.97.10 (Pl. 2, figs 6, 8); D, NMW.97.10G.1a (Text-fig. 2A); E, NMW.97.10G.1b (Text-fig. 2B). Scale bar represents 1 mm.

Paraloid glue soluble in acetone. Many of the best specimens were revealed by fortuitous fractures through the matrix. Rock splitting was accomplished using triangular tipped, leather-working needles struck with a toffee hammer. Specimens were kept dry at all times as contact with water results in fragmentation of the coalified plant material.

Illumination of specimens for both dégagement and photography was provided by a Schott KL 1500 light source, fitted with twin polarizing filters. A third polarizing filter was attached to either the microscope objective or the camera lens to reduce the glare from the micaceous matrix and to enhance edge definition. An Olympus OM system was used for all photography, using a variety of macro lenses.

LOCALITY INFORMATION AND STRATIGRAPHY

The '*Rhacophyton*' bed of the Avon Gorge occurs at the base of the Shirehampton Beds of the Upper Old Red Sandstone, which are immediately overlain in this locality by the basal Carboniferous Lower Limestone Shale. The exact location of the plant-bearing strata is given in Utting and Neves (1969). The plants are found in two distinct lithologies: green fine-grained sandstones (which represent fluvial channel in-fills) containing abundant plant debris; and green mudstones, containing intact (?autocthonous) plant material, interpreted as being vegetated overbank deposits (flood plain) with the plants having been rapidly covered with sediment during flood events. Further details of the entire plant assemblage will be presented elsewhere.

Collecting within the Avon Gorge is hampered by the locality being situated under approximately 2 metres of estuarine mud and being submerged at each high tide. As a consequence of the tidal nature of the estuary, rapidity in collecting is essential. It has proved impossible to remove all the mud from the rock surfaces at the field exposure, making sedimentological observations virtually impossible as bedding related features are obscured.

EXPLANATION OF PLATE 1

Figs 1–7. *Aglosperma avonensis* sp. nov.; Avon Gorge plant assemblage. 1, four isolated preovules at varying stages of dégagement, aligned on the same slab but each faces a different direction suggesting a random arrangement. This slab lacks a counterpart and the specimens are generally not well preserved or intact. The preovule to the left (NMW.97.10G.2a) lacks an uppermost preintegumentary lobe but its impression can be noted by the darker coloured imprint on the sediment below. The left middle preovule (NMW.97.10G.2b) possesses two preintegumentary lobes whilst the right middle preovule (NMW.97.10G.2c) is distally incomplete but has a well preserved pedicel and chalaza. The preovule to the right (NMW.97.10G.2d) is proximally incomplete and is enlarged in Pl. 2, fig. 7, showing the details of the nucellar apex; ×3·6. 2, NMW.97.10G.3; isolated preovule showing details of the long pedicel which tapers to a point; little of the integument remains in this poorly preserved specimen, although the positions of two preintegumentary lobes, one with a rounded apex, are visible; ×8·7. 3, NMW.97.10G.4; three preovules in close proximity to each other and to a short axis (right centre). The uppermost preovule has its distal apex pointing upwards, the central preovule is orientated towards the right and the lowermost preovule is orientated towards the upper right. None of these preovules or the axis are attached to each other. The pedicel on the central preovule is typical of this species when complete, tapering to a point; ×4·2. 4–5, part and counterpart of NMW.97.10G.5. 4, preovule with an entire pedicel and three well preserved preintegumentary lobes. At the distal apex the nucellar apex is visible. 5, details of the nucellar apex beside the distally recurved preintegumentary lobe on the right hand side. The distal extremes of both part and counterpart of this preovule are cnlarged in figs 6–7; ×9. 6–7, enlargement of the distal areas of NMW.97.10G.5 (figs 4–5). 6, nucellar apex comprising a pollen chamber and salpinx which protrudes beyond the distal reaches of the two preintegumentary lobes visiblc at each side. The tips of the preintegumentary lobes are slightly recurved, each tapering to a point and are observed in section; ×35. All specimens are illuminated by multi-directional, low angled, polarized light to reveal features otherwise not visible with conventional lighting.


1


2

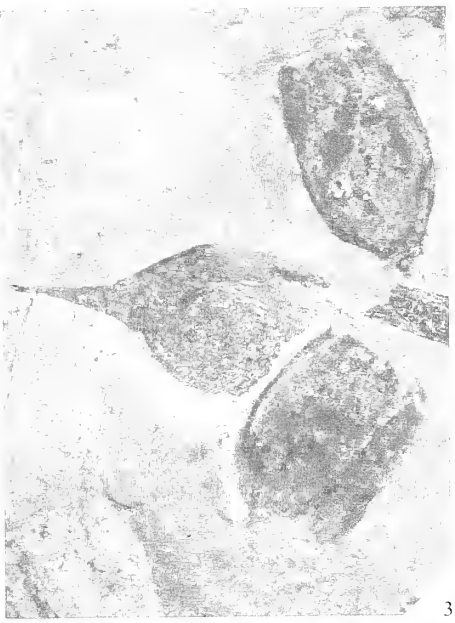
3


4


5

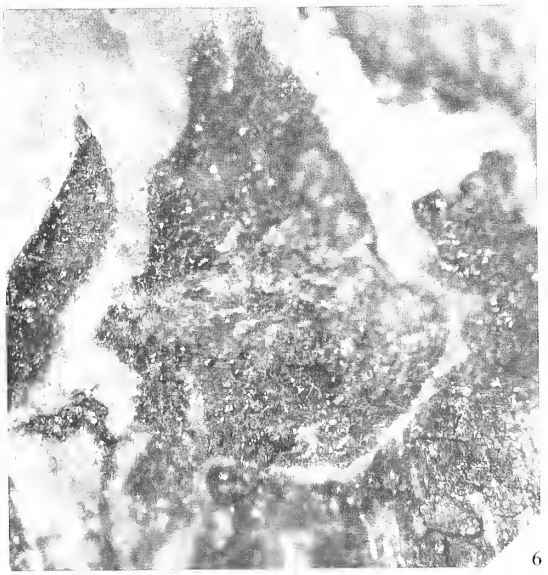
6

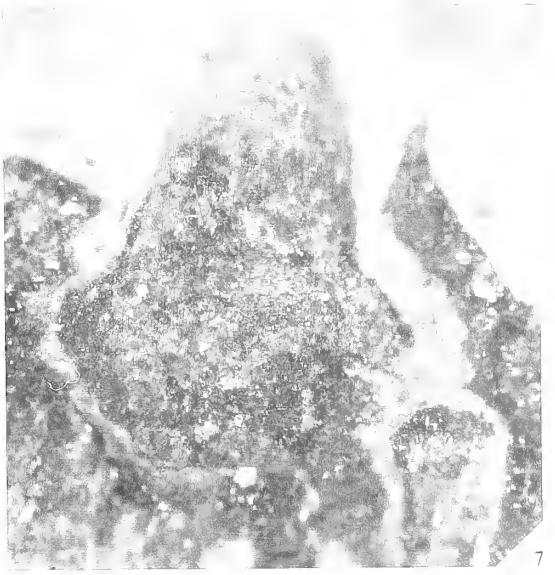
7

HILTON, *Aglosperma*

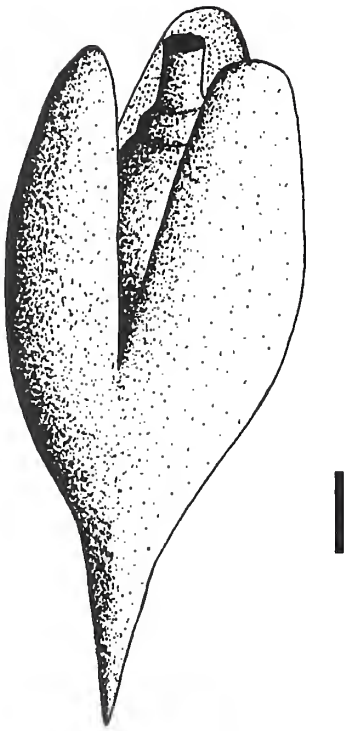

TEXT-FIG. 3. Reconstruction of *Aglosperma avonensis* sp. nov. Scale bar represents 1 mm.

Utting and Neves (1969) dated the Avon Gorge plant bed palynologically as within the VI spore zone (basal Tournaisian). This has been confirmed by re-examination of the palynoflora by Higgs *et al.* (1988), who assigned the Portishead Beds of the Avon Gorge to their LL biozone, whilst noting a change to the VI biozone in the Shirehampton Beds, including the plant-bearing strata in this younger biozone. This places the Avon Gorge plant bed stratigraphically younger than both the latest Devonian Taffs Well plant assemblage in Tongwynlais, Cardiff and the assemblage from Croyde Hoe Quarry on Baggy Point, north Devon (Fairon-Demaret 1986; Higgs *et al.* 1988; Hilton and Edwards 1996, in press), both of which contain abundant preovulate remains (Hilton 1996).

DESCRIPTION OF SPECIMENS

The description is based on 68 complete specimens and more than 30 incomplete ones. All specimens are detached from the parent plant and most show evidence of a highly prominent pedicel (Text-figs 1–2; Pl. 1, figs 1–4; Pl. 2, figs 1–4). The pedicel widens towards the chalaza of the preovule which is not clearly distinguishable because there is no distinction between the base of the preovule and the end of the pedicel. The pedicel is up to 5·1 mm long and tapers proximally to a point, presumably marking the place of preovule detachment (e.g. Text-fig. 1; Pl. 1, figs 1–3).

The overall outline of the preovule is ovate (Pl. 1, figs 1–4; Pl. 2, figs 1–3). Specimens typically have similarly convex outermost integumentary surfaces in all orientations encountered, indicating that the preovules were radially isodiametric prior to compression. The chalazal third of the integument is entire and the distal two-thirds are divided into three (rarely four) lobes (Pl. 1, figs 1, 4–5; Pl. 2, figs 1–4, 6). Each lobe is laminar in cross section and is curved around the outside of the nucellus and tapers distally to an obtuse apex (Pl. 2, figs 1–3). Both the inner and outer surfaces

of the preintegument are glabrous except for fine surface ribbing that is seen only on better preserved specimens, with ribs typically 1–2 μm wide and 5–10 μm apart from each other.

The nucellus is often visible between the preintegumentary lobes. The thin mineral film present between the preintegument and the nucellus indicates that the nucellus is free except for basal attachment where the nucellus is adnate to the chalazal portion of the preintegument (Text-fig. 1; Pl. 1, figs 1–7). This mineral film is similar to that described by Hilton and Edwards (1996), occurring between the preintegument and the nucellus of *Aglosperma quadrapartita* Hilton and Edwards, 1996. The outline of the nucellus follows the inner surface of the preintegument for approximately two-thirds of preovule length with the nucellar apex occurring above this point (Pl. 1, fig. 1; Pl. 2, fig. 6). The outer surface of the nucellus is usually glabrous. One specimen has preserved cellular detail, indicating that the outer layer of the nucellus consists of elongated epidermal cells which have a striated appearance. Another specimen possesses distinct ornamentation on the outer surface of the nucellus reminiscent of desiccation cracks, but this is not considered to be an original characteristic of the preovule.

Twelve specimens show well preserved nucellar apices and hence the form of the distal apparatus for microspore (pre-pollen/pollen) capture. The nucellus tapers towards the apex, presumably outlining the position of the functional megaspore (Text-fig. 1; Pl. 1, figs 4–7; Pl. 2, figs 6–8) although the latter has not been observed. The nucellar apex is cylindrical in form, comprising a dome-shaped pollen chamber where the approximate position of the pollen chamber floor can be discerned (Text-fig. 1; Pl. 1, figs 6–7; Pl. 2, figs 3–7). Above the pollen chamber is an elongate cylindrical salpinx (Text-fig. 1; Pl. 1, figs 6–7) the distal extremity of which commonly is irregular, suggesting it to be either incomplete or more probably with an irregular apex in life (Pl. 2, fig. 5). In some cases it flares outwards distally (Text-fig. 1A; Pl. 2, fig. 5) whilst in others it tapers distally (Text-fig. 1B; Pl. 1, figs 6–7; Pl. 2, figs 6–8). In certain specimens the salpinx protrudes beyond the exterior of the integument through the distal integumentary aperture (Text-fig. 1A, D–E; Pl. 1, figs 6–7) whilst in other specimens the nucellar apex is contained within the length of the integument (Text-fig. 1C; Pl. 2, figs 4–8). *Aglosperma avonensis* is reconstructed in Text-figure 3 showing the more commonly occurring three lobed form.

SYSTEMATIC PALAEONTOLOGY

Class LAGENOSPERMOPSIDA *sensu* Cleal, 1994
Order LAGENOSTOMALES Seward, 1917
Family GENOMOSPERMACEAE Long, 1975

Genus AGLOSPERMA Hilton and Edwards, 1996, nov. emend.

Type species. Aglosperma quadrapartita Hilton and Edwards, 1996.

Emended diagnosis. Acupulate preovule situated singly and terminally on long axis (pedicel). Preintegument lobate, fused in approximately basal third or less of preovule length, and widest at point where integumentary fusion ends. Preintegument vascularized with one strand per lobe. Micropyle absent. Nucellus free from the integument except at basal attachment. Nucellus glabrous and ovate in outline below pollen chamber. Distal nucellar apex with pollen chamber and long salpinx.

Remarks. The generic diagnosis is emended very slightly from that in Hilton and Edwards (1996) to incorporate characteristics of the new material and to remove characters which, with the discovery of an additional species, are now considered specific. Thus, characters relating to the number and shape of the preintegumentary lobes have been removed from the original diagnosis of the genus.

Aglosperma avonensis sp. nov.

Plates 1–2; Text-figures 1–3

Derivation of name. Avonensis from the Avon area, relating to the source of the material from the Avon Gorge, Bristol.

Holotype. NMW.97.10G.1a (part) NMW.97.10G.1b (counterpart), a complete adpressed preovule, National Museums and Galleries of Wales, Cardiff, Wales, UK.

Horizon and age. Shirehampton Beds, Upper Old Red Sandstone, Bristol district: VI miospore biozone of the Tournaisian, Lower Carboniferous.

Diagnosis. As for genus. Preovule excluding pedicel 4·7–7·1 mm long ($\bar{x}$ = 5·78 mm, n = 34), 2·6–4·2 mm wide ($\bar{x}$ = 3·56 mm, n = 34). Pedicel tapers, widening towards junction with preovule, up to 2·4 mm wide and < 5·1 mm long. Integument lobate in distal two-thirds or more with typically three preintegumentary lobes and less commonly four. Each preintegument lobe laminar in cross section and curved around the outside of the nucellus. Preintegument lobes tapering to an obtuse apex and with fine surface ribbing on inner and outer surfaces. Preintegument thickness 0·35 mm towards chalaza and thinning to 0·1 mm distally. Nucellus 3·9–5·5 mm long ($\bar{x}$ = 4·5 mm, n = 16) and 2·1–2·8 mm ($\bar{x}$ = 2·4 mm, n = 16) with maximum diameter towards the point of attachment. Pollen chamber with distinct pollen chamber floor 0·3–0·8 mm long ($\bar{x}$ = 0·7 mm, n = 12) and 0·7–1·1 mm wide ($\bar{x}$ = 0·85 mm, n = 12). Cylindrical salpinx *c.* one-third of pollen chamber width at distal end of pollen chamber.

EXPLANATION OF PLATE 2

Figs 1–8. *Aglosperma avonensis* sp. nov.; Avon Gorge plant assemblage. 1, NMW.97.10G.6; poorly preserved preovule where much of the organic material has lifted off. Two preintegumentary lobes are visible, each in approximate plan view, although only the right hand lobe has a complete rounded apex; ×8. 2, NMW.97.10G.7; single preovule with three preintegumentary lobes, each with a rounded apex and fused in the chalazal one-third of the preovule or less. The lobe to the right is in section while the central one is in plan view and the one to the left is obliquely orientated. The pointed pedicel is prominent; ×8. 3, NMW.97.10G.8; preovule with three preintegumentary lobes, the central one in plan view with a rounded apex and two lateral lobes each in an oblique orientation with the outer surface exposed. The integument is fused only towards the chalaza for approximately one-quarter of the preovule's length. The pedicel is incomplete but has the characteristic tapering appearance; ×9. 4, NMW.97.10G.9; preovule with long tapering pedicel and an incomplete preintegument. The nucellar apex is well preserved comprising a dome-shaped pollen chamber with a distally broadening salpinx situated distally from the pollen chamber. One integumentary lobe is visible to the right of the nucellus and another present to the left, below the nucellus. The third lobe has been removed to reveal the nucellus. The nucellar apex is enlarged in fig. 5; ×9. 5, NMW.97.10G.9; enlargement of the nucellar apex shown in fig. 4, showing the position of the pollen chamber and the salpinx and the irregular distal margin of the salpinx; ×27. 6, NMW.97.10G.10; basally incomplete preovule with two preintegumentary lobes beneath the central nucellus. A third lobe has been removed by dégagement to reveal the nucellus below, enlarged in fig. 8. The nucellar apex does not extend beyond the tips of the integumentary lobes; ×8. 7, NMW.97.10G.2d; enlargement of the right-most preovule in Pl. 1, fig. 1. This specimen displays two preintegumentary lobes, one either side of the nucellus. The lobe to the left is revealed in section whilst the one to the right is obliquely oriented. The nucellar apex comprises a cylindrical salpinx extending distally from a dome-shaped pollen chamber; ×15. 8, NMW.97.10G.10; enlargement of the nucellar apex shown in fig. 6 with long, cylindrical salpinx situated distally on a dome-shaped pollen chamber; ×14. All specimens are illuminated by multi-directional, low angled, polarized light to reveal features otherwise not visible in conventional lighting.


1


2


3


4

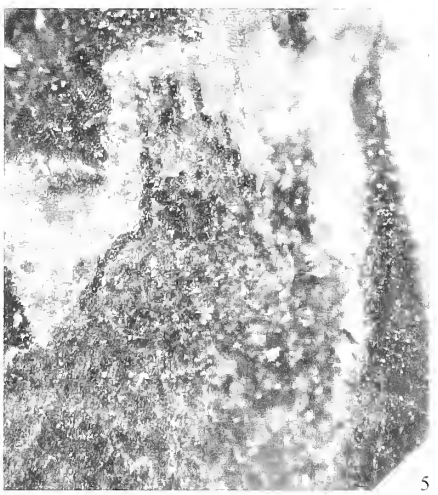
5


6

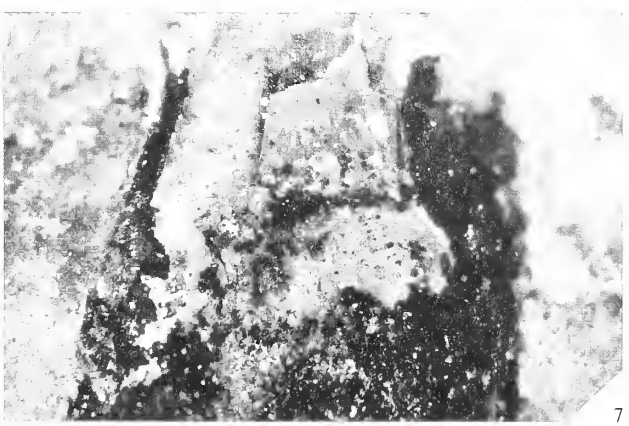
7

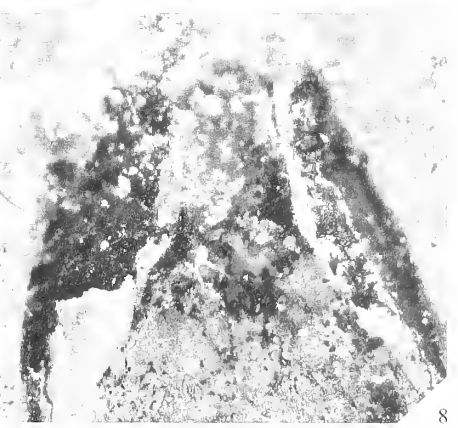
8

HILTON, *Aglosperma*

DISCUSSION

Comparison with other taxa

This new preovule is distinct from *Aglosperma quadrapartita* Hilton and Edwards, 1996 in a number of ways despite the presence of certain shared characteristics. Both *A. quadrapartita* and the new specimens are isodiametric in cross section and comprise a nucellus enveloped by a preintegument. Both species have similar levels of preintegumentary lobe fusion (fused in approximately the chalazal one-third) and have similar low levels of fusion of the preintegument to the nucellus. The preintegument of both species is finely striated, without hairs or glands, and is laminar when viewed in compressed transverse section. The size range of the two species overlap, although *A. quadrapartita* is typically longer and thinner. Preintegumentary size comparisons of the two species are shown in Text-figure 4.

The pedicel of *A. quadrapartita* is longer, and does not taper to a point as observed in the new material, with the detachment surface typically being an irregular fracture. *A. quadrapartita* has four preintegumentary lobes whilst the new preovules typically have three lobes, with only two specimens having four lobes. Therefore, the number of preintegumentary lobes between the two preovules is on the whole different, although the number of lobes observed in each species is not mutually exclusive. A further distinction relating to the preintegument is that in *A. quadrapartita* the lobes are lanceolate in outline, tapering to a distal point, whilst in the new species they are more obtuse and lack distinct pointed tips. These differences are confined to specimens at each locality. The nucellus of the new material is typically larger than in *A. quadrapartita* (Text-fig. 5) measured both in absolute terms and in size relative to the preintegument. Both species have a distinct nucellar apex, although in the new specimens the pollen chamber floor and pollen chamber are better defined than in *A. quadrapartita*. Features of the two species are compared in Table 1.

TABLE 1. Comparison of selected features of *Aglosperma quadrapartita* and *Aglosperma avonensis* sp. nov.

Character	*Aglosperma quadrapartita*	*Aglosperma avonensis* sp. nov.
Attachment	Pedicel max. length 12 mm, attenuated apex	Pedicel max. length 6 mm Tapering and with rounded apex
Form	Acupulate, radial symmetry	Acupulate, radial symmetry
Overall length	6–9 mm	6–9 mm
Overall diameter	2·3–4 mm	3–5·5 mm
Integument	4 lobes Fused basal one-third or less Laminar and ribbed Pointed apex 1 vascular strand per lobe	3 (rarely 4) lobes Fused basal one-third or less Laminar and ribbed Rounded apex ?1 vascular strand per lobe
Nucellus	Free from integument Small pollen chamber Long thin salpinx	Free from integument Large pollen chamber Long wide salpinx

The possibility that the new material represents an ontogenetic progression of *Aglosperma quadrapartita* is considered unlikely based on what is known about developmental sequences in other Late Devonian preovules. Rothwell and Scheckler (1988) showed an ontogenetic series in both *Moresnetia zalesskyi* (Stockmans) Fairon-Demaret and Scheckler, 1987 and *Elkinsia polymorpha* Rothwell, Scheckler and Gillespie, 1989, characterized by increases in overall dimensions with maturation post-pollination. If the two sets of specimens were conspecific, but represent different ontogenetic stages, based on size alone it would be expected that the new material would be a more

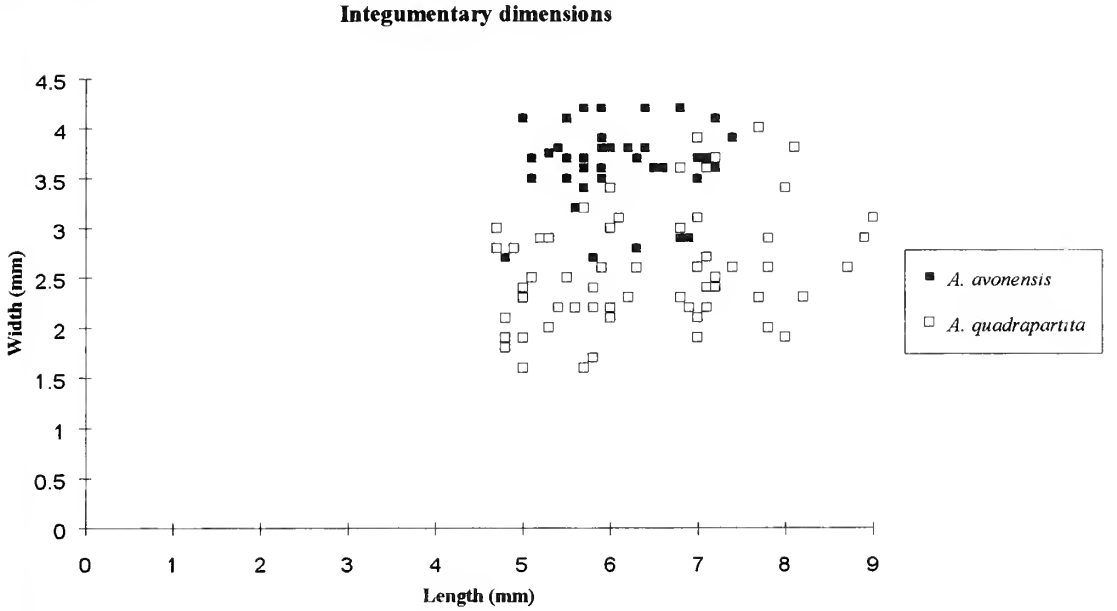

TEXT-FIG. 4. Graph comparing the integumentary dimensions of *Aglosperma quadrapartita* and *Aglosperma avonensis* sp. nov.

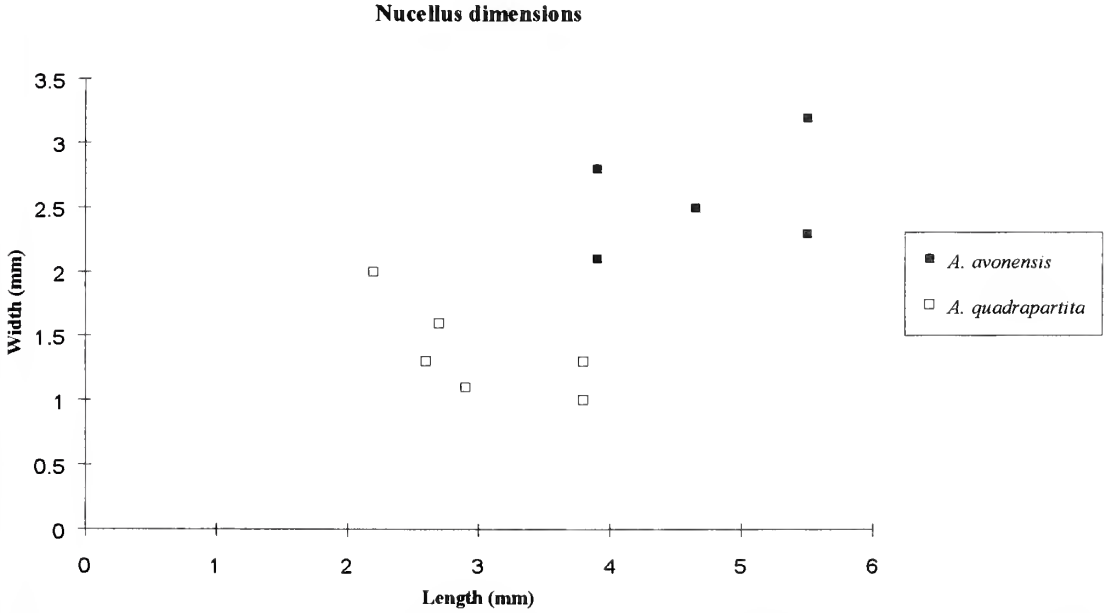

TEXT-FIG. 5. Graph comparing the nucellar dimensions of *Aglosperma quadrapartita* and *Aglosperma avonensis* sp. nov.

mature form of *A. quadrapartita*. Although it is possible that the greater overall nucellar dimensions of the new material could be explained through ontogenetic variation, the combination of other differences, in particular those relating to the form of the preintegument, suggests that this is not

the case. Whilst both species have a similar low degree of preintegumentary fusion at the chalazal end, the new material typically possesses three obtusely tipped integumentary lobes rather than the four lanceolate integumentary lobes observed in *A. quadrapartita*. This quantitative and morphological variation in preintegumentary lobe characteristics is very different from that reported through developmental sequences in other ovulate structures, where changes are in size rather than lobe shape and number (Rothwell and Scheckler 1988). Therefore, the combined differences of the integument and the nucellus are here considered sufficient to discount the new material as being an ontogenetic variant of *A. quadrapartita* resulting in the erection of a second species of the genus. For further comparison of the genus *Aglosperma* with other Palaeozoic preovule taxa, see Hilton and Edwards (1996).

Pollination biology

The material described here presents clear evidence from the external shape of the nucellar apex of *Aglosperma avonensis*, and shows a pollen chamber and tubular salpinx. This combination of characters is in general agreement with the external features present in other early seed plant ovulate structures, in particular those Late Devonian and Early Carboniferous forms displaying hydrasperman reproduction (Rothwell 1986). The distribution of the latter has been given considerable phylogenetic importance, implying monophylesis of the spermatophytes based on its ubiquitous distribution within the earliest seed plants and the improbability of this kind of elaborate reproductive structure having evolved independently more than once (Rothwell 1986; Rothwell and Scheckler 1988; Rothwell and Serbet 1994). In pre-Carboniferous spermatophytes this type of reproduction has previously been verified only in cupulate taxa (e.g. *Moresnetia* (Stockmans) Fairon-Demaret and Scheckler, 1987; *Elkinsia* Rothwell, Scheckler and Gillespie, 1989; *Kerryia* Rothwell and Wight, 1989). Thus, the presence of hydrasperman reproduction in ovulate structures with different architectural models (i.e. the acupulate taxa) has not been ascertained and currently adds no support to theories on the monophylesis of the spermatophytes.

Rothwell (1986) and Rothwell and Scheckler (1988) considered evidence from the exterior morphology of the nucellar apex insufficient to demonstrate the presence of hydrasperman reproduction. In the absence of permineralized preservation it is impossible to observe features within the nucellar apex characteristic of hydrasperman ovules, including a membraneous pollen chamber floor and a central column. The demonstration of internal morphology is essential because a nucellar apex comprising both a pollen chamber and salpinx (= nucellar beak) is not unique to hydrasperman ovules, with similar forms being observed in both medullosan and callistophytalean ovules also of Palaeozoic age (Serbet and Rothwell 1995). The presence of Late Devonian or basal Carboniferous examples of both of these other kinds of pollen chamber organizations is not supported by the fossil record (Serbet and Rothwell 1995).

Hydrasperman, medullosan and callistophytalean patterns of reproduction differ from each other primarily through the processes of post-pollination sealing of the megagametophyte (Serbet and Rothwell 1995). In hydrasperman ovules, sealing is achieved by the pollen chamber floor being pushed outwards by the developing megagametophyte so that the central column seals the base of the spine (Rothwell 1986; Rothwell and Scheckler 1988; Serbet and Rothwell 1995). In ovules displaying the medullosan pattern, sealing off is accomplished by a combination of reduction in the size of the opening of the nucellar beak and the deposition of mucilaginous or resinous substances at the tip of the nucellar beak (Serbet and Rothwell 1995). Therefore, the functioning of the central column characteristic of hydrasperman reproduction has become redundant in medullosan ovules (more typically absent), playing no part in post-pollination sealing off of the megagametophyte. In both hydrasperman and medullosan patterns, sealing of the megagametophyte is entirely through tissues of the nucellus. In the megagametophyte of callistophytalean ovules it occurs from the combination of the closure of the nucellar beak (either through deposition of mucilaginous/resinous substances or through enlargement of the cells at the nucellar beak) and closure of the micropyle of the integument around the nucellus.

To date, hydrasperman reproduction has been ascertained in all permineralized Devonian and basal Carboniferous ovulate structures where the combination of characteristics include both a pollen chamber and salpinx. Furthermore, only one preovulate structure of the same age has been proven to be non-hydrasperman, possessing a parenchymous nucellar beak rather than a hydrasperman-type pollen chamber (*Coumaisperma*; Galtier and Rowe 1989, 1991). In this regard it seems most probable that *Aglosperma avonensis* too was hydrasperman although further evidence in the form of permineralized anatomy is necessary to confirm this important point. Rather than presenting evidence for a diphyletic origin for the spermatophytes (as suggested by Hilton and Edwards 1996) it is here suggested that *Aglosperma* more probably presents evidence for a rapid morphological radiation of the seed-plants from a common ancestor. However, whether this hypothetical ancestor was cupulate or acupulate is a matter of considerable debate.

Further considerations

In the absence of evidence of the morphology of the parent plant, both species of *Aglosperma* have been interpreted as being acupulate (*sensu* Hilton and Edwards 1996). This implies that, beyond the known length of the pedicel, the preovule was attached directly to the parent plant and not enclosed within a cupule. The preintegument of *Aglosperma* is clearly distinct from definite cupulate preovules in being considerably larger (up to twice the size) and the free integumentary lobes of both species of *Aglosperma* are laminate in transverse section, rather than the terete cylindrical lobes observed in cupulate forms. This feature of preintegumentary lobe shape is so far unique to *Aglosperma* among contemporaneous spermatophytes. Furthermore, *Aglosperma* occurs terminally on a slender axis rather than on a short pedicel adnate to the cupule. From these distinguishing features Hilton and Edwards (1996) separated *Aglosperma* from contemporaneous cupulate morphologies and subsequently advocated an acupulate nature for the genus.

The discovery of *A. avonensis* indicates that the genus is not limited to a single location as previously thought (Hilton and Edwards 1996). As both the Avon Gorge and the Taff Gorge were situated on the southern margin of St George's land in the Late Devonian (Cope *et al.* 1992), the new discovery suggests that the genus (amongst other spermatophytes) was possibly common in this palaeogeographical region (Hilton 1996). Furthermore, from the stratigraphical occurrences of the two species of *Aglosperma* it may be deduced that the three lobed forms are derived from the older four lobed forms, although further species and occurrences would be desirable to verify this point.

Evidence for the cosmopolitan distribution of the genus comes from identification (by the author) of *Aglosperma quadrapartita* from a Late Devonian locality in Russia, dated on miospores as VCo miospore zone (M. Fairon-Demaret, pers. comm. 1995). This occurrence places acupulate preovules contemporaneous with the earliest cupulate forms and indicates that acupulate preovules were geographically widespread by the end of the Devonian. However, based on current evidence, acupulate preovules were not as widely distributed as cupulate forms, which have been recorded from North America (*Elkinsia polymorpha* Rothwell, Scheckler and Gillespie, 1989 and *Archaeosperma arnoldii* Pettit and Beck, 1968), Europe (*Moresnetia zalesskyi* (Stockmans) Fairon-Demaret and Scheckler, 1987; *Xenotheca devonica* (Arber and Goode) *emend.* Hilton and Edwards, in press and *Kerryia mattenii* Rothwell and Wight, 1989) and Russia (*Moresnetia* sp., Pettitt and Beck, 1968; *Lenlogia kryshtofovichii* (Radtchenko) Krassilov and Zakharova, 1995).

The distribution of *Aglosperma* has consequences for phylogenetic analyses of the seed plants (e.g. Crane 1985; Doyle and Donoghue 1986, 1992; Nixon *et al.* 1994; Rothwell and Serbet 1994) which identify the cupulate morphologies (i.e. those with the moresnetian architectural model *sensu* Hilton and Edwards in press) as characteristic of the earliest seed plants. In such analyses there is now the need to identify an additional (although lesser known) seed plant morphotype.

CONCLUSIONS

The possibility that the new material represents an ontogenetic stage of *Aglosperma quadrapartita* is discounted based on the overall morphological distinction from *A. quadrapartita*. This has led to

the taxonomic separation of the two sets of preovules although, due to their overall morphological similarity, they have been placed within the same genus. However, it is evident that without permineralized preservation it is impossible to ascertain unequivocally whether *Aglosperma* possessed hydrasperman pollination biology although this seems the most likely interpretation of the nucellar organization observed.

Aglosperma avonensis adds to the morphological diversity of the early seed plants and indicates that they were both widespread and numerous, constituting an increasingly more common component of earliest Carboniferous floras. Furthermore, new information on the distribution of the genus *Aglosperma* indicates that it was contemporaneous with the earliest cupulate preovules.

Acknowledgements. Financial support for this research was provided by a NERC research studentship GT4/92/277/G supervised by D. Edwards whom I acknowledge for helpful advice and criticism. R. H. Wagner (Cordoba, Spain) is thanked for making the initial collections from the Avon Gorge locality and for making the material available for this study. I am grateful to M. Fairon-Demaret (Liège) and S. E. Scheckler (Blacksburg, Virginia) for discussion and N. P. Rowe (Montpellier) for reviewing the manuscript. L. Axe, J. Crawley and V. Williams are thanked for technical assistance. I also acknowledge the time and effort given by my various field assistants in collecting from a truly horrible location: C. M. Berry, I. B. Butler, A. Faragher, A. R. Hemsley, M. Holmes, C. H. Wellman, E. Morel, Bao-Yin Geng, S. Morris, A. Miles and S. J. Woodland.

REFERENCES

CLEAL, C. J. 1994. Gymnospermophyta. 795–808. *In* BENTON, J. J. (ed.). *The fossil record 2*. Chapman and Hall, London, 845 pp.

COPE, J. C. W., INGHAM, J. K. and RAWSON, P. F. 1992. Atlas of palaeogeography and lithofacies. *Memoir of the Geological Society of London*, **13**, 1–153.

CRANE, P. R. 1985. Phylogenetic analysis of seed-plants and the origins of the angiosperms. *Annals of the Missouri Botanical Garden*, **72**, 716–793.

DOYLE, J. A. and DONOGHUE, M. J. 1986. Seed plant phylogeny and the origin of angiosperms: an experimental cladistic approach. *Botanical Review*, **52**, 321–431.

—— —— 1992. Fossils and seed plant phylogeny reanalyzed. *Brittonia*, **44**, 89–106.

FAIRON-DEMARET, M. 1986. Some uppermost Devonian megafloras: a stratigraphical review. *Annales de la Société Géologique de Belgique*, **109**, 43–48.

—— and SCHECKLER, S. E. 1987. Typification and redescription of *Moresnetia zalesskyi* Stockmans, 1948, an early seed plant from the Upper Famennian of Belgium. *Bulletin de l'Institut Royal des Sciences Naturelles de Belgique*, **57**, 183–199.

GALTIER, J. and ROWE, N. P. 1989. A primitive seed like structure and its implications for early gymnosperm evolution. *Nature*, **340**, 225–227.

—— —— 1991. A new permineralized seed-like structure from the basal-most Carboniferous of France. *Neues Jahrbuch für Geologie und Paläontologie*, **183**, 103–120.

HIGGS, K., CLAYTON, G. and KEEGAN, J. B. 1988. Stratigraphic and systematic palynology of the Tournasian rocks of Ireland. *Special Paper of the Geological Survey of Ireland*, **7**, 1–47.

HILTON, J. 1996. Famennian–Tournaisian plant assemblages from south-west Britain. Unpublished Ph.D. Thesis, University of Wales, Cardiff.

—— and EDWARDS, D. 1996. A new Late Devonian acupulate preovule from Taffs Well, South Wales. *Review of Palaeobotany and Palynology*, **93**, 235–252.

—— —— in press. New data on *Xenotheca devonica* Arber and Goode, an enigmatic early seed plant with cupulate preovules. *In* KURMANN, M. and HEMSLEY, A. R. (eds). *The evolution of plant architecture*. Royal Botanic Gardens, Kew, London.

KRASSILOV, V. A. and ZAKHAROVA, T. V. 1995. *Moresnetia*-like plants from the Upper Devonian of Minusinsk basin, Siberia. *Palaeontological Journal*, **29**, 35–43.

LECLERCQ, S. 1960. Refendage d'un reche fossilifière et dégagement de ses fossiles sous binoculaire. *Senckenberg Lethiaea*, **41**, 483–487.

LONG, A. G. 1975. Further observations on some Lower Carboniferous seeds and cupules. *Transactions of the Royal Society of Edinburgh*, **69**, 278–293.

NIXON, K. C., CREPET, W. L., STEVENSON, D. and FRIIS, E. M. 1994. A reevaluation of seed-plant phylogeny. *Annals of the Missouri Botanical Garden*, **81**, 484–533.

PETTITT, J. M. and BECK, C. B. 1968. *Archaeosperma arnoldii* – a cupulate seed from the Upper Devonian of North America. *Contributions to the Paleontological Museum, University of Michigan*, **22**, 139–154.

ROTHWELL, W. G. 1986. Classifying the earliest gymnosperms. 137–162. *In* SPICER, R. A. and THOMAS, B. A. (eds). *Systematic and taxonomic approaches in palaeobotany*. Systematics Association Special Volume No. 31. Clarendon Press, Oxford, 321 pp.

—— and SCHECKLER, S. E. 1988. Biology of ancestral gymnosperms. 85–134. *In* BECK, C. B. (ed.). *Origins and evolution of gymnosperms*. Columbia University Press, New York, 504 pp.

—— —— and GILLESPIE, W. H. 1989. *Elkinsia* gen. nov., a late Devonian gymnosperm with cupulate ovules. *Botanical Gazette*, **150**, 170–189.

—— and SERBET, R. 1994. Lignophyte phylogeny and the evolution of spermatophytes: a numerical cladistic analysis. *Systematic Botany*, **19**, 443–482.

—— and WIGHT, D. C. 1989. *Pullaritheca longii* gen. nov. and *Kerryia mattenii* gen. et sp. nov., Lower Carboniferous cupules with ovules of the *Hydrasperma tenuis*-type. *Review of Palaeobotany and Palynology*, **60**, 295–309.

SERBET, R. and ROTHWELL, G. W. 1992. Characterising the most primitive seed ferns. 1. A reconstruction of *Elkinsia polymorpha*. *International Journal of Plant Science*, **53**, 602–621.

—— —— 1995. Functional morphology and homologies of gymnospermous ovules: evidence from a new species of *Stephanospermum* (Medullosales). *Canadian Journal of Botany*, **73**, 650–661.

SEWARD, A. C. 1917. *Fossil plants*. Cambridge University Press, Cambridge, 318 pp.

STOCKMANS, F. 1948. Végétaux du Dévonien Supérior de la Belgique. *Mémoires du Musée Royal d'Histoire Naturelle de Belgique*, **110**, 1–85.

UTTING, J. and NEVES, R. 1969. Palynology of the Lower Limestone Shale Group (Basal Carboniferous Limestone series) and Portishead Beds, (Upper Old Red Sandstone) of the Avon Gorge, Bristol, England. *Colloque sur la Stratigraphie du Carbonifère, Congrès et Colloques, Université Liège*, **55**, 411–422, pl. 2.

JASON HILTON
Department of Earth Sciences
Cardiff University
PO Box 914
Cardiff CF1 3YE, UK

Typescript received 6 February 1997
Revised typescript received 20 October 1997

NOTES FOR AUTHORS

The journal *Palaeontology* is devoted to the publication of papers on *all aspects* of palaeontology. Review articles are particularly welcome, and short papers can often be published rapidly. A high standard of illustration is a feature of the journal. Six parts are published each year and are sent free to all members of the Association. *Typescripts* should conform in style to those already published in this journal, and should be sent (with a disk, if possible) to the Secretary of the Publications Committee, **Dr R. Wood, Department of Earth Sciences, University of Cambridge, Downing Street, Cambridge CB2 3EQ,** who will supply detailed instructions for authors on request (these are published in *Palaeontology* 1996, **39**, 1065–1075).

Special Papers in Palaeontology is a series of substantial separate works conforming to the style of *Palaeontology*.

SPECIAL PAPERS IN PALAEONTOLOGY

In addition to publishing *Palaeontology* the Association also publishes *Special Papers in Palaeontology*. **Members** may subscribe to this by writing to the Membership Treasurer: the subscription rate for 1998 is £55·00 (U.S. $120) for Institutional Members, and £20·00 (U.S. $36) for Ordinary and Student Members. A single copy of each *Special Paper* is available on a non-subscription basis to Ordinary and Student Members *only*, for their personal use, at a discount of 25 per cent. below the listed prices: contact the Marketing Manager. **Non-members** may obtain Nos 39–58 (excluding 44) at cover price from Blackwell Publishers Journals, P.O. Box 805, 108 Cowley Road, Oxford OX4 1FH, UK, and older issues from the Marketing Manager. For all orders of *Special Papers* through the Marketing Manager, please add £1·50 (U.S. $3) per item for postage and packing.

PALAEONTOLOGICAL ASSOCIATION PUBLICATIONS

Special Papers in Palaeontology

For full catalogue and price list, send a self-addressed, stamped A4 envelope to the Marketing Manager. Numbers 2–48, excluding 44, are still in print and are available together with those listed below:

49. (for 1993): Studies in palaeobotany and palynology in honour of Professor W. G. Chaloner, F.R.S. Edited by M. E. COLLINSON *and* A. C. SCOTT. 187 *pp.*, 38 *text-figs*, 27 *plates*. Price £50 (U.S. $100).
50. (for 1993): Turonian ammonite faunas from central Tunisia, *by* G. R. CHANCELLOR, W. J. KENNEDY *and* J. M. HANCOCK. 118 *pp.*, 19 *text-figs*, 37 *plates*. Price £40 (U.S. $80).
51. (for 1994): *Belemnitella* from the Upper Campanian and Lower Maastrichtian Chalk of Norfolk, England, *by* W. K. CHRISTENSEN. 84 *pp.*, 22 *text-figs*, 9 *plates*. Price £35 (U.S. $70).
52. (for 1994): Studies on Carboniferous and Permian vertebrates. Edited by A. R. MILNER. 148 *pp.*, 51 *text-figs*, 9 *plates*. Price £45 (U.S. $90).
53. (for 1995): Mid-Dinantian ammonoids from the Craven Basin, north-west England, *by* N. J. RILEY. 87 *pp.*, 51 *text-figs*, 8 *plates*. Price £40 (U.S. $80).
54. (for 1995): Taxonomy and evolution of Llandovery biserial graptoloids from the southern Urals, western Kazakhstan, *by* T. N. KOREN' *and* R. B. RICKARDS. 103 *pp.*, 23 *text-figs*, 14 *plates*. Price £40 (U.S. $80).
55. (for 1996): Studies on early land plant spores from Britain. Edited by C. J. CLEAL. 145 *pp.*, 23 *text-figs*, 28 *plates*. Price £45 (U.S. $90).
56. (for 1996): Fossil and Recent eggshell in amniotic vertebrates: fine structure, comparative morphology and classification, *by* K. E. MIKHAILOV. 80 *pp.*, 21 *text-figs*, 15 *plates*. Price £35 (U.S. $70).
57. (for 1997): Cambrian bradoriid and phosphatocopid arthropods of North America, *by* DAVID J. SIVETER *and* M. WILLIAMS. 69 *pp.*, 8 *text-figs*, 9 *plates*. Price £30 (U.S. $60).
58. (for 1997): Himalayan Cambrian trilobites, *by* P. A. JELL *and* N. C. HUGHES. 113 *pp.*, 10 *text-figs*, 32 *plates*. Price £40 (U.S. $80).
59. (for 1998): Late Ordovician brachiopods from the South China Plate and their palaeogeographical significance, *by* ZHAN REN-BIN *and* L. R. M. COCKS. 70 *pp.*, 15 *text-figs*, 9 *plates*. Price £30 (U.S. $60).

Field Guides to Fossils

These are available only from the Marketing Manager. Please add £1·00 (U.S. $2) per book for postage and packing *plus* £1·50 (U.S. $3) for airmail. Payments should be in Sterling or in U.S. dollars, with all exchange charges prepaid. Cheques should be made payable to the Palaeontological Association.

1. (1983): Fossil Plants of the London Clay, *by* M. E. COLLINSON. 121 *pp.*, 242 *text-figs*. Price £7·95 (U.S. $16) (Members £6 or U.S. $12).
2. (1987): Fossils of the Chalk, *compiled by* E. OWEN; *edited by* A. B. SMITH. 306 *pp.*, 59 *plates*. Price £11·50 (U.S. $23) (Members £9·90 or U.S. $20).
3. (1988): Zechstein Reef fossils and their palaeoecology, *by* N. HOLLINGWORTH *and* T. PETTIGREW. iv+75 *pp.* Price £4·95 (U.S. $10) (Members £3·75 or U.S. $7·50).
4. (1991): Fossils of the Oxford Clay, *edited by* D. M. MARTILL *and* J. D. HUDSON. 286 *pp.*, 44 *plates*. Price £15 (U.S. $30) (Members £12 or U.S. $24).
5. (1993): Fossils of the Santana and Crato Formations, Brazil, *by* D. M. MARTILL. 159 *pp.*, 24 *plates*. Price £10 (U.S. $20) (Members £7.50 or U.S. $15).
6. (1994): Plant fossils of the British Coal Measures, *by* C. J. CLEAL *and* B. A. THOMAS. 222 *pp.*, 29 *plates*. Price £12 (U.S. $24) (Members £9 or U.S. $18).
7. (1996): Fossils of the upper Ordovician, *edited by* D. A. T. HARPER *and* A. W. OWEN. 312 *pp.*, 52 *plates*. Price £16 (U.S. $32) (Members £12 or U.S. $24).

Palaeontology

VOLUME 41 · PART 5

CONTENTS

Printed in Great Britain at the University Press, Cambridge ISSN 0031–0239

Palaeontology

VOLUME 41 · PART 6 · DECEMBER 1998

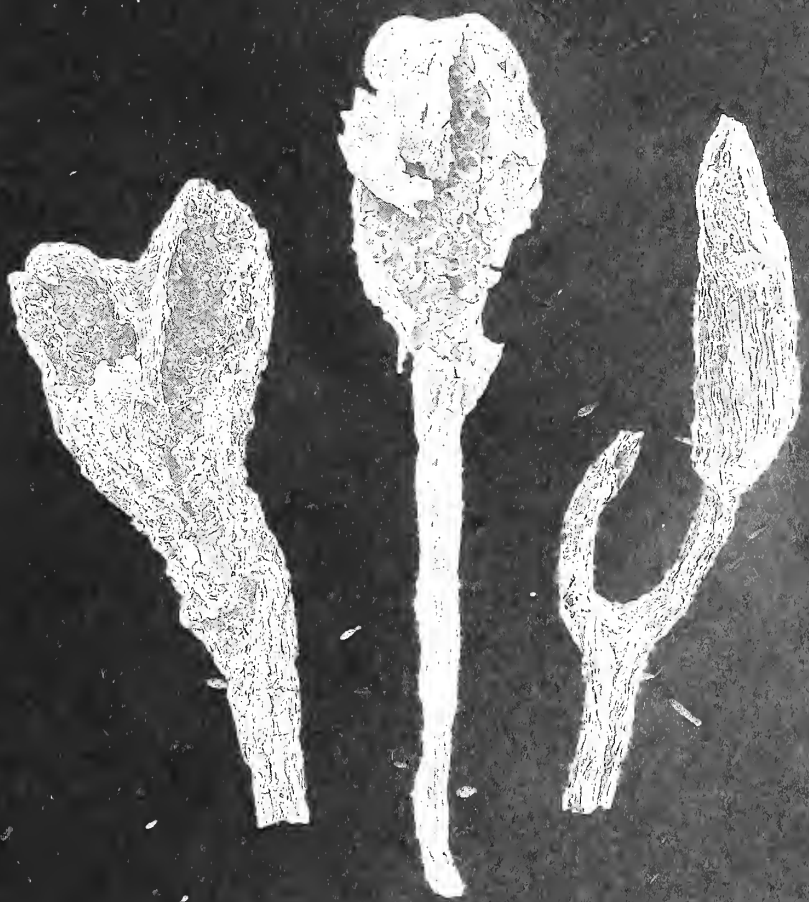

Published by
The Palaeontological Association · London
Price £38·00

THE PALAEONTOLOGICAL ASSOCIATION

(Registered Charity No. 276369)

The Association was founded in 1957 to promote research in palaeontology and its allied sciences.

COUNCIL 1997–1998

MEMBERSHIP

Membership is open to individuals and institutions on payment of the appropriate annual subscription. Rates for 1998 are:

Institutional membership . . .	£90·00 (U.S. $175)	Student membership	£10·00 (U.S. $20)
Ordinary membership . . .	£28·00 (U.S. $50)	Retired membership	£14·00 (U.S. $25)

There is no admission fee. Correspondence concerned with Institutional Membership should be addressed to **Dr J. E. Francis, Department of Earth Sciences, The University, Leeds LS2 9JJ.** Student members are persons receiving full-time instruction at educational institutions recognized by the Council. On first applying for membership, an application form should be obtained from the Membership Treasurer: **Dr M. J. Barker, Department of Geology, University of Portsmouth, Burnaby Road, Portsmouth PO1 3QL.** Subscriptions cover one calendar year and are due each January; they should be sent to the Membership Treasurer. All members who join for 1998 will receive *Palaeontology*, Volume 41, Parts 1–6. Enquiries concerning back numbers should be directed to the Marketing Manager.

Non-members may subscribe, and also obtain back issues up to five years old, at cover price through Blackwell Publishers Journals, P.O. Box 805, 108 Cowley Road, Oxford OX4 1FH, UK. For older issues contact the Marketing Manager.

US Mailing: Periodicals postage paid at Rahway, New Jersey. Postmaster: send address corrections to *Palaeontology*, c/o Mereury Airfreight International Ltd, 2323 E–F Randolph Avenue, Avenel, NJ 07001, USA (US mailing agent).

Cover: coalified terminal sporangia from the Lower Devonian of the Welsh Borderland containing permanent tetrads (far left) and dyads. Similar spores found dispersed in Ordovician rocks are considered the earliest evidence for embryophytic life on land (from left to right, NMW94.76G.1; NMW96.11G.6; NMW97.42G.4. All × 45).

RECENT DINOFLAGELLATE CYSTS IN A TRANSECT FROM THE FALKLAND TROUGH TO THE WEDDELL SEA, ANTARCTICA

by REX HARLAND, CAROL J. PUDSEY, JOHN A. HOWE *and* MERIEL E. J. FITZPATRICK

ABSTRACT. Dinoflagellate cyst analysis has been completed on core-top samples that form a transect from the area of the Falkland Islands to the Weddell Sea, Antarctica. This study is the first to document the distribution of the Recent dinoflagellate cyst thanatocoenosis in the area. All the dinoflagellate cysts recovered are described and at least two species, *Dalella chathamense* and *Selenopemphix antarctica*, are recognized as endemic to the southern hemisphere from the results of this study and from previous research. Data presented here reveal a clear latitudinal trend in the cyst distribution such that subdivision into two domains is possible. The first, to the south of 60° S, is characterized by low numbers of cysts, low diversity and the presence of *Impagidinium pallidum*, *Algidasphaeridium*? *minutum*, *Pentapharsodinium dalei*?, round brown *Protoperidinium* cysts and *Selenopemphix antarctica*. The second, to the north of 60° S, is characterized by richer assemblages, higher species diversity and the presence of *Dalella chathamense*, *Impagidinium sphaericum*, *Nematosphaeropsis labyrinthus* and high numbers of *Selenopemphix antarctica*. This division of the cyst assemblages coincides approximately with the northern winter limit of sea-ice and demonstrates the potential of dinoflagellate cyst analysis in the elucidation of the palaeoceanography of the area using this criterion.

THE seas around the continent of Antarctica play a major rôle in the production of the cold, dense bottom water which is largely responsible for driving the global thermohaline circulation system. Most of the world's bottom water is formed in the large embayments of Antarctica, namely the Weddell and Ross seas, with a minor secondary component deriving from the Nordic seas of the northern hemisphere. The Weddell Sea, under present interglacial conditions, is the source for about 80 per cent. of Antarctic Bottom Water (AABW), which in itself forms a major component of the thermohaline circulation (Foldvik and Gammelsrod 1988). AABW fills all of the deepest parts of the ocean basins bringing its properties of temperature, salinity and carbon isotope composition through the western Atlantic basins as far as 40° N (Kroopnick 1985).

The global thermohaline circulation system is now thought to be a major factor in driving general ocean circulation and its activity is also implicated in the fluctuations of climate that characterize the Quaternary (Broecker *et al.* 1985, 1990). Indeed, the relative stability and long residence time of water within the thermohaline circulation may well act as a buffer in preventing sudden reversals in the climate system. The production of AABW over time is an essential component to understanding of variation in the global thermohaline circulation and its response to changes in solar insolation throughout the Pleistocene. A factor in the production of this cold, dense bottom water is the seasonally variable extent and volume of Antarctic sea-ice. The greater the rate of ice growth the greater the potential formation and flux of AABW. Concern has been expressed recently over the amount of ice retreat in the Antarctic, thought to be as a result of global warming, and the possible consequences to the global circulation pattern.

The Antarctic region is also a well known and important area of upwelling and primary production, with the enhancement of diatom production being a particularly notable feature. Upwelling is caused by northward Ekman transport associated with the strong and persistent West Wind Drift or the Antarctic Circumpolar Current (ACC). This is reinforced by the action of

[Palaeontology, Vol. 41, Part 6, 1998, pp. 1093–1131, 2 pls]

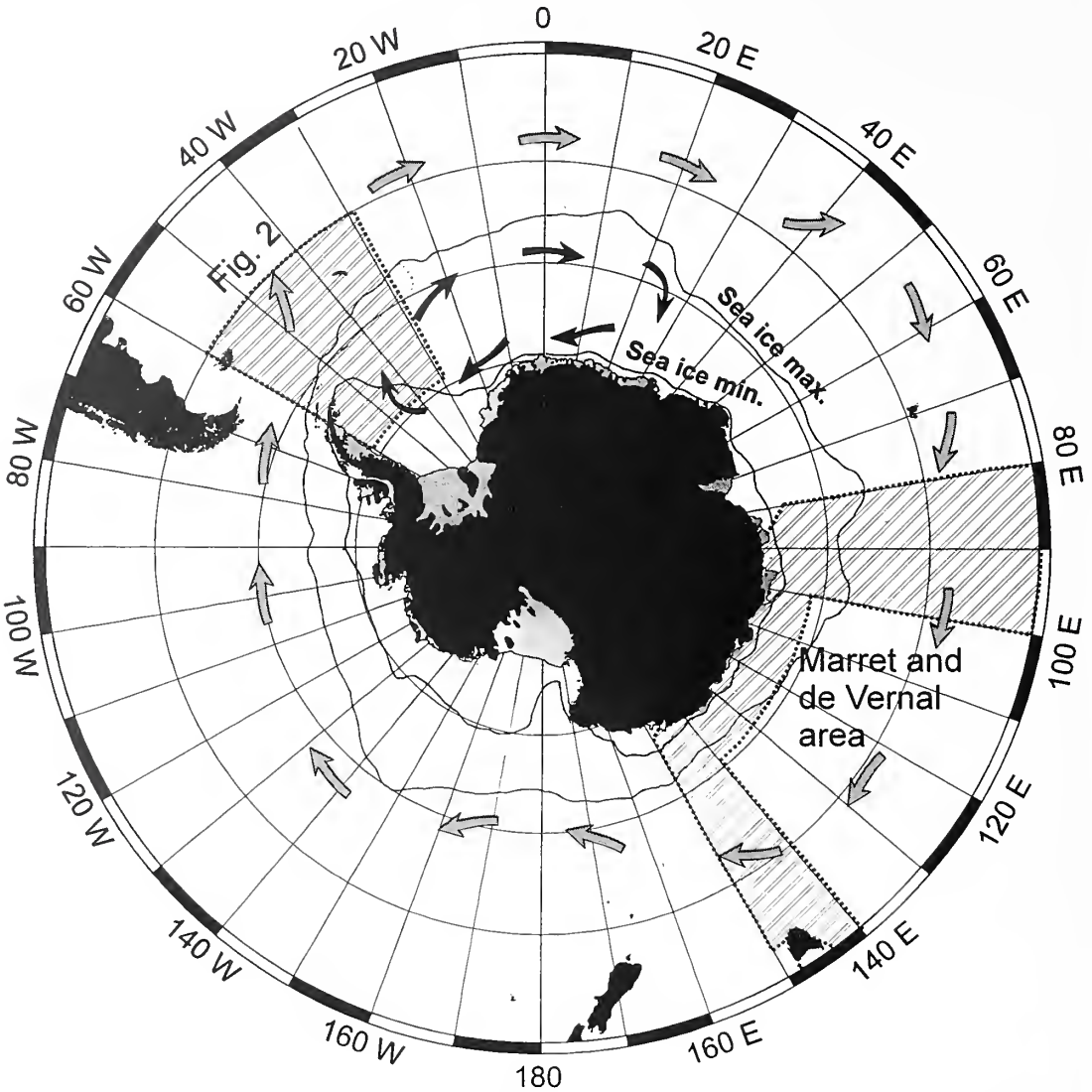

TEXT-FIG. 1. Map of the Antarctic continent and Southern Ocean showing the areas of the present study (Text-fig. 2) and that of Marret and de Vernal (1997). Also depicted are the maximum and minimum sea-ice limits as illustrated in the Sea Ice Climatic Atlas (1985) and the surface water circulation pattern from Nowlin and Klinck (1986). Black arrows, Weddell Gyre; grey arrows, Antarctic Circumpolar Current.

katabatic winds off the ice sheet, forcing surface water in an offshore direction and allowing the upwelling of nutrient-rich water from below the thermocline. This upwelling phenomenon occurs to the south of the Antarctic Convergence or Polar Front within the ACC in the area under discussion herein.

This unique juxtaposition of the production of cold, dense water to drive the global thermohaline circulation system and the upwelling of nutrient-rich water from depth to enhance primary production provides a potential wealth of important information to assist in detailing the changing oceanography of the area through time. In particular the enhanced primary production provides increased carbon fixing and production of a C_{ORG} flux to the accumulating bottom sediments. Also

important is the position of the Polar Front which serves to separate cold, nutrient-rich Antarctic surface water from the warmer, nutrient-poor surface waters of the South Atlantic Ocean. This feature is known to occur between about 55° S and 60° S in this area and, like its counterpart in the northern hemisphere, may have changed its geographical position over time with fluctuations in global climate.

It is, therefore, apparent that temporal fluctuations in the oceanography of the Antarctic region have the potential to provide clear proxy climate signals to assist in the elucidation of changing global climate and the construction of global climate models. In addition, such time series data on the production of oceanic deep water together with data on the fixing of carbon from nutrient rich surface waters will enhance our knowledge of the global carbon budget.

Changing oceanography as a consequence of changing climate produces temporal differences in the sediment record on the continental shelf and deep sea floor, particularly over the glacial to interglacial time scale. Deep sea sediment cores which preserve a complete depositional record are of particular interest. In the Weddell Sea, Scotia Sea and Falkland Trough (Text-figs 1–2) there are extensive areas of Quaternary deposition, mainly of hemipelagic and muddy contourite facies with some sandy contourites in the Falkland Trough. The sediments have been mapped and described by Pudsey *et al.* (1988), Pudsey (1992), Howe *et al.* (1997) and Pudsey and Howe (1998). The cores were dated by magnetostratigraphy (Pudsey *et al.* 1988; O'Brien 1989), diatom and radiolarian abundance stratigraphy (Jordan and Pudsey 1992; Pudsey and Howe 1998) and by chemostratigraphy (Shimmield *et al.* 1994). Sedimentation rates are generally low (4 mm/ky) in the central Weddell Sea and increase northwards to 30–40 mm/ky near 60° S (Grunig 1991) and 70–100 mm/ky in the northern Scotia Sea and Falkland Trough. Lithofacies include muddy diatom ooze and diatom-bearing mud, with a diatom content decreasing southwards and with foraminifera present only near the Polar Front. The high primary productivity of the area and the abundance of diatoms, particularly in the Scotia Sea, pointed to the possibility that a dinoflagellate cyst record may also be present. This is especially true for the heterotrophic dinoflagellates that may well be taking advantage of the high diatom crop (diatoms are known to be one of the prey groups of some of the heterotrophic dinoflagellates). A knowledge of the population of dinoflagellate cysts, produced by both autotrophic and heterotrophic motile forms, provides potential information on both the first and second tiers of the trophic web.

This study aims to establish the occurrence of Recent dinoflagellate cysts in the surface sediments of the Antarctic region and to examine their distribution. In order to fulfil this aim a transect of core-top samples has been examined from the Falkland Trough, to the south and east of the Falkland Islands, to the Weddell Sea, east of the Antarctic Peninsula, south of the Polar Front (Text-fig. 2). This information is essential before any attempt is made to look at the temporal dinoflagellate cyst record. This study establishes a Recent dinoflagellate cyst distribution baseline in relation to the present oceanography. In this context it is important to note that very little information is available on the occurrence of modern dinoflagellate cysts in Antarctica despite the seminal work of Balech (1973, 1976) and Balech and El-Sayed (1965) on the taxonomy and distribution of motile dinoflagellates in the plankton from the area.

Recently, Marret and de Vernal (1997) published a detailed and comprehensive account of the modern distribution of dinoflagellate cysts in the southern Indian Ocean (Text-fig. 1). They recognized the presence of a latitudinal distribution trend that is similar to the distribution patterns described for the Arctic and North Atlantic oceans in the northern hemisphere. Their latitudinal distribution of dinoflagellate cysts in bottom sediments includes circum-Antarctic, Subantarctic and Antarctic domains. McMinn (1995) suggested that there are no dinoflagellate cysts in the bottom sediments of the Antarctic region, an assumption that both Marret and de Vernal (1997) and we refute.

Before the work of Marret and de Vernal (1997), no information was available for the presence or distribution of modern and Recent dinoflagellate cysts in the Southern Ocean. This situation is in marked contrast to that for the North Atlantic Ocean and Nordic Seas where considerable data are now available (see de Vernal *et al.* 1994; Matthiessen 1995; Dale 1996). Some of the more

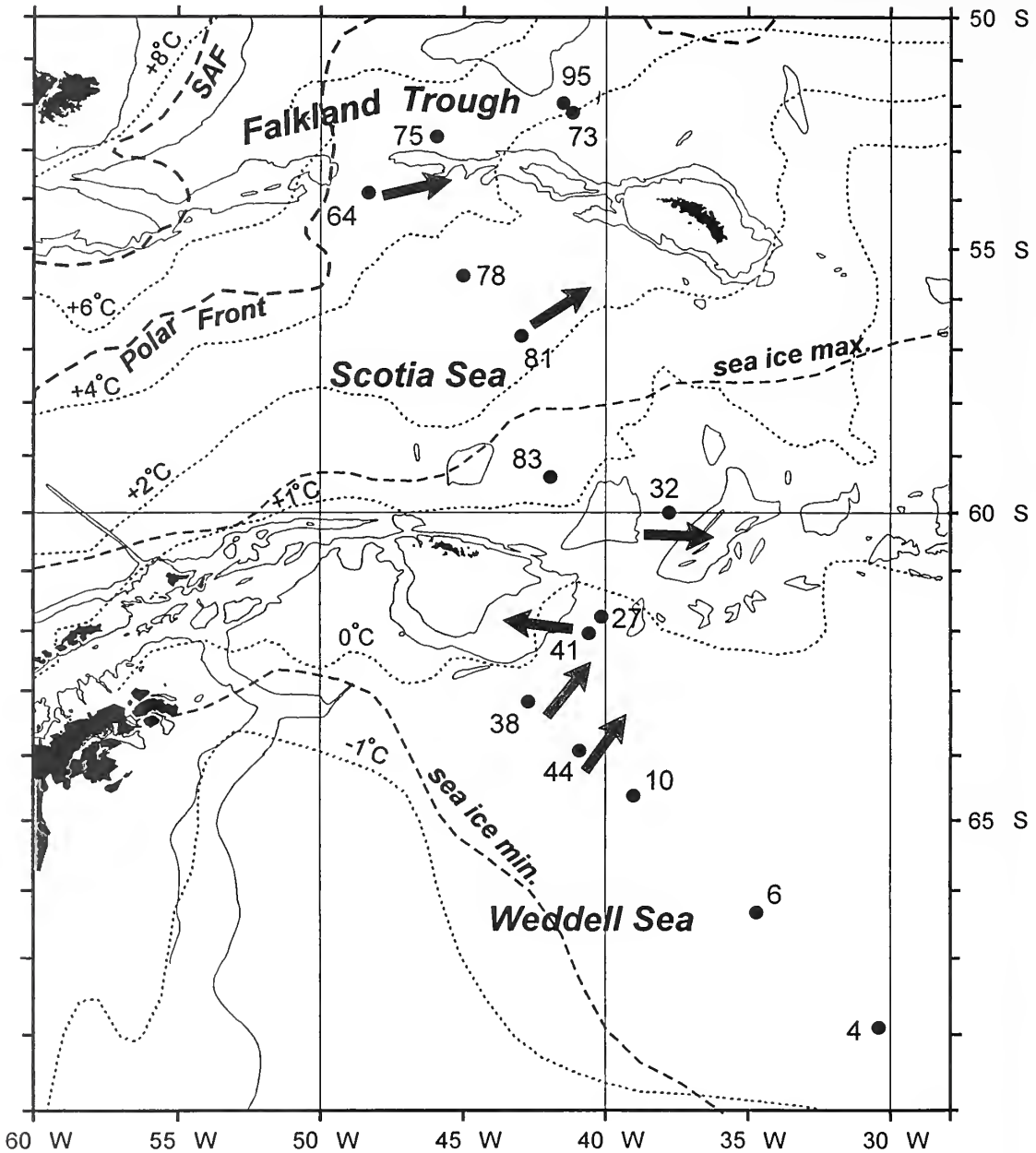

TEXT-FIG. 2. Location map showing the area of study including the Weddell Sea, Scotia Sea and the Falkland Trough with the sites of the core-top samples and various oceanographic parameters including bottom water circulation. Bathymetry (500 m and 2000 m contours) from Tectonic Map of the Scotia Arc (1985). Summer sea surface temperature isotherms from Olbers *et al.* (1992) and maximum and minimum sea-ice limits from Sea Ice Climatic Atlas (1985). SAF is the Subantarctic Front, the northern boundary of subantarctic surface water.

reliable data-sets have been reviewed by Edwards and Andrle (1992) and plotted against known winter and summer sea surface temperature, together with depth of recovery; this has produced the best summation of dinoflagellate cyst ecology to date from the study of bottom sediments. However, bottom sediment assemblages may not, in themselves, provide all the potential information on the modern ecology of dinoflagellate cysts as the data are always severely constrained by a number of factors. Not least is that bottom sediments are often not truly modern but are an integration of the record over hundreds of years due to bioturbation within the mixed layer.

This paper describes the occurrence of Recent dinoflagellate cysts along a transect from the Falkland Trough to the Weddell Sea (Text-fig. 2). This is a preliminary attempt at providing some ecological information, from the recognition of dinoflagellate cyst assemblages in core-top samples and their relationship to the oceanography of the area. A specific aim of this study was to identify any biogeographical signal that would prove useful in elucidating changing oceanographic and climatic conditions through the Pleistocene in the Antarctic region. This is an essential precursor to the analysis of dinoflagellate cysts through time and before any further detailed ecological work is available or attempted. We believe that the study of dinoflagellate cysts in the Antarctic realm will add to the understanding of the global dynamics of oceanographic and climatic change. In particular the extent of sea-ice, and any fluctuations in the nature and strength of the ACC will have an effect on the thermohaline circulation system and the primary production in the area respectively. Using the occurrence of dinoflagellate cysts as proxies for primary production and as a tool for reconstructing the oceanography of the area over time will add to our knowledge of the Antarctic region. The use of dinoflagellate cysts as proxies for climate and oceanographic change in the Quaternary of the Atlantic Ocean is now well established; this study is a first step in using dinoflagellate cysts in the Southern Ocean to this same end.

OCEANOGRAPHY

Comprehensive reviews of the oceanography of the area were given by Orsi *et al.* (1993, 1995). The Scotia Sea and Weddell Sea are dominated by two major current systems and their associated surface-water fronts. The eastward flowing ACC is wind driven, although the flow extends to the sea bed in many areas. The axis of strongest flow coincides with the position of the Polar Front. The Weddell Gyre extends from the western margin of the Weddell Sea (Text-fig. 2) to about 30° E. Flow is clockwise and mainly driven by thermohaline density contrasts in the deep water masses, although there is some wind forcing of surface waters near the coast.

Water masses

At the eastern end of the Weddell Gyre, Circumpolar Deep Water (CPDW) (Text-fig. 3) flows south and then west along the Antarctic continental margin. In the southern and western Weddell Sea, the relatively warm and saline CPDW mixes with very cold and dense shelf water. The resulting mixture is denser than the CPDW and sinks beneath it, flowing downslope as Weddell Sea Bottom Water (WSBW). Newly formed WSBW is the deepest water mass in the northern Weddell Sea; it is colder than −0·7 °C and has an oxygen content of 5·75–6·00 ml/l (Text-fig. 3; Carmack and Foster 1975; Foster and Middleton 1979). It is corrosive to siliceous and calcareous microfossil tests and this, combined with low productivity consequent on the short annual ice-free period, is the reason for the low organic content of Weddell Sea sediments (Pudsey and King 1998).

Between WSBW and the warm core of CPDW at 300–400 m depth is Weddell Sea Deep Water (WSDW) with temperatures of 0 to −0·7 °C. This water mass spreads through deep gaps in the topography into the southern Scotia Sea (Locarnini *et al.* 1993) and via the South Sandwich Trench into the south-western Atlantic where it is termed AABW.

In the northern Weddell Sea, CPDW has a temperature maximum of about 0·4 °C and its upper boundary with AASW is sharp (Text-fig. 3). In winter, the upper 150 m of the water column is close to freezing (Winter Water of Mosby 1934), but in summer a mixed layer develops, 20–30 m thick

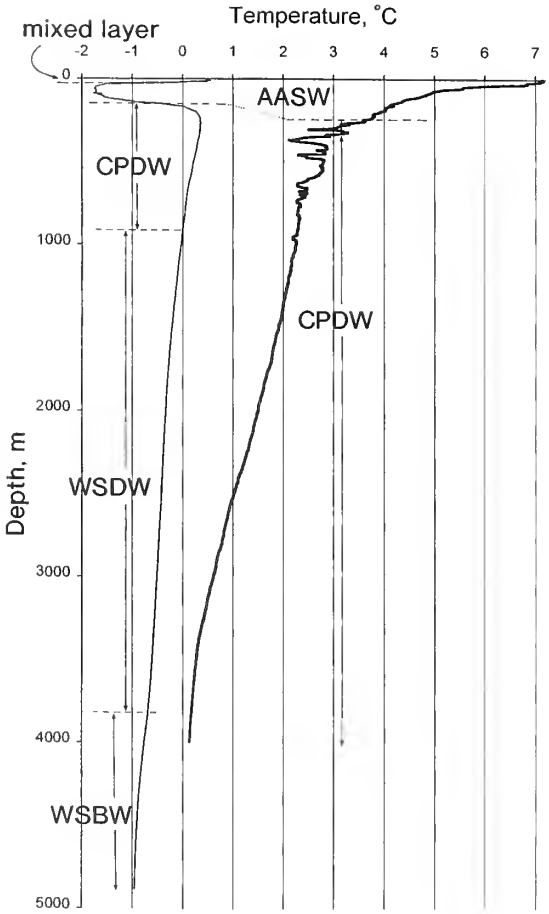

TEXT-FIG. 3. Full depth temperature profile compiled from CTD (conductivity-temperature-depth) and XBT (expendable bathythermograph) casts near the site of core-top 10 in the Weddell Sea (thin line) and near site of core-top sample 64 in the northern Scotia Sea just south-east of the Polar Front (thick line). AASW, Antarctic Surface Water; CPDW, Circumpolar Deep Water; WSBW, Weddell Sea Bottom Water; WSDW, Weddell Sea Deep Water.

and reaching 1 °C. Farther north, the summer mixed layer is deeper (to 80 m) and the AASW is warmer and merges more gradually with CPDW. Near the Polar Front, summer SST is 6–8 °C and temperature decreases downwards through the CPDW to sea bed values of 0–1 °C at 4000 m (Text-fig. 3). CPDW, being warmer and less oxygenated than WSBW, is less corrosive to siliceous and calcareous microfossil tests.

In Text-figure 4 we show temperature profiles at selected core sites, collected during several seasons from 1984–85 to 1992–93. The Weddell Sea sites (4 and 10) are characterized by low and stable temperatures. In the southern Scotia Sea (sites 81 and 83) there is considerable interannual variability, as well as spatial mixing of water masses shown by the small-scale irregularities in the profiles. Farther north at sites 64 and 78 the SST is 4–7 °C and the Winter Water from the south is scarcely discernible. North of the Polar Front at site 62, not included in this study, the region is more stable with less mixing. Interestingly, at sites 73 and 95 there is a Weddell-type temperature structure although these sites are a long way north.

Currents

From Drake Passage to 0° W, near surface velocities of 200–600 mm/s have been measured using current meters and drifting buoys (Nowlin and Clifford 1982; Hofmann 1985; Grose *et al.* 1995). There are few direct measurements of bottom water flow except in Drake Passage, where Bryden and Pillsbury (1977) and Whitworth *et al.* (1982) reported unsteady flow with speeds of up to

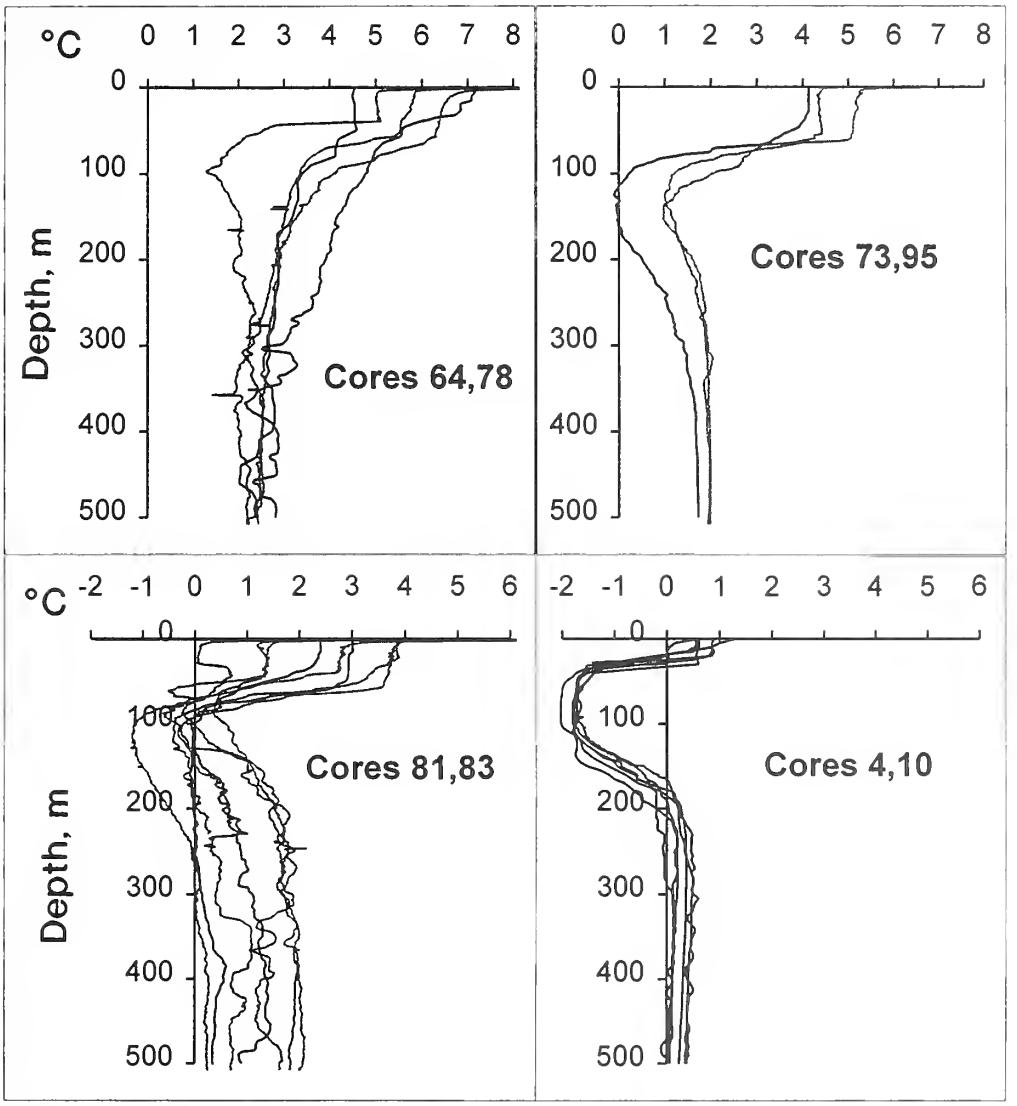

TEXT-FIG. 4. CTD and XBT profiles for the upper 500 m of the water column from areas close to the sites of the core-top samples used in this study. Cores 4 and 10 are typical of all sites from 41 southwards.

100 mm/s at *c.* 2700 m depth. Deep currents have been measured by several 1–2 year deployments of moored current meters within the area of Text-figure 2. The first results were reported by Barber and Crane (1995); bottom water flow was to the north-east at sites 44 and 38 (mean speeds of 28 and 97 mm/s respectively), to the west at site 41 (68 mm/s) and to the east near site 32 (76 mm/s). Two more moorings at the sites of cores 64 and 81 recorded mean speeds of 116 and 125 mm/s, with eastward flow (Pudsey and Howe 1998). These results are all from areas of Quaternary sediment deposition; considerably higher current speeds have been reported from rocky, non-depositional areas (Zenk 1981).

TABLE 1. Location and water depth for each of the core-top samples. All samples were taken from 0–1 mm except GC 027 which was taken from 0–2 mm. GC = gravity core; KC = Kasten core; PC = piston core; TC = trigger core.

Core	Latitude	Longitude	Water Depth (m)	Sea Area
TC 004	67° 55·7′ S	30° 25·50′ W	4546	Weddell Sea
TC 006	66° 20·3′ S	34° 42·99′ W	4694	Weddell Sea
TC 010	64° 37·9′ S	39° 01·20′ W	4802	Weddell Sea
TC 044	63° 56·8′ S	40° 55·90′ W	4548	Weddell Sea
PC 038	63° 10·1′ S	42° 43·40′ W	3802	Weddell Sea
TC 041	62° 03·9′ S	40° 35·20′ W	3310	Weddell Sea
GC 027	61° 47·3′ S	40° 08·30′ W	3470	Weddell Sea
TC 032	60° 00·1′ S	37° 47·20′ W	2915	Scotia Sea
KC 083	59° 22·2′ S	41° 57·90′ W	3900	Scotia Sea
KC 081	56° 44·3′ S	42° 58·10′ W	3662	Scotia Sea
PC 078	55° 33·0′ S	45° 00·90′ W	3840	Scotia Sea
KC 064	53° 52·1′ S	48° 20·30′ W	4304	Scotia Sea
KC 075	52° 40·7′ S	45° 57·60′ W	3388	Falkland Trough
KC 073	52° 09·2′ S	41° 10·70′ W	3760	Falkland Trough
KC 095	51° 56·5′ S	41° 30·40′ W	3402	Falkland Trough

Sea ice

The extent of sea ice varies from a minimum in early March when ice normally occupies only the western Weddell Sea, to a September maximum with the ice edge near 58° S (Sea Ice Climatic Atlas 1985, fig. 1). The pattern of melt-back is north to south in the Scotia Sea and north-west to south-east in the Weddell Sea, because of the continuous clockwise drift of the Weddell Gyre (Pudsey 1992). Cores from sites 4, 6, 10, 44 and 38 are covered by sea ice for eight to nine months of the year, sites 27, 32, 41 and 83 for three to seven months and sites 81 northwards have open water all year around. This is reflected in the diatom flora recovered in cores from the sites with the ice-related form *Fragilariopsis curta* (Van Heurck) Hustedt being rare north of 57° S (Jordan and Pudsey 1992).

MATERIALS AND METHODS

Fifteen core-top samples were used in this study and were taken from various types of core (Table 1) in a transect from the Falkland Trough, to the east of the Falkland Islands, through the Scotia Sea and into the Weddell Sea, to the east of the Antarctic Peninsula (Text-fig. 2; Table 1). The material was recovered as part of the British Antarctic Survey's deep-water coring programme, developed to study climate change and deep-ocean interaction across the area. Cores were taken during cruises onboard the *RRS Discovery* (1984–85 and 1987–88), and the *RRS James Clark Ross* (1993 and 1995). The core-top samples include the top 10 mm of material and, therefore, are an unavoidable integration of the dinoflagellate cyst record over the time span required to deposit that thickness of sediment. The samples were taken from the upper part of the mixed layer and their lithology and the interpreted environments of deposition are detailed in Table 2. All the samples are derived from hemipelagic and contourite areas avoiding any turbiditic sedimentation and are consistent with the known modern sedimentology.

Since we do not have unequivocal proof, from radiometric control, that this core-top material is modern we have, at this stage, made the assumption that the samples are, at least, Holocene in age. However, recent work in the north-east Atlantic Ocean has demonstrated the dynamism of the Holocene dinoflagellate cyst record through the Holocene (Harland and Howe 1995) and ongoing sedimentological research also points to the complexity of Holocene oceanography. For this preliminary study we believe that the data acquired is as close an approximation to a Recent age as can reasonably be expected, given the nature of the samples and their sedimentological regimen.

TABLE 2. Lithology, environment of deposition and mean bottom water current speed from the sampled localities.

Core	Lithology	Area	Process/Environment	Mean Current Speed	Comments
4	Clayey mud	Weddell Sea	Hemipelagic	?	Weddell abyssal plain
6	Clayey mud	Weddell Sea	Hemipelagic	16 mm/s	Weddell abyssal plain
10	Clayey mud	Weddell Sea	Hemipelagic	?	—
44	Clayey mud	Weddell Sea	Hemipelagic	32 mm/s	—
38	Clayey mud	Weddell Sea	Muddy contourite	97 mm/s	—
41	Clayey mud with diatoms	Weddell Sea	Hemipelagic	68 mm/s	—
27	Clayey mud with diatoms	Weddell Sea	Hemipelagic	?	—
32	Muddy diatom ooze	Scotia Sea	Muddy contourite	78 mm/s	—
83	Muddy diatom ooze	Scotia Sea	Pelagic biogenic	?	—
81	Diatom ooze	Scotia Sea	Muddy contourite	125 mm/s	On sediment drifts
78	Muddy diatom ooze	Scotia Sea	Muddy contourite	?	On sediment drifts
64	Diatomaceous mud with foraminifera	Scotia Sea	Muddy contourite	116 mm/s	On sediment drifts
75	Muddy diatom ooze with foraminifera	Falkland Trough	Muddy contourite	?	On sediment drifts
73	Diatom ooze	Falkland Trough	Pelagic biogenic	?	—
95	Muddy diatom ooze	Falkland Trough	Muddy/sandy contourite	?	—

TABLE 3. Raw counts of the dinoflagellate cysts in each of the core-top samples including trophic information where known or surmised. [A] = autotrophic species; [H] = heterotrophic species.

Sample Number	TC 004	TC 006	TC 010	TC 044	PC 038	TC 041	GC 027	TC 032	KC 083	KC 081	PC 078	KC 064	KC 075	KC 073	KC 095
Gonyaulacacean cysts															
Protoceratium reticulatum [A]	/	/	/	/	/	/	/	4	/	/	2	6	/	/	/
Dalella chathamense [A]	/	/	/	/	/	/	/	/	1	3	9	7	8	2	2
Impagidinium aculeatum [A]	/	/	/	/	/	/	/	/	/	/	2	1	/	/	/
Impagidinium pallidum [A]	/	3	6	/	/	/	1	/	/	2	12	/	4	/	/
Impagidinium patulum [A]	/	/	/	/	/	/	/	/	/	1	/	/	3	/	/
Impagidinium sphaericum [A]	/	/	/	/	/	/	/	1	16	31	34	42	23	1	5
Impagidinium spp. indet. [A]	/	/	/	/	/	/	/	2	6	/	4	1	/	1	4
Nematosphaeropsis labyrinthus [A]	/	/	/	/	/	/	/	/	/	2	8	13	5	1	2
Spiniferites ramosus [A]	/	/	/	/	/	/	/	/	/	/	2	4	/	/	1
Spiniferites spp. indet. [A]	/	/	/	/	/	/	/	/	/	/	/	/	1	/	1
Tectatodinium? sp. indet. [A]	/	/	/	/	/	/	/	/	/	/	2	/	1	/	/
Peridiniacean cysts															
Pentapharsodinium dalei? [A]	/	/	/	/	/	6	2	/	/	/	/	1	1	/	/
Congruentidiacean cysts															
Algidasphaeridium? *minutum* [H]	4	/	/	1	11	3	/	/	/	1	/	5	/	9	6
Protoperidinium conicoides [H]	/	/	/	/	/	1	/	3	/	/	3	8	2	2	/
Protoperidinium spp. indet. [round, brown] [H]	8	1	1	/	/	/	5	12	9	32	150	47	7	18	15
Protoperidinium spp. indet. [peridinioid] [H]	/	2	2	/	/	1	/	/	36	/	/	/	/	1	/
Selenopemphix antarctica [H]	5	/	/	/	3	12	11	47	220	289	70	24	163	166	194
Total (n)	17	6	9	1	14	23	19	69	288	361	298	159	218	201	230

TABLE 4. Percentage data of the dinoflagellate cysts in each of the core-top samples.

Sample Number	TC 004	TC 006	TC 010	TC 044	PC 038	TC 041	GC 027	TC 032	KC 083	KC 081	PC 078	KC 064	KC 075	KC 073	KC 095
Gonyaulacacean cysts															
Protoceratium reticulatum	/	/	/	/	/	/	/	5·8	/	/	0·7	3·8	/	/	/
Dalella chathamense	/	/	/	/	/	/	/	/	0·4	0·8	3	4·4	3·7	1	0·9
Impagidinium aculeatum	/	/	/	/	/	/	/	/	/	/	0·7	0·6	/	/	/
Impagidinium pallidum	/	50	66·7	/	/	/	5·3	/	/	0·6	4	/	1·8	/	/
Impagidinium patulum	/	/	/	/	/	/	/	/	/	0·3	/	/	1·4	/	/
Impagidinium sphaericum	/	/	/	/	/	/	/	1·5	5·6	8·6	11·4	26·4	10·6	0·5	2·2
Impagidinium spp. indet.	/	/	/	/	/	/	/	2·9	2·1	/	1·3	0·6	/	0·5	1·7
Nematosphaeropsis labyrinthus	/	/	/	/	/	/	/	/	/	0·6	2·7	8·2	2·3	0·5	0·9
Spiniferites ramosus	/	/	/	/	/	/	/	/	/	/	0·7	2·5	/	/	0·4
Spiniferites spp. indet.	/	/	/	/	/	/	/	/	/	/	/	/	0·5	/	0·4
Tectatodinium? spp. indet.	/	/	/	/	/	/	/	/	/	/	0·7	/	0·5	/	/
Peridiniacean cysts															
Pentapharsodinium dalei?	/	/	/	/	/	26·1	10·5	/	/	/	/	0·6	0·5	/	/
Congruentidiacean cysts															
Algidasphaeridium? *minutum*	23·5	/	/	100	78·5	13	/	/	/	0·3	/	3·2	/	4·5	2·6
Protoperidinium conicoides	/	/	/	/	/	4·4	/	4·4	/	/	1	5	0·9	1	/
Protoperidinium spp. indet. [round, brown]	47·1	16·7	11·1	/	/	/	26·3	/	3·1	8·9	50·3	29·6	3·2	9	6·5
Protoperidinium spp. indet. [peridinioid]	/	33·4	22·2	/	/	4·4	/	17·4	12·5	/	/	/	/	0·5	/
Selenopemphix antarctica	29·1	/	/	/	21·4	52·2	57·9	68·1	76·4	80·1	23·5	15·1	74·8	92·6	84·4
Total (n)	17	6	9	1	14	23	19	69	288	361	298	159	218	201	230

FOLDOUT

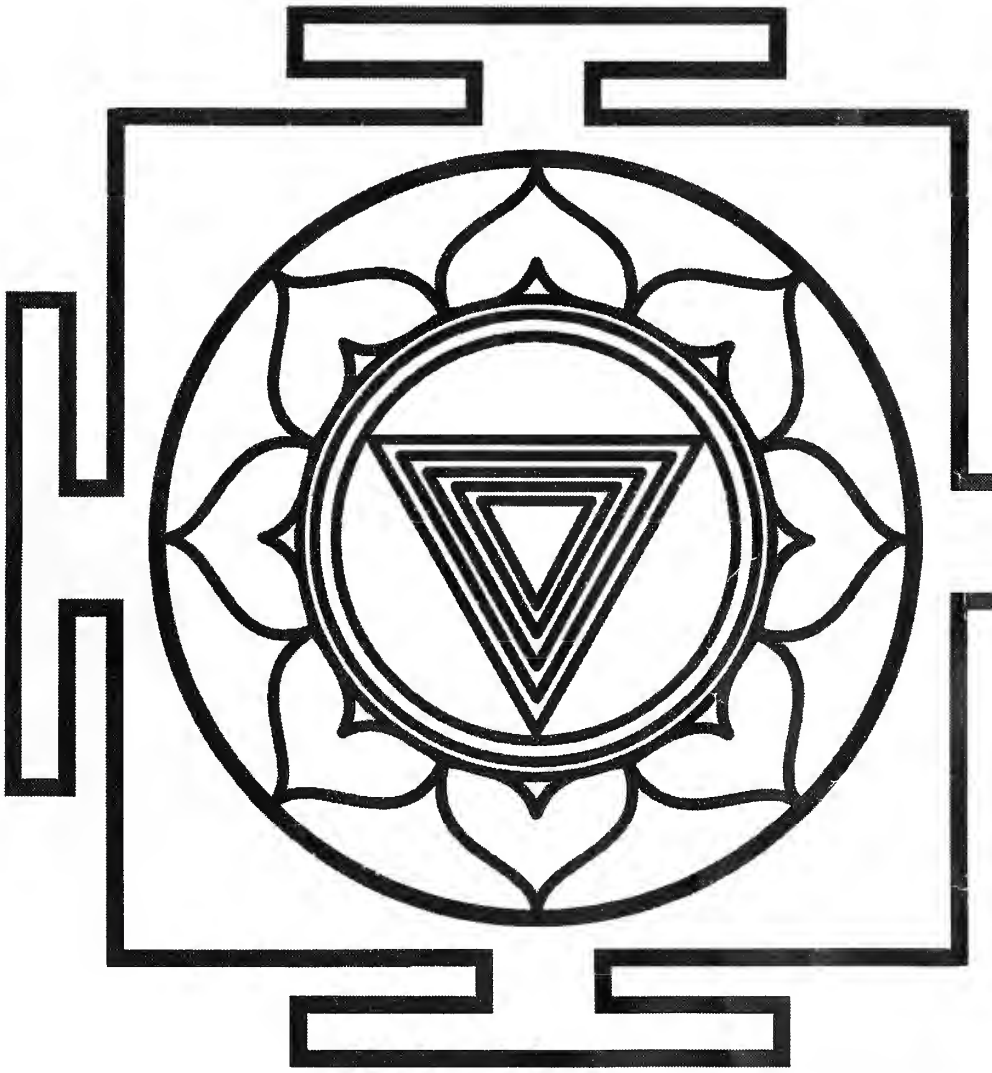

FOLDOUT

FOLDOUT

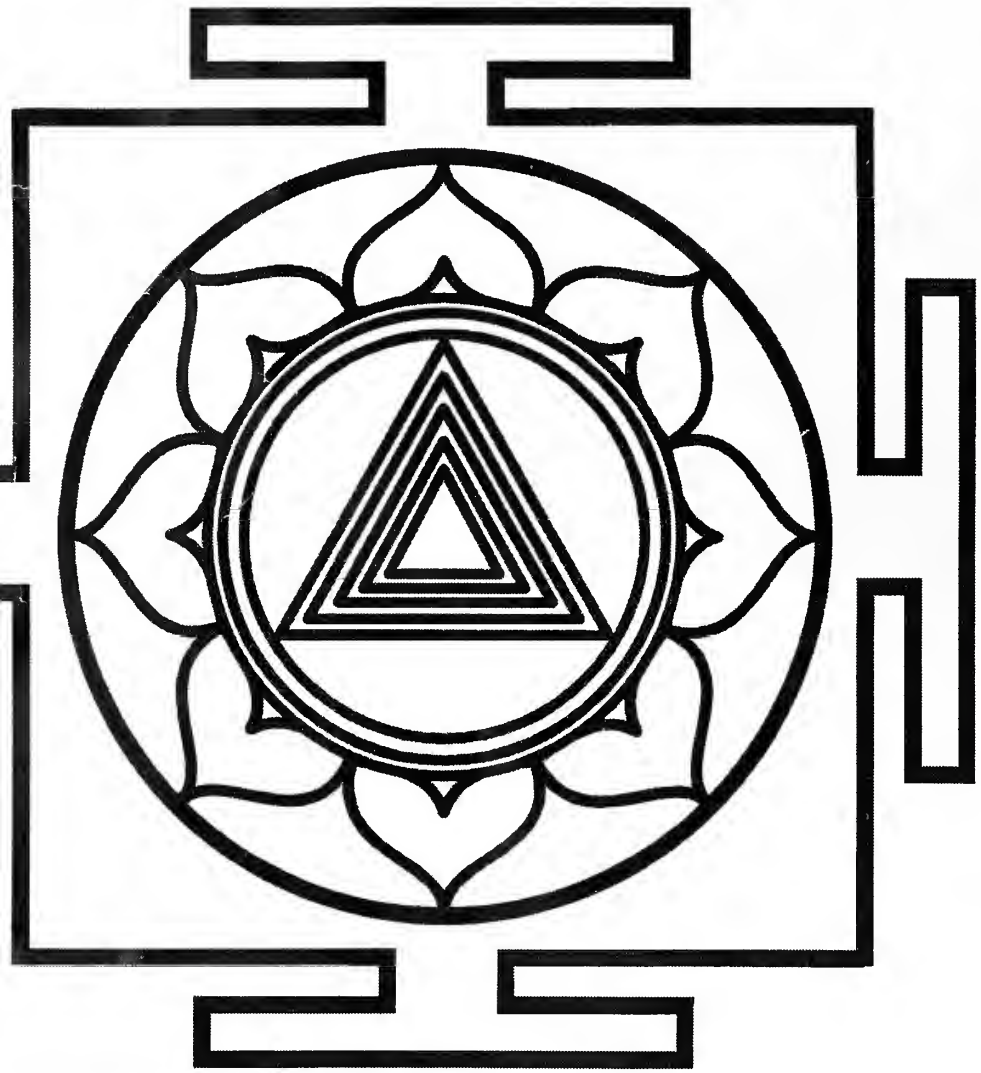

FOLDOUT

TABLE 5. Cysts per gramme of sediment information of the dinoflagellate cysts in each of the core-top samples.

Sample Number	TC 004	TC 006	TC 010	TC 044	PC 038	TC 041	GC 027	TC 032	KC 083	KC 081	PC 078	KC 064	KC 075	KC 073	KC 095
Gonyaulacacean cysts															
Protoceratium reticulatum	/	/	/	/	/	/	/	1	/	/	1	2	/	/	/
Dalella chathamense	/	/	/	/	/	/	/	/	2	2	3	2	8	2	2
Impagidinium aculeatum	/	/	/	/	/	/	/	/	/	/	1	1	/	/	/
Impagidinium pallidum	/	1	2	/	/	/	1	/	/	2	4	/	4	/	/
Impagidinium patulum	/	/	/	/	/	/	/	/	/	2	/	/	4	/	/
Impagidinium sphaericum	/	/	/	/	/	/	/	1	20	20	11	12	26	1	4
Impagidinium spp. indet.	/	/	/	/	/	/	/	1	8	/	1	1	/	1	4
Nematosphaeropsis labyrinthus	/	/	/	/	/	/	/	/	/	2	3	4	6	1	2
Spiniferites ramosus	/	/	/	/	/	/	/	/	/	/	1	1	/	/	1
Spiniferites spp. indet.	/	/	/	/	/	/	/	/	/	/	/	/	2	/	1
Tectatodinium? spp. indet.	/	/	/	/	/	/	/	/	/	/	1	/	2	/	/
Peridiniacean cysts															
Pentapharsodinium dalei?	/	/	/	/	/	2	1	/	/	/	/	1	2	/	/
Congruentidiacean cysts															
Algidasphaeridium? *minutum*	1	/	/	1	4	1	/	/	/	2	/	2	/	11	5
Protoperidinium conicoides	/	/	/	/	/	1	/	1	/	/	1	2	2	2	/
Protoperidinium spp. indet. [round, brown]	1	1	1	/	/	/	2	4	12	20	50	14	8	21	13
Protoperidinium spp. indet. [peridinioid]	/	1	1	/	/	1	/	/	46	/	/	/	/	1	/
Selenopemphix antarctica	1	/	/	/	1	4	3	15	276	186	23	7	182	195	169
Total (n)	3	4	4	1	5	9	7	23	364	236	100	49	246	235	201

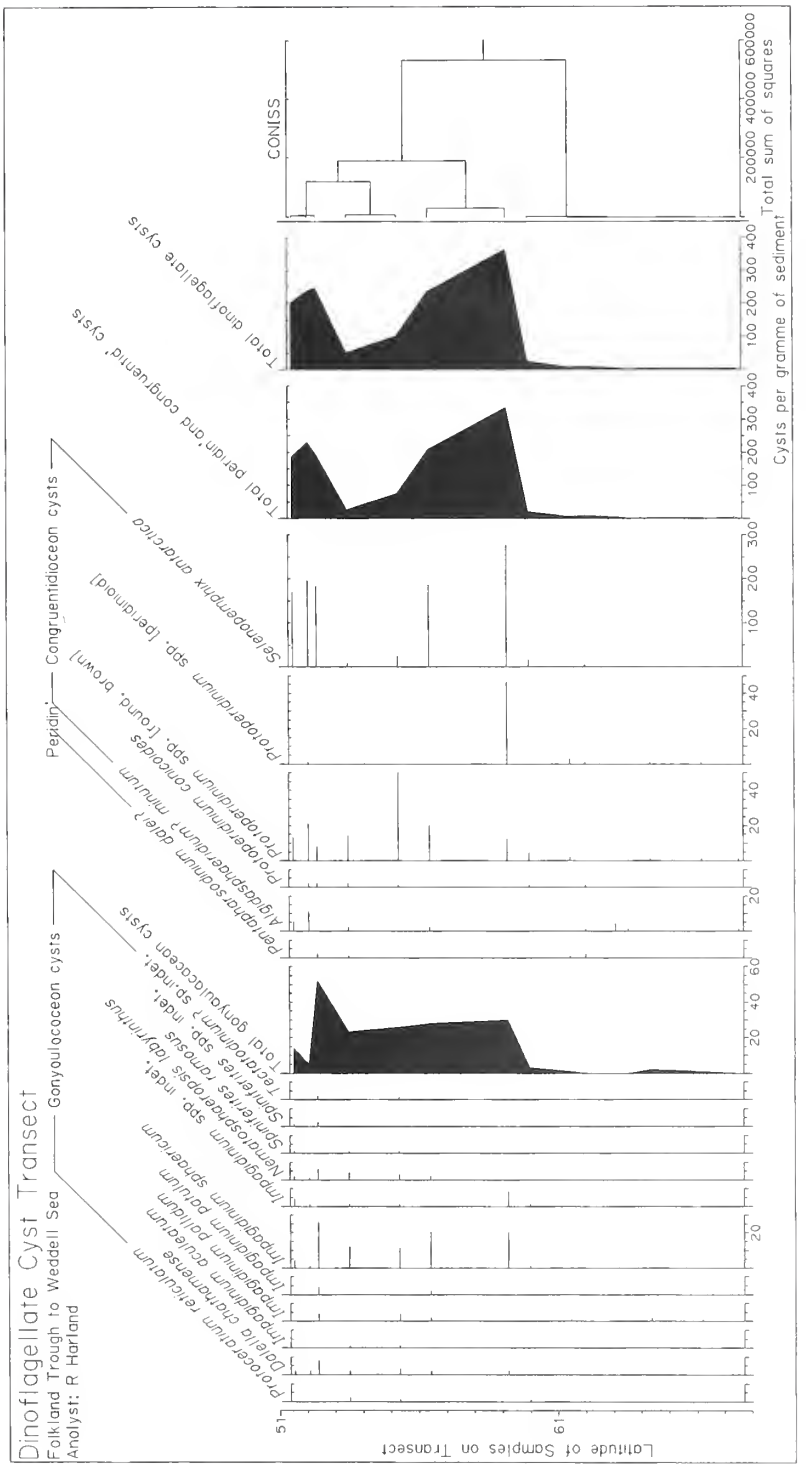

TEXT-FIG. 5. Cyst per gramme data from the core-top samples plotted along the transect against the latitude of the samples. Not to scale. Also plotted is the latitudinally constrained cluster analysis illustrating the division of the data into two distinct domains.

Most recently Pudsey and King (1998) have published AMS ^{14}C dates for the core-top samples from core 41 and 44, both included in this study. Dates, after subtraction of a reservoir age (1430 years), are 9560 ± 75 years and 11150 ± 190 years respectively, cautioning against the acceptance of a fully Recent thanatocoenosis. However, the presence of old carbon is known to be present (Pudsey and King 1998) which will have made the sample dates artificially too old. This study of the dinoflagellate cysts has disregarded the obviously reworked element of the palynological assemblages recovered from the core-top samples and has focused on the 'indigenous' component. Clearly some caution is required in the use of any data derived from core-top samples.

All the samples were subjected to normal palynological processing techniques, as outlined in general by Wood *et al.* (1996), with an avoidance of any oxidizing reagents, to prevent the loss of the more delicate and fragile cysts attributable to the peridiniacean and congruentidiacean dinoflagellates (Dale 1976). In addition, quantitative techniques were employed to enable the calculation of the numbers of dinoflagellate cysts per gramme of sediment and to avoid a reliance on the use of proportional data. To obtain quantitative data the original sample dry weight was noted and aliquot samples of the organic residues were taken, following the acid digestion stage, for mounting on strew slides and counting. The samples were stained with Safranin, mounted in Elvacite and were counted at $\times 10$ objective (Harland 1989). This method recovers only organic-walled dinoflagellate cysts and not the calcareous cysts that may be present (Dale and Dale 1992). All the material studied is housed in the palynological collections of the British Antarctic Survey, Cambridge.

Following counting, the data were compiled into Tables 3–5 which present the raw counts together with the percentage and cysts per gramme information respectively. Cluster analysis was performed on the cysts per gramme data-set using the CONISS programme, described by Grimm (1987), as part of the TILIA/TILIAGRAPH software used to construct Text-figure 5. The cluster analysis is stratigraphically constrained, or as used herein latitudinally constrained, so that adjacent samples are weighted to assist in the analysis along the studied transect rather than in a random fashion. This assumes that adjacent samples will be more likely to share a characteristic than others within the transect. The latitudinal information as plotted in the software gives the relative positions of the samples but is not to true scale.

Indigenous dinoflagellate cysts were recovered in all the core-top samples used in this study. The systematic palaeontology provides the first detailed account of Recent dinoflagellate cysts to be found in these southern waters.

SYSTEMATIC PALAEONTOLOGY

The dinoflagellate cyst species recovered from the core-top samples are listed systematically below. Since existing knowledge of Antarctic dinoflagellate cysts is so poor, extended comments are included for all the species encountered. The synonymies presented are selected to show the major taxonomic changes that the taxa have undergone since first published; they are not complete.

Division DINOFLAGELLATA (Bütschli 1885) Fensome, Taylor, Norris, Sarjeant, Wharton and Williams, 1993

Subdivision DINOKARYOTA Fensome, Taylor, Norris, Sarjeant, Wharton and Williams, 1993

Class DINOPHYCEAE Pascher, 1914

Subclass PERIDINIPHYCIDAE Fensome, Taylor, Norris, Sarjeant, Wharton and Williams, 1993

Order GONYAULACALES Taylor, 1980

Suborder GONYAULACINEAE (Autonym)

Family GONYAULACACEAE Lindemann, 1928

Subfamily CRIBROPERIDINIOIDEAE Fensome, Taylor, Norris, Sarjeant, Wharton and Williams, 1993

Remarks. Although the subfamily is known mostly from the fossil cyst record the modern cyst-forming genus *Protoceratium* has a recognizable cribroperidinoidean tabulation (see Dodge 1989).

Genus PROTOCERATIUM Bergh, 1882

Type species. Protoceratium aceros Bergh, 1882, original designation by monotypy.

Remarks. This genus was erected by Bergh (1882) to accommodate the type species only. Later it was accepted that *P. aceros* was a junior synonym of the previously described *Peridinium reticulatum* Claparède and Lachmann, 1859 and Bütschli (1885) effected the new combination.

Protoceratium reticulatum (Claparède and Lachmann 1859) Bütschli, 1885

Plate 1, figure 1

1859 *Peridinium reticulatum* Claparède and Lachmann, p. 405, pl. 20, fig. 3.
1882 *Protoceratium aceros* Bergh, p. 242, pl. 14, fig. 36.
1885 *Protoceratium reticulatum* (Claparède and Lachmann 1859) Bütschli, p. 1007, pl. 52, fig. 2.
1967 *Operculodinium centrocarpum* (Deflandre and Cookson 1955) Wall, p. 111 (*pars*), pl. 16, figs 1–2, 5.
1967 *Gonyaulax grindleyi* Reinecke, p. 157, pl. 1, figs A–C, text-fig. 1.
1997 *Operculodinium centrocarpum sensu* Wall and Dale, 1968; Marret and de Vernal, p. 387.

Remarks. Incubation experiments have firmly linked the cyst and motile stages of this species (Wall and Dale 1968). In the past, the cyst stage has been identified, in palynological literature, as *Operculodinium centrocarpum* (Deflandre and Cookson 1955) Wall, 1967. However, with the incubation evidence and the revision of the part of the family Gonyaulacaceae by Dodge (1989) it is now more appropriate to use the designation *Protoceratium reticulatum* (Claparède and Lachmann 1859) Bütschli, 1885 for modern cysts of this taxon and to reserve *O. centrocarpum* for those cysts clearly attributable to the separate and recognizably different Miocene taxon. Undoubtedly, there are many specimens in modern and fossil assemblages that will be difficult to assign definitively to either taxon until further information is available. In this study we agree with the views of Head (1996) and Harland and Long (1996) and use the modern extant taxon designation for our specimens.

Discussion. The specimens observed herein accord with the descriptions and size of material more commonly associated with the northern hemisphere and the North Atlantic Ocean (see Harland 1977). However, there was insufficient material available in this study to facilitate a full description and comparison of this southern hemisphere occurrence, let alone a full population analysis.

Occurrence. Protoceratium reticulatum occurs only in low numbers; never more than two cysts per gramme of sediment or more than 5·8 per cent. of the assemblages, and is confined to samples around and to the north of 61° S. Significantly, higher numbers of the cyst have not been seen by the authors until north of the Antarctic Convergence or Polar Front in the South Atlantic Ocean at about 48° S where we have recorded them at over 90 cysts per gramme of sediment. Marret and de Vernal (1997) recorded this species, as *Operculodinium centrocarpum*, north of the Subtropical Convergence in the southern Indian Ocean, where it dominates their Assemblage V in waters with a SST_w of 13–14 °C and a SST_s of 16–17 °C.

Ecology. This species is well known to possess an ubiquitous distribution pattern which has been summarized by Edwards and Andrle (1992) as estuarine to oceanic and of broad thermal tolerance.

There is evidence of some ecophenotypic variation (de Vernal *et al.* 1989) but the case has yet to be fully demonstrated Interestingly Wall *et al.* (1977, p. 146) reported that the species failed to develop distribution centres in environments with extensive coastal upwelling. It was also suggested that it may not be tolerant of non-stratified waters.

Subfamily GONYAULACOIDEAE Fensome, Taylor, Norris, Sarjeant, Wharton and Williams, 1993

Remarks. Most extant gonyaulacacean dinoflagellate cysts belong to this subfamily.

Genus DALELLA McMinn and Sun, 1994

Type species. Dalella chathamense McMinn and Sun, 1994, by original designation.

Dalella chathamense McMinn and Sun, 1994

Plate 1, figures 2–4

1994 *Dalella chathamense* McMinn and Sun, pp. 43, 45, pl. 1, figs 1–12.
1997 *Dalella chathamense* McMinn and Sun, 1994; Marret and de Vernal, p. 382, pl. 1, figs 1–4.

Remarks. This species is characterized, in particular, by its possession of a trabeculum which connects to the autocyst at the parasulcus, archeopyle margin and apex. The trabeculum consists of ribbon-like threads with a central thickened ridge. The paratabulation, as detailed by McMinn and Sun (1994) and Marret and de Vernal (1997), appears to be gonyaulacacean, sexiform with an S-type ventral organization. Specimens observed in the present study appear to conform with previous descriptions. This cyst has never undergone incubation experiments so the motile stage is unknown; the nature of the paratabulation suggests, however, an attribution to the modern genus *Gonyaulax* Diesing, 1866.

Occurrence. The present data show this cyst species to occur only to the north of 60° S in fairly low numbers never exceeding eight cysts per gramme of sediment or 4·4 per cent. of the assemblage. The occurrence of this species agrees well with the distribution pattern established by Marret and de Vernal (1997) and discussed below.

Ecology. Recent research from Marret and de Vernal (1997), using principal component analysis on a dataset of dinoflagellate cyst occurrences throughout the southern Indian Ocean, suggests that *Dalella chathamense* might be a Subantarctic endemic species, possibly oceanic in its preference, with its highest relative abundance in their Subantarctic domain (4·7 per cent.).

Genus IMPAGIDINIUM Stover and Evitt, 1978

Type species. Impagidinium dispertitum (Cookson and Eisenack 1965) Stover and Evitt, 1978, by original designation.

Impagidinium aculeatum (Wall 1967) Lentin and Williams, 1981

Plate 1, figure 5

1967 *Leptodinium aculeatum* Wall, p. 105, pl. 14, figs 18–19, text-fig. 3C–D.
1981 *Impagidinium aculeatum* Wall, 1967; Lentin and Williams, p. 153.

Remarks and occurrence. This species was identified in the present study in very minor amounts, about one cyst per gramme of sediment and less than 1 per cent of the assemblages, from two samples north of 56° S. It is probably attributable to an unidentified *Gonyaulax* species and until incubation data are available it is described under its palynological name.

Ecology. Edwards and Andrle (1992) summarized its ecology as outer neritic to oceanic and cool-temperate to tropical. Its occurrence in this study in such low numbers may have more to do with redeposition than with an autochthonous origin; however, it does occur in that part of the transect closest to the cool-temperate waters of the South Atlantic. Marret and de Vernal (1997) recognized *Impagidinium aculeatum* in their Subantarctic and Subtropical domains.

Impagidinium pallidum Bujak, 1984

Plate 1, figures 6–7

1984 *Impagidinium pallidum* Bujak, p. 187, pl. 2, figs 9–12.
1986 *Impagidinium*(?) *pallidum* Bujak, 1984; Mudie, p. 803, pl. 3, fig. 2.

Remarks. This species was attributed originally to the genus *Impagidinium* despite the absence of a clearly demonstrable paratabulation, because of the difficulty in deciphering the pale and thin-walled cysts. This led Mudie (1986) to question its affinity to the genus but without offering any extra information. Subsequent workers (Dale and Dale 1992; Matthiessen 1995) have accepted this species within *Impagidinium* and Dale and Dale (1992, pl. 3.1, figs 1–4), in particular, have published photomicrographs that are a convincing demonstration of some of the paratabulation and archeopyle formation, leading to the attribution as accepted herein. However, there remains the lack of published morphological description that adequately describes the paratabulation in detail. The material recovered in this study is not sufficiently well presented for the present authors to offer any further morphological information. This cyst is probably attributable to an unidentified *Gonyaulax* species and until incubation data are available it is described herein under its palynological name.

Occurrence. Impagidinium pallidum occurs in many of the samples analysed and was present in samples from both the Weddell Sea and the Scotia Sea together with the Falkland Trough. However, it never exceeds more than four cysts per gramme of sediment but may exceed 50 per cent. of the assemblages where the numbers of cysts recovered is very low. It was one of the few species of dinoflagellate cyst recovered in the Weddell Sea.

Ecology. Research to date suggests that this species is prevalent in high latitude regions and is particularly noted from the Greenland and Iceland seas (Matthiessen 1995). Marret and de Vernal (1997) recorded its most abundant distribution within the Antarctic domain where the SST_w is −1–0 °C and the SST_s is 3–5 °C. The occurrence of *I. pallidum* in this study is compatible with its known ecological preferences.

Impagidinium patulum (Wall 1967) Stover and Evitt, 1978

Plate 1, figure 8

1967 *Leptodinium patulum* Wall p. 105, pl. 14, fig. 20; pl. 15, figs 1–4; text-fig. 4.
1978 *Impagidinium patulum* (Wall 1967) Stover and Evitt, p. 166.

Remarks. This well-known dinoflagellate cyst has long been recognized from the northern hemisphere. Undoubtedly it has affinities to an unknown *Gonyaulax* species, but until incubation data are available the palynological name is preferred herein.

Occurrence. This *Impagidinium* species forms a minor component of two samples from the Scotia Sea and Falkland Trough, never exceeding more than four cysts per gramme of sediment or greater than 1·4 per cent. of the assemblages. It does not occur south of 57° S and probably has more affinity with waters to the north of the Antarctic Convergence.

Ecology Edwards and Andrle (1992) summarized the ecology of this species as being outer neritic to oceanic and with a broad thermal tolerance. This study is consistent with this information.

Impagidinium sphaericum (Wall 1967) Lentin and Williams, 1981

Plate 1, figures 9–12

1967 *Leptodinium sphaericum* Wall, p. 108, pl. 15, figs 11–15, text-fig. 2a–c.
1981 *Impagidinium sphaericum* (Wall 1967); Lentin and Williams, p. 154.

Remarks. This species has been identified often from bottom sediments in the northern hemisphere. As with other species of this genus, its affinities are with a species of *Gonyaulax*, but until incubation evidence is available the palynological designation is preferred.

Occurrence. In this study *Impagidinium sphaericum* forms an important part of the assemblages recovered in the core-top samples of both the Scotia Sea and the Falkland Trough. It does not occur south of 60° S but appears to be a major constituent in the northern part of the transect in contrast with other members of the genus. Numbers of cysts reach 26 cysts per gramme of sediment and up to 26·4 per cent. of the assemblages.

Ecology. Like other constituent species of the genus Edwards and Andrle (1992) summarized this species as having outer neritic to oceanic preferences in cool temperate to tropical environments.

EXPLANATION OF PLATE 1

Fig. 1. *Protoceratium reticulatum* (Claparède and Lachmann 1859) Bütschli, 1885; JR04/KC064/0.0-0.01/A2; Falkland Trough; orientation unknown, high focus showing the overall morphology.

Figs 2–4. *Dalella chathamense* McMinn and Sun, 1994. 2, JR04/KC064/0.0-0.01/B2; Falkland Trough; dorsal view, high focus showing the paratabulation outlined by the trabeculae. 3, JR04/PC078/0.0-0.01/B1; Scotia Sea; slightly oblique dorsal view, high focus showing the paratabulation and faint 3″ archeopyle. 4, JR04/KC075/0.0-0.01/A1; Falkland Trough; orientation unknown, high focus showing the overall appearance.

Fig. 5. *Impagidinium aculeatum* (Wall 1967) Lentin and Williams, 1981. JR04/PC078/0.0-0.01/A3; Scotia Sea; oblique dorsal view, high focus showing the overall morphology and the 3″ archeopyle.

Figs 6–7. *Impagidinium pallidum* Bujak, 1984. 6, JR04/KC081/0.0-0.01/A2; Scotia Sea; orientation unknown, possibly antapical, low focus, showing the enigmatic morphology of this cyst species. 7, JR04/PC078/0.0-0.01/A1; Scotia Sea; orientation unknown, low focus showing the general nature of the morphology.

Fig. 8. *Impagidinium patulum* (Wall 1967) Stover and Evitt, 1978. JR04/KC075/0.0-0.01/A7; Falkland Trough; oblique right lateral view, high focus showing the paratabulation on the hypocyst and the 3″ archeopyle at the top left of the photomicrograph.

Figs 9–12. *Impagidinium sphaericum* (Wall 1967) Lentin and Williams, 1981. 9–10, JR04/KC064/0.0-0.01/B1; Falkland Trough. 9, slightly oblique dorsal view, low focus showing the paratabulation and 3″ archeopyle. 10, ventral view, high focus showing the detail of the ventral paratabulation. 11–12, JR04/KC064/0.0-0.01/A1; Falkland Trough. 11, dorsal view, low focus showing the paratabulation and 3″ archeopyle. 12, ventral view, high focus showing the detailed paratabulation of the parasulcus and the prominent apical boss.

All photomicrographs taken under plane polarized light, except fig. 2 taken with Nomarski interference contrast; all × 500.

1

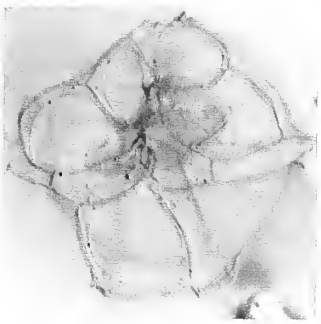

2

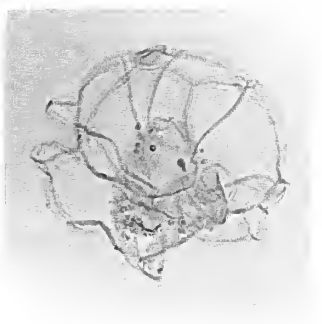

3

4

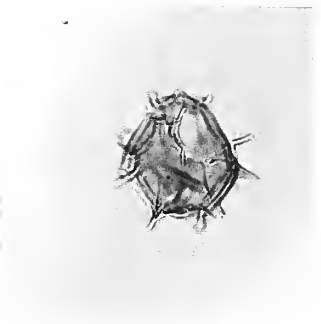

5

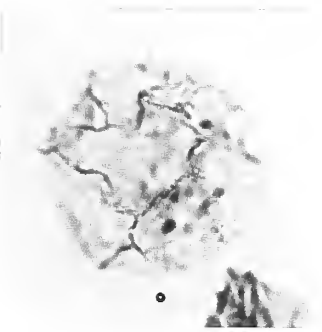

6

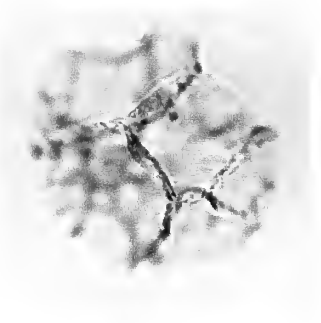

7

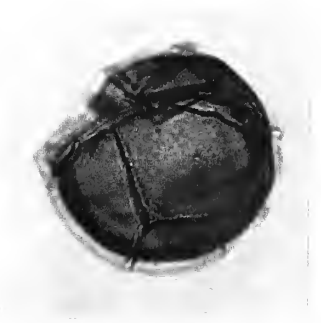

8

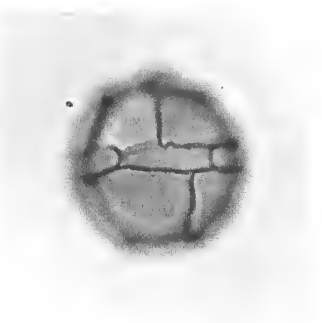

9

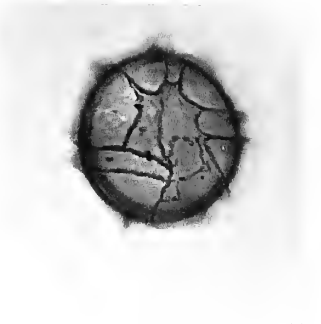

10

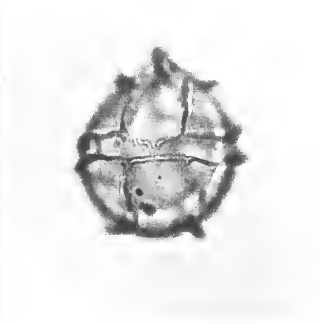

11

12

HARLAND *et al.*, Recent dinoflagellate cysts

The prominence of *I. sphaericum* in this study may suggest a potential indicator of particular ecological circumstances. Marret and de Vernal (1997) noted its presence in bottom sediments within their Subantarctic to Subtropical domains.

Impagidinium spp. indet.

Remarks. This category includes all those forms that are broken, crushed or in an unadvantageous orientation to preclude definitive identification to species level. This category forms a minor part of the assemblages north of about 60° S and so is consistent with the record of occurrence for most of the *Impagidinium* spp. described above except for *I. pallidum*.

Genus NEMATOSPHAEROPSIS Deflandre and Cookson, 1955 emend. Wrenn, 1988

Type species. Nematosphaeropsis balcombiana Deflandre and Cookson, 1955, by original designation.

Nematosphaeropsis labyrinthus (Ostenfeld 1903) Reid, 1974

Plate 2, figures 1–2

1903 *Pterosperma labyrinthus* Ostenfeld, p. 578, fig. 127.
1974 *Nematosphaeropsis labyrinthea* (Ostenfeld 1903); Reid, p. 592, pl. 1, figs 8–9.

Remarks. Despite this species being a well known component of modern dinoflagellate cyst assemblages its taxonomy is controversial (see Head and Wrenn 1992). Originally described as a prasinophyte from plankton collected in the Faeroes area, the species was recombined into the dinoflagellate cyst genus *Nematosphaeropsis* by Reid (1974). However, Wrenn (1988) argued that the species concept was untenable for a number of reasons: the original descriptions and line drawings could not be compared with Reid's (1974) material; there was no type material; and the morphology as described by Ostenfeld (1903) did not allow an unequivocal assignment to the Dinoflagellata. Wrenn (1988) suggested that the name *Nematosphaeropsis lemniscata* Bujak, 1984 emend. Wrenn, 1988 be applied to the species described by Reid (1974) with the original epithet remaining solely for the original discovery. For the moment, however, and until a comprehensive study of modern material from the type area has been achieved, the original epithet is preferred to maintain nomenclatural stability; to accept that Ostenfeld's *P. labyrinthus* is really a dinoflagellate cyst; and that Reid (1974) was correct in his recombination. Unfortunately the specimens recovered in the present study do not add any new useful information to support either case within the argument. This species is known to have affinities with *Gonyaulax spinifera* (Claparède and Lachmann 1859) Diesing, 1866 by incubation experiments (Wall and Dale 1968).

Occurrence. This species occurs only in the northern end of the transect to the north of 57° S always in small numbers, never exceeding six cysts per gramme of sediment or 8·2 per cent. of the assemblages.

Ecology. According to the summary published by Edwards and Andrle (1992) *Nematosphaeropsis labyrinthus* occurs in inner neritic to oceanic environments and has a broad thermal tolerance. However, Marret and de Vernal (1997) noted from their observations and those of McMinn and Sun (1994) that the species is most abundant where the SST_W are 6–13 °C and the SST_S are 8–17 °C. Baumann and Matthiessen (1992) suggested that the species prefers colder oceanic environments.

Recent research on high resolution samples of Holocene sediments from the North Atlantic (Harland and Howe 1995) suggested that the ecology of *N. labyrinthus* is perhaps rather more complex than it at first appears and is in need of further study.

Genus SPINIFERITES Mantell, 1850 emend. Sarjeant, 1970

Type species. Spiniferites ramosus (Ehrenberg 1838) Mantell, 1854, by subsequent designation.

Spiniferites ramosus (Ehrenberg 1838) Mantell, 1854

Plate 2, figure 3

1838 *Xanthidium ramosus* Ehrenberg, pl. 1, figs 1–2, 5.
1854 *Spiniferites ramosus* (Ehrenberg 1838) Mantell, p. 239.

Remarks. This species has a long history that dates back to the first discovery of dinoflagellate cysts. The holotype was not designated originally, but a lectotype was established by Davey and Williams (1966). Specimens of the species clearly belonging to the genus *Spiniferites* have long been recovered from modern sediments and many of them have been attributed to this species and also to *Spiniferites bulloideus* (Deflandre and Cookson 1955) Sarjeant, 1970. Harland (1977) discussed some of the difficulties in reconciling the identifications of specimens to either *S. ramosus* or to *S. bulloideus* and, after a review of the current literature, regarded. *S. bulloideus* as a subjective junior synonym of *S. ramosus*. Subsequent to this, various research workers have used both names for cysts with essentially identical morphologies (see Harland 1977, pl. 1, figs 5–6). The difficulty remains and is intrinsic in the use of a name established in the fossil literature for a modern cyst that is assumed to have an affinity to the thecate dinoflagellate *Gonyaulax spinifera* (Claparède and Lachmann 1859) Diesing, 1866; despite some references in the literature, *Spiniferites ramosus sensu stricto* has never been incubated whereas *Spiniferites bulloideus sensu* Wall and Dale 1968 has successfully hatched to produce *Gonyaulax scrippsae* Kofoid, 1911. Until further incubation work is completed, this taxon will remain the focus of much controversy. We follow the argument of Harland (1977) and maintain this species within the taxon *Spiniferites ramosus* until further evidence becomes available.

Occurrence. This species is a very minor component of the assemblages and is to be found at the northern end of the transect to the north of 56° S. It does not occur in numbers greater than one cyst per gramme of sediment or more than 2·5 per cent. of the assemblages.

Ecology. This well known if somewhat controversial species is regarded by Edwards and Andrle (1992) as estuarine to outer neritic in habit with a broad thermal tolerance. Marret and de Vernal (1997) do not record this cyst type in their Antarctic or Subantarctic domains. The extremely low numbers observed in this study are not inconsistent with the findings of Marret and de Vernal (1997).

Spiniferites spp. indet.

Remarks. This informal grouping includes all the dinoflagellate cyst specimens that show an affinity to the genus but cannot be identified to species level. It includes specimens that do not show clear morphological detail because of either poor orientation, being obscured by debris or by being broken. It is assumed that this informal grouping has affinities with the modern genus *Gonyaulax* Diesing, 1866.

Occurrence. These cysts form a minor component in samples that are found north of 53° S and never make up more than 0·5 per cent. of the assemblages.

Ecology. *Spiniferites* spp. are regarded as neritic in their habitat from the arctic to the tropics. Further comment is unwarranted on these indeterminate specimens.

Genus TECTATODINIUM Wall, 1967 emend. Head, 1994

Type species. *Tectatodinium pellitum* Wall, 1967 emend. Head, 1994, by original designation.

Tectatodinium? sp. indet.

Plate 2, figure 4

Remarks. Specimens attributed to this informal category are ovoidal and possess an indeterminate archeopyle. The wall structure has not been determined in detail, and this, with the indeterminate nature of the archeopyle, precludes firm assignation to the genus. It might prove to be the case that the specimens in question are the internal endocysts of reworked cavate cysts; the low numbers and sporadic occurrence preclude further comment.

Occurrence. These specimens occur only in two samples situated north of 56° S in the transect and never exceed 0·7 per cent. of the assemblages.

EXPLANATION OF PLATE 2

Figs 1–2. *Nematosphaeropsis labyrinthus* (Ostenfeld 1903) Reid, 1974. 1, JR04/KC064/0.0-0.01/A3; Falkland Trough; orientation unknown, high focus showing the overall trabeculate morphology. 2, JR04/KC073/0.0-0.01; Falkland Trough; orientation unknown, high focus showing the general morphology.

Fig. 3. *Spiniferites ramosus* (Ehrenberg 1838) Mantell, 1854; JR096/KC095/0.0-0.01; Falkland Trough; oblique ventral view, low focus showing the typical spiniferate morphology.

Fig. 4. *Tectadinium*? sp. indet.; JR04/KC075/0.0-0.01/A8; Falkland Trough; possible dorsal view, low focus showing the precingular archeopyle and overall morphology.

Fig. 5. *Pentapharsodinium dalei* Indelicato and Loeblich III, 1986?; D172/TC041/0.0-0.01; Weddell Sea; orientation unknown, high focus showing the overall nature and the bifurcations at the distal tips of the processes.

Figs 6–7. *Algidasphaeridium*? *minutum* (Harland and Reid 1980) Matsuoka and Bujak, 1988. 6, D154/TC004/0.0-0.01; Weddell Sea; orientation unknown, high focus showing the overall nature of the morphology. 7, D154/PC038/0.0-0.01; Weddell Sea; orientation unknown, high focus showing the general morphology.

Figs 8–9. *Protoperidinium conicoides* (Paulsen 1905) Balech, 1974. 8, D172/TC032/0.0-0.01; Scotia Sea; dorsal view, high focus showing the 2a archeopyle and nature of the overall morphology. 9, JR04/KC073/0.0-0.01/B1; Falkland Trough; dorsal view, high focus showing the intercalary 2a archeopyle with the operculum within the cyst.

Figs 10–12. *Selenopemphix antarctica* Marret and de Vernal, 1997. 10, JR04/KC075/0.0-0.01/A5; Falkland Trough; apical view, high focus showing the intercalary 2a archeopyle and the nature of the granulations on the surface of the cyst. 11, JR04/KC073/0·0-0.01/B3; Falkland Trough; apical view, high focus showing the archeopyle and surface ornamentation. 12, JR04/KC073/0.0-0.01/B2; Falkland Trough; apical view, high focus showing the overall morphology of the cyst.

All photomicrographs taken in plane polarized light; all × 500.

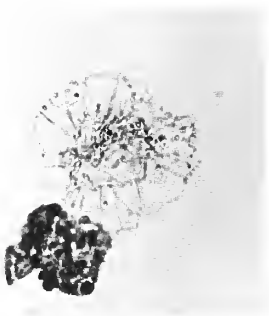

1

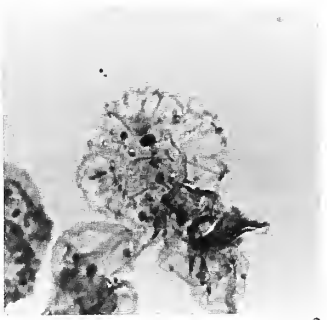

2

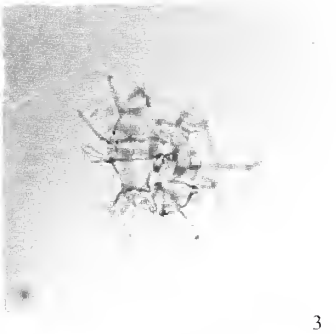

3

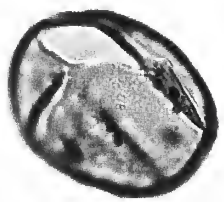

4

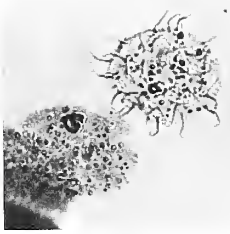

5

6

7

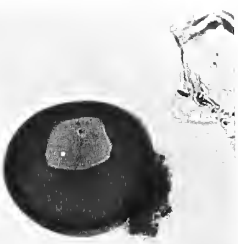

8

9

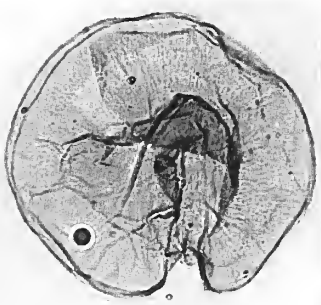

10

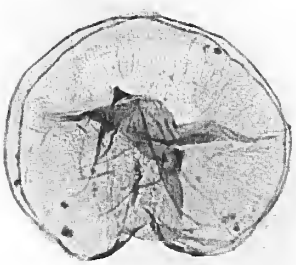

11

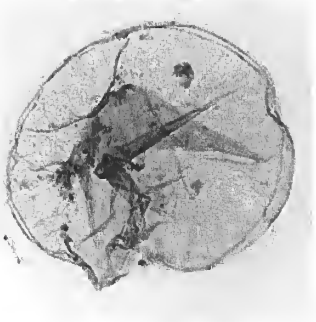

12

HARLAND *et al.*, Recent dinoflagellate cysts

Order PERIDINIALES Haeckel, 1894
Suborder PERIDINIINEAE (Autonym)
Family PERIDINIACEAE Ehrenberg, 1831
Subfamily uncertain

Genus PENTAPHARSODINIUM Indelicato and Loeblich III, 1986

Type species. *Pentapharsodinium dalei* Indelicato and Loeblich III, 1986, by original designation.

Remarks. This genus was erected as part of an attempt to clarify some of the taxonomic difficulties surrounding the scrippsielloid dinoflagellates. The genus is in part characterized by the possession of five cingular plates (4+t) and a wholly organic cyst.

Pentapharsodinium dalei? Indelicato and Loeblich III, 1986

Plate 2, figure 5

1977 *Peridinium faeroense* Paulsen, 1905; Dale, p. 243, figs 1–5, 7–8, 10–11, 14–19, 21, 23–25, 27–30.
1986 *Pentapharsodinium dalei* Indelicato and Loeblich III, p. 158.

Remarks. Cysts of this dinoflagellate were first incubated by Dale (1977) and identified as *Peridinium faeroense*. It is often a difficult cyst to identify in palynological preparations because of its small size and its propensity for attracting adhering organic material. Later Indelicato and Loeblich III (1986) described this taxon as a new species within their new genus *Pentapharsodinium*. The present authors have followed this taxonomic assignment. However we have questionably assigned some of our material to this taxon for the moment and until fuller comparisons with the northern hemisphere specimens are achieved. Recent work by Buck *et al*. (1992) on a dinoflagellate cyst morphotype from the Antarctic sea-ice opens the possibility that further cyst types might be present and that particular care should be exercised in the identification of small, inconspicuous cyst morphotypes.

Occurrence. This species occurs in small numbers, never more than two cysts per gramme of sediment but up to 26·1 per cent of assemblages with a low number total, at both the southern and northern ends of the transect. It is one of the few cyst species that occurs in some of the Weddell Sea core-top samples.

Ecology. Dale (1977) recorded this species from fjörds and embayments in the north temperate regions of the North Atlantic and north-eastern Pacific Ocean. Matthiessen (1995) noted its presence in the neritic, cold temperate regions of the Norwegian–Greenland seas. It is perhaps not inconsistent to record its presence in this study. It was observed by Marret and de Vernal (1997) only in surface samples from south-western Australia and, except for a single record, not from their Antarctic or Subantarctic domains.

Family CONGRUENTIDIACEAE Schiller, 1935
Subfamily CONGRUENTIDIOIDEAE (Autonym)

Genus ALGIDASPHAERIDIUM Matsuoka and Bujak, 1988

Type species. *Algidasphaeridium capillatum* Matsuoka and Bujak, 1988, by original designation.

Remarks. This genus was erected to accommodate small, spiny cysts with a chasmic archeopyle. Matsuoka and Bujak (1988) assigned the genus to the order Gymnodiniales Lemmermann, 1910 on

the basis that chasmic archeopyles had previously been observed on modern gymnodinialean cysts of the genera *Pheopolykrikos* Chatton, 1933 and *Cochlodinium* Schütt, 1896. However, there are no incubation data available to support their claim. For the moment, we prefer the more conservative assignment to the Peridiniales, on their general morphology and similarity to cysts described in the literature under the cyst genus *Multispinula* Bradford, 1975, which is attributable by incubation to the modern genus *Protoperidinium*. Incubation research will eventually provide unequivocal information on the assignment of this cyst taxon to its parental thecate dinoflagellate.

Algidasphaeridium? *minutum* (Harland and Reid 1980) Matsuoka and Bujak, 1988

Plate 2, figures 6–7

1980 ?*Multispinula minuta* Harland and Reid, p. 216, fig. 2M–O.
1988 *Algidasphaeridium*? *minuta* (Harland and Reid 1980) Matsuoka and Bujak, p. 36.

Remarks. In the present controversy over the correct assignment of this taxon, we are satisfied that the polygonal archeopyle as observed by Matthiessen (1995) and the similarity of the taxon to some forms previously attributed to *Multispinula* justify its inclusion within the Peridiniales. However, the general uncertainty over the detailed morphology and archeopyle type together with the lack of incubation data argues for its conservative interim retention in *Algidasphaeridium*, rather than any attempt to recombine the taxon into *Protoperidinium*. Incubation experiments will undoubtedly provide the necessary definitive information to allow the correct taxonomic and systematic assignment in the future.

Occurrence. This species occurs throughout the transect and is one of the few species that is present in the southern part within the Weddell Sea. However its most prominent occurrence, at 11 cysts per gramme of sediment and 4·5 per cent. of the assemblage, occurs at core-top KC 073. Higher percentages are recorded at other sites but based upon poor cyst recovery of only one or two specimens in total.

Ecology. *Algidasphaeridium*? *minutum* was noted in low percentages in the Subantarctic and Subtropical domains of Marret and de Vernal (1997). It is a species associated with polar and subpolar waters in the North Atlantic Ocean and Nordic Seas (Dale 1996). Its presence in this study lends support to its characterization as a high latitude cold water indicator.

Genus PROTOPERIDINIUM Bergh, 1881 emend. Balech, 1974

Type species. *Protoperidinium pellucidum* Bergh, 1881, by subsequent designation by Loeblich Jr and Loeblich III (1966).

Remarks. This genus accommodates, for the most part, the marine species formerly belonging to the genus *Peridinium* Ehrenberg, 1830. The diagnosis of the genus was emended by Balech (1974) who also provided a taxonomic framework at the subgeneric level on the detailed tabulation of the thecae. The consequence of this action on the systematics of various cyst taxa was explored by Harland (1982) but is not adopted by the present authors as insufficient taxa were available in the present study to warrant use of this further hierarchy. It should be noted that many species within this taxonomic grouping have a heterotrophic habit and therefore occupy quite a different position in the trophic web from the gonyaulacacean autotrophic dinoflagellates described above.

Protoperidinium conicoides (Paulsen 1905) Balech, 1974

Plate 2, figures 8–9

1905 *Peridinium conicoides* Paulsen, 1905, p. 3, fig. 2.
1974 *Protoperidinium conicoides* (Paulsen 1905) Balech, 1974, p. 58.

Remarks. Although a successful incubation experiment was not achieved by Wall and Dale (1968) acetolysis of thecae with enclosed cysts almost certainly established the relationship between the parent theca and cyst which, in palynological literature, has long been known as *Brigantedinium simplex* Wall, 1965 *ex* Lentin and Williams, 1993. This species is one of several that is often grouped within the so called 'round, brown' cysts whose morphology of a simple, brown spheroidal body can lead to confusion when the specimens are orientated unfavourably or are crushed so as to obscure the nature of the archeopyle. The archeopyle is virtually the only distinguishing morphological feature of this group of cysts.

Occurrence. Protoperidinium conicoides occurs in small numbers throughout the transect, never more than eight cysts per gramme of sediment were recorded or 5 per cent. of the assemblages, but it is more than likely that poorly orientated and crushed specimens have also been included in the counts for the unidentified, round, brown *Protoperidinium* cysts.

Ecology. Edwards and Andrle (1992) characterize the ecology of this cyst as inner neritic to oceanic and arctic to warm temperate. Dale (1996) also regards this taxon as having a polar to temperate distribution. The occurrence of this cyst species in the present study is, therefore, consistent with our present knowledge. Indeed Dale (1996) also noted its occurrence in the coastal regions of Antarctica and southern Chile. Marret and de Vernal (1997) described its presence as part of their *Brigantedinium* spp. grouping where it is especially dominant in the Subantarctic domain. They also noted that much of its distribution may be the result of its dependence on the distribution of diatoms, as it is a heterotrophic species and diatoms are often used as a food source. Its position in the trophic web is quite different from that of the autotrophic dinoflagellate species. Undoubtedly the heterotrophic nature of this taxon affects its distribution pattern as its survival strategy is different to that of autotrophs and it may not be so dependent on the intrinsic SST and SSS except inasmuch as it affects the distribution of its preferred food.

Protoperidium spp. indet. [round, brown]

Remarks. This taxonomic category includes all the round, brown *Protoperidinium* cysts that could not be speciated because of their orientation or compression. Many such cysts probably belong to the taxon *Protoperidinium conicoides* described above, but unless a clearly defined archeopyle is present a definitive identification cannot be made. It may also include other species of *Protoperidinium* that possess this conservative round, brown morphology.

Occurrence. These cysts were recovered throughout the transect but occurred in higher numbers to the north of 60° S where up to 50 cysts per gramme of sediment were recovered with percentages of up to 50·3 per cent.

Ecology. It is impossible to give any detailed ecological information for this taxon as it may include several species with different ecological requirements. However, it is likely that most if not all of this group are heterotrophic and are therefore largely controlled by the distribution and numbers of their preferred prey. It is not surprising that in this area of upwelling and high productivity that large numbers of this group, including *Protoperidinium conicoides*, should be strongly represented.

Protoperidinium spp. indet. [peridinioid]

Remarks. A second group of undifferentiated *Protoperidinium* cysts is included in this study and these have a recognizable pentagonal peridinioid morphology. Unfortunately, insufficient morphological detail was available to identify them to species level because of poor orientation,

compression or the obscuring of detail by organic debris. It is possible that a new species may be present in sample KC 083, but insufficient specimens were available for a detailed taxonomic study.

Occurrence. This group of cysts occurs in very low numbers and sporadically through the transect. High numbers, up to 46 cysts per gramme of sediment, occur in one sample only and may represent a new species. Further work is expected to clarify this observation.

Ecology. It is impossible to outline any meaningful ecology for this group of dinoflagellate cysts except to reiterate the possibility that, with their affinities to the genus *Protoperidinium*, they are also probably heterotrophic in their nutritional habits.

Genus *Selenopemphix* Benedek, 1972 emend. Head, 1993

Type species. Selenopemphix nephroides Benedek, 1972, by original designation.

Remarks. The emended definition published by Head (1993) recognizes polar compression as a key feature in its characterization and to separate it from *Lejeunecysta* Artzner and Dörhöfer, 1978 emend. Bujak, 1980. However, incubation evidence has for some considerable time linked cysts with a *Selenopemphix* morphology to the dinoflagellate genus *Protoperidinium*. Undoubtedly, cysts of this genus should be subsumed into *Protoperidinium*, as attempted by Harland (1982), but not largely recognized. For the moment we prefer the use of the newly published cyst taxonomy for the species until other definitive evidence is available.

Selenopemphix antarctica Marret and de Vernal, 1997

Plate 2, figures 10–12

1997 *Selenopemphix antarctica* Marret and de Vernal, p. 389, pl. 5, figs 1–5.

Remarks. This species is a conspicuous and characteristic component of dinoflagellate cyst assemblages in the present study. It is identifiable from its possession of two antapical horns and the granulations on the cyst surface that are concentrated around and on top of the apical and antapical horns. To date it has only been described by Marret and de Vernal (1997) and ourselves, but its prominence in southern hemisphere high latitude assemblages will undoubtedly lead to its recognition in other material. It is anticipated that this cyst species is derived from the genus *Protoperidinium* but confirmation of this must await incubation work.

Occurrence. Selenopemphix antarctica is a prominent component of the dinoflagellate cyst assemblages from the northern half of the transect to the north of 60° S where it forms the dominant species in the assemblages. Up to 276 cysts per gramme of sediment have been recorded and percentages as high as 92·6 per cent. It has also been observed in low numbers in the more southerly samples from the Weddell Sea.

Ecology. Marret and de Vernal (1997) recorded this species from the southern Indian Ocean to the south of 40° S dominating assemblages of their Antarctic and Subantarctic domains. In these areas the SST averages −1·8–0 °C in summer and freezes in the winter. They believed that *Selenopemphix antarctica* can be associated with cold waters and seasonal ice cover and that the species is endemic to high latitudes in the southern hemisphere.

RESULTS

Dinoflagellate cyst analysis of core-top samples has been completed on a transect from the Falkland Trough to the Weddell Sea (Text-fig. 6). The basic numerical data are shown in Tables 3 to 5 and include the raw counts, the percentages and the numbers of cysts per gramme of sediment. Rather than attempt to draw a whole series of distribution maps along the transect, one or two examples

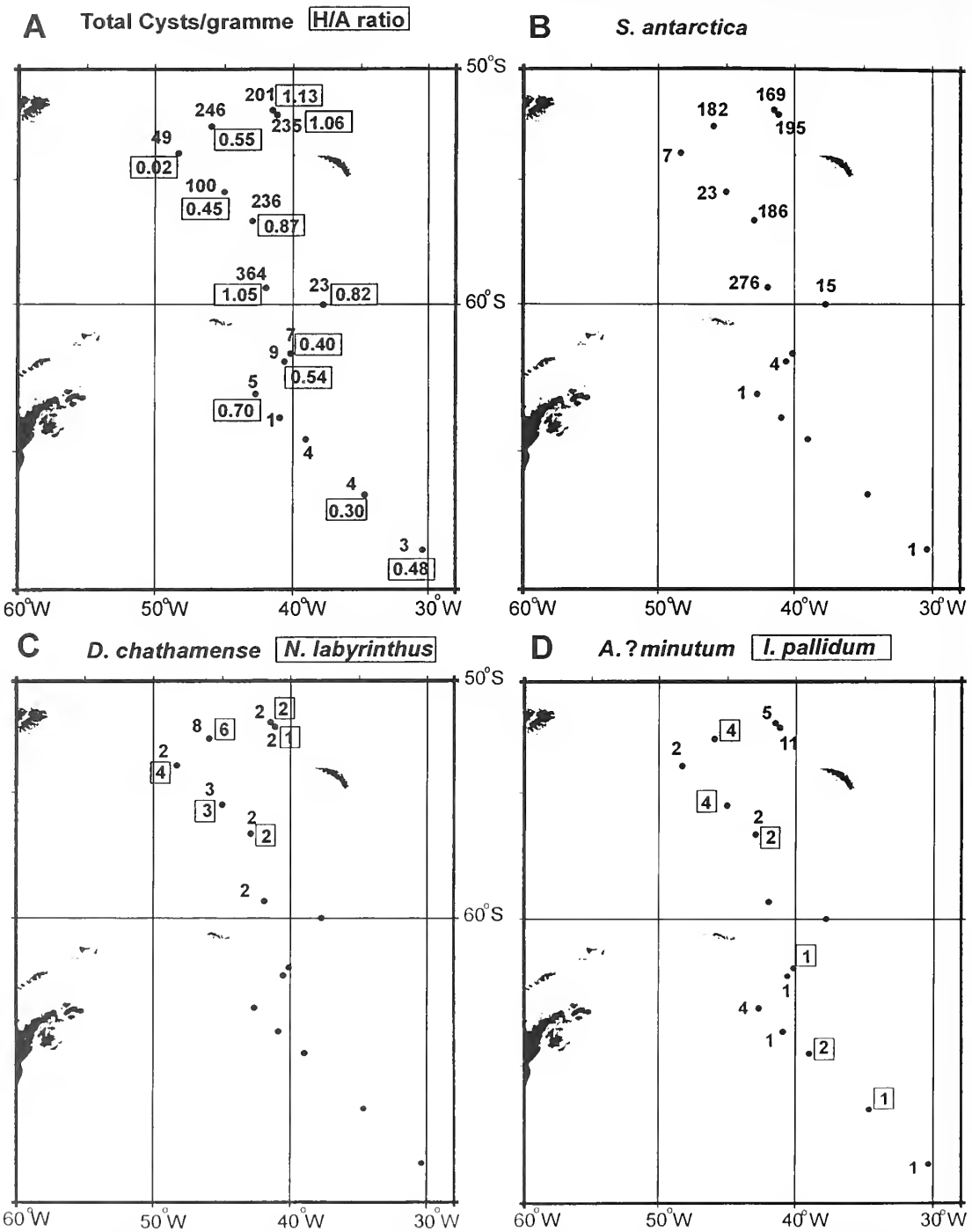

TEXT-FIG. 6. Maps of the distribution of dinoflagellate cysts along the studied transect. A, total cysts per gramme of sediment and H/A ratio. B, *Selenopemphix antartica*. C, *Dalella chathamense* and *Nematosphaeropsis labyrinthus*. D, *Impagidinium pallidum* and *Algidasphaeridium*? *minutum*.

are illustrated (Text-fig. 7) only, the data are arranged in a dinoflagellate cyst spectrum that is ordered according to latitude. The resulting cyst spectrum is illustrated in Text-figure 5. In order to aid the interpretation of results, a cluster analysis was performed on the data using CONISS (Grimm 1987) as part of the TILIA/TILIAGRAPH software package.

One of the first facts to emerge is that the number of cysts per gramme of sediment recovered in all the samples studied is much lower than from Recent and late Holocene sediments from the north-eastern Atlantic (Harland and Howe 1995). In that study some samples contained over 10000 cysts per gramme of sediment and certainly figures in excess of 1000 cysts per gramme of sediment were the norm. In this study none of the samples contained more than 364 cysts per gramme and many contained fewer than 20 cysts per gramme (see Text-fig. 6A). These figures are, however, not unlike the low numbers counted by Marret and de Vernal (1997) for material in the Southern Ocean where low dinoflagellate cyst concentrations typify their Antarctic and subAntarctic domains.

Second, it is immediately apparent from an inspection of the data, from the dinoflagellate cyst spectrum and from the cluster analysis, that there is a distinctive change in the data-set which is portrayed in the diagram between sites 032 and 083; that is between 60° 00.10′ S and 59° 22.20′ S. This change is manifested in the total numbers of dinoflagellate cysts per gramme of sediment and in the diversity of the assemblage, together with the species composition of the assemblages. The maps presented in Text-figure 6 of the cysts per gramme of sediment along the transect together with the occurrence of selected cyst species clearly show the influence of the 60° S line of latitude.

To the south of 60° S the assemblages are low in numbers of cysts per gramme, never exceeding 23 cysts per gramme of sediment. The assemblages are of low diversity and contain a maximum of six species with the common components including taxa such as *Impagidinium pallidum* (Pl. 1, figs 6–7; Text-fig. 7D) amongst the gonyaulacacean cysts and *Algidasphaeridium*? *minutum* (Pl. 2, figs 6–7; Text-fig. 7D), *Pentapharsodinium dalei*? (Pl. 2, fig. 5), round brown *Protoperidinium* cysts including *Protoperidinium conicoides* (Pl. 2, figs 8–9) and *Selenopemphix antarctica* (Pl. 2, figs 10–12; Text-fig. 7B) amongst the peridiniacean and congruentidiacean cysts. This sparse and low diversity assemblage has also been observed in additional assemblages at similar latitudes in the area. Indeed Marret and de Vernal (1997) recovered fewer than ten taxa in their Antarctic and subAntarctic domains. The cluster analysis clearly differentiates this assemblage from the data-set.

In contrast, the assemblages to the north of about 60° S are characterized by relatively rich dinoflagellate cyst assemblages with a high diversity cyst content. Cyst numbers can reach 364 cysts per gramme of sediment (Text-fig. 7A) with a diversity of 12 species. The assemblages are typically dominated by *Impagidinium sphaericum* (Pl. 1, figs 10–12), with subsidiary *Dalella chathamense* (Pl. 1, figs 2–4; Text-fig. 7C) and *Nematosphaeropsis labyrinthus* (Pl. 2, figs 1–2; Text-fig. 7C) amongst the gonyaulacacean cysts and *Selenopemphix antarctica* (Pl. 2, figs 10–12; Text-fig. 7B) amongst the congruentidiacean cysts, with subsidiary round brown *Protoperidinium* species. The cluster analysis is suggestive of a possible subdivision of this more northern assemblage. This subdivision is manifested in the higher numbers of the round, brown *Protoperidinium* species together with greater numbers of *Impagidinium sphaericum* and *Selenopemphix antarctica* in the more southerly part of this assemblage, and higher numbers of *Dalella chathamense*, *Nematosphaeropsis labyrinthus*, *Protoceratium reticulatum*, *Spiniferites* spp. and *Algidasphaeridium*? *minutum* in the more northerly part. We have insufficient evidence, at the moment, to substantiate this subdivision and certainly it is not as clearly defined as that at the 60° S line of latitude.

The latitude of 60° S appears to be clearly influential on the distribution of dinoflagellate cysts in the core-top samples from the studied samples of the transect and can be demonstrated clearly in terms of the numbers of cysts, in the cyst species diversity and in the composition of the recovered assemblages given all the constraints outlined previously.

COMPARISONS

We have already noted that few dinoflagellate cyst data are available from this part of the ocean. Indeed the lack of cyst information and the obvious importance of the Antarctic in the genesis of

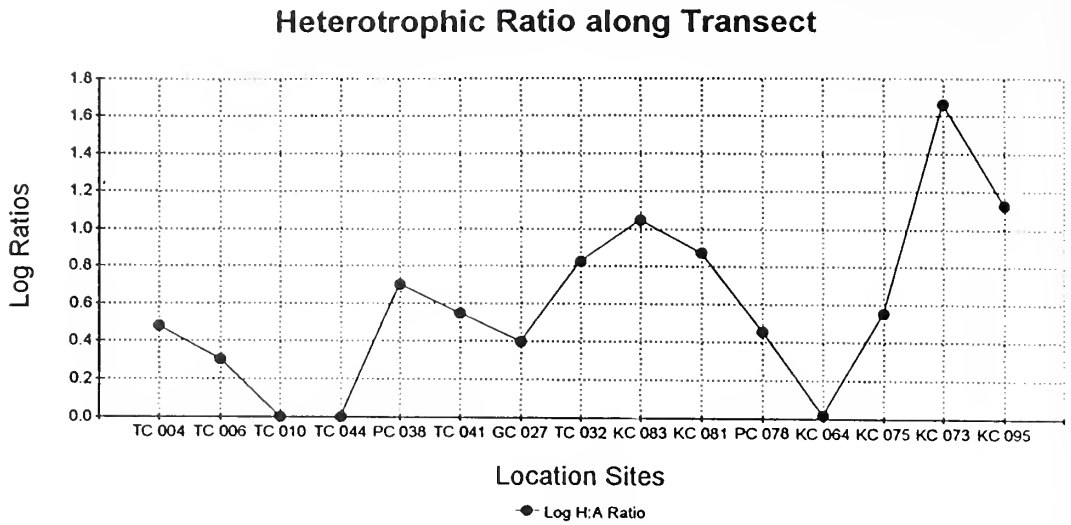

TEXT-FIG. 7. Graph of the heterotrophic ratio along the transect from the Weddell Sea (left) to Falkland Trough (right). Note the general increasing trend away from the Weddell Sea.

the global circulation pattern and providing a site of upwelling adds to the significance of this the first study of dinoflagellate cysts in the area of remit of the British Antarctic Survey.

However, it is pertinent to compare our results with those of Marret and de Vernal (1997) from the southern part of the Indian Ocean in the immediate vicinity of Antarctica. Using Principal Component Analysis on a data-set of 44 samples, Marret and de Vernal (1977) recognized two main groupings each of which contains three identified assemblages. Their most southerly group, a circum-Antarctic domain, contains identified dinoflagellate cyst assemblages to which the data presented herein can be compared. This circum-Antarctic domain is characterized by the high proportions of the cyst species *Selenopemphix antarctica*, *Impagidinium pallidum*, and round, brown *Protoperidinium* cysts referred to as *Brigantedinium* spp. It is immediately apparent from our data that our assemblages are also characterized by the same cyst taxa.

Within the circum-Antarctic domain Marret and de Vernal (1997) defined three separate assemblages: a proximal Antarctic assemblage (Assemblage I), an Antarctic assemblage (Assemblage II), and a Subantarctic assemblage (Assemblage III). Assemblage I contains *Selenopemphix antarctica* (> 70 per cent.), with *Impagidinium pallidum* (1–35 per cent.) and *Brigantedinium* spp. (2–15 per cent.); Assemblage II consists of *S. antarctica* (19–74 per cent.), with *Brigantedinium* spp. (8–56 per cent.) and *I. pallidum* (2–35 per cent.); Assemblage III is dominated by *Brigantedinium* spp. (16–72 per cent.), with *Nematosphaeropsis labyrinthus* (2–48 per cent.) and *S. antarctica* (0·6–20 per cent.).

We believe that our data are comparable to those of Marret and de Vernal (1997) and that our assemblages south of 60° S are similar to their Assemblage I, with high percentages of *S. antarctica* (0–68·1 per cent.), *I. pallidum* (0–66·7 per cent.) and round, brown *Protoperidinium* cysts (0–47·1 per cent.) and with significant proportions of *Algidasphaeridium*? *minutum* (0–78·5 per cent.). To the north of 60° S we believe that our assemblages are similar to Assemblage II of Marret and de Vernal (1997), with *S. antarctica* (15·1–92·6 per cent.), round, brown cysts (3·1–51·3 per cent.) and *I. pallidum* (0–4·0 per cent.). The possible subdivision of our data to the north of 60° S as intimated on the cluster analysis may be associated with Assemblage III of Marret and de Vernal (1997) especially on the increased presence of *Nematosphaeropsis labrinthus*, an important element of their

Assemblage III. However, we feel that there is insufficient evidence available at the moment to identify, with confidence, a subdivision of the dinoflagellate cyst assemblages north of 60° S. We are confident in identifying the two assemblages divided by the 60° S line of latitude and the clear similarity with Assemblages I and II of Marret and de Vernal (1997) which occur in the south Indian Ocean to the north and south of 65° S.

In addition to describing various dinoflagellate cyst assemblages from the area as a result of the Principal Component Analysis, Marret and de Vernal (1997) developed a transfer function relating the assemblages to SST and SSS. The best analogue methodology was used and all the procedures (described in de Vernal *et al.* 1994) yielded comparable reconstructions. Testing against the known modern environmental parameters of temperature and salinity yielded excellent coefficients of correlation. Since that time Drs Marret and de Vernal have included our data and have found it to be fully compatible with theirs and have utilized it in further refinements of their transfer function. This makes us confident that our data are meaningful within the constraints that we identified earlier.

DISCUSSION

To date, few data are available on Recent dinoflagellate cyst distributions in the southern hemisphere except for around Australia and New Zealand, e.g. Baldwin (1987), Bint (1988), Bolch and Hallaegraff (1990), McMinn (1990, 1991, 1992), McMinn and Sun (1994), Sun and McMinn (1994) and from the southern Indian Ocean (Marret and de Vernal 1997). In most cases the dinoflagellate cysts recovered can be assigned to species already known from the northern hemisphere. There are very few species that can be said to be endemic to the southern hemisphere. This is perhaps not surprising given the planktonic nature of the thecate dinoflagellate life stage, but it may also reflect the lack of a detailed systematic study of the taxonomy of the southern forms. However, two species are sufficiently taxonomically unique to be identified confidently as endemic to the southern hemisphere: *Dalella chathamense* and *Selenopemphix antarctica*. The increased interest in the dinoflagellate cyst flora of the southern oceans, as revealed in bottom sediments, may well lead to the description of other endemic species and *Impagidinium variaseptum* Marret and de Vernal, 1997 may prove to be one of these. However, the presence of the two species mentioned above in any palynological assemblage is, for the moment, a clear indication of deposition in the southern hemisphere and in the case of *Selenopemphix antarctica* to deposition in a circum-Antarctic domain.

In contrast with this rather limited evidence of endemism in dinoflagellate cyst distributions is the reinforcement that the major sea surface factor in controlling dinoflagellate cyst distributions is temperature. This is usually expressed in the latitudinal or climatic distribution trend and the biogeography of dinoflagellate cysts as first recognized by Wall *et al.* (1977) and later clearly demonstrated by Dale (1983). The results of the present study also show evidence of this latitudinal trend. As Dale (1996) pointed out, in coastal and neritic environments the distribution of dinoflagellate cysts follows a standard biogeographical zonation and appears to be bipolar on the global scale. The recognition of any of these biogeographical boundaries within Recent cyst distribution patterns provides a signal which can then be utilized in the sediment record to chart oceanographic and climatic changes.

The latitudinal distribution of the core-top dinoflagellate assemblages and the clear differentiation of dinoflagellate cyst assemblages at 60° S appears to provide such a biogeographical boundary. It remains to be proven as to whether this boundary can be utilized in the Quaternary fossil record. This 60° S boundary appears to coincide approximately with the limit of maximum sea-ice, and is the approximate position of the 1 °C summer SST isotherm (Text-fig. 2). To the north of 60° S there are about eight months of open water from mid October to mid June (Sea Ice Climatic Atlas 1985). The limit of sea-ice is important in its rôle in the suppression of light energy and therefore as a limiting factor for photosynthesis and primary production from phytoplankton including the autotrophic dinoflagellates. Indeed, it is interesting to note that Hasle (1969) observed a major decline in dinoflagellate numbers south of 60° S along transects at 90° W and 150° W. However, to

TABLE 6. Log ratio of heterotrophic dinoflagellates to autotrophic dinoflagellates. Total cyst numbers are given as cysts per gramme of sediment. A minimum value of 1 (shown in italics) was assigned to those assemblages without autotrophic forms to facilitate the calculation.

Core	Log H:A Ratio	Total Heterotroph Cysts	Total Autotroph Cysts
TC 004	0·4771	3	*1*
TC 006	0·301	2	1
TC 010	0	2	2
TC 044	0	1	*1*
PC 038	0·69897	5	*1*
TC 041	0·5441	7	2
GC 027	0·39794	5	2
TC 032	0·8239	20	3
KC 083	1·04663	334	30
KC 081	0·87091	208	28
PC 078	0·45426	74	26
KC 064	0·01773	25	24
KC 075	0·55091	192	54
KC 073	1·66276	230	5
KC 095	1·12571	187	14

the north of this line of latitude and beyond the winter sea-ice limit, numbers of dinoflagellates in the surface waters are controlled largely by nutrient availability.

The dinoflagellate cyst floras that have been recovered in the present study reveal that north of 60° S the diversity and recovery of dinoflagellate cysts increases markedly. Most of this increase derives from congruentidiacean cysts belonging, by inference or from incubation experiments, to the modern dinoflagellate genus *Protoperidinium*. Indeed Holm-Hansen *et al.* (1977) noted that this genus was the most important dinoflagellate genus to be found south of the Antarctic Convergence or Polar Front. *Protoperidinium* is heterotrophic in its nutritional strategy, often feeding upon diatoms which are the most predominant constituent of the phytoplankton in Antarctic waters (Jacques *et al.* 1979). These heterotrophic dinoflagellates are *r*-strategists and take advantage of the high nutrient content which encourages the increased diatom populations upon which the heterotrophic dinoflagellates feed. The diatoms, whilst autotrophic, are also *r*-strategists.

The area north of 60° S is a well-known area of upwelling from the effect of Ekman transport and katabatic winds off the Antarctic continent and it is to be expected that the effect of upwelling will be seen in the phytoplankton populations. We have already alluded to this in the increased numbers of *Protoperidinium* dinoflagellates and their cysts as seen in the core-top samples. An area of upwelling is also unstable and unpredictable and favours *r*-strategists. It is important, therefore, in this context to examine the numbers of autotrophic dinoflagellates and their cyst record in comparison with the heterotrophic dinoflagellates and their cysts. One of the ways of making this comparison is to look at the ratios between the two groups of dinoflagellate cysts. A simple intuitive approach was first described by Harland (1973) as the gonyaulacacean ratio although at the time it was not associated with nutritional strategies. Later it became more obvious that it was a measure of the numbers of peridiniacean cysts and hence of the importance of nutrient input into an environment encouraging heterotrophic nutrition. Recently, Powell *et al.* (1990) used the ratio of P-cysts to G-cysts as an indicator of nutrient enhancement and a guide to the history of coastal upwelling off the coast of Peru. They calculated a logarithmic ratio between peridiniacean and chorate cysts as a substitute for the peridiniacean/gonyaulacacean ratio. Dale (1996) argued the case to identify clearly the trophic categories, avoiding confusion with taxonomy or morphology.

In this study we have identified autotrophs and heterotrophs within our assemblages and have indicated the same on Table 3. Table 6 shows the numbers of cysts per gramme of sediment

assignable to each category and the calculated log ratios of heterotrophs to autotrophs (the 'H-cysts' and 'A-cysts' of Dale 1996). The results of plotting this ratio against the core-top samples along the transect (Text-fig. 6) reveals a general rising value from south to north with one of the major steps in the ratio occurring at about 60° S. This reinforces the other results presented in this paper and underscores the importance of the upwelling phenomenon in enhancing the numbers of the congruentidiacean dinoflagellate cysts and the position of the maximum limit of sea-ice. However, there is sufficient variation within the data for it to be treated with some caution. There is some potential, however, in using this methodology as a useful tool within the temporal record.

Relationships to productivity are less easy to disentangle, not least because of the possible allochthonous nature of the record and the difficulties in identifying modern sedimentation, as the congruentidiacean dinoflagellate cysts are representatives of the second tier within the trophic web feeding upon the dominant primary producers, the diatoms. A general assumption is that increased numbers of diatoms will inevitably lead to increased numbers of congruentidiacean dinoflagellate cysts; this also assumes that there is a simple relationship between the numbers of thecate forms, feeding upon diatoms, and the number of cysts produced as a result of sexual reproduction. This is perhaps rather too many assumptions to make at the moment and certainly none of these relationships is as yet proven nor has any quantitative model been established. Indeed, we have little information, for instance, on the competition faced by heterotrophic dinoflagellates from foraminifera and other planktonic organisms for food. We believe this will prove to be an extremely fruitful and exciting area for dinoflagellate research in the future. The importance of these relationships is becoming more and more apparent such that the link between dinoflagellate productivity, cyst production and positions in the first or second tier of the trophic web becomes paramount if ever the dinoflagellate cyst record is to be used as a proxy for productivity. It is to be welcomed that new data are becoming available on the numbers of cysts falling through the water column and being sampled in sediment trap arrays (Dale and Dale 1992). These data will assist in our understanding of cyst production and their final incorporation as a thanatocoenosis in bottom sediments.

In contrast to the discussion above on the role of the heterotrophic dinoflagellates, there is an increase in the absolute numbers of cysts derived from autotrophic dinoflagellates to the north along the studied transect (Text-fig. 6A). This trend increases toward the edge of the ACC and across the Antarctic Convergence as these *K*-strategists gain prominence in the more stable, predictable and nutrient-poor environments of the South Atlantic. Nonetheless, these autotrophic dinoflagellate cysts remain a minor component of the assemblages dominated by the congruentidiacean heterotrophs described herein. Further confirmation of this trend across the Antarctic Convergence must await further study on a more extensive dataset.

Finally, the relationship between the contained dinoflagellate cysts and the core-top sample lithologies also requires some comment. The poor recovery of dinoflagellate cysts south of 60° S also corresponds with an increase in the percentage of terrigenous sediment, low percentages of biogenic carbonate and silica and the presence of highly corrosive and oxygenated WSBW (Pudsey and Howe 1998). North of 60° S the increased numbers of dinoflagellate cysts is accompanied by increased percentages of biogenic material and a lower percentage of terrigenous sediment. This is further evidence to substantiate the effect of increased nutrient supply within the system leading to increased productivity and the importance of the sea-ice limit together with the nature of the bottom water masses. The relationships of biogenic material within core-top material is, however, also impossible to interpret without a clear understanding of the detailed sedimentation across the benthic boundary layer and the nature of the sedimentary record held in the uppermost millimetres of any sediment core and included in our core-top samples. Indeed, in Core 32 the Holocene in its entirety may be only 0·1 m thick. The different methods of core recovery may also be an important factor. However, the overall scale of this study and the comparisons with the work of Marret and de Vernal (1997) lead us to be confident in our identification of a biogeographical boundary for use within the palaeoceanographic history of the area. The biogeographical boundary identified herein is coincident with the maximum limit of sea-ice and, as a consequence, the length of time open sea

conditions prevail, as well as the availability of nutrients from upwelling. The detailed ecology of dinoflagellates within this particular environment is complex and will need further research before an adequate paradigm becomes available.

CONCLUSIONS

Our study is the first to describe in detail an indigenous dinoflagellate cyst thanatocoenosis from Recent bottom sediments in the Antarctic region. It provides distribution data and taxonomy of 17 taxa along a transect from the Falkland Trough to the Weddell Sea and it demonstrates a latitudinal trend in the cyst distributions. In comparison with the regional oceanography of the area the maximum limit of sea-ice appears to be the defining parameter in the cyst distributions. Hence the analysis of temporal (downcore) dinoflagellate cyst data should provide a proxy to recognize fluctuations in the limit of winter sea-ice through the more recent geological record. The recognition of this biogeographical and oceanographic boundary has implications for the extent and volume of sea-ice around the continent of Antarctica, the production of cold, dense bottom water and the dynamics of the thermohaline circulation system. The recognition of this and other biogeographical boundaries in the geological record also allows the detailing of climatic change in the region. Finally, the potential of using the dinoflagellate cyst record of autotrophic and heterotrophic dinoflagellates for investigating the trophic web, productivity, nutrient availability and upwelling histories has been discussed and identified as an area of future fundamental research.

Acknowledgements. The Centre for Palynology at the University of Sheffield and Mr S. Ellin and Mr B. Pigott, in particular, are thanked for their careful supervision of the qualitative palynological preparations of the core-top samples and for providing photographic facilities respectively. Particular thanks are due to Drs Anne de Vernal and Fabienne Marret who have been most generous with their help, advice and discussion as have the attendees of a recent workshop on 'Late Quaternary to Recent dinoflagellate cysts and their (palaeo-) ecological significance' held in Bremen, Germany, hosted by Professor Helmut Willems and Dr Karin A. F. Zonneveld. Finally Dr J. B. Riding and an anonymous referee are thanked for their constructive criticisms of the manuscript.

REFERENCES

ARTZNER, D. G. and DÖRHÖFER, G. 1978. Taxonomic note: *Lejeunecysta* nom. nov. pro. *Lejeunia* Gerlach 1961 emend. Lentin and Williams 1976 – dinoflagellate cyst genus. *Canadian Journal of Botany*, **56**, 1381–1382.

BALDWIN, R. P. 1987. Dinoflagellate resting cysts isolated from sediments in Marlborough Sounds, New Zealand. *New Zealand Journal of Marine and Freshwater Research*, **21**, 543–553.

BALECH, E. 1973. Segunda contribucion al conocimiento del microplancton del mar de Bellingshausen. *Contribucion del Instituto Antarctico Argentino*, **107**, 1–63.

—— 1974. El genero "Protoperidinium" Bergh, 1881 ("Peridinium" Ehrenberg, 1831, partim). *Revista del Museo Argentino de Ciencias Naturales "Bernardino Rivadavia", Hidrobiologia*, **4**(1), 1–79.

—— 1976. Clave ilustrada de dinoflagelados antarticos. *Publicacion Instituto Antarctico Argentino*, **11**, 1–99.

—— and EL-SAYED, S. Z. 1965. Microplankton of the Weddell Sea. *American Geophysical Union, Antarctic Research Series*, **5**, 107–124.

BARBER, M. and CRANE, D. 1995. Current flow in the north-west Weddell Sea. *Antarctic Science*, **7**, 39–50.

BAUMANN, K.-H. and MATTHIESSEN, J. 1992. Variations in surface water mass conditions in the Norwegian Sea: Evidence from Holocene coccolith and dinoflagellate cyst assemblages. *Marine Micropaleontology*, **20**, 129–146.

BENEDEK, P. N. 1972. Phytoplanktonten aus dem Mittel- und Oberoligozän von Tönisberg (Niederrheingebeit). *Palaeontographica, Abteilung B*, **137**, 1–71.

BERGH, R. S. 1881. Bidrag til Cilioflagellaternes Naturhistorie. Forelobige meddelelser. *Dansk Naturhistoriskforening i Kjobenhavn, Videnskabelige Meddelelser, Series 4*, **3**, 60–76.

—— 1882. Der Organismus der Cilioflagellaten. Eine phylogenetische Studie. *Morphologisches Jahrbuch*, **7**, 177–288.

BINT, A. N. 1988. Recent dinoflagellate cysts from Mermaid Sound, northwestern Australia. *Memoir of the Association of Australian Palaeontologists*, **5**, 329–341.

BOLCH, C. J. and HALLEGRAEFF, G. M. 1990. Dinoflagellate cysts in Recent marine sediments from Tasmania, Australia. *Botanica Marina*, **33**, 173–192.

BRADFORD, M. R. 1975. New dinoflagellate cyst genera from the recent sediments of the Persian Gulf. *Canadian Journal of Botany*, **53**, 3064–3074.

BROECKER, W. S., BOND, G., KLAS, M., BONANI, G. and WOLFLI, W. 1990. A salt oscillator in the glacial Atlantic? 1. The concept. *Paleoceanography*, **5**, 469–477.

—— PETEET, D. M. and RIND, D. 1985. Does the ocean-atmosphere system have more than one stable mode of operation? *Nature*, **315**, 21–26.

BRYDEN, H. L. and PILLSBURY, R. D. 1977. Variability of deep flow in the Drake Passage from year-long current measurements. *Journal of Physical Oceanography*, **7**, 803–810.

BUCK, K. R., BOLT, P. A., BENTHAM, W. N. and GARRISON, D. L. 1992. A dinoflagellate cyst from Antarctic sea ice. *Journal of Phycology*, **28**, 15–18.

BUJAK, J. P. 1980. Dinoflagellate cysts and acritarchs from the Eocene Barton Beds of southern England. 36–91. *In* BUJAK, J. P., DOWNIE, C., EATON, G. L. and WILLIAMS, G. L. Dinoflagellate cysts and acritarchs from the Eocene of southern England. *Special Papers in Palaeontology*, **24**, 1–100.

—— 1984. Cenozoic dinoflagellate cysts and acritarchs from the Bering Sea and northern North Pacific, DSDP Leg 19. *Micropaleontology*, **30**, 180–212.

BÜTSCHLI, O. 1885. Erster Band. Protozoa. 865–1088. *In Dr. H. G. Bronn's Klassen und Ordnungen des Thier-Reichs, wissenschaftlich dargestellt in Wort und Bild.* C. F. Winter'sche Verlagshandlung, Leipzig and Heidelberg.

CARMACK, E. C. and FOSTER, T. D 1975. On the flow of water out of the Weddell Sea. *Deep-Sea Research*, **22**, 711–724.

CHATTON, É. 1933. *Pheopolykrikos beauchampi* nov. gen., nov. sp., dinoflagellé polydinide autotrophe, dans l'Étang de Thau. *Bulletin de la Société zoologique de France*, **58**, 251–254.

CLAPARÈDE, É. and LACHMANN, J. 1859. Étude sur les infusoires et les rhizopods. *Mémoires de l'Institut National Génevois*, **6**, 261–482.

COOKSON, I. C. and EISENACK, A. 1965. Microplankton from the Browns Creek Clays, SW. Victoria. *Proceedings of the Royal Society of Victoria*, **79**, 119–131.

DALE, B. 1976. Cyst formation, sedimentation, and preservation: factors affecting dinoflagellate assemblages in Recent sediments from Trondheimsfjord, Norway. *Review of Palaeobotany and Palynology*, **22**, 39–60.

—— 1977. New observations on *Peridinium faeroense* Paulsen (1905), and classification of small orthoperidinioid dinoflagellates. *British Phycology Journal*, **12**, 241–253.

—— 1983. Dinoflagellate resting cysts: "benthic plankton". 69–136. *In* FRYXELL, G. A. (ed.). *Survival strategies of the algae*. Cambridge University Press, Cambridge, 144 pp.

—— 1996. Dinoflagellate cyst ecology: modeling and geological applications. 1249–1275. *In* JANSONIUS, J. and MCGREGOR, D. C. (eds). *Palynology: principles and applications*. 3. American Association of Stratigraphic Palynologists Foundation, Publishers Press, Salt Lake City, 911–1330.

—— and DALE, A. L. 1992. Dinoflagellate contributions to the deep sea. *Woods Hole Oceanographic Institution, Ocean Biocenosis Series*, **5**, 1–76.

DAVEY, R. J. and WILLIAMS, G. L. 1966. The genera *Hystrichosphaera* and *Achomosphaera*. 28–52. *In* DAVEY, R. J., DOWNIE, C., SARJEANT, W. A. S. and WILLIAMS, G. L. Studies on Mesozoic and Cainozoic dinoflagellate cysts. *Bulletin of the British Museum* (*Natural History*), *Geology*, *Supplement*, **3**, 1–248.

DEFLANDRE, G. and COOKSON, I. C. 1955. Fossil microplankton from Australian Late Mesozoic and Tertiary sediments. *Australian Journal of Marine and Freshwater Research*, **6**, 242–313.

DIESING, C. M. 1866. Revision der Prothelminthen, Abtheilung: Mastigophoren. *Sitzungsberichte der Akademie der Wissenschaften zu Wien, Mathematisch-naturwissenschaftliche Klasse*, **52**, 287–401.

DODGE, J. D. 1989. Some revisions of the Family Gonyaulacaceae (Dinophyceae) based on a scanning electron microscope study. *Botanica Marina*, **32**, 275–298.

EDWARDS, L. E. and ANDRLE, V. A. S. 1992. Distribution of selected dinoflagellate cysts in modern marine sediments. 259–288. *In* HEAD, M. J. and WRENN, J. H. (eds). *Neogene and Quaternary dinoflagellate cysts and acritarchs*. American Association of Stratigraphic Palynologists Foundation, Publishers Press, Salt Lake City, 438 pp.

EHRENBERG, C. G. 1830. Beiträge zur Kenntnis der Organisation der Infusorien und ihrer geographischen Verbreitung, besonders in Sibirien. *Königlich Akademie der Wissenschaften zu Berlin, Abhandlungen, Physikalische-Mathematische Klasse*, 1–88.

—— 1831. Animalia evertebrata. Unpaginated. *In* HEMPRICH, P. C. and EHRENBERG, C. G. *Symbolae physicae... Pars zoologica*. Akadamie der Wissenschaften zu Berlin, Abhandlungen, 10 pls.

—— 1838. Über das Massenverhältniss der jetz lebenden Kiesel-Infusorien und über ein neues Infusorien-Conglomerat als Polierschiefer von Jastraba in Ungarn. *Königlich Akademie der Wissenschaften zu Berlin, Abhandlungen*, 1836, **1**, 109–135.

FENSOME, R. A., TAYLOR, F. J. R., NORRIS, G., SARJEANT, W. A. S., WHARTON, D. I. and WILLIAMS, G. L. 1993. A classification of living and fossil dinoflagellates. *Micropaleontology, Special Publication*, **7**, 1–351.

FOLDVIK, A. and GAMMELSROD, T. 1988. Notes on Southern Ocean hydrography, sea-ice and bottom water formation. *Palaeogeography, Palaeoclimatology, Palaeoecology*, **67**, 3–17.

FOSTER, T. D. and MIDDLETON, J. H. 1979. Variability in the bottom water of the Weddell Sea. *Deep-Sea Research*, **26**, 743–762.

GRIMM, E. C. 1987. CONISS: a FORTRAN 77 program for stratigraphically constrained cluster analysis by the method of incremental sum of squares. *Computers and Geosciences*, **13**, 13–35.

GROSE, T. J., JOHNSON, J. A. and BIGG, G. R. 1995. A comparison between the FRAM (Fine Resolution Antarctic Model) results and observations in the Drake Passage. *Deep-Sea Research*, **42**, 365–388.

GRUNIG, S. 1991. Quaternary sedimentation processes on the continental margin of the South Orkney Plateau, NW Weddell Sea (Antarctica). *Berichte zur Polarforschung*, **75**, 1–196.

HAECKEL, E. 1894. *Systematische Phylogenie. Entwurf eines natürlichen Systems der Organismen auf Grund ihrer Stammegeschichte, I. Systematische Phylogenie der Protisten und Pflanzen*. Reimer, Berlin, 400 pp.

HARLAND, R. 1973. Dinoflagellate cysts and acritarchs from the Bearpaw Formation (Upper Campanian) of southern Alberta, Canada. *Palaeontology*, **16**, 665–706.

—— 1977. Recent and Late Quaternary (Flandrian and Devensian) dinoflagellate cysts from marine continental shelf sediments around the British Isles. *Palaeontographica, Abteilung B*, **164**, 87–126.

—— 1982. A review of Recent and Quaternary organic-walled dinoflagellate cysts of the genus *Protoperidinium*. *Palaeontology*, **25**, 369–397.

—— 1989. A dinoflagellate cyst record for the last 0·7 Ma from the Rockall Plateau, northeast Atlantic Ocean. *Journal of the Geological Society, London*, **146**, 949–951.

—— and HOWE, J. A. 1995. Dinoflagellate cysts and Holocene oceanography of the northeastern Atlantic Ocean. *The Holocene*, **5**, 220–228.

—— and LONG, D. 1996. A Holocene dinoflagellate cyst record from offshore north-east England. *Proceedings of the Yorkshire Geological Society*, **51**, 65–74.

—— and REID, P. C. 1980. Systematics Part I. *In* HARLAND, R., REID, P. C., DOBELL, P. and NORRIS, G. Recent and sub-Recent dinoflagellate cysts from the Beaufort Sea, Canadian Arctic. *Grana*, **19**, 211–225.

HASLE, G. R. 1969. Scientific results of marine biological research. *Hvalrådets Skriffter*, **52**, 1–168.

HEAD, M. J. 1993. Dinoflagellates, sporomorphs, and other palynomorphs from the Upper Pliocene St. Erth Beds of Cornwall, southwestern England. *Memoir of the Paleontological Society*, **31**, 1–62.

—— 1994. Morphology and paleoenvironmental significance of the Cenozoic dinoflagellate genera *Tectatodinium* and *Habibacysta*. *Micropaleontology*, **40**, 289–321.

—— 1996. Modern dinoflagellate cysts and their biological affinities. 1197–1248. *In* JANSONIUS, J. and McGREGOR, D. C. (eds). *Palynology: principles and applications*. 3. American Association of Stratigraphic Palynologists Foundation, Publishers Press, Salt Lake City, 911–1330.

—— and WRENN, J. H. (eds). 1992. A forum on Neogene and Quaternary dinoflagellate cysts. 1–31. *In* HEAD, M. J. and WRENN, J. H. (eds). *Neogene and Quaternary dinoflagellate cysts and acritarchs*. American Association of Stratigraphic Palynologists Foundation, Dallas, 438 pp.

HOFMANN, E. E. 1985. The large-scale horizontal structure of the Antarctic Circumpolar Current from FGGE drifters. *Journal of Geophysical Research*, **90**, 7087–7097.

HOLM-HANSEN, O., EL-SAYED, S. Z., FRANCESCHINI, G. A. and CUHEL, R. L. 1977. Primary production and factors controlling phytoplankton growth in the Southern Ocean. *Proceedings of the Third SCAR Symposium on Antarctic Biology*, 11–49.

HOWE, J. A., PUDSEY, C. J. and CUNNINGHAM, A. P. 1997. Pliocene–Holocene contourite deposition under the Antarctic Circumpolar Current, Western Falkland Trough, South Atlantic Ocean. *Marine Geology*, **138**, 27–50.

INDELICATO, S. R. and LOEBLICH, A. R. III 1986. A revision of the marine peridinioid genera (Pyrrhophyta) utilizing hypothecal-cingular plate relationships as a taxonomic guideline. *Japanese Journal of Phycology (Sôrui)*, **34**, 153–162.

JACQUES, G., DESCOLAS-GROS, C., GRALL, J.-R. and SOURNIA, A. 1979. Distribution du phytoplankton dans la partie Antarctique de l'Ocean Indièn en fin d'ete. *Internationale Revue der gesamten Hydrobiologie*, **64**, 609–628.

JORDAN, R. W. and PUDSEY, C. J. 1992. High-resolution diatom stratigraphy of Quaternary sediments from the Scotia Sea. *Marine Micropaleontology*, **19**, 201–237.

KOFOID, C. A. 1911. Dinoflagellata of the San Diego region. IV. The genus *Gonyaulax*, with notes on its skeletal morphology and a discussion of its generic and specific characters. *University of California Publications in Zoology*, **8**, 187–286.

KROOPNICK, P. M. 1985. The distribution of ^{13}C of ΣCO_2 in the world oceans. *Deep-Sea Research*, **32**, 57–84.

LEMMERMANN, E. 1910. III. Klasse Peridiniales. *In Kryptogamenflora der Mark Brandenburg und angrenzender Gebiete, III Algen I (Schizophyceen, Flagellaten, Peridineen)*. Gebrüder Borntraeger, Leipzig, 563–712, 869.

LENTIN, J. K. and WILLIAMS, G. L. 1981. Fossil dinoflagellates: index to genera and species, 1981 edition. *Bedford Institute of Oceanography, Report Series*, **BI-R-81-12**, 1–345.

—— —— 1993. Fossil dinoflagellates: index to genera and species 1993 edition. *American Association of Stratigraphic Palynologists Foundation, Contribution Series*, **28**, 1–856.

LINDEMANN, E. 1928. Abteilung Peridineae (Dinoflagellatae). 3–104. *In* ENGLER, A. and PRANTL, K. (eds). *Die Natürlichen Pflanzenfamilien nebst ihren Gattungen und wichtigeren Arten insbesonderen den Nutzpflanzen. Zweite stark vermehrte und verbesserte Auflage herausgegeben von A. Engler*. 2. Wilhelm Engelmann, Leipzig.

LOCARNINI, R. A., WHITWORTH, T., III and NOWLIN, W. D. Jr 1993. The importance of the Scotia Sea on the outflow of Weddell Sea Deep Water. *Journal of Marine Research*, **51**, 135–153.

LOEBLICH, A. R. Jr and LOEBLICH, A. R. III 1996. Index to the genera, subgenera, and sections of the Pyrrhophyta. *Studies in Tropical Oceanography, University of Miami*, **3**, 1–94.

MANTELL, G. A. 1850. *A pictorial atlas of fossil remains consisting of coloured illustrations selected from Parkinson's "Organic Remains of a former World", and Artis's "Antediluvian phytology"*. Henry G. Bohn, London, 207 pp.

—— 1854. *The medals of creation; or first lessons in geology and the study of organic remains*. 2nd edition. 1. Henry G. Bohn, London, 91, 239–242.

MARRET, F. and VERNAL, A. de 1997. Dinoflagellate cyst distribution in surface sediments of the southern Indian Ocean. *Marine Micropaleontology*, **29**, 367–392.

MATSUOKA, K. and BUJAK, J. P. 1988. Cenozoic dinoflagellate cysts from the Navarin Basin, Norton Sound and St. George Basin, Bering Sea. *Bulletin of the Faculty of Liberal Arts, Nagasaki University, Natural Science*, **29**(1), 1–147.

MATTHIESSEN, J. 1995. Distribution patterns of dinoflagellate cysts and other organic-walled microfossils in recent Norwegian–Greenland Sea sediments. *Marine Micropaleontology*, **24**, 307–334.

McMINN, A. 1990. Recent dinoflagellate cyst distribution in eastern Australia. *Review of Palaeobotany and Palynology*, **65**, 305–310.

—— 1991. Recent dinoflagellate cysts from estuaries on the central coast of New South Wales, Australia. *Micropaleontology*, **37**, 269–287.

—— 1992. Recent and late Quaternary dinoflagellate cyst distribution on the continental shelf and slope of southeastern Australia. *Palynology*, **16**, 13–24.

—— 1995. Why are there no post-Palaeogene dinoflagellate cysts in the Southern Ocean? *Micropaleontology*, **41**, 383–386.

—— and SUN XUEKUN 1994. Recent dinoflagellate cysts from the Chatham Rise, Southern Ocean, east of New Zealand. *Palynology*, **18**, 41–53.

MOSBY, H. H. 1934. The waters of the Atlantic Antarctic Ocean. *Scientific Results of the Norwegian Antarctic Expeditions 1927–1928*, **11**, 1–131.

MUDIE, P. J. 1986. Palynology and dinoflagellate biostratigraphy of Deep Sea Drilling Project Leg 94, Sites 607 and 611, North Atlantic Ocean. *Initial Reports of the Deep Sea Drilling Project*, **94**, 785–812.

NOWLIN, W. D. Jr and CLIFFORD, M. 1982. The kinematic and thermohaline zonation of the Antarctic Circumpolar Current at Drake Passage. *Journal of Marine Research*, **40**, 481–507.

—— and KLINCK, J. M. 1986. Physics of the Antarctic Circumpolar Current. *Reviews of Geophysics*, **24**, 469–491.

O'BRIEN, P. 1989. The magnetostratigraphy of marine sediments from Jane Basin, southeast of the South Orkney Microcontinent, Antarctica. Unpublished Ph.D. thesis, University of Southampton, England.

OLBERS, D., GOURETSKI, V., SEISS, G. and SCHROTER, J. 1992. *Hydrographic atlas of the Southern Ocean*. Alfred Wegener Institute, Bremerhaven, xvii + 82 pls.

ORSI, A. H., NOWLIN, W. D. Jr and WHITWORTH, T. III 1993. On the circulation and stratification of the Weddell Gyre. *Deep-Sea Research*, **40**, 169–203.

—— WHITWORTH, T. III and NOWLIN, W. D. JR 1995. On the meridional extent and fronts of the Antarctic Circumpolar Current. *Deep-Sea Research*, **42**, 641–673.

OSTENFELD, C. H. 1903. Phytoplankton from the sea around the Faeröes. *Botany of the Faeröes based upon Danish investigations*, 2. Det Nordiske Forlag, Copenhagen, 558–612.

PASCHER, A. 1914. Über Flagellaten und Algen. *Berichte der Deutsche Botanische Gesellschaft*, **32**, 136–160.

PAULSEN, O. 1905. On some Peridiniae and plankton diatoms. *Meddelelser fra Kommissionen for Havundsogelser, Serie Plankton*, **1**(3), 1–21.

POWELL, A. J., DODGE, J. D. and LEWIS, J. 1990. Late Neogene to Pleistocene palynological facies of the Peruvian continental margin upwelling, Leg 112. *Proceedings of the Ocean Drilling Program, Scientific Results*, **112**, 297–321.

PUDSEY, C. J. 1992. Late Quaternary changes in Antarctic Bottom Water velocity inferred from sediment grain size in the northern Weddell Sea. *Marine Geology*, **107**, 9–33.

—— BARKER, P. F. and HAMILTON, N. 1988. Weddell Sea abyssal sediments: a record of Antarctic Bottom Water flow. *Marine Geology*, **81**, 289–314.

—— and HOWE, J. A. 1998. Quaternary history of the Antarctic Circumpolar Current: evidence from the Scotia Sea. *Marine Geology*, **44**, 1841–1876.

—— and KING, P. in press. Particle fluxes, benthic processes and the palaeoenvironmental record in the northern Weddell Sea. *Deep-Sea Research*.

REID, P. C. 1974. Gonyaulacacean dinoflagellate cysts from the British Isles. *Nova Hedwigia*, **25**, 579–637.

REINECKE, P. 1967. *Gonyaulax grindleyi* sp. nov.: a dinoflagellate causing a red tide at Elands Bay, Cape Province, in December 1996. *Journal of South African Botany*, **33**, 157–160.

SARJEANT, W. A. S. 1970. The genus *Spiniferites* Mantell, 1850 (Dinophyceae). *Grana*, **10**, 74–78.

SCHILLER, J. 1935. Dinoflagellatae (Peridineae) in monographischer Behandlung. 2. Teil, Leiferung 2. 161–320. *In* RABENHORST, L. *Kryptogamen-Flora von Deutschland, Österreich und der Schweiz*. Akademische Verlagsgesellschaft, Leipzig.

SCHÜTT, F. 1896. Peridiniales (Peridineae, Dinoflagellata, Cilioflagellata, arthrodele Flagellaten). 1–30. *In* ENGLER, A. and PRANTL, K. (eds). *Die natürlichen Pflanzenfamilien nebst ihren Gattungen und wichtigeren Arten insbesondere den Nutzpflanzen unter Mitwirkung zahlreicher hervorragender Fachgelehrten, Teil. 1, Abteilung 1b*. Wilhelm Engelmann, Leipzig.

SEA ICE CLIMATIC ATLAS. 1985. *Volume 1, Antarctica*. Naval Oceanography Command, Asheville, North Carolina.

SHIMMIELD, G. B., DERRICK, S., MACKENSEN, A., GROBE, H. and PUDSEY, C. J. 1994. The history of biogenic silica, organic carbon and barium accumulation in the Weddell Sea and Antarctic Ocean over the last 150,000 years. 555–574. *In* ZAHN, R. *et al.* (eds). Carbon cycling in the Glacial Ocean: constraints on the ocean's role in global change. *NATO ASI Series*, **117**, 580 pp.

STOVER, L. E. and EVITT, W. R. 1978. Analyses of pre-Pleistocene organic-walled dinoflagellates. *Stanford University Publications, Geological Sciences*, **15**, 1–298.

SUN XUEKUN and MCMINN, A. 1994. Recent dinoflagellate cyst distribution associated with the Subtropical Convergence on the Chatham Rise, east of New Zealand. *Marine Micropaleontology*, **23**, 345–356.

TAYLOR, F. J. R. 1980. On dinoflagellate evolution. *BioSystems*, **13**, 65–108.

TECTONIC MAP OF THE SCOTIA ARC. 1985. *1:3000000, Sheet BAS (Miscellaneous), 3*. British Antarctic Survey, Cambridge.

VERNAL, A. de GOYETTE, C. and RODRIGUES, C. G. 1989. Contribution palynostratigraphique (dinokystes, pollen et spores) à la connaissance de la mer de Champlain: coupe de Saint-Césaire, Québec. *Canadian Journal of Earth Sciences*, **26**, 2450–2464.

—— TURON, J.-L. and GUIOT, J. 1994. Dinoflagellate cyst distribution in high-latitude marine environments and quantitative reconstruction of sea-surface salinity, temperature, and seasonality. *Canadian Journal of Earth Sciences*, **31**, 48–62.

WALL, D. 1965. Modern hystrichospheres and dinoflagellate cysts from the Woods Hole region. *Grana Palynologica*, **6**, 297–314.

—— 1967. Fossil microplankton in deep-sea cores from the Caribbean Sea. *Palaeontology*, **10**, 95–123.

—— and DALE, B. 1968. Modern dinoflagellate cysts and evolution of the Peridiniales. *Micropaleontology*, **14**, 265–304.

—— —— LOHMANN, G. P. and SMITH, W. K. 1977. The environmental and climatic distribution of dinoflagellate cysts in modern marine sediments from regions in the North and South Atlantic Oceans and adjacent seas. *Marine Micropaleontology*, **2**, 121–200.

WHITWORTH, T. III, NOWLIN, W. D. Jr and WORLEY, S. J. 1982. The net transport of the Antarctic Circumpolar Current through Drake Passage. *Journal of Physical Oceanography*, **12**, 960–971.

WOOD, G. D., GABRIEL, A. M. and LAWSON, J. C. 1996. Palynological techniques – processing and microscopy. 29–50. *In* JANSONIUS, J. and MCGREGOR, D. C. (eds). *Palynology: principles and applications*. 1. American Association of Stratigraphic Palynologists Foundation, Publishers Press, Salt Lake City, 462 pp.

WRENN, J. H. 1988. Differentiating species of the dinoflagellate cyst genus *Nematosphaeropsis* Deflandre & Cookson 1955. *Palynology*, **12**, 129–150.

ZENK, W. O. 1981. Detection of overflow events in the Shag Rocks Passage, Scotia Ridge. *Science*, **213**, 1113–1114.

REX HARLAND

DinoData Services
50 Long Acre, Bingham
Nottingham NG13 8AH, UK
and
Centre for Palynology
Department of Earth Sciences
University of Sheffield
Dainton Building
Brookhill
Sheffield S3 7HF, UK

CAROL A. PUDSEY

JOHN A. HOWE

British Antarctic Survey
High Cross, Madingley Road
Cambridge CB3 0ET, UK

MERIEL E. J. FITZPATRICK

Department of Geological Sciences
University of Plymouth
Drake Circus
Plymouth PL4 8AA, UK

Typescript received 5 August 1997
Revised typescript received 14 January 1998

CHAROPHYTES FROM THE LOWER CRETACEOUS OF THE IBERIAN RANGES (SPAIN)

by CARLES MARTÍN-CLOSAS *and* CARMEN DIÉGUEZ

ABSTRACT. In the Upper Barremian of the Iberian Ranges (Las Hoyas, Cuenca, Spain) an association of exceptionally well preserved charophyte thalli comprises four new form-species: *Palaeonitella vermicularis* sp. nov., *Charaxis spicatus* sp. nov., *Clavatoraxis robustus* gen. et sp. nov., and *Clavatoraxis diaz-romerali* sp. nov. This is the youngest fossil record of the genus *Palaeonitella*. The new form-genus *Clavatoraxis* is erected to include charophyte vegetative remains bearing spine-cell rosettes, a character attributed to the family Clavatoraceae. This is the first time an assemblage of charophyte vegetative remains has been described and related to assemblages of fructifications. This gives a good correlation at family level between the frequency of taxa found as vegetative remains and calcified fructifications. Two biocoenoses are represented: *Clavatoraxis robustus* displays adaptations found in extant charophytes living in permanent shallow water lakes whereas *Clavatoraxis diaz-romerali* was adapted to light-limited, probably deeper, environments. *Palaeonitella vermicularis* grew twisted round thalli of *Clavatoraxis*. Early Cretaceous freshwater communities appear to have been dominated by charophytes, and not by aquatic ferns as believed previously.

CHAROPHYTES include complex green algae, which are considered to be part of the evolutionary lineage leading to vascular plants (Kenrick 1994). The fossil record of these fresh- to brackish-water plants is rich, extends from the upper Silurian to the present, and is composed mainly of calcified fructifications called gyrogonites and utricles. Fossil whole plant remains are extremely scarce. Lower Cretaceous whole plant remains of charophytes consist of silicified specimens from the British Purbeck (Harris 1939), the Morrison Formation of the United States (Peck 1957) and the Barremian of Argentina (Musacchio 1971). Although small fragments of calcified vegetative remains of charophytes are not uncommon in marls prepared for the study of fructifications or in thin sections of lacustrine limestones, this is the first time that a complete association of large vegetative charophyte remains has been found in the post-Palaeozoic fossil record. The study of these fossils is not only necessary to increase knowledge of the morphology of the plants producing the fructifications currently studied, but also enables us description of the structure of an Early Cretaceous freshwater community and underlines the significance of charophytes in subaquatic freshwater environments prior to the radiation of angiosperms.

The material studied consists of exceptionally well preserved charophyte thalli from finely laminated lacustrine limestones in the La Huérguina Formation at Las Hoyas, near Cuenca, Spain (Text-fig. 1). The material was obtained in part by bed-by-bed sampling during the annual excavations of the site and also from the collection of Mr Armando Díaz-Romeral, from Cuenca, who discovered the charophyte remains. Charophyte thalli are calcified and preserved in three dimensions within laminites. In most specimens the surface is slightly corroded. This material was studied directly under light microscopy after immersion in an organic solvent. Limited etching with diluted acetic acid was necessary to prepare some specimens. Thin sections were also prepared to observe the internal anatomy of thalli. Since no three-dimensionally preserved fructifications were found attached to the thalli studied they have been named after already known or newly described form-taxa which are reserved for vegetative remains. A correlation between these taxa and the general systematics of fossil charophytes, which is based exclusively on fructifications, is currently only intended above the suprageneric level. For clavatoracean fructifications the systematics followed agrees with the phylogenetic system of Clavatoraceae proposed by Martín-Closas (1996).

[Palaeontology, Vol. 41, Part 6, 1998, pp. 1133–1152, 5 pls]

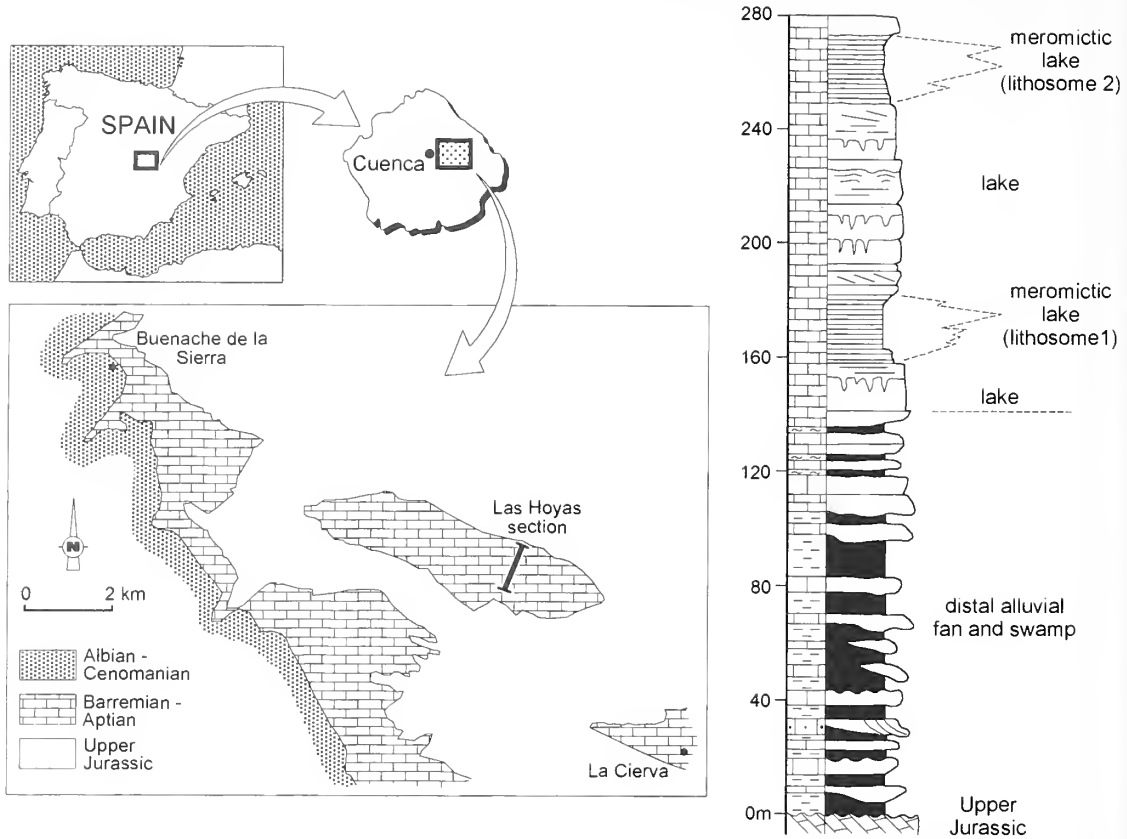

TEXT-FIG. 1. Geographical location and stratigraphical section of the palaeontological site of Las Hoyas; modified from Fregenal-Martínez and Meléndez (1993).

The marls and limestones of the La Huérguina Formation, which include the finely laminated limestones of Las Hoyas, were deposited in the south-eastern Iberian Basin, one of the Mesozoic intracontinental basins of the Iberian Plate. These basins contain up to 5000 m of Late Jurassic to Early Cretaceous sediments as a result of significant basement subsidence related to rifting of the Central Atlantic crust (Álvaro *et al.* 1979; Salas and Casas 1993). The south-eastern Iberian Basin was orientated following the general north-west to south-east trend of the Iberian Ranges. It opened towards the south-east to the Tethys sea, where the deposition of marine shallow water limestones dominated, whereas towards the opposite, north-western end of the basin, the sedimentation occurred mainly in freshwater facies, including the deposition of the La Huérguina Formation (Mas 1981; Meléndez 1983; Fregenal-Martínez and Meléndez 1994). This palustrine and lacustrine unit is up to 280 m thick in the area studied and includes two lithosomes, about 25 m thick, of finely laminated lacustrine limestones separated by palustrine and lacustrine stratified limestones and marls (Fregenal-Martínez and Meléndez 1993). The laminated limestones correspond to the distal, anoxic facies of a meromictic lake (Gómez-Fernández and Meléndez 1991), which preserved floral and faunal remains exceptionally well and provided the charophyte specimens studied here. Biostratigraphical analysis of charophyte and ostracod associations (Diéguez *et al.* 1995*a*) indicates that this unit is of Late Barremian age.

The fossils found at Las Hoyas include representatives of almost all Lower Cretaceous continental groups. The site has provided significant new taxonomic and phylogenetic data about

fish (Poyato-Ariza 1995), amphibians (McGowan and Evans 1995), dinosaurs (Pérez-Moreno *et al.* 1994) and birds (Sanz *et al.* 1996) along with invertebrates, such as insects (Martínez-Delclòs *et al.* 1995) and crustaceans (Rabadà 1993). Plant fossils are also very abundant and well preserved and include charophytes, bryophytes, ferns, conifers, cycadales, bennettitales, gnetales and early angiosperms (Sanz *et al.* 1988; Diéguez *et al.* 1995*b*). The enigmatic plant *Montsecchia vidali* (Zeiller 1902) Teixeira, 1954 is also present and constitutes one of the most abundant plant remains. Especially significant for this study is the absence of other freshwater macrophytes apart from charophytes.

SYSTEMATIC PALAEONTOLOGY

Division CHAROPHYTA Migula, 1897
Class CHAROPHYCEAE Smith, 1938
Order CHARALES Lindley, 1836

Form-genus PALAEONITELLA Pia, 1927 emend.

Type species. Palaeonitella cranii (Kidston and Lang 1921) Pia, 1927.

Original diagnosis. Vegetative shoot clearly organized in nodes and internodes with whorls of short branches. Reproductive organs so far unknown. Many details of organization are reminiscent of Characeae (Pia 1927, p. 91). ('Deutlich in Knoten und Internodien gegliederte vegetative Sprosse mit wirtelig gestellten Kurztrieben. Fortpflazungsorgane sind bis jetzt nicht bekannt. Viele Einzelheiten der Organisation erinnern an die Characeen').

Emended diagnosis. Vegetative shoot organized in nodes and internodes with whorls of short, non-branching branchlets. Thallus ecorticate. Reproductive organs so far unknown.

Remarks. The ecorticate thallus of *Paleonitella* is the main character to separate this genus from other post-Palaeozoic form-genera such as *Charaxis* Harris, 1939. The absence of furcations in branchlets of *Palaeonitella* distinguishes this genus from the Devonian ecorticate genus *Octochara* Gess and Hiller, 1995. Thalli of another Devonian genus, *Hexachara* Gess and Hiller, 1995, are similar in organization to *Palaeonitella* but the laterals of the former should be termed bract-cells since they always bear large gyrogonites.

Palaeonitella vermicularis sp. nov.

Plate 1, figures 1–4

Derivation of name. The name refers to the flexible and filamentous aspect of the thalli, which resemble worms (Latin, *vermis*).

Holotype. Specimen LH-16100 from the collection of Mr Armando Díaz-Romeral, Museo de Cuenca (Cuenca, Spain), deposited in the Unidad de Paleontología, Universidad Autónoma de Madrid.

Paratypes. Specimens LH-1319 and LH-16102 (the latter from the collection of Mr Armando Díaz-Romeral), Museo de Cuenca (Cuenca, Spain), deposited in the Unidad de Paleontología, Universidad Autónoma de Madrid.

Type layer and locality. Second lithosome of finely laminated limestones of the La Huérguina Formation at Las Hoyas (Cuenca, Spain).

Material. Specimen LH-16100 is an assemblage of abundant thalli, which are difficult to individualize. Specimens LH-1319, LH-16102, LH-16103 and LH-16104 contain individual portions of thalli.

Diagnosis. Extremely fine filamentous and flexible ecorticate thalli with nodes bearing about twelve, 1–2 mm long, single-celled branchlets and internodes separated at intervals of 1·5–3·5 mm.

Description. Charophyte vegetative remains flexible and filamentous in overall aspect, ecorticate and poorly calcified (Pl. 1, figs 1–2). Nodes bear about ten (probably 12) small (1–2 mm long) single-celled branchlets and are separated by ecorticate internodes, which lack a cortex of cells (Pl. 1, figs 3–4). Internodes 1·8–3·2 mm (mean 2·3 mm) long and 0·2–0·8 mm wide. No fructifications have been found attached to these thalli.

Comparisons. Palaeonitella cranii, from the Devonian Rhynie Chert, Scotland (Kidston and Lang 1921; Pia 1927), differs from *P. vermicularis* in its smaller size (relative difference 1:10) and possession of noded branchlets (single-celled in *P. vermicularis*). The other species described within the genus, *Palaeonitella tarafiyensis* Hill and El Khayal, 1983, from the Upper Permian of Saudi Arabia, is similar in general size and structure of branchlets to our material. However, the internodes of *P. tarafiyensis* are extremely long (up to 25 mm) and nodes are swollen to about twice the width of internodes, whereas in *P. vermicularis* internodes are short and nodes have about the same width as internodes. The Permian species appears much more rigid than the Cretaceous species, in spite of the similar preservation as lime-encrusted fossils.

Remarks. Palaeonitella vermicularis is relatively common in the samples studied and is associated with *Clavatoraxis robustus* and *Clavatoraxis diaz-romerali.* On the basis of the ecortication of *Palaeonitella* it has traditionally been accepted that this form-genus is reminiscent of extant Characeae Nitelleae. However, extant representatives bear furcated branchlets, unlike *Palaeonitella.* On the other hand, some Characeae Chareae are also ecorticate, and this may have been the condition of many other taxa which are exclusively fossil, such as the Devonian genera *Octochara* and *Hexachara.* Therefore, at present, assignment of *Paleonitella* to Nitelleae is a hypothesis.

Paleonitella vermicularis is the most modern species of the genus in the fossil record since other species were Palaeozoic. However, it is expected that the fossil record of the genus will increase and cover the gaps between fossil and present day charophytes bearing ecorticate thalli which are much like those described here.

Form-genus CHARAXIS Harris, 1939

Type species. Charaxis durlstonense Harris, 1939 from the Purbeck of Durlston (England), a lectotype proposed by Horn af Rantzien (1956).

Diagnosis. 'Vegetative charophyte organs agreeing in so far as they are known with *Chara.* Stem consisting of nodes and internodes, internode composed of a central cell surrounded by a ring of primary cortical cells which grow up and down from the nodes; and may cut off secondary cortical cells at their sides, primary cortical cells giving rise to spine cells. Leaves [branchlets] as in *Chara*, either corticated in the same way as the stem, or uncorticated' (Harris 1939, p. 67).

EXPLANATION OF PLATE 1

Figs 1–4. *Palaeonitella vermicularis* sp. nov.; LH-16100 (holotype). 1, partial view of thallus showing flexibility and variation in size; ×5. 2, detail of thallus with ecorticate internodes; ×6. 3, detail of thallus with branchlets preserved; ×6. 4, detail of node showing about ten branchlet scars; ×30.

Fig. 5. *Charaxis spicatus* sp. nov.; general view of LH-16110 (holotype); ×4.

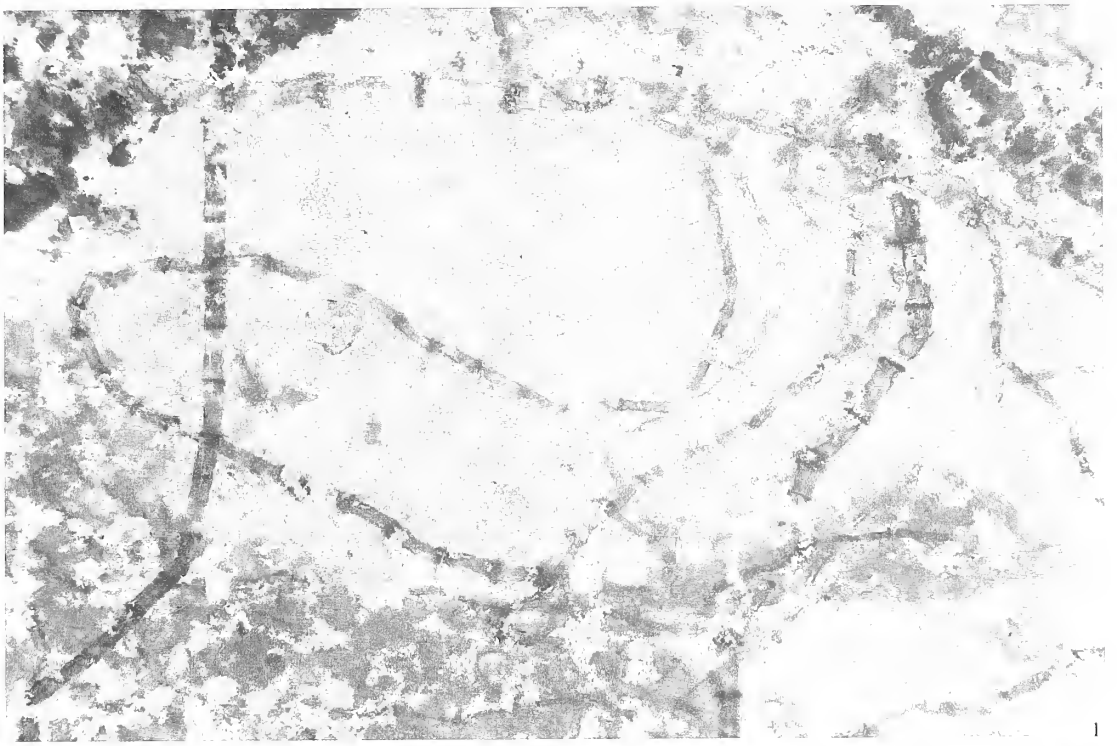

1

2

3

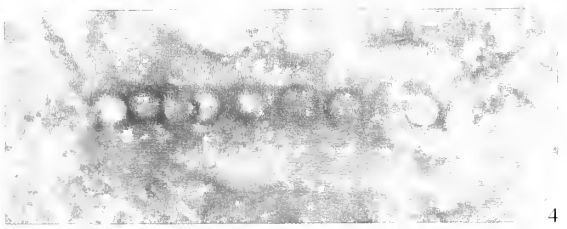

4

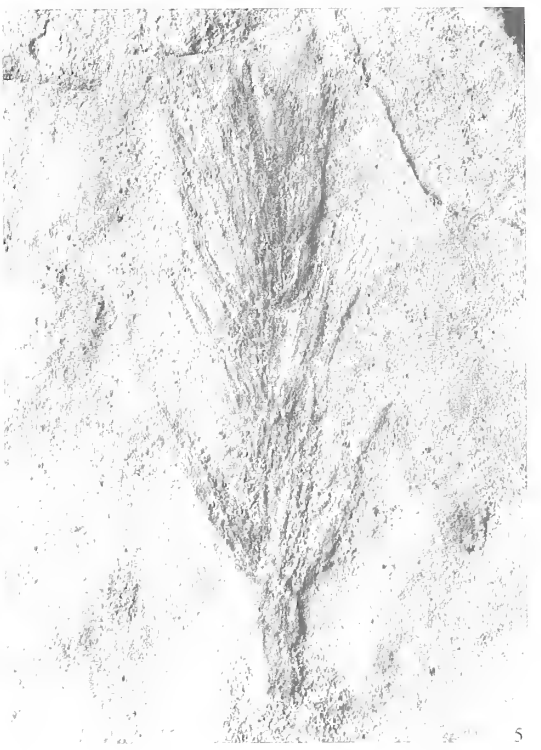

5

MARTÍN-CLOSAS and DIÉGUEZ, *Palaeonitella*, *Charaxis*

Charaxis spicatus sp. nov.

Plate 1, figure 5; Plate 2, figures 1–9

Derivation of name. Name refers to the spike-like form of the thallus.

Holotype. Specimen LH-16110 from the collection of Mr Armando Díaz-Romeral, Museo de Cuenca (Cuenca, Spain), deposited in the Unidad de Paleontología, Universidad Autónoma de Madrid.

Paratypes. Thin sections LH-16105–LH-16109, housed in the same museum. These samples were taken from a dark grey laminated mudstone.

Type horizon and locality. Second lithosome of finely laminated limestones of the La Huérguina Formation at Las Hoyas (Cuenca, Spain).

Material. LH-16110, which is an apical fragment of thallus, is the only three-dimensionally preserved specimen found to date. LH-16121 is a rock sample containing several horizons rich in charophyte remains which supplied the slices to prepare thin sections LH-16105–LH-16109.

Diagnosis. Thallus of *Charaxis* with nodes formed by six nodal cells bearing up to 18 ecorticate branchlets which are longer than the internodes above, completely covering them. Internodes several millimetres long and *c.* 1 mm wide formed by an internodal cell coated by first six then 18 cortical cells. Gyrogonites ellipsoidal (400–530 μm × 260–290 μm), showing *c.* 16–18 circumvolutions and probably apical and basal necks.

Description

Description of three-dimensionally preserved specimen LH-16110. Fragment of charophyte thallus bearing six large internodes (2·2–5·3 mm long and *c.* 1 mm wide) which are covered by vertical, non-spiralized cortical cells (Pl. 1, fig. 5). The preservation of this specimen does not allow a precise count of the number of cortical cells, which is, however, more than ten and less than 20. The five nodes preserved bear about 15 ecorticate, needle-like branchlets which are longer than the internode immediately above, covering it completely when not compressed. From this number of branchlets, which is similar to the most probable number of cortical cells, we deduce that the thallus was haplostichous, which means it had a cortex of primary cells only. Small scars at the base of nodes may correspond to bases of broken branchlets. No fructifications have been found attached to or in close association with this thallus.

Description of specimens from thin sections LH-16105–LH-16109. These specimens are about the half of the size of LH-16110, but are identical to it in external morphology, number of branchlets and general cortication (Pl. 2, fig. 1). Therefore we consider that samples LH-16105 to LH-16110 belong to the same species. Internodes are formed by a large nodal cell (200–330 μm in diameter) coated by small cortical cells (diameter 40–80 μm). Close to the nodes there are six large cortical cells (Pl. 2, fig. 6). At variable but short distances from nodes, these cortical cells trifurcate: two small laterals and a larger central tube arise from each original cell (Pl. 2, figs 3–4). This larger central cell becomes smaller towards the distal part of the internode. As a result,

---

EXPLANATION OF PLATE 2

Figs 1–9. *Charaxis spicatus* sp. nov. 1, thin section LH-16105; longitudinal section of thallus; × 20. 2, 7–8, thin section LH-16106. 2, longitudinal section through node showing insertion of three branchlets in each nodal cell (arrow); × 20. 7, oblique sections through distal part of internodes; × 30. 8, longitudinal section through fertile node showing three gyrogonites; × 20. 3, thin section LH-16107; tangential section of node and subjacent internode showing cortical cells branching downwards (arrow); × 20. 4, thin section LH-16108; longitudinal section through node and internode with secondary cortical cells formed by upwards branching of primary cortical cells (arrow); × 20. 5–6, 9, thin section LH-16109. 5, transverse section through apical internodal cell and branchlets; × 30. 6, transverse section through proximal part of internode showing primary and secondary cortical cells of different size; × 30. 9, longitudinal section of gyrogonite; × 50.


1


2

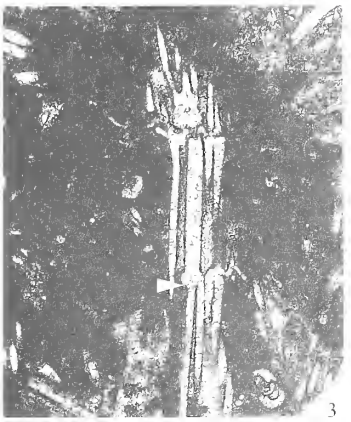
3

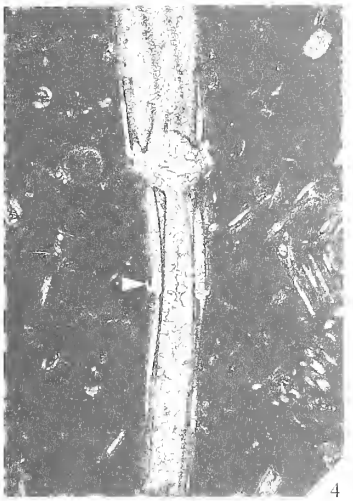
4

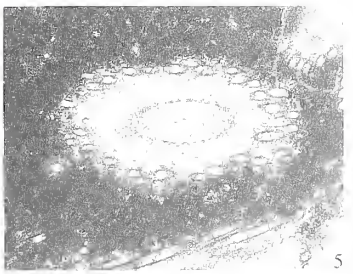
5

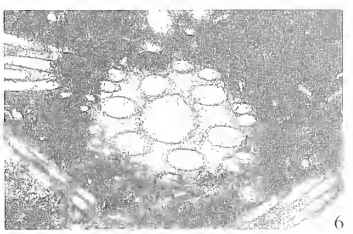
6


7


8

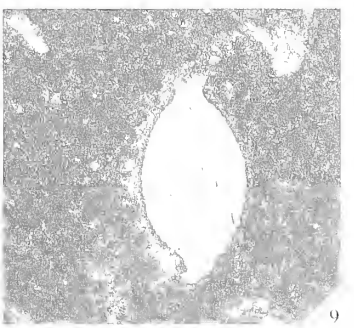
9

MARTÍN-CLOSAS and DIÉGUEZ, *Charaxis*

close to the centre of an internode there are about 18 cortical cells of equal diameter, three per original cortical cell (Pl. 2, fig. 7). In the centre of the internode, cortical cells coming from adjacent nodes do not interdigitate since corticated with 36 cells were not found. Nodes are formed by six large globular cells, from which three ecorticate branchlets emerge (Pl. 2, fig. 2). As a result about 18 extremely long branchlets develop and appear to cover completely the next internode and node in an apical direction (Pl. 2, fig. 5). Taking into account that the number of branchlets equals the final number of cortical cells per node, the cortex of this species could be termed haplostichous. Gyrogonites have been found attached to certain nodes and are ellipsoidal (400–530 μm × 260–290 μm) with an isopolarity index (height × 100/diameter) of 104–108 and about 16–18 circumvolutions (Pl. 2, fig. 8). Several gyrogonites found in the same thin sections, which appear to belong to the same species, show apical and basal necks (Pl. 2, fig. 9).

Comparisons. The new species has approximately as many branchlets and cortical cells as the lectotype of the genus *Charaxis durlstonense* but differs in the absence of cortication in branchlets. According to Groves (1933), the Tertiary species *Charaxis blassiana* (Heer 1855) Harris, 1939 and *Charaxis gypsorum* (Saporta 1862) Harris, 1939 are also haplostichous, like *Charaxis spicatus* sp. nov. However, they differ from the new species by their reduced number of branchlets. Other *Charaxis* species considered by Harris (1939) are either different from the point of view of cortex organization or are insufficiently known. *Charaxis striatus* Peck, 1957 is known only from internodal fragments which appear to be coated by an extremely large number of cortical cells in comparison with the number of nodal cells or branchlets. Using this character it may be distinguished easily from the new species described here. Schudack (1989, 1993) suggested that *Charaxis striatus* should be included in the form genus *Munieria* Deecke, 1883, and may be synonymous with *Munieria grambasti* subsp. *sarda* Cherchi, Gušić, Schmidt and Schroeder, 1981, which he considers a Clavatoraceae. However, the genus *Munieria*, as originally defined by Deecke (1883), includes incompletely calcified vegetative remains which may correspond to several of the charophyte form-genera presently known.

Remarks. Charaxis spicatus is strongly reminiscent of thalli of extant *Chara*, which may justify the inclusion of the new species in Characeae. However, the presence of gyrogonites bearing apical necks in the same horizon (but not in anatomical connection with thalli) makes this attribution unsure. In the Lower Cretaceous, gyrogonites with apical necks are typical of the extinct family Clavatoraceae.

Form-genus CLAVATORAXIS gen. nov.

Derivation of name. From Clavatoraceae, the extinct charophyte family bearing this type of vegetative remains and *axis* (Latin).

Type species. Clavatoraxis robustus sp. nov.

Diagnosis. Verticillate thalli organized in nodes with branchlets separated by corticate internodes. Spine-cell rosettes are present at least in some parts of the thalli.

Remarks. The presence of spine-cell rosettes was first noticed on thalli of *Clavator reidii* by Harris (1939). However, Harris found fructifications attached to the silicified vegetative remains that he studied, enabling him to ascribe such remains to a taxon using the fructification-based systematics of fossil charophytes. The new form-genus *Clavatoraxis* is created for sterile clavatoracean verticillated vegetative remains which cannot be attributed to any species of fructification.

EXPLANATION OF PLATE 3

Clavatoraxis robustus gen. et sp. nov.; holotype, LH-16111; young portion of thallus; × 2·5.

MARTÍN-CLOSAS and DIÉGUEZ, *Clavatoraxis*

Clavatoraxis robustus sp. nov.

Plate 3; Plate 4, figures 1–4; Plate 5, figures 1–9

Derivation of name. From its overall robust appearance, making it one of the largest and strongest thalli known from a Recent or fossil charophyte.

Holotype. Specimen LH-16111 from the collection of Mr Armando Díaz-Romeral, Museo de Cuenca (Cuenca, Spain), deposited in the Unidad de Paleontología, Universidad Autónoma de Madrid.

Paratypes. Specimens LH-16112–LH-16114 and thin sections LH-16116–LH-16120 housed in the same museum.

Type horizon and locality. Second lithosome of finely laminated limestones of the La Huérguina Formation at Las Hoyas (Cuenca, Spain).

Material. LH-450 A/B (portion of thallus), LH-823 A/B (portion of thallus), LH-1020 (portion of thallus), LH-1924 (small portion of thallus), LH-1941–LH-1943 (three small portions of branchlets in the same rock sample), LH-7087 (portion of thallus), LH-7361 (apical portion of thallus), LH-8016 (impression of portion of thallus), LH-8017 (portion of branched thallus), LH-8047 (impression of portion of thallus), LH-8114 (small portion of thallus), LH-8061 (portion of thallus), LH-13152 (portion of thallus with evidences of erosion), LH-13153 (impression of clavatoracean utricle), LH-13190 (portion of thallus with clavatoracean utricles scattered around), LH-13368 (portion of branchlet), LH-14114 (portion of thallus), LH-14180 (portion of thallus and impressions of utricles), LH-16111 (apical part of young thallus, holotype), LH-16112 (large mature thallus, paratype), LH-16113 (portion of mature thallus, paratype), LH-16114 (portion of mature thallus, paratype), LH-16115 (large sample with abundant fragments of thalli which supplied rock slices for thin sections), five thin sections (paratypes) LH-16116–LH-16120, LH-16122 (impression of two large portions of thalli and other smaller fragments).

Diagnosis. Several hundreds of millimetres long and 2–3 mm wide thalli of the *Clavatoraxis* type with first-order opposite branching and spine-cell rosettes completely covering internodes which are not terminal. In terminal, last order branchlets, spine cell rosettes are organized in nodes, separated by corticate, rosette-free internodes.

Description. Thalli supported by a main axis which is several hundreds of millimetres long and 2–3 mm wide, robust in overall appearance (Pl. 3). Branches attached to main axis are opposite and may further branch dichotomously or trichotomously (Pl. 3; Pl. 4, fig. 1). First and second order internodes are 16–44 mm long, spirally corticate (Pl. 5, fig. 1). Cortication formed by six cells near the nodes which interdigitate with the six cortical cells of an adjacent node giving the central part of an internode a 12-celled cortication (Pl. 5, figs 2–3). Internodes covered with spirally arranged, spine-cell rosettes, *c.* 0·5 mm in basal diameter (Pl. 4, fig. 2; Pl. 5, fig. 5). Up to 25 spiral rows of spine-cell rosettes are observed in lateral views of internodes of the main axis (Pl. 3). Spine-cell rosettes are hemispherical structures formed by a large number of club-shaped spine-cells, which are 200–250 μm long (Pl. 5, fig. 6). The apical swelling of such clubs is spherical, *c.* 100 μm in diameter and filled with sparite. As a result, the surface of a spine-cell rosette is covered by crystalline spheres. Club-shaped spine-cells radiate from the base of a rosette which is directly open to a cortical cell, leaving a gap in the cortical cell wall at the insertion point.

Last order branchlets organized in whorls of six are *c.* 3–4 mm long and formed by swollen nodes with short corticate internodes (Pl. 4, fig. 3). Nodes are formed by spine-cell rosettes with wedge-shaped (not club-shaped)

EXPLANATION OF PLATE 4

Figs 1–4. *Clavatoraxis robustus* gen. et sp. nov. 1, 3, paratype LH-16112. 1, mature portion of thallus showing opposite branching; ×1. 3, detail, showing six branchlets per node; ×4. 2, paratype LH-16113; young portion of thallus showing spiral arrangement of spine cell rosettes; ×2. 4, detail of mature branchlets in paratype LH-16114; ×4·5.

1

2

3

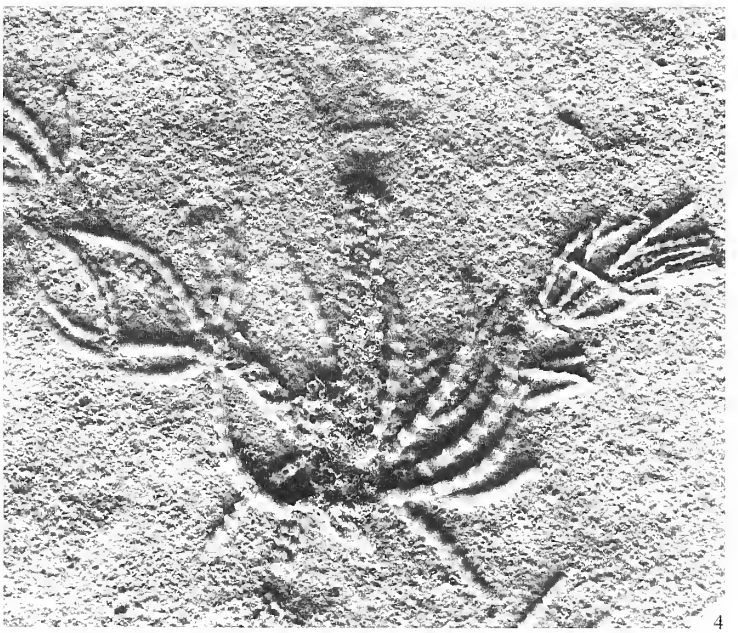

4

MARTÍN-CLOSAS and DIÉGUEZ, *Clavatoraxis*

spine cells, whereas internodes are rosette-free (Pl. 5, figs 7–8). Young, apical parts of thalli show closely packed last-order branchlets with nodes almost superimposed without leaving space for internodes. In the mature parts, last-order branchlets become loosely opened and their nodes are separated by short internodes. Since last order internodes are not covered by spine-cell rosettes, the cortication may be observed from the outside of thalli (Pl. 5, fig. 4). However, only the wall of cortical cells adjacent to the axis is calcified and this results in the fossil internode having a striated surface (Pl. 4, fig. 4).

No fructifications have yet been found attached to the thalli studied. The vegetative characters of *Clavator reidii* as described by Harris (1939) are largely like the last-order branchlets of thalli of *Clavatoraxis robustus* described here. This may be evidence that *Clavatoraxis robustus* bore fructifications of the clavatoroid type or even that it represents the vegetative remains of genus *Clavator*. However, this conclusion is not supported by the material studied, which only contains atopocharoid utricles dispersed in the sediment around the thalli. Such utricles are globular, bottle-shaped and do not present calcified gyrogonites (Pl. 5, fig. 9).

Comparisons. Young and closely packed, terminal branchlets of the thallus of *Clavatoraxis robustus* are similar in external appearance to *Munieria baconica* Deecke, 1883 as figured by Conrad and Radoičić (1971, fig. 4) and Bystrický (1976, pl. 4, fig. 7). Also, the mature, loosely packed terminal branchlets have a superficial similarity to *Munieria grambasti* Bystrický, 1976. However, our material differs by having the nodes of such branchlets formed by spine-cell rosettes whereas in the genus *Munieria* such nodes are devoid of rosettes and bear cylindrical cells.

Remarks. This is the most common charophyte found at Las Hoyas.

Clavatoraxis diaz-romerali sp. nov.

Text-figures 2A–C, 3A–D

Derivation of name. After Mr Armando Diaz-Romeral from Cuenca (Spain), in acknowledgement for collecting and making available the material upon which this study is based.

Holotype. Specimen LH-16123 from the collection of Mr Armando Díaz-Romeral, Museo de Cuenca (Cuenca, Spain), deposited in the Unidad de Paleontología, Universidad Autónoma de Madrid.

Paratype. Specimen LH-16101 and thin section LH-16124 prepared from the same sample (Museo de Cuenca).

Type horizon and locality. Second lithosome of finely laminated limestones of the La Huérguina Formation at Las Hoyas (Cuenca, Spain).

Material. Only the type material is known for this species.

Diagnosis. Thallus of *Clavatoraxis* filiform and rigid in overall appearance. Nodes, separated by long internodes. Spine-cell rosettes small and formed by a reduced number of wedge-shaped calcite crystals are dispersed on the main axis leaving large bare areas.

Description. Thalli filamentous and rigid in overall appearance. Internodes corticate and extremely long in comparison with the size of nodes and branchlets (Text-fig. 2A). Each internode is 6·9–20·1 mm long and

---

EXPLANATION OF PLATE 5

Figs 1–9. *Clavatoraxis robustus* gen. et sp. nov.; thin sections of rock sample LH-16115. 1, thin section LH-16116; tangential section through thallus showing cortical cells (c) covered by spine cell rosettes (r); ×15. 2, 7–8, thin section LH-16117. 2, transverse section through proximal part of internode. 7, oblique section of young branchlet. 8, longitudinal section of mature branchlet. All ×15. 3–4, thin section LH-16118. 3, transverse section through distal part of internode; ×15. 4, tangential section through branchlet; ×15. 5–6, thin section LH-16119. 5, tangential section through surface of internode showing arrangement of spine-cell rosettes; ×15. 6, detail of spine-cell rosette; ×25. 9, thin section LH-16120; longitudinal section of atopocharoid utricle; ×30.

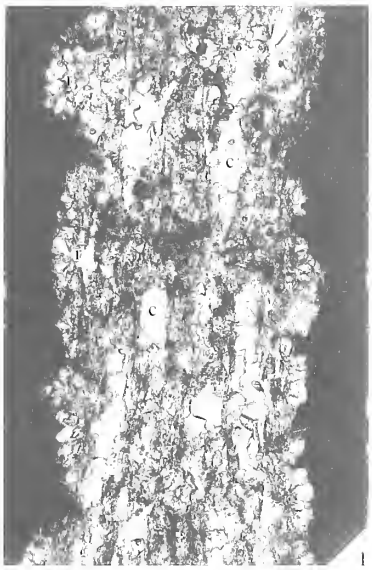

1

2

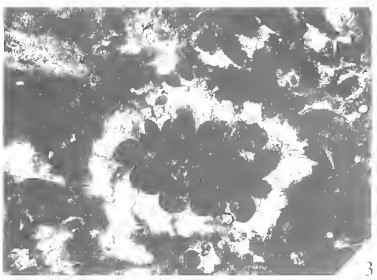

3

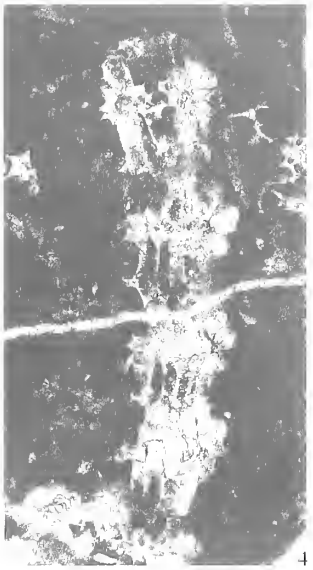

4

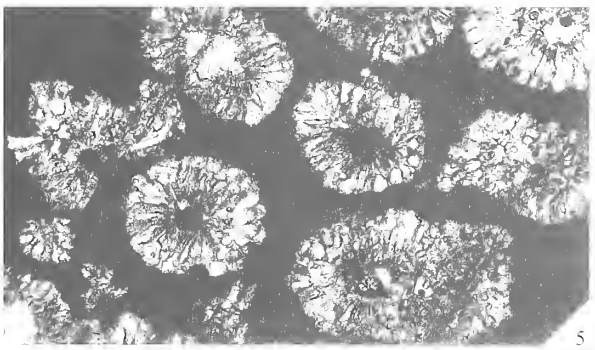

5

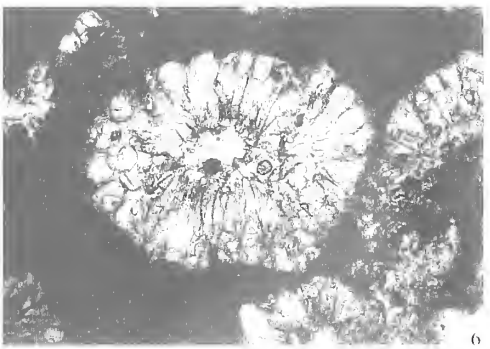

6

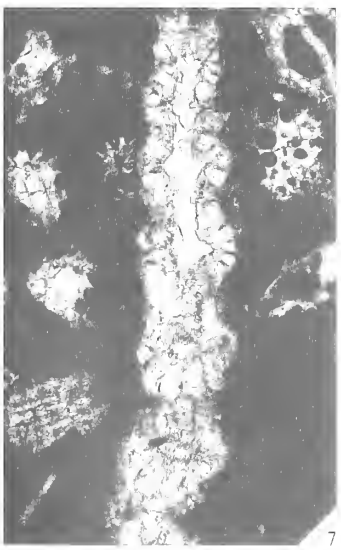

7

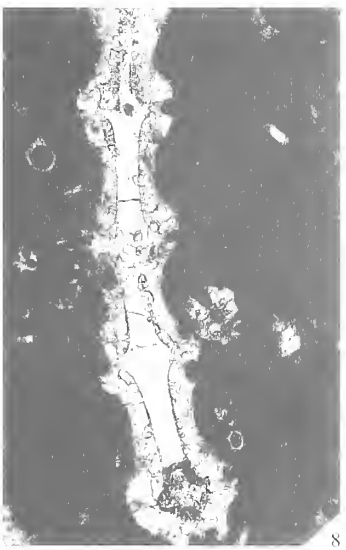

8

9

MARTÍN-CLOSAS and DIÉGUEZ, *Clavatoraxis*

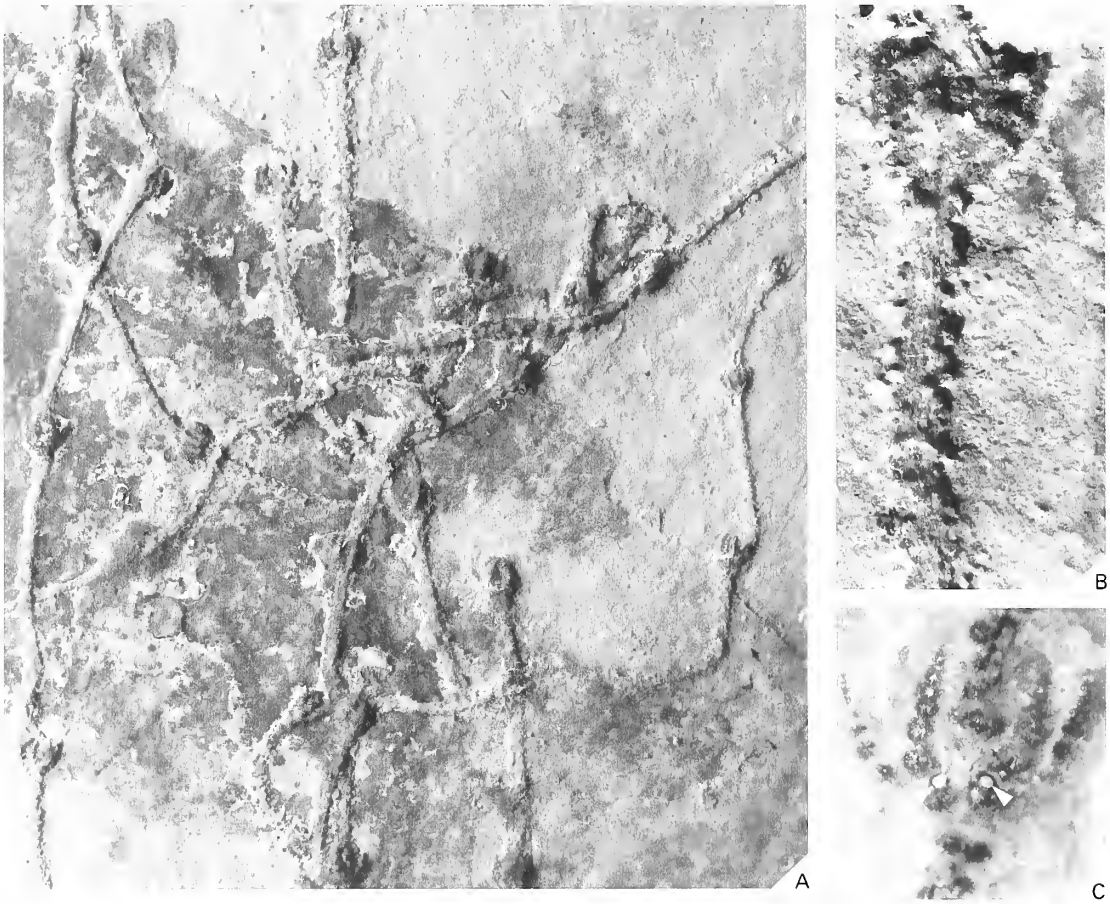

TEXT-FIG. 2. *Clavatoraxis diaz-romerali* sp. nov. A, LH-16123 (holotype); ×2·5. B, detail of internode of holotype; ×5. C, LH-16101 (paratype), detail of node bearing six branchlets (two cut off arrowed); ×15.

0·7–0·9 mm wide. Corticate cells, thin (80–100 μm in diameter) almost vertical or only slightly spiralized (Text-fig. 3B). Internodal cell 180–230 μm in diameter. Spine-cell rosettes hemispherical or hemiellipsoidal, 135–350 μm in maximum basal diameter, formed by wedge-shaped cells, inserted in the internodal cells or in last order branchlets leaving a gap in the wall at the insertion point (Text-fig. 3D). Spine-cell rosettes are dispersed on internodes, leaving large bare areas between them (Text-fig. 3C). Nodes bear six short, 1·2–2·2 mm long, last order branchlets which are identical to last order branchlets of *Clavatoraxis robustus* (Text-figs 2C, 3A). They are covered by swollen spine-cell rosettes inserted at regular intervals (Text-fig. 2B). This gives a noded appearance to such last order branchlets.

No fructifications have been found associated with the thalli of this species, but from the presence of spine-cell rosettes we infer that they are clavatoraceans.

Comparisons. This species differs from *C. robustus* in its filamentous appearance and by bearing dispersed, rather than closely distributed, spine-cell rosettes. However, last order branchlets of the two species are identical. The cortication of this filamentous *Clavatoraxis* makes it easy to distinguish from other filamentous species of genus *Palaeonitella* which are ecorticate.

Remarks. This species is rather uncommon in the lacustrine laminites studied. It has only been found in two samples which contain abundant thalli preserved together and associated with

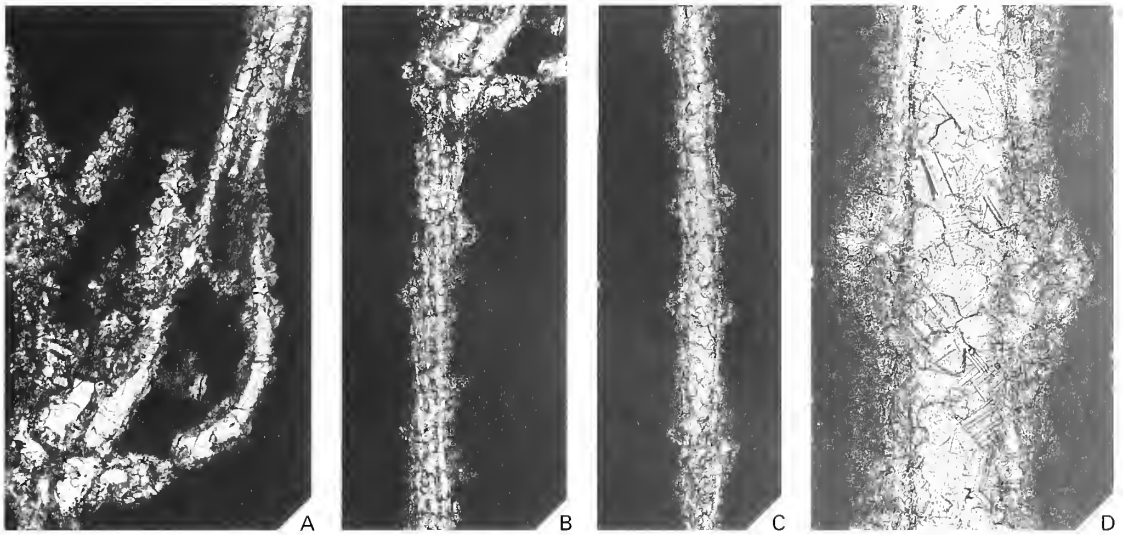

TEXT-FIG. 3. *Clavatoraxis diaz-romerali* sp. nov.; thin section LH-16124 of rock slice containing LH-16101. A, section through node; × 20. B, tangential section through internode; × 15. C, longitudinal section through internode; × 15. D, detail of spine-cell rosettes; × 55.

Palaeonitella vermicularis. This may indicate peculiar ecological conditions for this species of *Clavatoraxis*. Owing to the identical structure of last order branchlets in both species of *Clavatoraxis*, the hypothesis that they are merely ecotypes of the same biospecies cannot be ruled out.

COMPARISON WITH FRUCTIFICATIONS DISPERSED IN MARLY FACIES

This fossil assemblage of vegetative remains may be compared with the charophyte fructifications found dispersed in palustrine marly layers of the same age and formation underlying the site and described by Martín-Closas *in* Diéguez *et al.* (1995*b*). Marly layers provide the material to carry out current research on fossil charophytes, after sieving and sorting the calcified fructifications. In such palustrine facies, charophyte fructifications belong overwhelmingly to Clavatoraceae Atopocharoidae, and particularly to *Atopochara trivolvis* var. *triquetra* (Grambast 1968) Martín-Closas, 1996. Less common are Clavatoraceae Clavatoroidae such as *Clavator harrisii* Peck, 1941 and *Ascidiella cruciata* (Grambast 1969) Schudack, 1993 and only certain samples are enriched with the atopocharoidean *Globator maillardii* var. *trochiliscoides* (Grambast 1966) Martín Closas, 1996 and the characean *Mesochara harrisii* Mädler, 1952. These results correlate well with the relative abundance of *Clavatoraxis robustus*, vegetative remains probably related to Clavatoraceae Pia, 1927. Also, the rareness of *Charaxis spicatus* in the finely laminated limestones matches well the rarity of *Mesochara harrisii* in the laevigated marls if the affinity of *Charaxis* with Characeae Richard ex C. A. Agardh, 1824 is admitted. This is of special interest to palaeocharologists who, until now, have been unable to determine if the relative abundances of fossil fructifications reflect similar abundances of vegetative parts. However, there is also an inconsistency in the correlation of assemblages from different lithofacies. Nitellaceae Martín-Closas and Schudack, 1991 are not represented in assemblages of fructifications from marls whereas they may be represented by vegetative remains of *Palaeonitella vermicularis* if the affinity of the form-genus *Palaeonitella* with Nitellaceae Martín-Closas and Schudack, 1991 is accepted. This may be attributed to different ecological conditions during deposition of the lacustrine limestones and palustrine marls, but is most probably related to the slight calcification of reproductive remains of most Nitellaceae. The

lack of calcification of their gyrogonites, which accounts for their poor fossil record, is well documented in the charophyte literature (Feist and Brouwers 1990).

TAPHONOMY AND PALAEOECOLOGY

All charophyte vegetative remains found at Las Hoyas are preserved in calcite, unlike other whole remains of Lower Cretaceous charophytes (Harris 1939; Peck 1957; Musacchio 1971), which are silicified. The preservation in calcite accounts for the slight epidiagenetic corrosion which has obliterated some details of the surface of the thalli and of fructifications dispersed on the same rock samples containing thalli. From the point of view of biostratinomy the charophyte assemblage is parautochthonous. The fragility of the preserved vegetative structures and their high degree of connection, along with the absence of rootlets, indicate that only slight translocation occurred before deposition. This enables reconstruction of the composition and structure of the ancient charophyte community.

Extant charophyte communities display vertical zonation according to the adaptation of species to different light intensities, whereas horizontal zonations are strongly influenced by competition with angiosperms and by different tolerances to salinity and water level fluctuations (Corillion 1957). For the Early Cretaceous, horizontal zonations have been proposed based on the association of charophyte fructifications with the remains of other organisms, such as ostracodes or foraminifers, which are salinity markers (Schudack 1993). Vertical zonations have not yet been attempted since almost nothing was known about the adaptive morphology of fossil charophyte thalli and the relative abundances of the thalli that produce the fructifications usually found dispersed in the sediments. This is now possible with the material studied (Text-fig. 4). *Clavatoraxis robustus* is the most abundant taxon. It possessed a strong, self-supporting structure as deduced from the rigidity given by its large, branching and corticate thalli reinforced with a coat of spine-cell rosettes. In extant *Chara*, spine-cell rosettes have been interpreted as protective elements against herbivory. Amphipods, aquatic coleoptera and crayfish are significant charophyte grazers in permanent shallow water lakes and ponds (Proctor 1996). Thus, *Clavatoraxis robustus* probably lived in permanent shallow lacustrine facies, forming a dense framework of interconnected thalli, as do some extant associations dominated by robust *Chara*. *Clavatoraxis diaz-romerali*, although filamentous in overall appearance, was also rigid as demonstrated by its fracturation in long, straight fragments. These thalli probably stood upright at the bottom of the lake. The extremely long internodes of *Clavatoraxis diaz-romerali* are reminiscent of a similar adaptation we have observed in extant *Chara* when subjected to low light intensities. Also, the open distribution of spine-cell rosettes may indicate low grazing pressure, which is typical of deeper lacustrine facies (Proctor 1996). From these observations we deduce that *Clavatoraxis diaz-romerali* occurred in light-limited, probably deeper, habitats in comparison with *Clavatoraxis robustus*. This would also explain why the two taxa are not found in association. *Palaeonitella vermicularis* is a relatively common taxon in the charophyte associations studied. Its filamentous and flexible thalli were found twisted round thalli of both *Clavatoraxis* species. This does not indicate only a close ecological relationship between *Palaeonitella* and *Clavatoraxis* in the lake of Las Hoyas but also that *Palaeonitella vermicularis* was unable to stand upright in the bottom of the lake without the support of other plants. Thus, as in some recent associations containing *Nitella*, *Palaeonitella vermicularis* would have formed less-organized thickets that grew supported by the framework given by other charophytes, particularly *Clavatoraxis*. The palaeoecological role of *Charaxis spicatus* is not known, due to its scarcity in the fossil assemblage studied.

FRESHWATER PLANT COMMUNITY EVOLUTION

Charophytes are the only subaquatic macrophytes found in the palaeolake of Las Hoyas after ten years of systematic collection and study of large remains (both carbonaceous and calcitic) and palynomorphs. Plant remains other than charophytes, although abundant and well preserved, have been attributed to groups of land plants which occurred in subaerial habitats (Diéguez *et al.* 1995*b*).

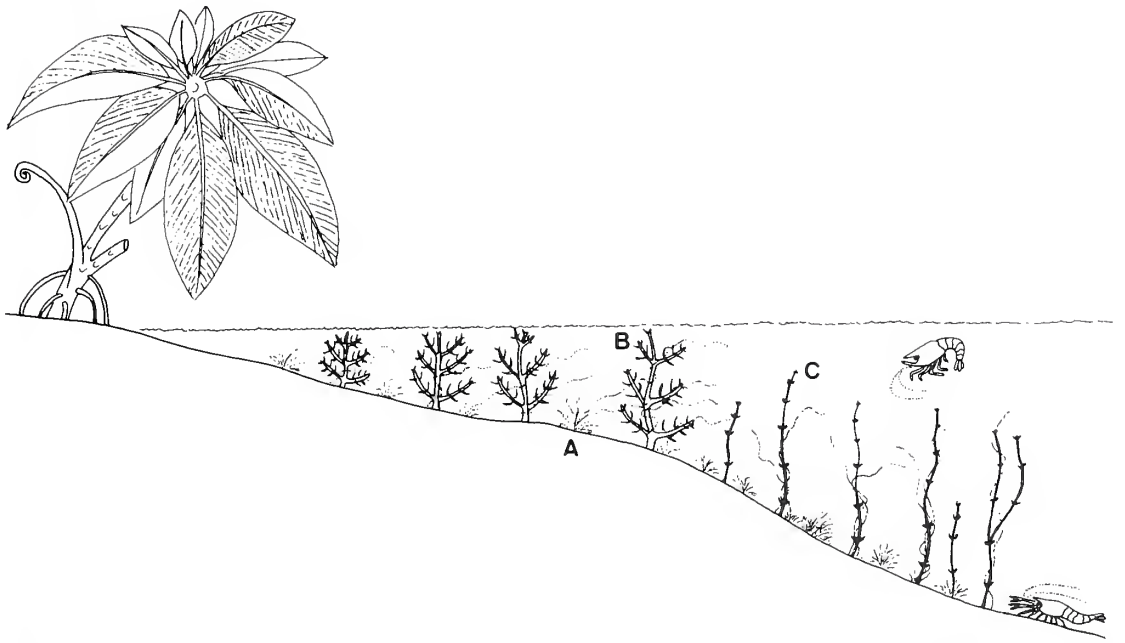

TEXT-FIG. 4. Proposed zonation of charophytes in the palaeolake of Las Hoyas. Near-shore associations were dominated by *Palaeonitella vermicularis* (A) and *Clavatoraxis robustus* (B) whereas in deeper facies the latter species was replaced by *Clavatoraxis diaz-romerali* (C). The tree-fern represented at the shore is *Weichselia reticulata*, one of the most abundant plants in Las Hoyas. Crayfish represented are *Delclosia martinelli*, a nektonic species and *Pseudastacus llopisi*, a benthic species which probably lived in association with charophytes.

The presence of a well structured and diverse charophyte community dominating the subaquatic environment in palustrine and lacustrine facies around the Barremian-Aptian boundary, along with the absence of other freshwater macrophytes, undermines current ideas on freshwater plant community evolution. To date it has been generally understood that 'aquatic pteridophytes may have... occupied many of the aquatic niches prior to angiosperm diversification', which occurred at the end of the Early Cretaceous (Collinson 1988, p. 326). This idea was based solely on the study of vascular plant remains. Although freshwater fern megaspores, particularly from *Azolla*, have been recorded in some Lower Cretaceous localities (Collinson 1980) they are far from being as abundant as charophyte fructifications. Besides this, freshwater ferns, which are small floating plants, have never been demonstrated to represent a serious competitor of charophytes. On the basis of evidence presented here we are now able to propose that before the radiation of freshwater angiosperms, continental subaquatic habitats were occupied extensively by well structured communities of charophytes in the absence of subaquatic embryophytes, whereas floating aquatic ferns were present only at certain localities. This hypothesis was suggested from the study of fossil charophyte fructifications by Martín-Closas and Serra-Kiel (1991) and is now supported by data from the fossil record of whole plant remains from Las Hoyas. The significance of subaquatic macrophytes for animal ecology is proposed to falsify this hypothesis. If charophytes were not the dominant macrophytes at Las Hoyas, benthic habitats would have remained devoid of any macrophytic vegetation, owing to the absence of subaquatic embryophytes during the whole Palaeozoic and early Mesozoic until the diversification of angiosperms. However, this is an untenable hypothesis, since huge populations of the crayfish *Pseudastacus llopisi* Via, 1971 were found at Las Hoyas, indicating that a significant macrophytic biomass existed to support them (Rabadà 1993). Extant astacid crayfish feed not only on macrophytes but also need a dense

macrophyte cover in which to shelter (Hobbs III 1991). The need for significant macrophytic cover formed by charophytes has also been given as an explanation for the development of particular groups of aquatic insects during the Early Cretaceous (Ponomarenko and Popov 1980).

A consequence of this conclusion is that freshwater vegetation remained extremely conservative during plant evolution. Charophytes, which are considered to be among land plant ancestors (Kenrick 1994), appear to have dominated the subaquatic macrophytic vegetation from the late Silurian, when they are first recorded (Ishchenko and Ishchenko 1982), until the radiation of subaquatic angiosperms, which occurred by the end of the Early Cretaceous (Mai 1985).

CONCLUSIONS

Four charophyte species, preserved as large plant remains, are described from the palaeontological site of Las Hoyas (Lower Cretaceous of the Iberian Ranges, Spain). A new genus (*Clavatoraxis*) has been created to include fossil vegetative remains related to Clavatoraceae. This genus includes two new species, *Clavatoraxis robustus* sp. nov. and *C. diaz-romerali* sp. nov. The other species are *Charaxis spicatus* sp. nov., probably related to fossil Characeae, and *Palaeonitella vermicularis* sp. nov., perhaps related to fossil Nitellaceae.

The abundance of taxa represented in the vegetative remains of charophytes found at Las Hoyas correlates well, at the family level, with the corresponding abundance of calcified fructifications found dispersed in sediments in the same formation.

The freshwater plant community of Las Hoyas was dominated by charophytes. *Clavatoraxis robustus* was the most abundant species and formed dense populations in the near-shore facies of the lake. *Clavatoraxis diaz-romerali* lived in deeper environments. Both species were associated with the filamentous *Palaeonitella vermicularis*, which was supported by other charophyte thalli.

Charophytes were the only subaquatic macrophytes of Las Hoyas, in the absence of submerged embriophytic macrophytes. This appears to indicate that submerged plant communities were dominated by charophytes until the radiation of subaquatic angiosperms, i.e. during most of the Palaeozoic and Mesozoic.

Acknowledgements. This paper is a contribution to the EU project ERBCHRX-CT93-0164 of the Human Capital and Mobility Program. It also contributes to the Spanish projects DGICYT PB93-0284 and DGICYT PB95-1142-CO2-01. We acknowledge some key references provided by Mme N. Grambast-Fessard (Université de Montpellier II). Constructive criticisms from M. Feist (Université de Montpellier II) and an anonymous reviewer improved the text.

REFERENCES

AGARDH, C. A. 1824. *Systema Algarum*. Lundae Literis Berlingianis, Lund, 312 pp.

ALVARO, M., CAPOTE, R. and VEGAS, R. 1979. Un modelo de evolución geotectónica para la Cadena Celtibérica. *Acta Geologica Hispanica*, **14**, 172–181.

BYSTRICKÝ, J. 1976. *Munieria grambasti* sp. nov. in Kalk-Gerölle der "Upohlav-Konglomerate" des Mittleren Váh-Gebietes (Klippenzone, Westkarpaten). *Geologica Carpathica*, **27**, 45–64.

CHERCHI, A., GUŠIĆ, I., SCHMIDT, M. and SCHROEDER, R. 1981. Lacustrine Middle Cretaceous with *Munieria grambasti* sarda n. ssp. (Charophyta?) of Alghero (NW Sardinia). *Revue de Micropaléontologie*, **23**, 138–150.

COLLINSON, M. E. 1980. A new multiple-floated *Azolla* from the Eocene of Britain with a brief review of the genus. *Palaeontology*, **23**, 213–229.

—— 1988. Freshwater macrophytes in palaeolimnology. *Palaeogeography, Palaeoclimatology, Palaeoecology*, **62**, 317–342.

CONRAD, M. A. and RADOIČIĆ, R. 1971. On *Munieria bakonica* Deecke (Characeae) and *Clypeina? solkani*, n. sp. (Dasycladaceae). A case of homeomorphism in calcareous green Algae. *Comptes Rendus des Séances de la Société de Physique et Histoire Naturelle de Genève, Nouvelle Série*, **6**, 87–95.

CORILLION, R. 1957. Les Charophycées de France et de l'Europe Occidentale. *Travaux du Laboratoire de Botanique, Faculté des Sciences, Angers*, **11–12**, 1–499.

DEECKE, W. 1883. Über einige neue Siphoneen. *Neues Jahrbuch für Mineralogie, Geologie und Paläontologie*, **1**, 1–14.

DIÉGUEZ, C., MARTÍN-CLOSAS, C., MELÉNDEZ, N., RODRÍGUEZ-LÁZARO, J. and TRINÇAO, P. 1995*a*. Biostratigraphy. 77–79. *In* MELÉNDEZ, N. (ed.). *Las Hoyas. A lacustrine Konservat-Lagerstätte, Cuenca, Spain.* Universidad Complutense de Madrid, Madrid, 89 pp.

—— TRINÇAO, P., MARTÍN-CLOSAS, C. and LÓPEZ-MORÓN, N. 1995*b*. Palaeobotany. 29–32. *In* MELÉNDEZ, N. (ed.). *Las Hoyas. A lacustrine Konservat-Lagerstätte, Cuenca, Spain.* Universidad Complutense de Madrid, Madrid, 89 pp.

FEIST, M. and BROUWERS, E. 1990. A new *Tolypella* from the Ocean Point dinosaur locality, North Slope, Alaska and the Late Cretaceous to Paleocene nitelloid Charophytes. *Bulletin of the United States Geological Survey*, **1990**, F1–F4.

FREGENAL-MARTÍNEZ, M. A. and MELÉNDEZ, N. 1993. Sedimentología y evolución paleogeográfica de la cubeta de Las Hoyas (Cretácico inferior, Serranía de Cuenca). *Cuadernos de Geología Ibérica*, **17**, 231–256.

—— 1994. Sedimentological analysis of the Lower Cretaceous lithographic limestones of the "Las Hoyas" fossil site (Serranía de Cuenca, Iberian Range, Spain). *Geobios, Mémoire Spéciale*, **16**, 185–193.

GESS, R. W. and HILLER, N. 1995. Late Devonian charophytes from the Witteberg Group, South Africa. *Review of Palaeobotany and Palynology*, **89**, 417–428.

GÓMEZ-FERNÁNDEZ, J. C. and MELÉNDEZ, N. 1991. Rhythmically laminated lacustrine carbonates in the Lower Cretaceous of La Serranía de Cuenca Basin (Iberian Ranges, Spain). *Special Publication of the International Association of Sedimentologists*, **13**, 245–256.

GRAMBAST, L. 1966. Un nouveau type structural chez les Clavatoracées, son intérêt phylogénétique et stratigraphique. *Comptes Rendus de l'Académie des Sciences, Paris*, **262**, 1929–1932.

—— 1968. Evolution of the utricle in the Charophyta genera *Perimneste* Harris and *Atopochara* Peck. *Journal of the Linnean Society (Botany)*, **61** (384), 5–11.

—— 1969. La symetrie de l'utricule chez les Clavatoracées et sa signification phylogénétique. *Comptes Rendus de l'Académie des Sciences, Paris*, **269**, 878–881.

GROVES, J. 1933. *Fossilium Catalogus, II: Plantae, Pars 19: Charophyta.* W. Junk, Berlin, 74 pp.

HARRIS, T. M. 1939. *British Purbeck Charophyta.* British Museum (Natural History), London, 83 pp.

HEER, O. 1855. *Flora Tertiaria Helvetiae* I. J. Winterthur, Wuster, 118 pp.

HILL, C. R. and EL-KHAYAL, A. A. 1983. Late Permian plants including Charophytes from the Khuff Formation of Saudi Arabia. *Bulletin of the British Museum (Natural History), Geology Series*, **37**, 105–112.

HOBBS III, H. H. 1991. Decapoda. 823–858. *In* THORP, J. H. and COVICH, A. P. (eds). *Ecology and classification of North American freshwater invertebrates.* Academic Press, San Diego, 911 pp.

HORN af RANTZIEN, H. 1956. An annotated check-list of genera of fossil Charophyta. *Micropaleontology*, **2**, 243–256.

ISHCHENKO, T. A. and ISHCHENKO, A. A. 1982. [Finding of charophytes in the Upper Silurian of Podolia.] 21–32. *In* TESLENKO, Yu. V. (ed.). [*Systematics and evolution of ancient plants.*] Nauk Dumka, Kiev, 132 pp. [In Russian].

KENRICK, P. 1994. Alternation of generations in land plants: new phylogenetic and palaeobotanical evidence. *Biological Review*, **69**, 293–330.

KIDSTON, R. and LANG, W. H. 1921. On Old Red Sandstone plants showing structure, from the Rhynie Chert Bed, Aberdeenshire. Part 5. The Thallophyta occurring in the Peat-Bed, the succession of the plants throughout a vertical section of the bed, and the conditions of accumulation and preservation of the deposit. *Transactions of the Royal Society of Edinburgh*, **52**, 855–902.

LINDLEY, J. 1836. *A natural system of botany.* 2nd edition. Longman, London, 526 pp.

MÄDLER, K. 1952. Charophyten aus dem Nordwestdeutschen Kimmeridge. *Geologisches Jahrbuch*, **67**, 1–46.

MAI, D. H. 1985. Entwicklung der Wasser- und Sumpfpflanzen-Gesellschaften Europas vor der Kreide bis ins Quartär. *Flora*, **176**, 449–511.

MARTÍN-CLOSAS, C. 1996. A phylogenetic system of Clavatoraceae (fossil Charophyta). *Review of Palaeobotany and Palynology*, **94**, 259–293.

—— and SCHUDACK, M. E. 1991. Phylogenetic analysis and systematization of post-Paleozoic Charophytes. *Bulletin de la Société Botanique de France, Actualités Botaniques*, **1**, 53–71.

—— and SERRA-KIEL, J. 1991. Evolutionary patterns of Clavatoraceae (Charophyta) analysed according to environmental change during Malm and Lower Cretaceous. *Historical Biology*, **5**, 291–307.

MARTÍNEZ-DELCLOS, X., NEL, A. and POPOV, Y. A. 1995. Systematic and functional morphology of *Iberonepa romerali* n. gen, n. sp. Belostomatidae Stygeonepinae from the Spanish Lower Cretaceous (Insecta, Heteroptera, Nepomorpha). *Journal of Paleontology*, **69**, 496–508.

MAS, J. R. 1981. El Cretácico inferior de la región noroccidental de la Provincia de Valencia. *Seminarios de Estratigrafía, Serie Monografías*, **8**, 1–408.

McGOWAN, G. and EVANS, S. E. 1995. Albanerpetontid amphibians from the Cretaceous of Spain. *Nature*, **373**, 143–145.

MELÉNDEZ, N. 1983. El Cretácico inferior de la región de Cañete-Rincón de Ademuz (Provincias de Cuenca y Valencia). *Seminarios de Estratigrafía, Serie Monografías*, **9**, 1–242.

MIGULA, W. 1897. Die Characeen Deutschlands, Österreichs und der Schweiz. 1–765. *In* RABENHORST, X. (ed.). *Kryptogamic Flora*. Vol. 5. E. Kummer, Leipzig, 765 pp.

MUSACCHIO, E. A. 1971. Charophytas de la Formación La Amarga (Cretácico inferior), Provincia de Neuquén, Argentina, *Revista del Museo de La Plata*, **4** (37), 19–38.

PECK, R. E. 1941. Lower Cretaceous Rocky Mountain nonmarine microfossils. *Journal of Paleontology*, **15**, 285–304.

—— 1957. North American Charophyta. *Professional Paper of the United States Geological Survey*, **294A**, 1–44.

PÉREZ-MORENO, B. P., SANZ, J. L., BUSCALIONI, A. D., MORATALLA, J. J., ORTEGA, F. and RASSKIN-GUTMAN, D. 1994. A unique multitoothed ornithomimosaur from the Lower Cretaceous of Spain. *Nature*, **370**, 363–367.

PIA, J. 1927. *Handbuch der Palaeobotanik*. Vol. I. R. Oldenbourg Verlag, Munich, 88 pp.

PONOMARENKO, A. G. and POPOV, Y. A. 1980. Palaeobiocenosis of Early Cretaceous Mongolia lakes. *Palaeontological Journal*, **3**, 1–10.

POYATO-ARIZA, F. J. 1995. A revision of the ostariophysan fish family Chanidae, with special reference to the Mesozoic forms. *Palaeo Ichtyologica*, **6**, 1–52.

PROCTOR, V. W. 1996. Charophytivory: 0·3 billion years of previously unexplored coevolution. *Abstracts from the Second International Symposium on Extant and Fossil Charophytes, Madison (Wisconsin)*, **1**, 29.

RABADÀ, D. 1993. Crustáceos decápodos lacustres de las calizas litográficas del Cretácico inferior de España: Las Hoyas (Cuenca) y el Montsec de Rubies (Lleida). *Cuadernos de Geología Ibérica*, **17**, 345–370.

SALAS, R. and CASAS, A. 1993. Mesozoic extensional tectonics, stratigraphy and crustal evolution during the Alpine Cycle of the Eastern Iberian Basin. *Tectonophysics*, **228**, 33–55.

SANZ, J. L., WENZ, S., YÉBENES, A., ESTES, R., MARTÍNEZ-DELCLÒS, X., JIMÉNEZ-FUENTES, E., BUSCALIONI, A. D., BARBADILLO, L. J. and VIA, L. 1988. An Early Cretaceous faunal and floral continental assemblage: Las Hoyas fossil-site (Cuenca, Spain). *Geobios*, **21**, 611–613.

—— CHIAPPE, L. M., PÉREZ-MORENO, B. B., BUSCALIONI, A. D., MORATALLA, J. J., ORTEGA, F. and POYATO-ARIZA, F. J. 1996. An Early Cretaceous bird from Spain and its implications for the evolution of avian flight. *Nature*, **382**, 442–445.

SAPORTA, M. de 1862. Études sur la végétation du Sud-est de la France à l'époque tertiaire. *Annales des Sciences Naturelles, Botanique*, **4** (17), 191–311.

SCHUDACK, M. E. 1989. Charophytenflora und fazielle Entwicklung der Grenzschichten mariner Jura/Wealden in den Nordwestlichen Iberischen Ketten (mit Vergleichen zu Asturien und Kantabrien). *Berliner geowissenschaftliche Abhandlungen, Reihe A*, **106**, 409–443.

—— 1993. Die Charophyten im Oberjura und Unterkreide Westeuropas. Mit einer phylogenetischer Analyse der Gesamtgruppe. *Berliner geowissenschaftliche Abhandlungen, Reihe E*, **8**, 1–209.

SMITH, G. M. 1938. *Botany. I. Algae and Fungi. Charophyceae*. McGraw Hill, New York, 127 pp.

TEIXEIRA, C. 1954. La flore fossile des calcaires lithographiques de Sta. María de Meyá (Lérida, Espagne). *Boletim da Sociedade Geologica de Portugal*, **12**, 1–14.

VIA, L. 1971. Crustáceos decápodos del Jurásico superior del Montsec (Lleida). *Cuadernos de Geología Ibérica*, **2**, 607–612.

ZEILLER, R. 1902. Sobre las impresiones vegetales del Kimmeridgiense de Sta. María de Meyá. *Memorias de la Real Academia de Ciencias y Artes de Barcelona*, **4** (26), 1–27.

CARLES MARTÍN-CLOSAS
Departament d'Estratigrafia i Paleontologia
Facultat de Geologia
08071 Barcelona, Catalonia, Spain

CARMEN DIÉGUEZ
Museo Nacional de Ciencias Naturales-C.S.I.C.
Calle José Gutiérrez Abascal 2
28006 Madrid, Spain

Typescript received 11 July 1997
Revised typescript received 12 January 1998

PORIFERA AND CHANCELLORIIDAE FROM THE MIDDLE CAMBRIAN OF THE GEORGINA BASIN, AUSTRALIA

by DORTE MEHL

ABSTRACT. A rich assemblage of poriferan spicules and sclerites of the Chancelloriidae has been found in Mid Cambrian phosphatic sediments of the Georgina Basin. The hexactinellid spicules are especially diverse, and contain several new types. These include pulvinusactins (nom. nov.) and follipinules, strongly inflated triaxons which probably formed an armouring dermal layer in *Thoracospongia*, and cometiasters which may be the first Cambrian evidence of the Hexasterophora. Demosponge spicules, especially triaenes, are moderately diverse. Polyactine spicules with central canals are interpreted as proto-aster megascleres, which may have evolved into aster microscleres. Calcarean, heteractinellid spicules are also common. These features suggest an early Cambrian diversification of the Porifera. The systematic position of the Chancelloriidae is still controversial.

CAMBRIAN phosphatic sediments of the Georgina Basin are well known because of their well preserved fossils. Trilobites, brachiopods and molluscs were documented early (e.g. Öpik 1961, 1970). The phosphates are also rich in microfossils showing soft-body preservation (Müller and Hinz 1992). Sponge spicules have been mentioned only in passing, although they are common, together with *Chancelloria* sclerites, in residues of washed sediments from the eastern Georgina Basin. In 1986, a joint venture project was initiated between K. J. Müller (Bonn) and J. H. Shergold (Canberra), new fossil collections in the Georgina Basin were made by Below, Laurie, Shergold and Walossek, and they also sampled from all the main formations. Material was collected in three main areas: most came from Rogers Ridge, some from Ardmore Outlier, and the remainder from the Thorntonia area. Sediments were processed in 15 per cent. acetic acid and the residues were screened and washed. The assemblage includes the rich fauna of sponge spicules and chancelloriid sclerites described herein. The purpose of this publication is the documentation of the Porifera and Chancelloriidae found in the Georgina Basin, and a discussion of phylogenetic and systematic aspects of these groups.

STRATIGRAPHICAL AND PALAEOECOLOGICAL BACKGROUND

The Georgina Basin covers about 325000 km^2 of central northern Australia and contains exposures of Cambro–Ordovician rocks deposited in a broad, shallow epicontinental sea. During the Mid Cambrian, a series of organic-rich muds, associated with phosphorites, was deposited. The stratigraphical framework of the Middle Cambrian has been provided by Öpik (1960, 1961), Smith (1972), Shergold and Druce (1980) and Shergold *et al.* (1985). Phosphogenesis persisted throughout most of the Mid Cambrian, and took place in the course of cyclic sedimentation related to upwelling during transgressions (Southgate and Shergold 1991). The stratigraphy and lithofacies have been described in detail by Shergold and Southgate (1986), so here only a short description of the formations is given, focusing on those in which sponge spicules and chancelloriian sclerites have been found. These are of early Mid Cambrian, Ordian to Undillan age. According to Southgate and Shergold (1991), the Mid Cambrian phosphorites of the Georgina Basin were deposited during two main transgressive episodes (Text-fig. 1).

[Palaeontology, Vol. 41, Part 6, 1998, pp. 1153–1182, 7 pls]

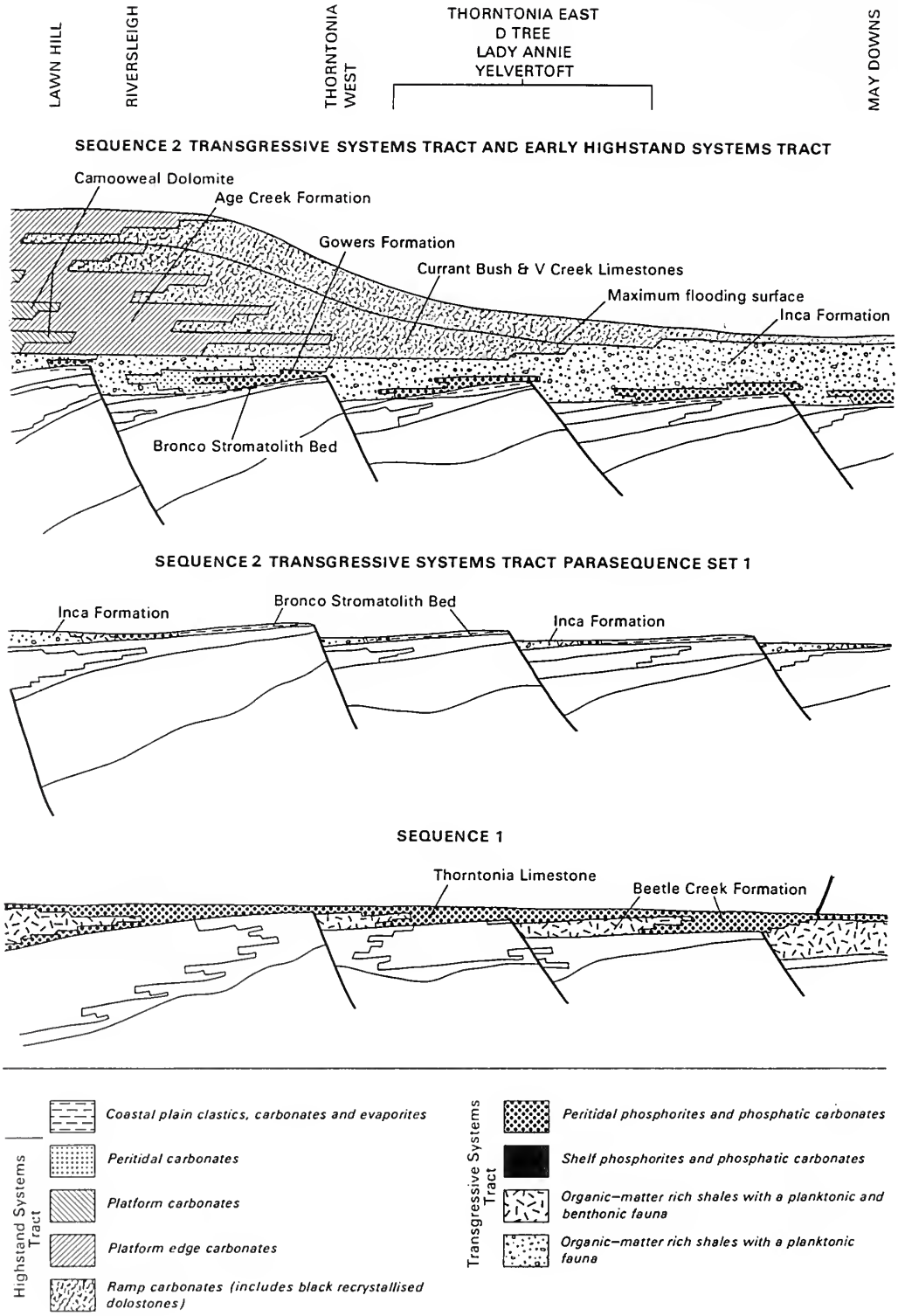

TEXT-FIG. 1. For caption see opposite.

Thorntonia Limestone Formation

This was deposited throughout the eastern and northern part of the Georgina Basin, and is particularly well exposed at Rogers Ridge and in the Ardmore Outlier. The formation consists mainly of dolostone, limestone and chert with recurring phosphatic hardgounds. The lower part of the Thorntonia Limestone represents a shallowing upward sequence. Oncolitic grainstones and stromatolitic algal boundstones indicate a shallow palaeoenvironment. Karst surfaces are recognized on top of the sequence. The Thorntonia Limestone contains a diverse fauna of mainly molluscs, trilobites, inarticulate brachiopods and sponge spicules. Age: Ordian.

Beetle Creek Formation

This formation comprises siliceous claystone, siltstone to sandstone, chert, thin-bedded limestone and phosphorite. This typically clastic formation is best developed in the Ardmore and Burke River outliers, where it is rich in fossils, mainly trilobites and molluscs, but also has produced a diverse assemblage of *Chancelloria* sclerites and sponge spicules. Age: Templetonian.

Inca Formation

This is a finely laminated siliceous shale with siltstone and chert layers and lenses of dark bituminous, dolomitic limestone. It is best developed in the Burke River Outlier. Fossil content is mainly planktic agnostid trilobites, sponge spicules and inarticulate brachiopods. The absence of benthic trilobite genera led Öpik (1970) to the conclusion that the sea floor was generally axoxic. Age: Upper Templetonian to Lower Undillan.

Gowers Formation

The formation consists of thin bedded mudstone to wackestone, commonly bituminous, with chert nodules and phosphate grains interrupted by series of hardgrounds with phosphatic cemented lag deposits. This unit, which crops out to the south and west of Thorntonia Station, represents a shallowing-upward sequence with emergent conditions at its top. Age: Upper Floran to Lower Undillan.

Devoncourt Limestone

This is a laminated and concretionary limestone, including black dolostones, probably deposited in deeper water (outer ramp environments). This unit is developed only in the Burke River Structural Belt and represents a highstand. Age: Upper Floran to Boomerangian, mainly Undillan.

MATERIALS AND METHODS

All the microfossils described here were examined by SEM. All specimens are housed at Australian Geological Survey Organisation, GPO Box 378, Canberra, Australia, where further lithostratigraphical data are available.

SYSTEMATIC PALAEONTOLOGY

Phylum PORIFERA Grant, 1836
Class HEXACTINELLIDA Schmidt, 1870

Genus THORACOSPONGIA Mehl, 1996

Type species. Thoracospongia follispiculata Mehl, 1996.

TEXT-FIG. 1. Schematic development of stratigraphical sequences, transgressive systems 1 and 2, in the north-eastern part of the Georgina Basin (after Southgate and Shergold 1991).

Diagnosis. Pinules, most probably dermal spicules, with their pinular rays extremely inflated, associated with other strongly inflated triaxons called pulvinusactins.

Thoracospongia follispiculata Mehl, 1996

Plate 1, figures 2–4, 6–16; Text-figure 2

Material. Fourteen specimens: CPC 33671 (holotype), 33668 (a, b), 33670, 33673–33674, 34201–34203, 34205–34209.

Description. This species is known only from isolated follipinules, which are pinules, 200–700 μm in diameter, with heavily inflated distal rays, covered by longitudinal ridges, and with outer rays being largely atrophied (Pl. 1, figs 8–13). Follipinules are normally associated with pulvinusactins, which are similarly swollen, normally four-rayed spicules, and it is assumed that the two types of spicule may have belonged originally to the same sponge. In a hypothetical reconstruction, Mehl (1996*a*) showed the possible spiculation of an armoured dermal layer consisting of heavily inflated follipinules and pulvinusactins.

The name *Pulvinusactin* is given to heavily inflated triaxons, mainly stauractins, 200–400 μm in diameter, with a pillow-like appearance (*pulvinus*, Lat. = pillow) (Mehl 1996*a*). This very common spicule type is basically triaxial, but rays are commonly atrophied to form pentactins (Pl. 1, fig. 3), mostly stauractins (Pl. 1, figs 2, 6, 14–15), tauactins (Pl. 1, figs 4, 7), or diactins (Pl. 1, fig. 16). Pulvinusactins are fairly abundant within the Georgina assemblage, and, like follipinules, may be interpreted functionally as spicules of a dermal cortex.

Remarks. Follipinule is the name for a special type of heavily inflated pinule (*follis*, Lat. = balloon) found commonly within the Georgina assemblage. Swelling of the distal ray sometimes extends to such a degree that the axial cross is completely buried and the paratangential rays are hardly visible, showing only as small spines protruding from the ball-shaped distal ray (Pl. 1, fig. 11). Thus, the proximal/paratangential rays might eventually be entirely buried, and the spicules would simply appear like spherical balls, which, especially in thin section, could easily be confused with demospongid sterrasters or radiolarians.

Archaeooides was introduced by Qian (1977) for smooth globular objects of uncertain phylogenetic association (for synonymy see Qian and Bengtson 1989). Within this assemblage, smooth spherical objects, *c.* 200–300 μm in diameter, are found associated with pinules. One must consider whether these spherical balls are poriferan spicules, either demospongid asters or hexactinellid follipinules. As described above, inflation of the pinulate rays beyond the axial crosses may eventually result in ball-shaped structures, which could easily be confused with asters. Smooth surfaces are sometimes found in follipinules, perhaps due to pre-depositional transport. The taxon *Archaeooides* is likely to cover various kinds of globular objects, such as radiolarians and sponge spicules.

Genus NABAVIELLA Mostler and Mosleh-Yazdi, 1976

Type species. Nabaviella gracilis Mostler and Mosleh-Yazdi, 1976.

EXPLANATION OF PLATE 1

Figs 1, 5. Regular hexactins. 1, CPC34200; Undillan; inflated hexactin with pointed rays; ×80. 5, CPC34204; Templetonian; inflated strongyl-hexactin; ×245.

Figs 2–4, 6–13. *Thoracospongia follispiculata* Mehl, 1996. 2–4, Upper Floran–Lower Undillan. 2, CPC34201; pulvinusactin; ×205. 3, CPC34202; inflated pentactin; ×160. 4, CPC34203; inflated tauactin; ×150. 6–7, pulvinusactins; ?Templetonian. 6 CPC33668a; ×90. 7, CPC33668b; ×120. 8–13, follipinules. 8–10, ?Templetonian. 8, CPC33671, holotype; ×155. 9, CPC33674; ×120. 10, CPC34205; ×125. 11, CPC33673; Undillan; ×125. 12–13, Templetonian. 12, CPC34206; ×145. 13, CPC34207; ×95. 14–15, pulvinusactins. 14, CPC33670; Upper Floran–Lower Undillan; ×200. 15, CPC34208; Templetonian; ×90. 16, CPC34209; Upper Floran–Lower Undillan; inflated diactin; ×180.

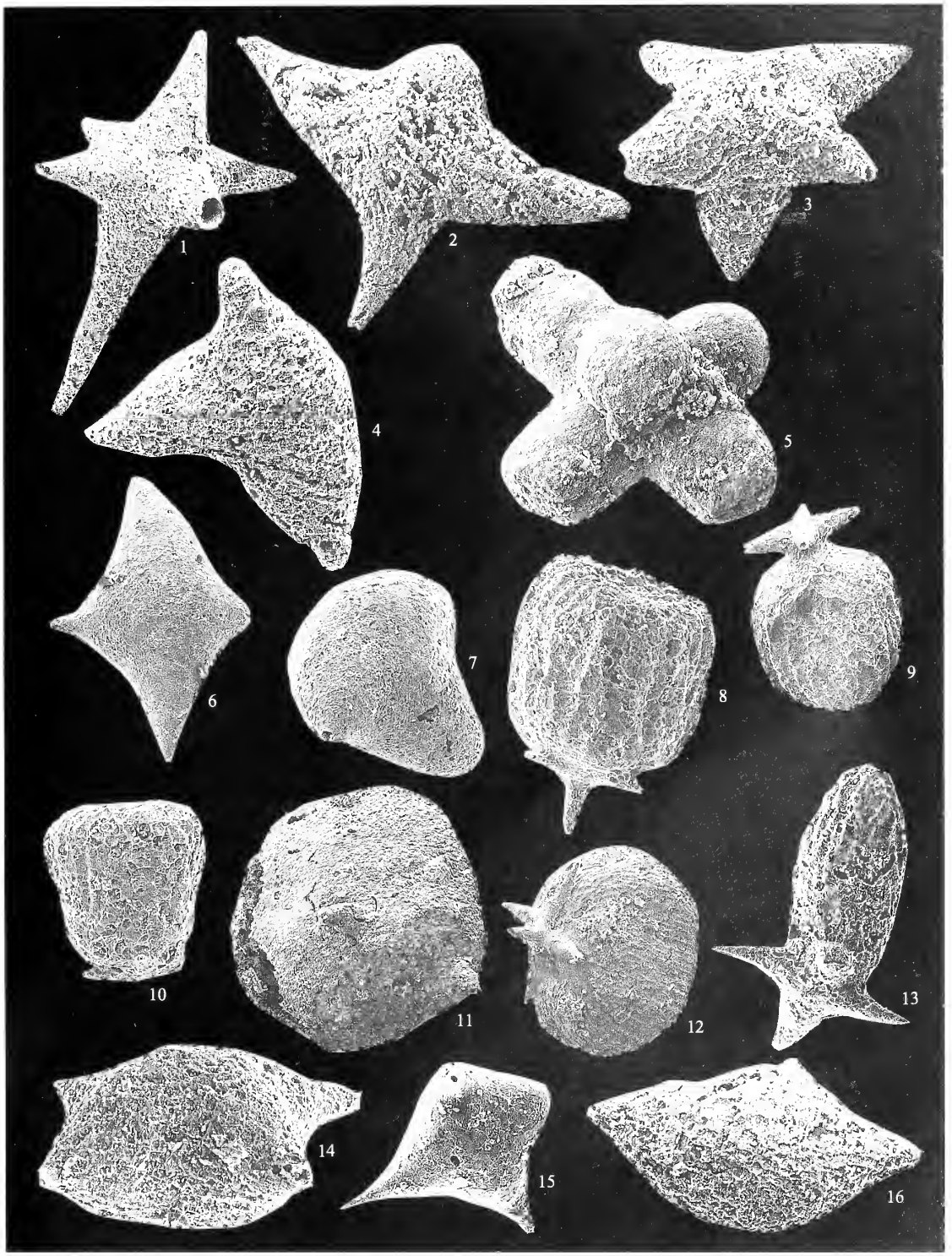

MEHL, regular hexactins, *Thoracospongia*

Diagnosis. Clavulate monaxons with umbels of at least five spines. Sometimes the spicules show distal swellings.

Nabaviella? sp.

Plate 2, figures 3–4, 8–9, 11, 14

Material. CPC 33667, 34234, 34236, 34239.

Description. In this assemblage, the clavulate spicules are from *c.* 500 μm to a few mm in length. Their umbels are mostly with few (two to four) spines (Pl. 2, figs 3–4). However, those clavulate spicules with five or six spines (Pl. 2, figs 8–9, 11, 14) may be considered as true paraclavules and correspond to the species *Nabaviella umbelliformis* Dong and Knoll, 1996. One was found to have a small distal swelling (Pl. 2, fig. 9) similar to *Nabaviella gracilis* Mostler and Mosleh-Yazdi, 1976, and may be considered as a tylodisc (Mehl 1992). The latter were probably marginal spicules without anchoring function.

Remarks. Paraclavules or tylodiscs may also in some cases be root-tuft anchoring spicules. Morphologically they are monactins with one clavulate end, known as an 'umbel', with four to six spines. Dong and Knoll (1996) classified *Nabaviella* as genus *incertae sedis*, but these spicules are definitely from hexactinellids, which are the only sponges known to possess clavules. Clavulate spicule types are difficult to distinguish when their locations within the sponge body are not known. In recent hexactinellids, clavules are normally marginal spicules associated with dermal or gastral membranes. Anchoring spicules are parts of root tufts in lyssacine hexactinellid sponges, protuding from the basal regions of the sponge body. In some cases, they are extremely large spicules (in some Recent amphidiscophoran hexactinellids, e.g. *Monorhaphis* and *Hyalonema*, they can be more than 1 m long). Functions of common clavulate spicules in Early Palaeozoic sponges remain unknown, because they are rarely found *in situ*. Paraclavules were documented in a dermal position in Devonian dictyosponges (Hall and Clarke 1899). However, such spicules are normally only found isolated in Palaeozoic sediments. Some authors (e.g. Finks 1970) have assumed closer phylogenetic relationships or even homology between paraclavules, clavules, and amphidiscs.

Although similar in appearance, amphidiscs and clavules are two basically different types of spicules, as proven by the different locations of the rudimentary crosses of their central axial canals. In sceptrules (scopules and clavules) the axial cross is located wtihin the inflated terminal end. These spicules, thus, can be considered to be true monactins. Amphidiscs have been documented to possess an axial cross in the middle of the shaft between the two terminal umbels; they are diactine spicules (Mehl 1992). Amphidiscs and clavules, thus, have different evolutionary histories, as documented by their phylogenetic relationships. Amphidiscs are a constituent character of the Amphidiscophora. True amphidiscs appear in the upper Silurian (Mostler 1986*a*). 'Hemidiscs' with one umbellate and one tylote end documented by Mostler and Mosleh-Yazdi (1986) from the Upper Cambrian, called tylodiscs by Mehl (1992), most probably evolved independently of amphidiscs and their reduced equivalents, hemidiscs. Clavules in the sense of sceptrules (Mehl 1992) are a constituent character of the Clavularia, Hexasterophora. The fossil record of scopules which are definitely sceptrules begins in the lower Ordovicium (Kozur *et al.* 1997*a*). The nature of most Early Palaeozoic monactins with umbels normally called clavules (e.g. Bengtson 1968) is uncertain though, and an assemblage of spicules from various hexactinellid taxa may have been included in this term. In order to avoid confusion with the definite sceptrules of Mesozoic and Recent hexactinellids, the name paraclavule seems appropriate for Palaeozoic forms.

Subphylum HEXASTEROPHORA Schulze, 1887

Genus FLOSCULUS Dong and Knoll, 1996

Type species. Flosculus gracilis Dong and Knoll, 1996.

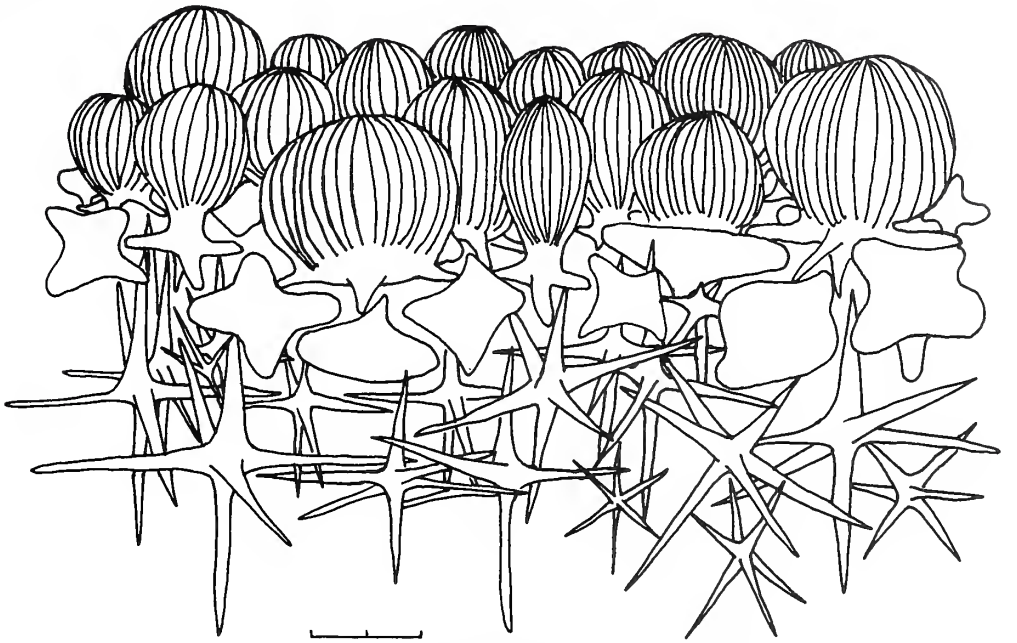

TEXT-FIG. 2. Hypothetical reconstruction of *Thoracospongia follispiculata*; for explanation see text. Scale bar represents 200 μm.

Diagnosis. Hexactine spicules with stout primary rays, some of which are split into numerous secondary rays.

Kometia gracilis (Dong and Knoll, 1996)

Plate 2, figures 1–2, 5

Material. Three specimens: CPC 33675, 34228, 34231.

Description. This name given for triaxons 400–800 μm in diameter with short, pointed, principal rays of which one or two split into 30–50 delicate secondary rays, 350–500 μm long. They are often gently curved and slightly barbed at their distal ends. When broken, it can be seen that the secondary rays are hollow, so each of them originally contained an extension of the axial filament.

Remarks. The genus *Flosculus* was erected by Dong and Knoll (1996) for Late Cambrian spicules from China and attributed to the Hexatinellida *incertae sedis*. However, hexactins in which all six rays are split into several secondary rays are called hexasters. This spicule type is a constituent character of the hexactinellid taxon, Hexasterophora, the sister group of the Amphidiscophora. In the most simple type, the oxyhexaster, the earliest record of which is from the lower Ordovician (Mostler 1986*a*), each of the six rays has simply two secondary, pointed rays. The more advanced discohexaster, known from the Mesozoic to the Recent, is characterized by small swellings or discs at the end of each terminal ray. The Middle Cambrian hexaster-like spicules described here have only one or two of the six hexactine rays split into numerous secondary rays. It is thus not entirely certain that these spicules are true hexasters. If this can be proven, e.g. by other Cambrian transitional forms, it will extend the palaeontological record of the Hexasterophora from lower Ordovician to the Middle Cambrian. A similar spicule fragment, maybe the same ?hexaster-type, was documented from Late Cambrian sediments of Argentinia (Heredia *et al.* 1987).

A very interesting hexactinellid spicule assemblage from the upper Ordovician of New South Wales has been documented by Webby and Trotter (1993). Spicules similar to those described here

from the Georgina Basin were figured and described, and *Kometia cruciformis* Webby and Trotter, 1993 was erected. Those hexasters possess six principal rays, one of which is split into a large number of barbed secondary rays. Their overall shape and size-range is almost identical to those of the Georgina specimens, and for this group of hexasters the name *kometiaster* may be given. However, the Ordovician hexasters, though most probably belonging to the same group as the Cambrian ones, differ in some respects: there are fewer secondary rays (only *c.* 15–25), and their terminal ends are more distinctly barbed and somewhat inflated. Kometiasters are the oldest ?hexaster spicules known. Thus, it is very probably that the major hexactinellid group, Hexasterophora, can be traced back to the Middle Cambrian.

OTHER HEXACTINELLID SPICULES

Regular hexactins

Plate 1, figures 1, 5

Material. Two specimens: CPC 34200, 34204

Description. Hexactins are regular triaxons with six rays at right angles (Pl. 1, fig. 1). They represent the original spicule symmetry of the Hexactinellida (Mehl 1991), but those hexactinellid spicules derived from hexactins, such as pinules, hexasters, pentactins, stauractins, tauactins and diactins, are by far the most common spicule types in this assemblage. Their sizes are highly variable, from about 100 μm to several mm in diameter. Some inflated hexactins are characterized by long rays that terminate in a point (Pl. 1, fig. 1). Similar 'blown-up' hexactins with inflated rays have been documented from the Late Cambrian La Cruz Formation of Argentinia (Heredia *et al.* 1987). Others show inflated rays with rounded ends of approximately equal length (Pl. 1, fig. 5). Transitions to other triaxone spicules with less than six rays are indicated by various degrees of reduction of one or several rays.

Regular pinules and their monactine and diactine derivatives

Plate 2, figures 7, 10; Plate 3, figure 18

Material. Three specimens: CPC 34227, 34233, 34235.

Description. These are triaxons, variable in size from *c.* 0·5–1 mm, and with spined, distal rays. The spines are commonly in an alternating arrangement, which gives a pine-tree like appearance (Pl. 3, fig. 18). Observations of Recent Hexactinellida indicate that the pinules are peripheral (dermal or gastral) spicules whose spined, distal ray often protrudes beyond the outer membrane of the sponge wall. Their proximal rays are often reduced, so these spicules are pinular pentactins. In long, slender pinules (Pl. 2, fig. 10) paratangential rays may be reduced, resulting in a variously spiny diactins (called uncinates) or monactins (Pl. 2, fig. 7).

Remarks. In modern Hexactinellida, pinular spicules are of widespread occurrence within many taxa of both Amphidiscophora and Hexasterophora. Consequently, such spicules must be

---

EXPLANATION OF PLATE 2

Figs 1–2, 5. *Kometia gracilis* (Dong and Knoll, 1996); ?Upper Templetonian; ?hexasters. 1, CPC33675; × 105. 2, CPC34228; × 130. 5, CPC34231; × 83.

Figs 3–4, 8–9, 11, 14. *Nabaviella*? sp. 3–4, 11, 14, clavules. 3–4, ?Upper Templetonian; possible anchoring spicules. 3, CPC34229; × 70. 4, CPC34230; × 75. 11, CPC34236; Templetonian; × 50. 14, CPC34239; Upper Floran–Lower Undillan; × 58. 8, CPC34234; ?Upper Templetonian; paraclavule; × 78. 9, CPC33667; ?Upper Templetonian; tylodisc; × 180.

Fig. 7. Monactin, 'uncinate' with atrophied proximal rays; CPC34233; ?Upper Templetonian; × 100.

Fig. 10. Pinular hexactin, with prolonged distal ray; CPC34235; ?Upper Templetonian; × 170.

Figs 12–13. Tauactins. 12, CPC34237; Templetonian; × 115. 13, CPC34238; ?Upper Templetonian; × 60.

MEHL, Cambrian spicules

considered to be either a primitive type of spicule or one that developed several times convergently within the Hexactinellida; both may be true. Various different shapes of pinules exist: most common is the classical, tree-like pinule with a densely spined distal ray (Pl. 3, fig. 18).

Many fossil and some recent hexactinellids, e.g. *Heterochone calyx* (Schulze, 1887), possess pinules with inflated distal rays. However, extremely inflated spicules, such as in the follipinules of *Thoracospongia*, seem to be a feature particular to Palaeozoic sponges. The Permian *Stioderma* (Finks 1960) was armoured by a dense surface layer of hexactins with swollen, ball-shaped distal and paratangential rays. Rigby (1975) figured pentactine pinules from the Cambrian of Texas and reconstructed these spicules with swollen rays as dermalia. Mostler and Mosleh-Yazdi (1976) described similar spicules from the Upper Cambrian of Iran and, based on them, erected the new genus and species *Rigbyella ruttneri*. The inflated hexactins documented by these authors are characterized by one main ray with a terminally split end. They do not show elongate ridges on their outer surfaces, such as are common in the Georgina Basin specimens.

Platy, spider-like pentactins

Plate 3, figures 6, 9–11

Material. Eight specimens: CPC 34215–34221, 34226.

Description. These abundant spicules are fairly large, up to 1 mm in diameter, bilaterally symmetrical with five unequal rays at oblique angles, which all lie more-or-less in one somewhat concave-convex level. One ray is short, flattened and plate-like; some show a fine tuberculation (Pl. 3, figs 6, 9–11). The remaining rays protrude symmetrically on each side of the inflated one. They are positioned at angles of *c.* 70–75° to neighbouring rays. Angles between rays on either side of the symmetry plane range between *c.* 90° and almost 170°.

Remarks. In spite of their irregular appearance, these spicules resemble some pentactins, whose rays have been modified into angles different from 90°, as is often the case, especially in Cambrian spicules. In this case the symmetrical rays are interpreted as paratangentialia, and the short inflated ray would then be the fifth, normally vertical, one, which has been strongly modified in shape and is totally bent out of a right angle. The common ornamentation of the inflated ray of these spicules indicates that they may be phylogenetically derived from pinulate pentactins, in which the distal ray is often inflated and shorter than the paratangential ones. Morphologically transitional forms between almost regular pentactins and 'spiderpentactins' have been observed. Similar pentactins have been documented from the Upper Cambrian by Heredia *et al.* (1987, fig. 6) and by Bengtson (1986, fig. 9).

EXPLANATION OF PLATE 3

Figs 1–5. Stauractins. 1, CPC34210; ?Upper Templetonian; aberrant stauractin with all four rays turned in one direction; × 50. 2, CPC34211; Undillan; platy stauractin; × 85. 3–5, Upper Floran–Lower Undillan; platy stauractins. 3, CPC34212; × 40. 4, CPC34213; × 83. 5, CPC34214; × 32.

Figs 6–12, 17–18. Pentactins. 6, 9–11, platy, spider-like pentactins. 6, 9–10, Upper Floran–Lower Undillan. 6, CPC34215; × 125. 9, PC34218; × 58. 10, CPC34219; × 75. 11, CPC34220; ?Upper Templetonian; × 110. 7, CPC34216; Templetonian; almost regular pentactin; × 88. 8, CPC34217; Upper Floran–Lower Undillan; × 125. 12, 17, ?Upper Templetonian. 12, CPC34221; small, two-dimensional pentactin; × 165. 17, CPC34226; two-dimensional pentactin; × 145. 18, CPC34227; Templetonian; pentactine pinule; × 113.

Figs 13–16. Polyactins, possibly triaenes with reduced rhabds. 13–14, 16, ?Upper Templetonian. 13, CPC34222; × 165. 14, CPC34223; × 140. 16, CPC34225; × 145. 15, CPC34224; Upper Floran–Lower Undillan; × 140.

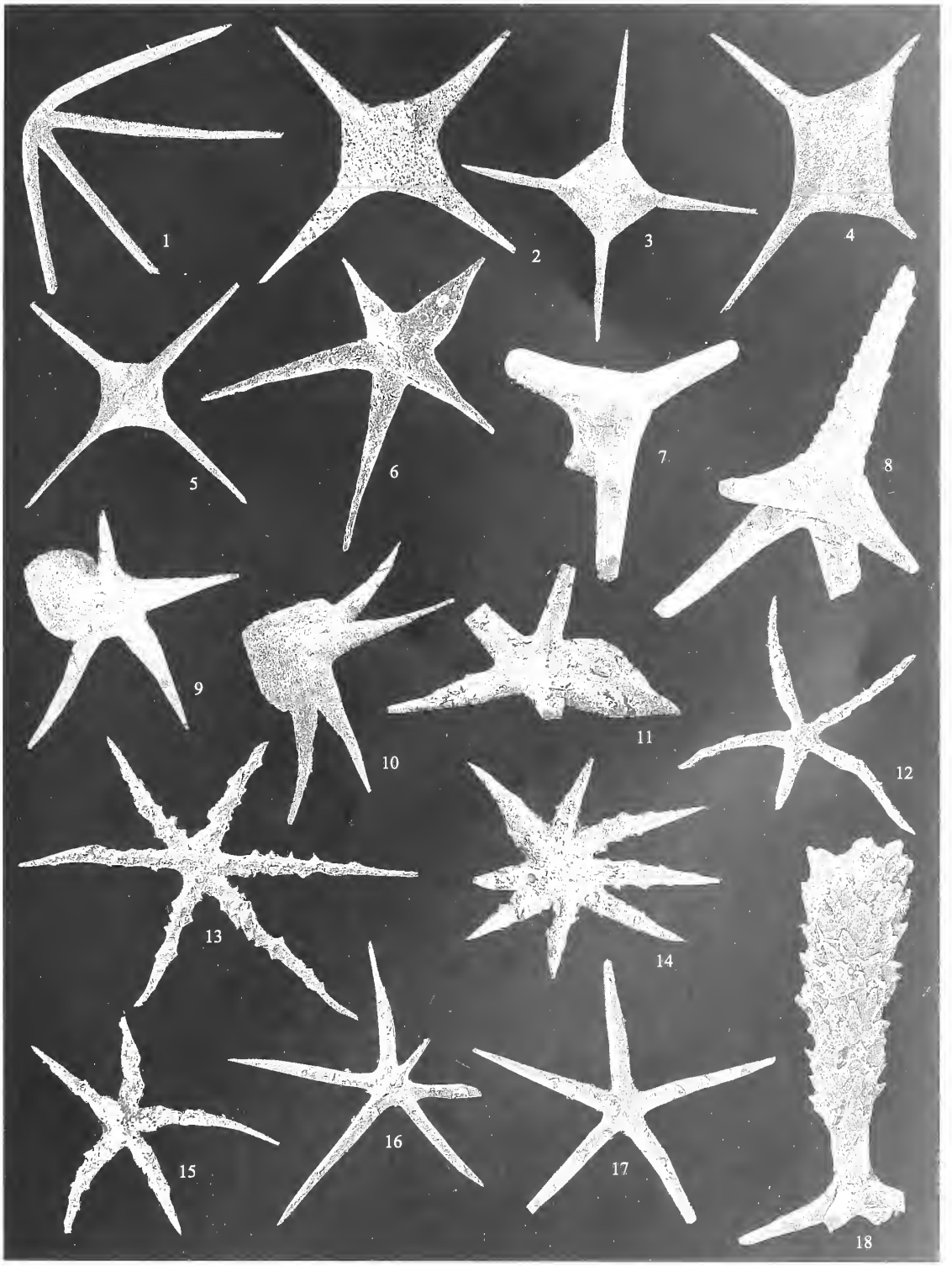

MEHL, stauractins, pentactins, polyactins

Stauractins

Plate 3, figures 1–5

Material. Five specimens: CPC 34210–34214.

Description. These are four-rayed spicules, present in great quantities within the Georgina Basin assemblage. The four rays are normally in a regular arrangement at right angles, but sometimes they seem to be 'compressed' with their rays at different angles (Pl. 3, fig. 1). Because all spicules are well-preserved, such 'deformation' is not likely to be due to post-depositional processes. Stauractins mostly range between 0·5–1 mm, but they are highly variable in both shape and size.

Platy stauractins. These represent a new spicule type. They are platy and flattened in their central area and, thus, appears almost shield-like (Pl. 3, figs 2–5). These platy stauractins are very common within the Georgina Basin assemblage, but have not been reported from elsewhere. Interpretation of these peculiar stauractins with regard to their position within the sponge body thus poses a problem, although they are most likely to be dermal.

Tauactins

Plate 2, figures 12–13

Material. Two specimens: CPC 34237–34238.

Description. T-shaped triactine spicules with only three rays at right angles occur (Pl. 2, figs 12–13) but are not very common within this assemblage. Similar tauactins were documented only from the Upper Cambrian of Queensland by Bengtson (1986, fig. 9L). Tauactins are of widespread occurrence in Recent lyssacine Hexactinellida, where they are normally mesenchymal rather than peripheral spicules, but their fossil record is poor, especially from the Lower Palaeozoic.

EARLY PALAEOZOIC RADIATION OF THE HEXACTINELLIDA

The oldest known well preserved body fossils of sponges are the earliest Cambrian hexactinellids from Hunan Province, China (Steiner *et al.* 1993). The sponges described by Chen *et al.* (1990) from the Lower Cambrian of Chenjiang, Yunnan Province as *Quadrolaminiella* were classified as demosponges, but should be attributed to the Hexactinellida, family Dictyospongidae Hall, 1884 (see also Hall and Clarke 1898). Because of the comparably high diversity of these Early Cambrian Hexactinellida and because of the occurrence of isolated spicules in the Late Proterozoic Shibatan Member in Hubei Province, Steiner *et al.* (1993) predicted the occurrence of hexactinellid sponges in the Upper Precambrian. The documentation of the sponge genus *Palaeophragmodictya* attributed to the Hexactinellida, family Dictyospongidae, from the Ediacara fauna, South Australia (Gehling and Rigby 1996), is a confirmation of this hypothesis, provided that the genus belongs in the Hexactinellida. However, according to my observations of type specimens, spicules cannot be identified with certainty in the Ediacara material. The reticulate pattern characterizing these fossils may be impressions of soft tissue only, e.g. collagen (which is probably the preservation state of all the Ediacara fossils). In fact, *Palaeophragmodictya* might well represent the first documentation so far of the hypothetical, aspicular, primitive sponges postulated by Reitner and Mehl (1996).

Triaxone hexactinellid spicules have been documented from the Upper Proterozoic of the Yangtze Platform, South China (Steiner *et al.* 1993). The monophylum Hexactinellida comprises the sister groups Amphidiscophora and Hexasterophora which can be traced back to the Lower Palaeozoic (Mehl 1996*a*). The oldest oxyhexasters, from the upper Ordovician, and amphidiscs, from the upper Silurian, were reported by Mostler (1986*a*), Mostler and Mosleh-Yazdi (1976) documented monaxone spicules with one clavulate and one swollen, barbed end, from the Upper Cambrian and based on these *Nabaviella elegans* was erected. These spicules, first classified by the authors as chancelloriides, then re-interpreted by Mostler (1986) as hemidiscs, are very large (*c.* 0·6–3·2 mm). They have only slight similarity to true hemidiscs, the oldest of which are known from

the Upper Carboniferous (Kling and Reif 1969) and most probably are reduced amphidiscs. Thus, it is uncertain whether the Amphidiscophora and Hexasterophora originated in the Cambrian. However, diverse assemblages of hexactinellid spicules, especially kometiasters, found in the Middle Cambrian of the Georgina Basin argue for a major radiation within the Hexactinellida that probably took place in the Early Cambrian.

Heavy silicification is a very common characteristic of Early Palaeozoic hexactinellid spicules; protection against predators or water turbulence may have been the reason for this defensive armouring. Similarly, massive surface spiculation of Cambrian hexactinellids might be interpreted as a defensive strategy against predators, such as *Aysheaia* that supposedly fed on sponges (Whittington 1978). Another possibility for such spiculation is the development of a dermal cortex for stabilization under conditions of variably high water-energy. A similar strategy is followed by the demosponges, e.g. the Geodidae, known from the Lower Cambrian to Recent (Reitner and Mehl 1995), with their massive cortex layers consisting of sterrasters. *Stioderma*, with its massive dermal pinular spicules, is the only similar hexactinellid sponge found among representatives of the Demospongiae and Calcarea in the shallow-water Pennsylvanian shelf facies in Texas (Finks 1960). Documentation of the Hexasterophora from the Lower Palaeozoic has been questioned by Wiedenmayer (1994), who claimed that some of the upper Ordovician to Permian hexasters described by Mostler (1986*a*) were pseudohexasters, in reality mesotrienes, attributable to the Demospongiae. The main argument for this re-interpretation is that some of Mostler's hexasters show secondary rays, each with an extension of the axial canal, but in hexactinellid spicules, according to Wiedenmayer (1994), axial canals should not continue into any of the distal rays. However, this 'rule' has been negated, because Liassic hexasters with axial canals continuing through the secondary rays have been documented (Mostler 1989, pls 1–2). Isolated amphidiscs are known from the upper Silurian, and entirely preserved amphidiscophoran sponges with amphidiscs and hemidiscs *in situ* were found in Late Carboniferous phosphorites from Uruguay by Kling and Reif (1969). In view of this strong evidence, there is little doubt that the Hexactinellida constitute an ancient and conservative group, whose major taxa reach back far into the Lower Palaeozoic.

Subphylum PINACOPHORA Mehl and Reitner, *in* Reitner, 1992

Diagnosis. This taxon was erected for the adelphotaxon of the Hexactinellida and comprises the sister groups Demospongiae and Calcarea. The main constituent character of the Pinacophora is the constant presence of pinacocytes in adult sponges. These are specialized flattened cells, differentiated into endo- and exopinacocytes, which are restricted to the inner and outer surfaces, respectively. Parts of the pinacocytes are specialized into porocytes, which line the pores to channels and in many cases make these pores contractile. Representatives of the Demospongiae and Calcarea in the fossil record are identified mainly by the mineralogy and symmetry of their spicules.

Class DEMOSPONGIAE Sollas, 1875

Diagnosis. This group is characterized by siliceous spicules, basically tetractins and monactins.

Tetractins

Plate 4, figures 1, 4–11

Material. Nine specimens: CPC 34240, 34243–34250.

Description. Basically regular orthotriaenes have three rays of equal length and distances of about 120° and a fourth longer ray, called the rhabd, at right angles to the other three. Regular orthotriaenes with long rhabds, although not common, are found (Pl. 4, figs 5, 11). Dichotriaenes with atrophied rhabds also occur (Pl. 4, fig. 6), as well as irregular triactins with variable angles between the rays and often with the rhabds partly or completely reduced (Pl. 4, figs 1, 4, 7–10).

Remarks. The tetractin represents the regular four-rayed calthrops symmetry, which is considered a plesiomorphic spicule within the Demospongiae (Mehl and Reitner 1991). Both orthotriaenes and calthropses have been found earlier in core samples from the Middle Cambrian of the Georgina Basin (van Kempen 1990). Since the presence of tetractins is an ancient, plesiomorphic character of the Demospongiae, in itself it does not contribute to the phylogenetic reconstruction of relationships within the Demospongiae. As stated by van Soest (1987, 1991), 'Tetractinomorpha' *sensu* Levi (1953) is not a monophyletic group. For this reason, Reitner (1992) introduced the taxon Aster-Tetractinellida for all tetractin-bearing demosponges with aster microscleres. Aster-Tetractinellida corresponds largely to Astrophora Sollas, 1888.

Demospongid diactins

Plate 4, figure 3

Material. CPC 34242.

Description. These are mainly oxeas and strongyles. In the Georgina Basin assemblage they are locally slightly acanthose (Pl. 4, fig. 3), they are of various sizes, mostly between 400 μm and 800 μm. Their phylogenetic attribution is uncertain, because various diactins are widespread within the Demospongiae.

Order SIGMATOPHORA Sollas, 1888

Diagnosis. Demospongiae with sigmata as microscleres.

Sigmata

Plate 4, figure 2

Material. CPC 34241.

Description. Only a single sigmatose spicule has been found (Pl. 4, fig. 2). This spicule is basically a diactin with both ends curved to point toward each other. It is a typical C-shaped sigma, except for its very large size (320 μm).

Remarks. Compared with most recent sigmata (*c.* 10–50 μm), this Middle Cambrian spicule is very large, which suggests that the sigma-microscleres might have evolved from Protosigma megascleres that were originally curved/bent oxeas.

Morphogroup DESMA-BEARING DEMOSPONGIAE = 'LITHISTIDA' Schmidt, 1870

Family ANTHASPIDELLIDAE Miller, 1889

Diagnosis. Demosponges with dendroclones arranged in ladder-like trabs, often with coring monaxons in the fusions between trabs.

EXPLANATION OF PLATE 4

Figs 1, 4–11. Tetractins: triaenes and probable triaene-derived polyactins. 1, CPC34240; Upper Floran–Lower Undillan; polyactin; ×80. 4, CPC34243; Upper Floran–Lower Undillan?; triaene? with reduced rhabd; ×70. 5, CPC34244; Templetonian; orthotriaene with curved rays; ×61. 6, CPC34245; Templetonian; trichotriaene; ×95.

Fig. 2. Oxea: sigmatose spicule; CPC3421; ?Upper Templetonian; proto-sigma?; ×200.

Fig. 3. Acanthose oxea: demospongid diactin; CPC34242; Upper Foran–Lower Undillan; ×125.

Figs 12–15. *Rankenella mors* (Gatehouse, 1968); ?Upper Templetonian. 12, CPC34251; ×135. 13, CPC34252; ×125. 14, CPC34253; ×140. 15, CPC34254; two dendroclones still fused; ×83.

MEHL, tetractins, oxeas, *Rankenella*

Genus RANKENELLA Kruse, 1983

Type species. Arborella mors Gatehouse, 1968.

Rankenella mors (Gatehouse, 1968)

Plate 4, figures 12–15

Material. Four specimens: CPC 34251–34254.

Description. Tubular, often branching sponges with deep oscula; encrusting forms also occur, normally with a distinctive dermal layer and many round oscula. The skeletal architecture is anthaspidellid (van Kempen 1978, 1983). Dendroclones in ladder-like series forming radial trabs between inner and outer surface. No coring monaxons have been observed within the fusions beween dendroclones. Irregular spicules known as desmas are not common within the Georgina Basin assemblages. In the Georgina Basin, *Rankenella mors* is known from isolated dendroclones as well as silicified, entirely preserved sponge fossils. The regular dendroclones, 200–400 μm long, show relatively long articulated cladomes and brachyomes at opposite ends of the smooth shafts. Two or three spicules are occasionally found still fused together by their articulated, root-like ends (Pl. 4, fig. 15).

Remarks. This type of isolated spicule from the Georgina Basin was originally described as *Arborella mors* Gatehouse, 1968. Later, entire sponge fossils were found by Kruse (1983) in Australia in the Mid Cambrian Ranken Limestone. These sponges were determined as representatives of the Anthaspidellidae with the typical spiculation of regular ladder-like trabs of dendroclones. The simple dendroclones of these sponges were recognized as identical with those documented by Gatehouse as *A. mors* on the basis of isolated spicules, and this species was assigned to a new genus *Rankenella* by Kruse (1983). Kruse (1996, fig. 3c) figured an encrusting specimen with a silicious covering sheet and round elevated oscula. According to my observations of this specimen, it seems definite that the covering sheet, which can be observed on other specimens as well, is not the result of secondary silicification only, but is a true dermal layer.

The anthaspidellid *Rankenella* is the earliest desma-bearing sponge so far described. Because the taxon 'Lithistida' is definitely not monophyletic (Gruber 1993), and no definite microscleres are known from *Rankenella* (or the Anthaspidellidae), it cannot be decided definitely whether this group belongs to the Astrophora or to the Sigmatophora. However, regular vertical and horizontal tracts of oxeas ('isodictyal architecture'), like those characteristic of the Anthaspidellidae, are known from some non-desma-bearing representatives of the Haplosclerida, Sigmatophora (Reitner and Kohring 1990). This skeletal architecture, which is probably symplesiomorphic within Haplosclerida, gives rise to the hypothesis that the Anthaspidellida may be a stem lineage representative of the Sigmatophora.

EXPLANATION OF PLATE 5

Figs 1–14. Polyactins, most of which show central canals (arrows), probably demospongiaen mesotriaenes and protoasters; Templetonian. 1–2, mesotriaenes. 1, CPC34255; ×168. 2, CPC34256; ×175. 3–11, protooxyasters. 3, CPC34257; ×165. 4, CPC34258; ×168. 5, CPC34359; ×125. 6, CPC34260; ×170. 7, CPC34261; ×160. 8, CPC34262; ×240. 9, CPC34263; ×110. 10, CPC34264; ×125. 11, CPC34265; ×120. 12, CPC34266; octactine?; ×125. 13, CPC34267; Upper Templetonian; problematical polyactin-radiolarian spicule; ×80. 14, CPC34268; polyactin, similar to large strongylacanthaster; ×98.

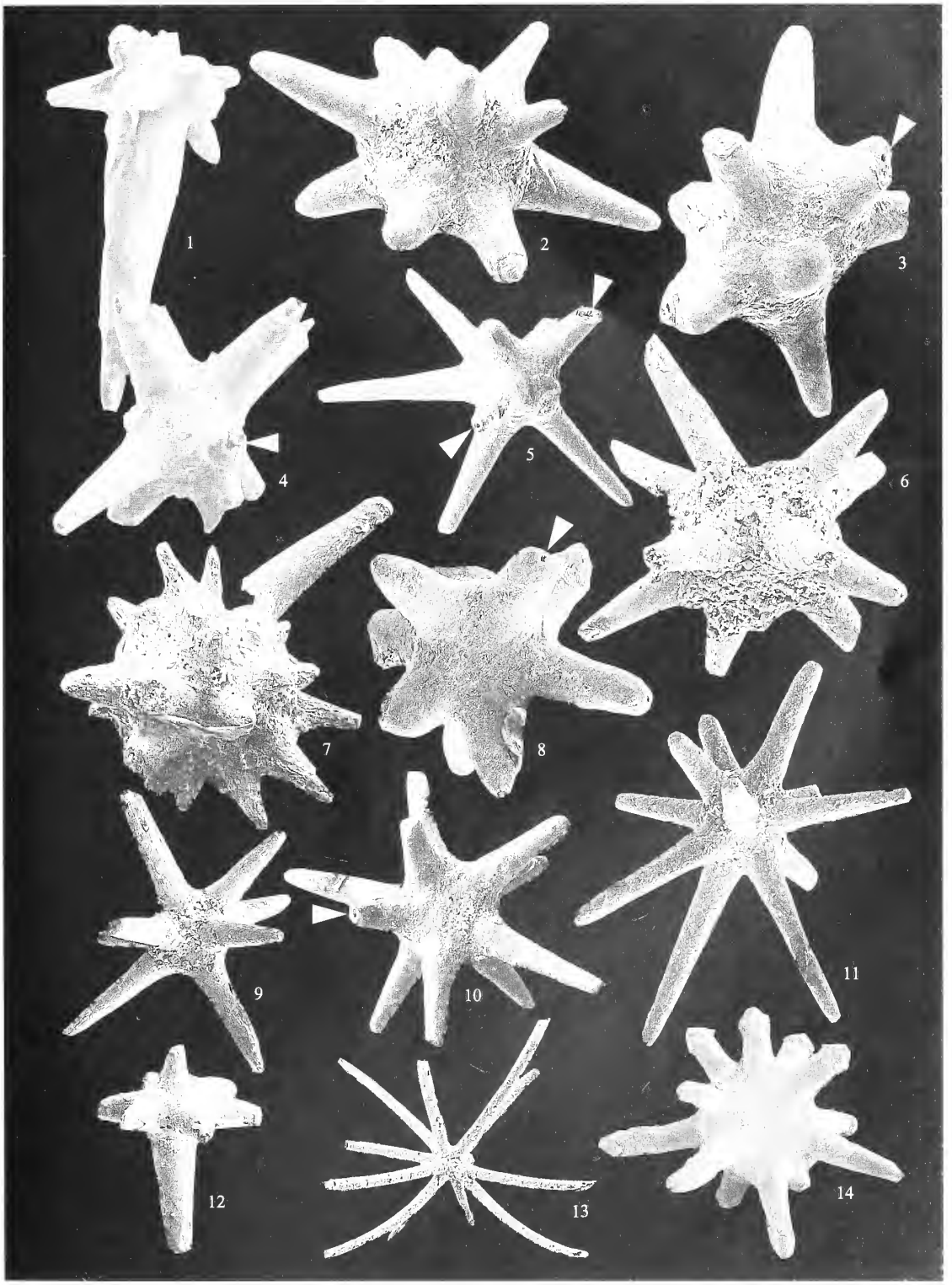

MEHL, polyactins

Order ASTROPHORA Sollas, 1888

Diagnosis. Demospongiae with aster.

Oxyasters

Plate 5, figures 1–11, 14

Material. Eleven specimens: CPC 34256–34265, 34268.

Description. These are fairly large (250–600 μm) spherical spicules with ten to 20 rays that radiate from the inflated centre (Pl. 5, figs 1–11, 14). Normally, these rays are of approximately equal length (*c.* 75–250 μm), but in some specimen a few rays are reduced, and in others one or two rays reach almost double length (Pl. 5, figs 1–5, 7, 12). Basal ray diameter is 40–50 μm, but one specimen (Pl. 5, fig. 13) has considerably thinner rays, and it is questionable whether it is a sponge spicule at all. Generally, these polyactins show radial symmetry. Some of them, however, show a somewhat bilateral-symmetrical shape (Pl. 5, figs 9, 12). When broken, most of the spicule rays show central canals (Pl. 5, arrows).

Remarks. Most of the polyactine spicules from the Georgina assemblage possess ten to 12 radial rays and thus show morphological similarity with those of some later Palaeozoic Heteractinellida, e.g. the Mississippian *Asteractinella.* Some of the polyactins show a bilateral-symmetrical arrangement of eight rays, six of which radiate in one level, with the remaining two pointing away at right angles (CPC 34266; Pl. 5, fig. 12). This pattern corresponds to the diagnosis of the Octactinellida, as given by Hinde (1887–1912). Octactinellida is a sub-taxon of Heteractinellida (e.g. Rigby 1983), and some of the spicules with bilateral symmetry that do not show axial canals might be heteractine polyactins. However, in most of the polyactins, the axial canals continue into the rays; these are not massive, like spicules of the Calcarea, but are definitely demospongiaen.

Most of the spherical spicules with few and relatively long, radiating rays look almost identical to oxyasters. A few polyactins show rounded or even spined ends to their rays (Pl. 5, fig. 14) and are similar to the asters of some recent demosponges, e.g. the strongylacanthasters of *Geodia* or acanthose euasters of *Timea.* Although much larger in size, the Cambrian polyactins show great morphological affinity with the oxyasters of some Recent tetractinellids. For these reasons, most of the polyactins from the Georgina Basin may be considered as true demospongid aster spicules. However, Recent oxyasters are normally ten to 15 times smaller than these Cambrian polyactins. This suggests that the Recent aster microscleres may be derived from Palaeozoic protoaster megascleres. Reif (1968, figs 10–12) figured similar polyactins from the upper Ordovician of Scandinavia, which he referred to as 'Aster-formige Megasklere' (aster-shaped megasclere). It is also possible that these Cambrian polyactins may be special mesotriaenes. Interesting analogues are the spherical polyactins from the Upper Triassic published as *Costamorpha zlambachensis* by Mostler (1986*b*, p. 345, pl. 4). The size range and overall morphology of these spicules, which also show central canals in all rays, is very similar to those from the Georgina Basin. However, in the Triassic spicules two rays are generally longer than the other ones, and Mostler (1986*b*) called the long rays 'Pseudorhabde' and interpreted his spicules as mesotriaenes. In many of the Georgina Basin polyactins the same phenomenon can be observed, and it cannot be discounted that these spicules are also derived mesotriaenes.

Thus, it must be considered whether the aster microscleres might have evolved from mesotriaene megascleres. This hypothesis is supported by the fact that the oxyaster seems to be a plesiomorphic form, probably very close to the original proto-aster (Reitner 1992, fig. 13a).

THE EARLY EVOLUTIONARY HISTORY OF THE DEMOSPONGIAE

Astrophora and Sigmatophora

These are the two major groups within the Demospongiae. They correspond only partly to the taxa 'Tetractinomorpha' and 'Ceractinomorpha' as defined by Lévi (1953), which have been shown to be polyphyletic (van Soest 1987, 1991). According to phylogenetic-systematic analyses of Recent

sponges, Aster-Tetractinellida and Sigmatophora are sister taxa. The presence of aster-microscleres is the constituent character of the Astrophora, and that of sigma-microscleres is a main autapomorphy of the Sigmatophora. Because of its distribution within this group, the oxyaster is considered as a phylogenetically early and original type of aster-microsclere, close to the hypothetical protoaster (Reitner 1992). So far, the Lower Cambrian oxyasters from Shanxi, China, (Zhang and Pratt 1994) are the earliest recorded oxyaster-type spicules.

Sigmata and asters. Sigmatose microscleres are a constituent character of the monophylum Sigmatophora. Middle Cambrian sigmata, as documented here and by Kruse (1990, pl. 24, fig. J), are the earliest reported. Thus, the existence of both main demospongid groups in the Middle Cambrian has been demonstrated. The sigma-microscleres may have evolved from Proto-sigma-megascleres that were originally curved/bent oxea. Similarly, the oxyasters in this assemblage are very large, more like average megascleres. These spicules would be 'megascleres' according to the common size-based classification of sponge spicules. However, the hypothesis that aster and sigma microscleres evolved from corresponding megascleres seems to be discordant with the fact that in Recent demosponges, mega- and microscleres are developed in different somatic layers by distinctly different types of sclerocytes. Demospongid megascleres are secreted by megasclerocytes, which originate ontogenetically from the large archaeocytes with nucleolate nuclei. They seem to be non-homologous with microscleres, which are secreted by smaller microsclerocytes with anucleolate nuclei (Simpson 1984). Consequently, I would expect the two spicule-types to have evolved independently within the Demospongiae rather than in the Hexactinellida, whose 'microscleres' have been documented to be reduced megascleres (Mehl 1992). It is possible, however, that sigmata and asters evolved independently of other spicules, but initially as larger spicules. Certain aster microscleres, e.g. sterrasters of Recent representatives of the Geodidae, are much larger than some size-reduced megascleres, such as microstrongyles or microcalthropses. According to the present stage of palaeontological knowledge, it seems likely that the microscleres evolved from megasclere prototypes: Sigmata from oxeas and asters from polyactine mesotriaenes.

Rankenella mors (Gatehouse, 1968) is by far the earliest representative of the 'lithistid' Anthaspidellidae. Desmata are of very widespread distribution and thus seem to be a plesiomorphic spicule-type within the Demospongiae. The taxon 'Lithistida', based on the presence of desmata megascleres, has proven to be polyphyletic, since it comprises representatives of various demospongid groups (Gruber 1993). Anthaspidellidae constitutes a well established monophylum characterized by the autapomorphic skeletal architecture of dendroclone desmas in ladder-like tracts fixed at radiating bundles of monaxons. They are the oldest desma bearing demosponges in the fossil record. Within these sponges, the desmas form skeletal strands by fusion of their cladomes and may be cored by monaxone spicules, such as styles and oxeas (van Kempen and ten Kate 1980; van Kempen 1983, 1989).

Class CALCAREA Bowerbank, 1864

Diagnosis. Pinacophoran sponges with calcitic spicules of basically triradiate symmetry, without axial canals.

Order HETERACTINELLIDAE Hinde, 1888

Diagnosis. Palaeozoic Calcarea with polyactine spicules.

Genus EIFFELIA Walcott, 1920

Type species. Eiffelia globosa Walcott, 1920.

Diagnosis. Calcarea with planiradiate, mostly six-rayed spicules.

Eiffelia sp.

Plate 6, figures 1–3, 7–9, 11–12

Material. Seven specimens: CPC 34269–34271, 34275–34277, 34281.

Description. *Eiffelia globosa* is known from the Burgess Shale as small globular sponges with deep oscula and a skeleton of normally hexiradiate, sometimes slightly concavo-convex spicules with six rays in one plane, radiating from a flattened centre. The diameter of the *Eiffelia* spicules in the Australian assemblage is highly variable, from *c.* 300 μm to almost 2 mm. The spicule surfaces are smooth, and the rays normally have rounded ends. All of the six rays diverge at angles of 50–70° (average 60°). As in all Heteractinellida (and Calcarea), the spicules of *Eiffelia* have no central canals. In most specimens the rays are of more-or-less equal length, and although some spicules have one or two rays greatly prolonged, whereas others are largely reduced (Pl. 6, fig. 7), they probably all belong to the genus *Eiffelia.*

Remarks. Entire specimens of *Eiffelia globosa* in body preservation from the Burgess Shale were studied by Rigby (1986), who found in these sponges up to four orders of six-rayed spicules. This may explain the remarkable variation in shape and size between the spicules attributed to *Eiffelia.* But, the possibility of more than one species within the isolated spicule assemblage from the Georgina Basin cannot be excluded.

Genus CANINSTRUMELLA Rigby, 1986

Type species. *Caninstrumella alternata* Rigby, 1986.

Diagnosis. Conical to basket-like sponges with skeletons of four- to six-, mostly five-rayed planiradiate spicules with short buttons on their convex, ?upper surfaces.

Caninstrumella? sp.

Plate 6, figures 6, 10

Material. Three specimens: CPC 34274, 34278–34279.

Description. Polyactine spicules, with five or six equally spaced rays and one to seven vertical rays, which are largely atrophied and appear as buttons (Pl. 6, figs 6, 10). Diameter normally varies between 300–600 μm. They are not very common.

Remarks. In a study of the sponges from the Burgess Shale, Rigby (1986) erected the genus *Caninstrumella* for heteractinids with four to six tangential rays and the proximal and distal rays reduced to short buttons. The polyactins from the Georgina Basin are highly variable: they generally have nodes on the convex side only, but sometimes possess as many as seven elevated nodes: one central one with the others equally distributed on the central plate in the central axis of

EXPLANATION OF PLATE 6

Figs 1–3, 7–9, 12. *Eiffelia* sp.: heteractinide hexiradiate spicules. 1–3, 7–8, 12, Templetonian. 1, CPC34269; ×56. 2, CPC34270; ×113. 3, CPC34271; ×68. 7, CPC34275; ×40. 8, CPC34276; ×55. 11, CPC34279; ×63. 12, CPC34280; ×130.

Figs 4–5. Undetermined triaene or heteractinellid(?) spicules; Templetonian. 4, CPC34272; ×68. 5, CPC34273; ×85.

Figs 6, 10. *Caninstrumella*? sp. spicules. 6, CPC34274; Upper Floran–Lower Undillan; ×83. 10, CPC34278; Templetonian; ×155.

MEHL, Cambrian spicules

each ray. In spite of these differences, these spicules may still be attributable to *Caninstrumella*, since no elevated nodes are seen on the spicules of any of the type specimens of *Eiffelia* (pers. obs.). The pyritic preservation of the Burgess Shale specimens may have obscured such fine structures. Further complete Cambrian Heteractinellida preserved differently might help complete the reconstruction of this genus.

Undetermined triaene or heteractinellid (?) spicules

Material. Two specimens: CPC 34272–34273.

Description. These spicules are more-or-less planiradiate with six to eight pointed rays. They are not uncommon in the Georgina assemblage (Pl. 6, figs 4–5). It is uncertain whether these are heteractinellid spicules or mesotriaenes with reduced rhabds.

ON THE SYSTEMATICS OF THE HETERACTINELLIDAE

This group was originally classified as belonging to the Hexactinellida by Hinde (1888). Heteractinellida was placed in Calcarea by Rietschel (1968) on account of their monocrystalline calcitic spicules and absence of central canals in their spicules. This placement was followed by later spongiologists (e.g. Rigby 1991; Reitner 1992). Reitner and Mehl (1996) considered the Heteractinellida in this sense to be a stem-group member of the Calcarea-taxon. The earliest known representatives of this group are from the Middle Cambrian. *Eiffelia globosa* and *Canistrumella alternata*, both from the Burgess Shale, possess planiradiate spicules very similar to those found in the Georgina Basin. *Jawonya gurumal* Kruse, 1987 from the Middle Cambrian of north Australia, the oldest heteractinellide sponge so far documented, has highly variable polyactine spicules. This indicates that the original heteractinellide spicules showed little symmetry, and the regular six-rayed, planiradial shape of *Eiffelia* spicules is a derived feature within the Heteractinellidae. *Eiffelia* is monospecific. The type species is *Eiffelia globosa* Walcott, 1920, the lectotype of which was designated by Rigby (1986). This and the reference specimens, and also the holotype of *Jawonya gurumal* have been recently re-studied by me. Some confusion still exists with regard to the Octactinellidae within the Heteractinellida. In his original description, Walcott (1920, p. 324, text-fig. 10) figured a six-rayed, composite chancelloriide sclerite and described this with 'a central hexagonal disc' as characteristic of his octactinellide species *Eiffelia globosa*. Sdzuy (1969, p. 132, pl. 14, figs 31–35; pl. 15, figs 1–3) classified *Eiffelia* within the Chancelloriidae and figured definitely chancelloriide sclerites as '*Eiffelia*? *hispanica* n. sp.' However, re-examination of the type specimens of *Eiffelia globosa* (U.S. Nat. Mus. cat. nos 66521–66523; Walcott 1920, pl. 86, figs 1, 1a–b) definitely excludes the presence of central discs or any composite spicules in *Eiffelia*, which has massive six-rayed, planiradial spicules only.

The Georgina collection also contains polyactin spicules that show no particular symmetry. They have variable numbers of pointed rays, generally of different lengths, radiating from the centre. No central canals have been observed within these spicules. Most of them are probably heteractinellid sponge spicules, but so far they cannot be attributed definitely to any particular group. Very irregular polyactins with similar ray-numbers are present in the dermal layer of the Middle Cambrian heteractinellide sponge *Jawonya gurumal* Kruse, 1987, from north Australia. Presumably, some of the irregular polyactins from the Georgina Basin belong to the same or some closely related species. Several authors (e.g. Rigby and Dixon 1979) have documented massive, irregular polyactins from Early Palaeozoic strata.

MICROFOSSILS OF UNCERTAIN SYSTEMATIC POSITION

Pseudo-poriferan spicules, probably Radiolaria

Plate 5, figure 13

Material. Two specimens: CPC 34232, 34267.

Description. Rather small (about 250–350 μm; only one exception found with 475 μm), thin-rayed polyactins with sometimes slightly curved, often hollow rays (Pl. 5, fig. 13) or they may be planiradiate. These fossils cannot be attributed definitely to any heteractinellid, demospongid or hexactinellid group, although some of them appear to show triaxial symmetry of the curved rays (Pl. 2, fig. 6). It is almost certain that most of these are not poriferan spicules. In some cases, such spicules are fused into a loose framework of a spherical ball, about 1 mm in diameter. Similar spherical frameworks of spicules from the Upper Cambrian were published as sponges by Bengtson (1986). However, according to new data by Kozur *et al.* (1997*b*) these spicules belong to large radiolaria, probably the oldest with mineralized skeletons.

CHANCELLORIIDAE Walcott, 1920

Genus CHANCELLORIA Walcott, 1920

Type species. Chancelloria eros Walcott, 1920.

Diagnosis. The completely preserved fossils, rarely found, are sessile, thin-walled, conical and with skeletons of polyactine, composite sclerites.

Chancelloria eros Walcott, 1920

Plate 7, figures 1, 3, 7–8, 12, 14–15

Material. Seven specimens: CPC 34281, 34383, 34287–34288, 34292, 34294–34295.

Description. The holotype, from the Burgess Shale, is a poorly preserved, pyritized specimen, characterized by (6–8 + 1) and rare (4 + 0) sclerites. Within the Georgina Basin collection, only isolated chancelloriide sclerites have been found. The (7 + 1) type is the most common type. It has a flat base with a comparably large central disc and wide, circular basal pores (Pl. 7, figs 6–8, 15). Total diameters of the sclerites are 0·7–1·0 mm. From the polygonal central disc the marginal rays radiate in a flat angle from 0 to *c.* 20°, exceptionally up to 45°. The length of marginal rays is variable, even between individual rays of the same sclerite, generally ranging between 200–400 μm. The central ray is normally somewhat longer.

Remarks. According to Bengtson *et al.* (1990), the chancelloriide scleritomes from the Burgess Shale, which Walcott (1920) included into the type species *Ch. eros*, are from several different species. The lectotype designated by Goryanskij (1973), figured by Walcott (1920, pl. 86, fig. 2; pl. 88, fig. 1f), has been re-studied by me. The (incomplete) scleritome is composed of rather large, 1–2 mm in total diameter, sclerites that are mainly (6–7 + 1). Individual rays are *c.* 1–1·6 mm long. Most chancelloriides in the Australian collection are only *c.* 0·7–1·0 mm in total diameter and thus are fairly small, compared with those reported by other authors (e.g. Walcott 1920; Rigby 1978). However, two or three size-ranges of sclerites are present within a chancelloriide scleritome. Also, sclerites become successively larger from the base upwards towards the ontogenetically younger part of the scleritome (Rigby 1978 and pers. obs. of new complete chancelloriides from the Wheeler Shale). Individual rays 1–2 mm long with polygonal basal outlines also occur within this assemblage. They obviously represent originally joined composites of larger, broken chancelloriide sclerites.

Chancelloria racemifundis Bengtson, *in* Bengtson *et al.*, 1990

Plate 7, figures 2, 6, 13

Material. Three specimens: CPC34282, 34286, 34293.

Description. The sclerites are generally rather small, 300–800 μm in diameter, with a highly variable number of long slender rays, (3–7 + 0) and (5–11 + 1) according to Bengtson (*in* Bengtson *et al.* 1990). Protruding ridges

and nodular deposits surround the basal foramina, and the entire circular base is rather small and bordered by a distinct ridge.

Chancelloria cf. *pentacta* Rigby, 1978

Plate 7, figure 10

Material. CPC 34290.

Description. The sclerites have the composition (5+1), (4+1) or (6+1). They are *c.* 0·8–1·0 mm in total diameter with rays 300–500 μm long. The polygonal outline of the basal disc, from which the rays curve away at steep angles of *c.* 60°, measures only 100–200 μm in diameter.

Remarks. It is uncertain whether these chancelloriide sclerites actually belong to the species *C. pentacta*. The type specimens of *C. pentacta*, as documented by Rigby (1978) from the Mid Cambrian Wheeler Shale, have generally larger sclerites with slightly more slender rays.

Chancelloria sp.

Plate 7, figure 9

Material. CPC 34289.

Description. A new type of sclerite (Pl. 7, fig. 9) with three to five marginal rays that bend away sharply, almost 90° from the base, is not very common within this assemblage. The basal pores are bordered by clearly elevated spines protruding above the basal surface. The thin outer wall is often in phosphatic preservation.

Genus ARCHIASTERELLA Sdzuy, 1969

Type species. Archiastrella pentactina Sdzuy, 1969.

Diagnosis. Sclerites in the configuration (3–6+0) with their rays radiating at steep angles from the central plate.

Archiasterella sp.

Plate 7, figure 11

Material. CPC 34291.

Description. This sclerite has steeply projecting marginal rays, but no central ray. Composition (5+0) is the most common type, according to Bengtson *et al.* (1990). One of the rays may be almost vertical to the base, whereas the others project at slightly more gentle angles.

EXPLANATION OF PLATE 7

Figs 1, 3, 7–8, 12, 14–15. *Chancelloria eros* Walcott, 1920. 1, 3, 12, 14–15, Ordian. 1, CPC34281; ×42. 3, CPC34283; ×42. 12, CPCCPC34292; ×41. 14, CPC34294; ×160. 15, CPC34295; ×50. 7–8, Templetonian. 7, CPC34287; ×70. 8, CPC34288; ×75.

Figs 2, 6, 13. *Chancelloria racemifundis* Bengtson, *in* Bengtson *et al.*, 1990; Templetonian. 2, CPC34282; ×120. 6, CPC34286; ×100. 13, CPC34293; ×105.

Figs 4–5. *Allonia erromenosa* Jiang, *in* Luo *et al.*, 1982; CPC34284; Ordian. 4, ×44. 5, ×39.

Fig. 9. *Chancelloria* sp.; Templetonian; ×105.

Fig. 10. *Chancelloria* cf. *pentacta* Rigby, 1978; CPC34290; Ordian; ×75.

Fig. 11. *Archiasterella* sp.; CPC34291; Ordian; ×31.

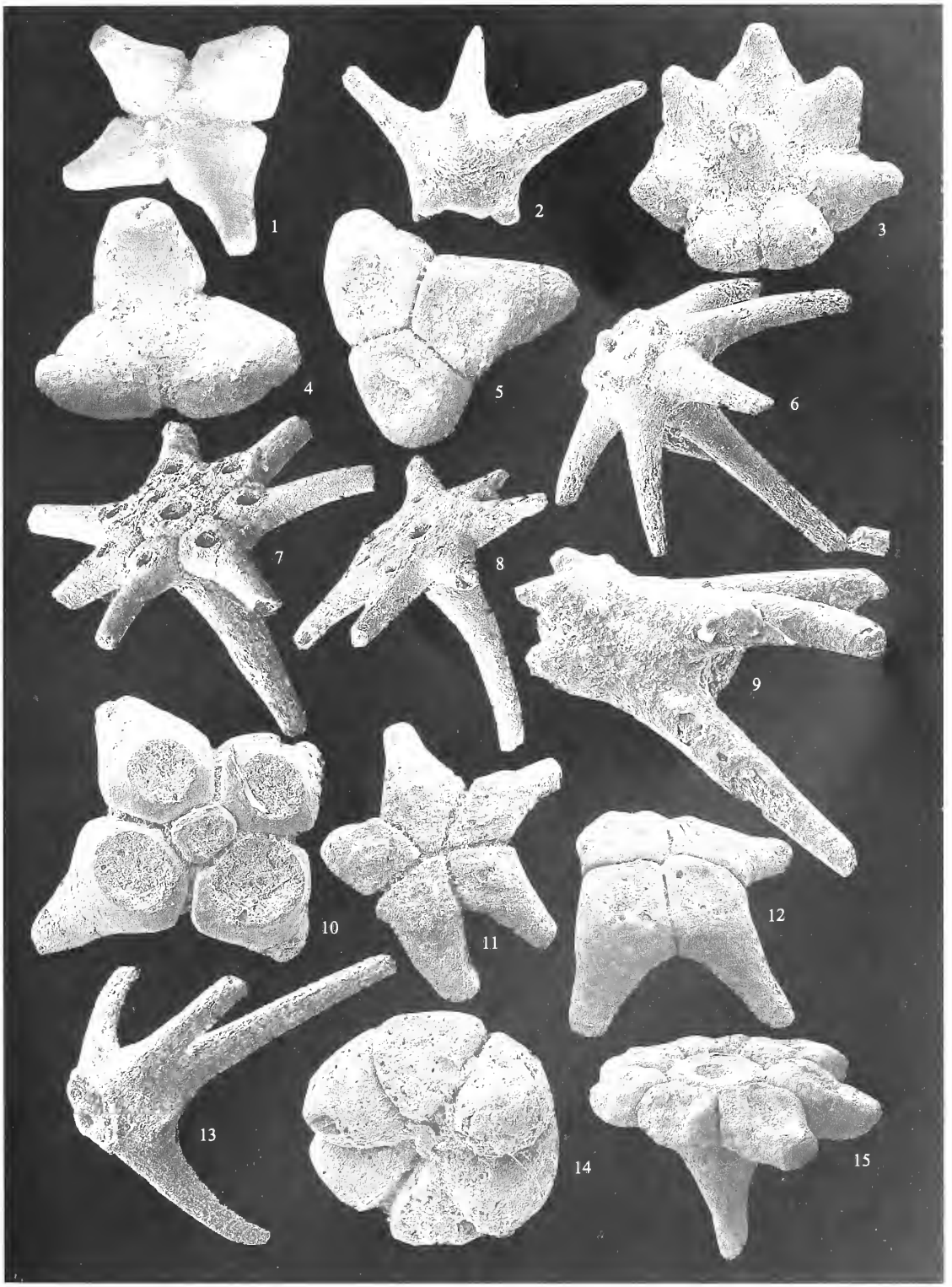

MEHL, *Chancelloria, Allonia, Archiasterella*

Genus ALLONNIA Doré and Reid, 1965

Type species. Allonnia triporata Doré and Reid, 1965.

Diagnosis. Sclerites with few, stout rays.

Allonnia erromenosa Jiang, *in* Luo *et al.*, 1982

Plate 7, figures 4–5

Material. Two specimens: CPC 34284–34285.

Description. Sclerites fairly large, *c.* 1 mm in diameter, with stout rays, normally in the configuration (3 + 0), but (4 + 0) also occurs. The rays bend away sharply (at 60–80°) from the wide, plane base which has large pores. A central ray is missing, but the base may be somewhat swollen in the central region.

SYSTEMATIC POSITION OF THE CHANCELLORIIDAE

Natural assemblages of chancelloriide sclerites are not common. The Burgess Shale material contains a few fairly complete specimens, which Walcott (1920) interpreted as sponges and described as a new genus *Chancelloria*. For a long time, the original classification of these sessile, sclerite-bearing Chancelloriidae as sponges was not questioned in the literature. On the contrary, Sdzuy (1969) classified the heteractinide genus *Eiffelia* within the Chancelloriidae, which he considered as the stem-group of all Porifera. For this reason, many authors (e.g. Mostler and Mosleh-Yazdi 1976) have attributed the chancelloriids to the Heteractinellida. Goryanskij (1973) was the first to argue for the necessity of excluding the Chancelloriidae from the Porifera. Bengtson and Missarzhevsky (1981) concluded, on account of the hollow, composite nature of chancelloriide sclerites, that it is impossible for them to be homologous with poriferan spicules. Consequently, they interpreted the sclerites as belonging to an exoskeleton and proposed the new class Coeloscleritophora to include the Chancelloriidae and, in their view, closely related families. Bengtson and Missarzhevsky (1981) considered the Coeloscleritophora, although of uncertain systematic position within the Metazoa, to be most probably a monophyletic group, which currently comprises the following taxa: Wiwaxiidae, Siphogonuchitidae and Chancelloriidae. However, the microstructure of chancelloriide sclerites is very different from those of the supposedly closely related *Wiwaxia*, and their homology is more than doubtful. The interpretation of the Chancelloriidae as Coeloscleritophora has been accepted also by most spongiologists (e.g. Rigby 1986).

New evidence (Butterfield and Nicholas 1996) of well-preserved chancelloriide sclerites, from which organic walls were dissolved with HF, appears to give reason to doubt the interpretation by Bengtson and Missarzhevsky (1981). The Chancelloriidae are known so far from the relatively complete scleritomes of the Mid Cambrian Burgess Shale (Walcott 1920; Rigby 1986) and Wheeler Shale (Rigby 1978). New, promising, complete and well-preserved chancelloriides from the Wheeler Shale are currently being studied by me. The results of preliminary studies of these specimens and the Georgina assemblage have been published (Mehl 1996*b*), but more detailed descriptions will probably provide new evidence on this enigmatic fossil group. Few sclerites from the Georgina Basin are found with their outer walls still present in a phosphatic preservation. These sclerite walls are composed of fibrous needles in a regular radial orientation. Most probably, these were originally crystals of aragonite, which have been diagenetically altered by heavy phosphatization (Mehl 1996*b*). This interpretation corresponds with the results of James and Klappa (1983) and Bengtson *et al.* (1990), who suggested that the chancelloriide sclerites were originally aragonitic. Although spicules have evolved convergently several times within the Porifera (Mehl and Reitner 1991; Reitner and Mehl 1996), no poriferan spicules of aragonitic mineralogy are known. Sponge spicules consist of either calcite or opaline silica. The calcitic spicules are monocrystalline, they are formed by an extracellular mode of secretion, and thus are massive without axial filaments or central canals

(Ledger and Jones 1977). Siliceous spicules, in contrast, are secreted intracellularly by sclerocytes and contain a thin axial filament in a central canal.

The chancelloriide composite type of sclerites, with large internal cavities and with inner and outer walls consisting of aragonitic needles, does not correspond with any known mode of spicule formation within the Porifera. Thus, Chancelloriide sclerites are not homologous with any known sponge spicules. However, many sponges do possess the ability to secrete $CaCO_3$ extracellularly, in addition to their spicules. Also, other types of skeletons are known, e.g. some horny sponges agglutinate sand grains between spongin fibres in their organic skeletons. According to Butterfield and Nicholas (1996), the organic walls of chancelloriide sclerites show remarkable similarity to the spongin spiculoids produced by some modern dendroceratid sponges. However, my observations of the massive spicules in different *Darwinella* species has so far provided no confirmation of a poriferan affinity of the Chancelloriidae.

Acknowledgements. The author thanks Prof. K. J. Müller (Bonn) and Dr J. Shergold (Canberra) for permission to work on the rich spicule assemblage from Georgina Basin, the Geological Survey of Canberra for loan of the material, Prof. J. K. Rigby (Provo, Utah) for critical review of the manuscript for this paper, and Dr R. A. Wood (Cambridge) for discussions. Deutsche Forschungsgemeinschaft is acknowledged for financing research on sponges (Me 1151/2, 1-3).

REFERENCES

BENGTSON, S. 1986. Siliceous microfossils from the Upper Cambrian of Queensland. *Alcheringa*, **10**, 195–216.

—— CONWAY MORRIS, S., COOPER, B. J., JELL, P. A. and RUNNEGAR, B. N. 1990. *Early Cambrian fossils of South Australia*. Association of Australasian Palaeontologists, Brisbane, 364 pp.

—— and MISSARZHEVSKY, V. V. 1981. Coeloscleritophora – a major group of enigmatic Cambrian metazoans. 19–21. *In* TAYLOR, M. E. (ed.). *Short papers for the Second International Symposium on the Cambrian System 1981*. U.S. Geological Survey Open-File Report, 662 pp.

BOWERBANK, J. S. 1864. *A monograph of the British Spongiadae. Volume I.* Ray Society, London, 289 pp.

BUTTERFIELD, N. J. and NICHOLAS, C. J. 1996. Burgess Shale-type preservation of both non-mineralizing and "shelly" Cambrian organisms from the Mackenzie Mountains, Northwestern Canada. *Journal of Paleontology*, **70**, 893–899.

CHEN JUN-YUAN, HOU XIAN-GUANG and LI GUO-XIAN 1990. New Lower Cambrian demosponges – *Quadrolaminiella* gen. nov. from Chenjiang, Yunnan. *Acta Palaeontologica Sinica*, **29**, 402–414.

DONG XIPING and KNOLL, A. H. 1996. Middle and Late Cambrian sponges from Hunan, China. *Journal of Paleontology*, **70**, 173–184.

DORÉ, F. and REID, R. E. H. 1965. *Allonia tripodophora* nov. gen., nov. sp., nouvelle éponge du Cambrien inférieur de Carteret (Manche). *Comptes Rendus Sommaires Séances Société Géologique de la France*, **1965**, 20–21.

FINKS, R. M. 1960. Late Paleozoic sponge faunas of the Texas region. The siliceous sponges. *Bulletin of the American Museum of Natural History*, **120**, 1–160.

—— 1970. The evolution and ecologic history of sponges during Paleozoic times. *Symposium of the Zoological Society, London*, **25**, 3–22.

GATEHOUSE, C. G. 1968. First record of lithistid sponges in the Cambrian of Australia. *Bulletin of the Bureau of Mineral Resources, Geology and Geophysics, Australia*, **92**, 57–68.

GEHLING, J. G. and RIGBY, K. 1996. Long expected sponges from the Neoproterozoic Ediacara Fauna of South Australia. *Journal of Paleontology*, **70**, 185–195.

GORYANSKIJ, V. Y. 1973. [On the necessity of excluding the genus *Chancelloria* from the sponge phylum.] *Trudy Institut Geologiki i Geofiziki So AN SSSR*, **49**, 39–44. [In Russian].

GRANT, R. E. 1836. Animal kingdom. 107–118. *In* TODD, R. B. (ed.). *The cyclopedia of anatomy and physiology*, 1. Gilbert and Piper, London, 813 pp.

GRUBER, G. 1993. Mesozoische und rezente desmentragende Demospongiae (Porifera, "Lithistidae") (Paläobiologie, Phylogenie und Taxonomie). *Berliner Geowissenschaftliche Abhandlungen, Reihe E*, **10**, 73.

HALL, J. 1884. Descriptions of the species of fossil reticulate sponges, constituting the family Dictyospongidae. *Annual Report of New York State Museum of Natural History*, **35**, 465–481.

—— and CLARKE, J. M. 1898. *A memoir on the Palaeozoic reticulate sponges constituting the family Dictyospongidae. Part 2.* Wynkoop Hallenbeck Crawford Co., Albany, New York, 105 pp.

HEREDIA, S., BORDONARO, O. and MATTEODA, E. 1987. Espiculas de poriferos de la formacion la Cruz, Cambrio Superior, Departamento Las Heras, provincia de Mendosa. *Ameghiniana*, **24**, 17–20.

HINDE, G. J. 1888. A monograph of the British fossil sponges. *Palaeontographica Part II: sponges of the Palaeozoic group*, **1887**, 93–188.

JAMES, N. P. and KLAPPA, C. F. 1983. Petrogenesis of Early Cambrian reef limestones, Labrador, Canada. *Journal of Sedimentary Petrology*, **53**, 1051–1096.

KEMPEN, T. M. G. van 1978. Anthaspidellid sponges from the Early Paleozoic of Europe and Australia. *Neues Jahrbuch für Geologie und Paläontologie, Abhandlungen*, **156**, 305–337.

—— 1983. The biology of aulocopiid lower parts (Porifera-Lithistida). *Journal of Paleontology*, **57**, 363–376.

—— 1990. On the oldest tetraxon megascleres. 9–16. *In* RÜTZLER, K. (ed.). *New perspectives in sponge biology*. Smithsonian Institution Press, Washington, 533 pp.

—— and KATE, W. G. H. Z. TEN 1980. The skeletons on two Ordovician anthaspidellid sponges; a semi-numerical approach. *Palaeontology, Proceeding Series B*, **83**, 437–453.

KLING, S. A. and REIF, W.-E. 1969. The Paleozoic history of amphidisc and hemidisc sponges: new evidence from the Carboniferous of Uruguay. *Journal of Paleontology*, **43**, 1429–1434.

KRUSE, P. D. 1983. Middle Cambrian '*Archaeocyathus*' from the Georgina Basin is an anthaspidellid sponge. *Alcheringa*, **7**, 49–58.

—— 1987. Further Australian Cambrian sphinctozoans. *Geological Magazine*, **124**, 543–553.

—— 1990. Cambrian paleontology of the Daly Basin. *Report of the Northern Territory Geological Survey*, **7**, 1–58.

—— 1996. Update on northern Australian Cambrian sponges *Rankenella*, *Jawonya* and *Wagima*. *Alcheringa*, **20**, 161–178.

KOZUR, H. W., MOSTLER, H. and REPETSKI, J. E. 1997*a*. 'Modern' siliceous sponges from the lowermost Ordovician (early Ibexian–early Tremadocian) Windfall Formation of the Antelope Range, Eureka County, Nevada, U.S.A. *Geologische Paläontologische Mitteilungen der Universität Innsbruck*, **21**, 201–221.

—— 1997*b*. Well-preserved Tremadocian primitive Radiolaria from the Windfall Formation of the Antelope Range, Eureka County, Nevada, U.S.A. *Geologische Paläontologische Mitteilungen der Universität Innsbruck*, **21**, 245–271.

LEDGER, P. W. and JONES, W. C. 1977. Spicule formation in the calcareous sponge *Sycon ciliatum*. *Cell Tissue Research*, **181**, 553–567.

LEVI, C. 1953. Sur une nouvelle classification des Démosponges. *Comptes Rendus de l'Académie des Sciences de Paris*, **236**, 853–855.

LUO HUILIN, JIANG ZHIWEN, WU XICHE, SONG XUELLIANG and OUYANG LIN 1982. [*The Sinian-Cambrian Boundary in Eastern Yunnan.*] 165 pp. [In Chinese with English summary].

MEHL, D. 1991. Are Protospongiidae the stem group of modern Hexactinellida? 43–53. *In* REITNER, J. and KEUPP, H. (eds). *Fossil and Recent sponges*. Springer Verlag, Berlin, 595 pp.

—— 1992. Die Entwicklung der Hexactinellida seit dem Mesozoikum – Paläobiologie, Phylogenie und Evolutionsökologie. *Berliner Geowissenschaftliche Abhandlungen, Reihe E*, **2**, 1–164.

—— 1996*a*. Phylogenie und Evolutionsökologie der Hexactinellida (Porifera) im Paläozoikum. *Geologische Paläontologische Mitteilungen der Universität Innsbruck, Sonderband*, **4**, 1–55.

—— 1996*b*. Organization and microstructure of the chancelloriid skeleton: implications for the biomineralization of the Chancelloriidae. *Bullétin de l'Institut Océanographique, Monaco, numéro spécial*, **14**, 377–385.

—— and REITNER, J. 1991. Monophylie und Systematik der Porifera. *Verhandlungen der Deutschen Zoologischen Gesellschaft*, **84**, 447.

MILLER, S. A. 1889. *North American geology and paleontology for the use of amateurs, students, and scientists*. Western Methodist Book Concern, Cincinnati, 718 pp.

MOSTLER, H. 1986*a*. Beitrag zur stratigraphischen Verbreitung und phylogenetischen Stellung der Amphidiscophora und Hexasterophora (Hexactinellida, Porifera). *Mitteilungen der Österreichchen Geologischen Gesellschaft*, **78**, 319–359.

—— 1986*b*. Neue Kieselschwämme aus der Zlambachschichten (Obertrias, Nördliche Kalkalpen). *Geologische Paläontologische Mitteilungen der Universität Innsbruck*, **13**, 331–361.

—— 1989. Mikroskleren hexatinellider Schwämme aus dem Lias der Nördlichen Kalkalpen. *Jahrbuch der Geologischen Bundesanstalt Wien*, **132**, 687–700.

—— and MOSLEH-YAZDI, A. 1976. Neue Poriferen aus oberkambrischen Gesteinen der Milaformation im Elburzgebirge (Iran). *Geologische Paläontologische Mitteilungen der Universität Innsbruck*, **5**, 1–36.

MÜLLER, K. J. and HINZ, I. 1992. Cambrogeorginidae fam. nov., soft-integumented problematica from the Middle Cambrian of Australia. *Alcheringa*, **16**, 333–353.

ÖPIK, A. A. 1960. Cambrian and Ordovician geology (of Queensland). *Journal of the Geological Society of Australia*, **7**, 89–109.

—— 1961. Geology and palaeontology of the headwaters of the Burke River, Queensland. *Bulletin of the Bureau of Mineral Resources, Australia*, 53, 1–249.

—— 1970. Nepeiid trilobites of the Middle Cambrian of northern Australia. *Bulletin of the Bureau of Mineral Resources, Australia*, **113**, 1–48.

QIAN YI 1977. [Hyolitha and some problematica from the Lower Cambrian Meishucun Stage in central and SW China.] *Acta Palaeontologica Sinica*, **16**, 255–278. [In Chinese].

—— and BENGTSON, S. 1989. Palaeontology and biostratigraphy of the Early Cambrian Meishunian Stage in Yunnan Province South China. *Fossils and Strata*, **24**, 1–56.

REIF, W. E. 1968. Schwammreste aus dem oberen Ordovizium von Estland und Schweden. *Neues Jahrbuch für Geologie und Paläontologie, Monatshefte*, **1968**, 733–744.

REITNER, J. 1992. 'Coralline Spongien'. Der Versuch einer phylogenetisch-taxonomischen Analyse. *Berliner Geowissenschaftliche Abhandlungen, Reihe E*, **1**, 1–352.

—— and KOHRING, R. 1990. Taxonomische Bedeutung freier Skleren in *Carpospongia globosa* (Eichwald, 1830) und *Aulocopium aurantium* Oswald, 1850 (Demospongiae, 'Lithistida') (Oberordovizium) aus dem Karolinsand von Braderup/Sylt. 219–230. *In* HACHT U. von (ed.). *Fossilien von Sylt, 3*. Inge-Maria von Hacht Verlag, Hamburg, 338 pp.

—— and MEHL, D. 1995. Early Paleozoic diversification of sponges: new data and evidences. *Geologische Paläontologische Mitteilungen der Universität Innsbruck*, **20**, 335–347.

—— 1996. Monophyly and systematics of the Porifera. *Verhandlungen des Naturwissenschaftlichen Vereins Hamburg, Neue Folge*, **36**, 5–32.

RIETSCHEL, R. 1968. Die Octactinellida und ihnen verwandte paläozoiche Kalkschwämme (Porifera, Calcarea). *Paläontologische Zeitschrift*, **42**, 13–32.

RIGBY, J. K. 1975. Some unusual hexactinellid sponge spicules from the Cambrian Wilberns Formation of Texas. *Journal of Paleontology*, **49**, 412–415.

—— 1978. Porifera of the Middle Cambrian Wheeler Shale, from the Wheeler Amphitheater, House Range, in Western Utah. *Journal of Paleontology*, **52**, 1325–1345.

—— 1983. Heteractinellida. 70–89. *In* RIGBY, J. K. and STEARN, C. W. (eds). Sponges and spongiomorphs. *University of Tennesee Department of Geological Sciences, Studies in Geology*, **7**, 1–220.

—— 1986. Sponges of the Burgess Shale (Middle Cambrian), British Columbia. *Palaeontographica Canadiana*, **2**, 1–105.

—— 1991. Evolution of Paleozoic heteractinellid calcareous sponges and demosponges – patterns and records. 83–101. *In* REITNER, J. and KEUPP, H. (eds). *Fossil and Recent sponges*. Springer Verlag, Berlin, 595 pp.

—— and DIXON, O. A. 1979. Sponge fauna of the Upper Silurian Read Bay Formation, Somerset Island, District of Franklin, Arctic Canada. *Journal of Paleontology*, **53**, 587–627.

SCHMIDT, O. 1870. *Grundzüge einer spongienfauna des Atlantischen gebietes*. Wilhelm Engelmann, Leipzig, 88 pp.

SCHULZE, F. E. 1887. Über den Bau und das System der Hexactinelliden. *Physische Abhandlungen der Königlichen Preussischen Akademie der Wissenschaften*, **1886**, 1–97.

SDZUY, K. 1969. Unter- und mittelkambrische Porifera (Chancelloriida und Hexactinellida). *Paläontologische Zeitschrift*, **43**, 115–147.

SHERGOLD, J. H. and DRUCE, E. C. 1980. Upper Proterozoic and Lower Palaeozoic rocks of the Georgina Basin. 149–174. *In* HENDERSON, R. A. and STEPHENSON, P. J. (eds). *The geology and geophysics of northeastern Australia*. Geological Society of Australia, Queensland Division, Brisbane, 468 pp.

—— JAGO, J. B., COOPER, R. A. and LAURIE, J. R. 1985. The Cambrian system in Australia, Antarctica and New Zealand. Correlation charts and explanatory notes. *Publication of the International Union of Geological Sciences*, **19**, 1–85.

—— and SOUTHGATE, P. N. 1986. Middle Cambrian phosphatic and calcareous lithofacies along the eastern margin of the Georgina Basin, Western Queensland. *Australasian Sedimentologists Group Field Guide Series*, **2**, 1–89.

SIMPSON, T. L. 1984. *The cell biology of sponges*. Springer, New York, Heidelberg, Berlin, 662 pp.

SMITH, K. G. 1972. Stratigraphy of the Georgina Basin. *Bulletin of the Bureau of Mineral Resources Australia*, **111**, 1–156.

—— 1991. Demosponge higher taxa re-examined. 54–71. *In* REITNER, J. and KEUPP, H. (eds). *Fossil and Recent sponges*. Springer Verlag, Berlin, 595 pp.

SOLLAS, W. J. 1875. Sponges. *In* BAYNES, T. S. (ed.). *Encylopaedia Britannica, a dictionary of arts, sciences and general literature*. 9th edition. Edinburgh, 421 pp.

—— 1885. A classification of the sponges. *Annals and Magazine of Natural History, Series 5*, **16**, 395.

—— 1888. Report on the Tetractinellida collected by H.M.S. Challenger during the years 1873–1876. *Report on the scientific results of the voyage of H.M.S. Challenger, Zoology*. Vol. 25. London, 458 pp.

SOUTHGATE, P. N. and SHERGOLD, J. H. 1991. Application of sequence stratigraphic concepts to Middle Cambrian phosphogenesis, Georgina Basin, Australia. *Bulletin of the Bureau of Mineral Resources, Journal of Australian Geology and Geophysics*, **12**, 119–144.

STEINER, M., MEHL, D., REITNER, J. and ERDTMANN, B.-D. 1993. Oldest entirely preserved sponges and other fossils from the lowermost Cambrian and a new facies reconstruction for the Yangtze Platform (China). *Berliner Geowissenschaftliche Abhandlungen, Reihe E*, **9**, 293–329.

WALCOTT, C. D. 1920. Middle Cambrian Spongiae. *Smithsonian Miscellaneous Collections*, **67**, 261–364.

WEBBY, B. D. and TROTTER, J. 1993. Ordovician sponge spicules from New South Wales. *Journal of Paleontology*, **67**, 21–48.

WHITTINGTON, H. B. 1978. The lobopod animal *Aysheaia pedunculata* Walcott, Middle Cambrian Burgess Shale, British Columbia. *Philosophical Transactions of the Royal Society, Series B*, **284**, 165–197.

WIEDENMAYER, F. 1994. Contributions to the knowledge of post-Palaeozoic neritic and archibenthal sponges (Porifera). *Schweizerische Paläontologische Abhandlungen*, **116**, 1–147.

ZHANG XI-GUANG and PRATT, B. R. 1994. A new and extraordinary Early Cambrian sponge spicule assemblage from China. *Geology*, **22**, 43–46.

DORTE MEHL

Institut für Paläontologie der
Freien Universität Berlin
Malteserstraße 74-100
D-12249 Berlin
Germany

Typescript received 6 September 1996
Revised typescript received 10 December 1997

PALAEOBIOLOGY OF THE PRIMITIVE ORDOVICIAN PELMATOZOAN ECHINODERM *CARDIOCYSTITES*

by JULIETTE DEAN *and* ANDREW B. SMITH

ABSTRACT. A new species of primitive cystoid, *Cardiocystites pleuricostatus*, is described from the Caradoc of Shropshire. Its superb preservation clarifies the morphology of this problematical taxon and shows it to belong to the Rhipidocystidae. Its highly flattened theca cannot be indicative of a recumbent mode of life, contrary to previous interpretations, since its arms and brachioles formed a conical filter. The flat, thin-plated theca may have been a specialization either for aiding gaseous exchange, or for providing hydrodynamic lift to the crown.

POORLY known taxa with apparently bizarre morphologies abound amongst early Palaeozoic echinoderms. They are of special interest for two reasons. First, they have proved difficult to place into a phylogenetic scheme, and in many cases have been elevated to high taxonomic rank. Determining their sister-group relationships is essential if we are to improve our understanding of the early evolution of echinoderms. It is especially important that the morphology of such poorly known taxa is interpreted correctly, so that estimates of disparity do not become overinflated. Second, where unexpected morphological combinations are encountered, these can shed light on the functional design and mode of life of primitive echinoderms.

Many of the taxa most difficult to place have traditionally been assigned to the eocrinoids, a paraphyletic group that comprises stem-group members of many of the better known cystoid groups (Smith 1984*a*; Paul 1988). Amongst the most poorly known of eocrinoids is *Cardiocystites*, erected by Barrande (1887) on the basis of two specimens from the middle Ordovician of the Czech Republic, neither of which was particularly well preserved. Although Barrande clearly recognized it to be a cystoid, he did not classify it further. Since its discovery no additional material of this species has been collected, and consequently its relationship to other cystoids has remained problematical. Ubaghs (1967, p. S491) accepted it as an eocrinoid, but left it unclassified within the class. Sprinkle (1973) redescribed and refigured Barrande's original material but was also unable to classify it, placing it in 'Order and Family indeterminate'. Broadhead (1982) placed *Cardiocystites* in the family Rhipidocystidae Jaekel, 1901, along with the other flattened eocrinoid genera *Rhipidocystis*, *Batherocystis*, *Petalocystis* and *Lingulocystis*. This placement was disputed by Lewis *et al.* (1987), when describing a new genus of rhipidocystid, *Mandalacystis*. They preferred to omit *Cardiocystites* and *Lingulocystis* from the Rhipidocystidae, but made no attempt to place either genus. Nevertheless, a cladistic analysis of cystoid genera carried out by Paul (1988) identified *Cardiocystites* as sister taxon to the clade *Rhipidocystis*, *Batherocystis* and *Petalocystis*.

Here we describe a new species of *Cardiocystites* which is much better preserved than the original and which consequently provides new information on the morphology and mode of life of this taxon. The material was collected more than 40 years ago by W. T. and J. F. Dean from the Caradoc of Shropshire. Although the Deans recognized that they had found a new and bizarre cystoid, the material remained undescribed in the collections of The Natural History Museum.

[Palaeontology, Vol. 41, Part 6, 1998, pp. 1183–1194]

MORPHOLOGY OF *CARDIOCYSTITES*

Cardiocystites can be recognized immediately by its flattened cordiform theca bounded by a narrow marginal frame. A cylindrical stem attaches to the marginal frame distally, whilst from the centre of the proximal face arise five short, free-standing arms which bear long brachioles (Text-fig. 1). The mouth was presumably situated at the point of ambulacral convergence, as in all echinoderms, although no specimen shows the actual opening. The periproct is also not visible on any specimen but was probably positioned at the anterior corner on one side of the theca, the only region not clearly seen in our new material.

Stem

The stem is at least as long as the theca and tapers only very slightly distally. It is composed of cylindrical holomeric columnals throughout. The stem is heteromorphic proximally, with alternating nodals and internodals established immediately beneath the theca (Text-fig. 2). Distally, however, columnals become more uniform and each has a small spinose flange, at least in the type species. The stem attachment is shared equally between the two lower marginal ossicles. The distal end of the stem is missing.

Theca

Thecal plating is very similar in *C. bohemicus* and *C. pleuricostatus* and comprises an outer series of frame plates and an internal series of large polygonal plates. Plating is clearly differentiated into a proximal and distal series separated by a horizontal suture line mid-way down the theca (Text-figs 1, 3). The marginal frame plates have a thickened external rim, *c.* 0·5–1·0 mm wide, which is smooth and slightly faceted. Upper right and upper left frame elements are similar, consisting of an L-shaped marginal ridge and a triangular internal flange. Sutures coincide exactly on the two surfaces. The flange arises from below the top of the marginal rim, so that the rim projects above the level of the central tesselate region on both surfaces.

In the lower half of the theca, frame elements differ on left and right sides. One side is formed of a single frame element similar to the proximal element. This is bow-shaped, with a short internal flange that narrows and more-or-less disappears at either end. An identical plate, again with coincidental sutures, is found directly underneath on the opposite surface. By contrast, the lower half of the other side of the frame is composed of two (*C. bohemicus*) or three (*C. pleuricostatus*) elements, each composed of a thickened rim and narrow internal flange. The plate sutures in this area are not clearly defined in any specimen, but the marginal sutures again coincide on each face. In side view the external face has a sharply defined longitudinal groove, raising the possibility that these lower frame plates may be composed of two elements tightly bound together.

The interior plates are large and very thin. Two large rectangular plates in the proximal half of the theca are subequal in size and meet down the midline along a straight suture. The lower half of the theca is probably composed of a single large triangular plate, although in neither species is the plating clearly seen. In *C. bohemicus* two ridges cross the theca, running from the oral mound and converging a little to one side of the stem attachment. These are also present in *C. pleuricostatus*, but are joined by a large number of other ridges set perpendicular to plate sutures. These appear to be structural ribs rather than pleats in the surface of the plate since, where they are displaced and seen in cross section, they appear solid.

The theca is unusual in that there appears to be almost no internal cavity between the two plated surfaces. The marginal rim, which in *C. pleuricostatus* is only 1 mm deep, is elevated above the central plates on both surfaces. In effect this means that the flanges and central plates are closely appressed, only a fraction of a millimetre apart. We initially thought that the part and counterpart

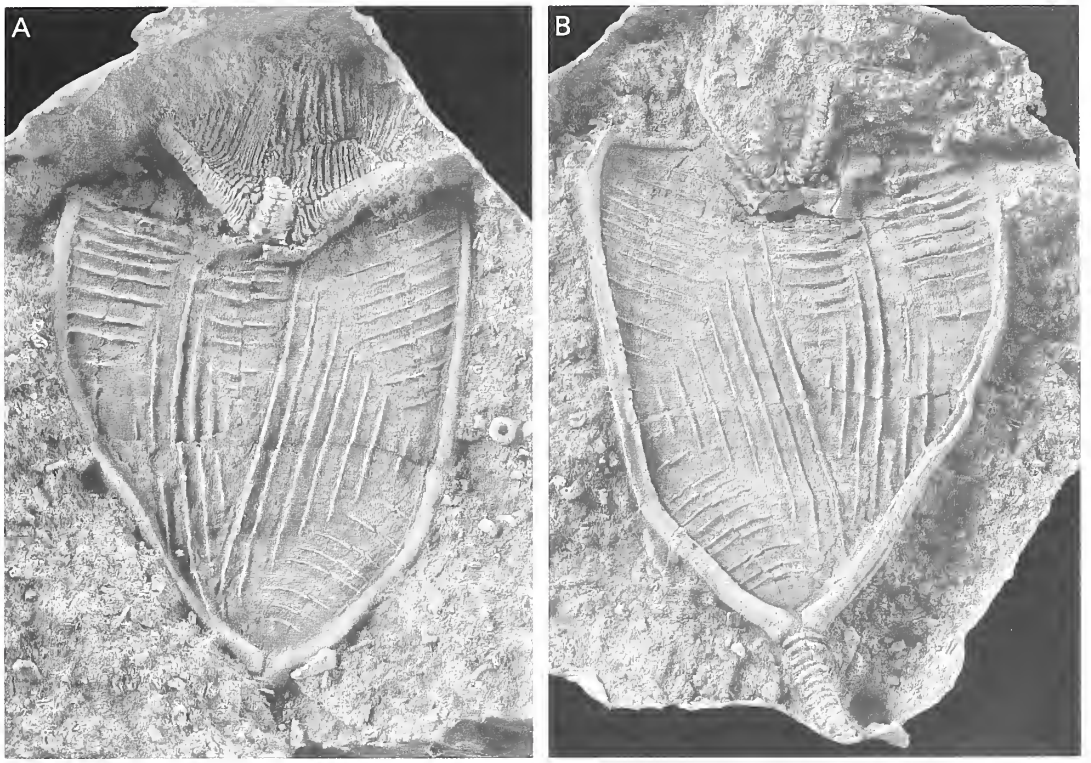

TEXT-FIG. 1. *Cardiocystites pleuricostatus* sp. nov.; BMNH E23706a–b, holotype; Smeathen Wood Beds, *Reuscholithus reuschi* Zone, Burrellian Stage, Harnagian Substage, Caradoc Series; Smeathen Wood, Horderley, Shropshire; part (A) and counterpart (B); × 3.

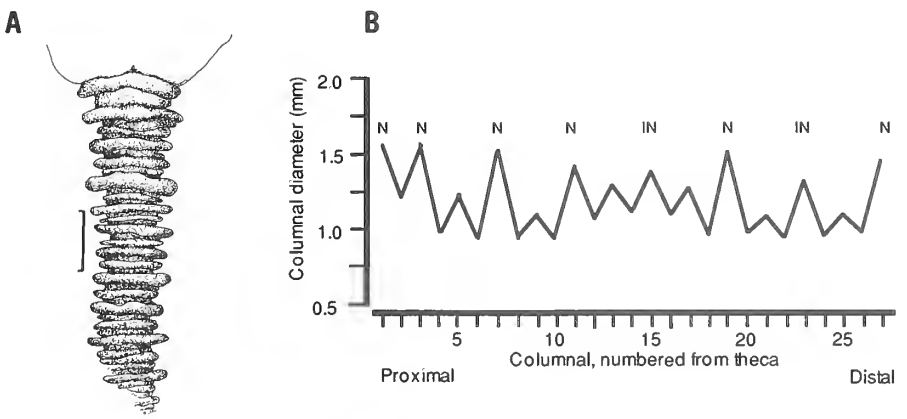

TEXT-FIG. 2. *Cardiocystites pleuricostatus* sp. nov. A, BMNH E23706b; *Camera lucida* drawing of stem; scale bar represents 1 mm. B, columnal diameter plotted against distance from theca; N = nodal, IN = internodal.

of the holotype of *C. pleuricostatus* were showing the internal and external of the same surface, since suture lines exactly coincided on the two surfaces. However, the ridging is not exactly identical on the two surfaces, and in some places the ridges on the underside can be seen to be weakly corrugating

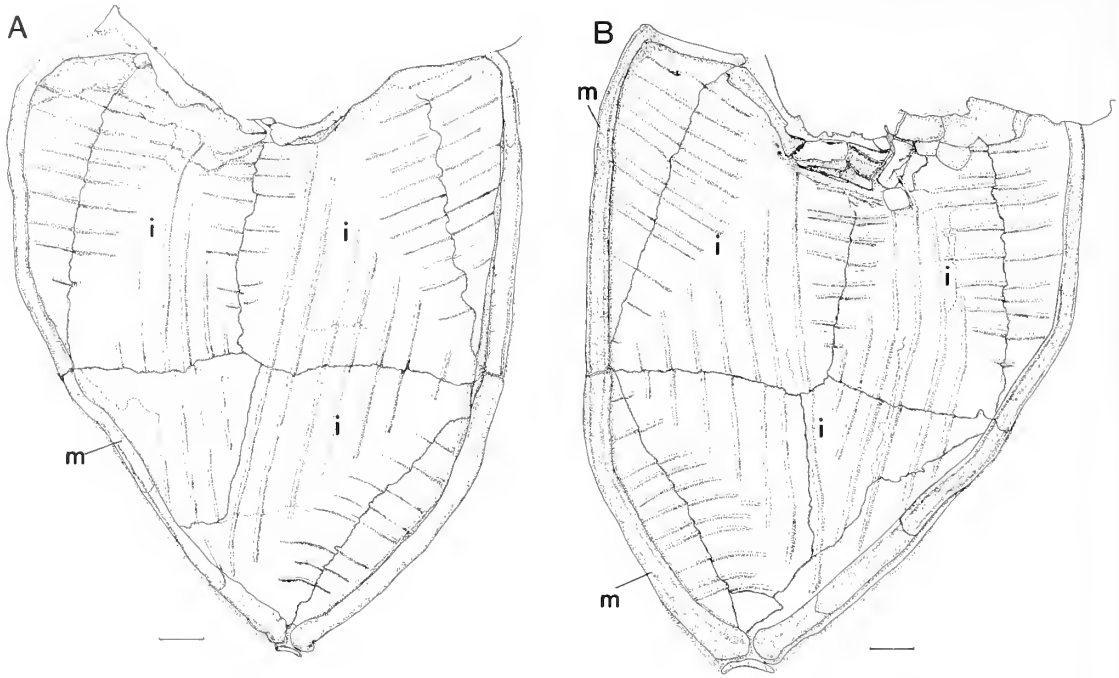

TEXT-FIG. 3. *Cardiocystites pleuricostatus* sp. nov.; BMNH E23706a–b, holotype; *Camera lucida* drawings of thecal plating, part (A) and counterpart (B). i = interior plate; m = marginal frame plate. Scale bars represent 1 mm.

the upper surface. The superb preservation of the arms and brachioles shows that there has been no skeletal disarticulation of the theca that might have resulted in the loss of a second plated surface.

Oral area

The oral area forms a small rounded and flat-topped region in the middle of the distal face of the theca. Its structure remains poorly known, but in *C. pleuricostatus* the five arms diverge from the centre of a ring of some seven plates, 1·5–4·5 mm long. Sutures of some of these plates appear to coincide with the mid-line of arm bases, but plating in this area has collapsed and the arrangement of these plates is uncertain. This is the only portion of the theca that appears to have any depth. On one side there is a small oval opening immediately adjacent to a sutural groove (Text-fig. 4C); we interpret these as the gonopore and hydropore slit.

Arms and brachioles

Five arms are seen in both species, but are better preserved in *C. pleuricostatus* (Text-fig. 5). They diverge upwards and outwards from the centre of the theca, are equal in length, relatively short and stubby, 6·5 mm long and 1·0–1·5 mm in diameter. They are thus only about one-third the length of the theca. Arm plating is biserial, composed of a double series of stout ossicles with a smooth outer surface slightly raised to form a rim at distal and proximal edges. There are *c.* 16 elements in each column. Each arm plate gives rise to a single brachiole (Text-fig. 4B). Basal arm elements are larger and more triangular in form than other elements (Text-fig. 4C).

Brachioles are much finer and very much longer than the arms. Each is biserial and the basal articulation occupies virtually the full width of the arm plate from which it arises. Brachioles are approximately 20 mm long and 0·1–0·2 mm wide and are formed of a large number of small

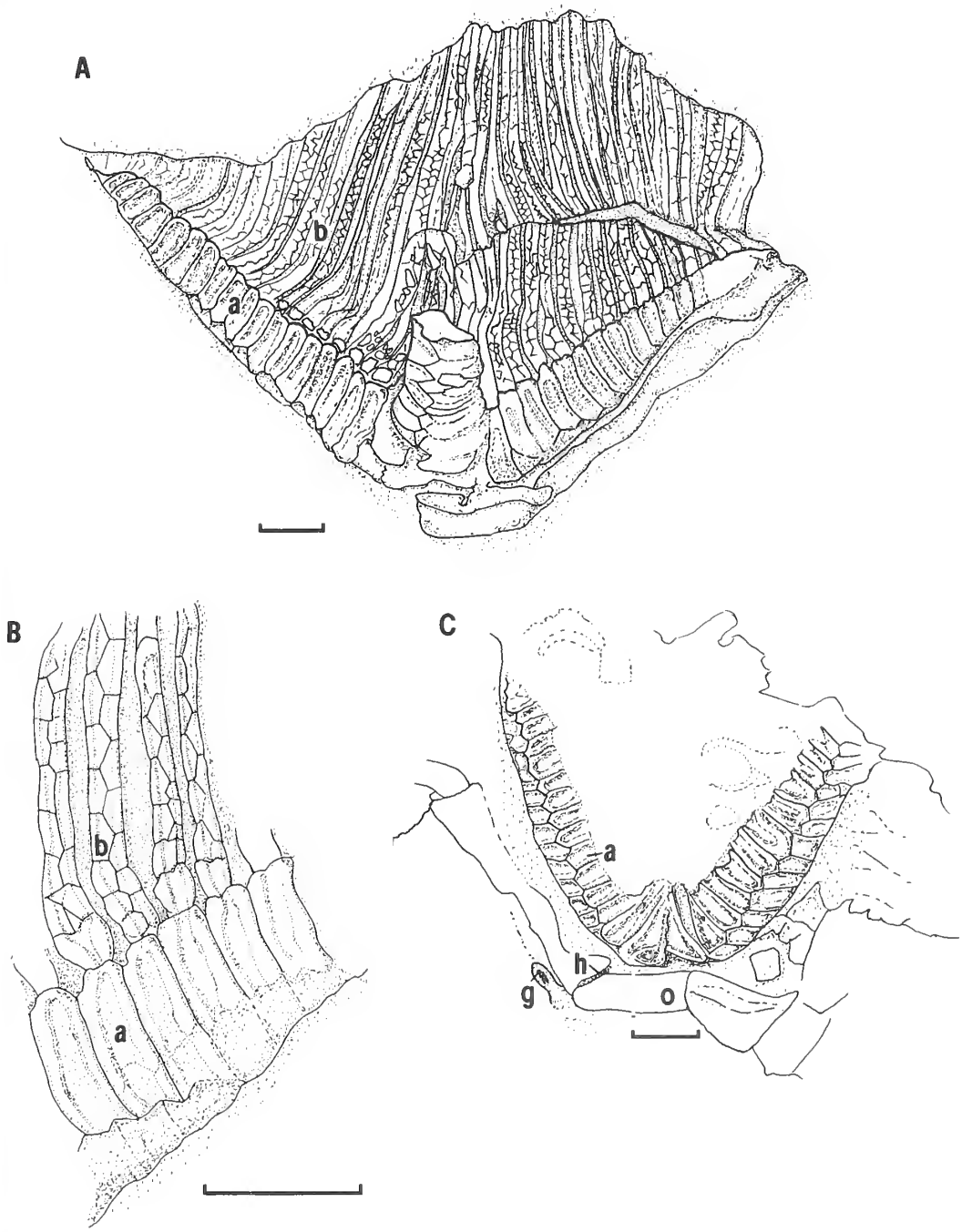

TEXT-FIG. 4. *Cardiocystites pleuricostatus* sp. nov.; BMNH E23706a–b, holotype; *Camera lucida* drawings. A, C, arms and brachioles of part and counterpart. B, detail showing biserial brachioles attaching to ambulacral ossicles of the arm. a = arm; b = brachiole; g = gonopore; h = hydropore slit; o = oral plates. Scale bars represent 1 mm.

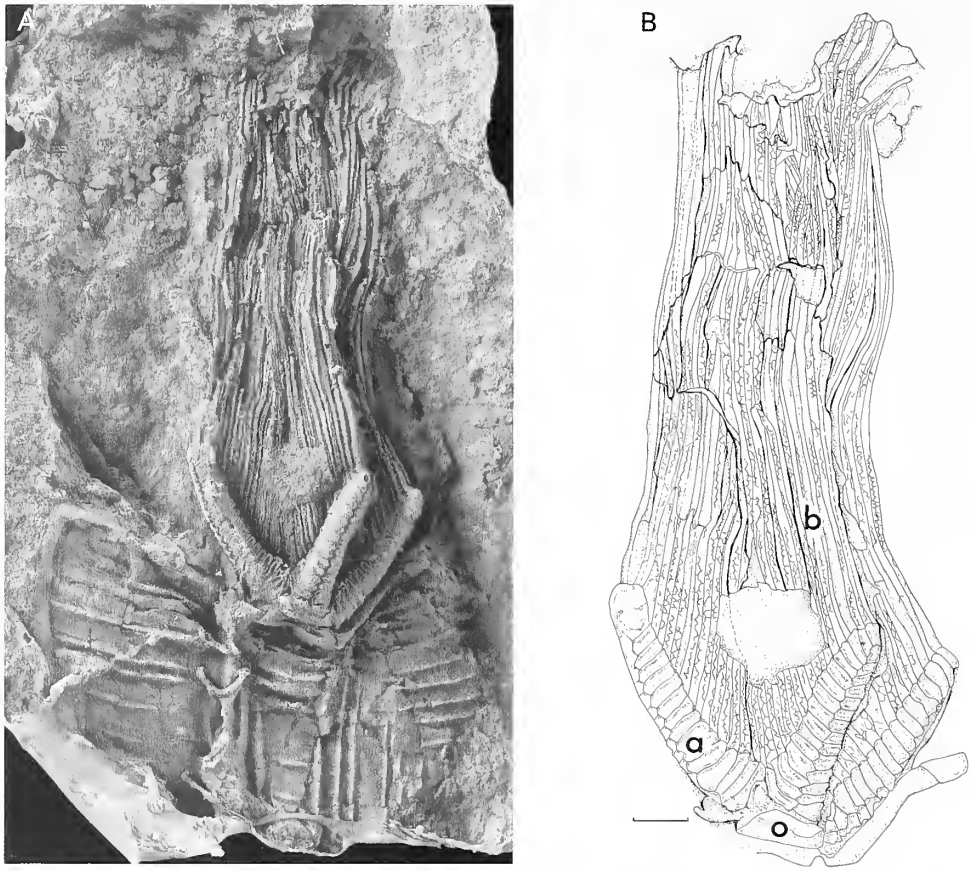

TEXT-FIG. 5. *Cardiocystites pleuricostatus* sp. nov.; BMNH E23709, paratype. A, latex cast; ×3. B, *Camera lucida* drawing of same showing arms (a), brachioles (b) and oral frame plates (o). Scale bar represents 1 mm.

pentagonal elements. Cover-plates appear to be absent. Brachioles arise from every arm ossicle and create a dense filtration fan. Basal elements are slightly enlarged, but otherwise there is no differentiation of plating either along the length of an individual brachiole, or distally along the length of the ambulacrum.

WHY DOES *CARDIOCYSTITES* HAVE SUCH A PECULIAR THECAL DESIGN?

The functional morphology and mode of life of cystoids such as rhipidocystids and *Cardiocystites* are not well understood. It has generally been assumed that their flattened thecal morphology indicates that they lived resting on the sea-floor (e.g. Bockelie 1981, p. 145; Lewis *et al.* 1987, p. 1229; Paul 1988, p. 206). The flattened theca is sometimes thought of as analogous to a snowshoe, functioning to distribute weight so that the animal remains on the surface when living on soft, unconsolidated sediment. Yet this is not the only possible explanation for why a flattened theca evolved, and there are now strong reasons for believing that flattened eocrinoids may have lived elevated above the sea-floor.

First, Lewis *et al.* (1987) discovered that the stem of the highly flattened rhipidocystid *Mandalacystis* ends in a holdfast, at least in smaller individuals. This is strong evidence that *Mandalacystis* lived attached by its stem in an upright posture rather than detached and recumbent. Lewis *et al.* were uncertain how to interpret this and, as a compromise, postulated that juveniles

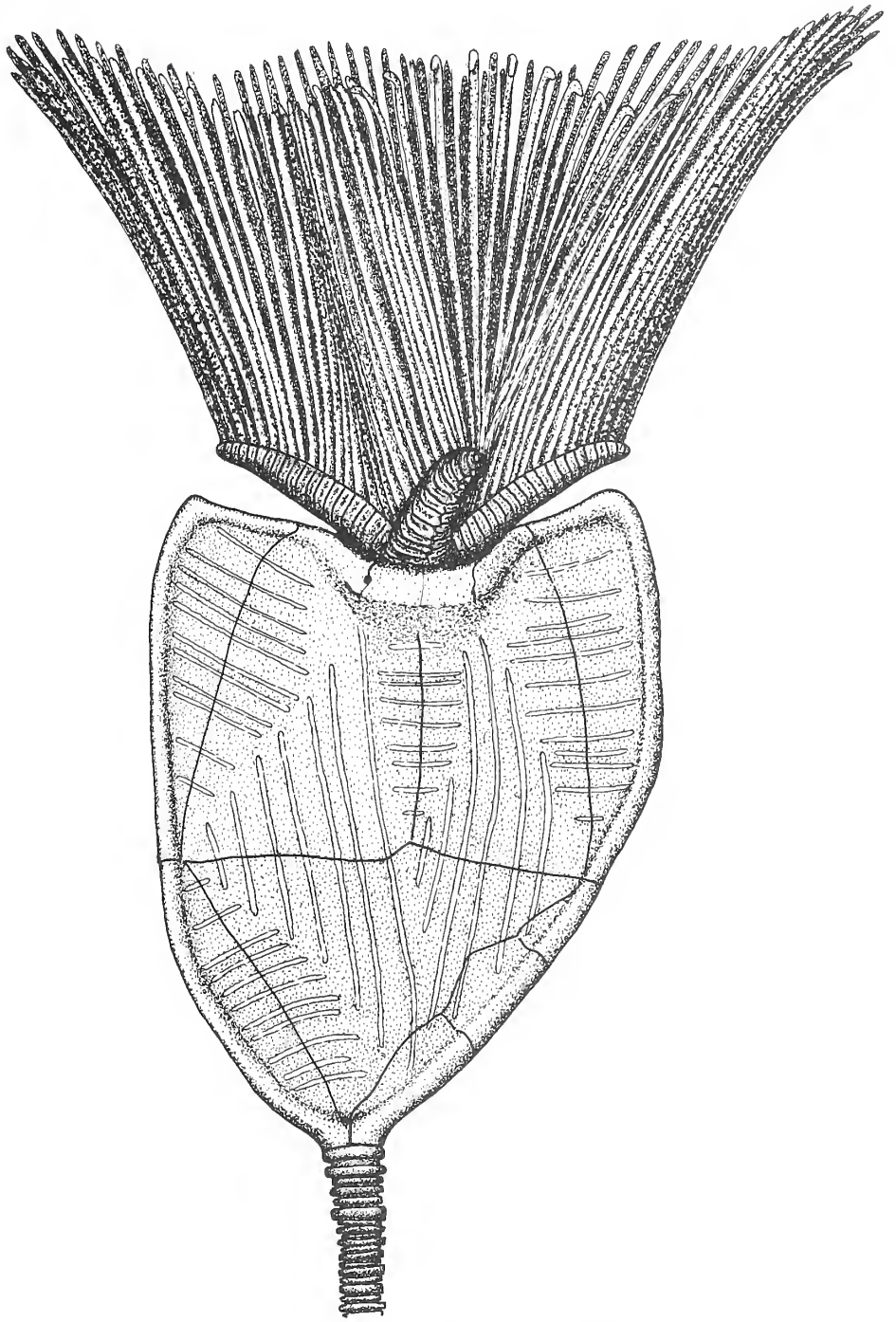

TEXT-FIG. 6. Reconstruction of *Cardiocystites pleuricostatus* sp. nov.

lived erect but that larger individuals became detached and adopted a recumbent mode of life similar to that postulated for other rhipidocystids. Wilson *et al.* (1992) later reported finding abundant holdfasts of rhipidocystids covering an early Ordovician hardground.

Secondly, we now know that *Cardiocystites* has five erect arms and a dense brachiolar filtration fan. Its five arms are splayed radially outwards and not confined to the plane of thecal flattening (Text-fig. 6). Furthermore, there is a complete absence of any bilateral symmetry to the conical filtration fan. Such a filtration fan could only have functioned if it was held well above the sediment-water interface and consequently *Cardiocystites* could not have lain on the sea-floor.

If the highly flattened body form seen in *Cardiocystites* and *Mandalacystis* is not an adaptation for a recumbent mode for life then it must have served another purpose. There are several possibilities: protective camouflage, providing hydrodynamic lift and/or stability, or enhancing rates of gaseous exchange.

Camouflage. Some modern cidaroid echinoids develop large paddle-shaped spines that are attractive to epiflora and epifauna and thus provide natural camouflage (Smith 1984*b*). It is therefore conceivable that the broad flat theca of eocrinoids might have served a similar purpose, since we know that encrusting biota were flourishing by this time. However, this explanation seems highly unlikely since none of the specimens shows any evidence of encrustation. Furthermore, the skeleton in echinoderms is mesodermal and thus tissue-covered in life. Cidaroid spines are exceptional in having a cortical overgrowth that is tissue-free, and thus attractive to epibionts. Such a cortex is clearly not developed on plates of *Cardiocystites*. Finally, this interpretation does not provide an explanation for the thinness of the plates forming the theca. It therefore seems highly implausible that the flattened theca served any role in camouflage.

Hydrofoil for lift or stability of filtration cone. The filtration cone of *Cardiocystites* needs to be elevated into the water column to function. The semi-rigid stem clearly serves to raise the crown, and enables the filtration cone to become orientated perpendicular to the current direction. However, there is also a possibility that lift could be generated from the current itself such that the crown acts in a manner analogous to a kite, and the stem its tether. The development of the theca into a broad blade-like foil immediately upstream of the filtration fan certainly had hydrodynamic consequences. Such a blade would presumably stabilize the orientation of the cone in the face of oscillating currents and possibly help optimize the angle of the crown.

Baumiller (1992) doubted whether crinoids ever utilized hydrodynamic lift because current velocities had to be extremely high before measurable lift was obtained. However, his calculations were based solely on the lift provided by a porous filtration cone. The foil-like theca of *Cardiocystites* may have provided additional and possibly more effective hydrodynamic lift, although we have no experimental evidence to support this. Furthermore, the light construction of the theca with its strengthening ribs is consistent with a hydrodynamic explanation.

Gaseous exchange. Efficiency of gaseous exchange was clearly an important issue for the survival of early Palaeozoic cystoids since many developed highly specialized respiratory structures (e.g. Paul 1979). These structures often dominate the theca and involve pores or thin-walled regions of the theca with large surface areas across which gases could diffuse readily. It is therefore possible that the flattened, thin-walled theca represents an adaptation for more efficient gaseous exchange. The thick-walled globular theca of standard eocrinoids must have been considerably more of a barrier to gases than the thin-walled, flattened theca of *Cardiocystites*. Internal volume was tiny, further enhancing the efficiency of the theca as an exchange surface. Thinness of thecal plates would have been crucial for effective gaseous exchange but also must have greatly reduced the mechanical strength of the theca. The ridges that cross the theca are unlikely to have functioned to increase the available surface area analogous to flanges on a radiator, since they appear to be solid and do not always coincide on the two surfaces. Rather, their primary rôle seems to have been in strengthening the plates.

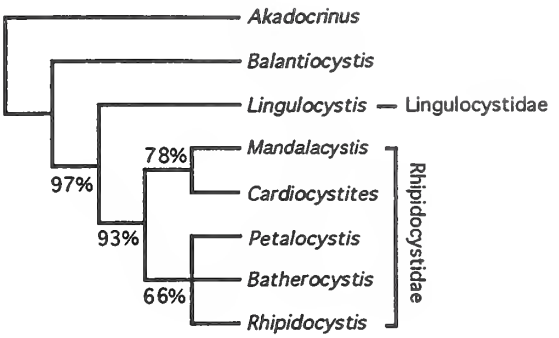

TEXT-FIG. 7. Single most parsimonious cladogram for flattened eocrinoid taxa. Tree length = 23, Consistency Index = 0·78, Retention Index = 0·76. Bootstrap values for internal branches are based on 1000 replicates.

On the other hand, one might question whether a flattened theca was really the most efficient way to improve gaseous exchange. Why, for example, did one surface not simply remain uncalcified?

PHYLOGENETIC RELATIONSHIPS

Paul (1988) provided the first serious assessment of the relationships of cystoids, including *Cardiocystites*. His cladistic analysis placed *Cardiocystites* as sister-group to rhipidocystids and identified *Lingulocystis* as the immediate outgroup to both taxa. In the light of our new data on the morphology of *Cardiocystites* we have undertaken a reanalysis of its relationships. For outgroups we include *Akadocrinus* (Paul's original outgroup) and *Balantiocystis*. *Balantiocystis* appears to be the most closely related eocrinoid; not only is its theca distinctly compressed but amongst its multiple polygonal plates are larger thickened nodulose plates that may be homologous to the marginals of rhipidocystids. Furthermore, its oral area and brachiole arrangement are very similar to that seen in *Rhipidocystis*. *Balantiocystis* comes from the lower Ordovician of the Montagne Noire, France and its morphology was superbly described by Ubaghs (1972).

The Appendix lists the character scorings used in our analysis along with our data matrix. Morphological information comes from the following sources: *Rhipidocystis* – Ubaghs (1967); Bockelie (1981); *Petalocystis* – Sprinkle (1973); *Mandalacystis* – Lewis *et al.* (1992); *Akadocrinus* – Sprinkle (1973); *Lingulocystis* – Ubaghs (1960, 1994); *Balantiocystis* – Ubaghs (1972); *Batherocystis* – Ubaghs (1967). *Batherocystis*, although clearly a member of the Rhipidocystidae, remains poorly known and no arm and brachiolar characters can be scored for this taxon.

Parsimony analysis using the exhaustive search option of PAUP (Swofford 1993) found one tree, which places *Petalocystis*, *Batherocystis* and *Rhipidocystis* in a trichotomy (Text-fig. 7). Lack of resolution in this part of the cladogram is due solely to the lack of information concerning the morphology of *Batherocystis* rather than conflict amongst characters. The remaining relationships are all supported with reasonably high bootstrap values. *Cardiocystites* is placed as sister taxon to *Mandalacystis*, and together these form the sister group to the clade *Rhipidocystis–Petalocystis–Batherocystis*. Since Lewis *et al.* (1992) accepted that *Mandalacystis* should be placed in the Rhipidocystidae, *Cardiocystites* must also belong in this family. *Lingulocystis* was identified as the immediate outgroup to Rhipidocystidae. This supports the findings of Paul (1988).

SYSTEMATIC PALAEONTOLOGY

Family RHIPIDOCYSTIDAE Jaekel, 1901

Genus CARDIOCYSTITES Barrande, 1887

Type species. By monotypy; *Cardiocystites bohemicus* Barrande, 1887, p. 120, pl. 31, figs 10–12, from the Zahořany Formation of Zahořany, Bohemia.

Diagnosis. Pelmatozoan with heteromorphic stem, flattened heart-shaped theca bounded by a thickened rim and composed of an upper and lower series of large polygonal plates, five erect arms and long brachioles.

Occurrence. Upper Ordovician (Caradoc Series) of the Czech Republic and England.

Cardiocystites pleuricostatus sp. nov.

Text-figures 1–6

Types. Holotype: Natural History Museum, London, BMNH E23706a, b; paratype BMNH E23709.

Other material. National Museum of Wales 97.43G.1 (arm fragment).

Occurrence. The holotype and NMW 97.43G.1 come from the Smeathen Wood Beds, *Reuscholithus reuschi* Zone, Burrellian Stage (Harnagian Substage), Caradoc Series at Smeathen Wood, Horderley, Shropshire. The paratype comes from the Harnagian Substage of 'Onny Valley', almost certainly from the Horderley district in the vicinity of Round House or Smeathen Wood.

Diagnosis. A *Cardiocystites* with multiple small corrugations running perpendicular to the plate margins towards the centre of the plate.

Description. The most proximal 6·5 mm of the stem is visible in the holotype, fully articulated. The stem is holomeric and heteromorphic with up to three series of internodals developed between nodals. Nodal and internodal cycles are readily discernible from sequential alternation in columnal diameter (Text-fig. 2). The nodal-internodal pattern becomes established rapidly beneath the theca, after the third nodal has formed.

The holotype, preserved as part and counterpart, has a maximum thecal width of 18 mm and a length from stem to the centre of the oral surface of 17·5 mm. It has a relatively narrow marginal rim, 0·75 mm wide and *c.* 0·5–1·0 mm deep; it is rectangular in cross section. On one face (?upper) the rim is weakly concave with rounded edges, while the other (?lower) is convex.

The organization of the distal series of plates is problematical. Marginal plates on either side bound a triangular area. The holotype shows possible fracture lines or sutures marking a small triangular area near the stem attachment and another approximately sagittal. However, the pattern of ribbing suggests that the entire area inside the marginal frame is composed of a single element.

All central plates are ribbed, with ribbing perpendicular to sutures. Ribs from adjacent plates meet across the suture line with little or no displacement. Ribs are *c.* 0·1 mm wide and 0·1 mm high. The median longitudinal ribs are the longest, with the two largest extending from the oral area to the marginal frame slightly to one side of the stem. Ribbing on upper and lower surface is often, but not always, coincidental.

Remarks. C. pleuricostatus is easily differentiated from *C. bohemicus* by its strongly ribbed thecal plates. In *C. bohemicus* just two ribs cross the theca, running obliquely from the oral area. These ribs are present in *C. pleuricostatus*, but are accompanied by a large number of other ribs, set perpendicular to plate sutures.

Acknowledgements. We are grateful to Professor W. T. Dean for the supply of extra material and stratigraphical information.

REFERENCES

BARRANDE, J. 1887. Classe des Échinodermes. Ordre des Cystidées. *Système silurien du centre de la Bohème*, Vol. 7. Part 1. Gerhard (Leipzig), Rivnác (Prague), 233 pp.

BAUMILLER, T. K. 1982. Importance of hydrodynamic lift to crinoid autoecology, or, could crinoids function as kites? *Journal of Paleontology*, **66**, 658–665.

BOCKELIE, J. F. 1981. The Middle Ordovician of the Oslo Region, Norway, 30. The eocrinoid genera *Cryptocrinites*, *Rhipidocystis* and *Bockia*. *Norsk Geologisk Tidsskrift*, **61**, 123–147.

BROADHEAD, T. W. 1992. Reappraisal of class Eocrinoidea (Echinodermata). 125–131. *In* LAWRENCE, J. M. (ed.). *Echinoderms: proceedings of the International Echinoderms Conference, Tampa Bay*. A. A. Balkema, Rotterdam, 529 pp.

JAEKEL, O. 1901. Über Carpoideen, eine neue Klasse von Pelmatozoen. *Zeitschrift der Deutsches Geologische Gesellschaft*, **1900**, 666–677.

LEWIS, R. D., SPRINKLE, J., BAILEY, B., MOFFIT, J. and PARSLEY, R. L. 1987. *Mandalacystis*, a new rhipidocystid eocrinoid from the Whiterockian Stage (Ordovician) in Oklahoma and Nevada. *Journal of Paleontology*, **61**, 1222–1235.

PAUL, C. R. C. 1979. Early echinoderm radiation. 415–434. *In* HOUSE, M. R. (ed.). *The origin of major invertebrate groups*. Systematics Association Special Volume, 12. Clarendon Press, Oxford, 442 pp.

—— 1988. The phylogeny of the cystoids. 199–213. *In* PAUL, C. R. C. and SMITH, A. B. (eds). *Echinoderm phylogeny and evolutionary biology*. Clarendon Press, Oxford, 373 pp.

SMITH, A. B. 1984*a*. Classification of the Echinodermata. *Palaeontology*, **27**, 431–459.

—— 1984*b*. *Echinoid palaeobiology*. George Allen & Unwin, London, 199 pp.

SPRINKLE, J. 1973. Morphology and evolution of blastozoan echinoderms. *Special Publication of the Museum of Comparative Zoology, Harvard University*, 1–284.

SWOFFORD, D. L. 1993. *Phylogenetic Analysis Using Parsimony, Version 3.1*. [Computer program, Apple Macintosh compatible].

UBAGHS, G. 1960. Le genre *Lingulocystis* Thoral. *Annales de Paléontologie, Invertébrés*, **46**, 81–116.

—— 1967. Eocrinoidea. S455–S495. *In* MOORE, R. C. (ed.). *Treatise on invertebrate paleontology. Part S. Echinodermata 1*. Geological Society of America and University of Kansas Press, Lawrence, Kansas, 650 pp.

—— 1972. Le genre *Balantiocystis* Chauvel (Echinodermata, Eocrinoidea) dans l'Ordovicien inférieur de la Montagne Noire (France). *Annales de Paléontologie, Invertébrés*, **58**, 1–27.

—— 1994. Échinodermes nouveaux (Stylophora, Eocrinoidea) de l'Ordovicien inférieur de la Montagne Noire (France). *Annales de Paléontologie*, **80**, 107–141.

WILSON, M. A., PALMER, T. J., GUENSBURG, T. E., FINTON, C. D. and KAUFMAN, L. E. 1992. The development of an early Ordovician hardground community in response to rapid sea-floor calcite precipitation. *Lethaia*, **25**, 19–34.

JULIETTE DEAN

ANDREW B. SMITH

Department of Palaeontology
The Natural History Museum
Cromwell Road
London SW7 5BD, UK

Typescript received 10 September 1997
Revised typescript received 20 November 1997

APPENDIX

Characters used in determining the phylogenetic position of *Cardiocystites*. The data matrix is given at the end.

1. Thecal form: globular to ovate (0); strongly flattened in one plane (1).
2. Stem: columnals, polyplated (0); holomeric (1).
3. Stem: homeomorphic (0); heteromorphic, with large and small columnals alternating (1); reduced to a few large elements (2).
4. Stem attachment to theca: attaches equally to two basals (0); attaches to three basals (1); attaches to four basals (2); attaches to five basals (3).
5. Marginal frame plates: undifferentiated (0); present (1).
6. Marginal plates with internal flanges: absent (0); present (1).
7. Marginal frame plates: double, at least distally (0); single (1).
8. Number of plates forming lateral and distal margins of theca: more than ten (0); seven or eight (1).
9. Centrals: tessellate (0); imbricate (1).
10. Number of centrals: more than six (0); three or four (1).
11. Transverse strutting: absent (0); present (1).
12. Arms: absent (oral frame plates give rise to brachioles direct) (0); present (1).
13. Oral area and arms: basically pentaradial (0); strongly bilateral (1).
14. Brachioles: biserial (0); uniserial (1).
15. Brachioles: contiguous forming filtration net (0); in scattered clumps (1).

16. Oral area: narrow, not stretching across entire proximal face (0); wide, occupying entire width of theca proximally (1).
17. Oral area: flush (0); depressed, below horn-like processes of the theca (1).
18. Periproct: lateral half-way down theca (0); in upper corner of theca close to peristome (1); on oral surface (2).

Cardiocystites	11101 10101 11001 011
Rhipidocystis	11201 10101 00110 101
Petalocystis	11201 10101 00100 001
Mandalocystis	11011 10101 01101 111
Lingulocystis	11121 01010 10100 000
Batherocystis	11201 10101 00??? 001
Balantiocystis	01110 0?000 00000 000
Akadocrinus	01030 0?000 00000 002

THE FIRST 'CICADA-LIKE HOMOPTERA' FROM THE TRIASSIC OF THE VOSGES, FRANCE

by FABRICE LEFEBVRE, ANDRÉ NEL, FRANCINE PAPIER, LÉA GRAUVOGEL-STAMM *and* JEAN-CLAUDE GALL

ABSTRACT. The first Cicadomorpha, *Gallodunstania grauvogeli* gen. et sp. nov., is described from the Triassic of the Vosges (France) and is provisionally attributed to the Palaeontinoidea family Dunstaniidae.

FOSSIL Cicadomorpha (Palaeontinoidea) are known from the Upper Permian of Southern Africa, the Triassic to the middle Cretaceous of Russia, the Triassic of Australia, the Lower Cretaceous of Brazil (Ueda 1997) and the Upper Jurassic to the Lower Cretaceous of Europe. Until now the group was unknown in the Triassic of Western Europe. The discovery, in the Lower–Middle Triassic of the Vosges, of a new species of Dunstaniidae, clearly belonging to a new genus, increases our knowledge on the diversity of this group.

SYSTEMATIC PALAEONTOLOGY

We follow the wing venation nomenclature proposed by Kukalová-Peck and Dworakowska (1988).

Infra-order CICADOMORPHA Latreille, 1802
Superfamily PALAEONTINOIDEA Handlirsch, 1906
Family DUNSTANIIDAE Tillyard, 1916

Genus GALLODUNSTANIA gen. nov.

Derivation of name. After *Gallia*, the ancient Latin name for France and after *Dunstania*, which is the type genus of the family Dunstaniidae.

Type species. *Gallodunstania grauvogeli* sp. nov.

Diagnosis. Vein CP well developed and bifurcated distally. Sc + R, M and Cu strongly approximate and parallel basally. CuA fused with Sc + R + M for a short distance; CuA closes distally the basal cell. Sc separates from R + M + CuA near the wing base and it distally fused with a costal branch of R + MA. AP is more-or-less parallel with the anal margin of the wing. AA and AP distally fused into a 'Y' vein. Sc, RA and a short branch of RP reach the nodus. CuA divided into three distal branches, the anterior one may be fused with the posterior branch of MP. There are no crossveins in the apical part of the wing.

Gallodunstania grauvogeli gen. et sp. nov.

Text-figures 1–3

Derivation of the species name. After the late Louis Grauvogel who collected the type material.

[Palaeontology, Vol. 41, Part 6, 1998, pp. 1195–1200]

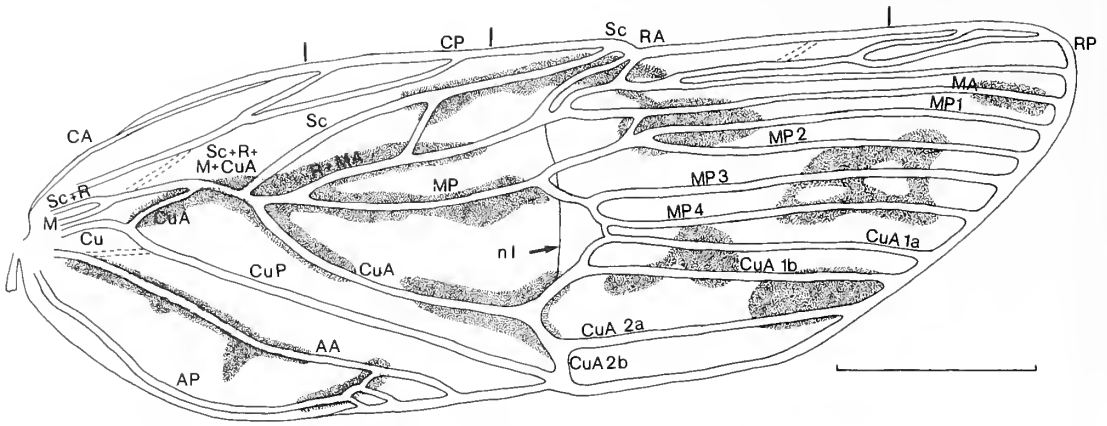

TEXT-FIG. 1. *Gallodunstania grauvogeli* gen. et sp. nov.; holotype, specimen 9152 a; forewing, Scale bar represents 5 mm.

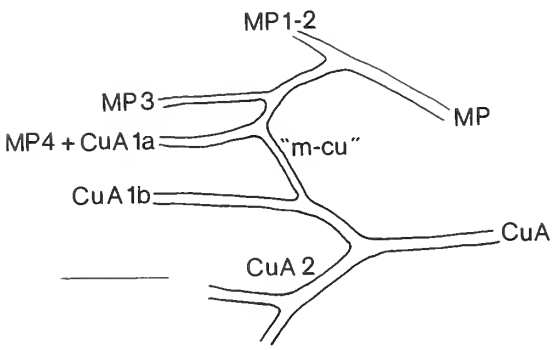

TEXT-FIG. 2. *Gallodunstania grauvogeli* gen. et sp. nov.; paratype, specimen 9151 a; area of the forewing crossvein 'm-cu'. Scale bar represents 2 mm.

Types. Holotype specimen 9152a (counterpart) and b (part) (Text-figs 1, 3); paratype specimen 9151a (part) and b (counterpart) (Text-fig. 2); Grauvogel and Gall coll., located at the Institut de Géologie, Université Louis Pasteur, Strasbourg.

Type locality and horizon. 'Grès à *Voltzia*', Upper Buntsandstein (Lower Anisian, Lower Triassic; Gall 1971), Vosges, Bust, Bas-Rhin, France.

Material. Two wings both represented by a part and counterpart 26 mm long: the holotype (9152) is entire, whereas the anal area is missing in the paratype (9151). The latter is surrounded by a lot of plant debris. The proposed reconstruction (Text-fig. 1) is based on both specimens. The three hypothetical 'veins', indicated by dotted lines in this reconstruction, may be due to artefacts. Thus, they are not taken into account in the description.

Diagnosis. As for genus (this is the only recognized species).

Description. Some traces of coloration are present on both wings and are indicated by stippled areas in the reconstruction. A nodal line (nl) is clearly visible but is not a vein. The nodus is located in the distal half of the wing, slightly after its middle. The nodal structures, which are poorly preserved, are indicated by a strong bend of the costal margin. Veins C and CA are joined basally and fused distally. The concave vein CP is well

TEXT-FIG. 3. Holotype; specimen 9152 a; × 5.

separated basally from C and CA, divided into two branches 6·3 mm from the base of the wing and reaches the costal margin basal of nodus. Veins Sc + R, M and Cu are respectively convex, concave and concave at their base, are well separated basally and are closely parallel over 1·5 mm (maximum distance between Sc + R and M = 0·15 mm, between M and Cu = 0·11 mm). Veins Sc + R and M are fused into a strong convex vein, 2·2 mm distal of base of wing. The convex vein CuA is fused with Sc + R + M over 1·3 mm, 3·7 mm distal of base of wing. Sc is separated from R, 5·7 mm distal of base of wing and reaching nodus. At 6 mm from base of wing, basal of nodal line, CuA is directed towards the anal area. R + MA and MP separate 7 mm from base of wing. A strong oblique branch of R + MA is directed towards Sc, 9·6 mm from base of wing. A short branch (RA?) of R + MA is aligned with the nodal line and reaches the nodus. More distally, RP(?) and MA(?) diverge. A short branch of RP(?) ends in the nodus. The main branch of RP(?) divides into two branches, RPa and RPb. RPa bifurcates before reaching the costal margin near the apex. RPb is more-or-less parallel with the costal margin and ends at the apex. MA(?) is nearly straight and parallel with RPb. MP forks into two branches, MP1-2 and MP3-4 (*sensu* Shcherbakov 1984), opposite the nodal line. The common stem of MP1-2 is twice as long as that of MP3-4. MP1-2 is divided into MP1 and MP2, and MP3-4 is divided into MP3 and MP4 (Text-figs 1–2). Distal branches of MP nearly straight and parallel with those of R + MA. A crossvein is present between MP1 and MA opposite the nodus. CuA is divided into CuA1 and CuA2 opposite the nodal line. CuA1 is directed towards the costal margin for a short distance, with an apical bend, and is parallel with the distal branches of MP, R and MA before reaching the apical margin. In the holotype, a strong supplementary vein, looking like a supplementary branch of CuA1, lies between MP4 and CuA1 opposite the nodus. In the paratype, the oblique 'crossvein' between CuA1 and MP4 looks like the basal part of a branch of CuA1 that would be fused distally with MP4, although this branch of CuA1 seems to be absent. CuA2 has two branches: the posterior one, CuA2b, fused with CuP at the anal margin opposite nodal line; and the anterior one, CuA2a, more-or-less parallel with posterior margin and distal branches of CuA1, MP, R and MA and reaching the apical margin. Cu is basally parallel with Sc + R and M but has a distal posterior bend opposite the point of fusion of Sc + R and M, and is divided into CuA and CuP, 2·7 mm from the base of the wing. The convex vein CuA is fused for a short distance with Sc + R + M. The concave CuP is nearly straight, and is strong and fuses with the anal margin and CuA2 opposite the nodal line. AA and AP (respectively convex and concave veins) are clearly separated at the base of the wing. AA is nearly straight, reaching the posterior margin distinctly basal of the nodal line and more-or-less parallel with CuP. AP is more-or-less parallel with the anal margin, and is divided into two short branches ending in posterior margin basal of AA, AA and AP distally fused into a 'Y' vein.

Dimensions of the holotype: wing 26·7 mm long and 8·5 mm wide; distance between base and nodus 15·7 mm; distance between nodus and apex 11·2 mm; distance between CP and nodus 4·3 mm; AP reaching posterior margin 9·9 mm from base; AA reaching posterior margin 11·2 mm from base; CuP reaching anal margin 13·4 mm from base.

Remarks. The two specimens probably belong to the same species since all the preserved characters are identical, except for the presence of a supplementary branch of CuA1 in the holotype, this branch probably being fused with MP4 in the paratype.

The wing venation of *Gallodunstania grauvogeli* gen. et sp. nov. is similar to that of the Cicadomorpha *sensu* Shcherbakov (1984) and Carpenter (1992). Nevertheless, because of the lack of an available phylogenetic analysis of this group, it is impossible to use cladistics to define the relationships of *Gallodunstania*. Thus, we attempt to classify it provisionally using the method of global similarity.

We include *Gallodunstania* gen. nov. in the infra-order Cicadomorpha (*sensu* Shcherbakov 1984) on the basis of the following shared characters: (1) CuA and CuP basally fused; (2) basal cell and basal part of CuA long; (3) fusion (at least partly) of AA and AP in distal third of anal area before reaching anal margin; (4) macrosculpture well developed; (5) nodal line clearly defined; (6) nodus well pronounced; (7) CA strongly curved at base of wing; and (8) basal cell closed by an anastomosis between CuA and Sc+R+M.

Wootton (1968) divided Cicadomorpha (Cicadoidea) into two evolutionary lines, one leading to the Tettigarctidae and Cicadidae and the second comprising Dunstaniidae, Mesogereonidae and Palaeontinidae. Later, Shcherbakov (1984) considered Cicadomorpha in a wider sense and divided it into Prosboloidea, Pereborioidea, Scytinopteroidea, Palaeontinoidea, Cicadoidea, Cercopoidea and Cicadelloidea. Affinities of *Gallodunstania* gen. nov. with Cercopoidea and Cicadelloidea are provisionally excluded because these groups do not share with it any nodal structures or nodal line. The structure of the anal veins in *Gallodunstania* gen. nov. is similar to that of the Cicadoidea Latreille, 1802 (Recent and fossil). Nevertheless, it cannot be included in this superfamily because of the following non-shared characters: (1) presence of a long CP (possible plesiomorphy); (2) absence of apical cells in radial and median areas; and (3) presence of a long and strong vein between CuA and MP4, looking like a branch of CuA and named 'crossvein m-cu' by Shcherbakov (1984, p. 89) and Carpenter (1992, p. 215) (possible derived character). We provisionally exclude *Gallodunstania* gen. nov. from the superfamily Prosboloidea Handlirsch, 1906 because: (1) it has a long and strong 'crossvein m-cu'; (2) CuA is bifurcated in the nodal line. The superfamily Pereborioidea Zalessky, 1930 is excluded because: (1) RA has no postnodal branches; (2) the nodal line is well pronounced; and (3) the 'crossvein m-cu' is long and strong. *Gallodunstania* gen. nov. does not share the following characters with the superfamily Scytinopteroidea Handlirsch, 1906: (1) the nodus is well pronounced; (2) the distal free part of Sc begins distad of the basal cell; and (3) CuA is bifurcated in the nodal line.

Only the superfamily Palaeontinoidea Handlirsch, 1906 shares with *Gallodunstania* gen. nov. the following diagnostic characters: (1) R is not divided at the base of the wing; (2) Sc and R are separated distad of the basal cell; (3) the nodal line is well developed; (4) there is a long and strong convex vein between CuA1 and MP4 (= 'crossvein m-cu' *sensu* Shcherbakov 1984), which could be a supplementary branch of CuA1; (5) CuA is bifurcated in the nodal line; and (6) the anal area is distally bent backward.

The long and strong vein that Shcherbakov considered as a 'crossvein m-cu' could be a synapomorphy of *Gallodunstania* gen. nov. and Palaeontinoidea because this character is only present in this group. The vein MP in the Palaeontinoidea is basally divided into two branches MP1-2 and MP3-4 which are distally subdivided into MP1 and MP2, and MP3 and MP4, and not into MP1 and MP2-4. If we accept this assumption for *Gallodunstania* gen. nov., then the supplementary vein between MP4 and CuA1 reaching the apical margin in the holotype has to be considered as a further branch of CuA1. Furthermore, in the paratype this vein seems to be fused with MP4, showing only its basal portion looking like a very strong oblique vein between CuA1 and MP4. This interpretation implies that the very long and strong oblique vein 'm-cu' between CuA1 and MP4, present in all Palaeontinoidea, is not a simple crossvein but the basal portion of a supplementary branch of CuA1 distally fused with MP4. This is particularly clear in *Pseudocossus turgaiensis* Becker-Migdisova and Wootton, 1965 in which the two veins are only partly fused (Becker-Migdisova and Wootton 1965).

The alternative hypothesis in which the vein MP of the Palaeontinoidea is basally divided into 'MP1' and 'MP2-4' does not explain: (1) the very strong oblique vein 'm-cu' present in all Palaeontinoidea; (2) the fusion of 'MP4' with 'MP3' in all Palaeontinidae; (3) the division of

'MP1' into two secondary branches 'MP1a' (= MP1 *sensu* Shcherbakov) and 'MP1b' (= MP2 *sensu* Shcherbakov) in all Paleontinoidea; and (4) the secondary branching of 'MP4' (= supplementary longitudinal vein between MP and CuA1) on 'MP3' in *Gallodunstania* gen. nov.

A specimen of *Fulgoridium* sp. (Fulgoroidea: Fulgoridiidae; Liassic of Germany) figured by Ansorge (1996, text-fig. 36) also shows a division of CuA into three main longitudinal branches. Even if the anterior branch of CuA of *Fulgoridium* sp. is not similar (and was probably acquired convergently) with those of the Palaeontinoidea, it gives some evidence of the possible presence of a three-branched CuA in some Euhemiptera.

Nevertheless, the attribution of *Galodunstania* gen. nov. to the Palaeontonoidea is provisional because vein AP of *Gallodunstania*, which is more-or-less parallel with the anal margin, looks different from those of the other known Palaeontinoidea.

Palaeontinoidea is divided into three fossil families (Shcherbakov 1984): Mesogereonidae Tillyard, 1921, Palaeontinidae Handlirsch, 1906 and Dunstaniidae Tillyard, 1916.

Gallodunstania galli gen. et sp. nov. differs from the Mesogereonidae since: (1) its nodus is well pronounced; (2) its veins MP1 and MP2 are not fused; (3) and the 'crossvein m-cu' is not close to the base of the wing. It differs from the Palaeontinidae since: (1) its CP (= Sc *sensu* Carpenter 1992) is well developed; and (2) its vein RP (= R *sensu* Carpenter 1992) is branched. The reduction of CP in the Palaeontinidae, as proposed by Carpenter (1992), is not very clearly established since *Asiocossus* Becker-Migdisova, 1962 (Triassic of Russia; included in the Palaeontinidae by Carpenter 1992), clearly shows a long and strong vein CP, with four or five costal branches. Thus character (1) listed above is not very convincing.

We provisionally include *Gallodunstania* gen. nov. in Dunstaniidae since it has the diagnostic characters proposed by Shcherbakov (1984) and Carpenter (1992): (1) a long CP reaching the costal margin close to the nodus; (2) long AA and AP; (3) postnodal and prenodal parts of forewing approximately equal in area; (4) RP branched (like in *Dunstaniodes* Becker-Migdisova and Wootton, 1965; Triassic of Russia); and (5) stem of MP1-2 more than twice as long as that of MP3-4.

As this attempt of classification is based on the method of global similarity, polarization of the characters is not possible and no phylogenetic conclusion can be inferred from this study. The superfamilies Prosboloidea, Palaeontinoidea and the families Dunstaniidae and Palaeontinidae are probably poly- or paraphyletic. Furthermore, Sorensen *et al.* (1995) considered that the various families included in Prosboloidea belong to the crown group of Cicadomorpha and that the latter is the polyphyletic.

CONCLUSIONS

The present classification of 'Cicadomorpha' probably does not reflect its phylogeny. A cladistic study should be undertaken in order to understand the phylogenetic history of this group. Therefore, any definite conclusion concerning the affinities of *Gallodunstania* gen. nov. has to wait.

Nevertheless, the present discovery strongly suggests that Palaeontinoidea were probably widespread during the Triassic, even if it is still impossible to make any palaeobiogeographical analysis, because of the lack of an accurate knowledge of their phylogeny.

Acknowledgements. We thank Dr Thierry Bourgoin (MNHN) for his suggestions concerning the vein nomenclature and for his kind help with the manuscript.

REFERENCES

ANSORGE, J. 1996. Insekten aus dem oberen Lias von Grimmen (Vorpommern, Norddeutschland). *Neue Paläontologische Abhandlungen*, **2**, 1–132.

BECKER-MIGDISOVA, E. F. 1962. [Some new fossil Hemiptera and Psocoptera.] *Paleontologicheskogo Zhurnal*, **1962**, 89–104. [In Russian].

—— and WOOTTON, R. J. 1965. Noviye paleontinoidy asii. [New palaeontinoids of Asia.] *Paleontologicheskogo Zhurnal*, **1965**, 63–79. [In Russian].

CARPENTER, F. M. 1992. Superclass Hexapoda. i–xxii + 1–655. *In* MOORE, R. C. and KAESLER, R. L. (eds). *Treatise on invertebrate paleontology. Part R. Arthropoda 4 (3/4)*. Geological Society of America and University of Kansas Press, Boulder, Colorado.

DWORAKOWSKA, I. 1988. Main veins of the wings of Auchenorrhyncha. *Entomologische Abdhandlungen, Staatliches Museum für Tierkunde Dresden*, **52**, 63–108.

GALL, J.-C. 1971. Faunes et paysages du grès à *Voltzia* du nord des Vosges. *Mémoire du Service de la Carte Géologique d'Alsace et de Lorraine*, **34**, 1–318.

HANDLIRSCH, A. 1906–08. *Die fossilen Insekten und die Phylogenie der rezenten Formen*. Leipzig, 1430 pp. [1–640 published 1906; 641–1430 published 1908].

KUKALOVÀ-PECK, J. 1991. Fossil history and the evolution of hexapod structures. 141–179. *In* NAUMANN, I. D., CRANE, P. B., LAWRENCE, J. F., NIELSEN, E. S., SPRADBERY, J. P., TAYLOR, R. W., WHITTEN, M. J. and LITTLEJOHN, M. J. (eds). *The insects of Australia, a textbook for students and research workers*. 1. 2nd edition. Melbourne University Press, Melbourne, Australia, 542 pp.

LATREILLE, P. A. 1802. *Histoire naturelle, générale et particulière, des Crustacés et des Insectes*. 3. Dufart, Paris, xii + 467 pp.

SHCHERBAKOV, D. Y. 1984. Systematics and phylogeny of Permian Cicadomorpha (Cimicida and Cicadina). *Paleontological Journal*, **1984**, 87–97.

SORENSEN, J. T., CAMPBELL, B. C., GILL, R. J. and STEFFEN-CAMPBELL, J. D. 1995. Non-monophyly of Auchenorrhyncha ('Homoptera'), based upon 18S rDNA phylogeny: eco-evolutionary and cladistic implications within pre-heteropterodea Hemiptera (s.l.) and a proposal for new monophyletic suborders. *Pan-Pacific Entomologist*, **71**, 31–60.

TILLYARD, R. J. 1916. Mesozoic and Tertiary insects of Queensland and New South Wales. *Publication of the Queensland Geological Survey*, **253**, 1–47.

—— 1921. Mesozoic insects of Queensland. No. 8. Hemiptera Homoptera (Contd.). The genus *Mesogereon*; with a discussion of its relationship with the Jurassic Palaeontinidae. *Proceedings of the Linnean Society of New South Wales*, **44**, 270–284.

UEDA, K. 1997. A new palaeontinid species from the Lower Cretaceous of Brazil (Homoptera: Palaeontinidae). *Bulletin of the Kitakyushu Museum of Natural History*, **16**, 99–104.

WOOTTON, R. 1971. The evolution of Cicadoidea (Homoptera). *International Congress of Entomology, Abstracts*, Moscow, (1968), **1**, 318–319.

ZALESSKIJ, M. 1930. Sur deux représentants nouveaux des Paléohémiptères du Permien de la Kama et du Perebore dans le bassin de la Pétchora. *Bulletin de l'Académie des Sciences del'URSS, Classe des sciences physico-mathématiques*, **7**, 1017–1027.

FABRICE LEFEBVRE

ANDRÉ NEL

Laboratoire d'Entomologie
Muséum National d'Histoire Naturelle
45 rue Buffon, F-75005 Paris, France
e-mail anel@mnhn.fr

FRANCINE PAPIER

LÉA GRAUVOGEL-STAMM

JEAN-CLAUDE GALL

Institut de Géologie
Université Louis Pasteur
1 rue Blessig
F-67084 Strasbourg Cedex, France

Typescript received 4 September 1997
Revised typescript received 3 December 1997

A NEW XENUSIID LOBOPOD FROM THE EARLY CAMBRIAN SIRIUS PASSET FAUNA OF NORTH GREENLAND

by GRAHAM E. BUDD *and* JOHN S. PEEL

ABSTRACT. Three incomplete specimens of a large lobopod, *Hadranax augustus* gen. et sp. nov. are described from the exceptionally preserved Sirius Passet fauna (Buen Formation, Lower Cambrian, North Greenland). Its overall appearance and size are similar to those of *Xenusion auerswaldi* Pompeckj from the Baltic, but *H. augustus* differs in its possession of four poorly defined dorsal nodes in each row rather than two, and in the probable possession of a pair of long, branched frontal appendages.

The new specimens further demonstrate that the lobopods were a widespread and diverse Cambrian group. The presence of a four-noded xenusiid refutes the hypothesis that lobopods were directly derived from tetraradial nemathelminthes and shows that both node number and form were fairly flexible, although their primary function remains unclear. The probable presence of a pair of long branched frontal appendages in *H. augustus* removes one of the major reasons for considering *Xenusion* to be a basal lobopod, and adds further to the characters that unite *Anomalocaris*-like taxa to the lobopods.

THE Sirius Passet fauna is an exceptionally well-preserved Early Cambrian fauna from the Buen Formation, which crops out in the far north of Greenland (Conway Morris *et al.* 1987; Text-fig. 1). Three major collecting expeditions, in 1989, 1991 and 1994, have now amassed almost 10000 specimens. About 40 species are present in the fauna, which is dominated by poorly sclerotized arthropods. Although primary description of Sirius Passet taxa is still at a relatively preliminary stage, 'conventional' Cambrian taxa such as sponges (Rigby 1986) and a nevadiid trilobite (Blaker 1988) have already been described. In addition, a remarkable articulated halkieriid, *Halkieria evangelista* (Conway Morris and Peel 1990, 1995), an *Opabinia*-like gilled lobopod, *Kerygmachela kierkegaardi* (Budd 1993), and an unusual trilobite-like arthropod, *Kleptothule rasmusseni* (Budd 1995), have been described.

GEOLOGICAL SETTING AND AGE

The Buen Formation consists of siliciclastic deposits which record the subsidence and subsequent transgression of an eroded carbonate platform, represented by the Portfjeld Formation, which developed on the currently southern margin of the Franklinian Basin sequence in North Greenland (Peel and Sønderholm 1991). In its type area of southern Peary Land, the formation is almost 420 m thick but it thickens northwards to about 700 m at the transition into a deep-water basin succession referred to the Polkorridoren Group, the latter cropping out immediately north of the Sirius Passet locality. Regionally, the Buen Formation consists of a lower sandstone-dominated member and an upper mudstone-dominated member, but the mudstones prevail in northern outcrops. The Sirius Passet fauna is derived from mudstones in the lowest part of the formation immediately adjacent to the edge of the underlying carbonate platform (Text-fig. 1).

The Buen Formation yields three stratigraphically distinct faunas of Early Cambrian age in eastern areas of North Greenland. The stratigraphically lowest, from near the base of the formation, contains the nevadiid *Buenellus higginsi* Blaker, 1988, considered by Palmer and Repina (1993) to

[Palaeontology, Vol. 41, Part 6, 1998, pp. 1201–1213, 3 pls]

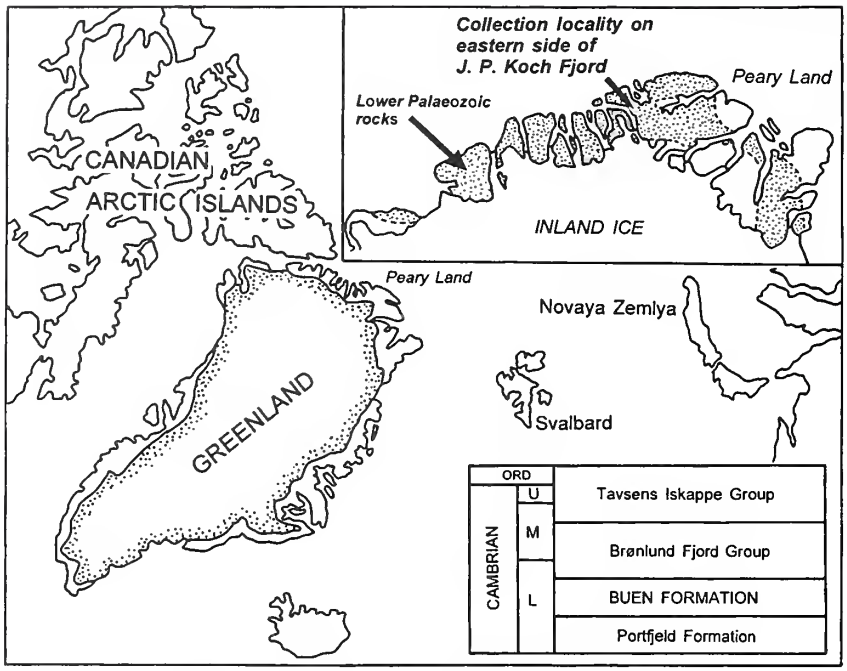

TEXT-FIG. 1. Locality map for the Sirius Passet fauna.

indicate the '*Nevadella*' Biozone of North American usage. Exposures in southern Peary Land yield *Olenellus* (*Mesolenellus*) *hyperboreus* Poulsen, 1974 and an undescribed new taxon of nevadiid form from the upper part of the formation, seemingly indicative of the boundary between the '*Nevadella*' and *Olenellus* Biozones. Uppermost beds of the formation yield *Olenellus svalbardensis*, Kielan, 1960, a typical *Olenellus* Biozone species, in eastern Peary Land, and the problematical *Alacephalus*? *davisi* Lane and Rushton, 1992 from a few kilometres south-west of the Sirius Passet locality.

Acritarchs retrieved from the upper parts of the Buen Formation indicate a general age of the *Holmia* Biozone (at least in part equivalent to the *Olenellus* Biozone of North America (Palmer and Repina 1993), and include the diagnostic forms *Skiagia ciliosa* and *Heliosphaeridium dissimilare* (Vidal and Peel 1993). Thus, the Sirius Passet fauna seems to be firmly dated as in the '*Nevadella*' Biozone. It therefore appears to predate the Chengjiang fauna (see e.g. Shu *et al.* 1995), which correlates with the *Heliosphaeridium dissimilare-Skiagia ciliosa* acritarch and *Holmia* trilobite biozones (Zang 1992).

Correlation within the Lower Cambrian has been thrown into some confusion recently, with the suggestion that the Tommotian may be rather younger than previously thought (Vidal *et al.* 1995). If this suggestion is correct, then the Buen Formation would correlate with the lower Tommotian as recognized by these authors. It is not clear, however, that such a reorganization of Lower Cambrian correlation will find universal recognition, and under more conventional schemata, the fauna is probably of Late Atdabanian age (Conway Morris and Peel 1995).

TAPHONOMY

The preservation of the Sirius Passet fauna is puzzling. The fossils show no clear signs of extensive transport, and are associated, perhaps directly, with trace fossils (e.g. Pl. 1; Pl. 2, fig. 1), implying that the environment of deposition was not permanently lethal. Although the central regions of many of the fossils seem certainly to have been mineralized, the outer regions, such as the carapaces

of many of the arthropods, seem also to have been replaced with clay minerals. Originally calcareous forms, such as the trilobite *Buenellus* (Blaker 1988) and the halkieriid *Halkieria* (Conway Morris and Peel 1995), have been decalcified, although they often retain a considerable amount of relief, and the original outer surface of the fossils is retained, implying a replacement process rather than the formation of external moulds.

SYSTEMATIC PALAEONTOLOGY

Super-phylum LOBOPODIA Snodgrass, 1938

Remarks. This grouping is taken to include all of the lobopodian taxa (including Tardigrada, Onychophora, Pentastomida and Cambrian forms) and all of the arthropods, i.e. the familiar fully sclerotized members of the clade, including the euarthropods (the smallest clade inclusive of all extant arthropods).

Family XENUSIIDAE Dzik and Krumbiegel, 1989

Emended diagnosis. Large lobopodians with robust trunk annulations; trunk nodes large; terminal limb claws apparently absent; annular nodes and long slender branched frontal appendages present in at least some forms.

Genera. Xenusion Pompeckj, 1927; *Hadranax* gen. nov.

Remarks. We do not consider that lobopodian monophyly has been satisfactorily demonstrated (*contra* Ramsköld 1992; Chen *et al.* 1995*a*). If the proposal of Budd (1993, 1996) that they constitute a paraphyletic assemblage is correct, then the supposed monophyly of any of the lobopodous groups including the Xenusiidae is suspect without further careful character analysis.

Genus HADRANAX gen. nov.

Derivation of name. From the Greek hadros (stout, sturdy) and anax (ruler) in reference to its large size and, no doubt in life, intimidating appearance. The gender is masculine.

Type species. Hadranax augustus sp. nov.

Diagnosis. Large, *Xenusion*-like lobopod, but differing in possessing rows of four trunk nodes instead of two, in the probable presence of annular nodes, and in the lack of fleshy limb outgrowths. *Hadranax* bears a pair of long, branched, probably frontal appendages that are not known from *Xenusion*.

Hadranax augustus sp. nov.

Plates 1–3; Text-figures 2–3

Derivation of name. From the Latin *augustus*, august.

Holotype. MGUH 24.527 from GGU collection 340103, an incomplete section of the trunk showing limbs and putative frontal appendages (Pls 1–2; Text-fig. 2).

Type horizon and locality. From the base of the Buen Formation ('*Nevadella*' Biozone, Lower Cambrian); east side of J. P. Koch Fjord, North Greenland.

Other material. MGUH 24.528 (Pl. 3, fig. 1). It is both poorly preserved and confused in the axial region (Text-fig. 3A; Pl. 3, fig. 1), and may represent exuviae (as Jaeger and Martinsson (1967) and Dzik and Krumbiegel (1989) suggested for the known specimens of *Xenusion*); however, a reasonable interpretation of the specimen may be made, showing how some of the limbs have been perturbed to lie under the trunk (Text-fig. 3B). ?MGUH 24.529 (Pl. 3, fig. 2), possibly an isolated pair of limbs, is assigned to this genus with some hesitation,

and may represent two poorly preserved limbs lying next to each other (Pl. 3, fig. 2). Any point of attachment to the body is not visible.

Diagnosis. As for the genus.

Description. Hadranax is a large lobopod: the longest specimen of the body as preserved is 69 mm long, but both terminations are missing. The head and caudal regions of *Hadranax* are unknown, apart from a possible anterior appendage (see below). The trunk is parallel along its preserved length, 11 mm wide, and in the largest specimen consists of eight alternating regions of rows of nodes separated by transverse annulations (see Ramsköld 1992 for terminology and its application to other Cambrian lobopods). There are four sub-equal and rather poorly defined nodes in each row. Five well-defined, broad annulations fill the trunk area between the nodal rows. They show some traces of relatively large but poorly defined 'annular nodes' (Text-fig. 2; Pls 1–2), i.e. small tubercular structures, although the possibility of these being crush structures cannot be discounted. In line with each nodal row is attached a pair of annulated lobopod limbs. Each limb is approximately 17 mm long, and there are 18–20 annulae per limb. The limb annulae bear small projections or tubercles (Pl. 2, fig. 2). The tips of the limbs are moderately pointed, but there is no convincing evidence for the presence of terminal claws.

The best preserved specimen has, mid-way along the trunk, a 28 mm long slender appendage projecting, which appears, as preserved, to underly the limbs (Pl. 1; Pl. 2, fig. 1; Text-fig. 2). It is also characterized by transverse annulations, although these are less prominent and more closely spaced than those along the limbs or the trunk. Near the distal end of the appendage is a short section of a somewhat more slender branch, which also appears faintly annulated. Just proximal to this branch and on the same side is a much smaller protuberance on the main appendage (Pl. 2, fig. 1, arrowed), which probably represents the base of a similar but considerably narrower branch.

The style of preservation and general character (transverse wrinkling and branching or spinosity developed along one margin) are consistent with it representing an appendage of a lobopod (compare the structures in *Aysheaia* (Whittington 1978) and *Kerygmachela* (Budd 1993)). Posterior appendages of lobopods tend to be identical with other trunk appendages, although some, such as in *Hallucigenia*, do appear to be differentiated at the anterior of the animal (Ramsköld 1992; Conway Morris 1997), and appear to be attached laterally, not ventrally, although in this case these appendages are not branched. If the appendage associated with *Hadranax* is either a frontal appendage or some other differentiated appendage, then it is bent backwards and under the body, and for it to be attached to the front of the body it would have to be at least 45 mm long (28 mm preserved plus at least 17 mm concealed under the trunk), and perhaps more than this. Even given these reservations, such an identification seems the most plausible: its overall appearance and preservation is close to that of the overlying specimen, and no other taxa within the fauna are known to possess such appendages.

Triangular extensions of the trunk, complete with annulations that converge distally (Pls 1–2; Text-fig. 2), appear to project out between the limbs of the best specimen. It is difficult to interpret these structures, as they may be taphonomic in origin, perhaps generated by the lateral margins of the trunk being squeezed up by the limbs during burial. However, if this was the case one would expect them to overly the limbs, which they do not, unless these portions are preserved in the (missing) counterpart. Conversely, they may represent genuine extensions of the trunk into fleshy lobes. Unfortunately the best specimen available that shows them does not resolve the issue, and the other convincing specimen is too distorted to be of any help.

Remarks. Whilst it is unfortunate that so little material is available (it is among the rarest taxa in the fauna), with only one good specimen, *Hadranax* nevertheless shows several interesting features, although a complete reconstruction will not be presented owing to the lack of knowledge of the head and tail. In particular, it shows the following important similarities to *Xenusion*, especially relative

---

EXPLANATION OF PLATE 1

Hadranax augustus gen. et sp. nov.; MGUH 24.527 (holotype). the most complete specimen; note branched appendage emerging from towards the top left of the specimen; the structure at the top right of the specimen is a trace fossil; ×2·7. Compare Text-figure 2.

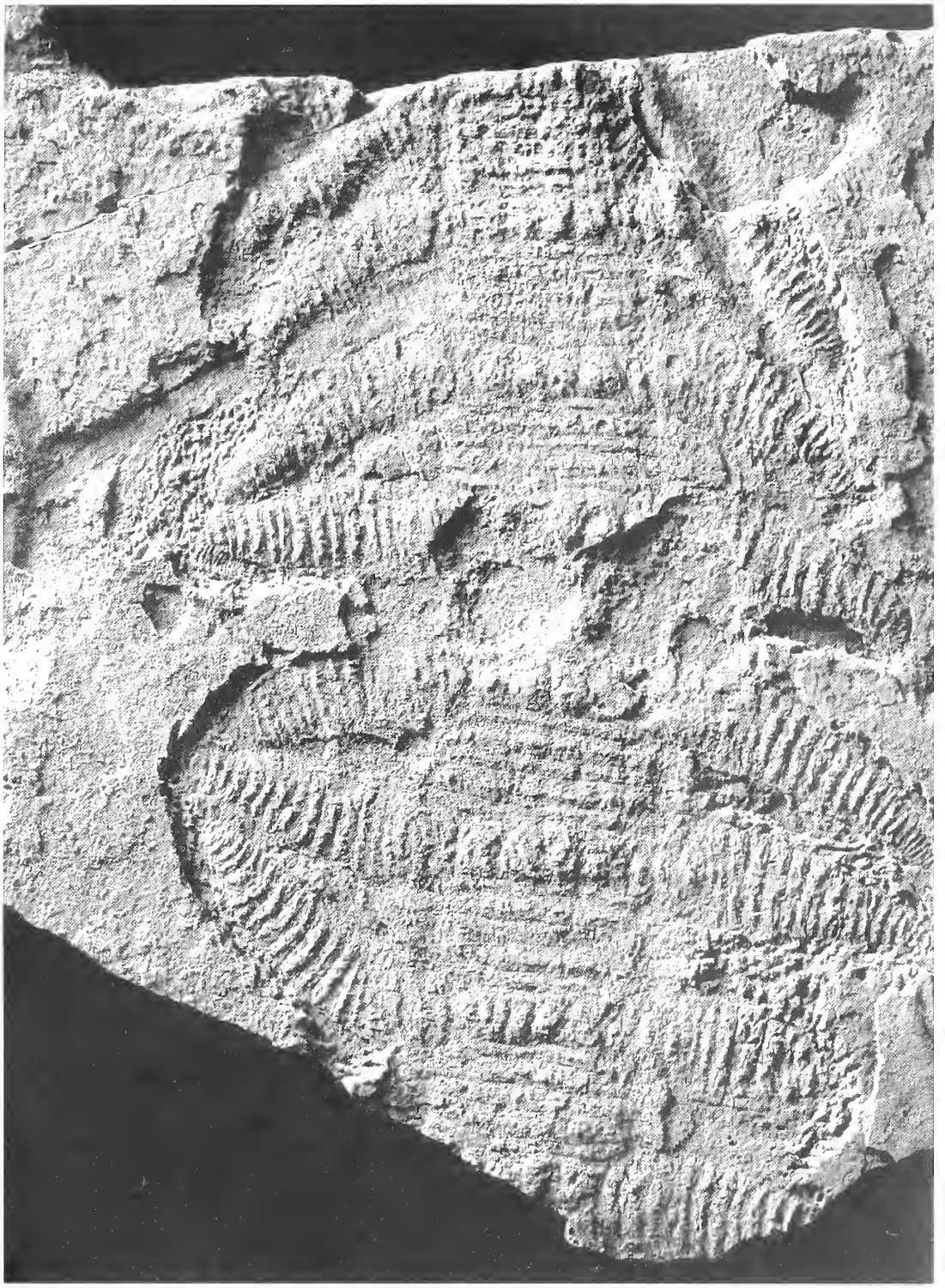

BUDD and PEEL, *Hadranax*

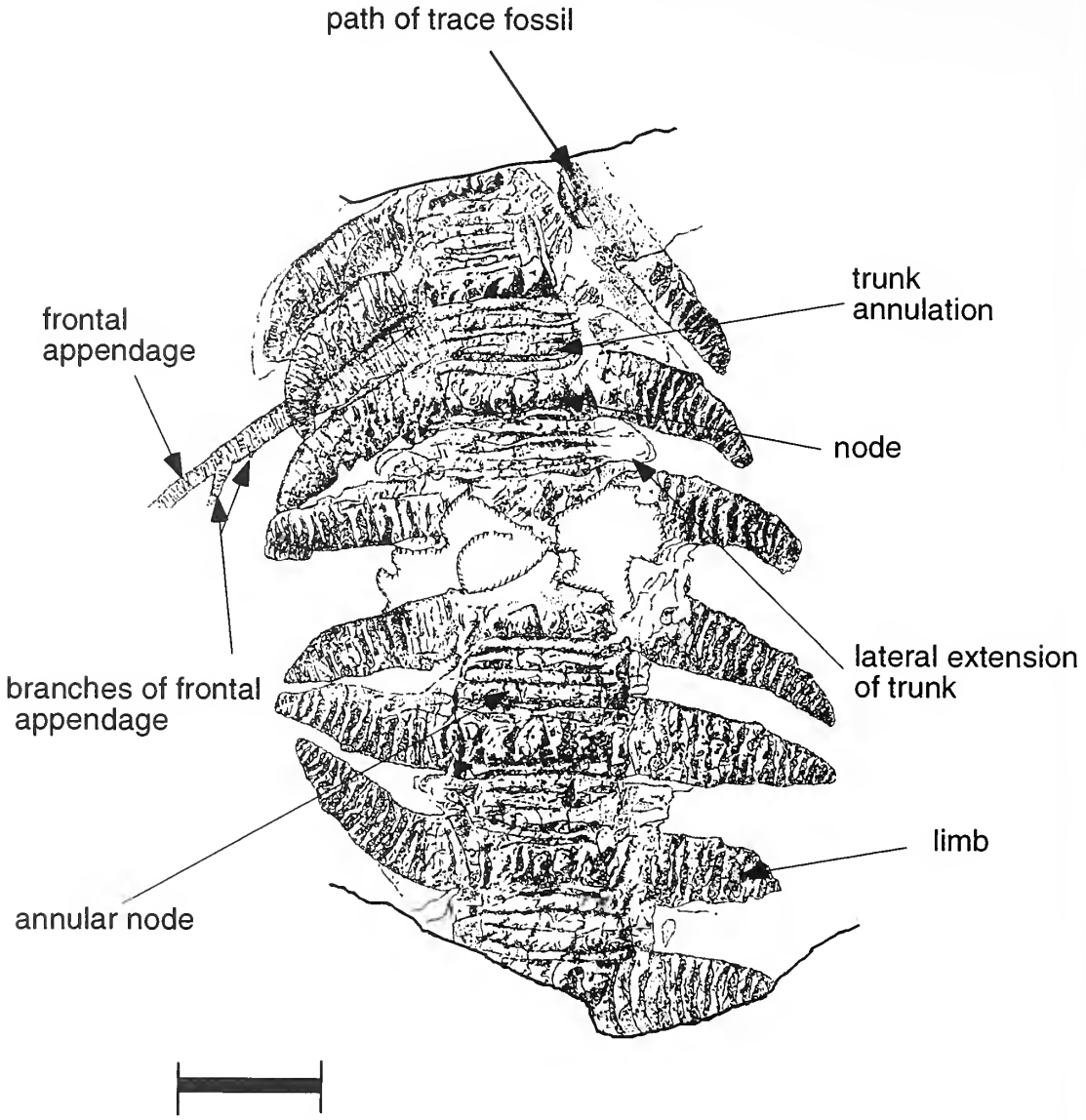

TEXT-FIG. 2. *Hadranax augustus* gen. et sp. nov.; explanatory drawing of MGUH 24.527 (holotype); compare Plate 1. Scale bar represents 10 mm.

to other Cambrian lobopods (no attempt to distinguish apomorphic and plesiomorphic characters is made here).

1. A large size, considerably greater than other Cambrian lobopods. The two known specimens of *Xenusion* have a nodal row spacing of *c.* 5·8 mm and 10 mm (Dzik and Krumbiegel 1989 argued that these two specimens represent posterior and anterior sections of a *c.* 200 mm long animal); for *Hadranax* the values are 8·1 mm for MGUH 24.527 and 8·3 mm for MGUH 24.528. Extrapolating these sizes to give about 20 limb pairs would give a total length of *c.* 150–160 mm, to which should be added the length of the frontal appendages.

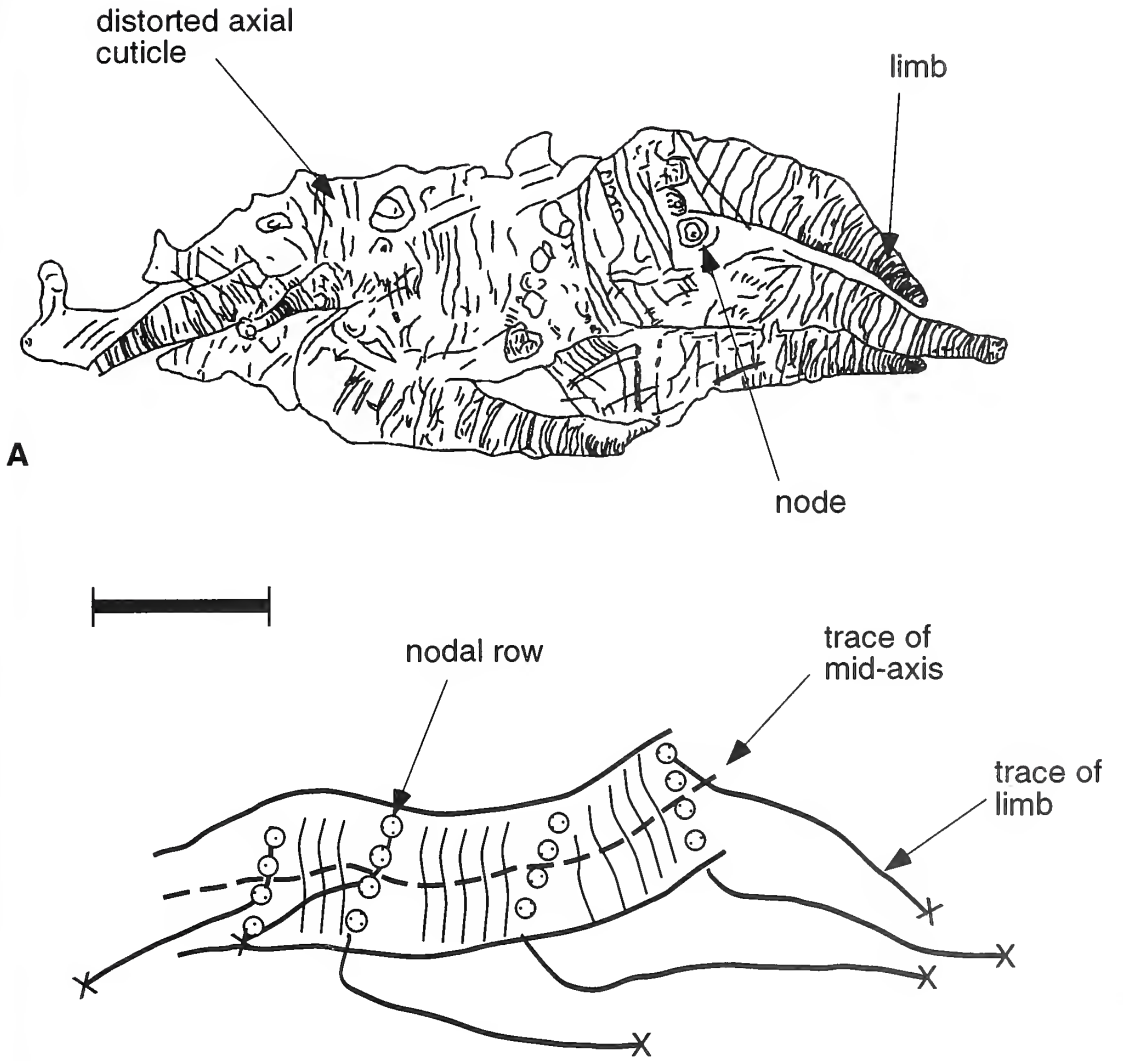

TEXT-FIG. 3. *Hadranax augustus* gen. et sp. nov. A, explanatory drawing of MGUH 24.528. B, schematic interpretation of MGUH 24.528 showing interpreted positions of nodal rows, limbs and their attachment sites. Scale bar represents 10 mm

2. Relatively wide, well-defined trunk annulations.
3. Similar limb morphologies with well-defined annulations and a lack of claws (but in both cases this may be a preservational artefact).
4. Large nodes that lack the plates of taxa such as *Microdictyon* and *Onychodictyon*.

Relative to *Xenusion*, *Hadranax* also possesses the following autapomorphic characters.

1. Annular nodes (see Ramsköld 1992 for definitions of terminology used herein).
2. Four rather than two nodes in each row, which do not appear to possess spines (although this lack may be a preservational artefact). The appearance of the nodes in the known Cambrian

lobopod genera is rather variable: *Paucipoda* possesses none (Chen *et al.* 1995), *Hadranax* and *Kerygmachela* possess rows of four, *Luolishania* rows of three, *Cardiodictyon*, *Hallucigenia* and *Onychodictyon* pairs and *Ayshaeia* a more irregular array of them.

3. Limbs that do not appear to bear fleshy protuberances, although they do appear to bear paired rows of tubercles.

4. The inferred presence of a pair of long, branched, probably frontal appendages. *Xenusion* is not known to possess such appendages. However, as only two specimens are known (Jaeger and Martinsson 1967 discussed a third specimen, now lost, but it is nowhere figured), and in neither is the preservation good enough to rule out such structures, this judgement is only provisional. The long 'proboscis'-like structure in the reconstruction of *Xenusion* by Dzik and Krumbiegel (1989) may not be accurate (L. Ramsköld, pers. comm.).

Although Pompeckj (1927) considered *Xenusion* to be an onychophoran, Heymons (1928) questioned the orientation of the specimen, and Tarlo (1967), basing his argument on the large size of the fossil and its superficial resemblance to the Vendian form *Rangea*, suggested a pennatulacean affinity, with the organism being interpreted as an upright, frond-like structure. Since then, more recently discovered material (Dzik and Krumbiegel 1989; Dzik 1991), together with the revolution that has occurred in our understanding of Cambrian lobopods (e.g. Ramsköld and Hou 1991; Hou and Bergström 1995) has really settled the question of affinities, although the poor preservation of the *Xenusion* specimens has hampered understanding of how precisely *Xenusion* relates to other lobopods. The xenusiid described here helps clarify the position somewhat, as it possesses a few more characters that other lobopods also possess, notably 'annular nodes' (widespread); four tubercles instead of two (possessed by *Kerygmachela*), and apparently a pair of branched, frontal appendages. In broad terms, this last seems to be most similar to the frontal appendage seen in *Aysheaia*, and also as argued by Budd (1993) to that of *Kerygmachela*, although in detail it is rather different from either of these examples. New discoveries of lobopods will undoubtedly alter our understanding of their systematics, but at present, the possibility that the xenusiids as defined herein will turn out to be paraphyletic (by being a grouping from within which the *Anomalocaris*-like taxa evolved) cannot be discounted.

Despite its pronounced similarity to *Xenusion*, at present the differing characters of *Hadranax*, in the important features of the nodal rows, annular nodes and probable frontal appendages, justify its placement in a new genus. However, this judgment may need amendation in the light of any new discoveries of xenusiid lobopods.

LOBOPOD DIVERSITY AND ECOLOGY IN THE CAMBRIAN

There are nine described genera of Cambrian taxa which would be broadly classified as 'lobopods' (*Aysheaia, Xenusion, Hadranax, Cardiodictyon, Microdictyon, Hallucigenia, Onychodictyon, Paucipodia, Luolishania*) and which more-or-less resemble the extant onychophorans (Bergström and Hou 1995; see also Chen *et al.* 1995*a*, 1995*b*). In addition to these, there have also been reports of a Cambrian tardigrade (Müller *et al.* 1995); a pentastomid (Walossek and Müller 1994) and a ?pentastomid-like worm, *Facivermis* (Hou and Chen 1989), all of which might be regarded as 'lobopods'. *Kerygmachela* and *Opabinia* should also both be considered to be at the lobopod grade of organization, as should some of the *Anomalocaris*-like taxa (Budd 1993, 1996, 1997).

EXPLANATION OF PLATE 2

Figs 1–2. *Hadranax augustus* gen. et sp. nov.; MGUH 24.527 (holotype). 1, details of ?frontal appendage, showing main branch and the tiny branch just proximal to it (arrowed); ×3·1. 2, details of trunk and limbs; note tubercles on limb at bottom left; ×4·5. Lighting in both from north-east. Lt = lateral extension of trunk.

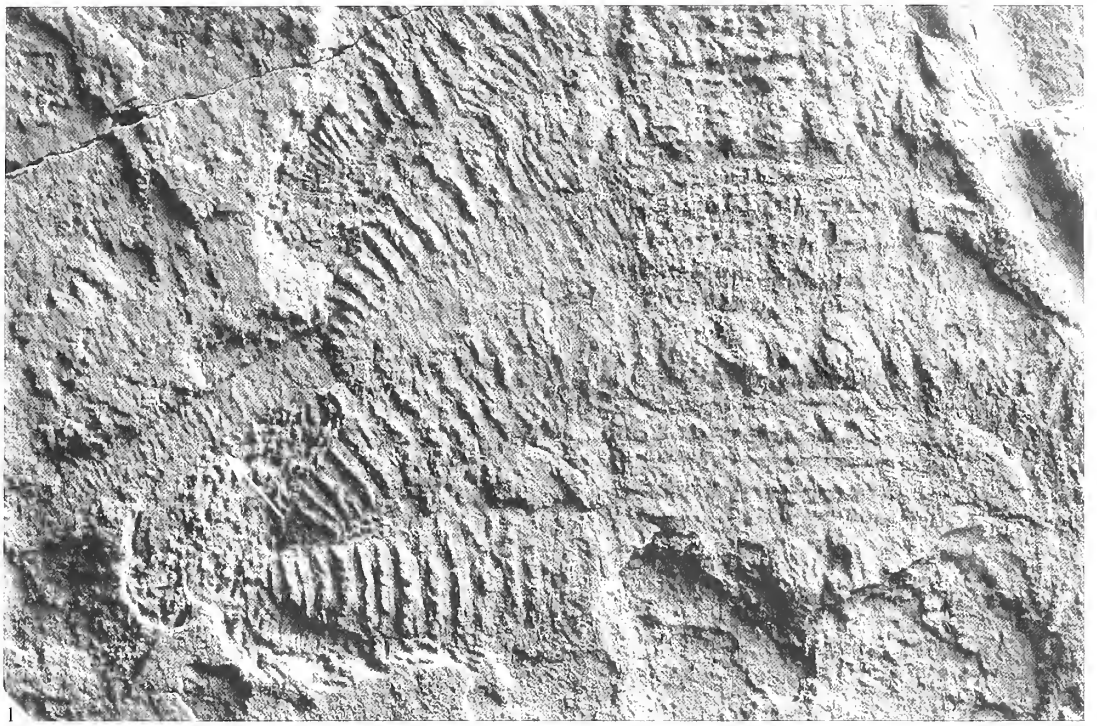

1

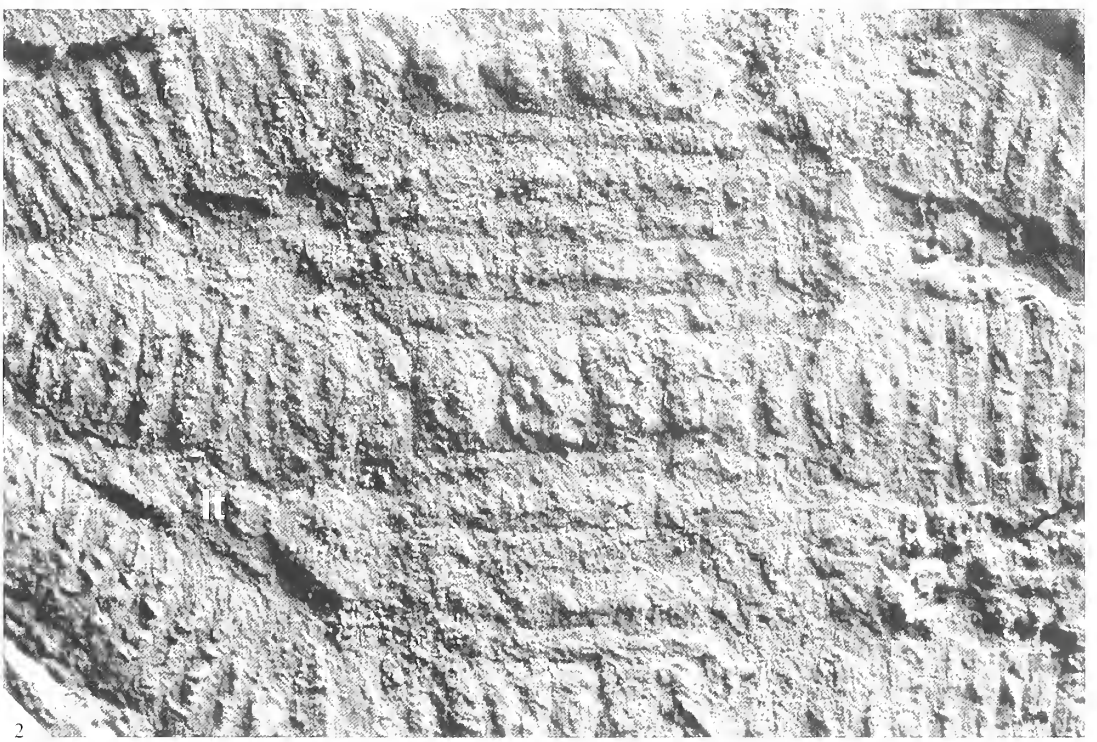

2

BUDD and PEEL, *Hadranax*

These forms exhibit a much wider morphological diversity than the extant onychophorans, notably in the details of the presence and form of ?defensive spines and frontal appendages. Most, if not all, of these forms, including *Hadranax*, were presumably benthic predators or scavengers, although the suggestion has been made that *Aysheaia* was parasitic on sponges (Whittington 1978), and that *Microdictyon* was a pseudo-pelagic commensal on the holothurian-like *Eldonia* (Chen *et al.* 1995*b*). The Cambrian lobopods may thus have fulfilled an important rôle in Cambrian benthic ecologies, perhaps similar to that occupied by the vagrant polychaetes today (see also Budd in press), although jawless polychaetes seem also to have been fairly diverse by the Mid Cambrian (e.g. Conway Morris 1979).

Almost all of these taxa are known only from exceptionally preserved faunas. It is probably fair to conclude that this broad grouping was widespread, diverse and important in the Cambrian. As was the case with the Cambrian 'arachnomorph' taxa (Briggs and Fortey 1989; Wills *et al.* 1994), this group became severely restricted, perhaps at the Mid-Late Cambrian boundary, and only a few vestiges survived into the rest of the Palaeozoic and beyond. No novel forms of lobopods (*qua* lobopods) seem to have arisen after the Mid Cambrian apart from the extant Tardigrada (first record, Upper Cambrian (Müller *et al.* 1995)) and the Onychophora (first record is probably the Carboniferous *Helenodora* (Thompson and Jones 1980), which most closely resembles *Aysheaia* of the Cambrian taxa). However, it would be a mistake to conclude from this fact alone that the 'lobopods' reached their acme in the Cambrian, as the group is likely to be paraphyletic (Budd 1993, 1997): both the uniramous and biramous arthropods are descended from them. Nevertheless, as a grade of organization, they were probably never as important as in the Early and Mid Cambrian.

There is a necessity, if at least some group of lobopods gave rise to the arthropods, of them having arisen before the arthropods. Unfortunately, at present, the details of Lower Cambrian stratigraphy do not allow any sort of accuracy in determining faunal successions of this nature. The oldest 'Burgess Shale'-like fauna is known from Polish borehole material (Dzik and Lendzion 1988), which may be placed as time-equivalent to the top of the Mazowsze Formation, probably corresponding to the top of the *Platysolenites* zone of Scandinavia and thus predating the earliest trilobites (Moczydłowska 1991; Palacios and Vidal 1995). The Polish material contains a probable relative of *Anomalocaris, Cassubia*, and a *Naraoia*-like form, *Liwia*. These taxa probably lie within the stem-group or near the base of the euarthropods respectively (Budd 1996), so at least some lobopods should therefore predate this time period. However, with the possible exception of the enigmatic form *Bomakellia* (Fedonkin 1994, fig. 5c; see also Waggoner 1996), this record is missing, and at present the origins of the lobopods themselves remain obscure; they are unlikely to be derived from annelids, as previously supposed (Eernisse *et al.* 1992, *contra* e.g. Snodgrass 1938). The suggestion of Dzik and Krumbiegel (1989) and Dzik (1991) that *Xenusion* should be considered to be a basal articulate, with its four-fold symmetry suggesting a derivation from the nemathelminth worms, seems also unlikely to be correct. The presence of a closely related form which does not have a four-fold limb and node arrangement probably implies that it is not some fundamental part of the construction of *Xenusion*; and the probable presence of a branched frontal appendage adds evidence that *Xenusion* need not be considered to be a basal form on the basis of its supposed extreme simplicity.

EXPLANATION OF PLATE 3

Figs 1–2. *Hadranax augustus* gen. et sp. nov. 1, MGUH 24.528; confused specimen, possibly exuviae; ×2·1. Lighting from south-east. Compare Text-figure 3. 2, MGUH 24.529; ?possible pair of limbs; tip of top limb arrowed; 'Is' indicates the wrinkled edge of an *Isoxys* specimen (see Williams *et al.* 1996); ×3·0. Lighting from west.

1

2

BUDD and PEEL, *Hadranax*

Acknowledgements. We thank J. Bergström and L. Ramsköld for discussion of the Chengjiang fauna. We gratefully acknowledge funding from the Carlsberg Foundation and National Geographic. GEB is funded by a Swedish Natural Sciences Research Council (NFR) post-doctoral fellowship. This is a contribution to IGCP Project 366.

REFERENCES

BLAKER, M. R. 1988. A new genus of nevadiid trilobite from the Buen Formation (Early Cambrian) of Peary Land, central North Greenland. *Rapport Gronlands Geologiske Undersøgelse*, **137**, 33–41.

BRIGGS, D. E. G. and FORTEY, R. A. 1989. The early radiation and relationships of the major arthropod groups. *Science*, **246**, 241–243.

BUDD, G. 1993. A Cambrian gilled lobopod from Greenland. *Nature*, **364**, 709–711.

BUDD, G. E. 1995. *Kleptothule rasmusseni* gen. et sp. nov.: an ?olenellinid-like trilobite from the Sirius Passet fauna (Buen Formation, Lower Cambrian, North Greenland). *Transactions of the Royal Society of Edinburgh: Earth Sciences*, **86**, 1–12.

—— 1996. The morphology of *Opabinia regalis* and the reconstruction of the arthropod stem-group. *Lethaia*, **29**, 1–14.

—— 1997. Stem-group arthropods from the Lower Cambrian Sirius Passet fauna of North Greenland. 125–138. *In* FORTEY, R. A. and THOMAS, R. H. (eds). *Arthropod relationships*. Chapman and Hall, London.

—— in press. Cambrian ecology of lobopods and non-trilobite arthropods. *In* ZHURAVLEV, A. Yu. and RIDING, R. (eds). *Ecology of the Cambrian radiation*. Columbia University Press, New York.

CHEN JUNYUAN, ZHOU GUIQING and RAMSKÖLD, L. 1995*a*. A new Early Cambrian onychophoran-like animal, *Paucipodia* gen. nov., from the Chengjiang fauna, China. *Transactions of the Royal Society of Edinburgh: Earth Sciences*, **85**, 275–282.

—— —— —— 1995*b*. The Cambrian lobopodian *Microdictyon sinicum*. *Bulletin of the National Museum of Natural Science (Taichung, Taiwan)*, **5**, 1–93.

CONWAY MORRIS, S. 1977. A new Metazoan from the Burgess Shale of British Columbia. *Palaeontology*, **20**, 623–640.

—— 1979. Middle Cambrian polychaetes from the Burgess Shale of British Columbia. *Philosophical Transactions of the Royal Society of London, Series B*, **385**, 227–274.

—— and PEEL, S. J. 1990. Articulated halkieriids from the Lower Cambrian of North Greenland. *Nature*, **345**, 802–804.

—— —— 1995. Articulated halkieriids from the Lower Cambrian of North Greenland and their role in early protostome evolution. *Philosophical Transactions of the Royal Society of London, Series B*, **347**, 305–358.

—— —— HIGGINS, A. K., SOPER, N. J. and DAVIS, N. C. 1987. A Burgess Shale-like fauna from the Lower Cambrian of North Greenland. *Nature*, **345**, 802–805.

DZIK, J. 1991. Is fossil evidence consistent with traditional views of the early metazoan phylogeny? 47–56. *In* SIMONETTA, A. M. and CONWAY MORRIS, S. (eds). *The early evolution of Metazoa and the significance of problematic taxa*. Cambridge University Press, Cambridge, ix + 296 pp.

—— and KRUMBIEGEL, G. 1989. The oldest 'onychophoran' *Xenusion*: a link connecting phyla? *Lethaia*, **22**, 169–181.

—— and LENDZION, K. 1988. The oldest arthropods of the East European Platform. *Lethaia*, **21**, 29–38.

EERNISSE, D. J., ALBERT, J. S. and ANDERSON, F. E. 1992. Annelida and Arthropoda are not sister taxa: a phylogenetic analysis of spiralian metazoan morphology. *Systematic Biology*, **41**, 305–330.

FEDONKIN, M. A. 1994. Vendian body fossils and trace fossils. 370–388. *In* BENGTSON, S. (ed.). *Early life on Earth*. Columbia University Press, New York, x + 630 pp.

HEYMONS, R. 1928. Uber Morphologie und verwandtschaftliche Beziehungen des *Xenusion auerswaldae* Pomp. aus dem Algonkium. *Zeitschrift für Morphologie und Ökologie der Tiere*, **10**, 307–329.

HOU XIANGUANG and BERGSTRÖM, J. 1995. Cambrian lobopodians – ancestors of extant onychophorans? *Zoological Journal of the Linnean Society of London*, **114**, 3–19.

—— and CHEN JUNYUAN 1989. Early Cambrian tentacled worm-like animal from Chengjiang, Eastern Yunnan. *Acta Palaeontologica Sinica*, **28**, 32–41.

JAEGER, H. and MARTINSSON, A. 1967. Remarks on the problematic fossil *Xenusion auerswaldae*. *Geologiska Föreningens i Stockholm Förhandlingar*, **88**, 435–452.

KIELAN, Z. 1960. On two olenellid trilobites from Vestspitsbergen. *Studia Geologica Polonica*, **4**, 83–92.

LANE, P. D. and RUSHTON, A. W. A. 1992. A problematical trilobite from the Lower Cambrian of Freuchen Land, central North Greenland. *Rapport Gronlands Geologiske Undersøgelse*, **154**, 5–12.

MOCZYDŁOWSKA, M. 1991. Acritarch biostratigraphy of the Lower Cambrian and the Precambrian-Cambrian boundary in south-eastern Poland. *Fossils and Strata*, **29**, 1–127.

MÜLLER, K. J., WALLOSSEK, D. and ZAKHAROV, A. 1995. 'Orsten' type phosphatized soft-integument preservation and a new record from the Middle Cambrian Kuonamka Formation in Siberia. *Neues Jahrbuch für Geologie und Paläontologie, Abhandlungen*, **197**, 107–118.

PALACIOS, T. and VIDAL, G. 1992. Lower Cambrian acritarchs from northern Spain: the Precambrian-Cambrian boundary and biostratigraphic implications. *Geological Magazine*, **129**, 421–436.

PALMER, A. R. and REPINA, L. N. 1993. Through a glass darkly: taxonomy, phylogeny, and biostratigraphy of the Olenellina. *University of Kansas Paleontological Contributions* (*New Series*), **3**, 1–35.

PEEL, J. S. and SØNDERHOLM, M. (eds). 1991. Sedimentary basins of North Greenland. *Bulletin Gronlands Geologiske Undersøgelse*, **160**, 1–164.

POMPECKJ, J. F. 1927. Ein neues Zeugnis uralten Lebens. *Paläontologische Zeitschrift*, **9**, 287–313.

POULSEN, V. 1974. Olenellacean trilobites from eastern North Greenland. *Bulletin of the Geological Society of Denmark*, **23**, 79–101.

RAMSKÖLD, L. 1992. Homologies in Cambrian Onychophora. *Lethaia*, **25**, 443–460.

—— and HOU XIANGHUANG 1991. New Early Cambrian animal and onychophoran affinities of enigmatic metazoans. *Nature*, **351**, 225–228.

RIGBY, J. K. 1986. Cambrian and Silurian sponges from North Greenland. *Rapport Gronlands Geologiske Undersøgelse*, **132**, 51–63.

SHU DEGAN, GEYER, G., CHEN LING and ZHANG XINGLIANG 1995. Redlichiacean trilobites with preserved soft-parts from the Lower Cambrian Chengjiang fauna (South China). *Beringeria*, Special Issue 2, 203–241.

SNODGRASS, R. E. 1938. Evolution of the Annelida, Onychophora and Arthropoda. *Smithsonian Miscellaneous Collections*, **97**, 1–159.

TARLO, L. B. H. 1967. *Xenusion* – onychophoran or coelenterate? *Mercian Geologist*, **2**, 97–99.

THOMPSON, I. and JONES, D. S. 1980. A possible onychophoran from the Middle Pennsylvanian Mazon Creek Beds of northern Illinois. *Journal of Paleontology*, **54**, 588–596.

VIDAL, G., MOCZYDLOWSKA, M. and RUDAVSKAYA, V. R. 1995. Constraints on the early Cambrian radiation and correlation of the Tommotian and Nemakit-Daldynian regional stages of eastern Siberia. *Journal of the Geological Society, London*, **152**, 499–510.

—— and PEEL, J. S. 1993. Acritarchs from the Lower Cambrian Buen Formation in north Greenland. *Bulletin Gronlands Geologiske Undersogelse*, **164**, 1–35.

WAGGONER, B. M. 1996. Phylogenetic hypotheses of the relationships of arthropods to Precambrian and Cambrian problematic fossil taxa. *Systematic Biology*, **45**, 190–222.

WALOSSEK, D. and MULLER, K. J. 1994. Pentastomid parasites from the Lower Palaeozoic of Sweden. *Transactions of the Royal Society of Edinburgh: Earth Sciences*, **85**, 1–37.

WHITTINGTON, H. B. 1978. The lobopodian animal *Aysheaia pedunculata* Walcott, Middle Cambrian, Burgess Shale, British Columbia. *Philosophical Transactions of the Royal Society of London, Series B*, **284**, 165–197.

WILLIAMS, M., SIVETER, D. J. and PEEL, J. S. 1996. *Isoxys* (Arthropoda) from the Early Cambrian Sirius Passet Lagerstätte, North Greenland. *Journal of Paleontology*, **70**, 947–954.

WILLS, M., BRIGGS, D. E. G. and FORTEY, R. A. 1994. Disparity as an evolutionary index: a comparison of Cambrian and Recent arthropods. *Paleobiology*, **20**, 93–130.

ZANG, W. L. 1992. Sinian and Early Cambrian floras and biostratigraphy of the South China Platform. *Palaeontographica*, **224**, 75–119.

GRAHAM E. BUDD

JOHN S. PEEL

Institute for Earth Sciences
Department of Historical
Geology and Palaeontology
Norbyvägen 22
Uppsala S-75236
Sweden

Typescript received 10 October 1996
Revised typescript received 19 November 1997

AETOSAURUS (ARCHOSAUROMORPHA) FROM THE UPPER TRIASSIC OF THE NEWARK SUPERGROUP, EASTERN UNITED STATES, AND ITS BIOCHRONOLOGICAL SIGNIFICANCE

by SPENCER G. LUCAS, ANDREW B. HECKERT *and* PHILLIP HUBER

ABSTRACT. Four specimens of the aetosaur *Stegomus* are known from Upper Triassic strata of the Newark Supergroup of the eastern United States. These specimens represent a small aetosaur with a long narrow carapace that is distinctly waisted in front of the hindlimbs, has paramedian scutes much wider than long and lateral scutes that lack spikes. *Stegomus* is thus remarkably similar to *Aetosaurus* Fraas, but has weaker sculpturing on its scutes. This is the principal difference between the two, so we regard *Stegomus* as a junior subjective synonym of *Aetosaurus* and recognize a distinct Newark species, *Aetosaurus arcuatus* (Marsh).

Aetosaurus in the Newark Supergroup is of biochronological significance because the genus has a broad distribution and one of its occurrences can be directly cross-correlated to Triassic marine biochronology. *Aetosaurus* is of early–mid Norian age in the German Lower and Middle Stubensandstein. *Aetosaurus* has been found in mid Norian marine limestones in Italy correlated to the *Himavatites columbianus* ammonite Zone, which directly cross-correlates the genus to the standard global chronostratigraphical scale. *Aetosaurus* is present in the Bull Canyon Formation (Chinle Group) of eastern New Mexico, USA and in the Ørsted Dal Member of the Fleming Fjord Formation in Greenland; both of these units are of early Norian age. *Aetosaurus* localities in the Newark Supergroup are of mid Norian age, a conclusion consistent with Newark palynostratigraphy and magnetostratigraphy. *Aetosaurus* is thus an index fossil of the lower–middle Norian.

AETOSAURS were herbivorous archosaurs of the Late Triassic. Their heads are extremely small relative to their bodies, their rostra lack teeth, and they have small, leaf-shaped maxillary and dentary teeth. The heavily armoured body has quadrangular plates that run form the back of the skull to the tip of the tail and encase much of the abdomen as well as the entire tail. The tarsus is crocodile normal, and the ichnogenus *Brachychirotherium* probably represents aetosaur footprints (Lockley and Hunt 1995).

Aetosaur fossils have a broad geographical distribution (Text-fig. 1) and are among the most common tetrapod fossils in many Late Triassic, non-marine strata. Distribution, abundance, and ease of identification make aetosaurs useful Late Triassic non-marine index fossils (Lucas and Heckert 1996; Hecker *et al.* 1996).

Here, we re-evaluate the taxonomy of one of the first aetosaurs described from North America, *Stegomus arcuatus* Marsh, 1896. We conclude that *Stegomus* is a junior subjective synonym of the European aetosaur genus *Aetosaurus* Fraas, 1877. This enables a robust correlation of *Aetosaurus* localities in the Unites States, Greenland, Germany and Italy, and thus further develops the biochronological utility of aetosaurs.

Institutional abbreviations. NCSM, North Carolina State Museum, Raleigh, North Carolina, USA; NJSM, New Jersey State Museum, Trenton, New Jersey, USA; NMMNH, New Mexico Museum of Natural History and Science, Albuquerque, New Mexico, USA; PU, Princeton University collection, now at Yale Peabody Museum; SMNS, Staatliches Museum für Naturkunde, Stuttgart, Germany; YPM, Yale Peabody Museum, New Haven, Connecticut, USA.

[Palaeontology, Vol. 41, Part 6, 1998, pp. 1215–1230, 2 pls]

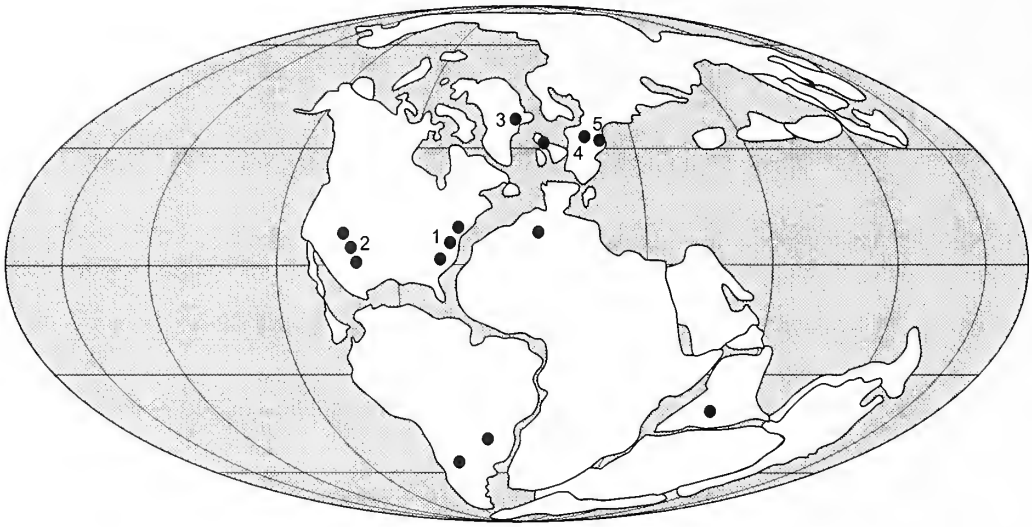

TEXT-FIG. 1. Map of Late Triassic Pangaea showing aetosaur localities and highlighting *Aetosaurus* records, which are: 1 = Newark Supergroup, eastern North America; 2 = Chinle Group, western United States; 3 = Fleming Fjord Formation, Greenland; 4 = Keuper Triassic, Germany; 5 = Alpine marine Triassic, Lombardian Alps, Italy.

SYSTEMATIC PALAEONTOLOGY

Order CROCODYLOTARSI Benton and Clark, 1988
Suborder AETOSAURIA von Huene, 1908
Family STAGONOLEPIDIDAE Lydekker, 1887

Genus AETOSAURUS Fraas, 1877

Aetosaurus arcuatus (Marsh, 1896)

Plates 1–2; Text-figures 2, 3B, 4; Table 1

1896 *Stegomus arcuatus* Marsh, p. 60, pl. 1.
1915 *Stegomus arcuatus*; Lull, p. 79, pl. 5
1948 *Stegomus arcuatus jerseyensis* Jepsen, p. 9, pls 1–2.
1953 *Stegomus arcuatus*; Lull, p. 79, pl. 5.
1986 *Stegomus arcuatus*; Baird, p. 142, figs 12–13, 14A.
1993*a* *Stegomus* cf. *Stegomus arcuatus*; Huber *et al.*, p. 179, fig. 5.

Holotype. YPM 1647 (Pl. 1), natural cast of the ventral aspect of part of the dorsal carapace (Marsh 1896, pl. 1; Lull 1915, pl. 5, 1953, pl. 5).

Horizon and locality of holotype. New Haven Formation, Fair Haven, Connecticut (see below).

EXPLANATION OF PLATE 1

Figs 1–3. *Aetosaurus arcuatus* (Marsh, 1896); YPM 1647, holotype; natural mould of ventral surface of part of dorsal carapace; lateral (1) and ventral (2) views and detail (3) of scute impressions showing articulation of paramedian (p) and lateral (l) scutes. 1–2, ×0·33; 3, ×0·66.

1

2

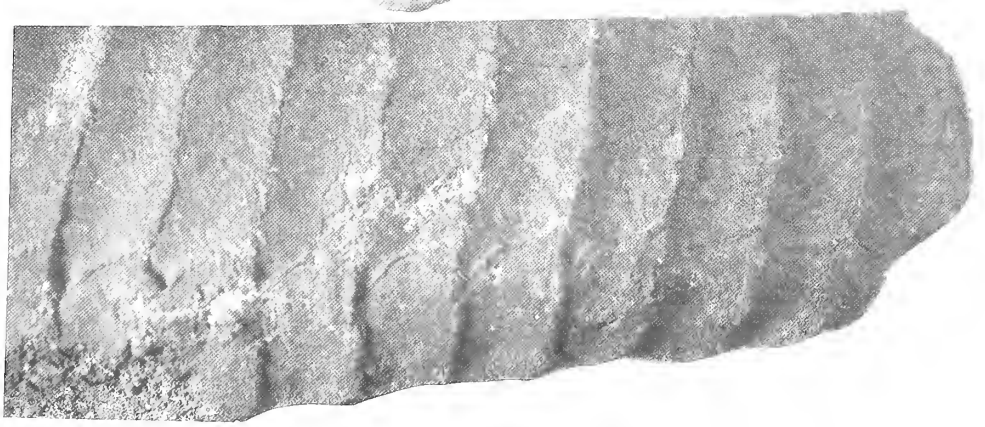

3

LUCAS *et al.*, *Aetosaurus*

TABLE 1. Measurements of scutes of specimens YPM 1647, NJSM 10740, NCSM 11756 and YPM [PU] 21750. Note that letter designations (A, B, C, etc.) of scutes of different specimens do not imply homology.

Paramedian scute row	Width (in mm)	Length (in mm)	W:L	Lateral scute row	Width (in mm)	Length (in mm)
			YPM 1647			
A	72	21	3·4	A	15	21
B	81	24	3·4	B	15	21
C	81	24	3·4	C	18	21
D	84	24	3·5	D	21	21
E	84	24	3·5	E	18	24
F	84	24	3·5	F	21	24
G	84	27	3·1	G	24	24
H	90	27	3·3	H	24	24
I	84	27	3·1	I	24	24
J	87	27	3·2	J	24	27
K	96	27	3·6	K	27	27
L	90	27	3·3	L	27	24
M	81	24	3·4	M	30	27
N	75	18	4·2	N	33	27
O	72	18	4·0	O	33	27
P	72	15	4·8	P	36	27
			NJSM 10740			
A	36	—	—	A	11*	13
B	39	24	1·6	B	13	20
C	31	18*	1·7	C	13	15
D	28	17*	1·6	D	12	16
E	28	16	1·7	E	11	18
F	21*	15	1·4	F	11	16
G	19	16	1·2	G	10	17
H	16	15*	1·1	H	—	—
I	—	14*	—	I	—	—
			NCSM 11756			
A	46*	19*	2·4	A	—	—
B	49	18	2·7	B	18	16
C	47	17	2·8	C	19	18
D	41	12	3·4	D	16	17
E	38	12	3·2	E	14	14
F	36	11	3·3	F	9	12
			YPM [PU] 21750			
A	19	6	3·2			
B	18	6	3·0			
C	17	6	2·8			
D	16	5	3·2			
E	19	5	3·8			
F	20	6	3·3			
G	19	5	3·8			
H	22	7	3·1			
I	24	5	4·8			
J	24	6	4·0			
K	27	6	4·5			
L	27	6	4·5			
M	28	8	3·5			
N	26	7	3·7			
O	28	7	4·0			
P	27	7	3·9			
Q	27	7	3·9			
R	25	7	3·6			
S	22	9	2·4			
T	16	7	2·3			

* Measurement of incompletely exposed or preserved scute.

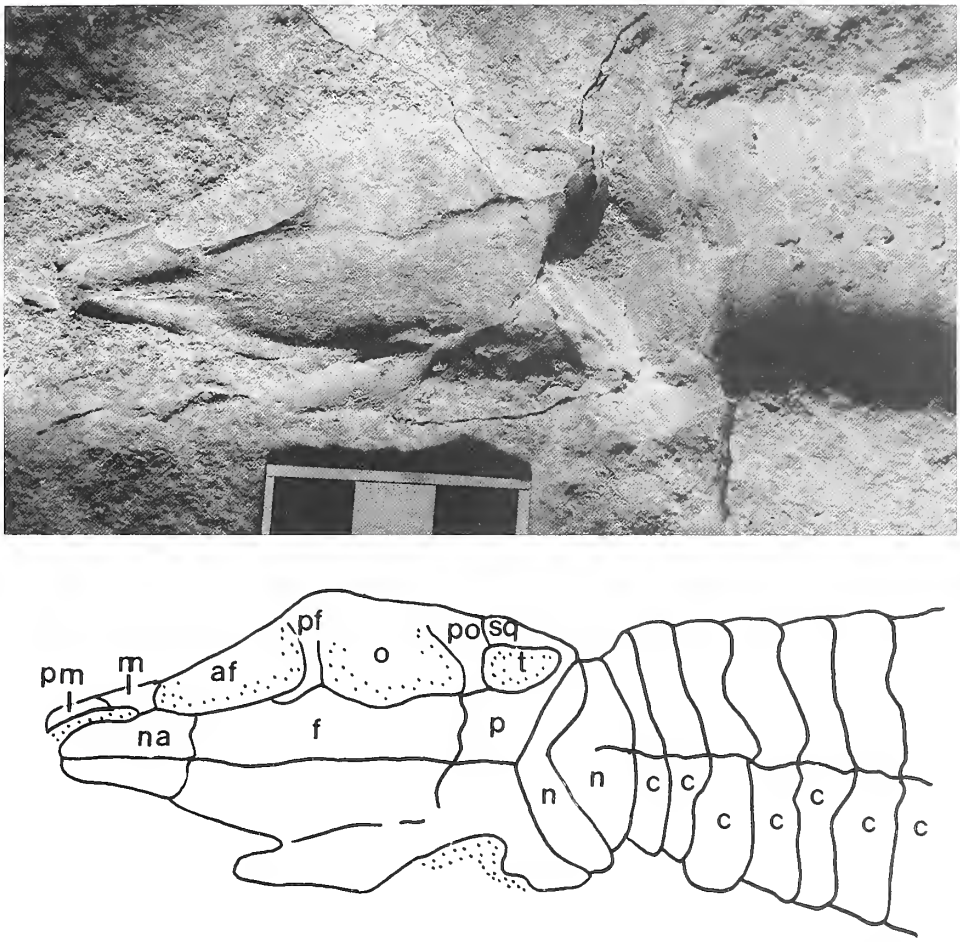

TEXT-FIG. 2. *Aetosaurus arcuatus* (Marsh, 1896); YPM [PU] 21759, skull and anterior portion of neck. Abbreviations: af = antorbital fenestra; c = cervical paramedian scutes; f = frontal; m = maxilla; n = nuchal scutes; na = nasals; o = orbit; p = parietal; pf = prefrontal; pm = premaxilla; po = postorbital; sq = squamosal; t = temporal fenestra. Skull drawing modified from Baird (1986); × 1·1.

Material. YPM [PU] 21750, natural cast of ventral aspect of skull and dorsal carapace (Baird 1986, figs 12, 14A; Pl. 2; Text-fig. 2); from the Passaic Formation on the bank of Nishisakawick Creek, Huntendon County, New Jersey.

NJSM 10740, partial tail (Jepsen 1948, pls 1–2; Baird 1986, fig. 13; Text-fig. 3B); from the Passaic Formation near Neshanic Station in Somerset County, New Jersey.

NCSM 11756 partial tail (Huber *et al.* 1993*a*, fig. 5) (Text-fig. 4A–B); from 'Lithofacies Association II' (= Lower Sanford Formation) at the Triangle Brick Quarry, North Carolina.

Revised diagnosis. A species of *Aetosaurus* distinguished from *A. ferratus* Fraas, 1877 and *A. crassicauda* Fraas, 1907 by the relatively large (3·5:1) width:length ratio of the dorsal paramedian scutes in adult specimens, very faint pitting on the scutes, and a tail that narrows rapidly posteriorly.

Description. Marsh (1896) and Lull (1915, 1953) described the holotype of *Stegomus arcuatus*, and Jepsen (1948) and Baird (1986) described the New Jersey specimens. Parker (1966) described the partial tail from North Carolina, and this specimen was later illustrated by Huber *et al.* (1993*a*, fig. 5).

The holotype, YPM 1647, consists of the natural mould of the median portion of a carcass that preserves 16 articulated rows of paramedian and lateral scutes and apparently was rolled and contracted dorsally before burial (pl. 1). The specimen is preserved as a natural sandstone mould of the ventral surface of the dorsal armour and also includes seven matrix blocks that include portions of the mould. No original bone is preserved, so YPM 1647 is a steinkern preserved in red, medium- to coarse-grained, arkosic sandstone and pebbly sandstone. The total length of the preserved carapace is about 440 mm.

The so-called 'pitting' of the scutes alleged by Lull (1915, 1953) actually is porosity of the sandstone matrix, not a morphological feature. Thus, this 'pitting' can be seen both on the scute impressions and on the surrounding sandstone matrix. The carapace is composed of two columns of 16 paramedian scutes that are rectangular in shape, much wider than long (width:length *c.* 3·1–4·8; Table 1). Smaller, trapezoidal lateral scutes occur at the margins of all the right paramedian scutes and are attached to six of the left paramedian scutes. There is no evidence that any of the lateral scutes has spikes or protuberances. Fine details of the surface morphology of all scutes are obscured by the coarse-grained fabric of the host matrix.

Baird (1986) provided a brief, but accurate description of YPM [PU] 21750, which is the most complete specimen previously assigned to *Stegomus* (Pl. 2; Text-fig. 2). This is the ventral impression of the skull roof and dorsal carapace from the skull to the pelvis. It represents a small aetosaur with a snout–pelvis length of approximately 210 mm. Skull length is about 69 mm, and width across the orbits is 17 mm. The snout tip is broken, but obviously tapered to a thin beak. The antorbital fenestra is antero-posteriorly long and dorso-ventrally short. The orbit is very large; with an antero-posterior length of 18 mm, it reaches *c.* 25 per cent. of skull length. This suggests that the specimen represents a juvenile (Baird 1986). Sutures for the premaxillary, maxillary, nasals, frontals, prefrontal, frontal, parietal, postorbital and squamosal are present, and are as Baird (1986, fig. 14A) indicated (Text-fig. 2).

A scute covers the occiput and is followed by two columns of 21 pairs of paramedian scutes. These scutes are rectangular – much wider than long (width:length ~ 3·0–4·0; Table 1) – and imbricated. The posterior edge of each scute overlaps (is dorsal to) the anterior edge of the scute behind it. This scute morphology is best illustrated by the natural cast of the scutes that infilled the posterior portion of the mould (Pl. 2, fig. 2). Scute morphology is strikingly similar to that of YPM 1647, although the New Jersey specimen is significantly smaller. The carapace of the New Jersey specimen narrows noticeably toward the pelvis.

NJSM 10740 is part of the dorsal portion of a tail (Text-fig. 3B). Jepsen (1948) provided an accurate description, and we only draw attention to a few key features. Note that the dorsal paramedian scutes are rectangular and wider than long (width:length ~ 1·6–1·7; Table 1). They are imbricated: the posterior edge of each scute overlaps (is dorsal to) the anterior edge of the scute behind it. The lateral scutes are square to trapezoidal in shape. The tail tapers very rapidly posteriorly.

NCSM 11756 is part of a tail that preserves six rows of scutes (Text-fig. 4). Most of the bone is exfoliated from the scutes, but some preserve the original external surface of the dermal bone. These surfaces have a distinct 'sunburst' pattern of grooves and small pits that radiate away from the scute's antero-posterior axis. As in the other specimens, the paramedian scutes are rectangular and much wider than long (Table 1). The lateral scutes are square to trapezoidal. None of the scutes bear bony spikes or protuberances. The tail tapers very rapidly posteriorly.

Remarks. The four specimens of *Stegomus* from the Newark Supergroup characterize an aetosaur with the following distinctive features: (1) it is relatively small in comparison to most other aetosaurs; (2) the paramedian scutes are much wider than long, with overlapping anterior bars; (3) the lateral scutes are small, trapezoidal and lack any bony spikes; (4) the paramedian scute surfaces bear a faint 'sunburst' pattern of pits and grooves; and (5) the carapace is 'waisted' (narrows, with a corresponding decrease in width:length ratios of dorsal scutes) immediately anterior to the pelvis.

EXPLANATION OF PLATE 2

Figs 1–2. *Aetosaurus arcuatus* (Marsh, 1896); YPM [PU] 21750. 1, natural mould of ventral aspect of skull and dorsal carapace, stereophotograph; ×0·5. 2, natural cast of infilling of posterior portion of mould, stereophotograph; ×1·5.

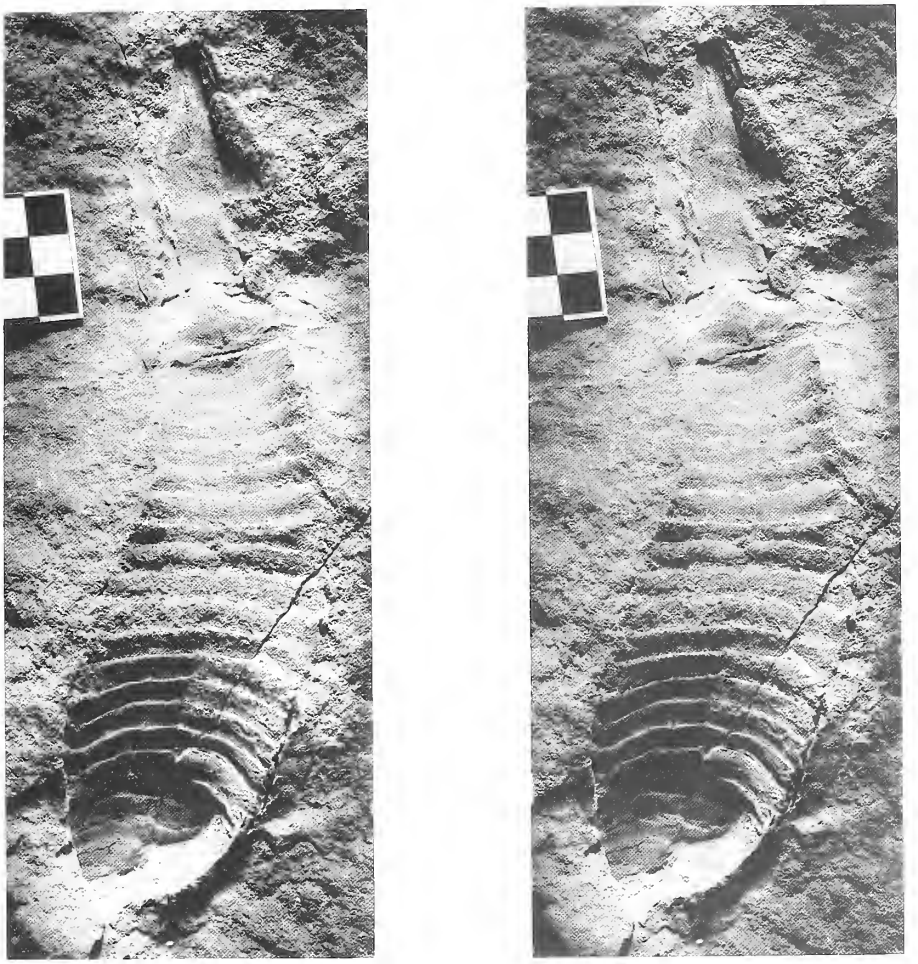

1

2

LUCAS *et al.*, *Aetosaurus*

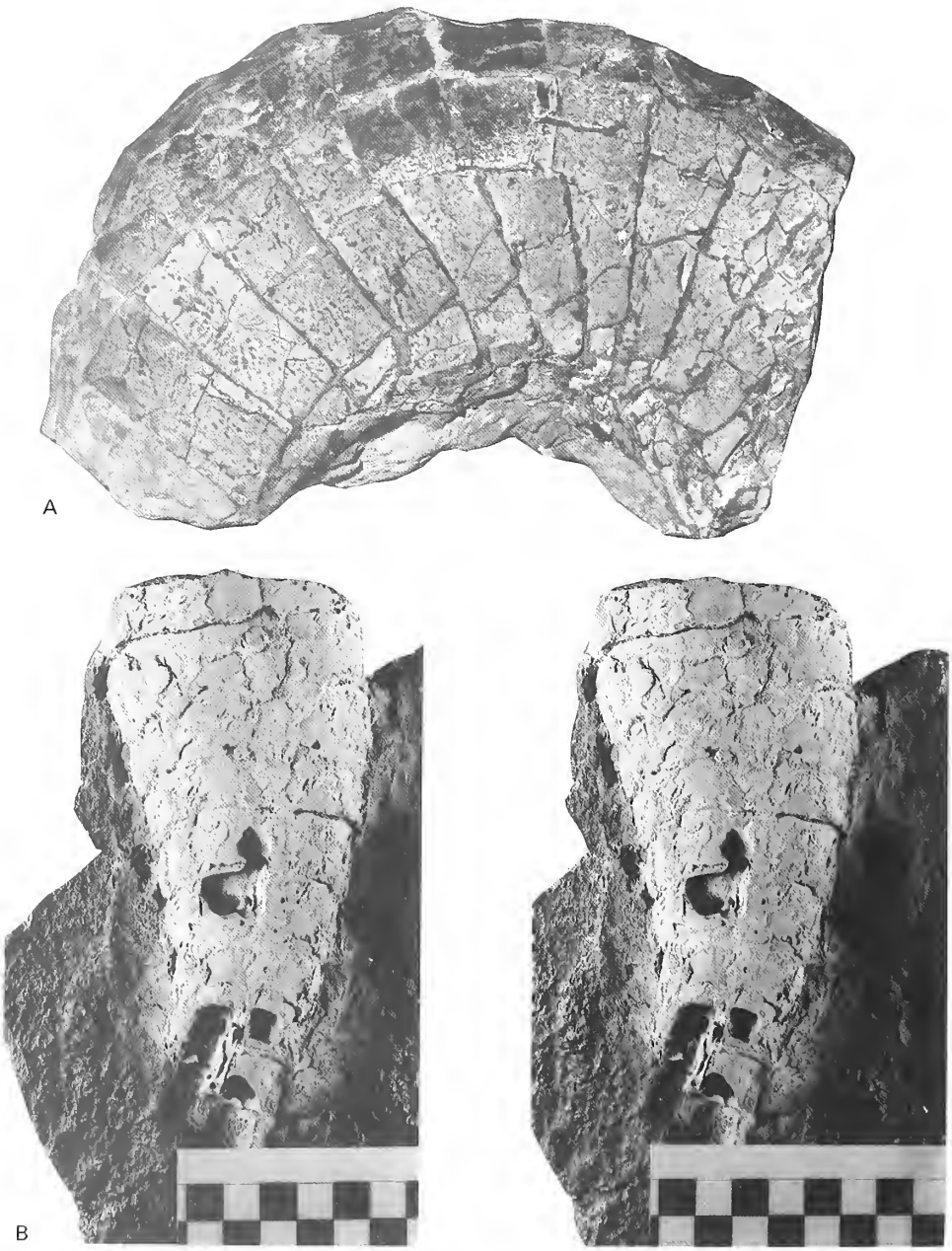

TEXT-FIG. 3. Selected specimens of *Aetosaurus*. A, SMNS 11837, holotype of *Aetosaurus crassicauda* Fraas, 1907; dorsal view of part of dorsal carapace. B, NJSM 10740; *Aetosaurus arcuatus* (Marsh, 1896); stereophotograph of partial tail. Both ×0·55.

Among the known aetosaurs, all these features are found only in *Aetosaurus* Fraas, 1877 (see Text-fig. 3A). Particularly significant is the pattern of pitting on the scutes and the lack of spikes or bosses. Most of the known aetosaurs have spikes on the scutes (e.g. Long and Murry 1995), but *Aetosaurus* lacks spikes and has a 'sunburst' pattern of pits and grooves on the scutes (e.g. Wild

TEXT-FIG. 4 *Aetosaurus arcuatus* (Marsh, 1896); NCSM 11756; North Carolina; partial tail, stereophotographs of dorsal (A) and ventral (B) aspects; ×0·66.

1989). Indeed, we are unable to distinguish specimens of *Stegomus* from *Aetosaurus* except by minor differences, so we consider the two genera to be synonymous.

On the holotype specimen of *Stegonus arcuatus* Marsh (1896), YPM 1647 (Pl. 1; Table 1), the pattern of sculpture on the scutes cannot be determined, but the specimen still preserves numerous details consistent with its assignment to *Aetosaurus*. The paramedian scutes lack ventral keels and are broadly rectangular, considerably wider than long, and do not appear to have possessed thickened lateral processes for articulation of the lateral scutes, as in some other aetosaurs, such as *Typothorax*. The lateral scutes are slightly wider than long, flat, and lack any indication of spinescence. In these characters, YPM 1647 clearly pertains to *Aetosaurus* as described originally by Fraas (1877) and subsequently by Fraas (1907), von Huene (1920), Walker (1961) and Wild (1989). We retain, however, a distinct North American species of the genus, *Aetosaurus arcuatus* (Marsh, 1896), based on the following features that distinguish it from *A. ferratus* Fraas, 1877 and *A. crassicauda* Fraas, 1907: the relatively high width:length ratio (3·5:1) of dorsal paramedian scutes in adult specimens, very faint pitting on the scutes, and rapid posterior narrowing of the tail.

DISTRIBUTION OF *AETOSARUS* IN THE NEWARK SUPERGROUP

Four specimens from the Newark Supergroup are referred to *Aetosaurus arcuatus*: (1) the holotype of *Stegomus arcuatus* Marsh from the New Haven Formation in Fair Haven, Connecticut; (2) the holotype of *S. arcuatus jerseyensis* Jepsen, an incomplete tail from the lower Passaic Formation at Neshanic Station, New Jersey; (3) the natural mould of the skull and dorsal armour of a juvenile from the Passaic Formation, Nishisakawick Creek, New Jersey; and (4) a partial tail from the 'Sanford Formation' at Triangle Brick Quarry, North Carolina.

The holotype of *Aetosaurus arcuatus* (Marsh, 1896) was collected by Freeman P. Clark in his brownstone quarry at Fair Haven, located within the city limits of New Haven, Connecticut. This quarry is developed in the New Haven Formation, a red-bed unit that consists mostly of arkosic sandstone and conglomeratic sandstone. The lower part of the New Haven Formation has yielded a Carnian–Norian palynoflora (Cornet 1977), and the upper part the procolophonid *Hypsognathus* and a sphenodontid (cf. *Sigmala*) indicative of a latest Triassic (probably Rhaetian) age (Huber *et al.* 1993*b*; Lucas and Huber 1993). The *Aetosaurus arcuatus* holotype is from the middle part of the New Haven Formation, which has been assigned a mid Norian age based on correlation with other, better dated Newark Supergroup strata (Lucas and Huber 1993).

The New Jersey specimens of *Aetosaurus* were both obtained from the Passaic Formation. The specimen described by Jepsen (1948) was recovered from a cellar excavation in strata belonging to the Neshanic Member of the Passaic Formation at Neshanic Station, New Jersey. The specimen described by Baird (1986) was obtained as a loose boulder from the bed of Nishisakawick Creek in nearby Frenchtown, New Jersey, from the stratigraphically lower Warford Member of the Passaic Formation. In the Newark basin, the thickness of the stratigraphical interval from the Warford to the Neshanic members of the Passaic Formation is about 600 m (Olsen *et al.* 1996, fig. 8). Based on palynostratigraphy, magnetostratigraphy, and cyclostratigraphy, Kent *et al.* (1995) assigned this interval to the early Norian with an estimated numerical age range of 215–218 Ma. The Newark basin occurrences of *Aetosaurus* in New Jersey thus establish the entire temporal range of *Aetosaurus* in the Newark Supergroup, and were used by Huber *et al.* (1993*b*) and Lucas and Huber (1993) to help define the Neschanician land-vertebrate faunachron (lvf), of early–mid Norian age.

The North Carolina specimen was described briefly in an abstract by Parker (1966). Its provenance is the Triangle Brick Quarry, near Glenlee, North Carolina, which exposes a 20 m thick section of fine–medium-grained arkosic and quartzose sandstone, siltstone and shale, mapped and informally named by Hoffman and Gallagher (1989) as 'Lithofacies Association II' of the Durham sub-basin of the Deep River basin, a unit that is the stratigraphical equivalent of the lower Sanford Formation in the adjacent Sanford sub-basin (Huber *et al.* 1993*a*). Other fossils from the Triangle Brick Quarry include megafossil plants (*Equisetum* stem fragments), darwinulid ostracodes,

abundant conchostracans, unionid bivalves, articulated crayfish, insects, bony fishes (*Synornichthys-Cionichthys*, *Turseodus*, *Semionotus*, *Osteplurus*), hybodontid elasmobranchs, several types of vertebrate coprolites, indeterminate labyrinthodont and phytosaur teeth and bone scrap, sphenosuchian and proterosuchian crocodylomorphs, and several, recently collected partial skeletons of a new rauisuchian currently under study by P. E. Olsen (pers. comm. 1995). Based on lithostratigraphical correlation of the Durham and Sanford sub-basin successions (Olsen *et al.* 1990), Lithofacies Association II is stratigraphically higher than the Cumnock Formation, which produced a tetrapod fauna of latest Carnian (late Tuvalian) age (Sanfordian lvf of the Newark Supergroup) (Huber *et al.* 1993*a*, 1993*b*). Hence, the Triangle Brick Quarry *Aetosaurus* comes from strata of early Norian age that belong to the early part of the Neshanician lvf, as defined by Huber *et al.* (1993*b*) and Lucas and Huber (1993).

BIOSTRATIGRAPHY AND BIOCHRONOLOGY

Tetrapod fossils provide one of the principal bases for the correlation of non-marine Triassic strata across Pangaea (Ochev and Shishkin 1989; Lucas 1990). During the Late Triassic, archosauromorph reptiles dominated tetrapod faunas. Two archosauromorph groups – phytosaurs (Parasuchidae) and aetosaurs (Stagonolepidae) – were broadly distributed across Pangaea, and their fossils are abundant in Late Triassic non-marine strata.

Phytosaurs have long been used for correlation of these strata (e.g. Camp 1930; Gregory 1957; Westphal 1976; Ballew 1989). However, they are not ideal index fossils because: (1) nearly an entire phytosaur skull is needed to make a genus- or species-level identification, whereas the vast majority of phytosaur fossils are isolated bones and skull fragments; and (2) phytosaur taxonomy is not well agreed on and generally oversplit, with three different taxonomic schemes (Ballew 1989; Hunt 1994; Long and Murry 1995).

An ideal index fossil should be widely distributed geographically, abundant, have a short temporal range, and be easily identifiable. Aetosaurs meet these four criteria:

1. Aetosaur fossils are found throughout most of Late Triassic Pangaea (Text-fig. 1). Indeed, they have a broader distribution than phytosaurs, most notably being known from Argentina, where phytosaurs have not been found (Lucas and Heckert 1996).
2. Aetosaurs are the most abundant tetrapod fossils in the Chinle Group (western USA) and the Ischigualasto Formation of Argentina (Lucas 1993; Rogers *et al.* 1993). They are common in many other Late Triassic deposits.
3. Stratigraphical/temporal ranges of aetosaur genera are usually relatively short – much less than a stage/age (Lucas and Heckert 1996) (Text-fig. 5).
4. Aetosaurs are easy to identify because their body armour is highly distinctive at the genus level (e.g. Long and Ballew 1985; Long and Murry 1995; Heckert *et al.* 1996; Lucas and Heckert 1996). A single piece or fragment of aetosaur armour, sometimes even as small as a postage stamp, can be precisely identified.

Recognition that *Stegomus* = *Aetosaurus* extends the record of this biostratigraphically significant taxon into the eastern United States. Here, we review the temporal distribution of *Aetosaurus* to establish its status as a non-marine index fossil of early–mid Norian time (Text-fig. 6).

Western United States

Hunt (1994) documented aetosaur scutes from the Bull Canyon Formation of the Chinle Group in east-central New Mexico. The holotype of a new genus he proposed, but did not publish, NMMNH P-17213, is a left dorsal paramedian scute, 75 mm wide and 31 mm long, so it has a low

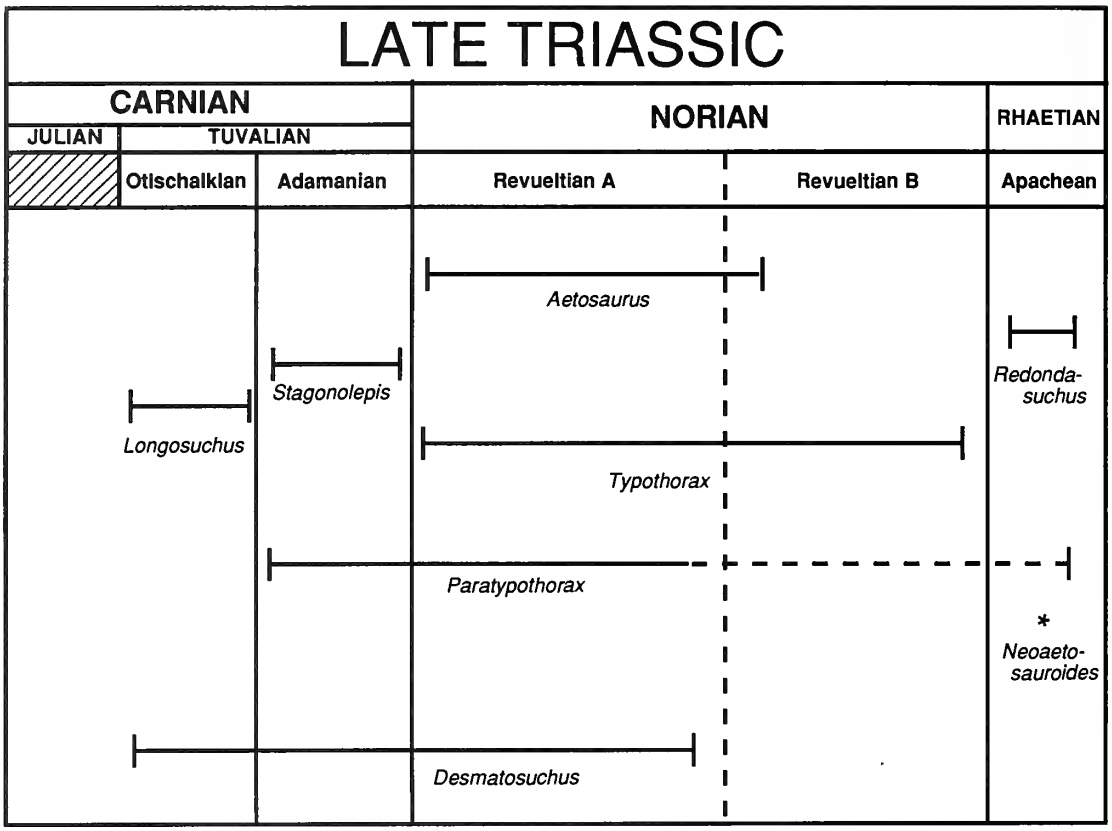

TEXT-FIG. 5. Late Triassic aetosaur biochronology (after Lucas and Heckert 1996).

width:length ratio of 2·4. The scute is slightly arched transversely, indicating that it is probably a caudal dorsal paramedian. The ornamentation consists of a very faint, radial pattern of elongate pits. It thus closely resembles the Newark specimens of *Aetosaurus arcuatus* reviewed here, and we assign it to that taxon. Another referred specimen from east-central New Mexico is NMMNH P-17615, a dorsal paramedian scute, 76 mm wide and 27 mm long, yielding a width:length ratio of 2·8. Associated scutes and possible material from the axial and the appendicular skeleton of these specimens will be described separately. The Bull Canyon Formation is considered to be of early–mid Norian age, based largely on the occurrence of the phytosaur *Pseudopalatus* and the aetosaur *Typothorax*, both of which are index taxa of the Revueltian lvf of Lucas and Hunt (1993).

Greenland

In Greenland, *Aetosaurus ferratus* occurs in the Ørsted Dal Member of the Fleming Fjord Formation (Jenkins *et al.* 1994). The Ørsted Dal Member has yielded a diverse assemblage of vertebrates: the plagiosaurid *Gerrothorax* cf. *pulcherrimus* Fraas, the cyclotosaur *Cyclotosaurus* cf. *posthumus* Fraas, the turtle cf. *Proganochelys*, the aetosaurs *Aetosaurus ferratus* Fraas and *Paratypothorax andressi* Long and Ballew, the prosauropod dinosaur *Plateosaurus engelhardti* Meyer, a theropod dinosaur, the mammals *Kuehneotherium* sp. and cf. *Brachyzostrodon*?, a pterosaur, coelacanth fishes, *Saurichthys*?, a lungfish, unidentified sphenodonts and lepidosaurs? and theropod dinosaur footprints (*Grallator* sp.) (Jenkins *et al.* 1994).

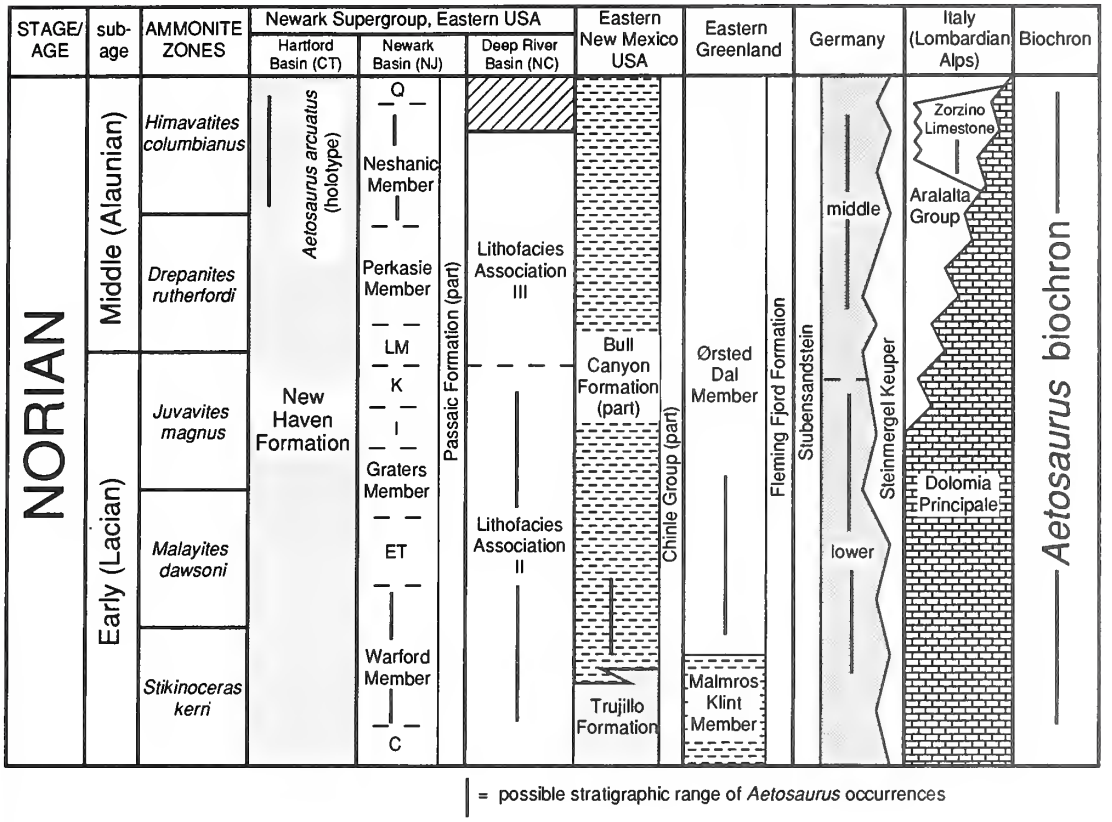

TEXT-FIG. 6. Correlation of *Aetosaurus*-yielding strata. Vertical bars indicate possible stratigraphical ranges of *Aetosaurus* occurrences. However, actual stratigraphical ranges are probably much shorter, but determination of this requires more precise stratigraphical data than are currently available for most *Aetosaurus* occurrences.

As Jenkins *et al.* (1994) concluded, this assemblage shares many taxa with the German Stubensandstein and clearly is of Norian age. The closest similarity to the Ørsted Dal assemblage is the vertebrate assemblage of the Lower Stubensandstein, especially the co-occurrence in both units of *Aetosaurus ferratus* and *Paratypothorax andressi*, as well as *Cyclotosaurus*, *Gerrothorax* and *Proganochelys*. We thus regard the Ørsted Dal Member vertebrates as of early Norian age (Text-fig. 6). However, we note that Jenkins *et al.* (1994) presented no precise stratigraphical ordering of vertebrate fossil localities in the 150–200-m thick Ørsted Dal Member and that some taxa from the Ørsted Dal Member (*Gerrothorax*, *Plateosaurus*) do not occur in the Lower Stubensandstein, but first appear in the Middle Stubensandstein (Benton 1993, table 1). Therefore, the possibility exists that the Ørsted Dal vertebrate assemblage includes temporal equivalents of both the Lower and Middle Stubensandstein.

Germany

In Germany, *Aetosaurus* is well documented from the Lower Stubensandstein (*A. ferratus*) and the Middle Stubensandstein (*A. crassicauda*) of the German Keuper (O. Fraas 1877; E. Fraas 1907; Wild 1989). Palynostratigraphy, vertebrate biostratigraphy, and sequence stratigraphy suggest that

the Stubensandstein is of early to mid Norian age (Brenner 1973; Brenner and Villinger 1981; Visscher and Brugman 1981; Benton 1986, 1993; Wild 1989; Aigner and Bachman 1992; Kozur 1993; Lucas and Huber 1994). The most precise correlation available suggests that the Lower Stubensandstein is early Norian, whereas the Middle Stubensandstein is mid Norian (e.g. Benton 1993). This suggests that *Aetosaurus* in Germany has an early–mid Norian temporal range comparable to its temporal range in the Newark Supergroup (Text-fig. 6).

Italy

Wild (1989) documented *Aetosaurus ferratus* from the marine Calcare di Zorzino Formation (= Zorzino Limestone) at Cene, near Bergamo in the Lombardian Alps of northern Italy. The Calcare di Zorzino Formation is a carbonate and turbidite facies that immediately overlies and is in part laterally equivalent to the Norian Dolomia Principale (= Hauptdolomit). After the regional progradation of platform carbonates (Dolomia Principale) during the early–mid Norian, extensional tectonism produced intraplatform depressions in which the Zorzino Limestone (Aralalta Group; Jadoul 1985) was deposited as patch reefs, turbiditic debris flows and lagoonal to freshwater facies (Jadoul *et al.* 1994). Palynostratigraphy and conodont biostratigraphy indicate that the fossil vertebrate locality in the Zorzino Limestone near Bergamo is very close to the Alaunian (mid Norian)–Sevatian (late Norian) boundary (Jadoul *et al.* 1994; Roghi *et al.* 1995; Tintori and Lombardo 1996). This indicates that the *Aetosaurus* occurrence documented by Wild (1989) is of late mid Norian age, and correlates with the younger part of the *Himavatites columbianus* Zone of the global Triassic ammonite biochronology (Tozer 1994). This provides a direct cross-correlation of an *Aetosaurus* occurrence to marine Triassic biochronology (Text-fig. 6).

Discussion

The direct cross-correlation of *Aetosaurus* from Italy to the middle Norian accords well with the inferred age of some *Aetosaurus* records in Germany and the United States. However, the German and American records suggest that *Aetosaurus* existed during both the early and mid Norian. Although this is consistent with cross-correlation to the Italian marine occurrence of *Aetosaurus*, the German and Newark Supergroup records obviously encompass a longer temporal range (Text-fig. 6) than the single Italian occurrence.

The total known temporal range of *Aetosaurus* thus equals about four ammonite zones, which is about half of Norian time, approximately 5–7 million years on most numerical time scales (e.g. Kent *et al.* 1995). *Aetosaurus* thus emerges as a tetrapod taxon capable of providing a robust correlation across much of Late Triassic Pangaea and is an index fossil of early–mid Norian time.

Acknowledgements. R. Barrick, P. Holroyd, D. Parris and M. A. Turner made it possible for us to study specimens of *Stegomus*. A. Tintori provided information on the age of the Zorzino Limestone, and A. Hunt provided useful discussion. The comments of two anonymous reviewers improved this article. The National Geographic Society (Grant 5412-95 to SGL) supported part of this research.

REFERENCES

AIGNER, T. and BACHMANN, G. H. 1992. Sequence-stratigraphic framework of the German Triassic. *Sedimentary Geology*, **80**, 115–135.

BAIRD, D. 1986. Some Upper Triassic reptiles, footprints and an amphibian from New Jersey. *The Mosasaur*, **3**, 125–135.

BALLEW, K. L. 1989. A phylogenetic analysis of Phytosauria from the Late Triassic of the western United States. 309–339. *In* LUCAS, S. G. and HUNT, A. P. (eds). *Dawn of the age of dinosaurs in the American Southwest*. New Mexico Museum of Natural History, Albuquerque, 414 pp.

BENTON, M. J. 1986. The Late Triassic tetrapod extinction events. 303–320. *In* PADIAN, K. (ed.). *The beginning of the age of dinosaurs*. Cambridge University Press, Cambridge, 378 pp.

—— 1993. Late Triassic terrestrial vertebrate extinctions: stratigraphic aspects and the record of the Germanic basin. *Paleontologia Lombardia, Nuova Series*, **2**, 19–38.

—— and CLARK, J. M. 1988. Archosaur phylogeny and the relationships of the Crocodylia. 295–338. *In* BENTON, M. J. (ed.). *The phylogeny and classification of the tetrapods. Volume 1: amphibians, reptiles, birds*. Clarendon Press, Oxford, 377 pp.

BRENNER, K. 1973. Stratigraphie und Paläogeographie des Oberen Mittelkeupers in Südost-Deutschland. *Arbeiten aus dem Institut für Geologie und Paläontologie der Universität Stuttgart*, **68**, 101–222.

—— and VILLINGER, E. 1981. Stratigraphie und Nomenklatur des südwesdeutschen Sandsteinkeupers. *Jahreshefte Geologische Landesamt von Baden-Württemberg*. **23**, 45–86.

CAMP, C. L. 1930. A study of the phytosaurs, with description of new material from western North America. *Memoirs of the University of California*, **10**, 1–161.

CORNET, B. 1977. The palynostratigraphy and age of the Newark Supergroup. Unpublished Ph.D. dissertation, Pennsylvania State University.

FRAAS, E. 1907. *Aëtosaurus crassicauda* n. sp., nebst Beobachtungen über das Becken der Arëtosaurier. *Jahreshefte des Vereins für vaterländische Naturkunde Württemberg*, **63**, 101–109.

FRAAS, O. 1877. *Aetosaurus ferratus* Fr. Die gepanzerte Vogel-Echse aus dem Stubensandstein bei Stuttgart. *Wurttemberger Naturwissenschaften Jahrbuch*, **33**(3), 1–22.

GREGORY, J. T. 1957. Significance of fossil vertebrates for correlation of the Late Triassic continental deposits of North America. *Report of the 20th Session, International Geological Congress*, Section 2, 7–25.

HECKERT, A. B., HUNT, A. P. and LUCAS, S. G. 1996. Redescription of *Redondasuchus reseri*, a Late Triassic aetosaur (Reptilia: Archosauria) from New Mexico (U.S.A.), and the biochronology and phylogeny of aetosaurs. *Geobios*, **29**, 619–632.

HOFFMAN, C. W. and GALLAGHER, P. E. 1989. Geology of the Southeast and Southwest Durham 7·5-minute quadrangles, North Carolina. *Bulletin of the North Carolina Geological Survey*, **92**, 1–34.

HUBER, P., LUCAS, S. G. and HUNT, A. P. 1993*a*. Revised age and correlation of the Upper Triassic Chatham Group (Deep River Basin, Newark Supergroup), North Carolina. *Southeastern Geology*, **33**, 171–193.

—— —— —— 1993*b*. Vertebrate biochronology of the Newark Supergroup Triassic, eastern North America. *Bulletin of the New Mexico Museum of Natural History and Science*, **3**, 179–186.

HUENE, F. von 1908. On the age of the reptile faunas contained in the Magnesian Conglomerate at Bristol and in the Elgin Sandstone. *Geological Magazine*, **5**, 99.

—— 1920. Osteologie von *Aetosaurus ferratus* O. Fraas. *Acta Zoologica*, **1**, 465–491.

HUNT, A. P. 1994. Vertebrate paleontology and biostratigraphy of the Bull Canyon Formation (Chinle Group, Upper Triassic), east-central New Mexico with revisions of the families Metoposauridae (Amphibia: Temnospondyli) and Parasuchidae (Reptilia: Archosauria). Unpublished Ph.D. dissertation, University of New Mexico.

JADOUL, F. 1985. Stratigrafia e paleogeografia del Norico nelle Prealpi Bergamasche occidentali. *Rivista Italiana di Paleontologia a Stratigrafia*, **91**, 479–512.

—— MASETTI, D., CIRILLI, S., BERRA, S., CLAPS, M. and FRISIA, S. 1994. Norian–Rhaetian stratigraphy and paleogeographic evolution of the Lombardy basin (Bergamasc Alps). *15th International Association of Sedimentologists, Regional Meeting, April 1994, Ischia, Italy, Field Excursion B1, Salermo, Italy*, 5–38.

JENKINS, F. A. Jr, SHUBIN, N. H., AMARAL, W. W., GATESY, S. M., SCHAFF, C. R., CLEMMENSEN, L. B., DOWNS, W. R., DAVIDSON, A. R., BONDE, N. and OSBÆCK, F. 1994. Late Triassic continental vertebrates and depositional environments of the Fleming Fjord Formation, Jameson Land, East Greenland. *Meddelelser om Grønland, Geoscience*, **32**, 1–25.

JEPSEN, G. L. 1948. A Triassic armored reptile from New Jersey. *State of New Jersey Department of Conservation Miscellaneous Geologic Paper*, 1–20.

KENT, D. V., OLSEN, P. E. and WITTE, W. K. 1995. Late Triassic–earliest Jurassic geomagnetic polarity sequence and paleolatitudes from drill cores in Newark rift basins, eastern North America. *Journal of Geophysical Research*, **100**, 14965–14998.

KOZUR, H. 1993. Annotated correlation tables of the Germanic Buntsandstein and Keuper. *Bulletin of the New Mexico Museum of Natural History and Science*, **3**, 243–248.

LOCKLEY, M. and HUNT, A. P. 1995. *Dinosaur tracks and other fossil footprints of the western United States*. Columbia University Press, New York.

LONG, R. A. and BALLEW, K. L. 1985. Aetosaur dermal armor from the Late Triassic of southwestern North America, with special reference to material from the Chinle Formation of Petrified Forest National Park. *Bulletin of the Museum of Northern Arizona*, **54**, 45–68.

LONG, R. A. and MURRY, P. A. 1995. Late Triassic (Carnian and Norian) tetrapods from the southwestern United States. *Bulletin of the New Mexico Museum of Natural History and Science*, **4**, 1–254.

LUCAS, S. G. 1990. Toward a vertebrate biochronology of the Triassic. *Albertiana*, **8**, 36–41.

—— 1993. The Chinle Group: revised stratigraphy and biochronology of Upper Triassic nonmarine strata in the western United States. *Bulletin of the Museum of Northern Arizona*, **59**, 27–50.
—— and HECKERT, A. B. 1996. Late Triassic aetosaur biochronology. *Albertiana*, **17**, 57–64.
—— and HUBER, P. 1993. Revised internal correlation of the Newark Supergroup Triassic, eastern United States and Canada. *Bulletin of the New Mexico Museum of Natural History and Science*, **3**, 311–319.
—— —— 1994. Sequence stratigraphic correlation of Upper Triassic marine and nonmarine strata, western United States and Europe. *Memoir of the Canadian Society of Petroleum Geologists*, **17**, 241–254.
—— and HUNT, A. P. 1993. Tetrapod biochronology of the Chinle Group (Upper Triassic), western United States. *Bulletin of the New Mexico Museum of Natural History and Science*, **3**, 327–329.
LULL, R. S. 1915. Triassic life of the Connecticut Valley. *Bulletin of the Connecticut Geologic and Natural History Survey*, **24**, 1–285.
—— 1953. Triassic life of the Connecticut Valley revised. *Bulletin of the Connecticut Geologic and Natural History Survey*, **81**, 1–336.
LYDEKKER, R. 1887. The fossil Vertebrata of India. *Records of the Geological Survey of India*, **20**, 51–80.
MARSH, O. C. 1896. A new belodont reptile (*Stegomus*) from the Connecticut River Sandstone. *American Journal of Science*, **2**, 59–62.
OCHEV, V. G. and SHISHKIN, M. A. 1989. On the principles of global correlation of the continental Triassic on the tetrapods. *Acta Palaeontologica Polonica*, **34**, 149–173.
OLSEN, P. E., FROELICH, A. J., DANIELS, D. L., SMOOT, J. P. and GORE, P. J. W. 1990. Rift basins of early Mesozoic age. 142–170. *In* HORTON, J. W. and ZULLO, V. A. (eds). *The geology of the Carolinas*. University of Tennessee Press, Knoxville, 180 pp.
—— KENT, D. V., CORNET, B., WITTE, W. K. and SCHISHE, R. W. 1996. High-resolution stratigraphy of the Newark rift basin (early Mesozoic, eastern North America). *Bulletin of the Geological Society of America*, **108**, 40–77.
PARKER, J. M. III 1966. Triassic reptilian fossil from Wake County, North Carolina. *Journal of the Elisha Mitchell Society*, **82**, 92.
ROGERS, R. R., SWISHER, C. C. III, SERENO, P. C., MONETTA, A. M., FORSTER, C. A. and MARTINEZ, R. N. 1993. The Ischigualasto tetrapod assemblage (Late Triassic, Argentina) and 40Ar/39Ar dating of dinosaur origins. *Science*, **260**, 794–797.
ROGHI, G., MIETTO, P. and DALLA VECCHIA, F. M. 1995. Contribution to the conodont biostratigraphy of the Dolomia di Forni (Upper Triassic, Carnian, NE Italy). *Memoire Scienze Geologie*, **47**, 125–133.
TINTORI, A. and LOMBARDO, C. 1996. *Gabonella agilis*, gen. n. sp. n., (Actinopterygii, Perleidiformes) from the Calcare di Zorzino of Lombardy (North Italy). *Rivista Italiana di Paleontologia e Stratigrafia*, **102**, 227–236.
TOZER, E. T. 1994. Canadian Triassic ammonoid faunas. *Bulletin of the Geological Survey of Canada*, **467**, 1–663.
VISSCHER, H. and BRUGMAN, W. A. 1981. Ranges of selected palynomorphs in the Alpine Triassic of Europe. *Review of Palaeobotany and Palynology*, **34**, 115–128.
WALKER, A. D. 1961. Triassic reptiles from the Elgin area: *Stagonolepis*, *Dasygnathus*, and their allies. *Philosophical Transactions of the Royal Society of London, Series B*, **248**, 103–204.
WESTPHAL, F. 1976. Phytosauria. 99–120. *In*: *Encyclopedia of paleoherpetology*. Vol. 13.
WILD, R. 1989. *Aëtosaurus* (Reptilia: Thecodontia) from the Upper Triassic (Norian) of Cene near Bergamo, Italy, with a revision of the genus. *Revista del Museo Civico di Scienze Naturali 'Enrico Caffi'*, **14**, 1–24.

SPENCER G. LUCAS
New Mexico Museum of Natural History and Science
1801 Mountain Road NW
Albuquerque, NM 87104, USA

ANDREW B. HECKERT
Department of Earth and Planetary Sciences
University of New Mexico
Albuquerque, NM 87131-1116, USA

PHILLIP HUBER
Virginia Museum of Natural History
1001 Douglas Avenue
Martinsville, VA 24112, USA

Typescript received 6 March 1997
Revised typescript received 3 November 1997

PALAEONTOLOGICAL ASSOCIATION

ANNUAL ADDRESS

ALL-TIME GIANTS: THE LARGEST ANIMALS AND THEIR PROBLEMS

by R. MCNEILL ALEXANDER

ABSTRACT. The largest known swimming, walking and flying animals are all vertebrates. They include the blue whale (up to 190 tonnes), the largest sauropod dinosaurs (probably about 80 tonnes) and two flying animals estimated to have had masses of at least 75 kg, the pterosaur *Quetzalcoatlus* and the bird *Argentavis*. Even larger sizes might be physically possible, but may not have been attained because problems associated with size may make excessively large animals competitively inferior. These problems are discussed with frequent reference to basic consequences of geometric similarity (areas are proportional to the squares of lengths and volumes to the cubes) and to the empirical rule that metabolic rates of similar animals tend to be proportional to (body mass)$^{0.75}$. Excessively large animals would be liable to overheat, both in water and on land. Larger animals tend to have fewer individuals in each species, suggesting the possibility that the largest whales and dinosaurs approach the limits of size above which numbers would be unlikely to be large enough for long term viability. Even the largest dinosaurs seem to have been well able to support their weight on land. Flying animal size may have been limited more by the problem of taking off than by the power requirement for flight. The largest swimming animals are filter feeders and the largest land animals were herbivores, so neither are at the top of a long food chain.

THIS paper reviews the largest animals known to have lived, at any time in the Earth's history. I will consider the problems associated with their size, and ask why they did not evolve to be even larger. Aquatic, terrestrial and flying animals will be considered separately. Invertebrates cannot match the size of the largest vertebrates, so I will be concerned almost exclusively with vertebrates. Colonial animals such as corals are excluded from consideration.

PRINCIPLES OF ALLOMETRY

It may be helpful to start by noting some of the consequences of size differences, starting with a geometrical point. Bodies of identical shape, but different sizes (that is, geometrically similar bodies) have surface areas proportional to the squares of their lengths and volumes proportional to the cubes of their lengths: for example, a cube with sides twice as long as another has faces of four ($= 2^2$) times the area and has eight ($= 2^3$) times the volume. If the bodies are made of the same material, they have masses proportional to their volumes. Thus for different-sized animals of the same shape we expect to find

$$\text{mass proportional to (length)}^3$$

from which follows

$$\text{length proportional to (mass)}^{0.33}$$

and since area is proportional to length squared

$$\text{area proportional to (mass)}^{0.67}$$

[Palaeontology, Vol. 41, Part 6, 1998, pp. 1231–1245]

Plainly, even closely related animals of different sizes are not precisely the same shape. Lions have relatively smaller brains and eyes than domestic cats (Davis 1962) but, in many other respects, groups of animals are remarkably close to geometric similarity. For example, the lengths of whales ranging from 30 kg dolphins to 100 tonne blue whales are proportional to (body mass)$^{0.34}$ (Economos 1983). The lengths of the limb bones of mammals ranging from shrews to elephants are proportional to (body mass)$^{0.35}$ (Alexander *et al.* 1979). However, in some cases we find marked deviations from geometric similarity. If Bovidae (antelopes, etc.) are considered separately from other mammals, their limb bone lengths are proportional to (mass)$^{0.26}$ (Alexander *et al.* 1979). The wing spans of birds other than hummingbirds tend to be proportional to (mass)$^{0.39}$ and those of hummingbirds to (mass)$^{0.53}$ (Rayner 1988).

Further to those geometrical points, we need to note that the pace of life is generally slower for larger animals. These generally make repetitive movements at lower frequencies than small animals: for example, sparrows in flight make about 20 wing beat cycles per second and swans about three cycles per second (see Rayner 1988). There is a tendency, in groups of related animals, for frequencies to be about proportional to (body mass)$^{-0.25}$. For example, wing beat frequencies of birds (excluding hummingbirds) are proportional to (mass)$^{-0.27}$ (Rayner 1988) and heart frequencies of mammals to (mass)$^{-0.25}$ (Stahl 1967). However, not all frequencies scale so steeply. The stride frequencies of mammals using corresponding gaits are about proportional to (shoulder height)$^{-0.5}$ and so to (mass)$^{-0.17}$ (Pennycuick 1975).

Another aspect of the slower pace of life for larger animals is that metabolic rates do not increase in proportion to body mass. The metabolic rate of a 2000 kg elephant is not 10000 times that of a 0·2 kg rat, but only about 1000 times. More generally, metabolic rates of similar animals of different sizes are found to be about proportional to (body mass)$^{0.75}$. This applies not only to resting rates (Calder 1984), but also approximately to field metabolic rates and maximum aerobic rates, both of which are proportional, for mammals, to (mass)$^{0.81}$ (Weibel and Taylor 1981; Nagy 1987). There are marked differences between groups, notably between ectotherms and endotherms; even with its body at a mammal-like temperature of 37 °C, a typical lizard uses oxygen only about one-quarter as fast as a mammal of equal mass (see Alexander 1981, fig. 11-4). However, within each group the 0·75 power law holds well.

Most of the attempts that have been made to explain this law apply only to a limited range of organisms. However, a recent very general theory (West *et al.* 1997) derives the law by considering the energy cost of distributing resources through a branching network of tubes (for example a blood system) in organisms of different sizes.

The 0·75 power law of metabolic rate is related to the −0·25 law of frequencies. Consider two muscles that exert equal stresses while shortening by equal fractions of their lengths. The forces they exert are proportional to their cross sectional areas, and the distances they shorten are proportional to their lengths, so the amounts of work they do (force multiplied by distance) are proportional to their volumes, and so to their masses. If these muscles make up equal fractions of body mass and contract with frequencies proportional to (body mass)$^{-0.25}$, their power outputs are proportional to (mass)$^{0.75}$.

There is another general rule (in this case, a very imprecise one) that is useful. Large species tend to have fewer members than small ones so that in most cases, for instance, the world population of a species of elephant will be fewer in number than the world population of a species of mouse. There is a general tendency for the population density of a species to be proportional to (body mass)$^{-0.75}$ (Cotgreave 1993). This has been interpreted as implying an energetic equivalence rule: if species of different sizes have numbers proportional to (mass)$^{-0.75}$ and metabolic rates proportional to (mass)$^{0.75}$, total rate of food intake will be the same for species of all sizes. However, several points should be noted. First, there is a great deal of scatter about the regression line: in many cases, a common species is 1000 times as numerous as a rare one of similar size. Second, some studies of particular groups have found exponents markedly different from −0·75. And finally, carnivore species tend to have many fewer members than herbivore species of similar size (Peters and Raelson 1984).

Subsequent sections of this paper apply the principles expounded in this one, in discussions of the consequences of large size for aquatic, terrestrial and flying animals. Crocodiles divide their time between land and water; they will be treated here as aquatic.

SWIMMING ANIMALS
(Text-fig. 1)

First, I shall consider aquatic animals. Before discussing the consequences for them of large size, I shall review some of the largest of them. The blue whale (*Balaenoptera musculus*) is not only the heaviest modern animal, but also the heaviest known to have lived at any time. Adult females, which grow larger than males, reach lengths of 30 m and masses (determined by weighing the carcase in pieces) of over 120 tonnes (Lockyer 1976). The heaviest recorded weighed 190 tonnes. There are eight other species of baleen whales, with adult masses ranging from 7 tonnes (the minke whale, *B. acutorostrata*) upwards. All of them are filter feeders, using the fringes of their baleen to strain small crustaceans or fishes from the plankton. Antarctic krill (Euphausioidea, about 50 mm long) are particularly important for the blue whale, but other species, with differently spaced bristles on their baleen, take mainly copepods or fishes (Nowak 1991).

There is a marked tendency for very large swimming animals to be filter feeders. The largest modern fishes are the whale shark, *Rhincodon typus*, which grows up to 13 m long with an estimated mass of at least 15 tonnes; and the basking shark, *Cetorhinus maximus*, which reaches 11 m and 8 tonnes (Matthews 1995). The basking shark feeds largely on copepods and crab larvae (Matthews and Parker 1950). The whale shark also feeds on zooplankton, but I know of no more precise description of its diet. Both these large sharks obtain their tiny prey by filtering. The largest known teleost fish, the Jurassic *Leedsichthys* (Martill 1988), was another filter feeder. It is known only from fragments, but these include the tail fin whose span of 2·7 m suggests a body length of 13 m.

Some other very large aquatic animals are predators on larger prey, mainly fishes and squid. By far the largest is the sperm whale, *Physeter catodon*, which attains 19 m and over 50 tonnes (Lockyer 1976). It feeds mainly on ammoniacal squid from substantial depths, prey whose bloated form suggests that they may not swim fast (Denton 1974). The killer whale (*Orcinus orca*; males reach 10 m and 9 tonnes) eats seals as well as fishes and squid (Nowak 1991). Male elephant seals, *Mirounga leonina*, have masses up to 3·7 tonnes and again feed mainly on fishes and squid (Nowak 1991). The great white shark, *Carcharodon carcharis*, preys on seals and dolphins as well as fishes (Wheeler 1975). The largest recorded modern specimen was 6·4 m long with a mass of 3·2 tonnes, but there are fossil *Carcharodon* teeth whose size indicates a body length of 13 m (Randall 1973). The largest known aquatic reptiles include the Cretaceous pliosaur *Kronosaurus* (12 m long; Romer 1959); the Triassic ichthyosaur *Shonisaurus* (14 m; Kosch 1990); and the Cretaceous crocodilian *Deinosuchus* (15 m; Steel 1989). All of these were apparently predators, but we have no direct evidence of their diets.

In comparison with these giants, the largest predatory teleosts are unimpressive. Current angling records are 0·71 tonnes for black marlin (*Makaira indica*) and 0·68 tonnes for bluefin tuna (*Thunnus thynnus*; Matthews 1995). Both feed mainly on schooling fish (Wheeler 1975). The ocean sunfish *Mola* grows larger, apparently to more than one tonne, but eats smaller prey such as jellyfishes and young fish (Wheeler 1975). Giant squid (*Architeuthis harveyi*) have immensely long tentacles, but the mantle is seldom more than 3 m long, and large specimens probably have masses of around 1 tonne (Clarke 1966).

We may ask why very large swimmers tend to be filter feeders. Consider first the rate (volume per unit time) at which water must be filtered. For animals taking the same food, this must be proportional to metabolic rate, and so to (body mass)$^{0·75}$. Blue whales and other rorquals take mouthfuls of water, which are then squeezed out through the baleen to filter out the food. If mouth volume is proportional to body mass and mouth-filling frequency (like other physiological frequencies, see above) to (mass)$^{-0·25}$, the rate of filtration will be proportional to (mass)$^{0·75}$, as

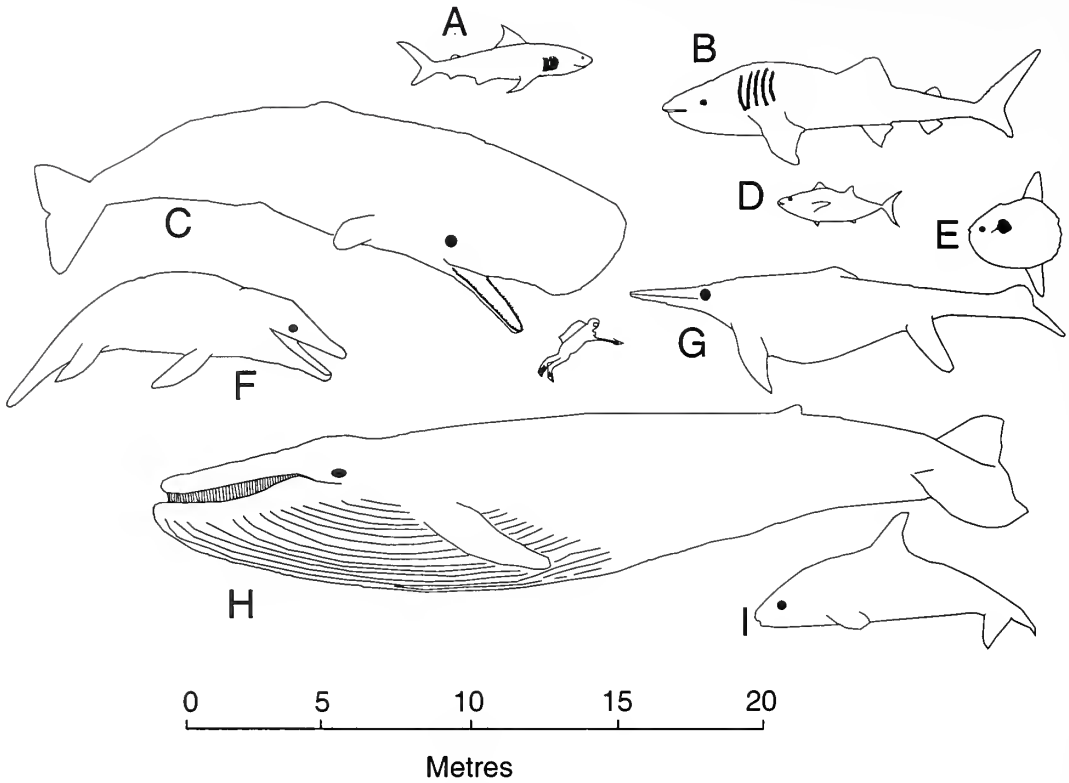

TEXT-FIG. 1. Some of the largest known swimming animals, drawn to a uniform scale. The names of extinct animals are asterisked. A, *Carcharodon*; B, *Rhincodon*; C, *Physeter*; D, *Thunnus*; E, *Mola*; F, *Kronosaurus**; G, *Shonisaurus**; H, *Balaenoptera*; and I, *Orcinus*.

required. Large size will present no problem. Right whales (*Balaena*) and filter-feeding sharks swim with their mouths open, straining out food with their baleen or gill rakers. Their rates of filtration will be mouth area multiplied by swimming speed. Geometric similarity would make mouth area proportional to $(\text{mass})^{0.67}$ so larger animals would have to swim a little faster to make filtration rates proportional to $(\text{mass})^{0.75}$ as required.

Considerations of energy cost suggest problems for very large filter feeders. Animals taking the same prey can be expected to have filters of equal mesh size, even if their bodies are very different in size. To obtain volumetric flow rates proportional to $(\text{mass})^{0.75}$ through filters whose areas are proportional to $(\text{mass})^{0.67}$, linear flow rates and so pressure drops must be proportional to $(\text{mass})^{0.08}$. The power required for filtration is the volumetric flow rate multiplied by the pressure drop, and so will be proportional to $(\text{mass})^{0.75} \times (\text{mass})^{0.08} = (\text{mass})^{0.83}$. Thus larger filter feeders may have to use a larger proportion of their food intake to drive the filtration process than smaller filter feeders. However, this conclusion could be avoided if fractal design made filter area increase with slight positive allometry (see Pennycuick 1992 on fractals). Also, at least some of the baleen whales appear to have fore stomachs which function as fermentation chambers, like the rumen of cattle (Herwig *et al.* 1984). If the chitin of crustacean exoskeletons is fermented, this may improve food utilization and so reduce the volume of water that must be filtered, alleviating the problem of energy cost for these very large filter feeders. In any case, the arguments in this paragraph fail to explain why the largest aquatic animals are filter feeders.

Now consider predation on prey which are too large to be filtered and must be pursued

individually. Slow prey may be able to escape from larger predators if they are better at swerving; the critical property is lateral acceleration (Howland 1974). The forces available for swerving can be expected to be proportional to muscle cross sectional area and so to $(\text{mass})^{0.67}$, and the accelerations they will provide will be proportional to $(\text{mass})^{-0.33}$. Thus predators can be expected to have trouble catching smaller prey. If the discrepancy of size between predators and prey is greater for larger predators, these may have most difficulty in catching prey. It may be significant that sperm whales feed largely on (probably) sluggish ammoniacal squid and killer whales hunt in groups, improving their chances of catching prey by making it harder for prey to escape by swerving (Howland 1974).

These arguments seem inconclusive; they fail to make it clear why so many of the largest swimmers are filter feeders. Another possible reason relates to the problem of maintaining a population of viable size, of very large animals. Filter feeders, taking food from relatively low in the food chain, have a more abundant energy supply than predators taking prey from higher in the food chain. If size were limited by the problem of obtaining enough energy to support a viable population, we would expect filter feeders to evolve to larger sizes than predators on large prey. Similarly, among terrestrial mammals herbivores have evolved to larger sizes than carnivores, and herbivore species have higher population densities than carnivore species of similar size. Similar reasoning might lead us to expect that because endotherms such as whales need more energy than ectotherms of similar size such as sharks, the largest animals should be ectotherms, which they are not. Similarly, terrestrial mammals need more energy than similar-sized (ectothermic) reptiles; thus we might expect reptiles to be more abundant than mammals of equal size, but they are not (Peters, 1983). These discrepancies show that we should be cautious in formulating arguments of this kind.

It seems unlikely that the blue whale has reached the maximum size consistent with a viable population. Prior to human exploitation, it is estimated that the world population comprised 200000 individuals (Nowak 1991). A recent estimate that the minke whale population of the north-east Atlantic is now about 120000 has raised confidence in the viability of this species to such an extent that it has been suggested that some hunting could be permitted (Motluk 1996). In their guidelines for assessing threats of extinction, Mace and Lande (1991) associated their lowest level of threat ('vulnerable') with a population size of only 10000 or less. However, they were concerned with extinction in periods of the order of centuries, whereas our concern is with viability over periods of millions of years. If smaller populations were viable, larger animals would be possible.

Another potential problem for very large animals is that excessively large ones would overheat. An animal may be thought of as a core, in which heat is liberated by metabolism and in which blood circulation maintains uniform temperature; enclosed by an insulating layer of skin with (in some cases) blubber, fur or feathers. The physics of heat conduction tells us that the temperature difference across the insulating layer is proportional to the metabolic rate divided by the thermal conductance of the insulation. Metabolic rate can be expected to be proportional to $(\text{body mass})^{0.75}$, as previously noted. Conductance should be proportional to surface area divided by insulation thickness, and so to $(\text{mass})^{0.67}/(\text{mass})^{0.33} = (\text{mass})^{0.33}$. Then the temperature difference across the insulating layer will be proportional to $(\text{mass})^{0.75}/(\text{mass})^{0.33} = (\text{mass})^{0.42}$, and excessively large animals would overheat. Ryg *et al.*'s (1993) calculations indicate that when a blue whale makes full use of the heat-insulating potential of its blubber, its basal metabolism is enough to heat it 40 K (centigrade degrees) above ambient, maintaining a typical mammalian body temperature of 38 °C in sea water at its freezing point of −2 °C. Field metabolic rates of large mammals are typically twice basal rates (Nagy 1987), so the whale's problem is not to keep warm, but to avoid overheating. It does this by sending blood to the dermis, bypassing the blubber. Hokkanen (1990) calculated that with maximal blood flow to the dermis, a blue whale metabolizing at 1·5 times the estimated basal rate could just avoid overheating in water at 29 °C. Tropical surface water temperatures are about 27 °C. These data suggest that the largest whales may be near the maximum size set by the overheating problem.

Even if this is the case, the largest fishes and aquatic reptiles are in no danger of overheating. They are much smaller than the blue whale, and their metabolic rates are presumably far below

those of similar-sized mammals. Tunnies and other 'warm blooded' fishes owe their elevated body temperatures more to vascular heat exchangers than to their size (Carey 1982). Leatherback turtles (*Dermochelys coriacea*) have metabolic rates intermediate between predictions for reptiles and mammals of their mass, enabling a 400 kg specimen to keep its body 18 K warmer than the water (Paladino *et al.* 1990).

TERRESTRIAL ANIMALS
(Text-fig. 2)

Now I will review and discuss the largest terrestrial animals. Among these, the largest known are sauropod dinosaurs, all of them extinct. The linear dimensions of sauropods are known from skeletons but their masses can only be estimated. This has been attempted in two ways. First, scale models have been made of the animals as they are believed to have appeared in life and their volumes have been determined, preferably by a method that depends on Archimedes' Principle. Then the volume of the living animal has been estimated by scaling up from the model, and the animal's mass calculated by assuming a density in the range observed for related modern animals (see Alexander 1985). Alternatively, the circumferences of fossil leg bones have been used to estimate body mass, by extrapolating from empirical relationships established for modern mammals (Anderson *et al.* 1985). A relationship based on mammals seems appropriate because we know from fossil footprints that dinosaurs did not adopt the sprawling stance of modern reptiles, but walked more like mammals (Thulborn 1990; Lockley 1991).

The largest dinosaur known from a reasonably complete (albeit composite) skeleton is *Brachiosaurus brancai*. It is about 25 m long, measured along the vertebral column (Paul 1988). Its mass has been estimated by both methods, yielding values ranging from 32 to 87 tonnes (Alexander 1989). Paul (1988) and Alexander (1989) both give values of 45–50 tonnes, and these are probably the best estimates. The Chicago skeleton of *B. altithorax* is a little smaller (Paul 1988). Other large sauropods known by more-or-less complete skeletons are *Apatosaurus louisae* (about 35 tonnes according to Alexander 1989, although Paul, who prefers very 'skinny' reconstructions, gives it only half that mass), and *Diplodocus carnegiei* (estimates range from 6 to 19 tonnes).

A few bones are known of sauropods that may have been heavier than *Brachiosaurus*. The bones described as '*Ultrasaurus*' seem to be from large specimens of *B. altithorax* of about 50 tonnes (Paul 1988). '*Supersaurus*' may be a *Diplodocus* species (Paul 1988). Its scapulocoracoid is 2·7 m long, compared with 1·542 m for *Diplodocus carnegiei*. Hence if *D. carnegiei* had a mass of 15 tonnes (within the range of estimates given above) the mass of *Supersaurus* may have been $15 \times (2700/1542)^3 = 80$ tonnes. The huge femur of *Antarctosaurus* is 2·31 mm long, compared with 1·785 m for *Apatosaurus louisae*. If the latter had a body mass of 35 tonnes, geometric scaling suggests a mass for *Antarctosaurus* of $35 \times (2310/1785)^3 = 75$ tonnes. However, the circumference of the femur is only 0·8 m, suggesting a more slender build and a lower mass (Paul 1988). It has been claimed that *Seismosaurus* may have had a mass of 100 tonnes (Gillette 1994), but the sparse remains (including no limb bones) seem inadequate to support the claim. These data suggest that the heaviest dinosaurs may have been between 50 and 80 tonnes. This is immensely heavier than the largest modern land animal, the African elephant (*Loxodonta africana*: large males are around 5·5 tonnes; Laws 1966). Adult male masses for other very large land mammals include 2·2 tonnes for white rhinoceros (*Ceratotherium simum*), 1·5 tonnes for hippopotamus (*Hippopotamus amphibius*) and 1·2 tonnes for giraffe (*Giraffa camelopardalis*; Owen-Smith 1988).

Although the large dinosaurs were sauropods, several other groups had members that were at least as heavy as any modern terrestrial animals. Mass estimates for herbivores include 5 tonnes for *Iguanodon* and 6 tonnes or more for *Triceratops* (Alexander 1989).

The only terrestrial animals known to have approached the size of the large sauropods are a few gigantic mammals. The largest of these was probably *Indricotherium*, a hornless Oligocene rhinocerotoid which Economos (1981) estimated to have had a mass of 20 tonnes. Others, including myself (Alexander 1989) have suspected it of being even heavier, up to 34 tonnes. However, it now appears that the early restoration on which these mass estimates were based is misleading. A careful

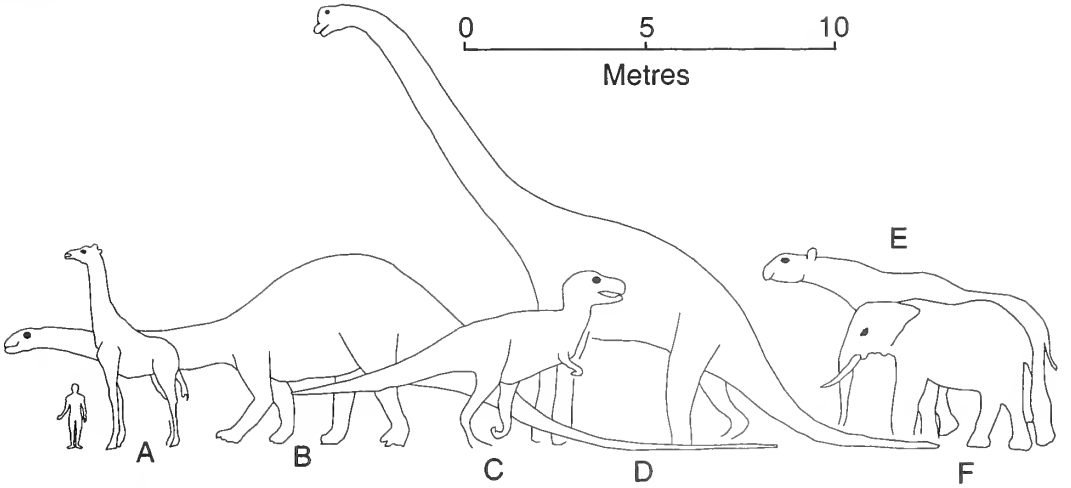

TEXT-FIG. 2. Some of the largest known terrestrial animals, drawn to scale. In the case of extinct animals (asterisked), only those known from reasonably complete skeletons are included. A, *Giraffa*; B, *Apatosaurus**; C, *Tyrannosaurus**; D, *Brachiosaurus**; E, *Indricotherium**; and F, *Loxodonta*.

analysis by Fortelius and Kappelman (1993) led to the conclusion that the bones that have been found come from specimens with an average mass of only 11 tonnes and that the largest specimens were probably little more than 15 tonnes. Two species of the related genus *Paraceratherium* were only a little smaller, and Fortelius and Kappelman argued that the largest complete mammoth (*Mammuthus*) skeleton may be from a 14 tonne animal. Other large extinct herbivores include pareiasaurs, dinocephalians and dicynodonts, but these were no larger than the largest modern mammals.

The largest known terrestrial carnivores are much smaller than the sauropods. The best known is *Tyrannosaurus rex*, which was about 12 m long with a mass of about 7 tonnes (Alexander 1989; Farlow *et al.* 1995). Two other theropods, *Giganotosaurus* (Coria and Salgado 1995) and *Carcharodontosaurus* (Sereno *et al.* 1996), may have been a little heavier.

The largest rauisuchids (early archosaurs) attained lengths of 6 m (Benton 1997). Apart from these, and the theropods, there seem to have been no terrestrial carnivores of more than 1 tonne, at any time. The largest modern examples are polar bears (*Ursus maritimus*; adult males are about 500 kg) and Siberian tigers (*Panthera tigris altaica*, about 250 kg; Nowak 1991). The crocodilians have been discussed already, as aquatic carnivores.

The question has often been asked, whether the largest dinosaurs could have supported their weight on land? The alternative would have been for them to have waded in water deep enough to have supported much of their weight by buoyancy. The question arises because for geometrically similar animals made of the same materials, weight increases as the cube of length, but bone and muscle cross sectional areas (and so strength) only in proportion to the square. Therefore, larger animals are expected to be less able to support their own weight.

Evidence that the large sauropods could support their weight on land comes from several sources. First, morphological comparisons with terrestrial mammals such as rhinoceroses and elephants, and with the semiaquatic hippopotamus, favour terrestrial habits (Bakker 1971). Second, many sauropod footprints are more sharply defined than seems consistent with their having been formed under water (Thulborn 1990). Third, the dimensions of leg bones of large sauropods such as *Apatosaurus* indicate that they were amply strong enough to support the animals' estimated weight. Alexander (1985) pointed out that bending moments due to components of force at right angles to

the long axes of bones are more likely to set up dangerous stresses than are axial forces. With that in mind, I defined a 'strength indicator' which expressed the strength in bending of a leg bone (estimated from its dimensions) in relation to the load that the weight of the body would impose on it. If the bones of an extinct animal have strength indicators equal to those of homologous bones of a similarly proportioned modern one, they were strong enough to allow the extinct animal to move in dynamically similar fashion to the modern one. The legs of *Apatosaurus* are quite similar in the relative lengths of the bones to those of the African elephant *Loxodonta*, and homologous leg bones of the two species have very similar strength indicators. This implies that *Apatosaurus* had leg bones strong enough for it to have moved as athletically as elephants, which easily support their weight on land and indeed can run moderately fast, although they cannot jump. Hokkanen (1986) discussed how large a dinosaur could be, and concluded that even a sauropod of well over 100 tonnes could have legs strong enough to support itself on land. Thus sauropod size seems not to have been limited by problems of support.

Another possibility we should consider is that dinosaur size was limited by the danger of overheating. Suppose first, as Bakker (1986) does, that the dinosaurs were endotherms with metabolic rates as estimated by extrapolation for mammals of their mass. We know that whales larger than any known dinosaur survive without overheating, even in the tropics where surface water temperatures may be as high as 27 °C. The effective temperatures of terrestrial habitats (averaged over day and night since we are considering very large animals which will heat and cool slowly) are probably seldom higher than this at the present day. In the Mesozoic, temperatures that we think of as tropical extended to higher latitudes than now, and equatorial temperatures seem to have been a few degrees higher (Hallam 1985).

It seems necessary to explain what I mean by the effective temperature of a habitat. Different parts of the environment (air, ground, vegetation, sky) will be at different temperatures, and heat balance may also be affected by solar radiation. The 'equivalent blackbody temperature' (Campbell 1977) is the temperature at which a body that was not producing heat or evaporating water would reach equilibrium in the environment. By the effective environmental temperature I mean the equivalent blackbody temperature averaged over 24 h. The observation that whales can live in tropical seas suggests that the largest dinosaurs could have avoided overheating at similar effective environmental temperatures on land, even if their metabolic rates were as high as would be predicted for mammals of the same mass. In this argument I have not referred to the difference in heat loss rates in air and in water because, although small animals lose heat much faster in water, the difference is trivial for animals of more than 100 kg (Bell 1980).

In another approach to the problem of overheating, Alexander (1989) considered the heat balance of a brachiosaur with mammal-like metabolism, estimating its rate of loss of heat by extrapolation from Bell's (1980) data on cooling rates for smaller reptiles. I estimated that, unless it dissipated excess heat by evaporation of water, an endothermic brachiosaur would be at least 60 K warmer than its environment, which would be lethal except in extreme cold. Comparison with whales (as in the previous paragraph) suggests that this temperature difference has been overestimated, but even so we must doubt the viability of a brachiosaur with mammal-like metabolism, especially in warm Mesozoic climates, where the quantities of water that would have to evaporate to prevent overheating would be enormous. A more sophisticated analysis by Hokkanen (1989) led to a similar conclusion, that a *Brachiosaurus* with mammal-like metabolism would probably not be viable in a hot climate.

Alexander (1989) also estimated body temperatures for ectothermic brachiosaurs, with metabolic rates as predicted for modern reptiles of equal mass. Unfortunately, my table 7.1 contained arithmetic inconsistency which has been pointed out to me by Dr Brian Bodenbender, to whom I am grateful. Also, my argument was simplistic: it should have taken account of the dependence of a reptile's resting metabolic rate on body temperature. A corrected form of the argument follows.

An animal with body temperature T_{body} in an environment at temperature T_{env} loses heat at a rate $(T_{body} - T_{env})\, C/\tau$, where C is the heat capacity of the body and τ is the thermal time constant (the quantity given by Bell 1980, for many reptiles). This formula is explained by Alexander (1989). At

equilibrium this heat loss is balanced by metabolic heat production at a rate $R(m, T_{body})$, that is at a rate that depends both on body mass and on body temperature.

$$(T_{body} - T_{env})\, C/\tau = R(m, T_{body}),$$

Bennett and Dawson (1976) gave equations relating metabolic rate to body mass, for several groups of reptiles at several temperatures. I will use their equations for lizards, which cover the widest temperature range. These give metabolic rates for a 50 tonne brachiosaur of 770 W at a body temperature of 20 °C, 3270 W at 30 °C and 4840 W at 37 °C. These enable us to estimate the metabolic rate of a brachiosaur with reptile-like metabolism at any likely body temperature.

The specific heat capacity of animal tissue is about 3500 J kg^{-1} K^{-1}, so a 50 tonne brachiosaur would have a heat capacity C of 175 MJ K^{-1}. We will assume a thermal time constant of 6×10^5 s (8 days). This is the shorter of the two estimates given by Alexander (1989; the other was 20 days), and is also shorter than an estimate of 12 days obtained by extrapolation from Loveridge's (1984) data for crocodiles. The shortest estimate has been chosen as the least likely to predict overheating. Thus C/τ will be taken to be 300 W/K and a temperature difference $(T_{body} - T_{env})$ of 10 K would be needed for equilibrium with a metabolic rate of 3000 W, the rate predicted for a body temperature of 29 °C. This tells us that with no evaporative cooling, a brachiosaur with a body temperature of 29 °C could be at equilibrium in an environment at 19 °C. Similarly, a brachiosaur with a body temperature of 38 °C could be at equilibrium in an environment at 23 °C. It seems unlikely that a brachiosaur with reptile-like metabolism could avoid overheating in hotter climates except by evaporative cooling.

The latent heat of vaporization of water at 30–40 °C is 2·4 MJ kg^{-1}, so the whole of the 4840 W produced by a brachiosaur at 37 °C could be dissipated by evaporation of 2 g of water per second, or 170 kg per day. This rate of loss seems entirely feasible; for example, a 3·7 tonne elephant lost 20 kg water per day by evaporation (Benedict 1936). Thus a brachiosaur with reptile-like metabolism could avoid overheating even in the hottest climates, provided it had an adequate water supply.

Thus the size of large dinosaurs may have been limited by the danger of overheating if they had a mammal-like metabolism but not if they had a reptile-like metabolism. Dinosaur metabolic rates have been controversial since Bakker (1972) put the case for endothermy, but most of the points made have been inconclusive. Bakker's most persuasive argument was that endothermic predators need bigger prey populations than ectothermic ones would do, to support their higher metabolic rates. He claimed to show that the ratio of predator to prey biomasses for dinosaur populations indicated endothermy, but Farlow (1976) showed that the evidence was equivocal. Weaver (1983) argued that *Brachiosaurus* could not have had mammal-like metabolism because, with a head of about the same size as that of a one tonne giraffe, it could not have eaten fast enough. If their metabolic rates are proportional to (body mass)$^{0.75}$ (see above) a 50 tonne endothermic brachiosaur would need to eat $50^{0.75} = 19$ times as much food as a 1 tonne giraffe with a similar-sized head. Barrick and Showers (1994) used the ratio of oxygen isotopes in *Tyrannosaurus* bone to argue that this dinosaur had a constant, uniform body temperature, like mammals (but see criticisms in Morell 1994 and Millard 1995). By contrast, Ruben *et al.* (1996) used computed axial tomography to show that the dinosaurs *Nanotyrannus, Dromaeosaurus* and *Hypacrosaurus* had no nasal turbinals. These structures are present in both birds and mammals, and serve as heat exchangers, cooling air as it is breathed out and condensing out much of its water vapour. Ruben *et al.* (1996) argued that, without nasal turbinals, endotherms with mammal-like metabolic rates would lose so much heat and water in their breath that endothermy was unlikely; dinosaurs were probably reptile-like in their metabolism.

Whether the dinosaurs had mammal-like or reptile-like metabolic rates, *Indricotherium* was presumably mammal-like. For it, overheating may have been a serious problem.

Another possibility is that dinosaur size was limited by the problem of maintaining a viable population (see Farlow 1993). Terrestrial habitats are more diverse and fragmented than the oceans, so world populations of terrestrial animals cannot be expected to comprise as many individuals as

populations of ocean-living animals of equal body mass. Africa was supporting a population of 1·3 million elephants in 1979 (Nowak 1991). Population densities tend to be proportional to (body mass)$^{-0.75}$ (Damuth 1981), with no clear difference between vertebrate ectotherms and endotherms (Peters 1983), so a continent capable of supporting 1·3 million 3 tonne elephants should be adequate to support 150000 50 tonne brachiosaurs, which would probably be enough for long-term (millions of years) viability.

We have seen that the largest terrestrial carnivores were a great deal smaller than the largest herbivores. Similarly, modern carnivorous mammal species have lower population densities than similar-sized herbivores (Peters and Raelson 1984) and the largest carnivores are much smaller than the largest herbivores.

FLYING ANIMALS
(Text-fig. 3)

Finally, I will review and discuss the largest flying animals. The Kori bustard (*Ardeotis kori*) seems to be the largest modern one, with masses of up to 16 kg (Maloiy *et al.* 1979). It takes off only with difficulty, and often runs instead of flying when approached. The largest albatrosses, vultures and swans all have masses around 10 kg and are much stronger fliers. The wandering albatross, *Diomedea exulans*, spends much of its time airborne, slope soaring over waves (Bevan *et al.* 1995). Vultures spend most of the day airborne, soaring either in thermals (*Gyps* species in Africa; Pennycuick 1972) or over the windward slopes of mountains (*Condor*; Pennycuick and Scholey 1984). By contrast, swans travel by flapping flight rather than soaring.

The largest extinct birds, like the largest modern ones, were plainly flightless; their wings are rudimentary or even absent. The elephant bird *Aepyornis* stood 3 m tall, with an estimated mass of 450 kg (Amadon 1947). The largest known birds with well developed wing skeletons are the vulture-like teratorns (Campbell and Tonni 1983). The largest of these, *Argentavis*, is unfortunately known from only a few bones. Its mass has been estimated from the circumference of the tibiotarsus as 80 kg, five times the mass of the Kori bustard. This estimate is very imprecise, with 95 per cent confidence limits of 37 and 166 kg, but even the lower limit is far heavier than any modern flying bird. If the wing span was in the same proportion to humerus length as in condors, it was about 6 m, far greater than the 2·7 m span of the condor or the largest of all modern spans, the 3·4 m of the wandering albatross.

All known pterosaurs had well developed wing skeletons and could presumably fly. Among them *Pteranodon ingens* is the largest known by a reasonably complete skeleton. Its wing span was 7 m, but it was remarkably lightly built, with an estimated mass of only 15 kg (Brower 1983). This mass was obtained by calculating the volume of the body and multiplying by 900 kg m^{-3}, approximately the density of a plucked bird. A larger species, *P. sternbergi*, is estimated to have had a span of 9 m, a typical span for an ultralight aircraft (Frey and Martill 1996). *Quetzalcoatlus northropi* was even larger (Lawson 1975; Langston 1981). Only an incomplete wing skeleton has been found, but there is better material of smaller *Quetzalcoatlus*, either young specimens or a smaller species. The wing span of the large individual must have been about 12 m. If it were geometrically similar to *Pteranodon* (span 7 m) it would have been $(12/7)^3$ times as heavy, about 75 kg. In fact, the wing skeleton was far from being geometrically similar to that of *Pteranodon* (the phalanges made up a smaller fraction of the span), so this estimate cannot be relied upon. Paul (1991) has estimated the mass of *Quetzalcoatlus northropi* as 250 kg. *Arambourgiania* (known only from a very few bones) may have had a slightly larger span than *Quetzalcoatlus* (Frey and Martill 1996).

Now I will consider whether large animals can be expected to be able to generate the power needed for flight. A simple argument predicts that for geometrically similar aircraft, the power required for flight will be proportional to (mass)$^{1.17}$ (see Rayner 1988), but the following argument predicts a lower exponent. Well-designed gliders of all sizes, from small gliders to large passenger-carrying craft, lose height at 0·5–1·0 m s^{-1} when gliding at optimum speed (Tucker and Parrott 1970). Thus they lose potential energy at rates proportional to their masses. This is the energy that keeps them airborne, so this observation suggests that the power required for flight is proportional

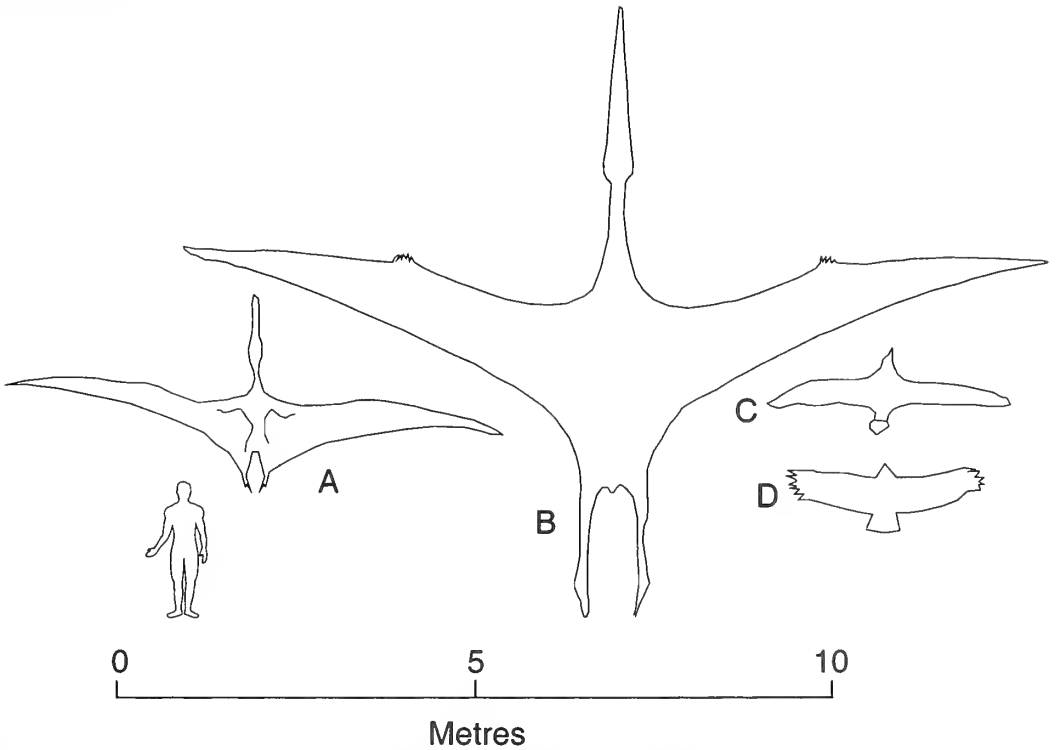

TEXT-FIG. 3. Some of the largest known flying animals, drawn to a uniform scale. Names of extinct animals are asterisked. A, *Pteranodon ingens**; B, *Quetzalcoatlus northropi**; C, *Diomedea*; and D, *Condor*.

to $(\text{mass})^{1.0}$. Whether power requirements increase in proportion to $(\text{mass})^{1.17}$ or to $(\text{mass})^{1.0}$, they increase faster than available metabolic power, which is expected to increase only in proportion to $(\text{mass})^{0.75}$. Thus large flying animals will have less power in reserve, and there must be an upper limit to the mass of flying animals.

A glider sinking at 0·5 m s^{-1} is losing potential energy at a rate of 5 W kg^{-1} of body mass. To do work at this rate, muscles operating at the expected efficiency of about 25 per cent. (Åstrand and Rodahl 1986) would have to use metabolic energy at a rate of 20 W kg^{-1} body mass. The maximum metabolic rates (calculated from oxygen consumption) of human endurance athletes are also about 20 W kg^{-1} (Åstrand and Rodahl 1986), suggesting that a man-sized bird such as *Argentavis* might be just able to fly. Confirmation of this seems to be provided by the *Gossamer Albatross*, an ultra-light propeller-driven aircraft powered by a pedalling athlete which flew successfully across the English Channel in 1979 (MacCready 1995). Some animals are much better endurance athletes than humans; maximum metabolic rates of 40 W kg^{-1} have been recorded for 500 kg horses, and a remarkable 100 W kg^{-1} for the pronghorn antelope (*Antilocapra americana*; mass about 32 kg; Lindstedt *et al.* 1991). Thus animals even larger than *Argentavis* and *Quetzalcoatlus* might well be able to produce enough power for flight.

A flying bird (or pterosaur) probably needs some capacity for powered flight, but most very large birds (albatrosses, vultures, etc.) spend most of their airborne time soaring. The success of man-made gliders serves as evidence that craft much larger than *Argentavis* and *Quetzalcoatlus* can soar successfully, both in thermals and on the windward sides of slopes.

There remains the question of whether such large animals could take off. Small birds can take off simply by jumping from the ground, hovering to keep themselves airborne, and then building up

speed. Simple helicopter theory tells us that the power needed for hovering is much greater than for forward flight and (for geometrically similar craft) increases in proportion to $(\text{mass})^{1.17}$ (Alexander 1982). Therefore, large birds cannot hover, even to take off. They may take off by diving from a high perch, but to take off from level ground they often have to run like taxiing aircraft, as bustards and vultures do. Similarly, swans run over the surface of water to take off.

The speed that a taxiing aircraft must reach, to take off, is the least speed at which the wings can provide enough lift to support it. It should correspond to the minimum gliding speed, which is between 5 and 10 m s^{-1} for various birds and a bat (Alexander 1982). Thus, animals that rely on running to take off may have to run moderately fast. The minimum speed is proportional to the square root of wing loading (that is, of body weight divided by wing area; Alexander 1982). It will generally be larger for larger animals because wing area is proportional only to $(\text{mass})^{0.67}$, in geometrically similar animals.

Pteranodon is the largest flying animal for which wing loading, and so take-off speed, can be estimated with any confidence. Even in this case there is considerable uncertainty; the mass estimate may be inaccurate, and there has been controversy about the area of the wings. Estimates for a *Pteranodon* of 7 m span range from 2·1 to 4·6 m^2 (Hazlehurst and Rayner 1992). Alexander (1994) argued on the basis of Unwin and Bakhurina's (1994) interpretation of the shape of pterosaur wings that an intermediate value, perhaps 3·4 m^2, was likely. If we accept this together with Brower's (1983) mass of 15 kg, and assume a maximum lift coefficient of 1·5, Brower's equation 2 gives a minimum speed of only 7 m s^{-1}. It seems unlikely that *Pteranodon* could run as fast as this (it is about the speed of a men's 1500 m race), but if the wind were blowing at 7 m s^{-1} or faster (a moderate breeze) it could take off simply by facing into the wind and spreading its wings. This depends on its wings being remarkably large for its weight; its estimated wing loading of 43 N m^{-2} is much lower than those of the largest albatrosses and vultures (about 170 and 100 N m^{-2}, respectively; Brower 1983).

Quetzalcoatlus is estimated to have had 1·7 times the span of *Pteranodon*, so if it had the same aspect ratio its wing area was $1{\cdot}7^2$ times that of *Pteranodon*, and can be estimated as 10 m^2. A 75 kg *Quetzalcoatlus* with this wing area would have had a wing loading of 74 N m^{-2}, still a little lower than those of the largest vultures. That does not necessarily mean that it could have taken off as easily as a vulture; its enormous wings must have been difficult to manage, while it was still on the ground. If, however, it had the 250 kg mass estimated by Paul (1991), its wing loading would have been 245 N m^{-2}, considerably higher than for albatrosses. Its minimum speed would then have been about 16 m s^{-1}, in the speed range of galloping racehorses. *Argentavis* is estimated to have had double the span, four times the wing area and eight times the mass of a large vulture. This would give it twice the wing loading of a vulture and $2^{0.5} = 1{\cdot}4$ times the take-off speed. The problem of taking off may well have set the upper limit to the size of flying animals.

CONCLUSIONS

It is tempting to look for limits to the range of animal sizes and then to ask whether animals have ever reached them, and if not why not. That approach seems misguided for two reasons. First, all postulated limits depend on assumptions based one extant animals which may be false for extinct ones. For example, the metabolic rate of an unknown or extinct large animal may not be as predicted by allometric equations based on modern animals. Second, the evolution of larger animals will not necessarily occur whenever larger animals are possible; it will occur only when larger animals are favoured by natural selection. Very large animals may fail to evolve because their movements would be cumbersome, or because their activity would be constrained by the precautions they would have to take to avoid overheating, or for some other reason, even if they would be capable of life in the absence of competition. This paper does not show that larger animals than have evolved would be physically impossible, but it does suggest reasons why they might have been at a disadvantage.

REFERENCES

ALEXANDER, R. McN. 1981. *The chordates*. 2nd edition. Cambridge University Press, Cambridge, 510 pp.

—— 1982. *Locomotion of animals*. Blackie, Glasgow, 163 pp.

—— 1985. Mechanics of posture and gait of some large dinosaurs. *Zoological Journal of the Linnean Society*, **83**, 1–25.

—— 1989. *Dynamics of dinosaurs and other extinct giants*. Columbia University Press, New York, 167 pp.

—— 1994. The flight of the pterosaur. *Nature*, **371**, 12–13.

—— JAYES, A. S., MALOIY, G. M. O. and WATHUTA, E. M. 1979. Allometry of the limb bones of mammals from shrews (*Sorex*) to elephant (*Loxodonta*). *Journal of Zoology*, **190**, 155–192.

AMADON, D. 1947. An estimated weight of the largest known bird. *Condor*, **49**, 159–164.

ANDERSON, J. F., HALL-MARTIN, A. and RUSSELL, D. A. 1985. Long bone circumference and weight in mammals, birds and dinosaurs. *Journal of Zoology Series A*, **207**, 53–61.

ÅSTRAND, P.-O. and RODAHL, K. 1986. *Textbook of work physiology*. 3rd edition. McGraw-Hill, New York, 756 pp.

BAKKER, R. T. 1971. Dinosaur physiology and the origin of mammals. *Evolution*, **25**, 636–658.

—— 1972. Anatomical and ecological evidence of endothermy in dinosaurs. *Nature*, **238**, 81–85.

—— 1986. *The dinosaur heresies*. Morrow, New York, 481 pp.

BARRICK, R. E. and SHOWERS, W. J. 1994. Thermophysiology of *Tyrannosaurus rex*: evidence from oxygen isotopes. *Science*, **265**, 222–224.

BELL, C. J. 1980. The scaling of the thermal inertia of lizards. *Journal of Experimental Biology*, **86**, 79–85.

BENEDICT, F. G. 1936. *The physiology of the elephant*. Carnegie Institution, Washington, 302 pp.

BENNETT, A. F. and DAWSON, W. R. 1976. Metabolism. 127–223. *In* GANS, C. (ed.). *Biology of the Reptilia 5*. Academic Press, London, 556 pp.

BENTON, M. J. 1997. *Vertebrate palaeontology*. 2nd edition. Chapman and Hall, London, 452 pp.

BEVAN, R. M., BUTLER, P. J., WOAKES, A. J. and PRINCE, P. A. 1995. The energy expenditure of free-ranging black-browed albatrosses. *Philosophical Transactions of the Royal Society, Series B*, **350**, 119–131.

BROWER, J. C. 1983. The aerodynamics of *Pteranodon* and *Nyctosaurus*, two large pterosaurs from the Upper Cretaceous of Kansas. *Journal of Vertebrate Paleontology*, **3**, 84–124.

CALDER, W. A. 1984. *Size, function and life history*. Harvard University Press, Cambridge, Ma., 431 pp.

CAMPBELL, G. S. 1977. *An introduction to environmental biophysics*. Springer, New York, 159 pp.

CAMPBELL, K. E. and TONNI, E. P. 1983. Size and locomotion in teratorns (Aves: Teratornithidae). *The Auk*, **100**, 390–403.

CAREY, F. G. 1982. Warm fish. 216–233. *In* TAYLOR, C. R., JOHANSEN, K. and BOLIS, L. (eds). *A companion to animal physiology*. Cambridge University Press, Cambridge, 365 pp.

CLARKE, M. R. 1966. A review of the systematics and ecology of oceanic squids. *Advances in Marine Biology*, **4**, 91–300.

CORIA, R. A. and SALGADO, L. 1995. A new giant carnivorous dinosaur from the Cretaceous of Patagonia. *Nature*, **377**, 224–226.

COTGREAVE, P. 1993. The relationship between body size and population abundance in animals. *Trends in Ecology and Evolution*, **8**, 244–248.

DAMUTH, J. 1981. Population density and body size in mammals. *Nature*, **290**, 699–700.

DAVIS, D. D. 1962. Allometric relations in lions vs. domestic cats. *Evolution*, **16**, 505–514.

DENTON, E. J. 1974. On buoyancy and the lives of fossil and modern cephalopods. *Proceedings of the Royal Society, Series B*, **185**, 273–299.

ECONOMOS, A. C. 1981. The largest land mammal. *Journal of Theoretical Biology*, **89**, 211–215.

—— 1983. Elastic and/or geometric similarity in mammalian design. *Journal of Theoretical Biology*, **103**, 167–172.

FARLOW, J. O. 1976. A consideration of the trophic dynamics of a late Cretaceous large-dinosaur community (Oldman Formation). *Ecology*, **57**, 841–857.

—— 1993. On the rareness of big, fierce animals: speculations about the body sizes, population densities, and geographic ranges of predatory mammals and large carnivorous dinosaurs. *American Journal of Science*, **293A**, 167–199.

—— SMITH, M. B. and ROBINSON, J. M. 1995. Body mass, bone 'strength indicator', and cursorial potential of *Tyrannosaurus rex*. *Journal of Vertebrate Paleontology*, **15**, 713–725.

FORTELIUS, M. and KAPPELMAN, J. 1993. The largest land mammal ever imagined. *Zoological Journal of the Linnean Society*, **107**, 85–101.

FREY, E. and MARTILL, D. M. 1996. A reappraisal of *Arambourgiania* (Pterosauria, Pterodactyloidea): one of the world's largest flying animals. *Neues Jahrbuch für Geologie und Paläontologie, Abhandlungen*, **199**, 221–247.

GILLETTE, D. D. 1994. *Seismosaurus, the earth shaker*. Columbia University Press, New York, 205 pp.

HALLAM, A. 1985. A review of Mesozoic climates. *Journal of the Geological Society, London*, **142**, 433–445.

HAZLEHURST, G. A. and RAYNER, J. M. V. 1992. Flight characteristics of Triassic and Jurassic Pterosauria: an appraisal based on wing shape. *Paleobiology*, **18**, 447–463.

HERWIG, R. P., STALEY, J. T., NERINI, M. K. and BRAHAM, H. W. 1984. Baleen whales: preliminary evidence for forestomach microbial fermentation. *Applied and Environmental Microbiology*, **47**, 421–423.

HOKKANEN, J. E. I. 1986. The size of the biggest land animal. *Journal of Theoretical Biology*, **118**, 491–499.

—— 1989. Heat exchange in large animals. Unpublished Ph.D. thesis, University of Leeds.

—— 1990. Temperature regulation of marine mammals. *Journal of Theoretical Biology*, **145**, 465–485.

HOWLAND, H. C. 1974. Optimal strategies for predator avoidance: the relative importance of speed and manoeuvrability. *Journal of Theoretical Biology*, **47**, 333–350.

KOSCH, B. F. 1990. A revision of the skeletal reconstruction of *Shonisaurus popularis* (Reptilia: Ichthyosauria). *Journal of Vertebrate Paleontology*, **10**, 512–514.

LANGSTON, W. 1981. Pterosaurs. *Scientific American*, **244** (2), 92–102.

LAWS, R. M. 1966. Age criteria for the African elephant, *Loxodonta africana*. *East African Wildlife Journal*, **4**, 1–37.

LAWSON, D. A. 1975. Pterosaur from the latest Cretaceous of West Texas: discovery of the largest flying creature. *Science*, **187**, 947–948.

LINDSTEDT, S. L., HOKANSON, J. F., WELLS, D. J., SWAIN, S. D., HOPPELER, H. and NAVARRO, V. 1991. Running energetics in the pronghorn antelope. *Nature*, **353**, 748–750.

LOCKLEY, M. 1991. *Tracking dinosaurs: a new look at an ancient world*. Cambridge University Press, Cambridge, 238 pp.

LOCKYER, C. 1976. Body weights of some species of large whales. *Journal du Conseil pour l'Exploration de la Mer*, **36**, 259–273.

LOVERIDGE, J. P. 1984. Thermoregulation in the Nile crocodile, *Crocodylus niloticus*. *Symposia of the Zoological Society of London*, **52**, 443–467.

MACCREADY, P. B. 1995. Gossamer aircraft and where they lead. 239–245. *In* ABBOTT, A. V. and WILSON, D. G. (eds). *Human-powered vehicles*. Human Kinetics, Champaign, Il., 279 pp.

MACE, G. M. and LANDE, R. 1991. Assessing extinction threats: toward a reevaluation of IUCN threatened species categories. *Conservation Biology*, **5**, 148–156.

MALOIY, G. M. O., ALEXANDER, R. MCN., NJAU, R. and JAYES, A. S. 1979. Allometry of the legs of running birds. *Journal of Zoology*, **187**, 161–167.

MARTILL, D. M. 1988. *Leedsichthys problematicus*, a giant filter-feeding teleost from the Jurassic of England and France. *Neues Jahrbuch für Geologie und Paläontologie, Monatshefte*, **1988**, 670–680.

MATTHEWS, L. H. and PARKER, H. W. 1950. Notes on the anatomy and biology of the basking shark (*Cetorhinus maximus* (Gunner)). *Proceedings of the Zoological Society of London*, **120**, 535–576.

MATTHEWS, P. 1995. *The new Guinness book of records 1996*. Guinness Publishing, London, 320 pp.

MILLARD, A. R. 1995. The body temperature of *Tyrannosaurus rex*. *Science* **267**, 1666.

MORELL, V. 1994. Warm-blooded dino debate blows hot and cold. *Science*, **265**, 188.

MOTLUK, A. 1996. Crisis looms over whaling ban. *New Scientist*, **150** (2036), 6.

NAGY, K. A. 1987. Field metabolic rate and food requirement scaling in birds and mammals. *Ecological Monographs*, **57**, 112–128.

NOWAK, R. M. 1991. *Walker's mammals of the world*. 5th edition. Johns Hopkins University Press, Baltimore, 1629 pp.

OWEN-SMITH, R. N. 1988. *Megaherbivores: the influence of very large body size on ecology*. Cambridge University Press, Cambridge, 369 pp.

PALADINO, F. V., O'CONNOR, M. P. and SPOTILA, J. R. 1990. Metabolism of leatherback turtles, gigantothermy, and thermoregulation of dinosaurs. *Nature*, **344**, 858–860.

PAUL, G. S. 1988. The brachiosaur giants of the Morrison and Tendaguru with a description of a new subgenus, *Giraffititan*, and a comparison of the world's largest dinosaurs. *Hunteria*, **2**, 1–13.

—— 1991. The many myths, some old, some new, of dinosaurology. *Modern Geology*, **16**, 69–99.

PENNYCUICK, C. J. 1972. Soaring behaviour and performance of some East African soaring birds observed from a motor-glider. *Ibis*, **114**, 178–218.

—— 1975. On the running of the gnu (*Connochaetes taurinus*) and other animals. *Journal of Experimental Biology*, **63**, 775–799.

—— 1992. *Newton rules biology*. Oxford University Press, Oxford, 111 pp.
—— and SCHOLEY, K. D. 1984. Flight behaviour of Andean condors *Vultur gryphus* and turkey vultures *Cathartes aura* around the Paracas Peninsula, Peru. *Ibis*, **126**, 253–256.
PETERS, R. H. 1983. *The ecological implications of body size*. Cambridge University Press, Cambridge, 329 pp.
—— and RAELSON, J. V. 1984. Relations between individual size and mammalian population density. *American Naturalist*, **124**, 498–517.
RANDALL, J. E. 1973. Size of the great white shark (*Carcharodon*). *Science*, **181**, 169–170.
RAYNER, J. M. V. 1988. Form and function in avian flight. *Current Ornithology*, **5**, 1–66.
ROMER, A. S. 1959. *The vertebrate story*. 4th edition. University of Chicago Press, Chicago, 437 pp.
RUBEN, J., HILLENIUS, W. J., GEIST, N. R., LEITCH, A., JONES, T. D., CURRIE, P. J., HORNER, J. R. and ESPE, G. 1996. The metabolic status of some late Cretaceous dinosaurs. *Science*, **273**, 1204–1207.
RYG, M., LYDERSEN, C., KNUTSEN, L. O., BJØRGE, A., SMITH, T. G. and ØRITSLAND, N. A. 1993. Scaling of insulation in whales and seals. *Journal of Zoology*, **230**, 193–206.
SERENO, P. C., DUTHEIL, D. B., IAROCHENE, M., LARSSON, H. C. E., LYON, G. H., MAGWENE, P. M., SIDOR, C. A., VARICCHIO, D. J. and WILSON, J. A. 1996. Predatory dinosaurs from the Sahara and Late Cretaceous faunal differentiation. *Science*, **272**, 986–991.
STAHL, W. R. 1967. Scaling of respiratory variables in mammals. *Journal of Applied Physiology*, **22**, 453–460.
STEEL, R. 1989. *Crocodiles*. Helm, London, 198 pp.
THULBORN, T. 1990. *Dinosaur tracks*. Chapman and Hall, London, 410 pp.
TUCKER, V. A. and PARROTT, G. C. 1970. Aerodynamics of gliding flight in a falcon and other birds. *Journal of Experimental Biology*, **52**, 345–368.
UNWIN, D. M. and BAKHURINA, N. N. 1994. *Sordes pilosus* and the nature of the pterosaur flight apparatus. *Nature*, **371**, 62–64.
WEAVER, J. C. 1983. The improbable endotherm: the energetics of the sauropod dinosaur *Brachiosaurus*. *Paleobiology*, **9**, 173–182.
WEIBEL, E. R. and TAYLOR, C. R. 1981. Design of the mammalian respiratory system. *Respiration Physiology*, **44**, 1–164.
WEST, G. B., BROWN, J. H. and ENQUIST, B. J. 1997. A general model for the origin of allometric scaling laws in biology. *Science*, **276**, 122–126.
WHEELER, A. 1975. *Fishes of the world: an illustrated dictionary*. Ferndale, London, 366 pp.

R. MCNEILL ALEXANDER
School of Biology
University of Leeds
Leeds LS2 9JT, UK

Typescript received 19 August 1996
Revised typescript received 1 October 1997

A PHYLOGENETIC TEST OF ACCELERATED TURNOVER IN NEOGENE CARIBBEAN BRAIN CORALS (SCLERACTINIA: FAVIIDAE)

by KENNETH G. JOHNSON

ABSTRACT. Documenting patterns of long-term faunal change is an important application of palaeontological data, but questionable results may be obtained if the potential effects of sampling bias are not considered. Analysis of fossil Caribbean reef coral occurrences indicates significant species turnover during the late Neogene. The goal of this study is to test this pattern for a subset of the entire fauna by using phylogenetic information to identify problematical taxa and periods of poor sampling. A phylogeny for 40 species from the faviid genera *Caulastraea*, *Colpophyllia*, *Diploria*, *Favia*, *Hadrophyllia*, *Manicina* and *Thysanus* was inferred using 23 multistate characters. Although the relationships are homoplasious, some stable groups emerged. One group includes the *Colpophyllia* species, another includes *Manicina*, *Hadrophyllia* and *Thysanus* species. As currently defined, both *Favia* and *Diploria* are paraphyletic stem groups. The inferred evolutionary tree was used to estimate species richness and proportional origination and extinction rates. When ghost lineages are considered, the magnitude of species richness estimates increases resulting in lower estimates of proportional origination and extinction. However, the pattern of faunal change within the group remains largely unchanged, with increased origination during the Late Miocene followed by extinction during the Late Pliocene and early Pleistocene.

PALAEONTOLOGICAL data are used to document patterns of long-term faunal change. As such they provide the primary data to assess the rôle of potential causes and to develop predictions of the potential consequences of periods of rapid turnover in the history of life. However, bias in sampling can lead to inconclusive or misleading results. Two strategies have been applied to overcome artefacts due to incomplete or uneven sampling (Smith 1994). One approach is to compile occurrences of high level taxa such as genera or families, and use these data to estimate taxonomic ranges. The distribution of ranges through time can then be analysed using evolutionary metrics. By including large numbers of taxa in their analysis, proponents of this approach are able to detect large-scale patterns free of sample bias. Supraspecific level taxa are likely to be better sampled (Gilinsky 1991), but suffer from problems of definition and comparability (Eldredge and Cracraft 1980) because they usually are defined as arbitrary subdivisions of a particular lineage rather than as holophyletic groups.

An alternative approach is to compare stratigraphical occurrence patterns at low taxonomic levels with phylogenetic information (Novacek and Norell 1982). Stratigraphical evidence has been widely used to test hypotheses of phylogeny. For example, the stratocladistic method proposed by Fisher (1991) explicitly includes stratigraphical information into the procedure for comparing competing hypotheses of relationship. Conversely, phylogeny can be used to assess the rôle of biased sampling in generating apparent patterns of faunal change (Benton 1994). Combining stratigraphical and phylogenetic data in an evolutionary tree will usually require interpretations of 'ghost lineages' and hypothetical range extensions (Norell 1992). Therefore, the estimates of rates of taxonomic evolution can change when phylogenetic information is included in an analysis of diversity patterns.

Recent work has provided evidence for rapid change in the Caribbean reef coral fauna during the late Neogene (Budd *et al.* 1996). Accelerated species turnover has been documented using a

[Palaeontology, Vol. 41, Part 6, 1998, pp. 1247–1268]

comprehensive compilation of all known reef coral occurrences from over 70 Miocene to Recent localities (Budd *et al.* 1992). Study of the patterns of species first and last occurrence using this database indicates a significant turnover event in the Late Pliocene to Pleistocene, with extinction rates as high as 30 per cent. of the fauna per million years during the late Pliocene. Furthermore, study of extinction selectivity among ecological groups indicates that species with small, short-lived colonies which reproduce sexually have overall higher rates of origination and extinction throughout the Neogene (Johnson *et al.* 1995). The origination and extinction of these types of taxa is the main mode of faunal change in late Neogene Caribbean reef corals. The goal of this study is to test the hypothesis of accelerated Pilo-Pleistocene faunal change by including phylogenetic information in the analysis.

There are over 170 species in the complete database, so developing a baseline phylogeny of the entire fauna is a prohibitively large task. Instead, a phylogeny has been inferred for the subset of taxa which experience the highest turnover. Most of these taxa come from the Faviidae, and have been classified into seven genera in which colonies form through primarily intratentacular division (Vaughan and Wells 1943). Three of these genera are restricted to the Caribbean region (*Manicina*, *Hadrophyllia* and *Thysanus*) whilst the others (*Caulastraea*, *Colpophyllia*, *Diploria* and *Favia*) have a broad geographical distribution including Mediterranean and Pacific occurrences. Several of the genera (*Manicina*, *Hadrophyllia*, *Favia* and *Thysanus*) include species which tend to live as small, free-living colonies in off-reef and reef marginal environments.

Previous attempts to reconstruct coral phylogeny using explicit cladistic techniques and skeletal characteristics have been hampered by the presence of excessive homoplasy and therefore poor resolution of species relationships (e.g. Budd and Coates 1992). But even homoplasious characters can be used to define groups (Pandolfi 1989), and analysis of skeletal characteristics on living material has been shown to be substantially in agreement with analyses of molecular and soft tissue characteristics (Potts *et al.* 1993; Budd *et al.* 1994). Furthermore, some workers (Veron 1995) have suggested that hybridization among disparate coral taxa is possible and has occurred repeatedly in the evolution of the Pacific coral fauna. If this is the case, then inferring phylogeny using parsimony is clearly an inappropriate approach for this group. Regardless, the cladistic approach applied to corals in this work resulted in useful interpretable hypotheses of relationships among the study taxa.

A cladistic analysis is used to reconstruct the phylogeny of meandroid faviid corals. The inferred phylogeny includes a high degree of homoplasy but groups are relatively stable. By combining the inferred phylogeny with the stratigraphical distribution of the study taxa, an evolutionary tree is constructed for the group with implications for evolution and biogeography. The tree suggests that the Caribbean fauna was largely isolated from the Mediterranean by the Miocene, and subsequent evolution was primarily moulded by extinction of Mediterranean lineages and radiation of Caribbean lineages.

Adding ghost lineages and extinctions resulting from cladistic branching events to analysis of faunal turnover does not alter the general pattern of increased richness and turnover in the late Neogene. Obviously, including ghost lineages will increase richness estimates, and, in general, decrease estimates of per taxon rates of origination and extinction. Proportional rates of species origination remain constant throughout much of the late Paleogene and Neogene, but decrease during the Pilo-Pleistocene. This pattern is similar whether or not ghost lineages and range extensions are included. Similarly, the pattern of variation in species extinction is not changed by considering phylogenetic information. Although estimates of the rate of both background origination and extinction are lower when range extensions and ghost lineages are included, estimates of the magnitude of the late Neogene period of accelerated extinction are comparable.

PHYLOGENY

Taxa

A total of 40 species from the Faviidae has been included in the present analysis (Appendix). Taxa with Neogene and Recent distributions were taken from a comprehensive compilation of Caribbean

TABLE 1. List of characters included in the analysis including the type of character (discrete or continuous), *a priori* ordering of character states (ordered or unordered), and the number of character states. Measures of character fit (consistency index (CI) retention index (RI) and rescaled consistency index (RC) on the consensus cladogram are also listed. These are in general minimum estimates across the range of all 72 equally parsimonious trees. Amb. = ambiguous.

Character	Type	Order	States	Amb.	CI	RI	RC
1. Attachment of skeleton	D	U	2	Y	0·25	0·70	0·17
2. Meandroid series sinuosity	D	U	3	Y	0·40	0·77	0·31
3. Frequency of wall development	C	O	4	N	0·50	0·92	0·46
4. Symmetry of bud geometry	D	U	3	Y	0·40	0·50	0·20
5. Calicular platform shape	D	U	2	Y	0·13	0·50	0·06
6. Calice relief	C	O	4	N	0·21	0·54	0·12
7. Calice or valley width	C	O	4	N	0·25	0·74	0·19
8. Epitheca	D	O	3	N	0·20	0·67	0·13
9. Relative costa thickness	D	U	2	Y	0·20	0·43	0·09
10. Coenosteum	C	U	5	Y	0·31	0·59	0·18
11. Exothecal dissepiments	D	O	2	N	0·33	0·60	0·20
12. Costa continuity	D	U	2	N	0·13	0·50	0·06
13. Complete septal cycles	C	O	4	N	0·17	0·35	0·06
14. Septal spacing	C	O	3	N	0·13	0·28	0·04
15. Septal thickness	D	U	2	Y	0·10	0·40	0·04
16. Columella width	C	O	3	Y	0·20	0·69	0·14
17. Columella continuity	D	U	2	N	1·00	1·00	1·00
18. Septal lobes	D	U	2	N	0·50	0·83	0·42
19. Paliform lobes	D	U	2	N	0·11	0·56	0·06
20. Endothecal dissepiments	C	O	3	Y	0·15	0·58	0·09
21. Wall structure	D	U	2	N	0·50	0·94	0·47
22. Double or single paratheca	D	U	2	N	0·33	0·75	0·25
23. Maximum colony size	C	U	3	N	0·25	0·70	0·18

Neogene coral occurrences (Budd *et al.* 1994). Several new taxa from the upper Neogene of the Dominican Republic (Budd and Johnson 1998) have also been included. Paleogene taxa were obtained from lists included in a review of the Eocene Caribbean faunas (Budd *et al.* 1992). Eocene species from Jamaica (Wells 1935; Zans *et al.* 1962), and Oligocene material from Antigua and Puerto Rico (Vaughan 1919; Frost and Weiss 1979; Frost *et al.* 1983) have been taken from published lists and new collections. The Paleogene and early Miocene fauna from Chiapas, Mexico (Frost and Langenheim 1974) was also considered. All extant Caribbean species from the seven genera as well as endemic species from the distinctive Brazilian fauna (Verrill 1901) were included. However, congeners from the Pacific and Mediterranean faunas have not been included. Although the exact biogeographical relations between the Mediterranean, Caribbean and Pacific biotas are not well understood, none of the included taxa has been described from outside the Caribbean Basin. However, Frost (1977) briefly compared the Mediterranean and Caribbean Oligocene faunas and suggested that some taxa might be synonymous, but he did not complete a full revision of the faunas. Species classified into *Favia*, *Diploria*, and possibly *Colpophyllia*, have been described from the Mediterranean.

Characters

Skeletal morphology was characterized using 23 characters with a total of 64 discrete character states (Table 1) scored from type material when possible. When type material was not available, characters were scored from published descriptions and examination of material in museum

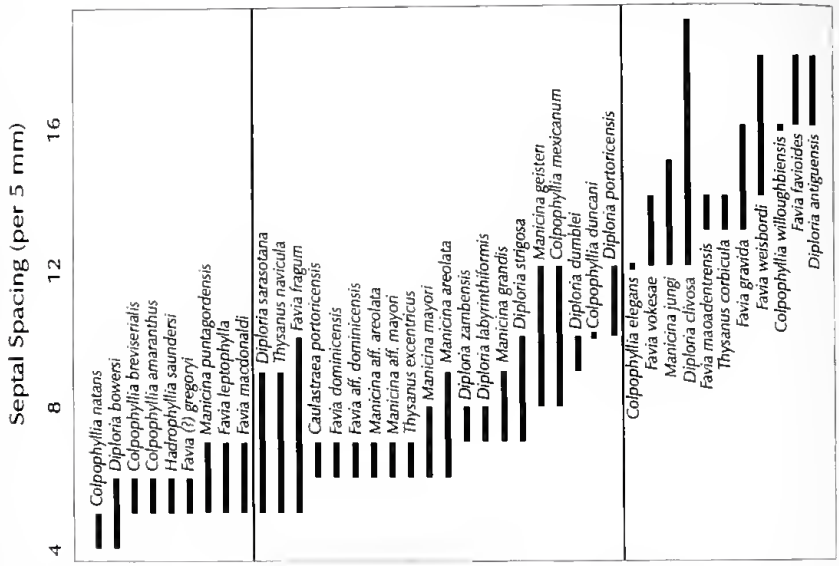

TEXT-FIG. 1. Distribution of septal spacing among the study taxa. Cut-offs to create discrete character states from this semi-quantitative measure were selected by visual examination of the distribution. Gaps are suggested at six and 12 septa per 5 mm resulting in three groups of species.

collections. Many of the characters are summaries of continuous variation in colony or corallite form which may not fall into non-overlapping (discrete) character states. Although some workers have criticized the use of characters with overlapping variation in phylogeny reconstruction (Chappill 1989), coral morphology is notoriously poor in features which are expressed as a few clearly non-overlapping states, so relationships among the study taxa are unlikely to be resolved if these attributes are not included. However, previous studies which used both overlapping and non-overlapping characters suggest that overlapping characters are more likely to be homoplasious (Stevens 1991).

A modified version of simple gap coding (Archie 1985) was used to subdivide continuous character distributions into discrete character states. The data for character coding are derived from a combination of measurement of type and accessory material and published species descriptions. Approximate ranges for each measured character were ranked by their midpoints, and plots examined for gaps in the character frequency distribution (Text-fig. 1). Where gaps were not evident, character state boundaries were defined at all levels where few taxa possessed ranges of variation which crossed the boundary between character states. Choosing the number of character states is a compromise between maximizing information content and maintaining consistency between characters (Archie 1985). Increasing the number of character states in a particular character increases that character's potential to resolve more groups but simultaneously increases the likelihood of homoplasy as random error in character scoring may obscure any phylogenetic signal. The division of a continuous character into discrete states remains an arbitrary act, but greater division of a character will not result in conflicting hypotheses of relationships (Thiele 1993).

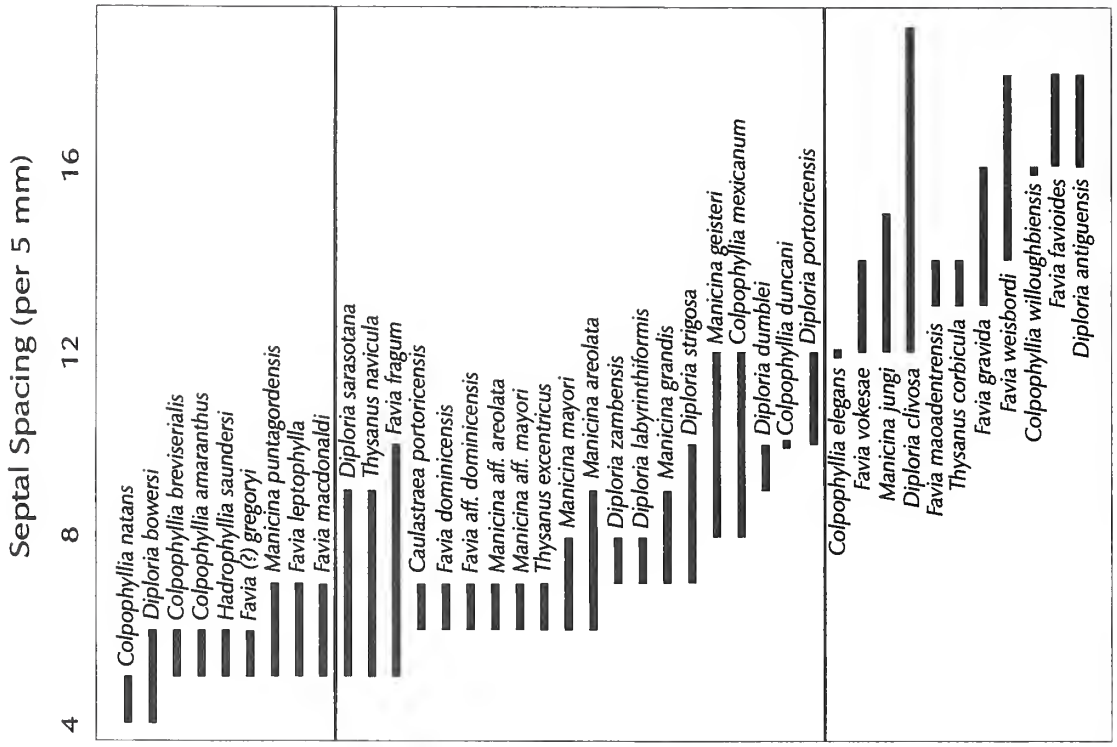

TEXT-FIG. 1. Distribution of septal spacing among the study taxa. Cut-offs to create discrete character states from this semi-quantitative measure were selected by visual examination of the distribution. Gaps are suggested at six and 12 septa per 5 mm resulting in three groups of species.

collections. Many of the characters are summaries of continuous variation in colony or corallite form which may not fall into non-overlapping (discrete) character states. Although some workers have criticized the use of characters with overlapping variation in phylogeny reconstruction (Chappill 1989), coral morphology is notoriously poor in features which are expressed as a few clearly non-overlapping states, so relationships among the study taxa are unlikely to be resolved if these attributes are not included. However, previous studies which used both overlapping and non-overlapping characters suggest that overlapping characters are more likely to be homoplasious (Stevens 1991).

A modified version of simple gap coding (Archie 1985) was used to subdivide continuous character distributions into discrete character states. The data for character coding are derived from a combination of measurement of type and accessory material and published species descriptions. Approximate ranges for each measured character were ranked by their midpoints, and plots examined for gaps in the character frequency distribution (Text-fig. 1). Where gaps were not evident, character state boundaries were defined at all levels where few taxa possessed ranges of variation which crossed the boundary between character states. Choosing the number of character states is a compromise between maximizing information content and maintaining consistency between characters (Archie 1985). Increasing the number of character states in a particular character increases that character's potential to resolve more groups but simultaneously increases the likelihood of homoplasy as random error in character scoring may obscure any phylogenetic signal. The division of a continuous character into discrete states remains an arbitrary act, but greater division of a character will not result in conflicting hypotheses of relationships (Thiele 1993).

Coding a larger range of character states will increase tree resolution, but this resolution is likely to be unstable.

Each character was assigned equal weight in the analysis regardless of its range. Determining the range of a character was an important aspect of character selection and scoring, and therefore already involved many *a priori* assumptions regarding character weighting. Adding additional assumptions to the analysis will only decrease the parsimony of the resulting hypothesis, and cannot add any additional information into the analysis (Farris 1990). Characters have been ordered where there is a clear set of steps between the states, but other characters were left unordered. Characters were not explicitly polarized prior to the selection of the most parsimonious tree. Instead, an outgroup was included in the analysis and the shortest unrooted trees including both an ingroup and an outgroup were subsequently rooted at an internal node with a basal polytomy (Maddison *et al.* 1984).

Character states

Analysis of character states is arguably the most important component of any phylogenetic analysis, so considerable space is devoted here to discussion of how coral morphology was reduced to a set of characters with discrete character states. A complete list of character states scored for each taxon is included in the Appendix.

1. *Attachment of skeleton.* Almost all reef-corals live permanently attached to a hard substrate, a few taxa are free-living during most of their lives. As in all scleractinian corals, a pelagic (or motile benthic) larval stage settles on a hard substrate prior to skeleton development. However, two strategies exist which allow free-living species to avoid permanent attachment. In some taxa, the original attachment points are small pieces of rubble (especially skeletal plates from the calcareous green algae *Halimeda* sp.), and as the coral grows, the lower surface becomes larger than its attachment substrate and so becomes effectively free on the sea floor. In other cases, colony attachment points are not well developed, and the colony is broken loose either by physical or biological agents. In either case, the strategy allows populations to live in habitats with high sedimentation (Gill and Coates 1977). *States*: 0 = free-living; 1 = attached.

2. *Meandroid series sinuosity.* Meandroid series result from intramural budding which is not followed by the construction of walls between daughter polyps. In meandroid colonies, the orientation of budding and subsequent extension of polyps is expressed in the meander form of the colony. Sinuosity of the meander valley ranges from straight to sinuous, but no intrinsic order is obvious from the geometry of colony formation. Therefore, this character has been left unordered in the analysis. If the meandroid series is branching, this character refers to the nature of the valley between branching points. This character has not been scored for phaceloid, plocoid, or cerioid taxa because the budding history cannot be clearly assessed from the arrangement of corallites on the surface of a colony. For these taxa, this character has been scored as missing. *States*: 0 = mostly straight; 1 = greatly curved; 2 = sometimes sinuous.

3. *Frequency of wall development.* All taxa considered in this analysis utilize intramural fission to some degree during colony development. However, various colony forms may be constructed depending on whether walls are erected between sister polyps. Phaceloid, plocoid and cerioid forms result when walls are constructed after the formation of a new bud, whilst flabellate and meandroid colonies result when walls develop only occasionally. However, strictly meandroid or cerioid/plocoid forms occupy the ends of a continuum of colony forms. The character is best coded by counting the number of continuous valley sections in a colony relative to the number of growth centres (stomodaea). Because soft tissue is not preserved in extinct taxa, this character was scored

by estimating the relative lengths of continuous sections of meander valley. This is a more-or-less continuous character, so there is some scope for variability with taxa, especially considering that mechanical damage to colonies during life can divide continuous series and trigger the formation of new calical walls during recovery and overgrowth of the damaged region. However, the terminal states (no new walls compared with inevitable wall development) is generally invariable within species. *States*: 0 = walls always develop; 1 = walls develop in most (approximately two-thirds) new buds; 2 = walls develop in few (approximately one-third) new buds; 3 = walls never develop between new buds.

4. *Symmetry of bud geometry*. Scleractinian polyps are characterized by hexagonal symmetry, so new centres may develop in any one of six directions. However, in many meandroid forms, the direction of budding is geometrically constrained to one, two or three directions (Text-fig. 2). Meander valleys in taxa that are constrained to uni- or bi-directional growth are straight or sinuous single series resulting in a flabellate colony form. If tri-directional growth is possible, branching meander series can develop. Morphometric analysis of colonies of *Manicina areolata* suggests that polyps may be polymorphic with respect to budding direction. In *M. areolata*, stomodaea are invariably located over branching points in the meander series, but can also be positioned between branching points, and new centres may originate on the margins or interior to meandroid series. However, as new centres which develop internally are limited to bi-directional grow, new branch points are invariably added to at the ends of the meander series. This character was illustrated by Matthai (1926) who distinguished between stomodaea which form in linear series by repeated intra-tentacular budding on the distomodaeal mode and stomodaea formed by dichotomous branching or terminal forking. *States*: 0 = only uni-directional; 1 = only bi-directional; 2 = sometimes multi-directional.

5. *Calicular platform shape*. In the taxa considered here, septa are elevated above the columella and provide support for tentacle attachment. When the polyp is completely retracted into the 'valley', the soft tissue is protected by the septal plates. The margins of the septal may be gently inclined to nearly vertical. Variable preservation of the study material results in uncertainty regarding this character in some of the less abundant species. *States*: 0 = sloping or V-shaped; 1 = steep-sided or U-shaped.

6. *Calice relief*. This character describes the difference in elevation (relative to the upward growth direction) of the columella and the upper surface of the septa. It is a semi-quantitative character with numerical ranges defined by dividing the range along approximate discontinuities in the distributions measure material. However, in some cases, material was excessively worn or damaged, so measurements might be considered as minima, and the character state assignment might be questionable. Because of its inherent order, this character has been left ordered in the analysis. *States*: 0 = low (< 2 mm); 1 = medium (2–4 mm); 2 = high (4–10 mm); 3 = very high (> 10 mm).

7. *Calice or valley width*. This semi-quantitative character describes the wall-to-wall distance across a meandroid valley or corallite diameter in non-meandroid colonies. It is roughly equivalent to two times the major septal length plus the width of the columella, and is closely conserved within the meandroid species. Previous work on cerioid faviids (*Montastraea*) suggests that this character is perhaps the most useful diagnostic for recognizing reef-coral morphospecies within generic groups (Budd 1993). Assuming that the character states really fall along a continuum, this is included as an ordered character. *States*: 0 = small (< 5 mm); 1 = medium (5–10 mm); 2 = large (10–15 mm); 3 = very large (> 15 mm).

8. *Epitheca*. In the meandroid faviids, the epitheca is a distinctive non-trabecular thecal tissue deposited in a modified cavity on the perimeter of the skeletal secreting layer (Sorauf 1972; Stolarski

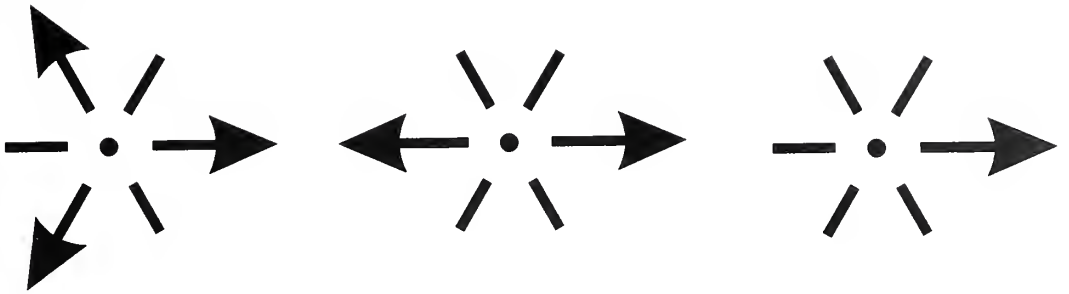

TEXT-FIG. 2. Illustration of three modes of bud geometry in meandroid faviid corals.

1995) which is thought to provide a protective cover for exposed skeleton. Such a function would be crucial for free-living corals in reef-marginal environments to deter infestation of boring organisms. Environmental variation may be significant in this character, but the states are general enough to include intraspecific variation. In several cases, outer surfaces of a colony were not preserved, so this character is coded as missing. *States*: 0 = absent or very reduced; 1 = reduced; 2 = well-developed.

9. *Relative costae thickness.* The relative thickness of major and minor costae may be equal, but in some forms, minor (third and fourth order) septa and costae can be less than half as thick as major septa. This character was used by Duncan (1863, 1864) to distinguish various forms of *Hadrophyllia*, *Thysanus* and *Manicina*. *States*: 0 = equal; 1 = unequal.

10. *Coenosteum.* Coenosteum is skeleton deposited by coenosarc tissues. In meandroid forms, coenosteum develops between adjacent series and reflects the complex packing of the meander network. In colonies restricted to only uni-directional or bi-directional budding (character 4), adjacent corallites are always sister polyps, so the development of coenosteum is geometrically forbidden. Therefore, taxa with restricted budding geometry are scored as 'absent'. Similarly, by definition, coenosteum is undeveloped in phaceloid colonies, and these taxa have been scored as 'absent'. No attempt was made to distinguish between these two character states to avoid overweighting the distinction between colony forms included as other characters. Transitions among the character states are not restricted to a linear sequence (e.g. it is possible to proceed from an absent coenosteum to a wide coenosteum without intermediate steps), so this character was left unordered. Coenosteum is invariably present or absent, but its width can be related to the stage of formation of a new bud. Therefore, maximum coenosteum widths were used when coding the character. *States*: 0 = absent; 1 = present with adjacent walls; 2 = present and narrow (less than meandroid valley width); 3 = present with medium width (equal to meandroid valley width); 4 = present and wide (greater than valley width).

11. *Exothecal dissepiments.* This character indicates the presence and relative abundance of tabular or vesicular horizontal structures extending between costal plates. Several taxa have been scored as 'missing' because of a shortage of well-preserved material in the current collection. *States*: 0 = absent; 1 = present.

12. *Continuity of costae.* A score for this character was determined by whether or not costae (or septa) are continuous between adjacent meander series. It is meaningless for flabellate or phaceloid colony forms and has been coded as 'missing' for several taxa. In meandroid forms, this character can in part reflect the relative sinuosity and proximity of the meander series to neighbouring series,

and possession of confluent septa suggests greater colony integration among adjacent meander series (Coates and Oliver 1973). *States*: 0 = discontinuous; 1 = continuous.

13. *Number of septal cycles*. The number of septal cycles has long been recognized as a significant character in corals. In forms with corallites formed by extramural budding, it can more easily scored by counting septa, but in meandroid forms the relative lengths and widths of septa must be examined. This character is related to septal spacing (character 14). *States*: 0 = three complete; 1 = more than three complete; 2 = nearly four complete; 3 = four or more complete.

14. *Septal spacing*. This character is scored using the number of septa per 5 mm along a meander series. It is related to septal width and the number of septal cycles. Because it is a relatively continuous character, discrete levels were assigned through visual inspection on a range of septal spacing measured on type material or taken from species descriptions (Text-fig. 1). Divisions were made between six and 12 septa per 5 mm reflecting discontinuities in the distribution at those points. Some taxa had overlap between adjacent character states. *Manicina puntagordensis*, *Favia leptophylla* and *F. macdonaldi* were scored as having fewer than six septal per 5 mm and *Colpophyllia elegans* was scored as having more than 12 septa per 5 mm. An alternative analysis with these four taxa scored between six and 12 septa per 5 mm did not change the hypothesized relationships among the taxa. *States*: septa per 5 mm: 0 = less than six; 1 = between six and 12; 2 = more than 12.

15. *Equality of septal thickness*. Major septa are generally longer than minor septa, and they may be thicker. In taxa with septothecal wall structures, this character should be structurally related to costal thickness (character 9), but often costae are equal and septa are unequal. *States*: 0 = equal; 1 = unequal.

16. *Columella width*. This character describes the width of the columella relative to the overall valley width. Absolute columella width is likely to be structurally correlated with overall valley width (character 7), so relative width was scored to avoid implicitly over-weighting corallite size. *States*: 0 = less than or equal to one-quarter valley width; 1 = one-third valley width; 2 = one-half width or wider.

17. *Columella continuity*. In meandroid colonies, the columella can be an continuous structure, with no easily recognizable corallite centres. But, in some taxa, corallite centres are clearly evident from the degree of septal inflection and by breaks in the columella. These breaks are often more clearly demonstrated in taxa with reduced or poorly developed columella and may be related to the process of budding. *States*: 0 = continuous; 1 = discontinuous.

18. *Septal lobes*. There is a great deal of confusion regarding septal and paliform lobes (character 19). As used here, septal lobes can only be found on lamellar septa composed primarily of a single fan system of simple trabeculae. Septal lobes are internal lobes formed by a second fan system. In contrast, paliform lobes are vertical extensions of septa formed by one or more trabecular bundles, and not generally composed of a second fan system. Some workers (Chevalier 1975; Veron *et al.* 1977) considered the presence of well-developed septal lobes to be significant, and based the definition of a new scleractinian family (Trachyphyllidae) largely on this character. However, this characteristic is widespread within the taxa considered here even though they are classified as members of the Faviidae. *States*: 0 = absent; 1 = present.

19. *Paliform lobes*. Paliform lobes are vertical extensions of the medial margins of septa formed by one or more trabeculae. They are not true pali because they do not form through the process of septal substitution (Wells 1956), in which the medial margin of a exoseptum bifurcates as it grows upwards and new septa are inserted into the calice. Paliform lobes are distinguished from septal

lobes by forming from a single or multiple trabeculae which are not arranged as a fan system. In general, paliform lobes are vertical extensions of skeleton with margins that are free from the parent septum, and are usually associated with a thickening of the inner ends of septa. Although these structures are considered distinct from septal lobes (character 18), they may represent proto-septal lobes. However, they have been coded as distinct because no specimens examined in this study have both well-developed septal and paliform lobes. *States*: 0 = absent; 1 = present.

20. *Endothecal dissepiments.* These structures are similar to exothecal dissepiments, but develop internally. *States*: 0 = absent or very few; 1 = intermediate; 2 = abundant.

21. *Wall structure.* Two distinct wall structures have been recognized in the study taxa. In all cases, septo-costal plates extend across the theca, but the margins of calices are defined by different structures. Septotheca is formed by septal skeleton and develops as a thickening and fusing of adjacent septo-costal plates. In contrast, thecal skeleton may not be not genetically related to the septa, in which case the theca is constructed by abundant and closely spaced dissepiments. This style of wall is termed paratheca (Wells 1956). *States*: 0 = septothecal; 1 = parathecal.

22. *Double or single wall.* In some parathecate colonies, wall development between adjacent meander series appears to be co-ordinated resulting in a distinctive double wall structure. In these forms, the walls appear as clearly defined thin plates separated by a constant distance. Although this character applies only to parathecal forms, it was scored for all taxa. This will increase the relative weight of wall structures in the phylogenetic inference. *States*: 0 = single wall; 1 = double wall.

23. *Size of colony.* Although colony growth is indeterminate, some species of corals tend to have smaller maximum colony sizes than others. This is no doubt a reflection of the life history or environmental tolerences of taxa, with some forms that utilize clonal reproduction through fragmentation possessing large (although not necessarily connected) colonies. Other taxa are rarely found as large colonies, especially free living species which depend on some degree of mobility to survive in sediment-rich environments (Johnson 1992). Although maximum colony size is clearly a continuous character, no effort was made here to define size categories statistically. Categories were defined by roughly dividing the total range of size variation of all known Neogene Caribbean coral taxa into three groups (Budd *et al.* 1994). *States*: 0 = small ($< 0{\cdot}1$ m); 1 = intermediate (0·1–0·3 m); 2 = large ($> 0{\cdot}3$ m).

Phylogenetic inference

Paup version 3.1.1 (Swofford 1993) was used to find the most parsimonious trees which describe the relationships among the taxa. Because of the relatively large number of taxa, a heuristic search was performed followed by total branch swapping of the set of all shortest unrooted trees. The maximum number of trees held in memory was 2000. The initial trees were found using random addition sequence with 100 iterations to help assure that the identified trees were close to global minima. Once the set of minimum trees was found, the tree was rooted and character state reconstructions were calculated relative to an outgroup consisting of *Caulastraea portoricensis*. Both Matthai (1928) and Wells (1956) present hypotheses of 'morphogenetic trends' in colonial corals with colonies formed by primarily extratentacular budding plesiomorphic to meandroid and flabellate colonies formed by exclusively intratentacular division. *Caulastraea* is the only genus in the Faviidae characterized by phaceloid colonies (Veron *et al.* 1977) and therefore most probably is part of a more pleisiomorphic lineage of the family than the other lineages included in this study. Extant species of *Caulastraea* are widely distributed across the Indo-Pacific region (Veron 1993) and have occurred since the Oligocene in the Caribbean, Indo-Pacific and Mediterranean regions (Chevalier 1961; Frost and Weiss 1979; Pfister 1980; Budd *et al.* 1994). Therefore, as a group,

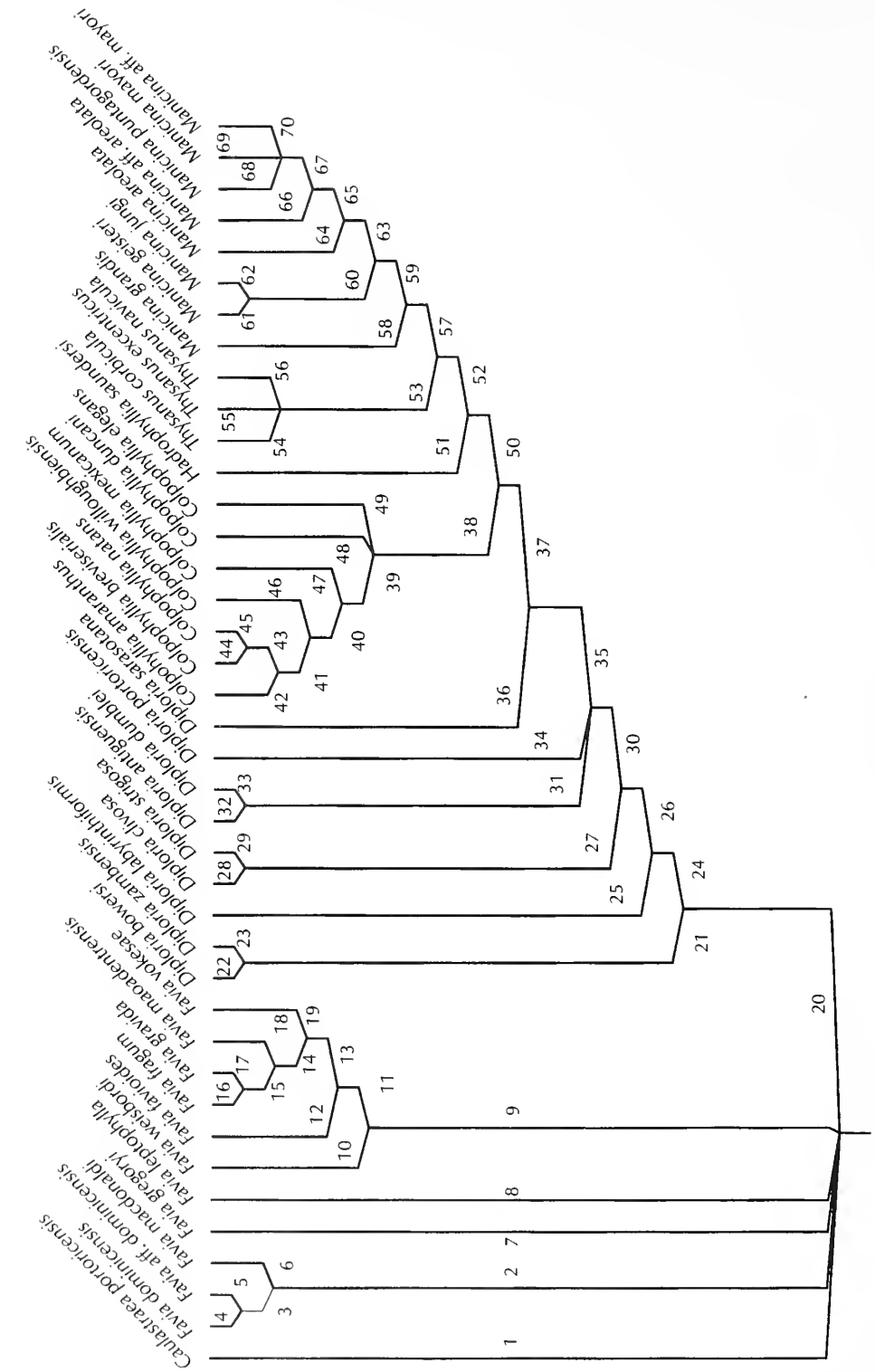

TEXT-FIG. 3. Strict consensus tree calculated from 78 trees with length 175. The relationships among species are ambiguous at three nodes. Apomorphies and support indices associated with branches are included as Table 2.

Caulastraea species are among the most widespread of all faviid corals. Strict consensus trees were formed from multiple equally parsimonious trees, and characters were optimized on the consensus cladogram assuming accelerated character transformation.

A cladistic permutation tail probability test (PTP) was used to assess the phylogenetic signal in the character matrix (Archie 1989; Faith and Cranston 1991). This test is a comparison of the length of the observed shortest tree with tree lengths for a set of 100 character matrices obtained by randomly reassigning character states for each taxon. The PTP test is designed to examine the amount of cladistic covariation in the data. The analysis was performed using code written by me for the automatic scripting of PAUP commands in NEXUS format. For each randomized data set, a heuristic search was used so the estimate of minimum tree length for each iteration is conservative.

The PTP test suggests that significant phylogenetic signal exists in the character matrix, with the observed most parsimonious tree shorter than 99 replicate trees ($P = 0{\cdot}01$). The initial heuristic search identified 78 equally parsimonious trees each with 175 steps. Five ambiguous nodes exist on a strict consensus of these trees (Text-fig 3); the relationships among some *Favia* species and the outgroup are not well resolved. Similarly, the relationships among *Colpophyllia elegans*, *C. duncani* and a group containing the other *Colpophyllia* species are not resolved. The relationships among *Manicina mayori*, *M. puntagordensis*, and *M.* species B and the relationships among the three *Thysanus* species are also not resolved. Some polytomies might be expected if several new lineages originate from another lineage which is not evolving new apomorphies, so further manipulation of the characters (e.g. reweighting) to increase resolution was not attempted.

Two randomization tests were also applied to assess the support for hypotheses of group monophyly. The 'evolutionary bootstrap' works by finding maximally parsimonious trees for a series of pseudo-random replicates of a character matrix constructed by randomly resampling (with replacement) the vector of character states for each taxon (Felsenstein 1985). The proportion of these trees which include a particular monophyletic group is used as a measure of support for that group. There may be serious objections to this test (reviewed by Sanderson 1995), but it is widely used in molecular systematics where large numbers of characters are available. Bootstrap support estimates were obtained using the Random Cladistics program with 100 pseudoreplicates (Siddall 1995).

Clade stability was also assessed using a modified jackknife procedure in which a series of cladograms were constructed for subsets of taxa with each taxon removed (Lanyon 1985). This is a way of examining the effects of individual taxa in the analysis. Although a different version of this test can be performed using the Random Cladistics package, this analysis was performed using a scripting program written by the author. Jackknife support values were calculated by determining group frequency from a total of 39 replicate trees constructed using heuristic searches. In each replicate, *Caulastraea portoricensis* was left in the analysis as the outgroup. If multiple shortest trees were found, a strict consensus tree was calculated for that replicate. The frequency distribution of all possible groups of taxa defined in the all-taxon consensus tree was then derived from the 39 replicate consensus trees by counting the number of trees in which each group was defined. The total number of iterations in which a group could possibly be found is equal to the number of iterations minus the number of taxa in the group, because if a taxon is not included in the analysis, it will not occur in the resulting tree. Jackknife percentages for each group were calculated by dividing the frequency of each group by the number of trees in which the group could possibly have occurred, the higher the percentage, the more stable the group to the effects of missing or 'problematical' taxa.

Character state reconstruction on the consensus tree is ambiguous for nine characters (Table 1). The tree as a whole has low consistency (rescaled consistency index = 0·14; retention index = 0·78), but high homoplasy levels are in part related to the large number of taxa included in the analyses (Sanderson and Donoghue 1989). Homoplasious characters include septal and costal architecture, but characters associated with budding and the corallite wall and columellae provide more support for the consensus tree. Contrary to expectation, results of a Kruskal–Wallace rank sum test suggest that discrete characters are not more consistent with the consensus cladogram than continuous characters ($\chi^2 = 0{\cdot}53$; 1 d.f. $P = 0{\cdot}47$).

TABLE 2. Branch stability measures and apomorphies for branches. Branch numbers refer to Text-figure 4. Jackknife frequencies and are shown with the maximum number of replicates for each group indicated in parentheses. Character states were optimized on the cladogram assuming accelerated change, and ambiguous apomorphies indicated by asterisk.

Branch	Jackknife	Apomorphies
1	—	6 (1–0), 8 (1–0), 10 (3–0), 11 (1–0), 13 (1–2), 16 (1–0), 19 (1–0), 23 (1–2)
2	0·69 (36)	10 (3–1)*, 12 (0–1), 16 (1–2)*, 20 (0–2)
3	0·76 (37)	19 (1–0), 21 (0–1)
4	—	6 (1–0), 10 (1–2)*
5	—	23 (1–0)
6	—	7 (1–2), 10 (1–4)*, 14 (1–0)
7	—	8 (1–0), 13 (1–0), 14 (1–0), 19 (1–0), 20 (0–2)
8	—	6 (1–0), 7 (1–0), 8 (1–2), 14 (1–0), 22 (0–1)
9	0·89 (33)	14 (1–2), 15 (1–0)*, 16 (1–2)*
10	—	13 (1–0)
11	0·97 (34)	7 (1–0), 10 (3–2), 23 (1–0)
12	—	4 (2–1)
13	0·97 (35)	13 (1–3), 15 (0–1)*, 19 (1–0)
14	0·53 (36)	6 (1–0), 9 (0–1)
15	0·51 (37)	8 (1–2)
16	—	13 (3–2), 14 (2–1)
17	—	3 (0–1), 16 (2–1)
18	—	1 (1–0), 10 (2–4), 20 (0–1)
19	—	10 (2–1), 12 (0–1)
20	0·64 (11)	3 (0–1), 10 (3–4), 15 (1–0), 16 (1–2)*, 20 (0–1)*
21	0·59 (37)	13 (1–0)
22	—	7 (1–0), 12 (0–1), 14 (1–0), 16 (2–1)*
23	—	19 (1–0)
24	0·53 (13)	3 (1–2)
25	—	—
26	0·50 (14)	5 (1–0), 10 (4–1)
27	0·97 (37)	11 (1–0), 15 (0–1), 23 (1–2)
28	—	7 (1–0), 8 (1–0), 13 (1–2), 14 (1–2)
29	—	12 (0–1)
30	0·44 (16)	16 (2–1)*, 20 (1–2)*
31	0·97 (37)	6 (1–0), 7 (1–0), 23 (1–0)
32	—	8 (1–2), 2 (1–3), 14 (1–2), 15 (0–1)
33	—	10 (1–3), 12 (0–1)
34	—	—
35	0·53 (19)	6 (1–2), 8 (1–0), 12 (0–1)
36	—	13 (1–0), 20 (2–0)
37	0·80 (20)	7 (1–2), 16 (1–0), 19 (1–0), 21 (0–1)
38	0·97 (32)	2 (1–2), 13 (1–2), 15 (0–1), 17 (0–1)
39	0·82 (34)	5 (0–1)*, 10 (1–2), 22 (0–1)
40	0·83 (35)	3 (2–1), 7 (2–3)
41	1·00 (36)	5 (1–0)*, 12 (1–0), 13 (2–1), 14 (1–0), 15 (1–0), 19 (0–1)
42	—	6 (2–3)
43	0·84 (37)	23 (1–2)
44	—	—
45	—	3 (1–2)
46	—	13 (2–3), 14 (1–2)
47	—	—
48	—	—
49	—	7 (2–1), 14 (1–2)

TABLE 2. (*cont.*)

Branch	Jackknife	Apomorphies
50	0·96 (27)	1 (1–0), 3 (2–3), 4 (2–1), 10 (1–0), 23 (1–0)
51	—	7 (2–3), 14 (1–0)
52	0·50 (28)	5 (0–1), 6 (2–1)
53	0·58 (36)	2 (1–0)*, 4 (1–0)*, 6 (1–0)*, 11 (1–0), 19 (0–1), 20 (2–0)
54	—	9 (0–1), 13 (1–3), 14 (1–2), 15 (0–1)
55	—	2 (0–1)*, 5 (1–0), 6 (0–1)*
56	—	4 (0–1)*, 20 (0–1)*
57	0·48 (31)	8 (0–2), 18 (0–1)
58	—	—
59	0·44 (32)	9 (0–1)*, 15 (0–1)
60	0·54 (37)	13 (1–2)
61	—	2 (1–2), 5 (1–0), 6 (1–2), 7 (2–3), 8 (2–1)
62	—	13 (2–3), 14 (1–2), 18 (1–0), 19 (0–1)
63	0·85 (34)	2 (1–0), 4 (1–2), 10 (0–2), 16 (0–1)
64	—	12 (1–0), 20 (2–1)
65	0·54 (35)	6 (1–3), 9 (1–0)*
66	—	—
67	0·92 (36)	1 (0–1)*, 5 (1–0)*, 7 (2–3), 22 (0–1), 23 (0–1)
68	—	1 (1–0)*, 6 (3–2), 14 (1–0)
69	—	5 (0–1)*, 9 (0–1)
70	—	15 (1–0), 16 (1–0)

Groups

The consensus tree suggests a distinct *Favia* subgroup, including *Favia maodentrensis*, *F. favioides*, *F. fragum*, *F. gravida*, and *F. vokesae*. This group is supported by three unambiguous apomorphies and can be found in a high proportion of the jackknife trees (Table 2). The shortest tree which does not include this group is two steps longer than the current hypothesis, and the three characters which support this group all have greater than median rescaled consistency indices. The group is characterized by decrease in both corallite and colony size and a narrowing of the coenosteum.

A second group, including *Colpophyllia*, *Hadrophyllia*, *Thysanus* and *Manicina* species, is also well supported. Apomorphies include deeper calices, a reduced epitheca, and the development of confluent costae. However, jackknife support for this group is not as strong as for some of the other groups, and only one additional step is required for an hypothesis which does not include this clade. Within this large group, two main subgroups are defined, one including the *Colpophyllia* species and the other including *Hadrophyllia*, *Thysanus* and *Manicina* species. Jackknife frequency for the *Colpophyllia* clade is very high (0·97) and the shortest tree which does not include the group is two steps longer than the current hypothesis. The *Colpophyllia* clade is supported by four unambiguous character state changes including the development of sinuous meandroid series, the insertion of minor septa which are thinner than the major septa. Most importantly, the *Colpophyllia* clade is characterized by the development of a discontinuous columella.

A smaller subgroup is stable within the *Colpophyllia* clade. This group includes the three Neogene species *Colpophyllia natans*, *C. amaranthus* and *C. breviserialis*, and is defined by a total of six character state changes, one of which is ambiguous. This is the most stable group in the current hypothesis, with support from all possible jackknife trees. This group is supported by a loss of fourth order septa, which results in a decrease in septal number accompanied by an increase in septal spacing, as well as the loss of septa with unequal thickness. Paliform lobes can be identified in all three Neogene *Colpophyllia* species. All of these characters are highly homoplasious with

rescaled consistency indices less than 0·10, demonstrating that homoplasious characters can be used to substantiate stable groups.

A group including species of *Manicina*, *Hadrophyllia* and *Thysanus* (MHT) is supported by five apomorphies, including the development of a free-living mode of growth and generally smaller colonies and the cessation of wall development between newly budded polyps. New buds are constrained to a linear series with no branching or forking resulting in a flabellate growth form and loss of coenosteum. These characters are related to loss of attachment to the substrate. Previous work has shown that colony size in the extant free-living coral *Manicina areolata* is constrained by the ratio of tissue surface area to colony mass (Johnson 1992) so that large colonies experience high mortality rates due to reduced colony mobility. Adopting a free-living mode allowed these taxa to occupy sediment-rich reef marginal environments equivalent to shallow or deep seagrass beds and mangrove fringe systems.

Stable subgroupings can be recognized within the MHT group. One node defines a group including the five meandroid *Manicina* species. This node is supported by four unambiguous apomorphies, and is characterized by the reacquisition of branched meandroid series with straight meander valleys between branch points accompanied by coenosteum development between adjacent branches. These characters are all more consistent with the hypothesis than average. However this group has relatively low jackknife support (0·85) and only one step is required for a tree which does not include the group. A second subgroup has high jackknife support (0·92) and includes three meandroid *Manicina* species with attached colonies. These taxa are also characterized by intermediate colony size and deeper calices with steeply sloping septal margins.

EVOLUTIONARY TREE

An evolutionary tree was constructed by superimposing cladistic relationships on to the stratigraphical range of species whilst minimizing hypothetical range extensions (Text-fig. 4). A single tree was selected from the set of most parsimonious trees by resolving ambiguous nodes using stratigraphical information (Smith 1994). The three ambiguous nodes in the more apomorphic part of the tree were treated first. For the ambiguous node in the *Colpophyllia* group, *C. duncani* was selected as the sister taxon to a group including *C. elegans* and the other *Colpophyllia* species. The alternative hypothesis places *C. elegans* as the pleisomorphic sister group to *C. duncani* and the other *Colpophyllia* species, and requires a range extension for *C. elegans* through the Mid Eocene. Similar reasoning was used to resolve the *Thysanus* and *Manicina* ambiguous nodes. A group including *Thysanus corbicula* and *Thysanus excentricus* is the hypothetical sister group of *Thysanus navicula*, and *Manicina puntagordensis* is identified as the pleisomorphic sister taxon to a group including *M. mayori* and *M.* aff. *mayori*. An ambiguous node involving the three Oligocene *Diploria* species was resolved by inferring a hypothetical monophyletic group including all three taxa. The alternative relationship identified two distinct stem groups, one including *D. antiguensis* and *D. dumblei* and the other including only *D. portoricensis*. The addition of stratigraphical information was not able to resolve the remaining ambiguous node which appears along the *Favia* stem groups. A single tree was selected from two remaining hypotheses which suggests that a group including *Favia dominicensis*, *F.* aff. *dominicensis*, and *F. macdonaldi* is a sister group to *F. gregoryi*.

The tree includes several hypotheses of ancestry when no apomorphies occur along cladogram branches. For example, *Colpophyllia breviserialis* is identified as the ancestor of *C. natans* because no autapomorphies are hypothesized for *C. breviserialis*. Branching events are drawn at or below boundaries for convenience; they are assumed to have occurred sometime within the time interval after the boundary. Last occurrences of taxa which are drawn at boundaries also reflect imprecise age assignment, and actual extinctions are assumed to have occurred in the time interval prior to the boundary.

Major range extensions are required for the more pleisomorphic taxa, and multiple origins of *Favia* and *Diploria* lineages are suggested. *Favia* is widely dispersed in both time and space. The genus has been described from the Cretaceous of Europe and the Caribbean (Vaughan and Wells

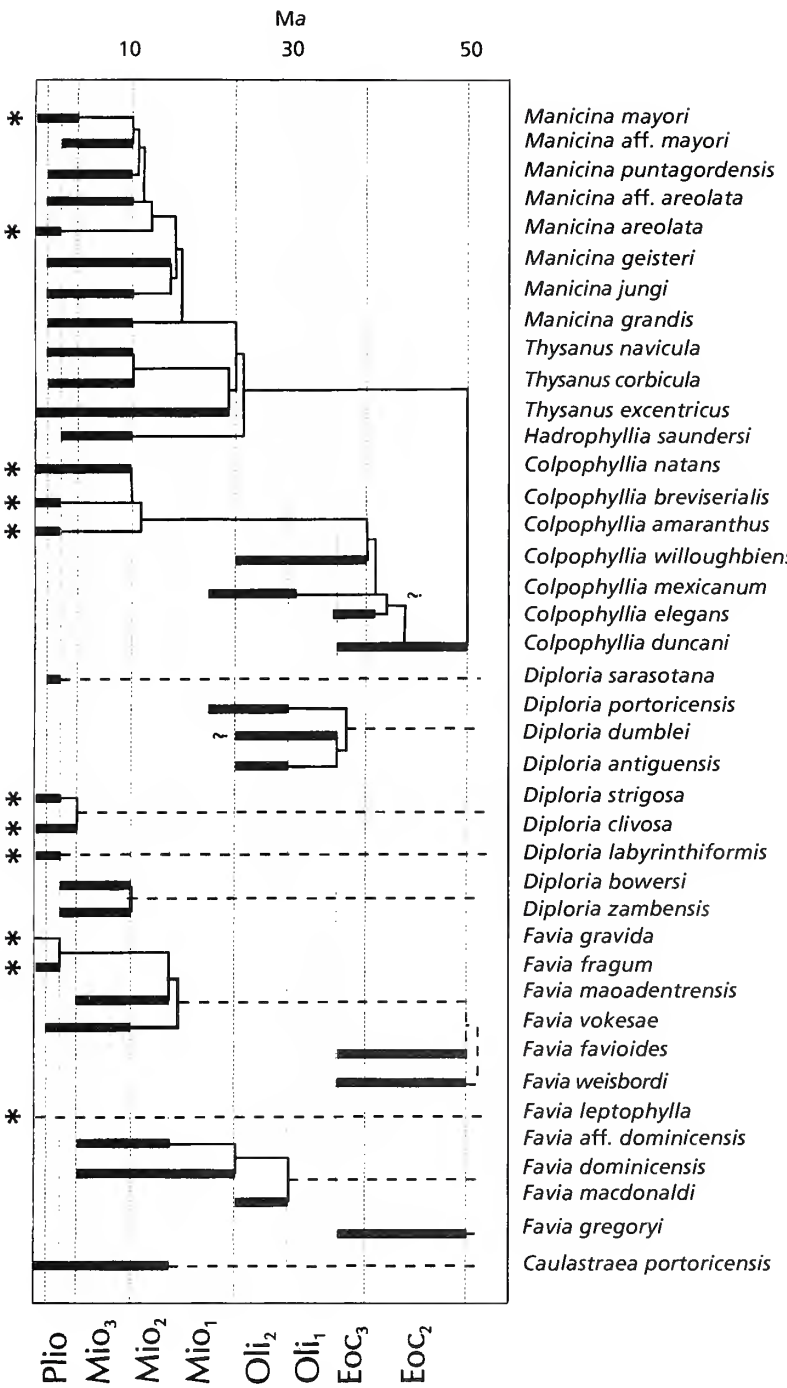

TEXT-FIG. 4. Evolutionary tree created by superimposing the selected cladogram onto stratigraphical ranges of the study taxa whilst minimizing hypothesized range extensions. Asterisks indicate extant species.

1943), and has developed a pan-tropical distribution since that time (Pfister 1980; Budd *et al.* 1992; Budd *et al.* 1994). The biogeographical origins of the distinctive coral fauna of north-eastern Brazil has never been demonstrated conclusively (Laborel 1967). However, this phylogeny suggests that the two endemic *Favia* species, *F. leptophylla* and *F. gravida*, are not closely related. Their most common ancestor is likely to be an unknown Paleogene species. Therefore, the biogeographical origins of this fauna is complex, including repeated migration of coral species from into and out of Caribbean and Brazilian reef communities.

As currently recognized, *Diploria* is also a paraphyletic group. Frost (1977) suggested close similarities among several Mediterranean and Caribbean species of *Diploria*, and species described from the Oligocene of Europe (Vaughan and Wells 1943; Pfister 1980) have been placed in the genus. However, the European forms have discontinuous columellar structures, and may represent a different lineage than the Caribbean forms (Chevalier 1961; Budd and Johnson 1998). Neogene *Diploria* species are restricted to the Caribbean region, but it is unlikely that the Miocene and later Caribbean *Diploria* species were directly derived from the Oligocene species.

In contrast, there is strong evidence of monophyly for both *Colpophyllia* and the MHT group. *Colpophyllia* was abundant in Europe during the Oligocene (Pfister 1980) and Miocene (Chevalier 1961), but became restricted to the Caribbean in the Neogene. The tree suggests that the Neogene Caribbean lineage originated from within the Paleogene lineage and has remained isolated from the Mediterranean fauna. No species of *Manicina*, *Hadrophyllia* or *Thysanus* has been described from outside the Caribbean, so a hypothesis of monophyly for this group is supported by the distribution data.

LATE NEOGENE TURNOVER

The evolutionary tree was used to compare evolutionary rates both with and without phylogenetic information. Phylogeny has two main effects on the distribution of taxa through time. First, the timing of species origination may be extended below the first occurrence of the species in the record, resulting in an hypothetical range extension. These range extensions will only alter estimates of origination rates and total species richness in earlier time intervals; they can have no effect on estimates of extinction rates. A phylogeny can also suggest the presence of undiscovered ancestral taxa termed 'ghost lineages' (Norell 1992). These are lineages predicted by tree topology. Since the age of both first and last occurrence of ghost lineages can be estimated on the evolutionary tree, including ghost lineages can alter estimates of species richness, origination and extinction through time.

Taxonomic turnover was analysed using standard techniques (Gilinsky 1991). The study interval has been divided into nine time periods of roughly equal duration, and an estimate of total species richness was obtained by counting the number of lineages which occur within or both before and after each interval. Some conventions were adopted to estimate the number of first and last occurrences in each time interval, so that first occurrences which correspond to boundaries are attributed to the interval after the boundary, but last occurrences mapped on to a boundary are attributed to the interval prior to the boundary (Text-fig. 5). All ghost lineages are counted if they were supported by at least one apomorphy. If both sister lineages associated with a branching event are supported by an apomorphy, then the branching event is assumed to be associated with the extinction of the parent lineage. If one of the sister lineages is not supported by an apomorphy, then it is assumed to be the parent lineage. Therefore, most branching events result in two first occurrences and one last occurrence. Proportional rates are used to estimate the magnitude and timing of taxonomic turnover. These are calculated as the number of first and last occurrences divided by the taxonomic richness within each time interval. Under a wide range of extinction models, these estimates of true branching and extinction rates are likely to be biased by differences in interval duration, but no individual metric has been proposed that provides unbiased estimates under a range of typical extinction models (Foote 1994).

As expected, the addition of ghost lineages increased estimated richness (Text-fig. 6A), with the

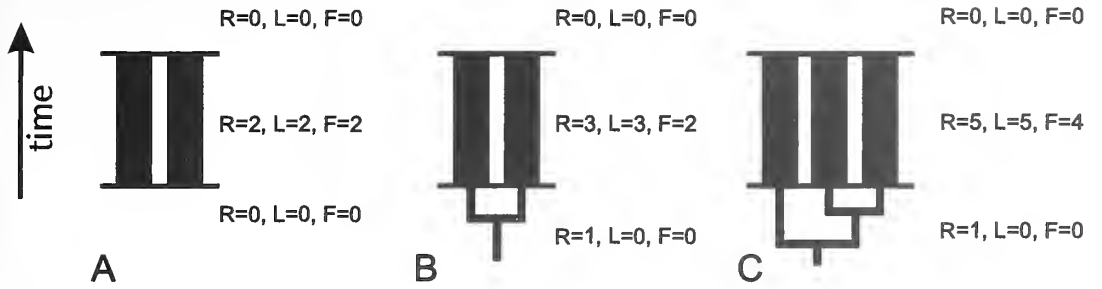

TEXT-FIG. 5. Rules for counting species richness and the number of first and last occurrences with and without hypothetical ancestors. In each case, vertical bars represent species ranges and horizontal lines are boundaries of stratigraphical intervals. Parts B and C include hypotheses of relationships and ghost lineages. A, when first occurrences are associated with interval boundaries, the species is assumed to have originated after the boundary, but last occurrences at boundaries are attributed to the prior time interval. B, hypothetical ancestors are assumed to become extinction during cladistic branching. C, all hypothetical ancestors are considered when multiple taxa appear to arise simultaneously.

long branches in the *Favia* and *Diploria* taxa increasing apparent richness during the Paleogene and Early Miocene. The general pattern remains unchanged with richness reaching a peak in the Late Miocene and Plio-Pleistocene faunas, but the highest total richness estimated including ghost lineages occurred during the Late Miocene with a decrease in richness during the Pliocene and Pleistocene. The number of first appearances (Text-fig. 6B) is also increased when phylogenetic predictions are included, but the overall pattern of high numbers of first appearances in the late Miocene is similar with and without ghost lineages. This increase might be caused by the increase in species richness during the Late Miocene. Proportional origination rates estimated including phylogeny suggest high origination throughout the Miocene. Patterns of species extinction through time are not changed by including phylogenetic information in the analysis. The estimates of pre-Pliocene background extinction rates are lower due to increased richness estimates when ghost lineages are counted, but neither the timing nor the magnitude of the Plio-Pleistocene extinction event is significantly altered. Including the ghost lineages has increased the relative difference between the Plio-Pleistocene time of species extinction relative to background extinction. For this group of reef-corals, there was radiation throughout the Miocene resulting in an increased number of species until the late Miocene. However, during the Plio-Pleistocene, most of the taxa suffered extinction.

Although the addition of phylogeny did not cause substantial change to the results of the analysis of taxonomic turnover, it does allow identification of periods with poor sampling, especially for the *Favia* and *Diploria* species during the Oligocene and early Miocene. Examination of the evolutionary tree also facilitates identification of potentially problematical occurrences of particular taxa. For example, the first appearance of *Thysanus excentricus* in the lower Miocene results in considerable range extension for the MHT lineage. As the database is refined, this occurrence will be examined in detail to insure that both the age assignment and identification are correct.

Therefore, although adding phylogenetic information to stratigraphical ranges can aid the detection of periods of poor sampling, the approach suffers from several potential sources of error. Most serious is the requirement for a stable phylogenetic hypotheses. This may not be possible for some problems, especially for large datasets or for groups without clearly defined discrete morphological characters. Alternate methods for detecting uneven sampling exist for such cases. For example, a sample completeness index can be calculated as the ratio of the number of taxa found in a particular interval to the number which occur both before and after the interval. A

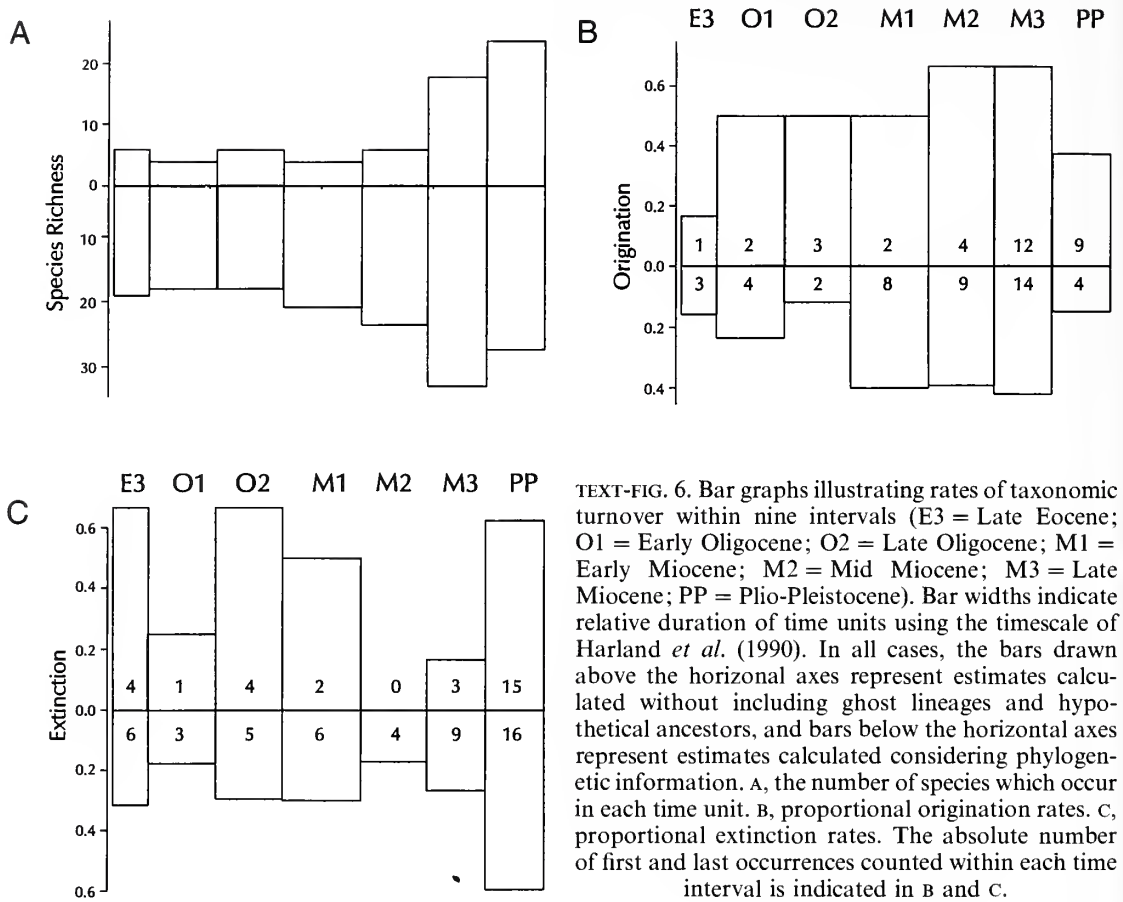

TEXT-FIG. 6. Bar graphs illustrating rates of taxonomic turnover within nine intervals (E3 = Late Eocene; O1 = Early Oligocene; O2 = Late Oligocene; M1 = Early Miocene; M2 = Mid Miocene; M3 = Late Miocene; PP = Plio-Pleistocene). Bar widths indicate relative duration of time units using the timescale of Harland *et al.* (1990). In all cases, the bars drawn above the horizonal axes represent estimates calculated without including ghost lineages and hypothetical ancestors, and bars below the horizontal axes represent estimates calculated considering phylogenetic information. A, the number of species which occur in each time unit. B, proportional origination rates. C, proportional extinction rates. The absolute number of first and last occurrences counted within each time interval is indicated in B and C.

combination of phylogenetic information and such phylogeny-free completeness indices will lead to a better understanding of the potential for uneven sampling to result in spurious patterns of taxonomic turnover.

SUMMARY

1. A new phylogeny for Caribbean faviid corals constructed from both continuous and discontinuous skeletal characters results in the definition of several lineages. One group includes all *Colpophyllia* species and another includes *Manicina*, *Hadrophyllia* and *Thysanus*. Within these groups the Neogene *Colpophyllia* species and the *Manicina* species with attached colonies are stable subgroups.

2. As currently recognized, *Diploria* and *Favia* are paraphyletic with respect to the meandroid taxa. This may be related to their biogeography with repeated migrations in and out of the Caribbean basin.

3. An evolutionary tree requires much hypothetical range extension for the poorly resolved taxa, but there is substantial agreement between branching order and order of first appearance within the *Colpophyllia* and *Manicina* groups.

4. Analysis of the rates of taxonomic turnover including ghost lineages and range extensions do not change the pattern detected when phylogenetic information was not included in the analysis; however, the evolutionary tree is useful in highlighting periods of relatively poor sampling and problematical occurrences of particularly sensitive taxa.

Acknowledgements. I thank A. F. Budd for invaluable help throughout this project. B. R. Rosen assisted with aspects of coral morphology and taxonomy, and discussion with T. McCormick and S. Peers provided useful insight into the problems of phylogenetic inference. The study was supported by a UK Natural Environment Research Council Advanced Postdoctoral Fellowship in Taxonomy.

REFERENCES

ARCHIE, J. W. 1985. Methods for coding variable morphological features for numerical taxonomic analysis. *Systematic Zoology*, **34**, 236–345.

—— 1989. A randomization test for phylogenetic information in systematic data. *Systematic Zoology*, **38**, 219–252.

BENTON, M. J. 1994. Palaeontological data and identifying mass extinctions. *Trends in Ecology and Evolution*, **9**, 181–185.

BUDD, A. F. 1993. Variation within and among morphospecies of *Montastraea*. *Courier Forschungsinstitut Senckenberg*, **164**, 241–254.

—— and COATES, A. G. 1992. Nonprogressive evolution in a clade of Cretaceous *Montastraea*-like corals. *Paleobiology*, **18**, 425–446.

—— and JOHNSON, K. G. 1998. Neogene paleontology in the northern Dominican Republic XX. The Family Faviidae (Anthozoa: Scleractinia) Part II. The Genera *Caulastraea*, *Favia*, *Diploria*, *Hadrophyllia*, *Thysanus*, *Manicina*, and *Colpophyllia*. *Bulletins of American Paleontology*.

—— —— and STEMANN, T. A. 1996. Plio-Pleistocene turnover and extinctions in the Caribbean reef coral fauna. 168–204. *In* JACKSON, J. B. C., BUDD, A. F. and COATES, A. G. (eds). *Evolution and environment in tropical America*. University of Chicago Press, Chicago, 408 pp.

—— STEMANN, T. A. and JOHNSON, K. G. 1994. Stratigraphic distributions of genera and species of Neogene to Recent Caribbean reef corals. *Journal of Paleontology*, **68**, 951–977.

—— —— STEWART, R. H. 1992. Eocene Caribbean reef-corals: a unique fauna from the Gatuncillo Formation of Panama. *Journal of Paleontology*, **66**, 570–594.

CHAPPILL, J. A. 1989. Quantitative characters in phylogenetic analysis. *Cladistics*, **5**, 217–234.

CHEVALIER, J. P. 1961. Recherches sur les madréporaires et les formations récifales Miocènes de la Méditerranée Occidentale. *Mémoires de la Société Géologique de France*, **93**, 1–563.

—— 1975. Les Scléractiniaires de las Mélanésie française (Nouvelle Calédonie, Iles Chesterfield, Ilse Loyauté, Nouvelles Hébrides). 2ème Partie, *Expédition française récifs coralliens, Nouvelle Calédonie Volume Septième*. Éditions de la Fondation Singer-Polignac, Paris, **7**, 5–407.

COATES, A. G. and OLIVER, W. A. 1973. Coloniality in zoantharian corals. 3–27. *In* BOARDMAN, R. S., CHEETHAM, A. H. and OLIVER, W. A., Jr (eds). 1973. *Animal colonies, development and function through time*. Dowden Hutchinson and Ross, Stroudsburg, Pennsylvania, 603 pp.

CORYELL, H. N. and OHLSEN, V. 1929. Fossil corals of Porto Rico, with descriptions also of a few Recent species. *New York Academy of Sciences, Scientific Survey of Porto Rico and the Virgin Islands*, **3**, 167–236, pls 26–44.

DANA, J. D. 1848. Zoophytes. *United States Exploring Expedition 1838–1842, Philadelphia*, **7**, 121–708, 721–740.

DUNCAN, P. M. 1863. On the fossil corals of the West Indian Islands, Part 1. *Quarterly Journal of the Geological Society, London*, **19**, 406–458, pls 13–16.

—— 1864. On the fossil corals of the West Indian Islands, Part 2. *Quarterly Journal of the Geological Society, London*, **20**, 20–44, pls 2–5.

ELDREDGE, N. and CRACRAFT, J. 1980. *Phylogenetic patterns and the evolutionary process. Method and theory in comparative biology*. Columbia University Press, New York, 349 pp.

ELLIS, J. and SOLANDER, D. 1786. *The natural history of many curious and uncommon zoophytes*. Benjamin White and Peter Elmsly, London, 208 pp.

ESPER, J. C. 1795. *Fortsetzungen der Pflanzenthiere*. Nürnberg, 1(3–4), 65–116, pls 32–100.

FAITH, D. P. and CRANSTON, P. S. 1991. Could a cladogram this short have arisen by chance alone? On permutation tests for cladistic structure. *Cladistics*, **7**, 1–28.

FARRIS, J. S. 1990. Phenetics in camouflage. *Cladistics*, **6**, 91–100.

FELSENSTEIN, J. 1985. Confidence limits on phylogenies: an approach using the bootstrap. *Evolution*, **39**, 783–791.

FISHER, D. C. 1991. Stratigraphic parsimony. 124–129. *In* MADDISON, W. P. and MADDISON, D. R. (eds). *MacClade version 3*. Sinauer Associates, Sunderland, Massachusetts, 398 pp.

FOOTE, M. 1994. Temporal variation in extinction risk and temporal scaling of extinction metrics. *Paleobiology*, **20**, 424–444.

FROST, S. H. 1977. Oligocene reef coral biogeography; Caribbean and western Tethys. *Memoires du Bureau de Recherches Géologiques et Minières*, **89**, 342–352.

—— and LANGENHEIM, R. L. 1974. *Cenozoic reef biofacies*. Northern Illinois University Press, Dekalb, Illinois, 388 pp.

—— and WEISS, M. P. 1979. Patch-reef communities and succession in the Oligocene of Antigua, West Indies: Summary. *Bulletin of the Geological Society of America*, **90**, 612–616.

—— HARBOUR, J. L., BEACH, D. K., REALINI, M. J. and HARRIS, P. M. 1983. *Oligocene reef tract development, southwestern Puerto Rico*. Rosenstiel School of Marine and Atmospheric Science, University of Miami, Miami Beach, Florida, 141 pp.

GILINSKY, N. L. 1991. The pace of taxonomic evolution. 157–174. *In* GILINSKY, N L. and SIGNOR, P. W. (eds). *Analytical paleobiology*. Short Courses in Paleontology Number 4. The Paleontological Society, University of Tennessee, Knoxville, Tennessee, 216 pp.

GILL, G. A. and COATES, A. G. 1977. Mobility, growth patterns and substrate in some fossil and Recent corals. *Lethaia*, **10**, 119–134.

HARLAND, W. B., ARMSTRONG, R. L., COX, A. V., CRAIG, L. E. SMITH, A. G. and SMITH, D. G. 1990. *A geologic time scale 1989*. Cambridge University Press, Cambridge, 263 pp.

HOUTTUYN, M. 1772. *Natuurlyke Historie of uitoverige Beschryving ver Dieren, Planten en Mineraalen, volgens het Samenstel van den Heer Linnaeus*. Amsterdam, Deel 1, vol. 17, 614 pp., pls 126–138.

JOHNSON, K. G. 1992. Population dynamics of a free-living coral: recruitment, growth, and survivorship of *Manicina areolata* on the Caribbean coast of Panamá, *Journal of Experimental Marine Biology and Ecology*, **164**, 171–191.

—— BUDD, A. F. and STEMANN, T. A. 1995. Extinction selectivity and ecology of Neogene Caribbean reef corals. *Paleobiology*, **21**, 52–73.

LABOREL, J. 1967. A revised list of Brazilian scleractinian corals and description of a new species. *Postilla*, **107**, 1–14.

LANYON, S. M. 1985. Detecting internal inconsistencies in distance data. *Systematic Zoology*, **34**, 397–403.

LINNAEUS, C. 1758. *Systema Naturae per regnia tria naturae, secundum classes, ordiners, genera, species. Tomus I. Regnum Animale*. Holmiae, Editio Decima, Reformata, 824 pp.

MADDISON, W. P., DONOGHUE, M. J. and MADDISON, D. R. 1984. Outgroup analysis and parsimony. *Systematic Zoology*, **33**, 83–103.

MATTHAI, G. 1926. Colony formation in astraeid corals. *Philosophical Transactions of the Royal Society, Series B*, **214**, 313–367.

—— 1928. Catalogue of the madreporarian corals in the British Museum (Natural History), Volume VII. *A monograph of the Recent meandroid Astraeidae*. British Museum (Natural History), London, 288 pp.

MILNE EDWARDS, H. and HAIME, J. 1849. Mémoire sur les polypiers appartenant à la familie des Oculinides, au groupe intermédiaire des Psuedastréides et à la famille des Fongides (extrait). *Compte Rendu de l'Academie de Sciences, Paris*, **29**, 67–73.

MÜLLER, P. L. S. 1775. Von den Korallen. *Des Ritters Carl von Linné Königlich Schweidischen Leibarztes vollständiges Natursystem nach der zwölften lateinischen Ausgabe mit einer ausführlichen Erklärung von P. L. S. Müller*, **6**, 672–708.

NORELL, M. J. 1992. Taxic origin and temporal diversity: the effect of phylogeny. 89–118. *In* NOVACEK, M. J. and WHEELER, Q. D. (eds). *Extinction and phylogeny*. Columbia University Press, New York, 253 pp.

NOVACEK, M. J. and NORELL, M. A. 1982. Fossils, phylogeny, and taxonomic rates of evolution. *Systematic Zoology*, **31**, 366–375.

PANDOLFI, J. M. 1989. Phylogenetic analysis of the early tabulate corals. *Palaeontology*, **32**, 745–764.

PFISTER, T. E. 1980. Systematische und paläoökologische Untersuchungen an oligozänen Korallen der umgebung von San Luca (Provinz Vicenza, Norditalien). *Schweizerische Paläontologisches Abhandulungen*, **103**, 1–121.

POTTS, D. C., BUDD, A. F. and GARTHWAITE, R. L. 1993. Soft tissue vs. skeletal approaches to species recognition and phylogeny reconstruction in corals. *Courier Forschungsinstitut Senckenberg*, **164**, 221–231.

SANDERSON, M. J. 1995. Objections to bootstrapping phylogenies. *Systematic Biology*, **44**, 299–320.

—— and DONOGHUE, M. J. 1989. Patterns of variation in levels of homoplasy. *Evolution*, **43**, 1781–1795.

SIDDALL, M. 1995. *Random Cladistics version 3.0*. Available by anonymous FTP from zoo.toronto.edu.ca.

SMITH, A. B. 1994. *Systematics and the fossil record*. Blackwell Scientific Publications, Oxford, 223 pp.

SORAUF, J. E. 1972. Skeletal microstructure and microarchitecture in Scleractinia (Coelenterata). *Palaeontology*, **15**, 88–107.

STEVENS, P. F. 1991. Character states, morphological variation, and phylogenetic analysis: a review. *Systematic Botany*, **16**, 553–583.
STOLARSKI, J. 1995. Ontogenetic development of the thecal structures in caryophylline scleractinian corals. *Acta Palaeontologica Polonica*, **40**, 19–44.
SWOFFORD, D. L. 1993. *Paup: Phylogenetic Analysis using Parsimony. Version 3.1.* Laboratory of Molecular Systematics, Smithsonian Institution, Washington, D.C.
THIELE, K. 1993. The holy grail of the perfect character: the cladistic treatment of morphometric data. *Cladistics*, **9**, 275–304.
VAUGHAN, T. W. 1917. The reef-coral fauna of Carrizo Creek, Imperial County, California and its significance. *Professional Paper of the United States Geological Survey*, **98T**, 355–386, pls 92–102.
—— 1919. Fossil corals from Central America, and Porto Rico, with an account of the American Tertiary, Pleistocene, and Recent coral reefs. *Bulletin of the United States National Museum*, **103**, 189–524.
—— and HOFFMEISTER, J. E. 1925. New species of fossil corals from the Dominican Republic. *Bulletin of the Museum of Comparative Zoology, Harvard College*, **67**, 315–326.
—— and WELLS, J. W. 1943. Revision of the suborders, families, and genera of the Scleractinia. *Special Paper of the Geological Society of America*, **104**, 1–363.
VERON, J. E. N. 1993. A biogeographic database of hermatypic corals. *Australian Institute of Marine Science Monograph Series*, **10**, 1–433.
—— 1995. *Corals in time and space. The biogeography and evolution of the Scleractinia.* Cornell University Press, Ithaca, 321 pp.
—— PICHON, M. and WIJSMAN-BEST, M. 1977. Scleractinia of eastern Australia Part II: families Faviidae, Trachyphylliidae. *Australian Institute of Marine Science Monograph Series*, **3**, 1–233.
VERRILL, A. E. 1868. Notice of the corals and echinoderms collected by Prof. C. F. Hartt, at the Abrolhos Reefs, Province of Bahia, Brazil, 1867. *Transactions of the Connecticut Academy of Arts and Sciences*, **1**, 351–359.
—— 1901. Variations and nomenclature of Bermudian, West Indian and Brazilian reef corals, with notes on various Indo-Pacific corals. *Transactions of the Connecticut Academy of Arts and Sciences*, **11**, 63–168.
WEISBORD, N. E. 1968. Some late Cenozoic stony corals from northern Venezuela. *Bulletins of American Paleontology*, **55**, 1–288.
—— 1974. Late Cenozoic corals of south Florida. *Bulletins of American Paleontology*, **66**, 259–544, pls 21–57.
WELLS, J. W. 1934. Eocene corals from Cuba. *Bulletins of American Paleontology*, **20**, 147–158.
—— 1935. Corals from the Cretaceous and Eocene of Jamaica. *Annals of Natural History, Tenth Series*, **5**, 183–194.
—— 1936. The nomenclature and type species of some genera of Recent and fossil corals. *American Journal of Science, Series 5*, **31**, 97–134.
—— 1945. West Indian Eocene and Miocene Corals. *Memoirs of the Geological Society of America*, **9**, 1–25.
—— 1956. Scleractinia. F328–444. *In* MOORE, R. C. (ed). *Treatise on invertebrate paleontology. Part F. Coelenterata.* Geological Society of America and University of Kansas Press, Lawrence, Kansas, 498 pp.
ZANS, V. A., CHUBB, L. J., VERSEY, H. R., WILLIAMS, J. B., ROBINSON, E. and COOKE, D. L. 1962. Synopsis of the geology of Jamaica. *Bulletin of the Geological Survey Department, Jamaica*, **4**, 1–72.

KENNETH G. JOHNSON
Department of Geology and Applied Geology
University of Glasgow
Glasgow G12 8QQ, UK

Typescript received 23 January 1996
Revised typescript received 10 June 1997

APPENDIX

Species and character matrix used in the phylogenetic inference. Wherever possible, type material was examined, but in other cases type material was not available and characters were scored by referring to non-type or to published descriptions. Missing characters are indicated by a question mark, characters which are inappropriate for a particular growth form are indicated by a dash.

Caulastrea portoricensis	(Coryell, *in* Coryell and Ohlsen, 1929)	1–021	01000	0–211	00000	002
Favia dominicensis	Vaughan, *in* Vaughan and Hoffmeister, 1925	1–021	10?02	11111	20002	101
Favia aff. *dominicensis*	Budd and Johnson, 1998	1–021	11?01	11111	20002	100
Favia favioides	(Wells, 1945)	1–01?	?0?02	10120	20010	000
Favia fragum	(Esper 1795)[1]	1–021	00212	10211	20000	000
Favia gregoryi	Wells, 1935	1–021	11003	10001	10002	001
Favia gravida	Verrill, 1868[2]	11121	00212	10321	10000	000
Favia leptophylla	Verrill, 1868[3]	1–021	00203	10101	10010	011
Favia macdonaldi	Vaughan, 1919	1–021	12?04	11101	20012	001
Favia maoadentrensis	Budd and Johnson, 1998	01021	00114	10321	20001	000
Favia vokesae	Budd and Johnson, 1998	1–021	10101	11321	20000	000
Favia weisbordi	Wells, 1934	1–02?	?1?03	10020	20010	001
Diploria antiguensis	(Vaughan, 1919)	11220	00201	?0321	10012	000
Diploria bowersi	Vaughan, 1917	11121	10?04	11000	10011	001
Diploria clivosa	(Ellis and Solander, 1786)[1]	11220	10001	00221	20011	002
Diploria dumblei	(Vaughan, 1919)	11220	00103	?1110	10012	000
Diploria labyrinthiformis	(Linneaus, 1758)[1]	11221	11104	10110	20011	001
Diploria portoricensis	(Vaughan, 1919)	11220	11101	?0110	1001?	001
Diploria sarasotana	Weisbord, 1974	11220	21001	?1010	10010	001
Diploria strigosa	(Dana, 1848)[1]	11220	11101	01111	20011	002
Diploria zambensis	Budd and Johnson, 1998	11121	11104	10010	20001	001
Colpophyllia amaranthus	(Müller, 1775)[1]	12120	33002	10100	01012	111
Colpophyllia breviserialis	Milne Edwards and Haime, 1849[1]	12120	23002	10100	01012	112
Colpophyllia duncani	Wells, 1935	12220	22001	?1211	01002	101
Colpophyllia elegans	Budd, *in* Budd, Stemann and Stewart, 1992	1222?	?1001	?1221	01002	101
Colpophyllia mexicanum	Frost, *in* Frost and Langenheim, 1974[2]	12221	22002	1?211	01002	111
Colpophyllia natans	Houttuyn, 1772	12220	23002	10100	01012	112
Colpophyllia willoughbiensis	(Vaughan, 1919)	12121	23002	11321	01002	111
Hadrophyllia saundersi	Budd and Johnson, 1998	01310	23000	1–100	00002	100
Thysanus corbicula	Duncan, 1863	00301	02010	0–321	00010	100
Thysanus excentricus	Duncan, 1863	01300	12000	0–100	00010	100
Thysanus navicula	Duncan, 1864	00311	02000	0–110	00011	100
Manicina areolata	(Linnaeus, 1758)[1]	00321	12212	10111	10101	100
Manicina aff. *areolata*	Budd and Johnson, 1998	00321	32202	11111	10102	100
Manicina grandis	Duncan, 1864	01311	12200	1–100	00102	100
Manicina geisteri	Budd and Johnson, 1998	02310	23110	1–211	00102	100
Manicina jungi	Budd and Johnson, 1998	01311	12210	1–321	00012	100
Manicina mayori	Wells, 1936[1]	10321	33212	11111	10102	111
Manicina aff. *mayori*	Budd and Johnson, 1998	10320	33202	11110	00102	111
Manicina puntagordensis	Weisbord, 1968	00320	23202	11101	10102	111

[1] collections from the Recent of Belize, Panama, and Anguilla were examined. All material is reposited in the Department of Geology, University of Iowa.
[2] characters scored from published descriptions.
[3] other material from type localities examined.

INDEX

D

E

L

M

N

O

VOLUME 41

Palaeontology

1998

PUBLISHED BY THE
PALAEONTOLOGICAL ASSOCIATION
LONDON

Dates of Publication of Parts of Volume 41

Part 1, pp. 1–192	13 February 1998
Part 2, pp. 193–381	23 March 1998
Part 3, pp. 383–573	10 June 1998
Part 4, pp. 575–806	14 August 1998
Part 5, pp. 807–1091	7 October 1998
Part 6, pp. 1093–1275	14 December 1998

THIS VOLUME EDITED BY B. M. COX, C. J. CLEAL, P. DOYLE, D. A. T. HARPER, A. HEMSLEY, D. K. LOYDELL, R. M. OWENS, D. M. UNWIN, R. A. WOOD

Printed in Great Britain
by Cambridge University Press

CONTENTS

NOTES FOR AUTHORS

The journal *Palaeontology* is devoted to the publication of papers on *all aspects* of palaeontology. Review articles are particularly welcome, and short papers can often be published rapidly. A high standard of illustration is a feature of the journal. Six parts are published each year and are sent free to all members of the Association. *Typescripts* should conform in style to those already published in this journal, and should be sent (with a disk, if possible) to the Secretary of the Publications Committee, **Dr R. Wood, Department of Earth Sciences, University of Cambridge, Downing Street, Cambridge CB2 3EQ,** who will supply detailed instructions for authors on request (these are published in *Palaeontology* 1996, **39**, 1065–1075).

Special Papers in Palaeontology is a series of substantial separate works conforming to the style of *Palaeontology*.

SPECIAL PAPERS IN PALAEONTOLOGY

In addition to publishing *Palaeontology* the Association also publishes *Special Papers in Palaeontology*. **Members** may subscribe to this by writing to the Membership Treasurer: the subscription rate for 1998 is £55·00 (U.S. $120) for Institutional Members, and £20·00 (U.S. $36) for Ordinary and Student Members. A single copy of each *Special Paper* is available on a non-subscription basis to Ordinary and Student Members *only*, for their personal use, at a discount of 25 per cent. below the listed prices: contact the Marketing Manager. **Non-members** may obtain Nos 39–58 (excluding 44) at cover price from Blackwell Publishers Journals, P.O. Box 805, 108 Cowley Road, Oxford OX4 1FH, UK, and older issues from the Marketing Manager. For all orders of *Special Papers* through the Marketing Manager, please add £1·50 (U.S. $3) per item for postage and packing.

PALAEONTOLOGICAL ASSOCIATION PUBLICATIONS

Special Papers in Palaeontology

For full catalogue and price list, send a self-addressed, stamped A4 envelope to the Marketing Manager. Numbers 2–48, excluding 44, are still in print and are available together with those listed below:

49. (for 1993): Studies in palaeobotany and palynology in honour of Professor W. G. Chaloner, F.R.S. Edited by M. E. COLLINSON *and* A. C. SCOTT. 187 *pp.*, 38 *text-figs*, 27 *plates*. Price £50 (U.S. $100).
50. (for 1993): Turonian ammonite faunas from central Tunisia, *by* G. R. CHANCELLOR, W. J. KENNEDY *and* I. M. HANCOCK. 118 *pp.*, 19 *text-figs*, 37 *plates*. Price £40 (U.S. $80).
51. (for 1994): *Belemnitella* from the Upper Campanian and Lower Maastrichtian Chalk of Norfolk, England, *by* W. K. CHRISTENSEN. 84 *pp.*, 22 *text-figs*, 9 *plates*. Price £35 (U.S. $70).
52. (for 1994): Studies on Carboniferous and Permian vertebrates. Edited by A. R. MILNER. 148 *pp.*, 51 *text-figs*, 9 *plates*. Price £45 (U.S. $90).
53. (for 1995): Mid-Dinantian ammonoids from the Craven Basin, north-west England, *by* N. J. RILEY. 87 *pp.*, 51 *text-figs*, 8 *plates*. Price £40 (U.S. $80).
54. (for 1995): Taxonomy and evolution of Llandovery biserial graptoloids from the southern Urals, western Kazakhstan, *by* T. N. KOREN' *and* R. B. RICKARDS. 103 *pp.*, 23 *text-figs*, 14 *plates*. Price £40 (U.S. $80).
55. (for 1996): Studies on early land plant spores from Britain. Edited by C. J. CLEAL. 145 *pp.*, 23 *text-figs*, 28 *plates*. Price £45 (U.S. $90).
56. (for 1996): Fossil and Recent eggshell in amniotic vertebrates: fine structure, comparative morphology and classification, *by* K. E. MIKHAILOV. 80 *pp.*, 21 *text-figs*, 15 *plates*. Price £35 (U.S. $70).
57. (for 1997): Cambrian bradoriid and phosphatocopid arthropods of North America, *by* DAVID J. SIVETER *and* M. WILLIAMS. 69 *pp.*, 8 *text-figs*, 9 *plates*. Price £30 (U.S. $60).
58. (for 1997): Himalayan Cambrian trilobites, *by* P. A. JELL *and* N. C. HUGHES. 113 *pp.*, 10 *text-figs*, 32 *plates*. Price £40 (U.S. $80).
59. (for 1998): Late Ordovician brachiopods from the South China Plate and their palaeogeographical significance, *by* ZHAN REN-BIN *and* L. R. M. COCKS. 70 *pp.*, 15 *text-figs*, 9 *plates*. Price £30 (U.S. $60).

Field Guides to Fossils

These are available only from the Marketing Manager. Please add £1·00 (U.S. $2) per book for postage and packing *plus* £1·50 (U.S. $3) for airmail. Payments should be in Sterling or in U.S. dollars, with all exchange charges prepaid. Cheques should be made payable to the Palaeontological Association.

1. (1983): Fossil Plants of the London Clay, *by* M. E. COLLINSON. 121 *pp.*, 242 *text-figs*. Price £7·95 (U.S. $16) (Members £6 or U.S. $12).
2. (1987): Fossils of the Chalk, *compiled by* E. OWEN; *edited by* A. B. SMITH. 306 *pp.*, 59 *plates*. Price £11·50 (U.S. $23) (Members £9·90 or U.S. $20).
3. (1988): Zechstein Reef fossils and their palaeoecology, *by* N. HOLLINGWORTH *and* T. PETTIGREW. iv+75 *pp.* Price £4·95 (U.S. $10) (Members £3·75 or U.S. $7·50).
4. (1991): Fossils of the Oxford Clay, *edited by* D. M. MARTILL *and* J. D. HUDSON. 286 *pp.*, 44 *plates*. Price £15 (U.S. $30) (Members £12 or U.S. $24).
5. (1993): Fossils of the Santana and Crato Formations, Brazil, *by* D. M. MARTILL. 159 *pp.*, 24 *plates*. Price £10 (U.S. $20) (Members £7.50 or U.S. $15).
6. (1994): Plant fossils of the British Coal Measures, *by* C. J. CLEAL *and* B. A. THOMAS. 222 *pp.*, 29 *plates*. Price £12 (U.S. $24) (Members £9 or U.S. $18).
7. (1996): Fossils of the upper Ordovician, *edited by* D. A. T. HARPER *and* A. W. OWEN. 312 *pp.*, 52 *plates*. Price £16 (U.S. $32) (Members £12 or U.S. $24).

Palaeontology

VOLUME 41 · PART 6

CONTENTS

Printed in Great Britain at the University Press, Cambridge ISSN 0031–0239